

# SITC 2016

NATIONAL HARBOR, MD

31<sup>ST</sup> ANNUAL MEETING

# ABSTRACTS

NOVEMBER 11-13, 2016



Society for Immunotherapy of Cancer

## Abstract & Poster Information

### Poster Hall Location

Prince George's Exhibition Hall AB

### Poster Set-Up Hours

Friday, November 11 7:00 – 10:00 a.m.

### Poster Tear-Down Hours

Saturday, November 12 8:00 – 9:30 p.m.

### Poster Hall Hours

Friday, November 11 noon – 8:00 p.m.

Saturday, November 12 7:00 a.m. – 8:00 p.m.

### Poster Presentation Times

#### Odd Numbered Posters (Poster Presenters are Present)

Friday, November 11 12:15 – 1:30 p.m. (Lunch)

Friday, November 11 6:15 – 7:30 p.m. (Poster Reception)

#### Even Numbered Posters (Poster Presenters are Present)

Saturday, November 12 11:45 a.m. – 1:00 p.m. (Lunch)

Saturday, November 12 6:45 – 8:00 p.m. (Poster Reception)

### Category

	<b>Poster Numbers</b>
Adoptive Cellular Therapy . . . . .	1 – 55
Biomarkers and Immune Monitoring . . . . .	56 – 125
Bispecific Antibodies . . . . .	126 – 131
Clinical Trials in Progress . . . . .	132 – 167
Clinical Trials: Cutting-Edge (Completed Trials) . . . . .	168 – 173
Coinhibition and Costimulation . . . . .	174 – 193
Combinations: Immunotherapy/Immunotherapy . . . . .	194 – 257
Combinations: Immunotherapy/Standard of Care . . . . .	258 – 269
Diet, Exercise and/or Stress and Impact on the Immune System . . . . .	270 – 274
Immune Metabolism . . . . .	275 – 281
Immune-related Adverse Event Management: Evidence Based Strategies and Clinical Care . . . . .	282 – 283
Immunogenomics and Oncogenetics . . . . .	284 – 292
Inflammation, Innate Immunity, and the Microbiome . . . . .	293 – 301
Not Listed/Other . . . . .	302 – 318
Oncolytic Viruses . . . . .	319 – 335
Promoting and Measuring Antitumor Immunity . . . . .	336 – 351
Survivorship Issues Related to Immunotherapy . . . . .	352 – 353
Therapeutic Cancer Vaccines . . . . .	354 – 381
Tumor Microenvironment . . . . .	382 – 437
Late-Breaking Abstracts . . . . .	438 – 469
Adoptive Cellular Therapy . . . . .	438 – 440
Biomarkers and Immune Monitoring . . . . .	441 – 445
Clinical Trials in Progress . . . . .	446 – 448
Clinical Trials: Cutting-Edge (Completed Trials) . . . . .	449
Coinhibition & Costimulation . . . . .	450
Combinations: Immunotherapy/Immunotherapy . . . . .	451 – 457
Combinations: Immunotherapy/Standard of Care . . . . .	458
Diet, Exercise and/or Stress and Impact on the Immune System . . . . .	459
Not Listed/Other . . . . .	460
Therapeutic Cancer Vaccines . . . . .	461 – 463
Tumor Microenvironment . . . . .	464 – 469



### Presidential Travel Award Recipient

This image denotes the four abstracts awarded Presidential Travel Awards. See abstracts 124, 125, 280, 300.



### Abstract Travel Award Recipient

This image denotes abstracts awarded Abstract Travel Awards. See abstracts 2, 7, 23, 25, 29, 30, 32, 34, 51, 78, 112, 117, 123, 156, 186, 216, 228, 247, 265, 268, 285, 338, 390, 416, 430, 432, 433.

## Table of Contents

Author Index ..... 2  
 Keyword Index..... 46  
 Abstract Listing ..... 49

### Don't Miss the SITC Oral Poster Sessions!

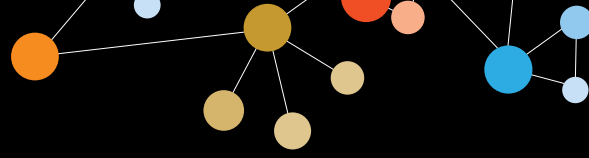
Beyond regular poster viewing, SITC welcomes the Oral Poster Sessions. These sessions provide select poster presenters with the opportunity to orally share their work with the SITC audience through brief, highlighted presentations. The Oral Poster Sessions will take place in the Prince George's Exhibition Hall AB in the presentation area in the far back right of the hall, adjacent to booth #538. The daily schedule of presenters is also available in the Exhibition Hall.

<b>Friday, November 11, 2016</b>		<b>Poster Number</b>
12:30 – 12:40 p.m.	Augmentation of tumor infiltrating CD8+ T cells and specific response to autologous tumor antigens in a phase I trial of in situ vaccination with CCL21 gene-modified dendritic cells <i>Jay M. Lee, MD – David Geffen School of Medicine, University of California, Los Angeles</i>	170
12:40 – 12:50 p.m.	Inflammatory activation via PKC-Syk pathway in macrophages lacking CD47-SIRPα restraint initiates potent phagocytosis toward cancer <i>Zhen Bian – Georgia State University</i>	294
12:50 – 1:00 p.m.	Phase II Study of Intratumoral plasmid Interleukin 12 (pIL-12) with Electroporation in Combination with Pembrolizumab in Stage III/IV Melanoma Patients with Low Tumor Infiltrating Lymphocytes <i>Alain Algazi, MD – University of California, San Francisco</i>	466
1:00 – 1:10 p.m.	Systemic immunotherapeutic efficacy of an immunocytokine, NHS-mull12, in a superficial murine orthotopic bladder cancer model <i>Amanda Vandevener, PhD – Center for Cancer Research, National Cancer Institute, National Institutes of Health</i>	460
1:10 – 1:20 p.m.	Effects of TLR7 agonist imiquimod combined with local radiotherapy on the tumor microenvironment in women with metastatic breast cancer in a prospective trial <i>Sylvia Adams, MD – New York University School of Medicine, Perlmutter Cancer Center</i>	464
<b>Saturday, November 12, 2016</b>		<b>Poster Number</b>
noon – 12:10 p.m.	Inhibitors of B cell activation reduce tumor growth and attenuate pro-tumorigenic phenotype of tumor immune infiltrates in a syngeneic mouse model of ovarian cancer <i>Nathalie Scholler, MD, PhD – Stanford Research Institute</i>	402
12:10 – 12:20 p.m.	Whole-blood RNA transcript-based signatures predict pre- and post-treatment response in two large independent clinical studies of patients with advanced melanoma treated with tremelimumab <i>Nina Bhardwaj, MD, PhD – The Tisch Cancer Institute at The Mount Sinai Medical Center</i>	62
12:20 – 12:30 p.m.	A test identifying advanced melanoma patients with long survival outcomes on nivolumab shows potential for selection for benefit from combination checkpoint blockade <i>Jeffrey Weber, MD, PhD – New York University Langone Medical Center</i>	107
12:30 – 12:40 p.m.	Pharmacodynamic gene expression changes from Talimogene Laherparepvec (T-VEC) plus Ipilimumab in a phase 1b study for metastatic melanoma <i>Abraham A. Anderson, PhD – Amgen, Inc.</i>	445
12:40 – 12:50 p.m.	Defining molecular mechanisms of resistance to tumor immunity <i>Natalie Collins, MD, PhD – Dana-Farber Cancer Institute</i>	285

## Author Index

Name	A	Poster Number	Name	A	Poster Number
Aarts, Craig		16	Agudo, Judith		232
Abassi, Yama		202	Aguilar, Ethan, G.		296
Abdallah, Rehab.		137	Aguilera, Todd		384
Abdul-Alim, Siddiq		26	Ahamadi, Malidi		197
Abelin, Jennifer, G.		312	Ahmad, Shamim		457
Abolhalaj, Milad		56, 382	Ahmed, Nabil		25
Abraham, Tara, S.		302	Ahn, Myung Ju.		165
Abtin, Fereidoun		170	Ahn, Yong-Oon		263
Abu-Eid, Rasha		457	Ahr, Katya		300
Acheson, Anupama		157	Ahrens, Eric, T.		338
Acquavella, Nicolas		160	Ai, Midan		177
Adam, Ammar		423	Aisner, Joseph		95
Adams, David		305	Aizer, Ayal		265
Adams, Gregory P		40	Ajina, Reham		385
Adams, Homer		411	Akerley, Wallace.		244
Adams, Katherine		5	Akporiaye, Emmanuel		446
Adams, Sarah, F.		383	Albershardt, Tina, C.		195, 354
Adams, Sharon		170	Albertini, Mark, R.		168, 171
Adams, Sylvia		464	Albiges, Laurence		135
Adamus, Tomasz		184, 350	Albrekt, Ann-Sofie		382
Addepalli, Murali		342, 343	Albright, Andrew		72, 73
Adekandi, Madhukara		130	Alekar, Shilpa		253
Adjei, Alex, A.		221	Aleman, Ramon		325, 326
Adurthi, Sreenivas		190	Alexander, Brian		265
Adusumilli, Prasad, S.		1	Algazi, Alain		117, 466
Aeffner, Famke		93	Ali, Siraj		95
Afentoulis, Michael		78	Alicea, Candido		7
Agapova, Larissa		223	Allbritton, Omaira		200
Agarwala, Sanjiv		333	Allen, Clint, T.		212
Ager, Casey		177, 194	Allen, Natalie		128
Aggarwal, Charu		368	Allersdorfer, Andrea		182
Aggouraki, Despoina		92	Alley, Evan, W.		261
Agnello, Giulia		275	Allison, James		246, 351, 352
Agrawal, Rajendra		79	Al-Muftah, Mariam		306
Agrawal, Sudhir		216	Alston, Tesha		250
Agrawal, Swati		79	Alt, Jürgen		262





## Author Index

<u>Name</u>	<u>A</u>	<u>Poster Number</u>	<u>Name</u>	<u>A</u>	<u>Poster Number</u>
Alteber, Zoya . . . . .		450	Aoki, Rhonda . . . . .		156
Alters, Susan . . . . .		275	Aquino-Michaels, Keston . . . . .		286
Althammer, Sonja. . . . .		443	Archer, Jacob, F. . . . .		195
Alva, Ajjai . . . . .		132	Arina, Ainhoa . . . . .		258
Amado, Rafael . . . . .		4	Armand, Philippe . . . . .		147, 153, 238
Amanda, Vandever . . . . .		460	Armenta, Paul . . . . .		467
Amaria, Rodabe . . . . .		216	Armet, Caroline, M. . . . .		423
Amatulli, Michael . . . . .		243	Armstrong, Adam . . . . .		144
Ameratunga, Malaka . . . . .		159	Arnoux, Thomas. . . . .		196
Amin, Asim . . . . .		106, 444	Arora, Kshitij . . . . .		116
Amrhein, John . . . . .		173	Arreaza, Gladys . . . . .		61
Anagnostou, Valsamo. . . . .		151	Ascarateil, Stephane . . . . .		355
Anand, Snjezana . . . . .		344, 345, 420	Ascierto, Paolo, A. . . . .		109, 449, 465
Andersen, Rikke. . . . .		9, 136	Ashworth-Sharpe, Julia . . . . .		118
Anderson, Abraham, A. . . . .		445	Askmyr, David . . . . .		56, 382
Anderson, Clark . . . . .		352	Asmellash, Senait . . . . .		107
Anderson, Mark . . . . .		386	Assadipour, Yasmine . . . . .		12
Andersson, Bengt. . . . .		364	Assenmacher, Mario . . . . .		33
Andersson, Emilia, K. . . . .		465	Athelogou, Maria . . . . .		110
Andre, Pascale . . . . .		196	Atkins, Michael, B. . . . .		106, 135, 161, 197, 425, 444
André, Thierry . . . . .		141	Atkinson, Victoria . . . . .		197
Andrijauskaite, Kristina . . . . .		454, 455	Attaf, Meriem . . . . .		9
Andtbacka, Robert, H.I. . . . .		140, 333, 334, 445, 466	Au, Gough . . . . .		319
Angela, Omilian . . . . .		99	Au, Katrina . . . . .		407
Angell, Helen, K. . . . .		57	Aung, Sandra . . . . .		462
Angiuoli, Sam . . . . .		291	Autio, Karen, A. . . . .		237
Annels, Nicola . . . . .		319	Au-Young, Janice . . . . .		97
Annunziata, Christina, M. . . . .		15	Avery, Kendra, N. . . . .		126, 127
Ansa-Addo, Ephraim, A. . . . .		2	Awad, Mark . . . . .		265
Ansari, Tameem . . . . .		59, 336	Ayers, Mark . . . . .		61, 72, 73
Antal, Joyce . . . . .		443	Azimi, Vahid . . . . .		119
Anthony, Scott . . . . .		427	Aznar, M. Angela . . . . .		174
Antilla, Marjukka . . . . .		41	Azrilevich, Alex. . . . .		449
Antonarakis, Emmanuel, S. . . . .		133, 137, 340	Azulay, Meir . . . . .		450
Antonia, Scott, J. . . . .		261, 449			
Anwar, Firoz. . . . .		309			

## Author Index

<u>Name</u>	<b>B</b>	<u>Poster Number</u>	<u>Name</u>	<b>B</b>	<u>Poster Number</u>
Backert, Linus		90	Bartlett, Nancy		147
Backes, Floor, J.		145	Barton, Sunjay, M.		292
Bagarazzi, Mark		368	Barve, Minal		371
Bagg, Eleanor, A. L.		3	Basher, Fahmin		252
Bahjat, Keith		91, 462	Bassett, Roland		104, 353
Bai, Dina		356	Basu, Samik		4
Baia, Gilson		339	Bath, Natalie		4
Baird, Jason		293	Batista, Luciana		341
Bajaj, Anshika		195	Bauer, Todd, W.		142, 155, 160, 237, 410
Bajorin, Dean		146	Baughman, Jan, E.		137
Baker, Daniel, M.		445	Bauman, Julie		396
Bakker, Lex		131	Baumgaertner, Petra		301
Balakumaran, Arun		134, 147, 153	Bauml, Joshua		368
Balatoni, Timea		408	Bavi, Prashant		465
Balboni, Tracy		265	Bayle, J. Henri		6
Balch, Leslie		208	Baylin, Stephen		151
Ballesteros-Merino, Carmen		78, 103, 114, 441, 462, 466	Beceren-Braun, Figen		427
Bander, Neil		55	Beck, Kristen		467
Bang, Andrew		265	Becker, Annette		424
Bang, Yung-Jue		61	Beckers, Johannes		419
Bannerji, Rajat		134	Beckett, Michael, A.		258
Bao, Riyue		432	Bedognetti, Davide		287, 288, 429
Bao, Yangyi		227, 367	Bedu-Addo, Frank		463
Barakat, David		388	Beechem, Joseph		67, 121, 122
Baratelli, Felicita, E.		170	Beeson, Craig		276
Barbee, Susannah, D.		175	Bel Aiba, Rachida-Siham		182
Barberi, Theresa		388	Bell, Bryan		293, 441
Barker, Christopher, A.		199	Bell, Charles, JM.		400
Barlesi, Fabrice		239	Bell, Peter		241
Barnea, Eytan		408	Bellmont, Joaquim		132, 146
Barras, David		301	Bellovin, David, I.		175
Barrett, Carl		57	Beltran, Nancy		69
Barrett, David		39	Beltran, Pedro		321
Barth, Carola		33	Ben Amor, Amira		96
Bartkowiak, Todd		177, 194	Bendell, Johanna		141, 449
Bartlett, David		222, 236, 346, 389	Bender, James		11, 42, 47



## Author Index

<u>Name</u>	<u>B</u>	<u>Poster Number</u>	<u>Name</u>	<u>B</u>	<u>Poster Number</u>
Bender, Lewis, H. . . . .		337	Bifulco, Carlo, B. . . . .		91, 103, 114, 157, 334, 462, 465, 466
Bender, Steven. . . . .		399	Bigley, Alison . . . . .		386
Benita, Yair. . . . .		450	Billingsley, James, M. . . . .		90
Bennett, Alan, D. . . . .		5	Binder-Scholl, Gwendolyn . . . . .		4, 5
Bennett, Mark, K. . . . .		155, 231	Bingham, Patrick . . . . .		253
Benz, Steven . . . . .		289	Biniszkiwicz, Detlev, M. . . . .		423
Bera, Tapan . . . . .		226	Binning, Gerd . . . . .		110, 443
Bergamaschi, Cristina . . . . .		7	Birditt, Brian . . . . .		121
Berger, Frank . . . . .		114	Bischoff, Helge. . . . .		262
Berger, Sven . . . . .		182	Bivalacqua, Trinity, J. . . . .		71
Bergeron, Derek. . . . .		96	Black, Joshua, C. . . . .		83, 93
Berglund, Anders . . . . .		124	Black, Lora . . . . .		458
Berglund, Peter . . . . .		195, 354	Black, Mary . . . . .		12
Berglund, Sofia . . . . .		89	Blacklock, Hilary . . . . .		163
Berkey, Sara . . . . .		389	Blackmon, Shauna. . . . .		106, 107, 444
Bernatchez, Chantale. . . . .		216, 387, 439	Blake, Zoe . . . . .		198, 467
Bernett, Matthew, J. . . . .		126, 127	Blakely, Collin . . . . .		409
Bernstein, Donna . . . . .		4	Blanchard, Miran . . . . .		458
Berrong, Zuzana . . . . .		457	Blaskovich, Michelle, A. . . . .		11, 14, 47
Berry, John S. . . . .		373	Blazar, Bruce, R. . . . .		48, 274
Berzofsky, Jay, A. . . . .		337	Blitzer, Grace . . . . .		21
Bessell, Catherine, A. . . . .		112	Blogowski, Wojciech . . . . .		303
Betts, Gareth . . . . .		4	Bloom, Anja, C. . . . .		337
Beyer, Sophie. . . . .		102	Boehm, Jesse . . . . .		285
Bhanot, Gyan . . . . .		95	Bokovanov, Vladimir. . . . .		223
Bhardwaj, Nina . . . . .		62, 148, 171, 400, 447	Bommareddy, Praveen, K. . . . .		320, 321, 327, 328
Bhardwaj, Rukmini. . . . .		176	Bono, Petri . . . . .		449
Bhatia, Shailender . . . . .		26, 45	Bonzon, Christine. . . . .		126, 127
Bhatt, Rupal . . . . .		444	Bookstaver, Michelle . . . . .		461
Bhaumik, Srabani . . . . .		118	Booth, Jamie . . . . .		414
Bian, Zhen . . . . .		294	Borch, Troels Holz . . . . .		136, 158
Bianchi, Valentina . . . . .		9	Borges, Luis. . . . .		175
Bianco, Alberto. . . . .		287	Borkar, Rohan, N. . . . .		119
Biediger, Ronald, J. . . . .		361	Bornschiagl, Svetlana . . . . .		63, 144, 271
Bielamowicz, Kevin . . . . .		25	Bosch, Marnix . . . . .		169
Bieniarz, Christopher . . . . .		118	Bose, Nandita . . . . .		179, 391

## Author Index

<u>Name</u>	<b>B</b>	<u>Poster Number</u>	<u>Name</u>	<b>B</b>	<u>Poster Number</u>
Bossen, Bolette . . . . .		81	Bryan, Jennifer . . . . .		328
Bossenmaier, Birgit . . . . .		226	Bryant, Bonita . . . . .		69
Bot, Adrian . . . . .		46	Bryant, Richard . . . . .		377
Botti, Gerardo . . . . .		109, 465	Bshara, Wiam . . . . .		99
Boudadi, Karim . . . . .		137	Bu, Xia . . . . .		186
Boughorbel, Sabri . . . . .		288	Buchbinder, Elizabeth . . . . .		265
Boulmay, Brian . . . . .		462	Buchner, Alexander . . . . .		110
Boussiotis, Vassiliki, A. . . . .		186	Bucsek, Mark . . . . .		270, 272
Boyer, Jean . . . . .		368	Budhani, Pratha . . . . .		177
Brahmer, Julie . . . . .		151	Budhu, Sadna . . . . .		199, 255
Bramante, Simona . . . . .		335	Budkowska, Marta . . . . .		303
Bramson, Jonathan . . . . .		16, 18	Bueno, Raphael . . . . .		409
Branstetter, Daniel . . . . .		402	Buettner, Florian . . . . .		419
Brech, Dorothee . . . . .		419	Buettner, Nico . . . . .		305
Brenin, David . . . . .		358	Bullock, Kim . . . . .		358, 370
Brenner, Malcolm, K. . . . .		123	Bullock, Timothy, N. . . . .		100, 101
Brett, Sara . . . . .		5	Burger, Michael, C. . . . .		50
Brevard, Julie . . . . .		216	Burgess, Melissa . . . . .		45
Brewer, Joanna . . . . .		5	Burgher, Blake . . . . .		98, 99
Brieu, Nicolas . . . . .		109	Burk, Chad . . . . .		37
Brisson, Ryan . . . . .		162	Burova, Elena . . . . .		200
Broadus, V.Courtney . . . . .		409	Burrill, Joel . . . . .		366
Brockstedt, Dirk, G. . . . .		261, 366	Bussler, Holm . . . . .		208
Brody, Joshua . . . . .		149, 232, 447	Butterfield, Lisa, H. . . . .		154, 222, 279
Bronson, Roderick . . . . .		297	Byrd, David . . . . .		26
Brooks, Alan, D. . . . .		249, 348	Byrd, John . . . . .		134
Broucek, Joseph . . . . .		418	Byrd, Tiara . . . . .		25
Brown, Alice . . . . .		323	Byrne-Steele, Miranda . . . . .		284
Brown, Brian . . . . .		232			
Brown, Brittany . . . . .		284	<b>C</b>		
Brown, Gail, L. . . . .		237	Cagney, Daniel . . . . .		265
Brown, Sheila . . . . .		240	Calderon, Hugo . . . . .		323
Browning, Erica . . . . .		466	Callahan, Margaret, K. . . . .		125, 238, 449
Bruce, Jeffrey, N. . . . .		292, 469	Calvo, Emiliano . . . . .		449
Brunazzi, Erin . . . . .		422	Campbell, Amanda . . . . .		451
Bruno, Tullia, C. . . . .		390, 422	Campbell, Jean . . . . .		466



## Author Index

<u>Name</u>	<u>C</u>	<u>Poster Number</u>	<u>Name</u>	<u>C</u>	<u>Poster Number</u>
Campbell, Mary		91	Cerkovnik, Logan		93
Campbell, Tracy		19	Cerullo, Vincenzo		201, 331
Campeato, Luis Felipe		224	Cervera-Carrascón, Víctor		41, 203
Campo, Meghan		282	Cesareni, Gianni		287
Campogan, Dwayne		340	Cha, John		344, 345, 420
Canoll, Peter		469	Chacon, Jessica		8
Canter, Robert, J.		49, 138	Chagin, Karen		4
Cao, Alexander		178	Chainsukh Loya, Anand		35
Cao, Felicia		322	Chajut, Ayelet		450
Capasso, Cristian		201, 331	Chakraborty, Paramita		276
Caplazi, Patrick		214	Champagne, Monique		173
Cappuccini, Federica		377	Champion, Brian		323
Carcaboso, Angel, M.		310	Chan, Anissa SH.		391
Carlino, Matteo, S.		197	Chan, Anthony T.C.		165
Carmichael, Lakeesha		168	Chan, Chanty		219
Caron, Christine		96	Chan, Christopher		450
Carpentier, Sabrina		341	Chan, Emily		449
Carpi, Sara		201	Chan, Ivan		237
Carpio, Cecilia		239	Chan, Leo		304
Carrasco, Ruben		297	Chan, Nancy		95
Carrera, Diego, A.		310	Chan, Timothy, A.		112, 374
Carretero-Iglesia, Laura		94	Chandran, Smita		139
Carson, Dennis, A.		242	Chandrasekhar,, Talapaneni		190
Carson, William		451	Chang, Alfred E		227, 367
Carvajal-Hausdorf, Daniel		64	Chang, Joe		352
Caspell, Richard		58	Chang, Nancy, N.		340
Castellini, Laura		384	Chang, Peter		6
Cathomas, Richard		262	Chang, Serena		65
Cauvin, Annick		421	Chang, Thomas		342
Cauwenberghs, Sandra		253	Chang, Young doo		85
Caux, Christophe		193, 247	Chanuc, Fabien		196
Cebon, Jonathan, S.		197	Chao, Mark		156
Ceccarelli, Michele		288	Chapelin, Fanny		338
Cecchi, Fabiola		111	Chaplin, Jenny		253
Celis, Esteban		10, 378	Chappel, Scott, C.		423
Cerignoli, Fabio		202	Charych, Deborah, H.		342, 343

**Author Index**

<u>Name</u>	<u>C</u>	<u>Poster Number</u>	<u>Name</u>	<u>C</u>	<u>Poster Number</u>
Chatterjee, Shilpak . . . . .		276	Chou, Margaret . . . . .		217
Chaudhri, Apoorvi . . . . .		186	Choueiri, Toni, K. . . . .		135, 146, 197
Chaudhuri, Amitabha . . . . .		392	Choy, Carmen . . . . .		218
Chaussabel, Damien . . . . .		288	Christian, Beth . . . . .		153
Cheever, Martin . . . . .		171	Chu, Liz . . . . .		26
Chen, Ada . . . . .		403, 424	Chu, Seung . . . . .		126, 127
Chen, Amanda . . . . .		175	Chunduru, Srinivas . . . . .		216
Chen, Gang . . . . .		393	Clark, Joseph, I. . . . .		106, 307, 444
Chen, Hui . . . . .		81	Clavijo, Paul, E. . . . .		212
Chen, Jason . . . . .		230, 231	Clayburgh, Daniel, R. . . . .		119
Chen, Jie Qing . . . . .		42	Clement, Amanda . . . . .		108
Chen, Lawrence . . . . .		117	Clements, Erin . . . . .		168
Chen, Lieping . . . . .		100	Clifton, Guy T . . . . .		373
Chen, Mei . . . . .		161	Clynes, Raphael . . . . .		238
Chen, Mingyi . . . . .		138	Cobbold, Mark . . . . .		305, 312, 356
Chen, Shuming . . . . .		66	Coder, Brandon . . . . .		257
Chen, Xiaomu . . . . .		339	Coffman, Robert, L. . . . .		242
Chen, Xin . . . . .		367	Cohen, Cyrille . . . . .		245
Chen, Xiufen . . . . .		295, 404	Cohen, Ezra, E.W. . . . .		242, 458
Chen, Yu . . . . .		393, 403	Cohen, Lewis . . . . .		65
Chenchik, Alex . . . . .		394	Cohen, Roger . . . . .		368
Cheng, Jonathan . . . . .		72, 73	Cohen, Zvi . . . . .		173
Cheng, Zhi-jie Jey . . . . .		181	Cojocar, Gady . . . . .		450
Chheda, Zinal . . . . .		310	Colen, Rivka . . . . .		237
Chiang, Eugene . . . . .		214	Colevas, A. Dimitrios . . . . .		156, 267
Chikina, Maria . . . . .		422, 428	Collins, Jennifer . . . . .		168
Chin, Renee . . . . .		177	Collins, Natalie . . . . .		285
Chinnasamy, Harshini . . . . .		12	Colrain, Jillian . . . . .		339
Chittenden, Thomas . . . . .		316	Coltharp, Carla . . . . .		395
Chiu, Hsiling . . . . .		215	Colyer, Duncan . . . . .		159
Chlosta, Sabine . . . . .		147, 153	Concha-Benavente, Fernando . . . . .		396
Cho, Charles . . . . .		399	Conder, Kristie . . . . .		446
Choi, Minsig . . . . .		129	Cong, Mei . . . . .		181
Chong Tan, Yann . . . . .		339	Conlin, Alison . . . . .		157
Chongyung, Fang . . . . .		360	Conlon, Kevin . . . . .		69
Choppin, Agnes . . . . .		454	Conn, Greg . . . . .		463



## Author Index

Name	C	Poster Number
Connolly, Eileen, P.		292
Conrad, Valerie.		91
Conroy, Jeff		98, 99
Conwell, Darwin.		228, 406
Copeland, Larry		145
Coppola, Domenico		85
Cordes, Lisa.		172
Cornfeld, Mark.		216
Corrales, Leticia, P.		295, 399
Cortés Salgado, Alfonso		282
Cortés, Javier.		282
Cortina, Luis		8
Coukos, George		375, 429
Coussens, Lisa, M.		119, 261, 409
Couto, Joseph		118
Coveler, Andrew, L.		150
Coyle, Scott, M.		440
Crabill, George		66
Craggs, Graham.		421
Craig, Andrew		407
Creasy, Caitlin		439
Cristescu, Razvan		61, 73
Crittenden, Marka		293
Crocker, Andrea		180
Cron, Kyle, R.		286
Cronstein, Bruce, N.		269
Crooks, James.		240
Crosby, Andrea.		421
Crosignani, Stefano		253
Crowder, Robert.		426
Crowley, Elizabeth		447
Cruickshank, Scott.		221
Csuka, Orsolya.		408
Cui, Weiguo		53
Culp, William		138
Cumberbatch, Kerwin		191

Name	C	Poster Number
Curbishley, Stuart.		305
Curiel, Tyler		389
Curran, Emily		295
Curran, Michael		177, 194
Curti, Brendan		91, 106, 140, 150, 244, 334, 444, 446

### D

D'Apuzzo, Massimo		434
Da Costa, Andre.		421
Dadey, Rebekah.		280
Daenthanasanmak, Anusara.		276
Dai, Fu.		227
Dai, Jie		200
Dai, Peihong		357
Dai, Zhimin		42
Dagleish, Angus		204
Dalvie, Deepak.		253
Daly, Megan, E.		448
Damare, Sherri		95
D'Amico, Leonard		67
Dammassa, Ernesta.		178
Danaher, Patrick		67, 171
Danforth, David		139
Daniels, Gregory, A.		307
Dassa, Liat.		450
Daud, Adil		117, 333, 466
Davar, Diwakar		154
Davenport, Anna		57
David, Justin, M.		379
David, Larry		78
Davies, Bronwyn		244, 319
Davies, Michael, A.		216, 353
Davis, Tom		171, 447
De Bono, Johann		133
de Braud, Filippo		449
de Groot, Patricia		352

## Author Index

Name	D	Poster Number	Name	D	Poster Number
de Gruijl, Tanja . . . . .		335	Deshpande, Vikram . . . . .		116
De Henau, Olivier . . . . .		199	Desjarlais, John . . . . .		126, 127
de Leon, Laura . . . . .		221	Deveraux, Quinn . . . . .		175
De Maeseneire, Coraline . . . . .		253	DeVito, Anna Marie . . . . .		26
De Sanctis, Francesco . . . . .		375	Devlin, Sean . . . . .		300
De Santis, Maria . . . . .		146	deVries, Michele . . . . .		366
de Silva, Suresh . . . . .		211	Dey, Chaitali . . . . .		130
de Wit, Ronald . . . . .		146	Dhudashia, Amit . . . . .		190
Deacon, Donna, H. . . . .		100, 101, 370, 429	Dhupkar, Pooja . . . . .		206
DeBenedette, Mark . . . . .		205, 259	di Pietro, Alessandra . . . . .		135
Declerck, Paul . . . . .		362	Diab, Adi . . . . .		216, 352, 359, 387
Decock, Julie . . . . .		288, 306	Diaz, Jr., Luis A. . . . .		141
Deeds, Michael . . . . .		144	Diaz, Luis . . . . .		291
DeFalco, Jeff . . . . .		339	Diaz-Lagares, Angel . . . . .		174
Dela Cruz, Filemon . . . . .		292	DiCostanzo, AriCeli . . . . .		271
Delcommenne, Marc . . . . .		75	Diede, Scott, J. . . . .		221
Delgoffe, Greg, M. . . . .		54, 278, 279, 280, 281, 389, 422	Dietz, Allan, B. . . . .		63, 144, 271
Delismon, Judy . . . . .		26	Dillhoff, Mary . . . . .		406
Delogu, Lucia . . . . .		287	Dillon, Patrick . . . . .		358
Delorenzi, Mauro . . . . .		301	Dilworth, Ryan . . . . .		395
Delrio, Paolo . . . . .		465	Dimberg, Anna . . . . .		325
Demaria, Sandra . . . . .		268, 269, 459, 464	Ding, Naiqing . . . . .		43
Deng, Liang . . . . .		357	Ding, Wei . . . . .		153
Deng, Weiwen . . . . .		366	Ding, Yueyun . . . . .		225
Deng, Wentao . . . . .		405	Disis, Mary, L. . . . .		67
Denies, Sofie . . . . .		253	Doberstein, Stephen, K. . . . .		343
Denis, Caroline . . . . .		196	Dobkin, Julie . . . . .		243
Denisova,, Galina . . . . .		18	Dobson, Jason, R. . . . .		178
Dennis, Lucas . . . . .		67, 121	Docta, Roslin . . . . .		3
Deol, Abhinav . . . . .		129	Doener, Fatma . . . . .		262
Derakhshandeh, Roshanak . . . . .		68	Dolegowska, Barbara . . . . .		303
DeRenzo, Christopher . . . . .		30	Doleschall, Zoltan . . . . .		408
Desai, Jayesh . . . . .		159	Dolstra, Harry . . . . .		131
Desai, Niyati . . . . .		116	Dolton, Garry . . . . .		9
Desbien, Anthony, L. . . . .		399	Doman, Thompson . . . . .		243
Deshpande, Amit . . . . .		76, 162	Dominguez, George . . . . .		221



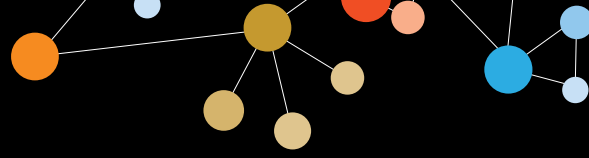


## Author Index

<u>Name</u>	<u>D</u>	<u>Poster Number</u>	<u>Name</u>	<u>D</u>	<u>Poster Number</u>
Donahue, Renee . . . . .		207, 212	Duncan, Brynn . . . . .		37
Donda, Alena . . . . .		94	Dundr, Pavel . . . . .		113
Donia, Marco . . . . .		9, 136, 158	Duong, MyLinh. . . . .		6
Donovan, Michael, Joseph. . . . .		148	Dutcher, Janice, P. . . . .		307
Dooddy, Jacqueline . . . . .		128	Dutour, Aurélie . . . . .		193
Doroodchi, Atbin . . . . .		457	Dutta, Panna . . . . .		463
Dorsey, Frank Charles . . . . .		243	Duttagupta, Priyanka . . . . .		434
Dotti, Gianpietro. . . . .		123	Duvvuri, Uma . . . . .		396
Dougherty, Janna. . . . .		24	Dwyer, Mary . . . . .		466
Dovedi, Simon . . . . .		250	Dyson, Gregory . . . . .		129
Downing, Sean . . . . .		108	Dyson, Mike. . . . .		317
Downs-Canner, Stephanie . . . . .		389			
Drabick, Joseph D . . . . .		452	<b>E</b>		
Dragnev, Konstanin . . . . .		143	Eagan, Maribeth, A. . . . .		121
Drake, Andrew, W. . . . .		450	Early, Brandon . . . . .		71
Drake, Charles, G. . . . .		133, 137, 340, 388, 399	Ebner, Peggy . . . . .		390
Dranoff, Glenn . . . . .		178	Eckelman, Brendan, P. . . . .		175
Draper, Lindsey, M. . . . .		19	Edwards, Robert, P. . . . .		222, 433, 389
Drechsel, Katharina . . . . .		33	Egevad, Lars . . . . .		188
Dreicer, Robert. . . . .		146	Ehrmann, Jon M. . . . .		102
Driessens, Gregory . . . . .		253	Eickhoff, Jens . . . . .		369
Driscoll, Kyla . . . . .		243	Einstein, Mark . . . . .		463
Druker, Brian, J. . . . .		411	Eisenhower, Mary . . . . .		284
Dubay, Christopher . . . . .		78, 91, 462	El Alaoui, Meddy . . . . .		317
Dubensky, Thomas, W. . . . .		366, 399	El Alaoui, Said . . . . .		317
Dubey, Aparajita. . . . .		130	El Rassi, Edward . . . . .		119
Dubinett, Steven, M. . . . .		170	Elashoff, David, A. . . . .		170
Dubois, Sigrid . . . . .		69	Eles, Klara . . . . .		408
Dudimah, Duafalia . . . . .		348	Ellies, Lesley . . . . .		384
Duff, Susan . . . . .		368	Elliott, Nathan . . . . .		121
Duhen, Rebekka . . . . .		70	Ellison, Christie . . . . .		458
Duhen, Thomas . . . . .		70	Elnaggar, Omar . . . . .		406
Dummer, Reinhard. . . . .		117	Elvecrog, James . . . . .		250
Dumontet, Charles . . . . .		317	Emberley, Ethan. . . . .		231
Dunai, Cordelia . . . . .		274, 296	Emens, Leisha. . . . .		149
Dunaway, Dwayne . . . . .		121, 122	Emerling, Daniel . . . . .		339

## Author Index

Name	<b>E</b>	Poster Number	Name	<b>F</b>	Poster Number
Emtage, Peter		440	Farren, Matthew		233
Enblad, Gunilla		123	Fast, Loren		189
Eng, Charis		220	Faustman, Denise		397
Engelhard, Victor, H.		415	Felber, Barbara		7
English, Jessie		254	Feldman, Steven, A.		12
Enstrom, Amanda		261	Femel, Julia		414
Erdag, Gulsun		100, 101	Feng, Dai		132
Eremeev, Artem		223	Feng, JunLi		253
Eriksson, Emma		324, 325, 326	Feng, Yan		399
Ernstoff, Marc, S.		106, 171, 444	Feng, Zipei		334, 462
Ertelt, Kathleen		391, 468	Feola, Sara		201
Espiritu Santo, Gregg		339	Fernandez, Christian		258
Essand, Magnus		123	Fernando, Ingrid		20, 379
Esteller, Manel		174	Ferris, Robert, L.		239, 267, 280, 396, 412, 413, 422, 456
Estevez Diz, Maria Del Pilar		145	Fesenkova, Valentyna		378
Eswarappa, Rajesh		225	Field, Jessica, J.		311
Evans, Elizabeth		208	Fieschi, Jacques		341
Evans, Kathy		277, 401	Fisher, Brenda		462
Evans, Lawrence		192	Fisher, George, A.		156
Eyquem, Justin		55	Fisher, Kerry		323
			Fisher, Terry		208
	<b>F</b>		Fitzharris, Bernie		197
Fa'ak, Faisal		359, 361	Flano, Emilio		374
Facciabene, Andrea		360, 375, 380	Flechtner, Jessica, B.		374
Facciponte, John		375, 380	Flies, Dallas, B.		383
Fakhrejahani, Farhad		172	Fling, Steven		67, 171
Falchook, Gerald		142, 237	Flint, Paul, W.		119
Fan, Aaron		10	Flynn, Patrick		409
Fan, Frank		181	Fogler, William		209
Fang, Victoria		24	Fong, Lawrence		342
Fantini, Massimo		20, 207, 212, 379	Formenti, Silvia, C.		268, 269, 464
Fardis, Maria		11, 47	Forrest-Hay, Alex		74
Faries, Mark		140	Fosco, Dominick		404
Farkas, Emil		408	Foster, Aaron E.		6
Faroudi, Mustapha		128	Foster, Cathie		208
Farrell, Michael		118	Foster, Rosemary		397



## Author Index

Name	F	Poster Number
Fotin-Mleczek, Mariola . . . . .		90, 262
Fousek, Kristen . . . . .		25
Fox, Bernard, A. . . . .		7, 78, 103, 114, 157, 334, 441, 453, 462, 465, 466
Fox, Maxine . . . . .		102
Francica, Brian. . . . .		399
Francis, Julie-Ann . . . . .		407
Francis, Nicole . . . . .		113
Frangou, Costa. . . . .		394
Frank, Ian . . . . .		11, 47
Frankel, Melissa. . . . .		95
Franklin, Marilyn . . . . .		209
Franklin, Wilbur . . . . .		390
Frascaro, Federica . . . . .		201
Fraser, Kathryn . . . . .		179, 391, 468
Frayssinet, Véronique. . . . .		341
Frederix, Kim . . . . .		253
Freeman, Gordon J. . . . .		186
Freese, Katharina. . . . .		33
Freimark, Bruce. . . . .		199, 210, 213
Frey, Alan. . . . .		24, 330
Fridman Kfir, Tal. . . . .		450
Fridman, Leticia. . . . .		395
Friedlander, Michael, L. . . . .		159
Friedlander, Philip . . . . .		62, 148, 171
Friedman, Alan. . . . .		388
Friedman, David. . . . .		293
Fritsch, Edward . . . . .		186
Fromm, George . . . . .		211
Früh, Martin. . . . .		262
Fry, Terry . . . . .		37
Fu, Siqing . . . . .		155
Fu, Yang-Xin . . . . .		258
Fu, Yichun . . . . .		198, 467
Fuertes Marraco, Silvia A. . . . .		301
Fugle, Caroline W. . . . .		416
Fuhrmann, Steven . . . . .		330

Name	F	Poster Number
Fujii, Rika. . . . .		20
Fukaya, Satoshi . . . . .		381
Fulton, Noreen . . . . .		256
Fulton, Ross, B. . . . .		179, 468
Fuoco, Claudia. . . . .		287
Fusciello, Manlio . . . . .		201
Fuseri, Nicolas . . . . .		196

### G

Gabitzsch, Elizabeth. . . . .		379
Gabraïl, Nashat . . . . .		328
Gabrilovich, Dmitry . . . . .		221
Gajewski, Thomas, F. . . . .		51, 150, 183, 238, 256, 286, 399, 429, 430, 432, 456
Galeassi, Nadejda . . . . .		370
Galon, Jérôme . . . . .		341, 465
Gamble, Alicia . . . . .		205, 259
Gameiro, Sofia, R. . . . .		207, 212
Gan, Hui. . . . .		159
Gan, Jacek. . . . .		168
Gandhi, Anita . . . . .		215
Ganesan, Shridar . . . . .		95
Gangadhar, Tara, C. . . . .		239
Ganguly, Sudipto . . . . .		450
Gangxiong, Huang . . . . .		22
Gao, Chan . . . . .		434
Gao, Qian. . . . .		3
Gardai, Shyra, J. . . . .		150, 311
Gardner, Kellie . . . . .		425
Gardner, Mark . . . . .		98
Gargosky, Sharron . . . . .		466
Garon, Edward, B. . . . .		143, 170
Garrabrant, Thomas. . . . .		8
Garrett-Mayer, Elizabeth. . . . .		276
Gartner, Jared J. . . . .		12, 44
Gartrell, Benjamin . . . . .		191
Gartrell, Robyn. . . . .		198, 292, 467

## Author Index

Name	G	Poster Number	Name	G	Poster Number
Garvin, Denise		181	Giralt, Sergio		300
Gasmi, Billel		255	Giri, Rajanish		18
Gastineau, Dennis, A.		63, 144, 271	Giri, Sanjeev		225
Gastman, Brian		171	Gitau, Mark		458
Gaughan, Elizabeth		370	Gitlitz, Barbara		151
Gause, Christine		165	Giver, Cynthia, R.		48
Gauthier, Audrey		240	Gladstone, Douglas		238
Gauthier, Kelsey, S.		399	Glenn, Sean		98, 99
Geib, James		216	Glitza, Isabella		216, 353
Geiss, Gary		121	Glod, John		4
Geissler, Michael		262	Gnad-Vogt, Ulrike		90, 262
Geller, Melissa		67	Godwin, John		267
George, Fiby		447	Goel, Sanjay		150
Georgoulas, V.		92	Goff, Stephanie, L.		12, 13, 139
Geppert, Carol		465	Gojo, Ivana		89
Gergel, Ivan		387	Gokuldass, Aishwarya		14, 47
Gerken, Claudia		30	Gold, Kathryn, A.		458
Gerry, Andrew		3, 5	Goldberg, Judith		464
Gershan, Jill		21	Goldinger, Simone		117
Gershenson, Zack		39	Goldman, Jonathan, W.		170
Geukens, Nick		362	Goldschmidt, Hartmut		163
Gfeller, David		301	Goldstein, Joel		180
Ghadially, Hormas		196	Gomes, Bruno		253
Ghaffari, Mahsa		118	Gomes, Tina		440
Ghamsari, Lila		374	Gong, Jian		210, 213
Ghandi, Leena		265	Gonzalez Gugel, Elena		400
Ghisoli, Maurizio		371	Gonzalez, Denise		175
Ghori, Razi		164	Gonzalez, Iliana		91
Giaccia, Amato		384	Gonzalez, Ricardo		34
Gianani, Roberto		83, 93	Gooding, William		222, 396
Gibney, Geoffrey		425	Goodman, Reid		409
Giffin, Louise		211	Gopal, Ajay		238
Gilden, Julia		181	Gorden, Keith		179, 468
Gill, Saar		23	Gordon, Keith		391
Gillies, Stephen, D.		168, 417	Gordon, Nancy		206
Giobbie-Hurder, Anita		282, 444	Gormley, Michael		77



## Author Index

<u>Name</u>	<b>G</b>	<u>Poster Number</u>	<u>Name</u>	<b>G</b>	<u>Poster Number</u>
Gorski, Kevin . . . . .		445	Grupp, Stephan . . . . .		39
Gottschalk, Stephen . . . . .		30, 36, 52, 322	Gschwendt, Juergen . . . . .		132
Gough, Michael . . . . .		293	Gu, Xuemin . . . . .		239, 267, 456
Govindappa, Nagaraja . . . . .		130	Guan, Wei . . . . .		178
Gowda, Nagaraj . . . . .		190, 225	Gudas, Jean . . . . .		442
Gowda, Nagesh . . . . .		190	Guenther, Garret . . . . .		202
Goyal, Sharad . . . . .		327	Guerrero, Jennifer . . . . .		297
Graff, Jeremy . . . . .		179, 391, 468	Guiducci, Cristina . . . . .		242
Graham, Charles . . . . .		407	Guindani, Michele . . . . .		104
Grailer, Jamison . . . . .		181	Guirado, Elizabeth . . . . .		298
Graves, Edward . . . . .		384	Gulley, James, L. . . . .		20, 172, 379
Gray, Michael . . . . .		210, 213	Gunderson, Andrew . . . . .		462
Graziano, Robert F. . . . .		102	Gunset, Gertrude . . . . .		55
Greasley, Samantha . . . . .		253	Guo, Jie . . . . .		253
Green, Daniel, S. . . . .		15	Guo, Zeng-qing . . . . .		393
Greenberg, Norman . . . . .		339	Gupta, Ashok . . . . .		443
Greenwald, Shirley . . . . .		450	Gupta, Ravi . . . . .		392
Gregory, Gareth . . . . .		134	Gupta, Sachin . . . . .		298
Greiff, Lennart . . . . .		56, 382	Gupta, Sumati . . . . .		244
Greiner, John, W. . . . .		234, 460	Gustafson, Michael, P. . . . .		63, 144, 271
Grenga, Italia . . . . .		207, 212	Gutierrez, Andres A . . . . .		238
Gressett, Monica, M. . . . .		417	Guttridge, Denis . . . . .		228
Griesinger, Frank . . . . .		262	Guy, Emily, I. . . . .		417
Grigoryeva, Olga . . . . .		223	Guyre, Cheryl, A. . . . .		75
Grigsby, Iwen . . . . .		250	Guzman, Wilson . . . . .		254
Grilley-Olson, Juneke, E. . . . .		150			
Grimaldi, Antonio . . . . .		109	<b>H</b>		
Grivas, MD, PhD, Petros . . . . .		313	Haanen, John, B. . . . .		135
Grogan, Elizabeth, W. . . . .		205	Habensus, Iva . . . . .		105, 118
Grogan, Jane . . . . .		214	Habtetsion, Tsadik . . . . .		438
Grose, Mark . . . . .		140, 244, 319, 328, 334	Hackl, Hubert . . . . .		89
Grosh, William . . . . .		370	Hacohen, Nir . . . . .		186
Gross, Matt . . . . .		166, 230, 231	Haddad, Robert . . . . .		456
Grossenbacher, Steven, K. . . . .		49, 138, 274	Hadrup, Sine Reker . . . . .		9
Grossmann, Kenneth . . . . .		333	Hagberg, Hans . . . . .		123
Gruber, Harry . . . . .		329	Hagihara, Katsunobu . . . . .		342

## Author Index

Name	H	Poster Number	Name	H	Poster Number
Hagner, Patrick		215	Harris-Bookman, Sarah		388
Hahn, Noah, M.		146	Hart, Philip		406
Hailemichael, Yared		359, 361	Hartig, Greg		168
Haining, W. Nicholas		285	Hartmann, Arndt		113, 465
Halaban, Ruth		107	Hartnett, Jim		181
Hale, Diane F.		373	Harvey, Christopher		162
Hall, Gerald		243	Hasapidis, Jeannette		221
Hall, MacLean		34	Hassan, Raffit		261
Hallmeyer, Sigrun		334	Hastings, William, D.		178
Halmos, Balazs		143	Hata, Chelsie, Y.		175
Hamadani, Mehdi		147	Hatz, Rudolf		114
Hamdy, Freddie		377	Hausler, David		38
Hamid, Omid		117, 445	Havel, Jonathan		112, 374
Hamieh, Mohamad		55	Havunen, Riikka		41, 203, 335
Hamilton, Garth		5	Hayakawa, Taeko		435
Hammerich, Linda		447	Hayashi, Tomoko		242
Hammill, Joanne		16, 18	Haydu, Lauren, E.		353
Hammond, Scott, A.		234	Haymaker, Cara		216, 387, 439
Hamzaoui, Kamel		96	Haynes, Heather		340
Han, Jian		284	He, Li-Zhen		180
Han, Yanyan		260	He, Ming-Xiao		84
Handy, John		114	Heath, Elisabeth		80
Hank, Jacquelyn, A.		168, 417	Hedvat, Michael		126, 127
Hanks, Brent, A.		171, 277, 401	Heery, Christopher R.		20, 172
Hanson, Bill		366	Hegde, Meenakshi		25
Hanson, Jodi		58, 60	Heinze, Clinton		417
Happel, Kyle		462	Hellmann, Matthew, D.		221, 255, 374
Harada, Yui		17	Hellström, Ann-Charlotte		324
Harari, Paul, M.		417	Helman, Sarah, R.		44
Harbell, Michael		339	Helming, Laura		299
Harder, Nathalie		109, 110	Helsen, Christopher		16, 18
Hardin, Mark O		373	Helwig, Christoph		172
Hardwick, James		253	Hembrough, Todd		111
Hare, Thomas W.		145	Hemmi, Silvio		335
Harrington, Kevin		244, 319	Hemminki, Akseli		41, 203, 335
Harris, Jaryse		383	Hemminki, Otto		335



## Author Index

<u>Name</u>	<u>H</u>	<u>Poster Number</u>	<u>Name</u>	<u>H</u>	<u>Poster Number</u>
Hendricks, Kyle . . . . .		169	Hodge, James, W. . . . .		20, 207, 212, 379
Hendrickx, Wouter . . . . .		287, 288, 306	Hodgson, Darren, R. . . . .		57
Hennicken, Delphine . . . . .		449	Hodi, F. Stephen. . . . .		197, 238, 265, 456
Henningsohn, Lars . . . . .		188	Hodkinson, Brendan, P. . . . .		77
Henrich, Ian . . . . .		217	Hoerr, Ingmar . . . . .		90
Henry, MaryBeth . . . . .		168	Hofmeister, Robert . . . . .		299
Heo, Dae Seog . . . . .		263	Höglund, Martin . . . . .		123
Herbert, Garth S. . . . .		373	Holdich, Tom . . . . .		4
Herbst, Ronald . . . . .		250	Holland, Pamela, M. . . . .		423
Hermitte, Fabienne. . . . .		341	Hollevoet, Kevin . . . . .		362
Heron, Dwight . . . . .		396	Hollingsworth, Robert E . . . . .		227, 367
Herzog, Thomas. . . . .		145	Holmgaard, Rikke . . . . .		243
Hess, Kenneth, R. . . . .		352	Holtzhausen, Alisha . . . . .		277, 401
Hessel, Harald . . . . .		110	Honarmand, Somayeh . . . . .		261
Heymach, John . . . . .		352	Hong, Bang-Xing . . . . .		322
Higgs, Brandon . . . . .		443	Hong, David . . . . .		177, 352
Higuchi, Tomoe . . . . .		383	Hong, Henoch, S. . . . .		90, 262
Hilbe, Wolfgang . . . . .		262	Hong, Peter . . . . .		200
Hill, Adrian . . . . .		377	Hong, Ruey-Long . . . . .		82, 165
Hill, Andrew, G. . . . .		197	Horne, William . . . . .		422
Hill, Jonathan, A. . . . .		423	Horst, Basil . . . . .		467
Hillairet de Boisferon, Marc . . . . .		240	Horton, Brendan. . . . .		183, 430
Hillringhaus, Lars. . . . .		315	Horvath, Szabolcs . . . . .		408
Hilton, Traci . . . . .		441, 462	Hoshida, Yujin . . . . .		444
Hiner, Rebecca. . . . .		459	Hotson, Andrew . . . . .		218
Hinner, Marlon, J. . . . .		182	Hou, Jinlin . . . . .		260
Hinrichs, Christian, S. . . . .		19, 44	Hou, Xiaohong . . . . .		284
Hipp, Madeleine. . . . .		262	Hou, Yafei. . . . .		310
Hirsch, Brooke . . . . .		83, 93	Houot, Roch . . . . .		239
Hirsch, Heather, A. . . . .		76, 162	Hovgaard, Dorrit. . . . .		35
Hirschhorn-Cymerman, Daniel . . . . .		255	Howe, Karen . . . . .		3
Hirshfield, Kim, M. . . . .		95	Howell, Alan. . . . .		208
Hix Glickman, Laura . . . . .		399	Howells-Ferreira, Ana. . . . .		91
Ho, Hanson . . . . .		440	Hoyt, Clifford . . . . .		108
Ho, Po . . . . .		218	Hsiao, Chin-Fu. . . . .		82
Hoch, Ute. . . . .		343, 359, 387	Hsu, Jennifer . . . . .		69

## Author Index

Name	H	Poster Number	Name	H	Poster Number
Hu, Hong-Ming		462	Hylander, Bonnie		270, 272
Hu, Xintao		7			
Hu, Yangyang		227, 367	<b>I</b>		
Hu, Zhiwei		451	Ibrahim, Nageatte		197
Hua, Hong		307	Ignacio, Eduardo		121
Hua, Ping		186	Iida, Shinsuke		163
Huang, Alan		121	Illingworth, Sam		323
Huang, Fei		411	Infante, Jeffrey		237
Huang, Hongying		191	Ioffe, Ella		200
Huang, Jing		260	Irmler, Martin		419
Huang, Shiang		227, 367	Irving, Bryan, A.		219
Huang, Tony		231	Itoh, Kyogo		465
Huang, Yuanhiu		219	Izaki, Daisuke		467
Hubbard, Antony		118			
Huber, Rudolf M.		114	<b>J</b>		
Hudson, Thomas, E.		366	Jablons, David		409
Huelsmann, Erica		418	Jablonski, Sandra		385
Huffman, Austin, P.		229	Jackson, Doreen O.		373
Huh, Warner		145	Jackson, Natalie		387
Huhn, Richard, D.		179	Jacobson, Caron		267
Hulett, Tyler		78	Jacques, Judy		374
Hu-Lieskovan, Siwen		208	Jaeger, Dirk		449
Humeau, Laurent		368	Jaen, Juan, C.		403, 424
Hunt, Donald, F.		312, 356	Jagannath, Sundar		163, 164
Hunter, John		450	Jäger, Dirk		141
Hurd, Mark		439	Jahan, Naznin		310
Hurt, Elaine		227, 367	Jahan, Thierry		261
Hurwitz, Michael		387	Jaini, Ritika		220
Huss, Ralf		109, 110	Jaiswal, Ashvin		177, 194
Hutchins, Jeff		199, 210, 213	Jakobsen, Bent		4, 5
Hutnick, Natalie, A.		77	Jallas, Anne-Catherine		193
Hutson, Thomas		106, 444	James, Marihella		216
Hwang, Jimmy		117	Jameson, Michael, B.		197
Hwu, Patrick		216, 387, 439	Jandus, Camilla		94
Hwu, Wen-Jen		197, 216	Jang, Dadi		384
Hyland, Fiona		97	Janku, Filip		237





## Author Index

Name	J	Poster Number	Name	J	Poster Number
Janne, Pasi, A. ....		221	Jolly, Douglas ....		329
Janssen, Louise ....		359	Joly, Nathalie ....		363
Jaquin, Thomas ....		182	Jonas, Adria. ....		391
Jarblad-Leja, Justyna ....		325	Jones, Frank ....		379
Jarushi, Sufyan ....		437	Jones, Jeremy ....		434
Jayant, kumar ....		79	Jones, Kyle, S. ....		175
Jennewein, Lukas ....		50	Jones, Lee ....		459
Jeng, Robert ....		300	Jones, Sian ....		291
Jensen, Ash ....		458	Jones, Tobin. ....		105, 118
Jensen, Shawn ....		7, 78, 453	Joseph, Sujith ....		25
Jeraj, Robert ....		369	Joshi, Bharat, H. ....		176, 431
Jessen, Katti ....		253	Joshi, Nikhil. ....		53
Jewell, Christopher, M. ....		461	Joy, Mary. ....		130
Jeyakumar, Ghayathri ....		80	Ju, Xiaoming ....		257
Jhawar, Sachin ....		320, 327	Juhler-Nøttrup, Trine ....		158
Ji, He ....		98, 99	June, Carl, H. ....		23
Jia, Dan Tong ....		467	Jung, Jaemyeong ....		122
Jia, Fang ....		442	Junker, Niels ....		35
Jiang, Aimin. ....		53	Jure-Kunkel, Maria ....		65
Jiang, Ziyue Karen ....		442	Jurisica, Igor ....		96
Jin, Benjamin. ....		19			
Jin, Ming ....		406	<b>K</b>		
Jin, Ping ....		464	Kadenhe-Chiweshe, Angela ....		292
Jin, Xiaoping ....		443	Kaiser, Andrew. ....		33
Jing, Junping ....		5	Kaiser, Stephen ....		253
Jing, Weiqing ....		21	Kalinski, Pawel. ....		222, 236, 346, 433
Jochems, Caroline ....		20, 172	Kallen, Karl-Josef. ....		90, 262
Joe, Andrew. ....		73	Kallergi, G. ....		92
Johnson, Brian. ....		402	Kalos, Michael. ....		243
Johnson, Bruce, D. ....		271	Kalra, Mamta ....		52
Johnson, Bryon, D. ....		21	Kamat, Ashish, M. ....		146, 173
Johnson, Donald ....		118	Kamenyeva, Olena ....		15
Johnson, Karen ....		250	Kammula, Udai ....		139
Johnson, Lisa ....		81	Kane, Lawrence, P. ....		412
Johnson, Melissa, L. ....		221	Kane, Michael ....		95
Johnson, Susan ....		175	Kanerva, Anna ....		335

## Author Index

Name	K	Poster Number	Name	K	Poster Number
Kang, Hyunseok . . . . .		456	Kemmer, Kathleen . . . . .		157
Kang, Kai . . . . .		308	Kenderian, Saad . . . . .		23
Kang, S. Peter . . . . .		72, 141	Kent, Michael, S. . . . .		138
Kangas, Takashi O . . . . .		179, 391, 468	Keppler, Jennifer, S. . . . .		442
Kanne, David, B. . . . .		399	Kern, Jeffrey . . . . .		390
Kantrowitz, Joel . . . . .		200	Khalil, Danny, N. . . . .		224
Kao, Hsiang-Fong . . . . .		82	Khattri, Arun. . . . .		162
Kapp, Kerstin . . . . .		314	Kher, Uma . . . . .		163
Kapralova, Marina . . . . .		223	Khleif, Samir . . . . .		457
Kari, Gabor. . . . .		4	Khong, Hiep . . . . .		359
Kariolis, Mihalis . . . . .		384	Khong, Hung . . . . .		333
Karlsson, Hannah. . . . .		123	Khuat, Lam, T. . . . .		274, 296
Karlsson-Parra, Alex. . . . .		364	Khushalani, Nikhil . . . . .		106, 239, 444
Karp, Judith, E. . . . .		89	Kiany, Simin. . . . .		22
Karpathy, Roberta . . . . .		244, 319	Kibel, Adam, S. . . . .		340
Karpov, Andrey. . . . .		223	Kidder, Koby. . . . .		294
Karulin, Alexey . . . . .		58, 60	Kiessling, Rolf . . . . .		27
Kasibhatla, Shailaja . . . . .		399	Kilgour, Elaine . . . . .		57
Kasler, Miklos . . . . .		408	Kim, Bong-Hyun. . . . .		37
Kates, Max. . . . .		71	Kim, Byoung-Gie . . . . .		145
Katibah, George. . . . .		366, 399	Kim, Chul-Ho . . . . .		271
Katsarlinos, P. . . . .		92	Kim, Dae Won . . . . .		85
Katz, Matthew, H.G. . . . .		160	Kim, Dongkyoon. . . . .		339
Kaufman, David, R. . . . .		72, 73, 244	Kim, Dong-Wan . . . . .		263
Kaufman, Howard, L. . . . .		95, 106, 307, 320, 321, 327, 328, 418, 444, 445, 467	Kim, Heejin . . . . .		80
Kaufmann, Daniel . . . . .		96	Kim, Jeffrey . . . . .		84
Kauh, John, S. . . . .		142, 243	Kim, Joseph, W. . . . .		172, 449
Kavanaugh, W. Michael . . . . .		219	Kim, Kyoung-Mee . . . . .		57
Kawakami, Yutaka . . . . .		435, 465	Kim, KyungMann . . . . .		168
Keam, Bhumsuk . . . . .		263	Kim, Miriam . . . . .		23
Kearney, Staci, J. . . . .		83, 93	Kim, Namyong. . . . .		86, 87, 88
Keefe, Stephen . . . . .		146	Kim, Rebecca. . . . .		93
Keler, Tibor. . . . .		171, 180, 447	Kim, Richard . . . . .		85
Kelly, Brian. . . . .		105, 118	Kim, Seongho . . . . .		80
Kelly, Karen . . . . .		448	Kim, Seulki . . . . .		263
			Kim, Seung-Tae. . . . .		57



## Author Index

<u>Name</u>	<u>K</u>	<u>Poster Number</u>	<u>Name</u>	<u>K</u>	<u>Poster Number</u>
Kim, Seungwon		396	Kohanbash, Gary		310
Kim, Soyeon		263	Kohlbacher, Oliver		90
Kim, Sung		57	Kohler, M. Eric		37
Kim, Tae Min		263	Kohlhapp, Frederick		320, 321
Kim-Schulze, Seunghee		447	Kohrt, Holbrook		65
Kindler, Hedy, L.		261	Koinis, Filippos		92
Kindt, Erick		253	Kokolus, Kathleen M		452
King, Michael		463	Kolarkar, Shalini		343
Kirchner, Thomas		110	Kollmeier, Jens		262
Kirk, Peter		342	Kolls, Jay		422
Kirksey, Yolanda		343	Kolrep, Ulrike		33
Kirkwood, John, M.		45, 154	Komar, Hannah, M.		233, 406
Kitaura, Kazutaka		242	Komarov, Andrey		394
Kjeldsen, Julie Westerlin		9	Konakova, Marina		342
Klebanoff, Christopher		139	Kongsted, Per		136, 158
Kleinerman, Eugenie S.		22, 206	Koon, Henry		106, 125, 444
Kler, Jasdeep		417	Koong, Albert		384
Klichinsky, Michael		23	Kopits, Charlene		14
Kline, Douglas		404	Koppolu, Bhanu		349
Kline, Justin		147, 295, 404	Koptez, Scott		439
Klingemann, Hans		45	Korman, Alan, J.		102, 417
Klinke, David, John		405	Kornacker, Michael		192
Klinkhardt, Ute		262	Kornbluth, Richard, S.		298
Klippel, Anke		215	Kortylewski, Marcin		184, 350, 434
Kluger, Harriet		107, 387	Kosaka, Yoko		411
Kmiecik, Katarzyna		128	Koshiji, Minori		141
Knapp, Alyssa		208	Kosmeder, Jerome		118
Knaus, Hanna, A.		89	Kosmides, Alyssa		185
Knudson, Karin, M.		207, 212	Kosoff, Rachele		257
Ko, Jenq-Yuh		82	Kostarelos, Kostas		287
Koch, Sven D.		90, 262	Kothari, Nishi		85
Kochenderfer, James N.		46	Koti, Madhuri		407
Kodumudi, Krithika		34, 264	Kotlan, Beatrix		408
Koegler, Sally		83	Kotsakis, Athanasios		92
Koelwyn, Graeme		459	Kotturi, Maya		450
Koguchi, Yoshinobu		91, 157, 446, 462	Koziol, Marie Eve		355

## Author Index

Name	<b>K</b>	Poster Number	Name	<b>L</b>	Poster Number
Kradjian, Giorgio		254	Labiano, Sara		174
Kraman, Matthew		128	Laderas, Ted		411
Krarup-Hansen, Anders		35	Lai, Shu-Chuan		82
Krasovskaia, Liudmila		223	Lai, Venus		200
Kraus, Manfred		253	Laing, Naomi		142
Kraynyak, Kim		368	Lake, Andrew, C.		423
Krejsa, Cecile, M.		402	Lam, Bao		141
Krenciute, Giedre		52	Lam, Elaine		166
Kriley, Isaac		12, 13	Lamble, Adam		411
Krishnan, Monica		265	Lamping, Elizabeth		172
Krishnan, Suba		65, 239, 267	Lan, Yan		254
Krisko, John		205	Landi, Daniel		25
Krogsgaard, Michelle		24	Landis, Benjamin, J.		83
Krueger, Joseph		93	Lane, Ryan		414
Ku, Yuan-Chieh		97	Langowski, John, L.		343
Kuai, Rui		365	Lapointe, Rejean		96
Kudchadkar, Ragini		142	Laport, Ginna		149, 218
Kulesz-Martin, Molly, F.		119	Larkin, James		135
Kulkarni, Anupriya		116	Larsson, Ola		27
Kumai, Takumi		10, 378	Lauer, Peter		366
Kumar, Sandeep		450	Law, Che-Leung		150, 311
Kumar, Shaji		134	Law, Debbie		76, 162
Kumar, Sushil		119, 261, 409	Lawrence, Donald P.		282
Kumar, Vikas		309, 318	Lazo, Suzan		297
Kummar, Shivaani		239	Lazorchak, Adam, S.		225
Kung, Andrew, L.		292	Le, Dung, T.		141, 267, 449
Kunk, Paul, R.		410	Le, Julie		34
Kuo, Peiwen		342	Le, Mai		466
Kuppen, Peter		288	Lee, Chen-Yu		442
Kurland, John		65	Lee, Cleo		118
Kuruvilla, John		147	Lee, Dean		304
Kyi, Chrisann		62, 148	Lee, Jay, M.		170
Kyruk, Lukasz		201	Lee, Jean, K.		142
			Lee, Jeeyun		57
			Lee, Jessica		368
			Lee, John		458

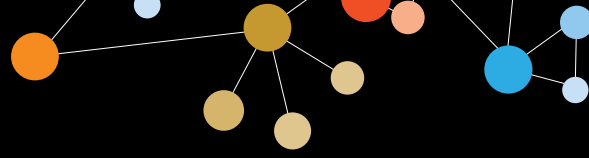


## Author Index

<u>Name</u>	<u>L</u>	<u>Poster Number</u>	<u>Name</u>	<u>L</u>	<u>Poster Number</u>
Lee, Mi-Heon . . . . .		170	Lewis, Whitney . . . . .		259
Lee, Sung Sook . . . . .		143	Lhuillier, Claire . . . . .		459
Lee, Sylvia . . . . .		26	Li, Amy . . . . .		466
Lee, Tien . . . . .		45	Li, Jian-Ming . . . . .		48
Lee, Tsai-Jan . . . . .		82	Li, Jin . . . . .		260
Lee, Victor . . . . .		165	Li, Jingxia . . . . .		48
Lee, Yu Soo . . . . .		263	Li, Kang . . . . .		159
Legut, Mateusz . . . . .		9	Li, Qiao . . . . .		227, 367
Lehmann, Paul . . . . .		58, 59, 60, 336	Li, Roger . . . . .		173
Lei, Liang . . . . .		469	Li, Rui . . . . .		462
Leidner, Rom . . . . .		293, 441, 446, 456	Li, Tianhong . . . . .		448
Leighl, Natasha . . . . .		143	Li, Weiqun . . . . .		231
Leland, Pamela . . . . .		176, 431	Li, Wenlin . . . . .		253
Leleti, Manmohan, R. . . . .		424	Li, Wenting . . . . .		152
Leleux, Jardin . . . . .		354	Li, Xia . . . . .		443
Lemmens, Edward, E. . . . .		261, 366	Li, Yanxia . . . . .		243
Leonard, John P. . . . .		238	Li, Yanyun . . . . .		125, 224, 255
Leonard, John, E. . . . .		208	Li, Zihai . . . . .		2, 416
Leonardo, Steven . . . . .		179, 391, 468	Liadi, Ivan . . . . .		24
Leong, Justin, L. . . . .		399	Liang, Shuo . . . . .		27
Leong, Meredith, L. . . . .		261, 366	Liang, Spencer . . . . .		450
Lepone, Lauren . . . . .		207, 212	Liang, Xiaoling . . . . .		260
Leshem, Yasmin . . . . .		226	Liang, Yan . . . . .		122
Lesinski, Gregory, B. . . . .		228, 233, 406	Liberman, Moishe . . . . .		96
Leslie, Gunatilaka, AA. . . . .		249	Lieber, Andre . . . . .		335
Lessey-Morillon, Elizabeth . . . . .		266	Lifke, Alexander . . . . .		315
Letai, Anthony . . . . .		297	Lifke, Valeria . . . . .		315
Letellier, Marie-Claire . . . . .		253	Lim, Wendell . . . . .		440
Leung, Ling . . . . .		450	Lin, Jin-Ching . . . . .		165
Levine, Zurit . . . . .		450	Lin, Jing . . . . .		393
Levitan, Diane . . . . .		61	Lin, Yan . . . . .		154
Levitsky, Victor . . . . .		188	Lin, Ying, Q. . . . .		170
Levy, Laurent . . . . .		376	Lind, Evan, F. . . . .		411
Levy, Ofer . . . . .		450	Lind, Kristin . . . . .		454
Levy, Ronald . . . . .		65, 239, 267	Lindner, Michael . . . . .		114
Lewis, Stacy . . . . .		157	Lindstedt, Malin . . . . .		56, 382

## Author Index

<u>Name</u>	<u>L</u>	<u>Poster Number</u>	<u>Name</u>	<u>L</u>	<u>Poster Number</u>
Lipson, Evan		238	Lorent, Julie		27
Liskay, Gabriella		408	Loriaux, Marc		411
Litton, Jennifer		373	Loriot, Yohann		132
Liu, Baorui		43	Loskog, Angelica		123, 324, 325, 326
Liu, Bei		416	Lossos, Izidore, S.		267
Liu, Biao		374	Lotze, Michael.T		11, 14, 42, 47
Liu, Cailian		255	Lou, Pei-Jen		82
Liu, Fang		61	Louis, Chrystal		52
Liu, Glenn		369	Lowe, David		275
Liu, Hao		264	Lowe, Jamie		179
Liu, Hongtao		256	Lowther, Daniel, E.		4
Liu, Jacqueline		117	Loya, Matthew		220
Liu, Jie		156	Lu, An		6
Liu, Linying		395	Lu, Bo		376
Liu, Matt		200	Lu, Lily		12
Liu, Shouchun		219	Lu, Shanhong		412, 413
Liu, Shuming		310	Lu, Yan		198, 292, 467
Liu, Tsang-Wu		82	Ludwig, Dale		243
Liu, Weiqun		261	Ludwig, Thomas		233
Liu, Xiao Qiao		73	Lugli, Alessandro		465
Liu, Xiu-fen		226	Lukaesko, Lisa		187
Liu, Yuan		294	Luke, Jason, J.		149, 171, 239, 432
Liu, Zhuqing		412, 413	Lum, Lawrence, G.		129, 227
Lo, Kin-Ming		254	Lumish, Melissa		300
Loboda, Andrey		72, 73	Luna, Jesus, I.		138
Loffredo, John T.		102	Lunceford, Jared		72, 73
Logan, Theodore		106, 239, 444	Lund, Amanda, W.		414
Logronio, Kathryn		450	Lundberg, Kristina		56, 382
Lohr, Michele		458	Lund-Johansen, Fridtjof		462
Loibner, Hans		417	Lundqvist, Andreas		27
London, Cheryl, A.		451	Lundy, Joanne		159
Long, Georgina, V.		197	Luo, Lusong		159
Longo, Dan		274	Luo, Yuling		84
Lonial, Sagar		163, 164	Luznik, Leo		89
Looney, Tim		97	Lye, Melvin		86, 87, 88
Lopez, Fernando		329	Lykov, Maxim		223



## Author Index

Lyngaa, Rikke . . . . . 9  
 Lyrsti, Z. . . . . 92

### M

Ma, Xiao-Jun . . . . . 84  
 Maas, Mary, L. . . . . 144  
 MacDonald, Andrew . . . . . 240  
 MacDonald, Cameron. . . . . 270, 272  
 MacDonald, Douglas . . . . . 200  
 Mace, Thomas . . . . . 228, 233, 406  
 Macedo Gonzales, Rodney, J.M. . . . . 229  
 Machlenkin, Arthur . . . . . 450  
 Mackall, Crystal . . . . . 4  
 MacKinnon, Andy . . . . . 166, 230, 231  
 Madan, Ravi . . . . . 172  
 Madonna, Gabriele . . . . . 109  
 Maecker, Holden . . . . . 65  
 Maegley, Karen . . . . . 253  
 Magalhaes, Isabelle . . . . . 28  
 Magazzù, Domenico . . . . . 135  
 Magee, Michael, S. . . . . 302  
 Magnani, John, L. . . . . 209  
 Mahendravada, Aruna . . . . . 6  
 Mahoney, Kathleen, M. . . . . 186  
 Mahvi, David . . . . . 168  
 Mailloux, Adam, W. . . . . 29  
 Maitra, Anirban . . . . . 439  
 Majeti, Ravindra. . . . . 156  
 Makarov, Vladimir . . . . . 374  
 Makhanov, Michael . . . . . 394  
 Makhijani, Neil . . . . . 228  
 Makkouk, Amani . . . . . 231  
 Malaker, Stacy, A. . . . . 312, 356  
 Malekzadeh, Parisa . . . . . 13  
 Malhotra, Jyoti . . . . . 95  
 Mallon, Zach . . . . . 344  
 Mallow, Crystal . . . . . 208  
 Malnassy, Gregory . . . . . 256

<u>Name</u>	<u>M</u>	<u>Poster Number</u>
Mandeli, John . . . . .		148
Mandloi, Nitin . . . . .		392
Mangin, Eric . . . . .		197
Mangrolia, Drishty . . . . .		368
Manguso, Robert . . . . .		285
Mani, Jiju. . . . .		190
Mani, Nikita . . . . .		64
Manieri, Nicholas . . . . .		214
Manji, Gulam, A. . . . .		142
Manley, Thomas. . . . .		150
Manning, Luisa . . . . .		371
Manning-Bog, Amy . . . . .		339
Manoharan, Malini . . . . .		392
Manro, Jason. . . . .		243
Mansfield, David . . . . .		244
Mansi, Laura . . . . .		239
Mao, Yumeng . . . . .		27
Marabelle, Aurélien . . . . .		193, 247
Marathi, Upendra, K. . . . .		361
Marchioni, Filippo . . . . .		442
Marelli, Bo . . . . .		254
Margolin, Kim . . . . .		26, 106, 444
Marguier, Gisele. . . . .		230, 231
Mariani, Mariangela . . . . .		135
Maric, Dragan . . . . .		235
Marillier, Reece . . . . .		253
Marincola, Francesco, M. . . . .		170, 287, 288, 429, 464, 465
Marinello, Patricia . . . . .		153, 163, 164
Market, Robert, V. . . . .		361
Markman, Ben . . . . .		159
Marks, Douglas . . . . .		467
Marliot, Florence . . . . .		341, 465
Marner, Erin . . . . .		118
Maroto, Miguel. . . . .		3
Marron, Thomas, U. . . . .		232, 447
Marrone, Kristen, A. . . . .		151

## Author Index

<u>Name</u>	<u>M</u>	<u>Poster Number</u>	<u>Name</u>	<u>M</u>	<u>Poster Number</u>
Marsh, Henry, C. . . . .		180	McFarland, Thomas . . . . .		168
Marshall, Netonia. . . . .		232	McGraw, Steven. . . . .		458
Marte, Jennifer . . . . .		172	McIntosh, Laura. . . . .		363
Martel, Maritza . . . . .		103, 157	McKenna, Jeffery, M. . . . .		399
Martin, Allison . . . . .		388	McMahon, Sheri. . . . .		172
Martin, Nathan, T. . . . .		93	McMichael, Elizabeth. . . . .		451
Martínez-Usatorre, Amaia . . . . .		94	McMiller, Tracee. . . . .		66
Martins, Beatriz . . . . .		201	McNamara, Michael. . . . .		462
Mascioni, Alessandro . . . . .		442	McNeel, Douglas, G. . . . .		369
Mason, Sean . . . . .		421	McNeil, Catriona . . . . .		197
Massarelli, Erminia . . . . .		239	McOlash, Laura . . . . .		21
Mastro, Andrea . . . . .		273	McQuade, Jennifer, L. . . . .		353
Masucci, Giuseppe, V. . . . .		120, 465	McQuinn, Christopher . . . . .		233
Masvidal Sanz, Laia . . . . .		27	McWeeney, Shannon . . . . .		411
Mata, Melinda . . . . .		30	McWhirter, Sarah, M. . . . .		399
Mateos, Maria Victoria . . . . .		163, 164	Means, Gary . . . . .		150
Mathieu, Mélissa . . . . .		31	Mederos, Eileen . . . . .		462
Matschiner, Gabriele . . . . .		182	Mediero, Aranzazu . . . . .		269
Matsumoto, Morio . . . . .		163	Medina, Daniel. . . . .		328
Matsutani, Takaji . . . . .		242	Meek, Megan. . . . .		276
Matthias Ahlers, Christoph . . . . .		65	Meek, Stephanie, M. . . . .		333
Mattsson, Jonas . . . . .		28, 188	Meeuwssen, Tanisha . . . . .		91
Mauceri, Helena, J. . . . .		258	Mehnert, Janice. . . . .		95, 328
Mauer, Daniela. . . . .		33	Mehrotra, Shikhar . . . . .		276
Mauldin, Ileana . . . . .		429	Mehta, Adi . . . . .		462
Maurer, Matthew . . . . .		238, 239	Mei, Qian . . . . .		121
Mazzeo, Christopher, F. . . . .		292	Meier, Roland. . . . .		239, 267
McArthur, Heather . . . . .		157	Melcher, Alan . . . . .		244, 319
McCafferty, John . . . . .		317	Melchiori, Luca . . . . .		4
McCaffery, Ian . . . . .		149, 218	Melero, Ignacio . . . . .		174, 238, 239
McCarter, Martin . . . . .		390	Mellinger, Staci . . . . .		157
McClanahan, Terrill, K. . . . .		72, 73	Melssen, Marit. . . . .		370, 415
McCulley, Kelsey . . . . .		304	Mendoza, Daniel . . . . .		329
McDaniel, Amanda. . . . .		344, 345, 420	Meniawy, Tarek . . . . .		159
McDermott, David, F. . . . .		106, 152, 197, 307, 444	Menk, Ashley, V. . . . .		54, 278, 279, 280, 281
McDonald, Dan . . . . .		239, 456	Mennel, Robert . . . . .		371



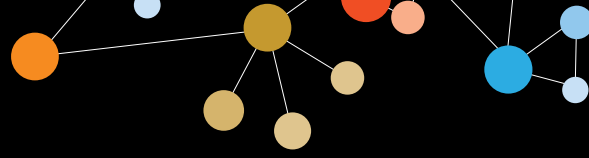


## Author Index

Name	M	Poster Number	Name	M	Poster Number
Mera, Toshi		397	Mlecnik, Bernhard		465
Merchant, Nipun		160	Mockel-Tenbrinck, Nadine		33
Merghoub, Taha	125, 199, 224, 255, 332, 357, 374		Moebius, Ulrich		182
Meric-Bernstam, Funda		166	Moeckly, Craig		250
Meridew, Jeffrey		105, 118	Mogg, Robin		61, 73
Merrick, Daniel		390	Mogundo, Frances-Mary		433
Merritt, Chris		122	Mohan, Aparna		392
Mes-Masson, Anne-Marie		96	Mohr, Ian		330
Messenheimer, David, J.		453	Mohrs, Markus		200
Met, Özcan		136	Molineaux, Chris	155, 166	
Metchette, Ken		399	Monaghan, Catherine		216
Metelli, Alessandra		416	Monette, Anne		96
Meunier, Liliane		96	Mongan, Ann	97, 98, 99	
Meyer, Christina		299	Monjazeb, Arta	138, 274, 448	
Meyers, Michael, L.		221	Monk, Bradley J.		145
Michaelson, Jennifer		76, 162	Montler, Ryan		70
Michot, Jean-Marie		153	Moogk, Duane		24
Mier, James, W.		444	Moon, James		365
Milenova, Ioanna		325, 326	Moore, Brandon		390
Milhem, Mohammed, M.		445	Moore, Gregory, L.	126, 127	
Millar, David		305	Moore, Kathleen M.	145, 248	
Miller, Lance		288	Moran, Amy, E.		187
Miller, Nichol		253	Moreci, Rebecca		280
Miller, Peter		395	Moreira, Dayson	184, 434	
Miller, Richard		149, 218	Morel, Yannis		196
Miller, William		91	Moreno, Rafael	325, 326	
Millward, Michael		159	Mori, Motomi		119
Milone, Michael		39	Morillon, Y. Maurice		234
Minor, David		445	Morishima, Chihiro		171
Minutolo, Nicholas		32	Mørk Petersen, Michael		35
Mitchell, John		390	Morou, Antigoni		96
Mitchell, Leah		329	Morris, Zachary, S.		417
Mitra, Priyam		238	Morrison, Carl	98, 99	
Mittelbronn, Michel		50	Morrison, Debra		464
Mittendorf, Elizabeth A.		373	Morrison, Larry		118
Mkrtichyan, Mikayel		175, 457	Morrow, Matthew		368

## Author Index

<u>Name</u>	<u>M</u>	<u>Poster Number</u>	<u>Name</u>	<u>N</u>	<u>Poster Number</u>
Morschhauser, Franck . . . . .		239	Nagasaka, Misako . . . . .		283
Morse, Jennifer . . . . .		264	Nagtegaal, Iris, D. . . . .		465
Morse, Michael . . . . .		307, 449	Nagy, Bethany . . . . .		7
Moskowitz, Craig . . . . .		147	Nail, Carmel . . . . .		358
Mostafid, Hugh . . . . .		319	Nailo, Rodrigo . . . . .		193
Motzer, Robert, J. . . . .		135	Naing, Aung . . . . .		237, 352
Moudgil, Tarsem . . . . .		441, 462	Nair, Nitya . . . . .		261
Mourelatos, Zissimos . . . . .		39	Nair, Rashmi . . . . .		190
Moxon, Nicole, M. . . . .		157	Najjar, Yana, G. . . . .		154
Mu, Song . . . . .		159	Nakagawa, Ryosuke . . . . .		29
Muchhal, Umesh . . . . .		126, 127	Nakamura, Yusuke . . . . .		256
Mudan, Satvinder . . . . .		204	Nam, Kijoeng . . . . .		146
Mueller, Sabine . . . . .		310	Nandoskar, Prachi . . . . .		466
Muir, Lincoln . . . . .		202	Narayanan, Sujata . . . . .		156
Mukherjee, Malini . . . . .		25	Narumiya, Kohei . . . . .		75
Mule, James, J. . . . .		29	Nath, Pulak, R. . . . .		235, 266
Müller, Jürgen . . . . .		69	Navale, Lynn . . . . .		46
Mullinax, John . . . . .		34, 264	Ndubaku, Chudi . . . . .		399
Mullins, Stefanie . . . . .		250	Nebozhyn, Michael . . . . .		72, 73
Mulvey, Matthew . . . . .		330	Nechaev, Sergey . . . . .		350
Mumm, John . . . . .		237	Necochea, Kevin . . . . .		185
Munday, Anthony . . . . .		329	Neelapu, Sattva, S. . . . .		238, 267
Muniz, Luciana . . . . .		400	Neely, Jaclyn . . . . .		239, 267
Munk, Adiel . . . . .		400	Nemoto, Satoshi . . . . .		29
Murakami, Masato . . . . .		178	Nemunaitis, John . . . . .		149, 371
Murphy, Aimee, L. . . . .		261, 366	Neou, Silinda . . . . .		231
Murphy, Erin . . . . .		72, 73	Netikova, Irena . . . . .		113
Murphy, William, J. . . . .		49, 138, 274, 296, 448	Neuberger, Michael . . . . .		114
Murray, Brion . . . . .		253	Neubert, Natalie J. . . . .		301
Murray, Shannon . . . . .		27	Neuman, Heather . . . . .		168
Murter, Benjamin, M. . . . .		450	Neves, Rogerio . . . . .		333
Murthy, Ravi . . . . .		169, 216	Newcomb, Eric . . . . .		424
Muthuswamy, Ravikumar . . . . .		222, 346	Newman, Jenna . . . . .		321, 418
Mwawasi, Kenneth . . . . .		18	Newman, Walter . . . . .		125
Myers, Paisley, T. . . . .		305, 312, 356	Ng, Quan Sing . . . . .		165
			Ng, Sinnie Sin Man . . . . .		7



## Author Index

<u>Name</u>	<u>N</u>	<u>Poster Number</u>	<u>Name</u>	<u>O</u>	<u>Poster Number</u>
Ngan, Roger, K.C.		165	Obeid, Joseph, M.		100, 101, 410, 429
Nghiem, Paul		45, 81	Obermajer, Nataša		222, 236, 346, 389
Ngo, Lisa, Y.		195	Ochoa, Augusto		462
Nguyen, Andrew		111, 289	Ochyl, Lukasz		365
Nguyen, Khue		349	Ocio, Enrique		163, 164
Nguyen, Linh, T.		465	O'Connor, Alison		81
Nguyen, Matthew		437	O'Connor, Rachel, W.		423
Nguyen, Ngan		339	Odunsi, Kunle		67, 389
Nguyen, Phuong		30	Oft, Martin		237
Nguyen, Sang		37	Ogasawara, Masahiro		372
Niazi, Kayvan		289	Ogden, Julia		57
Nicholas, Courtney		194	Oh, William		62
Nicolette, Charles		205, 223, 259	Ohanian, Arpy		26
Niederfellner, Gerhard		226	Ohashi, Pamela, S.		465
Nielsen Viller, Natasja		81	Ohr, James		396
Nielsen, Michael		361	Okada, Hideho		310, 338
Nielsen, Morten		35, 136, 158	Okada, Kaori		310
Nishimura, Michael		276	Okeley, Nicole, M.		311
Nishio, Hiroshi		435	Okubo, Yoshiaki		397
Noessner, Elfriede		419	Olafsen, Tove		442
Noffsinger, Lori		169	Olasz, Judit		408
Nonomura, John		466	Olencki, Thomas		106, 444
Normand, Sarah		437	Olson, Walter		358
Normant, Emmanuel		423	Olson, William		200
Norris, Christie		159	Omilian, Angela, R.		98
Nosrati, Adi		117	O'Neil, Bert		61
Novik, Yelena		464	O'Neill, Thomas		180
Novosiadly, Ruslan		243	Opat, Stephen		134
Nowak, Ryan, K.		458	Ophir, Eran		450
Nuccitelli, Richard		344, 345, 420	Opyrchal, Mateusz		221
Nunez-Cruz, Selene		39	Oratz, Ruth		464
Nutakki, Ravi		343	Ordentlich, Peter		221, 421
	<b>O</b>		Orecchioni, Marco		287
Oaknin, Ana		145	Orford, Keith, W.		155, 166
Obalapur, Palakshi		342	Ornatowski, Wojciech		383
			Osada, Toshihiro		381

## Author Index

<u>Name</u>	<b>O</b>	<u>Poster Number</u>	<u>Name</u>	<b>P</b>	<u>Poster Number</u>
Osman, Iman . . . . .		24	Papadopoulos, Kyriakos, P. . . . .		155, 237
Ostrowski, Michael, C. . . . .		406	Papot, Sébastien . . . . .		317
Oswald, Detlef . . . . .		314	Paramithiotis, Eustache . . . . .		363
Ota, Shuichi . . . . .		372	Pardoll, Drew . . . . .		66
Ott, Patrick, A. . . . .		73, 237, 239, 265, 267, 449	Paria, Biman . . . . .		139
Ott, Sascha . . . . .		9	Parihar, Robin . . . . .		36
Ottoson, Nadine . . . . .		179, 391	Paris, Mark . . . . .		208
Ou, Fang-Shu. . . . .		465	Paris, Sébastien. . . . .		376
Overacre, Abigail . . . . .		422	Park, Emily. . . . .		84
Overwijk, Willem, W. . . . .		216, 359, 361	Park, Ha-Ram . . . . .		263
Ovsepyan, Armen. . . . .		223	Park, Jae-Hyun . . . . .		256
Oyola, Sandra . . . . .		368	Park, Jiwon . . . . .		138
	<b>P</b>		Park, Johanna . . . . .		175
			Park, Timothy. . . . .		403
Pachynski, Russell, K. . . . .		426	Parlati, Francesco . . . . .		230, 231
Padda, Sukhmani, K. . . . .		156	Parney, Ian, F. . . . .		63, 144
Page, David . . . . .		103, 157, 441	Parsons, Andrea, J. . . . .		354
Pagès, Frank . . . . .		341, 465	Parviainen, Suvi. . . . .		41, 203, 335
Pai, Steven. . . . .		342	Pasetto, Anna. . . . .		44
Pal, Sumanta . . . . .		184, 434	Passey, Chaitali . . . . .		456
Palena, Claudia . . . . .		379	Pastan, Ira . . . . .		226
Pall, Georg . . . . .		262	Patel, Ashish . . . . .		441
Palmer, Brent. . . . .		390	Patel, Manish. . . . .		237
Palombella, Vito, J. . . . .		423	Patel, Prabhudas, S. . . . .		465
Pamer, Eric . . . . .		300	Patel, Sapna, P. . . . .		104, 216
Pan, Alison. . . . .		231	Patel, Shashank. . . . .		290
Pan, Fan . . . . .		66	Paterson, Alison, M. . . . .		423
Pan, Wenjing . . . . .		284	Patil, Ashwini . . . . .		392
Pan, Xiaoyu . . . . .		450	Patnaik, Amita . . . . .		149, 237
Panda, Anshuman . . . . .		95	Patsoukis, Nikolaos . . . . .		186
Pandha, Hardev . . . . .		244, 319	Patterson, James, W. . . . .		100
Pandite, Lini. . . . .		4	Patterson, Troy, D. . . . .		225
Paneque, Tomas. . . . .		320, 327	Paul, Kiran . . . . .		392
Pankov, Alex. . . . .		97	Paulos, Chrystal. . . . .		276
Pant, Shubham . . . . .		237	Paul-Wetterberg, Gabriella . . . . .		324
Papachristofilou, Alexandros . . . . .		262	Paustian, Christopher. . . . .		334, 441, 462



## Author Index

<u>Name</u>	<b>P</b>	<u>Poster Number</u>	<u>Name</u>	<b>P</b>	<u>Poster Number</u>
Pavlakis, George		7	Pfeil, Jacob		38
Pavlick, Anna, C.		171	Pferdekamper, Anne Marie		399
Payabyab, Eden		13	Pham, Hung		186
Paz-Ares Rodriguez, Luis		143	Phillips, Penny		456
Peace, Kaitlin M.		373	Pierce, Robert, H.		466
Pedersen, Magnus		136, 158	Pierobon, Mariaelena		385
Pegram, Mark, D.		156	Piha-Paul, Sarina, A.		72
Pei, Jerry		200	Pike, Luke		265
Peled, Jonathan		300	Pillai, Rathi, N.		449
Pelletier, Sandy		31	Pilon-Thomas, Shari		34, 264
Pellom, Samuel		347, 348	Pinczewski, Joel		429
Peltonen, Karita		201	Pinzon-Ortiz, Maria		178
Pena, Rhoneil		343	Piperdi, Bilal		143
Penny, Sarah, A.		305, 312, 356	Pirson, Romain		253
Peoples, George E		373	Plachco, Ana		205
Perales, Miguel		300	Pless, Miklos		262
Pérez Villarroel, Patricio		29	Plimack, Elizabeth		73
Perez, Myra		344	Poehlein, Christian		132, 133
Perez-Garcia, Arianne		24	Poggionovo, Cécile		341
Perini, Rodolfo		146	Polaske, Nathan		105, 118
Periyasamy, Sankar		130	Polesso, Fanny		187
Perlewitz, Kelly		157	Pollack, Ian, F.		310
Perna, Serena		238	Pollock, Emily		377
Perry, Kyle		257	Ponichtera, Holly		297
Persaud, Krishnadatt		243	Ponte, Jose		316
Pesonen, Sari		201, 331	Pope, Hans		285
Pestic-Dragovich, Lidija		105, 118	Poplin, Elizabeth		95
Petaccia De Macedo, Mariana		104	Poplonski, Tomasz		91
Petersen, Christopher		48	Porosnicu Rodriguez, Kori		300
Peterson, Nichole		407	Posner, Marshall		248
Peterson, Tim		144	Postow, Michael		125, 255
Petit, Robert		257	Pottier, Agnes		376
Petricoin III, Emanuel		385	Poueymirou, William		200
Petroni, Gina		160, 358, 370	Pourchet, Aldo		330
Petruzelka, Lubos		113	Pourdehnad, Michael		215
Petrylak, Daniel, P.		340	Pourzia, Alexandra		297

## Author Index

Name	P	Poster Number
Powderly, John		149
Powell, Daniel J.		8, 32, 40
Powell, Steven		458
Powers, Jay, P.		403, 424
Powles, Thomas		132, 161
Pramoonjago, Patcharin		410
Prantner, Andrew, M.		402
Pratte, Luke		93
Preillon, Julie		253
Presnell, Scott		288
Prickett, Todd D.		12, 44
Princiotta, Michael		257
Pritchard, Theresa		66
Profusek, Pam		313
Puhlmann, Markus		161
Puri, Raj, K.		176, 431
Puzanov, Igor		444, 445

### Q

Qi, Jin		254
Qi, Jingjing		125
Qian, Yingzhi		198
Qiao, Guanxi		270, 272
Qiao, Na		373
Qin, Guozhong		254
Qin, Haiying		37
Qin, Yong		104
Qin, Zhen		159
Qiu, Xiaohong		391
Quach, Phi		342
Quattrini, Adriano		5
Quick, Laura		217
Quinn, David, I.		178, 340

Name	R	Poster Number
Rabinovich, Brian		14, 47
Rabizadeh, Shahrooz		289
Rabolli, Virginie		253
Racolta, Adriana		105, 118
Rådestad, Emelie		188
Radfar, Arash		425
Radoja, Sasa		330
Radvanyi, Laszlo		254, 299
Rae, Chris, S.		366
Rafail, Stavros		360, 380
Rafat, Marjan		384
Rafelson, William		189
Rahma, Osama, E.		160, 410
Raje, Noopur		134
Rajopadhye, Milind		395
Rajurkar, Mihir		116
Rakhmilevich, Alexander, L.		417
Ralph, Christy		244
Ramachandra, Murali		190, 225
Ramachandra, Raghuv eer		190, 225
Ramachandran, Indu		4
Ramakrishna, Venky		180
Ramakrishnan, Rupal		124
Ramalingam, Suresh		221
Ramaswam, Bhuvan eswari		451
Ramchandren, Radhakrishnan		267
Ramos, Kimberly		257
Ranade, Kou stubh		443
Ranheim, Erik, A.		168
Ranki, Tuuli		201, 331
Rankin, Erinn		384
Rao, Arjun, A.		38
Rao, Tharak		307
Rapisuwon, Suthee		425
Rashid, Rumana		126, 127
Rattray, Rogan		91



## Author Index

<u>Name</u>	<u>R</u>	<u>Poster Number</u>	<u>Name</u>	<u>R</u>	<u>Poster Number</u>
Ravindranathan, Roshni . . . . .		346	Rickel, Erika . . . . .		192
Ravindranathan, Sruthi . . . . .		349	Riddell, Stanley . . . . .		26
Ray, Chad . . . . .		253	Ridnour, Lisa . . . . .		266
Razai, Amir, S. . . . .		175	Riedlinger, Greg . . . . .		95
Reagan, John, L. . . . .		189	Riemer, Joanne . . . . .		151
Rebelatto, Marlon. . . . .		443	Riess, Jonathan . . . . .		448
Rebhun, Robert . . . . .		274	Rifkin, Robert. . . . .		164
Reckamp, Karen . . . . .		170	Rimm, David . . . . .		64
Redchenko, Irina . . . . .		377	Rimoldi, Donata . . . . .		301
Reddy, Ashok . . . . .		78	Rina, Hui . . . . .		143
Reddy, Praveen . . . . .		130	Rinchai, Darawan . . . . .		288
Redmond, William . . . . .		462	Rini, Brian, I. . . . .		135, 161
Reeves, Jason . . . . .		76, 162	Rittase, William . . . . .		24
Reeves, Rebecca, S. . . . .		195, 354	Rivas, Charlotte . . . . .		36
Reid-Schachter, Gillian. . . . .		407	Rivas, Sarai . . . . .		427
Reilley, Matthew . . . . .		194	Rivera, Miguel . . . . .		116
Reilly, Christine . . . . .		208	Rizell, Magnus . . . . .		364
Reiter, Yoram . . . . .		226	Robbins, Paul F. . . . .		12, 44
Rekoske, Brian. . . . .		369	Roberts, David, D. . . . .		235, 266
Ren, Xiubao . . . . .		367	Robida, Mark . . . . .		105
Rennier, Keith, R. . . . .		426	Robinson, Matthew K Robinson . . . . .		40
Renrick, Ariana, N. . . . .		347	Robinson, William . . . . .		339
Repasky, Elizabeth, A. . . . .		270, 272, 452	Rocafiguera, Albert Oriol . . . . .		163
Reshef, Ran . . . . .		229	Roder, Heinrich . . . . .		106, 107, 444
Restifo, Nicholas, P. . . . .		19, 24, 290	Roder, Joanna . . . . .		106, 107, 444
Reu, Simone . . . . .		114	Rodriguez Canales, Jaime . . . . .		439
Reuben, Alex . . . . .		104	Rodriguez, Anthony . . . . .		415
Rhode, Peter . . . . .		455	Rodriguez-Cruz, Tania . . . . .		322
Ribas, Antoni . . . . .		72, 197, 208	Rodriguez-Garcia, Alba. . . . .		40
Ribeiro de Oliveira, Moacyr . . . . .		164	Rodríguez-Otero, Paula . . . . .		163, 164
Ribrag, Vincent. . . . .		147, 153, 239	Rodriguez-Rodriguez, Lorna. . . . .		95
Ricca, Jacob . . . . .		332	Roehrl, Michael H. . . . .		465
Richards, Allison . . . . .		34	Roelands, Jessica . . . . .		288
Richards, Jon. . . . .		140	Roell, Marina, K. . . . .		454
Richardson, Jennifer, H. . . . .		219	Roen, Diana . . . . .		60, 336
Richman, Sarah, A. . . . .		39	Rogers, Connie, J. . . . .		273

## Author Index

<u>Name</u>	<b>R</b>	<u>Poster Number</u>	<u>Name</u>	<b>S</b>	<u>Poster Number</u>
Roman, Kristin		108	Sacris, Erlinda		148
Romero, Jason		442	Sadelain, Michel		55
Romero, Pedro		94	Saeed, Abu, Z.		312
Rong, Xianhui		178	Saenger, Yvonne		148
Rooney, Cliona, M.		36	Saenger, Yvonne, M.		198, 292, 467
Rosa Brunet, Laura		240	Safyon, Einav		450
Rose, Jason		211	Saims, Dan		209
Rosen, Frances		170	Saini, Manoj		5
Rosenberg, Jonathan		449	Saito, Takuro		198
Rosenberg, Steven, A.		12, 13, 19, 44, 46, 139	Sakellariou-Thompson, Donastas		439
Rosenblum, Michael		117, 466	Salama, Sofie		38
Rosner, Gary		151	Salata, Daria		303
Ross, Ashley		137	Salazar, Andres, M.		148, 447
Ross, Brashonda		437	Salazar, Rachel		172, 254
Ross, Jeffrey		95	Saleh, Rachidi		416
Ross, Merrick		333	Salerno, Elise		429
Rossi, John M.		46	Salles, Gilles		239
Rothe, Christine		182	Salomon, Ran		450
Rothwell, William, T.		241	Samara, Raed		457
Rowlinson, Scott		275	Samiulla, Dodheri		190, 225
Roybel, Kole, T.		440	Sams, Lillian		243
Royster, Erica		34	Sanborn, J Zachary		289
Rubinstein, Mark		252, 454, 455	Sanborn, Rachel, E.		114, 238, 244, 456, 462
Ruchko, Sergey		223	Sanchez, Katherine		103
Ruella, Marco		23	Sander, Cindy		154
Rufer, Nathalie		94	Sanderson, Joseph, P.		3
Rupp, Levi, J.		440	Sandhu, Shahneen		159
Rush, Elizabeth Rush		154	Sandoval, Juan		174
Ruth, Nicola		305	Sankin, Alexander		191
Ruzich, Janet		157	San-Miguel, Jesus		163, 164
Ryan, Kevin		253	Santana Carrero, Rosa, M.		427
	<b>S</b>		Santiago, Laurelis		42, 47
Sabado, Rachel		148	Santoro, Stephen, P.		440
Sabesan, Arvind		139	Santos, João		41, 203
Sachsenmeier, Eliot		112	Santos, Patricia, M.		279
			Saraf, Sanatan		165





## Author Index

<u>Name</u>	<u>S</u>	<u>Poster Number</u>	<u>Name</u>	<u>S</u>	<u>Poster Number</u>
Sargent, Daniel, J. . . . .		465	Schluns, Kimberly, S. . . . .		427
Sarnaik, Amod, A . . . . .		34, 264	Schmidinger, Manuela . . . . .		135
Sasaki, Eiji . . . . .		381	Schmidt, Carl . . . . .		406
Saser, Kate, A. . . . .		411	Schmidt, Emmett . . . . .		244
Sasikumar, Pottayil . . . . .		190, 225	Schmidt, Guenter . . . . .		109, 110, 443
Sathian, Rekha . . . . .		392	Schmidt, Manuel . . . . .		314
Sathyanaryanan, Sriram . . . . .		76, 162	Schneck, Jonathan . . . . .		112, 185
Sato, Noriyuki . . . . .		465	Schoenberg, Mark . . . . .		191
Sato-Kaneko, Fumi . . . . .		242	Schoenfeld, Jonathan . . . . .		265
Satpayev, Daulet . . . . .		442	Schoenhals, Jonathan . . . . .		352
Saunders, Tracie . . . . .		95	Schoenmeyer, Ralf . . . . .		109
Sauntharajah, Yogen . . . . .		308	Scholler, John . . . . .		23
Sausen, Mark . . . . .		291	Scholler, Nathalie . . . . .		402
Savoldo, Barbara . . . . .		123	Scholz, Alexander . . . . .		339
Savolt, Akos . . . . .		408	Schreiber, Taylor, H. . . . .		71, 211
Sawant, Deepali . . . . .		428	Schroeder, Andreas . . . . .		262
Sayers, Thomas, J. . . . .		249, 348	Schüler, Julia . . . . .		182
Scales, Stephanie . . . . .		253	Schult, Silke . . . . .		33
Schad, Sara . . . . .		297	Schvartsman, Gustavo . . . . .		353
Schadendorf, Dirk . . . . .		239	Schwab, Matthias . . . . .		419
Schaeffeler, Elke . . . . .		419	Schwartz, Anthony, L. . . . .		235, 266
Schaer, David. . . . .		243	Schwartz, Sarit . . . . .		111
Schaffer, Michael, E. . . . .		77	Schwendeman, Anna . . . . .		365
Schalper, Kurt . . . . .		64	Schwitzer, Emily. . . . .		459
Scharping, Nicole. . . . .		54, 278, 280, 281	Scrivens, Maria . . . . .		208
Schauder, David. . . . .		53	Sebastian, Martin. . . . .		262
Schaue, Dorthe . . . . .		170	Secrest, Stephanie. . . . .		440
Scheel, Birgit . . . . .		90, 262	Sefrin, Julian, P. . . . .		315
Schell, Todd D . . . . .		452	Segal, Neil, H. . . . .		239, 267, 456
Schiller, Annemarie . . . . .		59	Seibel, Tobias. . . . .		262
Schindler, Ulrike. . . . .		403, 424	Seiwert, Tanguy . . . . .		72, 162, 456
Schjesvold, Fredrik . . . . .		164	Sellappan, Shankar . . . . .		111
Schlom, Jeffrey . . . . .		20, 172, 207, 212, 234, 379, 460	Senbabaoglu, Yasin . . . . .		255
Schloss, Charles . . . . .		152, 167	Senter, Peter, D. . . . .		311
Schlosser, Corinna . . . . .		182	Senzer, Neil . . . . .		371
Schlunegger, Kyle . . . . .		199	Serpa, Gregory. . . . .		406

## Author Index

Name	S	Poster Number	Name	S	Poster Number
Sethuraman, Jyothi		42, 47	Shen, Yueh-wei		46
Setiady, Yulius		316	Shepard, Dale		313
Sette, Alessandro		310	Shepard, Robert		463
Sevdali, Maria		291	Sher, Xinwei		73
Sewell, Andrew Kelvin		9	Sherman, Marika		46
Sexton, Holly		403, 424	Sherry, Lorcan		386
Seymour, Len		323	Sherry, Richard		13, 139
Sgarrella, Francesco		287	Shestova, Olga		23
Sgourakis, Nikolaos		38	Shi, Feng		305
Sha, Huizi		43	Shi, Jian		279
Shabanowitz, Jeffrey		312, 356	Shi, Li		443
Shafren, Darren		140, 244, 319, 328, 334	Shields, Anthony		129
Shah, Jatin		163, 164	Shih, Vincent, F.S.		311
Shah, Sumit, A.		156	Shimizu, Atsushi		381
Shakya, Reena		233	Shinners, Nicholas		6
Shamalov, Katerina		245	Shinwari, Nabeegha		143
Shamsili, Setareh		131	Shipp, Margaret		153
Shane, Olwill, A.		182	Shortt, Jake		134
Shankaran, Veena		72	Shree, Ankita		25
Shanker, Anil		347, 348	Shrestha, Yashaswi		285
Sharfman, William		239, 456	Shrimali, Rajeev		457
Sharma, Manish		267	Shrivastav, Shruti		310
Sharma, Meenu		359	Shu, Jenny		76, 162
Sharma, Naveen		246	Shukla, Sachet, A.		186
Sharma, Padmanee		352, 449	Shuman, Stewart		357
Sharma, Prannda		32	Shuster, Alexandr		223
Sharma, Sherven		170	Shwonek, Peter		230
Sharon, Elad		171	Sidhom, John-William		112
Sharpe, Alan, D.		57	Sidney, John		310
Shaw, Pamela		178	Siebenaler, Kristen		250
Shayan, Gulidanna		413, 422	Siefker-Radtke, Arlene		146
Shea, Sofia		429	Sievers, Eric		81
Shehade, Hussein		384	Signoretti, Sabina		152, 444
Sheikh, Nadeem, A.		340	Sikic, Branimir, I.		156
Shekarian, Tala		193, 247	Silk, Ann, W.		95, 320, 328
Shen, Rulong		451	Silk, Jonathan, D.		5



## Author Index

Name	S	Poster Number	Name	S	Poster Number
Silski, Cynthia		80	Somerville, Robert		12, 139
Silva, John		421	Sondel, Paul, M.		168, 417
Simard, François		193	Soneson, Charlotte		301
Simmons, John		291	Song, James		159
Simoës, Ines		198	Song, Xiao-Tong		322
Simpson, Guy		319	Song, Yang		161
Sims, Jennifer, S.		292, 469	Sonpavde, Guru		146
Singh, Manisha		359	Soon-Shiong, Patrick		20, 45
Singson, Victoria		219	Soria, Ainara		282
Sirard, Cynthia		125	Sosman, Jeffrey		106, 444
Siurala, Mikko		41, 203, 335	Sotayo, Alaba		297
Sivado, Eva		317	Sotirovska, Natalija		230
Sivan, Ayelet		286	Spacek, Jan		113
Sjöberg, Madeleine		201	Spada, Filomena		287
Skaletskaya, Anna		316	Spanos, William Chad		458
Skalova, Helena		113	Speers, Ellen		305
Skoble, Justin		366	Speiser, Daniel, E.		94, 301
Slansky, Jill		390	Spektor, Alexander		265
Slawin, Kevin		6	Spelman, Michael		440
Slingluff, Jr., Craig, L.		100, 101, 160, 358, 370, 410, 415, 429	Spencer, Christine		104
Slomovitz, Brian M.		248	Spencer, David M.		6, 30
Small, William		145	Spieler, Bradley		462
Smith, David, C.		150	Spiliopoulou, Pavlina		449
Smith, Ernest		208	Spires, Vanessa M.		102
Smith, Jill		385	Sprague, Isaac		122
Smith, Kelly		358, 370	Spranger, Stefani		183, 430
Smith, Leia		402	Spreafico, Anna		165
Smith, Sean, G.		349	Spurgeon, Stephen		238
Smolkin, Mark, E.		100, 358, 370, 410	Squalls, Oilivia		390
Snook, Adam, E.		302	Srinivasa, Sreesha, P.		130
Snzol, Mario		107, 387	Srirangam, Jay		253
Sodre, Andressa		124	Srivastava, Abhishek		139
Sokol, Levi		95	Srivastava, Raghvendra		396
Sokolove, Jeremy		339	Srivastava, Shivani		456
Solowiej, Jim		253	Staab, Mary Jane		369
Somanchi, Srinivas		304	Stack, Edward		467

## Author Index

Name	S	Poster Number	Name	S	Poster Number
Staelens, Ludovicus . . . . .		421	Su, Shu . . . . .		43
Staffas, Anna . . . . .		300	Su, Yu-Lin . . . . .		350
Stagg, John . . . . .		31	Subbiah, Vivek . . . . .		169
Ståhle, Magnus . . . . .		325	Sudarshan, Naremaddepalli . . . . .		190, 225
Starzynska, Teresa . . . . .		303	Sugarbaker, David . . . . .		409
Steadman, Lora . . . . .		305, 356	Sugiyama, Juri . . . . .		435
Stecha, Pete . . . . .		181	Suh, Robert . . . . .		170
Steele, Keith . . . . .		443	Suisham, Stacey . . . . .		80
Stefano, Pierini . . . . .		360, 375, 380	Sukari, Ammar . . . . .		283
Steggerda, Susanne . . . . .		230	Sullivan, Ryan J. . . . .		106, 107, 282, 444
Stein, Mark . . . . .		95	Sultan, Hussein . . . . .		378
Stein, Paul, L. . . . .		402	Sumey, Christopher . . . . .		458
Steinbach, Joachim, P. . . . .		50	Sun, Cheng . . . . .		115
Steingrimsson, Arni . . . . .		107	Sun, Shaoli . . . . .		416
Steinmetz, Sue . . . . .		144	Sun, Yongming . . . . .		97
Stelow, Edward, B. . . . .		410	Sundarapandiyan, Karuna . . . . .		180
Stern, Joshua . . . . .		191	Sundararaman, Srividya . . . . .		59, 336
Sternby, Malin . . . . .		364	Sundberg, Berit . . . . .		188
SternJohn, Julius . . . . .		250	Sung, Leonard . . . . .		399
Stevanovic, Sanja . . . . .		19, 44	Supan, Dana . . . . .		156
Stewart, Al . . . . .		253	Suresh, Rahul . . . . .		388
Stewart, John . . . . .		106, 444	Surguladze, David . . . . .		243
Stief, Christian . . . . .		110	Suryawanshi, Satyendra . . . . .		238, 239, 267
Stock, Wendy . . . . .		256	Sutcliffe, Kim . . . . .		446
Stone, Geoffrey, W. . . . .		298	Suzuki, Akiko . . . . .		176, 431
Storey, James . . . . .		180	Suzuki, Ryuji . . . . .		242
Stosnach, Claudia . . . . .		262	Svane, Inge Marie . . . . .		9, 35, 136, 158
Stramer, Amanda . . . . .		11, 47	Swaby, Ramona F. . . . .		165
Straub, Tobias . . . . .		419	Swann, Suzanne . . . . .		216
Straus, Jane . . . . .		369	Swanson, Ryan . . . . .		192
Streiner, Nicole . . . . .		253	Sweis, Randy, F. . . . .		432
Stroncek, David . . . . .		464	Swiderska-syn, Marzena . . . . .		454, 455
Stump, Julia . . . . .		114	Swiderski, Piotr . . . . .		184
Sturgill, Ian . . . . .		49	Szomolay, Barbara . . . . .		9
Su, Nan . . . . .		84			
Su, Paul . . . . .		37			

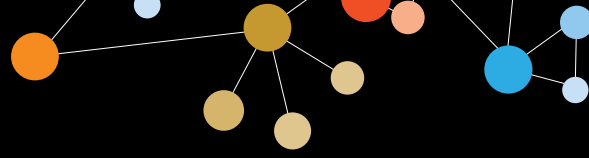


## Author Index

Name	T	Poster Number	Name	T	Poster Number
Taback, Bret		467	Thayer, Matt		209
Tagliaferri, Mary		387	Theiss, Noah		105
Tähtinen, Siri		201, 335	Theodoraki, Marie-Nicole		433
Takamura, Kathryn		466	Thibault, Guillaume		119
Takimoto, Chris, H.		156	Thimme, Robert		305
Talbert, Erin		228	Thomas, Lawrence, J.		180
Talia, Reneta		466	Thomas, Portia		347
Tallarico, John		399	Thomas, Remy		306
Tan, Joanne, BL		403, 424	Thomas, Vincent		317
Tan, Tze Heng		443	Thompson, John, A.		26, 197
Tan, Wei		330	Thompson, Lucas		70
Tan, Xuemei		159	Thompson, Seth		134, 147
Tanaka, Maki		333	Thounaojam, Menaka		347, 348
Tang, Chad		352	Throsby, Mark		131
Tang, Lei		105, 118	Thurston, Gavin		200
Tang, Shande		142	Thyparambil, Sheeno		111
Tannir, Nizar, M.		166, 237, 387	Tian, Zhigang		115
Tarhini, Ahmad, A.		154	Tighe, Rober		254
Tatangelo, Fabiana		465	Tilahun, Ashenafi		250
Taunton, Jack		440	Tillé, Laure		301
Taur, Ying		300	Tilman, Rau, T.		113, 465
Tawbi, Hussein		216, 353	Timmer, John, C.		175
Taylor, Allison		265	Timmerman, John		267
Taylor, Katrina A.		102	Ting, David		116
Taylor, Matthew		333, 449	Tipton, Kimberly, A.		219
Tcherepanova, Irina		205	To, Ka Fai		165
ter Meulen, Jan		195, 354	Tognon, Christina, E.		411
Terabe, Masaki		226, 337	Tom, Warren		97
Termini, James		298	Tomai, Mark, A.		250
Terrell, Andrew		458	Tomonobu, Fujita		465
Tetzlaff, Michael		387	Toms, Anne		373
Tewari, Krishnansu S.		145	Tonn, Torsten		50
Tewary, Poonam		249	Topalian, Suzanne		66
Teyssier, Noam		38	Toporik, Amir		450
Thakur, Archana		129	Torgov, Michael		442
Thakurta, Anjan		215	Torigoe, Toshihiko		465

## Author Index

Name	T	Poster Number	Name	U	Poster Number
Torno, Sebold . . . . .		208	Uecker, Darrin . . . . .		344, 345, 420
Torrey, Heather . . . . .		397	Uemura, Marc . . . . .		216
Torti, Vince . . . . .		253	Ugel, Stefano . . . . .		375, 380
Toth, Kyle . . . . .		276	Uger, Robert . . . . .		81
Toth, Laszlo . . . . .		408	Uhlik, Mark . . . . .		179, 391, 468
Trager, James, B. . . . .		340	Uhlin, Michael . . . . .		28, 188
Tran, Ben . . . . .		159	Ujhelyi, Mihaly . . . . .		408
Trappey, Alfred F . . . . .		373	Ullenhag, Gustav . . . . .		325
Trebska-McGowan, Kasia . . . . .		13	Unfricht, Darryn . . . . .		395
Trehu, Elizabeth . . . . .		76	Ungerleider, Richard . . . . .		333
Tribble, Nicholas . . . . .		3	Uraoka, Naohiro . . . . .		439
Trimble, Cornelia, L. . . . .		19	Urba, Walter . . . . .		91, 103, 157, 239, 441, 446, 462
Trivedi, Sumita . . . . .		396	Urban, Julie . . . . .		222, 346
Truesdell, Peter . . . . .		407	Uribe Herranz, Mireia . . . . .		380
Tsai, Katy . . . . .		117, 466	Uribe, Diana . . . . .		118
Tsang, Kwong Y. . . . .		20, 172, 207, 212, 379			
Tsao, Tsu-Shuen . . . . .		118	<b>V</b>		
Tsaparikos, Konstantinos . . . . .		253	Vaishampayan, Ulka . . . . .		80, 166
Tschaika, Marina . . . . .		449	Valsesia-Wittmann, Sandrine . . . . .		193, 247, 317
Tse, Tiffany . . . . .		440	van den Brink, Marcel R. M. . . . .		300
Tsouko, Efrosini . . . . .		352	Van den Eynde, Marc . . . . .		341, 465
Tsourkas, Andrew . . . . .		32	Van der Meijs, Pien . . . . .		402
Tsujikawa, Takahiro . . . . .		119, 261, 409, 414	van Hoef, Vincent . . . . .		27
Tsujiuchi, Takashi . . . . .		469	van Loo, Pieter Fokko . . . . .		131
Tuck, David . . . . .		225	van Vugt, Marianne . . . . .		197
Tufman, Amanda . . . . .		114	van Zutphen, Mariëlle . . . . .		197
Tumang, Joseph . . . . .		253, 299	Vanamee, Eva . . . . .		397
Tumeh, Paul, C. . . . .		117, 170	Vanderslice, Peter . . . . .		361
Turbitt, William, J. . . . .		273	VanderVeen, Laurie . . . . .		342
Turcotte, Simon . . . . .		31	Vandeven, Natalie . . . . .		81
Turk, Andrew, T. . . . .		292	Vankin, Ilan . . . . .		450
Twitty, Chris . . . . .		466	Vanpouille-Box, Claire, I. . . . .		268
Tykodi, Scott . . . . .		26	VanVlasselaer, Peter . . . . .		237
Tyner, Jeffery, W. . . . .		411	Varadarajan, Navin . . . . .		24
			Varadhachary, Gauri, R. . . . .		160
			Varhegyi, Nikole . . . . .		370



## Author Index

Name	V	Poster Number	Name	W	Poster Number
Vasaturo, Angela		341	Wakelee, Heather, A.		156
Vasilakos, John, P.		250	Waldman, Michelle		215
Vaske, Charles		111, 289	Waldman, Scott, A.		302
Vasselli, James		137	Waldmann, Anja		50
Vassilev, Lotta		335	Waldmann, Thomas		69
Veerapathran, Anandaraman		47	Wallace, William, D.		170
Velcheti, Vamsidhar		64, 125, 308	Waller, Edmund, K.		48
Velculescu, Victor		291	Waller, John		386
Veninga, Henrike		131	Wallraven, Gladice		371
Verma, Amita		309, 318	Walser, Tonya, C.		170
Verma, Vivek		457	Walsh, Richard		391, 468
Vetsika, E.-K		92	Walsh, William		143
Vetto, John		333	Walters, Ian, B.		337
Vianden, Christina		359	Wan, Ee		86, 87, 88
Vietsch, Eveline E.		251	Wang, Chichung		108
Vignali, Dario		390, 422, 428	Wang, Chun-Wei		82
Villabona, Lisa		120	Wang, Daqing		216
Villalobos, Victor, M.		156	Wang, Ena		288, 429, 464
Vink-Borger, Elisa		465	Wang, Gerald		170
Vitale, Laura, A.		171, 180	Wang, Hao		137
Vocka, Michal		113, 465	Wang, Hongjie		335
Vogel, Katharina		250	Wang, Judy, S.		142
Volkmer, Jens-Peter		156	Wang, Lai		159
Volkmoth, Wayne		339	Wang, Ping		426
Volz, Barbara		314	Wang, Shangzi		385
vonEbyen, Rie		384	Wang, Weiyi		357
Voss, Martin		166	Wang, Ximi, K.		229
Vreeland, Timothy J.		373	Wang, Yi		227
Vu, Tuyen		340	Wang, Yili		465
Vuyyuru, Raja		102	Wang, Ziming		49, 138, 274
<b>W</b>			Ward, Stephen, T.		312
Wada, Hiroshi		381	Wardell, Seth		11, 42
Wagner, Joel, P.		178	Wargo, Jennifer		104, 216
Wagtmann, Nicolai		196	Warren, Sarah		67, 121, 122
Wakefield, Jessica		151	Wassman, Karl		62
			Watkins, Simon		280

## Author Index

Name	W	Poster Number	Name	W	Poster Number
Waugh, Katherine		390	White, Mark		450
Webb, Mason		457	Whiteside, Melinda		237
Webb, Tonya, J.		68	White-Stern, Ashley		467
Weber, Amy		264	Whiting, Chan, C.		261, 366
Weber, James		21	Whiting, Sam		166
Weber, Jeffrey		106, 107, 124	Wicha, Max, S.		227, 367
Weber, Sharon		168	Widger, Jenifer		180
Webster, Philippa		122	Wieckowski, Eva		346
Wehler, Thomas		262	Wiedenmann, Alexander		182
Wei, Spencer		351	Wiedermann, Guy		5
Wei, Ziewn.		143	Wiegand, Volker		90
Weichselbaum, Ralph, R.		258	Wiener, Doris		47
Weidlick, Jeffrey		180	Wiestler, Tobias		443
Weigel, Tracey		168	Wigginton, Jon		137
Weinberg, Andrew		70, 187	Wijeratne, Kithsiri		249
Weiner, David		368	Wilhite, Tyler		265
Weiner, Louis M.		385	Wilkinson, Robert, W.		196, 250
Weinstein, Gregory		368	William, Loding		148
Weiss, Christian		262	Williams, Jason, B.		51
Weissbrich, Bianca		19	Williams, LaTerrica, C.		52
Weissman, Irving, L.		156	Williams, Matthew		333
Welden, Scott		333	Williamson, Kevin		339
Wellstein, Anton		251	Willingham, Stephen		218
Wels, Winfried, S.		50	Wilson, James, M.		241
Welsh, James		352	Wilson, Nicholas		299
Wennerberg, Erik		27, 269, 459	Winter, Hauke		114
Wenthe, Jessica		123, 324, 325	Winters, Kevin		410
Werner, Lauryn, R.		417	Wirth, Lori, J.		456
West, Brian		409	Withers, Sita		138, 274
West, James		219	Witjes, J. Alfred		146
Westergaard, Marie, Christine Wulff.		9, 158	Witt, Kristina		27
Wheatley, Courtney		271	Wittig, Burghardt		314
Whetstone, Ryan		278, 280, 281	Wolchok, Jedd, D.		125, 199, 224, 255, 332, 357, 374
White, Andrew, M.		67, 121	Wolfreys, Alison		421
White, Eileen		95	Wolfson, Martin		192
White, James		291	Won, Haejung		434





## Author Index

Name	W	Poster Number
Wondyfraw, Nebiyu		175
Wong, Chihunt		219
Wong, Deborah, J.		237
Wong, Gabriel		305
Wong, Hing		455
Wong, Kenneth, R.		219
Wong, Michael, KK.		307
Wong, Philip		125
Wong, Ryan		5
Wood, Laura		313
Woodman, Scott		216
Woods, David		124
Woodside, Darren, G.		361
Workman, Creg		422, 428
Wouters, Bradley, G.		465
Wrangle, John		455
Wu, Bill X.		416
Wu, Catherine, J.		186
Wu, Dongyun		260
Wu, Haiyan		133, 167
Wu, Jennifer		252, 416
Wu, Yeting		260
Wunderlich, John		12, 139
Wyant, Timothy		225
Wydro, Mateusz		128
Wythes, Martin		253

### X

Xi, Biao		202
Xia, Leiming		227
Xia, Yang		227, 367
Xiang, Bo		302
Xiao, Christine		277, 401
Xiao, Hong		293
Xiao, Weihua		115
Xiao, Zhilan		359

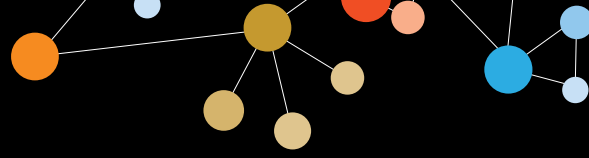
Name	X	Poster Number
Xin, Gang		53
Xu, Chun-wei		393
Xu, Chunxiao		254
Xu, Guifen		403
Xu, Hui		12
Xu, Tian		451
Xu, Xiaomei		254
Xu, Xin		211
Xu, Ya-Ming		249
Xu, Yitong		273
Xue, Allen		46

### Y

Yadav, Mahesh		214
Yagiz, Kader		329
Yaguchi, Tomonori		435
Yamamoto, Tori		8
Yamashiro, Darrell, J.		292
Yan, Jian		368
Yanagawa, Jane		170
Yang, Chou		260
Yang, James		139
Yang, Jason		159
Yang, Ning		357
Yang, Richard		168
Yang, Zane		368
Yano, Hiroshi		428
Yao, Shiyin		242
Yashar, David		457
Ye, Yun-bin		393
Yearley, Jennifer		72, 73
Yee, Andrew, J.		134
Yee, Cassian		216
Yehuda, Dina Ben		163
Yigitsoy, Mehmet		109
Yimer, Habte		164

## Author Index

Name	Y	Poster Number	Name	Z	Poster Number
Yin, Catherine		402	Zeng, Gang		170
Ylösmäki, Erkki		201, 331	Zeng, Weiping		311
Yonemitsu, Yoshikazu		17	Zeng, Xue		54, 278
Yoshino, Takayuki		141	Zha, Yuanyuan		51, 256
Young, Gregory		228, 233	Zhang, Bingqing		84
Young, Kristina		293	Zhang, Congcong		50
Young, Rob		217	Zhang, Danhui		339
Young, Steve, W.		403, 424	Zhang, Hongjun		118
Youssoufian, Hagop		248	Zhang, Hua		4
Yu, Evan, Y.		167	Zhang, Hui		45
Yu, Huakui		254	Zhang, Jian		118
Yu, Lianbo		451	Zhang, Jing		231
Yu, Ling		206	Zhang, Jinyu		252
Yu, Wendy		157	Zhang, Liping		105
Yu, Xuezhong		276	Zhang, Maggie		172
Yu, Zhiya		19, 24	Zhang, Ping		342
Yung-Wu, Chia		440	Zhang, Qifang		350
Yusko, Erik		71	Zhang, Shannon, S.		242
	<b>Z</b>		Zhang, Theresa		291
Zacharakis, Nikolaos		12	Zhang, Wenjun		118
Zafar, Sadia		335	Zhang, Winter		231
Zaharoff, David		349	Zhang, Xiaonan		27
Zalevsky, Jonathan		342, 343, 359, 387	Zhang, Yanping		254
Zamarin, Dmitriy		332	Zhang, Yayan		141, 153
Zamilpa, Charles		442	Zhao, Fei		277, 401
Zang, Xingxing		191	Zhao, Leyna		202
Zanhow, Cynthia		151	Zhao, Xingli		184, 434
Zappasodi, Roberta		125, 199, 255	Zhao, Zeguo		55
Zarour, Hassane		154	Zheng, Lianxing		399
Zauderer, Maurice		208	Zheng, Wenxin		258
Zavadova, Eva		113, 465	Zheng, Xianxian		253
Zea, Arnold		437	Zheng, Yi		395
Zeh, Herbert		222	Zhong, Hong		255
Zehn, Dietmar		94	Zhong, Shi		24
Zelenetz, Andrew, D.		267	Zhou, Gang		438
			Zhou, Li		367

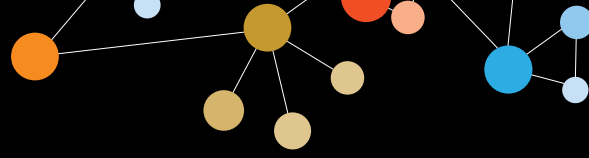


## Author Index

<u>Name</u>	<u>Z</u>	<u>Poster Number</u>
Zhou, Xiangjun . . . . .		260
Zhu, Baogong . . . . .		186
Zhu, Cheng . . . . .		24
Zhu, Yifei . . . . .		118
Zi, Tong . . . . .		76, 162
Zimarino, Carlo . . . . .		128
Zinzani, Pier Luigi . . . . .		147, 153
Zippelius, Alfred . . . . .		262
Zlobec, Inti . . . . .		465
Zloza, Andrew . . . . .		320, 321, 327, 328, 418
Zoon, Kathryn, C. . . . .		15
Zou, Jun . . . . .		257
Zuba-Surma, Ewa . . . . .		303
Zubkova, Olga . . . . .		223
Zuleger, Cindy . . . . .		168
Zureikat, Amer . . . . .		222

## Keyword Index

- Adoptive immunotherapy . . . . . 1, 2, 3, 4, 5, 6, 7, 8, 9, 10, 11, 12, 13, 14, 16, 17, 18, 19, 20, 21, 22, 23, 24, 25, 26, 29, 30, 31, 32, 33, 34, 35, 36, 37, 38, 39, 40, 41, 42, 43, 44, 45, 46, 47, 49, 50, 51, 52, 53, 54, 55, 56, 68, 123, 136, 138, 139, 158, 179, 185, 189, 203, 205, 220, 232, 259, 260, 290, 302, 304, 305, 310, 315, 333, 340, 347, 348, 356, 378, 385, 388, 430, 438, 439, 440, 441, 445
- Angiogenesis . . . . . 113, 414, 438, 451
- Antibody . . . . . 32, 43, 65, 78, 87, 88, 102, 104, 105, 108, 117, 118, 126, 127, 128, 130, 131, 132, 133, 134, 135, 141, 142, 143, 146, 150, 152, 153, 156, 161, 162, 163, 164, 165, 167, 168, 172, 174, 180, 181, 182, 183, 196, 199, 200, 202, 203, 212, 219, 223, 224, 227, 238, 241, 263, 267, 294, 299, 315, 316, 317, 339, 361, 362, 413, 416, 417, 421, 423, 426, 440, 445, 450, 451, 453, 454, 456, 460, 469
- Antigen Presenting Cells . . . . . 23, 38, 45, 48, 56, 68, 86, 120, 144, 150, 169, 171, 172, 179, 180, 181, 184, 185, 195, 213, 215, 236, 245, 248, 266, 269, 279, 287, 294, 298, 316, 323, 325, 346, 354, 355, 356, 367, 374, 382, 388, 390, 461, 463
- Autoimmunity . . . . . 2, 219, 294, 339
- B cell . . . . . 37, 58, 86, 180, 202, 262, 339, 355, 390, 395, 402
- Bioinformatics . . . . . 38, 67, 76, 77, 90, 93, 96, 98, 99, 101, 109, 110, 162, 178, 288, 289, 291, 292, 339, 392, 419, 432, 450, 469
- Biomarkers . . . . . 8, 11, 14, 29, 44, 46, 56, 57, 61, 62, 64, 65, 66, 67, 68, 70, 71, 72, 73, 74, 75, 76, 77, 78, 79, 80, 81, 82, 83, 84, 85, 86, 87, 88, 90, 91, 93, 94, 95, 96, 99, 100, 101, 102, 103, 105, 106, 107, 109, 110, 111, 113, 114, 116, 117, 118, 120, 121, 122, 123, 142, 148, 150, 155, 157, 162, 171, 176, 207, 218, 237, 267, 271, 285, 286, 288, 340, 343, 382, 392, 393, 395, 412, 413, 414, 416, 426, 429, 432, 441, 442, 443, 444, 445, 453, 465, 466, 467
- CAR T cells . . . . . 1, 6, 16, 18, 19, 23, 25, 28, 30, 32, 33, 36, 37, 39, 40, 46, 50, 55, 86, 123, 192, 202, 338, 430, 440
- Carcinogenesis . . . . . 79, 217, 266, 275, 293, 303, 306, 309, 318, 339, 405
- Checkpoint blockade . . . . . 21, 25, 31, 37, 48, 57, 61, 62, 64, 66, 72, 73, 74, 76, 84, 91, 92, 93, 95, 96, 97, 100, 102, 104, 106, 107, 109, 111, 115, 117, 126, 127, 128, 132, 133, 134, 135, 137, 140, 141, 142, 143, 146, 147, 149, 151, 152, 154, 155, 157, 159, 160, 161, 162, 163, 164, 165, 166, 167, 177, 178, 179, 181, 183, 184, 186, 188, 189, 190, 191, 192, 193, 194, 195, 196, 197, 198, 199, 200, 201, 202, 203, 205, 206, 209, 212, 213, 214, 215, 218, 219, 221, 222, 223, 224, 225, 226, 227, 228, 229, 230, 231, 232, 233, 235, 236, 237, 238, 240, 242, 243, 244, 246, 247, 248, 251, 255, 257, 265, 266, 273, 274, 282, 283, 285, 290, 291, 297, 307, 308, 315, 316, 330, 333, 334, 339, 350, 351, 357, 361, 365, 367, 369, 378, 383, 384, 387, 392, 400, 401, 402, 412, 413, 418, 425, 428, 430, 432, 437, 443, 445, 448, 449, 450, 452, 453, 454, 455, 456, 458, 466, 469
- Chemokine . . . . . 29, 45, 56, 84, 87, 88, 169, 170, 179, 183, 209, 217, 222, 229, 236, 250, 346, 357, 361, 364, 426, 430, 433, 440
- Chemotherapy . . . . . 15, 46, 82, 92, 111, 143, 154, 157, 189, 217, 231, 249, 261, 264, 297, 317, 318, 325, 329, 337, 380, 458
- Clinical study . . . . . 4, 51, 79, 87, 88, 100, 101, 109, 110, 136, 138, 143, 149, 156, 168, 172, 173, 189, 204, 221, 244, 260, 261, 265, 292, 313, 328, 333, 352, 369, 372, 443, 445, 449, 463, 465, 466
- Clinical trial . . . . . 4, 13, 17, 26, 46, 61, 62, 63, 65, 74, 80, 82, 87, 88, 90, 95, 111, 123, 132, 133, 134, 135, 136, 137, 138, 139, 140, 141, 142, 144, 145, 146, 147, 148, 149, 150, 151, 152, 153, 154, 155, 156, 157, 158, 159, 160, 161, 162, 163, 164, 165, 166, 167, 168, 169, 170, 171, 172, 197, 218, 221, 222, 237, 238, 248, 256, 261, 262, 267, 307, 313, 328, 333, 334, 352, 358, 364, 368, 369, 370, 371, 373, 377, 387, 442, 444, 446, 448, 449, 456, 458, 462, 463, 464, 466
- Coinhibition . . . . . 1, 66, 89, 100, 115, 128, 176, 178, 181, 183, 186, 187, 188, 190, 191, 192, 193, 194, 213, 214, 219, 226, 238, 243, 246, 255, 257, 412, 413, 450, 453
- Costimulation . . . . . 1, 6, 30, 48, 89, 150, 162, 174, 175, 176, 177, 179, 180, 182, 183, 185, 187, 189, 192, 194, 201, 211, 234, 247, 257, 290, 297, 298, 324, 325, 326, 339, 347, 413, 453
- Cytokine . . . . . 7, 15, 37, 41, 46, 62, 68, 69, 74, 84, 86, 87, 88, 106, 150, 169, 176, 179, 183, 203, 217, 233, 237, 250, 254, 287, 293, 294, 298, 303, 307, 309, 318, 340, 342, 343, 348, 357, 359, 361, 364, 374, 378, 383, 387, 388, 396, 407, 415, 426, 427, 428, 433, 434, 435, 437, 440, 441, 444, 451, 454, 455, 460, 466



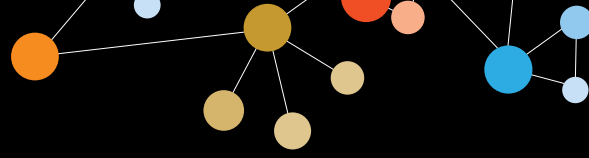
# Keyword Index

Dendritic cell . . . . .	48, 56, 144, 148, 150, 169, 170, 171, 179, 180, 186, 194, 195, 205, 223, 224, 236, 240, 259, 260, 269, 279, 287, 298, 311, 323, 326, 335, 346, 354, 357, 360, 364, 365, 367, 372, 379, 381, 382, 383, 419, 430, 435, 447, 461	279, 281, 389
Gene expression . . . . .	3, 37, 56, 67, 68, 70, 72, 73, 74, 76, 77, 84, 86, 89, 94, 95, 96, 97, 98, 99, 101, 111, 116, 121, 122, 162, 174, 176, 178, 183, 186, 195, 217, 284, 286, 287, 288, 289, 301, 306, 320, 335, 343, 382, 392, 394, 407, 426, 429, 432, 441, 444, 445, 460, 464, 468	
Genetic polymorphism . . . . .	57, 120	
Granulocyte . . . . .	45, 155, 224, 231, 352, 361	
Immune adjuvant. . . . .	10, 41, 56, 145, 171, 179, 184, 194, 201, 211, 222, 224, 227, 234, 240, 247, 249, 250, 264, 287, 292, 293, 298, 315, 316, 329, 331, 355, 357, 361, 364, 365, 370, 373, 375, 378, 380, 399, 461, 462, 464	
Immune contexture . . . . .	57, 83, 96, 97, 101, 105, 109, 110, 114, 119, 120, 121, 288, 301, 386, 394, 395, 407, 414, 419, 429, 432, 465, 467, 468	
Immune monitoring . . . . .	9, 11, 14, 31, 44, 48, 58, 59, 60, 61, 62, 63, 65, 68, 69, 70, 71, 74, 75, 77, 80, 82, 83, 84, 86, 87, 89, 90, 91, 92, 93, 97, 100, 102, 103, 104, 105, 113, 118, 119, 121, 122, 123, 144, 154, 202, 218, 237, 238, 256, 260, 261, 262, 267, 271, 284, 291, 292, 334, 336, 346, 369, 394, 442, 443, 446, 455, 464, 465, 468, 469	
Immune suppression . . . . .	36, 37, 53, 66, 81, 92, 93, 100, 101, 128, 130, 157, 178, 184, 188, 193, 207, 213, 225, 230, 231, 233, 243, 255, 266, 268, 269, 272, 281, 285, 290, 299, 301, 329, 347, 348, 350, 352, 385, 388, 389, 393, 396, 402, 403, 405, 406, 409, 412, 428, 435, 437, 450, 459, 468	
Immune tolerance . . . . .	2, 86, 88, 184, 189, 190, 203, 213, 219, 224, 294, 302, 360, 396, 397, 412, 413, 416, 417, 430	
Immune toxicity . . . . .	16, 18, 41, 86, 87, 88, 160, 177, 190, 219, 282, 283, 317, 458	
Immunoscore. . . . .	85, 94, 98, 99, 103, 109, 110, 113, 114, 176, 222, 286, 288, 386, 414, 429, 465, 467	
Inflammation . . . . .	15, 62, 64, 90, 101, 114, 169, 176, 177, 188, 273, 286, 293, 294, 301, 303, 309, 318, 361, 389, 392, 399, 406, 414, 427, 429, 432, 434, 469	
Leukemia/Lymphoma . . . . .	6, 65, 89, 123, 127, 131, 147, 202, 232, 238, 267, 294, 295, 296, 350, 411, 447	
MDSC . . . . .	36, 92, 123, 142, 155, 184, 194, 221, 225, 229, 231, 243, 273, 275, 308, 329, 350, 372, 402, 411, 434, 459	
Metabolism . . . . .	151, 155, 166, 187, 230, 231, 275, 278,	
Monocyte/Macrophage . . . . .	15, 23, 77, 86, 110, 118, 123, 142, 150, 156, 171, 242, 243, 246, 287, 294, 297, 299, 316, 322, 350, 388, 391, 409, 410, 419, 421, 423, 467, 468	
Myeloid cells . . . . .	23, 90, 123, 155, 171, 177, 184, 193, 194, 221, 231, 242, 243, 279, 297, 299, 322, 350, 361, 388, 402, 419, 421, 434, 468	
Neoantigens . . . . .	44, 70, 73, 78, 289, 305, 310, 312, 330, 345, 356, 363, 365, 366, 371, 374, 392, 408, 447	
NK/NKT cell . . . . .	17, 22, 36, 45, 49, 50, 68, 69, 90, 115, 138, 150, 155, 168, 202, 212, 231, 235, 263, 267, 296, 304, 325, 336, 342, 343, 380, 387, 394, 400, 410, 455, 456	
Pediatric tumors . . . . .	22, 36, 37, 38, 39, 193, 206, 217, 292, 310, 371, 388	
Proteomics . . . . .	87, 88, 106, 107, 111, 121, 122, 312, 356, 363, 385, 426, 441	
Radiotherapy . . . . .	138, 160, 199, 258, 262, 265, 268, 269, 272, 292, 327, 352, 376, 384, 417, 448, 458, 464	
Regulatory T cell (Treg cell) . . . . .	2, 76, 77, 92, 109, 114, 116, 118, 145, 175, 177, 178, 187, 188, 198, 209, 234, 240, 246, 255, 268, 281, 284, 311, 357, 359, 368, 386, 387, 388, 389, 390, 397, 402, 411, 413, 416, 417, 428, 457	
Solid tumors . . . . .	4, 9, 10, 12, 15, 19, 23, 29, 30, 34, 35, 36, 39, 40, 42, 43, 45, 49, 50, 52, 53, 61, 64, 65, 66, 68, 70, 74, 76, 77, 81, 82, 83, 85, 90, 93, 95, 97, 100, 101, 103, 111, 117, 118, 119, 120, 127, 130, 132, 133, 135, 136, 140, 141, 142, 146, 148, 149, 150, 152, 154, 156, 157, 158, 159, 160, 161, 165, 166, 167, 168, 169, 172, 173, 176, 182, 183, 184, 186, 187, 188, 191, 193, 194, 197, 198, 201, 203, 207, 210, 212, 213, 217, 218, 219, 221, 222, 224, 225, 227, 228, 234, 237, 238, 241, 246, 254, 260, 262, 263, 264, 267, 272, 283, 289, 290, 291, 292, 294, 301, 303, 306, 307, 308, 310, 312, 313, 315, 317, 322, 324, 325, 326, 327, 328, 330, 331, 333, 335, 337, 339, 340, 343, 344, 345, 347, 348, 350, 352, 361, 362, 363, 364, 365, 367, 369, 370, 372, 373, 375, 385, 386, 387, 388, 390, 395, 397, 400, 401, 402, 407, 408, 409, 414, 415, 417, 419, 420, 429, 430, 431, 434, 439, 440, 441, 446, 449, 450, 451, 452, 456, 460, 464, 466, 467	
Stem cell/cancer-initiating cell. . . . .	49, 131, 227, 303, 350, 367	
Surgery . . . . .	34, 100, 120, 191	
Systems biology . . . . .	76, 96, 111, 162, 271, 292, 405, 469	
T cell . . . . .	1, 2, 3, 4, 5, 6, 7, 8, 10, 11, 12, 14, 16, 17,	

## Keyword Index

- 18, 19, 21, 22, 23, 24, 25, 28, 29, 30, 32, 33, 34, 36, 37, 38, 39, 40, 42, 43, 44, 45, 46, 48, 49, 50, 51, 52, 53, 55, 58, 59, 60, 65, 68, 69, 70, 71, 72, 73, 75, 76, 77, 83, 85, 86, 89, 90, 91, 92, 94, 97, 102, 104, 109, 113, 114, 115, 116, 117, 118, 123, 126, 127, 131, 136, 138, 142, 145, 150, 155, 158, 168, 171, 172, 174, 175, 177, 178, 179, 181, 182, 183, 185, 187, 188, 189, 190, 192, 194, 195, 198, 201, 202, 203, 205, 209, 211, 212, 213, 214, 215, 217, 218, 219, 225, 227, 231, 232, 234, 235, 237, 238, 240, 242, 245, 246, 253, 254, 255, 256, 257, 258, 259, 260, 262, 263, 264, 266, 267, 268, 269, 272, 273, 274, 281, 284, 285, 289, 290, 292, 296, 301, 302, 304, 305, 307, 308, 310, 311, 312, 315, 323, 325, 326, 329, 331, 336, 337, 338, 340, 342, 343, 344, 345, 347, 348, 351, 354, 355, 356, 357, 358, 359, 361, 364, 365, 368, 370, 374, 377, 379, 380, 386, 387, 388, 389, 390, 394, 395, 397, 400, 401, 402, 403, 407, 409, 410, 411, 413, 415, 416, 417, 418, 420, 424, 425, 427, 428, 429, 430, 437, 438, 439, 440, 441, 442, 443, 445, 446, 447, 450, 452, 453, 454, 455, 456, 457, 459, 466, 467, 469
- T cell lineages . . . . . 4, 24, 29, 58, 59, 77, 114, 351, 389, 411, 417, 446, 454
- Targeted therapy . . . . . 3, 4, 6, 23, 24, 32, 41, 43, 50, 52, 56, 79, 102, 111, 130, 131, 132, 133, 134, 135, 136, 141, 142, 145, 146, 147, 152, 153, 161, 163, 164, 165, 167, 168, 176, 178, 193, 198, 201, 202, 207, 210, 213, 217, 220, 226, 227, 228, 234, 241, 245, 251, 253, 262, 267, 285, 307, 310, 315, 317, 320, 322, 331, 348, 350, 354, 362, 366, 371, 382, 385, 388, 389, 397, 416, 420, 421, 426, 431, 440, 445, 451, 457
- TLR . . . . . 56, 184, 224, 242, 246, 247, 249, 250, 314, 346, 350, 355, 358, 365, 434, 441, 447, 461, 464
- Tumor antigens . . . . . 3, 5, 10, 12, 19, 31, 38, 39, 40, 44, 56, 70, 94, 130, 131, 168, 171, 191, 195, 201, 211, 220, 227, 245, 260, 279, 289, 302, 305, 306, 310, 312, 315, 329, 330, 331, 337, 339, 340, 344, 345, 348, 354, 356, 357, 360, 361, 363, 365, 372, 374, 375, 377, 379, 381, 390, 408, 418, 440, 441, 447, 451, 462
- Tumor evasion . . . . . 4, 5, 25, 81, 101, 135, 184, 188, 189, 191, 201, 213, 243, 275, 285, 290, 294, 299, 348, 384, 401, 403, 419, 429, 430, 437
- Tumor infiltrating lymphocytes (TILs) . . . . . 4, 7, 8, 9, 11, 12, 13, 14, 24, 26, 29, 31, 34, 35, 38, 41, 42, 44, 45, 47, 51, 64, 67, 68, 71, 72, 74, 75, 76, 77, 83, 84, 93, 94, 96, 97, 103, 105, 109, 110, 116, 117, 120, 127, 130, 136, 137, 139, 142, 145, 154, 158, 172, 175, 179, 182, 188, 192, 196, 201, 203, 208, 209, 211, 213, 214, 218, 222, 229, 230, 233, 235, 240, 242, 246, 250, 254, 255, 258, 266, 269, 272, 278, 284, 286, 292, 299, 301, 308, 312, 315, 329, 330, 331, 334, 342, 343, 344, 346, 347, 348, 351, 357, 368, 385, 387, 388, 390, 393, 395, 399, 400, 401, 402, 403, 409, 410, 411, 412, 413, 415, 416, 419, 420, 425, 427, 428, 429, 430, 432, 438, 439, 441, 442, 443, 447, 450, 452, 457, 458, 459, 466, 467, 469
- Tumor microenvironment. . . . . 2, 4, 5, 15, 23, 25, 29, 36, 52, 64, 70, 71, 72, 73, 74, 76, 77, 81, 83, 84, 85, 93, 94, 97, 98, 99, 100, 101, 104, 105, 108, 109, 110, 114, 115, 117, 118, 119, 120, 123, 130, 135, 149, 154, 155, 162, 166, 176, 182, 183, 188, 193, 194, 198, 201, 209, 210, 213, 217, 218, 219, 222, 227, 229, 230, 231, 233, 235, 240, 242, 243, 244, 246, 250, 251, 254, 257, 258, 269, 273, 275, 281, 286, 292, 297, 298, 301, 311, 320, 321, 322, 323, 325, 326, 329, 330, 333, 334, 343, 347, 351, 357, 359, 382, 383, 384, 385, 386, 387, 388, 389, 390, 391, 392, 393, 394, 395, 396, 397, 399, 400, 401, 402, 403, 405, 406, 408, 409, 410, 411, 412, 413, 415, 417, 418, 419, 420, 421, 424, 425, 426, 427, 428, 429, 430, 431, 432, 433, 434, 440, 441, 443, 452, 457, 460, 464, 465, 466, 467, 468, 469
- Tumor stroma . . . . . 222, 243, 251, 325, 326, 361, 375, 385, 386, 394, 395, 401, 402, 405, 406, 414, 427, 430, 466, 467, 468
- Vaccine . . . . . 10, 37, 53, 56, 63, 75, 88, 90, 100, 102, 140, 144, 145, 148, 170, 171, 198, 201, 211, 220, 222, 234, 236, 244, 248, 250, 256, 257, 261, 262, 273, 289, 298, 310, 315, 330, 331, 337, 340, 344, 346, 355, 357, 358, 359, 361, 362, 364, 365, 366, 367, 368, 369, 370, 371, 372, 373, 374, 375, 376, 377, 378, 379, 380, 381, 441, 447, 457, 461, 462, 463





# Adoptive Cellular Therapy

Presenting author underlined; Primary author in italics

1

## Converting tumor-mediated PD-L1 inhibition into CAR T cell costimulation to potentiate adoptive T cell therapy

Prasad S Adusumilli

Memorial Sloan Kettering Cancer Center, New York, NY, USA

### Background

To overcome tumor-mediated inhibition of chimeric antigen receptor (CAR) T cells, we herein investigated the impact of tumor PD-L1 upregulation on CAR T cell exhaustion and anti-tumor efficacy, and further developed clinically translatable T cell-extrinsic as well as -intrinsic strategies to overcome PD-L1 inhibition in models of lung cancer (LC) and malignant pleural mesothelioma (MPM).

### Methods

Human T cells were transduced with MSLN-specific CAR with CD28 and CD3zeta domains (M28z) were tested *in vitro* and in clinically-relevant LC and MPM mouse models by bioluminescence imaging (BLI) of tumor burden progression. To counteract PD-1/PD-L1 inhibition *in vivo*, we evaluated the efficacy of PD-1 blocking antibody or cell-intrinsic genetic-engineering strategies by cotransducing M28z CAR T cells with a PD-1 dominant negative receptor (PD1-DNR) or with PD-1/4-1BB fusion protein.

### Results

A single, low-dose of M28z CAR T cells is able to resist the progression of established tumor for 40 days, but mice eventually died with progressing tumor. Tumor harvest analysis demonstrated the PD-1 and PD-L1 upregulation on CAR T cells and tumor cells (Figure Panel A). We then confirmed *in vitro* that PD-L1 inhibits M28z T cell effector functions (proliferation, cytotoxicity and cytokine secretion). The addition of PD-1 blocking potentiates CAR T cell therapy *in vivo* but its efficacy requires multiple injections (Panel B). In contrast, a single dose of M28z T cells coexpressing PD-1-DNR restore effector functions, enhance tumor burden control (Panel C) and prolong median survival (56 vs 82 days, p=0.001). Converting PD-L1 inhibition into a positive costimulatory signal by PD-1/4-1BB construct cotransduction into M28z CAR T cells enhanced cytokine secretion and T cell accumulation (Panel D).

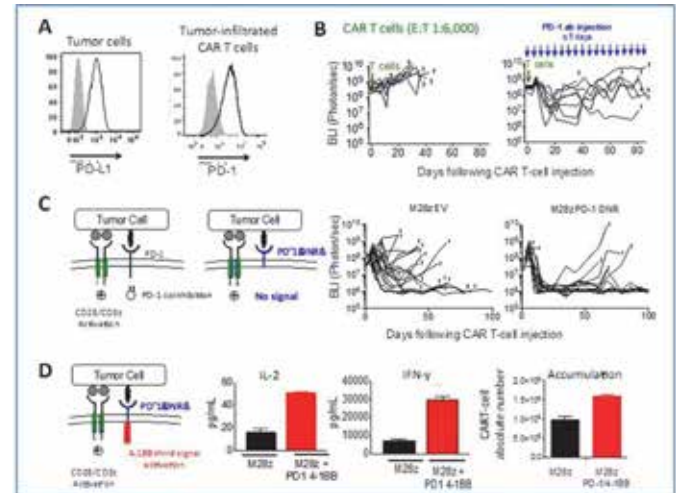
### Conclusions

Our results demonstrate the therapeutic benefit of providing optimal costimulation and coinhibitory blockade to counteract PD-L1/PD-1 immunosuppression, thus potentiate CAR T cell therapy for lung cancer and mesothelioma.

### References

1. Cherkassky L, Morello A, Villena-Vargas J, Feng Y, Dimitrov DS, Jones DR, *et al*: **CAR T cells with cell-intrinsic checkpoint**

**blockade resist tumor-mediated inhibition.** *J Clin Invest* 2016, PMID: 27454297.



## 2 Abstract Travel Award Recipient

### Lack of moesin improves adoptive T cell therapy by potentiating anti-tumor functions

Ephraim A Ansa-Addo, Zihai Li

Medical University of South Carolina, Charleston, SC, USA

### Background

Moesin is a member of the ezrin-radixin-moesin (ERM) protein family that are crucial for organizing membrane domains [1]. However, the role of ERM proteins in regulating signal transduction activities is still less clear and identifying new target proteins regulated by the ERMs for drug targeting remains an important area within the field due to their increased levels in multiple cancers. Whether ERM proteins play any role during the differentiation of naïve CD4<sup>+</sup> T cells to TGF-β-induced Tregs is completely unknown.

### Methods

We utilized a combination of knockout (MsnKO) mice, polyribosome profiling, RT-PCR and immunoblotting to demonstrate that a lack of moesin promotes efficient adoptive T cell therapy in mice by controlling translational upregulation of moesin by TGF-β in T cells.

### Results

The lack of moesin led to poorer development and function of both peripherally-inducible Tregs and *in vitro*-induced Treg cells (Figure 1). We found that the loss of moesin significantly delayed tumor recurrence in a mouse model of melanoma and supported the rapid expansion of adoptively transferred CD8<sup>+</sup> T cells against cancer-associated antigens (Figure 2). Of note, moesin knockout CD4<sup>+</sup> T cells exhibited no defects in T cell receptor activation, proliferation or cytokine production, suggesting no alternations in T cell activation in these mice.

**Adoptive Cellular Therapy**

*Presenting author underlined; Primary author in italics*

Instead, our data indicate that moesin interacts with TGF-β receptor II and controls its surface abundance and stability (Figure 3). Indeed, the lack of moesin significantly impaired optimal TGF-β signaling (Figure 4) and improved adoptive T cell therapy under cancer setting (Figure 5).

**Conclusions**

This finding is important and suggests that modulation of moesin (via inhibitors or agonists), such as developed recently for ezrin [2], could serve as a potential candidates for use in immunotherapy combinations for the treatment of cancer as well as advance our knowledge.

**Acknowledgements**

This work was supported by the US National Institutes of Health (R01DK098819 to D.C.R.; P01CA186866, R01CA188419 and R01AI070603 to Z.L.).

**References**

- Hirata T, Nomachi A, Tohya K, Miyasaka M, Tsukita S, Watanabe T, Narumiya S: **Moesin-deficient mice reveal a non-redundant role for moesin in lymphocyte homeostasis.** *Int Immunol* 2012, **24(11)**:705-717.
- Celik H, Bulut G, Han J, Graham GT, Minas TZ, Conn EJ, Hong SH, Pauly GT, Hayran M, Li X, Ozdemirli M, Ayhan A, Rudek MA, Toretsky JA, Uren A: **Ezrin inhibition up-regulates stress response gene expression.** *J Biol Chem* 2016, **291(25)**:13257-13270.

**Moesin knockout mice have fewer iTregs and evidence of polyclonal T cell activation**

Ansa-Addo et al.  
 Figure 1

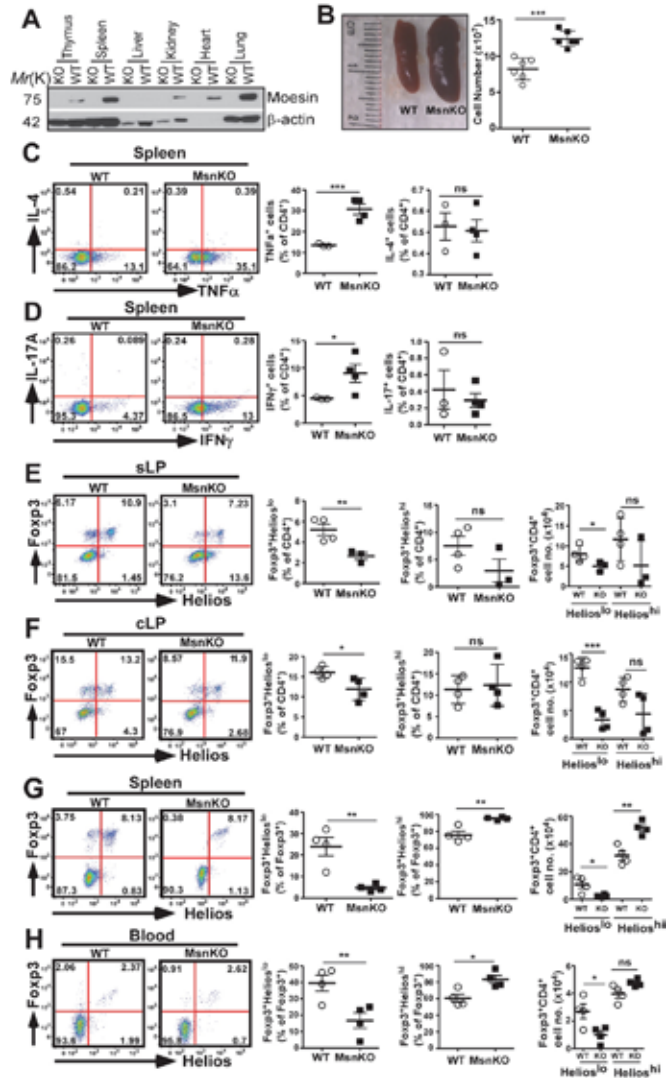


Figure 1. (A) Immunoblot of moesin knockout (KO or MsnKO) in multiple organs of mice. (B) Representative enlarged spleen size and increased cell number as observed in MsnKO mice. Data are reported as the mean ± SEM; \*\*\*P < 0.001 by Student's t-test. n = 6 per group. (C and D) Flow cytometry of inflammatory cytokines, TNF-α and IL-4 (C), and IFN-γ and IL-17A (D) produced by CD4+ T cells from spleens of WT and MsnKO mice after PMA-Ionomycin stimulation for 4 h. Data are reported as the mean ± SEM; \*P < 0.05 and \*\*\*P < 0.001 by Student's t-test. WT n = 3, MsnKO n = 4. (E and F) Flow cytometry analysis and absolute number of pTregs (Foxp3+Heliolo) in the small intestine lamina propria (sLP) (E) and colon lamina propria (cLP) (F) of 10-12 weeks old mice.



## Adoptive Cellular Therapy

Presenting author underlined; Primary author in italics

Data are reported as the mean  $\pm$  SEM; \*P < 0.05, \*\*P < 0.01 and \*\*\*P < 0.001 by Student's t-test. n = 4 per group, MsnKO sLP n = 3. (G and H) Flow cytometry analysis and absolute number of pTregs (Foxp3+Helioslo) in the spleen (G) and peripheral blood (H) of 10-12 weeks old mice. Data are reported as the mean  $\pm$  SEM; ns, not significant; \*P < 0.05 and \*\*P < 0.01 by Student's t-test. n = 4 per group.

### Loss of moesin augments adoptive T cell therapy of melanoma

Ansa-Addo *et al.*  
Figure 2

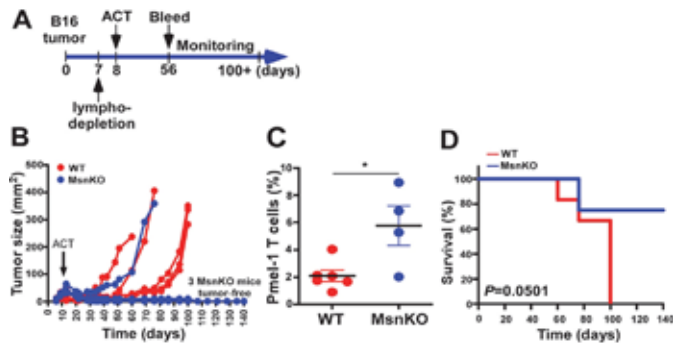


Figure 2. (A) Treatment scheme for B6 mice injected subcutaneously with B16-F1 melanoma tumor cells ( $2.5 \times 10^5$ ) 7 days prior to lympho- 31 depletion with 6Gy total body irradiation and adoptive transfer (ACT) of  $2 \times 10^6$  Pmel-1 T cells (i.v.) at day 8. (B) Tumor growth kinetics in individual mice treated as indicated in A, (each line represents one mouse); WT (n=6), MsnKO (n=4). (C) Frequency of donor Pmel-1 CD8+ T cells circulating in the blood of WT and MsnKO mice from B at 8 weeks. (D) Survival analysis of WT and MsnKO mice upon B16 melanoma tumor injection and adoptive cell transfer. \*P = 0.05 by Log-rank test (B and D), \*P < 0.05 by Student's t-test (C). Data are reported as the mean  $\pm$  SEM.

### Moesin interacts with TGF- $\beta$ receptor II to stabilize its surface abundance

Ansa-Addo *et al.*  
Figure 3

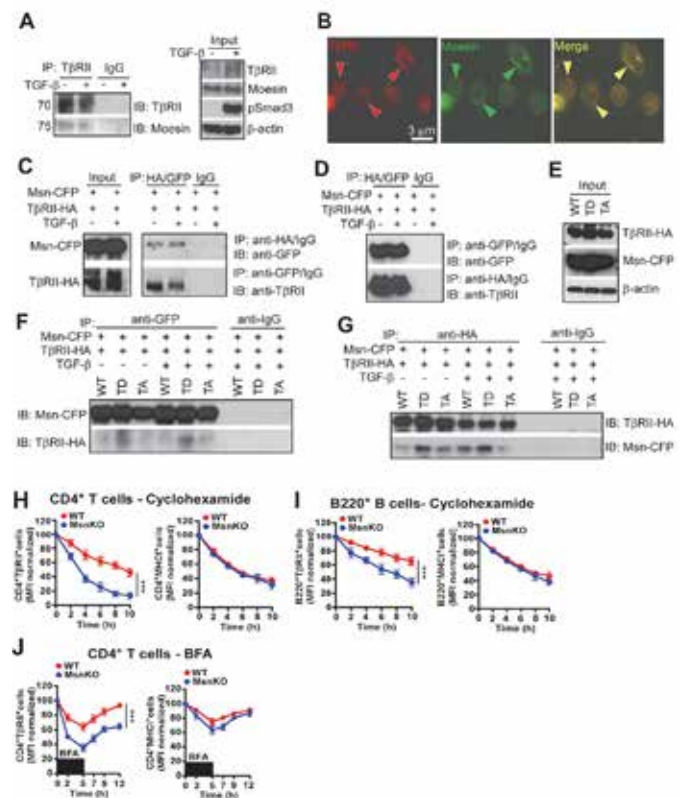


Figure 3. (A) Immunoprecipitation (IP), with anti-TjRRII and control immunoglobulin G antibodies of EL4 cell lysates, followed by immunoblot of pull-down and input samples with the indicated antibodies. (B) Confocal microscopy images of EL4 cells stimulated with TGF- $\beta$  (5 ng/ml for 1 h) and stained with anti-TjRRII and anti-moesin antibodies. (C and D) HEK293FT cells co-transfected with plasmids encoding wild-type moesin-tagged with CFP at the carboxy terminus (Msn-WT-CFP) and TjRRII-tagged with haemagglutinin at the carboxy terminus (TjRRII-HA). Immunoprecipitation of solubilised proteins using anti-GFP and anti-HA antibodies and immunoblot of the pull-down samples. Input - whole cell lysate immunoblotting (throughout). (E-G) Immunoprecipitation and immunoblot (as in C) of HEK293FT cells co-transfected with CFP-tagged wild-type or phosphomimetic moesin mutants and TjRRII-HA constructs. Data are representative of at least three (A-C) or four (D-F) independent experiments. (H and I) Primary CD4+ T cells (H) and B220+ B cells (I) from the spleen of WT and MsnKO mice were treated with cyclohexamide at the indicated times and surface TjRRII analyzed by flow cytometry. Data represents the mean  $\pm$  SD of at least three independent experiments. \*\*\*P < 0.001 by two-way analysis of variance (ANOVA). (J)

**Adoptive Cellular Therapy**

*Presenting author underlined; Primary author in italics*

Flow cytometry analysis of primary CD4+ T cells isolated from the spleen of WT and MsnKO mice, and treated with brefeldin A (BFA), 20 µg/ml for up to 5 h and then washed. Cell surface TβRII was left to recover for up to 12 h prior to analysis. Data represents the mean ± SD of at least three independent experiments. \*\*\*P <0.001 by two-way analysis of variance (ANOVA).

**Lack of moesin leads to inefficient TGF-β signaling**

Ansa-Addo et al. Figure 4

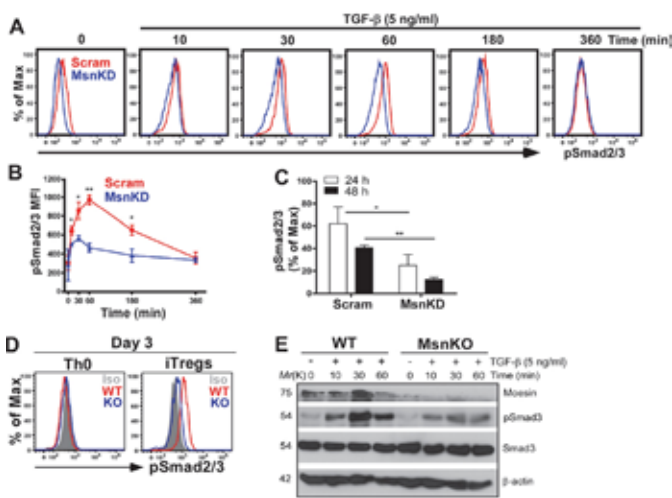


Figure 4. (A-C) EL4 LAF (EL4) cells transduced with lentiviral scrambled vector (Scram) or moesin shRNA (MsnKD), stimulated with TGF-β (5 ng/ml) and analyzed for intracellular pSmad2/3 by flow cytometry at the times indicated. Data are representative of the mean ± SD of at least three independent experiments. \*P <0.05 and \*\*P <0.01 by Student's t-test. (D and E) Analyses of phospho-Smad2/3 (pSmad2/3) by flow cytometry after 3-day cultures (D) and pSmad3 and total Smad3 by immunoblotting (E) stimulated at the indicated times in WT and MsnKO iTregs. Data are representative of at least two independent experiments.

**Schematic model on the roles of moesin in promoting cancer**

Ansa-Addo et al. Figure 9

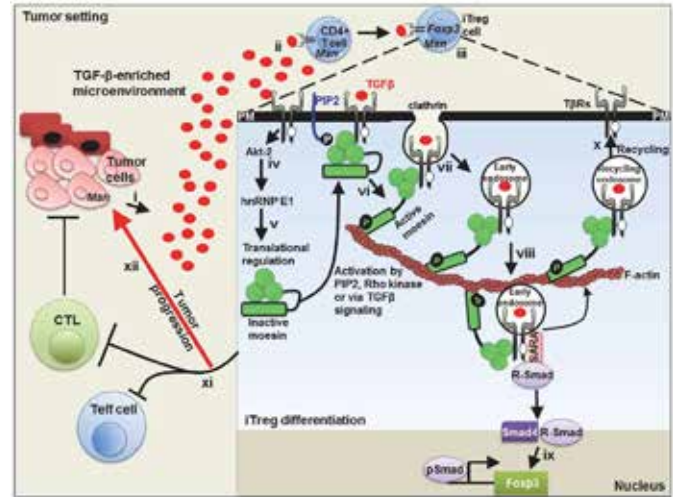


Figure 5. (i, ii) Under pathological conditions such as cancer, TGF-β production by tumor cells binds to cognate receptors on T cell surfaces and triggers signaling events that lead to Foxp3 expression and induced Treg cell development. (iii-iv) Signaling via the TGF-β non-canonical Akt-hnRNP E1-axis leads to post-transcriptional moesin expression. The TGF-β signaling pathway, Rho kinase and/or Phosphatidylinositol 4,5-bisphosphate[PtIn(4,5)P2] pathways, lead to phosphorylation/activation of moesin and aids moesin binding to the F-actin. (v-viii) Moesin-F-actin binding may promote internalization of TGF-β receptors possibly via early endosomes which feeds forward to promote optimal TGF-β signaling leading to efficient Foxp3 induction and iTreg cell differentiation. (ix) Moesin may also promote efficient recycling of TGF-β receptors to maintain the abundance of TβRII on the cell surface. (x) Differentiated induced Treg cells then suppress the proliferation of other immune cells such as cytotoxic T lymphocytes and effector T (Teff) cells to limit anti-tumor responses and promote tumor progression.

**3**

**Preclinical evaluation of an optimal-affinity MAG-EA4 T cell receptor for adoptive T cell therapy**

Andrew Gerry, Joseph P Sanderson, Karen Howe, Roslin Docta, Qian Gao, Eleanor A L Bagg, Nicholas Tribble, *Miguel Maroto*

Adaptimmune, Oxfordshire, England, UK



## Adoptive Cellular Therapy

Presenting author underlined; Primary author in italics

### Background

Adoptive immunotherapy employing optimal affinity T cell receptor (TCR) engineered T cells is a highly attractive treatment modality for multiple cancer indications. In order to ensure the safety of novel T cell receptor therapies, it is important both that expression of the target antigen is tightly restricted to tumor, and that the TCR does not display off-target activity. Here we describe development of an optimal-affinity MAGE-A4 TCR for adoptive T cell therapy.

### Methods

Expression profiling of the cancer-germline antigen MAGE-A4 was performed in tumor and normal tissues, determined by analyzing public RNAseq datasets and by in-house qPCR. We then generated an enhanced affinity TCR that recognizes a validated MAGE-A4 HLA-A\*02 peptide, selected based on potency and specificity in *in vitro* testing from panels of engineered TCRs originating from multiple parental TCRs. The selected TCR was subject to full preclinical characterization using Adaptimmune's extensive preclinical testing process. This process involves potency testing against both tumor cell lines and primary tumor tissue in 2D and 3D, and safety testing consisting of extensive screening of TCR-transduced T cell responses to a wide range of tumor lines, normal human primary cells and induced pluripotent stem cell-derived cells. In addition, the fine specificity of the TCR was characterized to allow the generation of a binding motif and the identification of putative mimotope peptides within the human proteome.

### Results

The MAGE-A4 antigen was found to be highly over-expressed in several clinically important solid tumor indications, such as lung squamous cell cancer (60%), head and neck cancer (42%), bladder cancer (34%) and esophageal cancer (33%), while expression in non-tumor material was limited to expression in the testes and placenta, both immune-privileged tissues. We generated an enhanced-affinity TCR that demonstrated enhanced potency against MAGE-A4-expressing tumor cell lines and fresh tumor tissue, whilst retaining absence of relevant response against MAGE-A4-negative cells and non-MAGE peptide mimotypes.

### Conclusions

MAGE-A4 is an attractive target antigen for adoptive T cell therapy using enhanced affinity TCRs. We have generated and characterized an optimal enhanced-affinity TCR, which shows enhanced potency against MAGE-A4-positive tumor targets whilst maintaining specificity. These data will be used to support an IND for the use of this TCR for investigatory clinical trials.

## 4

### Case report: specific peptide enhanced affinity receptor T cells (SPEAR® T cells) demonstrate long-term persistence and both *in vivo* and *ex vivo* tumoricidal activity

Gareth Betts<sup>1</sup>, Natalie Bath<sup>1</sup>, Luca Melchiori<sup>1</sup>, Daniel E Lowther<sup>1</sup>, Indu Ramachandran<sup>1</sup>, Gabor Kari<sup>1</sup>, Samik Basu<sup>1</sup>, Gwendolyn Binder-Scholl<sup>1</sup>, Karen Chagin<sup>1</sup>, Lini Pandite<sup>1</sup>, Tom Holdich<sup>1</sup>, Rafael Amado<sup>1</sup>, Hua Zhang<sup>2</sup>, John Glod<sup>2</sup>, Donna Bernstein<sup>2</sup>, Bent Jakobsen<sup>3</sup>, Crystal Mackall<sup>4</sup>

<sup>1</sup>Adaptimmune, Philadelphia, PA, USA

<sup>2</sup>National Cancer Institute, Bethesda, MD, USA

<sup>3</sup>Adaptimmune, Oxfordshire, England, UK

<sup>4</sup>Stanford University School of Medicine, Stanford, CA, USA

### Background

SPEAR® T cells reactive against the NY-ESO-1 specific HLA-A02:01 restricted peptide (SLLMWITQC) have demonstrated clinical activity (ORR 50%) in patients (n=12) with advanced synovial sarcoma (SS). The mechanisms underlying tumor relapse in the presence of persisting SPEAR® T cells remain unclear. Here, we report on phenotypic and functional studies on both engineered T cells and tumor biopsies from a patient with a NY-ESO-1<sup>+</sup> SS treated with NY-ESO-1<sup>C259</sup> SPEAR® T cells.

### Methods

Engineered T cell persistence was determined by qPCR for the vector backbone and flow cytometry for HLA-A2:01-SLLMWITQC reactive pentamer<sup>+</sup> T cells in post-infusion PBMC samples. Multi-parameter flow cytometric analyses were performed on pre-infusion manufactured product and post-infusion PBMCs to assess memory subsets using CD45RA and CCR7, exhaustion using CD28 and PD-1, and functionality by IFN- $\gamma$  and Gzmb. Tumor and NY-ESO-1<sup>C259</sup> T cells from patient PBMCs were isolated at 28 months post-infusion to determine their *ex vivo* killing capacity against a NY-ESO-1<sup>+</sup> cell line, A375. Antigen expression and immunomodulatory milieu (e.g. PD-L1) in baseline and post-treatment biopsies were assessed by immunohistochemistry. Serum cytokines were measured by a Luminex based immunoassay. Tumor response was determined by RECIST v1.1.

### Results

The patient achieved a partial response to NY-ESO-1<sup>C259</sup> SPEAR® T cells with progression at 9 months post-infusion. Persistence at 28 months with NY-ESO-1<sup>C259</sup> T cells was observed by qPCR and flow cytometry. Over the course of treatment, the phenotype of the engineered cells changed from a mix of T<sub>EMRA</sub> (CD45RA<sup>+</sup>CCR7<sup>-</sup>), T<sub>EM</sub> (CD45RA<sup>+</sup>CCR7<sup>-</sup>), and T<sub>SCM</sub> (CD45RA<sup>+</sup>CCR7<sup>+</sup>) populations at the time of infusion to a predominately T<sub>SCM</sub> (~98.7%) within five months. PBMC

## Adoptive Cellular Therapy

Presenting author underlined; Primary author in italics

derived NY-ESO-1<sup>C259</sup> SPEAR® T cells 28 months post-infusion exhibited substantial *ex vivo* killing of NY-ESO-1<sup>+</sup> A375 cells without additional *ex vivo* re-stimulation. Pre- and post-infusion biopsies showed NY-ESO-1 expression and exhibited minimal to moderate leukocytic (CD45<sup>+</sup>) infiltration accompanied by minimal lymphocytic infiltration post-infusion. Of note, PD-L1 expression was exclusive to CD45<sup>+</sup> cells.

### Conclusions

Despite an initial response to NY-ESO-1<sup>C259</sup> SPEAR® T cells, this patient eventually relapsed despite the persistence of functional SPEAR® T cells and antigen positive tumor. The basis for tumor progression following response remains unclear, but does not appear to result from T cell exhaustion. Other possibilities include loss of antigen expression and/or diminished tumor infiltration, which could result from the large peripheral T<sub>SCM</sub> population, known to traffic to lymphoid tissue rather than tumor.

### Trial Registration

ClinicalTrials.gov identifier NCT01343043.

### Consent

Written informed consent was obtained from patient for publication. A copy is available for editor review.

## 5

### Engineering 2nd generation SPEAR® T cells to overcome TGF-β-mediated immunosuppression for adoptive cell therapy

*Ryan Wong*<sup>1</sup>, Jonathan D Silk<sup>1</sup>, Katherine Adams<sup>1</sup>, Garth Hamilton<sup>1</sup>, Alan D Bennett<sup>1</sup>, Sara Brett<sup>2</sup>, Junping Jing<sup>2</sup>, Adriano Quattrini<sup>1</sup>, Manoj Saini<sup>1</sup>, Guy Wiedermann<sup>1</sup>, Andrew Gerry<sup>1</sup>, Bent Jakobsen<sup>1</sup>, Gwendolyn Binder-Scholl<sup>3</sup>, Joanna Brewer<sup>1</sup>

<sup>1</sup>Adaptimmune, Oxfordshire, England, UK

<sup>2</sup>GSK, Stevenage, England, UK

<sup>3</sup>Adaptimmune, Philadelphia, PA, USA

### Background

Adoptive cell therapy (ACT) with NY-ESO SPEAR® T cells, is showing promising initial clinical responses in phase I/II trials for both solid and liquid tumors including synovial sarcoma and multiple myeloma. However, the depth and durability of response may be affected by the inhibitory tumor microenvironment. Tumors utilize many different methods to inhibit anti-tumor immunity including secretion of inhibitory cytokines, such as transforming growth factor-β (TGF-β) and induction/recruitment of other inhibitory cells including regulatory T cells and myeloid-derived suppressor cells. These inhibitory cells also secrete cytokines such as IL-10 and TGF-β that potentially reduce the efficacy of T cells. TGF-β is expressed at high levels in a range of cancer indications.

### Methods

We investigated whether SPEAR® T cells can be engineered to express additional proteins, allowing them to overcome such immune resistance mechanisms, potentially improving clinical responses. TGF-β inhibits T cells by binding to a dimer of TGFβRII, which then recruits a dimer of TGFβRI forming a heterotetrameric complex that activates inhibitory intracellular SMAD signaling pathways. Truncating the intracellular signaling domain produces a dominant negative TGF-β receptor (dnTGFβRII) that, although capable of binding TGF-β, is unable to signal. We therefore generated SPEAR® T cells co-expressing enhanced affinity T cell receptors (TCR) that recognize a peptide from NY-ESO/LAGE-1A in the context of HLA-A2, together with dnTGFβRII and tested their function *in vitro*.

### Results

Firstly we showed that the function of NY-ESO SPEAR® T cells is inhibited with physiologically-relevant concentrations of TGF-β. We further show that dnTGFβRII can be co-expressed with enhanced affinity NY-ESO TCR in SPEAR® T cells. T cells expressing dnTGFβRII had reduced SMAD phosphorylation in response to TGF-β compared with cells expressing TCR alone, indicating that inhibitory signaling in response to TGF-β was reduced. Subsequently we showed that T cells expressing dnTGFβRII were partially or completely resistant to the effects of TGF-β, using assays for T cell proliferation, cytotoxicity (in 2D and with 3D microtissue models) and Th1 cytokine release (IFN-γ and IL-2) in response to antigen positive tumor cells.

### Conclusions

Together these data indicate that co-expression of dnTGFβRII may be a viable approach to improve the efficacy of SPEAR® T cells in treating cancer.

## 6

### Inducible MyD88/CD40 (iMC) costimulation drives ligand-dependent tumor eradication by CD123-specific chimeric antigen receptor T cells

*MyLinh Duong*<sup>1</sup>, An Lu<sup>1</sup>, Peter Chang<sup>1</sup>, Aruna Mahendravada<sup>1</sup>, Nicholas Shinnars<sup>1</sup>, Kevin Slawin<sup>1</sup>, David M Spencer<sup>2</sup>, Aaron E Foster<sup>1</sup>, J Henri Bayle<sup>1</sup>

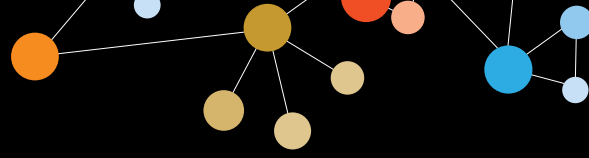
<sup>1</sup>Bellicum Pharmaceuticals, Houston, TX, USA

<sup>2</sup>Bellicum Pharmaceuticals and Baylor College of Medicine, Houston, TX, USA

### Background

CD123/IL-3Rα is a promising chimeric antigen receptor (CAR)-T cell target due to its high expression on both acute myeloid leukemia (AML) blasts and leukemic stem cells (AML-LSCs). However, the antigen is also expressed at lower levels on normal stem cell progenitors, presenting a major toxicity





## Adoptive Cellular Therapy

Presenting author underlined; Primary author in italics

concern should CD123-specific CAR-T cells show long-term persistence. Here, we describe a CAR platform, “GoCAR-T”, that uses a proliferation-deficient, first generation, CD123-specific CAR together with a ligand-dependent costimulatory switch (inducible MyD88/CD40 (iMC)) to provide physician-controlled eradication of CD123<sup>+</sup> tumor cells and regulate long-term CAR-T cell engraftment.

### Methods

T cells were activated and transduced with a bicistronic retrovirus encoding iMC (MyD88 and CD40 cytoplasmic signaling domains fused with tandem copies of FKBPv36 (binding domain for the dimerizing ligand rimiducid (Rim)) and a first generation CAR targeting CD123 (SFG-iMC-CD123.ζ). Ligand dependence for costimulation with iMC was assessed in coculture assays with CD123<sup>+</sup> AML cell lines (KG1, THP-1 and MOLM-13) by examination of cytokine production and observation by IncuCyte-based live cell imaging. *In vivo* efficacy was assessed by i.v. injection of 10<sup>6</sup> EGFP*luc*-expressing CD123<sup>+</sup> THP-1 tumor cells into immunodeficient NSG mice. After seven days 2.5x10<sup>6</sup> non-transduced or iMC-CD123.ζ-modified T cells were injected and Rim (1 mg/kg) or vehicle only administered i.p. on days 0 and 15 post-T cell injection. Animals were evaluated for tumor burden using IVIS bioluminescent imaging (BLI) and for T cell persistence by flow cytometry and qPCR at day 30 post-T cell injection.

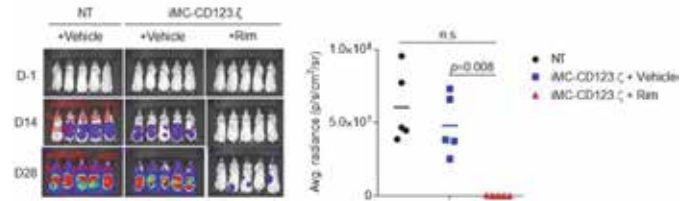
### Results

In coculture assays, both CD123 antigen recognition and Rim-dependent iMC costimulation were required for IL-2 production (285±41 versus 2,541±255 pg/ml for control and 1 nM Rim, respectively), robust CAR-T cell proliferation (87-fold increase with Rim stimulation) and enhanced KG1 cell killing. In NSG mice engrafted with CD123<sup>+</sup> THP-1-EGFP*luc* tumor cells, only animals treated with iMC-CD123.ζ-modified T cells and Rim controlled tumor growth, showing a 2-log reduction in tumor burden with Rim treatment. Two weeks after the second Rim injection, CAR-T cells were infrequent (<1.0%) in the spleen and bone marrow of both CAR groups, suggesting that active costimulation is required for CAR-T persistence.

### Conclusions

GoCAR-T, a platform comprising a ligand-dependent activation switch and a proliferation-deficient first generation CAR, efficiently eradicates CD123<sup>+</sup> leukemic cells when costimulation is provided by systemic rimiducid administration. Deprivation of iMC costimulation results in reduction of CAR-T levels, providing a user-controlled system for managing persistence and safety of CD123-specific CAR-T cells.

**Figure 1. Rimiducid-dependent MyD88/CD40 costimulation enhances antitumor activity of a first-generation CD123-specific CAR**



## 7 ★ Abstract Travel Award Recipient

### Heterodimeric IL-15 treatment enhances tumor infiltration, persistence and effector functions of adoptively transferred tumor-specific T cells in the absence of lymphodepletion

*Cristina Bergamaschi*<sup>1</sup>, Sinnie Sin Man Ng<sup>1</sup>, Bethany Nagy<sup>1</sup>, Shawn Jensen<sup>2</sup>, Xintao Hu<sup>1</sup>, Candido Alicea<sup>1</sup>, Bernard Fox<sup>2</sup>, Barbara Felber<sup>1</sup>, George Pavlakis<sup>1</sup>

<sup>1</sup>National Cancer Institute at Frederick, Frederick, MD, USA

<sup>2</sup>Providence Cancer Center, Portland, OR, USA

### Background

Adoptive cell transfer (ACT) is a promising immunotherapeutic approach for cancer. Host lymphodepletion is associated with favorable ACT therapy outcomes, but it may cause detrimental effects in humans. Among the benefits provided by lymphodepletion, ablation of cells forming a cytokine “sink” results in high levels of homeostatic cytokines that support proliferation and survival of the transferred lymphocytes. Interleukin-15 (IL-15) is a lymphocyte growth and activation factor presently in clinical trials for immunotherapy of metastatic cancers. We previously showed that bioactive IL-15 *in vivo* comprises a stable complex of the IL-15 chain with the IL-15 receptor alpha chain (IL-15Rα), termed heterodimeric IL-15 (hetIL-15). In this study, we tested the hypothesis that hetIL-15 administration enhances ACT in the absence of lymphodepletion.

### Methods

We evaluated the effects of the combination regimen ACT+hetIL-15 in the absence of lymphodepletion by transferring melanoma-specific Pmel-1 T cells into B16 melanoma-bearing mice. Tumors were analyzed by both flow cytometry and multi-parameter immunohistochemistry. Tumor-infiltrating transferred Pmel-1 were analyzed for their persistence, proliferation and effector functions.

### Results

hetIL-15 treatment delayed tumor growth by promoting infiltration and persistence of both adoptively transferred Pmel-1 cells and endogenous CD8<sup>+</sup> T cells into the tumor. In

## Adoptive Cellular Therapy

Presenting author underlined; Primary author in italics

contrast, persistence of Pmel-1 cells was severely reduced following irradiation in comparison to hetIL-15 treatment. Importantly, we found that hetIL-15 led to the preferential enrichment of Pmel-1 cells in B16 tumor sites in an antigen-dependent manner. Upon hetIL-15 administration, tumor-infiltrating Pmel-1 cells showed a “non-exhausted” effector phenotype, characterized by increased IFN-g secretion, proliferation and cytotoxic potential and low level of PD-1. hetIL-15 treatment also resulted in an improved Pmel-1 to Treg ratio in the tumor.

### Conclusions

This study shows that hetIL-15 administration improves the outcome of ACT in immunocompetent hosts and is able to replace the need for lymphodepletion prior ACT for cancer therapy. Applications of heterodimeric IL-15 to ACT will provide new tools and techniques for cancer immunotherapy protocols. Elimination of the need for lymphodepletion will make more patients eligible for cell transfer protocols. In addition, IL-15 could be a general method to place T cells into tumors, increasing the success rate of other immunotherapy interventions.

8

### WITHDRAWN

9

### Partially differentiated polyfunctional T cells dominate the periphery after tumor-infiltrating lymphocytes therapy for cancer

Marco Donia<sup>1</sup>, Julie Westerlin Kjeldsen<sup>2</sup>, Rikke Andersen<sup>1</sup>, Marie Christine Wulff Westergaard<sup>1</sup>, Valentina Bianchi<sup>3</sup>, Mateusz Legut<sup>3</sup>, Meriem Attaf<sup>3</sup>, Garry Dolton<sup>3</sup>, Barbara Szomolay<sup>4</sup>, Sascha Ott<sup>5</sup>, Rikke Lyngaa<sup>6</sup>, Sine Reker Hadrup<sup>6</sup>, Andrew Kelvin Sewell<sup>3</sup>, Inge Marie Svane<sup>1</sup>

<sup>1</sup>Department of Oncology, Center for Cancer Immune Therapy, Herlev Hospital, Herlev, Hovedstaden, Denmark

<sup>2</sup>Center for Cancer Immune Therapy, Herlev Hospital, Herlev, Hovedstaden, Denmark

<sup>3</sup>Cardiff University School of Medicine, Cardiff, Wales, UK

<sup>4</sup>Systems Immunology Institute, Cardiff University, Cardiff, Wales, UK

<sup>5</sup>Warwick Systems Biology Centre, University of Warwick, Coventry, England, UK

<sup>6</sup>Section for Immunology and Vaccinology, National Veterinary Institute, Technical University of Denmark, Frederiksberg, Hovedstaden, Denmark

### Background

Infusion of highly heterogeneous populations of autologous tumor-infiltrating lymphocytes (TILs) can result in tumor regression of exceptional duration. Initial tumor regression

has been associated with persistence of tumor-specific TILs one month after infusion, but mechanisms leading to long-lived memory responses are currently unknown. Here, we studied the dynamics of bulk tumor-reactive CD8<sup>+</sup> T cell populations in patients with metastatic melanoma following treatment with TILs.

### Methods

We analyzed the function and phenotype of tumor-reactive CD8<sup>+</sup> T cells contained in serial blood samples of sixteen patients treated with TILs.

### Results

Polyfunctional tumor-reactive CD8<sup>+</sup> T cells accumulated over time in the peripheral lymphocyte pool. Combinatorial analysis of multiple surface markers (CD57, CD27, CD45RO, PD-1 and LAG-3) showed a unique differentiation pattern of polyfunctional tumor-reactive CD8<sup>+</sup> T cells. This subpopulation acquired simultaneously expression of the early differentiation marker CD27, alongside typical features of late effector cells such as loss of CD45RO and up-regulation of PD-1 and CD57. The differentiation and functional status appeared very similar from 1 month to 1 year after infusion. Despite some degree of clonal diversification occurring *in vivo* within the bulk tumor-reactive CD8<sup>+</sup> T cells, further analyses showed that CD8<sup>+</sup> T cells specific for defined tumor-antigens had similar differentiation status.

### Conclusions

We demonstrated that tumor-reactive CD8<sup>+</sup> T cell subsets that persist after TIL therapy are mostly polyfunctional, and display a stable partially differentiated phenotype. These atypical CD27<sup>+</sup> incompletely differentiated polyfunctional TILs may have a high capacity for persistence and be crucial in keeping patients tumor free.

### Trial Registration

ClinicalTrials.gov identifier NCT00937625.

10

### Peptide vaccine enhances antitumor effect of adoptive cell transfer using genetically engineered T cells

Aaron Fan<sup>1</sup>, Takumi Kumai<sup>2</sup>, Esteban Celis<sup>2</sup>

<sup>1</sup>Augusta University, Augusta, GA, USA

<sup>2</sup>Georgia Cancer Center, Augusta University, Augusta, GA, USA

### Background

Adoptive cell therapy (ACT) has shown promise in tumor eradication in cancer, but current methods require harmful and toxic adjunct procedures. Our laboratory has developed a potent peptide vaccination strategy called TriVax that bypasses the necessity of these adjunct procedures. Previous studies show that retrovirally (RV)-transduced T cells are effective in ACT against various cancers. The present study

## Adoptive Cellular Therapy

Presenting author underlined; *Primary author in italics*

aimed to determine whether RV-transduced T cells could respond to TriVax specific for melanosomal tumor antigen gp100, and to see if the responses could be enhanced when transduced with a constitutively active form of STAT5 (CA-STAT5), which has been shown to increase survival of CD8 effector/effector memory T cell populations.

### Methods

CD8 T cells were purified from B6 mouse splenocytes and RV-transduced with a gene encoding the clonal T cell receptor (TCRs) for mouse gp100. In some experiments, cells were also co-transduced with a gene encoding for CA-STAT5 (co-expressing Thy1.1). Transduction efficiency was assessed using flow cytometry with gp100 tetramer and Thy1.1 antibody. Functional activity was measured using flow cytometry and EliSpot (IFN $\gamma$ ) assays. These cells were then adoptively transferred ( $1.0 \times 10^5$  tetramer+ cells) into naïve and tumor bearing congenic CD45.1 B6 mice, which were then vaccinated with TriVax. Tumor growth was assessed 3 times per week, and immune status was assessed in blood using flow cytometry every 7 days.

### Results

TriVax administration selectively expanded the ACT cell population expressing gp100-TCR. Cell numbers in spleen indicate a 14-fold expansion 25 days after vaccination from what was initially transferred. When co-transduced with CA-STAT5, an even higher fold expansion (55-fold) was observed. CA-STAT5+ cells also expanded more robustly than CA-STAT5- cells when stimulated with a subsequent vaccine boost, demonstrating a 5000-fold increase in cell numbers with 85% of CD8+ T cells also being positive for gp100 tetramer. ACT of these cell populations into tumor bearing mice also yielded a dramatic increase in cell numbers, which greatly enhanced the survival of mice in treatment groups.

### Conclusions

CD8 T cells RV-transduced to express a gp100 TCR and CA-STAT5 are capable of expansion in response to TriVax, bypassing the necessity of adjunct procedures. Co-expression of CA-STAT5 greatly enhances the boost effect of TriVax, leading to a dramatic anti-tumor effect.

11

### Stable tumor-infiltrating lymphocytes (TIL) phenotype following cryopreservation

Ian Frank, Amanda Stramer, Michelle A Blaskovich, Seth Wardell, Maria Fardis, James Bender, Michael T Lotze

Lion Biotechnologies, Inc., Tampa, FL, USA

### Background

Lion Biotechnologies focuses on the development and commercialization of cancer immunotherapies based on

tumor-infiltrating lymphocytes (TIL). Cryopreservation is a beneficial process which allows the final cell product to be shipped in a safe manner with less time constraints [1]. Clinical studies using cryopreserved TIL have not been conducted so far. Freezing and thawing of the cells may cause phenotypic changes such as loss of cell surface receptors [2]. Here, we tested fresh versus frozen/thawed TIL samples and evaluated the expression of phenotypic markers.

### Methods

Briefly, PreREP TILs were obtained by culturing melanoma tumor fragments in IL-2 (6000 IU/ml). Rapid expansion protocol (REP) cells were initiated using allogeneic PBMC feeder cells with OKT3 and IL-2 in a Grex-100 flask. When the desired confluency was reached, the cells were cryopreserved in a 5% DMSO solution. We used flow cytometry to phenotype the fresh and thaw/rested TIL at 0h, 24h and 7d following reREP TIL. Flow cytometric analysis was performed using fluorescent antibodies specific for TCR $\alpha$ /b, CD4, CD8, CD27, CD28, CD56, CCR7, CD45RA, CD95, PD-1, and CD25.

### Results

No significant differences in CD4, CD8 and TCR $\alpha$ /b expression or memory markers comparing fresh TIL versus thaw/rested TIL at 24h was noted. CD27 expression on TIL was reduced by 50% on thawed TIL, however after a 24h resting period the expression recovered. All other surface antigens that we tested were within 10% difference in their expression levels as compared to baseline.

### Conclusions

Cryopreservation did not affect the measured phenotypic characteristics of TIL. We are further investigating the possibility of using cryopreserved TIL in a clinical setting.

### References

1. Axelsson S, Faresjo M, Hedman M, Ludvigsson J, Casas R: **Cryopreserved peripheral blood mononuclear cells are suitable for the assessment of immunological markers in type 1 diabetic children.** *Cryobiology* 2008, **57**:201–208.
2. Sadeghi A, Ullenhag G, Wagenius G, Tötterman TH, Eriksson F: **Rapid expansion of T cells: Effects of culture and cryopreservation and importance of short-term cell recovery.** *Acta Oncol* 2013, **52**:978-986.

## Adoptive Cellular Therapy

Presenting author underlined; Primary author in italics

12

### Recognition of autologous neoantigens by tumor infiltrating lymphocytes derived from human breast cancer metastases

Stephanie L Goff<sup>1</sup>, Nikolaos Zacharakis<sup>1</sup>, Yasmine Assadipour<sup>1</sup>, Todd D Prickett<sup>1</sup>, Jared J Gartner<sup>1</sup>, Robert Somerville<sup>2</sup>, Mary Black<sup>1</sup>, Hui Xu<sup>1</sup>, Harshini Chinnasamy<sup>1</sup>, Isaac Kriley<sup>1</sup>, Lily Lu<sup>1</sup>, John Wunderlich<sup>1</sup>, Paul F Robbins<sup>1</sup>, Steven Rosenberg<sup>1</sup>, Steven A Feldman<sup>1</sup>

<sup>1</sup>Surgery Branch, National Cancer Institute, National Institutes of Health, Bethesda, MD, USA

<sup>2</sup>National Cancer Institute, Bethesda, MD, USA

#### Background

Adoptive transfer of tumor infiltrating lymphocytes (TIL) can effect long-term durable regression in patients with metastatic melanoma but has not been widely tested in common epithelial cancers. When examining the TIL of successfully treated patients with melanoma, a heterogeneous T cell population can be identified with reactivity against melanoma differentiation antigens, cancer germline antigens, and personalized non-synonymous somatic mutations. Common epithelial cancers, including breast cancer, express far fewer somatic mutations than melanoma, however, in a study of metastatic gastrointestinal cancer, lymphocytes targeting neoantigens were identified in the majority of specimens. This pilot study investigates the ability to grow TIL from breast cancer metastases, to identify personalized non-synonymous somatic mutations and potential neoantigens, and to adoptively transfer TIL into patients with breast cancer.

#### Methods

Eligible patients were evaluated and treated under IRB-approved protocols for tissue procurement, genomic testing, and adoptive cell transfer. Portions of resected tumors were placed in culture under standard TIL conditions. DNA was extracted from tumor and matched normal peripheral blood samples for whole exome sequencing (WES). Non-synonymous somatic mutations were identified and tested for potential immunogenicity using previously described tandem mini-gene and long (25mer) peptide techniques. Recognition was assessed by IFN $\gamma$  release on ELISPOT and/or CD137 (4-1BB) upregulation with appropriate controls.

#### Results

Nine patients underwent surgical resection in this ongoing pilot study, and TIL were successfully grown from the tumors of all patients. All were primarily CD3+ (median 79%) with a small population of natural killer cells. Of the CD3+ cells, 7 of 9 patients had a predominantly CD4+ population (median CD4:CD8 ratio 2.2, range 0.4-5.8). For eight tumors, WES was

performed, and non-synonymous somatic mutations were identified as potential neoantigens (median count 96.5, range 71-148). Autologous T cell reactivity has been identified against tumor-specific mutations in 6 of 8 patients.

#### Conclusions

Tumor-infiltrating lymphocytes derived from metastatic breast cancer can react to tumor-specific non-synonymous somatic mutations *in vitro*. TIL grown from breast cancers are predominantly CD4+ and can form the basis of an adoptive cell transfer experimental approach to patients with metastatic breast cancer.

#### Trial Registration

ClinicalTrials.gov identifier NCT01174121.

13

### Comparison of RECIST 1.0 to RECIST 1.1 in the evaluation of adoptive cell transfer

Kasia Trebska-McGowan<sup>1</sup>, Isaac Kriley<sup>1</sup>, Parisa Malekzadeh<sup>1</sup>, Eden Payabyab<sup>1</sup>, Richard Sherry<sup>2</sup>, Steven Rosenberg<sup>1</sup>, Stephanie L Goff<sup>1</sup>

<sup>1</sup>Surgery Branch, National Cancer Institute, National Institutes of Health, Bethesda, MD, USA

<sup>2</sup>National Cancer Institute, Bethesda, MD, USA

#### Background

Adoptive transfer of tumor infiltrating lymphocytes (TIL) can effect long-term durable regression in patients with metastatic melanoma. The earliest studies utilized WHO criteria for evaluation of response, but more recent studies replaced the bidimensional analysis with simplified unidimensional criteria of RECIST 1.0. With improved cross-sectional imaging, there became concern that the pathophysiology of lymph node response required distinct evaluation criteria, as tumor clearance may not completely eradicate normal structures. RECIST 1.1 was developed and validated in a variety of histologies with various treatments, but has not been evaluated for adoptive cell transfer.

#### Methods

Eligible patients were enrolled on an IRB-approved protocol of adoptive cell transfer, randomizing patients to receive one of two lymphodepleting regimens prior to transfer of TIL. This study was reported using RECIST 1.0 criteria, with 24 complete responders and 30 partial responders among 99 treated patients [1]. The official tumor measurements of target lesions and notations of non-target lesions were re-evaluated using RECIST 1.1 criteria, which limits the total number of target lesions, the number of target lesions/organ, and uses short-axis measurements for lymph node disease.



# Adoptive Cellular Therapy

Presenting author underlined; Primary author in italics

## Results

By design, the number of target lesions/patient was decreased, from 4 (range 1-10) to 3 (range 0-5). Thirty-eight lymph nodes did not meet short-diameter criteria for target lesions (10-14mm), and an additional 12 measured <10mm were reclassified as “non-pathologic”. With retrospective application of RECIST 1.1, three patients would not have met eligibility criteria for lack of evaluable disease. In assessing overall response to treatment, 25 patients met CR criteria, with an additional 27 with PR. While there were five patients who achieved CR at an earlier time point, overall time to response was not significantly different (median 16.0 v 19.8 months p=0.19). One patient with lymph node disease did not achieve CR by original criteria, was an early CR in this analysis, but recurred three months later.

## Conclusions

Adoption of RECIST 1.1 demonstrated comparable response rates for this trial. A hallmark of our modern studies is the durability of complete responses with RECIST 1.0, and only by further application of the new criteria will we be able to confirm the validity of lymph node response criteria in adoptive cell transfer.

## Trial Registration

ClinicalTrials.gov identifier NCT01319565.

## References

1. Goff SL, Dudley ME, Citrin DE, Somerville RP, Wunderlich JR, Danforth DN, *et al*: **Randomized, Prospective Evaluation Comparing Intensity of Lymphodepletion Before Adoptive Transfer of Tumor-Infiltrating Lymphocytes for Patients with Metastatic Melanoma.** *J Clin Oncol* 2016, **34(20)**:2389-2397.

14

## Bioluminescent redirected lysis assay (BRLA) as an efficient potency assay to assess tumor-infiltrating lymphocytes (TILs) for immunotherapy

Aishwarya Gokuldass, Michelle A Blaskovich, Charlene Kopits, Brian Rabinovich, Michael T Lotze

Lion Biotechnologies, Inc., Tampa, FL, USA

## Background

Administration of TILs is a promising treatment for patients with melanoma and other solid tumors. TIL therapy involves culturing and expanding T cells isolated from a patient’s tumor *in vitro* and then reinfusing them back into the patient. TIL antitumor activity is commonly measured using tumor cells from the patient’s tumor, when available. However, autologous tumor cell lines are difficult to grow consistently. In order to test the potency of TILs that are infused into patients, we developed a surrogate target cell line that can be used to assess the lytic potential of TILs in a BRLA.

## Methods

Mouse mastocytoma P815 cells expressing endogenous CD16, transduced with eGFP and firefly luciferase were selected as a surrogate for autologous tumor cells. The CD16 Fc receptor binds anti-CD3 antibodies providing a potent TCR activation signal. The P815 cells were sorted and cloned and then co-cultured with TILs +/- anti-CD3 antibodies to assess tumor reactivity through TCR activation and basal non-specific killing. Following 4 hours of incubation, luciferin was added to the wells for 5 minutes. After the incubation, bioluminescence intensity was determined. The % cytotoxicity and survival were calculated thus: % Survival = (experimental luminescence-background)/ (maximum luminescence-background)\*100; % Cytotoxicity = 100-(% Survival); and Interferon-γ release in the media of the co-cultured TILs and P815 cells was analyzed by ELISA and LAMP1 (CD107a) expression analyzed by flow cytometry to evaluate the cytotoxicity of TILs.

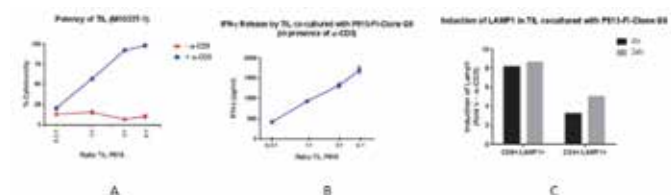
## Results

TCR-mediated TIL cytotoxicity can be measured in a highly sensitive dose-dependent manner. As shown below, this assay is highly sensitive. The following data will be presented: Highly Sensitive Potency Assay for TILs. A) % cytotoxicity of TIL (from patient M1033T-1) when co-cultured with P815 Clone G6 (with and without anti-CD3 antibody) at different ratios of effector to target cells. B) ELISA data showing amount of IFN-γ released at different ratios of effector to target cells. C) % LAMP1 marker expressed by the M1033T-1 when co-cultured with P815 Clone G6 and anti-CD3 at 1:1 effector to target cells for 4 and 24hr co-culture.

## Conclusions

Our ‘Bioluminescent Redirected Lysis Assay’ (BRLA) using an engineered P815 cell line can be used as an assay to measure TIL potency. It requires no radionuclides and is more efficient than traditional cytotoxicity assays.

Figure 1



A) % cytotoxicity of TIL (from patient M1033T-1) when co-cultured with P815 Clone G6 (with and without anti-CD3 antibody) at different ratios of effector to target cells. B) ELISA data showing amount of IFN-γ released at different ratios of effector to target cells. C) % LAMP1 marker expressed by the M1033T-1 when co-cultured with P815 Clone G6 and anti-CD3 at 1:1 effector to target cells for 4 and 24hr co-culture.

## Adoptive Cellular Therapy

Presenting author underlined; *Primary author in italics*

15

### Culturing and live cell confocal imaging of ovarian cancer spheroids with monocytes and interferons

Daniel S Green<sup>1</sup>, Olena Kamenyeva<sup>2</sup>, Kathryn C Zoon<sup>3</sup>, Christina M Annunziata<sup>1</sup>

<sup>1</sup>Translational Genomics Section, Women's Malignancy Branch, National Cancer Institute, Bethesda, MD, USA

<sup>2</sup>Biological Imaging Section, Research Technologies Branch, National Institute of Allergy and Infectious Disease, National Institutes of Health, Bethesda, MD, USA

<sup>3</sup>Laboratory of Infectious Diseases, National Institute of Allergy and Infectious Disease, National Institutes of Health, Bethesda, MD, USA

#### Background

Ovarian cancer is the number one cause of death due to gynecological malignancies and the fifth leading cause of death in cancer in women. 75% of patients will have recurrent disease. Recurrent disease is chemotherapy refractive that progresses to chemotherapy resistant disease. Currently there are no definitive second-line treatments for patients. Patients with ovarian cancer have a 5-year survival rate of 25-30%, making it one of the most lethal malignancies.

#### Methods

One of the limitations of *in vitro* studies is the use of immortalized cell lines grown in two-dimensional flasks. To address this issue, many laboratories have been growing spheroids. We have employed 3-dimensional culturing techniques to create complex spheroids from ovarian cancer cell lines that have phenotypic structure similar to metastatic ovarian cancer. To further characterize spheroids we have created a system for sorting spheroids based on size. The spheroids can then be cultured in 2-dimensions for the study of chemotherapy sensitivities, and the efficacy of monocyte and interferon therapies for the treatment of ovarian cancer. Further, we have developed a single-photon confocal microscopy protocol for the multi-parameter imaging of live spheroids and monocytes with and without interferons. To create experimental robustness, we have employed a technique to image multiple conditions (4) over long periods of time (14-16 hours), allowing for the simultaneous imaging of both control and experimental conditions. Post-acquisition analysis of the images can be used to study migration of the individual cells within the spheroids, loss of cell dye viability, and migration of monocytes into the spheroids.

#### Results

We have found that the size of the spheroid defines, in part its sensitivity to standard chemotherapy agents. Post-acquisition analysis of the images have been used to study migration

of the individual cells within the spheroids, loss of cell dye viability, and migration of monocytes into the spheroids. The addition of interferons with or without monocytes significantly reduces the movement of the individual cells within the spheroids. Furthermore, we have found that the addition of interferons slows monocyte migration and initiates monocyte attachment and entry into the spheroids.

#### Conclusions

The combination of novel cell culturing techniques with modern imaging and post-acquisition data analysis will increase our understanding of ovarian cancer response to both standard chemotherapy and novel cell based therapies.

#### Acknowledgements

This work was supported by the Intramural Research Program of the National Institutes of Health (NIH), National Institute of Allergy and Infectious Diseases (NIAID), and National Cancer Institute (NCI).

16

### A novel xenograft model of chimeric antigen receptor-mediated toxicity sheds light on the influence of T cell source on the severity of the toxic sequelae

Joanne Hammill, Christopher Helsen, Craig Aarts, *Jonathan Bramson*

McMaster University, Hamilton, ON, Canada

#### Background

Chimeric antigen receptor (CAR)-engineered T lymphocytes are demonstrating striking clinical success, yet these treatments can be accompanied by severe on- and off-tumor toxicities. The availability of murine models to study these toxic phenomenon are currently lacking.

#### Methods

In our model, human T lymphocytes are engineered with a second-generation CD28-based CAR, targeted with a designed ankyrin repeat protein (DARPin) with picomolar affinity against HER2 (anti-HER2 DARPin CAR-T cells), and adoptively transferred into NRG mice at doses ranging from  $6 \times 10^5$  –  $1.2 \times 10^7$  CAR-T cells/mouse.

#### Results

Toxicity manifested in a drop in core body temperature and weight and, in some cases, lethality. The onset and severity of the toxicity varied with the source of the T lymphocytes (i.e., donor) used to generate CAR-T cells. We evaluated seven different donors and the toxicities associated with each donor's cell product was reproducible across multiple experiments and multiple manufacturing runs. Anti-HER2 DARPin CAR-T cells were toxic in tumor-free mice, but toxicities were most severe in the presence of HER-2+ tumors demonstrating both on-tumor and off-tumor effects. The

## Adoptive Cellular Therapy

Presenting author underlined; *Primary author in italics*

CAR-T cells did not respond to murine HER-2 indicating that the toxicity was both off-tumor and off-target. The toxicity was not due to the DARPin itself, as CAR-T cells bearing DARPins with other specificities were not toxic in this model. Further characterization of the model indicated that severity of toxicity was dose-dependent and could be exacerbated by the presence of a HER2<sup>+</sup> tumor. Moribund mice were found to have aggregates of T cells in their lungs, liver, and heart and displayed a cytokine storm in the blood. The toxicity was triggered by CD4<sup>+</sup> T cells in the anti-HER2 DARPin CAR-T cell product. While anti-HER2 DARPin CAR-T cells generated from donors demonstrating reduced toxicity were able to mediate anti-tumor efficacy *in vivo* in a xenograft model of ovarian carcinoma at low doses, they exhibited a narrow therapeutic window consistent with data emerging from the clinic where CAR-T therapy is effective.

### Conclusions

This model offers a promising avenue to test strategies for the prevention or mitigation of toxicities associated with adoptive CAR-T cell transfer as well as insights into the contribution of T cell source to toxicities. Investigations are ongoing.

### Acknowledgements

This work was supported by the Samuel Family Foundation, the Terry Fox Foundation, the Canadian Breast Cancer Foundation, and Triumvira Immunologics.

17

### **Ex vivo generation of highly purified and activated natural killer cells from human peripheral blood in accordance with GMP/GCTP for clinical studies**

Yui Harada, Yoshikazu Yonemitsu

Kyushu University, Fukuoka, Fukuoka, Japan

### Background

Natural killer (NK) cells play a crucial role during the innate immune responses, and as such form part of the body of immunological defense against various diseases, including infectious diseases and malignancies. Therefore, adoptive immunotherapy using NK cell is emerging as promising treatments for intractable malignancies; however, there has been still developing because of difficulties in culture, shortage of overall effector numbers, contamination of considerable numbers of T cells, and their limited anticancer potencies. We here established the simple feeder-free method to generate purified (>90%) and highly activated NK cells from human peripheral blood-derived mononuclear cells (PBMCs) in accordance with GMP/GCTP for clinical studies.

### Methods

Under approval of the institutional ethical committee, PBMCs were collected from healthy volunteers by using CliniMACS

Prodigy<sup>®</sup> (automatic/closed system). CD3<sup>+</sup> cells were depleted by CliniMACS CD3 beads, and CD3-depleted PBMCs were cultured at a concentration of 5 x 10<sup>5</sup> cells/ml with high concentration of hIL-2 and 5% human AB serum for 14 days. Fresh medium was added every 4-5 days throughout the culture period. Then, we confirmed the expression of surface markers, CD107a mobilization and cell-mediated cytotoxicity against various tumor cells and normal cells with or without monoclonal antibody drugs *in vitro* and antitumor effects against K562 *in vivo*.

### Results

Among the several parameters, we found that simply 1) only CD3-depletion, 2) high dose IL-2, and 3) use of specific culture medium were sufficient to obtain the highly purified, expanded (~200-fold) and activated CD3<sup>+</sup>/CD56<sup>+</sup> NK cells from PBMCs. Almost all activated NK cells expressed lymphocyte-activated marker CD69, and showed dramatically high expression of NK activation receptors (i.e. NKG2D, NKp30, NKp46, etc.), interferon- $\gamma$ , perforin and granzyme B. Importantly, only 2 hours reaction at effector/target ratio=1:1 was sufficient to kill almost all K562 cells, and antitumor activity was also representative on tumor bearing mice *in vivo*. Cytolysis was specific for various tumor cells, but not for normal cells, irrespective of MHC class I expression.

### Conclusions

These findings strongly support that NK cells activated by our method is purified, expanded, and near fully activated. The cells were currently under investigation in clinical trial (phase I/IIa).

18

### **T cell antigen couplers (TAC) demonstrate strong effectivity against solid tumors with no measurable toxicities, demonstrating an enhanced therapeutic index**

Christopher Helsen<sup>1</sup>, Joanne Hammill<sup>1</sup>, Kenneth Mwawasi<sup>1</sup>, Galina Denisova<sup>1</sup>, Jonathan Bramson<sup>1</sup>, Rajanish Giri<sup>2</sup>

<sup>1</sup>McMaster University, Hamilton, ON, Canada

<sup>2</sup>Indian Institute of Technology Mandi, India

### Background

Engineering T cells with chimeric antigen receptors (CARs) is proving to be an effective method for directing T cells to attack tumors in an MHC-independent manner [1, 2]. Current generation CARs aim to recapitulate T cell signaling by incorporating modular functional components of the TCR and co-stimulatory molecules. We sought to develop an alternate method to re-direct the T cell receptor which employs the native TCR. To this end, we developed the T cell Antigen Coupler (TAC) technology, a membrane-anchored receptor redirects the TCR and co-receptor in the presence of tumor antigen.

## Adoptive Cellular Therapy

Presenting author underlined; *Primary author in italics*

### Methods

The utility of the TAC receptor has been assessed using *in vitro* and *in vivo* assays. *In vitro* assays are based on receptor surface staining, cytokine release and cytotoxicity assays. *In vivo* studies examined the anti-tumor effect of TAC-engineered T cells against established xenografts.

### Results

*In vitro* testing has demonstrated robust and specific cytokine production and cytotoxicity by TAC-engineered human T cells directed against either HER-2 or CD19. *In vivo* TAC-engineered T cells revealed strong activity against HER-2 expressing solid xenograft tumor models such as MDA-MB-231 and OVCAR-3. Curiously, the TAC-engineered T cells outperformed a matched CD28-based second generation CAR in these models, demonstrating both increased anti-tumor efficacy and reduced toxicity. Whereas, mice treated with CAR engineered T cells showed serious toxicities that were both donor- and dose-dependent, we did not observe any toxicities arising from the TAC-engineered T cell, even at doses that produced complete tumor regression.

### Conclusions

These differences in toxicities and efficacy highlight the biological differences of TAC and CAR receptors and indicated the potential for a superior therapeutic index for TAC engineered T cells. Current TAC's in development target lymphatic malignancies and have shown great promise in early *in vitro* and *in vivo* assays.

### Acknowledgements

Samuel Family Foundation, the Terry Fox Foundation, the Canadian Breast Cancer Foundation and Triumvira Immunologics.

### References

1. Barrett DM, Singh N, Porter DL, Grupp S, June CH: **Chimeric antigen receptor therapy for cancer**. *Annu Rev Med* 2014, **65**:333–347.
2. Gill S, June CH: **Going viral: chimeric antigen receptor T-cell therapy for hematological malignancies**. *Immunol Rev* 2015, **263** :68–89.
3. Zhao Z, *et al*: **Structural Design of Engineered Costimulation Determines Tumor Rejection Kinetics and Persistence of CAR T Cells**. *Cancer Cell* 2015, **28**:415–428.
4. Sadelain M, Brentjens R, Rivière I: **The basic principles of chimeric antigen receptor design**. *Cancer Discov* 2013, **3**:388–398.

## 19

### T cell receptor gene engineered T cells targeting human papillomavirus (HPV)-16 E7 induce regression of HPV-16+ human tumors in a murine model

Benjamin Jin<sup>1</sup>, Tracy Campbell<sup>1</sup>, Lindsey M Draper<sup>2</sup>, Sanja Stevanovic<sup>1</sup>, Zhiya Yu<sup>3</sup>, Bianca Weissbrich<sup>4</sup>, Nicholas P Restifo<sup>3</sup>, Cornelia L Trimble<sup>5</sup>, Steven Rosenberg<sup>3</sup>, Christian S Hinrichs<sup>3</sup>

<sup>1</sup>Experimental Transplantation and Immunology Branch, National Cancer Institute, Bethesda, MD, USA

<sup>2</sup>National Cancer Institute, Bethesda, MD, USA

<sup>3</sup>Surgery Branch, National Cancer Institute, Bethesda, MD, USA

<sup>4</sup>Kite Pharma EU, Amsterdam, Noord-Holland, Netherlands

<sup>5</sup>Johns Hopkins University, Baltimore, MD, USA

### Background

The human papillomavirus (HPV)-16 E7 oncoprotein is constitutively expressed by HPV-16-associated cancers and absent from healthy tissues, and it is therefore an attractive therapeutic target for T cell receptor (TCR) gene engineered T cell therapy. However, E7 displays manifold mechanisms of immune evasion, and its potential as a target for TCR-T cell therapy is unknown.

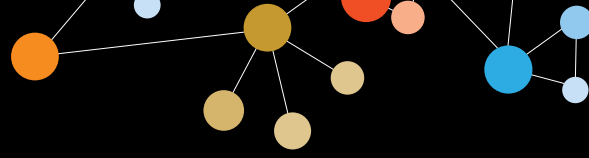
### Methods

The nucleotide sequence of a TCR targeting HPV-16 E7<sub>11-19</sub> was determined by study of cervix-infiltrating T cells from a subject with HPV-16+ cervical intraepithelial neoplasia. Expression of the TCR was optimized by hydrophobic substitutions in the alpha chain transmembrane region and introduction of an additional inter-chain TCR constant region disulfide bond. Second-party T cells genetically engineered to express the optimized TCR (E7 TCR T cells) were evaluated in *in vitro* immunologic assays and in an *in vivo* murine model of human cervical cancer.

### Results

E7 TCR T cells displayed binding to HLA-A\*02:01-E7<sub>11-19</sub> tetramers. HLA-A\*02:01 restriction was confirmed with major histocompatibility complex (MHC) blocking and with testing for recognition of target cells either expressing or lacking HLA-A\*02:01. In functional assays, E7 TCR T cells recognized and killed a panel of HLA-A\*02:01+ HPV-16+ cervical and oropharyngeal cancer cells lines but not cell lines that lacked either the restriction element or target antigen. Tumor recognition by CD8 and CD4 T cells that expressed the E7 TCR was observed. They displayed minimal if any cross-reactivity against peptides from human proteins that were identified by BLAST search based on protein sequence similarity or the presence of key shared residues mapped by alanine scanning of E7<sub>11-19</sub>. E7 TCR T cells recognized E7<sub>11-19</sub> peptide-pulsed T2





## Adoptive Cellular Therapy

Presenting author underlined; Primary author in italics

cells at concentrations as low as  $10^{-11}$  M indicating relatively high functional avidity. Direct comparison to a previously described E6-specific TCR revealed greater functional avidity, a slower TCR-pMHC Koff-rate, and superior tumor cell recognition for the E7 TCR. In a murine xenograft model, a single intravenous injection of E7 TCR T cells induced complete regression of tumors from one human cervical cancer line and controlled tumors from another human cervical cancer line.

### Conclusions

E7 TCR T cells specifically recognized and killed HPV-16+ cancer cells *in vitro* and mediated regression of HPV-16+ tumors *in vivo*. These findings provide the preclinical basis for a new personalized TCR-T cell therapy for metastatic HPV-16+ cancers including many cervical, oropharyngeal, and anal malignancies. A clinical trial for E7 TCR T cells is now active (NCI-16-C-0138).

### 20

#### **haNK, a cytotoxic human high affinity natural killer cell line, exerts enhanced ADCC mediated by avelumab (an anti-PD-L1 antibody) against multiple human tumor cell lines**

*Kwong Tsang*<sup>1</sup>, Massimo Fantini<sup>1</sup>, James W Hodge<sup>2</sup>, Rika Fujii<sup>2</sup>, Ingrid Fernando<sup>1</sup>, Caroline Jochems<sup>1</sup>, Christopher Heery<sup>1</sup>, James Gulley<sup>1</sup>, Patrick Soon-Shiong<sup>3</sup>, Jeffrey Schlom<sup>4</sup>

<sup>1</sup>Laboratory of Tumor Immunology and Biology, National Cancer Institute, National Institutes of Health, Bethesda, MD, USA

<sup>2</sup>National Cancer Institute, National Institutes of Health, Bethesda, MD, USA

<sup>3</sup>NantKwest, Inc., Culver City, CA, USA

<sup>4</sup>Center for Cancer Research, National Cancer Institute, National Institutes of Health, Bethesda, MD, USA

### Background

Immune checkpoints have been implicated in the down-regulation of antitumor immunity. Anti-PD-1/PD-L1 checkpoint inhibitory monoclonal antibodies (mAbs) can restore immune function in the tumor microenvironment, and have demonstrated clinical benefit in patients with melanoma, Hodgkin's lymphoma, lung and bladder carcinomas, and other tumor types. In addition to its checkpoint inhibitory function, avelumab, a fully human IgG1 anti-PD-L1 mAb, can mediate antibody-dependent cellular cytotoxicity (ADCC) to lyse human tumor cells in the presence of natural killer (NK) cells [1]. NK cells can be used for cancer therapy. However, obtaining sufficient numbers of functionally active NK cells from patients is technically challenging since only about 10% of the population expresses on NK cells the high-affinity FcR that provides maximum ADCC. One alternative is to use

established NK cell lines that have antitumor activity. High affinity NK cells (haNK), provided by NantKwest, derived from the human NK cell line NK-92, are genetically engineered to express high-affinity human CD16 (FcγRIIIA-V158) and transduced with the human IL-2 gene. In addition, haNK cells have little inhibitory killer-cell immunoglobulin-like receptor (KIR) expression, a unique feature that may be a factor in their highly cytotoxic activity against a broad range of malignancies. We report here our investigation of 1) whether haNK cells used in combination with avelumab can lyse human tumor cells via the ADCC mechanism, and 2) the factors that may influence this cytotoxic activity.

### Methods

Cell lines used in our experiments included human carcinomas of the head and neck, cervix, bladder, and colon, as well as prostate and pancreatic cancers. haNK cells irradiated with 10 Gy were used as effector cells at various effector-to-target-cell ratios in all experiments. Four- and 18-hour <sup>111</sup>In release assays were performed to evaluate ADCC activity.

### Results

Our results show that 1) haNK cells can lyse a range of human carcinoma cells when avelumab is used to target PD-L1 expression; 2) the addition of anti-CD16 neutralizing antibody significantly inhibits ADCC lysis, implicating CD16 ligation as a major mechanism of action for ADCC lysis mediated by haNK and avelumab; and 3) in combination with avelumab, haNK cells mediate significantly higher levels of ADCC lysis than do NK cells isolated from healthy donor peripheral blood mononuclear cells (PBMC).

### Conclusions

These results provide a rationale for using haNK cells in combination with avelumab or other ADCC-mediating cytotoxic mAbs to treat human malignancies.

### 21

#### **Adoptive transfer of ex vivo-expanded PD-1+ CD8+ and CD4+ T cells eliminates myeloma in mice**

*Weiqing Jing*, Jill Gershan, Grace Blitzer, James Weber, Laura McOlash, Bryon D Johnson

Medical College of Wisconsin, Milwaukee, WI, USA

### Background

Adoptive T cell therapy (ACT) has emerged as a potential curative therapy for patients with advanced solid tumors. However, for hematologic cancers, identifying and enriching the cancer antigen-reactive T lymphocytes for ACT remains a challenge. Our lab previously demonstrated that blockade of the PD-1/PD-L1 pathway (in the context of non-myeloablative, lymphodepleting whole body irradiation) was capable of eliminating established myeloma in mice [1, 2].

## Adoptive Cellular Therapy

Presenting author underlined; Primary author in italics

In the current study, we tested whether PD-1 is a marker for myeloma-reactive T cells.

### Methods

C57BL/KaLwRij (KaLwRij) mice were inoculated with 5T33 myeloma cells intravenously, and 28 days later, splenic PD-1+ and PD-1- T cells (CD8+ and CD4+) were isolated by flow cytometric sorting. The purified T cells were expanded in culture for 7 days on plate-bound CD3 and soluble CD28 antibodies plus IL-2, IL-7 and IL-15. Some of the expanded T cells were assayed *in vitro* for myeloma reactivity. Equal mixtures of expanded CD4+ and CD8+ T cells, or each subset alone, were infused to myeloma-bearing Rag1-deficient recipients, and the mice were followed for myeloma progression.

### Results

We found that numbers of cancer antigen-reactive T lymphocytes in myeloma-bearing mice were enriched in PD-1+ CD8+ and CD4+ T cell subsets. PD-1+ T cells could be efficiently expanded *ex vivo* for adoptive transfer, and the expanded cells maintained their anti-myeloma reactivity. Adoptive transfer of the *ex vivo*-expanded PD-1+ T cells effectively eliminated established myeloma in Rag1-deficient recipients. In contrast, adoptive transfer of expanded PD-1- T cells failed to demonstrate anti-myeloma efficacy *in vivo*. Notably, both CD8+ and CD4+ PD-1+ T cell subsets played a role in eradicating myeloma, but combined administration of the *ex vivo*-expanded subsets was most efficacious.

### Conclusions

Our results show that PD-1 is a biomarker for myeloma-specific CD8+ and CD4+ T cells in mice. Furthermore, these PD-1-expressing T cells can be expanded in culture for effective adoptive cell immunotherapy of myeloma-bearing recipients.

### Acknowledgements

Support from the Midwest Athletes Against Childhood Cancer (MACC) Fund, Children's Research Institute, and a former grant from the Multiple Myeloma Research Foundation.

### References

- Jing W, Gershan JA, Weber J, Tlomak D, McOlash L, Sabatos-Peyton C, Johnson BD: **Combined immune checkpoint protein blockade and low dose whole body irradiation as immunotherapy for myeloma.** *J Immunother Cancer* 2015, **3**:2.
- Kearl TJ, Jing W, Gershan JA, Johnson BD: **Programmed death receptor-1/programmed death receptor ligand-1 blockade after transient lymphodepletion to treat myeloma.** *J Immunol* 2013, **190**:5620-5628.

## 22

### Entinostat sensitized osteosarcoma cells for cytotoxic effect of natural killer cells

Simin Kiany, Huang Gangxiong, Eugenie S Kleinerman

University of Texas MD Anderson Cancer Center, Houston, TX, USA

### Background

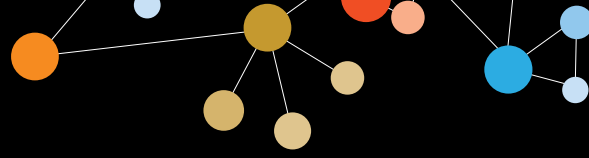
The goal of this study is to find an alternate therapy for osteosarcoma (OS) lung metastasis. We previously showed that NK cell therapy significantly decreased, but did not cure, OS lung metastasis in a mouse model. Other studies have shown that histone deacetylase inhibitors (HDACi) sensitize tumor cells to NK cell cytotoxicity, primarily by increasing expression of ligands for NK cells on tumor cells; thus, to augment NK cell therapy, we combined it with the HDACi, entinostat.

### Methods

Flow cytometry, western blot analysis, and Q-PCR were used to determine whether entinostat increased expression of NK cell ligands on OS cells. Effects of entinostat on NK cell viability, receptor expression, and cytotoxicity were explored using a viability test, flow cytometry, and calcein release assay, respectively. NK cells were isolated from blood buffy coats and were expanded *ex vivo* using genetically engineered K562 cells and human IL-2. Q-PCR was used to measure microRNAs expression in OS cells and a CHIP assay was used to determine increased histone acetylation at the MICA/B gene promoters. For the *in vivo* study, mice were given 10, 5, or 2.5 mg/kg of entinostat orally to determine the subtherapeutic dose of the drug.

### Results

We demonstrated that 2  $\mu$ M entinostat for 48 h upregulated expression of NK cell ligands on OS cell lines. Increased expression of ligands on OS cells resulted in increased susceptibility of OS cell lines to NK cell cytotoxicity *in vitro*. NK cell treatment with up to 2  $\mu$ M entinostat did not affect NK cell viability or NK cell receptor (NKG2D, NKp30, NKp44, NKp46, and DNAM-1) expression. NK cells pretreated with entinostat for 24 h did not decrease cytotoxicity of NK cells to OS cell lines. We also showed two mechanisms by which entinostat controls MICA/B expression on OS cells: 1) by increasing H4 acetylation at the MICA/B genes promoters and 2) by down-regulating mir-20a, mir-93, and mir-106b expression. We demonstrated that the sub-therapeutic dose of entinostat that significantly increased MICA/B on OS lung metastasis was 5 mg/kg three times a week for 5 weeks. Combining 5mg/kg entinostat and NK cell therapy is our ongoing *in vivo* experiment.



# Adoptive Cellular Therapy

Presenting author underlined; Primary author in italics

## Conclusions

We demonstrated that entinostat immunosensitized OS cells to NK cell lysis by inducing upregulation of ligands for NK cells on OS cells. Our results suggest that NK cell therapy combined with entinostat provides an innovative approach to enhance the immunotherapeutic effect of NK cells against OS pulmonary metastases.

## 23 Abstract Travel Award Recipient

### Chimeric antigen receptor macrophages (CARMA) for adoptive cellular immunotherapy of solid tumors

Michael Klichinsky, Marco Ruella, Olga Shestova, Saad Kenderian, Miriam Kim, John Scholler, Carl H June, Saar Gill

Center for Cellular Immunotherapies, University of Pennsylvania, Philadelphia, PA, USA

## Background

Anti-CD19 chimeric antigen receptor (CAR) redirected T cells have demonstrated profound efficacy in relapsed/refractory B cell malignancies. However, CAR T cells have thus far failed to recapitulate these results in solid tumors. Accumulating evidence suggests that macrophages naturally traffic to and persist in solid tumors. The goal of this study was to evaluate the anti-tumor function of genetically engineered CAR macrophages (CARMA) and assess their potential for translation as a novel immunotherapeutic platform for solid tumors.

## Methods

To examine the function of CARs in macrophages, first generation CARs with a CD3 $\zeta$  intracellular domain were introduced into the THP-1 macrophage model. *In vitro* function was assessed via quantitative phagocytosis and luciferase-based specific killing assays. To assess the function of the CD3 $\zeta$ -domain, CD3 $\zeta$ -null CAR constructs were compared. Ad5f35 was used to transduce primary human monocyte derived macrophages with an anti-HER2 CAR construct, and anti-tumor function was tested *in vitro* and *in vivo*. The impact of inhibiting the CD47/SIRP $\alpha$  “do-not-eat-me” signal was tested with blocking antibodies and CRISPR-Cas9 mediated SIRP $\alpha$  knockout. Macrophage M1/M2 phenotype was determined by flow cytometry. Immunodeficient mouse xenograft models of a human HER2(+) ovarian cancer cell-line (SKOV3) were used for *in vivo* efficacy studies.

## Results

CAR19, but not untransduced macrophages, phagocytosed CD19+ (but not CD19-) K562 cells. Deletion of CD3 $\zeta$  in CAR19 macrophages abrogated phagocytosis and significantly reduced specific killing. Phagocytosis was inhibited by pharmacologic blockade of phagocytic signaling - suggesting that CAR activation drives productive cell-signaling in

macrophages. Phagocytosis was also demonstrated in HER2 and mesothelin CARMA models. Blockade of the inhibitory CD47/SIRP $\alpha$  “do-not-eat-me” signal enhanced CARMA phagocytosis of antigen-bearing target cells in a dose-dependent manner (Figure 1). We identified Ad5f35 as an efficient transduction approach for engineering primary human macrophages, resulting in >70% CAR transduction efficiency. Primary human anti-HER2 CARMA demonstrated targeted phagocytosis and specific killing. Ad5f35 transduction polarized human macrophages to the pro-inflammatory M1 phenotype, and rendered them resistant to downstream M2 subversion by immunosuppressive cytokines and cell lines. Anti-HER2 CARMA was evaluated *in vivo* in an ovarian cancer xenograft model. Mice that received CARMA had a decrease in tumor burden of approximately two orders of magnitude and had a 30-day survival benefit relative to untreated or control macrophage treated mice ( $p=0.018$ , Figure 2).

## Conclusions

Here, we introduce for the first time that human macrophages engineered with a CAR exert antigen-specific tumor phagocytosis and killing, and propose a novel immunotherapeutic platform for the treatment of diverse solid tumors.

### CAR driven phagocytosis and synergy with CD47/SIRP $\alpha$ blockade

Figure 1

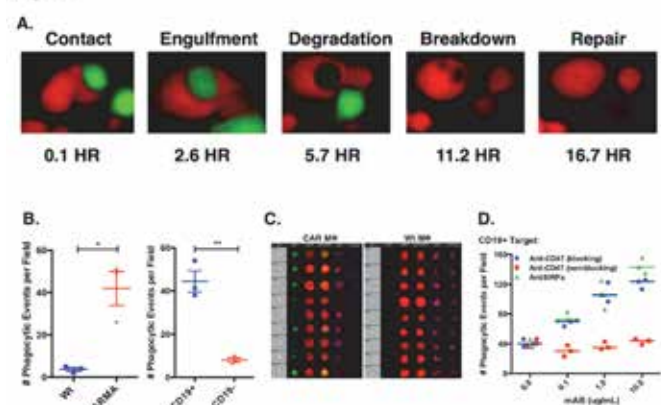


Figure 1. Timelapse of a CAR19 macrophage (mRFP+) phagocytosing a CD19+ K562 cells (GFP+) cell (A). CARMA but not Wt macrophages phagocytosed CD19+ but not CD19- tumor cells (B). Phagocytosis was confirmed by Imagestream cytometry, gating on mRFP+GFP+ events (C). Blockade of CD47 and SIRP $\alpha$  led to a dose dependent increase in CARMA phagocytosis. Non-blocking anti-CD47 clone 2D3 (opsonization control) did not enhance phagocytosis (D).

## Adoptive Cellular Therapy

Presenting author underlined; Primary author in italics

### CARMA prolonged survival in an ovarian cancer xenograft model

Figure 2

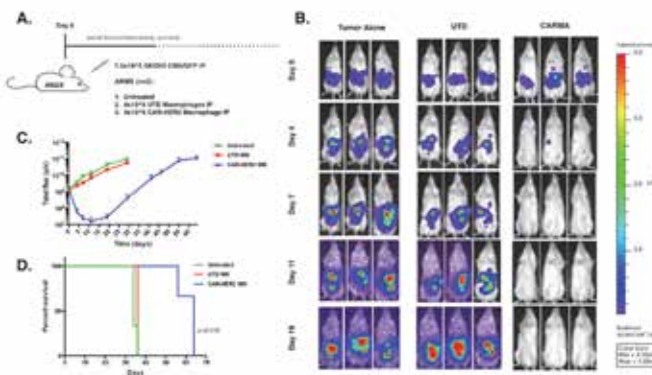


Figure 2. Anti-HER2 primary human CARMA were tested in immunodeficient mouse models of human HER2+ ovarian cancer (schema, A). CARMA but not control untransduced macrophages reduced tumor burden (B, C) and prolonged survival by 30 days ( $p=0.018$ , D).

24

### Regulation of T cell sensitivity by TCR-proximal signaling components during anti-melanoma responses

Duane Moogk<sup>1</sup>, Shi Zhong<sup>2</sup>, Zhiya Yu<sup>3</sup>, Ivan Liadi<sup>4</sup>, William Rittase<sup>5</sup>, Victoria Fang<sup>6</sup>, Janna Dougherty<sup>1</sup>, Arianne Perez-Garcia<sup>7</sup>, Iman Osman<sup>8</sup>, Cheng Zhu<sup>5</sup>, Navin Varadarajan<sup>4</sup>, Nicholas P Restifo<sup>3</sup>, Alan Frey<sup>9</sup>, Michelle Krogsaard<sup>10</sup>

<sup>1</sup>Perlmutter Cancer Center, NYU School of Medicine, New York, NY, USA

<sup>2</sup>Xiangxue Pharmaceutical Co., Ltd., Guangdong, Guizhou, People's Republic of China

<sup>3</sup>Surgery Branch, National Cancer Institute, Bethesda, MD, USA

<sup>4</sup>University of Houston, Houston, TX, USA

<sup>5</sup>The George W. Woodruff School of Mechanical Engineering, Georgia Institute of Technology, Atlanta, GA, USA

<sup>6</sup>Skirball Institute of Biomolecular Medicine, NYU School of Medicine, New York, NY, USA

<sup>7</sup>Kite Pharma, Inc., Santa Monica, CA, USA

<sup>8</sup>Ronald O. Perelman Department of Dermatology and Department of Medicine and Urology, Perlmutter Cancer Center at NYU School of Medicine, New York, NY, USA

<sup>9</sup>New York University Langone School of Medicine, New York, NY, USA

<sup>10</sup>Department of Pathology and Perlmutter Cancer Center at NYU School of Medicine, New York, NY, USA

### Background

Immunotherapies for cancers have made great strides in recent years, yet new and improved approaches are required to achieve more durable responses in a greater number of patients. The *in vitro* expansion phase of adoptive T cell therapy prior to reinfusion into the patient present opportunities to genetically enhance T cell subsets to improve *in vivo* performance. While the most common genetic modification is the incorporation of engineered antigen-specific TCRs or chimeric antigen receptors, modification to signaling pathways in T cell memory subsets in order to enhance T cell sensitivity is an underexplored strategy. This is mainly because contributions of TCR signaling components that confer differences in activation sensitivity and functional outcomes between CD8+ T<sub>cm</sub> and T<sub>em</sub> are unclear.

### Methods

To understand how TCR-proximal signaling differs significantly between T cell memory subsets, we derived T<sub>CM</sub> and T<sub>EM</sub> from the humanized TCR-transgenic melanoma mouse model (JR209). We quantified differences in TCR activation and feedback regulation by novel live-cell imaging technologies, phospho-specific protein assays and used modeling of early TCR signaling to reveal the physiological significance of these differences.

### Results

One of the critical steps of T cell triggering is the coordinated phosphorylation and binding of CD3 and Zap-70 by Lck following TCR ligation by pMHC. Here, we show that T<sub>cm</sub> and T<sub>em</sub> possess differential constitutive Lck activities. Immediately proximal to Lck signaling, we observed enhanced Zap-70 phosphorylation in TEM following TCR ligation compared with TCM. Further, we observed increased intracellular calcium influx and cytotoxic effector function in TEM compared with TCM, and provide evidence that this results from a lower probability of TCM reaching threshold activation signaling due to the decreased magnitude of TCR-proximal signaling. We show that the differences in Lck constitutive activity between CD8+ T<sub>cm</sub> and T<sub>em</sub> are driven in part by differential regulation by SH2 domain-containing phosphatase-1 (Shp-1) and C-terminal Src kinase (Csk). We demonstrate that inhibition of Shp-1 results in increased constitutive Lck and cytotoxic activity in T<sub>CM</sub> to levels similar to that of T<sub>EM</sub>.

### Conclusions

Together, this work demonstrates that differential activities of TCR-proximal signaling components may contribute to establishing the divergent effector properties of T<sub>CM</sub> and T<sub>EM</sub>. Inhibition of negative regulatory molecules, for example Shp-1 or Csk, or generalized augmentation of T cell sensitivity with miRNA offer potential therapeutic approaches in T cell immunotherapy but must be considered in the context of specificity and optimal targeting.





## Adoptive Cellular Therapy

Presenting author underlined; Primary author in italics

### 25 Abstract Travel Award Recipient

#### Co-expression of synthetic PD-1 fusion proteins augments HER2 CAR T cell functionality against glioblastoma

Daniel Landi, Kristen Fousek, Malini Mukherjee, Ankita Shree, Sujith Joseph, Kevin Bielamowicz, Tiara Byrd, Nabil Ahmed, Meenakshi Hegde

Baylor College of Medicine, Houston, TX, USA

#### Background

HER2-CAR T cells home to the central nervous system (CNS) and induce tumor regression in patients with glioblastoma (GBM) [1]. However, most responses are transient, as CAR T cells fail to expand and have limited persistence. *Ex vivo* analyses of tumor infiltrating lymphocytes demonstrate high levels of inhibitory receptors, including PD-1. Monoclonal antibodies blocking PD-1/PD-L1 induce responses in some patients with solid tumors and potentiate anti-tumor T cell activity. However, because antibodies exhibit erratic CNS pharmacokinetics, combining this approach with CAR T cells is not optimal for CNS tumors. We hypothesize that co-expression of a synthetic PD-1 fusion protein will convert PD-L1 into a costimulatory T cell signal, improving expansion, persistence, and anti-tumor activity of adoptively transferred HER2-CAR T cells.

#### Methods

We generated an array of bicistronic vectors encoding our clinically utilized 2<sup>nd</sup> generation HER2-CAR (CD28 $\zeta$ -endodomain) and a PD-1 fusion protein. All PD-1 fusion proteins contained the native PD-1 ectodomain fused to either the CD28 transmembrane and endodomain (PD-1/CD28) or CD8 $\alpha$ -transmembrane and 4-1BB-endodomain (PD-1/4-1BB). T cell expansion, persistence, and exhaustion (LAG3, TIM3, PD-1) were measured using flow cytometry following coculture with autologous HER2+/PD-L1+ GBM cells for 2-4 weeks. Cytokine release at 24 hours was measured using standard ELISA, and the xCELLigence impedance-based system was used to evaluate cytolytic activity. Using high-resolution immunofluorescence imaging, we interrogated differences at the CAR T cell/GBM contact point, also referred to as the immunologic synapse (IS).

#### Results

Compared to conventional HER2-CAR T cells, PD-1/CD28 T cells expanded more quickly with significantly higher IL2/IFN $\gamma$ -release at 24 hours (Figure 1), whereas PD-1/4-1BB T cells demonstrated enhanced cytolytic ability against autologous GBM cells in prolonged killing assays (Figure 2) and better long-term persistence. Inhibitory receptor expression following coculture was comparable among T cell products, but PD-1/4-1BB T cells maintained a greater

percentage of central memory cells (CCR7+/CD45RA-). HER2-CAR T cells bearing PD-1 fusion proteins demonstrated increased levels of activated kinases in CD28/4-1BB signaling pathways. Three-dimensional reconstitution and quantification of confocal images of the CAR T cell/tumor interface revealed increased stability of the IS between the HER2-CAR and the HER2 molecule on GBM.

#### Conclusions

We conclude that PD-L1 can be converted into a costimulatory signal using synthetic PD-1 fusion molecules to drive key T cell activation pathways and enhance stability of the CAR-target antigen interface, leading to improved HER2-CAR T cell functionality against GBM.

#### References

1. Ahmed N: **Autologous HER2 CMV bispecific CAR T cells for progressive glioblastoma: Results from a phase I clinical trial.** *J Clin Oncol* 2015, **33**:3008.

#### T cell cytokine release after 24 hr coculture with autologous GBM

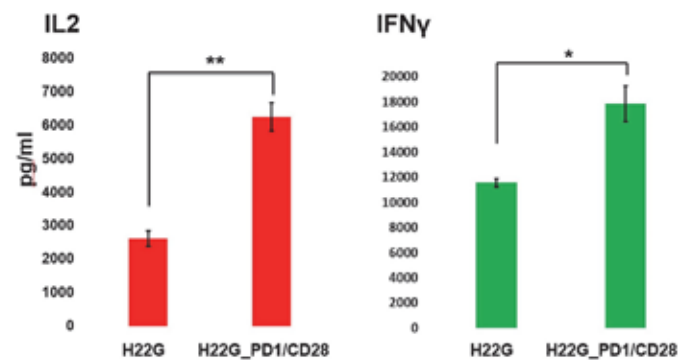
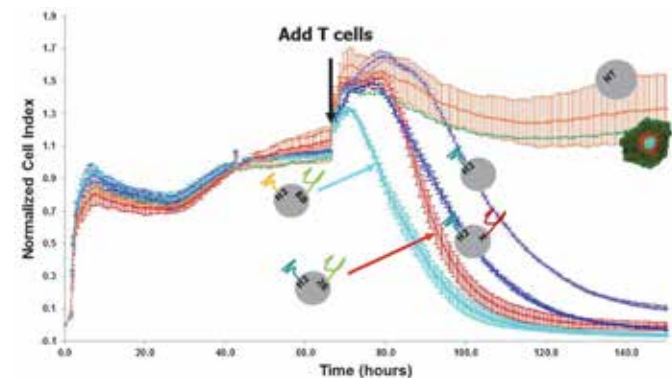


Figure 1. 2<sup>nd</sup> generation HER2 CAR T cells with and without PD-1/CD28 fusion proteins were incubated with autologous GBM cells at a 1:1 ratio. Cytokine concentrations from culture supernatant collected at 24 hours were measured using standard ELISA.

#### GBM killing by PD-1 fusion CAR T cells



## Adoptive Cellular Therapy

Presenting author underlined; *Primary author in italics*

Figure 2. The xCELLigence platform uses impedance across resistor-coated plates to measure adherant tumor cell viability. Once 10,000 tumor cells became adherant and confluent, 1,000 T cells were added that expressed either a HER2 CAR only (H2) or a HER2 CAR with a truncated PD-1 protein (X), PD-1/CD28 protein (28), or PD-1/4-1BB protein (BB). Non-transduced T cells and tumor only wells served as controls.

### 26

#### Adoptive therapy with tumor-infiltrating lymphocytes for melanoma: interim results of a phase II single-institution study

Sylvia Lee<sup>1</sup>, David Byrd<sup>2</sup>, John Thompson<sup>3</sup>, Shailender Bhatia<sup>4</sup>, Scott Tykodi<sup>4</sup>, Judy Delismon<sup>5</sup>, Liz Chu<sup>5</sup>, Siddiq Abdul-Alim<sup>5</sup>, Arpy Ohanian<sup>5</sup>, Anna Marie DeVito<sup>6</sup>, Stanley Riddell<sup>5</sup>, Kim Margolin<sup>7</sup>

<sup>1</sup>Seattle Cancer Care Alliance, Fred Hutchinson Cancer Research Center, University of Washington, Seattle, WA, USA

<sup>2</sup>University of Washington, Seattle, WA, USA

<sup>3</sup>Clinical Research Division at Fred Hutch Cancer Center, University of Washington, Seattle, WA, USA

<sup>4</sup>Fred Hutchinson Cancer Research Center, University of Washington, Seattle, WA, USA

<sup>5</sup>Fred Hutchinson Cancer Research Center, Seattle, WA, USA

<sup>6</sup>Seattle Cancer Care Alliance, Seattle, WA, USA

<sup>7</sup>Department of Medical Oncology, City Of Hope, Duarte, CA, USA

#### Background

Adoptive cell therapy using tumor-infiltrating lymphocytes (TIL) has been established as an effective treatment option for metastatic melanoma but is available at only a small number of institutions. We have developed a TIL program at the Fred Hutchinson Cancer Research Center and present our initial results in melanoma patients.

#### Methods

Patients with metastatic melanoma were enrolled in a two-step fashion to a nonrandomized, phase II TIL trial: Step 1 for TIL generation and Step 2 for TIL treatment. TIL are cultured from tumor fragments, using standard methodologies developed at the NCI. At a time of future disease progression, patients are given cyclophosphamide 60mg/kg/day x 2 days, fludarabine 25mg/m<sup>2</sup>/day x 5 days, then TIL up to 1.5 x 10<sup>11</sup>, followed by high-dose IL-2, 600,000 units/kg every 8 hours, up to 14 doses as tolerated. TIL populations are selected for infusion based on growth, phenotype, and MHC-class-I-dependent autologous tumor recognition, as assessed by interferon-gamma release.

#### Results

Thirty-two patients have been enrolled on Step 1 for TIL generation. Of these, 23(72%) achieved adequate TIL number of >40 x10<sup>6</sup> by 5 weeks of culture. TIL in 17(53%) patients also demonstrated positive autologous tumor reactivity. To date, 7 patients have received TIL therapy on Step 2; all had progressed on prior immunotherapy (Table 1). In these 7 patients, the RECIST 1.1 responses are: 2 CR, 1 PR, 3 SD, 1PD. All patients experienced tumor regression of some or all baseline target lesions; the patient with PD progressed in the brain, but experienced a partial response of extracranial sites. Two patients were on concurrent BRAF therapy and had reached a plateau in their response to BRAF inhibitors prior to start of TIL treatment, and both experienced further tumor reduction after TIL. Responses were associated with a higher percent CD8+TIL, a lower percent Treg(CD4+CD25+CD127-), and TCR oligoclonality, while functional markers PD-1 and TIM3 did not associate with response.

#### Conclusions

Our single-institution study validates the utility of TIL therapy in patients with advanced melanoma, refractory to other immunotherapy. TIL can induce durable CRs and can also mediate additional tumor regression in patients on active BRAF inhibition. The replication of TIL methodology across different institutions, with reproducible clinical efficacy, supports the feasibility of its widespread application, as well as further investigation into optimizing elements of this treatment modality.

#### Acknowledgements

We wish to thank the NCI Surgery Branch and MD Anderson for their generous guidance with the development of our TIL therapy program, and Prometheus for their generous IL-2 support.

**Table 1. Characteristics and responses of treated patients**

	Age/ Gender	Prior Treatments	M Classification and Metastatic Sites	Response	Response Duration (months)
1	54 F	Anti-CTLA-4, interferon (IFN)	M1c: Mesentery, small bowel, lymph nodes (LN)	PR	8
2	34 F	Anti-PD1, anti-CTLA-4, IFN, IL-2 + radiation (XRT), temozolomide	M1c: Brain, kidneys, adrenals, bone, liver, LN, subcutaneous (SC)	SD	3
3	61 M	IL-2, BRAF inhibitor	M1c: Brain, liver, lungs, mediastinum, SC, mesentery, chest wall	PD (Progression in brain, but PR in extracranial sites)	8, for extracranial response
4	27 F	IL-2, anti-CTLA-4+IL-21, anti-CTLA-4 + XRT, recombinant IL-15	M1c: Brain, SC, LN, pleura, kidneys, peritoneum	SD	3
5	63 M	Anti-CTLA-4	M1a: Intramuscular, LN	CR	17, ongoing
6	52 M	Anti-CTLA-4	M1a: SC, LN	CR	20, ongoing
7	31 F	Anti-PD1, anti-CTLA-4, dacarbazine, BRAF/MEK inhibitor	M1c: Brain, lungs, liver, SC	SD	5



## Adoptive Cellular Therapy

Presenting author underlined; *Primary author in italics*

27

### **IL-15 primes an mTOR-regulated gene-expression program to prolong anti-tumor capacity of human natural killer cells**

Andreas Lundqvist<sup>1</sup>, Vincent van Hoef<sup>1</sup>, Xiaonan Zhang<sup>1</sup>, Erik Wennerberg<sup>2</sup>, Julie Lorent<sup>1</sup>, Kristina Witt<sup>1</sup>, Laia Masvidal Sanz<sup>1</sup>, Shuo Liang<sup>1</sup>, Shannon Murray<sup>3</sup>, Ola Larsson<sup>1</sup>, Rolf Kiessling<sup>1</sup>, Yumeng Mao<sup>1</sup>

<sup>1</sup>Karolinska Institutet, Stockholm, Stockholms Lan, Sweden

<sup>2</sup>Weill Cornell Medical College, New York, NY, USA

<sup>3</sup>Nova Southeastern University, Cell Therapy Institute, Fort Lauderdale, FL, USA

#### **Background**

NK cell-based immunotherapy is a potential therapeutic modality in patients with advanced cancers as transfer of haploidentical NK cells induces beneficial responses in patients with hematological malignancies; and leukemia clearance correlates with persistence and *in vivo* expansion of NK cells after infusion. Thus, sustained NK cell activity *in vivo* likely represents a therapy performance-limiting factor.

#### **Methods**

We performed genome-wide analysis of cytosolic and polysome-associated mRNA from interleukin (IL)-2 and IL-15 activated NK cells. Furthermore, the ability of IL-2 and IL-15 to sustain human NK cell activity following cytokine withdrawal as well as their effect on NK cells to resist tumor-induced immunosuppression was compared.

#### **Results**

After cytokine withdrawal, IL-15-treated NK cells maintained a higher level of cytotoxicity ( $p < 0.05$ ) and showed lower levels of apoptosis ( $p < 0.05$ ) compared with cells treated with IL-2. IL-15 augmented mTOR signaling, which correlated with increased expression of genes related to cell metabolism and respiration. Consistently, mTOR inhibition abrogated IL-15-induced cell function advantages. Moreover, mTOR-independent STAT-5 signaling contributed to improved NK cell function during cytokine activation but not following cytokine withdrawal. Upon co-culture with tumor cells or exposure to tumor cell supernatant, IL-15 activated NK cell maintained a significantly higher level of proliferation and cytotoxic activity ( $p < 0.05$ ). Mechanistically, tumor-derived prostaglandin-E2 suppressed IL-2 cultured NK cells while IL-15 cultured NK cells remained activated. The superior performance of IL-15 stimulated NK cells was also observed using a clinically applicable protocol for NK cell expansion *in vitro* and *in vivo*.

#### **Conclusions**

This study adds to our understanding about establishment and maintenance of tumor-reactive NK cells and supports clinical implementation of IL-15 for adoptive NK cell

therapy. More broadly, our studies suggest that a large aspect of cytokine-mediated gene expression programs and downstream cellular functions, including anti-tumor capacity, are overlooked if post-activation conditions are omitted. This is likely not limited to NK cells and should hence be considered in similar studies of other immune cells.

28

### **Functional characterization of CD4+ and CD8+ CD19 chimeric antigen receptor T cells**

Isabelle Magalhaes, Jonas Mattsson, Michael Uhlin

Karolinska Institutet, Stockholm, Stockholms Lan, Sweden

#### **Background**

Chimeric antigen receptor (CAR) T cells targeting CD19 have shown dramatic results in patients with refractory B cell malignancies but the precise mechanisms of how CD19 CAR T cells kill tumor cells are not all well understood.

#### **Methods**

Second generation CD19 CAR T cells were produced from peripheral blood mononuclear cells (PBMCs) obtained from pediatric patients with acute lymphoblastic leukemia (ALL) and adult patients with chronic lymphocytic leukemia (CLL). Here we present the phenotype, cytokine and cytotoxic profile of CD4+ and CD8+ CD19 CAR T cells generated from patients and healthy donors (HDs).

#### **Results**

T cell frequency in PBMCs from patients (ALL and CLL) was low (<4% of lymphocytes). In patients with CLL, 90% of lymphocytes were CD19+ B cells. In patients with CLL, as compared to HDs, the majority of CD8+ T cells displayed a terminally differentiated phenotype, while CD4+ T cells were mostly effector memory cells. Retroviral transduction was performed on PBMCs without prior B cell depletion or T cell enrichment step. CAR T cell cytotoxicity towards CD19+ target cells was mediated via granzymes, but not perforin, Fas-L or TRAIL. In patients and HDs, CD4+ and CD8+ CD19 CAR T cells showed a comparable cytokine (IL-2, IFN-g, TNF) production, CD107a expression in response to stimulation with K562 CD19+ cells. The majority of CAR T cells were polyfunctional ( $\geq 2$  functions). However, patients with CLL, as compared to HDs and patients with ALL, displayed a higher frequency of IFN-g producing and polyfunctional CD4+ and CD8+ CD19 CAR T cells. When stimulated with autologous CD19+ B cells, as compared to K562 CD19+, lower frequencies of CD4+ and CD8+ CD19 CAR T cells produced IL-2, IFN-g and TNF. The frequency of polyfunctional CD19 CAR T cells was lower when stimulated with autologous B cells as compared to K562 CD19+ cells. Stimulation with other CD19+ cell lines induced a different cytokine production profile of CD19 CAR T cells.

## Adoptive Cellular Therapy

Presenting author underlined; Primary author in italics

### Conclusions

CD4+ and CD8+ CD19 CAR T cells display comparable differentiation phenotype, cytokine production and cytotoxic capacity. The presence of a high frequency of CD19+ B cells during the generation of CAR T cells did not have an impact on CAR T cell phenotype. However CAR T cells from patients with CLL produced more cytokines when stimulated with CD19+ target cells suggesting that activation of CD19 CAR T cells by B cells during cell expansion impacts the cytokine profile. Furthermore, our data show that the level of CD19 cell surface expression modulates CAR T cells cytokine production.

### 29 Abstract Travel Award Recipient

#### Directing traffic: fostering chemokine receptor expression on tumor-infiltrating lymphocytes improves re-trafficking in vivo

Satoshi Nemoto<sup>1</sup>, Patricio Pérez Villarroya<sup>1</sup>, Ryosuke Nakagawa<sup>1</sup>, James J Mule<sup>2</sup>, Adam W. Mailloux<sup>1</sup>

<sup>1</sup>Translational Science, H. Lee Moffitt Cancer Center, Tampa, FL, USA

<sup>2</sup>Immunology Program, Cutaneous Oncology Program, H. Lee Moffitt Cancer Center, Tampa, FL, USA

### Background

Previously, a critical role for chemokines was found in a unique immune-related gene expression signature (GES) for immune cell recruitment and tertiary lymphoid structure formation in metastatic melanoma [1]. Regarding adoptive cell therapy (ACT) of tumor-infiltrating lymphocytes (TIL), we hypothesized that expression of chemokine receptors (CCR)2, CCR5, and CCR7, which bind multiple GES chemokines, favor TIL re-trafficking to the tumor, thereby bolstering ACT efficacy.

### Methods

We utilized a preclinical ACT model in which TIL from syngeneic MC-38 colon carcinomas grown in wild-type (WT) C57BL/6 mice, or gene knock-out (KO) C57BL/6 mice lacking CCR2, CCR5, or CCR7, were expanded *ex vivo*, and adoptively transferred into MC-38-bearing C57BL/6 recipient mice bearing congenic CD45.1. After seven days, tumor burden was assessed, and Spanning-tree Progression Analysis of Density-normalized Events (SPADE) of 18-parameter cytometry data was used to identify and quantify TIL subsets, and <sup>51</sup>Cr-release assays quantified cytotoxicity among sorted TIL populations.

### Results

ACT of WT TIL reduced tumor burden by 50% compared to untreated mice (p=0.0098). This benefit was lost when transferring CCR5KO or CCR7KO TIL, and reduced when transferring CCR2KO TIL (all p < 0.05). MC-38 tumors contained 90%, 85%, and 70% less transferred TIL with ACT of CCR2KO, CCR5KO, or CCR7KO TIL, respectively, compared to WT TIL (all p < 0.01). SPADE identified eight novel subsets in

re-trafficked TIL with unique patterns of activation, memory, and immune checkpoint markers (Table 1). Nearly all subsets displayed impaired re-trafficking with CCR2KO, CCR5KO, or CCR7KO TIL ACT (all p < 0.05). Cytotoxicity assays suggest a range of cytotoxic potential among identified subsets, with CD8<sup>+</sup>TIL3 and 4 subsets being most cytotoxic (all p < 0.05). During TIL expansion, IL-2 up-regulated CCR2, CCR5, and CCR7 in a cell density-dependent fashion (all p < 0.007). ACT of TIL with up-regulated CCRs increased tumor re-trafficking three-fold (p < 0.05), and decreased tumor burden by an additional 25% (p < 0.05) versus WT TIL without up-regulated CCRs.

### Conclusions

CCR2, CCR5, and CCR7 are vital for TIL re-trafficking to MC-38 tumors following ACT, including cytotoxic subsets among eight novel TIL phenotypes. Fostering CCR expression during TIL expansion augments ACT efficacy in murine MC-38 colon carcinoma. Translational studies to human TIL ACT are currently underway.

### Acknowledgements

Supported by NCI-NIH (CA148995-01; P30CA076292; P50CA168536), V Foundation, Dr. Miriam and Sheldon G. Adelson Medical Research Foundation, and the Chris Sullivan Foundation.

### References

1. Messina JL, Fenstermacher DA, *et al*: **12-Chemokine gene signature identifies lymph node-like structures in melanoma: potential for patient selection for immunotherapy?** *Scientific Reports* 2012, **2**:765-770.

**Table 1**

Table 1: Marker Expression on Novel TIL Subsets*													
Subset	CD4	CD8	CD127	CD4	CD27	CD45RA	CD69	CD62L	KLRG1	TIM-3	PD-1	LAG-3	CTLA4
CD8TIL	+++	-	**	+++	*	*	*	-	*	-	**	+++	-
CD8TIL1	*	**	-	-	*	-	*	-	-	-	-	+++	-
CD8TIL2	*	**	-	-	-	-	*	**	*	-	**	**	-
CD8TIL3	+++	+++	*	-	**	-	*	-	*	-	**	+++	-
CD8TIL4	**	+++	*	-	**	-	*	-	*	-	**	+++	-
CD8TIL5	+++	**	**	-	*	-	*	**	**	**	**	+++	-
CD8TIL6	-	**	+++	-	-	*	**	**	+++	+++	+++	**	+++
CD8TIL7	+++	**	*	-	-	-	*	*	*	*	*	**	-

\* Marker expression defined as: - 0-25 percentile expression, + 25-50 percentile expression, ++ 50-75 percentile expression, +++ 75-100 percentile expression.



## Adoptive Cellular Therapy

Presenting author underlined; Primary author in italics

### 30 Abstract Travel Award Recipient

#### Provision of inducible MyD88 and CD40 co-stimulation in CAR T cells results in potent antitumor activity in preclinical solid tumor models

Melinda Mata<sup>1</sup>, Phuong Nguyen<sup>1</sup>, Claudia Gerken<sup>1</sup>, Christopher DeRenzo<sup>1</sup>, David M Spencer<sup>2</sup>, Stephen Gottschalk<sup>1</sup>

<sup>1</sup>Baylor College of Medicine, Center for Cell and Gene Therapy, Houston, TX, USA

<sup>2</sup>Bellicum Pharmaceuticals and Baylor College of Medicine, Houston, TX, USA

#### Background

Although adoptive immunotherapy using T cells expressing chimeric antigen receptors (CAR) is successful in refractory hematological malignancies, limited clinical responses have been observed in solid tumors. We reasoned that introducing an inducible co-stimulation (iCO-STIM) gene into T cells would allow for improved activation of CAR T cells, resulting in enhanced antitumor activity. Due to the co-stimulatory properties of MyD88 and CD40 in T cells, we explored whether CAR T cells expressing an iCO-STIM molecule consisting of a myristoylation-targeting sequence, two FKBP dimerizing domains, MyD88 $\Delta$ TIR, and the intracellular domain of CD40, have superior effector function relative to standard CAR T cells *in vitro* and *in vivo*.

#### Methods

T cells expressing a HER2-CAR and iCO-STIM (HER2-CAR/iCO-STIM T cells) were generated by transduction with a retroviral vector encoding FRP5. $\zeta$  (HER2-CAR), a 2A peptide, and iCO-STIM. HER2-CAR/iCO-STIM T cell effector function was then evaluated *in vitro* and in murine xenograft models.

#### Results

In the presence of CID (AP20187), HER2-CAR/iCO-STIM T cells produced significantly higher levels of IL2 ( $p < 0.05$ ) compared to HER2-CAR/iCO-STIM T cells in the absence of CID or HER2-CAR.CD28. $\zeta$  T cells in co-culture assays with HER2+ tumor cells (MDA-HER2, LM7, A549). In contrast, HER2-negative tumor cells (MDA) did not induce IL2 production by HER2-CAR/iCO-STIM T cells +/- CID or HER2-CAR.CD28. $\zeta$  T cells. In repeat stimulation assays, HER2-CAR/iCO-STIM T cells showed robust antigen-dependent expansion in the presence of CID and were able to lyse HER2-positive LM7 cells after 4 re-stimulations compared to HER2-CAR.CD28. $\zeta$  T cells ( $p < 0.0001$ ). *In vivo*, a low dose of HER2-CAR/iCO-STIM T cells ( $3 \times 10^5$ ) + CID had superior antitumor activity in the metastatic LM7 osteosarcoma murine xenograft model compared to HER2-CAR/iCO-STIM T cells without CID or HER2-CAR.CD28. $\zeta$  T cells, resulting in a significant survival advantage ( $p < 0.001$ ). In 3 mice that

developed late recurrences after HER2-CAR/iCO-STIM T cell + CID therapy, a second dose of CID, given 100 days post T cell injection, eliminated 2/3 tumors. Superior antitumor activity of HER2-CAR/iCO-STIM T cell + CID therapy was confirmed in the HER2+ A549 lung cancer murine xenograft model.

#### Conclusions

CID-mediated activation of MyD88 and CD40 co-stimulatory signals in HER2-CAR T cells results in superior effector function compared to standard HER2-CAR T cells. Thus, expressing iCO-STIM molecules in CAR T cells has the potential to improve the efficacy of CAR T cell therapy approaches for solid tumors. In addition, our results indicate that the CID/iCO-STIM system will enable the 'remote control' of infused T cells.

### 31

#### In vivo administration of immune checkpoint inhibitors prior to tumor harvest enhances the function of tumor-infiltrating T lymphocytes expanded for adoptive T cell transfer

Mélissa Mathieu, Sandy Pelletier, John Stagg, Simon Turcotte  
CRCHUM, Montréal, PQ, Canada

#### Background

T cell reactivity against mutated antigens, derived from cancer genomic alterations, is a key mediator of immunotherapy efficacy. Adoptive cell transfer (ACT) of mutation-reactive tumor-infiltrating T lymphocytes (TILs) however has been only effective in a minority of patients with metastatic gastrointestinal cancers. We hypothesize that the low frequency of mutation-reactive TILs and their exhaustion features may contribute to the lack of efficacy of TIL ACT, and that these factors can be overcome by *in vivo* administration of blocking antibodies against CTLA-4 or PD-1 prior to tumor harvest and TIL expansion.

#### Methods

We selected the mouse MC-38 colorectal cancer model to study CD8+ TIL reactive to 2 mutated, 2 self, and 1 retroviral antigens using co-cultures with peptide-pulsed splenocytes followed by IFN- $\gamma$  intracellular staining. MC-38 cancer cells were inoculated subcutaneously and allowed to grow until 20mm<sup>2</sup>. Then anti-CTLA-4 (9H10) and/or anti-PD-1 (RPM1-14) antibodies were administered twice (4 days interval). Three days following the last antibody injection, tumors were harvested and analyzed for immune cell infiltration, phenotype and functionality. TILs were also expanded *in vitro* and characterized regarding the specificity and the functionality against the known antigens.

#### Results

The administration of anti-CTLA-4 prior to tumor harvest increased immune cell infiltration, decreased the proportion

## Adoptive Cellular Therapy

Presenting author underlined; *Primary author in italics*

of myeloid derived suppressor cells and regulatory T cells in the tumors and enhanced CD8+ T cell IFN- $\gamma$  and TNF- $\alpha$  production. Administration of both anti-CTLA-4 and anti-PD-1 was more effective to eliminate the tumor burden and recapitulated the effects observed following anti-CTLA-4 injection alone. Anti-CTLA-4 and/or anti-PD-1 alone did not appear to change the relative frequency of TIL reactive to mutated, self, or viral antigens but increased their polyfunctionality.

### Conclusions

*In vivo* pre-conditioning of MC-38-bearing mice with immune checkpoint blocking antibodies may generate TILs more fit for ACT immunotherapy. Experiments are underway to compare the efficacy of this approach to conventional TIL ACT in this mouse model.

### 32 Abstract Travel Award Recipient

#### Redirecting gene-engineered T cells through covalent attachment of targeting ligands to a universal immune receptor

Nicholas Minutolo<sup>1</sup>, Prannada Sharma<sup>1</sup>, Andrew Tsourkas<sup>2</sup>, Daniel J Powell<sup>1</sup>

<sup>1</sup>Department of Pathology and Laboratory Medicine, Perelman School of Medicine, University of Pennsylvania, Philadelphia, PA, USA

<sup>2</sup>Department of Bioengineering, University of Pennsylvania, Philadelphia, PA, USA

### Background

Infusion of T cells genetically engineered to express a chimeric antigen receptor (CAR) is a promising approach for the treatment of certain cancers. Though CAR T cells are highly efficacious against CD19+ hematological malignancies, limitations exist in broadening their use. Conventional CAR T cells target a single tumor associated antigen (TAA), limiting their effectiveness against tumors with heterogeneous TAA expression as well as emerging antigen loss variants, as observed in CD19 CAR trials. Additionally, stably engineered CAR T cells may continually proliferate and activate in the presence of antigen, potentially causing fatal toxicity, without a method of elimination. To overcome these issues, we and others have developed a variety of universal immune receptors (UIRs) that allow for targeting of multiple TAAs with a single receptor-expressing T cell. Although these UIRs are a promising new technology, their reliance on noncovalent interactions between receptor and targeting ligand can lead to potential issues of affinity, specificity and activity.

### Methods

Our UIR platform employs the use of the SpyCatcher and SpyTag proteins that, when combined, can form a covalent bond with high efficiency both *in vitro* and *in vivo*. Our

SpyCatcher immune receptor is composed of an extracellular SpyCatcher domain attached to intracellular T cell signaling motifs in a lentiviral expression vector. Anti-TAA antibodies conjugated to SpyTag are used to confer redirected specificity to SpyCatcher expressing T cells. Measurements of T cell effector function include T cell cytokine secretion, activation, and targeted tumor cell lysis *in vitro*.

### Results

In this study, we demonstrate the first universal immune receptor platform that allows for the endowment of function through post-translational covalent attachment of targeting ligands, securing their loading on the T cell surface while expanding recognition specificity. We demonstrate that the SpyCatcher immune receptor is expressed in primary human T cells and allows for specific T cell activation and cytokine secretion against plate bound SpyTag. Notably, in the presence of SpyTag-labeled targeting antibody, SpyCatcher T cells recognize and lyse antigen-expressing human tumor cells in a target-specific and dose-dependent fashion.

### Conclusions

The SpyCatcher immune receptor is the first universal immune receptor designed for its capacity to covalently bind targeting ligands and redirect T cells against a diverse array of antigens, addressing current limitations of conventional CAR T cell therapy.

### 33

#### Simple automated manufacturing of gene engineered T cells under serum free conditions for adoptive T cell therapy

Nadine Mockel-Tenbrinck, Daniela Mauer, Katharina Drechsel, Carola Barth, Katharina Freese, Ulrike Kolrep, Silke Schult, Mario Assenmacher, Andrew Kaiser

Miltenyi Biotec, Bergisch Gladbach, Nordrhein-Westfalen, Germany

### Background

Adoptive immunotherapy using gene-modified T cells redirected against cancer has proven clinical efficacy and tremendous potential in several medical fields. However, such personalized medicine faces several challenges in the complexity associated with the current clinical manufacturing methods. The processes are mostly suboptimal requiring cell manufacturers to deal with open steps, liquid handlings between devices used, manual interventions, removal of activation beads and often the use of reagents for which commercial availability is not in line with the high and increasing demand. GMP compliant human AB serum is one of such reagents. Therefore, developing improved methods to generate gene-engineered T cells suitable for clinical use



## Adoptive Cellular Therapy

Presenting author underlined; *Primary author in italics*

that do not require serum are essential for the commercial scalability of such therapies.

### Methods

We have developed a robust and reproducible automated manufacturing process for the lentiviral gene-modification and expansion of selected T cells. The CliniMACS Prodigy TCT (for T Cell Transduction) process software allows automated purification and polyclonal T cell stimulation followed by gene-modification and expansion of T cells in a single-use closed tubing set.

### Results

Here we show that the TCT process enables the manufacturing of gene-modified T cells without the need for serum supplementation (human AB serum) when using TexMACS GMP Medium. Furthermore, implementation of a humanized recombinant activation reagent TransAct allows for a simplification of the process whereby the “bead removal” step is unnecessary. Comparable results from healthy donor or patients starting cells are demonstrated.

### Conclusions

Taken together the TCT process in combination with the CliniMACS Prodigy and minimal user interactions enables the preparation of gene-modified T cells in serum free conditions. Process risks, due to use of different devices, unnecessary manipulations, or potential shortage of human AB serum availability can be minimized by automation of the entire process as developed and shown here. Overall, these improvements are meant to fully support commercial treatment of a large number of patients.

### 34 ★ Abstract Travel Award Recipient

#### Tumor Infiltrating lymphocytes from soft tissue sarcoma have tumor-specific function

John Mullinax, MacLean Hall, Julie Le, Krithika Kodumudi, Erica Royster, Allison Richards, Ricardo Gonzalez, Amod Sarnaik, Shari Pilon-Thomas

H. Lee Moffitt Cancer Center, Tampa, FL, USA

#### Background

Adoptive Cell Transfer (ACT) using Tumor Infiltrating Lymphocytes (TIL) for unresectable metastatic melanoma results in a median overall survival of 52 months at our institution. This stands in contrast to the median overall survival for metastatic soft tissue sarcoma (mSTS) which is 12 months. The purpose of this report is to describe the phenotype and function of TIL from fresh surgical sarcoma specimens as a rationale for applying ACT to mSTS.

#### Methods

Fresh surgical sarcoma specimens were acquired under an IRB-approved protocol. Half of the specimen was digested

and phenotyped by flow cytometry. The remaining half was plated as fragments for the isolation of TIL, which were expanded *in vitro* with conditions validated for melanoma-derived TIL. Cultured TIL were phenotyped by flow cytometry and propagated further with a rapid expansion protocol (REP). Tumor-specific reactivity was assessed by co-culture of TIL with autologous tumor or HLA-matched cell lines with measurement of IFN-gamma using ELISA.

#### Results

Sixteen patient-derived sarcoma specimens were collected. Histology of primary tumor included dedifferentiated liposarcoma (9), well-differentiated liposarcoma (2), undifferentiated pleomorphic sarcoma (2), and one each of gastrointestinal stromal tumor, myxofibrosarcoma and synovial sarcoma. Analysis of tumor digests indicated an average of 48% of cells from the lymphocyte gate were CD3+ (range 3.6%-76%). TIL were grown from all specimens, with TIL observed in 152 out of 192 (79%) fragments. The phenotype of the CD3+ subpopulations from TIL cultures included a median of 90.8% (range 2-99.9%) CD8+ and 2.3% (range 0-96.4%) CD4+ T cells. TIL were expanded in a REP to clinically meaningful numbers (mean 1385-fold) with no change in the CD8+ T cell proportion. Tumor-specific function of TIL generated from fragments was measured in two patients. There was tumor-specific IFN-gamma release (mean  $148.8 \pm 13.5$  pg/ml) in TIL co-cultured with HLA-matched cell lines and also in TIL co-cultured with autologous tumor digest (mean  $259.9 \pm 14.7$  pg/ml). The degree of IFN-gamma release was significantly greater when TIL were co-cultured with autologous digest compared to an HLA-mismatched cell line ( $p=0.0295$ ).

#### Conclusions

CD3+CD8+ TIL can be isolated from human sarcoma tumors *in vitro*, expanded to meaningful numbers for therapeutic use, and demonstrate reactivity to the tumor from which they were cultured. These data form the basis for efforts to develop a clinical trial using ACT for patients with advanced sarcoma.

#### Acknowledgements

Work funded by a grant from the Chotiner Family

## Adoptive Cellular Therapy

Presenting author underlined; Primary author in italics

Foundation.

35

### Preclinical development of tumor infiltrating lymphocyte (TIL) based adoptive cell transfer (ACT) immunotherapy for patients with sarcoma

Morten Nielsen<sup>1</sup>, Anders Krarup-Hansen<sup>2</sup>, Dorrit Hovgaard<sup>3</sup>, Michael Mørk Petersen<sup>3</sup>, Anand Chainsukh Loya<sup>4</sup>, Niels Junker<sup>5</sup>, Inge Marie Svane<sup>5</sup>

<sup>1</sup>Center for Cancer Immune Therapy and Department of Oncology, Herlev Hospital, Herlev, Hovedstaden, Denmark

<sup>2</sup>Department of Oncology, Herlev University Hospital, Herlev, Hovedstaden, Denmark

<sup>3</sup>Department of Orthopaedic Surgery, Copenhagen University Hospital, Copenhagen, Hovedstaden, Denmark

<sup>4</sup>Department of Pathology, Copenhagen University Hospital, Copenhagen, Hovedstaden, Denmark

<sup>5</sup>Department of Oncology, Center for Cancer Immune Therapy, Herlev University Hospital, Herlev, Hovedstaden, Denmark

#### Background

ACT based on infusion of autologous TILs has the ability to induce complete and durable response in some patients with advanced malignant melanoma [1]. We believe that this approach could also be effective in sarcoma. In this preclinical study we are investigating feasibility of expanding TILs from sarcoma, as well as performing functional *in vitro* analyses on these TILs. This abstract is an update on our results so far.

#### Methods

A portion (> 1 cm<sup>3</sup>) of the excised sarcoma tumor tissue is cut into fragments and placed in a growth medium containing IL-2 for initial TIL expansion. Afterwards, TIL cultures undergo a rapid expansion protocol (REP) expansion by adding OKT-3 and feeder cells. Phenotype and functional analyses are performed using flow cytometry and Elispot.

#### Results

To this date we were able to expand TILs from 18 of 20 tumor samples. TILs were harvested and frozen when an estimated number of 100x10<sup>6</sup> to 200x10<sup>6</sup> cells were reached. Mean expansion time was 32 days (16 - 61). 87.7% (36.4 – 99.1) of these cells were CD3+, and of these 66.7% (16.3 – 99.1) were CD4+, and 21.8 % (0.1 – 50.6) were CD8+. Most of the expanded TILs were effector memory subtype, while a smaller fraction was the more differentiated effector T cells. REP expansion rates ranged from 630 fold to 2.300 fold, and followed expansion pattern similar to TILs from malignant melanoma. TILs from 6 of 10 tested tumor samples with 4 different sarcoma subtypes (undifferentiated pleomorphic sarcoma, myxofibrosarcoma, myxoid liposarcoma and

osteosarcoma) demonstrated reactivity against autologous tumor cells using Elispot. Further assessment is ongoing.

#### Conclusions

We were able to expand TILs from 90% of the included tumor samples to numbers needed for possible future clinical implementation. TILs were a mix of CD4+ and CD8+ with CD4+ being predominant. As of yet we have demonstrated TIL reactivity against autologous tumor cells from 6 of 10 tested patients. Thus, we conclude that it is feasible to translate TIL based ACT into clinical testing in sarcoma patients.

#### References

1. Rosenberg SA, Yang JC, Sherry RM, *et al*: **Durable complete responses in heavily pretreated patients with metastatic melanoma using T-cell transfer immunotherapy.** *Clin Cancer Res* 2011, **17(13)**:4550-4557.

36

### Human natural killer cells engineered to express a chimeric NK activating receptor have activity against highly suppressive cells of the solid tumor microenvironment

Charlotte Rivas<sup>1</sup>, Robin Parihar<sup>1</sup>, Stephen Gottschalk<sup>2</sup>, Cliona M Rooney<sup>1</sup>

<sup>1</sup>Baylor College of Medicine, Houston, TX, USA

<sup>2</sup>Center for Cell and Gene Therapy, Baylor College of Medicine, Houston, TX, USA

#### Background

The suppressive microenvironment of solid tumors inhibits the anti-tumor activity of endogenous and chimeric antigen receptor (CAR)-bearing T cells, thereby limiting the efficacy of adoptive T cell therapies. Myeloid-derived suppressor cells (MDSCs; CD33<sup>+</sup> CD11b<sup>+</sup> HLA-DR<sup>low</sup>) and regulatory T cells (Tregs; CD4<sup>+</sup> CD25<sup>high</sup> FoxP3<sup>+</sup> Helios<sup>+</sup>) contribute to the inhibitory tumor microenvironment (TME) through secretion of suppressive cytokines, expression of inhibitory ligands, and by promoting tumor neo-vascularization. NKG2D is an activating surface receptor expressed on natural killer (NK) cells, whose ligands are highly expressed by human Tregs and MDSCs. We genetically modified primary human NK cells to express a chimeric NKG2D molecule (ectodomain of endogenous NKG2D fused to the cytotoxic CD3-zeta chain; called NKG2D.z) in order to promote NK cell activation against Tregs and MDSCs. We hypothesized that NKG2D.z NK cells would exhibit enhanced cytolytic activity against suppressive autologous Tregs and MDSCs via the chimeric NKG2D, as well as secrete chemokines and cytokines that recruit and activate tumor-specific T cells. The objective of the current study was to compare the activity of NKG2D.z NK cells vs. non-transduced (NT)-NK cells on Tregs, MDSCs, or the combination.



## Adoptive Cellular Therapy

Presenting author underlined; Primary author in italics

### Methods

We isolated MDSCs and Tregs from normal donors and patients with solid tumors, confirmed their phenotype by flow cytometry and their suppressive activity in T and NK cell proliferation assays, and used them as targets in NK cell cytotoxicity and co-culture assays.

### Results

NT (endogenous) and mock-engineered (empty vector control) NK cells were unable to mediate cytotoxicity or release pro-inflammatory cytokines in response to autologous MDSCs or Tregs, either alone or in combination. In contrast, NKG2D.z NK cells exhibited enhanced cytolysis and secreted T cell-recruiting and -activating cytokines in response to both suppressive cell types alone. Further, when NKG2D.z NK cells were co-cultured in a highly suppressive environment containing both MDSCs and Tregs, their cytolytic and cytokine-secreting activities against either cell type were unimpaired. We have established an *in vivo* TME model comprising tumor cells with MDSCs and Tregs, and experiments testing the ability of NKG2D.z NK cells to eliminate suppressive cells and recruit endogenous or CAR-T cells *in vivo* are underway.

### Conclusions

Our results suggest that our modified NK cells may reverse immune suppression by the TME and improve T cell-based immune therapies for solid tumors.

### Acknowledgements

Authors thank Charles L. Sentman, PhD for initial use of the NKG2D.zeta sequence.

37

### Cytokines induced by pre-B leukemia progression mediates irreversible T cell dysfunction

Haiying Qin<sup>1</sup>, Sang Nguyen<sup>1</sup>, Paul Su<sup>1</sup>, Chad Burk<sup>1</sup>, Brynn Duncan<sup>1</sup>, Bong-Hyun Kim<sup>2</sup>, M. Eric Kohler<sup>1</sup>, Terry Fry<sup>1</sup>

<sup>1</sup>National Cancer Institute, NIH, Bethesda, MD, USA

<sup>2</sup>Frederick National Laboratory for Cancer Research Leidos Biomedical Research, Inc., Frederick, MD, USA

### Background

Acute lymphoblastic leukemia (ALL) is the most common childhood malignancy. The cure rate has reached up 90% with modern therapy, outcomes are still very poor for patients who relapse. Immunotherapy with donor lymphocyte infusions for ALL has not demonstrated the success seen in other hematologic malignancies, suggesting there are characteristics inherent to ALL that make it less amenable to detection and elimination by the immune system. T cell dysfunction in the setting of leukemia has been well described, but the mechanisms have not been

fully elucidated. It is also unclear if this T cell dysfunction underlies some of the treatment failures seen in patients receiving adoptive therapy with chimeric antigen receptor (CAR) expressing T cells. Immune checkpoint blockade has led to advances in the treatment of many solid tumors, but it has yet to demonstrate similar success in ALL.

### Methods

Using two preclinical models of pre-B cell ALL, we studied the negative impact of ALL progression on T cell function and the efficacy of CAR T cell therapy and immune checkpoint blockade. We also dissected the mechanism underlying the observed T cell dysfunction.

### Results

Prophylactic vaccination protects mice against the murine pre-B ALL in a T cell-dependent manner. However, therapeutic vaccination is ineffective, even in the setting of low disease burden. Adoptive transfer of primed T cells from immunized donors can completely eradicate established leukemia; however, this efficacy is not seen with the adoptive transfer of T cells from leukemia-bearing mice. Expression of a CD19 CAR in T cells from leukemic mice fails to eradicate ALL, while the CAR T cells derived from naïve mice can. T cells from leukemic mice express markers of T cell dysfunction. The expression of these molecules was associated with elevated levels of IL6, TNF $\alpha$  and IL10 in the serum of leukemia-bearing mice. Incubation of naïve T cells in these cytokines *ex vivo* recapitulated the upregulation of exhaustion markers seen *in vivo*, suggesting these cytokines play a role in the observed T cell dysfunction. Blockade of PD-1, its ligand, PD-L1, or Tim3 were ineffective at reversing T cell dysfunction and preventing leukemia progressions *in vivo*, suggesting other mechanisms must be targeted to restore immune function in leukemia bearing hosts.

### Conclusions

Cytokines induced by Pre-B Leukemia progression mediates irreversible T cell dysfunction. These findings underscore the need to elucidate the mechanisms of leukemia-induced immune suppression to fully optimize the use of CAR-expressing T cells in the treatment of ALL.

38

### Identification of a recurrent high-affinity MHC class I restricted neopeptide in neuroblastoma using ProTECT

Arijun A Rao<sup>1</sup>, Noam Teyssier<sup>1</sup>, Jacob Pfeil<sup>1</sup>, Nikolaos Sgourakis<sup>1</sup>, Sofie Salama<sup>1</sup>, David Haussler<sup>2</sup>

<sup>1</sup>University of California, Santa Cruz, Santa Cruz, CA, USA

<sup>2</sup>UC Santa Cruz Genomics Institute, University of California, Santa Cruz, Santa Cruz, CA, USA

## Adoptive Cellular Therapy

Presenting author underlined; Primary author in italics

### Background

T cells are trained to differentiate between cell-surface MHC-displayed peptide sequences from self- and non-self proteins and act on the latter. The numerous mutations often associated with cancers can occur in coding regions of the genome and modify the sequence of wild-type proteins, potentially creating targets for immunotherapies. We have developed an analysis pipeline ProTECT (Prediction of T cell Epitopes for Cancer Therapy) to identify and rank neo-epitopes in terms of immunogenicity. Running ProTECT on a set of recurrent neuroblastomas showed that recurrent tumors share neo-epitopes with their corresponding primary tumors suggesting that immunotherapies could provide long-term protection.

### Methods

ProTECT accepts paired tumor and normal DNA sequencing fastq files, and tumor RNA sequencing fastqs. Mutations are called using a panel of callers, and are annotated to identify coding mutations. Prediction of self-MHC:mutated-peptides is carried out and the final binding predictions are ranked using an in-house algorithm. We support both MHCI and MHCII predictions.

### Results

Running ProTECT on 6 recurrent neuroblastoma samples (NBL) from the TARGET (Therapeutically Applicable Research To Generate Effective Treatments) project revealed that the relapsed tumor inherits neo-epitopes predicted in the primary tumor. We also predicted neo-epitopes from 2 well-known hotspot mutations in NBL (NRAS Q61K and ALK R1275Q) that bind to common MHC alleles (HLA-A\*01:01, HLA-A\*03:01 and HLA-B\*15:01). We carried out *in vitro* refolding and crystallization assays [1] for the five highest-ranking mutant NRAS and ALK predictions. Properly conformed MHC trimers were verified by a single, monodisperse peak after anion exchange chromatography and validated by SDS gel electrophoresis. Mass spec confirmed bound peptide for 4/5 tested predictions and 3 of these were used to set up hanging-drop crystallization trials in various conditions. Positive hits were obtained for one (MAQDIYRASY::HLA-B\*15:01). ProTECT has also been run on a large subset of The Cancer Genome Atlas (TCGA). We aim to reveal clinically relevant hotspot-mutation:MHC pairs.

### Conclusions

We have described a pipeline for identification and ranking of therapeutically relevant neo-epitopes. We have predicted potentially therapeutic targets for NBL that have been validated *in vitro*.

### References

1. Garboczi DN, Hung DT, Wiley DC: **HLA-A2-peptide complexes: refolding and crystallization of molecules**

expressed in *Escherichia coli* and complexed with single antigenic peptides . *PNAS* 1992, **89**:8.

### 39

#### **A higher-affinity variant of a GD2-specific CAR significantly enhances potency in vivo and allows for a novel model of on-target off-tumor toxicity**

*Sarah A Richman*<sup>1</sup>, Selene Nunez-Cruz<sup>2</sup>, Zack Gershenson<sup>2</sup>, Zissimos Mourelatos<sup>3</sup>, David Barrett<sup>1</sup>, Stephan Grupp<sup>1</sup>, Michael Milone<sup>3</sup>

<sup>1</sup>Children's Hospital of Philadelphia Division of Oncology, Philadelphia, PA, USA

<sup>2</sup>University of Pennsylvania, Philadelphia, PA, USA

<sup>3</sup>Department of Pathology and Laboratory Medicine, Division of Neuropathology, University of Pennsylvania, Philadelphia, PA, USA

### Background

As many potential targets of chimeric antigen receptor (CAR) T cell immunotherapy are self-antigens that are over-expressed in tumors but also present at lower levels on some normal tissue, understanding the nature of on-target off-tumor toxicity and how to overcome it is important in the development of new CAR T cell therapies. Preclinical modeling of such toxicity is complicated by the fact that most antigens are not shared between humans and mice, and strategies have largely relied on co-injection of antigen-low tumors or introduction of human antigen into mouse tissue by viral gene delivery. The GD2 tumor antigen would provide an excellent model in which to study on-target off-tumor toxicity as the exact glycolipid antigen is naturally shared between mice and humans. However, as of yet, GD2-specific CAR T cells have yielded modest efficacy and little toxicity in preclinical studies. Here we have engineered a higher potency GD2 CAR by introducing an affinity-enhancing mutation (E101<sub>H</sub>K), previously described by Horwacik et al., that we show significantly enhances CAR T cell activity and provides a model for toxicity.

### Methods

Primary human T lymphocytes were transduced with lentivirus encoding either wild-type 14G2a-based anti-GD2 CAR, E101K mutant GD2 CAR, or a negative control CAR. After standard stimulation and expansion, T cells were analyzed for CAR surface expression by flow cytometry and for *in vitro* effector function by chromium release and IFN gamma ELISA. To evaluate *in vivo*, NOD-SCID-IL2R $\gamma$ c<sup>-/-</sup> (NSG) mice were injected with the luciferase-expressing GD2-high human neuroblastoma cell line SY5Y, and four days later 3,000,000 CAR+ T cells were injected via tail vein. Tumor burden was measured using *in vivo* bioluminescence, and tumor and



## Adoptive Cellular Therapy

Presenting author underlined; Primary author in italics

normal tissues were evaluated histologically by H&E staining and immunohistochemistry.

### Results

The higher affinity mutant displayed comparable surface expression and T cell expansion but significantly enhanced GD2-specific cytotoxicity and cytokine release *in vitro* and tumor control *in vivo*. However, this enhanced efficacy was associated with severe CNS toxicity causing neurologic symptoms and death, and post-mortem evaluation of tissues revealed extensive CAR T cell infiltration into certain brain structures, particularly cerebellum, known to contain GD2.

### Conclusions

The introduction of an affinity-enhancing mutation into the GD2-specific CAR dramatically increases CAR T cell potency and permits off-tumor CAR T cell activity in areas of the brain containing GD2. This scenario provides a new opportunity to investigate the mechanism of this toxicity and test strategies to achieve a therapeutic window.

40

### Evaluating the potential of Müllerian inhibiting substance type II receptor (MISIIR) as a target for CAR T cell therapy against ovarian cancer

Alba Rodriguez-Garcia<sup>1</sup>, Matthew K Robinson<sup>2</sup>, Gregory P Adams<sup>2</sup>, Daniel J Powell<sup>3</sup>

<sup>1</sup>University of Pennsylvania, Philadelphia, PA, USA

<sup>2</sup>Fox Chase Cancer Center, Philadelphia, PA, USA

<sup>3</sup>Department of Pathology and Laboratory Medicine, Perelman School of Medicine, University of Pennsylvania, Philadelphia, PA, USA

### Background

Ovarian cancer is responsible for 5% of cancer-related deaths among women, and the majority of the cases are diagnosed at a late stage, accounting for a 5-year survival rate of 27%. Therefore, there is a dire need for effective therapies. The recent success of adoptive cell therapy using T cells engineered to express anti-CD19 chimeric antigen receptors (CARs) for the treatment of hematologic malignancies, rationalizes the development of similar strategies for solid tumors such as ovarian cancer. The achievement of safe, effective therapy requires the selection of a target antigen that is overexpressed in malignant cells but present in few to no normal cells. The Müllerian inhibiting substance type 2 receptor (MISIIR) is a member of the TGF- $\beta$  receptors family involved in the regression of the primordial female reproductive tract in male embryos. This action is exerted through its interaction with soluble Müllerian inhibiting substance (MIS), triggering a downstream signaling cascade that induces apoptosis. MIS signaling through MISIIR has been shown to cause growth inhibition in ovarian, breast,

prostate and endometrial cancer cell lines *in vitro*. In humans, MISIIR is expressed at very low levels in a restricted set of healthy tissues but is overexpressed in gynecologic cancers, including 69% of epithelial ovarian cancers, making it a candidate target antigen.

### Methods

Here, we evaluate for the first time the potential of MISIIR as a target for CAR T cell therapy. In this work, we generated and functionally tested 5 distinct CARs comprised of different human MISIIR-specific single-chain antibody variable fragments (scFv) isolated from a phage display library coupled to the T cell signaling domains from CD27 and CD3Z.

### Results

All the CARs were efficiently expressed primary human T cells transduced using recombinant lentivirus technology and showed specific binding and reactivity against recombinant MISIIR protein. Interestingly, when co-cultured with target cells engineered to overexpress MISIIR, just one of the CARs, GM7-27Z, showed specific reactivity in terms of cytolytic function and proinflammatory cytokines secretion. The activity of this CAR was further evaluated *in vitro* and *in vivo* in a panel of tumor cells lines expressing different levels of the target antigen.

### Conclusions

Although the assessment of CAR-mediated antitumor activity and on-target off-tumor toxicity potential *in vivo* is required, the results obtained so far support the further exploration of an anti-MISIIR CAR-based therapy for the effective treatment of ovarian cancer as well as other gynecologic malignancies.

41

### IL-2 in adoptive cell therapy—local production from an adenovirus vector instead of systemic administration results in safety and efficacy gains

João Santos<sup>1</sup>, Riikka Havunen<sup>2</sup>, Mikko Siurala<sup>2</sup>, Víctor Cervera-Carrascón<sup>1</sup>, Suvi Parviainen<sup>1</sup>, Marjukka Antilla<sup>3</sup>, Akseli Hemminki<sup>2</sup>

<sup>1</sup>TILT Biotherapeutics, Helsinki, Uusimaa, Finland

<sup>2</sup>University of Helsinki, Helsinki, Uusimaa, Finland

<sup>3</sup>Finnish Food Safety Authority, Helsinki, Uusimaa, Finland

### Background

The use of interleukin-2 (IL-2) has been a major asset to boost the therapeutic anti-tumor efficacy of adoptive cell therapy, including tumor infiltrating lymphocyte (TIL) therapy in the context of solid tumors. However, clinical assessments have revealed that its systemic administration results in poor accumulation at solid tumor sites. Additionally, the half-life of this recombinant molecule is short. High dose administration has therefore been used but this results in severe adverse

## Adoptive Cellular Therapy

Presenting author underlined; Primary author in italics

events, including mortality. Hence, local production at the tumor is an attractive concept which might retain or even increase the useful aspects of IL-2, while reducing systemic side effects.

### Methods

We aimed to evaluate the efficacy and safety of, intratumoral delivered IL-2-armed adenoviruses combined with T cell transfer in rodents. Experiments were set up using the syngeneic CB57BL/6 mouse B16.OVA melanoma tumor model infused with OVA-specific T cells, and the syngeneic Syrian hamsters Hapt1 pancreatic tumor model infused with TILs. Both therapeutic schedules involved once-a-week intratumoral administration of replication deficient serotype 5 (mice) or oncolytic serotype 5/3 chimeric (hamsters) IL-2-armed adenoviruses comparing with weekly-continuous systemic administration of recombinant IL-2.

### Results

In both models, local production of IL-2 successfully replaced that need for systemic IL-2. In fact, efficacy was even higher than with systemic IL-2. Furthermore, the vectored delivery of IL-2 significantly potentiated the infiltration of CD8+ T cells and, significantly decreased the percentage of regulatory T cells. In animals that received systemic recombinant IL-2 therapy, significant histological changes were observed in the lungs, liver, heart, spleen and kidneys that should be considered as side-effects of the treatment.

### Conclusions

In summary, local production of IL-2 seems appealing from the point of view of efficacy and safety in the context of adoptive cell therapy. This preclinical assessment provides the rationale for clinical translation, which is ongoing by TILT Biotherapeutics Ltd.

## 42

### Successful expansion and characterization of tumor infiltrating lymphocytes (TILs) from non-melanoma tumors

Jyothi Sethuraman, Laurelis Santiago, Jie Qing Chen, Zhimin Dai, Seth Wardell, James Bender, Michael T Lotze

Lion Biotechnologies, Inc., Tampa, FL, USA

### Background

Adoptive cell therapy (ACT) has shown promise in comparison to other methods of cancer immunotherapy that rely on the active development of antitumor T cells *in vivo* to mediate cancer regression [1]. Administration of autologous TILs in melanoma patients has shown an overall response rate of 55% at NCI, 38% at Moffitt Cancer Center, 48% at MD Anderson Cancer Center and 40% in Sheba at the Ella Cancer Institute, Israel [1]. TILs have been found in a

variety of solid tumors, and their presence has been shown to be a prognostic indicator of improved survival. Here, we demonstrate the feasibility of growing TILs and the potential to develop TIL therapies to treat other solid tumors, such as lung, breast, and bladder cancers.

### Methods

Upon receiving surgically resected tumor specimens, samples were washed in HBSS and cut into small fragments prior to propagating *in vitro* in G-REX-10 cell culture flasks with interleukin-2 (commonly referred to as a pre-rapid expansion protocol [pre-REP]). After culture initiation, media was exchanged. The media was changed every 3 days subsequently for 2 weeks. TILs were harvested to assess cell count and viability, followed by immunophenotyping and cryopreservation.

### Results

The average yield of TILs cultured and expanded from bladder, cervical, head & neck, lung, and triple-negative breast tumors is listed in Table 1. Phenotypic characterization of TILs from bladder, cervical and lung cancer were >60-70% CD8+ T cells whereas TILs from head and neck demonstrated variable distribution of CD8+ and CD4+ T cells. TILs propagated from TNBC were >80% CD4+ T cells. Regardless of the tumors, most cultures had < 20% CD56+ NK cells.

### Conclusions

We have been successful in culturing and expanding TILs from various non-melanoma solid tumors. We will initiate REP from pre-REP TILs from non-melanoma tumors to enable product development for subsequent possible clinical trials. Efforts are currently focused on culturing TILs from smaller tumor specimens/biopsies to assess utility in promoting expansion of TILs with central and effector memory phenotypes and selecting for mutanome reactive TILs.

### References

1. Rosenberg SA, Restifo NP: **Adoptive cell transfer as personalized immunotherapy for human cancer.** *Science* 2015, **348**:62-68.

**Table 1**

Tumor	Number of patient tumors	Average yield (and range) of TILs from pre-REP (10 <sup>6</sup> )
Bladder	2	290 (97-600)
Cervical	4	360 (147-800)
H&N	7	539 (132-738)
Lung	8	688 (50-915)
TNBC	13	429 (81-665)



## Adoptive Cellular Therapy

Presenting author underlined; Primary author in italics

43

### A tumor-penetrating recombinant protein anti-EGFR-iRGD enhances efficacy of antigen-specific CTL in gastric cancer in vivo

Huizi Sha, Shu Su, Naiqing Ding, Baorui Liu

The Comprehensive Cancer Center of Drum-Tower Hospital, Medical School of Nanjing University & Clinical Cancer Institute of Nanjing University, Nanjing, Jiangsu, People's Republic of China

#### Background

Strategies that enhance the function of T cells are critical for immunotherapy. Targeted delivery of T cells through BiTE (bispecific T cell engager) platform to cancerous tissues shows potential in sparing unaffected tissues. However, it has been a major challenge for cells penetration in solid tumor tissues due to the complicated tumor microenvironment. Activated T cells expression integrin, which is the target of peptide RGD. Peptide iRGD (CRGDK/RGPD/EC) increased vascular and tissue permeability in a tumor-specific and neuropilin-1-dependent manner, allowing co-administered drugs to penetrate into extravascular tumor tissue. Recombinant protein anti-EGFR-iRGD was purified and examined.

#### Methods

Recombinant protein anti-EGFR-iRGD consisting of an anti-EGFR VHH (the variable domain from the heavy chain of the antibody) fused to iRGD, a tumor-specific binding peptide with high permeability were expressed in *E. coli* BL21 (DE3) and purified by nickel-nitrilotriacetic acid affinity chromatography. We use tumor cell lines and mice to analyze the targeting, penetrating and antitumor activity of antigen-specific T cells together with recombinant protein.

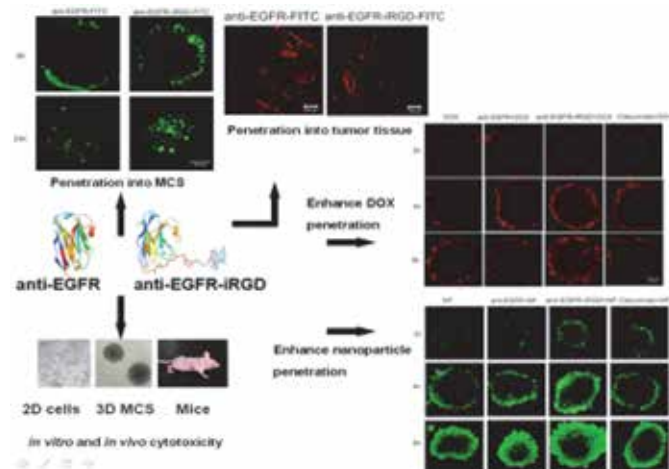
#### Results

We have successfully constructed a recombinant protein named anti-EGFR-iRGD, a dual targets of EGFR and integrin and high permeable protein. It could spread extensively throughout both the multicellular spheroids and the tumor mass. The recombinant protein anti-EGFR-iRGD could help more T cells infiltrating into tumor mass and also exhibited antitumor activity in tumor cell lines and mice.

#### Conclusions

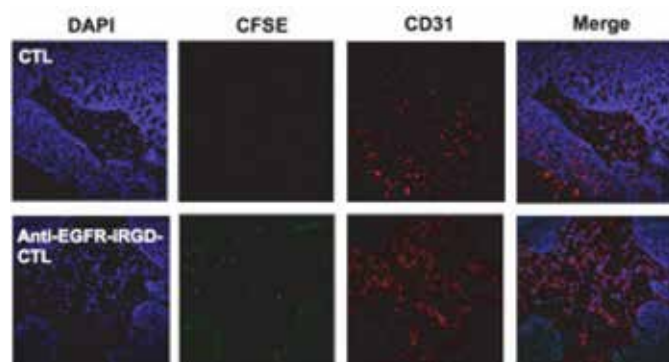
Our results provide impetus for further studies for potentially using iRGD based fusion protein anti-EGFR-iRGD with immune therapy regimens for enhancing therapy of gastric cancer patients.

Figure 1. Purification and verification of recombinant protein



purification and verification of recombinant protein

Figure 2. Penetration of CTL together with recombinant protein



penetration of CTL together with recombinant protein

44

### Immunodominance of cancer neoantigen and cancer-germline antigen T cell reactivities in successful immunotherapy of virally-induced epithelial cancer

Sanja Stevanovic<sup>1</sup>, Anna Pasetto<sup>2</sup>, Sarah R Helman<sup>1</sup>, Jared J Gartner<sup>2</sup>, Todd D Prickett<sup>2</sup>, Paul F Robbins<sup>2</sup>, Steven A Rosenberg<sup>2</sup>, Christian S Hinrichs<sup>1</sup>

<sup>1</sup>Experimental Transplantation and Immunology Branch, National Cancer Institute, National Institutes of Health, Bethesda, MD, USA

<sup>2</sup>Surgery Branch, National Cancer Institute, National Institutes of Health, Bethesda, MD, USA

#### Background

Immunotherapy has clinical activity in human papillomavirus (HPV)-induced epithelial cancers, but the tumor antigens

## Adoptive Cellular Therapy

Presenting author underlined; Primary author in italics

targeted by T cells resulting in cancer regression are poorly defined. The viral proteins expressed by these malignancies are generally considered the primary targets of T cell based immune attack. However, HPV+ cancers also harbor somatic mutations and express cancer-germline antigens that may be targets of tumor-specific T cells. Here, we aimed to elucidate the landscape of tumor antigens targeted by T cells in two patients with metastatic HPV+ cervical cancer who experienced durable complete tumor regression after adoptive transfer of tumor-infiltrating lymphocytes (TIL).

### Methods

To this end, reactivity of therapeutic TIL was assessed in immunological assays against HPV-derived antigens (L1, L2, E1, E2, E4, E5, E6 and E7), mutated neoantigens and cancer-germline antigens identified by whole-exome and/or RNA sequencing of patient's tumors. T cell receptor (TCR) clonotypes conferring specificity to tumor antigens were elucidated and quantified, and their *in vivo* persistence was profiled by TCR deep sequencing.

### Results

T cell reactivity against the HPV-E6 and/or -E7 antigens was detected in both patient's infused TIL, consistent with previously reported results. No T cell reactivity was detected against other six HPV-derived antigens. However, our data indicated that these patient's infused TIL distinctly recognized mutated neoantigens or a cancer-germline antigen. Detailed TCR clonotype analysis showed that in one patient multiple CD8+ clonotypes (35% of infused TIL) recognized somatically mutated gene products ( $n=3$ ) unique to patient's tumor in addition to several CD8+ and/or CD4+ clonotypes (14% of TIL) targeting HPV-E6 and/or -E7. In the other patient, one CD8+ clonotype (67% of TIL) recognized the cancer-germline antigen Kita-kyushu lung cancer antigen 1 in addition to one CD4+ clonotype (14% of TIL) that targeted HPV-E7. Administered viral and non-viral tumor antigen-specific T cells in both patients remained functional and persisted at elevated levels in the circulation for months during ongoing remission.

### Conclusions

Our data show that both patients who experienced complete tumor regression received TIL that contained low frequency of HPV-targeted T cells but a high frequency of mutated neoantigen- or cancer-germline antigen-targeted T cells. These results reveal a previously unappreciated role for T cells targeting non-viral antigens in HPV+ cervical cancer. By expanding the categories of potential tumor regression antigens for cervical cancer and possibly other HPV-induced malignancies, our findings provide new targets for personalized cancer vaccines and/or adoptive T cell therapies as well as for immune-monitoring of various cancer immunotherapies.

### Consent

Written informed consent was obtained from patients.

### 45

## Adoptive cellular therapy (ACT) with allogeneic activated natural killer (aNK) cells in patients with advanced Merkel cell carcinoma (MCC): preliminary results of a phase II trial

Shailender Bhatia<sup>1</sup>, Melissa Burgess<sup>2</sup>, Hui Zhang<sup>3</sup>, Tien Lee<sup>4</sup>, Hans Klingemann<sup>4</sup>, Patrick Soon-Shiong<sup>4</sup>, Paul Nghiem<sup>1</sup>, John M Kirkwood<sup>5</sup>

<sup>1</sup>Fred Hutchinson Cancer Research Center, University of Washington, Seattle, WA, USA

<sup>2</sup>University of Pittsburgh Cancer Institute, Pittsburgh, PA, USA

<sup>3</sup>NantBioScience, Inc., Culver City, CA, USA

<sup>4</sup>NantKwest, Inc., Culver City, CA, USA

<sup>5</sup>UPMC Cancer Center, University of Pittsburgh Cancer Institute, Pittsburgh, PA, USA

### Background

MCC is an aggressive skin cancer associated with Merkel cell polyomavirus (MCPyV). Downregulation of class I major histocompatibility complex (MHC) expression in >80% of MCC tumors suggests potential susceptibility to adoptively transferred NK cells. aNK cells are derived from a NK cell line that is highly cytotoxic to a broad range of tumor cells. Phase I studies suggest that aNK cell therapy is well tolerated and has antitumor activity in patients with advanced hematologic or solid cancers. This study seeks to determine the efficacy of aNK cell therapy in patients with advanced MCC.

### Methods

In this open-label phase II study, advanced MCC patients (planned N=24) receive aNK cells ( $2 \times 10^9$  cells/m<sup>2</sup>) intravenously on two consecutive days (1 cycle) every 2 weeks. Key eligibility criteria include age  $\geq 18$  years, unresectable stage III or IV MCC, and ECOG performance status  $\leq 2$ . Up to two prior systemic chemotherapies and/or immunotherapies are allowed. The study uses a Simon optimal two-stage design. The primary efficacy endpoint is 4-month progression-free survival (PFS) rate. Secondary endpoints include objective response rate by RECIST 1.1, time to progression, overall survival, safety, and quality of life assessment (FACT-G). Planned correlative studies include genomic and proteomic tumor profiles, MCPyV status, and immunohistochemical assessment of MHC-1, correlated to treatment outcome.

### Results

As of August 2016, 3 patients have been enrolled. Treatment-related adverse events have been grade 2 or milder with no serious adverse events. The efficacy criterion for the first stage of the study has been met, with a patient with

## Adoptive Cellular Therapy

Presenting author underlined; *Primary author in italics*

advanced MCC refractory to multiple prior therapies including PD-1 blockade demonstrating an impressive partial response (PR) with >70% regression, ongoing at 20 weeks. Intriguing changes were observed clinically in another patient's superficial tumors just a few hours after aNK infusions, although this patient developed progressive disease at 4 weeks. Correlative studies on tumor biopsies of the patient with PR are ongoing.

### Conclusions

ACT with allogeneic aNK cells has been safe and well tolerated in the initial three patients with advanced MCC. Encouraging antitumor activity has been observed with an impressive PR in a patient with advanced MCC refractory to PD-1 blockade. The pre-specified efficacy criterion for the first stage of the trial has been met and enrollment continues on the trial. Updated results will be presented at the meeting.

### Trial Registration

ClinicalTrials.gov identifier NCT02465957.

## 46

### Low dose conditioning chemotherapy and CD19-directed CAR T cells may elicit distinct immune programs associated with clinical responses

*John M Rossi<sup>1</sup>, Marika Sherman<sup>1</sup>, Allen Xue<sup>1</sup>, Yueh-wei Shen<sup>1</sup>, Lynn Navale<sup>1</sup>, Steven A Rosenberg<sup>2</sup>, James N Kochenderfer<sup>3</sup>, Adrian Bot<sup>1</sup>*

<sup>1</sup>Kite Pharma, Inc, Santa Monica, CA, USA

<sup>2</sup>Surgery Branch, National Cancer Institute, Bethesda, MD, USA

<sup>3</sup>Experimental Transplantation and Immunology Branch, National Cancer Institute, Bethesda, MD, USA

### Background

Anti-CD19 CAR T cell therapy has shown promising clinical efficacy. Recent evidence points to a critical role for non-myeloablative conditioning chemotherapy, influencing the expansion, persistence and activity of CAR T cells. To diminish toxicities, Kochenderfer, *et al.* pioneered a conditioning chemotherapy regimen with low dose cyclophosphamide (300-500mg/m<sup>2</sup>) and fludarabine (30mg/m<sup>2</sup>) administered daily for 3 days [1]. This resulted in a response rate of 73% in patients with advanced Non-Hodgkin lymphoma, with lower rate of hematologic toxicities. Post CAR T cell-treatment peak levels of cytokines in blood were associated with T cell expansion, clinical efficacy or neurotoxicity [1].

### Methods

We analyzed 41 blood biomarkers in 22 patients treated with anti-CD19 CAR T cells, preceded by low dose conditioning chemotherapy. We also measured cytokine levels produced by CAR T cells *ex vivo*, upon culture with CD19-expressing

target cells. The expansion of CAR T cells in blood was measured by quantitative PCR.

### Results

Conditioning chemotherapy enhanced IL-15 and decreased lymphocytes and perforin blood levels. Several cytokines peaked sequentially in blood post CAR T cell infusion: among those, IL-15 and GM-CSF at days 2-3, followed by IL-10 and Granzyme B, at day 6. CAR T cell expansion in blood occurred within 7-14 days. IL-15 blood levels associated with T cell expansion, clinical response and toxicities. In addition, early post-CAR T cell treatment levels GM-CSF and peak blood levels of IL-10 and Granzyme B, were associated with clinical efficacy or neurotoxicity. When stimulated *ex vivo* with CD19-expressing cells, CAR T cells produced a broad range of molecules including GM-CSF, IL-10 and Granzyme B, but not IL-15.

### Conclusions

In conclusion, these preliminary findings suggest that three immune programs impact clinical outcome of CAR T cell treatment: a T cell proliferative program initiated by conditioning chemotherapy, together with an inflammatory and a cytotoxic program deployed by CAR T cells. In addition, this analysis highlights the need to carefully optimize the conditioning chemotherapy regimen.

### Acknowledgements

This study was conducted under a CRADA between NCI and Kite Pharma.

### Trial Registration

ClinicalTrial.gov identifier NCT00924326.

### References

1. Kochenderfer J, Somerville R, Lu T, Shi V, Yang JC, Sherry R, *et al*: **Anti-CD19 chimeric antigen receptor T cells preceded by low-dose chemotherapy to induce remissions of advanced lymphoma [abstract]**. *J Clin Oncol* 2016, **34** Suppl:LBA3010.

## 47

### Artificial antigen presenting cells promote expansion of tumor infiltrating lymphocytes (TILs)

*Anandaraman Veerapathran, Aishwarya Gokuldass, Amanda Stramer, Jyothi Sethuraman, Michelle A Blaskovich, Doris Wiener, Ian Frank, Laurelis Santiago, Brian Rabinovich, Maria Fardis, James Bender, Michael T Lotze*

Lion Biotechnologies, Inc., Tampa, FL, USA

### Background

For more than a decade, allogeneic peripheral blood mononuclear cells (PBMC) have been used as accessory feeder cells that provide "costimulatory signals" necessary for the expansion of tumor-infiltrating lymphocytes (TILs) in



## Adoptive Cellular Therapy

Presenting author underlined; Primary author in italics

the presence of IL-2 and CD3 stimulation (Rapid Expansion Protocol [REP]) [1]. The intrinsic heterogeneity of allogeneic PBMC is an important variable when considering the expansion and resulting phenotype of post-REP TIL prepared for transplantation. The procurement of allo-PBMC in large numbers is also challenging and expensive. Our objective was to evaluate artificial antigen presenting cells (aAPC) as a potential substitute for PBMC. As such, we developed a novel aAPC from the CD64<sup>+</sup> MOLM-14 human leukemia cell line, genetically engineered to express recombinant CD86 (B7-2) and CD137-L (41BBL) (MOLM14-86/137).

### Methods

The MOLM-14-86/137 cell line was generated via transduction of wild type MOLM-14 with lentiviral virions encoding genomic RNA of CD86 or CD137 downstream of the U3 promoter from MSCV. MOLM-14-86/137 was  $\gamma$ -irradiated at 100Gy and co-cultured with TILs at a 1:100 ratio (TIL:aAPC) in media containing OKT3 (30 ng/ml) and IL-2 (3000 IU/ml) for 14 days. On Day 14, we calculated their expansion and examined their differentiation (flow cytometry), metabolic rate, and cytotoxicity.

### Results

Compared to TIL co-cultured with PBMC or wild type MOLM-14, we obtained 95-100% TILs via co-culture with MOLM-14-86/137. This value was within the expected range using PBMC (Figure 1). TIL differentiation, cellular respiration (OXPHOS) and redirected cytotoxicity were also within the range expected via co-culture with PBMC.

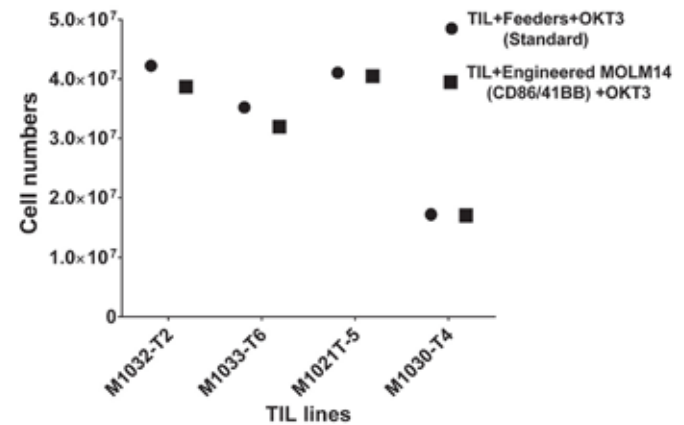
### Conclusions

According to our measurements, co-culture of TIL with MOLM-14-86/137 aAPC resulted in expansion, metabolic activity and cytotoxicity that were sufficiently similar to that obtained with PBMC. This data suggests that investigation of a MOLM-14-86/137 based REP protocol in a clinical setting is warranted.

### References

1. Dudley ME, Wunderlich JR, Shelton TE, Even J, Rosenberg SA: **Generation of tumor-infiltrating lymphocyte cultures for use in adoptive transfer therapy for melanoma patients.** *J Immunother* 2003, **26**:332–342.

Figure 1



Rapid expansion of TILs using irradiated engineered MOLM-14 or PBMC feeders. TIL were co-cultured with PBMC Feeders or MOLM14 (CD86/41BBL) at 1:100 ratios plus OKT3(30ng/ml) and IL-2 (3000 IU/ml). Cells were counted and split on Day 6 and 11. Each dot represents cell numbers determined on Day 14.

### 48

#### Blocking vasoactive intestinal peptide signaling modulates immune checkpoints and graft-versus-leukemia in allogeneic transplantation in mice

*Edmund K Waller*<sup>1</sup>, Jian-Ming Li<sup>1</sup>, Christopher Petersen<sup>1</sup>, Bruce R Blazar<sup>2</sup>, Jingxia Li<sup>1</sup>, Cynthia R Giver<sup>1</sup>

<sup>1</sup>Emory University, Atlanta, GA, USA

<sup>2</sup>University of Minnesota, Minneapolis, MN, USA

#### Background

The goal of allogeneic bone marrow transplantation (allo-BMT) is the elimination of leukemia cells through the graft-versus-leukemia (GvL) activity of donor cells, while limiting graft-versus-host disease (GvHD). Immune checkpoint pathways regulate GvL and GvHD activities, but blocking these pathways can cause lethal GVHD. Vasoactive intestinal peptide (VIP) is an immunosuppressive neuropeptide that regulates co-inhibitory pathways.

#### Methods

Murine models of MHC-mismatched allogeneic bone marrow transplantation were used to evaluate the effect of blocking VIP-signaling on the graft-versus-leukemia (GvL) and graft-versus host disease (GvHD) effect of donor T cells. Mice were transplanted with donor grafts from VIP-KO mice or recipients of wild-type grafts were treated with seven daily injections of a peptide antagonist to VIP (VIPhyb). Survival, GvHD and the growth of luciferase+ LBRM, a T cell lymphoblastic leukemia cell line, or C1498, a myeloid

## Adoptive Cellular Therapy

Presenting author underlined; Primary author in italics

leukemia cell line, were monitored by bio-luminescent imaging. Expression of chemokine receptors, cytokines and check-point molecules were measured by flow cytometry. VIP expression on donor and host cells was visualized using a transgenic mouse in which GFP expression is driven by the VIP promoter. T cell repertoire from T cells in mice with GvHD or GvL was analyzed by deep sequencing.

### Results

VIP is expressed transiently in donor NK, NKT, dendritic cells, and T cells after allo-transplant, as well as in host leukocytes. A peptide antagonist of VIP signaling (VIPhyb) increased T cell proliferation *in vitro* and reduced IL-10 expression in donor T cells. Treatment of allo-BMT recipients with VIPhyb, or transplanting donor grafts lacking VIP (VIP-KO), activated donor T cells in lymphoid organs, reduced T cell homing to GvHD target organs, and enhanced GvL without increasing GvHD in multiple allo-BMT models. Genetic or *ex vivo* depletion of donor NK cells or CD8+ T cells from allografts abrogated the VIPhyb-enhanced GvL activity (Figure 1A). VIPhyb treatment led to downregulation of PD-1 and PD-L1 expression on donor immune cells (Figure 1B), increased effector molecule expression, and expanded oligoclonal CD8+ T cells that protected secondary allo-transplant recipients from leukemia (Figure 1C & D).

### Conclusions

VIP production by donor immune cells is dynamically regulated after allo-BMT, and transplanting VIP-KO cells, or daily treatment with VIPhyb, significantly enhanced survival of leukemia-bearing transplant recipients via a CD8+ T cell dependent GvL effect without increased GvHD in murine models of MHC mis-matched allo-BMT. Blocking VIP-signaling thus represents a novel pharmacological approach to separate GvL from GvHD and enhance adaptive T cell responses to leukemia-associated antigens in allo-BMT.

Figure 1

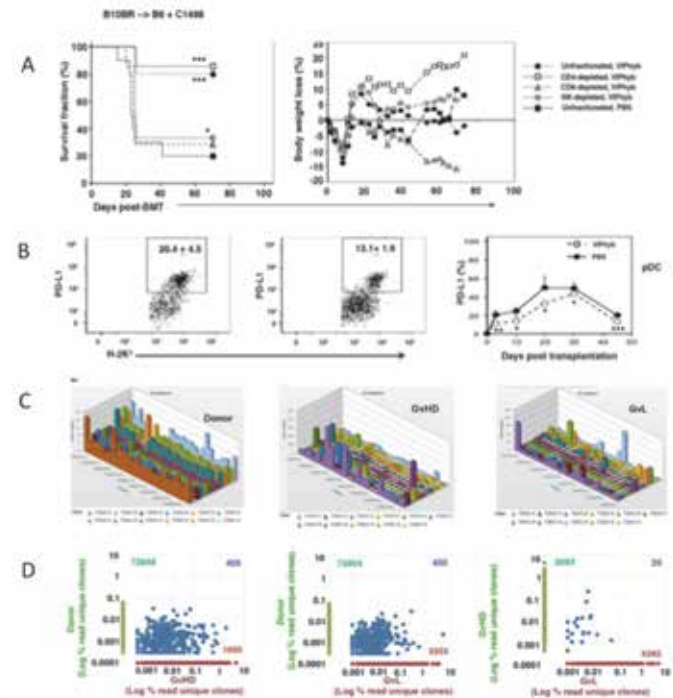


Figure 1. Treatment of allo-BMT recipients with a VIP antagonist induces a CD8+ donor T cell-dependent GvL response associated with down-regulation of PD-L1 on donor pDC and expansion of oligoclonal donor CD8+ T cells. A: Survival curves and GVHD clinical scores for B10.BR->B6 allo-BMT harboring C1498 leukemia cells. Donor T cell subsets were depleted of specific populations by MACS prior to transplantation as shown. B: Expression of PD-L1 on donor pDC in B6->B10.BR transplants. C: TCR Vbeta and J gene segments present in donor CD8+ T cells (left), CD8+ T cells from mice with GVHD (middle) and Cd8+ T cells from mice with GvL (right). D: Lack of correspondence between TCR Vbeta and J genes sequenced in mice with GVHD and mice with GvL.

## 49

### Bortezomib sensitizes cancer stem cells from solid human tumors to natural killer cell-mediated killing

Ziming Wang<sup>1</sup>, Steven K Grossenbacher<sup>1</sup>, Ian Sturgill<sup>2</sup>, Robert J Canter<sup>1</sup>, William J Murphy<sup>1</sup>

<sup>1</sup>University of California, Davis, Sacramento, CA, USA

<sup>2</sup>California State University, Sacramento, Sacramento, CA, USA

### Background

Cancer stem cells (CSCs) from solid and hematopoietic tumors resist conventional cytotoxic therapies that target rapidly

## Adoptive Cellular Therapy

Presenting author underlined; Primary author in italics

proliferating cells. Thus, residual CSCs can hide within the tumor niche and seed relapse and metastasis. Due to their relapse potential there is an urgent need to identify ways to therapeutically target CSCs. We previously found that cells expressing high amounts of the stem cell associated protein aldehyde dehydrogenase (ALDH) are effectively killed by activated natural killer (NK) lymphocytes. NK cells are known to kill malignant cells through apoptotic processes inherent to the target cell, such as TRAIL-DR5 or Fas-FasL binding, without prior immunization. We and others have also found that the FDA approved proteasome inhibitor, bortezomib, sensitizes tumor cells to NK cell killing by upregulating DR5 and intracellular machinery associated with apoptosis. Based on this previous work, we investigated the effects of bortezomib to promote NK cell killing of ALDH<sup>bright</sup> CSCs. We evaluated CSCs derived from solid tumors, *in vitro* and *in vivo*, for the induction of receptors associated with NK cell mediated killing, and for their susceptibility to NK killing after treatment.

### Methods

*In vitro* sensitization and cytotoxicity assays were performed using cultured NK cells isolated from human peripheral blood. The glioblastoma and sarcoma cell lines, U87 and A673, respectively, were first treated with bortezomib, then co-cultured with activated NK cells at serial effector:target ratios. Target tumor cells were analyzed using flow cytometry for cell survival, and expression of Fas, DR4, DR5, and MICA/B on both ALDH<sup>bright</sup> and ALDH<sup>dim</sup> cells.

### Results

Bortezomib led to a 3-fold increase in the percentage of viable ALDH<sup>bright</sup> glioblastoma and sarcoma cells, *in vitro*, compared to untreated controls. Bortezomib enhanced the expression of Fas and DR5 by 10% and 40%, respectively, in ALDH<sup>bright</sup> U87 cells. It increased the expression of DR4 by 20% in ALDH<sup>bright</sup> A673 cells. However, bortezomib had little effect on ALDH<sup>dim</sup> cells. Bortezomib pretreatment led to a 98% decrease in viable ALDH<sup>bright</sup> cells following NK cytotoxicity assays *in vitro*. *In vivo*, bortezomib improved the efficacy of adoptive NK cell therapy in multiple mouse xenograft models.

### Conclusions

ALDH<sup>bright</sup> CSCs are resistant to the cytotoxic effects of bortezomib. Bortezomib resistance is marked by increases in the expression of Fas, DR4, and DR5 and leads to increased susceptibility to lysis by activated NK cells. The combined use of bortezomib with activated natural killer cells could act as a potential anti-CSC strategy to improve outcomes for patients with solid tumors.

50

## Targeted NK cells display potent activity against glioblastoma and induce protective antitumor immunity

Congcong Zhang<sup>1</sup>, Michael C Burger<sup>2</sup>, Lukas Jennewein<sup>3</sup>, Anja Waldmann<sup>1</sup>, Michel Mittelbronn<sup>3</sup>, Torsten Tonn<sup>4</sup>, Joachim P Steinbach<sup>2</sup>, Winfried S Wels<sup>1</sup>

<sup>1</sup>Georg-Speyer-Haus, Institute for Tumor Biology and Experimental Therapy, Frankfurt, Germany

<sup>2</sup>Institute for Neurooncology, Goethe University, Frankfurt, Germany

<sup>3</sup>Elinger Institute, Goethe University, Frankfurt, Frankfurt, Germany

<sup>4</sup>German Red Cross Blood Donation Service North-East, Dresden, Dresden, Germany

### Background

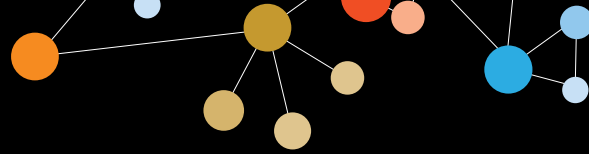
Significant progress has been made over the last decade towards realizing the potential of natural killer (NK) cells for cancer immunotherapy. In addition to donor-derived primary NK cells, also continuously expanding cytotoxic cell lines such as NK-92 are being considered for adoptive cancer immunotherapy. High cytotoxicity of NK-92 has previously been shown against malignant cells of hematologic origin in preclinical studies, and general safety of infusion of NK-92 cells has been established in phase I clinical trials. To enhance their therapeutic utility, here we genetically modified NK-92 cells to express a chimeric antigen receptor (CAR), consisting of an ErbB2 (HER2)-specific scFv antibody fragment fused via a linker to a composite CD28-CD3 $\zeta$  signaling domain. GMP-compliant protocols for vector production, lentiviral transduction and expansion of a genetically modified NK-92 single cell clone (NK-92/5.28.z) were established.

### Methods

Functional analysis of NK-92/5.28.z cells revealed high and stable CAR expression, and selective cytotoxicity against ErbB2-expressing but otherwise NK-resistant tumor cells of different origins *in vitro*. Ongoing work focuses on the development of these cells for adoptive immunotherapy of ErbB2-positive glioblastoma (GBM). ErbB2 expression in primary tumors and cell cultures was assessed by immunohistochemistry and flow cytometry. Cell killing activity of NK-92/5.28.z cells was analyzed in *in vitro* cytotoxicity assays. *In vivo* antitumor activity was evaluated in NOD-SCID IL2R $\gamma$  null (NSG) mice carrying orthotopic human GBM xenografts and C57BL/6 mice carrying orthotopic ErbB2-expressing murine GBM tumors.

### Results

We found elevated ErbB2 protein expression in >40% of primary GBM samples and in the majority of GBM cell lines investigated. In *in vitro* assays, NK-92/5.28.z in contrast to



## Adoptive Cellular Therapy

Presenting author underlined; *Primary author in italics*

untargeted NK-92 cells lysed all ErbB2-positive established and primary GBM cells analyzed. Potent *in vivo* antitumor activity of NK-92/5.28.z was observed in orthotopic GBM xenograft models in NSG mice, leading to a marked extension of symptom-free survival upon repeated stereotactic injection of CAR NK cells into the tumor area. In immunocompetent mice, local therapy with NK-92/5.28.z cells resulted in cures of transplanted syngeneic GBM in the majority of animals, induction of endogenous antitumor immunity and long-term protection against tumor rechallenge at distant sites.

### Conclusions

Our data demonstrate the potential of ErbB2-specific NK-92/5.28.z cells for adoptive immunotherapy of glioblastoma, justifying evaluation of this approach for the treatment of ErbB2-positive GBM in clinical studies.

### 51 Abstract Travel Award Recipient

#### Shared T cell receptor sequences between HLA-A2+ patients vaccinated against a Melan-A epitope correlate with clinical benefit

Jason B Williams<sup>1</sup>, Yuanyuan Zha<sup>1</sup>, Thomas F Gajewski<sup>2</sup>

<sup>1</sup>University of Chicago, Chicago, IL, USA

<sup>2</sup>University of Chicago Medical Center, Chicago, IL, USA

### Background

Adoptive T Cell Therapy (ACT) of *in vitro* expanded T cell clones or transduced T cells redirected against defined tumor antigens has shown therapeutic efficacy in some patients. Ideas to improve upon this therapy are multifaceted, including combining ACT with checkpoint blockade, increasing the number of defined T cell receptors (TCR) against defined antigens, identifying new tumor-specific somatic mutations to target, and engineering TCRs to have increased avidity. However, even for well characterized antigens such as Melan-A, the optimal TCR is not known. Some engineered TCRs have shown off-tumor toxicity, and so selecting TCRs with maximal therapeutic efficacy but at the same time giving minimal side effects remains an important goal.

### Methods

We reasoned that one strategy for selecting optimal TCRs might be to identify T cells expanded after active immunization against defined epitopes in patients who experienced clinical benefit but no apparent side effects. To this end, we performed deep TCR sequencing of HLA-A2/Melan-A<sup>+</sup> CD8<sup>+</sup> T cells from 16 metastatic melanoma patients vaccinated against a Melan-A epitope.

### Results

While changes in overall TCR clonality measured before and after vaccination did not correlate with clinical benefit, many TCRs showed a significant increase in representation of

the total TCR repertoire after vaccination. Of the 6 patients that received a clinical benefit we found 122 public TCR $\beta$  and 124 public TCR $\alpha$  sequences. 105 of these sequences showed expansion after vaccination in 2 or more patients. Surprisingly, we did not observe the defined Melan-A-specific TCRs used previously in redirected ACT clinical trials, designated DMF4 and DMF5. Mapping of public sequences by frequency per patient and aligning TCR $\alpha$ /TCR $\beta$  sequences highlighted several potential TCR $\alpha$ /TCR $\beta$  pairings. One patient was of particular interest as he had participated in two vaccine trials, with a 32-month interim between trials and clinical benefit each time. By the end of the second treatment period, the patient's TCR repertoire contained 55 public sequences. Interestingly, 7 of these sequences showed an initial contraction at the end of the first trial followed by a significant expansion by the end of the second trial, suggesting a strong clonotypic response to Melan-A.

### Conclusions

Together, these data highlight multiple TCR $\alpha$  and TCR $\beta$  sequences correlating with clinical benefit in the setting of no treatment-related toxicities. Similar results have been observed in other trials utilizing CEA peptide or WT1 peptide immunization. These sequences should enable full-length cloning of TCRs to be used in redirect adoptive cell therapy.

### Trial Registration

ClinicalTrials.gov identifier NCT00515528.

### 52

#### T cells redirected to TEM8 have antitumor activity but induce 'on target/off cancer toxicity' in preclinical models

LaTerrica C Williams<sup>1</sup>, Giedre Krenciute<sup>1</sup>, Mamta Kalra<sup>1</sup>, Chrystal Louis<sup>1</sup>, Stephen Gottschalk<sup>2</sup>

<sup>1</sup>Baylor College of Medicine, Houston, TX, USA

<sup>2</sup>Center for Cell and Gene Therapy, Baylor College of Medicine, Houston, TX, USA

### Background

Targeting the tumor vasculature holds promise to improve the outcome for patients with refractory solid tumors. Tumor endothelial marker (TEM) 8 is an attractive target for T cell therapies since it is expressed at higher levels in malignant cells and the tumor endothelium as judged by studies using monoclonal antibodies (mAbs). However T cells do not require high expression of the targeted antigen for activation, because of the higher overall avidity of a multivalent T cell compared to bivalent mAbs. Thus, the aim of this project was to determine the safety and antitumor activity of T cells expressing TEM8/CD3-specific T cell engagers (TEM8-ENG).



## Adoptive Cellular Therapy

Presenting author underlined; Primary author in italics

### Methods

qPCR and FACS analysis was used to determine the expression of TEM8 in solid tumor and endothelial cells. TEM8-ENG T cells were generated by transducing T cells with a retroviral vector encoding a TEM8-ENG consisting of the TEM8-specific scFv L2 linked to a scFv recognizing CD3. TEM8-ENG T cell effector function was evaluated *in vitro* and *in vivo*. Appropriate controls were used including ENG T cells specific for an irrelevant antigen (CD19).

### Results

To confirm the specificity of TEM8-ENG T cells we used targets that did not express TEM8 (BV173) or BV173 cells that were genetically modified to express human TEM8, murine TEM8, or murine TEM1. TEM8-ENG T cells recognized TEM8<sup>pos</sup> targets (BV173.hTEM8, BV173.mTEM8) as judged by their ability to secrete IFN $\gamma$  in coculture assays and kill both targets in cytotoxicity assays; in contrast, TEM8<sup>neg</sup> cells (BV173, BV173.mTEM1) were not recognized. Specificity of TEM8-ENG T cells was further confirmed with TEM8<sup>pos</sup> U373 glioma cells and U373.k/oTEM8 cells. TEM8-ENG T cells recognized a panel of TEM8<sup>pos</sup> solid tumor cells (A431, A549, LM7, LAN1, U87), and primary endothelial cells (HHSEC, HPAEC) in contrast to TEM8<sup>neg</sup> tumor cells (KG1a, Daudi). *In vivo*, intratumoral administration of TEM8-ENG T cells induced regression of U373 gliomas in an orthoptic xenograft model. Intravenous administration of  $1 \times 10^7$  TEM8-ENG T cells resulted in antigen-dependent expansion and death of 7/10 mice; no toxicity was observed after the injection of  $1 \times 10^6$  TEM8-ENG T cells.

### Conclusions

TEM8 is expressed in tumor endothelium, normal endothelial cells and solid tumor cells as judged by qPCR, FACS, and functional assays. TEM8-ENG T cells had antitumor activity *in vivo*, but displayed dose-dependent toxicity. Our studies highlight that mAbs and T cells may have different toxicity profiles, most likely due to differences in their avidity for the targeted antigen. TEM8-ENG T cell xenograft models represent an ideal model to study genetic approaches to prevent 'on target/off cancer toxicities' of cell therapies.

53

### A pathogen boosted adoptive cell transfer immunotherapy to treat solid tumors

Gang Xin<sup>1</sup>, David Schauder<sup>1</sup>, Aimin Jiang<sup>2</sup>, Nikhil Joshi<sup>3</sup>, Weiguo Cui<sup>1</sup>

<sup>1</sup>Blood Center of Wisconsin, Milwaukee, WI, USA

<sup>2</sup>Department of Immunology, Roswell Park Cancer Institute, Buffalo, NY, USA

<sup>3</sup>Koch Institute for Integrative Cancer Research and Department of Biology, Massachusetts Institute of Technology, Cambridge, MA, USA

### Background

Despite the remarkable success in treating hematological malignancies, adoptive cell transfer (ACT) still faces several challenges in treating solid tumors. The main stumbling blocks include insufficient quantity of tumor-specific T cells for transfer, impaired migration of transferred T cells into the tumor and the immunosuppressive microenvironment within the tumor.

### Methods

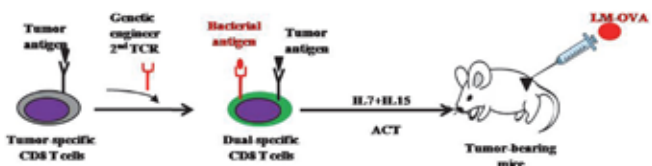
To overcome these problems, we designed an innovative approach that not only overcomes immunosuppression, but also induces robust anti-tumor T cell responses in the tumor. We first genetically engineered dual-specific CD8 T cells that can recognize both a tumor associated antigen and a bacterial antigen *in vitro*. Then, we treated tumor-bearing mice with ACT using a small number of the dual-specific CD8 T cells. This was accompanied by intratumoral injection of a low dose of the bacteria, which was sufficient to break local immunosuppression.

### Results

The dual-specific CD8 T cells expanded robustly and migrated to the tumor bed in response to the infection. At the same time, the second TCR of these effector CD8 T cells recognized tumor antigen and executed effector function, causing tumor regression. As a result of this enhanced anti-tumor effect, 60% of the treated mice successfully eradicated their solid tumor at the primary site.

### Conclusions

Our approach not only overcomes immunosuppression, but also recruits robust anti-tumor T cell responses to the tumor. Overall, our study harnesses the power of multiple arms of the immune system with promising translational value, which can be used to target many types of solid tumors.



54

### Pharmacologic rejuvenation of exhausted T cells to improve adoptive TIL therapy

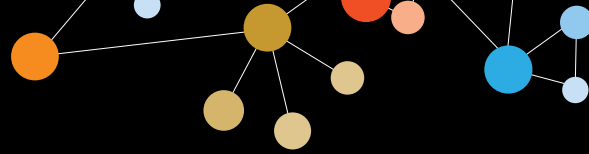
Xue Zeng<sup>1</sup>, Ashley V Menk<sup>1</sup>, Nicole Scharping<sup>2</sup>, Greg M Delgoffe<sup>2</sup>

<sup>1</sup>University of Pittsburgh Cancer Institute, Pittsburgh, PA, USA

<sup>2</sup>University of Pittsburgh, Pittsburgh, PA, USA

### Background

Immunotherapy has emerged as a strategy for the treatment of cancer. One of these immunotherapies is adoptive tumor-



## Adoptive Cellular Therapy

Presenting author underlined; Primary author in italics

infiltrating lymphocyte (TIL) therapy, in which T cells from resected tumors are expanded *in vitro* and then given to patients. However adoptive TIL therapy has little efficacy for many patients, because the tumor microenvironment creates an extreme environment for T cells. Our lab has revealed that T cells display metabolic defects, especially a loss of mitochondria, when they infiltrate the tumor microenvironment. This loss is related to T cell exhaustion. We hypothesize that these exhausted T cells were the most functional cells as they responded to tumor earliest and strongest. However their loss of mitochondria prevents them from further expansion when removed and cultured *in vitro*. Thus, we are utilizing what we have identified about their metabolic dysfunction to rejuvenate those T cells during *ex vivo* expansion. Our goal is to make exhausted T cells more metabolically active and provide a potent method for TIL therapy.

### Methods

**Tumor injection:** mice were given either 250,000 B16 or MC38 tumor cells injected intradermally in the center of the back. **T cell activation:** TILs are activated with 3  $\mu\text{g}/\text{ml}$  anti-CD3 (plate bound), 2  $\mu\text{g}/\text{ml}$  anti-CD28, 50 units/ml IL-2. **Adoptive TIL transfer:** treated and non-treated TIL are given to the mice that bear tumors by intravascular injection.

### Results

PD-1<sup>hi</sup> cells remain mitochondrially deficient and fail to proliferate *ex vivo*. Rosiglitazone can rescue mitochondrial mass and proliferation. PD-1 Tim-3<sup>hi</sup> cells are over proliferated by PD-1 Tim-3<sup>lo</sup> cells. Preliminary data has shown that glitazone compounds to long-term expansion protocols prevents loss of the previously-exhausted T cells during expansion.

### Conclusions

Cells expressing high levels of PD-1 and Tim-3 have low mitochondrial mass and fail to proliferate effectively *in vitro*. Mixing congenically marked cells from the non-exhausted or exhausted compartment shows exhausted cells are quickly overtaken by the non-exhausted (less than 1 week). Adding glitazone compounds to stimulate mitochondrial biogenesis results in short-term improvement of T cell proliferation *in vitro*. Preliminary data has shown that glitazone compounds to long-term expansion protocols prevents loss of the previously-exhausted T cells during expansion.

### Acknowledgements

UPCI Cytometry Core and Animal Facility (supported by NCI P30CA047904), University of Pittsburgh Department of Immunology, University of Pittsburgh Cancer Institute, Tumor Microenvironment Center, Chinese Scholar Council.

### References

1. Delgoffe GM, Powell JD: **Feeding an army: The metabolism of T cells in activation, energy, and exhaustion.** *Mol Immunol* 2015, **68(2 Pt C)**:492–496.

### 55

#### A turbocharged chimeric antigen receptor against prostate cancer

Zeguo Zhao<sup>1</sup>, Mohamad Hamieh<sup>1</sup>, Justin Eyquem<sup>1</sup>, Gertrude Gunset<sup>1</sup>, Neil Bander<sup>2</sup>, Michel Sadelain<sup>1</sup>

<sup>1</sup>Center for Cell Engineering, Memorial Sloan Kettering Cancer Center, New York, NY, USA

<sup>2</sup>Department of Urology, Weill Cornell Medical College, New York, NY, USA

#### Background

Both CD28- and 4-1BB-based second-generation CAR T cells elicit dramatic clinical responses in patients with refractory/relapsed CD19 positive malignancies, especially patients with acute lymphoblastic leukemia. We recently demonstrated that co-expressing the second-generation 19-28z CAR with 4-1BBL yields balanced tumoricidal function and T cell persistence, resulting in the greater therapeutic efficacy (Turbocharged CAR). However, due in part to their tumor microenvironment, solid tumors often resist CAR T cell therapy. We hypothesized that CD28-based second-generation CAR T cells coexpressing 4-1BBL would have better therapeutic efficacy against solid tumors than current second-generation CARs, owing to their unique intrinsic and immunomodulatory qualities.

#### Methods

Prostate-specific membrane antigen (PSMA) is a dimeric type II integral membrane glycoprotein, which is overexpressed in castrate-resistant, metastatic prostate cancer. We constructed a tricistronic PSMA-targeted CAR vector encoding the Pd28z CAR, 4-1BBL and a truncated, nonfunctional EGFR as a safety control (Pd28z–4-1BBL–EGFRt). Two second-generation CARs (Pd28z and PdBBz) served as controls.

#### Results

In a high tumor burden model of disseminated prostate cancer, we used the *in vivo* “stress test” in which the T cell dose is gradually lowered to levels where CAR therapy begins to fail, in order to compare the relative functionality and persistence of these CAR T cells. CAR T cells coexpressing Pd28z with 4-1BBL exhibited higher tumor eradication and T cell persistence in NSG mice bearing diffuse metastatic prostate cancer, compared to both second-generation CARs Pd28z and PdBBz.

#### Conclusions

4-1BBL Turbocharged CAR T cells thus seem to possess striking therapeutic potential against solid tumors.

## Biomarkers and Immune Monitoring

Presenting author underlined; Primary author in italics

56

WITHDRAWN

57

### PD-L1 and immune infiltrates are prognostic and differentially expressed in distinct subtypes of gastric cancer

Helen K Angell<sup>1</sup>, Kyoung-Mee Kim<sup>2</sup>, Seung-Tae Kim<sup>2</sup>, Sung Kim<sup>3</sup>, Alan D Sharpe<sup>4</sup>, Julia Ogden<sup>4</sup>, Anna Davenport<sup>5</sup>, Darren R Hodgson<sup>4</sup>, Carl Barrett<sup>6</sup>, Jeeyun Lee<sup>3</sup>, Elaine Kilgour<sup>4</sup>

<sup>1</sup>AstraZeneca, Cambridge, England, UK

<sup>2</sup>Samsung Medical Center, Seoul, Norway

<sup>3</sup>Samsung Medical Center, Sungkyunkwan University School of Medicine, Norway

<sup>4</sup>AstraZeneca, Macclesfield, England, UK

<sup>5</sup>University Hospital of South Manchester, Manchester, England, UK

<sup>6</sup>AstraZeneca, Waltham, MA, USA

#### Background

Gastric cancer (GC) is often diagnosed at an advanced stage, for which therapeutic options are largely limited to cytotoxic chemotherapy and five-year survival is less than 20%. Immune checkpoint blockade with anti-programmed cell death-1 (PD-1) or anti-programmed cell death ligand-1 (PD-L1) antibodies is emerging as a promising therapeutic approach for several cancer types. An important question is whether the clinical efficacy of PD-1/PD-L1 checkpoint blockade can be improved through combination with targeted agents, such as trastuzumab, for use in human epidermal growth factor receptor 2 (HER2)-positive disease and olaparib, a poly (ADP-ribose) polymerase (PARP) inhibitor. This study determines the association of PD-L1 expression and immune cell infiltrates with clinical outcome and investigates the overlap of these with microsatellite instability (MSI)-high, ATM low and HER2 high segments.

#### Methods

PD-L1 membrane expression on tumour cells (TC) and infiltrating immune cells (IC), CD3+ T lymphocytes, CD8+ cytotoxic T cells, ATM and HER2 were assessed by immunohistochemistry (IHC) in a cohort of 380 Korean gastric cancer patients. PD-L1 positivity was assessed by a pathologist (positive < 0%). CD3 and CD8 were quantified by HALO® image analysis (cells/mm<sup>2</sup>). EBV status was determined using *in situ* hybridization and MSI status was performed using PCR and MLH1 IHC.

#### Results

The ATM-low and HER2-high segments are mutually exclusive and differ markedly in their immune profile; the ATM-low segment being enriched for MSI ( $p < 0.01$ ), PD-L1 TC

positivity ( $p < 0.01$ ) and CD8+ cytotoxic immune infiltrates ( $p=0.033$ ), while the HER2 segment is enriched for MSS, with no enrichment for immune markers. The PD-L1 segment is associated with increased T cell infiltrates: CD3 ( $p < 0.01$ ) and CD8 ( $p < 0.01$ ), while the MSI-high segment is enriched for PD-L1 TC ( $p < 0.01$ ), PD-L1 IC ( $p < 0.001$ ), CD3 ( $p < 0.05$ ) and CD8 ( $p < 0.01$ ), and has significant overlap with the ATM-low but not HER2 segments. Multivariate analysis confirmed PD-L1 TC positivity ( $p < 0.01$ ), high CD3 (overall survival [OS]  $P < 0.01$ ; disease-free survival [DFS]  $p=0.021$ ) and high CD8 (OS  $p < 0.01$ ; DFS  $p=0.027$ ) as independent prognostic factors for both DFS and OS. Patients with MSI-high tumours had better overall survival by both univariate ( $p < 0.01$ ) and multivariate ( $p < 0.05$ ) analysis.

#### Conclusions

Here we present evidence for segmentation of gastric cancers into four distinct molecular segments, namely ATM-low, HER2-high, PD-L1 positive and MSI-high. This illustrates the potential for subsets of GC patients to respond differently to immune therapy and the opportunity to employ different strategies for maximising the benefit from immune therapies in these segments.

58

### Four color T and B cell ELISPOT assays for simultaneous detection of analytes

Jodi Hanson, Richard Caspell, Alexey Karulin, Paul Lehmann

Cellular Technology Ltd, Shaker Hts, OH, USA

#### Background

ELISPOT assays are a key research tool for enumerating antigen-specific T and B cells in PBMC. As both T and B cells occur in major classes, immune monitoring has to be concerned with identifying these as well. So far, ELISPOT assays have been primarily done single or double color. In this report, we demonstrate the development of four color T and B cell ELISPOT assays.

#### Methods

PBMC were cultured for 4 days with a peptide pool of CMV-, EBV- and Flu- viruses for T cell assays or polyclonal B cell activators for B cell assays. On day 4, cells were washed, counted and plated in a low autofluorescence PVDF plate. Plates were precoated with capture antibodies for detection of IFN-g, IL-2, GzB, or TNF- $\alpha$  (T cell assays) or Ig secretion (B cell assays). During a 4h culture, the cytokine or antibodies secreted by the individual T or B cells respectively was captured on the membrane. The plate-bound "spots" were visualized using cytokine-specific or IgG subclass- or Ig class-specific detection reagents, whereby each detection reagent is distinguished from the other 3 reagents through its unique





## Biomarkers and Immune Monitoring

*Presenting author underlined; Primary author in italics*

fluorescence. The four-color assays were analyzed using an ImmunoSpot® S6 Analyzer.

### Results

We show that the four color assay has the same sensitivity for detecting individual cells secreting analytes as the respective single color assays, and that the four fluorescent colors can be discerned unambiguously, without overlap. Cells secreting any of the four analytes can therefore be identified unambiguously in an automated fashion, without the need for compensation. Cells co-expressing analytes can be identified by superimposing the individual colors. Studying B cells and T cells experimentally has permitted us to verify the accuracy of co-expression measurements. Each B cell secretes only one type of Ig class/subclass. T cells, in contrast, frequently coexpress cytokines. Serial dilution experiments showed that for T cells the numbers of co-expressors linearly decreased with the numbers of cells plated. For B cells, no coexpressors were found.

### Conclusions

The feasibility of four color T and B cell assays have been shown here. This is particularly important when conserving cell material thereby allowing researchers the opportunity for comprehensive immune monitoring spanning multiple cytokines.

59

### **A positive control for the detection of functional CD4 T cells in human PBMC – CPI protein pool**

Tameem Ansari, Annemarie Schiller, Srividya Sundararaman, Paul Lehmann

Cellular Technology Ltd, Shaker Heights, OH, USA

### Background

Testing of PBMC for immune monitoring purposes requires verification of their functionality. This is of particular concern when testing cryopreserved PBMC or cells that have been shipped, stored for prolonged periods of time. The CEF peptide pool has been developed as a positive control for CD8 cell functionality. A positive control for detecting CD4 memory cell functionality so far is lacking.

### Methods

Protein antigens from infectious/ environmental organisms have been selected that are ubiquitous. T cell reactivity to these antigens has been tested in an IFN-g Immunospot® assay from CTL. Cryopreserved PBMC from 100 Caucasian donors were selected from CTL's ePBMC database for testing. Magnetic bead depletion experiments were performed to verify CD4 or CD8 response.

### Results

Of an initial selection of 12 antigenic systems, (Varicella, Influenza, Parainfluenza, Mumps, Cytomegalovirus, Streptococcus, Mycoplasma, Lactobacillus, Neisseria, Candida, Rubella, and Measles) 3 were selected as a) eliciting CD4 cells exclusively and b) eliciting recall responses in the majority of donors. While individually none of the antigens triggered recall responses in all of the donors, the pool of these three antigens did. Only 2 of 100 donors did not respond to the CPI (Cytomegalo-, Epstein Barr-, and Influenza- virus) protein pool. These two however were impaired functionally non-viable cells with increased numbers of dead and apoptotic cells and showed increased apoptotic progression. Comparisons with CEF peptide pool, showed clear cut responses in ~50% of donors, borderline responses in xx and no responses in 30% of donors.

### Conclusions

CPI protein pool is suited as a positive control in Caucasians. Studies are on the way to establish the suitability of this pool for functionality testing in Asians and Africans.

60

### **Maximizing odds for detecting a positive T cell response by ELISPOT**

Jodi Hanson, Diana Roen, Alexey Karulin, Paul Lehmann

Cellular Technology Ltd, Shaker Heights, OH, USA

### Background

It has been a matter of debate to determine the best cutoffs in ELISPOT assay analysis for the unambiguous identification of a positive T cell response. At present, the answers to the above question is largely based on empirical or mixed criteria. To come up with scientifically validated answers, parametric statistical analysis has to be used, which in turn requires knowledge about the distributional properties of ELISPOT counts in replicate wells.

### Methods

PBMC of HLA-A2-0201 positive human subjects who had been infected with HCMV were plated with a HCMV peptide antigen (CEF-7 peptide, pp65 (495-503)) at 100,000 cells per well in IFH-g ELISPOT assays. However, we selected donors whose PBMC, when tested at 100,000 cells per well and challenged with the HLA-A2-0201-restricted HCMV peptide, pp65(495-503) did not display spot counts over medium background. We tested the PBMC for pp65 reactivity in 96 replicate wells to establish the distributional properties of these low frequency ELISPOTS. The distributional properties of the spot counts in the replicate wells were analyzed using diagnostic plots (QQ plots) and the Shapiro-Wilk normality tests.

## Biomarkers and Immune Monitoring

Presenting author underlined; Primary author in italics

### Results

We observed that increasing the number of PBMC plated per well resulted in higher positive to negative count ratio, lower relative experimental error (CV), and higher power for detecting pp65-induced positive responses without causing false positive results from HCMV negative subjects. This decrease of CV and increase in the power of the test was directly proportional to the numbers PBMC plated. The distributional properties showed that the spot counts in replicate wells follow Normal distribution. We showed that parametric statistics, such as Student's t test can be used and provide higher statistical power detecting weak positive HCMV responses than nonparametric methods (Wilcoxon or DFR). We also show that compared to increasing cell numbers per well, the increase of replicate wells is a more efficacious means of establishing positivity when statistical analysis is at the limits of confidence.

### Conclusions

The Normal distribution of ELISPOT counts permits us to make precise predictions regarding the numbers of replicate wells needed, and cut off values, especially when responses from donors are low.

### 61

#### Association between microsatellite instability and clinical response across tumor types in the phase Ib KEYNOTE-012 and KEYNOTE-028 studies of pembrolizumab in PD-L1-expressing advanced solid tumors

Mark Ayers<sup>1</sup>, Diane Levitan<sup>2</sup>, Gladys Arreaza<sup>2</sup>, Fang Liu<sup>2</sup>, Robin Mogg<sup>2</sup>, Yung-Jue Bang<sup>3</sup>, Bert O'Neil<sup>4</sup>, *Razvan Cristescu*<sup>2</sup>

<sup>1</sup>Merck & Co., Inc., West Point, PA, USA

<sup>2</sup>Merck & Co., Inc., Kenilworth, NJ, USA

<sup>3</sup>Seoul National University College of Medicine, Seoul, Republic of Korea

<sup>4</sup>Indiana University Health University Hospital, Indianapolis, IN, USA

### Background

High levels of microsatellite instability (MSI-H) can occur in some patients with colorectal cancer (CRC) due to defects in mismatch repair (MMR). In the phase II KEYNOTE-016 study, MSI-H CRC patients were more responsive to PD-1 inhibition with pembrolizumab, as were MSI-H non-CRC patients. Here, we evaluate loss of *MLH1* gene expression across tumor types, and effect of MSI status on clinical response to pembrolizumab in the KEYNOTE-012 and KEYNOTE-028 studies in patients with recurrent, metastatic tumors including breast, gastric, urothelial, and CRC tumors.

### Methods

Microarray analysis of loss of *MLH1* gene expression was used as a surrogate for MSI-H status to assess prevalence of MSI-H in the proprietary Moffitt database of approximately 18,000 annotated, archived tumors. MSI status of tumors from KEYNOTE-012 and KEYNOTE-028 was evaluated using the Promega MSI Analysis system v1.2. Microsatellite markers were amplified from DNA isolated from tumors and separated and size analyzed by capillary electrophoresis. MSI-H status was identified by comparison of formalin-fixed, paraffin-embedded tumor samples to matched blood DNA. Samples were MSI-H if 2 or more markers changed or non-MSI-H if 1 or no markers changed relative to blood. Logistic regression analyses assessed the correlation between MSI status and overall response rate (ORR, centrally-assessed RECIST v1.1).

### Results

In the Moffitt database, loss of *MLH1* expression mirrored results from a clinical MSI immunohistochemistry assay in CRC patients. Loss of *MLH1* expression also correlated with mutational load. Inferred MSI-H status was identified across multiple tumor types (aggregate prevalence 3.2%) in the Moffitt database (Figure 1). In KEYNOTE-012 (n=96) and KEYNOTE-028 (n=265), MSI-H status was identified in 6% and 2% of patients, respectively, (3% overall), similar to the unselected population in the Moffitt database. Gastric cancer had the highest prevalence (n=4 patients), with estrogen receptor positive breast, biliary, esophageal, triple negative breast, endometrial, CRC, and bladder tumors also having MSI-H in at least one patient. For patients with MSI and response data (n=310), ORR was 70% versus 12% (1-sided p=0.0001) in those with MSI-H and non-MSI-H status, respectively.

### Conclusions

In this retrospective analysis, identification of MSI-H status was associated with a statistically relevant increase in response to pembrolizumab. This suggests that determination of MSI-H status may be predictive of response to pembrolizumab regardless of histology. The association between MSI-H status and clinical benefit of anti-PD-1 therapy is being evaluated in ongoing studies (KEYNOTE-158 [NCT02628067], KEYNOTE-164 [NCT02460198], and KEYNOTE-177 [NCT02563002]).

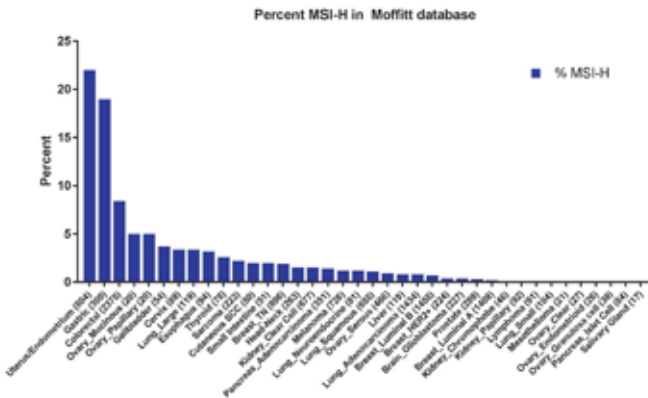
### Trial Registration

ClinicalTrials.gov identifier NCT01848834 and NCT02054806.

# Biomarkers and Immune Monitoring

Presenting author underlined; Primary author in italics

**Figure 1**



62

## Whole-blood RNA transcript-based signatures predict pre- and post-treatment response in two large independent clinical studies of patients with advanced melanoma treated with tremelimumab

*Philip Friedlander*<sup>1</sup>, Karl Wassman<sup>2</sup>, Chrisann Kyi<sup>1</sup>, William Oh<sup>1</sup>, Nina Bhardwaj<sup>3</sup>

<sup>1</sup>Icahn School of Medicine at Mount Sinai, New York, NY, USA

<sup>2</sup>Check Point Sciences, Cambridge, MA, USA

<sup>3</sup>Tish Cancer Institute, Icahn School of Medicine at Mount Sinai, New York, NY, USA

### Background

Tremelimumab is a cytotoxic T lymphocyte-associated antigen-4-blocking monoclonal antibody. An unmet clinical need exists for blood-based response-predictive gene signatures to facilitate use of cancer immunotherapy in the most clinically effective and cost-efficient manner.

### Methods

Pre- and post-treatment (30 days) peripheral blood samples were taken from 210 treatment-naïve melanoma patients receiving tremelimumab in a worldwide, multicenter phase III study. Objective response was determined by an expert panel of radiologists using RECIST criteria. 169 mRNA transcripts were measured for the n=210 patients using reverse transcription polymerase chain reaction (RT-PCR) [1]. Pre- and post-treatment response-predictive signatures were identified in the n=210 training dataset. An independent population of n=150 refractory/relapsed melanoma patients receiving tremelimumab after chemotherapy enrolled in a worldwide, multicenter phase II study [2] was the test dataset.

### Results

A 16-gene pre-treatment and 8-gene post-treatment mRNA signatures were identified in the n=210 training dataset. These pre- and post-treatment signatures were tested in the

n=150 test dataset first, for objective response as determined by RECIST criteria, and second for one-year survival after treatment. The same genes, coefficients and constant from the training dataset were used in the test cases with the results in Table 1. Both the 16-gene pre- and 8-gene post-treatment response-prediction training gene signatures validated when compared to objective response in the test dataset. The one-year survival criteria also validated with even higher AUC's for both pre- and post-treatment.

### Conclusions

This is the first large clinical study of tremelimumab, independently validated in a second large clinical study, to show both pre- and post-treatment response-predictive mRNA signatures in blood. The pre-treatment biological signature may represent expression levels of particular immune system genes that are needed for a robust immune response against cancer. They may identify patients whose immune systems are already primed to fight the cancer and are particularly amenable to a boost in effectiveness provided by immunotherapy. The 30-day post-treatment biological signature represents a timely way to determine whether the patient is responding positively to the immunotherapy.

### Trial Registration

ClinicalTrials.gov identifier NCT00257205.

### References

- Ribas A, *et al*: Phase III randomized clinical trial comparing tremelimumab with standard-of-care chemotherapy in patients with advanced melanoma. *J Clin Oncol* 2013, **31(5)**:616-622.
- Kirkwood JM, *et al*: Phase II trial of tremelimumab (CP-675,206) in patients with advanced refractory or relapsed melanoma. *Clin Cancer Res* 2010, **16(3)**:1042-1048.

**Table 1**

	Pre-Treatment Blood-Based 16-Gene mRNA Signature			Post-Treatment Blood-Based 8-Gene mRNA Signature		
	Training Cases N=210	Test Response N=150	Test Survival N=150	Training Cases N=210	Test Response N=150	Test Survival N=150
Biomarker Response	96.4%	65.0%	74.4%	85.7%	70.0%	69.8%
Sensitivity	96.4%	65.0%	74.4%	85.7%	70.0%	69.8%
Specificity	66.5%	59.2%	55.1%	64.3%	60.8%	59.8%
NPV	99.2%	91.7%	84.3%	96.7%	92.9%	83.1%
AUC	0.8634	0.6376	0.6785	0.7853	0.6125	0.6512

63

## Extensive analysis of PD-1 and CTLA-4 in HVs and GBM patients: implications for monitoring patients on checkpoint inhibitors

*Svetlana Bornschlegl*, Michael P Gustafson, Dennis A Gastineau, Ian F Parney, Allan B Dietz

Mayo Clinic, Rochester, MN, USA

## Biomarkers and Immune Monitoring

Presenting author underlined; Primary author in italics

### Background

Checkpoint inhibitors are becoming widely used for immunotherapy but methods to monitor dosing and duration for each individual patient needs to be more fully understood. Immune monitoring by flow cytometry is a tool that can be utilized for measuring responses to immunotherapy in patients. In this study we assessed the expression of PD-1 and CTLA-4 on numerous cell types in healthy volunteers (HVs) and glioblastoma (GBM) patients enrolled in a dendritic cell clinical trial.

### Methods

Peripheral blood was collected from 20 HV and 20 GBM patients receiving a DC vaccine in a clinical trial. Whole blood was stained using a previously established method for the identification of multiple cell populations by flow cytometry and novel analysis that captures data on over 120 phenotypes [1]. An extended analysis focused on T cell phenotypes was performed using markers for CD154, CD45RO, CD56, CD3, CD8, CD28, CD4, and CD45. T cell parent populations were characterized by SS, FS, CD45<sup>+</sup>, CD3<sup>+</sup>, CD4<sup>+</sup>, CD8<sup>+</sup>, CD4<sup>+</sup>/CD8<sup>+</sup> sub populations. Non-T cell populations were assessed by various gating strategies. These populations were measured for PD-1<sup>+</sup>, CTLA4<sup>+</sup>, DP, and DN populations.

### Results

We identified 15 parent populations, of which 11 expressed PD-1 and 9 expressed CTLA-4. Within subsets of the parent populations we found statistically significant differences ( $p < 0.001$ ) in PD-1 between CD8<sup>+</sup> memory and CD8<sup>+</sup> naïve cells, CD4<sup>+</sup> memory and CD4<sup>+</sup> naïve cells, CD8<sup>+</sup> NKT and CD8<sup>+</sup>CD3<sup>+</sup> cells, as well as NKT and NK cells. These statistical differences hold true for both HV and GBM patients. We also found HVs to have higher levels of CTLA-4 on CD4<sup>+</sup>CD8<sup>+</sup> cells and B cells compared to GBM patients, and lower levels of PD-1 on CD8<sup>+</sup> and naïve CD8<sup>+</sup> cells.

### Conclusions

This panel allows us to measure approximately 60 phenotypes related to checkpoint proteins. The data presented here identify PD-1 and CTLA-4 phenotypic differences within parent populations, within subsets of parent populations, and differences in healthy volunteers compared to GBM patients. These results may help optimize the targeting of checkpoint proteins as well as other immunotherapeutic approaches in clinical trials.

### Acknowledgements

This study is funded in part by the Ivy Foundation.

### Trial Registration

ClinicalTrials.gov identifier NCT01957956.

### References

1. Gustafson MP, *et al*: **A method for identification and analysis of non-overlapping myeloid immunophenotypes in humans.** *PLoS ONE* 2015, **10.3**:e0121546.

### 64

#### Objective measurement and clinical significance of IDO1 protein in hormone receptor-positive breast cancer

Daniel Carvajal-Hausdorf<sup>1</sup>, Nikita Mani<sup>1</sup>, Vamsidhar Velcheti<sup>2</sup>, Kurt Schalper<sup>1</sup>, David Rimm<sup>1</sup>

<sup>1</sup>Yale University School of Medicine, New Haven, CT, USA

<sup>2</sup>Cleveland Clinic Main Campus, Cleveland, OH, USA

### Background

Immunostimulatory therapies targeting immune suppressive pathways produce durable clinical responses in advanced solid tumors. Indoleamine 2, 3-dioxygenase (IDO) is the rate-limiting oxidoreductase that catalyzes the degradation of tryptophan to kynurenine. IDO induces immune tolerance by downregulating CD8<sup>+</sup> and effector CD4<sup>+</sup> T cell responses. IDO1, the most active isoform, is expressed in diverse tumor types and can be targeted using small molecule inhibitors. Here, we used a validated quantitative in situ assay to measure the levels of IDO1 protein in a retrospective collection of hormone receptor-positive breast cancer (BC).

### Methods

IDO1 was measured using quantitative immunofluorescence (QIF) in 362 stage I-III hormone-receptor-positive breast carcinomas represented in tissue microarray format. The levels of IDO1 were determined in the tumor compartment; and were stratified using the median as cut-point. The association between IDO1 levels, clinico-pathological features, CD3<sup>+</sup>, CD8<sup>+</sup> and CD20<sup>+</sup> tumor-infiltrating lymphocytes (TIL) and survival was studied.

### Results

IDO1 protein was detected in 76.2% of hormone receptor-positive BC. There was no significant association between IDO1 levels and major clinico-pathological characteristics. Increased IDO1 correlated with decreased CD20<sup>+</sup> infiltration ( $P=0.0004$ ) but not with changes in CD3<sup>+</sup> or CD8<sup>+</sup> levels. Elevated IDO1 expression was associated with worse 20-year overall survival (log-rank  $P=0.02$ , HR=1.39, 95% C.I.: 1.05-1.82). IDO1 scores were independently associated with outcome in multivariable analysis.

### Conclusions

IDO1 protein is expressed in the majority of hormone receptor-positive BC and is an independent negative prognostic marker. Additionally, IDO1 expression is negatively associated with tumor B cell infiltration. Measurement of IDO1 has the potential to identify a population that might derive benefit from IDO1 blockade.





## Biomarkers and Immune Monitoring

Presenting author underlined; Primary author in italics

### References

1. Munn DH, Zhou M, Attwood JT, Bondarev I, Conway SJ, Marshall B, *et al*: **Prevention of allogeneic fetal rejection by tryptophan catabolism.** *Science* 1998, **281(5380)**:1191-1193.
2. Uyttenhove C, Pilotte L, Theate I, Stroobant V, Colau D, Parmentier N, *et al*: **Evidence for a tumoral immune resistance mechanism based on tryptophan degradation by indoleamine 2,3-dioxygenase.** *Nat Med* 2003, **9(10)**:1269-1274.
3. Ling W, Zhang J, Yuan Z, Ren G, Zhang L, Chen X, *et al*: **Mesenchymal stem cells use IDO to regulate immunity in tumor microenvironment.** *Cancer Res* 2014, **74(5)**:1576-1587.
4. Schalper KA, Carvajal-Hausdorf D, McLaughlin J, Altan M, Velcheti V, Gaule P, *et al*: **Differential expression and significance of PD-L1, IDO-1 and B7-H4 in human lung cancer.** *Clin Cancer Res* 2016.

### 65

#### **CD8+ T cell subsets may be associated with response to anti-CD137 agonist antibody treatment**

Serena Chang<sup>1</sup>, Ronald Levy<sup>1</sup>, John Kurland<sup>2</sup>, Suba Krishnan<sup>2</sup>, Christoph Matthias Ahlers<sup>2</sup>, Maria Jure-Kunkel<sup>2</sup>, Lewis Cohen<sup>2</sup>, Holden Maecker<sup>1</sup>, Holbrook Kohrt<sup>1</sup>

<sup>1</sup>Stanford University School of Medicine, Stanford, CA, USA

<sup>2</sup>Bristol-Myers Squibb, Princeton, NJ, USA

#### **Background**

Cancer immunotherapies historically, have low success rates. One way to increase these success rates involves investigating baseline or early response biomarkers that predict success. Selecting patients with early biomarkers for success and competent immune status are essential when choosing the best therapeutic strategy. CD137 agonists, activators of T and NK cells and a promising newer immunotherapy, have dramatically reduced tumor size and disease in murine tumor models [1] and are currently being examined in clinical trials [2].

#### **Methods**

This study investigated the immune response and potential early immune biomarkers in both solid tumor and hematologic cancer patients participating in the phase I BMS-663513 NCT01471210 clinical trial of urelumab monotherapy. We used peripheral blood mononuclear cells to determine the circulating immune competence of patients (n=8) before treatment (baseline/C1D1), 24 hours after the first treatment (C1D2), before the second treatment (C2D1), and up to 30 days after the third treatment (C3R). Analysis was performed using mass cytometry, surveying 38 different immune proteins simultaneously.

### Results

At all time points, we observed a trend toward higher central memory and naïve CD8+ T cells in patients with stable disease (n=3) or partial response (n=1) vs. progressors (n=4), while the opposite was true in effector and effector memory RA cells. The most striking difference was seen when considering all CD8+CD27+ T cells, which were higher in those with stable disease or partial response, at all time points. CD8+FcεR1α+ T cells showed a similar trend, albeit to a lesser extent, while CD57+CD8+ T cells showed the opposite trend. CD8+ T cells in both groups were comparably responsive to PMA/ionomycin stimulation, producing multiple cytokines. These trends were not seen in CD4+ T cells or with head and neck solid tumor patients treated with cetuximab.

### Conclusions

The aforementioned trends suggest that CD27+CD8+ T cells, and possibly other subsets of CD8+ T cells, should be further explored to determine whether they predict response to anti-CD137 agonist therapy. They also suggest that potential predictive measures of immune status prior to immunotherapy are detectable in peripheral blood.

### References

1. Sabel MS, *et al*: **Monoclonal antibodies directed against the T-cell activation molecule CD137 (interleukin-A or 4-1BB) block human lymphocyte-mediated suppression of tumor xenografts in severe combined immunodeficient mice.** *J Immunother* 2000, **23(3)**:362-368.
2. Sznol M, *et al*: **Phase I study of BMS-663513, a fully human anti-CD137 agonist monoclonal antibody, in patients (pts) with advanced cancer** *J. Clin Oncol* 2008.

### 66

#### **Regulation of PD-L1 expression in melanoma and immune cells**

Shuming Chen<sup>1</sup>, George Crabill<sup>1</sup>, Theresa Pritchard<sup>1</sup>, Tracee McMiller<sup>1</sup>, Drew Pardoll<sup>2</sup>, Fan Pan<sup>2</sup>, Suzanne Topalian<sup>1</sup>

<sup>1</sup>Department of Surgery, Johns Hopkins University School of Medicine, Sidney Kimmel Comprehensive Cancer Center, and Bloomberg-Kimmel Institute for Cancer Immunotherapy, Baltimore, MD, USA

<sup>2</sup>Department of Oncology, Johns Hopkins University School of Medicine, Sidney Kimmel Comprehensive Cancer Center, and Bloomberg-Kimmel Institute for Cancer Immunotherapy, Baltimore, MD, USA

#### **Background**

The therapeutic effects of PD-1/PD-L1 inhibition in multiple cancers indicates a critical role for this pathway in immunosuppression in the tumor microenvironment (TME), but factors regulating PD-L1 expression on tumor

## Biomarkers and Immune Monitoring

*Presenting author underlined; Primary author in italics*

and immune cells are poorly understood. The dichotomous transcription factors STAT1 and STAT3 have both been reported to bind the PD-L1 promoter. The current study investigates the role of STAT1/3 and other signaling in cytokine-induced PD-L1 expression on human melanoma (MEL) cells and monocytes.

### Methods

Seventeen cultured MELs or short-term monocyte cultures were treated with recombinant cytokines including IFN-g, IL-6, IL-10, IL-32g, or TNF-a. PD-L1 cell surface protein expression was detected by flow cytometry, and mRNA by quantitative real-time RT-PCR (qRT-PCR). STAT1 or/and STAT3 were knocked down by small interfering RNAs (siRNAs). Total and phosphorylated STAT1/3 proteins were quantified by Western blotting.

### Results

While PD-L1 is expressed on 35-40% of MELs *in situ*, it was not expressed on 17 cultured MELs. IFN-g significantly enhanced PD-L1 protein expression on MELs ( $p=0.0003$ ), increasing PD-L1 mRNA expression (qRT-PCR) in association with PD-L1 cell surface protein expression (FACS) in all MELs tested ( $p=0.0004$ ). This suggests that IFN-g regulates PD-L1 expression primarily at the transcriptional level and not via translocation of intracellular protein stores. Enhanced PD-L1 expression in IFN-g-treated MELs correlated with increased STAT1 phosphorylation ( $p=0.05$ ). Consistent with this, siRNA knockdown of STAT1 reduced PD-L1 expression by 40-70% in 2 MELs after 24-48hr IFN-g exposure. In contrast, STAT3 knockdown reduced IFN-g-induced PD-L1 expression by only 12-15%, on one of two MEL lines. In cultured monocytes from two donors, PD-L1 mRNA expression was induced by IFN-g, IL-10, IL-32-g and TNF-a, and significantly correlated with PD-L1 cell surface protein expression, suggesting that these cytokines acted at the transcriptional level. In monocytes, IFN-g was associated with markedly increased pSTAT1, and IL-10 with increased pSTAT3. These cytokines were not associated with increased pp65 or focal adhesion kinase (FAK) phosphorylation in monocytes.

### Conclusions

In addition to IFN-g, other cytokines in the TME may play important, coordinate and selective roles in promoting PD-L1 expression on different cell types including tumor and stromal cells. pSTAT1 and pSTAT3 are associated with PD-L1 protein expression in response to different cytokine stimuli. Future studies will further characterize cytokine-triggered transcription factors and signaling pathways responsible for PD-L1 expression on tumor cells and immune cells. Understanding mechanisms regulating PD-L1 expression will help guide the development of more optimal predictive biomarkers and combinatorial therapies based on anti-PD-1.

67

## Gene expression markers of tumor infiltrating leukocytes

*Patrick Danaher*<sup>1</sup>, Sarah Warren<sup>1</sup>, Lucas Dennis<sup>1</sup>, Andrew M White<sup>1</sup>, Leonard D'Amico<sup>2</sup>, Melissa Geller<sup>3</sup>, Mary L Disis<sup>2</sup>, Joseph Beechem<sup>1</sup>, Kunle Odunsi<sup>4</sup>, Steven Fling<sup>2</sup>

<sup>1</sup>NanoString Technologies, Seattle, WA, USA

<sup>2</sup>University of Washington, Seattle, WA, USA

<sup>3</sup>University of Minnesota, Minneapolis, MN, USA

<sup>4</sup>Roswell Park Cancer Institute, Buffalo, NY, USA

### Background

Assays of the abundance of immune cell populations in the tumor microenvironment promise to inform immune oncology research and the choice of immunotherapy for individual patients. We propose to measure the intratumoral abundance of various immune cells populations with gene expression. In contrast to IHC and flow cytometry, gene expression assays yield high information content from a clinically practical workflow. Previous studies of gene expression in purified immune cells have reported hundreds of genes showing enrichment in a single cell type, but the utility of these genes in tumor samples is unknown. We describe a novel statistical method for using co-expression patterns in large tumor gene expression datasets to validate previously reported candidate cell type marker genes.

### Methods

We used co-expression patterns in 9986 samples from The Cancer Genome Atlas (TCGA) to validate previously reported cell type marker genes. We compared immune cell scores derived from these genes to measurements from flow cytometry and immunohistochemistry. We characterized the reproducibility of our cell scores in replicate runs of RNA extracted from FFPE tumor tissue.

### Results

We identified a list of 60 marker genes whose expression levels quantify 14 immune cell populations. Cell type scores calculated from these genes are concordant with flow cytometry and IHC readings, show high reproducibility in replicate RNA samples from FFPE tissue and reveal an intricate picture of the immune infiltrate in TCGA. Most genes previously reported to be enriched in a single cell type have co-expression patterns inconsistent with cell type specificity.

### Conclusions

Due to their concise gene set, computational simplicity and utility in tumor samples, these cell type gene signatures may be useful in future discovery research and clinical trials to understand how tumors and therapeutic intervention shape the immune response.



# Biomarkers and Immune Monitoring

Presenting author underlined; Primary author in italics

**Figure 1. Comparison of gene expression and flow cytometry cell type measurements in PBMCs.**

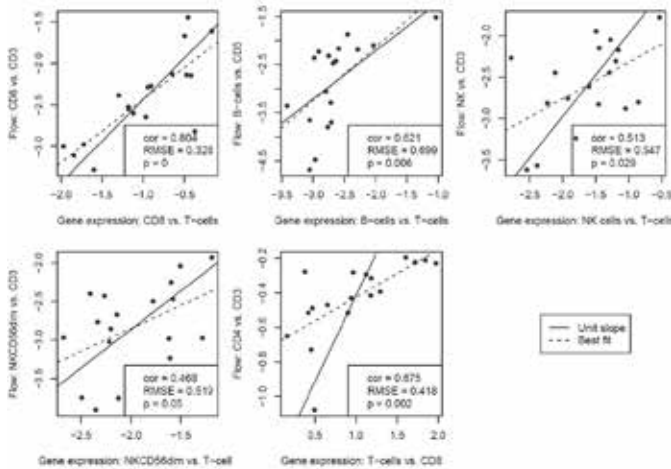


**Figure 2. Comparison of gene expression and IHC cell type measurements in FFPE.**

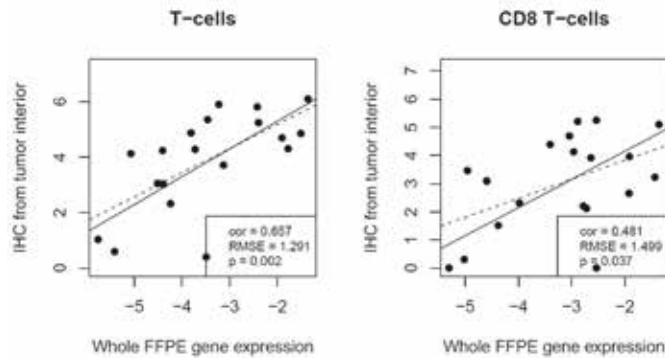
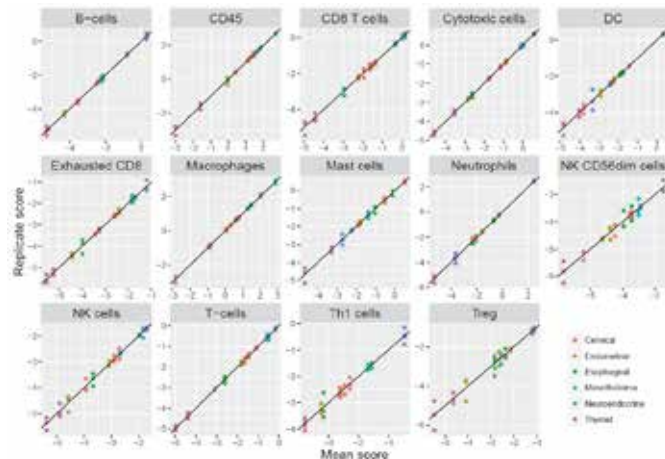


**Figure 3. Reproducibility of gene expression measurements of immune cell types**



68

## Quantitative real-time PCR based diagnostic to assess NKT cell function in breast cancer patients

Roshanak Derakhshandeh, Tonya J Webb

University of Maryland, Baltimore, Baltimore, MD, USA

### Background

Breast cancer is a leading cause of cancer-related death among women worldwide. Although, surgery, radiotherapy, and chemotherapy have improved the 5-year survival rate, new treatment methods are needed to combat this disease. To date, significant efforts have been invested into harnessing the therapeutic potential of the immune system for the treatment of cancer. However, tumor tolerance and immune suppression can severely limit its therapeutic efficacy. In fact, natural killer T (NKT) cells play an important role in cancer immune surveillance, but are reduced in cancer patients. In order to assess which patients will likely benefit from immune cell-based therapies, we have developed a quantitative method to rapidly assess the baseline function of NKT cells using stimulation with artificial antigen presenting cells followed by and quantitative real-time PCR (aAPC-qPCR).

### Methods

In this study, we assessed NKT cell number and function in healthy donors and breast cancer patients by flow cytometry, ELISA, and qPCR. In addition, we assessed the percentage of tumor-infiltrating lymphocytes and PD-L1 expression within the tumor microenvironment by immunohistochemistry.

### Results

Although % circulating NKT cell were significantly reduced in breast cancer patients (BCP), compared to healthy donors (HD), we detected NKT cell function in 82% HD (n=22) and 70% BCP (n=30). We compared high responders (high IFN- $\gamma$  induction) to low responders and found that there was no significant difference in NKT cell number between these two groups. Following further characterization of these groups, it was found that low responders had a significant reduction in the induction of TNF $\alpha$ , LAG3, and LIGHT.

### Conclusions

In summary, this data we have developed a novel diagnostic platform using aAPC-qPCR to determine NKT cell function in patients. This technology is important because NKT cell number did not correlate with function in our breast cancer patient cohort. Thus, our studies demonstrate that there is a critical need to assess baseline immune function prior to the initiation of immunotherapy. Future studies can focus identifying new breast cancer classifications according to immune gene expression patterns, and these tumor subtypes may provide a basis for new therapeutic opportunities.

## Biomarkers and Immune Monitoring

Presenting author underlined; Primary author in italics

### Acknowledgements

Supported by NIH/NCI 1R21CA162273, R21CA184469, and R21CA199544 grants to Tonya Webb.

### References

1. Siegel RL, Miller KD, Jemal A: **Cancer Statistics 2015**. *CA Cancer J Clin* 2015, **65(1)**: 5-29.
2. Hermans IF, *et al*: **NKT cells enhance CD4+ and CD8+ T cell responses to soluble antigen in vivo through direct interaction with dendritic cells**. *J Immunol* 2003, **171(10)**: 5140-5147.

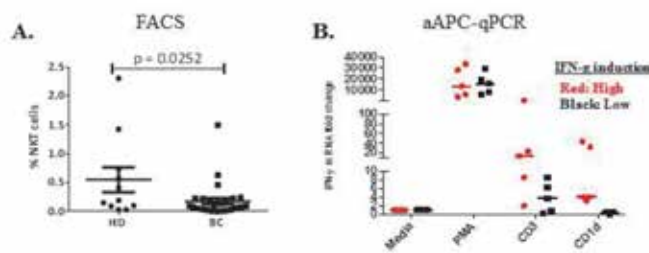


**Figure 1.** (A) Circulating % NKT cells are reduced in BC patients. Peripheral blood mononuclear cells (PBMC) were collected from healthy donors (HD) and breast cancer patients (BC), stained for NKT TCR and analyzed by flow cytometry. (B) NKT cell function correlates total T cell function in BC patients. PBMCs from BC patients were stimulated with CD1D-Ig aAPC loaded with  $\alpha$ -GalCer to specifically activate NKT cells or anti-CD3/CD28 to activate T cells. Media serves as a negative control and PMA/ionomycin was the positive control. After 4 hours, RNA was extracted and qPCR was performed to assess IFN-g and 18S. Fold induction was calculated relative to the control.

Figure 1. (A) Circulating % NKT cells are reduced in BC patients. Peripheral blood mononuclear cells (PBMC) were collected from healthy donors (HD) and breast cancer patients (BC), stained for NKT TCR and analyzed by flow cytometry. (B) NKT cell function correlates total T cell function in BC patients. PBMCs from BC patients were stimulated with CD1D-Ig aAPC loaded with  $\alpha$ -GalCer to specifically activate NKT cells or anti-CD3/CD28 to activate T cells. Media serves as a negative control and PMA/ionomycin was the positive control. After 4 hours, RNA was extracted and qPCR was performed to assess IFN-g and 18S. Fold induction was calculated relative to the control.

69

### Arming of CD56<sup>dim</sup> and CD56<sup>bright</sup> NK cells in IL-15-infused cancer patients

Sigrid Dubois, Kevin Conlon, Bonita Bryant, Jennifer Hsu, Nancy Beltran, Jürgen Müller, Thomas Waldmann

Lymphoid Malignancies Branch, Center for Cancer Research, National Cancer Institute, Bethesda, MD, USA

### Background

Survival and expansion of NK cells depends on interleukin (IL)-15. It has recently been shown that IL-15 infusions caused NK cell expansions in cancer patients. The objectives

of our study were to assess the effects of IL-15 on functions of CD56<sup>dim</sup> and CD56<sup>bright</sup> subpopulations of NK cells in IL-15-treated cancer patients.

### Methods

We monitored numbers, phenotypic changes, cytokine production and lytic activities of CD56<sup>dim</sup> and CD56<sup>bright</sup> NK cell subpopulations in the blood of cancer patients that had received daily infusions of 2  $\mu$ g/kg IL-15 for 10 days .

### Results

Ten-day continuous infusion of IL-15 led to expansions of both CD56<sup>dim</sup> and CD56<sup>bright</sup> subpopulations of NK cells. Phenotypic analyses revealed that IL-15 infusions caused the expression of CD56<sup>bright</sup>-typical surface proteins on CD56<sup>dim</sup> NK cells that included Trail, CD62L, NKG2D, CD94 and the IL-18 receptor, while CD56<sup>bright</sup> NK cells remained essentially unchanged. CD56<sup>bright</sup> NK cells retained their superior ability to produce IFN $\gamma$ /TNF $\alpha$  in responses to IL-12/IL-18 when compared with CD56<sup>dim</sup> NK cells, and IL-15 infusions increased the percentage of cytokine-producing CD56<sup>bright</sup> NK cells. The cytotoxic capacity of CD56<sup>dim</sup> NK cells remained superior to CD56<sup>bright</sup> NK cells even after IL-15 infusions. However, cytotoxic competencies were increased for both subpopulations after IL-15 infusions that resulted in substantial lytic activities via natural cytotoxicity receptors, stress receptors, and antibody-dependent cytotoxicity even among CD56<sup>bright</sup> NK cells.

### Conclusions

These data show that IL-15 infusions increase the functional abilities of both types of NK cells in cancer patients.

70

### Identification of a novel subset of tumor-resident human CD8+ T cells, marked by dual expression of CD103 and CD39

Rebekka Duhén<sup>1</sup>, Thomas Duhén<sup>2</sup>, Lucas Thompson<sup>3</sup>, Ryan Montler<sup>2</sup>, Andrew Weinberg<sup>1</sup>

<sup>1</sup>Earle A. Chiles Research Institute, Providence Cancer Center, Portland, OR, USA

<sup>2</sup>AgonOx, Inc., Portland, OR, USA

<sup>3</sup>Juno Therapeutics, Portland, OR, USA

### Background

Homing and retention of T cells in tissues is mediated by the interaction of adhesion molecules with their respective ligands. Among those, the integrin CD103 interacts with its ligand E-cadherin and allows T cells to home to epithelial tissues. T cells expressing high levels of CD103 have recently been identified as tissue-resident memory (T<sub>RM</sub>) cells and play a crucial role in protecting epithelial tissues against viral infections. Previous reports have shown that CD103+



## Biomarkers and Immune Monitoring

Presenting author underlined; Primary author in italics

CD8+ T cells were present in some but not all human solid malignancies.

### Methods

Cell sorting, gene expression analysis, and TCR sequencing.

### Results

Here, while confirming these data, we identify a subset of CD103+ CD8+ T cells that co-express the ectonucleotidase CD39. This subset is enriched in primary tumors and metastatic lymph nodes but absent in the blood and normal lymph nodes of cancer patients. We compared several tumor histologies and found highest frequencies in head and neck squamous cell carcinomas (HNSCC), ovarian, lung and rectal cancers (ranging from 20-80% of tumor-infiltrating CD8+ T cells), whereas those cells were absent or low in primary colon cancer and colorectal liver metastasis. Gene expression analysis of CD103/39 double positive CD8+ T cells revealed a gene signature reminiscent of T<sub>RM</sub> cells (CCR7<sup>lo</sup>, L-selectin<sup>lo</sup>, S1PR1<sup>lo</sup> and CD69<sup>hi</sup>), and their activated phenotype (HLA-DR<sup>hi</sup>, Ki67<sup>hi</sup>, Granzyme B<sup>hi</sup>) implies strong tumor reactivity. Furthermore, TCR repertoire analysis shows high clonality and distinct CDR3 sequences in this subset compared to other CD8+ T cells present in the tumor. Based on this phenotype, gene signature, circulation pattern and clonality, we believe that CD103/39 double positive CD8+ T cells are being chronically stimulated within the tumor microenvironment, and may recognize neoantigens. In support of this finding, our *in vitro* data suggests that expression of CD39 is upregulated as a result of strong, sustained TCR stimulation in naïve CD8+ T cells. Finally, to better address the role of those cells *in vivo* we examined 9 different solid murine tumor models. Unexpectedly, CD103/39 double positive CD8+ T cells were only found in the transgenic MMTV-PyMT breast cancer model. Utilizing this model, we plan to study their differentiation and function *in vivo* and address their antigenic specificity and role in tumor development.

### Conclusions

Taken together our findings suggest that targeting tumor-resident CD103/39 CD8+ T cells may be a promising approach to enhance immune-mediated tumor regression.

71

### Characterization of tumor infiltrating T cell receptor (TCR) repertoire in non-muscle invasive bladder cancer (NMIBC) patients treated with Bacillus Calmette-Guérin (BCG)

Max Kates<sup>1</sup>, Brandon Early<sup>2</sup>, Erik Yusko<sup>3</sup>, Taylor H Schreiber<sup>2</sup>, Trinity J Bivalacqua<sup>1</sup>

<sup>1</sup>Johns Hopkins University, Baltimore, MD, USA

<sup>2</sup>Heat Biologics, Durham, NC, USA

<sup>3</sup>Adaptive Biotechnologies, Seattle, WA, USA

### Background

Bladder cancer is the 5<sup>th</sup> most common malignancy in the US, and the majority of bladder cancer is diagnosed while confined to the most superficial layer (non-muscle invasive bladder cancer, NMIBC) [1]. Treatment goals in this minimal residual disease setting are ideal for immunotherapy: reduce local disease recurrence following surgical resection and prevent progression to muscle invasive bladder cancer (MIBC). Bacillus Calmette-Guérin (BCG), an attenuated form of *Mycobacterium bovis*, is an intravesical immunotherapy which remains the mainstay of NMIBC treatment since 1976. Despite the tenure in bladder cancer treatment, full characterization of the immunologic mechanism of action of BCG is still lacking [2]. In a pilot study, we sought to investigate the diversity of T cells infiltrating bladder tumors and compare the changes in T cell diversity among patients who were responders and unresponsive to BCG.

### Methods

Six patients were selected from the IRB-approved Johns Hopkins bladder cancer tumor repository. All patients had T1 disease without concurrent *carcinoma in situ* (CIS) and received standard of care BCG induction and maintenance. Three patients were classic “responders” to BCG, with disease-free intervals of 8, 28, and 34 months. Three patients were unresponsive to BCG: two patients progressed to MIBC and ultimately died of metastatic bladder cancer and one had recurrent disease requiring cystectomy. Pre-treatment and post-treatment tumor tissue samples were compiled; genomic DNA was isolated, amplified, and sequenced using Adaptive Biotechnologies’ ImmunoSeq assay.

### Results

ImmunoSeq technology surveyed the T cells in all 12 samples. Median fraction of T cells in the samples pre-treatment was 0.16 (95% CI, -0.419 to 0.731) while post-treatment median was 0.36 (95% CI, 0.184 to 0.532), indicating a trend towards a higher T cell fraction after treatment. Clonality, an objective measure of T cell diversity, was low in most patients and unchanged post-treatment: some T cell clones in the tumor samples expanded or contracted, though most clones were stable post-treatment, and no clones expanded to be dominant. Clonality likewise did not appear to correlate with patient response to BCG.

### Conclusions

Tumor infiltrating T cell kinetics do not appear to correlate with response to BCG in this pilot sample of patients. These data suggest that an alternative mechanism involving the innate immune cell population may be the primary driver of BCG response.

## Biomarkers and Immune Monitoring

Presenting author underlined; Primary author in italics

### References

1. **SEER Cancer Statistics Factsheets: Bladder Cancer.** National Cancer Institute. <http://seer.cancer.gov/statfacts/html/urinb.html>. Accessed 25 Jul 2016.
2. Biot C, *et al*: **Preexisting BCG-specific T cells improve intravesical immunotherapy for bladder cancer.** *Sci Transl Med* 2012, **4**:137ra72.

### 72

#### **An immune-related gene expression profile delineates features of the tumor microenvironment required for clinical response to PD-1 blockade**

Mark Ayers<sup>1</sup>, Jared Lunceford<sup>1</sup>, Michael Nebozhyn<sup>1</sup>, Erin Murphy<sup>1</sup>, Andrey Loboda<sup>1</sup>, David R Kaufman<sup>1</sup>, Andrew Albright<sup>1</sup>, Jonathan Cheng<sup>1</sup>, S Peter Kang<sup>1</sup>, Veena Shankaran<sup>2</sup>, Sarina A Piha-Paul<sup>3</sup>, Jennifer Yearley<sup>1</sup>, Tanguy Seiwert<sup>4</sup>, Antoni Ribas<sup>5</sup>, Terrill K McClanahan<sup>1</sup>

<sup>1</sup>Merck & Co., Inc., Kenilworth, NJ, USA

<sup>2</sup>University of Washington, Seattle, WA, USA

<sup>3</sup>University of Texas MD Anderson Cancer Center, Houston, TX, USA

<sup>4</sup>University of Chicago, Chicago, IL, USA

<sup>5</sup>University of California, Los Angeles, CA, USA

#### **Background**

PD-L1 expression, which predicts response to PD-1-directed therapies such as pembrolizumab in many cancer types, is often associated with an active T cell infiltrate in the tumor microenvironment, suggesting that the presence of activated intratumoral T cells may be a determinant of response to PD-1 checkpoint blockade. This study describes the stepwise derivation of an immune-related gene expression profile (GEP) that identifies key biological features of a T cell inflamed tumor microenvironment and predicts clinical response to pembrolizumab across a wide variety of solid tumors.

#### **Methods**

Associations between clinical response to pembrolizumab and gene expression signatures of IFN- $\gamma$  signaling and activated T cell biology were evaluated using RNA isolated from formalin-fixed paraffin-embedded baseline samples of patients with multiple tumor histologies. Gene expression was analyzed on the NanoString nCounter system.

#### **Results**

Preliminary signatures, comprised of genes associated with IFN- $\gamma$  and activated T cell biology, were initially evaluated in a discovery set of 19 patients with melanoma, and subsequently validated in an independent cohort of 62 melanoma patients [1, 2]. Refined versions of these signatures were independently tested and shown to predict objective response and progression free survival (PFS) in

40 patients with head and neck squamous cell carcinoma (HNSCC) and 33 patients with gastric cancer [3, 4]. Using data combined from 220 pembrolizumab-treated patients across 9 cancer types, a final 18-gene GEP was derived that included immune-related genes related to antigen presentation, chemokine expression, cytotoxic activity, and adaptive immune resistance. The predictive value of the GEP compared favorably with that of PD-L1 immunohistochemistry when evaluated in an additional independent cohort of PD-L1-unselected HNSCC patients (n=96).

#### **Conclusions**

The pan-tumor GEP described in this study, typified by indicators of a T cell inflamed microenvironment, captures hallmark characteristics of tumors that are responsive to anti-PD-1 therapy. Our data suggest that these immune-related components are generally necessary, but not always sufficient, for clinical response to pembrolizumab. The GEP represents a potential tumor type-agnostic determinant of response to PD-1 checkpoint blockade, and has undergone analytical validation as a potential diagnostic assay with a clinical utility profile that suggests good performance for maintaining high negative-predictive value and sensitivity [5].

#### **Acknowledgements**

Joanne Tomassini, Merck & Co., Inc., writing support.

#### **Trial Registration**

ClinicalTrials.gov identifier NCT01295827, NCT01848834, and NCT02054806.

#### **References**

1. Ribas A, *et al*: *J Clin Oncol* 2015, **33(suppl)**:Abstr 3001.
2. Shankaran V, *et al*: *J Clin Oncol* 2015, **33(suppl)**:Abstr 3026.
3. Seiwert T, *et al*: *J Clin Oncol* 2015, **33(suppl)**:Abstr 6017.
4. Doi T, *et al*: Presented at ASCO GI Cancers Symposium. 2016.
5. Wallden B, *et al*: *J Clin Oncol* 2016, **34(suppl)**:Abstr 3034.

### 73

#### **Tumor mutational load and T cell inflamed microenvironment are independent determinants of response to pembrolizumab**

Razvan Cristescu<sup>1</sup>, Robin Mogg<sup>1</sup>, Mark Ayers<sup>1</sup>, Andrew Albright<sup>1</sup>, Erin Murphy<sup>1</sup>, Jennifer Yearley<sup>1</sup>, Xinwei Sher<sup>1</sup>, Xiao Qiao Liu<sup>2</sup>, Michael Nebozhyn<sup>1</sup>, Jared Lunceford<sup>1</sup>, Andrew Joe<sup>1</sup>, Jonathan Cheng<sup>1</sup>, Elizabeth Plimack<sup>3</sup>, Patrick A Ott<sup>4</sup>, Terrill K McClanahan<sup>1</sup>, Andrey Loboda<sup>1</sup>, David R Kaufman<sup>1</sup>

<sup>1</sup>Merck & Co., Inc., Kenilworth, NJ, USA

<sup>2</sup>MSD China, Beijing, People's Republic of China

<sup>3</sup>Fox Chase Cancer Center, Philadelphia, PA, USA

<sup>4</sup>Dana-Farber Cancer Institute, Boston, MA, USA



## Biomarkers and Immune Monitoring

Presenting author underlined; *Primary author in italics*

### Background

Non-synonymous, single-nucleotide variant mutational load (ML) is associated with response to cancer immunotherapies, including CTLA-4 and PD-1/L1 blockade, in some tumor types. A presumptive mechanism is increased tumor antigenicity through generation of neoepitopes not subject to central immune tolerance. A T cell inflamed microenvironment characterized by T cell infiltration, an IFN $\gamma$ -centric gene-expression profile (GEP), and PD-L1/PD-L2 upregulation, likewise associates with response to PD-1/PD-L1-directed therapies. However, the interaction and independent predictive values of these two distinct aspects of tumor biology have not been well studied. This study evaluates the association between ML and outcome, as well as the independent predictive values of ML and GEP, in pembrolizumab-treated cancer patients across 21 indications.

### Methods

Whole-exome sequencing and gene-expression profiling were performed on FFPE specimens from patients pooled from two multi-cohort, advanced solid tumor trials (KEYNOTE-028, n=80 and KEYNOTE-012, n=39). The previously defined GEP score was calculated as a weighted sum of normalized expression values for 18 genes. ML and neoantigen analytical approaches included public tools (GATK, MuTect, NetMHC). Statistical testing was pre-specified and adjusted for multiple-testing. Association of ML and GEP was further explored across cancer types using a proprietary database (Moffitt) of tumor gene expression (microarray RNA, n=16,000) and targeted exome (~1300 genes, n=2500) profiles, and TCGA datasets.

### Results

ML and neoantigen load were both significantly associated with objective response (AUROC=0.76 and 0.78, nominal 1-sided p=0.0036 and 0.0083, respectively). Median numbers of mutations were 180 in responders and 61 in non-responders. The overall response rate (ORR) in all patients was 15 %. At a ML cutoff of 102 (associated with ROC Curve Youden Index), the ORR was 32.3%, with a prevalence of 31.0% and negative-predictive value of 92.8 %. GEP was also significantly associated with objective response (AUROC=0.76, nominal 1-sided p=0.0071). ML and GEP were modestly correlated (r=0.28), consistent with associations observed between ML and GEP in Moffitt (r=0.11) and TCGA databases (r=0.29). When jointly modeled, ML showed significant association with response (p=0.0078) after adjusting for GEP (also significant, p=0.0251).

### Conclusions

These data validate the utility of ML and GEP across tumor types as independently predictive, complementary biomarkers of response to pembrolizumab. Moreover, these data suggest that tumor antigenicity and T cell infiltration have a non-linear, rather than tightly covariant, relationship.

As measures of distinct, yet common features of a PD-1 checkpoint-blockade-responsive tumor, ML and GEP may have utility in characterizing responses to PD-1 blockade and potentially other cancer immunotherapies.

### Acknowledgements

Joanne Tomassini, Merck & Co., Inc., writing support.

### Trial Registration

ClinicalTrials.gov identifier NCT01848834 and NCT02054806.

### 74

## Next generation techniques for biomarker development, validation and implementation reveal the importance of non-coding RNAs in predicting response to immunotherapy

Alex Forrest-Hay

Thermo Fisher Scientific, Newburyport, MA, USA

### Background

Cancer immunotherapies are changing treatment paradigms and expanding the therapeutic landscape for cancer patients. The current success of these therapies is well documented, however not all patients respond to immunotherapy and those that do can experience toxicities. There is a growing need to identify predictive and prognostic biomarkers to enhance understanding of the mechanisms underlying the interactions between the immune system and cancer. This presentation will discuss emerging biomarker techniques.

### Methods

Several new technologies will be showcased in this presentation: (1) The ability to obtain deep transcriptomic data including both coding and non-coding transcripts from a single FFPE section - less than 1ng of RNA and from 50pg of RAN from exosomes; (2) RNA *in situ* methodologies to explore ncRNAs and secreted cytokines/chemokines and quantify their expression levels in the tumor micro-environment; and (3) immuno-assays for assessing soluble checkpoint markers from 25ul of serum/plasma.

### Results

Data will be showcased that demonstrates the importance of exploring different isoforms of genes and non-coding RNA when searching for biomarkers. A new ncRNA discovered through single cell sequencing and microarray work is a surrogate marker for CD8+ T cell infiltration in a melanoma cohort and correlates with response to nivolumab in this initial small dataset (n=13). Additional data will be available by November. Finally, data will be presented that demonstrates that it is possible to detect "cleaved" or soluble PD-L2 upregulation in the serum of a glioblastoma patient who has undergone immunotherapeutic vaccine therapy via a novel multiplexed Luminex assay.

## Biomarkers and Immune Monitoring

Presenting author underlined; *Primary author in italics*

### Conclusions

Biomarkers are critical as we move further into the age of combination immunotherapies. It is important to cast the net as broadly as possible and not restrict studies to small subsets of known genes as the likely next generation of clinically useful biomarkers will be non-coding elements or endogenous retroviruses. It is also critical to understand which spliced variant of any given transcript is differentially expressed to fully understand the mechanism that drives any given cancer or response to treatment. New technologies are now available to do this cost effectively from clinical samples such as fine needle aspirates, FFPE tissue sections and blood. This presentation demonstrates the importance of using the latest molecular tools to advance the field of immunotherapy to facilitate the next wave of therapeutic advances.

### References

1. Das R, *et al*: **Combination Therapy with Anti-CTLA-4 and Anti-PD-1 Leads to Distinct Immunologic Changes In Vivo.** *J Immunol* 2015, **194**:950–959.

75

### Rapid generation of new specificity MHC tetramers for the detection of antigen-specific T cells using a novel peptide exchange tetramer kit that allows for quantification of peptide exchange

Cheryl A Guyre<sup>1</sup>, Kohei Narumiya<sup>2</sup>, Marc Delcommenne<sup>2</sup>

<sup>1</sup>MBL International, Woburn, MA, USA

<sup>2</sup>MBL International, Des Plaines, IL, USA

### Background

Major histocompatibility complex (MHC)-encoded glycoproteins bind peptide antigens through non-covalent interactions to generate complexes that are displayed on the surface of antigen-presenting cells for recognition by T cells. Peptide-binding site occupancy is necessary for stable assembly of newly synthesized MHC proteins and export from the endoplasmic reticulum. During this stage peptides produced in the cytosol compete for binding to MHC molecules, resulting in extensive peptide exchanges.

### Methods

We have developed a kit based on the principle of peptide exchange to generate novel specificity MHC tetramer reagents in a four-hour assay. While alternate methodologies rely on UV cleavage of exiting peptide on monomeric MHC complexes and a subsequent lengthy tetramerization procedure, we have developed a fully formed fluorescently labeled MHC tetramer that requires only the addition of the peptide of interest and a proprietary peptide exchange factor to complete the reaction.

### Results

A human HLA-A\*02:01 tetramer made from monomer units folded with an irrelevant exchangeable peptide, along with peptide exchange factor, was used with exogenous peptides to generate new specificity tetramers. The efficiency of peptide exchange was quantified using a novel flow cytometry-based sandwich immunoassay using magnetic beads conjugated with an anti-HLA-A,B,C capture antibody and a FITC conjugated antibody reacting against the exiting peptide. Exogenous peptide exchange rates correlated with their theoretical binding affinity to HLA-A\*02:01. Tetramers generated using peptides specific for CMV and Influenza demonstrated efficient exchange and detected similar percentages of antigen-specific CD8+ T cells as classically folded MHC tetramers in flow cytometry staining assays.

### Conclusions

The application of this technology to screening and neoantigen cytotoxic T lymphocyte (CTL) epitope discovery will be discussed.

### References

1. Reaper DR, Cresswell P: **Regulation of MHC class I assembly and peptide binding.** *Annu Rev Cell Dev Biol* 2008, **24**:343-368.

2. Mayerhofer PU, Tampé R: **Antigen translocation machineries in adaptive immunity and viral immune evasion.** *J Mol Biol* 2015, **427**(5):1102-1118.

76

### Selection of indications for JTX-2011 ICONIC clinical trial

Heather A Hirsch, Amit Deshpande, Jason Reeves, Jenny Shu, Tong Zi, Jennifer Michaelson, Debbie Law, Elizabeth Trehu, *Sriram Sathyanaryanan*

Jounce Therapeutics, Cambridge, MA, USA

### Background

ICOS (inducible co-stimulator of T cells) is a co-stimulatory molecule expressed primarily on T lymphocytes. Clinical data identified ICOS as a potentially key molecule in providing optimal anti-tumor benefit following anti-CTLA-4 therapy, with preclinical data confirming that engagement of the ICOS pathway plays a significant role in mediating anti-CTLA-4 driven anti-tumor responses. JTX-2011 is an ICOS agonist antibody that will be entering early phase clinical development for the treatment of advanced solid tumors in the ICONIC trial. JTX-2011 is designed to generate an anti-tumor immune response through stimulation of T effector cells and preferential reduction of intratumoral T regulatory (Treg) cells. Efficacy of an ICOS agonist in mouse syngeneic tumor models is greatest in tumors with the highest levels of intra-tumoral ICOS, suggesting a potential predictive





## Biomarkers and Immune Monitoring

Presenting author underlined; *Primary author in italics*

biomarker approach for clinical development. In this study we report assessment of indications for enrollment in the clinic trial using *in silico* and IHC analyses across multiple tumor types.

### Methods

Integrated analyses of RNA, DNA, and clinical data from the Cancer Genome Atlas (TCGA) were performed within multiple indications to understand the context in which ICOS is expressed. Using a proprietary ICOS IHC assay, ICOS expression analysis was performed on a subset of indications based on ranking from *in silico* analysis. ICOS expression was also compared to histology and molecularly defined indication subtypes as well as signatures of immune cell infiltrates to understand context of ICOS positivity.

### Results

We analyzed ICOS mRNA expression in ~10,000 solid tumors samples across ~30 indications. These data were used to rank indications, and ICOS expression in key indications was orthogonally confirmed using IHC. Consistent with previous data showing ICOS protein expression on Treg cells, ICOS RNA expression significantly correlated with Treg marker expression across multiple indications in TCGA tumor samples. Based on frequency of high ICOS expression, we determined non-small cell lung cancer, head and neck squamous cell carcinoma, triple negative breast carcinoma, gastric adenocarcinoma, and melanoma to be potential indications for JTX-2011 therapy. We further compared ICOS expression to PD-L1 expression to understand if there is a distinct population within an indication that is not a candidate for PD-1/PD-L1 therapy but could benefit from JTX-2011 therapy. A subset of patients in multiple indications exhibit high ICOS levels but low PD-L1 expression.

### Conclusions

In conclusion, these data support the prioritization of specific tumor types for treatment with JTX-2011 in the ICONIC trial.

77

### A large-scale analysis of immune cell type proportions in diverse solid tumors

Brendan P Hodkinson, Natalie A. Hutnick, Michael E. Schaffer, Michael Gormley

Janssen R&D, Spring House, PA, USA

### Background

Anticancer immunotherapies eliminate cancer cells by targeting immune cells to promote immune activation or block immune suppression. Ipilimumab and nivolumab, targeting CTLA-4 and PD-1 respectively, have demonstrated dramatic responses in melanoma and lung cancer [1, 2]. However, poor response rates in other types

of cancer underscore the need to better understand immunomodulatory mechanisms [3]. In this work, we extend previous methods for inferring immune cell type proportions from gene expression profiles [4], applying them to tumor and normal tissue samples from different tissue types to investigate interactions between tumors and the immune system.

### Methods

Proportions of 22 immune cell types were inferred from breast, colorectal, lung, and prostate microarrays representing tumors and normal tissue using machine learning. Statistical hypothesis testing was used to investigate immune cell proportion differences (1) between tumor and normal tissues and (2) between tumor types. Prostate tumors were further investigated to determine whether particular cell types (1) were associated with androgen receptor (AR) signaling or (2) could serve as prognostic markers.

### Results

All tumor types showed significantly higher proportions of M1 macrophages than normal tissues of the corresponding type, a characteristic of early-stage tumors and tumors of patients with better prognosis. Immunosuppressive regulatory T cells (Tregs), were detected more often at higher levels in tumors than normal tissue (significantly in breast and lung). Tumors of the prostate were most similar to normal tissue, possibly reflecting low immune infiltrate. Deeper research into prostate cancer showed (1) tumor AR activity to be positively correlated with plasma cells and negatively correlated with CD8+ T cells, Tregs, and monocytes and (2) indicated that more M1 macrophages (and lower M2/M1 ratios) were associated with better prognosis.

### Conclusions

Our results indicate that immune cell infiltration differs greatly between (1) healthy and cancerous tissues and (2) different tumor types. With further development, the inference of immune cell type proportions from gene expression profiles may lead to improved prognosis, predictive biomarkers for immunotherapy to assist in patient stratification, and new immunoncology targets by indicating immunosuppressive mechanisms.

### References

1. Hodi FS, *et al*: **Improved survival with Ipilimumab in patients with metastatic melanoma.** *N Engl J Med* 2010, **363**:711-723.
2. Risvi NA, *et al*: **Activity and safety of Nivolumab.** *Lancet Oncol* 2015, **16**:257-265.
3. Topalian SL, *et al*: **Safety, activity, and immune correlates of anti-PD-1.** *N Engl J Med* 2012, **366**:2443-2454.

## Biomarkers and Immune Monitoring

*Presenting author underlined; Primary author in italics*

4. Newman AM, *et al*: **Robust enumeration of cell subsets from tissue expression profiles.** *Nat Methods* 2015, **12**:453-457.

### 78 Abstract Travel Award Recipient

#### **Increased antibody and T cell responses to neoepitope site peptides following combination immunotherapy with a complex cell-derived cancer vaccine**

*Tyler Hulett*<sup>1</sup>, Shawn Jensen<sup>1</sup>, Carmen Ballesteros-Merino<sup>2</sup>, Christopher Dubay<sup>1</sup>, Michael Afentoulis<sup>1</sup>, Ashok Reddy<sup>3</sup>, Larry David<sup>3</sup>, Bernard Fox<sup>1</sup>

<sup>1</sup>Providence Cancer Center, Portland, OR, USA

<sup>2</sup>Earle A. Chiles Research Institute at Portland Providence Cancer Center, Portland, OR, USA

<sup>3</sup>Oregon Health & Science University, Portland, OR, USA

#### **Background**

Here, we report novel correlations between the antibody and T cell responses that develop to tumor-specific molecular targets following complex cancer vaccination. Further investigation of these correlations might lead to new methods of monitoring T cell immune responses via their corresponding antibody responses.

#### **Methods**

This study involves a complex autophagosome-enriched vaccine (DRibbles) made from 4T1 murine mammary carcinoma cells combined with poly-IC adjuvant. Animals pre-treated with 4T1 DRibbles and poly-I:C benefit from a significant delay in 4T1 tumor growth upon tumor challenge ( $p < .001$ ), and an increase in CD3+CD8+ tumor infiltrates by multi-spectral immunohistochemistry ( $p < .001$ ).

#### **Results**

We designed an array of 150 paired mutant neoepitope and wild-type 4T1 variant site 15mer peptides; this array included all single-nucleotide polymorphism (SNP) variant sites which were an exact match between a published 4T1 sequence and variants identified from sequencing our own 4T1 cell bank. In pooled data from three independent biological experiments, we observed an increase in antibody responses to both the mutant and wild-type variant site peptides in combination vaccinated animals versus adjuvant alone ( $p=.0002$ ). Surprisingly, we found that these antibody response increases strongly correlated with a higher maximum predicted MHC I binding score from NetMHCpan. To investigate T cell responses, we performed an *ex vivo* screen with a selection of predicted MHC I binding minimal peptides. IL2 expanded splenocytes from vaccinated animals were more likely than those from naïve animals to make an interferon gamma response to the SNP peptides whose parent proteins we had previously identified in the vaccine by mass spectrometry ( $p=.01$ ). A similar trend was seen for mass spectrometry

identified wild-type variant site peptides; these results are from a pool of three independent biological experiments.

#### **Conclusions**

This study identifies a previously unknown link between predicted MHC I binding affinity and the anti-tumor antibody response, a link which correlates with pooled T cell response data found in screening assays. We are confirming these data with larger scale T cell studies of screening assay hits *ex vivo*.

#### **Acknowledgements**

Chiles Foundation, Robert W. and Elise Franz, Lynn and Jack Loacker, Wes and Nancy Lematta, M.J. Murdock Charitable Trust, Harder Family, OCTRI-OSLER TL1, the Providence Medical Foundation, and the ARCS Foundation – Portland.

### 79

#### **miRNA a real kid for early recognition for PANcreatic adenocarcinoma (MARKER PAN study)**

*Kumar Jayant*, Swati Agrawal, Rajendra Agrawal

Sudha Hospital and Medical Research Center, Kota, Rajasthan, India

#### **Background**

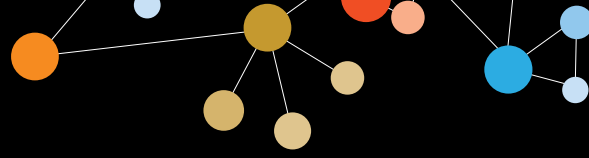
Pancreatic ductal adenocarcinoma constitutes the majority of malignant pancreatic tumours. Pancreatic adenocarcinoma is one of the deadliest cancers for humankind to tackle. More so over, its lethality has increased in the presence of late presentation. The median survival in advanced stage is 5-6 months. The present state CA 19.9 is the most commonly used marker though its sensitivity is questionable regarding terms of any help in early diagnosis. One of the promising evolving entities is miRNA, which has recently come to light, as a possible biomarker and cellular target for pancreatic cancer. The main aim of this study is to create a potential pool of circulatory miRNA panel for diagnosis of pancreatic cancer.

#### **Methods**

We have evaluated the current literature for various reported miRNA of diagnostic value in the serum by using MeSH terms: pancreatic adenocarcinoma, serum miRNA, and urinary miRNA. Six studies related to miRNA were evaluated in detail and discussed here.

#### **Results**

Details analysis of various studies have outlined many promising miRNA as potential candidates for the biomarker pool. The most notable ones are miRNA 143, miRNA 223, miRNA 30e, miRNA 204, miRNA 486, miRNA 145, miRNA 150, miRNA 223, miRNA 200, miRNA 21, miRNA 155 are few notable ones. Details of all potential miRNA are outlined in the Table 1.



# Biomarkers and Immune Monitoring

Presenting author underlined; Primary author in italics

## Conclusions

miRNA will be a great potential tool to help in the disease diagnosis in the very early stage of a disease. Creating the database of these circulatory miRNAs will be of great potential in creating a panel that will aid in the development of a screening tool.

## References

1. Debernardi S, *et al*: **Noninvasive urinary miRNA biomarkers for early detection of pancreatic adenocarcinoma.** *Am J Cancer Res* 2015, **5(11)**:3455–3466.
2. Xu J, *et al*: **Plasma miRNAs Effectively Distinguish Patients With Pancreatic Cancer From Controls.** *Ann Surg* 2015, **00(00)**:1.
3. Schultz N, *et al*. **MicroRNA biomarkers in whole blood for detection of pancreatic cancer.** *JAMA* 2014, **311(4)**:392–404.
4. Liu J, *et al*. **Combination of plasma microRNAs with serum CA19-9 for early detection of pancreatic cancer.** *Int J cancer* 2012, **131(3)**:683–691.
5. Bauer AS, *et al*: **Diagnosis of pancreatic ductal adenocarcinoma and chronic pancreatitis by measurement of microRNA abundance in blood and tissue.** *PLoS One* 2012, **7(4)**:e34151.6.
6. Liu R, *et al*. **Serum microRNA expression profile as a biomarker in the diagnosis and prognosis of pancreatic cancer.** *Clin Chem* 2012, **58(3)**:610–618.

Table 1

Study	Body Fluid Examined	Sample Size of pancreatic cancer	miRNA	Remarks
<u>Debernardi et al. 2016</u>	Urine	59	miRNA143, miRNA 223, miRNA 30e, 204	Sensitivity-83.3% Specificity-96.2%
Xu et al. 2016	Plasma	192	miRNA486	AUC-0.861 Sensitivity-75% Specificity-87%
Schultz et al. 2014	Blood	409	miRNA145,miRNA150, miRNA223, miRNA 636	AUC-0.86 Sensitivity-85% Specificity-64%
Liu et al. 2012	Serum	197	miR20a, miRNA21, miRNA24, miRNA25, miRNA 99a, miRNA 99a, miRNA185, miRNA191	AUC-0.992 Sensitivity-89% Specificity-100%
Bauer et al. 2012	Blood	345	miRNA320, miRNA159, miRNA225	AUC-0.973
Liu et al. 2012	Plasma	140	miRNA 16, miRNA21, miRNA155, miRNA181a, miRNA181b, miRNA196a, miRNA210, miRNA199	AUC-95.6

Table showing pool of potential miRNA with diagnostic values

## 80

### Neutrophil lymphocyte ratio as a biomarker predictive of clinical outcome with nivolumab therapy in RCC

Ghayathri Jeyakumar<sup>1</sup>, Seongho Kim<sup>1</sup>, Heejin Kim<sup>1</sup>, Cynthia Silski<sup>1</sup>, Stacey Suisham<sup>1</sup>, Elisabeth Heath<sup>1</sup>, *Ulka Vaishampayan*<sup>2</sup>

<sup>1</sup>Department of Oncology, Barbara Ann Karmanos Cancer Institute, Wayne State University, Detroit, MI, USA  
<sup>2</sup>Karmanos Cancer Institute, Detroit, MI, USA

## Background

With numerous therapies available for treatment of RCC, there is a need to evaluate factors predictive of response to enable patient selection. We are reporting a preliminary analysis evaluating the neutrophil lymphocyte ratio (NLR) and response to prior vascular endothelial growth factor (VEGF) inhibitors as factors predictive of response and clinical outcome in RCC patients treated with nivolumab. We also evaluated factors such as race, smoking status and prognostic scoring by MSKCC (Memorial Sloan Kettering Cancer Center) and Heng criteria.

## Methods

Regulatory approval was obtained. A retrospective chart review of RCC patients at Karmanos Cancer Institute treated with PD-1/PD-L1 inhibitors was conducted. Data was collected on demographics, smoking status, prognostic scoring (MSKCC and Heng), NLR pre and post 4 doses of nivolumab, response to prior therapies and correlated with clinical outcomes on immunotherapy therapies. Univariable and multivariable analyses were performed to evaluate any association with response rate (RR), progression free survival (PFS) and overall survival (OS).

## Results

Twenty-six patients were evaluated; 25 received nivolumab and 1 received nivolumab and ipilimumab. The median age was 61 years (39-82). 7 patients (27%) were African American (AA) and 12 patients (46%) were smokers. Pretherapy NLR > 6 months and 2 prior therapies. On univariable Cox analysis, pretherapy NLR ≥ 4 was not a significant predictor of response, but approached borderline statistical significance in the prediction of shorter PFS and OS (PFS: p= 0.06, HR 2.532, OS: p=0.058, HR 4.926). Median OS was 2.79 months in the group with NLR ≥ 4 and 18.39 months in the group with NLR > 6 months had a negative impact on PFS and OS (PFS: p= 0.067, HR= 2.98; OS: p=0.028, HR=10.834). In univariable logistic analysis, AA patients had higher risk of non-response (OR 10.5, p=.018), and demonstrated shorter OS (HR15.81, p=0.01) with nivolumab therapy in RCC.

## Biomarkers and Immune Monitoring

Presenting author underlined; Primary author in italics

### Conclusions

NLR is worthy of future investigation as a predictor of clinical outcomes with immune checkpoint inhibition therapy in RCC. Prior therapy that was  $\geq 6$  months had a negative effect on the PFS and OS with immunotherapy. Validation of this preliminary observation is required in a larger sample size.

81

### CD47 is overexpressed on Merkel cell carcinoma and a target for SIRP $\alpha$ therapy

*Natalie Vandeven*<sup>1</sup>, *Natasja Nielsen Viller*<sup>2</sup>, *Alison O'Connor*<sup>2</sup>, *Hui Chen*<sup>2</sup>, *Bolette Bossen*<sup>2</sup>, *Eric Sievers*<sup>2</sup>, *Robert Uger*<sup>2</sup>, *Paul Nghiem*<sup>1</sup>, *Lisa Johnson*<sup>2</sup>

<sup>1</sup>Fred Hutchinson Cancer Research Center, University of Washington, Seattle, WA, USA

<sup>2</sup>Trillium Therapeutics, Mississauga, ON, Canada

### Background

Merkel cell carcinoma (MCC) is an aggressive, neuroendocrine skin cancer with currently no effective, durable treatments for advanced disease. CD47 delivers an anti-phagocytic (“do not eat”) signal by binding SIRP $\alpha$  on the surface of macrophages. While CD47 has recently emerged as a promising drug target in oncology, its role in MCC is unknown. In this study, we evaluated CD47 expression in MCC tumor samples in conjunction with markers of immune infiltrate, Merkel cell polyomaviral (MCPyV) status, and survival. In addition, we assessed the ability of TTI-621 (SIRP $\alpha$ Fc), a CD47-blocking decoy receptor, to enhance macrophage-mediated phagocytosis of MCC tumor lines.

### Methods

A formalin-fixed paraffin-embedded (FFPE) tissue microarray (TMA) from 23 MCC patients (Table 1) was simultaneously stained for DAPI, CD3, CK20, CD47, CD64, CD68, and CD163 and analyzed using multispectral imaging and inForm software (Perkin Elmer). An *in vitro* assay was used to determine the effect of TTI-621 on the phagocytosis of the MCC tumor cell line MCC26. Monocyte-derived macrophages were primed with IFN- $\gamma$  and co-cultured with violet proliferation dye (VPD) labeled MCC26 cells +/- TTI-621 or control Fc for two hours. Phagocytosis was determined by flow cytometry as the percentage of VPD+CD14+ macrophages.

### Results

Mean membranous CD47 levels on CK20+ tumor cells ranged from 0.55-17.63 (median 4.5) compared to 0.55-9.55 (median 3.33) on CD3+ cells. Using median CD47 expression on MCC cells, Kaplan-Meier analysis suggested that patients with lower CD47 expression have improved survival rates however, this did not reach statistical significance ( $p=0.121$ ) in this small number of patients. There were few intratumoral T cells ( $146 \pm 434.9$  CD3+/mm<sup>2</sup>) compared to infiltrating macrophages

( $519 \pm 1781$  CD68+/mm<sup>2</sup>). Spearman correlation analysis indicated a weak correlation between higher expression of tumor CD47 and decreased numbers of infiltrating T cells ( $r=-0.352$ ,  $p=0.012$ ). Additionally, MCPyV+ patients (17/23) had slightly higher mean expression levels of CD47 (6.08), and it was not significantly higher than the small number of MCPyV negative (6/23) patients represented on the TMA (mean = 4.17;  $p=0.223$ ). Phagocytosis of MCC26 was increased in the presence of TTI-621, in a dose-dependent manner.

### Conclusions

CD47 is over-expressed in MCC, regardless of MCPyV status, suggesting that blockade of CD47 by TTI-621 may be particularly beneficial to patients with sparse T cell infiltrate. A phase I dose escalation clinical trial of TTI-621 in patients with solid tumors, including MCC, will initiate enrollment this year. This study will examine changes in the tumor microenvironment in response to TTI-621.

Table 1 Patient Demographics

Characteristic	CD47 High (n = 13)	CD47 Low (n = 10)	P
<b>Sex</b>			
Male (n=14)	9 (69.2)	5 (50.0)	0.306
Female (n=9)	4 (30.8)	5 (50.0)	
<b>Age at dx</b>			
$\geq 65$ (n=15)	10 (76.9)	5 (50.0)	0.184
$<65$ (n=8)	3 (23.1)	5 (50.0)	
<b>Immune suppressed</b>			
Yes (n=1)	1 (7.69)	0 (0.0)	1.000
No (n=22)	12 (92.31)	10 (100.0)	
<b>MCPyV Viral Status</b>			
Positive (n=17)	10 (76.9)	7 (70.0)	0.637
Negative (n=6)	3 (23.1)	3 (30.0)	
<b>Stage at Diagnosis</b>			
Local disease (n = 10)	5 (46.1)	4 (40.0)	0.552
Regional/distant disease (13)	7 (53.9)	6 (60.0)	
<b>Received Initial Radiation Therapy?</b>			
Yes (n=14)	7 (53.0)	7 (70)	0.454
No (n=8)	5 (38.5)	3 (30.0)	
Unknown (n=1)	1 (7.7)	0	
<b>Received Chemotherapy?</b>			
Yes (n=5)	3 (23.1)	2 (20.0)	0.594
No (n=17)	9 (69.2)	8 (80.0)	
Unknown (n=1)	1 (7.6)	0 (0)	
<b>Survival Status</b>			
Alive (n=13)	5 (46.2)	7 (70.0)	0.101
Died of Non-MCC (n=2)	0 (0)	2 (20.0)	
Died of MCC (n=6)	9 (69.5)	1 (10.0)	
Died of unknown causes (n=2)	2 (15.7)	0 (0)	

Demographics of MCC patients on TMA by CD47 status



## Biomarkers and Immune Monitoring

Presenting author underlined; Primary author in italics

82

### **Neutrophil-to-lymphocyte ratio (NLR) as a predictive biomarker of induction chemotherapy for stage IVA or IVB nasopharyngeal carcinoma (NPC) patients – a post-hoc analysis on Taiwan cooperative oncology group (TCOG) 1303 study**

Hsiang-Fong Kao<sup>1</sup>, Chin-Fu Hsiao<sup>2</sup>, Shu-Chuan Lai<sup>2</sup>, Chun-Wei Wang<sup>1</sup>, Jenq-Yuh Ko<sup>3</sup>, Pei-Jen Lou<sup>3</sup>, Tsai-Jan Lee<sup>1</sup>, Tsang-Wu Liu<sup>4</sup>, Ruey-Long Hong<sup>1</sup>

<sup>1</sup>Department of Oncology, National Taiwan University Hospital, Taipei, Taipei, Taiwan (People's Republic of China)

<sup>2</sup>Institute of Population Health Sciences, National Health Research Institutes, Taiwan, Zhunan, Miaoli, Taiwan (People's Republic of China)

<sup>3</sup>Department of Otorhinolaryngology, National Taiwan University Hospital, Taipei, Taipei, Taiwan (People's Republic of China)

<sup>4</sup>Taiwan Cooperative Oncology Group, National Health Research Institutes, Taiwan, Zhunan, Miaoli, Taiwan (People's Republic of China)

#### **Background**

Neutrophil-to-lymphocyte ratio (NLR) is considered as a prognostic biomarker for many kinds of cancers [1], including NPC [2]. However, its predictive role for a more intensive treatment is not known.

#### **Methods**

TCOG 1303 was a phase III trial (NCT00201396) comparing induction chemotherapy (IC) followed by concurrent chemoradiation (CCRT) versus CCRT alone in stage IVA or IVB NPC patients. In both arms, radiotherapy was delivered with weekly cisplatin (30mg/m<sup>2</sup>). For patients in the IC arm, chemotherapy with mitomycin C, epirubicin, cisplatin, 5-fluorouracil, and leucovorin were administered for 3 cycles before the CCRT. The primary endpoint was disease free survival (DFS). The secondary endpoint was overall survival (OS). NLR analysis was a post-hoc analysis. Patients with available data were included in the analysis. NLR = 3 was chosen as the cut-point for analysis [1].

#### **Results**

From September 2003 to August 2009, 479 patients were enrolled. The pre-treatment NLR were available in 319 patients. The median follow-up was 60 months. There were 89 patients with NLR ≥ 3.0 (NLR-H), and 230 patients with NLR < 3.0 (NLR-L). Between these two groups, there was no significant difference between NLR-H and NLR-L groups in DFS (5-year disease-free rate (median (95% CI) 0.57 (0.46-0.67) vs 0.58 (0.51-0.64), log-rank p = 1.00) and OS (5-year OS rate: 0.71 (0.60-0.80) vs 0.74 (0.67-0.80), log-rank p=0.30). In the NLR-L group, there were 119 patients in the IC-CCRT

arm, and 111 patients in the CCRT arm. The characteristics between both arms in NLR-L group were similar. There was a borderline significance in NLR-L group on DFS (IC-CCRT vs CCRT, 5-year DFS rate: 0.64 (0.55-0.72) vs 0.50 (0.41-0.60), log-rank p=0.058). The OS between two arms is not significant (IC-CCRT vs CCRT, 5-year-OS rate: 0.78 (0.68-0.85) vs 0.70 (0.60-0.78), log-rank p=0.20). In the NLR-H group, there were 43 patients in the IC-CCRT arm, and 46 patients in the CCRT arm. Between IC-CCRT and CCRT arm in NLR-H group, there was no significant difference in DFS (IC-CCRT vs CCRT, 5-year DFS rate: 0.61 (0.43-0.74) vs 0.54 (0.38-0.67), log-rank p=0.37) and OS (IC-CCRT vs CCRT, 5-year-OS rate: 0.74 (0.57-0.86) vs 0.68 (0.52-0.80), log-rank p=0.95).

#### **Conclusions**

NLR is not a predictive biomarker for advanced (stage IVA-IVB) NPC patients to take induction chemotherapy. In advanced NPC, the prognostic role of NLR is not significant.

#### **References**

1. Templeton AJ, *et al*: **Prognostic role of neutrophil-to-lymphocyte ratio in solid tumors: a systematic review and meta-analysis.** *J Natl Cancer Inst* 2014, **106(6)**:dju124.
2. He JR, *et al*: **Pretreatment levels of peripheral neutrophils and lymphocytes as independent prognostic factors in patients with nasopharyngeal carcinoma.** *Head & Neck* 2012, **34**:1769-1776.

83

### **WITHDRAWN**

84

### **Combining the best of both worlds: immune profiling the tumor microenvironment with RNA and protein biomarkers by fluorescence multiplex RNA in situ hybridization and immunohistochemistry**

Jeffrey Kim, *Ming-Xiao He*, Bingqing Zhang, Nan Su, Yuling Luo, Xiao-Jun Ma, Emily Park

Advanced Cell Diagnostics, Newark, CA, USA

#### **Background**

Recent triumphs in cancer immunotherapy have benefited many cancer patients across multiple malignancies, generating much interest from all sides. At the same time, there is an urgent need to develop predictive biomarkers to identify patients who are most likely to benefit from various immunotherapeutic strategies. While many biomarker analysis technologies are available, most do not provide spatial and cell type-specific information critical for assessing the specific immune cell types with lineage and functional information in the evolving microenvironment of each tumor. Furthermore, multiplexing capabilities are highly

## Biomarkers and Immune Monitoring

*Presenting author underlined; Primary author in italics*

desirable in order to obtain comprehensive single cell-level co-expression information and to maximize the use of limited biopsied sample material.

### Methods

In this study, we demonstrate the development of an improved fluorescence multiplex *in situ* hybridization (ISH) method to detect three RNA biomarkers simultaneously in FFPE and fresh frozen tissues on the Leica BOND RX automated slide staining system. The presented method detects RNA biomarkers in a highly specific and sensitive manner, overcoming the inherent challenge of auto-fluorescence in FFPE tissues. Individual RNA molecules are visualized as distinct bright dots using any fluorescence microscopy or multi-spectral fluorescence imaging system.

### Results

We applied this technique to archived non-small cell lung cancer FFPE tissues to detect (1) the co-expression of various immune checkpoint markers (such as PD-1, LAG-3, TIM-3) in PD-L1 positive and negative tumor environments and (2) immune functional markers such as cytokines and chemokines in combination with cell lineage markers. We further demonstrate the flexibility of this technique to allow for detection of both RNA and protein biomarkers, where immune checkpoint and functional markers are detected by ISH and cell lineage markers (such as CD3, CD8) by IHC. The data on the co-expression and localization of multiple combinations of markers derived from serial sections of FFPE tissues provide comprehensive information regarding the immune network in each tumor microenvironment.

### Conclusions

The newly developed multiplex fluorescence RNAscope assay and its combination with IHC presents a powerful tool to interrogate the various cell types and spatial heterogeneity within tumor tissues. Information revealed through simultaneous detection of multiple RNA and/or protein markers may provide new insights to maximize the benefits of current therapeutic approaches. This fully automated assay platform is well suited for developing and validating clinically relevant biomarkers in FFPE tissue.

85

### Expression and prognostic significance of CD8/CD45RO tumor-infiltrating lymphocytes (TIL) and PD-L1 in cholangiocarcinoma

Dae Won Kim, Domenico Coppola, Nishi Kothari, Young doo Chang, Richard Kim

H. Lee Moffitt Cancer Center, Tampa, FL, USA

### Background

Cholangiocarcinoma is a malignancy arising from the epithelial cells of the biliary tract with poor prognosis. TILs and PD-L1 have a prognostic impact in various solid tumors. We aimed to investigate TILs and PD-L1 expression and their clinical relevance in cholangiocarcinoma.

### Methods

Formalin-fixed paraffin-embedded tumor samples from 41 patients with resected and histologically verified cholangiocarcinoma between 1990 and 2015 were identified and immunohistochemically (IHC) stained with anti-CD8, anti-CD45RO and the anti-PD-L1 mouse IgG1 (clone 5H1; Thompson) antibodies. Stained tumor samples were reviewed and enumerated by a GI pathologist. PD-L1 positivity was defined  $\geq 5\%$  of tumor cells with a minimum of 100 evaluable tumor cells. The association between expression of PD-L1, CD8 or CD45RO and survival was investigated using Kaplan-Meier survival and COX proportional hazard regression analyses.

### Results

The median age of patients was 64 (41-85) with 53% male. 22%, 41% and 37% were stage I, II and III, respectively. 29 patients, 4 patients and 2 patients had R0 resection (microscopically margin-negative), R1 (microscopic residual tumor) and R2 (macroscopic residual tumor), respectively. 11 patients received post-surgical adjuvant treatment. CD8 was positive in 16 (39%), CD8CD45RO (memory CD8 cells) was positive in 5 (12%), and PD-L1 was positive in 19 (46%). With a median follow-up of 21.4 months, tumors with CD8+CD45RO+ TIL has better cancer specific survival (median: unreached vs 41.2mo, HR=0.27, 95% CI: 0.09-0.83, P=0.023) and overall survival (median: unreached vs 21.4mo, HR=0.34, 95%CI: 0.14-0.82, P=0.016) than CD45RO-. The expression of CD8 alone or PD-L1 in tumor was not associated with prognosis. Multivariate analysis showed that CD8+CD45RO+ TIL (HR=0.13, 95% CI: 0.02-0.99, P=0.049) as well as stage, adjuvant treatment and R0 resection were independent predictors of OS.

### Conclusions

Presence of CD8 memory T cells (CD8+CD45RO+) in tumor microenvironment was associated with significant better clinical outcome, and the expression of PD-L1 on cholangiocarcinoma cells may suggest a potential therapeutic target of anti-PD-L1 antibody therapy in cholangiocarcinoma.

86

### Immune cell based assay with suspension cells and wall-less DropArray plate

Namyong Kim, Melvin Lye, Ee Wan

Curiox Biosystems, San Carlos, CA, USA





## Biomarkers and Immune Monitoring

Presenting author underlined; Primary author in italics

### Background

The promising advances of immunotherapy in cancer patient suggest a need of parallel innovative solution to facilitate study and manipulation of immune cells. The design of cell based assays for studying patient T or B cells in conventional microtiter plate suffers from key limitations. The large microwell volume of classical microtiter plate is poorly suited to the limited amount of primary immune cells available and especially when a rare subpopulation study is needed. Furthermore, a cell based assay with multi-step staining procedures and immune cells often leads to significant cell loss and require a complex washing process optimization. Here, we present the use of DropArray wall-less microtiter plate for cell based assays with immune cells.

### Methods

DropArray 384 well plates are designed with hydrophobic/hydrophilic patterning and hold an array of 2  $\mu$ l drops in which cell based assays can be conducted conveniently and where cells and reagent consumption can be minimized by up to 90%. DropArray wall-less plates employ surface tension to retain suspension cells efficiently on the plate surface during a wash process with a convenient automatic washing station with no optimization required. DropArray plates are used in conjunction with common high content imaging platforms for analysis.

### Results

DropArray plates display efficient retention of suspension cells such as PBMC, plasmacytoid dendritic cells, and B or T cells in a range of 70 to 90% after multiple wash steps. Among few cell based assays we highlight how the DropArray plate is used to visualize/quantify events of cytotoxic T cells mediating tumor cell killing and where bi-specific antibody efficacy is evaluated with high content imaging platforms in a real time assay.

### Conclusions

DropArray wall-less plates constitute the next generation microtiter plate for running immune cell based assay with suspension cells.

87

### Miniaturization of Luminex based multiplex cytokine assay with 96 and 384 DropArray plates

*Namyong Kim, Melvin Lye, Ee Wan*

Curiox Biosystems, San Carlos, CA, USA

### Background

Luminex<sup>®</sup> magnetic bead-based assays have contributed to the expansion of biomarker discovery by providing tools for simultaneous measurement of multiple analytes. However, high cost and sample volume requirements limit the use of

this technology in drug discovery and research, especially when analyzing cerebrospinal fluid, tears and limited organic and body fluids. In this poster, we use Curiox's DropArray technology to reduce Luminex reagents and sample use by 80% while generating similar or enhanced data as obtained by traditional Luminex<sup>®</sup> methods.

### Methods

DropArray 96 (DA-96) plate is a wall-less plate that can accommodate 5 to 20  $\mu$ l drops in each of its 96 circular imprints. DA-96 plate follows standard SLAS/ANSI format, compatible with standard microtiter instruments and follows the same Luminex workflow for magnetic bead-based assays. Each circular hydrophilic area of the DA-96 plate can hold 5 $\mu$ l of each Luminex reagent and samples thus effectively miniaturizing the Luminex assay by at least 80%. DA-96 plate is used sequentially on vortex/orbital shakers, washed in a fully automated station and used in Luminex instruments for data acquisition. We use Milliplex<sup>®</sup>, Bio-Plex<sup>®</sup> or Procartaplex<sup>™</sup> kits coupled with DA-96 plates for cytokine analysis.

### Results

Using Milliplex<sup>®</sup>, Procartaplex<sup>™</sup> or Bio-Plex<sup>®</sup> based kits with DropArray 96 (DA-96) plate and washer, produce interpolated concentration, which correlates 99% with classic high multiplexing methods. Precision and accuracy analysis with DA-96 plates equals or excels conventional Luminex methods with intra assay CV% below 10% and recovery within acceptable range of 70-130%. Range of concentration detection conforms conventional methods with 3.5 to 4 logs range depending on analytes and produce similar sensitivities down to the pg/ml level. DA-96 plate offers excellent reproducibility well-to-well and plate to plate. 2 $\mu$ l and 5 $\mu$ l cytokine supernatant analysis from stimulated immune cells with Milliplex or Bio-Plex based kit DA-Bead method are presented as a functional example. Analysis of 150 serum samples with DA-96 plates indicate enhanced data detection of various analytes when compared to a conventional microtiter plate method.

### Conclusions

The DA-96 plate and washer is an effective miniaturization platform for Luminex assays that provides similar or enhanced performance reducing costs and sample use by up to 80%. DA-96 plates maximise sample use by requiring only 1/5 of the sample volume. DA-96 plates workflow is similar to standard Luminex workflow. DA-96 plates can be used with Luminex xMAP based kit (Milliplex, Bio-plex, Procartaplex) and any Luminex based instrument.

## Biomarkers and Immune Monitoring

Presenting author underlined; Primary author in italics

88

### Miniaturization of Singulex/Erenna based multiplex cytokine assay with wall-less DropArray 96 plates

*Namyong Kim*, Melvin Lye, Ee Wan

Curiex Biosystems, San Carlos, CA, USA

#### Background

Recent expansion in biomarker discovery has been possible by the use of bead-based assays and single molecule detection capabilities such as the Singulex assay. Minimal volume requirement with the Singulex methodology requires 50-100µl per well and can be a major bottleneck with limited clinical samples. Furthermore, requirement of multiple plate transfers with the Singulex workflow present a significant delay and obstacle during the workflow when multiple plates are processed simultaneously. Here, we combine DropArray 96 plates (DA-96) and the Singulex assay to achieve similar performance with 80% less volume than the current method.

#### Methods

DA-96 plate is a wall-less plate with 96 circular hydrophilic imprints on a hydrophobic/plastic surface displayed in SLAS/ANSI format, compatible with standard microtiter instruments. Each circular hydrophilic area can hold conventional Singulex reagents such as magnetic beads/ antibody/sample/standards up to a total of 20µl volume. Following a highly similar Singulex workflow and using conventional multichannel pipettes, DA-96 plates are used sequentially on vortex shakers and washed in a fully automated wash station. DA-96 to DA-96 plate bead transfer is performed conveniently with a Magnet Transfer Jig™ tool to bypass the need for multiple pipetting steps required in the conventional method. Finally, Beads on DA-96 plate are eluted out in a 384 well plate in a highly convenient manner which avoids centrifugation of beads and laborious plate transfer before acquisition into Singulex reader.

#### Results

Using Singulex Erenna based kits for cardiac Troponin-I, DA-96 plate miniaturized workflow displayed precision and accuracy analysis in line with conventional methods with intra assay CV% below 20% and recovery within acceptable range of 80-120%. Reliable sensitivity LLOQ reached 0.35pg/ml. DA-96 plate and washer offer excellent reproducibility well to well and plate to plate with 20µl of sample volume per well.

#### Conclusions

With similar performance as conventional plates, faster and streamlined workflow, DA-96 plate is the next generation plate for Singulex assay providing similar or improved sensitivity and a smaller sample volume requirement.

89

### Phenotype, function and gene expression signatures of CD8+ T cells in patients with acute myeloid leukemia (AML)

*Hanna A Knaus*<sup>1</sup>, Sofia Berglund<sup>1</sup>, Hubert Hackl<sup>2</sup>, Judith E Karp<sup>3</sup>, Ivana Gojo<sup>1</sup>, Leo Luznik<sup>1</sup>

<sup>1</sup>Johns Hopkins University, Baltimore, MD, USA

<sup>2</sup>Biocenter, Division of Bioinformatics Medical University of Innsbruck, Innsbruck, Tirol, Austria

<sup>3</sup>Sidney Kimmel Comprehensive Cancer Center, Johns Hopkins University, Baltimore, MD, USA

#### Background

T cell dysfunction in AML remains poorly understood. Therefore, we aimed to genotypically, phenotypically and functionally characterize T cells of AML-patients before and after induction-chemotherapy.

#### Methods

To study transcriptional signatures, FACS-purified peripheral blood (PB) CD8<sup>+</sup>T cells from 6 patients [3 responders (R) and 3 non-responders (NR)] and 4 healthy controls (HCs) were analyzed by microarray. Significantly differentially expressed genes were selected based on >2FC between patient and HC, and  $p < 0.01$ . We phenotypically characterized PB T cells from 69 AML-patients before and after induction-chemotherapy, and from 55 HCs, by flow cytometry (FLC). To study AML-blast/T cell interactions, we FACS-purified and *in vitro* cultured T cells and primary AML-blasts from newly diagnosed patients for 3 days. T cells were cultured alone or in co-culture with blasts (1:10) and analyzed by FLC.

#### Results

The transcriptional profile of CD8<sup>+</sup> T cells at AML diagnosis included significant upregulation of the immune inhibitory receptors genes 2B4, KLRG1, CD160 and TIGIT compared to HCs. In contrast, co-stimulatory receptor genes were downregulated, including CD40LG, CD28 and CD30LG. Ingenuity pathway analysis (IPA) revealed that the co-stimulatory CD28, ICOS and OX40 signaling pathways were downregulated. We performed confirmatory T cell phenotype characterization by FLC in a larger patient cohort (n=69). CD8<sup>+</sup> T cells were phenotypically senescent (CD27<sup>-</sup>CD28<sup>-</sup>CD57<sup>+</sup>) and %T cells co-expressing 2-4 co-inhibitory receptors (2B4/KLRG1/CD160/CD57) was significantly higher in AML patients compared to HCs. Next, we compared R to NR after induction chemotherapy. R-patients upregulated immune-stimulatory receptor genes like ICOS, whereas NR-patients upregulated immune-inhibitory receptor TIM3; LST1 (inhibits lymphocyte proliferation); TWEAK-APRIL (T cell apoptosis); and CD39 (terminally exhausted T cells). In accordance with these findings, IPA showed enrichment of the co-stimulatory



## Biomarkers and Immune Monitoring

Presenting author underlined; Primary author in italics

ICOS and OX40 signaling pathways in R-patients. In the confirmatory patient cohort, %senescent T cells and T cells co-expressing 2-4 co-inhibitory receptors was significantly decreased in R-patients (n=52), but unchanged in NR-patients (n=17) compared to pretreatment levels. The co-culture assay showed that the presence of AML blasts also significantly decreased the %primary AML T cells expressing co-stimulatory receptors 41BB, ICOS and OX40, while it increased the frequency of HC T cells expressing 2B4 and CD57.

### Conclusions

Our study provides insight into AML-associated phenotypical and transcriptional changes in T cells. Our data suggest that the AML-blasts influence the T cell phenotype and genotype. Response is associated with reversion to HC pattern, whereas NR patient remain in an exhausted/senescent state. Identification of their immune signature will hopefully help to rationally designing future clinical trials of immune-modulating strategies in AML.

90

### Distinct transcriptional changes in non-small cell lung cancer patients associated with multi-antigenic RActive® CV9201 immunotherapy

*Henoch S. Hong<sup>1</sup>, Sven D. Koch<sup>1</sup>, Birgit Scheel<sup>1</sup>, Ulrike Gnad-Vogt<sup>2</sup>, Karl-Josef Kallen<sup>1</sup>, Volker Wiegand<sup>2</sup>, Linus Backert<sup>3</sup>, Oliver Kohlbacher<sup>3</sup>, Ingmar Hoerr<sup>1</sup>, Mariola Fotin-Mleczek<sup>1</sup>, James M. Billingsley<sup>4</sup>*

<sup>1</sup>CureVac AG, Tübingen, Baden-Württemberg, Germany

<sup>2</sup>CureVac AG, Frankfurt am Main, Hessen, Germany

<sup>3</sup>Eberhard-Karls-Universität Tübingen, WSI/ZBIT, Applied Bioinformatics Group, Tübingen, Baden-Württemberg, Germany

<sup>4</sup>Division of Immunology, New England Primate Research Center, Harvard Medical School, Southborough, MA, USA

### Background

RActive® CV9201 is a novel mRNA-based therapeutic vaccine targeting five lung cancer-associated antigens. A phase I/IIa clinical trial was conducted in 46 patients with stage III or IV non-small cell lung cancer (NSCLC). We sought to comprehensively analyze changes in peripheral blood during the vaccination period to generate hypotheses facilitating the identification of potential biomarkers correlating with differential clinical outcomes post mRNA-based immunotherapy.

### Methods

Whole-genome expression profiling was performed in peripheral blood mononuclear cells (PBMCs) derived from a subgroup of 22 stage IV NSCLC patients before and after initiation of treatment with CV9201. We used a modular approach to gene expression data analysis based blood

transcriptional modules (BTMs), a previously described, sensitive tool for blood transcriptome data analysis. In addition, phenotypic T cell, B cell and NK cell analyses were performed by flow cytometry on the same PBMC samples.

### Results

Patients segregated into two major clusters based on transcriptional changes post treatment with CV9201. The first group of patients was characterized by the upregulation of an expression signature associated with myeloid cells and inflammation, whereas the other group exhibited an expression signature associated with T and NK cells. Patients with an enrichment of T and NK cell modules exhibited significantly longer progression-free and overall survival compared to patients with an upregulation of myeloid cell and inflammatory modules. Notably, these gene expression signatures were mutually exclusive and inversely correlated. Furthermore, our findings correlated with phenotypic data derived by flow cytometry as well as the neutrophil-to-lymphocyte ratio suggesting changes in the cellular composition of peripheral blood leukocytes after mRNA immunotherapy.

### Conclusions

We demonstrate non-overlapping, distinct transcriptional signatures associated with differential survival outcomes. These results warrant further validation in controlled, prospective clinical trials for the development of biomarker candidates for mRNA-based immunotherapy.

### Trial Registration

ClinicalTrials.gov identifier NCT00923312.

91

### Persistence and turnover of therapy-induced peripheral CD4+ T cell clones in patients with metastatic melanoma upon ipilimumab therapy

*Yoshinobu Koguchi<sup>1</sup>, Valerie Conrad<sup>1</sup>, William Miller<sup>1</sup>, Iliana Gonzalez<sup>1</sup>, Tomasz Poplonski<sup>1</sup>, Tanisha Meeuwssen<sup>1</sup>, Ana Howells-Ferreira<sup>1</sup>, Rogan Rattray<sup>1</sup>, Mary Campbell<sup>1</sup>, Carlo Bifulco<sup>2</sup>, Christopher Dubay<sup>3</sup>, Keith Bahjat<sup>1</sup>, Brendan Curti<sup>1</sup>, Walter Urba<sup>1</sup>*

<sup>1</sup>Earle A. Chiles Research Institute, Providence Cancer Center, Portland, OR, USA

<sup>2</sup>Robert W. Franz Cancer Research Center, Earle A. Chiles Research Institute, Providence Cancer Center, Portland, Oregon, USA, Portland, OR, USA

<sup>3</sup>Providence Cancer Center, Portland, OR, USA

### Background

Ipilimumab is a human monoclonal antibody targeting CTLA-4, which is expressed in activated T cells and involved in negative regulation. 22% of patients with metastatic

## Biomarkers and Immune Monitoring

Presenting author underlined; Primary author in italics

melanoma who received ipilimumab monotherapy are alive 3 years after treatment and the majority of these patients have had a durable response lasting ten years or more [1]. It is important to uncover underlying resistance mechanisms as most patients still fail to benefit from ipilimumab or other immunotherapies.

### Methods

We assessed whether activation and/or proliferation of peripheral T cells correlated with clinical outcome of patients with metastatic melanoma treated with ipilimumab. PBMCs from patients at baseline and 12 weeks following initiation of treatment participating in a compassionate use trial of ipilimumab [2] were evaluated for ICOS+ or Ki-67+ frequencies on CD4+ and CD8+ T cells, as well as regulatory T cells, using flow cytometry. We conducted T cell receptor (TCR) CDR3 sequencing for sorted bulk CD4+ T cells from baseline, weeks 7 and 12 of ipilimumab treatment to understand their clonal behaviors in patients with metastatic melanoma upon treatment.

### Results

Ipilimumab treatment significantly increased the frequency of ICOS+ T cells regardless of clinical outcome as previously reported by others [3]. Increased Ki-67+ CD4+ T cells upon ipilimumab treatment (> 1.7 fold) was associated with prolonged overall survival. Our results suggest that ipilimumab's anti-tumor effects may be mediated in part by proliferation of CD4+ T cells. However, some patients with melanoma progression showed increased Ki-67 expression in CD4+ T cells after ipilimumab, implying that CD4+ T cell proliferation alone is not a predictive biomarker. When we tracked destiny of newly emerging CD4+ T cell clones upon treatment (present at weeks 7 but not present at baseline), we found prominent turnover at weeks 12 in patients who progressed upon treatment. In contrast, a patient who showed complete response and later survived longer than 3 years showed persistence of new CD4+ T cell clones upon treatment.

### Conclusions

Our results suggest that successful treatment with ipilimumab may be, in part, explained by appearance and persistence of potentially tumor-specific CD4+ T cell clones. We will be conducting TCR CDR3 sequencing for DNA extracted from tumor FFPE blocks to see whether clones of interests can be detected in tumor.

### Trial Registration

ClinicalTrials.gov identifier NCT00495066.

### References

- Schadendorf D, *et al*: *J Clin Oncol* 2015, **33**:1889-1894.
- Koguchi Y, *et al*: *Cancer Res.* 2015, **75**:5084-5092.
- Ng Tang D, *et al*: *Cancer Immunol Res* 2013, **1**:229-234.

92

### High frequencies of PD-1+CD8+ T cells are correlated with PD-L1+ circulating tumor cells (CTC) and have predictive/prognostic value in non-small cell lung cancer (NSCLC) patients

E-K Vetsika, G Kallergi, Despoina Aggouraki, Z Lyrusti, P Katsarlinos, Filippos Koinis, V Georgoulas, Athanasios Kotsakis

Laboratory of Translational Oncology, University of Crete, School of Medicine, Heraklion, Greece

### Background

The use of antibodies against the negative immune checkpoints, PD-1 and PD-L1 proteins, is an effective therapy for NSCLC patients. In this study, we evaluated the levels of PD-1+ and PD-L1+ expressing- immune cells (ICs) and CTCs, and their association with the clinical outcome in advanced/metastatic NSCLC.

### Methods

Peripheral blood was collected from 37 advanced/metastatic chemotherapy-naïve NSCLC patients before treatment. Flow cytometry was performed to enumerate the PD-1 and PD-L1 expressing-ICs with anti-tumor (CD4+ and CD8+ T cells, B cells, Dendritic cells) and suppressive functions [CD4+ and CD8+ Treg, Bregs, Myeloid-derived Suppressor cells (MDSC)]. Moreover, PD-1+ and PD-L1+ CTCs were enumerated by immunofluorescence. Correlation between the levels of PD-1+ and PD-L1+-expressing ICs and CTCs and their association with overall (OS) and progression-free survival (PFS) was evaluated; high expression of ICs was defined as the percentage of the cells above the mean value.

### Results

The detection and quantification of all PD-1 and PD-L1-expressing ICs and CTCs, in NSCLC is presented. PD-1 and PD-L1 expression was detected on all tested effector cells and CTCs. In addition, PD-1 and PD-L1 expression was found on all immunosuppressive cells, except Bregs and monocytic-MDSCs. Importantly, the increased percentages of PD-1+CD8+ T cells were associated with worse response to treatment ( $p=0.032$ ) and shorter PFS ( $p=0.023$ ), indicating its clinical relevance. In contrast, the high expression of PD-1 on naive CD4+ Treg was correlated with longer PFS ( $p=0.017$ ), implying that PD-L1/PD-1 axis could be a mechanism leading to Treg apoptosis and hence re-activation of immune system. In multivariate analysis, high percentage of PD-1+CD8+ T cells was an independent predictor for decreased PFS (HR: 4.1,  $p=0.0007$ ), while the increased percentages of naive PD-1+CD4+ Treg cells were independently associated with increased PFS (HR: 3.8,  $p=0.018$ ). Interestingly, high levels of PDL-1+ CTCs were correlated high levels of PD-1+CD8+T cells ( $p < 0.04$ ), indicating a likely immune escape mechanism of



## Biomarkers and Immune Monitoring

*Presenting author underlined; Primary author in italics*

CTCs. The levels of all other PD-1 and PD-L1 expressing cells were not associated with the clinical outcome.

### Conclusions

For the first time the current study provides evidence for a possible interaction between the ICs and CTCs in NSCLC patients via the PD-1/PD-L1 axis. Moreover, these results indicate that PD-1 expression, on two distinct ICs with opposite functions, differentially impact NSCLC patient's clinical outcome.

93

### Objective and consistent scoring of a PD-L1 complementary diagnostic with Computational Tissue Analysis (cTA™)

Nathan T Martin, Famke Aeffner, Staci J Kearney, Joshua C Black, Logan Cerkovnik, Luke Pratte, Rebecca Kim, Brooke Hirsch, Joseph Krueger, Roberto Gianani

Flagship Biosciences, Inc, Westminster, CO, USA

### Background

The PD-1/PD-L1 pathway mediates immunosuppression in the tumor microenvironment. Therapies targeting this pathway have been approved along with corresponding diagnostic assays for selected indications. These assays predict patient responses to therapy by measuring the percentage of tumor cells (Keytruda, Opdivo) or immune cells (durvalumab) that stain positive for PD-L1. The AACR-ASCO-FDA Blueprint Project seeks to facilitate harmonization of PD-L1 tests in order to enable their practical use, with the goal of building a method for objective, consistent, proper test interpretation. In response, we have developed Computational Tissue Analysis (cTA™) approaches that enable objective, consistent assessments of staining. In addition to evaluating staining concurrently in multiple cell types (eg, tumor epithelium, immune infiltrate) and ensuring reproducible scoring, these approaches may help clarify the differences between various PD-L1 assays. The present study evaluated Flagship's cTA™ approaches to scoring samples stained with the Dako PD-L1 pharmDx (28-8) immunohistochemistry complementary diagnostic assay. The current manual scoring method considers any patient with at least 1% PD-L1–positive tumor cells a candidate for Opdivo treatment. However, a trend toward increased overall survival was observed in patient groups with greater PD-L1 positivity (5% and 10%), suggesting the importance of reliably distinguishing between positivity thresholds.

### Methods

We developed a cTA™ approach to test the hypothesis that it could provide more consistent scoring around these low thresholds, which are challenging for pathologists. We stained 40 formalin-fixed, paraffin-embedded nonsquamous

non–small cell lung cancer samples with the aforementioned Dako assay; a subset of these we stained on consecutive days to evaluate assay and scoring precision. The cTA strategy digitally identified tumor cells and quantified membrane staining intensity consistent with the manufacturer's scoring guidelines. We also evaluated scoring of PD-L1 expression in immune infiltrate in the same analysis.

### Results

The cTA™ membrane scoring approach for tumor cells met Flagship's Clinical Laboratory Improvement Amendments (CLIA) validation criteria, with the manually scored assay as the reference standard. This approach was accurate and provided greater reproducibility of scoring over the dynamic range of PD-L1–positive cell frequencies.

### Conclusions

This study demonstrated the utility of cTA™ approaches for consistently and objectively scoring PD-L1 expression in tumor cells within the CLIA environment. It also highlighted the challenge pathologists face in differentiating between 1%, 5%, and 10% positivity. cTA™ approaches could be used for consistent scoring of a single assay or to understand differences between assays in performance or relationship to clinical response.

94

### Antigen recognition avidity dependent miR-155 upregulation in melanoma tumors correlates with increased CD8+ T cell infiltrates

Amaia Martínez-Usatorre<sup>1</sup>, Camilla Jandus<sup>1</sup>, Alena Donda<sup>1</sup>, Laura Carretero-Iglesia<sup>2</sup>, Daniel E. Speiser<sup>1</sup>, Dietmar Zehn<sup>3</sup>, Nathalie Rufer<sup>4</sup>, Pedro Romero<sup>1</sup>

<sup>1</sup>Department of Fundamental Oncology, Ludwig Cancer Research Center, University of Lausanne, Epalinges, Vaud, Switzerland

<sup>2</sup>Department of Fundamental Oncology, Centre Hospitalier Universitaire Vaudois (CHUV), Epalinges, Vaud, Switzerland

<sup>3</sup>School of Life Sciences Weihenstephan, Technical University Munich, Freising, Bayern, Germany

<sup>4</sup>Department of Oncology, Centre Hospitalier Universitaire Vaudois (CHUV), Epalinges, Vaud, Switzerland

### Background

MicroRNAs (miRs) are noncoding small RNAs that regulate protein expression at the post-transcriptional level in all cells, including those forming the immune system. We previously showed that a single miR, miR-155, promotes effector CD8+ T cell responses in viral infection, vaccination and adoptive cell transfer for tumor therapy in mice [1]. However, little is known yet about miR-155 expression regulation in tumor infiltrating CD8+ T cells.

## Biomarkers and Immune Monitoring

Presenting author underlined; Primary author in italics

### Methods

Our goal here was to study the dynamics of miR-155 expression, i) in tumor specific effector CD8+ T cells from mouse spleen and melanoma tumors expressing high or low affinity antigen ligands, and ii) in *ex vivo* sorted human CD8+ T cell subsets from melanoma patient's blood, non-tumor infiltrated lymph nodes (NLNs), tumor infiltrated lymph nodes (TILNs) and non-lymphoid tumor masses.

### Results

We report that antigen recognition and T cell avidity are major determinants in the regulation of miR-155 expression in tumor antigen specific CD8+ T cells. Moreover tumor specific mouse and human effector memory (EM) CD8+ T cells from melanoma patients showed increased miR-155 expression levels in melanoma tumors and TILNs compared to T cells from tumor-free areas. In addition, high miR-155 expression levels correlated with increased tumor specific effector CD8+ T cell infiltrates and tumor control in mice. In agreement with these observations in mouse model systems, miR-155 expression levels in human EM CD8+ T cells positively correlated with their frequencies in TILNs and tumor masses in melanoma patients. In addition, high EM CD8+ T cell frequencies correlated with increased overall patient survival.

### Conclusions

We propose miR-155 expression levels in CD8+ T cells from tumor infiltrated tissues as a surrogate marker for antigen specific CD8+ T cell responses *in situ* and a possible prognostic biomarker in melanoma.

### References

- Dudda JC, *et al*: **MicroRNA-155 is required for effector CD8+ T cell responses to virus infection and cancer.** *Immunity* 2013, **38(4)**:742-753.

95

### Immune activation and prolonged benefit to avelumab (anti-PD-L1) therapy in a patient with metastatic EBV+ gastric cancer

Anshuman Panda<sup>1</sup>, Janice Mehnert<sup>2</sup>, Kim M Hirshfield<sup>2</sup>, Greg Riedlinger<sup>2</sup>, Sherri Damare<sup>2</sup>, Tracie Saunders<sup>2</sup>, Levi Sokol<sup>3</sup>, Mark Stein<sup>2</sup>, Elizabeth Poplin<sup>2</sup>, Lorna Rodriguez-Rodriguez<sup>2</sup>, Ann Silk<sup>2</sup>, Nancy Chan<sup>2</sup>, Melissa Frankel<sup>2</sup>, Michael Kane<sup>2</sup>, Jyoti Malhotra<sup>2</sup>, Joseph Aisner<sup>2</sup>, Howard L. Kaufman<sup>2</sup>, Siraj Ali<sup>4</sup>, Jeffrey Ross<sup>4</sup>, Eileen White<sup>2</sup>, Gyan Bhanot<sup>2</sup>, Shridar Ganesan<sup>2</sup>

<sup>1</sup>Rutgers Cancer Institute of New Jersey, Rutgers University, Piscataway, NJ, USA

<sup>2</sup>Rutgers Cancer Institute of New Jersey, New Brunswick, NJ, USA

<sup>3</sup>University Radiology, New Brunswick, NJ, USA

<sup>4</sup>Foundation Medicine, Inc., Cambridge, MA, USA

### Background

The molecular basis for response to immune checkpoint therapy in different cancers is not well understood. In some cases response correlates with high tumor mutation burden, due to environmental exposure to carcinogens (UV exposure/tobacco), or intrinsic DNA repair defects (mismatch repair defects/*POLE* mutations) leading to generation of immunogenic neoantigens. However, some tumors with low mutation burdens are sensitive to immune checkpoint therapy, suggesting other mechanisms of immune activation.

### Methods

Exceptional clinical benefit was observed in a patient with advanced gastric cancer treated with the PD-L1 inhibitor avelumab. Informed consent was obtained and she was enrolled to the Rutgers Cancer Institute of New Jersey genomic tumor-profiling protocol. Comprehensive genomic profiling was performed using the FoundationOne platform. *In situ* hybridization was performed to evaluate expression of Epstein Barr Virus (EBV)-encoded RNA. Data from The Cancer Genome Atlas (TCGA) dataset of gastric cancer was analyzed to review associations between EBV status, mutation burden, gene expression based immune signatures and histologic lymphocytic infiltration.

### Results

This 57-year-old female presented with chemotherapy refractory metastatic gastric cancer causing complete esophageal obstruction, cervical and thoracic lymphadenopathy, and chronic anemia from tumor blood loss. Avelumab 10 mg/kg every 2 weeks was administered in a clinical trial. She experienced tumor reduction after 4 cycles. After 10 cycles, further tumor regression, improved anemia, and improved ability to ingest solid foods with > 15 lb weight gain was observed and continues at 20+ cycles. Genomic analysis of a pre-treatment tumor specimen did not show a high mutation burden or evidence of mismatch repair defects, but was strongly positive for EBV-encoded RNA. Approximately 9% of gastric cancers in the TCGA dataset have evidence of EBV RNA expression. These EBV+ cancers were micro-satellite stable with relatively low mutation burden, but high expression of immune checkpoint genes including PD-1 and PD-L1, and gene expression evidence of immune infiltration.

### Conclusions

These data suggest that EBV+ gastric cancers are a subset of micro-satellite stable gastric cancers with low mutation burden that respond to immune checkpoint therapy. Tumor EBV expression may be a marker of sensitivity to immune checkpoint therapy that is independent of total mutation burden and microsatellite instability. A phase III trial of avelumab in patients with recurrent gastric cancer is ongoing.



## Biomarkers and Immune Monitoring

*Presenting author underlined; Primary author in italics*

### Acknowledgements

We acknowledge our patient's participation.

### Trial Registration

ClinicalTrials.gov identifier NCT01772004.

### Consent

Written informed consent was obtained from the patient for publication of protocol data in this abstract and accompanying images. A copy of the consent is available for review.

96

### Immune-enriched NSCLC biopsy tissue microarrays demonstrate that proliferating and checkpoint expressing TIL correlate with positive outcome

*Anne Monette*<sup>1</sup>, Derek Bergeron<sup>1</sup>, Amira Ben Amor<sup>2</sup>, Liliane Meunier<sup>3</sup>, Christine Caron<sup>3</sup>, Antigoni Morou<sup>1</sup>, Daniel Kaufmann<sup>1</sup>, Moishe Liberman<sup>4</sup>, Igor Jurisica<sup>5</sup>, Anne-Marie Mes-Masson<sup>1</sup>, Kamel Hamzaoui<sup>2</sup>, Rejean Lapointe<sup>1</sup>

<sup>1</sup>Université de Montréal, Centre de recherche du CHUM (CRCHUM), Montreal, PQ, Canada

<sup>2</sup>University of Tunis El Manar II, Tunis, Tunisia

<sup>3</sup>Institut du Cancer de Montréal (ICM), Centre de recherche du CHUM (CRCHUM), Montreal, PQ, Canada

<sup>4</sup>Centre Hospitalier de l'Université de Montréal (CHUM), Université de Montréal, Montreal, PQ, Canada

<sup>5</sup>Ontario Cancer Institute, University of Toronto, Toronto, ON, Canada

### Background

Immune checkpoint (ICP) blockade therapies using anti-PD-1 have elicited positive responses in non-small cell lung cancer (NSCLC) patients, where non-responders are suspected to arise from the downstream expression of additional ICP on effector TIL. In this age of companion diagnostics, during the expanding of the list of predictive biomarkers like PD-L1, it will become invaluable to: 1) define which ICP impact prognosis; 2) determine whether ICP expression is co-dependent, ordered, and can be used to stratify patients; and 3) develop standardized methods for their use in scoring patients ahead of ICP blockade therapies.

### Methods

An immune-cell-specific biopsy-based tissue microarray (TMA) from untreated NSCLC patients (n=81) was fabricated to profile TIL-ICP using multiplex immunofluorescence (MP-IF). ICP distributions and coexpression were correlated with clinical data, and results were compared to The Cancer Genome Atlas (TCGA) RNA-Seq lung adenocarcinoma (LUAD; n=520) and lung squamous cell carcinoma (LUSC; n=504) datasets. Using microfluidic qRT-PCR, coexpression of ICP with numerous effector TIL genes was assessed in CD8+ and CD4+

TIL isolated from freshly resected untreated tumors, normal tissues, and peripheral blood mononuclear cells (PBMC).

### Results

TIL that are proliferating and expressing certain ICP positively correlate with the overall survival (OS) of NSCLC patients. From TMA staining data, ICP expression is increased (CTLA4) or decreased (PD-1, CD26, CD57, CD244) relative to patient mortality, and ICP coexpression (CD57-CD39, CD26-CD39) or TIL-ICP expression (CD3-CTLA4, CD3-TIM-3, increased; CD3-CD26, CD3-CD73, decreased) enhance statistical significance. Increased expression of ICP (TIM-3, CD26, LAG-3) or TIL-ICP (CD3-TIM-3, CD3-BTLA, CD3-LAG-3, CD3-CD26, CD3-CD39) correlates with improved OS. From both TMA results and TCGA datasets, ICP subset expression is observed to have heightened importance relative to OS at earlier time points, suggesting an ordered accruing of ICP by TIL. Hierarchical cluster analysis reveals ICP groupings (CD26, CD39, TIM-3; TIGIT, CTLA4, PDCD1; CD244, CD57) reflected by qRT-PCR results also revealing ICP distributions on CD8+ and CD4+ TIL and PBMC. TCGA datasets also provide evidence that overall ICP expression positively correlates with OS, and that advanced cancer stages have lowered ICP expression. Finally, ICP expression analysis defines an ordered build of ICP on NSCLC TIL.

### Conclusions

This multi-cohort analysis performed using an array of techniques has resulted in the discovery of TIL ICP expression having the greatest benefit for different NSCLC subtypes. ICPs are coexpressed, and their early, stepwise acquisition may be an important determinant of OS. In this era of personalized medicine, use of ICP MP-IF panels may better stratify patients for ICP blockade therapies.

97

### High sensitivity detection of low expressing interleukins and interferons for biomarker research analysis from FFPE samples using multiplexed NGS

*Ann Mongan*, Yuan-Chieh Ku, Warren Tom, Yongming Sun, Alex Pankov, Tim Looney, Janice Au-Young, Fiona Hyland

Thermo Fisher Scientific, South San Francisco, CA, USA

### Background

There is growing evidence supporting the association of tumor infiltrating lymphocytes, inflammatory signaling molecules, and drug sensitivity to cancer checkpoint blockade therapy. At the same time, the exact markers that are predictive of response for each therapeutic agent are still the subject of active investigations. To address the need for better understanding of the effect of different T cell subsets, antigen presentation, and tumor killing, gene expression profiling presents an attractive means to simultaneously evaluate the

## Biomarkers and Immune Monitoring

*Presenting author underlined; Primary author in italics*

tumor microenvironment and cancer cells. Furthermore, as most of the samples available for drug sensitivity research studies are derived from formalin-fixed paraffin-embedded (FFPE) slides with typically low RNA quality, target sequencing offers a cost-effective solution that provides significantly higher sensitivity and specificity over whole transcriptome sequencing or other gene expression profiling methods.

### Methods

Here we report the results of a 395-gene expression panel profiling FFPE non-small cell lung cancer (NSCLC) and melanoma tumor research samples. The panel uses Ion AmpliSeq™ technology to measure the expression of genes involved in T cell activation, markers of different leukocyte subsets, antigen presentation, and tumor characteristics (proliferation, adherence/migration, epithelial-to-mesenchymal transition, etc).

### Results

Gene expression measured by the panel stratified NSCLC samples into groups that are consistent with histopathology classification and tumor infiltrating levels provided by pathologists. The panel offers reproducibility between replicates and high sensitivity of detection for low expressing genes such as IL-2, IL-10, IL-21, and IFNG, among others. We further demonstrated excellent concordance between fresh frozen and FFPE samples (correlation >0.95) as well as concordance with TaqMan<sup>(R)</sup> qPCR. With a series of limiting dilution experiments between two cell lines, the assay showed broad dynamic range and linearity up to 200 fold. This OncoPrint™ Immune Response Research Assay\* is accompanied by a Torrent Suite™ software package that provides run quality metrics, normalized gene expression, and hierarchical clustering among multiplexed samples.

### Conclusions

In summary, the current gene panel offered an accurate and accessible tool for evaluating biomarkers that may be relevant to cancer immunotherapy.\*For Research Use Only. Not for use in diagnostic procedures.

98

### Validation of a custom RNA-Seq approach to cancer immune profiling

Jeff Conroy<sup>1</sup>, Carl Morrison<sup>1</sup>, Sean Glenn<sup>2</sup>, Blake Burgher<sup>2</sup>, He Ji<sup>2</sup>, Mark Gardner<sup>2</sup>, Ann Mongan<sup>3</sup>, Angela R Omilian<sup>1</sup>

<sup>1</sup>Roswell Park Cancer Institute, Buffalo, NY, USA

<sup>2</sup>OmniSeq, LLC, Buffalo, NY, USA

<sup>3</sup>Thermo Fisher Scientific, South San Francisco, CA, USA

### Background

Immune checkpoint blockade with monoclonal antibodies directed at the inhibitory immune receptors has emerged

as a successful treatment for cancer patients. Evaluation of tumor checkpoint blockade by IHC is subjective, not reproducible, and importantly not scalable. We have designed a custom 362 gene RNA-Seq immune profiling panel that uses a multi-analyte algorithmic analysis (MAAA) to evaluate checkpoint blockade, tumor infiltrating lymphocytes (TILs), and cytokine/chemokine interactions.

### Methods

269 cancer samples of diverse histologies with both frozen and FFPE samples were evaluated by RNA-Seq with a custom 362-gene Ion AmpliSeq Immune Response Profiling Assay using the Ion Chef™ and Proton. RNA-Seq analysis was performed with the Torrent Suite™ followed by normalization. All samples were also included in a custom TMA and IHC was performed for 61 different markers for various immunotherapy targets. Custom TaqMan assays were also performed for each of the 61 different markers.

### Results

Correlation of frozen and FFPE samples was directly related to level of expression at the gene level. High expression genes showed a better correlation than low expression genes. RNA-Seq and TaqMan results were highly correlated for all 61 genes evaluated. As compared to IHC the results for RNA-Seq were continuous rather than bimodal and allowed for a much more detailed analysis of the immune repertoire. Frequent difficult-to-interpret results for IHC for PD-L1 and other markers were easily interpreted by RNA-Seq, while subsets of TILs were identified allowing for a detailed analysis of this important parameter.

### Conclusions

Immune profiling by RNA-Seq allows for the identification of samples with over-expression of multiple genes involved in checkpoint blockade, TILs, and cytokine/chemokine interactions. Subjectivity of interpretation of IHC as well as the lack of scalability will require a more high-throughput approach such as RNA-Seq. Our results show that such an approach is feasible with FFPE specimens and is more accurate and reproducible than IHC.

99

### An algorithmic approach to cancer immune profiling

Jeff Conroy<sup>1</sup>, Wiam Bshara<sup>1</sup>, Omilian Angela<sup>1</sup>, Blake Burgher<sup>2</sup>, He Ji<sup>2</sup>, Sean Glenn<sup>2</sup>, Carl Morrison<sup>1</sup>, Ann Mongan<sup>3</sup>

<sup>1</sup>Roswell Park Cancer Institute, Buffalo, NY, USA

<sup>2</sup>OmniSeq, LLC, Buffalo, NY, USA

<sup>3</sup>Thermo Fisher Scientific, South San Francisco, CA, USA

### Background

Immune checkpoint blockade with monoclonal antibodies directed at the inhibitory immune receptors has emerged



## Biomarkers and Immune Monitoring

*Presenting author underlined; Primary author in italics*

as a successful treatment for cancer patients. Evaluation of tumor checkpoint blockade by IHC is subjective, not reproducible, and importantly not scalable. We have designed a custom 362 gene RNA-Seq immune profiling panel that uses a multi-analyte algorithmic analysis (MAAA) to evaluate checkpoint blockade, tumor infiltrating lymphocytes, and cytokine/chemokine interactions. Additionally, we have previously profiled several hundred samples that are used for ranking of expression of each gene.

### Methods

269 FFPE cancer samples of diverse histologies were evaluated by RNA-Seq with a custom 362-gene Ion AmpliSeq Immune Response Profiling Assay using the Ion Chef™ and Proton. RNA-Seq analysis was performed with the Torrent Suite™ followed by normalization. Results for each sample were then evaluated with a MAAA to provide a prediction score for 61 known immunotherapy drugs. Predictions were reported for a continuous scale of 1-100 and interpreted as low, neutral, or high. All samples were also included in a custom TMA and IHC was performed for known targets of various immunotherapies when available.

### Results

At least one over expressed immunotherapeutic target was identified in more than 50% of the samples. By evaluating upstream and downstream mediators for each overexpressed target at least one high prediction score was identified in almost one-third of the samples. Not surprisingly the class of immune recognition, including checkpoint blockade, was the most frequently identified group of high prediction scores. High prediction scores were also identified for immune therapy drugs for the classes of immune inhibition (eg IDO1), tumor targeting mAbs (eg CD56), and microbe-associated (TLR7).

### Conclusions

Profiling by RNA-Seq allows for the identification of samples with over expression of multiple genes involved in the tumor immune repertoire. By applying a MAAA to these results in the context of a known database of results we can provide a prediction score that guides selection of various immune therapies, including more than just checkpoint blockade. As immune therapy moves from treatment of last resort to first and second line treatment an accurate scalable interrogation of the total tumor immune microenvironment will be required.

100

### **PD-L1, PD-L2 and PD-1 expression in metastatic melanoma: correlation with tumor infiltrating immune cells and clinical outcome**

Joseph M Obeid<sup>1</sup>, Gulsun Erdag<sup>2</sup>, Mark E Smolkin<sup>3</sup>, Donna H Deacon<sup>1</sup>, James W Patterson<sup>4</sup>, Lieping Chen<sup>5</sup>, Timothy N Bullock<sup>4</sup>, Craig L Slingsluff<sup>6</sup>

<sup>1</sup>Department of Surgery, University of Virginia, Charlottesville, VA, USA

<sup>2</sup>Department of Pathology, Johns Hopkins Medicine, Baltimore, MD, USA

<sup>3</sup>Department of Public Health Sciences, University of Virginia, Charlottesville, VA, USA

<sup>4</sup>Department of Pathology, University of Virginia, Charlottesville, VA, USA

<sup>5</sup>Department of Immunobiology, Yale University, New Haven, CT, USA

<sup>6</sup>University of Virginia, Charlottesville, VA, USA

### Background

The expression of PD-L1 in melanoma metastases limits immune control of tumor progression. Reliable biomarkers of patient survival, and response to treatment, are critical for patient care and selection. Yet the prognostic ability of PD-L1, or highly related PD-L2, remain controversial. We hypothesized that the expression of PD-L1 and PD-L2 by melanoma cells would correlate with both immune cell infiltration and patient survival, independent of checkpoint blockade therapy.

### Methods

Tissue microarrays of metastatic melanoma samples from 147 patients were evaluated (median follow-up: 19 months). None had been treated with PD-1/PD-L1 blockade. Cancer vaccines had been administered to 49 of the patients (33%). Melanoma cells were assessed by immunohistochemistry for surface and cytoplasmic expression of PD-L1 (clone 5H1) and PD-L2 (R&D Systems, AF1224). Immune cells were enumerated with stains for PD-L1, PD-1, CD8, CD45, CD4, CD3, CD163, CD20, CD138, and FoxP3. Relationships between the proportions of PD-L1 and PD-L2 expressing tumor cells with immune cell counts were assessed (by Spearman correlation), and with immune cell distribution (Immunotype, by Wilcoxon rank sum tests). Associations with patient survival were evaluated using Kaplan-Meier curves and Log-rank tests. P values less than 0.05 were considered significant.

### Results

Surface expression of either PD-L1 or PD-L2 by melanoma cells correlated significantly with increasing intratumoral densities of immune cells expressing each of the following: CD45, CD3, CD4, CD8, PD-1 and FoxP3 ( $p \leq 0.001$ ). PD-L1

## Biomarkers and Immune Monitoring

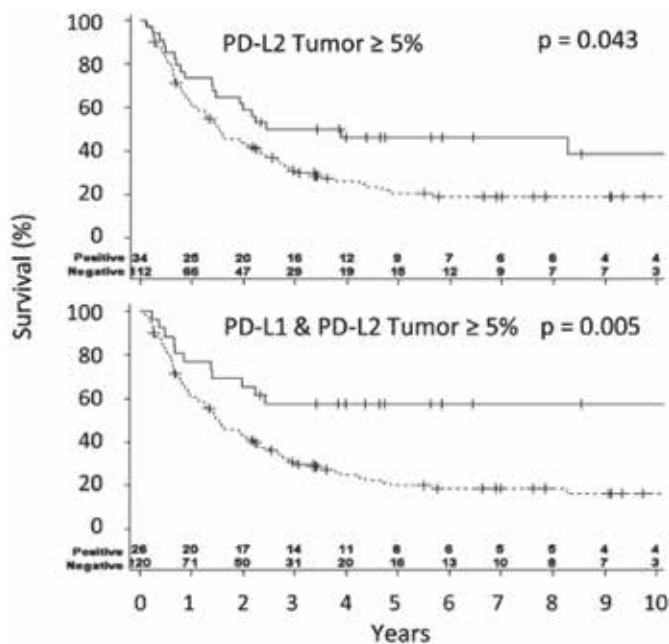
Presenting author underlined; Primary author in italics

expression was more common in tumors of patients who had previously participated in melanoma vaccine trials ( $p = 0.034$ ). Diffuse infiltration (Immunotype C), as opposed to infiltration limited to the perivascular spaces (Immunotype B), was associated with increased PD-L1 ( $p = 0.058$ ) and PD-L2 ( $p = 0.033$ ) expression by melanoma cells. Expression of PD-L2 on  $\geq 5\%$  of tumor cells was associated with improved overall survival ( $p = 0.043$ ), and the simultaneous positive expression of both PD-1 ligands was even more strongly associated with improved survival ( $p = 0.005$ , Figure).

### Conclusions

Both PD-L1 and PD-L2 are markers of immune infiltration. PD-L2 alone, or in combination with PD-L1, is a marker for prognosis in metastatic melanoma patients. The prognostic associations of the combination of PD-L1 and PD-L2 support future studies of the predictive value of these ligands in the setting of combination checkpoint blockade therapy.

### Association between PD-L2 expression on tumor cells and patient overall survival



101

### PD-L1 is expressed in inflamed non-small cell lung cancer (NSCLC) specimens and its expression predicts longer patient survival, despite co-expression of other checkpoint molecules

*Joseph M Obeid*<sup>1</sup>, Gulsun Erdag<sup>2</sup>, Donna H Deacon<sup>1</sup>, Craig L Slingluff<sup>3</sup>, Timothy N Bullock<sup>4</sup>

<sup>1</sup>Department of Surgery, University of Virginia, Charlottesville, VA, USA

<sup>2</sup>Department of Pathology, Johns Hopkins Medicine, Baltimore, MD, USA

<sup>3</sup>University of Virginia, Charlottesville, VA, USA

<sup>4</sup>Department of Pathology, University of Virginia, Charlottesville, VA, USA

### Background

PD-L1 expression is induced by IFN $\gamma$ , providing a feedback mechanism to control inflammation locally. There are conflicting data concerning its prognostic implication in patients with NSCLC. We hypothesized that PD-L1 is a positive prognostic indicator in NSCLC and that tumors expressing PD-L1 also express other immune checkpoint molecules and are highly infiltrated by T cells.

### Methods

Tissue microarrays (TMA) were constructed using two 1 mm cores from formalin-fixed paraffin embedded surgical specimens of 151 NSCLC (90 adenocarcinomas (AdCA), 58 squamous cell, and 3 mixed histology). Patients were not treated with PD-1/PD-L1 antibodies, 93% had stage I/II disease (median follow-up: 27 months). TMAs were evaluated by immunohistochemistry for PD-L1 (clone 5H1, membranous or cytoplasmic staining), GAL9, CD155, and PD-1 on tumor cells and CD8, FoxP3, PD-1 and LAG3 on immune cells. PD-L1 expression was recorded as the percent of staining tumor cells (scale 0-4). GAL9, CD155, and PD-1 were assessed by intensity of staining on tumor cells (scale 0-4). Stained immune cells were enumerated per core. Overall survival (OS) was assessed as a function of PD-L1 expression using Cox-proportional hazard. Correlations between PD-L1 expression and other markers were assessed using Pearson correlation coefficients. The Cancer Genome Atlas (TCGA) data were explored for validation of co-expression profiles using Fisher exact tests.

### Results

Increased percentages of PD-L1<sup>+</sup> tumor cells were associated with longer OS (univariate:  $p = 0.03$  and multivariate accounting for stage, age, histology, CD8 counts and tumor grade:  $p = 0.04$ ). PD-L1 expression also correlated with increasing CD8 ( $p = 0.002$ ), FoxP3 (0.013), LAG3 (0.007) or PD-1 ( $p = 0.049$ ) expressing lymphocytes and with the expression of



## Biomarkers and Immune Monitoring

Presenting author underlined; Primary author in italics

PD-1, GAL9 and CD155 on tumor cells ( $p \leq 0.02$ ). Tumors with high PD-L1 and CD8 expression (21%) also highly expressed inhibitory markers (FoxP3, LAG3, CD155 and GAL9, Figure). Similar significant correlations with PD-L1 mRNA expression were found in the TCGA cohort of 517 AdCA patients with PD-1 and CD8, and with checkpoint molecules LAG3, TIM3, and PD-L2, as well as the TIM3 ligand Gal9 (Table 1).

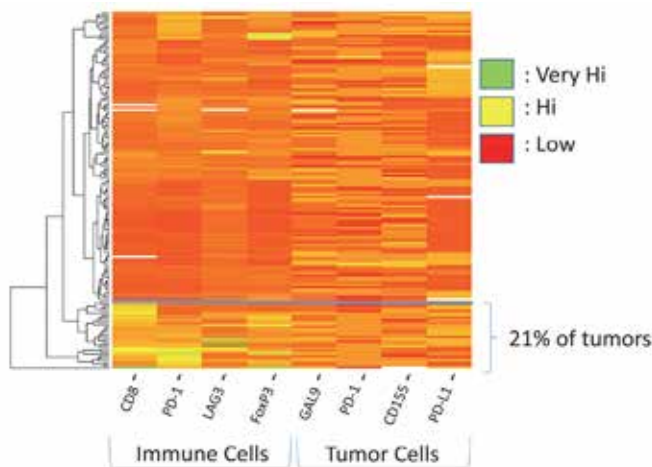
### Conclusions

Tumor cell expression of PD-L1 is a favorable prognostic indicator and correlates with CD8<sup>+</sup> T cell infiltration and co-expression of other inhibitory checkpoint molecules and ligands. The simultaneous presence of additional tumor protective signals in these tumors may influence their response to PD-1/PD-L1 blockade. Patterns of co-expression of checkpoint molecules may guide selection of combination checkpoint blockade therapy.

### Acknowledgements

Results presented are in part based upon data generated by the TCGA Research Network (<http://cancergenome.nih.gov>) (Cerami E, et al., PMID:22588877; Gao J, et al., PMID:23550210).

### The expression of different immune markers



Heatmap depicts protein expression intensities as determined by IHC in the 151 NSCLC tumors

### Genes expressed in association with PD-L1 in NSCLC

Gene	Co-Expression with PD-L1 in AdenoCA / SCCA		Test of Co-Occurrence or Mutual Exclusivity with PD-L1 in AdenoCA / SCCA		
	Spearman Score (r)	Percentile Rank	Fisher Exact Test P-value	Log Odds Ratio	Association Tendency*
PD-L2	0.76 / 0.73	0 / 0	<0.001 / <0.001	3.07 / 2.49	CO-O / CO-O
Tim-3	0.66 / 0.40	0 / 0	0.002 / 0.077	1.26 / -0.94	CO-O / ME
PD-1	0.53 / 0.34	1 / 1	<0.001 / 0.282	1.56 / 0.41	CO-O / CO-O
CD8A	0.54 / 0.40	1 / 0	0.001 / 0.042	1.48 / 0.87	CO-O / CO-O
TIGIT	0.56 / 0.38	1 / 1	0.143 / 0.090	0.63 / 0.88	CO-O / CO-O
FoxP3	0.48 / 0.30	2 / 3	0.193 / 0.553	0.58 / 0.04	CO-O / CO-O
LAG3	0.47 / 0.36	2 / 1	<0.001 / 0.007	1.63 / 1.11	CO-O / CO-O
CD8B	0.43 / 0.16	3 / 10	0.016 / 0.460	1.09 / <0.01	CO-O / ME
GAL9	0.29 / 0.36	8 / 1	0.029 / 0.209	-1.37 / 0.55	ME / CO-O
CD155	0.08 / -0.02	30 / 49	0.085 / 0.016	0.61 / -1.03	CO-O / ME
CD56	0.01 / 0.05	48 / 27	0.655 / 0.645	-0.21 / -0.06	ME / ME

\* CO-O = co-occurrence; ME = mutual exclusivity

Gene expression analysis in the 517 adenocarcinoma and 501 squamous cell carcinoma specimens from the TCGA provisional database.

### 102

### Enhanced vaccine-induced T cell responses observed with ipilimumab (anti-CTLA-4) treatment in a nonhuman primate pharmacodynamic model

*John T Loffredo*, Raja Vuyyuru, Sophie Beyer, Vanessa M Spires, Maxine Fox, Jon M Ehrmann, Katrina A Taylor, Alan J Korman, Robert F Graziano

Bristol-Myers Squibb, Princeton, NJ, USA

### Background

Currently, the preclinical assessment of immuno-oncology (I-O) agents relies heavily on murine tumor efficacy models, typically necessitating surrogate antibodies. Although nonhuman primate studies enable the use of human clinical candidate antibodies, such studies rely on limited pharmacodynamic (PD) markers. To more thoroughly evaluate the ability of I-O therapies to impact T cell immunity, we took advantage of the limited major histocompatibility complex (MHC) diversity in Mauritian cynomolgus macaques (MCMs) and utilized a highly immunogenic vaccine containing known MCM T cell epitopes. This design enabled longitudinal tracking of vaccine-elicited responses using antigen-specific T cell readouts. We then evaluated the effects of ipilimumab (anti-CTLA-4) in this nonhuman primate PD model.

### Methods

Pre-selected MCMs with specific MHC class I alleles that restrict known CD8<sup>+</sup> T cell epitopes were vaccinated intramuscularly with two non-replicating adenovirus serotype 5 (Ad5) viral constructs, one encoding simian immunodeficiency virus (SIV) Gag protein and the second



## Biomarkers and Immune Monitoring

*Presenting author underlined; Primary author in italics*

encoding SIV Nef protein. Following vaccination, MCMs received intravenous administration of either saline as control or ipilimumab (anti-CTLA-4) at 10 mg/kg. Vaccine-induced SIV-specific T cell responses were longitudinally evaluated via flow cytometry, including the use of peptide loaded MHC class I tetramers and IFN-gamma ELISPOT assays.

### Results

All vaccinated MCMs generated detectable levels of Gag- and Nef-specific T cell responses that typically peaked 2 to 3 weeks post-vaccination with a consistent immunodominance hierarchy. Addition of a single dose of ipilimumab resulted in robust augmentation of vaccine-induced CD8<sup>+</sup> T cell responses both at the peak of the vaccine response and after the vaccine response waned (>6 weeks post-vaccination). Enhanced Ki-67 expression was also detected on bulk CD8<sup>+</sup> and CD4<sup>+</sup> T cells, signifying increased proliferative capacity with ipilimumab treatment.

### Conclusions

Using this nonhuman primate PD model, we observed that the administration of ipilimumab enhanced the magnitude of vaccine-induced Ag-specific T cell responses. The ability to demonstrate such PD effects in monkeys allows for the testing of human clinical candidate antibodies in pharmacologically relevant models. This vaccine system can be used to provide early proof-of-concept data as well as aid in lead candidate selection by comparing antibodies targeting different epitopes or expressing different Fc domain formats (e.g., human IgG1 vs human IgG4). The described findings highlight the feasibility of this approach to investigate the impact of immunomodulatory antibodies/therapies on T cell immunity, particularly at an antigen-specific T cell level, and warrant the study of additional I-O agents.

103

### **Multispectral immunofluorescence as a novel and complementary method of characterizing tumor-infiltrating lymphocytes (TILs) in early stage breast cancer (ESBC)**

*David Page*<sup>1</sup>, Katherine Sanchez<sup>2</sup>, Carmen Ballesteros-Merino<sup>1</sup>, Maritza Martel<sup>2</sup>, Carlo Bifulco<sup>3</sup>, Walter Urba<sup>4</sup>, Bernard Fox<sup>3</sup>

<sup>1</sup>Earle A. Chiles Research Institute, Providence Portland Medical Center, Portland, OR, USA

<sup>2</sup>Providence Portland Medical Center, Portland, OR, USA

<sup>3</sup>Robert W. Franz Cancer Research Center, Earle A. Chiles Research Institute, Providence Cancer Center, Portland, Oregon, USA

<sup>4</sup>Earle A. Chiles Research Institute, Providence Cancer Center, Portland, OR, USA

### Background

In ESBC, TILs by gold-standard H&E Salgado criteria are prognostic for survival. Salgado criteria employ a single-slide “average” pathologist estimation of stromal TILs and excludes analysis of immune cell “hotspots.” Alternatively in colorectal cancer, the immunoscore methodology is prognostic for survival but employs CD8<sup>+</sup> assessment of immune cell “hotspots.” Recently, immune cell hotspots predicted response to anti-PD-L1 in breast cancer. Therefore, we wished to preliminarily evaluate both gold-standard and immune hotspot strategies for scoring TILs in ESBC, and to evaluate the utility of multispectral immunofluorescence (fluorescent mIHC), which allows for single-slide quantification of numerous immune cell subsets.

### Methods

From 8 sequentially diagnosed ESBC specimens, FFPE-preserved diagnostic core biopsies and subsequent excision specimens were obtained via an IRB-approved biospecimen protocol. Adjacent slides were submitted for routine H&E and fluorescent mIHC. H&E TILs were scored by a trained breast pathologist using Salgado criteria. Fluorescent mIHC was conducted using the PerkinElmer Vectra platform using a validated antibody panel (CD3, CD8, FoxP3, CD163, PD-L1, cytokeratin, and DAPI) [1]. To recapitulate the Salgado “TIL average” scoring method using fluorescent mIHC, 9 randomly-selected tumor-bearing 20x fields were selected from a single slide, then stromal TIL scores were averaged across these fields. To recapitulate the immunoscore “immune hotspot” methodology, CD8<sup>+</sup> high-density areas were visually identified at 4x magnification, then subsequently scored at 20x magnification.

### Results

Representative images are shown in Figure 1; all 16 specimens were high quality without significant crush artifact or nonspecific staining. Cytokeratin staining delineated stroma from tumor, allowing for automated quantification of both stromal and intratumoral TILs by fluorescent mIHC. H&E Salgado TIL scores ranged from 0-60%; core biopsy and excisional H&E TIL scores were highly correlated ( $r^2=0.7$ , Figure 2). By the “TIL average” fluorescent mIHC method, core biopsy and excisional biopsy immune cell counts were highly correlated (Table 1). By the “immune hotspot” fluorescent mIHC method, at least one hotspot was identified in each of the 16 specimens; however, core biopsy and excisional hotspot immune cell counts were only weakly correlated.

### Conclusions

In ESBC, fluorescent mIHC provides complementary data on TIL phenotype that may ultimately prove useful in personalizing immunotherapy. A “TIL average” strategy of assessing TILs by fluorescent mIHC may more stably

# Biomarkers and Immune Monitoring

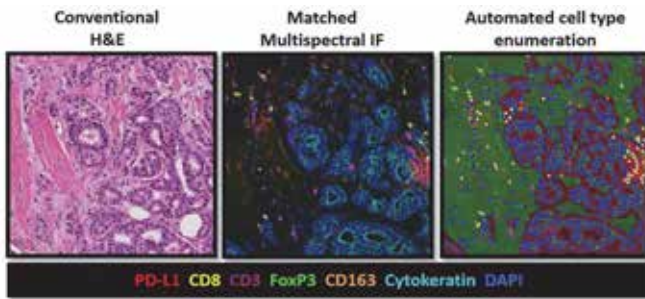
Presenting author underlined; Primary author in italics

characterize individual tumors compared to an “immune hotspot” approach; however, further evaluation is warranted.

## References

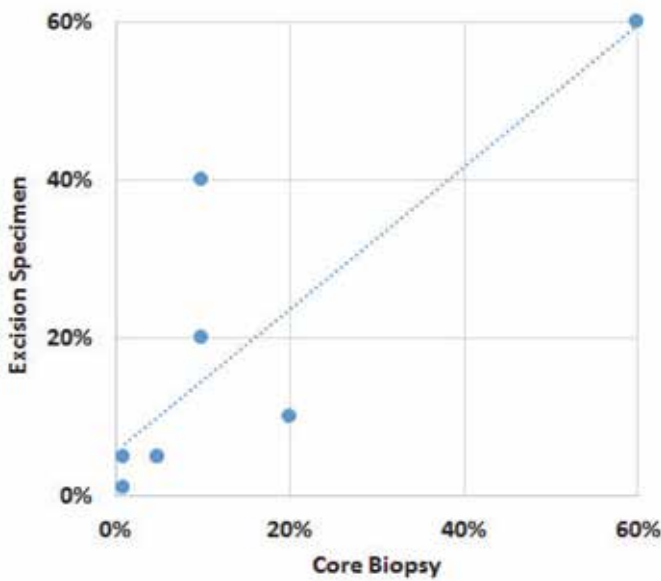
1. Feng Z, Puri S, Moudgil T, *et al*: **Multispectral imaging of formalin-fixed tissue predicts ability to generate tumor-infiltrating lymphocytes from melanoma.** *J Immunother Cancer* 2015, **3**:47.

Figure 1.



Representative H&E and IF Images

Figure 2.



Correlation of H&E Salgado score, core biopsy versus excisional specimen

Table 1.

Cell Type	“TIL average” method, $r^2$	“Immune hotspot” method, $r^2$
CD3+	0.67	0.04
CD8+	0.63	0.06
PD-L1+	0.42	0.34
PD-L1+ CD3+	0.74	0.29
CD163+	0.61	0.43

Correlation of IF cell densities, core biopsy versus excisional specimen

## 104

### Changes in uveal melanoma immune infiltrate in response to checkpoint blockade

*Sapna P Patel*, Mariana Petaccia De Macedo, Yong Qin, Alex Reuben, Christine Spencer, Michele Guindani, Roland Bassett, Jennifer Wargo

University of Texas MD Anderson Cancer Center, Houston, TX, USA

#### Background

Uveal melanomas are a subset of melanomas that contain few genomic mutations, thereby generating few neo-epitopes, and making them of low immunogenic potential. What is unknown is how systemic treatment for metastatic disease changes the immunogenicity of metastatic uveal melanomas. Previous work has demonstrated the immune infiltrate in cutaneous melanomas changes in response to treatment with checkpoint blockade. We undertook a pilot study to describe the changes in uveal melanoma immune infiltrate in response to treatment with systemic checkpoint blockade.

#### Methods

Twenty-two uveal melanoma patients who had received checkpoint blockade for metastatic disease, and who had archival pathologic tissue, were identified. Formalin-fixed paraffin-embedded tissue sections were obtained on available cases, and bleaching protocols were utilized to reduce heavy melanin pigmentation. Immunohistochemistry was performed using validated antibodies for CD3, CD8, CD68, FOXP3, PD-1, and PD-L1.

#### Results

Eleven uveal melanoma patients had at least one time point of tumor tissue collected and evaluated, most commonly before treatment initiation. Nine patients had at least two time points collected and evaluated, some while on treatment, others at progression of disease. In a representative case, a pre-treatment metastatic liver biopsy

## Biomarkers and Immune Monitoring

*Presenting author underlined; Primary author in italics*

showed low level of CD8+ lymphocytes infiltrating the tumor. After 4 doses of ipilimumab, with best overall clinical response of disease progression, the patient had another liver biopsy. This tissue sample showed a notable increase in CD8+ lymphocyte infiltration via immunohistochemistry compared to the pre-treatment sample. This is consistent with similar data from cutaneous melanoma patients receiving checkpoint blockade, where CD8+ infiltrates at progression is lower than during treatment response, but higher than at baseline. Full details of all cases will be presented at the SITC Annual Meeting.

### Conclusions

Immune infiltration does change in metastatic uveal melanoma in response to systemic checkpoint blockade. Some patients did experience an increase in infiltrating CD8+ T lymphocytes while on immunotherapy. The change in immune infiltrate did not, however, correlate with clinical response to treatment. Future analysis includes an evaluation for immune suppressive molecules, such as indoleamine 2,3-dioxygenase and transforming growth factor-beta, and evaluation of immune infiltration in response to combination checkpoint blockade as well as to targeted therapy.

### Acknowledgements

The authors would like to acknowledge Zac Cooper, PhD, for his time at MD Anderson crafting the grant that funded this research.

### 105

#### Development of an automated brightfield duplex IHC for simultaneous detection of PD-L1 and CD8 on lung carcinoma and tonsil FFPE tissue sections

*Adriana Racolta*, Brian Kelly, Tobin Jones, Nathan Polaske, Noah Theiss, Mark Robida, Jeffrey Meridew, Iva Habensus, Liping Zhang, Lidija Pestic-Dragovich, Lei Tang

Ventana Medical Systems, Inc., Tucson, AZ, USA

### Background

Behavior of various tumor-infiltrating immune cells in the tumor environment correlates with patient responses to therapies. Particularly, the localization of CD8+ T cells within and around a tumor mass containing immune and tumor cells expressing the programmed death-ligand 1 (PD-L1) checkpoint marker is positively correlated with response to immunotherapy targeting PD-L1 blockade. Simultaneous detection of CD8+ T cells and PD-L1+ cells could become a valuable diagnostic tool. We developed a fully automated duplex immunohistochemistry (IHC) assay to detect these two biomarkers on a single formalin-fixed, paraffin-embedded (FFPE) tissue section using VENTANA BenchMark ULTRA stainers and brightfield microscopy.

### Methods

The duplex IHC assay uses anti-PD-L1 (SP263) and anti-CD8 (SP239) rabbit monoclonal primary antibodies and goat anti-rabbit secondary antibodies conjugated to either horseradish peroxidase (HRP) or alkaline phosphatase (AP). The detection and amplification of signal is achieved upon activation of tyramide- or quinone methide-conjugated chromogens by the corresponding enzymes and covalent binding of chromogens. The detection of PD-L1, with a purple chromogen and CD8 with either yellow or cyan is performed sequentially and fully automated on the VENTANA BenchMark ULTRA stainers and includes a heat deactivation (HD) step between the two rounds of detection to prevent cross-reactivity of same species antibodies. The assay was developed and tested using normal human tonsil tissue, lung carcinomas, and multi tissue arrays. The staining was assessed by trained pathologists or measured using commercially available imaging software.

### Results

The PD-L1/CD8 duplex assay showed equivalent staining to the single PD-L1 or CD8 DAB staining (Figure 1) on normal tonsil and lung carcinomas. The reproducibility test showed 100% agreement between three lots of reagents and 89% (blue detection) and 100% (yellow and purple detection) agreement between three testing laboratories. The staining precision is acceptable as the coefficient of variation of staining intensity was less than 2%. Effectiveness of heat deactivation was validated for the conditions of the duplex assay as we did not detect cross-reactivity or adverse effects on the epitopes and the chromogens.

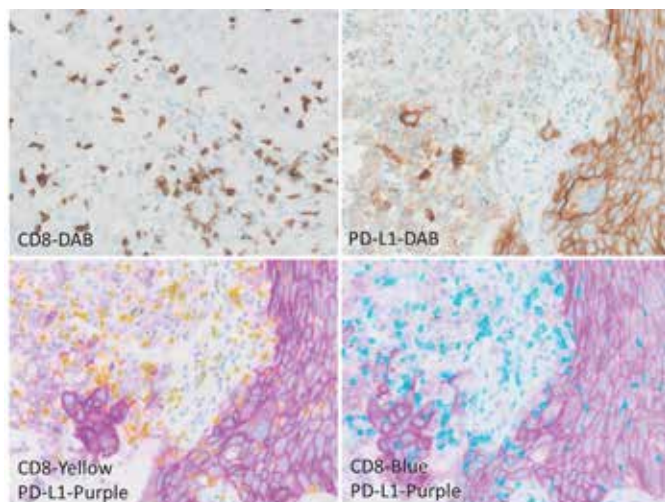
### Conclusions

We developed a fully automated and robust dual IHC staining assay for detection of PD-L1 and CD8 markers on the same slide. The chromogens used in this assay are compatible with regular counterstains and alcohol dehydration. The dual IHC assay could facilitate mining of spatial relationship between the two markers for evaluation of tumor microenvironment.

## Biomarkers and Immune Monitoring

Presenting author underlined; Primary author in italics

**Figure 1. Comparative single and dual staining of PD-L1 and CD8 in lung tumor tissue**



106

### Application of a test developed for prediction of response to high dose interleukin-2 (HDIL-2) and the BDX008 test for prediction of outcomes following checkpoint inhibitors to cohorts of patients treated with HDIL-2 or nivolumab

Ryan J Sullivan<sup>1</sup>, Theodore Logan<sup>2</sup>, Nikhil Khushalani<sup>3</sup>, Kim Margolin<sup>4</sup>, Henry Koon<sup>5</sup>, Thomas Olencki<sup>6</sup>, Thomas Hutson<sup>7</sup>, Brendan Curti<sup>8</sup>, Joanna Roder<sup>9</sup>, Shauna Blackmon<sup>10</sup>, Heinrich Roder<sup>9</sup>, John Stewart<sup>11</sup>, Asim Amin<sup>12</sup>, Marc S Ernstoff<sup>13</sup>, Joseph I Clark<sup>14</sup>, Michael B Atkins<sup>15</sup>, Howard L Kaufman<sup>16</sup>, Jeffrey Sosman<sup>17</sup>, Jeffrey Weber<sup>18</sup>, David F McDermott<sup>19</sup>

<sup>1</sup>Medical Oncology Department, Massachusetts General Hospital, Boston, MA, USA

<sup>2</sup>Simon Cancer Center, Indiana University, Indianapolis, IN, USA

<sup>3</sup>H. Lee Moffitt Cancer Center, Tampa, FL, USA

<sup>4</sup>Department of Medical Oncology, City Of Hope, Duarte, CA, USA

<sup>5</sup>Case Western Reserve University, Cleveland, OH, USA

<sup>6</sup>The Ohio State University, Columbus, OH, USA

<sup>7</sup>Texas Oncology-Baylor Charles A. Sammons Cancer Center, Dallas, TX, USA

<sup>8</sup>Earle A. Chiles Research Institute, Providence Cancer Center, Portland, OR, USA

<sup>9</sup>Biodesix, Inc., Boulder, CO, USA

<sup>10</sup>Massachusetts General Hospital Cancer Center, Boston, MA, USA

<sup>11</sup>Wake Forest Baptist Medical Center, Winston Salem, NC, USA

<sup>12</sup>Levine Cancer Institute, Carolinas HealthCare System,

Charlotte, NC, USA

<sup>13</sup>Roswell Park Cancer Institute, Buffalo, NY, USA

<sup>14</sup>Loyola University Medical Center, Maywood, IL, USA

<sup>15</sup>Georgetown-Lombardi Comprehensive Cancer Center, Washington DC, DC, USA

<sup>16</sup>Rutgers Cancer Institute of New Jersey, New Brunswick, NJ, USA

<sup>17</sup>Robert Lurie Comprehensive Cancer Center of Northwestern University, Chicago, IL, USA

<sup>18</sup>NYU Langone Medical Center, New York, NY, USA

<sup>19</sup>Beth Israel Deaconess Medical Center, Boston, MA, USA

### Background

With multiple approved immunotherapies for metastatic melanoma (MM), tests that enable optimal treatment selection are needed. BDX008 is a serum protein-based test that identifies patients with better (BDX008+) or worse (BDX008-) survival (OS) on nivolumab [1]. Using similar methods and samples from the IL-2 Select trial, a test for prediction of progression-free survival (PFS) after HDIL-2 treatment has been developed that divides patients into two groups, A and B (better and worse PFS, respectively). Performance of these tests is compared in two cohorts of MM patients treated with either HDIL-2 or nivolumab.

### Methods

MALDI mass spectra were generated for pre-treatment samples from 114 pts in the IL-2 Select trial and 119 patients from a trial of nivolumab with or without a peptide vaccine. (The IL-2 trial was used for development of the IL-2 test, the nivolumab/peptide trial for development of BDX008.) Both the IL-2 test and BDX008 were applied to all spectra generated from these trial samples. Outcomes included PFS (HDIL-2), time to progression (TTP; nivolumab/peptide), and OS (both), depending on the test and the trial agent (Figure 1 and results).

### Results

Of the 112 patients treated with HDIL-2 (2 failed BDX008 QC), 39 (35%) were classified as group A, and 89 (79%) as BDX008+. All group A samples were BDX008+. PFS was strongly correlated with IL-2 test classification: IL-2 test group B had inferior PFS compared with IL-2 test group A, but no difference whether BDX008+ or not. In contrast, OS was favorable with BDX008+ regardless of IL-2 test group. Hence, patients classified as IL-2 test group B and BDX008+ had a similar OS to group A patients despite an inferior PFS, possibly due to subsequent checkpoint inhibitor therapy or to pre-IL-2 factors with prognostic importance but not predictive for PFS after IL-2. In the nivolumab patients, 72 (61%) samples were BDX008+ and 37 (31%) fell into IL-2 test group A; all 37 were BDX008+. Both TTP and OS correlated closely with BDX008: BDX008+ had better outcomes than BDX008-; also, BDX008- outcomes were independent of IL-2 test status.



## Biomarkers and Immune Monitoring

Presenting author underlined; Primary author in italics

### Conclusions

Patients classified into poor outcome categories by both BDx008 and the IL-2 test have poor outcomes on both immunotherapeutic regimens. For the remaining patients, the two tests perform differently, identifying partially overlapping groups of patients likely to have good outcomes with one or the other therapy.

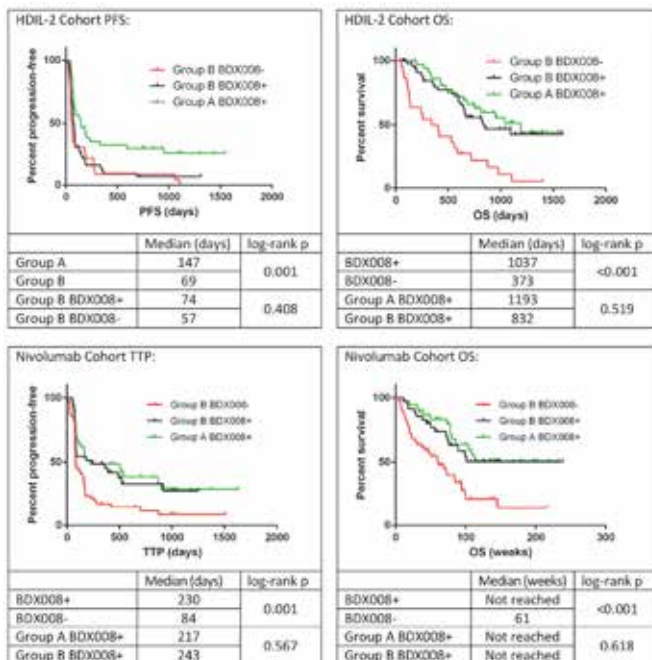
### Trial Registration

ClinicalTrials.gov identifier NCT01288963 and NCT01176461.

### References

1. Weber J, *et al*: Pre-treatment patient selection for nivolumab benefit based on serum mass spectra. SITC2015.

Figure 1



107

### A test identifying advanced melanoma patients with long survival outcomes on nivolumab shows potential for selection for benefit from combination checkpoint blockade

Jeffrey Weber<sup>1</sup>, Harriet Kluger<sup>2</sup>, Ruth Halaban<sup>3</sup>, Mario Snzol<sup>2</sup>, Heinrich Roder<sup>4</sup>, Joanna Roder<sup>4</sup>, Senait Asmellash<sup>4</sup>, Arni Steingrimsson<sup>4</sup>, Shauna Blackmon<sup>5</sup>, Ryan J Sullivan<sup>6</sup>

<sup>1</sup>NYU Langone Medical Center, New York, NY, USA

<sup>2</sup>Yale Medical Oncology, New Haven, CT, USA

<sup>3</sup>Yale University School of Medicine, New Haven, CT, USA

<sup>4</sup>Biodesix, Inc., Boulder, CO, USA

<sup>5</sup>Massachusetts General Hospital Cancer Center, Boston, MA, USA

<sup>6</sup>Medical Oncology Department, Massachusetts General Hospital, Boston, MA, USA

### Background

Multiple immunotherapeutic regimens for the treatment of metastatic melanoma (MM) are now approved and can provide long term benefit to a proportion of patients. Blood-based assays that can assist treatment selection are of significant clinical relevance. Using serum mass spectrometry, a test has been developed to predict good outcomes on anti-PD-1 therapy. We present results on the development and validation of this test.

### Methods

MALDI mass spectra were generated for pretreatment serum samples from 119 patients treated with nivolumab at Moffitt Cancer Center. Using a classifier development platform optimized for creation of multivariate molecular diagnostic tests which can generalize well to independent datasets, a test was created to identify patients with particularly good outcomes. This test classifies samples into two groups: group 1 (very good outcome) and group 2 (inferior outcome). This test was validated in two independent cohorts of MM patients receiving anti-PD-1 agents: 30 patients from Yale University (YU) and 25 patients, most treated with pembrolizumab, from Massachusetts General Hospital (MGH). The test was also applied to pretreatment samples collected from 21 patients from YU receiving combination PD-1/CTLA-4 blockade. Difference in outcomes between patients classified as group 1 and group 2 within each cohort were assessed using log-rank p values and Cox proportional hazard ratios (HRs).

### Results

Of the 119 patients used in test development, 34 (29%) were classified as group 1. Group 1 had better survival (OS) and time-to-progression (p=0.002 and p=0.014, respectively), with two-year survival of 67%. In the YU cohort receiving an anti-PD-1 agent, 13 (43%) classified as Group 1, which had better OS than Group 2 (p<0.001) and two-year survival above 80%. Eleven (44%) patients from the MGH cohort were classified as Group 1. There was a trend to improved OS for Group 1 compared to Group 2 (p=0.062, HR= 0.17). Within the cohort of patients receiving combination PD-1/CTLA-4 blockade, 13 (62%) classified as Group 1. Two-year survival was 83% in Group 1 and 63% in Group 2.

### Conclusions

The test identifies a subgroup of patients with extremely good outcomes on anti-PD-1 therapy. High two-year survival in the Group 1 cohorts may indicate that the test has potential utility in identifying patients who derive significant benefit from anti-PD-1 monotherapy and might gain little benefit from the addition of an anti-CTLA-4 agent. As follow-





## Biomarkers and Immune Monitoring

Presenting author underlined; *Primary author in italics*

up was only 2 years for OS, and the numbers are small, further validation is necessary.

### Trial Registration

ClinicalTrials.gov identifier NCT01176461.

108

### Reproducibility of automated and semi-automated seven-color immunofluorescence staining with tyramide signal amplification

Chichung Wang, Kristin Roman, Amanda Clement, Sean Downing, Clifford Hoyt

PerkinElmer, Hopkinton, MA, USA

#### Background

Multiplexed immunohistochemistry has become increasingly important as cancer immunologists seek understanding of specific cell-to-cell interactions within tumor and its microenvironment. To support this need, we have developed staining approaches that leverage the properties of tyramide signal amplification (TSA) to increase signals above background and to provide photostable balanced signals. However, automation is needed before broad adoption occurs in research and eventually in clinical practice. We present two methods for automation, one fully automated on a Leica Bond Rx and the other semi-automated on a Biocare Intellipath. The fully automated approach uses sodium dodecyl sulfate (SDS) to denature endogenous myeloperoxidase (MPO) and eliminate cross reactivity among antibodies without affecting previously applied fluorescence labels. The semi-automated on the Intellipath automates all staining steps, except for antibody stripping which occurs off-line using microwave. In this presentation, we present detailed protocols and assess analytical performance.

#### Methods

Previously, we demonstrated reproducible immunofluorescence labeling with a manual protocol utilizing microwave exposure to remove antibodies between each marker (Methods 70 (2014) 46–58). In the fully automated approach using the Bond Rx, we replace the microwave step with a 7-minute exposure to 5% SDS at 50C. Tonsil and breast cancer sections were stained with a 6-plex, 7-color panel for PD-1, PD-L1, CD8, CD68, Foxp3, cytokeratin, plus DAPI counterstain. Serial sections were used to assess reproducibility, cross talk, interference, and signal-to-background ratio. Slides were scanned and analyzed using multispectral imaging (Vectra™) to isolate fluorescence signals for accurate measurement.

#### Results

Balanced specific staining was achieved with both methods. Crosstalk was below the limit of detection. Signal-to-

background was above 10:1 for each label, as measured by looking at signal strength on and off cells positive for the marker of interest. Coefficient of variation of measured signals was generally less than 20% for the semi-automated approach and less than 15% for the fully automated approach.

#### Conclusions

This is the first demonstration of reproducible and independent fully-automated TSA-based automated multiplexed immunofluorescence using SDS to perform antibody denaturation. It is also a demonstration of a semi-automated approach that performs antibody stripping off of the autostaining instrument and is compatible with a broad range of mid-range and conventional autostaining platforms.

#### References

1. Stack EC, Wang C, Roman KA, Hoyt CC : **Multiplexed immunohistochemistry, imaging, and quantitation: A review, with an assessment of Tyramide signal amplification, multispectral imaging and multiplex analysis** . *Methods* 2014 , **70**:46-58.

109

### Spatial distribution of CD8+ T cells predicts response to ipilimumab in malignant melanoma

*Nathalie Harder*<sup>1</sup>, Guenter Schmidt<sup>1</sup>, Ralf Schoenmeyer<sup>1</sup>, Nicolas Brieu<sup>1</sup>, Mehmet Yigitsoy<sup>1</sup>, Gabriele Madonna<sup>2</sup>, Gerardo Botti<sup>2</sup>, Antonio Grimaldi<sup>3</sup>, Paolo A Ascierto<sup>3</sup>, Ralf Huss<sup>1</sup>

<sup>1</sup>Definiens AG, Munich, Bayern, Germany

<sup>2</sup>Istituto Nazionale dei Tumori di Napoli Fondazione “G. Pascale”, Naples, Campania, Italy

<sup>3</sup>Istituto Nazionale Tumori Fondazione, Napoli, Italy

#### Background

Although checkpoint blockade immunotherapies are successful in some cancer patients, the majority of patients still do not benefit from these therapies. The advances of digital pathology and the availability of quantitative whole slide image analysis allows for a systematic search for novel tissue-based biomarkers to predict therapy response and overall survival. Here, we present a Tissue Phenomics case study to discover a potential companion diagnostic test for ipilimumab (IPI) in malignant melanoma.

#### Methods

The patient cohort is a subset of the MISIPI study [1], comprising 30 melanoma patients. Consecutive sections from FFPE tissue were immunohistochemically stained with CD3, CD8, and FoxP3. The sections were digitized and automatically aligned using an advanced staining-independent image registration algorithm. Tumor regions were manually annotated by a pathologist, excluding

## Biomarkers and Immune Monitoring

*Presenting author underlined; Primary author in italics*

artifacts and necrotic regions. A novel parameter-free cell segmentation approach was used to automatically detect and classify cells with respect to their protein expression profile [2] and to the spatial distance to the annotated tumor border. We computed for each of the CD3+, CD8+ and FoxP3+ cell populations the average cell density in the tumor in a border region within the tumor and in a border region just outside the tumor. By computing a potentially predictive score for each ratio of the measured cell densities, we identified the most promising patient stratification algorithm in terms of predictive values for therapy response and the Kaplan-Meier statistics p-value for overall survival.

### Results

We identified a promising scoring algorithm which is based on the ratio of the CD8+ cell density at the inner tumor border to the CD8+ cell density in the tumor. It enables patient stratification into IPI responders and non-responders with high predictive values (positive predictive value 68%, negative predictive value 79%, prevalence 39%) and at the same time, excellent prediction of overall survival (p-value < 0.0015).

### Conclusions

A novel companion diagnostic algorithm for ipilimumab in malignant melanoma was discovered by Tissue Phenomics. It provides high predictive power and enables considerably improved treatment decisions. However, the results are still preliminary and need to be further validated.

### References

1. Bifulco C, Capone M, Feng Z, *et al*: **MISIPI study: Melanoma ImmunoScore evaluation in patients treated with ipilimumab**. *J Transl Med* 2014, **12(Suppl 1)**:P11.
2. Brieu A, Pauly O, Zimmermann J, Binnig G, Schmidt G: **Slide-specific models for segmentation of differently stained digital histopathology whole slide images**. *Proc SPIE* 2016, **9784**:978410.

110

### Tumor-associated Macrophages (TAMs) as a prognostic marker for prostate cancer progression

*Maria Athelou<sup>1</sup>, Harald Hessel<sup>2</sup>, Nathalie Harder<sup>1</sup>, Alexander Buchner<sup>3</sup>, Günter Schmidt<sup>1</sup>, Christian Stief<sup>3</sup>, Ralf Huss<sup>1</sup>, Gerd Binnig<sup>1</sup>, Thomas Kirchner<sup>2</sup>*

<sup>1</sup>Definiens AG, Munich, Germany

<sup>2</sup>Institute of Pathology, Ludwig-Maximilians-University, Munich, Germany

<sup>3</sup>Department of Urology, Ludwig-Maximilians-University, Munich, Klinikum Grosshadern, Germany

### Background

Tumor-associated macrophages (TAMs) and tumor infiltrating T-cells (TILs) have been associated with tumor progression

in various tumor entities. In this study, we applied the Tissue Phenomics technology to discover new TAM-related prognostic factors to predict prostate cancer progression. This technology correlates clinical outcome data with image analysis results from (virtually) multiplexed tissue slides. Multiplexing enables the co-analysis of multiple immunohistochemically (IHC) stained tissue sections. Using this method, we investigated the prognostic relevance of M1/M2 TAMs (CD68/CD163) and TILs (CD3/CD8) within prostate cancer (PCa) resection specimens from low-risk and intermediate-risk patients with respect to Prostate Specific Antigen (PSA) recurrence after radical prostatectomy (RP).

### Methods

Analysis and quantification were performed on three consecutive duplex stained FFPE tissue sections from 89 patients (on which 40 with PSA recurrence) with low- to intermediate-risk PCa after RP with a Gleason-Score ≤ 7a. M1- and M2-type macrophages were characterized by CD68 and CD163, T-cells by CD3 and CD8, tumor and non-tumor epithelial tissue regions by CK18 and p63. CK18 positive glands without any p63-stained basal cell nuclei are considered as tumor glands. The three duplex stained slides were analyzed and converted into one virtual tissue slide through image co-registration. TAMs and TILs were quantified separately in the distinct tumor regions and the tumor microenvironment. Both, the overall number of TILs and TAMs and the ratio of M1- and M2-positive macrophages were analyzed using the Tissue Phenomics technology. The correlation between various TIL and TAM cell densities within the different regions of interest (tumor and tumor microenvironment), the tumor grading and tumor stage, and clinical parameters (PSA recurrence, overall and disease-free survival) were performed.

### Results

Prostate cancer patients without PSA recurrence show a significantly higher ratio of CD8 to CD163 positive cell densities in the tumor microenvironment. The PSA recurrence prediction accuracy is 76.8% with a Kaplan-Meier log-rank test p-value of 2.7e-5 for the disease free survival time.

### Conclusions

These first results indicate a considerable prognostic potential of TAMs to predict PSA recurrence in PCa. The application shows that the Tissue Phenomics Technology enables the investigation and the evaluation of the prognostic relevance of certain immune cell populations. The analysis of the relation of TILs to TAMs is an excellent example for such kind of applications with a potentially high impact for prostate cancer patient treatment decisions.

## Biomarkers and Immune Monitoring

Presenting author underlined; Primary author in italics

111

### Co-expression of PD-L1 and other targetable protein and genomic markers: opportunities for combination therapy

Shankar Sellappan<sup>1</sup>, Sheeno Thyparambil<sup>1</sup>, Sarit Schwartz<sup>1</sup>, Fabiola Cecchi<sup>1</sup>, Andrew Nguyen<sup>2</sup>, Charles Vaske<sup>2</sup>, Todd Hembrough<sup>1</sup>

<sup>1</sup>NantOmics, Rockville, MD, USA

<sup>2</sup>NantOmics, Culver City, CA, USA

#### Background

Several immune checkpoint inhibitors have been approved to treat multiple solid tumor types. Immune responses could be modulated by targeted therapies as well as cytotoxic agents. The opportunity to combine immunotherapies with agents against targetable proteomic and genomic biomarkers may lead to improved outcomes and reduced toxicities; however, analysis of multiple biomarkers creates an increased demand for tissue. Using a multi-omic approach that incorporates mass spectrometry based proteomic analysis and NGS, we were able to objectively detect the expression of multiple therapeutically-relevant proteins and genomic alterations from a minimum two FFPE sections. Here, we report on patient samples that express the PD-L1 protein and either co-express therapeutically-relevant proteins (EGFR, HER2, MET, ROS1, TOPO1, etc.) or gene mutations (MET, KIT, BRAF, JAK3, etc.).

#### Methods

Formalin-fixed, paraffin-embedded (FFPE) sections of tumor tissue from patients with different cancer indications were obtained. For proteomics analysis, tumor area of 8 mm<sup>2</sup> was marked by a board-certified pathologist. Following laser microdissection of the marked areas, tumor cell proteins were extracted using the Liquid Tissue<sup>®</sup> process and subjected to selected reaction monitoring mass spectrometry to quantify 27 targeted proteins in each patient sample. For genomics analysis, genomic content was isolated from the FFPE tumor tissue sections as well as from corresponding normal samples and subjected to NGS for whole genome sequencing (tumor and normal) and whole transcriptome sequencing (tumor only) analysis.

#### Results

Quantitative proteomic analyses of 1710 cancer patient samples across multiple indications revealed a wide range (144 – 1025 amol/mg) of PD-L1 protein expression. Several actionable protein targets were co-expressed with PD-L1, including targeted therapy markers (EGFR (80%), HER2 (29%), MET (56%), ROS1 (22%)) and chemotherapy markers (TOPO1 (100%), etc.). PD-L1 protein expressing tumors were also found to harbor therapeutically-relevant genomic mutations, including MET (N375S and T1010I), JAK3 (V722I), KIT (M541L), BRAF (V600E), CDKN2A (D84H), etc.

#### Conclusions

Tumor molecular profiling by both proteomic and genomic analysis revealed co-expression of targetable proteins (EGFR, HER2, MET, TOPO1, etc.) and genomic alterations (MET, KIT, BRAF, etc.) in patients that express the PD-L1 protein. From minimal amounts of tissue, we were able to assess multiple therapeutically-associated biomarkers using mass spectrometry based targeted quantitative proteomics and NGS based comprehensive genomic (DNA and RNA) analysis. Ongoing clinical trials involving immunotherapy and chemo/targeted therapies could benefit from molecularly stratifying patients by proteomic and genomic testing to increase efficacy and reduce toxicity.

### 112 Abstract Travel Award Recipient

#### ImmunoMap: a novel bioinformatics tool for analysis of T cell receptor repertoire data in model systems and clinical settings

John-William Sidhom<sup>1</sup>, Catherine A Bessell<sup>2</sup>, Jonathan Havel<sup>3</sup>, Jonathan Schneck<sup>4</sup>, Timothy A Chan<sup>3</sup>, Eliot Sachsenmeier<sup>5</sup>

<sup>1</sup>Johns Hopkins University School of Medicine, Baltimore, MD, USA

<sup>2</sup>Immunology Program, Johns Hopkins University, School of Medicine, Columbia, MD, USA

<sup>3</sup>Memorial Sloan Kettering Cancer Center, New York, NY, USA

<sup>4</sup>Johns Hopkins Medical Institute, Baltimore, MD, USA

<sup>5</sup>University of Rochester, Monrovia, MD, USA

#### Background

There has been a dramatic increase in T cell receptor (TCR) sequencing spurred, in part, by the widespread adoption of this technology across academic medical centers and by the rapid commercialization of TCR sequencing. While the raw TCR sequencing data has increased, there has been little in the way of approaches to parse the data in a biologically meaningful fashion. The ability to parse this new type of ‘big data’ quickly and efficiently to understand the T cell repertoire in a structurally relevant manner has the potential to open the way to new discoveries about how the immune system is able to respond to insults such as cancer and infectious diseases.

#### Methods

Here we describe a novel method utilizing phylogenetic and sequencing analysis to visualize and quantify TCR repertoire diversity. To demonstrate the utility of the approach, we have applied it to understanding the shaping of the CD8 T Cell response to self (Kb-TRP2) and foreign (Kb-SIY) antigens in naïve and tumor bearing B6 mice. Additionally, this method was applied to tumor infiltrating lymphocytes (TILs) from patients undergoing Nivolumab (anti-PD-1) therapy in a clinical trial for metastatic melanoma to understand TCR repertoire characteristics between responders and non-responders.

## Biomarkers and Immune Monitoring

Presenting author underlined; *Primary author in italics*

### Results

Analysis of the naïve CD8 response to SIY showed a lower clonality yet more closely structurally related response whereas CD8 responses to TRP2 were highly clonal yet less structurally related. Presence of tumor exhibited interesting differential effects on SIY vs. TRP2. We believe that differences in TCR repertoire suggest effects from central and peripheral tolerance on self vs. foreign antigens. In clinical trial data, the phylogenetic analysis revealed unique TCR repertoire signatures that differentiated responders from non-responders to anti-PD-1 therapy, including some that could be detected prior to initiation of therapy. Additionally, this analysis revealed that patients whose CD8 response had a larger contribution from novel and unique structural clones responded better to therapy.

### Conclusions

In summary, we have developed and demonstrated a novel method to meaningfully parse and interpret TCR repertoire data and have applied it to yield a novel understanding of CD8 T Cell responses to different types of antigens as well as key characteristics in those who respond to anti-PD-1 therapy.

### Naive SIY vs. TRP2 TCR Repertoire

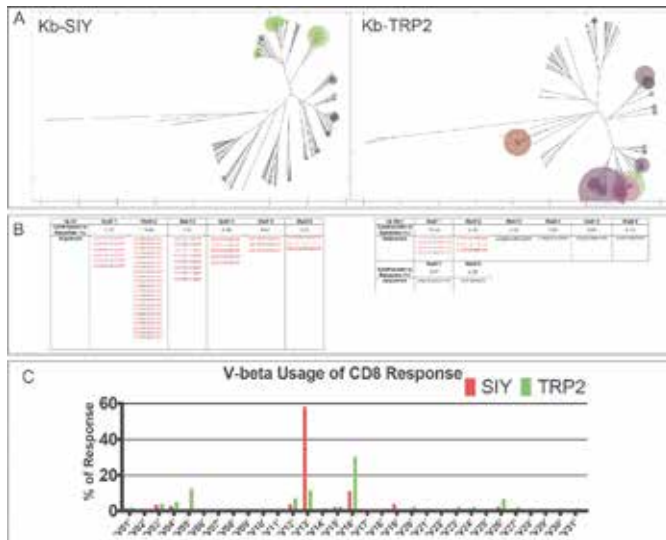


Figure 1. A) Weighted Phylogenetic Trees Comparing Kb-SIY vs Kb-TRP2 TCR Repertoire. Size of circles proportional to frequency of sequence. Color of circle corresponds to V-Beta Usage. B) Dominant Motifs gathered from phylogenetic trees determined by homologous sequences and their contribution to the response C) V-Beta Usage of Kb-SIY vs Kb-TRP2 Response

### Effects of Tumor on TCR Repertoire

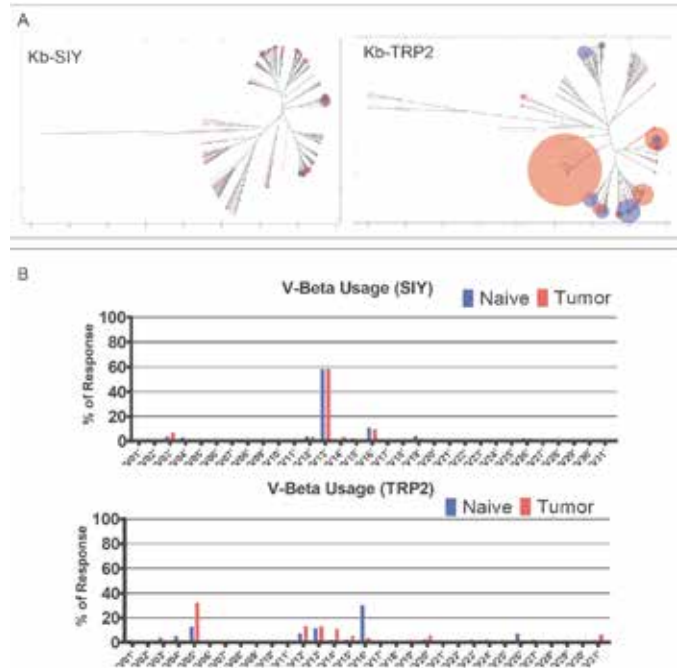


Figure 2. A) Weighted Phylogenetic Trees comparing Naive to Tumor-Bearing TCR Repertoire from spleen. Size of Circles proportional to frequency of sequence. Blue Circles = Naive Repertoire. Red Circles = Tumor-Bearing Repertoire. B) V-Segment Usage of Kb-SIY vs Kb-TRP2 Responses for Naive vs Tumor-Bearing Response

### Effect of anti-PD-1 (Nivolumab) therapy on Tumor Infiltrating Lymphocyte TCR Repertoire

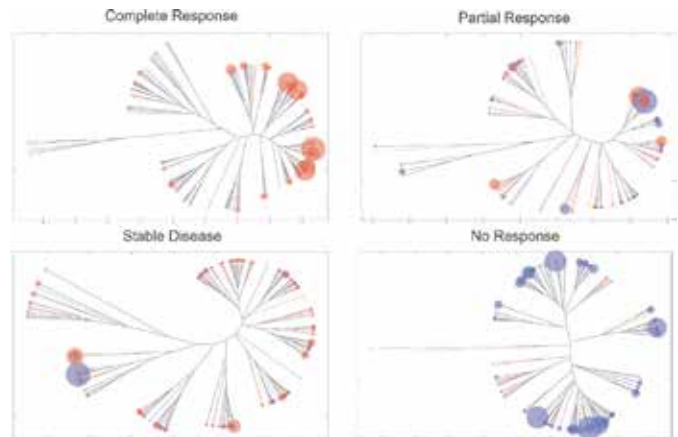


Figure 3. Examples of weighted phylogenetic trees from four cohorts of responders on anti-PD-1 therapy. Size of circles proportional to frequency of sequence. Blue = TCR repertoire prior to therapy. Red = TCR repertoire on therapy.



## Biomarkers and Immune Monitoring

*Presenting author underlined; Primary author in italics*

113

### Immunomonitoring of patients with colorectal cancer

Jan Spacek<sup>1</sup>, Michal Vocka<sup>1</sup>, *Eva Zavadova*<sup>1</sup>, Helena Skalova<sup>1</sup>, Pavel Dundr<sup>1</sup>, Lubos Petruzelka<sup>1</sup>, Nicole Francis<sup>1</sup>, Rau T Tilman<sup>2</sup>, Arndt Hartmann<sup>3</sup>, Irena Netikova<sup>1</sup>

<sup>1</sup>General Hospital First Medical Faculty, Prague, Hlavni mesto Praha, Czech Republic

<sup>2</sup>Institut für Pathologie, Universität Bern, Bern, Switzerland

<sup>3</sup>Pathologie, Friedrich-Alexander-Universität Erlangen-Nürnberg, Erlangen, Germany

#### Background

Colorectal cancer is the second leading cause of cancer death worldwide. This high mortality is because almost half of colorectal cancers are detected at an advanced stage of disease, and the currently used prognostic factors are not always accurate. Recently, the prognostic impact of the body's immune response to cancer has been demonstrated. Immunoscore (*in situ* immune cell infiltrate in tumours) has been shown to be a very powerful prognostic indicator in patients with clinically localized colorectal cancer. These patients are usually treated with only surgical removal of the tumour; however, approximately 25% of these patients will have recurrence of their disease, indicating that occult metastases were already present at the time of curative surgery. No tumour-associated marker predicts the recurrence of this subgroup of patients that could benefit from adjuvant therapy. These days are investigated other parameters of the immune response – mostly cellular immunity and the production of immunosuppressive and neoangiogenic markers. VEGF is the factor responsible for neoangiogenesis and it is being considered as a possible prognostic marker of disease progression. Transforming growth factor-beta (TGF-beta) is also neoangiogenic and a highly immunosuppressive factor, as it suppresses the body's natural immunity against tumours. TGF-beta is also being considered as another possible prognostic marker of disease progression. The purpose of this study was to monitor the immune response in patients with stage II colorectal cancer, with a focus on cellular as well as humoral immunity. TGF-beta and VEGF levels were followed.

#### Methods

22 patients with stage II colon cancer included in the research project received routine cancer treatment. Basic parameters – histological type and grade, proliferative markers – were established at baseline. Patients were evaluated by a clinical immunoncologist to exclude any immune disorders of allergic or autoimmune origin. TGF-beta and VEGF were measured using ELISA, and anti-tumour cellular immunity (CD4, CD8, T-reg, B cells) were measured via flow cytometry.

#### Results

In patients with stage II colorectal cancer, predominantly a depression in cellular immunity was seen. Plasma levels of immunoglobulins were also reduced, particularly the IgG4 subtype. Most patients showed some clinical symptoms of immunodeficiency, such as frequent respiratory tract infections and/or herpetic infections. TGF-beta and VEGF plasma levels were increased.

#### Conclusions

The correlation of these neoangiogenic and immunosuppressive factors, as well as the state of anticancer immunity, could help in the future as a prognostic marker and contribute to the selection of targeted immune therapy in patients with colorectal cancer.

114

### Evaluation of immune cell infiltrates in non-small cell lung cancer as a potential comprehensive prognosticator

Carmen Ballesteros-Merino<sup>1</sup>, Julia Stump<sup>2</sup>, Amanda Tufman<sup>2</sup>, Frank Berger<sup>3</sup>, Michael Neuberger<sup>4</sup>, Rudolf Hatz<sup>5</sup>, Michael Lindner<sup>6</sup>, Rachel E Sanborn<sup>7</sup>, John Handy<sup>7</sup>, Bernard Fox<sup>7</sup>, Carlo Bifulco<sup>7</sup>, Rudolf M Huber<sup>2</sup>, Hauke Winter<sup>4</sup>, Simone Reu<sup>8</sup>

<sup>1</sup>Earle A. Chiles Research Institute at Portland Providence Cancer Center, Portland, OR, USA

<sup>2</sup>Ludwig Maximilian University of Munich and Thoracic Oncology Centre Munich, Germany; Comprehensive Pneumology Center (CPC) and Member of the German Center for Lung Research (DZL, CPC-M), Munich, Bayern, Germany

<sup>3</sup>Department of Clinical Radiology, University of Munich, Munich, Bayern, Germany

<sup>4</sup>Comprehensive Pneumology Center (CPC) and Member of the German Center for Lung Research (DZL, CPC-M); Department of General, Visceral, Transplantation, Vascular and Thoracic Surgery, Hospital of the Ludwig Maximilian University, Munich, Bayern, Germany

<sup>5</sup>Comprehensive Pneumology Center (CPC) and Member of the German Center for Lung Research (DZL, CPC-M), Munich; Hospital of the Ludwig Maximilian University, Munich; Asklepios Clinic, Munich, Bayern, Germany

<sup>6</sup>Comprehensive Pneumology Center (CPC) and Member of the German Center for Lung Research (DZL, CPC-M), Munich, Germany; Asklepios Clinic Munich-Gauting, Germany, Munich-Gauting, Bayern, Germany

<sup>7</sup>Robert W. Franz Cancer Research Center, Earle A. Chiles Research Institute, Providence Cancer Center, Portland, Oregon, USA

<sup>8</sup>Comprehensive Pneumology Center (CPC) and Member of the German Center for Lung Research (DZL, CPC-M); Institute of Pathology, University of Munich, Munich, Bayern, Germany



## Biomarkers and Immune Monitoring

*Presenting author underlined; Primary author in italics*

### Background

Therapeutic strategies in non-small cell lung cancer (NSCLC) are based on the histopathological evaluation of the tumor tissue which, in conjunction with the TNM staging system, remains the gold standard for prognostic assessment. Nevertheless, histopathology and stage-specific clinical outcomes vary significantly, indicating that there is a need for additional prognosticators. A previous study reported that intense lymphocytic infiltrates were found in 6-11% of NSCLC and were associated with a significant increase in disease-free and overall survival [1]. The aim of our study was to use multispectral imaging and digital quantification to assess relationships between T cells and FoxP3+ or PD-L1+ cells in tissue microarrays (TMAs) cored from "hot spots" of dense infiltrates at the invasive margin and center of the NSCLC.

### Methods

Tissue microarrays (TMA) were generated from formalin-fixed paraffin-embedded tissue of 98 curatively resected patients with stage IA-IIIa NSCLC. TMAs included 3 cores for tumor center and 3 cores for invasive margin selected from the areas with the most dense (hot spot) lymphocytic infiltrate. TMAs were immunolabeled with mIHC technique for the following antibodies: PD-L1, CD8, CD3, FoxP3, CD163, cytokeratin and DAPI and quantified with InForm software. Results were compared between groups of patients with squamous and non-squamous cell carcinoma and correlated with the course of the disease, overall/progression-free survival, metastases or relapse and clinicopathological parameters.

### Results

In contrast to reports evaluating whole sections, analysis of "hot spots" in this cohort of patients failed to provide a prognostic biomarker for survival. Current studies are evaluating how an evaluation of the whole section correlates with results of this "hot-spot" analysis. Our preliminary data suggests that the "hot-spot" analysis of CD8, FoxP3 and PD-L1 does not allow us to identify outcome in NSCLC.

### Conclusions

Multispectral assessment of CD8, FoxP3, and PD-L1 performed on "hot-spots" of stage I-III NSCLC did not provide a prognostic biomarker. Given other reports that immune infiltrates are associated with improved outcome, this suggests it may be important to evaluate a larger percentage of the tumor. These findings appear to contrast with the colon immunoscore project which identified a correlation with an enumeration of CD3+ and CD8+ T cell numbers in hot-spots and disease-free and overall survival.

### Acknowledgements

C. Ballesteros-Merino and J. Stump contributed equally to this study. Supported by the Harder Family, Lynn and Jack

Loacker, Robert W. Franz, Wes and Nancy Lematta, the Murdock Trust and Providence Medical Foundation.

### References

1. Brambilla E, Le Teuff G, Marguet S, Lantuejoul S, Dunant A, Graziano S, *et al*: **Prognostic Effect of Tumor Lymphocytic Infiltration in Resectable Non-Small-Cell Lung Cancer.** *J Clin Oncol* 2016, **34**:1223-1230.

### 115

#### **High NKG2A expression contributes to NK cell exhaustion and predicts a poor prognosis of patients with liver cancer**

*Cheng Sun, Weihua Xiao, Zhigang Tian*

Institute of Immunology, The Key Laboratory of Innate Immunity and Chronic Disease (Chinese Academy of Medical Science), School of Life Sciences and Medical Center, University of Science & Technology of China, Hefei, Anhui, People's Republic of China

### Background

As the predominant lymphocyte subset in the liver, nature killer (NK) cells have been shown to be highly associated with the outcomes of patients with chronic hepatitis B virus infection (CHB) and hepatocellular carcinoma (HCC). Previously, we reported that NKG2A, a checkpoint candidate, mediates human and murine NK cell dysfunction in CHB. However, NK cell exhaustion and, particularly, the level of NKG2A expression within liver tumours have not been reported.

### Methods

In this study, we analysed NKG2A expression and the related dysfunction of NK cells located in intra- or peritumour regions of liver tissue samples from 207 HCC patients, in addition to analysing disease outcomes.

### Results

The expression of NKG2A in NK cells and the NKG2A ligand, HLA-E, in intratumour HCC tissues was observed to be increased. These NK cells, and particularly CD56<sup>dim</sup> NK cells, with higher NKG2A expression showed features of functional exhaustion and were associated with a poor prognosis. The increase in NKG2A expression might be induced by IL-10, which was present at a high level in the plasma of HCC patients. Blocking IL-10 could specifically inhibit NKG2A expression in NK cells.

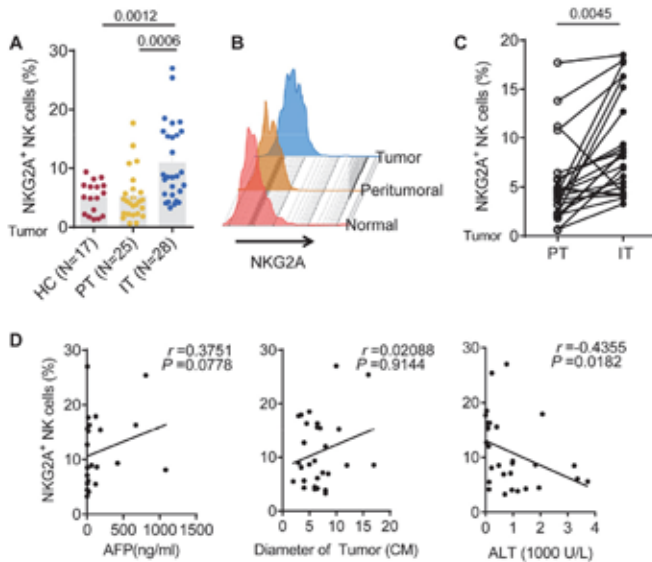
### Conclusions

These findings indicate that NKG2A expression is influenced by factors from cancer nests and contributes to NK cell exhaustion, suggesting that NKG2A blockade has the potential to restore immunity against liver tumours by reversing NK cell exhaustion.

## Biomarkers and Immune Monitoring

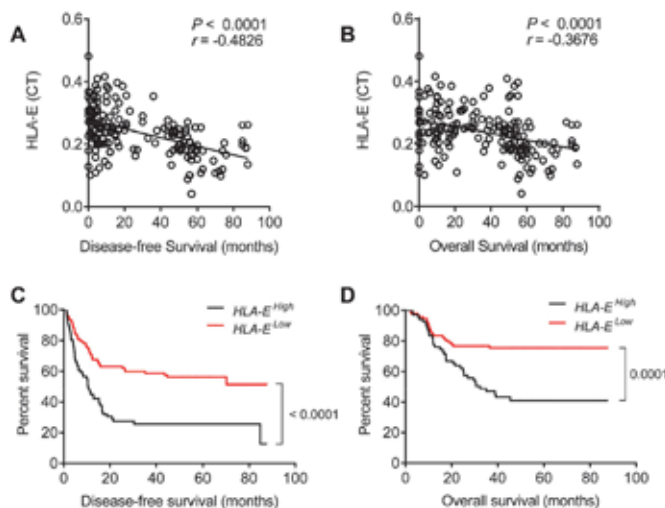
Presenting author underlined; Primary author in italics

**Figure 1. The frequency of intratumour NKG2A+ NK cells is increased in HCC.**



(A, B) The percentage of NKG2A-expressing NK cells in healthy livers (N=17) and IT (N=28) and PT (N=25) from HCC patients. The differences in the cumulative data were calculated using a two-tailed paired Student's t test. (C) NKG2A expression in NK cells from the paired central tumour and PT from each HCC patient (N=23). (D) The correlation between NKG2A expression in hepatic NK cells from IT and the serum AFP and ALT levels and tumour diameters of HCC patients. Spearman's correlation coefficients are shown.

**Figure 4. Shorter survival of patients with higher densities of HLA-E+ cells within tumours.**



(A, B) Correlations between DFS or OS and the density of HLA-E+ cells in the IT regions of HCC patients (N=177). Pearson's correlation coefficients (R) and P values are shown.

(C, D) Kaplan–Meier survival curves for the duration of DFS (C) and OS (D) in months, according to the HLA-E+ cells density in IT (low densities, Red line; high densities, Black line) (log-rank test).

### 116

#### Association of non-coding repeat RNA expression with immune infiltrates

*Kshitij Arora*<sup>1</sup>, Niyati Desai<sup>1</sup>, Anupriya Kulkarni<sup>1</sup>, Mihir Rajurkar<sup>1</sup>, Miguel Rivera<sup>1</sup>, Vikram Deshpande<sup>2</sup>, David Ting<sup>1</sup>

<sup>1</sup>Massachusetts General Hospital Cancer Center, Harvard Medical School, Charlestown, MA, USA

<sup>2</sup>Massachusetts General Hospital, Harvard Medical School, Boston, MA, USA

#### Background

Colorectal cancer (CRC) is the third most common type of cancer in the United States. There have been exciting responses to immunotherapy in CRC, but the ability to predict which patients would benefit from these drugs remains elusive. Recent work has demonstrated the aberrant expression of non-coding repeat RNAs across cancers including colon cancer [1, 2]. These repeats appear to trigger elements of the innate immune response that may have implications for response to immunotherapy [1]. To determine if repeat RNAs are linked to the tumor immune microenvironment, we developed a novel combined repeat RNA *in situ* hybridization (RNA-ISH) with T cell immunohistochemistry (IHC) on fixed formalin paraffin embedded (FFPE) tissues. We assessed two different repeat types (HSATII and HERV-H) that have been well documented in human cancers and reported to have an association with innate immune responses [2]. To investigate correlation of host immune T cells with these repeats a pilot study of seventy-five patients of CRC was performed.

#### Methods

FFPE tissue sections of 75 patients were stained by RNA-ISH and IHC on the Leica Bond RX. HSATII and HERV-H repeat RNA-ISH and CD8 (cytotoxic) and FOXP3 (regulatory) T cell marker IHC was performed on each case. Repeat RNA scores were determined as HIGH or LOW based on relative cancer cell expression to normal adjacent tissues. T cell density was determined by counting the number of positive cells in a 400 x 200  $\mu\text{m}$  area. T cell density differences were calculated by t-test.

#### Results

We found HSATII was HIGH in 47 (63%) and HERV-H was HIGH in 36 (48%) of CRC cases with a concordance between repeats of 51%. Analysis with T cell subsets revealed lower CD8+ T cells in HSATII HIGH tumors (306 vs 686 CD8+ T cells/mm<sup>2</sup>; p<sub>2</sub>; p=0.03).

## Biomarkers and Immune Monitoring

Presenting author underlined; Primary author in italics

### Conclusions

Repeat RNAs are expressed across malignancies with varying levels that correlate with different immune infiltrates. Cancer expression of HSATII and HERV-H repeats offers a novel surrogate biomarker of cytotoxic and regulatory T cell tumor infiltration. The mechanistic effects of these repeats on immune cell function merits further investigation.

### Acknowledgements

We thank Alex Forrest-Hay, Manoj Gandhi, Frank Witney, and Affymetrix, Inc. for sponsored research support.

### References

- Chiappinelli KB, Strissel PL, Desrichard A, Li H, Akman B, *et al*: **Inhibiting DNA Methylation Causes an Interferon Response in Cancer via dsRNA Including Endogenous Retroviruses.** *Cell* 2015, **162**:974-986.
- Ting DT, Lipson D, Brannigan BW, Akhavanfard S, Coffman EJ, *et al*: **Aberrant overexpression of satellite repeats in pancreatic and other epithelial cancers.** *Science* 2011, **331**:593-596.

**Colon adenocarcinoma FFPE sections stained with Dual color RNAISH (Red) for HERVH, HSAT II and IHC (Brown) for FOXP3 & CD8**

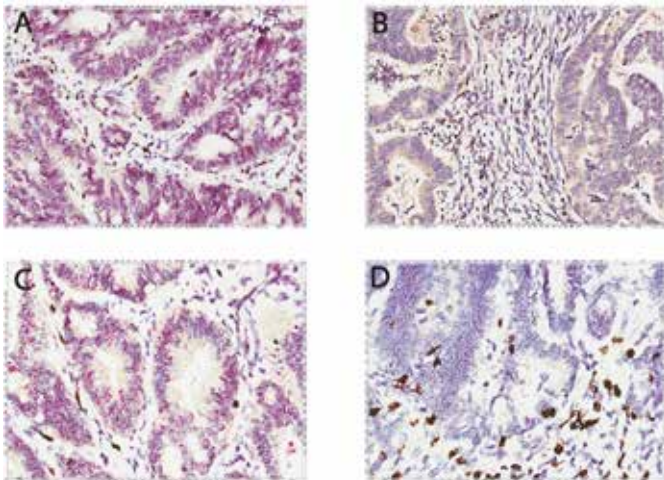


Figure 1. Colon adenocarcinoma FFPE tissue stained with dual color RNA-ISH (Red) for HERVH, HSATII and IHC (Brown) for FOXP3 & CD8. 400X magnification A) High HervH and Low FOXP3 B) Low HERVH and High FOXP3 C) High HSATII and Low CD8 D) Low HSATII and High CD8.

### 117 Abstract Travel Award Recipient

#### Outcome disparities by sex in melanoma patients treated with anti-PD-1 therapy

*Katy Tsai*<sup>1</sup>, Adi Nosrati<sup>1</sup>, Simone Goldinger<sup>2</sup>, Omid Hamid<sup>3</sup>, Alain Algazi<sup>1</sup>, Paul Tume<sup>4</sup>, Jimmy Hwang<sup>1</sup>, Jacqueline Liu<sup>1</sup>, Lawrence Chen<sup>1</sup>, Reinhard Dummer<sup>2</sup>, Michael Rosenblum<sup>1</sup>, Adil Daud<sup>1</sup>

<sup>1</sup>University of California, San Francisco, San Francisco, CA, USA

<sup>2</sup>University Hospital of Zurich, Zurich, Switzerland

<sup>3</sup>The Angeles Clinic & Research Institute, Los Angeles, CA, USA

<sup>4</sup>University of California, Los Angeles, Los Angeles, CA, USA

### Background

PD-1 antibodies have shown significant clinical activity against advanced melanoma, but ORR with PD-1 monotherapy remains less than 50%. We previously reported and validated a clinical scoring model to predict response to anti-PD-1, and in our logistic regression analysis, female sex was found to be associated with lower response rate (OR 0.36, 95% CI 0.19-0.67). We report further on outcomes in immunotherapy-treated patients by sex and correlate this with results of T cell profiling of an exhausted, antigen-experienced phenotype (% PD-1<sup>high</sup>CTLA-4<sup>high</sup> CD8 cells) from pre-treatment biopsy samples.

### Methods

336 patients (118 women, 218 men) with advanced cutaneous melanoma were treated with pembrolizumab or nivolumab at 4 academic cancer centers between December 2011 and October 2013. Baseline demographics and clinical characteristics were collected from electronic health records. Tumor response was assessed using RECIST v1.1 criteria. Pre-treatment flow cytometry data from 122 patients (45 women, 77 men) treated with both PD-1 monotherapy and PD-1/CTLA-4 combination therapy were analyzed by sex for correlative data.

### Results

In the PD-1 monotherapy cohort, median ORR was 33.1% (95% CI 24.4-41.2) in females and 54.6% (95% CI 47.9-61.3) in males ( $p=0.0001$ ). Median PFS was 5.5 months (95% CI 3.4-7.1) in females and 18 months (95% CI 11.3-23.8) in males ( $p=0.0004$ ) (Figure 1). Flow cytometry analysis of pre-treatment tumor biopsies revealed a statistically significant reduced proportion of exhausted PD-1<sup>high</sup>/CTLA-4<sup>high</sup> CD8 T cells that persisted across age groups (Figure 2).

### Conclusions

There is a significant discrepancy between response to PD-1 monotherapy between men and women with advanced melanoma. The mechanisms of this may have immunologic

## Biomarkers and Immune Monitoring

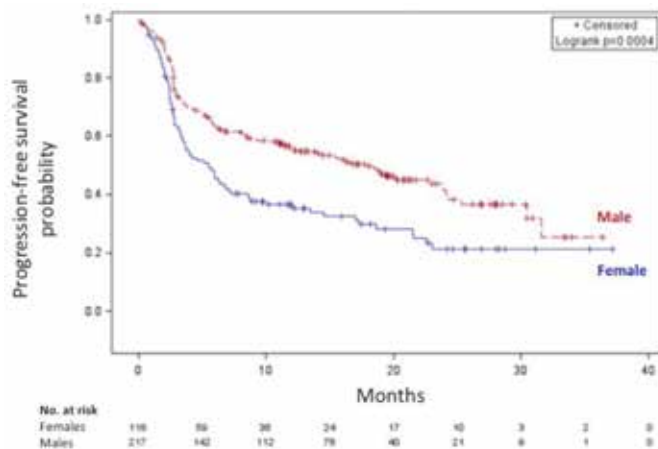
Presenting author underlined; Primary author in italics

basis given the difference in pre-treatment T cell profiles between men and women.

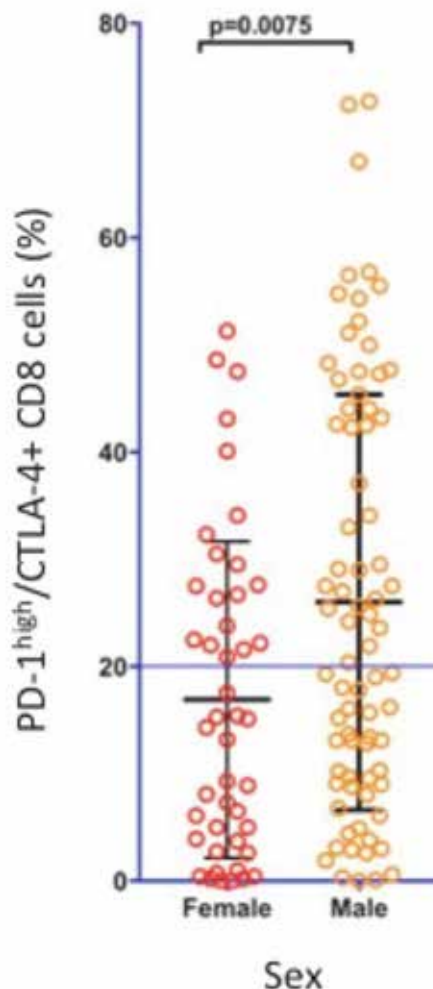
### Trial Registration

ClinicalTrials.gov identifier NCT01295827, NCT01704287, NCT01721746, and NCT02156804.

**Figure 1. Progression-free survival estimates by sex in advanced melanoma patients receiving anti-PD-1 monotherapy**



### Pre-treatment of PD-1<sup>high</sup>/CTLA-4<sup>high</sup> CD8 T cells by sex



### 118

#### A flexible and versatile toolbox for parallel multiplex immunohistochemical detection using recombinant epitope-tagged antibodies and monoclonal anti-tag antibodies

Tsu-Shuen Tsao<sup>1</sup>, Julia Ashworth-Sharp<sup>1</sup>, Donald Johnson<sup>1</sup>, Srabani Bhaumik<sup>1</sup>, Christopher Bieniarz<sup>1</sup>, Joseph Couto<sup>2</sup>, Michael Farrell<sup>1</sup>, Mahsa Ghaffari<sup>1</sup>, Iva Habensus<sup>1</sup>, Antony Hubbard<sup>1</sup>, Tobin Jones<sup>1</sup>, Brian Kelly<sup>1</sup>, Jerome Kosmeder<sup>1</sup>, Cleo Lee<sup>2</sup>, Erin Marner<sup>1</sup>, Jeffrey Meridew<sup>1</sup>, Nathan Polaske<sup>1</sup>, Adriana Racolta<sup>1</sup>, Diana Uribe<sup>1</sup>, Hongjun Zhang<sup>1</sup>, Jian Zhang<sup>1</sup>, Wenjun Zhang<sup>1</sup>, Yifei Zhu<sup>2</sup>, Larry Morrison<sup>1</sup>, Lidija Pestic-Dragovich<sup>1</sup>, *Lei Tang*<sup>1</sup>

<sup>1</sup>Ventana Medical Systems, Inc., Tucson, AZ, USA

<sup>2</sup>Spring Bioscience, Pleasanton, CA, USA



## Biomarkers and Immune Monitoring

Presenting author underlined; Primary author in italics

### Background

Contextual detection of multiple biomarkers on single formalin-fixed, paraffin-embedded (FFPE) slides for clinical applications remains an unmet need. Current multiplex immunohistochemistry (IHC) procedures entail successive rounds of antibody application and fluorophore attachment followed by antibody inactivation. We developed a parallel multiplex IHC approach using series of epitope-tagged antibodies and anti-epitope antibodies conjugated to fluorophores, haptens, or enzymes, and demonstrated feasibility by 5-plex fluorescent and duplex brightfield assays of markers relevant for immuno-oncology.

### Methods

DNA sequences corresponding to peptide epitope tags were fused in-frame to rabbit monoclonal antibody cDNAs for expression in mammalian cells. Recombinant tagging bypasses the potential antibody inactivation associated with chemical-based tagging. Conjugation of fluorophores or haptens to antibodies was performed using NHS ester precursors. Horseradish peroxidase (HRP) and alkaline phosphatase (AP) were conjugated to reduced antibodies via NHS-maleimide linkers. Affinity of anti-epitope antibodies to peptides was assessed using biolayer interferometry. IHC of FFPE tissue sections was performed on VENTANA BenchMark ULTRA platform.

### Results

Rabbit monoclonal antibodies against CD3, CD8, CD68, FoxP3, and PD-L1 were each engineered with a unique epitope tag. Epitope-tagged primary antibodies produced identical diaminobenzidine (DAB) staining intensity and pattern as untagged native antibodies. Multiple clones of recombinant rabbit monoclonal antibodies against each of the five epitope tags were conjugated and screened for retention of affinity, stability, and appropriate staining intensity and pattern in validated tissue microarrays. At least one clone of each anti-epitope antibody met the functional requirements and these were used to stain FFPE lung and tonsil tissue sections in conjunction with cocktail epitope-tagged antibodies. Epitope-tagged antibodies were detected using one of three detection configurations in order of sensitivity: 1) fluor-conjugated anti-epitope antibodies, 2) hapten-conjugated anti-tag antibodies and fluor-conjugated anti-hapten antibodies, and 3) attachment of tyramide- or quinone methide-fluors to tissue specimens with HRP- or AP-conjugated anti-epitope antibodies. Titration of antibodies and assay optimization enabled pairings of particular biomarkers with detection configurations to generate specific fluorescence patterns and relative intensities similar to those produced by DAB stains using untagged antibodies and HRP-conjugated anti-species antibodies. Two-color brightfield

stains were generated using enzyme-conjugated anti-tag antibodies and HRP- and AP-activated chromogens.

### Conclusions

We have demonstrated feasibility of parallel multiplex IHC using a series of epitope-tagged antibodies and fluor-, hapten-, or enzyme-conjugated anti-epitope antibodies. Applying tagged antibodies and anti-tag antibody probes as cocktails streamlines multiplex detection and avoids the inactivation of antibodies that is necessary in multiplex approaches based on serially applied antibodies.

119

### Multiplex immunohistochemistry and image cytometry analysis for phenotyping spatial immune characteristics

Takahiro Tsujikawa<sup>1</sup>, Rohan N Borkar<sup>2</sup>, Vahid Azimi<sup>2</sup>, Sushil Kumar<sup>1</sup>, Guillaume Thibault<sup>1</sup>, Motomi Mori<sup>1</sup>, Edward El Rassi<sup>1</sup>, Daniel R Clayburgh<sup>1</sup>, Molly F Kulesz-Martin<sup>1</sup>, Paul W Flint<sup>1</sup>, Lisa M Coussens<sup>1</sup>

<sup>1</sup>Oregon Health & Science University, Portland, OR, USA

<sup>2</sup>Intel Corporation, Hillsboro, OR, USA

### Background

While immune therapies targeting select checkpoint molecules have revolutionized cancer medicine, the fact that many patients fail to respond underscores the need for improved patient stratification and application of multi-nodal biomarkers reflecting *in situ* status of the tumor immune microenvironment.

### Methods

We developed a multiplexed immunohistochemical (IHC) imaging approach based on sequential IHC with iterative labeling, digital scanning and subsequent stripping of sections. To elucidate contextual information on leukocyte presence, complexity and functional phenotype *in situ*, we investigated these parameters in head and neck squamous cell carcinoma (HNSCC) utilizing multiplex IHC analyses in de-identified tissue microarray sections reflecting human papilloma virus (HPV)-positive and negative oropharyngeal HNSCC and normal pharynx. Quantitative multiparameter image cytometry was developed to enable quantification of cell density, composition and location of 16-immune cell lineages, along with monitoring of programmed cell death-1 (PD-1) receptor and ligand (PD-L1) expression.

### Results

Intratatumoral immune cell densities were comprehensively evaluated by multiplex IHC/image cytometry via unsupervised clustering analysis and revealed presence of lymphoid, myeloid, and hypo-inflamed profiles correlating with HPV-status. Myeloid-inflamed profiles with low ratios of CD163<sup>-</sup>/CD163<sup>+</sup> of CD68<sup>+</sup> CSF1R<sup>+</sup> macrophages and CD8<sup>+</sup> T cell/CD68<sup>+</sup>



## Biomarkers and Immune Monitoring

*Presenting author underlined; Primary author in italics*

ratios was significantly associated with poor prognosis in both HPV-positive and negative HNSCC. Neoplastic cell nest vs. stroma region analyses revealed distinct distribution patterns for T<sub>H</sub>1 and T<sub>H</sub>2 lymphocytes, showing intratumoral T<sub>H</sub>1 orientation in HNSCC. Intratumoral CD66b<sup>+</sup> granulocyte infiltration was associated with unfavorable prognosis. Further analysis for spatial characteristics of immune complexity revealed high T<sub>H</sub>1/T<sub>H</sub>2 ratios and CD8<sup>+</sup> T cell infiltration within a distance of 20 μm to PD-L1<sup>+</sup> cells, indicating an association between PD-L1 expression and regional characteristics of immune complexity.

### Conclusions

These results demonstrate the capability of multiplex IHC-based image cytometry analysis toward improved understanding of heterogeneous tumor microenvironments.

### Acknowledgements

This project was supported by Oregon Clinical and Translational Research Institute (OCTRI), grant number (UL1TR000128) from the National Center for Advancing Translational Sciences (NCATS) at the National Institutes of Health (NIH), and P30 CA069533-17 OHSU Knight Cancer Institute. LMC acknowledges support from the NIH/NCI, DOD BCRP Era of Hope Scholar Expansion Award, Susan G. Komen Foundation, Stand Up To Cancer – Lustgarten Foundation Pancreatic Cancer Convergence Dream Team Translational Research Grant, Breast Cancer Research Foundation, and the Brenden-Colson Center for Pancreatic Health.

120

### Analysis of immunerelated prognostic markers in colon cancer patients randomized to surgery alone or surgery and adjuvant cytostatic treatment

*Lisa Villabona*, Giuseppe V Masucci

Karolinska Institutet, Stockholm, Stockholms Lan, Sweden

### Background

We have previously shown that human leukocyte antigen (HLA)-A\*02, a common allele in the Scandinavian population, is a negative prognostic factor in epithelial ovarian cancer [1]. It is a strong predictor of patient outcome, only inferior to clinical staging. We have also shown that this prognostic trait in epithelial ovarian cancer is stronger by the presence of the gene compared with the expression of its protein, MHC class I [2]. Finally, we have shown that HLA-G expression in ovarian cancer is a negative prognostic marker [3]. Our aim was to analyse the prognostic markers HLA-A\*02 genotype, MHC class I and HLA-G expression on tumour cells and the CD8<sup>+</sup> lymphocyte infiltration in colon cancer.

### Methods

Clinical information and primary tumours were collected from 520 colon cancer patients and followed for overall survival for 120 months. HLA-A\*02 genotype was determined by conventional PCR. MHC class I expression and CD8<sup>+</sup> lymphocyte infiltration were determined by immunohistochemistry.

### Results

Patients with a stage III tumour and HLA-A\*02 genotype had a better outcome if randomized to adjuvant chemotherapy versus surgery alone (P=0.03). There was an indication that patients with complete absence of MHC class I expression had a better overall survival compared to patients with a decreased or increased expression. Expression of HLA-G was a negative prognostic marker for the male patients (P=0.002). Also a high infiltration of CD8<sup>+</sup> lymphocytes was important in the male patients, where a high frequency of infiltration correlated with a good prognosis (P=0.002). These factors were not, however, significant in the female population. The superior negative prognostic marker in the female patients was HLA-A\*02 genotype.

### Conclusions

HLA-A\*02 positivity may be an important marker to determine which colon cancer patients should receive adjuvant chemotherapy. It also seems to determine the outcome of the female patients, which raises new questions as to why this gene, which most likely has the same function in both genders, can be devastating to one gender and not the other.

### References

1. Gamzatova Z, *et al*: **Human leucocyte antigen (HLA) A2 as a negative clinical prognostic factor in patients with advanced ovarian cancer.** *Gynecol Oncol* 2006, **103**(1):145-150.
2. Andersson E, *et al*: **Correlation of HLA-A02\* genotype and HLA class I antigen down-regulation with the prognosis of epithelial ovarian cancer.** *Cancer Immunol Immunother* 2012, **61**(8):1243-1253.
3. Andersson, *et al*: **Non-classical HLA-class I expression in serous ovarian carcinoma: correlation with the HLA-genotype, tumor infiltrating immune cells and prognosis.** *Oncoimmunology* 2015, **5**(1):e1052213.

## Biomarkers and Immune Monitoring

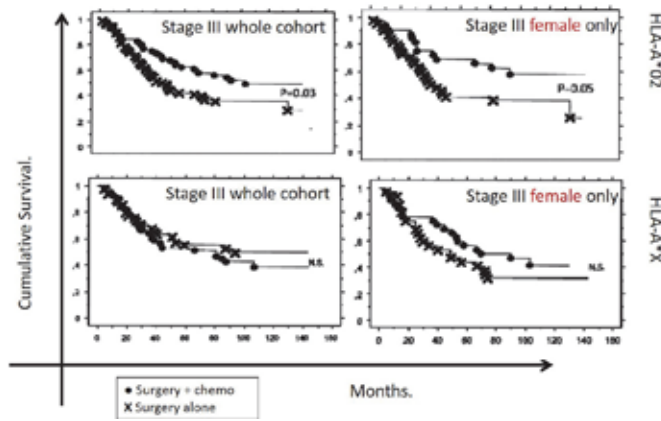
Presenting author underlined; Primary author in italics

**Table 1**

		N:o	%
Cohort		520	100
Genus	Women	249	47.8
	Men	271	52.2
Localisation	Colon dx	241	46.3
	Transversum	47	9
	Colon sin	41	8
	Sigmoidum	182	35
	Undetermined	9	1.7
Stage	Duke B	230	44.2
	Duke C	290	55.8
Treatment	Surgery	275	52.9
	Surgery + adj chemotherapy	245	47.1

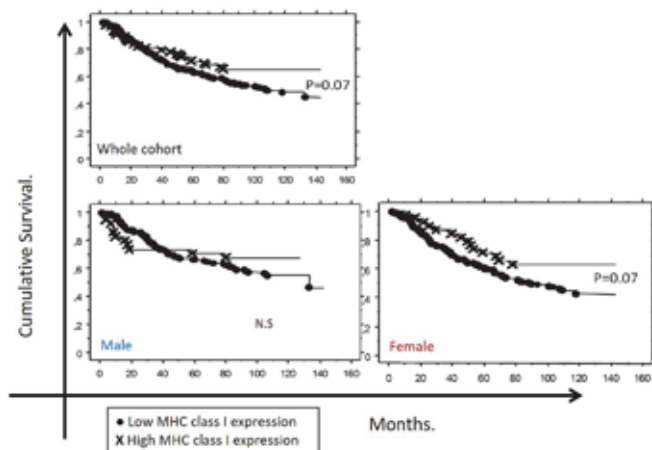
Cohort description

**Figure 1**



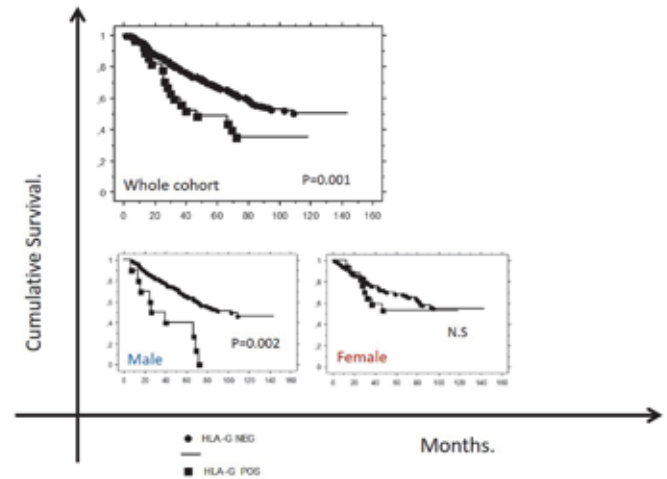
HLA-genotype and treatment.

**Figure 2**



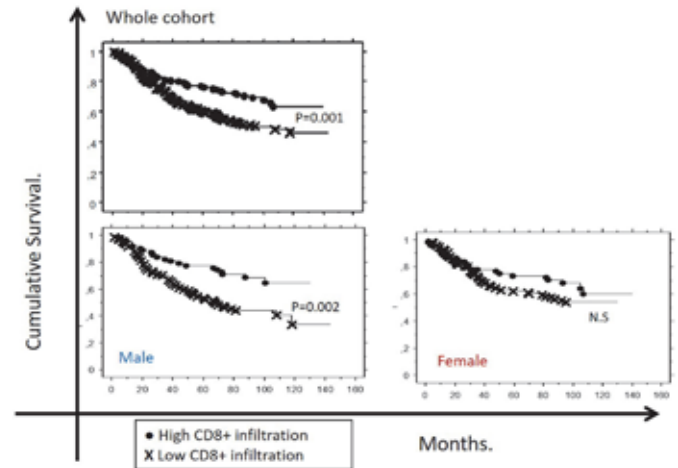
MHC class I expression

**Figure 3**



HLA G expression

**Figure 4**

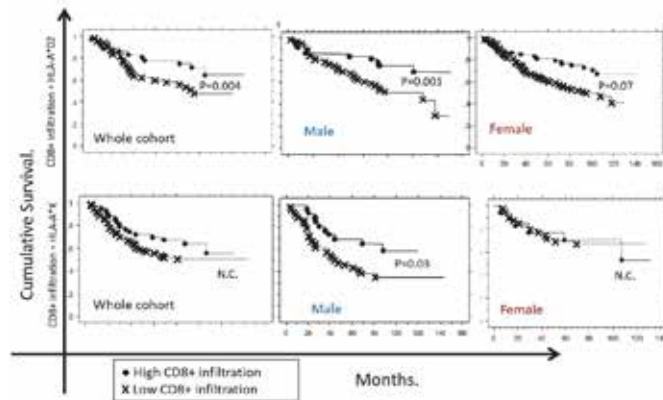


CD8+ infiltration

## Biomarkers and Immune Monitoring

Presenting author underlined; Primary author in italics

Figure 5



CD8+ infiltration and HLA-genotype

121

### Profiling immune cell populations and functional state with simultaneous, multiplexed detection of RNA and protein on the nCounter® platform

Gary Geiss, Brian Birditt, Qian Mei, Alan Huang, Andrew M White, Maribeth A Eagan, Eduardo Ignacio, Nathan Elliott, Dwayne Dunaway, Lucas Dennis, Sarah Warren, *Joseph Beechem*

NanoString Technologies, Seattle, WA, USA

#### Background

One of the biggest challenges facing the field of immunoncology is development of a comprehensive understanding of how the immune system responds to a tumor. Multi-analyte profiling (DNA, RNA, and protein) from limited sample is crucial to furthering our understanding of tumor immunity. NanoString's nCounter® technology has become an important platform for quantification of transcriptional responses by enabling direct digital quantification of up to 800 RNA targets from a single sample.

#### Methods

Now the nCounter technology can simultaneously quantify 770 RNA transcripts plus 30 proteins from as few as 20,000 cells (up to 50,000 primary cells such as PBMCs). NanoString has developed content and methods to allow digital quantification of both cell surface and intracellular protein targets that are essential to immuno-oncology research. These key targets include immune cell population markers, immune checkpoint proteins, transcription factors, chemokines, and cytokines. Protein detection is enabled via primary antibodies, which are covalently linked to single stranded DNA indexing oligos. Cells are stained with a multiplexed cocktail of labeled antibodies, and DNA oligos are subsequently released via cell lysis for hybridization

to optical barcodes in the standard NanoString workflow. This technique enables quantitative, multiplexed protein detection over 5 logs of dynamic range.

#### Results

As proof of concept, RNA and protein were measured simultaneously from just 50,000 PBMCs treated with phorbol 12-myristate 13-acetate (PMA) and ionomycin, TNF $\alpha$ , IFN $\gamma$ , or anti-CD3/CD28. NanoString's multiplex RNA and protein detection provides a thorough evaluation of the immunological response in these experiments and demonstrates the value of multi-analyte profiling from the same sample by characterizing the breadth of the response (via 770 RNA measurements) and providing depth to the analysis (via tandem measurements of RNA and protein for key targets). As independent confirmation, the findings were validated with flow cytometry.

#### Conclusions

This advance in multi-analyte, multiplexed digital molecular profiling with low sample input will accelerate immunoncology research and may enable the discovery and development of novel immunotherapies and their associated companion diagnostics.

122

### Spatially-resolved, multiplexed digital characterization of protein and mRNA abundance in FFPE tissue sections: application to immuno-oncology

Dwayne Dunaway, Jaemyeong Jung, Chris Merritt, Isaac Sprague, Philippa Webster, Yan Liang, Sarah Warren, Joseph Beechem

NanoString Technologies, Seattle, WA, USA

#### Background

Characterization of the abundance, distribution, and colocalization of key immunoregulatory proteins within the tumor microenvironment is necessary for a thorough understanding of tumor immune responses. Historically, immunohistochemistry and immunofluorescence have been used to assess spatial heterogeneity of proteins and nucleic acids in tissue slices, but these techniques are of limited utility due to the challenge of measuring multiple targets in parallel. We have developed a platform to enable spatially-resolved protein and RNA detection with the potential to simultaneously quantify up to 800 targets with greater than 5 logs of dynamic range from a single formalin-fixed paraffin-embedded (FFPE) slide.

#### Methods

The technology uses DNA oligo tags covalently linked to detection reagents (primary antibodies or mRNA-binding probes) via a UV photocleavable linker to identify targets

## Biomarkers and Immune Monitoring

Presenting author underlined; *Primary author in italics*

in situ and enable quantitation via the standard nCounter<sup>®</sup> technology. A slide-mounted FFPE tissue section is incubated with a cocktail of oligo-labeled primary antibodies or mRNA binding probes, and a serial section is stained with low-plex visible/fluorescent probes (e.g., nuclear staining probes, or select antibody pairs such as anti-CD3 and anti-CD8) to generate an image of the FFPE tissue slice morphology. Regions of interest (ROI) in the tumor are then identified and sequentially illuminated with UV light to release the DNA-oligos. Following UV illumination, the photocleaved oligos are released into the aqueous layer above the tissue slice, collected via microcapillary aspiration, and stored in an individual well of a microtiter plate. Oligos are then hybridized to nCounter optical barcodes to permit *ex situ* digital counting of as many as 800 different analytes localized within a single ROI in the tumor, which can be referenced using image capture software.

### Results

We demonstrate validation of this technology by characterization of a panel of immune proteins on FFPE tumor biopsies and tissue microarrays. We extend this technology to spatially-resolved multiplexed detection of RNA on a number of important immune targets (e.g., CD3, CD45). We further demonstrate that this approach enables protein detection at single cell resolution and enables simultaneous multiplexed detection of CD3, CD4, CD8, CD45, CD45RO, PD-1, PD-L1, Vista, TIM-3, B7-H3, Ki67 and additional key immuno-oncology-(IO) targets. Finally, we demonstrate detection of key IO RNA targets using direct hybridization of oligo-labeled probes.

### Conclusions

The ability to measure DNA, RNA, and protein at up-to 800-plex from single slices of FFPE tissue may enable the discovery of key immune biomarkers in tumors and accelerate the development immunotherapy and their associated companion diagnostics.

### 123 Abstract Travel Award Recipient

#### Immunological biomarkers correlate to survival in CAR19-treated patients

Jessica Wenthe<sup>1</sup>, Gunilla Enblad<sup>1</sup>, Hannah Karlsson<sup>1</sup>, Magnus Essand<sup>1</sup>, Barbara Savoldo<sup>2</sup>, Gianpietro Dotti<sup>2</sup>, Martin Höglund<sup>1</sup>, Malcolm K Brenner<sup>2</sup>, Hans Hagberg<sup>1</sup>, Angelica Loskog<sup>1</sup>

<sup>1</sup>Uppsala University, Uppsala, Uppsala Lan, Sweden

<sup>2</sup>Baylor College of Medicine, Houston, TX, USA

#### Background

CD19-targeting chimeric antigen receptor (CAR) T cell therapy achieved remarkable results in patients with acute lymphoblastic leukemia. However, few studies have

shown promising results in patients with other CD19<sup>+</sup> B cell malignancies, including lymphomas. We have completed a trial treating 15 patients with various B cell malignancies with third generation CD19-targeting (CD28/4-1BB) CAR T cells with or without preconditioning using a moderate dose of cyclophosphamide (500mg/m<sup>2</sup>) and fludarabine (25mg/m<sup>2</sup>). Herein, we report the results of a biomarker screening pre and post CAR T cell treatment using the trial biobank.

#### Methods

A biobank consisting of plasma and peripheral blood mononuclear cells obtained from CAR T cell treated patients with relapsed or refractory CD19<sup>+</sup> B cell malignancy was analyzed for immunological biomarkers. Samples were analyzed for immunosuppressive cells by flow cytometry and for systemic biomarkers using a 233-analyte proteomic analysis (ProSeek). Of the 15 treated patients, 11 patients had lymphoma and 6 had leukemia. During CAR T cell manufacture, lymphoma patients received standard treatment to control tumor burden. All patients were treated with one infusion of CAR T cells with dose ranges from 2x10<sup>7</sup> to 2x10<sup>8</sup> cells/m<sup>2</sup>. The two last patients received anti-PD-1 antibody therapy post CAR infusion. Correlation of biomarkers with survival was assessed by Spearman correlation.

#### Results

The patients were grouped into initial complete responders (6/15) and long-term survivors (4/15). In patient blood, CAR mRNA peaked at 1 week post infusion and could still be detected with varying levels over time up to 12 months post infusion. Baseline levels of monocytic myeloid-derived suppressor cells were negatively correlated with survival (P=0.0231) and M2-like macrophages tended to be increased at the time of relapse compared to the time of complete response (Mean %HLA-DR<sup>+</sup>CD80<sup>+</sup>CD163<sup>+</sup> of CD11b<sup>+</sup> cells: 15.4% vs. 8.3%). The proteomic analysis is ongoing. So far, several chemokines (CXCL16, CCL16, CCL15) as well as Th2 response and macrophage-associated molecules (IL8, IL10, IL33R, GDF-15) are correlated negatively with survival, whereas IL12, 41BB, TRAIL and transferrin receptor show a positive correlation.

#### Conclusions

In summary, we analyzed immunological biomarkers in 15 patients treated with CAR T cells in Sweden. An increase of M2-like macrophages was seen prior to relapse and molecules connected with suppressive responses were correlated negatively to survival including angiogenic drivers such as IL8 and CCL16 warranting a trial combining CAR T cells with angiogenic inhibitors. Instead, Th1-related IL12 and 41BB correlated with a longer survival time.





## Biomarkers and Immune Monitoring

Presenting author underlined; *Primary author in italics*

### Trial Registration

ClinicalTrials.gov identifier NCT02132624.

### 124 Presidential Travel Award Recipient

#### Increased STAT3 signaling and decreased suppressive function of regulatory T cells are biomarkers of positive patient outcome to nivolumab therapy

David Woods<sup>1</sup>, Anders Berglund<sup>2</sup>, Rupal Ramakrishnan<sup>2</sup>, Andressa Sodre<sup>1</sup>, Jeffrey Weber<sup>1</sup>

<sup>1</sup>NYU Langone Medical Center, New York, NY, USA

<sup>2</sup>H. Lee Moffitt Cancer Center, Tampa, FL, USA

#### Background

Antibody-mediated blockade of the inhibitory receptor PD-1 on T cells has shown clinical efficacy in the treatment of various malignancies. However, biomarkers of response and mechanisms of resistance remain largely unidentified. To address this gap, we sought to identify the role(s) of regulatory T cells (Tregs) in metastatic melanoma patients treated with the PD-1 antibody nivolumab.

#### Methods

Pre and post-treatment Tregs were isolated from the peripheral blood of surgically resected stage III/IV metastatic melanoma patients treated with adjuvant nivolumab. Suppressive capacity was assessed in an allogeneic mixed lymphocyte reaction. Paired (pre vs. post-treatment) Tregs were assessed by flow cytometry for phosphorylated STAT3 (pSTAT3) expression. Finally, paired Treg samples were assessed for gene expression by RNA-sequencing.

#### Results

Tregs from non-relapsing patients demonstrated a significant decrease in suppressive capacity post-treatment ( $p < 0.05$ ). However, suppressive capacity in relapsing patients did not decrease and their Tregs were significantly more suppressive post-treatment relative to non-relapsers ( $p < 0.01$ ). Significantly increased levels of pSTAT3 post treatment were observed in non-relapsers ( $p < 0.05$ ) but not in relapsers ( $p < 0.40$ ). Significantly increased pSTAT3 was not seen in conventional T cells after nivolumab therapy. Culturing treatment-naïve T cells with PD-1 blocking antibodies *in vitro* resulted in increased levels of pSTAT3 in Tregs compared to IgG controls ( $p < 0.01$ ). *In vitro* PD-1 blockade also significantly increased the number of Tregs ( $p < 0.01$ ), and significant increases were seen in paired patient samples ( $p < 0.05$ ). Paired analysis of Treg RNA-seq data using Panther and GeneGo. Metacore showed several significantly increased pathways associated with proliferation in non-relapsers. Changes in these pathways were absent in relapsers. Gene Set Enrichment Analysis of non-relapser Tregs showed significant ( $q=8.2e-18$ ) overlap with known STAT3 target genes. Conversely, Enrichr analysis of relapsers showed

significant upregulation of STAT1 and STAT2 target genes. No overlap of significantly changed gene expression or pathways in Tregs vs. conventional CD4+ T cells were observed.

#### Conclusions

These results highlight the potential importance of Tregs in mediating benefit with PD-1 blockade, demonstrating pSTAT3 induction and reduced suppressive capacity as biomarkers of clinical benefit. PD-1 blockade also increased the percentages of Tregs, consistent with the known roles of STAT3 in promoting cell survival and proliferation. RNA-seq data demonstrated increased STAT3 and proliferation associated gene expression. Intriguingly, Tregs from relapsing patients had increased expression of genes associated with STAT1/2 signaling, warranting further investigation of these pathways. In addition to highlighting STAT signaling as a biomarker of relapse, these results demonstrate distinct differences in the impact of PD-1 blockade in Treg vs. conventional T cells.

### 125 Presidential Travel Award Recipient

#### Analysis of pharmacodynamic biomarkers in the first in-human trial of GITR co-stimulation with the agonist antibody TRX-518 in advanced solid cancer patients

Roberta Zappasodi<sup>1</sup>, Yanyun Li<sup>1</sup>, Jingjing Qi<sup>2</sup>, Philip Wong<sup>2</sup>, Cynthia Sirard<sup>3</sup>, Michael Postow<sup>4</sup>, Walter Newman<sup>3</sup>, Henry Koon<sup>5</sup>, Vamsidhar Velcheti<sup>6</sup>, Margaret K Callahan<sup>7</sup>, Jedd D Wolchok<sup>4</sup>, Taha Merghoub<sup>1</sup>

<sup>1</sup>Ludwig Collaborative Laboratory, Memorial Sloan Kettering Cancer Center, New York, NY, USA

<sup>2</sup>Immune Monitoring Core Facility, Memorial Sloan Kettering Cancer Center, New York, NY, USA

<sup>3</sup>Leap Therapeutics, Cambridge, MA, USA

<sup>4</sup>Department of Medicine, Memorial Sloan Kettering Cancer Center, New York, NY, USA

<sup>5</sup>Case Western Reserve University, Cleveland, OH, USA

<sup>6</sup>Cleveland Clinic Main Campus, Cleveland, OH, USA

<sup>7</sup>Memorial Sloan Kettering Cancer Center, New York, NY, USA

#### Background

GITR is a tumor necrosis factor receptor expressed at high levels on regulatory T cells (Tregs) and up-regulated on T cells upon activation. GITR stimulation abrogates Treg suppression and enhances T cell effector function. These observations suggest that GITR could be an attractive target for immunotherapy with agonist antibodies. GITR stimulation in tumor-bearing mice has shown therapeutic activity associated with both Treg reduction and modulation. Here we report results of pharmacodynamic analyses in the first in-human phase I trial with the fully humanized agonist anti-GITR antibody TRX518 as monotherapy in patients with advanced refractory solid tumors.



## Biomarkers and Immune Monitoring

*Presenting author underlined; Primary author in italics*

### Methods

Patients were accrued to 9 cohorts (up to 6 patients/cohort) to receive a single dose of TRX518 (dose range: 0.0001-8 mg/kg). Pharmacodynamic analyses included flow cytometric evaluation of frequency and phenotype of circulating T cells and cytokine quantification in serum samples at different time points up to 12 weeks after treatment. Relevant changes observed with these analyses were monitored in pre- and post-treatment tumor biopsies by immunofluorescence staining.

### Results

Here we report results obtained in 37 patients treated with  $\geq 0.005$  mg/kg TRX518 (cohorts 3-9), including 6 melanoma, 7 non-small cell lung cancer (NSCLC) and 7 colorectal cancer (CRC) patients and 17 patients with 11 other solid tumors. Among the T cell parameters analyzed, we found frequent reduction in circulating Tregs after treatment with TRX518 across all cohorts, with some exceptions. Importantly, this effect could be maintained over the 12-week observation period. When the analysis was performed by disease type, it revealed a pronounced TRX518 dose-dependent down-regulation of peripheral Tregs in both melanoma and CRC patients. Interestingly, in NSCLC cancer patients, Tregs did not always decrease after treatment. In a subset of patients (n=6; 2 melanoma, 2 CRC, 2 lung), for whom we had pre- and post-treatment tumor biopsies in addition to PBMCs, we tested whether intra-tumor Tregs were consistently affected. In melanoma and CRC patients, intra-tumor Foxp3<sup>+</sup> Tregs were significantly reduced after treatment, in agreement with the peripheral Treg down-modulation observed in the same patients. In lung cancer patients, lack of circulating Treg reduction was consistently associated with stable or increased intra-tumor Treg infiltration after TRX518.

### Conclusions

Circulating Treg reduction is a potential pharmacodynamic biomarker of TRX518 biological activity. This parameter may allow predictive correlation with changes in intratumoral Treg infiltration. We plan to further investigate this effect and its relevance for the association with clinical responses in our recently opened TRX518 multi-dose study.

### Trial Registration

ClinicalTrials.gov identifier NCT01239134.

### Consent

Written informed consent was obtained from the patient for publication of this abstract and any accompanying images. A copy of the written consent is available for review by the Editor of this journal.

## Bispecific Antibodies

Presenting author underlined; Primary author in italics

126

### Multiple bispecific checkpoint combinations enhance T cell activity

Matthew J. Bennett, Gregory L. Moore, Michael Hedvat, Christine Bonzon, Seung Chu, Rumana Rashid, Kendra N Avery, Umesh Muchhal, John Desjarlais

Xencor, Inc., Monrovia, CA, USA

#### Background

Combination checkpoint blockade has demonstrated increased clinical responses relative to single checkpoint blockade. However, the combination of nivolumab plus ipilimumab has also exhibited increased immune-related adverse events. We reasoned that dual checkpoint blockade could be accomplished using a bispecific antibody format, with the potential benefits of reduced cost and more selective targeting of tumor-reactive lymphocytes to improve safety. Numerous checkpoint receptors exist, including PD-1, CTLA-4, LAG-3, BTLA, and others, encouraging the exploration of multiple bispecific combinations.

#### Methods

Antibodies specific to PD-1, CTLA-4, LAG-3, and BTLA were assembled into a bispecific antibody format in select combinations and optimized for stability and affinity. *In vitro* T cell stimulation activity of these bispecific antibodies was measured in a SEB stimulation assay. IL-2 and IFN $\gamma$  production was measured by ELISA. *In vivo* activity was evaluated by engrafting human PBMCs into NSG mice (huPBMC-NSG) and measuring the extent of T cell engraftment by flow cytometry after weekly treatment. An anti-tumor model was also developed with the huPBMC-NSG system, in which KG1a AML cells were first inoculated and allowed to establish tumors, followed by engraftment of huPBMC and treatment with antibody.

#### Results

We produced PD-1 x CTLA-4, PD-1 x LAG-3, CTLA-4 x LAG-3, and PD-1 x BTLA bispecific antibodies. All of the bispecifics enhanced IL-2 production in an *in vitro* SEB stimulation assay relative to control, indicating functional checkpoint blockade. In most cases, IL-2 production was similar or superior to that of anti-PD-1 alone. Treatment of huPBMC-NSG mice with checkpoint bispecifics promoted enhanced T cell engraftment relative to control. Engraftment levels promoted by bispecifics were generally superior to those found for anti-PD-1 treatment alone, and in some cases comparable to a combination of anti-PD-1 and anti-CTLA-4 antibodies. In one run of the model, while anti-PD-1 treatment alone promoted a 7-fold increase in human CD45<sup>+</sup> cells, a PD-1 x CTLA-4 bispecific antibody induced a 22-fold increase, and a CTLA-4 x LAG-3 bispecific promoted a 12-fold increase. Combining

CTLA-4 x LAG-3 with anti-PD-1 to achieve triple checkpoint blockade promoted a 67-fold increase in human CD45<sup>+</sup> cells, leading to severe graft versus host disease. The bispecific antibodies also exhibited compelling anti-tumor activity in a mouse AML model.

#### Conclusions

Dual checkpoint blockade with bispecific antibodies is feasible and promotes strong T cell activation *in vitro* and *in vivo*. Multiple combinations display compelling activity, suggesting clinical development is warranted for the treatment of human malignancies.

127

### Dual blockade of PD-1 and CTLA-4 with bispecific antibodies promotes human T cell activation and proliferation

Michael Hedvat, Matthew J Bennett, Gregory L Moore, Christine Bonzon, Rumana Rashid, Seung Chu, Kendra N Avery, Umesh Muchhal, John Desjarlais

Xencor Inc., Monrovia, CA, USA

#### Background

Treatment of melanoma patients with nivolumab plus ipilimumab increases progression-free-survival compared to each monotherapy. The increase in efficacy of the combination regimen is accompanied by an increase in adverse events. Since PD-1+CTLA-4<sup>+</sup> tumor-infiltrating-lymphocytes are dysfunctional in the tumor microenvironment, we attempted to specifically target PD-1+CTLA-4<sup>+</sup> double-positive T cells with a PD-1 x CTLA-4 bispecific antibody in an effort to recapitulate efficacy of the combination regimen while reducing toxicity.

#### Methods

Antibodies binding to PD-1 and CTLA-4 with favorable stability and functional properties were assembled in a bispecific antibody platform with substitutions in the Fc domain to suppress effector function. PD-1 x CTLA-4 bispecific antibodies were evaluated *in vitro* by measuring antibody binding and de-repression of super-antigen stimulated peripheral blood lymphocytes (PBMCs) and *in vivo* by monitoring the engraftment of human PBMCs in NSG mice (huPBMC-NSG) by flow cytometry. To evaluate anti-tumor efficacy we monitored the growth of established KG1a AML cancer cells in huPBMC-NSG following treatment.

#### Results

Optimized candidate single-chain Fvs were confirmed to bind PD-1 and functionally block PD-L1 and PD-L2 binding to PD-1. We also generated optimized anti-CTLA-4 Fabs. Anti-PD-1 and anti-CTLA-4 targeting components were assembled into a bispecific format and displayed favorable biophysical and

## Bispecific Antibodies

Presenting author underlined; *Primary author in italics*

manufacturing properties. PD-1 x CTLA-4 bispecific antibodies enhanced IL-2 secretion 5-fold relative to control ( $p < 0.001$ ,  $n = 18$  donors) in response to antigenic challenge of previously stimulated T cells, with 2-fold superior activity compared to anti-PD1 bivalent antibody ( $p < 0.001$ ,  $n = 18$  donors). PD-1 x CTLA-4 bispecific antibodies significantly enhanced T cell engraftment in huPBMC-NSG mice compared to vehicle controls ( $p < 0.001$ ,  $n = 10$ /group). PD-1 x CTLA-4 bispecific antibodies promoted higher T cell engraftment than anti-PD-1 alone ( $p < 0.01$ ,  $n = 10$ /group) and similar engraftment to a combination of anti-PD-1 and anti-CTLA-4 bivalent antibodies. PD-1 x CTLA-4 bispecific antibodies also exhibited compelling anti-tumor activity in a mouse AML model.

### Conclusions

Dual blockade of PD-1 and CTLA-4 with a bispecific antibody results in T cell activation that is comparable to a combination of bivalent antibodies targeting PD-1 and CTLA-4. Specific targeting of human lymphocytes positive for both PD-1 and CTLA-4 with a bispecific antibody may promote similar efficacy compared to a combination of bivalent antibodies while reducing adverse events. These data suggest that clinical development of a PD-1 x CTLA-4 bispecific antibody is warranted for the treatment of human malignancies.

128

### A LAG-3/PD-L1 bispecific antibody inhibits tumor growth in two syngeneic colon carcinoma models

Matthew Kraman, Katarzyna Kmiecik, Natalie Allen, Mustapha Faroudi, Carlo Zimarino, Mateusz Wydro, Jacqueline Doody

F-star Biotechnology Ltd., Cambridge, England, UK

### Background

Lymphocyte activation gene-3 (LAG-3) is a member of the immunoglobulin superfamily expressed on activated T cells, NK cells, pDCs, B cells, and  $\gamma\delta$  T cells, and participates in immune suppression, particularly through persistent strong expression in a percentage of regulatory T cells (Tregs). Programmed cell death receptor (PD-1) binds to its ligand PD-L1, expressed not only on activated immune cells to inhibit cellular immune responses but also on tumor cells. Expression of LAG-3 and PD-1 leads to T cell exhaustion, allowing tumor escape from immune surveillance. Combining inhibitory antibodies to PD-1 and LAG-3 reactivates T cells leading to efficacy in murine models over single treatment [1] and prompted interest in combining these two in the development of a LAG-3 and PD-L1 bispecific antibody for inhibiting tumor growth. This format may additionally result in novel mechanisms of action that are impossible to attain with combinations.

### Methods

A murine-specific anti-LAG-3 and PD-L1 bispecific antibody was engineered and analyzed for binding, blocking, and preventing LAG-3 and PD-L1-mediated T cell suppression *in vitro*. In addition, the LAG-3/PD-L1 bispecific antibody was tested in 2 syngeneic murine tumor models for its ability to suppress tumor growth.

### Results

Not only is the bispecific anti-LAG-3/PD-L1 antibody (mAb<sup>2</sup>™) able to bind both antigens simultaneously and with nanomolar affinities, but it also demonstrates functional activity against both targets *in vitro*. This potency translates into *in vivo* efficacy, where the anti-LAG-3/PD-L1 mAb<sup>2</sup> decreased tumor burden in the MC38 colon carcinoma tumor model, both in early-established or well-established tumors. At the end of the study tumor-free animals were more numerous in the LAG-3/PD-L1 bispecific group than in the group given a combination of individual anti-LAG-3 and PD-L1 antibodies. The results were recapitulated in the CT26 murine colon cancer model, where the LAG-3/PD-L1 mAb<sup>2</sup> showed an increase of anti-tumor activity as compared to the combination of anti-LAG-3 and anti-PD-L1 antibodies.

### Conclusions

The promising preclinical results from this anti-mouse LAG-3/PD-L1 bispecific antibody supports continuing to progress with the development of an anti-human LAG-3/PD-L1 mAb<sup>2</sup> for use in the treatment of cancer patients.

### Acknowledgements

Alasdair Bell, Maude Berthelot, Katy Everett, Alexander Koers, Teresa Mallia, Emma McConnell, and Sarka Pechouckova.

### References

1. Woo SR, *et al*: Immune inhibitory molecules LAG-3 and PD-1 synergistically regulate T-cell function to promote tumoral immune escape. *Cancer Res* 2012, **72(4)**:917-927.

129

### Clinical responses in advanced pancreatic patients treated with bispecific antibody armed T cells (BATS)

Lawrence G Lum<sup>1</sup>, Minsig Choi<sup>2</sup>, Archana Thakur<sup>1</sup>, Abhinav Deol<sup>3</sup>, Gregory Dyson<sup>3</sup>, Anthony Shields<sup>3</sup>

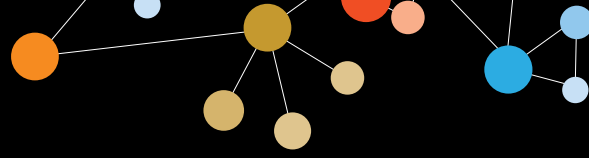
<sup>1</sup>University of Virginia Cancer Center, Charlottesville, VA, USA

<sup>2</sup>Stony Brook University Medical Center, Stony Brook, NY, USA

<sup>3</sup>Karmanos Cancer Institute, Detroit, MI, USA

### Background

Conventional chemotherapy (chemo) for locally advanced pancreatic cancer (LAPC) and metastatic pancreatic cancer (PC) is associated with dismal responses and poor survival rates. Arming activated T cells (ATC) with anti-CD3 x anti-EGFR bispecific antibody (EGFRBi) turns every ATC into a



## Bispecific Antibodies

Presenting author underlined; *Primary author in italics*

non-MHC restricted EGFR-specific cytotoxic T lymphocyte [1]. Engagement of CD3 on T cells and EGFR on Mia PACA-2 leads to cytokine secretion, proliferation, cytotoxicity by ATC and inhibition of tumor growth [2]. An earlier study using Infusions of anti-CD3 x anti-HER2 (HER2Bi) armed ATC in metastatic breast cancer provided encouraging survival (OS = 36 months) and evidence of anti-breast cancer immunity [3].

### Methods

In this study, we used anti-CD3 x anti-EGFR bispecific antibody (EGFRBi)-armed T cells (EGFR BATs) to target EGFR in 5 metastatic PC patients and 6 colorectal cancer patients treated at Karmanos Cancer Institute on Protocol #2014-025 in a phase I dose escalation involving 3 weekly infusions of 10, 20, and 40 x 10<sup>9</sup> BATs/infusion followed by a booster infusion 3 months later.

### Results

In the 5 PC patients, we report 1 patient was stable for 6.5 months and 2 patients in whom infusions of EGFR BATs may have “sensitized” the tumor to subsequent chemotherapy. The patient with stable disease had a near partial response. The median overall survival in 5 patients is 23.5 months with the median time to progression (TTP) of 7.0 months. Patient IT20102 received BATs and was stable (decreased marker lesion by 27%) at 6.5 mos. IT20091 had a remarkable clinical response to chemotherapy after progressing after immunotherapy at 4.6 months. After 3 BATs infusions, patient IT2010 had a “flare” or progression and subsequently had a complete response to Xeloda and remains in remission. This phase I study shows: 1) long-term stabilization in one patient; 2) a persistent complete responder after BATs “progression” followed by chemotherapy; 3) improved chemotherapy responsiveness after EGFRBi-BATs therapy; and 4) two patients with slow progressive disease who survived beyond 400 days. Survival for the 5 patients was 13.6, 14.5, 23.3 (alive in CR), 24.9 (alive, stable), and 31.0 months after enrollment, respectively (as of 7-20-16).

### Conclusions

Targeting PC with EGFR BATs resulted in improved survival and remarkable post-immunotherapy chemotherapy responses in a small series of patients. The series provides evidence for anti-tumor activity of EGFR BATs as well as evidence that BATs infusions can sensitize tumors to subsequent chemotherapy.

### Acknowledgements

Funding for this study was provided by Helen Kay Trust and Philanthropy and Startup Funds at KCI. We acknowledge the efforts of clinical coordinating staff, the clinical trials office staff, GMP laboratory staff, and clinical nursing support staff to making this study possible. The study was conducted at KCI.

### References

1. Reusch U, Sundarum M, Davol PA, Olson SD, Davis JB, Demel K, *et al*: **Anti-CD3 x anti-EGFR Bispecific Antibody Redirects T Cell Cytolytic Activity to EGFR-Positive Cancers In Vitro and in an Animal Model.** *CCR* 2006, **12**:183-190.
2. Grabert RC, Cousens LP, Smith JA, Olson S, Gall J, Young WB, *et al*: **Human T Cells Armed with Her2/neu Bispecific Antibodies Divide, Are Cytotoxic, and Secrete Cytokines with Repeated Stimulation.** *CCR* 2006, **12**:569-576.
3. Lum LG, Thakur A, Al-Kadhimi Z, Colvin G, Cummings F, Legare R, *et al*: **Targeted T cell Therapy in Stage IV Breast Cancer: A Phase I Clinical Trial.** *CCR* 2015, **21**:2305-2314.

**Table 1**

Pt	Age	Disease	Prior Tx	BATs (x 10 <sup>9</sup> )	TTP (mo)	OS (mo)	Comments
IT20087	58	Mets to liver	Folifirinox	47	6 mo	Died 13.5 mo	Progressed after Immunotherapy
IT20091	63	T3 N1 Mets to liver, S/P Whipple	5FU, Leu/5FU, Folifirinox	9, 79	4.8 mo	Died 31 mo	Folifirinox induced CR after IT and responded a 2 <sup>nd</sup> time to Folifirinox
IT20092	64	T2b Abd Nodes, S/P Whipple	Gemzar, 5FU, radiation	36	7 mo	Died 14.5 mo	Slowly progress with chronic diarrhea
IT20102	56	T4, Mets to liver, lungs	Folifirinox	74	6.5 mo	Alive 24.9 mo	Progressed after 6.5 mo
IT20104	51	T4, Abd Node	FOLFOLX, eloda	72	2.2 mo	Alive 29.3 mo	Chemo induced CR after IT; On Xeloda

### 130

#### **A fusion monoclonal antibody (FmAb2) to target tumors and the immune system with a unique mechanism of action: preclinical proof-of-concept**

Sreesha P Srinivasa, Nagaraja Govindappa, Praveen Reddy, Aparajita Dubey, Sankar Periyasamy, Madhukara Adekandi, Chaitali Dey, Mary Joy

Biocon Research Ltd, Bangalore, India

#### **Background**

We describe a novel therapeutic molecule that simultaneously inhibits two important targets which control pathways that are hallmarks of tumorigenesis. Epidermal growth factor receptor (EGFR) is important for the growth and survival of tumor cells, and transforming growth factor beta (TGFβ) is a pleiotropic cytokine expressed in the tumor microenvironment that regulates important processes such as epithelial-to-mesenchymal cell transition (EMT), migration, invasion, and tumor-specific immunosuppression. To date, therapies have targeted these pathways individually; monoclonal antibodies (mAbs) and small molecule inhibitors of EGFR are in clinical use, and modulators of TGFβ pathway are in late-stage clinical development.

#### **Methods**

FmAb2 is a recombinant fusion mAb consisting of the TGFβ receptor II extracellular domain (T-ECD) fused to cetuximab,

## Bispecific Antibodies

Presenting author underlined; Primary author in italics

an anti-EGFR mAb. We hypothesized that using FmAb2 to block the EGFR and TGFb pathways simultaneously would have a synergistic effect on inhibition of tumor growth and EMT, and also induce a tumor-specific immune response. Furthermore, this agent would neutralize TGFb preferentially in the tumor microenvironment, thereby improving efficacy while reducing systemic toxicity.

### Results

FmAb2 was expressed in Chinese hamster ovary (CHO) cells, purified using standard methodology and tested using *in vitro* and *in vivo* models. FmAb2 is secreted as an intact fusion protein and simultaneously binds both targets in *in vitro* binding assays. In surface plasmon resonance kinetic binding assays (Biacore), FmAb2 binds EGFR with a  $K_D$  of ~2.5 nM and TGFb1 with a  $K_D$  of ~60 nM. FmAb2 binds EGFR on the cell surface, neutralizes tumor cell-secreted TGFb1, inhibits proliferation of sensitive tumor cell lines and activates NK cell-mediated antibody-dependent cellular cytotoxicity (ADCC). Using fluorescently labeled FmAb2, we demonstrate that systemically administered FmAb2 in mice preferentially localizes to tumors and is 10-fold more effective in neutralizing tumor TGFb1 compared to T-ECD fused to IgG-Fc (T-ECD-Fc). Consistent with this, we also observe significantly better inhibition of tissue inhibitor of metalloproteinase-1 (TIMP-1) in FmAb2-treated tumors compared to T-ECD at equivalent doses. In a head-and-neck mouse xenograft model, FmAb2 administration is significantly superior to cetuximab or T-ECD-Fc alone at equivalent doses. Furthermore, FmAb2 treatment is more efficacious than the co-administration of cetuximab + T-ECD-Fc at equivalent doses, most likely due to better neutralization of tumor TGFb1.

### Conclusions

FmAb2 is currently in preclinical development and is expected to enter clinical testing soon.

### 131

#### **MCLA-117, a CLEC12AxCD3 bispecific IgG targeting a leukemic stem cell antigen, induces T cell mediated AML blast lysis**

*Pieter Fokko van Loo*<sup>1</sup>, Henrike Veninga<sup>1</sup>, Setareh Shamsili<sup>1</sup>, Mark Throsby<sup>1</sup>, Harry Dolstra<sup>2</sup>, Lex Bakker<sup>1</sup>

<sup>1</sup>Merus N.V., Utrecht, Netherlands

<sup>2</sup>Department of Laboratory Medicine, Radboud University Medical Center, Nijmegen, Gelderland, Netherlands

### Background

Patients with acute myeloid leukemia (AML) have a dismal prognosis despite improvements in chemotherapy and supportive care. Novel, more effective therapies are needed for these patients. We report the characterization of MCLA-117, a novel T cell redirecting antibody for the treatment

of AML that targets CLEC12A on leukemic cells and CD3 on T cells. CLEC12A is a myeloid differentiation antigen that is expressed on 90-95% of newly diagnosed and relapsed AML. Moreover, CLEC12A is selectively expressed on leukemic stem cells (LSCs) but not on normal early hematopoietic progenitors, including hematopoietic stem cells (HSCs).

### Methods

MCLA-117 is a human common light chain CLEC12AxCD3 full length IgG1 bispecific antibody. Heterodimerization of the bispecific IgG is facilitated by amino acid residues introduced at the CH3 interface. MCLA-117 lacks Fc effector function following amino acid substitutions in the CH2 region.

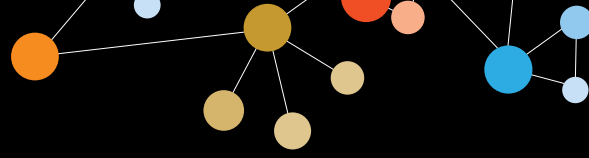
### Results

MCLA-117 specifically binds to CLEC12A expressing myeloid cells and CD3 expressing T cells, as evaluated using healthy donor samples. In line with the CLEC12A expression MCLA-117 did not bind the HSCs, nor the common myeloid progenitor cells. The potency of MCLA-117 to induce T cell mediated lysis of CLEC12A<sup>POS</sup> tumor cells was evaluated in cytotoxicity assays. In co-cultures with resting healthy donor T cells and AML tumor cells, MCLA-117 efficiently induced CLEC12A antigen dependent T cell activation ( $EC_{50}$  of 44 ng/mL), T cell proliferation and tumor target cell lysis ( $EC_{50}$  of 66±37 ng/mL). The efficacy of MCLA-117 to induce lysis of AML blasts by autologous T cells in primary AML samples with low T cell to AML blast ratios was examined in an *ex vivo* culture system. We demonstrated robust eradication of AML blasts by MCLA-117, even at low E:T ratios (Figure 1). In 9/11 AML patient samples taken at diagnosis, MCLA-117 induced expansion of autologous T cells (7-226-fold) and killing (31-99%) of AML blasts at low E:T ratios (E:T 1:3–1:97).

### Conclusions

MCLA-117 efficiently induced CLEC12A-mediated lysis of AML blasts by T cells present in AML samples, even at very low E:T ratios, and it provoked robust T cell proliferation. Based on its binding profile within the hematopoietic compartment, MCLA-117 is expected to specifically target myeloid blasts and LSCs while sparing the normal HSCs. A phase I clinical study (MCLA-117-CL01) is ongoing to evaluate the preliminary safety and efficacy of MCLA-117 in adult AML patients.

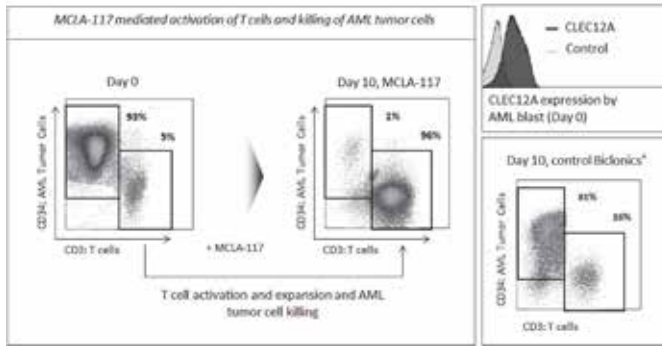




# Bispecific Antibodies

Presenting author underlined; Primary author in italics

Figure 1



MCLA-117 efficiently induced T cell expansion and redirected lysis of AML blast in primary AML samples even at a low E:T ratio. Primary AML blast sample taken at diagnosis was incubated with MCLA-117 and a control Bionics (binding CD3 and an irrelevant antigen). CLEC12A expression, T cell proliferation and primary AML blast lysis was quantified using flow cytometry.

## Clinical Trials in Progress

Presenting author underlined; Primary author in italics

132

### **KEYNOTE-361: randomized phase III study of pembrolizumab with or without chemotherapy versus chemotherapy alone in advanced urothelial carcinoma**

Ajjai Alva<sup>1</sup>, Juergen Gschwendt<sup>2</sup>, Yohann Loriot<sup>3</sup>, Joaquim Bellmunt<sup>4</sup>, Dai Feng<sup>5</sup>, Christian Poehlein<sup>5</sup>, Thomas Powles<sup>6</sup>

<sup>1</sup>University of Michigan, Ann Arbor, MI, USA

<sup>2</sup>Technical University of Munich, Munchen, Germany

<sup>3</sup>Gustave Roussy, Université Paris-Saclay, Villejuif, France

<sup>4</sup>Dana-Farber Cancer Institute, Harvard Medical School, Boston, MA, USA

<sup>5</sup>Merck & Co., Inc., Kenilworth, NJ, USA

<sup>6</sup>Barts Cancer Institute, Queen Mary University of London, London, England, UK

#### **Background**

Cisplatin-based combination chemotherapy is standard first-line treatment for patients with advanced bladder cancer. The median survival with these regimens is 13-15 months, and only 5-15% of patients attain long-term survival. Programmed death ligand 1 (PD-L1) is expressed in select urothelial cancer lesions. In the phase Ib KEYNOTE-012 study, monotherapy with the anti-programmed death 1 antibody pembrolizumab demonstrated antitumor activity (objective response rate, 28%; 95% CI, 13%-47%) and acceptable safety in patients with chemotherapy-refractory metastatic PD-L1-positive urothelial carcinoma, and higher tumor PD-L1 expression was associated with higher response rates. KEYNOTE-361 is a randomized, open-label, phase III study of pembrolizumab with or without chemotherapy versus chemotherapy alone in patients with advanced urothelial carcinoma.

#### **Methods**

Key eligibility criteria include age  $\geq 18$  years; histologically or cytologically confirmed diagnosis of advanced/unresectable or metastatic urothelial carcinoma of the bladder, renal pelvis, ureter, or urethra; measurable disease based on RECIST v1.1 as determined by the local site investigator/radiology assessment; no prior systemic chemotherapy for advanced/metastatic urothelial carcinoma (with the exception of neoadjuvant platinum-based chemotherapy with recurrence  $>12$  months after completion of therapy; or adjuvant platinum-based chemotherapy following radical cystectomy with recurrence  $>12$  months after completion of therapy); ECOG performance status 0-2; and provision of a fresh tissue sample for biomarker analysis. Approximately 990 patients will be randomized 1:1:1 to receive: pembrolizumab 200 mg on day 1 of each 3-week cycle (Q3W) alone or in combination with investigator's choice of chemotherapy (gemcitabine [1000 mg/m<sup>2</sup> on days 1 and 8 of each 3-week cycle] plus cisplatin [70 mg/

m<sup>2</sup> Q3W] or gemcitabine plus carboplatin [AUC 5 Q3W] for cisplatin-ineligible patients), or investigator's choice of chemotherapy alone. Patients will be stratified based on chemotherapy regimen (cisplatin or carboplatin, chosen before randomization) and tumor PD-L1 expression (positive or negative). Treatments will continue until progressive disease, unacceptable adverse events (AEs), investigator decision, or 35 doses of pembrolizumab (pembrolizumab arms only). Response will be assessed per RECIST v1.1 by blinded independent central review (BICR) every 9 weeks until week 54, then every 12 weeks thereafter. AEs will be evaluated throughout treatment and for 30 days thereafter (90 days for serious AEs) and graded per National Cancer Institute Common Terminology Criteria for Adverse Events, version 4.0. The primary end points are PFS per RECIST v1.1 as assessed by BICR and OS; key secondary end points include objective response rate and safety and tolerability. Enrollment in KEYNOTE-361 is ongoing.

#### **Trial Registration**

ClinicalTrials.gov identifier NCT02853305.

133

### **Phase II study of pembrolizumab in patients with metastatic castration-resistant prostate cancer previously treated with targeted endocrine therapy and taxane chemotherapy: KEYNOTE-199**

Emmanuel S Antonarakis<sup>1</sup>, Charles G Drake<sup>2</sup>, Haiyan Wu<sup>3</sup>, Christian Poehlein<sup>3</sup>, Johann De Bono<sup>4</sup>

<sup>1</sup>Johns Hopkins University, Sidney Kimmel Cancer Center, Baltimore, MD, USA

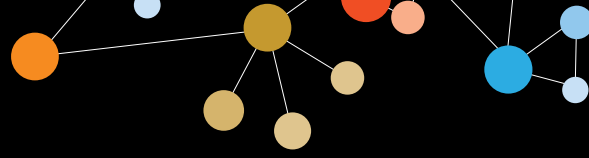
<sup>2</sup>Johns Hopkins University Cancer Center, Baltimore, MD, USA

<sup>3</sup>Merck & Co., Inc., Kenilworth, NJ, USA

<sup>4</sup>Royal Marsden Hospital, London, England, UK

#### **Background**

Treatment for patients with metastatic castration-resistant prostate cancer (mCRPC) has focused on suppression of testosterone and androgen receptor signaling, palliative radiation therapy, and chemotherapy. As expression of the programmed death-1 (PD-1) receptor and its ligand PD-L1 is present in mCRPC lesions, particularly after initial treatment with antiandrogen and/or chemotherapy, targeting this pathway may be an attractive treatment option. Pembrolizumab, an anti-PD-1 antibody that blocks interaction between PD-1 and its ligands, PD-L1 and PD-L2, produced durable responses in patients with heavily pretreated PD-L1-positive prostate cancer in the KEYNOTE-028 study. KEYNOTE-199 is a nonrandomized, multinational, open-label phase II study to evaluate pembrolizumab monotherapy in patients with mCRPC previously treated with chemotherapy.



## Clinical Trials in Progress

Presenting author underlined; *Primary author in italics*

### Methods

Eligible patients must be  $\geq 18$  years old with histologically or cytologically confirmed adenocarcinoma of the prostate without small-cell histology, measurable disease per RECIST v1.1 or detectable bone metastases by whole-body bone scintigraphy and no RECIST v1.1 measurable tumors, supplied tumor sample for PD-L1 expression (new or archived), progression of disease within 6 months before screening, and ECOG performance status 0-2. Patients must have been treated with  $\geq 1$  targeted endocrine therapy (abiraterone or enzalutamide) and  $\leq 2$  chemotherapy regimens, 1 of which must have contained docetaxel. Patients also must have ongoing androgen deprivation with serum testosterone  $< 50$  ng/dL. Patients will be enrolled into 1 of 3 cohorts based on PD-L1 status and RECIST v1.1 measurability: patients with PD-L1-positive, RECIST v1.1 measurable disease (cohort 1, n=100), patients with PD-L1-negative, RECIST v1.1 measurable disease (cohort 2, n=100), and patients with bone metastases and RECIST v1.1 nonmeasurable disease (cohort 3, n=50). Patients will receive pembrolizumab 200 mg every 3 weeks until documented confirmed disease progression, unacceptable adverse events (AEs), or illness that prevents further treatment. Imaging response will be assessed every 9 weeks for approximately 1 year and every 12 weeks thereafter, per central imaging vendor review using RECIST v1.1 criteria and the Prostate Cancer Clinical Trials Working Group 3 guidelines. AEs will be monitored throughout the study and graded per Common Terminology Criteria for Adverse Events, version 4.0. Primary end points are the objective response rate and duration of response for cohorts 1 and 2 combined and by each cohort. Key secondary end points include safety and tolerability, disease control rate, radiographic progression-free survival, and overall survival for each cohort and all 3 combined. Exploratory translational analyses and expression of other immune checkpoints will also be evaluated.

### Trial Registration

ClinicalTrials.gov identifier NCT02787005.

### Methods

Based on this pre-clinical data, we are undertaking a clinical trial of chemo-immunotherapy using the immunomodulatory drug gemcitabine (GEM) to suppress tumor infiltrating suppressor cells such as myeloid-derived suppressor cells (MDSC) and regulatory T cells (Tregs) with a dendritic cell (DC) vaccine pulsed with the above six HLA-A2-presented TBVA-derived peptides (DC-TBVA) in 30 HLA-A2+ patients with metastatic breast cancer (MBC). Eligible patients will first undergo leukapheresis for the generation of the DC-TBVA vaccine. Patients will then receive 3 cycles of GEM, 1000 mg/m<sup>2</sup> IV on days 1 and 8 of a 21-day cycle for 3 cycles. Patients will then receive the DC-TBVA vaccine administered twice intradermally 7 days apart. Patients must be HLA-A2+ and

have radiologically measurable MBC, an ECOG performance status of 0-1 and not have any active immune disorders. Prior GEM therapy is acceptable as long as the last dose was  $\geq 3$  months from registration on this study. Patients may not be on steroids. The 4 specific aims are to 1) assess the safety of GEM +  $\alpha$ DC1-TBVA vaccination, 2) assess the clinical response of MBC to GEM +  $\alpha$ DC1-TBVA vaccination, 3) determine the clinical efficacy of GEM +  $\alpha$ DC1-TBVA vaccination in generating Tc1 immunity, and 4) correlate changes in MDSC and Tregs with the generation of anti-TBVA Tc1-cell immunity.

### Results

We will report the results of this study once it has been completed.

### Conclusions

This is a clinical trial in progress and conclusions will be forthcoming at the end of the study.

### Acknowledgements

Funded by Susan G. Komen (IIR13261822; IND 15722).

### 134

#### **KEYNOTE-155: phase Ib study of pembrolizumab in combination with dinaciclib in patients with hematologic malignancies**

Rajat Bannerji<sup>1</sup>, John Byrd<sup>2</sup>, Gareth Gregory<sup>3</sup>, Stephen Opat<sup>4</sup>, Jake Shortt<sup>4</sup>, Andrew J Yee<sup>5</sup>, Noopur Raje<sup>5</sup>, Seth Thompson<sup>6</sup>, Arun Balakumaran<sup>6</sup>, Shaji Kumar<sup>7</sup>

<sup>1</sup>Rutgers Cancer Institute of New Jersey, New Brunswick, NJ, USA

<sup>2</sup>The Ohio State University, Columbus, OH, USA

<sup>3</sup>Monash Health and Peter MacCallum Cancer Centre, Clayton, Victoria, Australia

<sup>4</sup>Monash Health, Clayton, Victoria, Australia

<sup>5</sup>Massachusetts General Hospital, Boston, MA, USA

<sup>6</sup>Merck & Co., Inc., Kenilworth, NJ, USA

<sup>7</sup>Mayo Clinic, Rochester, MN, USA

### Background

Pembrolizumab, a PD-1 immune checkpoint inhibitor, and dinaciclib, a cyclin-dependent kinase inhibitor, have demonstrated antitumor activity as monotherapies in various tumor types, including hematologic malignancies. In a preclinical study using a solid-tumor syngeneic model (MC38), enhanced antitumor activity was observed with the combination of pembrolizumab and dinaciclib, with no significant toxicities. KEYNOTE-155 is a phase Ib study designed to evaluate the safety and efficacy of the combination of pembrolizumab and dinaciclib in patients with relapsed or refractory chronic lymphocytic leukemia (CLL), multiple myeloma (MM), or diffuse large B cell lymphoma (DLBCL).

## Clinical Trials in Progress

Presenting author underlined; Primary author in italics

### Methods

Key eligibility criteria include  $\geq 18$  years, ECOG performance status 0-1, and confirmed diagnosis of one of the following: CLL as defined by 2008 iwCLL criteria with  $\geq 1$  prior therapy; active MM with measurable disease and  $\geq 2$  prior therapies including an IMiD and proteasome inhibitor; or DLBCL with progression following  $\geq 2$  prior therapies including autologous stem cell transplantation (ASCT; or ineligible for ASCT). An initial cohort of 12 patients ( $\geq 3$  with each disease type) will be enrolled in the dose-evaluation phase (two 21-day cycles) to determine dose-limiting toxicities (DLTs). In cycle 1, patients will receive pembrolizumab 200 mg on day 1, dinaciclib 7 mg/m<sup>2</sup> on day 1, and dinaciclib 10 mg/m<sup>2</sup> on day 8. In cycle 2 and beyond, patients will receive pembrolizumab 200 mg on day 1 and dinaciclib 14 mg/m<sup>2</sup> on days 1 and 8. If  $\leq 4$  patients experience DLTs in the first 2 cycles, expansion cohorts (~30 patients each) will be opened for signal detection. If  $\geq 5$  DLTs occur in the first 2 cycles, a lower dose of dinaciclib will be studied in up to 24 patients. Treatment will continue until disease progression, unacceptable toxicity, or 35 cycles. Response will be assessed every 3 cycles for CLL and DLBCL, and at the start of each cycle for MM. Primary end points are safety and tolerability in both phases and objective response rate within each disease type per investigator assessment in the signal-detection phase. Secondary end points include duration of response, progression-free survival, and overall survival within each disease type in the signal-detection phase. Exploratory objectives include assessment of treatment effect on CD4, CD8, and quantitative immunoglobulins; the relationship between candidate biomarkers and antitumor activity; and the relationship between genomic variation and response to treatment. KEYNOTE-155 will enroll up to 138 patients from multiple sites.

### Trial Registration

ClinicalTrials.gov identifier NCT02684617.

### 135

#### **Avelumab in combination with axitinib versus sunitinib as first-line treatment for patients with advanced renal cell carcinoma: the phase III JAVELIN Renal 101 trial**

Brian I Rini<sup>1</sup>, Toni K Choueiri<sup>2</sup>, Mariangela Mariani<sup>3</sup>, Laurence Albiges<sup>4</sup>, John B Haanen<sup>5</sup>, Michael B Atkins<sup>6</sup>, James Larkin<sup>7</sup>, Manuela Schmidinger<sup>8</sup>, Domenico Magazzù<sup>3</sup>, Alessandra di Pietro<sup>3</sup>, Robert J Motzer<sup>9</sup>

<sup>1</sup>Cleveland Clinic Taussig Cancer Institute, Cleveland, OH, USA

<sup>2</sup>Dana-Farber Cancer Institute, Brigham and Women's Hospital, Boston, MA, USA

<sup>3</sup>Pfizer Inc., Milano, Lombardia, Italy

<sup>4</sup>Gustave Roussy Cancer Campus, University of Paris Sud, Department of Cancer Medicine, Villejuif, Ile-de-France, France

<sup>5</sup>Netherlands Cancer Institute, Amsterdam, Noord-Holland, Netherlands

<sup>6</sup>Georgetown-Lombardi Comprehensive Cancer Center, Washington DC, USA

<sup>7</sup>Royal Marsden Hospital, London, England, UK

<sup>8</sup>Medical University of Vienna, Vienna, Wien, Austria

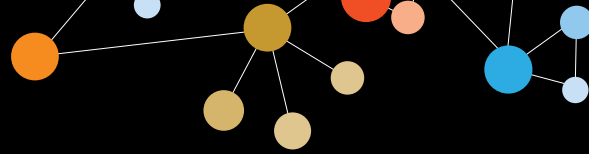
<sup>9</sup>Memorial Sloan Kettering Cancer Center, New York, NY, USA

### Background

Checkpoint inhibitors and tyrosine kinase inhibitors may have complementary mechanisms of action in advanced renal cell carcinoma (aRCC), providing a rationale for investigating combination treatment. Inhibition of the programmed death-1 receptor ligand (PD-L1) pathway leads to reactivation of an effective antitumor immune response against multiple cancers, including RCC. Avelumab (MSB0010718C) is a fully human IgG1 anti-PD-L1 antibody that has shown clinical activity in patients with several tumor types. Axitinib is an anti-VEGF receptor tyrosine kinase inhibitor approved for treatment of aRCC after failure of 1 prior systemic therapy. In an ongoing phase Ib study, avelumab plus axitinib administered at standard monotherapy doses showed encouraging safety and antitumor activity in treatment-naïve patients with aRCC. JAVELIN Renal 101 is a global phase III trial comparing avelumab plus axitinib versus sunitinib as first-line treatment for patients with aRCC.

### Methods

The primary objective of this randomized, multicenter trial is to demonstrate superiority of first-line avelumab plus axitinib versus sunitinib monotherapy in prolonging progression-free survival (PFS). Eligibility criteria include: aRCC with a clear cell component, availability of archival or fresh tumor biopsy, ECOG PS  $\leq 1$ , no prior systemic therapy for advanced disease or prior immunotherapy, and measurable disease per RECIST v1.1. Approximately 583 patients will be randomized 1:1 to



## Clinical Trials in Progress

*Presenting author underlined; Primary author in italics*

receive either: Arm A, avelumab intravenously over 1 hour every 2 weeks plus axitinib orally twice daily continuously (cycle length 6 weeks); or Arm B, sunitinib orally once daily for 4 weeks followed by 2 weeks off. Stratification factors are: ECOG PS (0 vs 1) and region (US vs Canada/Europe vs rest of world). Treatment is discontinued for unacceptable toxicity or if any criteria for withdrawal are met. Patients may continue treatment beyond progression if investigator-assessed clinical benefit is achieved and treatment is well tolerated. The primary endpoint is PFS per RECIST v1.1 by blinded independent central review. Secondary endpoints include overall survival, PFS by investigator assessment, objective response, duration of response, time to response, safety, and patient-reported outcomes. Pharmacokinetics, immunogenicity, and tumor tissue biomarkers will also be assessed. Enrollment in this pivotal trial began in March 2016.

### Trial Registration

ClinicalTrials.gov identifier NCT02684006.

### 136

#### **T cell therapy in combination with vemurafenib in BRAF mutated metastatic melanoma patients**

Troels Holz Borch, Rikke Andersen, Per Kongsted, Magnus Pedersen, Morten Nielsen, Özcan Met, Marco Donia, Inge Marie Svane

Department of Oncology, Center for Cancer Immune Therapy, Herlev University Hospital, Herlev, Hovedstaden, Denmark

### Background

Adoptive T cell therapy (ACT) with tumor infiltrating lymphocytes (TIL) has proven to be a powerful treatment option for patients with metastatic melanoma with response rates of approximately 50% and durable complete responses in about 15%. However, there is still a need for improving TIL efficacy and a promising strategy is combination with immunomodulating agents. One such agent is vemurafenib (vem), a selective BRAF inhibitor, which induces objective responses in about 50% of melanoma patients with tumors expressing BRAF<sup>V600E/K</sup>. In addition to the direct anti-cancer effect, vem has been shown to increase T cell infiltration into tumors, upregulate melanoma antigen expression and increase the frequency of TIL recognizing autologous melanoma cells. This trial was previously presented at the Society for Immunotherapy of Cancer annual meeting [1]. In this abstract an update on clinical responses is provided.

### Methods

A total of 12 patients will be included in this open phase II non-randomized trial primarily to investigate safety when combining ACT and vem. Secondly, clinical responses will

be evaluated according to RECIST and extensive immune monitoring will be performed. Patients are treated with vem orally 960 mg BID one week prior to excision of tumor material for T cell generation and continue vem until hospital admission (4-7 weeks). During hospitalization patients will receive a preparative lymphodepleting regimen consisting of cyclophosphamide 60 mg/kg for 2 days and fludarabine 25 mg/m<sup>2</sup> for 5 days. TIL infusion consists of 5-10 x 10<sup>10</sup> T cells and patients are subsequently treated with continuous interleukin-2 infusion following the decrescendo regimen for 5 days. Patients are evaluated for up to 5 years or until progression.

### Results

So far 5 patients have been treated. No unexpected toxicity has been observed. Three patients achieved confirmed ongoing partial response (9+ months, 5+, and 4+) and 2 patients had progressive disease at evaluation after TIL. Immune analyses are pending.

### Conclusions

So far treatment combining vem and ACT using TILs has been safe with no unexpected toxicity and encouraging clinical benefit with durable responses has been observed.

### Trial Registration

ClinicalTrials.gov identifier NCT02354690.

### References

1. Borch TH, Andersen R, Kongsted P, *et al*: **T cell therapy in combination with Vemurafenib in BRAF mutated metastatic melanoma patients.** *J Immunother Cancer* 2014, **2(Suppl 3)**:67.

### 137

#### **Neoadjuvant enoblituzumab (MGA271) in men with localized intermediate and high-risk prostate cancer—a pilot and biomarker study**

Karim Boudadi<sup>1</sup>, Hao Wang<sup>1</sup>, James Vasselli<sup>2</sup>, Jan E Baughman<sup>3</sup>, Jon Wigginton<sup>2</sup>, Rehab Abdallah<sup>1</sup>, Ashley Ross<sup>1</sup>, Charles G Drake<sup>4</sup>, Emmanuel S Antonarakis<sup>5</sup>

<sup>1</sup>Johns Hopkins Hospital, Baltimore, MD, USA

<sup>2</sup>MacroGenics, Inc., Rockville, MD, USA

<sup>3</sup>MacroGenics, Inc., South San Francisco, CA, USA

<sup>4</sup>Johns Hopkins University Cancer Center, Baltimore, MD, USA

<sup>5</sup>Johns Hopkins University, Sidney Kimmel Cancer Center, Baltimore, MD, USA

### Background

B7-H3 is part of the B7 superfamily of immune checkpoint molecules. While its regulation and mechanism of action are not completely understood, B7-H3 expression correlates with adverse pathology and clinical outcomes in men with prostate cancer. B7-H3 expression appears to be associated



## Clinical Trials in Progress

Presenting author underlined; *Primary author in italics*

with biochemical and clinical progression following treatment. The correlation between B7-H3 overexpression and poor prognosis suggests a role in tumor immune escape. In addition, B7-H3 levels remain high in the presence of androgen deprivation. These results suggest a potential role for B7-H3 in prostate cancer progression and support its use as a therapeutic target. Enoblituzumab is an anti-B7-H3 humanized monoclonal antibody with a proposed mechanism of action of antibody directed cellular cytotoxicity. We propose a neoadjuvant study to determine the anti-tumor, immunological and biological effects of enoblituzumab in men with localized prostate cancer. We hypothesize that administration of enoblituzumab will be safe and feasible in the neoadjuvant setting for men with localized intermediate and high-risk prostate cancer. We also hypothesize that enoblituzumab will produce measurable tumor cell death and antitumor immune responses in harvested prostate glands.

### Methods

This is a single-center, single-arm, open-label pilot study of enoblituzumab 15mg/kg IV weekly for 6 doses beginning 50 days prior to radical prostatectomy. The target population (N=16) is men with localized, intermediate or high-risk prostate adenocarcinoma (Gleason sum  $\geq 7$ ), with adequate organ function, no adverse indications for standard radical prostatectomy, and no previous local treatment to the prostate, anti-androgen exposure, or immunotherapy. The primary endpoint will be frequency/severity of adverse events from time of first administration of enoblituzumab until the 90<sup>th</sup> post-op day. Prostate glands will be harvested at time of radical prostatectomy and prostate tissue will be examined for the secondary endpoints and compared to pre-treatment biopsies. The secondary biological endpoint is tumor cell death, which will be quantified by caspase 3 staining and post-treatment apoptotic index. The trial will meet its biological endpoint if tumor cell apoptosis is two-fold higher after treatment, which we will be able to detect with an 80% power based on a one-sided t-test with a significance level of 0.05, with 16 subjects. Other secondary endpoints will include CD8+ T cell infiltration, CD8/Treg ratio, TCR repertoire, and B7-H3 expression, and will be exploratory in nature. If this study shows preliminary evidence of clinical activity and reasonable safety, our future goal will be to use enoblituzumab in the adjuvant and salvage settings.

138

## Radiotherapy enhances natural killer cell homing and function in canine bone and soft tissue sarcoma

Robert J Canter<sup>1</sup>, Jiwon Park<sup>1</sup>, Ziming Wang<sup>1</sup>, Steven Grossenbacher<sup>1</sup>, Jesus I Luna<sup>1</sup>, Sita Withers<sup>2</sup>, William Culp<sup>2</sup>, Mingyi Chen<sup>1</sup>, Arta Monjazeb<sup>1</sup>, Michael S Kent<sup>2</sup>, *William J Murphy*<sup>1</sup>

<sup>1</sup>University of California, Davis, Sacramento, CA, USA

<sup>2</sup>University of California, Davis, Davis, CA, USA

### Background

We have previously shown that radiotherapy (RT) increases natural killer (NK) cytotoxicity and homing in diverse pre-clinical models of human solid malignancies, including sarcomas. Since sarcomas commonly afflict dogs, we hypothesized that dog PBMC-derived NK cells would be effective in canine models of sarcoma, including adoptive transfer in a canine RT/NK clinical trial.

### Methods

Canine NK cells were isolated from 15 mls whole blood using Ficoll separation and CD5 depletion. Isolated NK cells were expanded in co-culture with irradiated K562c9IL21 for 2-3 weeks. Using 6-month metastasis-free survival as the primary endpoint, a canine clinical trial is underway evaluating RT and adoptive intratumoral NK immunotherapy. For this trial, treatment consists of palliative RT weekly for one month followed by two intra-lesional injections of autologous canine NK cells. In correlative studies, including dog patient-derived xenografts (PDX), we assessed NK homing using eFluor 670 cell proliferation dye and NK function by expression of activation markers including IFN $\gamma$ , granzyme B, and perforin.

### Results

We have treated 7 of planned 14 dogs with osteosarcoma on protocol. Of 3 evaluable dogs who have reached the 6-month primary endpoint, we have observed 1 partial response and 2 are metastasis-free, including 1 dog with complete resolution of a suspicious 3 mm pulmonary nodule. In dog patients on trial, phenotyping of expanded NK cells from all patients showed > 90% granzyme B and IFN $\gamma$  expression prior to adoptive transfer. Tagging experiments 1 week after intratumoral injection revealed that 11 – 60% of CD45+ cells are eFluor 670 positive, confirming persistence of injected NK cells post injection. Analysis of unactivated circulating PBMCs post-injection demonstrated a significant increase in granzyme B expression ( $2.25X \pm 0.42$ ,  $P < 0.01$ ). Dog PDX studies demonstrate that focal RT increases NK homing to sarcomas on average  $3.8X \pm 0.3$  ( $P < 0.001$ ) compared to unirradiated controls. Immunohistochemical analysis of irradiated dog sarcomas (historical controls) shows a significant increase in CD3+ tumor-infiltrating lymphocytes

## Clinical Trials in Progress

Presenting author underlined; Primary author in italics

post RT ( $P < 0.04$ , see figure). Co-culture experiments of dog PDX sarcomas *ex vivo* with allogeneic NK cells showed RT-induced sensitization to NK killing at doses of 10 - 20 Gy ( $P < 0.01$ ).

### Conclusions

RT and NK immunotherapy appear synergistic in dog models of sarcoma, and preliminary results from a canine clinical trial of palliative RT and autologous NK transfer for osteosarcoma are promising, including possible abscopal effects. Further evaluation of this novel radio-immunotherapy approach is warranted.

### Acknowledgements

The authors are grateful to Teri Guerrero and Heather Schrader for veterinary clinical trials support.

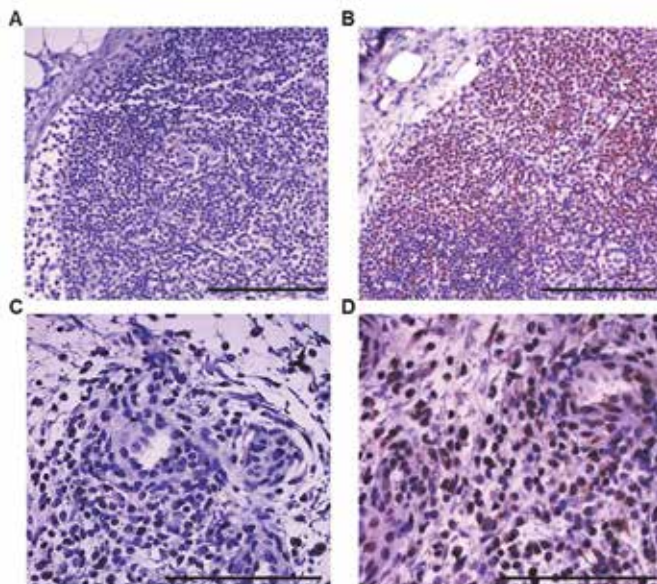


**Figure 1. Canine Sarcomas Show Increased CD3+ Lymphocytes after Radiotherapy.** (A) High power view of normal dog lymph node in the absence of mouse anti-dog CD3 antibody. (B) High power view of normal dog lymph node shows diffuse expression of CD3+ lymphocytes. (C) High power view shows absence of CD3+ lymphocytes following amputation of distal tibia dog osteosarcoma. (D) High power view positive increased CD3+ cells in a dog osteosarcoma following palliative RT (scale bars 100  $\mu\text{m}$ ).

139

### Interim results of a phase II trial of adoptive transfer of tumor infiltrating lymphocytes in patients with metastatic uveal melanoma

Smita Chandran<sup>1</sup>, Robert Somerville<sup>1</sup>, John Wunderlich<sup>1</sup>, David Danforth<sup>1</sup>, James Yang<sup>1</sup>, Richard Sherry<sup>1</sup>, Christopher Klebanoff<sup>1</sup>, Stephanie Goff<sup>1</sup>, Biman Paria<sup>1</sup>, Arvind Sabesan<sup>1</sup>, Abhishek Srivastava<sup>1</sup>, Steven A Rosenberg<sup>2</sup>, Udai Kammula<sup>1</sup>

<sup>1</sup>National Cancer Institute, Bethesda, MD, USA

<sup>2</sup>Surgery Branch, National Cancer Institute, National Institutes of Health, Bethesda, MD, USA

### Background

Uveal melanoma (UM) is a rare tumor variant with no established treatments once metastases develop. Although a variety of immune based therapies have demonstrated anti-tumor activity in metastatic cutaneous melanoma, their use in UM has been disappointing. Recently, adoptive T cell therapy has shown salvage responses in multiple refractory solid tumors. Based upon our identification from UM liver metastases of tumor infiltrating lymphocytes (TIL) with strong autologous reactivity, we sought to determine if clinical adoptive transfer of such TIL could mediate regression in patients with metastatic UM. Here we present an interim analysis of the ongoing clinical trial, NCT01814046.

### Methods

In the main arm of this phase II study, patients with metastatic melanoma of ocular origin received nonmyeloablative lymphodepleting conditioning chemotherapy consisting of intravenous cyclophosphamide (60 mg/kg/daily) for 2 days and fludarabine (25 mg/m<sup>2</sup>/daily) for 5 days followed by an intravenous infusion of autologous TIL and high-dose interleukin-2 (720,000 IU/kg). Clinical responses were evaluated using Response to Evaluation Criteria in Solid Tumors (RECIST), version 1.0. The study was designed to initially enroll 19 patients and if 4 or more patients achieved an objective clinical response, accrual would expand in a second phase to a total of 33 patients.

### Results

At the current time, 17 patients with metastatic UM have completed TIL treatment; 16 of these patients are evaluable for response assessment. Five of 16 (31%) UM patients demonstrated objective tumor regression. Among the responders, four patients demonstrated partial tumor regression lasting between 4 and 10 months. One patient achieved complete tumor regression, ongoing 15 months after TIL infusion. In the year prior to TIL therapy, this patient demonstrated marked progression of multiple liver metastases after anti-CTLA-4 and anti-PD-1 checkpoint therapy. However, after a single infusion of TIL, we observed rapid and complete tumor regression. Circulating serum tumor DNA specific for the patient's *GNAQ* driver mutation demonstrated complete clearance by 10 days following cell therapy consistent with the patient's clinical response. Overall in the trial, the frequency of tumor-reactive T cells within the administered infusion and the levels of IFN- $\gamma$  released after autologous tumor stimulation were positively associated with clinical response ( $P=0.04$ , respectively).

### Conclusions

To our knowledge, these clinical findings represent the first demonstration that autologous T cell transfer is capable of inducing complete and durable tumor regression of metastatic UM. Refinement of this cell therapy is aimed

## Clinical Trials in Progress

Presenting author underlined; Primary author in italics

at identifying the antigenic targets associated with clinical response.

140

### **A phase Ib study of intratumoral CAVATAK (coxsackievirus A21) and ipilimumab in patients with advanced melanoma**

Brendan Curti<sup>1</sup>, Jon Richards<sup>2</sup>, Mark Faries<sup>3</sup>, Robert H I Andtbacka<sup>4</sup>, Mark Grose<sup>5</sup>, Darren Shafren<sup>6</sup>

<sup>1</sup>Earle A. Chiles Research Institute, Providence Cancer Center, Portland, OR, USA

<sup>2</sup>Oncology Specialists, S.C., Niles, IL, USA

<sup>3</sup>John Wayne Cancer Institute, Santa Monica, CA, USA

<sup>4</sup>University of Utah, Huntsman Cancer Institute, Salt Lake City, UT, USA

<sup>5</sup>Viralytics, Inc., Sydney, New South Wales, Australia

<sup>6</sup>Viralytics Limited, Newcastle, New South Wales, Australia

#### **Background**

CAVATAK™ is a bio-selected oncolytic and immunotherapeutic strain of coxsackievirus A21 (CVA21). In a phase II study, intratumoral (i.t.) CVA21 injection of advanced melanoma lesions resulted in regression in 28.1% of patients including non-injected lesions, increases in tumor immune-cell infiltration, up-regulation of IFN $\gamma$  response and immune-checkpoint genes, including CD122 which may be a marker for enhanced anti-tumor activity by anti-CTLA-4 blockade. Preclinical models using B16 ICAM confirmed enhanced antitumor effects when CVA21 was combined with anti-CTLA-4 or anti-PD-1. The preliminary data are presented from the open-label, phase Ib MITCI (Melanoma Intra-Tumoral Cavatak and Ipilimumab) in patients (pts) with advanced melanoma.

#### **Methods**

Pts received up to 3 x 10<sup>8</sup> TCID<sub>50</sub> CVA21 i.t. on study days 1, 3, 5, 8 and 22, and then q3w for up to 14 additional i.t. injections. Ipilimumab (3 mg/kg) was administered q3w for 4 doses starting at Day 22. The first response assessment (irRC) occurred on Day 106. The primary endpoint was to assess safety of CVA21 in combination with ipilimumab treatment (tx). Immune monitoring samples were obtained to analyze T cells with regulatory, memory, and effector phenotypes. Biopsies of injected lesions have been obtained in some patients.

#### **Results**

No DLT's have been reported in the 18 patients enrolled. Combination tx has been well-tolerated with only one grade 3 or higher treatment-related AE being ipilimumab-related fatigue. Colitis or other immune related toxicities have been grade 1 or 2. The study met its primary statistical futility endpoint of achieving  $\geq 4$  confirmed objective responses

(CR or PR) in the first 12 pts enrolled. Of the first 11 pts eligible for investigator response assessment, ORR for the ITT population is 57.1% (4/7), with the ORR for ipilimumab-naïve pts being 67% (4/6). The DCR (CR+PR+SD) on the ITT population is currently 86% (6/7). All responses were observed by 3.5 months with complete tumor responses being observed in individual injected and non-injected lesions. One three-fold increase in peripheral blood CD4+ and CD8+ T cells with central and effector memory phenotypes were observed comparing baseline to day 85 in most of the patients analyzed thus far.

#### **Conclusions**

CVA21 + ipilimumab tx of pts with advanced melanoma has been well tolerated. This combination immunotherapy induced anti-tumor activity in local, visceral and non-visceral lesions in a number of patients that have failed previous immunotherapies. Increases in T cell effector and memory subsets were also observed.

#### **Trial Registration**

ClinicalTrial.gov identifier NCT01636882.

141

### **KEYNOTE-177: randomized phase III study of pembrolizumab versus investigator-choice chemotherapy for mismatch repair-deficient or microsatellite instability-high metastatic colorectal carcinoma**

Luis A Diaz, Jr.<sup>1</sup>, Dung T Le<sup>1</sup>, Takayuki Yoshino<sup>2</sup>, Thierry André<sup>3</sup>, Johanna Bendell<sup>4</sup>, Minori Koshiji<sup>5</sup>, Yayan Zhang<sup>5</sup>, S Peter Kang<sup>5</sup>, Bao Lam<sup>5</sup>, Dirk Jäger<sup>6</sup>

<sup>1</sup>Sidney Kimmel Comprehensive Cancer Center at Johns Hopkins University, Baltimore, MD, USA

<sup>2</sup>National Cancer Center Hospital East, Kashiwa-shi, Chiba, Japan

<sup>3</sup>Saint Antoine Hospital, Paris, Ile-de-France, France

<sup>4</sup>Sarah Cannon Research Institute and Department of Medical Oncology, Tennessee Oncology, Nashville, TN, USA

<sup>5</sup>Merck & Co., Inc., Kenilworth, NJ, USA

<sup>6</sup>National Center for Tumor Diseases, Heidelberg, Baden-Wuerttemberg, Germany

#### **Background**

A subset of colorectal carcinomas (CRCs) have deficiencies in the mismatch repair (MMR) system, resulting in microsatellite instability (MSI). MSI-high tumors contain high levels of lymphocyte infiltrates and strong expression of the programmed death 1 (PD-1) immune checkpoint receptor and its ligand, PD-L1. Pembrolizumab is an anti-PD-1 monoclonal antibody that blocks the interaction between PD-1 and its ligands, thereby enabling an antitumor





## Clinical Trials in Progress

Presenting author underlined; Primary author in italics

immune response. In the phase II KEYNOTE-016 study, pembrolizumab showed promising antitumor activity against MMR-deficient tumors in patients with treatment-refractory metastatic CRC, with an objective response rate of 47% (95% CI, 23%-72%). KEYNOTE-177 (ClinicalTrials.gov, NCT02563002) is an international, randomized, open-label phase III study designed to evaluate the efficacy and safety of pembrolizumab compared with standard-of-care chemotherapy as a first-line treatment for MMR-deficient or MSI-high metastatic CRC.

### Methods

Key eligibility criteria include age  $\geq 18$  years, confirmed MSI-high or MMR-deficient stage IV CRC, measurable disease per RECIST v1.1 by local site assessment, Eastern Cooperative Oncology Group performance status 0-1, no active autoimmune disease or brain metastases, and no prior therapy for metastatic disease. Patients are to be randomized 1:1 to receive either pembrolizumab 200 mg every 3 weeks (Q3W) or investigator's choice of standard-of-care chemotherapy. Chemotherapy must be chosen prior to randomization; options include mFOLFOX6 or FOLFIRI alone or in combination with bevacizumab or cetuximab. Treatment is to continue until progressive disease, unacceptable toxicity, patient/investigator decision, or completion of 35 cycles (pembrolizumab only). Response is to be evaluated by CT or MRI every 9 weeks per RECIST v1.1 by central imaging vendor review and per RECIST adapted for immunotherapy response patterns. Eligible patients may continue pembrolizumab beyond initial RECIST-defined progression. Patients in the standard-of-care arm who have progressive disease and meet crossover criteria may be eligible to receive pembrolizumab for up to 17 treatment cycles. Adverse events (AEs) are to be assessed throughout treatment and for 30 days thereafter (90 days for serious AEs) and graded per NCI CTCAE v4.0. Patients are to be followed for survival every 9 weeks. The primary end point is progression-free survival per RECIST v1.1; secondary end points are overall survival, objective response rate per RECIST v1.1, and safety and tolerability. Exploratory end points include duration of response and health-related quality of life. Enrollment in KEYNOTE-177 is ongoing, with 270 patients planned to be enrolled.

### Trial Registration

ClinicalTrials.gov identifier NCT02563002.

142

### Phase Ia/Ib trial investigating the CSF-1R inhibitor LY3022855 in combination with durvalumab (MEDI4736) or tremelimumab in patients with advanced solid malignancies

*Todd M Bauer*<sup>1</sup>, *Judy S Wang*<sup>2</sup>, *Jean K Lee*<sup>3</sup>, *Gulam A Manji*<sup>4</sup>, *Ragini Kudchadkar*<sup>5</sup>, *John S Kauh*<sup>6</sup>, *Shande Tang*<sup>6</sup>, *Naomi Laing*<sup>7</sup>, *Gerald Falchook*<sup>8</sup>

<sup>1</sup>Sarah Cannon Research Institute, Tennessee Oncology, PLLC, Nashville, TN, USA

<sup>2</sup>Sarah Cannon Research Institute, Florida Cancer Specialists, Sarasota, FL, USA

<sup>3</sup>Laura and Isaac Perlmutter Cancer Center at NYU Langone Medical Center, New York, NY, USA

<sup>4</sup>Columbia University Medical Center, New York, NY, USA

<sup>5</sup>Winship Cancer Institute at Emory University, Atlanta, GA, USA

<sup>6</sup>Eli Lilly and Company, Bridgewater, NJ, USA

<sup>7</sup>AstraZeneca Pharmaceuticals, Waltham, MA, USA

<sup>8</sup>Sarah Cannon Research Institute at HealthONE, Denver, CO, USA

### Background

Checkpoint inhibitors of programmed cell death-1 protein (PD-1)/programmed cell death-ligand 1 (PD-L1) and cytotoxic T lymphocyte associated protein 4 (CTLA-4) pathways have demonstrated clinically meaningful improvement in survival for patients with various tumor types. Preclinical data demonstrate significant interplay between innate and adaptive immune systems. Targeting colony-stimulating factor 1 receptor (CSF-1R) may lead to disruption of the immunosuppressive effects of innate immune cells expressing CSF-1R. Treatment with an anti-CSF-1R monoclonal antibody (mAb) induces anti-tumor responses in multiple murine tumor models when combined with CTLA-4 blockade [1], suggesting that combining a checkpoint inhibitor with a CSF-1 pathway inhibitor may potentiate the anti-tumor response. Study I5F-MC-JSCC will evaluate the effects of CSF-1R inhibition using LY3022855 (anti-CSF-1R mAb) in combination with durvalumab (MEDI4736; anti-PD-L1 mAb) or tremelimumab (anti-CTLA-4 mAb) in participants with advanced solid malignancies.

### Methods

JSCC is a phase Ia/Ib open-label, 3+3 dose-escalation (Part A), followed by dose-expansion (Part B) study of LY3022855 in combination with either durvalumab or tremelimumab. Eligible patients have confirmed solid malignancies (regardless of PD-L1 status) and ECOG PS 0-1. Patients must not have received small molecule therapy, chemotherapy, radiation therapy, monoclonal antibody treatment, or

## Clinical Trials in Progress

Presenting author underlined; Primary author in italics

immunosuppressive medication within 14-28 days of start of study treatment, but prior immune checkpoint therapy is permitted. Pretreatment and on-treatment biopsies will be obtained (Part A all patients, Part B ovarian cohort). In the LY3022855+durvalumab regimen, LY3022855 (IV) will be administered at increasing dose levels as tolerated; durvalumab (IV) will be administered at a fixed dose. In the LY3022855+tremelimumab regimen, both LY3022855 and tremelimumab (IV) will be administered at increasing dose levels as tolerated. Once a maximum tolerated dose has been identified for each combination, enrollment to Part B (5 disease-specific expansion cohorts of 20 patients per cohort: LY3022855+durvalumab- non-small cell lung cancer, ovarian, melanoma; LY3022855+tremelimumab- mesothelioma, melanoma) will begin. The primary objective is to characterize the safety and tolerability of each combination in treatment of patients with advanced solid malignancies, as well as define a recommended phase II dose. Secondary objectives include assessment of antitumor activity of each combination, immunogenicity, and pharmacokinetics. Exploratory objectives are to assess immunomodulatory effects of the combinations. Approximately 178 patients are planned.

### Trial Registration

ClinicalTrials.gov identifier NCT02718911.

### References

1. Holmgaard RB, Brachfeld A, Gasmi B, *et al*: **Timing of CSF-1/CSF-1R signaling blockade is critical to improving responses to CTLA-4 based immunotherapy.** *Oncol Immunology* 2016, 5:e1151595.

### 143

#### **Phase III study of carboplatin-paclitaxel/nab-paclitaxel chemotherapy with or without pembrolizumab for first-line metastatic, squamous non-small cell lung carcinoma: KEYNOTE-407**

*Edward B Garon*<sup>1</sup>, Balazs Halmos<sup>2</sup>, Hui Rina<sup>3</sup>, Natasha Leighl<sup>4</sup>, Sung Sook Lee<sup>5</sup>, William Walsh<sup>6</sup>, Konstantin Dragnev<sup>7</sup>, Bilal Piperdi<sup>8</sup>, Luis Paz-Ares Rodriguez<sup>9</sup>, Nabeegha Shinwari<sup>8</sup>, Ziewn Wei<sup>8</sup>

<sup>1</sup>David Geffen School of Medicine at UCLA, Santa Monica, CA, USA

<sup>2</sup>Montefiore Medical Center, White Plains, NY, USA

<sup>3</sup>The Crown Princess Mary Cancer Centre Westmead, Westmead, New South Wales, Australia

<sup>4</sup>Princess Margaret Cancer Centre, Toronto, ON, Canada

<sup>5</sup>Inje University Haeundae Paik Hospital, Busan, Republic of Korea

<sup>6</sup>University of Massachusetts Medical School, Worcester, MA, USA

<sup>7</sup>Dartmouth Hitchcock Medical Center, Lebanon, NH, USA

<sup>8</sup>Merck & Co., Inc., Kenilworth, NJ, USA

<sup>9</sup>Gabinete Radiológico del Dr. Pita, NA, Madrid, Spain

### Background

Chemotherapy with a platinum doublet has traditionally been the standard of care for most patients with treatment-naive non-small cell lung carcinoma (NSCLC). Preliminary data from the phase I/II KEYNOTE-021 (ClinicalTrials.gov, NCT02039674) study suggest manageable toxicity and encouraging efficacy of carboplatin and paclitaxel chemotherapy plus the anti-PD-1 antibody pembrolizumab in treatment-naive NSCLC. KEYNOTE-407 (ClinicalTrials.gov, NCT02775435) is a randomized, double-blind, placebo-controlled phase III study to compare the efficacy and safety of paclitaxel or nab-paclitaxel plus carboplatin with or without pembrolizumab as first-line treatment in advanced squamous NSCLC.

### Methods

Eligible patients are aged  $\geq 18$  years and have stage IV squamous NSCLC, an ECOG PS 0-1, and no prior systemic chemotherapy. Patients with mixed histology (e.g., adenosquamous) are allowed if there is a squamous component in the specimen; small cell histology is excluded. Approximately 560 patients will be randomly assigned (1:1) to pembrolizumab 200 mg every 3 weeks (Q3W) plus carboplatin area under the curve (AUC) 6 Q3W and paclitaxel 200 mg/m<sup>2</sup> Q3W or nab-paclitaxel 100 mg/m<sup>2</sup> day 1, day 8, and day 15 Q3W for 4 cycles followed by pembrolizumab 200 mg Q3W or to the same regimen in which pembrolizumab is replaced by a normal saline placebo. Patients are to be stratified by choice of taxane (paclitaxel vs nab-paclitaxel), PD-L1 status (tumor proportion score [TPS]  $\geq 1\%$  vs  $< 1\%$ ; and geographic region of the enrolling site (East Asia vs non-East Asia) before randomization. Pembrolizumab/placebo will continue for 35 cycles or until disease progression, intolerable toxicity, or investigator or patient decision to withdraw. Patients who received placebo may be able to cross over to pembrolizumab at the time of documented progression. Adverse events (AEs) will be monitored throughout the study and for 30 days (90 days for serious AEs) after treatment completion and graded per NCI CTCAE v4.0. Response will be assessed by RECIST v1.1 by independent central radiologic review at weeks 6, 12, and 18, then every 9 weeks until week 45, and every 12 weeks thereafter. The primary end points are progression-free survival (PFS) by independent radiologic review and overall survival; secondary end points are objective response rate, duration of response, and safety. Exploratory objectives include PFS by PD-L1 TPS status ( $\geq 1\%$  vs  $< 1\%$ ) and choice of taxane (paclitaxel or nab-paclitaxel), patient-reported outcomes (EORTC QLQ-C30 and LC13 and EuroQoL-5D), pharmacokinetics, and biomarkers.



## Clinical Trials in Progress

Presenting author underlined; Primary author in italics

### Trial Registration

ClinicalTrials.gov identifier NCT02775435.

**144**

### **Preliminary manufacturing, safety, and immune monitoring results of an allogeneic tumor lysate-pulsed dendritic cell vaccine for patients with newly diagnosed glioblastoma**

Michael P Gustafson, Mary L Maas, Michael Deeds, Adam Armstrong, Svetlana Bornschlegl, Tim Peterson, Sue Steinmetz, Dennis A Gastineau, Ian F Parney, Allan B Dietz  
Mayo Clinic, Rochester, MN, USA

#### Background

Clinical responses to dendritic cell (DC) vaccines for brain tumors have been demonstrably inconsistent. Several factors, including tumor and treatment related immunosuppression, poor DC maturation, and suboptimal antigen sources, likely contribute to this phenomenon. We report preliminary data from a clinical trial for patients with newly diagnosed glioblastoma (GBM) that combines current standard of care treatment with an autologous DC vaccine using mature DCs pulsed with allogeneic cultured GBM lysates.

#### Methods

Twenty adult patients with resected newly diagnosed GBM who had completed radiation/concurrent temozolomide were enrolled. DCs were manufactured *in vitro* from CD14+ monocytes purified from patient leukapheresis products and cultured to produce highly pure CD83+ mature DCs. The mature autologous DCs were pulsed with allogeneic tumor lysates with defined tumor-associated antigen expression. Patients received temozolomide plus intradermal injections of the vaccine (10-20  $\times 10^6$  DCs) for up to 6 cycles followed by vaccine alone for up to 6 cycles. In some cases, patients received injections using a novel intradermal delivery device (3M human microstructured transdermal system).

#### Results

Allogeneic cultured GBM lysate pulsed DCs were manufactured successfully to produce 15 doses of at least  $10 \times 10^6$  DCs/injection in 100% (19/19) of patients to date. Vaccines were manufactured consistently as DCs collectively averaged 91.4% CD83+ and 98.1% CD80-positive for these maturation markers. Patients on trial have received a median of 8 injections and three patients have received all 15 doses. Of the toxicities potentially related to the vaccine, only grade 1 and 2 toxicities (fever, rash, fatigue) have been observed. Mean follow-up to date is 0.98 years (range 0.19 – 1.77 years); 15/20 patients are still alive. In the first 8 patients, median survival has not been reached with median follow-up 1.56 years. To assess immune responses to the vaccine, patients were monitored for over 120 immunophenotypes

and circulating tumor antigen specific T cells by flow cytometry with up to 8 longitudinal samples for some patients.

#### Conclusions

The combination of adjuvant temozolomide with an autologous mature DC pulsed with allogeneic tumor lysate vaccine was shown to be safe, feasible, and able to produce tumor antigen-specific immune responses in newly diagnosed GBM patients. This successful strategy is well suited for continuing into later stage clinical trials.

#### Acknowledgements

This study is funded in part by the Ben and Catherine Ivy Foundation.

#### Trial Registration

ClinicalTrials.gov identifier NCT01957956.

**145**

### **AIM2CERV: a randomized phase III study of adjuvant AXAL immunotherapy following chemoradiation in patients who have high-risk locally advanced cervical cancer (HRLACC)**

Thomas Herzog<sup>1</sup>, Floor J Backes<sup>2</sup>, Larry Copeland<sup>3</sup>, Maria Del Pilar Estevez Diz<sup>4</sup>, Thomas W Hare<sup>5</sup>, Warner Huh<sup>6</sup>, Byoung-Gie Kim<sup>7</sup>, Kathleen M Moore<sup>8</sup>, Ana Oaknin<sup>9</sup>, William Small<sup>10</sup>, Krishnansu S Tewari<sup>11</sup>, Bradley J Monk<sup>12</sup>

<sup>1</sup>University of Cincinnati, Cincinnati, OH, USA

<sup>3</sup>James Cancer Hospital, The Ohio State University, Columbus, OH, USA

<sup>4</sup>Instituto do Câncer do Estado de São Paulo - Faculdade de Medicina da Universidade de São Paulo, São Paulo, Brazil

<sup>5</sup>Advaxis Immunotherapies, Princeton, NJ, USA

<sup>6</sup>University of Alabama at Birmingham, Department of Obstetrics & Gynecology, Birmingham, AL, USA

<sup>7</sup>Samsung Medical Center, Sungkyunkwan University School of Medicine, Seoul, Republic of Korea

<sup>8</sup>Stephenson Oklahoma Cancer Center, Oklahoma City, OK, USA

<sup>9</sup>Vall d'Hebron University Hospital, Vall d'Hebron Institute of Oncology (VHIO), Barcelona, Spain

<sup>10</sup>Loyola University, Maywood, IL, USA

<sup>11</sup>University of California, Irvine Medical Center, Orange, CA, USA

<sup>12</sup>University of Arizona Cancer Center-Phoenix Creighton University School of Medicine at Dignity Health St. Joseph's Hospital and Medical Center, Phoenix, AZ, USA

#### Background

Patients with HRLACC experience a 50% chance of disease recurrence/death following cisplatin-based chemoradiation (CCRT) plus brachytherapy, and represent a group with

## Clinical Trials in Progress

Presenting author underlined; Primary author in italics

a significant unmet need for new treatments. Persistent infection with oncogenic strains of human papillomavirus (HPV) is the most common cause of CC, and provides rationale for therapeutic targeting of HPV. Axalimogene filolisbac (AXAL/ADXS11-001) is an irreversibly attenuated *Listeria monocytogenes*-listeriolysin O immunotherapy that secretes a HPV E7 fusion protein that induces HPV-specific cytotoxic T cell generation and reduces immune tolerance in the tumor microenvironment. Previous studies demonstrated AXAL was well tolerated and associated with objective tumor response and survival benefits in patients with recurrent/metastatic CC. AXAL has received FDA Fast Track Designation for the treatment of HRLACC.

### Methods

This double-blind, placebo-controlled, multinational, multicenter randomized phase III trial is being conducted under a Special Protocol Assessment agreement with the FDA. The study will evaluate adjuvant AXAL in patients with HRLACC, defined as histologically confirmed squamous cell, adenocarcinoma, or adenosquamous carcinoma of the cervix and  $\geq 1$  of the following: 1) FIGO stage IB2, IIA2, IIB with biopsy-proven pelvic nodes, or  $\geq 2$  positive nodes by MRI/CT  $\geq 1.5$ -cm diameter, or  $\geq 2$  positive pelvic nodes by PET; 2) all FIGO stage IIIA, IIIB, IVA; 3) any FIGO stage with para-aortic lymph node metastases criteria, defined by biopsy-proven para-aortic node(s), or  $\geq 1$  positive para-aortic node(s) by MRI/CT  $> 1.5$ -cm shortest dimension, or  $\geq 1$  positive para-aortic node(s) by PET with SUV  $> 2.5$ . Eligible patients must be disease free per RECIST 1.1 following completion of CCRT with curative intent and aged  $\geq 18$  with GOG performance status 0–1. Patients will be randomized 2:1 to AXAL ( $1 \times 10^9$  colony-forming units) or placebo and receive a 60-minute infusion of treatment every 3 weeks for 3 doses (weeks 1, 4, and 7) for the first 3 months (Induction Phase). Thereafter, patients will receive treatment every 8 weeks for 5 doses or until disease recurrence (Maintenance Phase); patients will receive a 7-day course of oral antibiotics/placebo 72 hours after completion of each treatment in both phases. Primary objective is to compare disease-free survival (DFS) of AXAL with placebo; secondary objectives are safety and overall survival (OS). Exploratory objectives will determine if there is an association between HPV subtypes and DFS/OS, and patient-reported outcomes. The design provides 85% power for a sample size of 450 to demonstrate a reduction in the hazard of recurrence by 38%.

### Trial Registration

ClinicalTrials.gov identifier NCT02853604.

146

### KEYNOTE-057: phase II study of pembrolizumab in patients with *Bacillus Calmette Guérin* (BCG)–unresponsive, high-risk non–muscle-invasive bladder cancer (NMIBC)

Ashish M Kamat<sup>1</sup>, Joaquim Bellmunt<sup>2</sup>, Toni K Choueiri<sup>3</sup>, Kijoeng Nam<sup>4</sup>, Maria De Santis<sup>5</sup>, Robert Dreicer<sup>6</sup>, Noah M Hahn<sup>7</sup>, Rodolfo Perini<sup>4</sup>, Arlene Siefker-Radtke<sup>1</sup>, Guru Sonpavde<sup>8</sup>, Ronald de Wit<sup>9</sup>, J. Alfred Witjes<sup>10</sup>, Stephen Keefe<sup>4</sup>, Dean Bajorin<sup>11</sup>

<sup>1</sup>University of Texas MD Anderson Cancer Center, Houston, TX, USA

<sup>2</sup>Dana-Farber Cancer Institute, Harvard Medical School, Boston, MA, USA

<sup>3</sup>Dana-Farber Cancer Institute/Brigham and Women's Hospital, Boston, MA, USA

<sup>4</sup>Merck & Co., Inc., Kenilworth, NJ, USA

<sup>5</sup>University of Warwick, Coventry, England, UK

<sup>6</sup>University of Virginia School of Medicine, Charlottesville, VA, USA

<sup>7</sup>Sidney Kimmel Comprehensive Cancer Center at Johns Hopkins University, Baltimore, MD, USA

<sup>8</sup>University of Alabama at Birmingham Comprehensive Cancer Center, Birmingham, AL, USA

<sup>9</sup>Erasmus MC Cancer Institute, Rotterdam, Netherlands

<sup>10</sup>University Radboud, Nijmegen, Netherlands

<sup>11</sup>Memorial Sloan Kettering Cancer Center, New York, NY, USA

### Background

A large percentage of patients with NMIBC experience disease recurrence/progression after standard-of-care therapy with transurethral resection of bladder tumor (TURBT) and intravesical BCG instillation. The programmed death-1/programmed death ligand 1 (PD-1/PD-L1) pathway is frequently altered in cancer, leading to inhibition of active T cell-mediated immune surveillance of tumors. PD-L1 is widely expressed in urothelial tumors, providing a therapeutic rationale for targeting this pathway in NMIBC. KEYNOTE-057 is an open-label, phase II study designed to evaluate the efficacy and safety of the anti-PD-1 antibody pembrolizumab in patients with high-risk, BCG-unresponsive NMIBC.

### Methods

Eligibility criteria include age  $\geq 18$  years, histologically confirmed diagnosis of high-risk, BCG-unresponsive NMIBC (high-grade Ta, T1, and/or carcinoma *in situ* [CIS] despite adequate BCG treatment), ineligible for or declined radical cystectomy, and ECOG performance status 0–2. Eligible patients must have undergone  $\geq 2$  cystoscopic procedures with the most recent  $\leq 8$  weeks before study start, including complete TURBT (tissue sample must be available). Patients



## Clinical Trials in Progress

Presenting author underlined; *Primary author in italics*

will receive pembrolizumab 200 mg every 3 weeks for 24 months or until disease recurrence, progression, or unacceptable toxicity. Patients will be placed into cohorts based on presence (cohort A) or absence (cohort B) of CIS as determined by tissue pathology at screening. Response will be assessed using cystoscopy and urine cytology every 12 weeks for the first 2 years, every 24 weeks for the next 2 years, and every 52 weeks thereafter. CT imaging will be used to assess for metastatic or nodal disease. At 18 months, patients with no evidence of disease may discontinue treatment. Low-grade Ta recurrence will not be considered treatment failure; these patients may undergo repeat TURBT and remain on treatment. Adverse events (AEs) will be monitored throughout the study and for 30 days after end of treatment (90 days for serious AEs and events of clinical interest) and graded per Common Terminology Criteria for Adverse Events, version 4.0. Primary end points are complete response (cohort A) and disease-free survival (cohort B); secondary end points include progression-free survival, overall survival, duration of response, and the relationship between PD-L1 expression and response to treatment. Enrollment will continue until approximately 260 patients have enrolled.

### Trial Registration

ClinicalTrials.gov identifier NCT02625961.

**147**

### **KEYNOTE-013: an open-label, multicohort phase Ib trial of pembrolizumab in patients with advanced hematologic malignancies**

Justin Kline<sup>1</sup>, Philippe Armand<sup>2</sup>, John Kuruvilla<sup>3</sup>, Craig Moskowitz<sup>4</sup>, Mehdi Hamadani<sup>5</sup>, Vincent Ribrag<sup>6</sup>, Pier Luigi Zinzani<sup>7</sup>, Sabine Chlosta<sup>8</sup>, Seth Thompson<sup>8</sup>, Arun Balakumaran<sup>8</sup>, Nancy Bartlett<sup>9</sup>

<sup>1</sup>Committee on Immunology and Department of Medicine, University of Chicago, Chicago, IL, USA

<sup>2</sup>Dana-Farber Cancer Institute, Boston, MA, USA

<sup>3</sup>Princess Margaret Cancer Centre and University of Toronto, Toronto, ON, Canada

<sup>4</sup>Memorial Sloan Kettering Cancer Center, New York, NY, USA

<sup>5</sup>Medical College of Wisconsin, Milwaukee, WI, USA

<sup>6</sup>Institut Gustave Roussy, Villejuif, Ile-de-France, France

<sup>7</sup>Institute of Hematology "L. e A. Seràgnoli," Università di Bologna, Bologna, Emilia-Romagna, Italy

<sup>8</sup>Merck & Co., Inc., Kenilworth, NJ, USA

<sup>9</sup>Washington University School of Medicine in St. Louis, St Louis, MO, USA

### Background

Pembrolizumab, a humanized monoclonal antibody that blocks interaction between PD-1 and its ligands, has

demonstrated robust antitumor activity and a manageable toxicity profile in advanced solid tumors. KEYNOTE-013 is a multicenter, open-label, multicohort phase Ib trial designed to assess the safety and efficacy of single-agent pembrolizumab in patients with hematologic malignancies. The KEYNOTE-013 trial design has been updated to include a cohort evaluating combination therapy of pembrolizumab and lenalidomide in patients with relapsed/refractory (R/R) diffuse large B cell lymphoma (DLBCL) who have failed, are ineligible for, or refused stem cell transplantation (SCT). Combination therapy of pembrolizumab, lenalidomide, and dexamethasone in R/R multiple myeloma (MM) in KEYNOTE-023 has demonstrated synergistic efficacy and manageable toxicity [1].

### Methods

Cohorts include patients with: (1) intermediate 1, intermediate 2, or high-risk myelodysplastic syndrome (MDS) that failed  $\geq 4$  cycles of prior treatment with a hypomethylating agent; (2) R/R MM that failed  $\geq 2$  lines of prior therapy, including a proteasome inhibitor and IMiD; (3) R/R nodular sclerosing or mixed cellularity Hodgkin lymphoma (HL) (cohort 3); (4) R/R non-Hodgkin lymphoma (NHL) who failed, were ineligible for, or refused SCT, including: (4a) R/R primary mediastinal large B cell lymphoma (PMBCL), (4b) any other R/R PD-L1–positive NHL, (4c) R/R follicular lymphoma (FL), (4d) R/R DLBCL; and (5) R/R DLBCL. Key eligibility criteria for all cohorts are age  $\geq 18$  years, ECOG performance status 0/1, measurable disease, and adequate hematologic, renal, and hepatic function. Patients in cohorts 1-4 enrolled under amendments 1-3 will be treated with pembrolizumab intravenously (IV) 10 mg/kg every 2 weeks; those enrolled under amendments 4-6 will be treated with pembrolizumab IV 200 mg every 3 weeks (Q3W) because of updated program-wide PK/PD information. Patients enrolled in cohort 5 will be treated with pembrolizumab IV 200 mg Q3W in combination with lenalidomide taken orally once daily for 21 days of each 28-day cycle. Treatment will continue until disease progression, intolerable toxicity, or up to 35 doses of pembrolizumab ( $\sim 2$  years). The primary end points are objective response rate and safety. Secondary objectives include duration of response, progression-free survival, overall survival, and association between PD-L1 expression and response. Enrollment is open for MM (cohort 2), PMBCL (cohort 4a), and FL (cohort 4c), evaluating single-agent pembrolizumab; and for DLBCL (cohort 5), evaluating pembrolizumab in combination with lenalidomide. Approximately 222 patients will be enrolled.

### Trial Registration

ClinicalTrials.gov identifier NCT01953692.

### References

1. Mateos MV, et al: *J Clin Oncol* 2016, **34**[suppl]:Abstr 8010.

## Clinical Trials in Progress

Presenting author underlined; Primary author in italics

148

### **Trials in progress: a phase II study of in situ therapeutic vaccination against refractory solid cancers with intratumoral poly-ICLC**

Chrisann Kyj<sup>1</sup>, Rachel Sabado<sup>1</sup>, Yvonne Saenger<sup>2</sup>, Loging William<sup>3</sup>, Michael Joseph Donovan<sup>3</sup>, Erlinda Sacris<sup>1</sup>, John Mandeli<sup>3</sup>, Andres M. Salazar<sup>4</sup>, Philip Friedlander<sup>1</sup>, *Nina Bhardwaj*<sup>1</sup>

<sup>1</sup>Tish Cancer Institute, Icahn School of Medicine at Mount Sinai, New York, NY, USA

<sup>2</sup>Hematology and Oncology Division, Columbia University Medical Center, New York, NY, USA

<sup>3</sup>Icahn School of Medicine at Mount Sinai, New York, NY, USA

<sup>4</sup>Oncovir, Inc., Washington, DC, USA

#### **Background**

Poly-ICLC, a double-stranded RNA complex, can directly activate dendritic cells and trigger NK cells to kill tumor cells. It can be given intramuscularly (IM) to induce systemic inflammation and intratumorally (IT) to induce immune infiltration of tumors.

#### **Methods**

In this phase II study, eligible subjects are head and neck, skin (melanoma and non-melanoma), and sarcoma patients with recurrent or metastatic disease who have failed prior systemic therapy. In each treatment cycle, one accessible tumor site was targeted for IT injection of 1 mg of Poly-ICLC 3 times a week for 2 weeks followed by IM boosters biweekly for 6 weeks and then a 2 week rest period. This 10-week cycle was repeated in cycle 2, followed by a 6 week no-treatment period. Tumor biopsies were performed at baseline, week 3, and week 26. Pre- and post-vaccination tumors were evaluated by quantitative multiplex immunohistochemistry (IHC) and RNA sequencing. Blood samples were collected at baseline and prior to each cycle for immune response evaluations.

#### **Results**

A phase I pilot portion of this study showed 1 patient who achieved clinical benefit with stable disease (progression-free survival of 6 months). Poly-ICLC was well tolerated with principal side effects of fatigue and inflammation at injection site (< grade 2). One case of grade 3 tumor necrosis was observed. In the patient with clinical benefit, IHC analysis of tumor showed increased CD4(60x), CD8(10x), PD-1(20x) and PD-L1(3x) compared to patients with progressive disease whose tumor biopsies showed unchanged/decreased CD4, CD8, PD-1, and PD-L1 levels over treatment period. Furthermore, RNASeq analysis of the same patient's tumor and peripheral blood mononuclear cells (PBMC) showed dramatic changes such as upregulation of interferon-

stimulated genes, chemokines, and genes associated with T cell activation and antigen presentation indicative of local and systemic immune activation in response to Poly-ICLC treatment.

#### **Conclusions**

Preliminary findings show that Poly-ICLC is well tolerated in advanced solid cancer patients, and generates local immune response in tumor microenvironment and systemic immune response as evident in the patient achieving clinical benefit. These results warrant further investigation, and are currently being explored in this ongoing larger multicenter adaptive phase II clinical trial.

#### **Trial Registration**

ClinicalTrials.gov identifier NCT01984892.

#### **References**

1. Martins KA, Bavari S, *et al*: **Vaccine adjuvant uses of poly-IC and derivatives**. *Expert Rev Vaccines* 2015, **14**:447-459.
2. Salazar A, Erlich R, *et al*: **Therapeutic in situ autovaccination against solid cancers with intratumoral poly-iclc: case report, hypothesis, and clinical trial**. *Cancer Immunol Res* 2014, **2(8)**:720-724.

149

### **Phase I/Ib multicenter trial of CPI-444, an adenosine A2a receptor (A2aR) antagonist as a single agent and in combination with atezolizumab (atezo) in patients with advanced solid tumors**

John Powderly<sup>1</sup>, Joshua Brody<sup>2</sup>, John Nemunaitis<sup>3</sup>, Leisha Emens<sup>4</sup>, Jason J Luke<sup>5</sup>, Amita Patnaik<sup>6</sup>, Ian McCaffery<sup>7</sup>, Richard Miller<sup>7</sup>, *Ginna Laport*<sup>7</sup>

<sup>1</sup>Carolina BioOncology Institute, PLLC, Huntersville, NC, USA

<sup>2</sup>Icahn School of Medicine at Mount Sinai, New York, NY, USA

<sup>3</sup>Mary Crowley Cancer Research Centers, Texas Oncology, P.A., Gradalis, Inc., Medical City Dallas Hospital, Baylor University Medical Center, Dallas, TX, USA

<sup>4</sup>Johns Hopkins University School of Medicine, Baltimore, MD, USA

<sup>5</sup>University of Chicago School of Medicine, Chicago, IL, USA

<sup>6</sup>South Texas Accelerated Research Therapeutics, LLC, San Antonio, TX, USA

<sup>7</sup>Corvus Pharmaceuticals, Burlingame, CA, USA

#### **Background**

Adenosine is elevated within the tumor microenvironment and signaling through the A2aR is immunosuppressive. CPI-444 is an oral, selective A2aR antagonist that inhibits A2aR and demonstrates antitumor efficacy in mouse models alone and combined with PD-1/PD-L1 blockade. CPI-444 was well-tolerated in previous clinical trials in the non-oncology



## Clinical Trials in Progress

*Presenting author underlined; Primary author in italics*

setting. This is the first report of adenosine blockade in cancer patients (pts).

### Methods

This phase I/Ib, open label clinical trial uses a two-step adaptive design to study CPI-444 alone and combined with atezo in pts with selected advanced cancers. The objectives are to evaluate safety and efficacy and to optimize dose/schedule. Eligible pts have failed standard therapies with histologies: non-small cell lung (NSCLC), melanoma (MEL), triple-negative breast (TNBC), renal (RCC), prostate, head and neck (H&N), colorectal (CRC) or bladder cancers. In step 1 of the trial, pts are randomized to one of 4 cohorts (12 pts/cohort) including 3 single-agent cohorts or combined with atezo. Step 2 contains multiple disease-specific expansion cohorts to evaluate CPI-444 alone and combined with atezo.

### Results

Step 1 has enrolled 19 pts to date, median age 67 years (range, 36-84); three pts each with NSCLC, TNBC, RCC and CRC, 2 pts each with MEL, prostate and bladder cancer and one pt with H&N. Median number of prior regimens was 3 (range, 1-5). Seven pts received prior anti PD-1/PD-L1 therapy; 4 pts were resistant and 3 were refractory. Twelve pts remain on study (range 1- 17 weeks) and 7 have discontinued due to disease progression. Of 8 pts evaluable for response at 2 months, 3 had stable disease (2 received CPI-444 alone); 11 pts have not reached the first response assessment timepoint. A prostate cancer pt in the combination cohort remains on treatment for >4 months with minimal regression of nodal disease and a transient decrease in serum PSA. A TNBC pt on CPI-444 alone showed 15% reduction in tumor burden. No grade 3 or 4 adverse events or DLTs related to CPI-444 alone or in combination with atezo were observed. Dose-dependent inhibition of A2aR signaling was demonstrated in peripheral blood mononuclear cells using a CREB phosphorylation assay. Evidence of immune activation was observed in some pts treated with CPI-444 alone as reflected by an increase in circulating activated PD-1+/CD8+ T cells.

### Conclusions

Early data demonstrate that CPI-444 is well-tolerated alone and combined with atezo and demonstrates preliminary evidence of immune activation and clinical activity. Enrollment is ongoing.

### Trial Registration

ClinicalTrials.gov identifier NCT02655822.

## 150

### **SEA-CD40 is a CD40 agonist with early evidence of pharmacodynamic and antitumor activity: preliminary results from a phase I study in advanced solid malignancies**

Andrew L Covel<sup>1</sup>, David C Smith<sup>2</sup>, Juneko E Grilley-Olson<sup>3</sup>, Thomas F Gajewski<sup>4</sup>, Sanjay Goel<sup>5</sup>, Shyra J Gardai<sup>6</sup>, Che-Leung Law<sup>6</sup>, Gary Means<sup>6</sup>, Thomas Manley<sup>6</sup>, Brendan Curti<sup>7</sup>

<sup>1</sup>Seattle Cancer Care Alliance, University of Washington, Seattle, WA, USA

<sup>2</sup>University of Michigan, Ann Arbor, MI, USA

<sup>3</sup>University of North Carolina Lineberger Comprehensive Cancer Center, University of North Carolina Chapel Hill, Chapel Hill, NC, USA

<sup>4</sup>University of Chicago Medical Center, Chicago, IL, USA

<sup>5</sup>Montefiore Medical Center, Bronx, NY, USA

<sup>6</sup>Seattle Genetics, Inc., Bothell, WA, USA

<sup>7</sup>Earle A. Chiles Research Institute, Providence Cancer Center, Portland, OR, USA

### Background

SEA-CD40 is a non-fucosylated, humanized IgG1 monoclonal antibody which binds CD40, an immune-activating TNF receptor. Binding to CD40 on antigen-presenting cells (APCs) and enhanced crosslinking via FcγRIIIa stimulates pro-inflammatory cytokine production and induction of immune co-stimulatory receptors, leading to T cell activation and antitumor activity. Further, when CD40 is expressed on malignant cells, SEA-CD40 induces antibody-dependent cellular cytotoxicity through enhanced NK cell binding.

### Methods

This ongoing phase I dose-escalation study evaluates the safety, tolerability, pharmacodynamic biomarkers, and antitumor activity of SEA-CD40 in adult patients with advanced metastatic solid tumors (relapsed, refractory, or progressive disease after ≥1 prior systemic therapy). Antitumor activity is assessed after every 4 cycles of treatment by immune-related response criteria and RECIST v1.1.

### Results

To date, 22 patients (median age 59 years; range, 28–76) with solid tumors have received a median of 2.5 cycles (range, 1–16) of SEA-CD40, 0.6–60 mcg/kg IV q3wk. Two dose-limiting toxicities occurred at 60 mcg/kg (1 G3 and 1 G4 infusion-related reaction [IRR]). AEs were primarily infusion-related toxicities. Treatment-emergent AEs in ≥25% of patients were: chills (77%), nausea (55%), fatigue (45%), vomiting (41%), dyspnea and headache (32% each), and flushing and lymphopenia (27% each). Changes in pharmacodynamic biomarkers consistent with CD40



## Clinical Trials in Progress

*Presenting author underlined; Primary author in italics*

and CD16 engagement were observed, including: dose-proportional increases in inflammatory cytokine levels; B cell depletion with partial recovery by next cycle; reduction in T regulatory cells; transient margination of monocytes and NK cells with recovery by Day 8; and upregulation of MHC class II on APCs. In 18 efficacy-evaluable patients, 4 had SD and 1 had PR by RECIST (28% disease control rate [DCR]). Two patients had durable SD (gastroesophageal junction tumor, 10 mcg/kg, PD after 12 cycles; mesothelioma, 10 mcg/kg, PD after 8 cycles). The patient with PR achieved PR after Cycle 4 (basal cell carcinoma, 60 mcg/kg, PD following Cycle 8). Four patients remain on treatment.

### Conclusions

SEA-CD40 is a biologically and clinically potent molecule in heavily pre-treated patients with advanced solid tumors. Strategies to manage IRRs are being evaluated. Cytokine elevations correlate with preclinical models and the proposed mechanism of action through CD40 activation on APCs. Pharmacodynamic data and evidence of clinical activity (28% DCR), along with preclinical evidence for synergy when SEA-CD40 is combined with checkpoint inhibitors [1], presents a compelling opportunity to enhance immunotherapy for cancer.

### Trial Registration

ClinicalTrials.gov identifier NCT02376699.

### References

1. Gardai SJ, *et al*: **A sugar-engineered non-fucosylated anti-CD40 antibody, SEA-CD40, with enhanced immune-stimulatory activity alone and in combination with immune checkpoint inhibitors.** *J Clin Oncol* 2015, **33(15Suppl)**:3074.

### 151

#### **A randomized phase II study of epigenetic therapy with azacitidine and entinostat with concurrent nivolumab versus nivolumab alone in recurrent metastatic non-small cell lung cancer**

*Kristen A Marrone*<sup>1</sup>, Gary Rosner<sup>2</sup>, Valsamo Anagnostou<sup>1</sup>, Joanne Riemer<sup>1</sup>, Jessica Wakefield<sup>1</sup>, Cynthia Zanhov<sup>1</sup>, Stephen Baylin<sup>1</sup>, Barbara Gitlitz<sup>3</sup>, Julie Brahmer<sup>1</sup>

<sup>1</sup>Sidney Kimmel Comprehensive Cancer Center at Johns Hopkins University, Baltimore, MD, USA

<sup>2</sup>School of Medicine Oncology Biostatistics, Baltimore, MD, USA

<sup>3</sup>Keck School of Medicine of USC, Los Angeles, CA, USA

### Background

While survival results with immune checkpoint blockade in the second-line treatment setting of non-small cell lung cancer (NSCLC) are impressive, many patients' cancer progresses or becomes resistant to these therapies.

Combinatorial approaches are being investigated to improve response and outcomes with these agents. Epigenetic therapy has been found to be effective component of cancer treatment. Hypermethylation of DNA promoter regions by DNA methyltransferases (DNMT) and histone deacetylation by histone deacetylases (HDAC) represent two of these critical epigenetic mechanisms of tumor-specific gene silencing. Interestingly, 5 of 5 patients treated with combination epigenetic therapy followed by PD-1/PD-L1 therapy achieved long-term clinical benefit at our institution while on clinical trial. Preclinical studies have also shown that combined HDAC/DNMT inhibition can induce susceptibility to immune checkpoint therapy and inhibit tumor growth [1].

### Methods

This is a multi-institution, open-label, randomized phase II study of azacitidine and entinostat with concurrent nivolumab compared to nivolumab alone in patients with recurrent, metastatic NSCLC. Patients with metastatic NSCLC who have received 1-2 prior therapies and are Eastern Cooperative Group (ECOG) performance status (PS) 0-1 are stratified by histology and randomized to receive azacitidine (40 mg/m<sup>2</sup> subcutaneous (SQ) days 1-5, 8-10), entinostat (4 mg orally days 3 and 10) and nivolumab (3 mg/kg intravenous (IV) days 1 and 15) for 6 28-day cycles, followed by nivolumab (3 mg/kg IV days 1 and 15) alone [Arm D] or nivolumab (3 mg/kg IV days 1 and 15) on a 28-day cycle alone [Arm C] until disease progression (Figure 1). Statistics: The primary endpoint of this trial is the percentage of patients progression-free at 24 weeks. Using planned study enrollment of 60 patients on each Arm (n=120) and using the exact Mantel-Haenszel test for analysis, this will provide 90% power to detect an odds ratio of 3 for combination therapy over single-agent nivolumab with respect to being progression-free at 24 weeks. Secondary endpoints include objective response rate, progression-free survival, time to progression, overall survival and safety and tolerability. Correlative Study: All patients are required to have pre- and post- treatment biopsies; Arm D patients will also have biopsies while on combination therapy. Plasma and peripheral blood mononuclear cells will also be drawn for analysis.

### Trial Registration

ClinicalTrials.gov identifier NCT01928576.

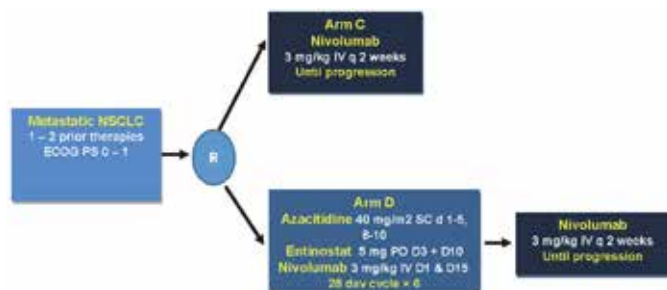
### References

1. Cameron EE, Bachman KE, Myohanen S: **Synergy of demethylation and histone deacetylase inhibition in the re-expression of genes silenced in cancer.** *Nat Genet* 1999, **21**:103-107.

## Clinical Trials in Progress

Presenting author underlined; Primary author in italics

**Figure 1: Study Schema**



152

### **KEYNOTE-427: phase II study of pembrolizumab in patients with locally advanced/metastatic renal cell carcinoma (mRCC)**

David F McDermott<sup>1</sup>, Sabina Signoretti<sup>1</sup>, Wenting Li<sup>2</sup>, Charles Schloss<sup>2</sup>

<sup>1</sup>Beth Israel Deaconess Medical Center, Boston, MA, USA

<sup>2</sup>Merck & Co., Inc., Kenilworth, NJ, USA

#### **Background**

Targeting the programmed death 1 (PD-1) pathway has been found to be effective in patients with previously treated, advanced or clear cell mRCC. Pembrolizumab is an anti-PD-1 antibody that blocks the interaction between PD-1 and its ligands, enabling an increased antitumor immune response. Most patients with mRCC progress within 1 year following the initiation of standard first-line treatment with antiangiogenic therapy, highlighting the need for therapies that provide more durable benefit in mRCC.

#### **Methods**

KEYNOTE-427 (ClinicalTrials.gov, NCT02853344) is a phase II, open-label study designed to evaluate the efficacy and safety of pembrolizumab monotherapy as a first-line treatment for advanced, recurrent or metastatic clear cell or non-clear cell mRCC. Target enrollment in KEYNOTE-427 is 105 patients in a clear cell cohort (cohort A) and 150 patients in a non-clear cell cohort (cohort B). Key eligibility criteria include locally advanced, metastatic or recurrent disease, measurable disease per RECIST v1.1 assessed by blinded independent central review (BICR), no prior systemic therapy for advanced RCC, provision of a tumor tissue sample for biomarker analysis, and Karnofsky performance status  $\geq 70\%$ . Patients are to receive pembrolizumab intravenously 200 mg once every 3 weeks until progressive disease, the occurrence of unacceptable adverse events (AEs), or for up to 35 doses in patients without progressive disease. Patients who stop pembrolizumab after 35 doses without progressive disease or who stop treatment after a complete response will be allowed treatment with an additional 17

doses of pembrolizumab upon progression. Response will be assessed per RECIST v1.1 by BICR using CT and/or MRI. Bone scans will be performed at baseline and throughout the study for patients with a positive bone scan at baseline. AEs will be graded per National Cancer Institute Common Terminology Criteria for Adverse Events, version 4.0. The primary objective is estimation of the objective response rate in each cohort per RECIST v1.1. An interim analysis for response rate will be performed for the non-clear cell RCC cohort when the 30th patient in this cohort has completed the third scan. Secondary objectives include estimation of duration of response, disease control rate, progression-free/overall survival, and safety and tolerability of pembrolizumab treatment by cohort.

#### **Trial Registration**

ClinicalTrials.gov identifier NCT02853344.

153

### **KEYNOTE-170: phase II study of pembrolizumab in patients with relapsed/refractory primary mediastinal large B cell lymphoma (rrPMBCL) or relapsed or refractory Richter syndrome (rrRS)**

Jean-Marie Michot<sup>1</sup>, Philippe Armand<sup>2</sup>, Wei Ding<sup>3</sup>, Vincent Ribrag<sup>1</sup>, Beth Christian<sup>4</sup>, Arun Balakumaran<sup>5</sup>, Patricia Marinello<sup>5</sup>, Sabine Chlosta<sup>5</sup>, Yayan Zhang<sup>5</sup>, Margaret Shipp<sup>2</sup>, Pier Luigi Zinzani<sup>6</sup>

<sup>1</sup>Institut Gustave Roussy, Villejuif, Ile-de-France, France

<sup>2</sup>Dana-Farber Cancer Institute, Boston, MA, USA

<sup>3</sup>Mayo Clinic, Rochester, MN, USA

<sup>4</sup>The Ohio State University, Columbus, OH, USA

<sup>5</sup>Merck & Co., Inc., Kenilworth, NJ, USA

<sup>6</sup>Institute of Hematology "L. e A. Seràgnoli," Università di Bologna, Bologna, Emilia-Romagna, Italy

#### **Background**

The 9p24.1 locus is frequently amplified in rrPMBCL, leading to overexpression of the PD-L1 and PD-L2 immune checkpoint ligands and providing a potential mechanism of immune evasion. Pembrolizumab is an anti-PD-1 monoclonal antibody that blocks the interaction between PD-1 and PD-L1 and PD-L2, thereby enabling an antitumor immune response. In the multicohort, phase Ib KEYNOTE-013 study, pembrolizumab was associated with a tolerable safety profile and promising antitumor activity (overall response rate [ORR] of 38% 6/16) in patients with rrPMBCL. In the phase II MC1485 study, pembrolizumab demonstrated promising preliminary efficacy (ORR, 43% [3/7]) in patients with rrRS. The multicenter, phase II KEYNOTE-170 study was designed to further evaluate the safety and efficacy of pembrolizumab in patients with rrPMBCL or rrRS.

## Clinical Trials in Progress

*Presenting author underlined; Primary author in italics*

### Methods

Eligible patients must be at least 18 years of age and fit into 1 or 2 profiles: (1) diagnosis of rrPMBCL according to World Health Organization 2008 criteria, failed to achieve a complete response (CR) or relapsed after autologous stem cell transplantation (auto-SCT), or are ineligible for auto-SCT and have failed to respond or relapsed after  $\geq 2$  lines of prior treatment; or (2) pathologic diagnosis per local institutional review of rrRS that transformed from underlying chronic lymphocytic leukemia (CLL), received at  $\geq 1$  prior therapy for rrRS, and have relapsed or refractory disease. Patients are to receive pembrolizumab 200 mg intravenously every 3 weeks for until disease progression, unacceptable toxicity, or 35 cycles of treatment. In patients with rrRS, additional standard therapies to treat the underlying CLL may be added according to the physician's discretion. Eligible patients who attain a CR as determined by the independent central imaging vendor may stop trial treatment and may be eligible for retreatment upon disease progression. Response is to be assessed every 12 weeks by independent central imaging vendor review based on International Working Group (IWG) response criteria. Adverse events (AEs) are to be assessed throughout treatment and for 30 days thereafter (90 days for serious AEs) and graded per NCI CTCAE v4.0. Patients will be followed for survival every 12 weeks. The primary end point is ORR by independent central imaging vendor review according to IWG response criteria or IWG response criteria with special considerations for rrRS; secondary end points include progression-free survival, overall survival, and safety and tolerability. Enrollment is ongoing and will continue until approximately 106 patients are enrolled.

### Trial Registration

ClinicalTrials.gov identifier NCT02576990.

**154**

### **Dose-seeking and efficacy study of anti-PD-1 therapy with pembrolizumab (P) combined with BRAF inhibitor (BRAFi) therapy with vemurafenib (V) for therapy of advanced melanoma**

*Yana G Najjar*<sup>1</sup>, Lin<sup>1</sup>, Lisa H. Butterfield<sup>1</sup>, Ahmad A. Tarhini<sup>1</sup>, Diwakar Davar<sup>1</sup>, Hassane Zarour<sup>1</sup>, Elizabeth Rush<sup>1</sup>, Cindy Sander<sup>1</sup>, John M Kirkwood<sup>2</sup>

<sup>1</sup>University of Pittsburgh Cancer Institute, Pittsburgh, PA, USA

<sup>2</sup>University of Pittsburgh Cancer Institute, UPMC Cancer Center, Pittsburgh, PA, USA

### Background

BRAF inhibitors induce antitumor responses in >50% of patients (pts) with BRAF V600E/K mutant metastatic melanoma, but some patients do not respond and most responders have only partial responses, the median duration

of which is 7-9 months. BRAFi markedly increase tumor infiltrating lymphocytes (TIL), although markers of T cell exhaustion and PD-L1 are increased. We hypothesize that BRAFi will drive TIL into the tumor parenchyma, and that by blocking PD-1/PD-L1 disinhibitory signals, pembrolizumab may improve the function and durability of TILs.

### Methods

This study is an investigator-initiated phase I/II dose-seeking and efficacy trial of P and V for pts with unresectable/metastatic BRAF mutant melanoma. Primary objectives are to determine safety and maximum tolerated dose (MTD) of V combined with P in this population, and to assess ORR with the combination, in comparison to historical benchmarks. Secondary objectives are to evaluate PFS and OS. Exploratory objectives are to assess whether the combination favorably modulates the tumor microenvironment and decreases T cell exhaustion in sequential biopsies of tumor and blood samples. We aim to accrue up to 50 patients to this study. Using the modified toxicity probability interval (mTPI) will allow efficient identification of the MTD; we expect at least 30 patients to be enrolled at the recommended phase II dose. Pts will receive P 200 mg q3 wks, and V 480 mg, 720 mg, or 960 mg BID, per mTPI. Treatment with both V & P will start on day 1. The DLT monitoring period is 3 wks. Pts will have CT scans at baseline and wk 9, then q12 wks. For pts with biopsiable disease, biopsies at baseline and wk 3 are mandatory. Blood for correlative studies will be drawn at baseline, wk 3, wk 9 and progression. Pts will be treated until DLT or PD for up to 2 years.

### Results

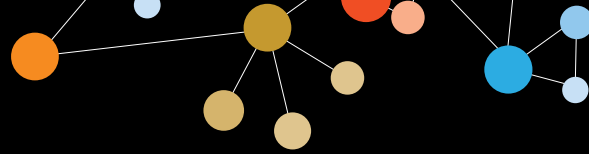
One patient has been started on therapy and is in wk 2 of the 3 wk DLT monitoring period, with no significant toxicities thus far.

### Conclusions

We anticipate that treatment with pembrolizumab and vemurafenib will be safe and well tolerated. In addition to the primary efficacy endpoint of ORR and secondary endpoints of PFS and OS, this study includes extensive immune correlative analyses, including analysis of PD-1/PD-L1 and levels of Treg, MDSC, and inhibitory cytokines in the tumor parenchyma and peripheral blood. One patient on trial thus far is tolerating treatment well, with no significant toxicities to date.

### Trial Registration

ClinicalTrials.gov identifier NCT02818023.



## Clinical Trials in Progress

Presenting author underlined; Primary author in italics

155

### **CX-1158-101: a first-in-human phase I study of a small molecule inhibitor of arginase (CB-1158) as monotherapy and in combination with an anti-PD-1 checkpoint inhibitor in patients with solid tumors**

Siqing Fu<sup>1</sup>, Todd Bauer<sup>2</sup>, Chris Molineaux<sup>3</sup>, Mark K Bennett<sup>3</sup>, Keith W Orford<sup>3</sup>, Kyriakos P Papadopoulos<sup>4</sup>

<sup>1</sup>Department of Investigational Cancer Therapeutics, The University of Texas MD Anderson Cancer Center, Houston, TX, USA

<sup>2</sup>Sarah Cannon Research Institute, Nashville, TN, USA

<sup>3</sup>Calithera Biosciences, South San Francisco, CA, USA

<sup>4</sup>South Texas Accelerated Research Therapeutics, San Antonio, TX, USA

#### **Background**

T cells and natural killer (NK) cells require L-arginine for proliferation and activation. Arginine depletion by arginase in the tumor microenvironment induces immunosuppression and is associated with tumor immune evasion, advanced disease stage and poor outcomes. Arginase is secreted by granulocytic myeloid-derived suppressor cells (G-MDSCs) and its pharmacological inhibition is expected to restore arginine levels and relieve immunosuppression. CB-1158 is a potent, selective, and orally-bioavailable small molecule inhibitor of arginase (IC<sub>50</sub>=98 nM). CB-1158 reverses G-MDSC-mediated immunosuppression by blocking arginine depletion in an *ex vivo* human model. T cells activated in the presence of G-MDSC-conditioned media demonstrate reduced proliferation and suppressed production of Th1 cytokines; this effect is reversed by the addition of CB-1158. *In vivo*, twice daily dosing of CB-1158 causes dose-dependent increases in plasma and tumor arginine levels and is associated with single agent anti-tumor efficacy in multiple syngeneic models. CB-1158 also enhances the antitumor efficacy of checkpoint inhibitors.

#### **Methods**

CX-1158-101 is a phase I first-in-human study of CB-1158 in patients with solid tumors. The primary objective is to evaluate the safety and tolerability of CB-1158, as monotherapy and in combination with nivolumab. Secondary objectives include selection of the recommended phase II dose (RP2D), determination of CB-1158 pharmacokinetics and evaluation the anti-tumor effect, for monotherapy and nivolumab combination. Exploratory objectives include an evaluation of pharmacodynamic biomarkers, including plasma arginine, plasma arginase activity, and effects on immune function in the peripheral blood and tumor biopsies. In Part 1a, safety/tolerability of escalating doses of CB-1158 will be evaluated in patients with solid tumors of any

type. In Part 2, three expansion cohorts will open at the monotherapy RP2D. These cohorts include non-small cell lung cancer (NSCLC, Cohort A), colorectal cancer (CRC, Cohort B), and Cohort C, which will include patients with squamous cell carcinoma of the head and neck (SCCHN), renal cell cancer (RCC), gastric or gastroesophageal junction (GEJ) cancer, urothelial cell cancer (UCC), and/or melanoma. Upon demonstration of sufficient PK and/or PD effect of CB-1158 in Part 1a, dose escalation of CB-1158 in combination with full dose nivolumab will open in Part 1b. The dose escalation will enroll patients with NSCLC, RCC, and melanoma. In Part 3, two expansion cohorts will enroll patients to the combination of CB-1158 and nivolumab at the RP2D. These cohorts will enroll NSCLC and melanoma patients that have received prior anti-PD-1/PD-L1 therapy and had progressive disease or prolonged (>24 weeks) stable disease.

### 156 Abstract Travel Award Recipient

#### **A first-in-human, first-in-class phase I trial of the anti-CD47 antibody Hu5F9-G4 in patients with advanced cancers**

Sukhmani K Padda<sup>1</sup>, Sumit A Shah<sup>1</sup>, A Dimitrios Colevas<sup>1</sup>, Sujata Narayanan<sup>1</sup>, George A Fisher<sup>1</sup>, Dana Supan<sup>1</sup>, Heather A Wakelee<sup>1</sup>, Rhonda Aoki<sup>1</sup>, Mark D Pegram<sup>1</sup>, Victor M Villalobos<sup>2</sup>, Jie Liu<sup>3</sup>, Chris H Takimoto<sup>4</sup>, Mark Chao<sup>4</sup>, Jens-Peter Volkmer<sup>5</sup>, Ravindra Majeti<sup>6</sup>, Irving L Weissman<sup>3</sup>, Branimir I Sikic<sup>1</sup>

<sup>1</sup>Stanford University School of Medicine, Stanford, CA, USA

<sup>2</sup>University of Colorado Anschutz Medical Campus, Aurora, CO, USA

<sup>3</sup>Institute for Stem Cell Biology and Regenerative Medicine and Forty Seven, Inc., Palo Alto, CA, USA

<sup>4</sup>Institute for Stem Cell Biology and Regenerative Medicine, Forty Seven, Inc., Stanford University School of Medicine, Palo Alto, CA, USA

<sup>5</sup>Forty Seven, Inc., Menlo Park, CA, USA

<sup>6</sup>Institute for Stem Cell Biology and Regenerative Medicine; Stanford University School of Medicine, Stanford, CA, USA

#### **Background**

Hu5F9-G4 is a humanized monoclonal antibody that targets CD47, blocking its anti-phagocytic “don’t eat me” signal through macrophage receptor SIRPα, leading to tumor phagocytosis. CD47 is overexpressed on human cancers and also on red blood cells (RBCs). In primate toxicology studies, Hu5F9-G4 caused a transient anemia that was improved with a single lower priming dose allowing higher maintenance doses.

#### **Methods**

Relapsed/refractory solid tumors and lymphomas were included. This dose escalation study included: Part A, to



## Clinical Trials in Progress

Presenting author underlined; Primary author in italics

determine the priming dose and Part B, to determine the maintenance dose. The maximum tolerated dose (MTD) in part A was used for the single priming dose in part B (Hu5F9-G4 dosed weekly). The primary objective is to determine safety and secondary objectives are to determine PK and PD. Preliminary data reported from data cutoff of July 22, 2016.

### Results

21 patients have enrolled. Part A included 0.1 (N=1), 0.3 (N=2), 1 (N=6), and 3 mg/kg (N=2). There were 2 dose-limiting toxicities (DLTs) in Part A at the 3 mg/kg dose: grade (G) 3 abdominal pain and G3 hemagglutination (H) (protocol-specific scale of 1+ H on peripheral blood smear (PBS) and G2 headache). 1 mg/kg was selected as the priming dose, with no >G2 anemia and almost 100% RBC receptor occupancy. Treatment-related adverse events (TRAE) in Part A included: anemia (3 G1, 3 G2), hyperbilirubinemia (3 G1, 2 G2; unconjugated), headache (6 G1, 1 G2), H on PBS (8 G1), and nausea (3 G1). Part B included 3 (N=4), 10 (N=3), and 20 mg/kg (N=3, ongoing). There have been no DLTs in 3 patients on 10 mg/kg (last fully evaluable cohort). Most toxicity was associated with the single priming dose and reversible. TRAE in Part B at 3 mg/kg included: anemia (2 G1, 2 G2), hyperbilirubinemia (1 G1, 1 G3; unconjugated), headache (3 G1), H on PBS (1 G1), retinal toxicity (G2 protocol-specific scale, asymptomatic). TRAE at 10 mg/kg included: anemia (3 G1), headache (2 G1), and nausea (1 G1). Target trough levels associated with preclinical activity are being achieved at the 10 mg/kg dose, and half-life increases with repeated dosing. Two patients with adenoid cystic carcinoma in Part A had stable disease for 16 and 8 months.

### Conclusions

Hu5F9-G4 is well tolerated at 10 mg/kg weekly, with 1 mg/kg priming dose. Part B maintenance dose 20 mg/kg enrolling.

### Acknowledgements

Stanford Clinical and Translational Research Unit; California Institute for Regenerative Medicine; Forty Seven, Inc.

### Trial Registration

ClinicalTrials.gov identifier NCT02216409.

## 157

### A pilot/phase II study evaluating pembrolizumab plus standard-of-care chemotherapy in metastatic triple-negative breast cancer, with companion comprehensive immunological monitoring

David Page<sup>1</sup>, Wendy Yu<sup>2</sup>, Alison Conlin<sup>3</sup>, Janet Ruzich<sup>4</sup>, Stacy Lewis<sup>5</sup>, Anupama Acheson<sup>6</sup>, Kathleen Kemmer<sup>7</sup>, Kelly Perlewitz<sup>8</sup>, Nicole M Moxon<sup>3</sup>, Staci Mellinger<sup>3</sup>, Carlo Bifulco<sup>9</sup>, Maritza Martel<sup>3</sup>, Yoshinobu Koguchi<sup>10</sup>, Bernard Fox<sup>9</sup>, Walter Urba<sup>10</sup>, Heather McArthur<sup>11</sup>

<sup>1</sup>Earle A. Chiles Research Institute, Providence Portland Medical Center, Portland, OR, USA

<sup>2</sup>Providence St. Vincent Medical Center, Portland, OR, USA

<sup>3</sup>Providence Portland Medical Center, Portland, OR, USA

<sup>4</sup>Providence Medical Group, Clackamas, OR, USA

<sup>5</sup>Providence Medical Group, Portland, OR, USA

<sup>6</sup>Providence Cancer Center, Portland, OR, USA

<sup>7</sup>Oregon Health & Science University, Portland, OR, USA

<sup>8</sup>Providence Medical Group, Newberg, OR, USA

<sup>9</sup>Robert W. Franz Cancer Research Center, Earle A. Chiles Research Institute, Providence Cancer Center, Portland, Oregon, USA

<sup>10</sup>Earle A. Chiles Research Institute, Providence Cancer Center, Portland, OR, USA

<sup>11</sup>Memorial Sloan Kettering Cancer Center, New York, NY, USA

### Background

While sustained cytotoxic chemotherapy may be associated with lymphopenia and immunosuppression, chemotherapy may also facilitate antigen release/presentation, adaptive expression of PD-L1, and relative depletion of suppressive immune cell populations. Metastatic triple-negative breast cancer (MTNBC) is an aggressive and incurable disease associated with high mutational load and tumor-infiltrating lymphocytes, and is treated conventionally with sequential, sustained cytotoxic chemotherapy. In heavily pre-treated patients, anti-PD-1/L1 monotherapy yielded modest response rates of 9-19% [1]. However, we hypothesize that up-front treatment with 1<sup>st</sup>/2<sup>nd</sup> line chemotherapy plus anti-PD-1/L1 might minimize immunosuppression (by treating patients before they are exposed to prolonged chemotherapy) and maximize immunostimulation (by treating less chemo-resistant disease and maximizing antigen release). In a preliminary cohort, anti-PD-L1 plus chemotherapy (nab-paclitaxel) was safe, with favorable response rates compared to historical controls [2].

### Methods

In a pilot/phase II investigator-initiated trial, we will evaluate the safety and tolerability of anti-PD-1 (pembrolizumab 200mg IV every three weeks) plus investigator-selected





## Clinical Trials in Progress

Presenting author underlined; Primary author in italics

1<sup>st</sup>/2<sup>nd</sup> line standard-of-care chemotherapy with either weekly paclitaxel (80mg/m<sup>2</sup> IV) or oral capecitabine (2,000mg twice daily, weekly 1 on/1 off). Secondly, we will evaluate efficacy of each combination employing a Simon 2-stage design, as measured by week 12 radiographic response. Because chemotherapy-associated immunosuppression could potentially influence immunotherapy efficacy, we will serially characterize general immune status and T cell activation using a validated real-time multi-parametric flow cytometry platform and peripheral blood T cell receptor sequencing (to measure clonal repertoire diversity). Via a companion biospecimen protocol, these data will be compared with data from MTBNC subjects receiving paclitaxel or capecitabine alone. Furthermore, baseline and post-treatment tumor-infiltrating lymphocytes will be characterized using multi-spectral immunofluorescence (using a validated panel including CD3, CD8, CD163, FOXP3, PD-L1, DAPI, and CK) and T cell receptor sequencing.

### Results

As of 8/7/2016, five subjects have been registered for enrollment.

### Conclusions

This investigator-initiated trial will provide important data, evaluating the efficacy of commonly used chemotherapies (paclitaxel or capecitabine) plus anti-PD-1, as well as evaluating the effect of these regimens on general immune status, peripheral T cell activation, and tumor infiltrating lymphocytes. A registrational MTBNC trial of nab-paclitaxel +/- anti-PD-L1 is ongoing.

### Trial Registration

ClinicalTrials.gov identifier NCT02734290.

### References

1. Emens LA, Kok M, Ojalvo LS: **Targeting the programmed cell death-1 pathway in breast and ovarian cancer.** *Curr Opin Obstet Gynecol* 2016, **28**:142-147.
2. Adams S, Diamond J, Hamilton E, *et al*: **Phase Ib trial of atezolizumab in combination with nab-paclitaxel in patients with metastatic triple-negative breast cancer (mTNBC).** *ASCO Annual Meeting* 2016.

158

### T cell therapy for patients with advanced ovarian cancer: a pilot study in progress

Magnus Pedersen<sup>1</sup>, Marie Christine Wulff Westergaard<sup>1</sup>, Troels Holz Borch<sup>1</sup>, Morten Nielsen<sup>1</sup>, Per Kongsted<sup>1</sup>, Trine Juhler-Nøttrup<sup>2</sup>, Marco Donia<sup>1</sup>, Inge Marie Svane<sup>1</sup>

<sup>1</sup>Department of Oncology, Center for Cancer Immune Therapy, Herlev University Hospital, Herlev, Hovedstaden, Denmark

<sup>2</sup>Department of Oncology, Herlev Hospital, Herlev, Hovedstaden, Denmark

### Background

Adoptive cell therapy (ACT) with tumor infiltrating lymphocytes (TILs) is based on infusion of activated and expanded cells isolated from autologous tumor tissue. The treatment has shown a clinical effect in approximately 50% of malignant melanoma patients with 20% obtaining a complete response [1]. Recent studies suggest that TIL based ACT can potentially be used with success in other cancers, including ovarian cancer (OC). OC is the 5<sup>th</sup> leading cause of cancer death among women. If inoperable, the treatment is a combination of chemotherapy. Recurrent disease has a poor prognosis. The primary aim of this study is to assess feasibility and tolerability of T cell therapy for OC. Secondly, to describe objective response using RECIST 1.1 and clarify if the treatment can induce measurable immune responses against tumor cells. This trial is presented at the European Society of Medical Oncology (ESMO) 2016 conference. In this abstract an update on clinical responses is provided.

### Methods

Six patients will be included. Patients with progressive/recurrent OC and histologically verified serous adenocarcinoma are potential candidates. Surgical removal of tumor tissue for T cell expansion is performed. Stem cells are harvested for potential use if patients are having difficulties recovering from lymphodepleting chemotherapy. The treatment consists of lymphodepleting chemotherapy (60 mg/kg cyclophosphamide for 2 days, 25 mg/m<sup>2</sup> fludarabine for 5 days) followed by T cell administration and high-dose decrescendo interleukin-2 for up to 5 days. Patients are evaluated for up to 5 years/until progression.

### Results

Five patients have received treatment. The first had a partial metabolic response, stable disease (SD) with nearly 20% tumor regression and >50% reduction in CA-125 at 6 weeks, but progressive disease (PD) at 12 weeks. The second had SD at 6 weeks with a small decrease in CA-125, but PD at 12 weeks. The third had SD at 6 weeks with a 25% drop in CA-125, but PD at 12 weeks. The fourth had SD at 6 weeks with stable CA-125 and awaits 12 weeks evaluation. The fifth patient has not been evaluated yet. Only expected and manageable toxicities have been observed. All patients recovered without stem cell support. Immune analyses are pending.

### Conclusions

So far, T cell therapy for patients with advanced OC seems to be manageable and tolerable.

## Clinical Trials in Progress

Presenting author underlined; Primary author in italics

### Trial Registration

ClinicalTrials.gov identifier NCT02482090.

### References

1. Rosenberg SA, Yang JC, Sherry RM, *et al*: **Durable complete responses in heavily pretreated patients with metastatic melanoma using T-cell transfer immunotherapy.** *Clin Cancer Res* 2011, **17(13)**:4550-4557.

### 159

#### **Updated safety, efficacy, and pharmacokinetics (PK) results from the phase I study of BGB-A317, an anti-programmed death-1 (PD-1) mAb in patients with advanced solid tumors**

Jayesh Desai<sup>1</sup>, Ben Markman<sup>2</sup>, Shahneen Sandhu<sup>3</sup>, Hui Gan<sup>4</sup>, Michael L Friedlander<sup>5</sup>, Ben Tran<sup>6</sup>, Tarek Meniawy<sup>7</sup>, Joanne Lundy<sup>2</sup>, Duncan Colyer<sup>3</sup>, Malaka Ameratunga<sup>8</sup>, Christie Norris<sup>9</sup>, Jason Yang<sup>10</sup>, Kang Li<sup>10</sup>, Lai Wang<sup>10</sup>, Lusong Luo<sup>10</sup>, Zhen Qin<sup>10</sup>, Song Mu<sup>11</sup>, Xuemei Tan<sup>10</sup>, James Song<sup>11</sup>, Michael Millward<sup>7</sup>

<sup>1</sup>Royal Melbourne Hospital and Peter MacCallum Cancer Centre, Melbourne, Victoria, Australia

<sup>2</sup>Monash Cancer Center, East Bentleigh, Victoria, Australia

<sup>3</sup>Peter MacCallum Cancer Center, Melbourne, Victoria, Australia

<sup>4</sup>Austin Hospital, Melbourne, Victoria, Australia

<sup>5</sup>Prince of Wales Hospital, Sydney, New South Wales, Australia

<sup>6</sup>Royal Melbourne Hospital, Melbourne, Victoria, Australia

<sup>7</sup>Linear Clinical Research, Sir Charles Gairdner Hospital, Nedlands, Western Australia, Australia

<sup>8</sup>Austin Health and Olivia Newton-John Cancer Research Institute, Melbourne, Victoria, Australia

<sup>9</sup>The Prince of Wales Hospital, Randwick, New South Wales, Australia

<sup>10</sup>BeiGene (Beijing) Co., Ltd, Beijing, People's Republic of China

<sup>11</sup>BeiGene (US) Co. Ltd., Fort Lee, NJ, USA

### Background

BGB-A317 is a humanized IgG4 anti-PD-1 mAb with high specificity and affinity ( $K_D=0.15$  nM) for PD-1. It blocks PD-L1 and PD-L2 binding and inhibits PD-1-mediated negative signaling in T cell lines and tumor growth in a number of allogeneic xenograft models.

### Methods

A phase I, multicenter study was conducted to evaluate the safety, tolerability, PK and antitumor activity of BGB-A317 in patients with advanced solid tumors. A 3+3 dose escalation design was undertaken. Patients received escalating doses of BGB-A317 intravenously at 0.5, 2, 5 and 10 mg/kg once every

two weeks (Q2W). Additional patients were treated at 2 and 5 mg/kg once every three weeks (Q3W).

### Results

As of 27 July 2016, 103 patients were treated across 4 dose-escalating cohorts of BGB-A317 Q2W (0.5 mg/kg, n=3; 2 mg/kg, n=6; 5 mg/kg, n=6 and 10 mg/kg, n=7) and 4 dose-expansion cohorts (2 mg/kg, Q2W, n=20; 2 mg/kg, Q3W, n=21; 5 mg/kg Q2W, n=20 and 5 mg/kg, Q3W, n=20). One DLT (1/6) of grade 3 colitis was observed in the 5 mg/kg Q2W dose-escalating cohort. Maximum tolerated dose was not reached. Recommended phase II dose is 5 mg/kg Q3W. The most common treatment-emergent adverse events (AEs) were grade (G) 1-2 fatigue (42%), nausea (30%), diarrhea (25%), abdominal pain (22%) and constipation (21%). Treatment-related G3 AEs included fatigue (n=2), hypotension (n=2), back pain (n=1), colitis (n=1), diabetes mellitus (n=1), diabetic ketoacidosis (n=1), dyspnea (n=1), elevated ALT (n=1), hyperglycaemia (n=1), hypoxia (n=1) and pneumonitis (n=1). Population PK analysis was conducted using 411 observed BGB-A317 serum concentrations from 31 patients who received doses of 0.5, 2, 5 and 10 mg/kg Q2W and 13 patients who received doses of 2 and 5 mg/kg Q3W. BGB-A317 PK is linear and the terminal elimination half-life is 16 days. Patients' body weight is not a significant covariate on the clearance of A317. Among 99 evaluable patients, preliminary evidence of anti-tumor activities included 16 patients have partial responses (5 to be confirmed) and 20 patients exhibit stable disease. 13 responding patients remain on treatment, ranging from 18 to 38 weeks.

### Conclusions

BGB-A317 demonstrates a favorable safety profile with AEs in keeping with the class effect. Early promising anti-tumor activity has been observed. BGB-A317 PK is linear and systemic clearance is not affected by body weight, which supports fixed dosing. The expanded phase IB study in selected cancer types is ongoing.

### Trial Registration

ClinicalTrials.gov identifier NCT02407990.

## Clinical Trials in Progress

Presenting author underlined; Primary author in italics

### Time to Response and Duration of Response

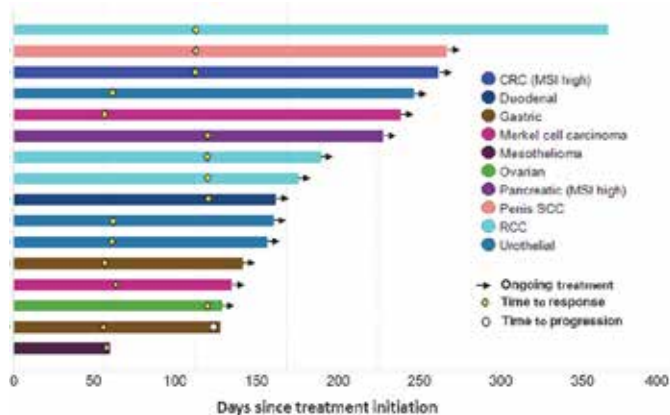


Figure 1. Sixteen patients demonstrated partial response (confirmed and unconfirmed), including 3 PRs in 5 urothelial carcinoma patients, 3 PRs in 9 RCC patients, 2 PRs in 4 gastric cancer patients, 2 PRs in 2 Merkel cell carcinoma patients, 1 PR in 1 colorectal cancer (CRC) patient with microsatellite instability high (MSI-h) status, among 12 CRC patients, 1 PR in 1 pancreatic cancer patient with MSI-h status, between 2 pancreatic cancer patients, 1 PR in 1 penis squamous cell carcinoma patient, 1 PR in 1 duodenal carcinoma patient, 1 PR in 22 ovarian cancer patients, and 1 PR in 7 mesothelioma patients.

160

### Preliminary safety data from a randomized multicenter phase Ib/II study of neoadjuvant chemoradiation therapy (CRT) alone or in combination with pembrolizumab in patients with resectable or borderline resectable pancreatic cancer

Matthew H G Katz<sup>1</sup>, Todd W Bauer<sup>2</sup>, Gauri R Varadhachary<sup>3</sup>, Nicolas Acquavella<sup>4</sup>, Nipun Merchant<sup>4</sup>, Gina Petroni<sup>5</sup>, Craig L Slingluff Jr.<sup>6</sup>, Osama E Rahma<sup>7</sup>

<sup>1</sup>Department of Surgical Oncology, Division of Surgery, The University of Texas MD Anderson Cancer Center, Houston, TX, USA

<sup>2</sup>Department of Surgery, University of Virginia, Charlottesville, VA, USA

<sup>3</sup>Department of Gastrointestinal (GI) Medical Oncology, Division of Cancer Medicine, The University of Texas MD Anderson Cancer Center, Houston, TX, USA

<sup>4</sup>Sylvester Comprehensive Cancer Center, University of Miami, Miami, FL, USA

<sup>5</sup>University of Virginia, Charlottesville, VA, USA

<sup>6</sup>Division of Surgical Oncology, University of Virginia, Charlottesville, VA, USA

<sup>7</sup>Dana-Farber Cancer Institute, Harvard University, Boston, MA, USA

### Background

Tumor-infiltrating lymphocytes (TILs) do not reach the pancreatic cancer (PC) cells in significant numbers due to the presence of stroma and a suppressive microenvironment [1]. Neoadjuvant chemoradiation (CRT) can increase the presence of TILs in the PC microenvironment (PCME) [2]. We tested the combination of CRT and pembrolizumab for the first time in patients with pancreatic cancer in the neoadjuvant setting.

### Methods

Patients with resectable or borderline resectable pancreatic cancer are randomized 2:1 to receive pembrolizumab intravenously every 3 weeks during concurrent CRT with capecitabine (825 mg/m<sup>2</sup> orally twice daily, 5 days/week, on days of radiation only) and radiation (50.4 Gy in 28 fractions over 28 days) or Arm B to receive only concurrent CRT with capecitabine.

### Results

As of July 5, 2016 a total of 13 patients have been enrolled on the study (9 on Arm A and 4 on Arm B). Six patients had resectable disease (4 on arm A and 2 on arm B) while 7 patients had borderline resectable disease (5 on Arm A and 2 on arm B). Post-neoadjuvant therapy, 2 patients were determined to have unresectable disease (both on arm B) and 4 patients underwent surgery (2 on each arm). Seven patients remain on neoadjuvant treatment. All grade toxicities related to treatment are summarized in Table 1. There were five grade 3 toxicities reported in Arm A: 2 patients had diarrhea attributed to CRT and resolved after holding the treatment; 2 patients had lymphopenia attributed to pembrolizumab or the combination; and one patient had elevated alkaline phosphatase related to the combination that met the definition of DLT and resolved after holding the treatment and receiving steroids. There was only one grade 3 toxicity reported on Arm B: lymphopenia attributed to CRT. There were no surgical complications reported within 30 days post-surgery in all patients who underwent surgery.

### Conclusions

The study safety stopping boundaries have not been met and the study will continue enrolling patients.

### Trial Registration

ClinicalTrials.gov identifier NCT02305186.

### References

1. Kunk PR, Bauer TW, Slingluff CL, Rahma OE: **From bench to bedside a comprehensive review of pancreatic cancer immunotherapy.** *J Immunother Cancer* 2016, **15**:4-14.
2. Homma Y1, Taniguchi K, Murakami T, Nakagawa K, Nakazawa M, Matsuyama R, *et al*: **Immunological impact of neoadjuvant chemoradiotherapy in patients with borderline resectable pancreatic ductal adenocarcinoma.** *Ann Surg Oncol* 2014, **21**(2):670-676.

Clinical Trials in Progress

Presenting author underlined; Primary author in italics

Table 1. Maximum Grade Toxicities Related to Treatment

Table with columns for adverse events and toxicity grades (N=11, N=10, N=10, N=10, Total). Rows include events like anemia, neutropenia, thrombocytopenia, etc.

161

KEYNOTE-426: randomized phase III study of pembrolizumab in combination with axitinib versus sunitinib monotherapy in treatment-naive advanced/metastatic renal cell carcinoma (mRCC)

Brian I Rini<sup>1</sup>, Thomas Powles<sup>2</sup>, Mei Chen<sup>3</sup>, Yang Song<sup>3</sup>, Markus Puhlmann<sup>3</sup>, Michael B Atkins<sup>4</sup>

- 1Cleveland Clinic Taussig Cancer Institute, Cleveland, OH, USA
2Barts Cancer Institute, Queen Mary University of London, London, England, UK
3Merck & Co., Inc., Kenilworth, NJ, USA
4Georgetown-Lombardi Comprehensive Cancer Center, Washington DC, USA

Background

Standard first-line treatments for mRCC include antiangiogenic agents sunitinib, pazopanib, and bevacizumab plus interferon, which yield a median progression-free survival (PFS) of approximately 10-11 months and median survival of 23-29 months. 5-year survival in mRCC remains low. Pembrolizumab, a programmed death 1 immune checkpoint inhibitor, has been tested in combination with axitinib, a vascular endothelial growth factor receptor inhibitor, in patients with treatment-naive mRCC. This combination has demonstrated manageable toxicity and promising clinical efficacy. The combination of pembrolizumab plus axitinib is being further tested for efficacy and safety in this open-label randomized phase III study, KEYNOTE-426 (ClinicalTrials.gov, NCT02853331), versus sunitinib monotherapy in patients with treatment-naive mRCC.

Methods

Key eligibility criteria include age >=18 years, treatment-naive advanced/metastatic renal cell carcinoma with clear cell histology, measurable disease per RECIST v1.1, adequate organ function, and Karnofsky performance status >=70%. Patients will be stratified per International Metastatic RCC Database Consortium risk category and geographic region, and then randomly assigned 1:1 to receive pembrolizumab 200 mg once every 3 weeks plus axitinib 5 mg twice daily or sunitinib 50 mg once daily for 4 weeks, then 2 weeks off. Treatment will continue until progressive disease, unacceptable adverse events, death, or withdrawal of consent. The primary end points are PFS per RECIST v1.1, as assessed by blinded independent central review, and overall survival. Secondary end points include objective response rate, duration of response, disease control rate, safety, and patient-reported outcomes. Approximately 840 patients will be enrolled globally.

Trial Registration

ClinicalTrials.gov identifier NCT02853331.

162

Translational studies identify ICOS agonist antibody JTX-2011 as a novel immunotherapy option for HNSCC patients

Sriram Sathyanaryanan<sup>1</sup>, Heather A Hirsch<sup>1</sup>, Jenny Shu<sup>1</sup>, Amit Deshpande<sup>1</sup>, Arun Khattri<sup>2</sup>, Jason Reeves<sup>1</sup>, Tong Zi<sup>1</sup>, Ryan Brisson<sup>2</sup>, Christopher Harvey<sup>1</sup>, Jennifer Michaelson<sup>1</sup>, Debbie Law<sup>1</sup>, Tanguy Seiwert<sup>3</sup>

- 1Jounce Therapeutics, Cambridge, MA, USA
2University of Chicago School of Medicine, Chicago, IL, USA
3University of Chicago, Chicago, IL, USA

Background

ICOS (Inducible CO-Stimulator molecule) is a co-stimulatory molecule expressed primarily on T lymphocytes. Clinical data identified ICOS as a potentially key molecule in providing optimal anti-tumor benefit following anti-CTLA-4 therapy. JTX-2011 is an ICOS agonist antibody that will be entering early phase clinical development for the treatment of advanced solid tumors. JTX-2011 has a dual mechanism of action whereby it amplifies an immune response in T effector (Teff) cells while preferentially reducing the number of T regulatory cells (Treg).

Methods

An mRNA based gene-expression signature for ICOS expression and an IHC assay for ICOS and for T cell markers were developed. ICOS expression on intra-tumoral T cells and PD-L1 were analyzed in a cohort of 126 HNSCC patients collected at University of Chicago and in RNA sequencing data collected from The Cancer Genome Atlas (TCGA). ICOS





## Clinical Trials in Progress

*Presenting author underlined; Primary author in italics*

expression was correlated with other immune signatures associated with response or resistance to anti-PD-1 therapy.

### Results

Preclinical studies show that tumor models with the highest levels of intra-tumoral ICOS are most responsive to treatment with an ICOS agonist antibody. We hypothesize that tumors expressing high levels of ICOS would be expected to benefit from JTX-2011 treatment, we analyzed ICOS mRNA expression in ~10000 solid tumors across 30 indications. Highest levels of ICOS mRNA were observed in HPV+ and HPV- HNSCC. Flow cytometry showed highest expression of ICOS on intra-tumoral CD4+ Tregs, followed by CD4+ Teff and CD8+ T cells. We confirmed these results in a large set of clinical samples using a multiplex immunofluorescence (IF) assay. A wide range of ICOS cell density was observed in this dataset suggesting that identification of an ICOS “high” group may enrich for patients most likely to benefit from anti-ICOS targeted therapy. We further correlated ICOS expression to expression of PD-L1, a marker associated with response to anti-PD-1 therapy. Using IHC and gene-expression analyses, we identified a subset of patients that is less likely to respond to PD-1 therapy and more likely to respond to ICOS agonist therapy. In preclinical studies, treatment with anti-PD-1 therapy increased ICOS expression, suggesting that administration of JTX-2011 together with PD-1 blockade may provide an effective combination strategy.

### Conclusions

These results support development of JTX-2011 in HNSCC patients expressing high levels of ICOS and suggest that combination of JTX-2011 with an anti-PD-1 agent may be an effective treatment paradigm.

163

### **KEYNOTE-183: randomized, open-label, phase III study of pembrolizumab in combination with pomalidomide and low-dose dexamethasone in patients with refractory or relapsed/refractory multiple myeloma**

*Jatin Shah*<sup>1</sup>, Maria Victoria Mateos<sup>2</sup>, Morio Matsumoto<sup>3</sup>, Hilary Blacklock<sup>4</sup>, Albert Oriol Rocafiguera<sup>5</sup>, Hartmut Goldschmidt<sup>6</sup>, Shinsuke Iida<sup>7</sup>, Dina Ben Yehuda<sup>8</sup>, Enrique Ocio<sup>2</sup>, Paula Rodríguez-Otero<sup>9</sup>, Sundar Jagannath<sup>10</sup>, Sagar Lonial<sup>11</sup>, Uma Kher<sup>12</sup>, Patricia Marinello<sup>12</sup>, Jesus San-Miguel<sup>9</sup>

<sup>1</sup>University of Texas MD Anderson Cancer Center, Houston, TX, USA

<sup>2</sup>Complejo Asistencial Universitario de Salamanca/IBSAL, Salamanca, Castilla y Leon, Spain

<sup>3</sup>National Hospital Organization, Shibukawa Medical Center, Gunma, Japan

<sup>4</sup>Middlemore Hospital, Otahuhu, Auckland, New Zealand

<sup>5</sup>Hospital Germans Triasi Pugo, Barcelona, Spain

<sup>6</sup>University Hospital Heidelberg, Heidelberg, Germany

<sup>7</sup>Nagoya City University Graduate School of Medical Sciences, Nagoya, Japan

<sup>8</sup>Hadassah Medical Center, Jerusalem, Italy

<sup>9</sup>Clinica Universidad de Navarra, Pamplona, Navarra, Spain

<sup>10</sup>The Mount Sinai Medical Hospital, New York, NY, USA

<sup>11</sup>Winship Cancer Institute, Emory University, Atlanta, GA, USA

<sup>12</sup>Merck & Co., Inc., Kenilworth, NJ, USA

### Background

Response rates remain low for refractory or relapsed/refractory multiple myeloma (rrMM) treated with currently approved therapies, including proteasome inhibitors and immunomodulatory drugs (IMiDs). Lenalidomide reduces PD-L1 and PD-1 expression on MM cells and enhances checkpoint blockade–induced cytotoxicity; PD-1 blockade with pembrolizumab may thus act synergistically with IMiDs to enhance tumor suppression. In the phase I KEYNOTE-023 study, the combination of pembrolizumab + lenalidomide and low-dose dexamethasone was associated with an acceptable safety profile and a promising overall response rate (ORR) of 50% (20/40) in patients with rrMM, supporting further evaluation of pembrolizumab in combination with immunomodulatory agents. The randomized, open-label, multicenter, phase III KEYNOTE-183 study (ClinicalTrials.gov, NCT02576977) was designed to compare the efficacy and safety of pomalidomide and low-dose dexamethasone with or without pembrolizumab in patients with rrMM.

### Methods

Key eligibility criteria include age  $\geq 18$  years, Eastern Cooperative Oncology Group performance status 0-1,



## Clinical Trials in Progress

*Presenting author underlined; Primary author in italics*

confirmed diagnosis of rrMM with measurable disease,  $\geq 2$  lines of prior treatment, and documented progression on the last line of therapy. Prior therapies must have included an IMiD, such as lenalidomide or thalidomide, and a proteasome inhibitor, such as bortezomib, ixazomib, or carfilzomib. Patients are randomly assigned 1:1 to receive pomalidomide 4 mg daily on days 1-21 and low-dose dexamethasone 40 mg (20 mg for patients aged  $>75$  years) daily on days 1, 8, 15, and 22 of repeated 28-day cycles, with or without pembrolizumab 200 mg every 3 weeks. Stratification is based on prior lines of treatment (2 vs  $\geq 3$ ) and disease status (refractory vs. sensitive to lenalidomide). Patients receiving pomalidomide must receive appropriate anticoagulation prophylaxis therapy. Treatment will continue until disease progression or unacceptable toxicity. Response will be assessed every 28 days by Clinical Adjudication Committee blinded central review and investigator review based on International Myeloma Working Group (IMWG) 2011 response criteria. Adverse events (AEs) will be assessed throughout treatment and for 30 days thereafter (90 days for serious AEs) and graded per NCI CTCAE v4.0. Patients will be followed for survival every 12 weeks. The primary endpoint is progression-free survival (PFS) based on IMWG criteria and overall survival; secondary endpoints are ORR, safety and tolerability, disease control rate, duration of response, and second PFS. Enrollment is ongoing and will continue until approximately 300 patients are enrolled.

### Trial Registration

ClinicalTrials.gov identifier NCT02576977.

164

### **KEYNOTE-185: randomized, open-label, phase III study of pembrolizumab in combination with lenalidomide and low-dose dexamethasone in patients with newly diagnosed and treatment-naïve multiple myeloma (MM)**

*Jatin Shah*<sup>1</sup>, Sagar Lonial<sup>2</sup>, Moacyr Ribeiro de Oliveira<sup>3</sup>, Habte Yimer<sup>4</sup>, Maria Victoria Mateos<sup>5</sup>, Robert Rifkin<sup>6</sup>, Fredrik Schjesvold<sup>7</sup>, Enrique Ocio<sup>5</sup>, Paula Rodríguez-Otero<sup>8</sup>, Jesus San-Miguel<sup>8</sup>, Razi Ghori<sup>9</sup>, Patricia Marinello<sup>9</sup>, Sundar Jagannath<sup>10</sup>

<sup>1</sup>University of Texas MD Anderson Cancer Center, Houston, TX, USA

<sup>2</sup>Winship Cancer Institute, Emory University, Atlanta, GA, USA

<sup>3</sup>Jane Thompson Russell Cancer Care Center, Tacoma, WA, USA

<sup>4</sup>Texas Oncology, Tyler, TX, USA

<sup>5</sup>Complejo Asistencial Universitario de Salamanca/IBSAL, Salamanca, Castilla y Leon, Spain

<sup>6</sup>Rocky Mountain Cancer Centers, Denver, CO, USA

<sup>7</sup>Oslo University Hospital, Oslo, Norway

<sup>8</sup>Clinica Universidad de Navarra, Pamplona, Navarra, Spain

<sup>9</sup>Merck & Co., Inc., Kenilworth, NJ, USA

<sup>10</sup>The Mount Sinai Medical Hospital, New York, NY, USA

### Background

Lenalidomide in combination with low-dose dexamethasone is one of the standard-of-care treatments for MM. Preclinical and experimental data has shown that lenalidomide reduces PD-L1 and PD-1 expression on MM cells and enhances checkpoint blockade-induced cytotoxicity; thus, PD-1 blockade with pembrolizumab may act synergistically with lenalidomide to enhance tumor suppression. In the phase I KEYNOTE-023 study, the combination of pembrolizumab + lenalidomide and low-dose dexamethasone was associated with an acceptable safety profile and a promising overall response rate (ORR) of 50% (20/40) in patients with relapsed/refractory MM, supporting further evaluation of pembrolizumab in combination with lenalidomide. The randomized, open-label, phase III KEYNOTE-185 study was designed to compare the efficacy and safety of lenalidomide and low-dose dexamethasone with or without pembrolizumab in patients with newly diagnosed and treatment-naïve MM not eligible for transplantation.

### Methods

Key eligibility criteria include age  $\geq 18$  years; newly diagnosed, treatment-naïve, active MM with measurable disease; ineligibility for autologous stem cell transplantation; and Eastern Cooperative Oncology Group performance status 0-1. Patients are randomized 1:1 to receive lenalidomide 25 mg daily on days 1-21 and low-dose dexamethasone 40 mg (20 mg for patients aged  $>75$  years) on days 1, 8, 15, and 22 of

## Clinical Trials in Progress

Presenting author underlined; Primary author in italics

repeated 28-day cycles, with or without pembrolizumab 200 mg every 3 weeks. Stratification is based on age (<75 vs ≥75 years) and International Staging System (ISS) stage (ISS I or II vs ISS III). Treatment will continue until disease progression or unacceptable toxicity. Response will be assessed every 28 days by Clinical Adjudication Committee blinded central review and by investigator review based on International Myeloma Working Group (IMWG) 2011 response criteria. Adverse events will be assessed throughout treatment and for 30 days thereafter (90 days for events of clinical interest) and graded per NCI CTCAE v4.0. Patients will be followed for survival every 12 weeks. The primary end point is progression-free survival (PFS) as assessed by central review according to IMWG criteria; secondary end points are overall survival, overall response rate, duration of response, second PFS, and safety and tolerability. Enrollment is ongoing and will continue until approximately 640 patients are enrolled.

### Trial Registration

ClinicalTrials.gov identifier NCT02579863.

165

### **KEYNOTE-122: phase II study of pembrolizumab versus standard-of-care chemotherapy in platinum-pretreated, recurrent or metastatic nasopharyngeal carcinoma**

Anna Spreafico<sup>1</sup>, Victor Lee<sup>2</sup>, Roger K C Ngan<sup>3</sup>, Ka Fai To<sup>4</sup>, Myung Ju Ahn<sup>5</sup>, Quan Sing Ng<sup>6</sup>, Ruey-Long Hong<sup>7</sup>, Jin-Ching Lin<sup>8</sup>, Ramona F Swaby<sup>9</sup>, Christine Gause<sup>9</sup>, Sanatan Saraf<sup>9</sup>, Anthony T C Chan<sup>4</sup>

<sup>1</sup>Princess Margaret Cancer Centre, Toronto, ON, Canada

<sup>2</sup>Li Ka Shing Faculty of Medicine, The University of Hong Kong, People's Republic of China

<sup>3</sup>Queen Elizabeth Hospital, Hong Kong, People's Republic of China

<sup>4</sup>The Chinese University of Hong Kong, Hong Kong, People's Republic of China

<sup>5</sup>Samsung Medical Center, Sungkyunkwan University, Seoul, Republic of Korea

<sup>6</sup>National Cancer Centre Singapore, Singapore, Singapore

<sup>7</sup>National Taiwan University Hospital, Taipei City, Taiwan (People's Republic of China)

<sup>8</sup>Taichung Veterans General Hospital, Taichung City, Taiwan (People's Republic of China)

<sup>9</sup>Merck & Co., Inc., Kenilworth, NJ, USA

### Background

Current treatment for recurrent/metastatic nasopharyngeal carcinoma (NPC) that progresses on a platinum-based regimen includes monotherapy with gemcitabine, capecitabine, or docetaxel. Although these treatments are used in clinical practice, they have not been formally approved for second-line NPC. Prolonged exposure to

Epstein-Barr virus (EBV) in NPC leads to increased expression of programmed death-1 (PD-1), resulting in suppressed T cell immunity and tumor surveillance. Pembrolizumab is a monoclonal anti-PD-1 antibody designed to block the interaction between PD-1 and its ligands, PD-L1 and PD-L2. In the phase Ib KEYNOTE-028 study, pembrolizumab was associated with an overall response rate of 22% (6/27) in mostly heavily pretreated (≥3 lines) patients with NPC. KEYNOTE-122 is a multicenter, open-label, randomized phase II study designed to evaluate the efficacy and safety of pembrolizumab monotherapy versus chemotherapy in patients with platinum-pretreated, recurrent or metastatic NPC.

### Methods

Key eligibility criteria include age ≥18 years, histologically confirmed nonkeratinizing differentiated NPC (WHO Class II) or undifferentiated NPC (WHO Class III), metastatic or recurrent disease, EBV positivity determined locally or centrally by EBV-encoded small RNA *in situ* hybridization, previous treatment with platinum-containing regimen, ECOG performance status 0-1, and measurable disease per RECIST v1.1. Patients will be randomly assigned 1:1 to receive pembrolizumab 200 mg every 3 weeks (Q3W) or investigator's choice of chemotherapy (capecitabine 1000 mg/m<sup>2</sup> twice daily on days 1-14 of each 3-week cycle, gemcitabine 1250 mg/m<sup>2</sup> once per week on days 1 and 8 of each 3-week cycle, or docetaxel 75 mg/m<sup>2</sup> Q3W). Treatment will continue until disease progression, unacceptable toxicity, investigator decision, or 35 cycles of pembrolizumab. Patients who complete 35 pembrolizumab cycles or discontinue pembrolizumab following a complete response may receive an additional 17 pembrolizumab cycles upon disease progression. Response will be evaluated every 6 weeks for the first year of treatment and every 9 weeks thereafter per RECIST v1.1 by central imaging assessment. Adverse events (AEs) will be assessed throughout treatment and for 30 days thereafter (90 days for serious AEs) and graded per National Cancer Institute Common Terminology Criteria for Adverse Events, version 4.0. Upon disease progression, patients will be followed for survival every 12 weeks. Primary end points are overall survival and progression-free survival per RECIST v1.1 by central imaging assessment; secondary end points include objective response rate and duration of response per RECIST v1.1 by central imaging assessment. Enrollment is ongoing and will continue until approximately 160 patients have enrolled.

### Trial Registration

ClinicalTrials.gov identifier NCT02611960.

## Clinical Trials in Progress

Presenting author underlined; Primary author in italics

166

### **CX-839-004: a phase I/II study of the safety, pharmacokinetics, and pharmacodynamics of the glutaminase inhibitor CB-839 combined with nivolumab in patients with renal cell carcinoma, melanoma, and non-small cell lung cancer**

Elaine Lam<sup>1</sup>, Nizar M Tannir<sup>2</sup>, Funda Meric-Bernstam<sup>2</sup>, Ulka Vaishampayan<sup>3</sup>, Keith W Orford<sup>4</sup>, Chris Molineaux<sup>4</sup>, Matt Gross<sup>4</sup>, Andy MacKinnon<sup>4</sup>, Sam\_Whiting<sup>4</sup>, *Martin Voss*<sup>5</sup>

<sup>1</sup>University of Colorado Denver, Aurora, CO, USA

<sup>2</sup>University of Texas MD Anderson Cancer Center, Houston, TX, USA

<sup>3</sup>Karmanos Cancer Institute, Detroit, MI, USA

<sup>4</sup>Calithera Biosciences, South San Francisco, CA, USA

<sup>5</sup>Memorial Sloan Kettering Cancer Center, New York, NY, USA

#### **Background**

T cells require glucose and glutamine for activation and proliferation. Tumor consumption of nutrients within the tumor microenvironment may contribute to localized immune suppression, termed a “metabolic checkpoint,” and selective inhibition of tumor metabolism may reverse this immunosuppression. CB-839 is a potent, first-in-class, oral inhibitor of glutaminase 1 that inhibits the tumor TCA cycle by blocking glutaminase 1-mediated conversion of glutamine to glutamate. *In vitro* studies of CB-839 demonstrated that blocking glutaminolysis in tumor cells increased extracellular glutamine and stimulated proliferation of T cells. In the CT26 syngeneic colon carcinoma model, combining CB-839 with a PD-1/PD-L1 inhibitor doubled the rate of complete regressions over the checkpoint inhibitor alone. Safety and preliminary evidence of activity of CB-839 as monotherapy and in combination with everolimus and paclitaxel were reported previously.

#### **Methods**

CX-839-004 is a phase I/II trial evaluating CB-839 + nivolumab in patients with clear cell RCC (ccRCC), melanoma (mel), and NSCLC. The primary objectives are to evaluate (i) safety and tolerability and (ii) anti-tumor effect of the combination. Secondary objectives include determining the MTD/RP2D of CB-839 in combination with standard dose nivolumab. Exploratory objectives include characterization of the pharmacodynamics of the combination and evaluation of biomarkers that may predict anti-tumor effect. Eligibility criteria include incurable metastatic or locally advanced ccRCC, mel or NSCLC previously treated with standard of care therapy, ECOG 0-1, and measurable disease by RECIST 1.1. In the phase I portion, a minimum of 6-9 patients will receive escalating doses of CB-839 orally BID and nivolumab 3 mg/kg IV on Days 1 and 15 every 28 days. Subsequent

to determining the MTD or RP2D, patients will be enrolled into phase II cohorts as follows: Cohort 1 ccRCC checkpoint inhibitor naïve; Cohort 2 ccRCC with documented progressive disease (PD) or stable disease (SD) > 6 mo on nivolumab in most recent line of therapy; Cohort 3 ccRCC with no better than SD before documented PD on any checkpoint inhibitor in any prior line of therapy; Cohort 4 melanoma with documented PD on a PD-1/PD-L1 inhibitor in most recent line of therapy; Cohort 5 NSCLC with documented PD or SD > 6 mo on PD-1/PD-L1 inhibitor in most recent line of therapy. Tumor burden will be assessed approximately every 8 weeks by RECIST 1.1 and irRECIST. Adverse events will be graded per NCI CTCAE. Samples obtained for pharmacodynamic and biomarker analyses will include pre-treatment and on-treatment tumor biopsies, blood and plasma.

#### **Trial Registration**

ClinicalTrials.gov identifier NCT02771626.

167

### **KEYNOTE-365: multicohort, phase Ib/II study of pembrolizumab combination therapy in patients with metastatic castration-resistant prostate cancer (mCRPC)**

Evan Y Yu<sup>1</sup>, Haiyan Wu<sup>2</sup>, Charles Schloss<sup>2</sup>

<sup>1</sup>Seattle Cancer Care Alliance, Seattle, WA, USA

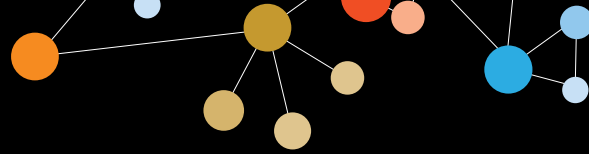
<sup>2</sup>Merck & Co., Inc., Kenilworth, NJ, USA

#### **Background**

Approved treatments for mCRPC include second-generation endocrine therapies (abiraterone and enzalutamide) and taxanes (docetaxel and cabazitaxel). These agents may increase programmed death ligand 1 (PD-L1) expression and/or facilitate release of neoantigens. Additionally, the PARP inhibitor, olaparib, has activity in patients with mCRPC who have DNA-repair defects. Pembrolizumab is an anti-programmed death 1 (PD-1) antibody that blocks the interaction between the immune checkpoint receptor PD-1 and its ligands. KEYNOTE-365 (ClinicalTrials.gov, NCT02861573) is an international, nonrandomized, multicohort, open-label phase Ib/II study evaluating the safety and response rate of pembrolizumab in combination with olaparib (cohort A), docetaxel + prednisone (cohort B), or enzalutamide (cohort C) in patients with mCRPC.

#### **Methods**

Key eligibility criteria include: histologically or cytologically confirmed adenocarcinoma of the prostate without small-cell histology, documented prostate cancer progression within 6 months preceding screening, and ongoing androgen deprivation with serum testosterone < 50 ng/dL. Cohort A will include patients previously treated with docetaxel (prior treatment with 1 other chemotherapy is allowed, as well as ≤2 second-generation hormonal manipulations);



## Clinical Trials in Progress

Presenting author underlined; *Primary author in italics*

cohort B will include patients previously treated with either abiraterone acetate or enzalutamide (but not both) before chemotherapy; and cohort C will include patients previously treated with abiraterone acetate before chemotherapy. Patients will receive pembrolizumab 200 mg once every 3 weeks (Q3W) (all cohorts) and either olaparib 400 mg twice daily (cohort A), docetaxel 75 mg/m<sup>2</sup> Q3W + prednisone 5 mg twice daily (cohort B), or enzalutamide 160 mg every day (cohort C). Treatments will continue until disease progression or unacceptable adverse events (AEs). There will be a maximum of 35 cycles of pembrolizumab (all cohorts) and 10 cycles of docetaxel + prednisone (cohort B). Patients who must discontinue a combination component may continue with the other drug until progression/unacceptable AEs. Response will be assessed by evaluating prostate-specific antigen (PSA) levels Q3W, and with radiologic imaging every 9 weeks for the first year and every 12 weeks thereafter. Primary endpoints are safety/tolerability and PSA response rate (decline of  $\geq 50\%$  from baseline measured twice at least 3 weeks apart). Secondary end points include time to PSA progression, radiographic progression-free survival based on investigator-assessed RECIST v1.1 per the Prostate Cancer Working Group 3 guidelines, and overall survival. Approximately 70 patients will be enrolled in each cohort.

### **Trial Registration**

ClinicalTrials.gov identifier NCT02861573.

## Clinical Trials: Cutting-Edge (Completed Trials)

Presenting author underlined; Primary author in italics

168

### Final statistical analysis of a pilot trial of hu14.18-IL2 in patients with completely resectable recurrent stage III or stage IV melanoma

Mark R Albertini<sup>1</sup>, Erik A Ranheim<sup>2</sup>, Jacquelyn A Hank<sup>2</sup>, Cindy Zuleger<sup>1</sup>, Thomas McFarland<sup>1</sup>, Jennifer Collins<sup>3</sup>, Erin Clements<sup>4</sup>, Sharon Weber<sup>1</sup>, Tracey Weigel<sup>4</sup>, Heather Neuman<sup>1</sup>, Greg Hartig<sup>1</sup>, David Mahvi<sup>5</sup>, MaryBeth Henry<sup>1</sup>, Jacek Gan<sup>1</sup>, Richard Yang<sup>1</sup>, Lakeesha Carmichael<sup>1</sup>, KyungMann Kim<sup>1</sup>, Stephen D Gillies<sup>6</sup>, Paul M Sondel<sup>2</sup>

<sup>1</sup>University of Wisconsin, Madison, WI, USA

<sup>2</sup>University of Wisconsin School of Medicine and Public Health, Madison, WI, USA

<sup>3</sup>University of Wisconsin Carbone Cancer Center, Madison, WI, USA

<sup>4</sup>Westchester Medical Center, New York Medical College, Valhalla, NY, USA

<sup>5</sup>Department of Surgery, Medical University of South Carolina, Charleston, SC, USA

<sup>6</sup>Provenance Biopharmaceuticals Corp., Carlisle, MA, USA

#### Background

Phase I testing of the hu14.18-IL2 immunocytokine (IC), a mAb reactive with GD2 disialoganglioside, linked to IL2, in patients (pts) with melanoma showed immune activation, reversible toxicities, and a maximal tolerated dose of 7.5 mg/m<sup>2</sup>/day. Preclinical data in IC-treated tumor bearing mice with low tumor burden documented striking antitumor effects. The main goal of this study was to obtain pilot data with hu14.18-IL2 in subjects with advanced melanoma who achieved a complete response (CR) through surgery.

#### Methods

Pts with completely resectable recurrent stage III or stage IV melanoma were scheduled to receive 3 cycles of IC at 6 mg/m<sup>2</sup>/d IV over 4 hours on days 1, 2 and 3 of each 28-day cycle. Pts were randomized to surgical resection of all sites of disease either following (Group A) or prior to (Group B) IC cycle 1. Primary objectives were 1) to evaluate histological evidence of anti-tumor activity in terms of apoptosis/necrosis of hu14.18-IL2 and 2) to evaluate recurrence-free survival (RFS) and overall survival (OS). The secondary objectives were 1) to evaluate adverse events associated with treatment and 2) to evaluate biological endpoints.

#### Results

Twenty melanoma pts (11 recurrent stage III, 8 stage IV, one unknown primary) were randomized to Group A (11 pts) or B (9 pts). Two Group B pts did not receive IC due to persistent disease following surgery. Six of 18 IC-treated patients remained free of recurrence, with a median recurrence-free survival of 5.7 months (95% CI: 1.8-not

reached). The 24-month RFS rate was 38.9% (95% CI: 17.5-60.0%). The median follow-up of surviving patients was 50.0 months (range: 31.8-70.4). The 24-month OS rate was 65.0% (95% CI: 40.3-81.5%). Twelve pts had evaluable tumor samples for GD2 analysis and 6/12 showed expression of GD2 on melanoma cells. There was no significant difference in RFS (p=0.791) or OS (p=0.567) based on GD2 expression. There was a significant difference in the change in C-reactive protein values from baseline to cycle 1, day 3 (p < 0.02). There were significant differences in the change in lymphocyte counts from baseline to post-baseline time points. Toxicities were similar to those previously reported for IC. Immunohistologic evaluations of resected tumors showed variable inflammation and tumor necrosis between pts and no clear differences between Groups A and B.

#### Conclusions

Prolonged tumor-free survival was seen in some melanoma pts at high risk for recurrence who were treated with IC.

#### Trial Registration

ClinicalTrials.gov identifier NCT00590824.

169

### Cytokine production by intratumorally administered activated dendritic cells correlates with survival in a phase I clinical trial

Vivek Subbiah<sup>1</sup>, Ravi Murthy<sup>1</sup>, Lori Noffsinger<sup>2</sup>, Kyle Hendricks<sup>2</sup>, Marnix Bosch<sup>3</sup>

<sup>1</sup>University of Texas MD Anderson Cancer Center, Houston, TX, USA

<sup>2</sup>Cognate Bioservices, Inc, Hanover, MD, USA

<sup>3</sup>Northwest Biotherapeutics, Bellevue, WA, USA

#### Background

Activated, autologous dendritic cells (aaDC) can be used to induce anti-tumor immune responses. A unique method of applying aaDC is through intratumoral injection, where the tumor cells serve as the source of antigen required for an adaptive anti-tumor response. A local effect may also occur as a result of cytokine production by the injected DC which makes the tumor more susceptible to a pre-existing or an induced immune attack.

#### Methods

Forty patients with locally advanced or metastatic solid tissue cancers were treated in a dose escalation trial in which aaDC were injected percutaneously under image guidance into a single tumor. Subjects had a median of 3 tumors (range 1 – 5) and had received an average of 3.1 prior treatments. To generate the aaDC, autologous monocytes were converted *ex vivo* into DC which were then activated. All batches of DC were released based on pre-specified criteria which included



## Clinical Trials: Cutting-Edge (Completed Trials)

Presenting author underlined; Primary author in italics

immunophenotyping and a T cell-stimulation assay, as well as sterility and endotoxin levels. Cytokine levels produced by the activated DC during manufacturing were measured and patient outcomes were correlated to these expression levels.

### Results

All three doses levels were well tolerated. The main adverse events related to treatment were grade 1 and 2 fevers. Twenty-one patients achieved stable disease (SD) 8 weeks after initiating treatment, and this was found to correlate with survival ( $p=0.01$ ). Levels of certain cytokines, such as such IL-8 and IL-12 p40, and TNF $\alpha$  were substantially elevated *in vitro* and IL-8 and IL-12 p40 production were predictive of survival ( $p=0.001$  and  $p=0.008$ , respectively). TNF $\alpha$  levels also correlated with SD at week 8 ( $p=0.01$ ). More than 70% of patients tested were found to have significant T cell responses, and/or *de novo* or significantly enhanced PD-L1 expression in the tumor post treatment, with a trend towards improved survival ( $p=0.1$ ).

### Conclusions

Study outcomes such as stabilization of disease and survival correlated with high DC cytokine levels, in the absence of meaningful toxicity. The DCVax treatment may be mediated through direct cytotoxic effects, as well as modulation of the tumor microenvironment to increase tumor infiltration by T cells, and attraction of inflammatory cells to the tumor. The development of PD-L1 expression likely reflects an induced immune response.

170

### Augmentation of tumor infiltrating CD8+ T cells and specific response to autologous tumor antigens in a phase I trial of *in situ* vaccination with CCL21 gene-modified dendritic cells

Jay M Lee<sup>1</sup>, Mi-Heon Lee<sup>1</sup>, Edward B Garon<sup>1</sup>, Jonathan W Goldman<sup>1</sup>, Felicita E Baratelli<sup>1</sup>, Dorthe Schaeue<sup>1</sup>, Gerald Wang<sup>1</sup>, Frances Rosen<sup>1</sup>, Jane Yanagawa<sup>1</sup>, Tonya C Walser<sup>1</sup>, Ying Q Lin<sup>1</sup>, Sharon Adams<sup>2</sup>, Franco M Marincola<sup>3</sup>, Paul C Tumeh<sup>1</sup>, Fereidoun Abtin<sup>1</sup>, Robert Suh<sup>1</sup>, Karen Reckamp<sup>4</sup>, William D Wallace<sup>1</sup>, Gang Zeng<sup>1</sup>, David A Elashoff<sup>1</sup>, Sherven Sharma<sup>5</sup>, Steven M Dubinett<sup>1</sup>

<sup>1</sup>David Geffen School of Medicine at UCLA, Los Angeles, CA, USA

<sup>2</sup>National Institutes of Health Clinical Center, Bethesda, MD, USA

<sup>3</sup>Sidra Medical and Research Center, Doha, Qatar

<sup>4</sup>City of Hope and Beckman Research Institute, Duarte, CA, USA

<sup>5</sup>VA Greater Los Angeles Healthcare System, Los Angeles, CA, USA

### Background

Intratumoral (IT) infiltration by activated immune effector cells is associated with a significantly better prognosis, however, tumor-associated immune suppression commonly occurs in non-small cell lung cancer (NSCLC). CD8<sup>+</sup> T cell or dendritic cell (DC) infiltration is an independent favorable prognostic indicator. CCL21 is a lymphoid chemokine that chemoattracts both lymphocytes and DC. Our preclinical studies revealed potent systemic antitumor immune responses following IT *in situ* vaccination with DC overexpressing CCL21. In clinical evaluation of this strategy, we investigated anti-tumor specific systemic immune responses and tumor-infiltrating CD8<sup>+</sup> T cells (CD8<sup>+</sup> TIL) in NSCLC patients in response to *in situ* vaccination via IT administration of autologous DC transduced with a replication-deficient adenoviral (Ad) vector expressing the secondary lymphoid chemokine (SLC/CCL21) gene.

### Methods

In a phase I trial, sixteen stage IIIB/IV NSCLC subjects received two vaccinations ( $1 \times 10^6$ ,  $5 \times 10^6$ ,  $1 \times 10^7$ , or  $3 \times 10^7$  dendritic cells/injection) by CT- or bronchoscopic-guided IT injection (days 0 and 7). Immune responses were assessed by tumor antigen-specific peripheral blood lymphocyte induction of IFN- $\gamma$  in ELISPOT assays. Tumor biopsies were evaluated for CD8<sup>+</sup> T cells and tumor PD-L1 by immunohistochemistry.

### Results

Twenty-five percent (4/16) of patients had stable disease at day 56 follow-up by RECIST criteria. Four possible vaccine-related grade 1 adverse events (AE) occurred in 3 patients with no clear association to dose or schedule; the AE included flu-like symptoms, blood-tinged sputum after each injection, nausea, and fatigue. ELISPOT assays revealed 38% (6/16) of patients had systemic responses against autologous tumor associated antigens (TAA). Tumor CD8<sup>+</sup> T cell infiltration was induced in 54% of subjects (7/13; 3.4 fold average increase in the number of CD8<sup>+</sup> T cells per mm<sup>2</sup>). Patients with increased intratumoral CD8<sup>+</sup> T cells following vaccination showed significantly increased PD-L1 mRNA expression ( $p=0.02$ ).

### Conclusions

Intratumoral vaccination with Ad-CCL21-DC was well-tolerated and resulted in 1) induction of systemic tumor antigen-specific immune responses and 2) enhanced tumor CD8<sup>+</sup> T cell infiltration accompanied by increased PD-L1 expression. DC-CCL21 *in situ* vaccination may be an effective approach to induce tumor CD8<sup>+</sup> T cell infiltration in combination with checkpoint inhibitor therapy. This will be assessed in combination with PD-1/PD-L1 checkpoint inhibition.

## Clinical Trials: Cutting-Edge (Completed Trials)

Presenting author underlined; Primary author in italics

### Acknowledgements

Supported by NCI R21CA105705, VA 2I01BX000359-05, NIH/NCATS UL1TR000124, NIH/NCI K23CA131577, NIH NCI L30CA142223, NIH NCI 5K12CA076905, the Thoracic Surgery Foundation and the NCI Experimental Therapeutics (NExT) Program.

### Trial Registration

ClinicalTrials.gov identifier NCT00601094.

171

### Increased immune responses in melanoma patients pre-treated with CDX-301, a recombinant human Flt3 ligand, prior to vaccination with CDX-1401, a dendritic cell targeting NY-ESO-1 vaccine, in a phase II study

Nina Bhardwaj<sup>1</sup>, Philip Friedlander<sup>2</sup>, Anna C Pavlick<sup>3</sup>, Marc S Ernstoff<sup>4</sup>, Brian Gastman<sup>5</sup>, Brent Hanks<sup>6</sup>, Mark R Albertini<sup>7</sup>, Jason J Luke<sup>8</sup>, Tibor Keler<sup>9</sup>, Tom Davis<sup>9</sup>, Laura A Vitale<sup>9</sup>, Elad Sharon<sup>10</sup>, Patrick Danaher<sup>11</sup>, Chihiro Morishima<sup>12</sup>, Martin Cheever<sup>13</sup>, Steven Fling<sup>13</sup>

<sup>1</sup>Tish Cancer Institute, Icahn School of Medicine at Mount Sinai, New York, NY, USA

<sup>2</sup>Icahn School of Medicine at Mt Sinai, New York, NY, USA

<sup>3</sup>NYU Perlmutter Cancer Center, New York, NY, USA

<sup>4</sup>Roswell Park Cancer Institute, Buffalo, NY, USA

<sup>5</sup>Cleveland Clinic, Cleveland, OH, USA

<sup>6</sup>Duke Cancer Institute, Durham, NC, USA

<sup>7</sup>University of Wisconsin, Madison, WI, USA

<sup>8</sup>University of Chicago School of Medicine, Chicago, IL, USA

<sup>9</sup>Celldex Therapeutics, Hampton, NJ, USA

<sup>10</sup>Cancer Therapy Evaluation Program, National Cancer Institute, National Institutes of Health, Rockville, MD, USA

<sup>11</sup>NanoString Technologies, Seattle, WA, USA

<sup>12</sup>University of Washington, Seattle, WA, USA

<sup>13</sup>Cancer Immunotherapy Trials Network, Fred Hutchinson Cancer Research Center, Seattle, WA, USA

### Background

Patients with high-risk melanoma have a 20-60% recurrence rate with 5-year OS between 45% and 70%. We evaluated vaccination with CDX-1401, a fusion protein consisting of human monoclonal IgG1 antibody targeting the dendritic cell (DC) receptor DEC-205 linked to the full-length NY-ESO-1 tumor antigen, with or without pretreatment with CDX-301, a recombinant human Flt3 ligand (Flt3L), in a phase II, randomized study of subjects with resected Stage IIb-IV melanoma. The primary objective was to determine whether the immune response to NY-ESO-1 elicited by vaccination with CDX-1401 and Hiltonol® (Poly-ICLC, from Oncovir) is substantially increased by prior expansion of circulating dendritic cells (DC) with CDX-301 therapy. Prevention of disease recurrence was not a clinical endpoint for this study.

### Methods

60 pts with resected melanoma were randomized to two cohorts. Cohort 1 (CH1) received CDX-301 pretreatment (25 mcg/kg SQ daily x 10 days) in the first 2 of 4 monthly cycles of vaccination with CDX-1401 (1 mg IC day 1) + poly-ICLC (2 mg SQ, days 1 and 2). Cohort 2 (CH2) received 4 monthly cycles of vaccine with CDX-1401 and poly-ICLC w/o prior CDX-301. Antigen-specific immune responses were measured by Elispot and ELISA; flow cytometry and T cell assays were performed to evaluate the effects on immune cell subsets.

### Results

The combination regimens of Flt3L, DC targeted NY-ESO-1 and poly-ICLC were well tolerated. Substantial increases in innate immune cells (DCs, NK cells and monocytes) were elicited in Flt3L treated (CH1) patients and w Flt3L treatment was associated with significant increases in activated T cells. T cell responses were elicited in both cohorts but were elicited earlier in CH1 and the number of individual responders to NY-ESO-1 in CH1 was significantly greater than in CH2. In addition, anti-NY-ESO-1-specific T cell responses in CH1 were significantly more robust. Significant increases in antibody titer were noted in both cohorts, but the average peak titer was significantly higher in CH1 vs CH2. Additional flow analyses, gene expression profiling and functional phenotyping of antigen-specific T cells are in progress.

### Conclusions

In melanoma patients, DC mobilization with Flt3L is safe and leads to substantially enhanced B and T cell responses to DC targeted vaccines.

### Trial Registration

ClinicalTrials.gov Identifier NCT02129075.

## Clinical Trials: Cutting-Edge (Completed Trials)

Presenting author underlined; Primary author in italics

### Antigen-specific (anti-NY-ESO-1) T cell responses

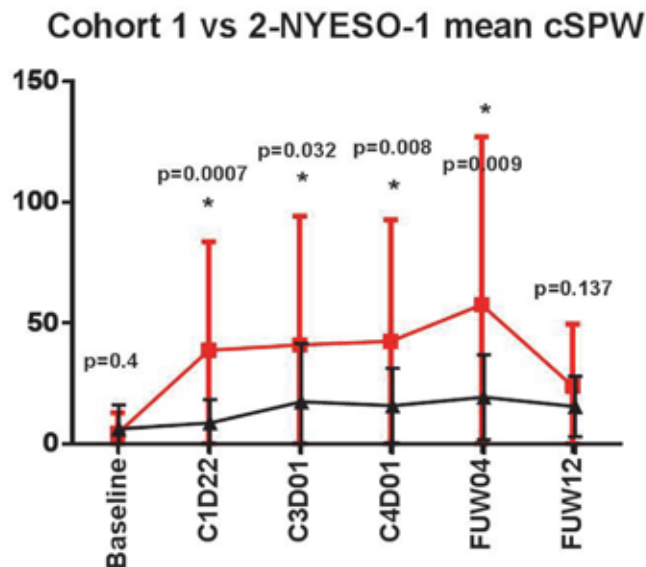


Figure 1. Anti-NY-ESO-1 specific responses in Cohort 1 are more robust and detected earlier vs Cohort 2. Differences between Cohort 1 and Cohort 2 at each time point are shown for Mean (of cohort) corrected SPW. Asterisks (\*) indicate highly significant differences.

172

### A first-in-human phase I dose-escalation study of NHS-IL12 in solid tumors

Christopher R Heery<sup>1</sup>, Joseph W Kim<sup>2</sup>, Elizabeth Lamping<sup>3</sup>, Jennifer Marte<sup>3</sup>, Sheri McMahon<sup>3</sup>, Lisa Cordes<sup>3</sup>, Farhad Fakhrehjani<sup>3</sup>, Ravi Madan<sup>3</sup>, Kwong Tsang<sup>4</sup>, Caroline Jochems<sup>1</sup>, Rachel Salazar<sup>5</sup>, Maggie Zhang<sup>5</sup>, Christoph Helwig<sup>6</sup>, Jeffrey Schlom<sup>7</sup>, James L Gulley<sup>8</sup>

<sup>1</sup>Laboratory of Tumor Immunology and Biology, National Cancer Institute, Bethesda, MD, USA

<sup>2</sup>Yale Cancer Center, New Haven, CT, USA

<sup>3</sup>National Cancer Institute, Bethesda, MD, USA

<sup>4</sup>Laboratory of Tumor Immunology and Biology, National Cancer Institute, NIH, Bethesda, MD, USA

<sup>5</sup>EMD Serono, Billerica, MA, USA

<sup>6</sup>Merck KGaA, Darmstadt, Hessen, Germany

<sup>7</sup>Laboratory of Tumor Immunology and Biology, Center for Cancer Research, National Cancer Institute, Bethesda, MD, USA

<sup>8</sup>Genitourinary Malignancies Branch, Center for Cancer Research, National Cancer Institute, National Institutes of Health, Bethesda, MD, USA

### Background

NHS-IL12 (MSB0010360N; M9241), a tumor-targeting immunocytokine comprising 2 heterodimers of IL-12 fused to the H-chain of the NHS76 antibody, has affinity for single- and double-stranded DNA and is designed to target necrotic tissue and deliver IL-12 to tumor. In previous trials with human recombinant IL-12, clinical activity was limited by toxicity. The goal is to reduce toxicity associated with systemic IL-12 through highly specific delivery to the tumor.

### Methods

A 3+3 dose-escalation study in patients with advanced solid tumors was designed to demonstrate the safety of NHS-IL12 while evaluating pharmacokinetic (PK) and pharmacodynamic (PD) effects. Dosing started at 0.1 mcg/kg, with a planned maximum DL9 (21.8 mcg/kg). Patients were admitted for PK/PD draws and 48-hour observation after the first 2 doses. Restaging evaluations were performed every 8 weeks using standard RECIST 1.1 and immune-related response criteria. An expansion cohort (n=10) was enrolled at the maximum-tolerated dose (MTD) for further PK/PD analysis.

### Results

From 12/2011–05/2016, 58 patients enrolled in DLs 1–9. 22 patients enrolled in single-dose cohorts (SDC); 36 patients in multiple-dose cohorts (MDC; q4wk). In SDC, all patients completed treatment; there was 1 death unrelated to study treatment. In MDC, 32 patients discontinued due to: progression (20), adverse events (AEs, 4), alternative treatment (3), treatment-schedule conflict or withdrawal (4), and 1 death unrelated to study treatment. Median administrations in the MDC was 2.5 doses (range 1–22). Treatment-related AEs occurred in 47/58 patients (81%). Dose-limiting toxicities were observed in 1/6 patients on DL8 (16.8 mcg/kg, grade 3 alanine aminotransferase (ALT) elevation) and 2/6 patients in DL9 (21.8 mcg/kg, grade 3 aspartate aminotransferase (AST) and ALT elevation and lipase elevation), making the MTD 16.8 mcg/kg. 10 patients were enrolled in expanded DL8 at 16.8 mcg/kg. Most common AEs in DL8 (n=16) were decreased lymphocyte count (81.3%), increased AST (81.3%), decreased white blood cell count (75%), increased ALT (75%), and fever (62.5%). Most AEs were transient and resolved within 10 days. Most symptoms were controlled with NSAIDs or acetaminophen. Serum cytokines showed time- and dose-dependent changes for IFN-gamma, IL-10, IL-12P70, and TNF- $\alpha$ . Best overall response was stable disease in 15/30 evaluable subjects. Five patients stayed on study treatment  $\geq$ 182 days.

### Conclusions

NHS-IL12 administered s.c. q4wk was safe and well-tolerated with predictable adverse events. Analysis of paired tumor biopsies to determine intratumoral effects are ongoing. Updated data will be presented at the conference.

## Clinical Trials: Cutting-Edge (Completed Trials)

Presenting author underlined; Primary author in italics

### Trial Registration

ClinicalTrials.gov identifier NCT01417546.

173

### Salvage intravesical Mycobacterium phlei cell wall-nucleic acid complex (MCNA) for BCG-unresponsive patients

Roger Li<sup>1</sup>, John Amrhein<sup>2</sup>, Zvi Cohen<sup>3</sup>, Monique Champagne<sup>3</sup>, Ashish Kamat<sup>1</sup>

<sup>1</sup>University of Texas MD Anderson Cancer Center, Houston, TX, USA

<sup>2</sup>McDougall Scientific Ltd., Toronto, ON, Canada

<sup>3</sup>Telest Therapeutics Inc., Saint-Laurent, PQ, Canada

### Background

A standardized definition of BCG-unresponsive disease has been recently agreed upon to assess the efficacy of salvage treatments for patients with bladder cancer recurrence despite intravesical BCG therapy. Previously, we have reported the results from a single-arm trial of intravesical MCNA treatment in patients who have previously failed BCG [1]. We now report the results of a retrospective analysis, looking at efficacy with attention paid to the specific category of BCG-unresponsive patients.

### Methods

High-risk NMIBC patients with either papillary and/or carcinoma *in situ* (CIS) having failed intravesical BCG treatment were enrolled. BCG treatment failure was defined as cancer recurrence after at least 2 courses of BCG (at least 5 of 6 induction instillations and at least 2 of 3 maintenance instillations, or 2 induction courses). Patients received induction treatment with 6 weekly doses of 8 mg MCNA intravesically, followed up by maintenance treatment of 3 weekly instillations at months 3, 6, 12, 18 and 24. Treatment efficacy was evaluated by cystoscopy, urine cytology and biopsy, with disease-free status achieved when central review of biopsy reveals absent high grade disease.

### Results

Of the 129 patients originally enrolled, 94 fit the newly defined BCG unresponsive criteria. The cohort consisted of 68 (72.3%) with CIS, with/without papillary tumor, and 26 (27.7%) with exclusively papillary tumor upon recurrence after BCG. In the CIS-containing group, the complete response rate measured at months 6, 12, and 24 were 39.7% (28-52.3%), 23.5% (14.1-35.4%), and 13.2% (6.2-23.6%), respectively. In the group with only papillary tumors, the corresponding disease-free survival rates were 61.2% (38.2-77.8%), 61.2% (38.2-77.8%), and 50.1% (27.5-69%).

### Conclusions

Intravesical MCNA therapy is an alternative therapy to radical cystectomy in the patients with recurring disease after intravesical BCG treatment. It has the potential to offer 24% of patients with CIS and 60% of patients with papillary tumors a chance to safely preserve their bladder.

### References

- Morales A, Herr H, Steinberg G, Given R, Cohen Z, Amrhein J, Kamat AM: **Efficacy and Safety of MCNA in Patients with Nonmuscle Invasive Bladder Cancer at High Risk for REcurrence and Progression after Failed Treatment with bacillus Calmette-Guerin.** *J Urol* 2015, **193**:1135-1143.

Figure 1. Study Design

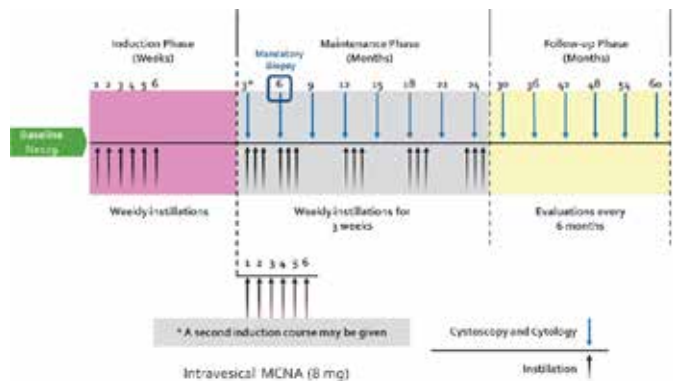


Table 1. Disease Free Survival

Population	N	6-Month DFS or CR Rate <sup>a</sup> %	1-Year DFS or CR Rate <sup>a</sup> %	2-Year DFS or CR Rate <sup>a</sup> %	Median Duration of Response in Months (1-Yr responders)
Overall	94	48.9 (38.6, 59.0)	34.8 (24.7, 45.0)	28.3 (17.3, 36.3)	34.0
CIS (± papillary)	68	39.7 (28.6, 52.3)	23.5 (14.4, 35.4)	13.2 (6.4, 23.6)	26.0
Papillary tumors only	26	61.2 (38.2, 77.8)	61.2 (38.2, 77.8)	50.1 (27.5, 69.0)	39.0





## Coinhibition and Costimulation

Presenting author underlined; *Primary author in italics*

174

### **DNA methylation changes in CD8+ T cells following 4-1BB costimulation**

*M Angela Aznar*<sup>1</sup>, Sara Labiano<sup>1</sup>, Angel Diaz-Lagares<sup>2</sup>, Manel Esteller<sup>3</sup>, Juan Sandoval<sup>4</sup>, Ignacio Melero<sup>1</sup>

<sup>1</sup>Center for Applied Medical Research (CIMA), University of Navarra, Pamplona, Navarra, Spain

<sup>2</sup>Bellvitge Biomedical Research Institute (IDIBELL), Barcelona, Catalonia, Spain

<sup>3</sup>Bellvitge Biomedical Research Institute (IDIBELL), Barcelona, Navarra, Spain

<sup>4</sup>Medical Research Institute La Fe, Valencia, Comunidad Valenciana, Spain

#### **Background**

4-1BB costimulation imprints long term changes in the behavior of costimulated T cells [1]. There is not a satisfactory mechanistic explanation yet.

#### **Methods**

To determine the specific DNA methylation changes occurring upon 4-1BB costimulation, purified human CD8+ T cells from three healthy donors were activated *in vitro* for 5 days with anti-CD3 monoclonal antibody (OKT3) and either with anti-4-1BB monoclonal antibody urelumab or its corresponding isotype (hulgG4). Activated lymphocytes were left 5 days in culture with hUL-7 without further stimulation. Such back-to-resting CD8+ lymphocytes were reactivated with OKT3 for 12, 24 and 36h to validate the expression of the genes differentially methylated upon primary stimulation at mRNA and protein levels. DNA methylation profiles of both activated and resting cell subsets were characterized with Infinium 450K DNA methylation array (Illumina). To further confirm our observations, identical experimental procedure was performed with anti-4-1BB 6B4 agonist antibody in a CD8+ T cell donor. Differentially methylated genes between OKT3+anti-4-1BB versus their corresponding control counterparts were validated by pyrosequencing on activated and resting CD8+ from independent group of healthy donors (n=8 for Urelumab and n= 11 for 6B4). Expression changes were confirmed by qRT-PCR and flow cytometry in activated, rested and reactivated CD8+.

#### **Results**

853 genes were differentially methylated in urelumab-treated CD8+ T cells compared with their controls, 52 of which were shared with 6B4-costimulated CD8+ T lymphocytes. A number of differentially methylated genes are involved in i) T cell migration, ii) T cell activation, survival and homeostasis and iii) regulation of gene expression including key T cell transcription factors.

#### **Conclusions**

4-1BB costimulation induces CD8+ T lymphocytes that are poised to respond more effectively to a second antigen exposure. These acquired functions are imprinted in the genomic DNA of the CD8+ T cells by DNA methylation during 4-1BB co-stimulation, and involve key genes for CD8+ T cells.

#### **References**

1. Hendriks J, Xiao Y, Rossen JW, van der Sluijs KF, Sugamura K, Ishii N, Borst J: **During viral infection of the respiratory tract, CD27, 4-1BB, and OX40 collectively determine formation of CD8+ memory T cells and their capacity for secondary expansion.** *J Immunol* 2005, **175**:1665-1676.

175

### **Novel tetravalent anti-GITR antibody is a potent anti-tumor agent in vivo**

*Susannah D Barbee*<sup>1</sup>, David I Bellovin<sup>1</sup>, John C Timmer<sup>2</sup>, Nebiyu Wondyfraw<sup>1</sup>, Susan Johnson<sup>1</sup>, Johanna Park<sup>1</sup>, Amanda Chen<sup>1</sup>, Mikayel Mkrtichyan<sup>1</sup>, Amir S Razai<sup>2</sup>, Kyle S Jones<sup>2</sup>, Chelsie Y Hata<sup>2</sup>, Denise Gonzalez<sup>1</sup>, Quinn Deveraux<sup>2</sup>, Brendan P Eckelman<sup>2</sup>, Luis Borges<sup>1</sup>

<sup>1</sup>Five Prime Therapeutics, South San Francisco, CA, USA

<sup>2</sup>Inhibrx, La Jolla, CA, USA

#### **Background**

Glucocorticoid-induced TNFR-related (GITR, TNFRSF18) is a member of the TNFR superfamily with pleiotropic T cell modulatory activity. In the mouse, GITR is expressed at high levels on regulatory T cells (T<sub>reg</sub>) and has been reported to antagonize their suppressive capacity, whereas it is expressed at moderate levels on conventional effector T cells (both CD4<sup>+</sup> and CD8<sup>+</sup>) for which where it exerts stimulatory activity. Studies have indicated that GITR-targeting agents mediate anti-tumor control via two mechanisms: depletion and possibly suppression of T<sub>reg</sub> and/or direct agonism of effector T cells.

#### **Methods**

We have developed a novel anti-GITR antibody with enhanced agonist activity using single-domain antibodies (sdAbs) in a multivalent format. A tetravalent anti-GITR agonist antibody induces NF- $\kappa$ B activation and T cell stimulation *in vitro* that is superior to a conventional bivalent antibody; multivalency confers agonist activity in the absence of Fc-mediated crosslinking. T<sub>reg</sub>-depleting activity is obtained with an Fc effector-competent format.

#### **Results**

The tetravalent antibody potently controls tumor growth *in vivo* following a single dose with activity as low as 0.08 mg/kg. Treatment reduces T<sub>reg</sub> frequency, thereby altering the ratio to effector T cells within the tumor to create a favorable



## Coinhibition and Costimulation

Presenting author underlined; Primary author in italics

environment for an effective anti-tumor immune response. CD8<sup>+</sup> T cell activation and proliferation is observed *in vivo*, and treatment confers long-term immunity to tumor re-challenge.

### Conclusions

In summary, multivalent GITR agonist antibodies are a promising modality for the treatment of cancer and we are exploring candidates for clinical development.

176

### Evaluation of AP-1 signaling by interleukin-13 in human glioblastoma cells

Rukmini Bhardwaj, *Raj K Puri*, Akiko Suzuki, Pamela Leland, Bharat H Joshi

Centre for Biologics Evaluation and Research (CBER), U.S Food and Drug Administration, Silver Spring, MD, USA

### Background

Glioblastoma (GBM) is one of the deadliest and most aggressive forms of brain cancer with a median survival of  $\leq$  two years. Previously, our lab has demonstrated that Interleukin-13 receptor (IL-13R) alpha2 ( $\alpha$ 2) is a novel tumor antigen and is overexpressed in  $\sim$ 78% of the GBM tumors. IL-13R $\alpha$ 2 can be targeted by cancer vaccines, chimeric antigen receptor modified T cells (CAR-T) and a chimeric fusion immunotoxin consisting of IL-13 and truncated *Pseudomonas* exotoxin (IL-13-PE). However, the significance and regulation of the IL-13/IL-13R axis is not completely understood in the context of cancer immunology and in particular IL-13 signaling through the IL-13R $\alpha$ 2 chain.

### Methods

We characterized and confirmed IL-13R $\alpha$ 2 expression in GBM tumor cell lines and its biological function by performing RT-qPCR and testing their sensitivity to the cytotoxic effect of IL-13-PE. We examined the activation of AP-1 family of transcription factors after treating GBM cell lines; U251, A172, U87MG (IL-13R+) and T98G (IL-13R-) with IL-13. Five members of the AP-1 family (c-Jun, Jun-D, Jun-B, c-Fos and Fra-1) were studied by immunocytochemistry (ICC) after treating 40,000 glioma tumor cells with IL-13 (20ng/ml) for 30 minutes in a glass chamber slide. We used IL-2 treatment as a negative control, since these cell lines did not express IL-2 receptors.

### Results

We observed an overexpression of IL-13R $\alpha$ 2 mRNA in three of four GBM cell lines (U251, A172 and U87MG), which also showed high sensitivity to IL-13-PE immunotoxin. By ICC analysis of tumor cells, we found that three members of AP-1 family (c-Jun, Jun-D and Fra-1) were activated only in IL-13R $\alpha$ 2 positive glioma cells when treated with IL-13.

In contrast, IL-13R $\alpha$ 2 negative T98G cells did not show activation of any of the AP-1 members. Two other members of the AP-1 family, Jun-B and c-Fos, were not activated after treatment with IL-13. We also observed that the extent of immunostaining and percent positive cells for c-Jun and Fra-1 in IL-13R $\alpha$ 2 positive glioma cells were significantly higher than IL-13R negative cells ( $P < 0.001$ ).

### Conclusions

Our results show that IL-13 mediates signaling in IL-13R $\alpha$ 2 positive GBM cell lines through the AP-1 pathway by activating c-Jun, Jun-D and Fra-1. IL-13 did not activate any of the AP-1 family members in a receptor negative GBM cell line. These results indicate that IL-13R $\alpha$ 2 is a key player in the IL-13/IL-13R $\alpha$ 2 axis for initiating signal transduction through the AP-1 pathway in GBM tumor cells and may be a good target for immunotherapy.

177

### Activation of liver-resident myeloid cells to produce IL-27 initiates 4-1BB hepatotoxicity

*Todd Bartkowiak*<sup>1</sup>, Ashvin Jaiswal<sup>1</sup>, Casey Ager<sup>1</sup>, Midan Ai<sup>2</sup>, Pratha Budhani<sup>2</sup>, Renee Chin<sup>2</sup>, David Hong<sup>2</sup>, Michael Curran<sup>1</sup>

<sup>1</sup>Department of Immunology, University of Texas MD Anderson Cancer Center, Houston, TX, USA

<sup>2</sup>University of Texas MD Anderson Cancer Center, Houston, TX, USA

### Background

4-1BB agonist antibodies were the second T cell co-stimulatory agents to enter the clinic after  $\alpha$ CTLA-4. Despite impressive efficacy against both hematologic and solid tumors and an ability to suppress adverse events associated with checkpoint blockade, their development has been stymied by poor understanding of their underlying mechanism and the resulting inability to separate off-target liver toxicity from on-target anti-tumor immunity. We sought to uncover the mechanisms by which 4-1BB agonist antibodies trigger hepatotoxicity in hopes of discovering approaches by which the anti-tumor and hepatotoxic effects could be separated.

### Methods

C57BL6/J mice (Taconic) were treated every 3 days for 3 doses with the 4-1BB antibody 3H3 (250ug),  $\alpha$ PD-1 (RMP1-14, 250ug),  $\alpha$ CTLA-4 (9D9 or 9H10 100ug), or  $\alpha$ CD40 (FGK4.5 100ug). For 4-1BB knockout reconstitution experiments, mice were sublethally irradiated and then transferred with  $2 \times 10^6$  splenocytes as on d-1. CCR5, CXCR3, CCR2, Ebi3, IL27Ra, MHCII, and B2m knockout mice and FoxP3-DTR and OT-1 transgenics were purchased from Jackson. Serum liver enzymes were read on day 16 by the MDACC mouse pathology core.

## Coinhibition and Costimulation

Presenting author underlined; Primary author in italics

### Results

We find that  $\alpha$ 4-1BB mediated liver damage initiates through stimulation of myeloid cells, followed by subsequent recruitment and activation of CD8 and CD4 T cells in the liver. Moreover, we show that the inflammatory cytokine IL-27 is essential in myeloid conversion of T cells into mediators of liver damage. Conversely, FoxP3<sup>+</sup> regulatory T cells (Treg) act to suppress 4-1BB agonist induced liver inflammation, and liver pathology worsens significantly when they are ablated. Further, we show that concomitant CTLA-4 blockade ameliorates 4-1BB hepatotoxicity by expanding peripheral Tregs, but that this effect is lost with addition of  $\alpha$ PD-1. Additional differences exist between the tumor and liver microenvironments, which may be exploited to selectively promote on target activation of 4-1BB by agonist antibodies in the future.

### Conclusions

4-1BB activation of liver-resident myeloid cells promotes the subsequent recruitment and activation of T cells in an IL-27 dependent manner. These T cells mediate the liver pathology associated with 4-1BB antibodies unless their activity is suppressed by Tregs. Our results support the use of 4-1BB agonists in rational combinations, in particular with CTLA-4 blockade, which may expand Tregs in the liver to ameliorate  $\alpha$ 4-1BB mediated toxicities.

### Acknowledgements

We thank the MD Anderson IRG program and DOD PRCRP grant CA140792 for funding. Dr. Robert Mittler kindly provided 4-1BB knockout mice and Drs. Aymen Al-Shamkhani, Martin Glennie, and Stephen Beers kindly provided LOB12 antibody.

178

### Restoration of tumor-infiltrating lymphocyte function by panobinostat and tumor eradication with the combination of panobinostat and PD-1 blockade

*William D Hastings*<sup>1</sup>, Maria Pinzon-Ortiz<sup>1</sup>, Masato Murakami<sup>2</sup>, Jason R Dobson<sup>1</sup>, David Quinn<sup>1</sup>, Joel P Wagner<sup>1</sup>, Xianhui Rong<sup>1</sup>, Pamela Shaw<sup>3</sup>, Ernesta Dammasa<sup>2</sup>, Wei Guan<sup>1</sup>, Glenn Dranoff<sup>1</sup>, Alexander Cao<sup>4</sup>

<sup>1</sup>Novartis Institutes for BioMedical Research, Inc., Cambridge, MA, USA

<sup>2</sup>Novartis Institutes for BioMedical Research, Inc., Werk Klybeck, Basel-Landschaft, Switzerland

<sup>3</sup>Cellaria Biosciences, LLC, Cambridge, MA, USA

<sup>4</sup>Bristol-Myers Squibb, Princeton, NJ, USA

### Background

Tumor immunotherapy is a unique therapeutic modality in our fight against human cancers. The recent success of immune checkpoint therapies highlights the value and

potential of this approach. Epigenetic regulation of tumor immunology is becoming a key area of investigation. Experimental data have linked HDAC-inhibition to the enhancement of tumor antigen expression and presentation, the activation of effector T and NK cells, and the suppression of T regulatory cells. These observations are confounded by the potential immune-inhibitory effects by HDAC-inhibitors on DC and T cell activation. Here, we have examined the immune modulatory effects of pan-HDAC-inhibitor, panobinostat (LBH589), and its interaction with a PD-1 antibody, in preclinical settings.

### Methods

Panobinostat was tested *in vitro* in human peripheral blood mononuclear cell (hPBMC) cultures at concentrations from 5 nM to 500 nM. Next, panobinostat was examined *in vivo* as single agent and in combination with the PD-1 antibody, 1D2, in MC38, a murine syngeneic tumor model.

### Results

Panobinostat restored IL-2, IFN $\gamma$ , and TNF $\alpha$  expression that was inhibited during T cell exhaustion. Elevation of tumor-infiltrating lymphocytes (TIL) was observed by both flow cytometry and immunohistochemistry. Of note, the proportion of CD8<sup>+</sup> effector-memory cells was increased by panobinostat. Proteomic analysis of the treated MC38 tumors revealed increases in IFN $\gamma$  levels under panobinostat treatment. Molecular profiling of tumor samples by NanoString indicated that panobinostat treatment led to increases of MHC class I, II and invariant chain expression. This is coupled with inductions of chemokine and cytokine expression and increases in effector T cell functions as measured by Granzyme A and B expression. Finally, while panobinostat and PD-1 antibody each achieved some level of anti-tumor efficacy, the combination of panobinostat and PD-1 antibody achieved complete responses in 10 out of 10 mice tested. The tumor regression was durable as none of the treated mice had any recurrence of tumors more than 60 days after the cessation of treatment.

### Conclusions

Our preclinical data point to a dichotomy of immune modulation by panobinostat. While it may be immune-suppressive during priming, panobinostat is immune-stimulatory under antigen-experienced, immune-exhaustive environment. With the latter more reflective of the tumor microenvironment, we saw evidence of panobinostat being immune-stimulatory on TIL in a preclinical setting, with induction of both TIL percentages as well as activity. The positive effects on TIL and the promising combination efficacy with PD-1 antibody *in vivo* support further testing of panobinostat as a possible immuno-oncology agent both in preclinical and clinical settings.

## Coinhibition and Costimulation

*Presenting author underlined; Primary author in italics*

179

### **Imprime PGG, a soluble yeast $\beta$ -glucan, is a systemically administered PAMP that activates DCs and supports T cell priming, showing synergy with cancer immunotherapies**

Ross B Fulton, Steven Leonardo, Kathryn Fraser, Takashi O Kangas, Nadine Ottoson, Nandita Bose, Richard D Huhn, Jeremy Graff, Jamie Lowe, Keith Gorden, Mark Uhlik

Biothera Pharmaceuticals Inc., Eagan, MN, USA

#### **Background**

Pathogen-associated molecular patterns (PAMPs) provide crucial activating signals to the immune system. Importantly, due to their potent ability to induce pro-inflammatory cytokines that can cause systemic toxicity, most PAMPs are limited to local administration such as subcutaneous or intratumoral injection. Imprime PGG (Imprime) is a soluble yeast  $\beta$ -1,3/1,6 glucan that has been administered intravenously (i.v) to >400 healthy volunteers and cancer patients with minimal adverse effects. Imprime has shown promising efficacy when combined with other therapeutic antibodies in multiple clinical trials. Imprime has been previously shown to have promising efficacy in combination with immune checkpoint inhibitors in pre-clinical mouse tumor models and is currently being explored clinically in combination with anti-PD-1 therapy. In data presented here, we sought to further understand how Imprime functions to link the innate and adaptive immune systems via dendritic cells (DCs) to induce T cell priming providing benefit to checkpoint inhibitor therapy.

#### **Methods**

To examine *in vivo* effects of Imprime, C57BL/6 mice were injected i.v. with 1.2 mg of Imprime. 16hr post treatment, lymph nodes (LNs) were harvested and mRNA levels were determined using the QuantiGene Plex platform (Affymetrix). To study Imprime's effect on CD8 T cell priming,  $1 \times 10^5$  OT-I CD8 T cells were transferred into congenic hosts and immunized with H-2K<sup>b</sup>/OVA<sub>257-264</sub> peptide +/- Imprime. Separately, healthy human volunteers were infused with 4mg/kg Imprime and serum cytokines/chemokines were examined using the Luminex platform.

#### **Results**

Following i.v. administration of Imprime in non-tumor bearing mice, Imprime rapidly bound resident and migratory DC subsets, caused DC maturation, and increased DC recruitment into LNs. Transcriptional profiling in LNs showed increased mRNA levels of chemokines important in immune cell trafficking, pro-inflammatory cytokines, and a strong type I interferon signature. Many of these chemokines were also increased in the blood of healthy volunteers, as was detection

of Imprime binding to DCs. In congenic mouse recipients that were immunized with peptide +/- Imprime after transfer of OVA-specific OT-I CD8 T cells, those primed in the presence of Imprime demonstrated greater overall expansion and acquisition of effector functions than peptide alone. Imprime's transcriptional profile and ability to enhance T cell priming was dependent on the C-type lectin receptor Dectin-1.

#### **Conclusions**

Together, these data demonstrate that Imprime acts as a unique i.v.-administered PAMP that primes the immune system and inspires a coordinated adaptive immune response. These qualities make Imprime an attractive candidate to synergize with cancer immunotherapies.

180

### **Functional characterization of CDX-1140, a novel CD40 antibody agonist for cancer immunotherapy**

Laura A Vitale<sup>1</sup>, Thomas O'Neill<sup>1</sup>, Jenifer Widger<sup>1</sup>, Andrea Crocker<sup>1</sup>, Li-Zhen He<sup>1</sup>, Jeffrey Weidlick<sup>1</sup>, Karuna Sundarapandiyani<sup>1</sup>, Venky Ramakrishna<sup>1</sup>, James Storey<sup>2</sup>, Lawrence J Thomas<sup>2</sup>, Joel Goldstein<sup>1</sup>, Henry C Marsh<sup>2</sup>, Tibor Keler<sup>1</sup>

<sup>1</sup>Celldex Therapeutics, Hampton, NJ, USA

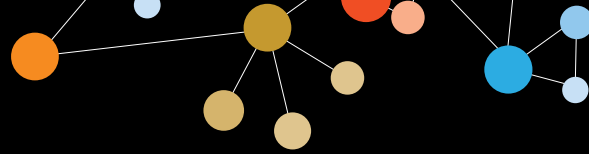
<sup>2</sup>Celldex Therapeutics, Needham, MA, USA

#### **Background**

For the development of agonist antibodies that stimulate immune responses, a balance is required between sufficiently strong immune stimulation and the untoward effects of systemic immune activation. This is particularly true for CD40, a molecule expressed by antigen presenting cells, which is critical in the regulation of immune responses. Agonist CD40 antibodies are highly effective in preclinical tumor models either through direct interaction with CD40-expressing lymphomas, or indirectly through the activation of adaptive anti-tumor immunity. There are several agonist CD40 antibodies in clinical development, but limited data are available with regard to their clinical activity and safety profile. Data reported for the agonist anti-CD40 mAb CP-870,893 (Roche/Pfizer) [1] demonstrated clinical activity in cancer patients, but its low maximum tolerated dose (0.2 mg/kg) may impede the full potential of activating this pathway. We set out to develop a CD40 agonist antibody with strong immune stimulating properties and a safety profile that allows for systemic dosing.

#### **Methods**

Anti-CD40 monoclonal antibodies (mAbs) were generated by immunization of human Ig transgenic mice with recombinant and cell surface expressed human CD40. We selected hybridomas that produced human antibodies with an assay using a reporter cell line engineered to express CD40 and



## Coinhibition and Costimulation

Presenting author underlined; *Primary author in italics*

NFκB-responsive luciferase. The variable regions of lead antibodies that displayed differential activity were cloned in human IgG1 or IgG2 constant domains and expressed in CHO cells.

### Results

From this panel, CDX-1140, a human IgG2 antibody, was selected for further development. CDX-1140 is a potent inducer of human B cell proliferation and activation, and similarly directly stimulates dendritic cells to upregulate costimulatory molecules and secrete cytokines. Importantly, CD40 stimulation with CDX-1140 is independent of the Fc domain of the antibody. *In vivo*, CDX-1140 has potent anti-lymphoma activity in xenograft models, and a pilot study in non-human primates has shown good pharmacodynamic and safety profiles. A summary of these functional activities will be presented.

### Conclusions

These data support CDX-1140 as a novel CD40 agonist with potential for immunotherapy of cancer patients.

### References

1. Vonderheide RH, *et al*: **Clinical activity and immune modulation in cancer patients treated with CP-870,893, a novel CD40 agonist monoclonal antibody.** *J Clin Oncol* 2007, 25:876–883.

181

### Releasing the breaks: quantitative cell-based bioassays to advance individual or combination immune checkpoint immunotherapy

Jamison Grailer, Julia Gilden, Pete Stecha, Denise Garvin, Jim Hartnett, Frank Fan, Mei Cong, Zhi-jie Jey Cheng

Promega Corporation, Madison, WI, USA

### Background

Blockade of immune checkpoint receptors (e.g., PD-1, CTLA-4) has emerged as a promising new approach to enhance anti-tumor responses. While immunotherapies directed against PD-1 and CTLA-4 are showing unprecedented efficacy in the treatment of cancer, some patients and tumor types remain refractory to these therapies. This has resulted in a broadening of immunotherapy research and development to include additional inhibitory receptors (e.g., LAG-3, TIGIT, Tim-3) targeted individually or in combination with other immune checkpoint receptors. A major challenge in the development of biologics is access to quantitative and reproducible functional bioassays. Existing methods rely on primary cells and measurement of complex functional endpoints. These assays are cumbersome, highly variable, and fail to yield the data quality required for drug development. To address this need, we have developed a

suite of immune cell line-based bioluminescent reporter bioassays for individual and combination immune checkpoint immunotherapy targets including PD-1 (PD-L1 or PD-L2), CTLA-4, LAG-3, TIGIT, PD-1+TIGIT and more.

### Methods

These reporter-based bioassays were rationally designed to reflect the mechanism of action (MOA) of drug candidates targeting individual and combination immune checkpoint receptors. Each assay consists of an effector cell and an artificial antigen presenting cell (aAPC). Effector cell lines were engineered on a T cell background to express inhibitory receptor(s) and a luciferase reporter driven by specific response elements under the precise control of intracellular signals mediated by the T cell receptor (TCR) and inhibitory receptor target(s). The aAPCs were specially engineered to be able to activate the TCR in an antigen-independent manner and also stably express the ligand(s) of checkpoint receptor(s). These cell lines were developed in Thaw-and-Use format and can be used in assays without cell culture.

### Results

Upon co-culture of effector cells with aAPCs, TCR activation in effector cells is suppressed by signaling from immune checkpoint receptor(s), which can then be specifically reversed by blocking antibodies targeting the inhibitory receptor(s) and/or their ligand(s). The bioassays were demonstrated to be specific to research-grade antibodies with known blocking activity as well as FDA-approved drugs (e.g., nivolumab, ipilimumab). In addition, the bioassays are pre-qualified according to ICH guidelines and demonstrate the performance required for use in antibody screening, potency testing and stability studies.

### Conclusions

We have developed a suite of MOA-based bioassays for immune checkpoint receptors. These assays are easy to use and demonstrate high assay specificity, sensitivity and reproducibility. They are suitable for drug development in a quality-controlled environment.

182

### Costimulatory T cell engagement by PRS-343, a CD137 (4-1BB)/HER2 bispecific, leads to tumor growth inhibition and tumor-localized CD8+ T cell expansion in a humanized mouse model

*Marlon J Hinner*<sup>1</sup>, Rachida-Siham Bel Aiba<sup>1</sup>, Corinna Schlosser<sup>1</sup>, Thomas Jaquin<sup>1</sup>, Andrea Allersdorfer<sup>1</sup>, Sven Berger<sup>1</sup>, Alexander Wiedenmann<sup>1</sup>, Gabriele Matschiner<sup>1</sup>, Julia Schüler<sup>2</sup>, Ulrich Moebius<sup>1</sup>, Christine Rothe<sup>1</sup>, Olwill A Shane<sup>1</sup>

<sup>1</sup>Pieris Pharmaceuticals, Inc., Freising, Bayern, Germany

<sup>2</sup>Oncotest GmbH, Freiburg, Baden-Wuerttemberg, Germany



## Coinhibition and Costimulation

Presenting author underlined; Primary author in italics

### Background

CD137 (4-1BB) is a key costimulatory immunoreceptor and a highly promising therapeutic target in cancer. To overcome limitations of current mAb-based approaches which monospecifically target CD137, we generated PRS-343, a CD137/HER2 bispecific designed to promote CD137 clustering by bridging CD137-positive T cells with HER2-positive tumor cells, thereby providing a potent costimulatory signal to tumor antigen-specific T cells.

### Methods

We have previously described the generation of PRS-343 as a fusion of a CD137-specific Anticalin® protein to a variant of the HER2-targeting monoclonal antibody trastuzumab with an engineered IgG4 backbone. PRS-343 was found to efficiently activate T cells *ex vivo* in the presence of HER2-positive cells. Here, *in vivo* proof of concept data is presented utilizing a humanized mouse model in immunocompromised mice and the SK-OV-3 cell line as a HER2-positive xenograft. Tumor-bearing mice received human PBMC and weekly injections of PRS-343 for three weeks. An IgG4 isotype antibody served as the negative control, while a CD137-targeting benchmark antibody and trastuzumab with an engineered IgG4 backbone (“tras-IgG4”) served as controls for monospecific targeting of CD137 and HER2, respectively.

### Results

PRS-343 activity was investigated at four different weekly doses, ranging from 4µg to 200µg. We found that PRS-343 dose-dependently led to strong tumor growth inhibition compared to treatment with the isotype control. Tumor response was accompanied by a significantly higher frequency of hCD45(+) tumor infiltrating lymphocytes (TIL) as determined by immunohistochemistry (IHC). Single IHC stainings against the T cell markers hCD3, hCD4 and hCD8 indicated that the rise in TIL frequency was due to an expansion of CD3+CD8+ T cells, while CD4+ lymphocytes remained at a low frequency both in the treatment and control groups. Interestingly, we observed neither tumor growth inhibition nor an increase in human TIL frequency with the anti-CD137 benchmark. The tras-IgG4 control was also devoid of lymphocyte infiltration into the tumor, but displayed a tumor growth inhibition comparable to PRS-343.

### Conclusions

We report potent costimulatory T cell engagement of the immunoreceptor CD137 in a HER2-dependent manner, utilizing the CD137/HER2 bispecific PRS-343. PRS-343 displays dual activity *in vivo* based on monospecific HER2-targeting and bispecific, tumor-localized costimulation of CD137. Compared to known CD137-targeting antibodies in clinical development, PRS-343 has the potential to provide a more localized activation of the immune system with higher efficacy and reduced peripheral toxicity. The positive

functional data of PRS-343 support investigation of its anti-cancer activity in clinical trials.

### 183

#### IL-2 signaling on tumor-infiltrating CD8+ T cells is not required for successful 4-1BB combination immunotherapy

Brendan Horton<sup>1</sup>, Stefani Spranger<sup>2</sup>, Thomas F Gajewski<sup>3</sup>

<sup>1</sup>University of Chicago, Chicago, IL, USA

<sup>2</sup>The Department of Pathology, The University of Chicago, Chicago, IL, USA

<sup>3</sup>University of Chicago Medical Center, Chicago, IL, USA

### Background

Antibodies against the PD-1/PD-L1 pathway have yielded impressive clinical results; however, not all patients benefit from these treatments, and many experience only partial responses. There is therefore a continued interest in developing new strategies to further boost anti-tumor immune responses and maximize therapeutic efficacy. CD8<sup>+</sup> Tumor infiltrating lymphocytes (TIL) in both human and mouse tumors have been shown to express the co-stimulatory molecule 4-1BB. In addition to PD-1, 4-1BB agonists can induce tumor regression in pre-clinical models that is further boosted by anti-PD-L1 mAbs, but the detailed mechanism remains unclear.

### Methods

We utilized the murine melanoma cell line B16, expressing the model antigen SIY, implanted subcutaneously into syngeneic C57BL/6 mice for these experiments.

### Results

To determine if TIL already present in the tumor were sufficient for tumor regression, we utilized the S1P inhibitor FTY720. Therapeutic efficacy was preserved when anti-41BB combination immunotherapy was administered with FTY720, arguing it works directly on T cells in the tumor microenvironment. A markedly augmented number of antigen-specific CD8<sup>+</sup> TIL occurred after combination immunotherapy even with FTY720 administration, arguing that antigen-specific TIL were expanded directly in the tumor microenvironment. To assess the mechanism of TIL accumulation, we performed BrdU labeling to measure proliferation, and detection of active caspase-3 to measure apoptosis. Unexpectedly, we found that proliferation of CD8<sup>+</sup> TIL was not affected by combination immunotherapy. Instead, a significant decrease of active caspase-3 levels occurred in CD8<sup>+</sup> TIL after immunotherapy, arguing that the accumulation of antigen specific TIL was due to decreased apoptosis. To further study the molecular mechanism of intratumoral TIL accumulation, we performed a gene expression profiling on untreated and immunotherapy-





## Coinhibition and Costimulation

*Presenting author underlined; Primary author in italics*

treated CD8<sup>+</sup> TIL. Pathway analysis revealed that IL-2 and NF- $\kappa$ B were major hubs of differentially regulated genes. Consistently, we found increased IL-2 production in CD8<sup>+</sup> TIL after immunotherapy. Therefore, we tested if T cell-intrinsic IL-2 signaling within the tumor site was required for successful immunotherapy. Intratumoral antibody-mediated blockade of IL-2 did not decrease the efficacy of combination immunotherapy. Mixed bone marrow chimeras of wild type (WT) and CD25<sup>-/-</sup> bone marrow confirmed that there was no defect in CD25<sup>-/-</sup> CD8<sup>+</sup> TIL accumulation after immunotherapy.

### Conclusions

These results suggest that restored IL-2 production by TIL is a marker of successful immunotherapy but is not required for therapeutic efficacy. Current studies are focusing on the role of T cell-intrinsic NF- $\kappa$ B signaling in successful combination immunotherapies that utilize agonist 4-1BB antibodies.

184

### Dual function STAT3 inhibitor (CpG-STAT3ASO) generates systemic antitumor immune responses resulting in eradication of bone-localized prostate tumors in mice

*Dayson Moreira*, Tomasz Adamus, Xingli Zhao, Piotr Swiderski, Sumanta Pal, Marcin Kortylewski

City of Hope, Duarte, CA, USA

### Background

STAT3 transcription factor promotes prostate cancer progression and sustains potently immunosuppressive tumor microenvironment. STAT3 activity in both cancer cells and in tumor-associated immune cells is likely responsible for resistance of metastatic prostate cancers to current treatments, including immunotherapy.

### Methods

We previously demonstrated that ligands for endosomal Toll-like Receptor 9 (TLR9), CpG oligonucleotides, allow for cell-selective delivery of therapeutics to TLR9<sup>+</sup> myeloid immune cells and tumor-propagating cells in prostate cancers. Here, we describe new CpG-conjugated STAT3 antisense oligonucleotides (ASO), chemically modified for improved nuclease resistance ( $T_{1/2}$  = 106 h in human serum).

### Results

CpG-STAT3ASOs are quickly and efficiently internalized by human (DU145, LN-TLR9) and mouse (Myc-CaP, Ras/Myc-driven RM9) prostate cancer cells as well as by TLR9<sup>+</sup> immune cells, including polymorphonuclear myeloid-derived suppressor cells (PMN-MDCs) derived from blood of prostate cancer patients. In contrast to STAT3ASO alone, the naked CpG-STAT3ASO was internalized by rapid scavenger receptor-mediated mechanism even at low concentrations. Correspondingly, CpG-STAT3ASOs showed

improved potency of STAT3 knockdown at mRNA and protein levels in target cells. As assessed by biodistribution studies in mice, the intravenous (IV) injections of fluorescently-labeled CpG-STAT3ASO<sup>Cy3</sup> effectively targeted TLR9<sup>+</sup> myeloid cells and cancer cells in organs, such as spleen and bone marrow. For efficacy studies, we used syngeneic (RM9) and xenotransplanted (LN-TLR9, DU145), castration-resistant prostate tumors implanted intratibially in mice. Repeated IV injections of 5 mg/kg CpG-STAT3ASO resulted in regression of bone-localized RM9 tumors while treatments using STAT3ASO alone or CpG-scrambled ODN failed to control tumor progression. Antitumor effects of CpG-STAT3ASO depended on combination of direct and immune mediated cancer cell killing as suggested by reduced antitumor efficacy in xenotransplanted tumor models in immunodeficient mice. Both STAT3ASO and CpG-STAT3ASO reduced STAT3 activity in tumor and tumor-associated immune cells, but only the latter resulted in tumor infiltration by neutrophils and T cells. These effects were associated with reduced PD-L1 expression on MDSCs and the reduced percentage of regulatory T cells. Our preliminary results using blood samples from prostate cancer patients' suggest that CpG-STAT3ASO effectively alleviates tolerogenic effects of human PMN-MDCs on T cell activity.

### Conclusions

Overall, our strategy allows for two-pronged targeting of metastatic, castration-resistant prostate cancers using safer and more efficient reagents based on TLR9-targeted oligonucleotide delivery.

185

### A nanoparticle based approach for optimizing T cell activation, signaling, and proliferation for adoptive immunotherapy

*Alyssa Kosmides*<sup>1</sup>, Kevin Necochea<sup>2</sup>, Jonathan Schneck<sup>3</sup>

<sup>1</sup>Johns Hopkins School of Medicine, Baltimore, MD, USA

<sup>2</sup>Johns Hopkins, Irvine, CA, USA

<sup>3</sup>Johns Hopkins Medical Institute, Baltimore, MD, USA

### Background

Artificial antigen presenting cells (aAPCs) are platforms that present the two necessary signals for T cell activation. Traditionally, aAPCs have signaling molecules randomly dispersed on their surface, although data has shown the importance of nanoscale signal organization and costimulatory molecule choice on stimulation [1]. Traditional aAPCs are thus inefficient for studying the dynamics of T cell activation. Here, we have developed a novel platform where signal 1 and 2 molecules are on distinct nanoparticles that are co-clustered on the T cell surface within a magnetic field. By manipulating nanoparticle properties and the types of co-

## Coinhibition and Costimulation

Presenting author underlined; Primary author in italics

stimulatory molecules, we show the benefit of this platform as a tool to study T cell stimulation.

### Methods

Iron-dextran or polystyrene particles were conjugated with signal 1 peptide-MHC and signal 2 anti-CD28 mAb either on the same or separate 30-4500nm particles. Murine CD8+ cells were stimulated with nanoparticles and a 0.2T magnetic field. Activation was measured by cell proliferation, cytokine secretion, and cytotoxicity.

### Results

We first showed that signal 1 and 2 can be separated onto distinct particles when these particles are clustered within a magnetic field (Figure 1a). The resultant CD8+ T cells have equivalent cytotoxicity as compared to cells stimulated with traditional aAPCs (Figure 1b). T cell activation is dependent on the co-clustering of both signaling molecules – when either is presented on a non-paramagnetic polystyrene particle, proliferation is decreased (Figure 2a). The two signaling molecules also must be clustered sufficiently close, at the scale of tens of nanometers, as there was an inverse correlation between particle size and T cell proliferation (Figure 2b). Finally, signal separation allows for greater enrichment of the clonal T cell subsets using signal 1 only particles, and thus greater activation over the same time period after the addition of signal 2 particles and a magnetic field. Signal separation also allows for easy optimization of signal 2 type and ratio (preliminary data not shown).

### Conclusions

Here, we have demonstrated a novel T cell activation platform that involves simpler aAPC synthesis without sacrificing activation potential. This platform enables the study of the clustering of signaling molecules as well as easy manipulation of the types and ratios of different co-stimulatory signals.

### Acknowledgements

AKK thanks the NSF (DGE-1232825), JHU INBT (2T32CA153952-06), and NCI (F31CA206344) for fellowship support.

### References

1. Perica K, *et al*: **Magnetic Field-Induced T Cell Receptor Clustering by Nanoparticles Enhances T Cell Activation and Stimulates Antitumor Activity.** *ACS Nano* 2014, **8**(3):2252-2260.

### Novel platform activates CD8+ T cells equivalently to traditional aAPCs

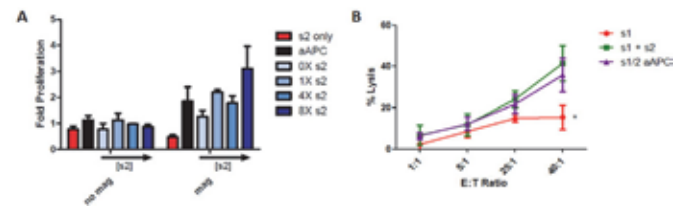


Figure 1. A) TCR transgenic PMEL CD8+ T cells were stimulated for 7 days with Db-gp100 signal 1 only particles with increasing molar doses of anti-CD28 signal 2 (s2) only particles (i.e. 2X = 2:1 molar excess signal 2). aAPC refers to traditional signal 1 and 2 aAPCs. Cells were incubated in the presence or absence of a magnetic field for the first three days, and cell counts were taken on day 7. B) PMEL CD8+ T cells were stimulated for 7 days with signal 1 (s1) only particles, signal 1 and 2 on separate particles (s1 + s2), or signal 1 and 2 on the same particle (s1/2 aAPC). After 7 days, T cell mediated killing of target B16-F10 cells was measured (\* $p < 0.05$  by two-way ANOVA).

### Signal 1 and 2 co-clustering is necessary for CD8+ T cell activation

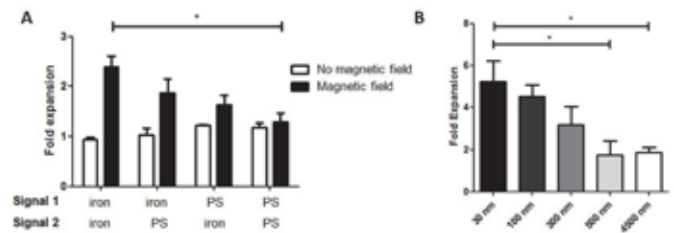
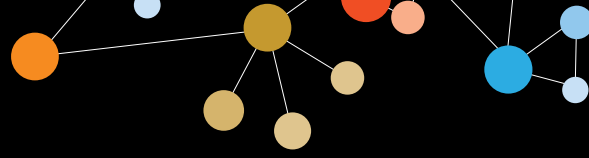


Figure 2. A) Db-gp100 signal 1 and anti-CD28 signal 2 mAbs were conjugated to the surface of 100 nm iron dextran or polystyrene nanoparticles. PMEL CD8+ T cells were stimulated with different combinations of these particles in the presence or absence of a magnetic field, and cell counts were taken after 7 days (\* $p < 0.05$  by two-way ANOVA). B) PMEL CD8+ T cells were stimulated with signal 1 and 2 on separate iron-dextran particles of increasing size within a magnetic field. Cell counts were taken after 7 days (\* $p < 0.05$  by one-way ANOVA).



## Coinhibition and Costimulation

Presenting author underlined; Primary author in italics

### 186 Abstract Travel Award Recipient

#### **A secreted PD-L1 splice variant expressed across tumor types inhibits lymphocyte function**

Kathleen M Mahoney<sup>1</sup>, Sachet A Shukla<sup>2</sup>, Nikolaos Patsoukis<sup>3</sup>, Apoorvi Chaudhri<sup>2</sup>, Hung Pham<sup>2</sup>, Ping Hua<sup>2</sup>, Xia Bu<sup>2</sup>, Baogong Zhu<sup>2</sup>, Nir Hacohen<sup>4</sup>, Catherine J Wu<sup>2</sup>, Edward Fritsch<sup>5</sup>, Vassiliki A Boussiotis<sup>3</sup>, Gordon J Freeman<sup>2</sup>

<sup>1</sup>Beth Israel Deaconess Medical Center, Dana-Farber Cancer Institute, Boston, MA, USA

<sup>2</sup>Dana-Farber Cancer Institute, Boston, MA, USA

<sup>3</sup>Beth Israel Deaconess Medical Center, Boston, MA, USA

<sup>4</sup>Massachusetts General Hospital, Boston, MA, USA

<sup>5</sup>Neon Therapeutics, Inc., Cambridge, MA, USA

#### **Background**

Targeting immune checkpoint pathways, such as programmed death ligand-1 (PD-L1, also known as CD274 or B7-H1) or its receptor programmed cell death-1 (PD-1) have shown clinical benefit in patients with many different types of tumors. While PD-L1 expression is not a reliable biomarker for predicting response to therapy, the expression of the coinhibitory molecule PD-L1 on the surface of tumor cells is associated with worse prognosis in many tumors. This negative effect of PD-L1 expression is seen even when only a small fraction of the tumor expressed PD-L1 on the tumor cell surface. Here we describe a splice variant (secPD-L1) that does not splice into the transmembrane domain, producing a secreted form of PD-L1.

#### **Methods**

Lymphoma, kidney and breast cancer cell lines were analyzed for full length and secPD-L1 mRNA expression by qRT-PCR. RNASeq analysis in the Cancer Cell Line Encyclopedia confirmed expression of secPD-L1 in human tumor cell lines. RNASeq analysis of full-length PD-L1 and secPD-L1 was performed on The Cancer Genome Atlas, the GTEx database of non-malignant human tissue and sorted immune cells from healthy donors. Monocyte-derived dendritic cells were generated from healthy donors, stimulated with TNF $\alpha$ /PGE, polyI:C, or LPS and assayed for expression of full-length PD-L1 and secPD-L1. Recombinant His-tagged secPD-L1 was produced to test whether it functioned as an inhibitor of proliferation and IFN $\gamma$  production in coactivation assays with T lymphocytes isolated from healthy donors.

#### **Results**

The secPD-L1 variant is expressed by cancer cell lines that also express the full-length PD-L1, as well as non-malignant immune cells particularly activated monocyte-derived dendritic cells. In The Cancer Genome Atlas, expression of secPD-L1 is found in primary tumors with higher expression of full-length PD-L1. Furthermore using recombinant

secPD-L1 we found that secPD-L1 contains a unique 18 amino acid tail containing a cysteine and can dimerize, and inhibit T cell proliferation and IFN- $\gamma$  production *in vitro*.

#### **Conclusions**

This is the first report that a secreted splice variant of PD-L1 is expressed in a subset of many types of tumors, homodimerizes and is functionally active. Since secPD-L1 does not require cell-to-cell interaction to mediate its inhibitory effect, it may function as a paracrine negative immune regulator within the tumor microenvironment.

#### **Acknowledgements**

2014 AACR Basic Cancer Research Fellowship, Grant Number 14-40-01-MAHO, the 2014 ASCO Young Investigator Award supported by Kidney Cancer Association, and Claudia Adams Barr Program for Innovative Cancer Research (KMM); DF/HCC Kidney Cancer SPORE P50CA101942.

### 187

#### **Combined targeting of OX40 and PD-L1 metabolically reprograms T cells promote regression of large established tumors**

Amy E Moran<sup>1</sup>, Fanny Polesso<sup>1</sup>, Lisa Lukaesko<sup>2</sup>, Andrew Weinberg<sup>1</sup>

<sup>1</sup>Earle A. Chiles Research Institute, Providence Cancer Center, Portland, OR, USA

<sup>2</sup>Oregon Health & Science University, Portland, OR, USA

#### **Background**

The protective capability of tumor antigen specific T cells is regulated by both co-stimulatory and inhibitory signals in the tumor microenvironment. Current approaches in cancer immunotherapy seek to restore the function of unresponsive T cells by blocking inhibitory pathways. However, providing exogenous co-stimulatory signals are showing clinical promise and provide novel approaches for combination therapy.

#### **Methods**

Multiple solid tumor mouse models in multiple different mouse strains were used (MCA205/B6, CT26/Balb/C, d42m1T3/129) to determine the synergy of aOX40 (clone OX86) with aPD-L1 (clone 10F.9G2) in large, established tumors. Tumors were allowed to grow until they were ~50-70mm<sup>2</sup> before treatment began. Animals were treated either alone or concurrently with 250 $\mu$ g aOX40 or 200 $\mu$ g aPD-L1 for a total of 500 $\mu$ g aOX40 and 600 $\mu$ g aPD-L1. Animals were euthanized and T cells isolated from secondary lymphoid organs and tumors. T cells were sorted for TCR $\beta$  chain sequencing based on Nur77GFP expression and or Foxp3RFP expression. TCR $\beta$  chain sequencing was performed by Adaptive Biotechnologies. T cell metabolic function was

## Coinhibition and Costimulation

*Presenting author underlined; Primary author in italics*

assessed using 2NBDG and TMRE as well as a Seahorse Analyzer. Phenotyping and functional assays were performed using traditional methods of flow cytometry.

### Results

We demonstrate for the first time that agonist OX40 monoclonal antibodies metabolically reprogram CD4 Th1 skewed and CD8 effector T cells. In addition, using tetramers to track tumor-antigen specific CD8 T cells, we observe a significant expansion of effector memory CD8 T cells with enhanced cytotoxic function. Moreover, despite increased regulatory T cell (Treg) proliferation in the periphery, the CD8/Treg and CD4/Treg ratio is significantly increased in the blood and tumor of combination therapy treated animals. Furthermore, using a TCR signal strength reporter system, we observed the clonal expansion of a number of tumor infiltrating CD8 T cells that were actively receiving strong TCR signals *in situ*. Unlike aOX40 or aPD-L1 alone, combination immunotherapy focused the CD8 T cell repertoire response such that the 10 most frequent clones within the tumor made up almost 40% of the total CD8 T cell response.

### Conclusions

Our findings suggest that concurrently targeting both positive (OX40) and negative (the PD-1/PD-L1 axis) T cell pathways can restore the function of failed tumor antigen specific T cells and promote tumor regression of well established tumors.

188

### Characterization of infiltrating lymphocytes in benign, malignant, and healthy prostate tissue

Emelie Rådestad<sup>1</sup>, Lars Egevad<sup>1</sup>, Jonas Mattsson<sup>1</sup>, Berit Sundberg<sup>1</sup>, Lars Henningsohn<sup>1</sup>, Victor Levitsky<sup>2</sup>, Michael Uhlin<sup>1</sup>

<sup>1</sup>Karolinska Institutet, Stockholm, Stockholms Lan, Sweden

<sup>2</sup>Molecular Partners, Schlieren-Zurich, Zurich, Switzerland

### Background

Prostate cancer (PC) is the second most common cancer type among men worldwide. Other non-malignant conditions of the prostate, such as benign prostatic hyperplasia (BPH), affect a majority of the older male population. Furthermore, chronic prostatic inflammation is common and is discussed to be a potential driver of benign and malignant prostate conditions. We aimed to compare the phenotype of lymphocytes present in prostates without pathologic changes with those infiltrating PC or BPH lesions, focusing on characterization of co-inhibitory receptor expression.

### Methods

Lymphocytes were isolated from prostates of patients with PC (n=5), BPH (n=31), and deceased transplantation

donors (n=5). Two tissue samples per PC patient were processed, one primary malignant and one adjacent non-malignant. Prostate-infiltrating lymphocytes were isolated using mechanical dissociation followed by density gradient centrifugation and flow cytometric analysis.

### Results

Analysis showed that the majority of prostate-infiltrating T cells in all prostate conditions were CD8<sup>+</sup> and had a CD45RO<sup>+</sup>CCR7<sup>-</sup> effector memory phenotype. The ratio of CD4<sup>+</sup>/CD8<sup>+</sup> T cells was comparable in all conditions, except BPH, where it was slightly higher than in healthy prostates. T cells expressing CD25 were more abundant in prostate tissue of PC patients (median 13.7% at malignant site, 15.1% at non-malignant site) and BPH (13.6%) compared to healthy controls (3.3%). Analysis of co-inhibitory receptor expression revealed that PD-1 was expressed by a larger proportion of T cells in PC specimens (71.0%, 60.0%) than in BPH (34.6%) and control prostates (47.2%). The opposite was found for LAG-3, which was expressed by a larger proportion of T cells in BPH (18.1%) than in PC (8.6%, 2.6%). Median frequency in control prostates was 13.1%. There were no differences between the sample types regarding frequencies of T cells expressing TIM-3 or CTLA-4, nor in quantity of Tregs or  $\gamma\delta$  T cells. Compared to peripheral blood, the frequency of Tregs was significantly higher in all prostate tissue types; 17.0%, 16.6%, 16.5% and 20.5% in control, BPH, malignant and non-malignant site compared to 7.2% and 5.4% in blood of BPH and PC patients.

### Conclusions

Many prostate-infiltrating T cells seem to express co-inhibitory receptors LAG-3 and PD-1, regardless of prostate condition. Furthermore, presence of Tregs does not seem to be unique to the PC environment. However, we did find an increased frequency of T cells expressing PD-1 in PC lesions. It is of great importance to elucidate expression of co-inhibitory receptors for different solid cancers to narrow down patient groups that might benefit from different immunotherapies.

189

### Understanding the therapeutic effectiveness of alloreactive immune responses in both murine and human acute myeloid leukemia during nonegraftment cellular therapy

William Rafelson<sup>1</sup>, John L Reagan<sup>2</sup>, Loren Fast<sup>2</sup>

<sup>1</sup>Rhode Island Hospital, Warren Alpert School of Medicine, Brown University, Providence, RI, USA

<sup>2</sup>Warren Alpert School of Medicine, Brown University, Providence, RI, USA

### Background

In stem cell transplant, few have studied the recipient lymphocytes' recognition of mismatched donor antigens





## Coinhibition and Costimulation

*Presenting author underlined; Primary author in italics*

and MHC molecules, and how these primed host T cells may then recognize and kill leukemic cells. Previously, our group infused haploidentical, G-CSF mobilized, donor T cells into patients with refractory hematological malignancies preconditioned with 100cGy total body irradiation. Strong recipient immune responses, with some durable remissions, were seen in hematologic malignancies. In a second trial without G-CSF mobilization or recipient radiation, patients exhibited weaker inflammatory and anti-leukemic responses [1]. We therefore decided to characterize the alloreactive antileukemic response in a murine preclinical model with the AML leukemic cell line, C1498.

### Methods

B6D2F1 mice were injected with C1498 leukemic cells and subsequently on day 7 were injected with haploidentical spleen cells from C57BL/6 mice. They were then monitored for signs of tumor progression and euthanized when they became moribund. T lymphocytes obtained from these euthanized mice were also tested for their ability to generate anti-C1498 responses when stimulated with haploidentical stimulator cells. We performed *in vitro* experiments whereby healthy B6D2F1 splenocytes were stimulated with mitomycin-treated haploidentical spleen cells from a C57BL/6 mouse, and grown in mixed lymphocyte culture and tested on day 5 for their ability to lyse Cr51-labeled syngeneic blasts and C1498 leukemic target cells.

### Results

Results of the murine model demonstrated the ability of alloreactive cytolytic T lymphocytes to lyse C1498 leukemic cells but not syngeneic blast cells. In addition, isolated CD3+ cells obtained from C1498 bearing mice were able to generate anti-C1498 lytic activity when stimulated with haploidentical cells *in vitro*. These responses are being explored further *in vivo*.

### Conclusions

In previous trials, increased PD-1 expression in recipients following initial markers of T cell activation suggest that T cell exhaustion mediates leukemic cell survival. Increased PD-L1 expression on leukemic cells provides one explanation for their eluding the host inflammatory response. Total body irradiation may be disrupting the equilibrium of host-tumor tolerance. G-CSF mobilization of donor lymphocytes increases donor antigens for host recognition and subsequent alloreactivity. The murine model shows that alloreactive T cells can generate lysis specific to tumor but not self antigens. This model of alloreactive tumor response can be explored as an adjuvant therapy to other therapeutic approaches, including checkpoint inhibition.

### Acknowledgements

NIH/NRSA funding is acknowledged in this study.

### References

1. Reagan JL, Fast LD, Nevola M, *et al*: **Nonengraftment donor lymphocyte infusions for refractory acute myeloid leukemia.** *Blood Cancer J* 2015, **5**:e371.

### 190

#### **First-in-class orally bioavailable checkpoint inhibitors targeting single and multiple immune inhibitory pathways**

*Pottayil Sasikumar*, Naremaddepalli Sudarshan, Raghuvver Ramachandra, Nagesh Gowda, Dodheri Samiulla, Talapaneni Chandrasekhar, Sreenivas Adurthi, Jiju Mani, Rashmi Nair, Amit Dhudashia, Nagaraj Gowda, Murali Ramachandra

Aurigene Discovery Technologies Limited, Bangalore, Karnataka, India

#### **Background**

Immune checkpoint inhibitors have changed the landscape of cancer therapy with the general acceptance that they will be the mainstay of future therapies. This is evident from a large number of ongoing clinical trials evaluating checkpoint inhibitors as a single agent or in combination with other therapeutic modalities. While these antibody-based therapies show impressive clinical activity, they suffer from the shortcomings including the failure to show responses in a majority of patients, immune-related adverse events (irAEs) due to the breaking of immune self-tolerance and need to administer by intravenous injection. The recent reports on severe demyelinating polyradiculoneuropathy leading to death observed in two patients with the anti-PD-1 immunotherapy also point to the need for short-acting agents for the better management of irAEs. Towards addressing these shortcomings, we are developing small molecule agents targeting one or more immune checkpoint pathways to increase the response rate and dosing by oral route with relatively shorter pharmacokinetic exposure.

#### **Methods**

We at Aurigene have devised a strategy to identify agents targeting single or multiple immune checkpoint proteins by taking advantage of the sequence/structural similarities among immune checkpoint ligands and receptors. In this strategy, high affinity shortest pharmacophore derived from the extracellular domain of checkpoint proteins are first identified and transformed into therapeutic agents with optimized drug-like properties. Our strategy has resulted in the identification of agents targeting PD-L1 alone, VISTA alone, PD-L1 and VISTA, and PD-L1 and TIM-3. The first compound from this approach AUPM-170/CA-170, a first-in-class dual antagonist targeting PD-L1 and VISTA, is undergoing clinical trials.



## Coinhibition and Costimulation

Presenting author underlined; Primary author in italics

### Results

Herein we report the pharmacological evaluation of another novel small molecule antagonist dually antagonizing PD-L1 and TIM-3 pathways. Potent functional activity comparable to that obtained with an anti-PD-1 or anti-TIM-3 antibody in rescuing T cell proliferation and effector functions was observed with the lead compound, AUPM-327. AUPM-327 showed selectivity against other immune checkpoint proteins as well as in a broad panel of receptors and enzymes. In preclinical models of melanoma, breast and colon cancers, AUPM-327 showed significant efficacy in inhibition of tumor growth upon oral dosing with excellent tolerability.

### Conclusions

These findings support further development of AUPM-327 in the clinic.

### 191

#### A new target for immune checkpoint inhibition in urothelial carcinoma

Alexander Sankin, Benjamin Gartrell, Kerwin Cumberbatch, Hongying Huang, Joshua Stern, Mark Schoenberg, Xingxing Zang

Montefiore Medical Center, Bronx, NY, USA

### Background

Tumor cells evade immune surveillance by expressing cell surface ligands such as PD-L1 that are known to disrupt normal T cell function. Inhibition of these immunologic checkpoints has led to durable clinical remissions in metastatic melanoma, lung cancer, and bladder cancer [1-3]. We have recently described a new checkpoint family member HHLA2 that plays a significant role in inhibiting T cell activity [4]. We sought to characterize HHLA2 expression patterns in human urothelial carcinoma.

### Methods

After obtaining IRB approval, we identified urothelial tumor cases from our institutional database and obtained paraffin-embedded tissue specimens originating from either transurethral resections (TUR) or radical cystectomies. A validated immunohistochemistry (IHC) protocol for HHLA2 staining has been previously described by the authors [4]. Tumor slides were examined by a single pathologist with no prior knowledge of patient clinical characteristics. Tumors were considered positive for HHLA2 expression (HHLA2+) if the number of positively stained tumor cells exceeded 1/100.

### Results

We identified 46 urothelial tumor specimens with adequate tissue for staining (Table 1). 37/46 (80%) specimens were obtained from TUR and 9/46 (20%) were obtained from radical cystectomy. Our cohort was enriched with aggressive

tumor characteristics, specifically 45/46 (98%) were high grade, 34/46 (76%) were stage pT2 or higher, and 15/46 (33%) had metastases to lymph nodes and/or distant organs. HHLA2 was expressed in 28/46 (61%) tumors (Figure 1).

### Conclusions

This is the first study to demonstrate a robust expression pattern of the newly discovered immune checkpoint ligand HHLA2 in human urothelial tumors. Future studies will need to be conducted to further characterize the functional role of HHLA2 in bladder cancer immune evasion pathways and to develop therapeutic strategies to enhance immune mediated tumor destruction.

### References

1. Brahmer JR, Tykodi SS, Chow LQ, Hwu WJ, Topalian SL, Hwu P, *et al*: **Safety and activity of anti-PD-L1 antibody in patients with advanced cancer.** *N Engl J Med* 2012, **366(26)**:2455-2465.
2. Powles T, Eder JP, Fine GD, Braiteh FS, Loriot Y, Cruz C, *et al*: **MPDL3280A (anti-PD-L1) treatment leads to clinical activity in metastatic bladder cancer.** *Nature* 2014, **515(7528)**:558-562.
3. Topalian SL, Hodi FS, Brahmer JR, Gettinger SN, Smith DC, McDermott DF, *et al*: **Safety, activity, and immune correlates of anti-PD-1 antibody in cancer.** *N Engl J Med* 2012, **366(26)**:2443-2454.
4. Zhao R, Chinai JM, Buhl S, Scandiuzzi L, Ray A, Jeon H, *et al*: **HHLA2 is a member of the B7 family and inhibits human CD4 and CD8 T-cell function.** *Proc Natl Acad Sci* 2013, **110(24)**:9879-9884.

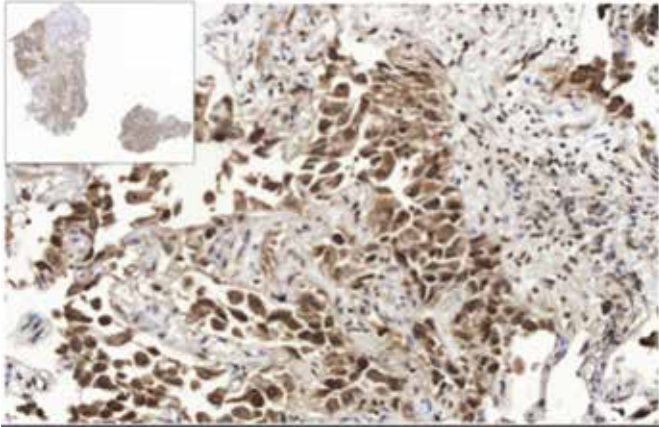
**Table 1. Clinicopathologic characteristics of patients by HHLA2 staining status**

	Total (n=46)	HHLA2+ (n=28)	HHLA2- (n=18)
Median age	75	75	74
Gender (%)			
Male	34 (74%)	19 (68%)	15 (83%)
Female	12 (26%)	9 (32%)	3 (17%)
Specimen type (%)			
TUR	37 (80%)	27 (96%)	10 (56%)
Cystectomy	9 (20%)	1 (4%)	8 (44%)
Grade (%)			
Low	1 (2%)	1 (4%)	0 (0%)
High	45 (98%)	27 (96%)	18 (100%)
Tumor stage (%)			
Ta	1 (2%)	1 (4%)	0 (0%)
T1	11 (24%)	10 (36%)	1 (6%)
T2	20 (43%)	10 (36%)	10 (56%)
T3	11 (24%)	6 (21%)	5 (28%)
T4	3 (7%)	1 (4%)	2 (11%)
Metastasis (%)			
None	31 (67%)	18 (64%)	13 (72%)
N1-3 or M1	15 (33%)	10 (36%)	5 (28%)
Concomitant CS (%)			
Yes	8 (17%)	4 (14%)	4 (22%)
No	38 (83%)	24 (86%)	14 (78%)

## Coinhibition and Costimulation

Presenting author underlined; Primary author in italics

**Figure 1. Example of a human urothelial tumor that expresses HHLA2**



192

### Therapeutic T cell activation using engineered variant IgSF domains

Ryan Swanson, Michael Kornacker, Lawrence Evans, Erika Rickel, Martin Wolfson

Alpine Immune Sciences, Seattle, WA, USA

#### Background

The large number of immunoglobulin super family (IgSF) receptors on immune cells and tumors are attractive targets for the development of cancer immunotherapies. While nearly all commercial strategies targeting this family are focused on antibody-based biologics, we have developed a novel affinity ligand platform based upon yeast affinity maturation of human IgSF family extracellular domains (ECDs), which we term variant Ig Domains (vIgDs). vIgDs unique biochemical properties, including small size, monomeric/single domain structure, and capacity to interact with multiple counterstructures, combined with the near universal expression of IgSF family members and their counterstructures on immune cells and tumors, position the vIgD platform as an exciting new option for development of immuno-oncology biologics with first-in-class mechanisms of action.

#### Methods

IgSF domains of interest were mutagenized and cloned as yeast display libraries. Soluble counterstructure ligands were used to stain the display libraries, and yeast clones exhibiting the highest binding were isolated by flow cytometry sorting. vIgDs from the sorting outputs were subcloned into a mammalian Fc fusion expression vector, and individual vIgD-Fc fusions were recombinantly expressed in HEK293 cells. Purified preparations of vIgD-Fc fusions were used to stain eukaryotic cells transfected to surface express the

target counterstructure. vIgD-Fc fusion proteins possessing desirable binding properties were tested for functional activity using *in vitro* assays with human primary T cells.

#### Results

Random and rationally designed mutant vIgD libraries were stained with counterstructure ligands and successfully sorted to isolate vIgDs with increased binding to the target counterstructures as demonstrated by elevated binding curves of successive selection outputs. vIgDs were expressed as recombinant Fc fusion protein constructs and demonstrated superior binding of transfectants expressing counterstructures compared to their parental wild-type IgSF domain Fc fusion protein. The resulting variants also demonstrated superior costimulatory activity when co-immobilized with anti-CD3 in human primary T cells.

#### Conclusions

Receptors built from IgSF domains are critical orchestrators of cellular communication in the immune system. However, IgSF receptors typically exhibit relatively low affinities for their target counterstructures, prohibiting their use as oncology therapeutics. Engineering of IgSF domains using yeast display affinity maturation allows the generation of variant proteins possessing superior binding to single or multiple native counterstructures. These binding improvements translate into beneficial alterations of functional activity, including improved costimulatory activity. The vIgD therapeutic platform is a new option for both development of soluble recombinant therapeutics or improvement of engineered cellular therapies.

193

### Impact of BTK/ITK inhibition with ibrutinib on neuroblastoma and osteosarcoma syngeneic solid tumor models

Sandrine Valsesia-Wittmann<sup>1</sup>, Tala Shekarian<sup>1</sup>, François Simard<sup>2</sup>, Rodrigo Nailo<sup>2</sup>, Aurélie Dutour<sup>2</sup>, Anne-Catherine Jallas<sup>1</sup>, Christophe Caux<sup>3</sup>, Aurélien Marabelle<sup>4</sup>

<sup>1</sup>Centre Leon Berard, Lyon, Rhone-Alpes, France

<sup>2</sup>Centre Leon Berard CRCL UMR Inserm 1052/CNRS 5286, Lyon, Rhone-Alpes, France

<sup>3</sup>UCBL1, Centre Leon Berard UMR Inserm 1052/CNRS 5286, Lyon, Rhone-Alpes, France

<sup>4</sup>CRCL, UMR Inserm 1052/CNRS 5286, IHOP, Centre Léon Bérard, Gustave Roussy, Université Paris-Saclay, Lyon, Rhone-Alpes, France

#### Background

Ibrutinib, a covalent inhibitor of BTK, is currently revolutionizing B cell lymphoma treatment. Most solid tumors do not express BTK. However, BTK has been identified as a critical pathway in synthetic lethality assays in MYC

## Coinhibition and Costimulation

Presenting author underlined; *Primary author in italics*

dependent tumor cell lines. Interestingly, BTK can also be expressed in myeloid cells downstream to Fcγ receptors. Also, ibrutinib inhibits interleukin-2-inducible T cell kinase (ITK), with potential ability to shift the balance from Th2 to Th1 T cells. Therefore, ibrutinib might have immunomodulatory effects in addition to its direct effects on cancer cells.

Interestingly, aggressive MYCN amplified neuroblastoma (NB) are also highly infiltrated by myeloid cells. In osteosarcoma (OS), osteoclasts are derived from myeloid lineage. Thus, BTK blockade could be of double interest in NB and OS through both tumor- and immune-targeted effects.

### Methods

We analyzed BTK expression by quantitative RT-QPCR and FACS analysis in different NB or OS cell lines and tumors from patients. We assessed the impact of ibrutinib on macrophage differentiation assays. *In vivo* anti-tumoral ibrutinib efficacy was evaluated in a mouse transplantable NB and rat orthotopic OS syngeneic models.

### Results

High levels of BTK expression in some neuroblastoma tumor samples and variable levels of expression of BTK in patient tumor cell lines were observed. Interestingly, ibrutinib therapy had a positive impact on Neuro2A syngeneic NB models. No synergic effect of ibrutinib and anti-PD-L1 therapy could be obtained. In the rat OS model, ibrutinib had also therapeutic activity with a positive impact on growth of orthotopic bone tumors. However, we observed a negative impact of ibrutinib therapy on the number of spontaneous OS lung metastasis. Ibrutinib had no impact on the viability and differentiation of M1, M2 or Mo-DCs. However, it impaired human M1 macrophages differentiation towards a more immunosuppressive M2 phenotype with lower CD86 and CD163 expression, but no variation of HLA-DR and PD-L1. This negative effect was reversed by a TLR4 agonist.

### Conclusions

Ibrutinib therapy has shown a positive therapeutic efficacy on the growth of primary tumors of a mouse NB and rat OS syngeneic models. However, in the OS model, ibrutinib therapy resulted in a higher number of spontaneous lung metastasis. This effect could be due to a negative impact of ibrutinib on anti-tumoral M1 macrophage differentiation. However this effect can be blocked by TLR4 stimulation suggesting that combinations of ibrutinib with TLR agonists might be of interest in solid tumors.

### Acknowledgements

Pharmacyclics for providing ibrutinib.

## Combinations: Immunotherapy/Immunotherapy

Presenting author underlined; *Primary author in italics*

194

### **Rational combinations of intratumoral T cell and myeloid agonists mobilize abscopal responses in prostate cancer**

Casey Ager<sup>1</sup>, Matthew Reilley<sup>2</sup>, Courtney Nicholas<sup>1</sup>, Todd Bartkowiak<sup>1</sup>, Ashvin Jaiswal<sup>1</sup>, Michael Curran<sup>1</sup>

<sup>1</sup>Department of Immunology, University of Texas MD Anderson Cancer Center, Houston, TX, USA

<sup>2</sup>Department of Cancer Medicine, University of Texas MD Anderson Cancer Center, Houston, TX, USA

#### **Background**

Despite the success of checkpoint blockade immunotherapy in characteristically immunogenic cancers such as melanoma, these antibodies remain ineffective against poorly T cell-infiltrated malignancies including prostate cancer. Sensitizing these “cold” tumors to immunotherapy will require interventions which enhance tumor antigen presentation and T cell priming, while suppressing microenvironmental signals which constrain T cell expansion, survival, and effector function independent of coinhibitory signaling. We investigated whether intratumoral administration of either the STING agonist c-di-GMP (CDG) or dendritic cell (DC) growth factor Flt3-ligand can potentiate the therapeutic effects of T cell checkpoint modulation with  $\alpha$ CTLA-4,  $\alpha$ PD-1, and  $\alpha$ 4-1BB in a bilateral subcutaneous model of prostate adenocarcinoma. Additionally, we tested whether intratumoral delivery of low-dose checkpoint modulators with CDG at a single lesion can achieve abscopal control of distal lesions.

#### **Methods**

Male C57BL/6 mice were challenged subcutaneously on both flanks with TRAMP-C2 prostate adenocarcinoma, and treatment was administered intraperitoneally and/or intratumorally for 3 doses every 4 days, beginning on day 14 post-implantation for survival experiments or day 31 for flow analysis experiments.

#### **Results**

Intratumoral delivery of STING agonist CDG alone potently rejects all injected TRAMP-C2 tumors, but fails to generate systemic control of uninjected lesions. Systemic administration of  $\alpha$ CTLA-4,  $\alpha$ PD-1, and  $\alpha$ 4-1BB cures 40% of mice with bilateral TRAMP-C2, and concurrent administration of CDG at one or both flanks enhances survival to 75%. Similar effects are observed with intratumoral Flt3L, although administration at both flanks is required for full effect. Intratumoral low-dose  $\alpha$ CTLA-4,  $\alpha$ PD-1, and  $\alpha$ 4-1BB at a single flank induces abscopal effects in 20% of mice, and concurrent administration of CDG enhances systemic immunity to cure up to 50% of mice. We observe that the level of STING activation required to mediate rejection

without inducing ulcerative toxicity is proportional to initial tumor size. Functionally, local STING activation complements intratumoral checkpoint modulation to reduce local MDSC infiltration, enhance CD8:Treg ratios, and downregulate the M2 macrophage marker CD206. In contrast, local Flt3L robustly enhances immune infiltration of injected and distal tumors, but therapeutic benefit is attenuated due to concomitant induction of FoxP3+ Treg.

#### **Conclusions**

Intratumoral STING activation via CDG or DC expansion with Flt3L potentiates the therapeutic effects of systemically-delivered  $\alpha$ CTLA-4,  $\alpha$ PD-1, and  $\alpha$ 4-1BB against multifocal TRAMP-C2 prostate cancer. The abscopal potential of CDG alone is weak, in contrast to prior observations, but combining CDG with low-dose checkpoint blockade intratumorally can induce systemic immunity, suggesting an alternative approach for clinical implementation of combination immunotherapies at reduced doses.

195

### **Multi-genome reassortant dendritic cell-tropic vector platform (ZVex®-Multi) allows flexible co-expression of multiple antigens and immune modulators for optimal induction of anti-tumor CD8+ T cell responses**

Tina C Albershardt, Anshika Bajaj, Jacob F Archer, Rebecca S Reeves, Lisa Y Ngo, Peter Berglund, Jan ter Meulen

Immune Design, Seattle, WA, USA

#### **Background**

Induction of immune responses against multiple antigens expressed from conventional vector platforms is often ineffective for reasons not well understood. Common methods of expressing multiple antigens within a single vector construct include the use of fusion proteins, endoprotease cleavage sites, or internal ribosome entry sites. These methods often lead to decreased expression of antigens-of-interest and/or reduced induction of T cell responses against the encoded antigens. Circumventing these limitations, we have developed a novel production process for our integration-deficient, dendritic cell-targeting lentiviral vector platform, ZVex, enabling highly flexible and effective multigene delivery *in vivo*, making it possibly the most versatile vector platform in the industry.

#### **Methods**

Up to five vector genome plasmids, each encoding one full-length antigen or immuno-modulator, were mixed with four constant plasmids, each encoding vector particle proteins, prior to transfection of production cells. Due to the propensity of lentiviruses forming genomic reassortants, the resulting vector preparations hypothetically contain a mix of homozygous and heterozygous vector particles. qRT-PCR was



## Combinations: Immunotherapy/Immunotherapy

Presenting author underlined; *Primary author in italics*

used to determine total and antigen-specific titers of ZVex-Multi vectors, defined as vector genome counts. Mice were immunized with ZVex-Multi vectors or monozygous vectors expressing multiple antigens from the same backbone to compare immunogenicity via intracellular cytokine staining. Two tumor models were used to evaluate therapeutic efficacy: 1) a B16 melanoma model, where tumor cells were inoculated in the flank and measured 2-3 times per week; and 2) a metastatic CT26 colon carcinoma model, where tumor cells were inoculated intravenously, and lung nodules were enumerated 17-19 days post-tumor inoculation.

### Results

Titration by qRT-PCR of multiple ZVex-Multi vector lots demonstrated that production yields of ZVex-Multi expressing up to four different tumor-associated antigens (e.g., NY-ESO-1, MAGE-A3) and two immuno-modulators (e.g., IL-12, anti-CTLA-4 or anti-PD-L1) were highly reproducible. Compared to mice immunized with vectors expressing multiple antigens from the same backbone, mice immunized with ZVex-Multi vectors consistently developed T cells against all targeted TAAs and exhibited improved tumor growth control and survival.

### Conclusions

ZVex-Multi is a next generation DC-tropic vector platform designed to overcome limitations of single-genome vector platforms with respect to efficient co-expression of any combination of desired genes. Unlike other vector platforms, ZVex-Multi eliminates multiple cloning steps modifying the vector backbone, which can often result in unpredictable expression patterns of coded gene products. Its versatility and agility makes ZVex-Multi potentially the best-in-class vector platform for co-expression of multiple tumor antigens and immuno-modulators for enhanced cancer immunotherapy against a broad range of tumors.

196

### **NK, T cells and IFN-gamma are required for the anti-tumor efficacy of combination-treatment with NKG2A and PD-1/PD-L1 checkpoint inhibitors in preclinical models**

*Caroline Denis*<sup>1</sup>, *Hormas Ghadially*<sup>2</sup>, *Thomas Arnoux*<sup>1</sup>, *Fabien Chanuc*<sup>1</sup>, *Nicolas Fuseri*<sup>1</sup>, *Robert W Wilkinson*<sup>2</sup>, *Nicolai Wagtmann*<sup>1</sup>, *Yannis Morel*<sup>1</sup>, *Pascale Andre*<sup>1</sup>

<sup>1</sup>Innate Pharma, Marseille, Provence-Alpes-Cote d'Azur, France

<sup>2</sup>MedImmune, Cambridge, England, UK

### Background

Monalizumab (IPH2201) is a first-in-class humanized IgG<sub>4</sub> targeting NKG2A, which is expressed as heterodimer with CD94 on the surface of NK,  $\gamma\delta$ T and tumor infiltrating CD8+ T

cells. This inhibitory receptor binds to HLA-E in humans and to Qa-1<sup>b</sup> in mice. HLA-E is frequently up-regulated on cancer cells, protecting from killing by NKG2A<sup>+</sup> cells. Monalizumab blocks binding of CD94-NKG2A to HLA-E, reducing inhibitory signaling thereby enhancing NK and T cell responses. PD-1/PD-L1 inhibitors are successfully being used to treat patients with a wide variety of cancers. Combined blockade of NKG2A/HLA-E and PD-1/PD-L1 may be a promising strategy to better fight cancer by activating both the adaptive and innate immune systems.

### Methods

To assess the effect of combined blockade of NKG2A/HLA-E and PD-1/PD-L1 *in vivo*, anti-mouse NKG2A and PD-1 antibodies were used in mice engrafted with A20 mouse B lymphoma cell line. For *in vitro* assays, anti-PD-L1 antibody durvalumab, and monalizumab were tested in human PBMC staphylococcal enterotoxin b assays.

### Results

When cultured *in vitro*, the A20 cells express ligands for PD-1 but not for NKG2A. Exposure to IFN- $\gamma$  *in vitro*, or subcutaneous injection into mice, induced expression of Qa-1<sup>b</sup>, resulting in a tumor model co-expressing PD-L1 and Qa-1<sup>b</sup>. Monotherapy with PD-1 or NKG2A blockers resulted in moderate anti-tumor efficacy while treatment with combination of NKG2A and PD-1 blockers resulted in a significantly higher anti-tumor immunity, and an increased rate of complete tumor regression. Depletion of either NK, or CD8+ T cells, or IFN- $\gamma$  was enough to abrogate the efficacy of PD-1 and NKG2A blockade, indicating that both of these effector populations contribute to the efficacy of the combination treatment. To further explore this possibility and to assess the potential therapeutic relevance in humans, well-validated PBMC-based assays were used which showed that blocking both axes with a combination of durvalumab and monalizumab led to increased production of cytokines by both T and NK cells. Furthermore, the magnitude of the increase in cytokine secretion was dependent on the production of high levels of IFN- $\gamma$ . Since IFN- $\gamma$  is known to induce HLA-E this suggests that blockade of NKG2A could have a beneficial role in activation of immune cells through the combined blockade of PD-1/PD-L1.

### Conclusions

Together, these data indicate that blocking NKG2A in conjunction with PD-1/PD-L1 checkpoint inhibitors provides increased anti-tumor efficacy mediated by IFN- $\gamma$  and support the rationale for assessing this combination in clinical trials.





## Combinations: Immunotherapy/Immunotherapy

Presenting author underlined; Primary author in italics

197

### Pharmacokinetics and immunogenicity of pembrolizumab when given in combination with ipilimumab: data from KEYNOTE-029

Michael B Atkins<sup>1</sup>, Matteo S Carlino<sup>2</sup>, Antoni Ribas<sup>3</sup>, John A Thompson<sup>4</sup>, Toni K Choueiri<sup>5</sup>, F Stephen Hodi<sup>5</sup>, Wen-Jen Hwu<sup>6</sup>, David F McDermott<sup>7</sup>, Victoria Atkinson<sup>8</sup>, Jonathan S Cebon<sup>9</sup>, Bernie Fitzharris<sup>10</sup>, Michael B Jameson<sup>11</sup>, Catriona McNeil<sup>12</sup>, Andrew G Hill<sup>13</sup>, Eric Mangin<sup>14</sup>, Malidi Ahamadi<sup>14</sup>, Marianne van Vugt<sup>15</sup>, Mariëlle van Zutphen<sup>15</sup>, Nageatte Ibrahim<sup>14</sup>, Georgina V Long<sup>16</sup>

<sup>1</sup>Georgetown-Lombardi Comprehensive Cancer Center, Washington, DC, USA

<sup>2</sup>Westmead and Blacktown Hospitals, Melanoma Institute Australia, and the University of Sydney, Westmead, New South Wales, Australia

<sup>3</sup>University of California, Los Angeles, CA, USA

<sup>4</sup>University of Washington, Seattle, WA, USA

<sup>5</sup>Dana-Farber Cancer Institute/Brigham and Women's Hospital, Harvard University, Boston, MA, USA

<sup>6</sup>University of Texas MD Anderson Cancer Center, Houston, TX, USA

<sup>7</sup>Beth Israel Deaconess Medical Center, Boston, MA, USA

<sup>8</sup>Gallipoli Medical Research Foundation, Greenslopes Private Hospital, and the University of Queensland, Greenslopes, Queensland, Australia

<sup>9</sup>Olivia Newton-John Cancer Research Institute, Heidelberg, Victoria, Australia

<sup>10</sup>Canterbury District Health Board, Christchurch Hospital, Christchurch, New Zealand

<sup>11</sup>Waikato Hospital Regional Cancer Centre, Hamilton, New Zealand

<sup>12</sup>Royal Prince Alfred Hospital, Melanoma Institute Australia, the University of Sydney, and Chris O'Brien Lifecare, Camperdown, New South Wales, Australia

<sup>13</sup>Tasman Oncology Research, Southport Gold Coast, Queensland, Australia

<sup>14</sup>Merck & Co., Inc., Kenilworth, NJ, USA

<sup>15</sup>Quantitative Solutions, a Certara company, Oss, Netherlands

<sup>16</sup>Melanoma Institute Australia, the University of Sydney, Mater Hospital, and Royal North Shore Hospital, Wollstonecraft, New South Wales, Australia

#### Background

The pharmacokinetics of pembrolizumab given as monotherapy are well characterized. Consistent with other monoclonal antibodies, pembrolizumab has low clearance (0.202 L/day), limited central (3.53 L) and peripheral (3.85 L) volume of distribution, and low variability in the central volume of distribution (19% coefficient of variation). Pembrolizumab monotherapy has low immunogenicity

potential, with an observed incidence of treatment-emergent anti-drug antibodies (ADA) of < 1%. We present data on the pharmacokinetics and immunogenicity of pembrolizumab when given in combination with ipilimumab in the phase I KEYNOTE-029 study.

#### Methods

KEYNOTE-029 included 2 cohorts that assessed the safety and antitumor activity of pembrolizumab plus ipilimumab: a safety run-in that included patients with advanced melanoma or renal cell carcinoma (RCC) (N=22) and a melanoma expansion cohort (N=153). In both cohorts, patients received 4 doses of pembrolizumab 2 mg/kg plus ipilimumab 1 mg/kg Q3W followed by pembrolizumab 2 mg/kg Q3W for up to 2 years. Pembrolizumab serum concentration was quantified with an electrochemiluminescence-based immunoassay (lower limit of quantitation, 10 ng/mL). A validated bridging electrochemiluminescence immunoassay using a standard 3-tiered approach (drug tolerance level, 124 µg/mL) was used to detect ADA in serum.

#### Results

Across cohorts, 175 patients received pembrolizumab plus ipilimumab: 165 with melanoma and 10 with RCC. At least 1 evaluable sample for pharmacokinetic assessment was available for all 10 patients with RCC and 162 patients with melanoma. The predose serum concentration versus time profiles for pembrolizumab were similar in patients with RCC and melanoma (Figure 1). Observed serum concentrations were within the range predicted for pembrolizumab 2 mg/kg Q3W given as monotherapy (Figure 2). Of the 160 patients with melanoma who provided postdose ADA samples, 156 (97.5%) were negative, 2 (1.3%) were inconclusive, and 2 (1.3%) were positive for treatment-emergent ADA. Best overall response in the ADA-positive patients was stable disease in one and progressive disease in the other. No patient with RCC had treatment-emergent ADA.

#### Conclusions

The addition of ipilimumab does not appear to impact pembrolizumab serum concentration or increase the risk of developing ADA in patients with advanced melanoma or RCC.

#### Trial Registration

ClinicalTrials.gov identifier NCT02089685.

## Combinations: Immunotherapy/Immunotherapy

Presenting author underlined; Primary author in italics

**Figure 1. Arithmetic mean (SE) predose serum concentration-time profile of pembrolizumab following multiple doses of pembrolizumab plus ipilimumab (linear-linear scale).**

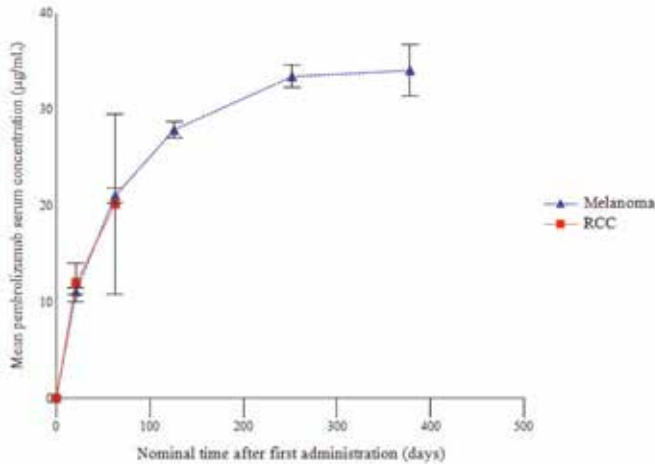
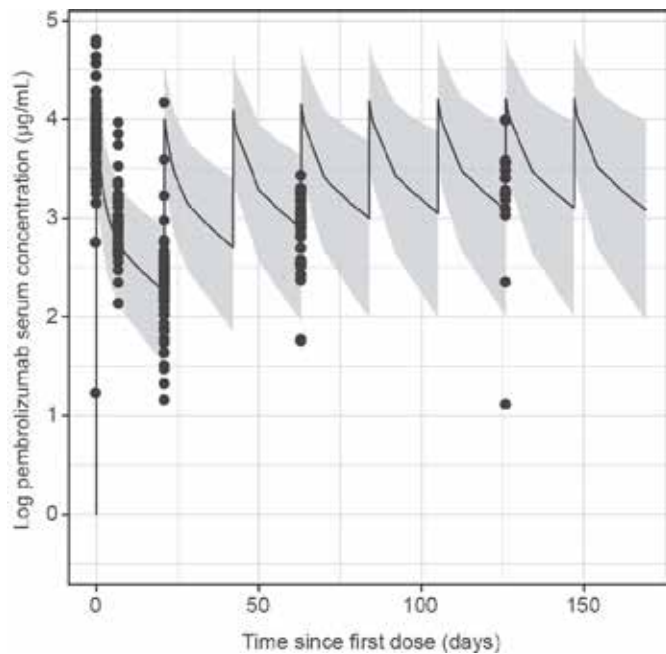


**Figure 2. Observed pembrolizumab serum concentrations from patients with melanoma treated with pembrolizumab plus ipilimumab in relation to the predicted concentration interval (gray) for pembrolizumab 2 mg/kg Q3W monotherapy (log scale).**



198

### Establishing a model for successful immunotherapy with T-Vec combined with BRAF inhibition and anti-PD-1 in genetically engineered murine melanoma

Robyn Gartrell<sup>1</sup>, Zoe Blake<sup>1</sup>, Ines Simoes<sup>2</sup>, Yichun Fu<sup>1</sup>, Takuro Saito<sup>3</sup>, Yingzhi Qian<sup>1</sup>, Yan Lu<sup>1</sup>, *Yvonne M Saenger*<sup>4</sup>

<sup>1</sup>Columbia University Medical Center, New York, NY, USA

<sup>2</sup>Institut d'Investigacions Biomediques August Pi i Sunyer, Barcelona, Catalonia, Spain

<sup>3</sup>Icahn School of Medicine at Mount Sinai, New York, NY, USA

<sup>4</sup>New York Presbyterian/Columbia University Medical Center, New York, NY, USA

#### Background

Talimogene laherparepvec (T-Vec) is the first oncolytic virus to be U.S. Food and Drug Administration (FDA) approved for the treatment of cancer. T-Vec, a modified herpes simplex type I (HSV I) virus, has two proposed mechanisms of action: direct cell lysis and immune activation. Combination immunotherapy using T-Vec and checkpoint blockade has shown promise in clinical trials. In preliminary work, our laboratory has shown that T-Vec causes up-regulation of programmed cell death protein 1 (PD-1) on infiltrating T cells in mice, suggesting potential synergy of T-Vec and anti-PD-1 (αPD-1).

#### Methods

In a temporally and spatially regulated murine model of BRAF<sup>CA</sup> PTEN<sup>-/-</sup> spontaneous melanoma [1], tumors are induced on right flank. When tumors reach >5mm in diameter, mice are randomized into 6 treatment groups comparing combinations of BRAF inhibition (BRAFi), αPD-1, and T-Vec (Table 1). Tumor growth is measured twice a week until end of study. Flow cytometry is performed on tumor, lymph node, and spleen to assess immune microenvironment.

#### Results

Mean tumor volume and survival was plotted to compare groups (Figure 1 & 2). Mice treated with triple combination have decreased tumor growth. Mice treated with combination T-Vec + BRAFi with or without αPD-1 have longer survival compared to mice treated with control or single drug arms. Flow cytometry shows increase in percent CD3+/CD45+ cells in tumors of mice treated with combination αPD-1 + T-Vec compared to the control and single drug arms. Percent CD8+/CD3+ cells in tumors treated with immunotherapy appears to be increased compared to the control and BRAFi only group (Figure 3). Additionally, percent of FOXP3+/CD4+ cells in tumors appears to be decreased in groups receiving T-Vec (Figure 4) while no change in FOXP3+/CD4+ populations was observed in tumors from groups receiving αPD-1 without T-Vec or in draining lymph node or spleen.

# Combinations: Immunotherapy/Immunotherapy

Presenting author underlined; Primary author in italics

## Conclusions

Initial findings show that combination therapy of BRAFi +  $\alpha$ PD-1 + T-Vec is more effective than any single treatment. Combination immunotherapy increases infiltration of T cells into tumor. Furthermore, oncolytic virus appears to decrease regulatory T cells infiltrating tumor. This study is ongoing and further analysis will continue as we further evaluate the immune microenvironment using flow cytometry and immunohistochemistry.

## Acknowledgements

The study was funded by the Melanoma Research Alliance and Amgen (Amgen-CUMC-MRA Established Investigator Academic-Industry Partnership Award).

## References

1. Dankort, Curley, Cartlidge, *et al*: **Braf(V600E) cooperates with Pten loss to induce metastatic melanoma.** *Nature Genetics* 2009, **41**:544-552.

## Treatment Groups Table

Group	Treatment
Group 1 (Red)	Control Chow + IP 2A3 + IT PBS
Group 2 (Orange)	BRAFi Chow + IP 2A3 + IT PBS
Group 3 (Yellow)	BRAFi Chow + IP $\alpha$ PD1 + IT PBS
Group 4 (Green)	BRAFi Chow + IP 2A3 + IT T-Vec
Group 5 (Blue)	BRAFi Chow + IP $\alpha$ PD1 + IT T-Vec
Group 6 (Purple)	Control Chow + IP $\alpha$ PD1 + IT T-Vec

IP= intraperitoneal, IT= intratumoral, BRAFi = Braf inhibitor,  $\alpha$ PD1=anti programmed cell death 1, T-Vec = Talimogene Laherparepvec

Table 1. Treatment groups

## Tumor Volume Comparison of All Mice Figure

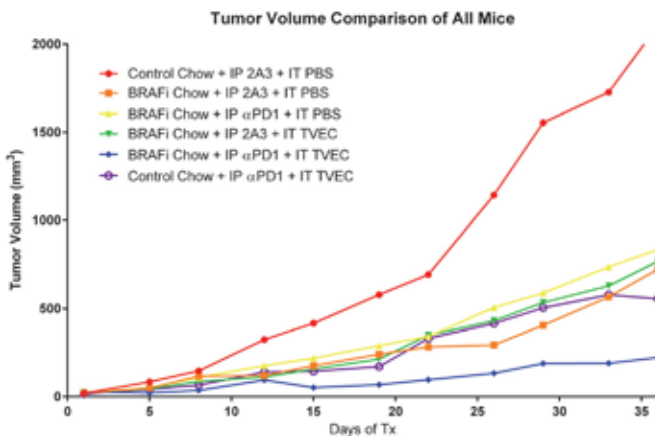


Figure 1. Tumor volume comparison of all mice

## Survival Comparison of Treatment Groups Figure

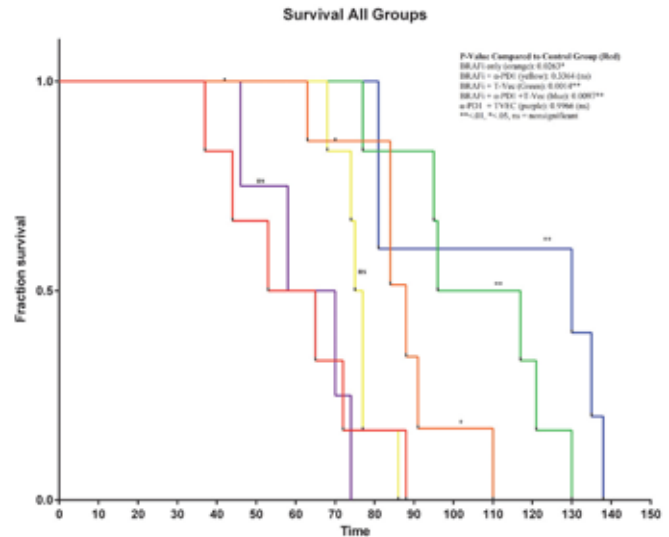


Figure 2. Survival comparison of treatment groups

## Flow cytometry data of CD8+ cells per CD3+ cell populations Figure

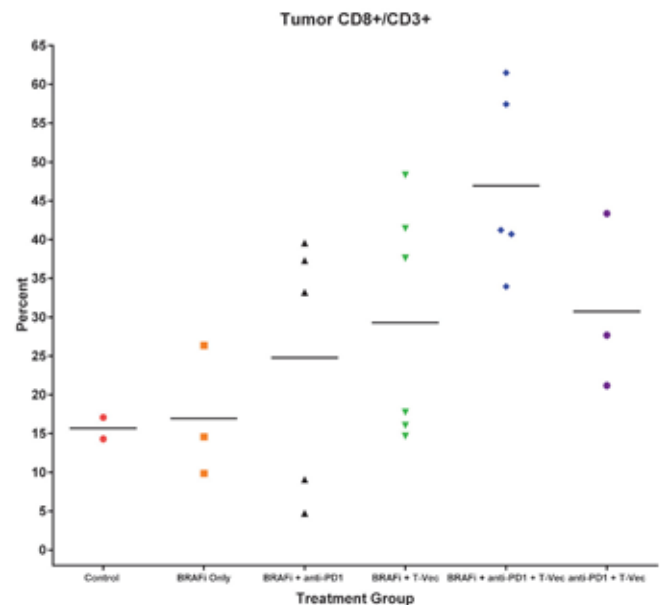


Figure 3. Flow cytometry data of CD8+ cells per CD3+ cell populations

## Combinations: Immunotherapy/Immunotherapy

Presenting author underlined; Primary author in italics

### Flow cytometry data of CD4+/FOXP3+ cells per CD4+ cell populations

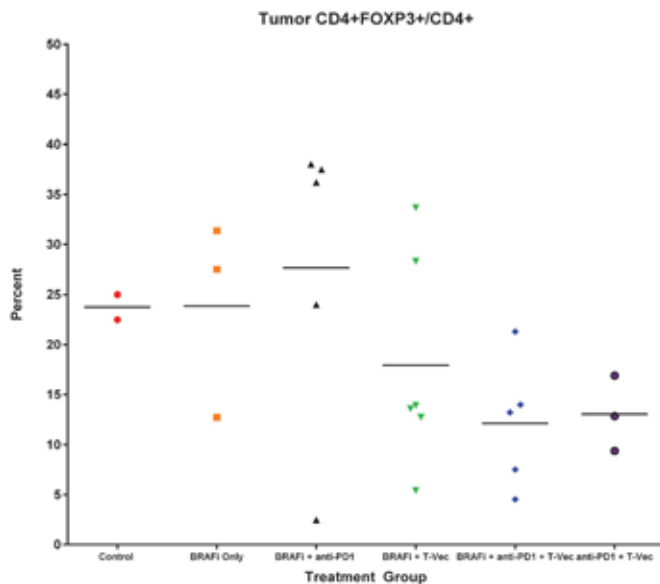


Figure 4. Flow cytometry data of CD4+/FOXP3+ cells per CD4+ cell populations

199

### Phosphatidylserine targeting antibody in combination with checkpoint blockade and tumor radiation therapy promotes anti-cancer activity in mouse melanoma

Sadna Budhu<sup>1</sup>, Olivier De Henau<sup>1</sup>, Roberta Zappasodi<sup>1</sup>, Kyle Schlunegger<sup>2</sup>, Bruce Freimark<sup>2</sup>, Jeff Hutchins<sup>2</sup>, Christopher A Barker<sup>1</sup>, Jedd D Wolchok<sup>1</sup>, Taha Merghoub<sup>1</sup>

<sup>1</sup>Memorial Sloan Kettering Cancer Center, New York, NY, USA

<sup>2</sup>Peregrine Pharmaceuticals, Inc., Tustin, CA, USA

#### Background

Phosphatidylserine (PS) is a phospholipid that is exposed on the surface of apoptotic cells, some tumor cells and tumor endothelium. PS has been shown to promote anti-inflammatory and immunosuppressive signals in the tumor microenvironment. Antibodies that target PS have been shown to reactivate anti-tumor immunity by repolarizing tumor associated macrophages to a M1-like phenotype, reducing the number of MDSCs in tumors and promote the maturation of dendritic cells into functional APCs. In a B16 melanoma model, targeting PS in combination with immune checkpoint blockade has been shown to have a significantly greater anti-cancer effect than either agent alone. This combination was shown to enhance CD4+ and CD8+ T cell infiltration and activation in the tumors of treated animals. Radiation therapy is an effective focal treatment of primary solid tumors, but is less effective in treating metastatic solid

tumors as a monotherapy. There is evidence that radiation induces immunogenic tumor cell death and enhances tumor-specific T cell infiltration in irradiated tumors. In addition, the abscopal effect, a phenomenon in which tumor regression occurs outside the site of radiation therapy, has been observed in both preclinical and clinical trials with the combination of radiation therapy and immunotherapy.

#### Methods

We examined the effects of combining tumor radiation therapy with an antibody that targets PS (1N11) and an immune checkpoint blockade (anti-PD-1) using the mouse B16 melanoma model. Tumor surface area and overall survival of mice were used to determine efficacy of the combinations.

#### Results

We examined the expression of PS on immune cells infiltrating B16 melanomas. CD11b+ myeloid cells expressed the highest levels of PS on their surface whereas T cells and B16 tumor cells express little to no PS. These data suggest that targeting PS in B16 melanoma would induce a pro-inflammatory myeloid tumor microenvironment. We hypothesize that therapies that induce apoptotic cell death on tumor cells would enhance the activity of PS-targeting antibodies. We therefore examined the effects of combining a PS-targeting antibody with local tumor radiation. We found that the PS-targeting antibody synergizes with both anti-PD-1 and radiation therapy to improve anti-cancer activity and overall survival. In addition, the triple combination of the PS-targeting antibody, tumor radiation and anti-PD-1 treatment displayed even greater anti-cancer and survival benefit.

#### Conclusions

This finding highlights the potential of combining these three agents to improve outcome in patients with advanced-stage melanoma and may inform the design of future clinical trials with PS targeting in melanoma and other cancers.

200

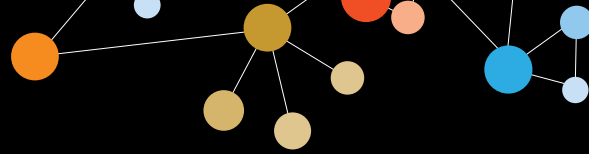
### A novel anti-human LAG-3 antibody in combination with anti-human PD-1 (REGN2810) shows enhanced anti-tumor activity in PD-1 x LAG-3 dual-humanized mice and favorable pharmacokinetic and safety profiles in cynomolgus monkeys

Elena Burova, Omaira Allbritton, Peter Hong, Jie Dai, Jerry Pei, Matt Liu, Joel Kantrowitz, Venus Lai, William Poueymirou, Douglas MacDonald, Ella Ioffe, Markus Mohrs, William Olson, Gavin Thurston

Regeneron, Tarrytown, NY, USA

#### Background

In the tumor microenvironment, T cell inhibitory checkpoint receptors trigger signals that suppress T cell effector



## Combinations: Immunotherapy/Immunotherapy

Presenting author underlined; *Primary author in italics*

function, resulting in tumor immune evasion. Clinical antibodies blocking one of these receptors, PD-1, yield positive responses in multiple cancers; however, their efficacy is limited. Simultaneously targeting more than one inhibitory checkpoint receptor has emerged as a promising therapeutic strategy. In support of this concept, mice deficient in PD-1 and LAG-3, an inhibitory checkpoint receptor often co-expressed with PD-1 in the tumor microenvironment, exhibit enhanced anti-tumor activity. Here, we demonstrate increased anti-tumor efficacy of a combined anti-human PD-1 (hPD-1) and anti-human LAG-3 (hLAG-3) therapy using fully human monoclonal antibodies in dual humanized PD-1 x LAG-3 mice. The pharmacokinetics and toxicology of the novel anti-hLAG-3 antibody were assessed in non-human primates to support clinical development.

### Methods

REGN2810, a high affinity anti-hPD-1 monoclonal antibody that blocks PD-1 interaction with PD-L1 and PD-L2, and a novel high affinity monoclonal anti-hLAG-3 antibody, which blocks the LAG-3/MHC II interaction were generated. Dual humanized PD-1 x LAG-3 mice were engineered by replacing the extracellular domains of mouse *Pdcd1* and *Lag3* with the corresponding regions of *hPD-1* and *hLAG-3* and were used for testing antibody efficacy in a MC38.ova syngeneic tumor model. Expression of humanized PD-1 and LAG-3 were analyzed by flow cytometry. Binding of hLAG-3 to mouse MHC II was confirmed with a cell adhesion assay, and binding of hPD-1 to mouse PD-L1 was confirmed using surface plasmon resonance. The pharmacokinetics of anti-hLAG-3 antibody following a single i.v. dose, and the safety profile in a 4-week weekly i.v. dose regimen of up to 50 mg/kg/dose, were determined in cynomolgus monkeys.

### Results

Treatment of MC38.ova tumor-bearing humanized mice with a combination of anti-hPD-1 and anti-hLAG-3 antibodies triggered activation of intratumoral and peripheral T cells. Importantly, the combination treatment exhibited an additive, dose dependent anti-tumor effect compared to the respective monotherapies. Anti-hLAG-3 antibody pharmacokinetics in cynomolgus monkeys followed a standard mean concentration-time profile characterized by an initial brief distribution phase and a linear beta elimination phase. Exposure to anti-hLAG-3 increased in a dose-proportional manner, with elimination half-lives ranging from 10.8 to 11.5 days. Anti-hLAG-3 antibody was well tolerated, and no-observed-adverse-effect level (NOAEL) could be established up to 50 mg/kg.

### Conclusions

Preclinical anti-tumor efficacy of combined REGN2810 and anti-hLAG-3 antibody treatment, together with favorable pharmacokinetic and safety data for anti-hLAG-3 antibody in

cynomolgus monkeys, support clinical development of this cancer combination immunotherapy.

### 201

#### Combination of PD-L1 blockade with oncolytic vaccines re-shapes the functional state of tumor infiltrating lymphocytes

*Cristian Capasso*<sup>1</sup>, Federica Frascaro<sup>2</sup>, Sara Carpi<sup>3</sup>, Siri Tähtinen<sup>1</sup>, Sara Feola<sup>4</sup>, Manlio Fusciello<sup>1</sup>, Karita Peltonen<sup>1</sup>, Beatriz Martins<sup>1</sup>, Madeleine Sjöberg<sup>1</sup>, Sari Pesonen<sup>5</sup>, Tuuli Ranki<sup>5</sup>, Lukasz Kyruk<sup>1</sup>, Erkki Ylösmäki<sup>1</sup>, Vincenzo Cerullo<sup>1</sup>

<sup>1</sup>University of Helsinki, Helsinki, Uusimaa, Finland

<sup>2</sup>University of Siena, Supersano (LE), Puglia, Italy

<sup>3</sup>University of Pisa, Pisa, Toscana, Italy

<sup>4</sup>University of Napoli Federico II, Helsinki, Uusimaa, Finland

<sup>5</sup>PeptiCRAd Oy, Helsinki, Uusimaa, Finland

### Background

The immunological escape of tumors represents one of the main obstacles to the treatment of malignancies. The blockade of PD-1 or CTLA-4 receptors represented a milestone in the history of immunotherapy. However, immune checkpoint inhibitors seem to be effective in specific cohorts of patients. It has been proposed that their efficacy relies on the presence of an immunological response. Thus, we hypothesized that disruption of the PD-L1/PD-1 axis would synergize with our oncolytic vaccine platform PeptiCRAd.

### Methods

We used murine B16OVA *in vivo* tumor models and flow cytometry analysis to investigate the immunological background.

### Results

First, we found that high-burden B16OVA tumors were refractory to combination immunotherapy. However, with a more aggressive schedule, tumors with a lower burden were more susceptible to the combination of PeptiCRAd and PD-L1 blockade. The therapy significantly increased the median survival of mice (Figure 1). Interestingly, the reduced growth of contralaterally injected B16F10 cells suggested the presence of a long lasting immunological memory also against non-targeted antigens. Concerning the functional state of tumor infiltrating lymphocytes (TILs), we found that all the immune therapies would enhance the percentage of activated (PD-1<sup>pos</sup> TIM-3<sup>neg</sup>) T lymphocytes and reduce the amount of exhausted (PD-1<sup>pos</sup> TIM-3<sup>pos</sup>) cells compared to placebo. As expected, we found that PeptiCRAd monotherapy could increase the number of antigen specific CD8+ T cells compared to other treatments. However, only the combination with PD-L1 blockade could significantly increase the ratio between activated and exhausted pentamer positive cells (p=0.0058), suggesting that by disrupting the PD-1/



## Combinations: Immunotherapy/Immunotherapy

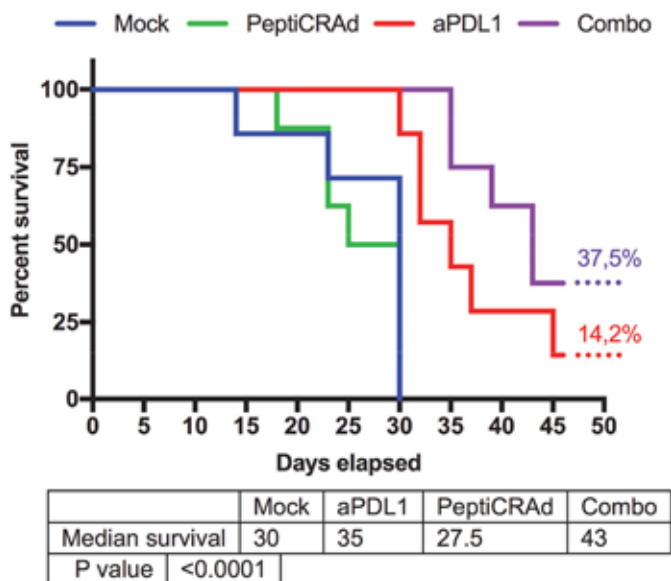
Presenting author underlined; Primary author in italics

PD-L1 axis we could decrease the amount of dysfunctional antigen specific T cells. We observed that the anatomical location deeply influenced the state of CD4+ and CD8+ T lymphocytes. In fact, TIM-3 expression was increased by 2 fold on TILs compared to splenic and lymphoid T cells. In the CD8+ compartment, the expression of PD-1 on the surface seemed to be restricted to the tumor micro-environment, while CD4+ T cells had a high expression of PD-1 also in lymphoid organs. Interestingly, we found that the levels of PD-1 were significantly higher on CD8+ T cells than on CD4+ T cells into the tumor microenvironment ( $p < 0.0001$ ).

### Conclusions

In conclusion, we demonstrated that the efficacy of immune checkpoint inhibitors might be strongly enhanced by their combination with cancer vaccines. PeptiCRAAd was able to increase the number of antigen-specific T cells and PD-L1 blockade prevented their exhaustion, resulting in long-lasting immunological memory and increased median survival.

Figure 1.



Survival of C57 mice bearing B16OVA tumors and treated on day 6 post-implantation with either PBS, PDL1 blockade, OVA-targeting PeptiCRAAd or the combination of PDL1-blockade and OVA-PeptiCRAAd.

### 202

#### **In vitro evaluation of immunotherapy protocols through a label-free impedance-based technology allows dynamic monitoring of immune response and reagent efficacy**

*Fabio Cerignoli*, Biao Xi, Garret Guenther, Naichen Yu, Lincoln Muir, Leyna Zhao, Yama Abassi

ACEA Biosciences Inc., San Diego, CA, USA

### Background

*In vitro* characterization of reagent efficacy in the context of cancer immunotherapy is a necessary step before moving to more expensive animal models and clinical studies. However, current *in vitro* assays like Chromium-51, ATP-based luminescence or flow cytometry are either difficult to implement in high throughput environments or are mainly based on endpoint methodologies that are unable to capture the full dynamic of the immune response. Here, we present the adaptation of an impedance-based platform to monitor cytotoxic activity of immune cells activated through different means.

### Methods

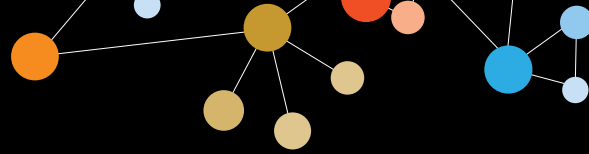
Impedance technology detects cell death and proliferation of adherent cells by measuring changes in conductance of microelectrodes embedded in 96 and 384-wells cell culture plates. We utilized adherent and B cell leukemia/lymphoma cell lines as well as primary tumor cells as *in vitro* models for immunotherapy reagent evaluation. We seeded the cells on electrodes coated 96-well plates and monitored cell adhesion and proliferation for 24 hours. The following day effector cells were added at multiple effector:target ratios in presence of BiTEs antibodies and/or anti PD-1/PD-L1 antibodies. Impedance signal was monitored for up to seven days. Control wells were set up with effector cells only or with target plus effector cells but without antibodies. We adapted such adhesion-based technology to monitor non-adherent B-leukemia/lymphoma cells, by developing a strategy where the wells are coated with an anti-CD40 antibody. The coating allows specific adhesion and retention of B cells and measurement of changes in impedance that are proportional to cell number.

### Results

Using increasing concentrations of EpCAM/CD3 BiTE, we demonstrated the suitability of an impedance-based approach to quantitatively monitor the efficacy of immune cells-mediated cancer cell killing both under different effector:target ratios and antibody concentrations. Combination treatments with checkpoint reduced timing and increased amount of killed cancer cells. Similar results were also obtained with engineered CAR-T cells against CD19 or NK cell lines, demonstrating specific killing of tumor B cells at very low effector:target ratios. The results were also confirmed by flow cytometry.

### Conclusions

Overall, our results demonstrate the value of an impedance-based approach in measuring the cytotoxic response across the temporal scale, an aspect that is otherwise very difficult to assess with more canonical end point assays. Furthermore, the availability of 384-well format and minimal sample handling place the technology in an ideal spot



## Combinations: Immunotherapy/Immunotherapy

*Presenting author underlined; Primary author in italics*

for applications in large reagent validation screening or personalized medicine, like therapeutic protocol validation directly on patient samples.

**203**

### **Tumor necrosis factor alpha and interleukin-2 expressing adenovirus plus PD-1 blockade as a boost for T cell therapy in the context of solid tumor therapies**

Victor Cervera-Carrascón<sup>1</sup>, Mikko Siurala<sup>1</sup>, João Santos<sup>1</sup>, Riikka Havunen<sup>2</sup>, Suvi Parviainen<sup>1</sup>, Akseli Hemminki<sup>1</sup>

<sup>1</sup>TILT Biotherapeutics, Helsinki, Uusimaa, Finland

<sup>2</sup>University of Helsinki, Helsinki, Uusimaa, Finland

#### **Background**

Because of the immunosuppressive tumor microenvironment, the immune system is unable to develop effective responses against tumor cells. This phenomenon also acts against the effectiveness of adoptive T cell therapy. In order to overcome this situation in the tumor, an attractive therapeutic combination is the combination of oncolytic viruses and immune checkpoint inhibitors. In this case, besides the last two therapies mentioned above, combinations with T cell therapy were also included. The virus used was engineered to express tumor necrosis factor  $\alpha$  (TNF $\alpha$ ) and interleukin (IL)-2, two cytokines that will boost the immunogenicity of the virus and thus its antitumor properties. On the other hand, the use of anti-PD-1 will avoid exhaustion on tumor infiltrating T cells and hence remove the barriers that could dampen the desired immune response against the tumor.

#### **Methods**

In the study of the antitumor effect of this three armed treatment we used an *in vivo* model of subcutaneous B16-OVA melanoma-bearing mice. Two experiments were carried out; the first one (n=47) to establish the differences between the triple, double, and single armed combination therapies and the second experiment (n=84) was focused on study the differences between the groups that showed the best outcomes in the first one and also optimize viral and anti-PD-1 administration regimes.

#### **Results**

Preliminary results show a statistically significant positive effect coming out from the combination of virus therapy and immune checkpoint blockade with regard to both tumor progression and overall survival, with up to 43% complete tumor regression achieved in some of the groups after 96 days post treatment. On the other hand, the effect of adoptive cell therapy in this combination is not completely clear. More results will be presented after analyzing biological samples collected during both experiments.

#### **Conclusions**

Preclinical studies are a key step to detect which combinations are more suitable for success in human trials. In this study we developed a rationale for the combination relying on two concepts: to make silent tumors more visible to the immune system and to counter immunosuppressive mechanisms to unleash the full potential of T cells against the tumor, rendering in a modification of the tumor microenvironment that makes it more susceptible for T cell mediated killing. According to the results displayed from these experiments, the combination of this genetically modified adenovirus and PD-1 blockade is an efficient combination to be considered for future application in humans.

**204**

### **IMM-101 primes for increased complete responses following checkpoint inhibitors in metastatic melanoma; 3 case reports**

Angus Dalgleish<sup>1</sup>, Satvinder Mudan<sup>2</sup>

<sup>1</sup>St George's University of London, London, UK

<sup>2</sup>The Royal Marsden Hospital and Imperial College London, London, UK

#### **Background**

IMM-101, a heat-killed borate-buffered whole cell product of *Mycobacterium obuense* has been shown to enhance cell mediated cytokine responses and innate immune responses involving NK and gamma delta cells [1]. Complete responses (CR) in patients with melanoma lung metastases demonstrated. Follow up of original publication [2] has shown a 30% 5-year survival. Combined with gemcitabine in metastatic pancreatic cancer a significant survival advantage over gemcitabine monotherapy is seen [3].

#### **Methods**

We present 3 patients with metastatic melanoma, progressed after initial stabilisation with IMM-101, who showed CR after check point inhibitors (CPI) ipilimumab (n=2), pembrolizumab (n=1). Patient 1: 2006 46M melanoma left forearm, BT 3.7 mm, 1 positive lymph node. Recurrent disease treated with surgery, Aldara and low dose IL-2. 2010 pulmonary mets, commenced IMM-101, no response (initial SD). 2011 given ipilimumab. Patient 2: 2011 50F axillary lump removed, melanoma (no primary). Concomitant mediastinal, lung, gastric and peritoneal deposits. Gastric surgery, decarbazine. Commenced IMM-101 with cyberknife to lung lesion. 2013 Small bowel obstruction from new disease. Started ipilimumab. Patient 3: 2014 79M melanoma, left cheek, BT 2.4 mm. Regional lymph node recurrence, treated with a left neck dissection in April 2014. Developed paracardiac nodes, adrenal, lung and multiple large subcutaneous deposits.

## Combinations: Immunotherapy/Immunotherapy

Presenting author underlined; *Primary author in italics*

Commenced IMM-101 with initial shrinkage. However, new large subcutaneous lesions. Commenced pembrolizumab.

### Results

Patient 1 - CR on Pet CT, maintained through 2016. Patient 2 - CR maintained for 2 years. Patient 3 - CR of subcutaneous deposits four days after first injection.

### Conclusions

The CR rate to CPI's is disappointing, < 1% for Ipilimumab. PDL-1 expression is predictive for PD-1 responses and although CPI combinations are clearly needed, most are very toxic. IMM-101 is relatively free of toxicity, enhances PD-1 expression in pre-clinical models but may also prime tumour response to check point inhibitors by its action on macrophage function. Based on these observations, we speculate that IMM-101 primes for CPI's and propose a trial priming with IMM-101, followed by anti-PD-1 antibodies.

### References

1. Fowler D, *et al*: **Mycobacteria activate  $\gamma\delta$  T-cell anti-tumour responses via cytokines from type 1 myeloid dendritic cells: a mechanism of action for cancer immunotherapy.** *Cell* 2012, **61(4)**:535-547.
2. Stebbing J, *et al*: **An intra-patient placebo-controlled phase I trial to evaluate the safety and tolerability of intradermal IMM-101 in melanoma.** *Ann Oncol* 2012, **23(5)**:1314-1319.
3. Dalglish, *et al*: **Randomised open-label, phase II study of Gemcitabine with and without IMM-101 for advanced pancreatic cancer (IMAGE-1 Trial).** *BJC* 2016, in press.

## 205

### Immunological impact of checkpoint blockade on dendritic cell driven T cell responses: a cautionary tale

Mark DeBenedette, Ana Plachco, Alicia Gamble, Elizabeth W Grogan, John Krisko, Irina Tcherepanova, Charles Nicolette

Argos Therapeutics Inc., Durham, NC, USA

### Background

AGS-003 is an individualized, autologous, tumor antigen-loaded, dendritic cell (DC) immunotherapy currently in phase III development for the treatment of metastatic renal cell carcinoma (mRCC) in combination with standard-of-care. Antibodies to PD-1 on activated T cells or PD-L1 expressed on APCs have now been approved for treatment of several cancer indications including RCC. While there is a strong mechanistic rationale for the potential synergy of these agents in combination, data supporting the importance of sequencing the administration of these agents are limited. Since the DC-based immunotherapy, AGS-003, expresses high levels of PD-L1, combinations with checkpoint blockade may remove a critical signal protecting DCs during the early CTL activation

phase *in vivo*. Concurrent administration of checkpoint inhibitors with AGS-003 may, therefore, impede the proposed mechanism of action of AGS-003, which is the induction of tumor-specific CTL responses. Results derived from *in vitro* modeling of DCs inducing T cell responses can demonstrate how to better mobilize the immune system to overcome the immunosuppressive environment of cancer. Therefore, it was of interest to test anti-PD-1/anti-PD-L1 antibody therapy *in vitro* in combination with DCs representative of AGS-003, to observe the effects combination therapy would have on antigen-specific CTL proliferation and functional responses.

### Methods

DCs derived from monocytes were co-electroporated with MART-1 RNA and CD40 ligand RNA to represent AGS-003 DC products. *In vitro* co-cultures were set up with autologous CTLs and MART-1/CD40L DCs in the presence of anti-PD-1 or anti-PD-L1 antibodies. In some instances, PD-1 expression was hyper expressed on CTLs by electroporating MART-1-specific CTLs with PD-1 RNA. Subsequent expansion of MART-1-specific CTLs and multi-functional responses in the presence of checkpoint blockade were mapped using multi-color flow cytometry.

### Results

Combination with anti-PD-1 antibody did not negatively affect the expansion of MART-1-specific CTL responses; however, if PD-1 was hyper-expressed on previously stimulated MART-1-specific CTLs responses were diminished. Anti-PD-1 antibody blocking restored CTL function in the presence of high levels of PD-1 expression. Interestingly, anti-PD-L1 antibody blocking resulted in suppression of early MART-1-specific CTL expansion and subsequent downstream effector function.

### Conclusions

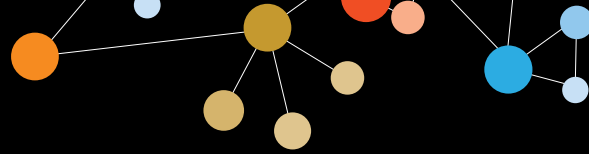
Our results suggest that the sequencing of AGS-003 therapy and checkpoint blockade is important to allow full CTL activation by the DCs prior to anti-PD-1/PD-L1 therapy. Moreover the high expression of PD-L1 on DCs may serve as a "don't kill the messenger" signal, critical to prevent deletion of the DC prior to full signal delivery during early phases of CTL activation.

## 206

### Targeting the PD-1/PD-L1 signaling pathway for the treatment of OS lung metastasis

Pooja Dhupkar, Ling Yu, Eugenie S Kleinerman, Nancy Gordon

University of Texas MD Anderson Cancer Center, Houston, TX, USA



## Combinations: Immunotherapy/Immunotherapy

Presenting author underlined; *Primary author in italics*

### Background

Osteosarcoma (OS) is a primary bone malignancy, commonly culminating into aggressive pulmonary metastasis. Despite chemotherapy advances, the 5-year survival of pulmonary metastatic OS remains 25-30%. Immunotherapy is one of the promising novel approaches to target minimal residual and relapsed disease. The objective of this study is to determine if blocking the PD-1/PD-L1 immunosuppressive signaling pathway using a PD-1 checkpoint inhibitor will have an effect in OS lung metastasis. Anti-PD-1 and anti-PD-L1 antibodies have exhibited therapeutic benefit in melanoma, and non-small cell lung carcinoma. We hypothesize that disruption of the PD-1/PD-L1 signaling pathway using anti-PD-1 antibody has an effect against OS lung metastasis and improves overall survival.

### Methods

Flow cytometry and western blotting were used to analyze PD-L1 expression in 7 different OS cell lines. Immunohistochemistry (IHC) analysis was used to determine PD-L1 expression in OS lung metastases from patients and mice. LM7 human OS mouse model was used to test the effect of blocking murine PD-1 in OS lung metastases. Therapeutic effect of anti-PD-1 treatment was measured by the number of macro and micro-metastases. IHC was used to measure cell proliferation (Ki-67), apoptosis (TUNEL) and cleaved-caspase 3 expression in addition to NK cells and macrophages infiltration. Western blotting was used to address the downstream components of the signaling pathway such as p-Stat3 and p-Erk1/2. The Simple PCI software was used to quantify the IHC data.

### Results

Our studies revealed surface and total PD-L1 expression in five out of seven human OS cell lines. Primary and metastatic OS lung tumor samples from patients demonstrated membranous and cytoplasmic PD-L1 expression. Using a human OS mouse model we demonstrated therapeutic effect of anti-PD-1 therapy as the number of macro and micro-metastases decreased in the anti-PD-1 treated group as compared to the untreated. Anti-PD-1 treatment led to a significant increase in the number of NK cells and macrophages in the OS lung tumors suggesting these cells to have a potential therapeutic benefit against OS lung metastases. In addition, anti-PD-1 therapy caused a decrease in PD-L1 expression in the lung tumors, possibly due to a decrease in p-ERK1/2 and p-Stat3 expression.

### Conclusions

We conclude that targeting the PD-1/ PD-L1 axis could be used to treat OS lung metastasis. Therapeutic efficacy of anti-PD-1 may be due to an increased activity of NK cells and/or macrophages in the lung tumors and that inhibition of the

p-Stat3/ PD-L1 pathway may be the mechanism implicated in OS lung metastases after anti-PD-1 treatment.

### 207

#### **Effect of the class I-HDAC inhibitor entinostat and the pan-HDAC inhibitor vorinostat on peripheral immune cell subsets**

*Italia Grenga, Lauren Lepone, Sofia Gameiro, Karin M Knudson, Massimo Fantini, Kwong Tsang, James Hodge, Renee Donahue, Jeffrey Schlom*

Laboratory of Tumor Immunology and Biology, National Cancer Institute, National Institutes of Health, Bethesda, MD, USA

### Background

Cancer immunotherapy requires effective recognition and elimination of tumor cells identified as non-self; however, tumors can evade host immune surveillance through multiple mechanisms, including epigenetic silencing of genes involved in antigen processing and immune recognition. Epigenetic therapy with histone deacetylase (HDAC) inhibitors has shown limited benefit as a monotherapy in patients with solid tumors; however, recent reports suggest the potential for synergy when combined with immunotherapy. Entinostat is a class I-HDAC inhibitor undergoing trials for the treatment of various cancers, while vorinostat is a pan-HDAC inhibitor approved in the United States for the treatment of cutaneous T cell lymphoma. The aim of this study was to extensively evaluate the effects of entinostat and vorinostat on human peripheral immune cell subsets in order to examine the potential for combination of HDAC inhibitors with cancer immunotherapy.

### Methods

Peripheral blood mononuclear cells (PBMCs) from metastatic breast cancer patients (n=7) were exposed *in vitro* for 48 hours to clinically relevant exposures of entinostat, vorinostat, or vehicle control. PBMCs were then analyzed by multicolor flow cytometry using 27 unique markers to identify 123 immune cell subsets, which included 9 classic cell types [CD4<sup>+</sup> and CD8<sup>+</sup> T cells, regulatory T cells (Treg), B cells, conventional dendritic cells (cDC), plasmacytoid dendritic cells (pDC), natural killer cells (NK), natural killer T cells (NKT), and myeloid derived suppressor cells (MDSC)], and 114 refined subsets relating to their maturation and function.

### Results

Treatment with entinostat and vorinostat induced several notable alterations in peripheral immune cells, suggesting mainly immune activating properties. Exposure to entinostat increased the frequency of activated CD4<sup>+</sup> T cells, activated mature NK cells, antigen presenting cells (cDCs), and highly



## Combinations: Immunotherapy/Immunotherapy

*Presenting author underlined; Primary author in italics*

immature MDSCs, as well as decreased total Tregs and those with a suppressive phenotype. Exposure to vorinostat induced fewer changes than entinostat, including increasing the frequency of activated CD4<sup>+</sup> T cells, highly immature MDSCs, and NKT cells.

### Conclusions

These findings show that while entinostat and vorinostat have overall immune activating properties, entinostat induced a greater number changes than vorinostat. This study supports the combination of HDAC inhibitors with immunotherapy, including therapeutic cancer vaccines and/or checkpoint inhibitors.

208

### Shifting the balance of tumor-mediated immune suppression and augmenting immunotherapy with antibody blockade of semaphorin 4D to facilitate immune-mediated tumor rejection

Elizabeth Evans<sup>1</sup>, Holm Bussler<sup>1</sup>, Crystal Mallow<sup>1</sup>, Christine Reilly<sup>1</sup>, Sebold Torno<sup>1</sup>, Maria Scrivens<sup>1</sup>, Cathie Foster<sup>1</sup>, Alan Howell<sup>1</sup>, Leslie Balch<sup>1</sup>, Alyssa Knapp<sup>1</sup>, John E Leonard<sup>1</sup>, Mark Paris<sup>1</sup>, Terry Fisher<sup>1</sup>, Siwen Hu-Lieskovan<sup>2</sup>, Antoni Ribas<sup>2</sup>, Ernest Smith<sup>1</sup>, Maurice Zauderer<sup>1</sup>

<sup>1</sup>Vaccinex, Rochester, NY, USA

<sup>2</sup>University of California, Los Angeles, Los Angeles, CA, USA

### Background

We report a novel role for semaphorin 4D (SEMA4D, CD100) in modulating the tumor microenvironment (TME) to exclude activated antigen presenting cells and cytotoxic T lymphocytes so as to promote tumor growth. Antibody blockade reduces expansion of MDSC, shifts the balance of M1/M2, T effector/T regulatory cells and associated cytokines and chemokines, and augments tumor rejection with immune checkpoint inhibition.

### Methods

Anti-SEMA4D antibodies were evaluated, alone and in combination with immune checkpoint antibodies. Immune response was characterized by immunohistochemistry, flow cytometry, functional assays, and cytokine, chemokine and gene expression analysis. Anti-tumor activity was evaluated in various preclinical models. A phase I trial for single agent VX15/2503 was completed.

### Results

SEMA4D restricts migration of macrophages and promotes expansion of suppressive myeloid cells *in vitro*. Strong expression of SEMA4D at the invasive margins of actively growing tumors *in vivo* modulates the infiltration and polarization of leukocytes in the TME. Antibody neutralization facilitated recruitment of activated APCs

and T lymphocytes into the TME in preclinical models. M-MDSCs were significantly reduced in both tumor and blood following treatment. This was accompanied by a significant shift towards increased Th1 cytokines and CTL-recruiting chemokines, with concurrent reduction in Treg-, MDSC-, and M2-macrophage promoting chemokines (CCL2, CXCL1, CXCL5). Accordingly, an increase in Teff:Treg ratio (3x, p < 0.005) and CTL activity (4x, p < 0.0001) was observed. NanoString gene expression analysis of on-treatment tumors confirms an increase in the gamma-inflammatory gene signature (Ribas, ASCO 2015), including significant increases in CXCL9, Gzmb, CCR5, Stat1, Lag3, Ptprc, Ciita, Pdc1 (PD-1), and Itga1. These coordinated changes in the tumoral immune context are associated with durable tumor rejection and immunologic memory in preclinical colon, breast, and melanoma models. Importantly, anti-SEMA4D antibody can further enhance activity of immune checkpoint inhibitors and chemotherapy. Strikingly, the combination of anti-SEMA4D with anti-CTLA-4 acts synergistically, with maximal increase in survival (p < 0.01) and complete tumor regression in 100% of mice, as compared to 22% with monotherapy (p < 0.01). SEMA4D antibody treatment was well tolerated in nonclinical and clinical studies; including a phase I multiple ascending dose trial in patients with advanced refractory solid tumors. Patients with the longest duration of treatment, 48-55 weeks, included colorectal, breast, and a papillary thyroid patient, who had a partial response by RECIST.

### Conclusions

Inhibition of SEMA4D represents a novel mechanism and therapeutic strategy to promote functional immune infiltration into the tumor and inhibit tumor progression. Phase Ib/IIa trials of combination therapy with immune checkpoint inhibition are planned.

209

### Combination of a glycomimetic antagonist to E-selectin and CXCR4, GMI-1359, with an anti-PD-L1 antibody attenuates regulatory T cell infiltration and accelerates time to complete response in the murine CT26 tumor model

William Fogler<sup>1</sup>, Marilyn Franklin<sup>2</sup>, Matt Thayer<sup>2</sup>, Dan Saims<sup>2</sup>, John L. Magnani<sup>1</sup>

<sup>1</sup>GlycoMimetics, Inc., Rockville, MD, USA

<sup>2</sup>MI Bioresearch, Ann Arbor, MI, USA

### Background

Regulatory T cells (T<sub>reg</sub>) modulate anti-tumor immunity by suppressing T cell activation. T<sub>reg</sub> are induced and maintained by immunoregulatory receptors, such as PD-L1, and respond to homing signals within the inflamed tumor microenvironment that include the endothelial cell protein,





## Combinations: Immunotherapy/Immunotherapy

Presenting author underlined; Primary author in italics

E-selectin, and the CXCR4 ligand, SDF-1. GMI-1359 is a small molecule glycomimetic beginning clinical evaluation with dual inhibitory activity against E-selectin and SDF-1. The aim of the current study was to determine if GMI-1359 alone or in combination with anti-mPD-L1 antibody affected the *in vivo* growth of CT26 colon carcinoma and to assess percentages of infiltrative intratumoral cells expressing immune markers.

### Methods

Female Balb/c mice were implanted subcutaneously with  $5 \times 10^5$  CT26.WT tumor cells. Three days post tumor injection, mice ( $n=15$ /group) were treated with saline, GMI-1359 (40 mg/kg for 12 consecutive days), isotype control antibody (anti-KLH) or anti-mPD-L1 antibody (10F.9G2, 10 mg/kg on days 3, 6, 10, 13, and 17), or the combination of GMI-1359 and anti-mPD-L1 or anti-KLH. On day 15, tumors and spleens ( $n=5$ /group) were excised and T cells (total CD4+ and CD8+, and CCR7+/CD62L+ subsets of each), regulatory T cells ( $T_{reg}$ ; CD4/CD25/FoxP3), and myeloid derived suppressor cells (MDSC; CD11b+/Gr1+) were determined by flow cytometry. The remaining mice were followed for tumor response.

### Results

Treatments were well tolerated. Mice in control groups and single agent GMI-1359 were all identified with progressive disease. In contrast, treatment with anti-mPD-L1 alone or in combination with GMI-1359 produced a 40% complete response (CR) rate. The median time to CR was shorter when anti-mPD-L1 was combined with GMI-1359 compared to anti-mPD-L1 alone (14 vs. 23 days, respectively,  $p < 0.0471$ ). Evaluation of tumor infiltrating cells showed that combination therapy with GMI-1359 and anti-mPD-L1 reduced the percentage of  $T_{reg}$  compared to treatment with saline, GMI-1359 or anti-mPD-L1 as single treatments (0.9% vs. 3.3%, 2.9% and 1.9%, respectively). No other T cell subsets were affected. In spleens, the median percentage of  $T_{reg}$  were unaffected by any of the treatments and suggest that the reduction in intratumoral  $T_{reg}$  by combined treatment with anti-PD-L1 and GMI-1359 was an attenuated response to maintenance and homing signals in the tumor microenvironment.

### Conclusions

In conclusion, these studies demonstrate that the dual E-selectin/CXCR4 antagonist, GMI-1359, in combination with anti-mPD-L1 antibody attenuates the induction and distribution of intratumoral  $T_{reg}$  and this reduction in  $T_{reg}$  is associated with a more rapid immunotherapeutic anti-tumor response.

## 210

### Antibody targeting of phosphatidylserine enhances the anti-tumor responses of ibrutinib and anti-PD-1 therapy in a mouse triple negative breast tumor model

Jian Gong, Michael Gray, Jeff Hutchins, Bruce Freemark

Peregrine Pharmaceuticals, Tustin, CA, USA

### Background

Phosphatidylserine (PS) is a phospholipid normally residing in the inner leaflet of the plasma membrane that becomes exposed on vascular endothelial cells and tumor cells in the tumor microenvironment, particularly in response to chemotherapy and irradiation. Binding of antibodies targeting PS induces the recruitment of immune cells and engages the immune system to destroy tumor and associated vasculature and by blocking the immunosuppressive action of PS. Recent studies have demonstrated that PS-targeting antibodies enhance the anti-tumor activity of immune checkpoint antibody blockade to CTLA-4 and PD-1 in mouse breast and melanoma tumor models. Ibrutinib is an approved anticancer drug targeting B cell malignancies that is a selective, covalent inhibitor Bruton's tyrosine kinase (BTK) in B cell tumors. Data from recent mouse tumor studies demonstrate that ibrutinib in combination with anti-PD-1 antibody blockade inhibits growth of solid tumors, lacking BTK expression, suggesting that ibrutinib may inhibit interleukin-2 inducible T cell kinase (ITK) and promote Th1 anti-tumor responses.

### Methods

The present study was conducted to evaluate a combination therapy including PS-targeting antibody mch1N11, ibrutinib and anti-PD-1 antibody in C57Bl/6 mice bearing triple negative E0771 breast tumors. Tumors were staged to an initial volume of  $\sim 100\text{mm}^3$  and randomized to treatment groups ( $N=10$ ) with mch1N11 or isotype control at 10 mg/kg qw, anti-PD-1 at 2.5 mg/kg qw or ibrutinib 6 mg/kg or vehicle qd x 8. Tumor volumes were measured twice per week to determine tumor growth inhibition (TGI) relative to control treated animals. The *in vitro* sensitivity of E0771 tumor cells to ibrutinib was compared to the drug sensitive Jeko-1 cell line in a 72 hour growth and viability assay.

### Results

The E0771 cell line is resistant *in vitro* to 10 mM ibrutinib. Tumor bearing mice treated with mch1N11, ibrutinib or anti-PD-1 alone had 22.2%, 23.5% and 32.6% TGI respectively. The TGI for mch1N11 and ibrutinib was 30.5%, ibrutinib and anti-PD-1 was 34.5%, mch1N11 and anti-PD-1 was 36.1%. The triple combination therapy had statistically greater TGI compared to control treated mice (59.9%,  $p=0.0084$ ).

## Combinations: Immunotherapy/Immunotherapy

Presenting author underlined; *Primary author in italics*

### Conclusions

Treatment of solid tumors with a combination of inhibitors that target PS, ITK and the PD-1/PD-L1 axis in the tumor microenvironment provides a novel treatment for solid tumors, including triple negative breast cancer.

211

### Gp96-Ig/costimulator (OX40L, ICOSL, or 4-1BBL) combination vaccine improves T cell priming and enhances immunity, memory, and tumor elimination

George Fromm, Suresh de Silva, Louise Giffin, Xin Xu, Jason Rose, Taylor H Schreiber

Heat Biologics, Inc., Durham, NC, USA

### Background

The excitement in the field of immuno-oncology over the last several years, driven largely by the clinical success of the first-wave of checkpoint inhibitors, is tempered by the fact that only 10-40% of patients respond to these drugs given as monotherapy. It is widely believed that to improve efficacy and patient outcome, new approaches that combine treatments with more than one functionality are needed. Novel approaches that provide combination therapy in a single product, will likely lead the way.

### Methods

We have developed a next generation cellular vaccine platform – referred to as *ComPACT* (COMbination Pan-Antigen Cytotoxic Therapy), that incorporates a tumor antigen chaperone (gp96-Ig) with T cell costimulation (Fc-OX40L), into a single tumor cell line that secretes them both (recently published in *Cancer Immunology Research* 2016).

### Results

The current data extend these findings in additional preclinical settings. Specifically, *ComPACT* is capable of priming antigen-specific CD8+ T cells (peak: 13.3% of total CD8+), even more so than a leading OX40 agonist antibody (8.4%) or vaccine alone (5.6%), and this is associated with increased CD127+KLRG-1- memory precursor cells and antigen-specific CD4+ proliferation, with reduced off-target inflammation. Importantly, vaccine-expressed Fc-OX40L stimulated IFN $\gamma$ +, TNF $\alpha$ +, granzyme-b+ and IL-2+ by antigen-specific CD8+ T cells. This pharmacodynamic signature of an anti-tumor immune response predicted enhanced rejection of established MC38, CT26 and B16.F10 tumors. Additionally, tetramer analysis of antigen-specific CD8+ T cells (in all 3 tumor models), identified significant accumulation of tumor infiltrating lymphocytes (TIL), suggesting that *ComPACT* is not only capable of amplifying antigen-specific T cells, but these T cells can efficiently target and eliminate tumors. We have expanded our repertoire of '*ComPACT*' vaccines to secrete gp96-Ig along with either Fc-TL1A, Fc-4-1BBL or Fc-

ICOSL. Each costimulator/vaccine has a unique functionality, which may be context or tumor dependent. We are currently exploring these mechanistic differences.

### Conclusions

Taken together, we show that the magnitude and specificity of vaccination can be enhanced by locally secreted costimulatory molecules when delivered within a single product. This may simplify clinical translation and importantly, provide significant patient benefit by improving safety and lowering costs.

212

### Modulation of antibody-dependent cell-mediated cytotoxicity (ADCC) mediated by the anti-PD-L1 antibody avelumab on human lung and prostate carcinoma cell lines using the HDAC inhibitors vorinostat and entinostat

Massimo Fantini<sup>1</sup>, Sofia R Gameiro<sup>1</sup>, Karin M Knudson<sup>1</sup>, Paul E Clavijo<sup>2</sup>, Clint T Allen<sup>2</sup>, Renee Donahue<sup>1</sup>, Lauren Lepone<sup>1</sup>, Italia Grenga<sup>1</sup>, James W Hodge<sup>1</sup>, Kwong Y Tsang<sup>1</sup>, Jeffrey Schlom<sup>1</sup>

<sup>1</sup>National Cancer Institute, National Institutes of Health, Bethesda, MD, USA

<sup>2</sup>National Institute on Deafness and Other Communication Disorders, National Institutes of Health, Bethesda, MD, USA

### Background

Chromatin deacetylation is a major determinant in epigenetic silencing of immune-associated genes, a key factor in tumor evasion of host immune surveillance. Deregulation of epigenetic enzymes, including aberrant expression of histone deacetylases (HDACs), has been associated with poor prognosis in several cancer types, including of prostate and lung origin. Vorinostat is a pan-HDAC inhibitor currently approved in the United States for the treatment of cutaneous T cell lymphoma. Entinostat is a class I HDAC inhibitor under clinical investigation for the treatment of various malignancies. HDAC inhibitors have been shown to delete immunosuppressive elements and promote synergistic antitumor effects in combination with various immunotherapies. Checkpoint inhibitors targeting PD-1/PD-L1 interactions are promising immunotherapies shown to elicit objective responses against multiple tumors. Avelumab is a fully human IgG1 mAb monoclonal antibody that inhibits PD-1/PD-L1 interaction by targeting PD-L1, and mediates ADCC against PD-L1-expressing tumor cells *in vitro*. We examined the sensitivity of human lung and prostate carcinoma cells to avelumab-mediated ADCC following clinically-relevant exposure to vorinostat or entinostat.

### Methods

Carcinoma cells were exposed daily to vorinostat (3 $\mu$ M) or DMSO for 4 consecutive days, or to entinostat (500 nM) or



## Combinations: Immunotherapy/Immunotherapy

Presenting author underlined; *Primary author in italics*

DMSO for 72h, prior to being examined for (a) cell-surface PD-L1 expression or (b) used as target cells lysis assay where NK cells from healthy donors were used as effectors. To examine the effect of HDAC inhibitors on PD-L1 expression *in vivo*, female nu/nu mice were implanted with NCI-H460 (lung) or PC-3 (prostate) carcinoma cells. When tumors reached 0.5-1 cm<sup>3</sup>, animals received 4 daily doses of DMSO or vorinostat (150 mg/kg, p.o.). Alternatively, animals received a single dose of entinostat (20 mg/kg, p.o.) or DMSO 72h prior to tumor excision. Frozen specimens were examined for cell-surface expression of PD-L1 by immunofluorescence.

### Results

Our results show that 1) vorinostat and entinostat significantly increase the sensitivity of human lung and prostate carcinoma cells to ADCC mediated by avelumab; 2) the anti-CD16 neutralizing mAb significantly decreases avelumab-mediated lysis of target cells exposed to either HDAC inhibitor; 3) both HDAC inhibitors can enhance tumor PD-L1 expression *in vitro* and *in vivo* in prostate and/or lung xenograft models; 4) increased avelumab-mediated ADCC of tumor targets exposed to HDAC inhibitors can occur without increased tumor PD-L1 expression.

### Conclusions

These studies provide a rationale for combining vorinostat or entinostat with mAbs targeting PD-L1, including for patients that have failed monotherapy regimens with HDAC or checkpoint inhibitors.

### 213

#### **Monoclonal antibodies targeting phosphatidylserine enhance combinational activity of the immune checkpoint targeting agents LAG3 and PD-1 in murine breast tumors**

Michael Gray, Jian Gong, Jeff Hutchins, Bruce Freimark

Peregrine Pharmaceuticals, Tustin, CA, USA

#### **Background**

Our previous work demonstrated that the addition of phosphatidylserine (PS) targeting antibodies to anti-programmed death ligand 1 (PD-1) therapy in murine triple negative breast cancers (TNBC) significantly enhanced immune system activation and tumor growth inhibition. In these studies, NanoString immune profile analysis showed that intratumoral levels of lymphocyte activation gene 3 (LAG3) mRNA increased in response to PS and PD-1 treatments. This suggests LAG3 may act to attenuate T cell activation in TNBC during I/O therapeutic regimens; however, it is unknown if PD-1 and LAG3 function cooperatively in regulating T cell energy, and whether adding PS blocking antibodies can further enhance the effectiveness of LAG3 and/or LAG3 + PD-1 therapies.

### Methods

Animal studies utilized C57bl/6 mice implanted with the murine TNBC model E0771. Immunoprofiling analysis was performed by flow cytometry and the NanoString nCounter<sup>®</sup> PanCancer Immune Profiling Panel. Antibody treatments utilized a specific phosphatidylserine targeting antibody (ch1N11), anti-PD-1, or anti-LAG3 alone or in combination. All statistical analysis utilized the student t-test (significant with  $p < 0.05$ ).

### Results

LAG3 and PD-1 were co-expressed on T cells in E0771. Mice treated with antibodies targeting PS, PD-1, and LAG3 alone in combination with each other demonstrated that the addition of PS blocking antibodies to anti-PD-1 therapy or LAG3 had significantly greater anti-tumor activity than either single agent. Comparison of PD-1 + LAG3 combinational therapy vs. single PD-1 or LAG3 treatments showed moderately more anti-tumor activity than single treatments; however, the addition of PS blocking antibodies to either checkpoint inhibitor was as equally effective in inhibiting tumor growth as observed in the combination of LAG3 + PD-1 treatment. Further comparison of PD-1 + LAG3 vs. PS + PD-1 + LAG3 treatments demonstrated that the addition of PS blocking antibodies resulted in a significant decrease in tumor growth accompanied by complete tumor regression in a greater number of animals than observed in the PD-1 + LAG3 treatment group. FACS and NanoString immunoprofiling analysis on each treatment group showed that the addition of PS blocking antibodies to all checkpoint treatment groups, including the combination of PD-1 + LAG3, resulted in enhanced tumor infiltrating lymphocytes (TILs), a reduction of myeloid derived suppressor cells (MDSCs), and enhanced cytokines associated with immune system activation.

### Conclusions

Overall, our data demonstrate that while PS, LAG3, and PD-1 therapies each have efficacy in TNBC as single agents, I/O treatments that include PS blocking antibodies offer significantly improved growth inhibition and are capable of increasing TILs compared to single and combinational treatments by T cell checkpoint targeting inhibitors alone.

### 214

#### **The immunoreceptor TIGIT regulates anti-tumor immunity**

Jane Grogan, Nicholas Manieri, Eugene Chiang, Patrick Caplazi, Mahesh Yadav

Genentech, South San Francisco, CA, USA

#### **Background**

Strategies to re-activate exhausted anti-tumor immune responses with antibody blockade of key T cell co-inhibitory

## Combinations: Immunotherapy/Immunotherapy

Presenting author underlined; *Primary author in italics*

receptors such as PD-1/PD-L1 or CTLA-4 have demonstrated transformational potential in the clinic. TIGIT (a PVR-nectin family member) is a dominant immuno-inhibitory receptor on tumor-specific T and NK cells, shown to regulate anti-tumor immunity. Activation of TIGIT on T and NK cells limits proliferation, effector cytokine production, and killing of target tumor cells. The high affinity receptor for TIGIT is PVR, and the counter agonist receptor is CD226, all of which are members of the PVR-nectin family. TIGIT is elevated in the tumor microenvironment in many human tumors and coordinately expressed with other checkpoint immune receptors such as PD-1. However, the spatial and coordinate expression of these receptors and ligands required for these functions, and the cell-types involved in anti-tumor immunity, remains unknown.

### Methods

TIGIT, CD226 and PD-L1 blockade will be assessed in preclinical syngeneic tumor model CT26 and MC38. To determine which immune cells are important for allowing tumor progression early and late in disease mice with cell-specific gene ablation for these family members were challenged with tumors. Tumor growth was determined and tumor sections labeled and probed by fluorescence microscopy to assess TIGIT, CD226 and PVR cellular expression.

### Results

In mouse models of both cancer, antibody co-blockade of TIGIT and PD-L1 enhanced CD8<sup>+</sup> T cell effector function, resulting in significant tumor clearance. TIGIT is expressed on CD8<sup>+</sup> T cell, Treg and NK cells. Specific ablation of TIGIT on CD8<sup>+</sup> T cells resulted in tumor clearance, and was dependent on PVR in the host tissue. Immunofluorescence studies will be presented.

### Conclusions

Therapeutic blockade of TIGIT may result in improved eradication of malignancies when used in conjunction with other anti-cancer therapies including those that modulate anti-tumor immune responses, and is currently being tested in phase I clinical trials. Models indicate that inhibition of TIGIT with a blocking mAb may release CD226 to activate tumor-specific T cells. Another mechanism could involve regulation of T cell suppression by TIGIT on regulatory T cells. A better understanding of the coordinate interaction between these receptors and ligands in tumors will be informative for the appropriate application of checkpoint-therapy combinations.

215

### CC-122 in combination with immune checkpoint blockade synergistically activates T cells and enhances immune mediated killing of HCC cells

Patrick Hagner<sup>1</sup>, Hsiling Chiu<sup>1</sup>, Michelle Waldman<sup>1</sup>, Anke Klippel<sup>1</sup>, Anjan Thakurta<sup>1</sup>, Michael Pourdehnad<sup>2</sup>, Anita Gandhi<sup>1</sup>

<sup>1</sup>Celgene Corporation, Summit, NJ, USA

<sup>2</sup>Celgene Corporation, San Francisco, CA, USA

### Background

CC-122 binds the E3 ubiquitin ligase CRL4<sup>CRBN</sup> resulting in the degradation of the transcription factor Aiolos and activation of T cells. Preclinical and clinical data obtained in hematologic malignancies indicate that CC-122 exerts immunomodulatory activity through enhanced antibody dependent cell-mediated cytotoxicity and a shift in T cell subsets from a naïve to effector and memory subsets. CC-122 is in clinical development in multiple hematologic diseases and in solid tumors such as hepatocellular carcinoma (HCC) as a single agent (NCT01421524) and in combination with nivolumab (nivo). The effects of combining CC-122 with immune checkpoint antibodies in *in vitro* models of T cell activation and immune co-culture models with HCC cells were examined.

### Methods

Carboxyfluorescein succinimidyl ester (CFSE) based proliferation, cytokine production and immune co-culture assays were performed with stimulated peripheral blood mononuclear cells (PBMC) from healthy donors followed by drug treatment. Drug combinations were investigated in mixed lymphocyte reactions (MLR) with monocyte derived dendritic cells and T cells from separate donors. Apoptosis was measured via Annexin V/ToPro3 staining. Synergy calculations were performed with the fractional product method.

### Results

In a 3-day CD3-stimulated PBMC assay, CC-122 (1-10 $\mu$ M) treatment elevated HLA-DR, a marker of T cell activation, by 3.4-5.5 and 3.2-5.3 fold in CD4<sup>+</sup> and CD8<sup>+</sup> T cells, respectively. Proliferation of CD4<sup>+</sup> and CD8<sup>+</sup> T cells from CD3-stimulated PBMC treated with vehicle, CC-122 (50nM), nivo (50 $\mu$ g/ml) or the combination was assessed via CFSE staining. The percentage of proliferating vehicle-treated CD4<sup>+</sup> and CD8<sup>+</sup> cells was 37% and 40%, compared to nivo (45% and 47%), CC-122 (54% and 68%) and the combination (61% and 74%). SEB stimulated PBMC were treated with CC-122 (40nM), and nivo or  $\alpha$ -PD-L1 (0.1-100 $\mu$ g/ml) resulting in secretion of 424, 160 and 154 ng/ml IL-2, respectively. The combination of CC-122 with either nivo or  $\alpha$ -PD-L1 (10 $\mu$ g/ml) resulted in synergistic





## Combinations: Immunotherapy/Immunotherapy

*Presenting author underlined; Primary author in italics*

IL-2 secretion levels of 873 and 813 ng/ml, respectively. In an MLR assay, the combination of CC-122 (100nM) with nivo (10µg/ml) or α-PD-L1 (10µg/ml) resulted in synergistic IL-2 and IFNγ secretion. Finally, the combination of CC-122 and nivo or CC-122 and α-PD-L1 significantly increased PBMC-mediated cytotoxicity of HCC cells compared to either single agent or isotype control ( $p \leq 0.05$ ).

### Conclusions

CC-122 in combination with nivo or anti-PD-L1 antibodies results in synergistic activation of T cells and significantly enhanced immune mediated cytotoxicity against HCC cells. Given the novel mechanism of immunomodulation by CC-122 and synergistic combination with checkpoint blockade, clinical investigation in HCC is currently in progress.

### 216 Abstract Travel Award Recipient

#### **Reactivating the anti-tumor immune response by targeting innate and adaptive immunity in a phase I/II study of intratumoral IMO-2125 in combination with systemic ipilimumab in patients with anti-PD-1 refractory metastatic melanoma**

*Cara Haymaker*<sup>1</sup>, Marc Uemura<sup>1</sup>, Ravi Murthy<sup>1</sup>, Marihella James<sup>1</sup>, Daqing Wang<sup>2</sup>, Julie Brevard<sup>2</sup>, Catherine Monaghan<sup>2</sup>, Suzanne Swann<sup>2</sup>, James Geib<sup>2</sup>, Mark Cornfeld<sup>2</sup>, Srinivas Chunduru<sup>2</sup>, Sudhir Agrawal<sup>2</sup>, Cassian Yee<sup>1</sup>, Jennifer Wargo<sup>1</sup>, Sapna P Patel<sup>1</sup>, Rodabe Amaria<sup>1</sup>, Hussein Tawbi<sup>1</sup>, Isabella Glitza<sup>1</sup>, Scott Woodman<sup>1</sup>, Wen-Jen Hwu<sup>1</sup>, Michael A Davies<sup>1</sup>, Patrick Hwu<sup>1</sup>, Willem W Overwijk<sup>1</sup>, Chantale Bernatchez<sup>1</sup>, Adi Diab<sup>1</sup>

<sup>1</sup>University of Texas MD Anderson Cancer Center, Houston, TX, USA

<sup>2</sup>Idera Pharmaceuticals, Inc., Cambridge, MA, USA

### Background

While checkpoint inhibitor (CPI) therapy has transformed metastatic melanoma (MM) treatment, many patients remain refractory. We reasoned that combining CPI with an agent that activates antigen presenting cells and improves T cell priming may result in improved response. Our approach is to modulate the tumor microenvironment through intratumoral (i.t.) injection of the TLR9 agonist, IMO-2125, in combination with ipilimumab (ipi). We hypothesize that this will result in dendritic cell (DC) activation and induction of tumor-specific CD8<sup>+</sup>T cells which will synergize with ipilimumab to overcome immune-escape. Based on this rationale we initiated a phase I/II clinical trial.

### Methods

Adults with refractory MM despite up to 2 lines of CPI including PD-1 blockade therapy (with or without a BRAF inhibitor) are eligible. IMO-2125, in doses escalating from

4mg to 32mg, is given i.t. weeks 1, 2, 3, 5, 8, and 11 along with ipilimumab i.v. 3 mg/kg weeks 2, 5, 8, and 11. Dose-limiting toxicity (DLT) is evaluated using a modified Toxicity Probability Interval design. Primary endpoints are safety, tumor response, and PK. Blood and injected and distal tumor biopsies are obtained pre- and on-treatment. Immune analyses include DC subsets and their activation status as well as T cell activation, function and proliferation. T cell repertoire diversity will be evaluated by high throughput CDR3 sequencing.

### Results

As of August 2, 2016, 11 pts have been enrolled. DLT has not been observed. Grade 3 hypophysitis (2 subjects) is the only immune-related AE observed to date. No other drug-related grade 3-5 AEs were documented and only 1 subject experienced a grade 2 fever. Five patients are evaluable for response - 2 PR, 2SD, 1PD per investigator assessment. Fresh tumor biopsies show maturation (upregulation of HLA-DR) of the myeloid DC1 subset (CD1c<sup>+</sup>CD303<sup>-</sup>) in the IMO-2125 injected tumor lesion 24 hrs post-treatment compared to pre-treatment biopsy. On-treatment biopsy results are consistent with a higher rate of proliferative (Ki67) effector CD4<sup>+</sup> and CD8<sup>+</sup> T cells in responders. Cytokine analysis shows a 2-3 fold increase in circulating IFNγ levels compared to pretreatment in responders.

### Conclusions

Though preliminary, these results demonstrate that the combination of ipi and IMO-2125 is well tolerated with encouraging preliminary activity in a PD-1 refractory population. Dose escalation is ongoing and a phase II expansion will include IMO-2125 in combination with both ipi and anti-PD-1. Updated safety, antitumor activity, and biomarker data will be presented.

### Trial Registration

ClinicalTrials.gov identifier NCT02644967.

### 217

#### **Ubiquitin-specific protease 6 (USP6) oncogene confers dramatic sensitivity of sarcoma cells to the immunostimulatory effects of interferon**

*Ian Henrich*<sup>1</sup>, Laura Quick<sup>2</sup>, Rob Young<sup>2</sup>, Margaret Chou<sup>2</sup>

<sup>1</sup>University of Pennsylvania, Philadelphia, PA, USA

<sup>2</sup>Children's Hospital of Pennsylvania, Philadelphia, PA, USA

### Background

Bone and soft tissue tumors (BSTTs) represent a heterogeneous class of neoplasms that disproportionately affect children. Compared to other malignancies, BSTTs are poorly understood, which has hampered the development of effective therapies. Our lab previously discovered that



## Combinations: Immunotherapy/Immunotherapy

Presenting author underlined; Primary author in italics

the oncogenic de-ubiquitylating enzyme USP6 is the key etiologic agent in several benign BSTTs, and is selectively overexpressed in multiple sarcomas, a malignant class of BSTTs [1]. USP6 drives tumorigenesis by directly de-ubiquitylating the Jak1 kinase, leading to its stabilization and activation of STAT transcription factors [2]. Since the Jak1-STAT pathway is a central mediator of interferon (IFN) signaling, we hypothesized that USP6 overexpression in sarcomas would render them hypersensitive to the immune stimulatory effects of IFN, which could be exploited for therapeutic benefit.

### Methods

USP6 was expressed in a doxycycline-inducible manner in various patient-derived sarcoma cell lines, including Ewing sarcoma, rhabdomyosarcoma, leiomyosarcoma, and liposarcoma. USP6 expression levels were confirmed to approximate those in primary patient tumor samples.

### Results

USP6 conferred exquisite sensitivity of sarcoma cells to the immuno-modulatory effects of IFN. Activation of STAT1 and STAT3 were both enhanced and prolonged in sarcoma cells expressing USP6 upon IFN treatment. RNA-sequencing confirmed that USP6 induces an IFN response signature by itself, and that it synergizes with IFN to dramatically induce interferon-stimulated gene (ISG) expression. The ISGs synergistically induced by USP6 and IFN include a large group of anti-tumor and immunomodulatory genes: the pro-apoptotic ligand TRAIL was dramatically elevated and mediated apoptosis of USP6-expressing sarcoma cells. Immunomodulatory factors synergistically induced by USP6 and IFN included chemokines and cytokines that drive migration and differentiation of T cells.

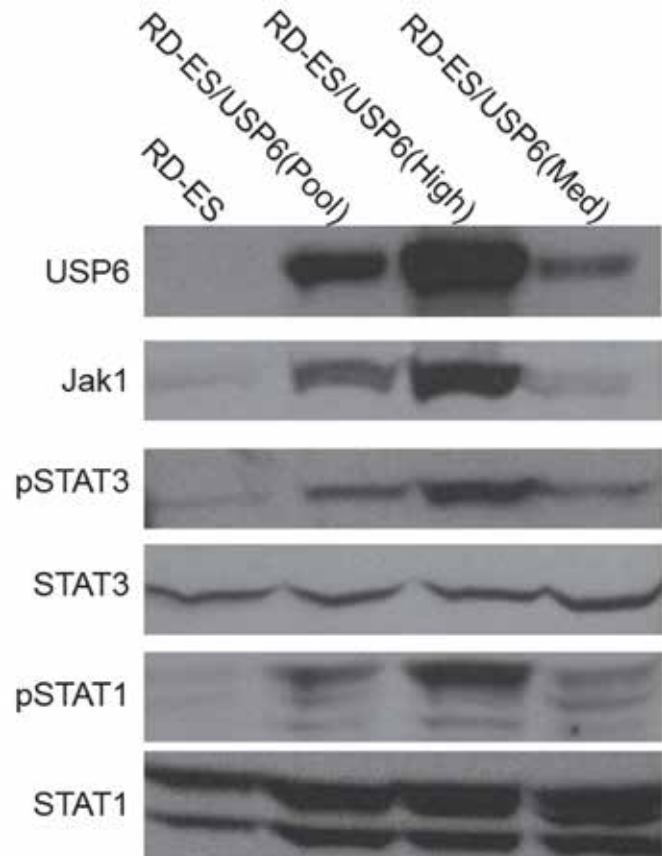
### Conclusions

USP6 overexpression sensitized sarcoma cells to IFN, simultaneously inducing TRAIL-mediated death and stimulating sarcoma cells to produce immune stimulatory/anti-tumorigenic chemokines and cytokines. This dual mechanism of action may position IFN as an extremely effective therapeutic agent for treatment of sarcomas that overexpress USP6.

### References

1. Oliveira A, Chou M: **The TRE17/USP6 oncogene: a riddle wrapped in a mystery inside an enigma.** *Front Biosci (Schol Ed)* 2012, **4**:321-340.
2. Quick L, Young R, Henrich I, Wang X, Asmann Y, Oliveira A, Chou M: **Jak1-STAT3 signals are essential effectors of the USP6/TRE17 oncogene in tumorigenesis.** *Cancer Res* 2016, in press.

Figure 1. USP6 Expression in RD-ES Cell Line

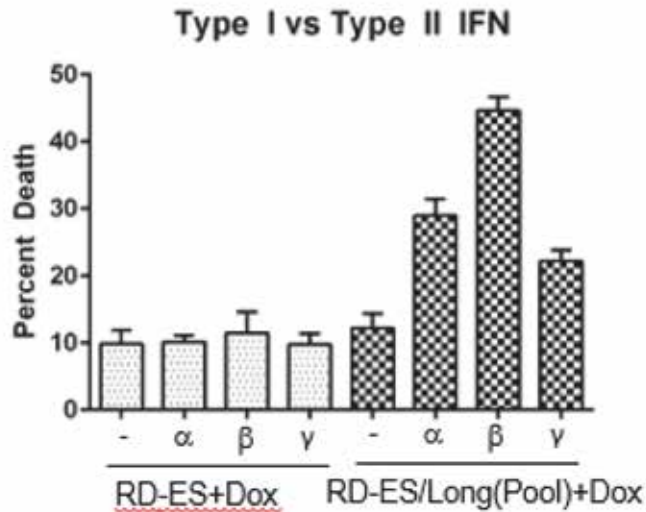


USP6 was expressed in a doxycycline-inducible in the patient derived Ewing sarcoma cell line. Clonal lines that express high or medium amounts of USP6 were isolated from the initial pooled population. Expression of USP6 increased Jak1 levels and activation of downstream effectors STAT1 and STAT3 in an USP6 dose dependent manner. Note: Similar lines were/are being created for other sarcomas. RD-ES is used as an example.

## Combinations: Immunotherapy/Immunotherapy

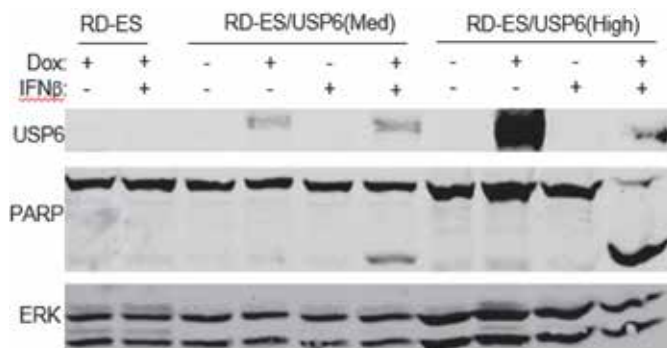
Presenting author underlined; Primary author in *italics*

**Figure 2. USP6 Sensitizes Cells to IFN-Induced Death**



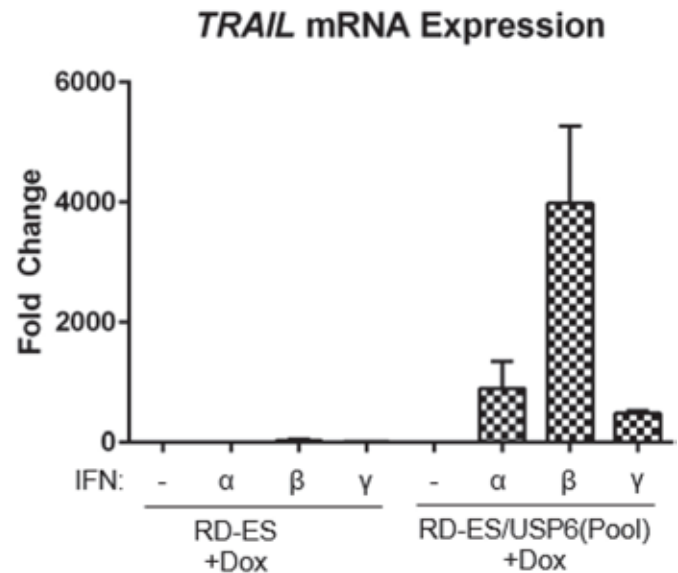
RD-ES were treated with 1000 U/mL IFN $\alpha$ , IFN $\beta$ , or IFN $\gamma$  for 24 hours with or without USP6 expression. IFN $\beta$  was most effective in inducing death (~50%). Death was monitored via trypan blue exclusion.

**Figure 3. USP6 Expression Determines Sensitivity to IFN-Induced Death**



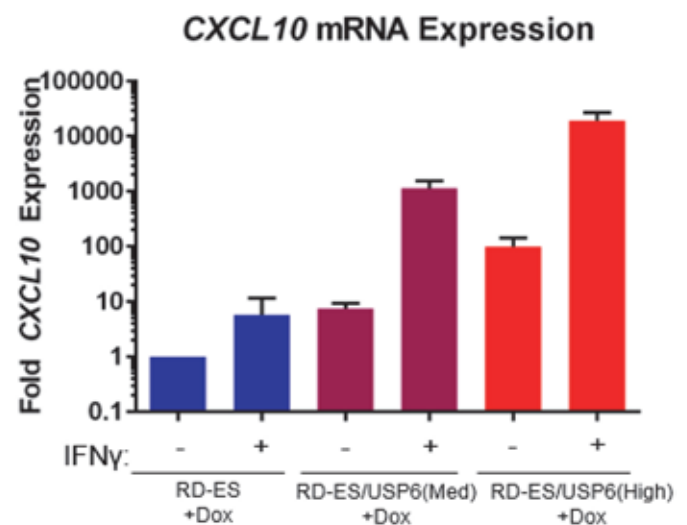
RD-ES, RD-ES/USP6(Med), and RD-ES/USP6(High) were treated with 1000 U/mL IFN $\beta$  overnight. Higher USP6 increases the sensitivity of the cells to IFN $\beta$  induced death. Death was monitored by PARP cleavage.

**Figure 4. USP6 Synergizes with IFN to Massively Upregulate TRAIL**



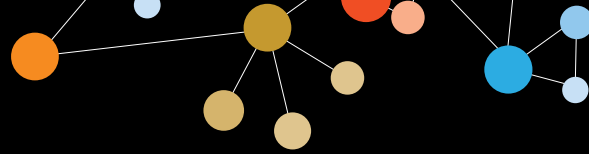
RD-ES were treated with 1000 U/mL IFN $\alpha$ , IFN $\beta$ , or IFN $\gamma$  for 24 hours with or without USP6 expression. TRAIL was found to be synergistically induced by IFN in the presence of USP6. IFN $\beta$  was the most potent at near 5000-fold over baseline.

**Figure 5. USP6 Synergizes with IFN $\gamma$  to Increase Chemokine Expression**



RD-ES, RD-ES/USP6(Med), and RD-ES/USP6(High) were treated with 10 U/mL IFN $\gamma$  overnight. The chemokine CXCL10 was synergistically induced in an USP6 dose-dependent manner. Similar expression patterns were seen for other chemokines like CXCL9 and CXCL11





## Combinations: Immunotherapy/Immunotherapy

Presenting author underlined; *Primary author in italics*

consistent with increased capacity to generate adenosine. The adenosine analog NECA inhibited TCR-mediated ERK phosphorylation and production of IL-2 and IFN $\gamma$  in human PBMCs; these inhibitory effects were blocked by CPI-444. Treatment of MC38 with CPI-444 led to inhibition of tumor growth, with tumor elimination in ~30% of mice. Combining CPI-444 with anti-PD-L1 synergistically inhibited tumor growth and eliminated tumors in 90% of mice. When cured mice were re-challenged with MC38, tumors were uniformly rejected, indicating CPI-444 induced systemic anti-tumor memory. CD8<sup>+</sup> depletion abrogated efficacy of CPI-444  $\pm$  anti-PD-L1 treatment. Biomarker results from the ongoing phase Ib trial demonstrate CPI-444 neutralizes A2AR signaling and activates markers of an immune response. To measure A2AR inhibition, peripheral blood samples were activated with NECA and pCREB quantified using flow cytometry. A2AR signaling was robustly inhibited in 8 of 9 patients in an exposure dependent manner. Of the patients evaluated so far, immune activation was observed by flow cytometry analysis of PD-1/CD8 frequency in all continuously treated patients and a subset of patients on the 14 day schedule. IHC and gene expression of pathway markers in serial tumor biopsies will be discussed.

### Conclusions

In total, this shows that CPI-444 exhibits functional inhibition of adenosine signaling, and treatment is associated with activation of markers of anti-tumor immunity. This is the first demonstration of immune modulation in cancer patients receiving an adenosine antagonist.

219

### **Probody™ therapeutics targeting the PD-1/L1 axis provide preclinical anti-tumor efficacy while minimizing induction of autoimmunity as single agents and in combination with CTLA-4 blockade**

Kimberly A Tipton, Kenneth R Wong, Victoria Singson, Chihunt Wong, Chanty Chan, Yuanhiu Huang, Shouchun Liu, Jennifer H Richardson, W Michael Kavanaugh, James West, *Bryan A Irving*

CytomX Therapeutics, Inc., South San Francisco, CA, USA

### Background

Immunotherapy has transformed cancer treatment by unleashing potent and durable anti-tumor immunity against many cancers. However, because many of the same mechanisms control anti-tumor immunity and self-tolerance, these therapies can also induce systemic autoimmunity by activating autoreactive T cells in normal tissues. Combinations of checkpoint inhibitors targeting PD-1 and CTLA-4 increase clinical response rates, but similarly increase toxicities, thereby reducing their clinical potential. New

approaches are therefore needed that provide anti-tumor activity without dysregulating systemic immunity.

### Methods

CytomX has developed Probody therapeutics (Pb-Tx) that are proteolytically-activated antibodies designed to widen the therapeutic index by minimizing drug interaction with normal tissue while retaining anti-tumor activity. Pb-Tx are “masked” to attenuate binding to target in healthy tissue, but can become “unmasked” in the tumor microenvironment by tumor-specific protease activity.

### Results

*In vitro*, the masked PD-1 Pb-Tx had reduced affinity for mouse PD-1 relative to the parental antibody. Binding affinity was completely restored following addition of appropriate proteases. In mice, single-agent antibodies to CTLA-4 and to PD-1, and the PD-1 Pb-Tx induced 10%, 30%, and 20% complete tumor regressions (CRs) against established MC38 tumors, respectively. In combination with anti-CTLA-4, both PD-1 antibody and Pb-Tx induced 80% CRs and generated effective T cell memory against tumor re-challenge. In 10-week-old NOD mice, a 1 or 10 mpk single dose of anti-PD-1 antibody induced diabetes in 43% and 57% of mice, respectively, while a 10 mpk dose of PD-1 Pb-Tx yielded only 14% disease incidence with delayed onset. In younger NOD mice, the CTLA-4/PD-1 antibody combination induced diabetes in 50% of mice. In contrast, mice administered the PD-1 Pb-Tx/CTLA-4 antibody combination were completely protected. Similar data were generated with a PD-L1-targeted Pb-Tx.

### Conclusions

A PD-1 targeted Pb-Tx provided equivalent anti-tumor efficacy in mice to that of its parental antibody while protecting from anti-PD-1-mediated autoimmunity, both as a single agent and in combination with a CTLA-4 antibody. These results demonstrate that PD-1 Pb-Tx retain anti-tumor efficacy with improved safety profiles preclinically and therefore have promise to enable safer combination immunotherapies.

220

### **Enhancement of target expression on breast tumors via hormone receptor antagonism: a novel strategy for enhancing immunotherapeutic efficacy**

Ritika Jaini, Matthew Loya, Charis Eng

Lerner Research Institute, Cleveland Clinic, Cleveland, OH, USA

### Background

Immunotherapy has historically been successful in highly antigenic tumors but mostly failed in non-antigenic tumors.



## Combinations: Immunotherapy/Immunotherapy

Presenting author underlined; Primary author in italics

Our studies in autoimmunity have shown that increased antigen load within a tissue enhances immune reactivity against it. We hypothesize that enhancing protein target expression on breast tumors can increase the efficacy of targeted immunotherapy. Lactation proteins have recently been shown to be effective immunotherapeutic targets on breast tumors. Since lactation proteins are negatively regulated by signaling via the estrogen receptor (ER), we hypothesize that target lactation protein expression on breast tumors can be increased by antagonism of the ER in order to enhance efficacy of antigen specific immunotherapy/vaccination.

### Methods

Enhancement of target protein expression in human breast tumors was tested *in vitro* by treatment of ER+ (MCF7 cells) and ER+PR+ (T47D cells) with different doses of the clinically approved ER modulator, tamoxifen. *In vivo* modulation of target antigen expression was tested by inoculating 6-7 week old Balb/cJ female mice with 4T1 breast tumors followed by oral treatment with tamoxifen. Increase in lactation protein expression (e.g. alpha lactalbumin) was assayed by *in vitro* Luciferase assays followed by confirmation by immunoblotting and immunohistochemistry at different time points post treatment. Effect of increased antigen expression on efficacy of targeted immunotherapy was assessed by antigen specific immunization of 4T1 tumor bearing mice with or without tamoxifen administration and comparing tumor growth.

### Results

Our *in vitro* studies on human tumors and *in vivo* murine studies show that antagonism of the ER via tamoxifen treatment can substantially increase expression of target lactation proteins such as alpha lactalbumin on breast tumors. We show that whereas at least a 2-3 fold increased expression of the target protein can be achieved on tumors, normal breast tissue remains unaffected. Tumor progression studies revealed that in spite of increased target expression, no enhancement in efficacy of immunotherapy was achieved via active immunization protocols. However, efficacy of cell based targeted immunotherapies can possibly be enhanced when applied in combination with our proposed strategy to increase target expression.

### Conclusions

Singular increase in target antigen expression on tumors is not effective in enhancing efficacy of immunotherapy probably due to associated limiting factors such as DC trafficking, antigen presentation and effective priming. However, the efficacy of cell-based targeted immunotherapeutic strategies that circumvent the limitations around active priming can be enhanced by using our combinatorial strategy of enhancing antigen expression on tumors via hormone receptor antagonism.

### Acknowledgements

The PhRMA Foundation for funding support.

### 221

#### **Dose escalation/confirmation results of ENCORE 601, a phase Ib/II, open-label study of entinostat (ENT) in combination with pembrolizumab (PEMBRO) in patients with non-small cell lung cancer (NSCLC)**

Melissa L Johnson<sup>1</sup>, Alex A Adjei<sup>2</sup>, Mateusz Opyrchal<sup>3</sup>, Suresh Ramalingam<sup>4</sup>, Pasi A Janne<sup>5</sup>, George Dominguez<sup>6</sup>, Dmitry Gabrilovich<sup>6</sup>, Laura de Leon<sup>7</sup>, Jeannette Hasapidis<sup>7</sup>, Scott J Diede<sup>8</sup>, Peter Ordentlich<sup>7</sup>, Scott Cruickshank<sup>7</sup>, Michael L Meyers<sup>9</sup>, *Matthew D Hellmann*<sup>10</sup>

<sup>1</sup>Sarah Cannon Research Institute, Nashville, TN, USA

<sup>2</sup>Mayo Clinic, Rochester, MN, USA

<sup>3</sup>Roswell Park Cancer Institute, Buffalo, NY, USA

<sup>4</sup>Emory University, Atlanta, GA, USA

<sup>5</sup>Dana-Farber Cancer Institute, Boston, MA, USA

<sup>6</sup>The Wistar Institute, Philadelphia, PA, USA

<sup>7</sup>Syndax Pharmaceuticals, Inc., Waltham, MA, USA

<sup>8</sup>Merck Research Laboratories, North Wales, PA, USA

<sup>9</sup>Syndax Pharmaceuticals, Inc., New York, NY, USA

<sup>10</sup>Department of Medicine, Memorial Sloan Kettering Cancer Center, New York, NY, USA

### Background

ENT is an oral, class I selective histone deacetylase (HDAC) inhibitor shown in animal models to reduce immunosuppressive myeloid derived suppressor cells (MDSCs) and regulatory T cells (Tregs) and produce synergistic anti-tumor responses when combined with immune checkpoint inhibition. ENCORE 601 is a phase Ib/II study designed to evaluate ENT plus PEMBRO in patients with advanced NSCLC. The objective of the phase Ib dose escalation/confirmation portion was to determine the recommended phase II dose (RP2D).

### Methods

Patients with stage III/IV NSCLC (previous anti-PD-1/PD-L1 therapy was permitted) were enrolled in a 3+3 dose escalation phase. ENT 3mg and 5mg QW PO + PEMBRO 200mg Q3W IV in 21-day cycles were explored to determine the safety and RP2D, followed by a dose-confirmation cohort (n=9). Pre-treatment biopsies were required. Correlative studies included tumor PD-L1 expression and phenotypic and functional evaluation of immune cell subsets in peripheral blood and tumor tissue.

### Results

Twenty-two NSCLC patients (9 of which progressed on prior anti-PD-1/PD-L1 therapy) were treated with ENT plus PEMBRO; 13 in the dose escalation phase (6 at ENT 3mg and 7 at ENT 5mg) and 9 in the dose confirmation phase





## Combinations: Immunotherapy/Immunotherapy

Presenting author underlined; Primary author in italics

(ENT 5mg). Of 20 patients with PD-L1 expression results, 7 patients (35%) had PD-L1 <1%, 8 (40%) had PD-L1 1-49%, and 5 (25%) had PD-L1 ≥ 50%. During dose escalation, 1 patient previously treated with anti-PD-1 therapy experienced a DLT at Cycle 2 Day 15 (ENT 3mg, Grade 3 immune-mediated hepatitis), and no other DLTs were observed. Among all 22 patients treated, Grade 3/4 treatment-related AEs included hypophosphatemia (9%), neutropenia (5%), anemia (5%), acute respiratory failure (5%), elevated alkaline phosphatase (5%) and immune-mediated hepatitis (5%). Of 6 evaluable patients previously exposed to anti-PD-1/PD-L1, best response includes 3 SD and 3 PD. Of 11 evaluable anti-PD-1/PD-L1 naïve patients, best response includes 1 PR, 1 SD and 9 PD. A reduction in peripheral MDSC levels was observed between pre-treatment and Cycle 2 Day 1 in 7 of 11 patients assessed (median decrease of 40.7% PMN-MDSCs; 67.3% M-MDSCs).

### Conclusions

5mg ENT weekly combined with PEMBRO has a manageable safety profile, expected pharmacodynamic effects on reducing MDSCs, and will be further explored in the phase II expansion cohorts including NSCLC and melanoma.

### Trial Registration

ClinicalTrials.gov identifier NCT02437136.

## 222

### Combinatorial reprogramming of chemokine environment in colorectal and ovarian cancer patients to promote intratumoral CTL infiltration

Pawel Kalinski<sup>1</sup>, Amer Zureikat<sup>2</sup>, Robert Edwards<sup>3</sup>, Ravi Muthuswamy<sup>3</sup>, Nataša Obermajer<sup>4</sup>, Julie Urban<sup>3</sup>, Lisa H Butterfield<sup>2</sup>, William Gooding<sup>2</sup>, Herbert Zeh<sup>3</sup>, David Bartlett<sup>4</sup>

<sup>1</sup>Department of Surgery; University of Pittsburgh Cancer Institute; Department of Infectious Diseases and Microbiology, University of Pittsburgh, Pittsburgh, PA, USA  
<sup>2</sup>University of Pittsburgh Cancer Institute, Pittsburgh, PA, USA  
<sup>3</sup>University of Pittsburgh, Pittsburgh, PA, USA  
<sup>4</sup>Department of Surgery, University of Pittsburgh, Pittsburgh, PA, USA

### Background

Since the infiltration of tumor tissues with effector CD8<sup>+</sup> T cells (CTLs) is associated with improved clinical outcomes and predicts patients' responsiveness to checkpoint blockers, we developed a combinatorial approach to selectively enhance the production of CTL chemokines in tumor lesions, while avoiding the activation of healthy tissues. Our preliminary data from human *ex vivo* tissue culture models demonstrate that a) TLR3-based combinatorial adjuvants selectively induce CTL-attracting chemokines in tumor-associated stromal and myeloid cells, while avoiding undesirable activation of cancer

cells and surrounding non-tumor tissues; b) combination of TLR3 ligands with IFN $\alpha$  synergistically amplifies the production of CTL-attracting chemokines and allows to uniformly induce their production in all tumor lesions; and c) that the inclusion of COX2 blockers prevents the induction of Treg-attractants.

### Methods

Based on these preclinical data, we developed a phase I/II clinical trial (UPCI 10-131/NCT01545141) to determine the safety and local effectiveness of intravenous infusion of rintatolimod (Ampligen; selective TLR3 ligand) combined with Intron A and oral celecoxib, in patients with resectable recurrent colorectal cancer. Our phase I/II trial UPCI 11-128 (NCT02432378) evaluates the safety, feasibility and local effectiveness of the intraperitoneal delivery of rintatolimod and Intron A (with oral celecoxib) in cisplatin-treated patients with recurrent ovarian cancer.

### Results

In the completed phase I of UPCI 10-131, we observed very good safety profile of this combination and, in accordance with our expectations, selective disappearance of CTL-, TH1- and NK cell markers from circulation, lasting 24-48 hours after rintatolimod/Intron A infusion. Comparison of the resected tumors demonstrated enhanced intratumoral ratios of CXCL10 (CTL-attractant) to CCL22 (Treg-attractant) and CD8 $\alpha$  (CTL marker) to FoxP3 (Treg marker), in the treatment cohort, compared to patients receiving standard care at our center (non-randomized control). The randomized phase II portion of this clinical study is ongoing. Our recently-implemented study UPCI 11-128 provides preliminary indication of the feasibility and local effectiveness of intraperitoneal modulation of tumor microenvironments in cisplatin-treated ovarian cancer patients.

### Conclusions

Our data provide early indications of the safety and feasibility of using combinatorial adjuvants to selectively enhance intratumoral CTL infiltration. Verification of these results in randomized phase II portions of our trials may provide new means to enhance the clinical effectiveness of checkpoint inhibitors, therapeutic vaccines and adoptive T cell therapies (ACT) against "cold tumors", enhancing the scope of their applications.

### Acknowledgements

This project was supported by the NIH grants P01 CA132714 and P50 CA159981. Rintatolimod was provided under MTA by Hemispherx Bio.

### Trial Registration

ClinicalTrials.gov identifier NCT01545141.

## Combinations: Immunotherapy/Immunotherapy

Presenting author underlined; Primary author in italics

223

### A model system to characterize the personalized cell immunotherapy, AGS-003, and predict functional activity in combination with PD-1 checkpoint inhibitor and sunitinib

*Olga Zubkova*<sup>1</sup>, Larissa Agapova<sup>1</sup>, Marina Kapralova<sup>1</sup>, Liudmila Krasovskaia<sup>1</sup>, Armen Ovsepyan<sup>2</sup>, Maxim Lykov<sup>2</sup>, Artem Ereemeev<sup>1</sup>, Vladimir Bokovanov<sup>1</sup>, Olga Grigoryeva<sup>1</sup>, Andrey Karpov<sup>1</sup>, Sergey Ruchko<sup>1</sup>, Charles Nicolette<sup>3</sup>, Alexandr Shuster<sup>2</sup>

<sup>1</sup>LLC Cellthera Pharm, Volginsky, Vladimir, Russia

<sup>2</sup>LLC IBC Generium, Volginsky, Vladimir, Russia

<sup>3</sup>Argos Therapeutics Inc., Durham, NC, USA

#### Background

AGS003 is an immunotherapy consisting of autologous dendritic cells (DCs) electroporated with amplified total tumor RNA plus synthetic CD40L RNA and is currently being tested in combination with standard of care to extend survival of newly diagnosed metastatic RCC patients in the phase III ADAPT clinical trial. We set out to establish an animal model system to more thoroughly study the AGS-003 mechanism of action and assess the functionality in combination with other therapeutic agents.

#### Methods

Mouse DC precursors were processed in a similar manner to how human monocytes are processed to manufacture AGS-003. Bone marrow cells from 7-10 week old Balb/c mice were incubated with GM-CSF and IL4 and matured with TNF $\alpha$ , IFN $\gamma$  and PGE2. Mature DCs were electroporated with total tumor RNA from RENCA tumor plus synthetic mCD40L RNA and injected i.p. to treat syngeneic BALB/c mice in an orthotopic RCC model. This model system was utilized to test the AGS-003-like mouse DCs as a single agent or in combination with the mPD-1 checkpoint inhibitor.

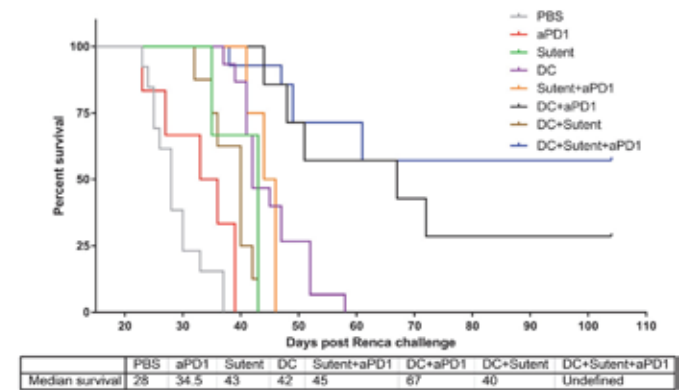
#### Results

Here we report on successfully developing murine DCs with similar properties to AGS003, including phenotype (CD80, CD83, CD86, MHC1, CCR7), secretion of IL12 induced by CD40L RNA and induction of CD8+CD28+CD45RA- memory T cells *in vivo*. Results showed that, as a single agent, the DC therapy was superior to PBS controls at increasing median survival, slowing tumor growth and decreasing lung metastases. These effects were dependent on inclusion of the amplified total RENCA cell RNA based on comparison with irrelevant RNA controls. In addition, the greatest control of tumor growth rate and median survival occurred when combined with the PD-1 checkpoint inhibitor and sunitinib.

#### Conclusions

These data demonstrate the importance of amplified total tumor RNA in directing immune responses against the corresponding tumor target and support the strategy of generating and/or augmenting preexisting antitumor immune responses with active immunotherapy to maximize clinical benefit when combined with PD-1 checkpoint inhibition and sunitinib as the standard therapy drug for renal cell carcinoma. This model system may be useful to explore additional combination therapies with other therapeutic agents.

**Figure 1. Survival curve of DC-based combination therapy in RCC mouse model**



DC monotherapy showed a 50% increase in median OS compared to the PBS group (42 vs 28 days). DC + Sunitinib combination therapy did not show increased OS compared to monotherapy with DCs or Sunitinib (40 vs 42 or 43 days). DC + aPD-1 combination therapy showed significantly increased median OS compared to monotherapy with DCs or aPD-1 (67 vs 42 or 34.5 days). DC + Sunitinib + aPD-1 combination therapy showed significantly increased media OS (>104 days) compared to all other groups tested.

224

### Local intratumoral treatment with low-dose CD40 and TLR4 agonists overcomes resistance to PD-1 blockade to control tumors systemically

Danny N. Khalil<sup>1</sup>, Luis Felipe Campesato<sup>1</sup>, Yanyun Li<sup>2</sup>, Taha Merghoub<sup>2</sup>, Jedd D. Wolchok<sup>3</sup>

<sup>1</sup>Memorial Sloan Kettering Cancer Center, New York, NY, USA

<sup>2</sup>Ludwig Collaborative Laboratory, Memorial Sloan Kettering Cancer Center, New York, NY, USA

<sup>3</sup>Department of Medicine, Memorial Sloan Kettering Cancer Center, New York, NY, USA

#### Background

Multiple cancer types resistant to immune checkpoint blockade (i.e., anti-PD-1, PD-L1, and/or CTLA-4) also



## Combinations: Immunotherapy/Immunotherapy

Presenting author underlined; Primary author in italics

demonstrate impaired antigen presenting cell (APC) activation. We hypothesized that intratumoral administration of agents designed to enforce APC activation would convert a living tumor into a source of immunogenic APCs capable of priming anti-tumor T cells.

### Methods

Using a checkpoint-blockade resistant syngeneic B16 murine model with established (0.5 - 1 cm) bilateral tumors, we screened and characterized agents associated with APC activation for their ability to overcome resistance to anti-PD-1 therapy. Such agents were administered either systemically, or intratumorally to one of the two tumors, allowing us to distinguish the effect at the injected tumor from that at the contralateral tumor.

### Results

In the setting of PD-1 blockade, we found that intratumoral treatment with the TLR4 agonist monophosphoryl lipid A (MPL) and low-dose CD40 agonist monoclonal antibody (mAb) induces an anti-tumor T cell response. CD8+ T cells subsequently infiltrate and control noninjected tumors at a distant site. Interestingly, locally injected tumors were heavily infiltrated with neutrophils expressing costimulatory markers including CD86 within 3 hours of treatment, and then rapidly regressed. In addition, there was persistence of activated dendritic cells and monocytes in the injected-tumor's draining lymph node. Within 1 week, distant tumors were infiltrated with activated CD8+ T cells, and showed a marked increase in the T effector to T regulatory ratio. The control of distant tumors was abolished in RAG1-deficient animals lacking lymphocytes. Cured animals fully resisted tumor re-implantation at 90 days, developing fur depigmentation at both the site of initial treatment and the untreated tumor reimplantation site, but not elsewhere, suggesting a highly specific anti-tumor response. Notably, systemic administration of MPL and CD40 at 25-fold higher dose was less effective than intratumoral treatment.

### Conclusions

In conclusion, low-dose intratumoral treatment with combined TLR4 and CD40 agonists induces anti-tumor T cells which in turn infiltrate tumors at distant sites and provide durable immunity such that animals are resistant to tumor re-implantation. Given that this regimen relies on agents that are FDA-approved for other indications, or in clinical development, it can readily be translated into clinical trials across a broad range of malignancies that are currently refractory to immunotherapy.

### 225

## CA-170, a first in class oral small molecule immune checkpoint antagonist, promotes T cell immune activation and inhibits tumor growth in pre-clinical models of cancer

Adam S Lazorchak<sup>1</sup>, Troy D Patterson<sup>1</sup>, Yueyun Ding<sup>1</sup>, Pottayil Sasikumar<sup>2</sup>, Naremadepalli Sudarshan<sup>2</sup>, Nagaraj Gowda<sup>2</sup>, Raghuvveer Ramachandra<sup>2</sup>, Dodheri Samiulla<sup>2</sup>, Sanjeev Giri<sup>2</sup>, Rajesh Eswarappa<sup>2</sup>, Murali Ramachandra<sup>2</sup>, David Tuck<sup>1</sup>, Timothy Wyant<sup>1</sup>

<sup>1</sup>Curis, Inc., Lexington, MA, USA

<sup>2</sup>Aurigene Discovery Technologies Limited, Bangalore, Karnataka, India

### Background

Antibody-mediated immune checkpoint blockade has transformed cancer therapy. However, the majority of patients fail to respond to antibody therapies targeting single immune checkpoint pathways and antibodies exhibit a long *in vivo* half-life which may contribute to the emergence of immune-related adverse events. Additionally, antibody therapies must be administered by intravenous infusion in a hospital or clinic setting, which places additional burden on patients who may have mobility challenges. CA-170 is a small molecule, orally bioavailable antagonist of the PD-L1, PD-L2 and VISTA/PD-1H immune checkpoint pathways, currently undergoing phase I clinical testing. CA-170 was developed through a rational design and a screening strategy which identified small molecules that could antagonize T cell suppression independently mediated by PD-L1, PD-L2 and VISTA/PD-1H in functional assays.

### Methods

CA-170 inhibition of the PD-1/PD-L1/2 or VISTA/PD-1H signaling has been inferred through *in vitro* T cell effector function rescue studies using human, monkey or mouse cells stimulated in the presence of inhibitory PD-L1, PD-L2 or VISTA/PD-1H proteins. CA-170 selectivity was tested against the related inhibitory immune checkpoint pathways CTLA-4, LAG-3, BTLA or the immune co-stimulatory B7/CD28 pathway in functional assays. CA-170 *in vivo* antitumor activity and immune stimulatory activity was tested in multiple syngeneic mouse tumor models. Definitive toxicology and pharmacokinetic profiling studies were performed in mouse and cynomolgus monkey.

### Results

CA-170 exhibits potent immune rescue activity, comparable to that of blocking PD-1 or VISTA/PD-1H antibodies when tested in cell culture assays that measure the proliferation or IFN- $\gamma$  secretion of T lymphocytes stimulated in the presence of inhibitory PD-L1, PD-L2 or VISTA/PD-1H proteins. CA-170

## Combinations: Immunotherapy/Immunotherapy

Presenting author underlined; Primary author in italics

does not exhibit off target activity against CTLA-4, LAG-3, BTLA pathways or the B7/CD28 pathway in functional assays. In immune competent mice, orally administered CA-170 inhibits the growth of syngeneic tumors, enhances peripheral T cell activation, and promotes the immune activation of tumor infiltrating CD8<sup>+</sup> T cells in a dose dependent manner. In preclinical safety studies conducted in rodents and non-human primates, orally administered CA-170 shows no signs of toxicity when dosed up to 1000 mg/kg for 28 consecutive days. CA-170 exhibits an oral bioavailability of approximately 40% and <10% in mouse and monkey, respectively, and the plasma half-life ranges from approximately 0.5 hours for mouse to approximately 3.25-4.0 hours for cynomolgus monkey.

### Conclusions

These non-clinical data provide a strong rationale for the continued clinical development of CA-170, the first oral, small molecule immune checkpoint antagonist for the treatment of advanced cancers.

226

### Combination of local immunotoxins with CTLA-4 blockade eradicates murine tumors by promoting anti-cancer immunity

Yasmin Leshem<sup>1</sup>, Xiu-fen Liu<sup>1</sup>, Tapan Bera<sup>1</sup>, Masaki Terabe<sup>1</sup>, Birgit Bossenmaier<sup>2</sup>, Gerhard Niederfellner<sup>2</sup>, Yoram Reiter<sup>3</sup>, Ira Pastan<sup>1</sup>

<sup>1</sup>National Cancer Institute, NIH, Bethesda, MD, USA

<sup>2</sup>Roche Pharmaceutical Research & Early Development, Discovery Oncology, Innovation Center Penzberg, Roche Diagnostics GmbH, Penzberg, Germany

<sup>3</sup>Technion Institute, Haifa, Iceland

### Background

Immune check point blockade therapy using antibodies to cytotoxic T-lymphocyte-associated protein 4 (CTLA-4) benefits only a limited number of cancer patients. Combination therapies are being pursued to augment the immune activation and drug efficacy. SS1P and RG7787 are immunotoxins that consist of an anti-mesothelin antibody fragment genetically fused to a portion of Pseudomonas exotoxin A. We previously observed in patients delayed onset of responses to SS1P treatment that persisted long after discontinuation of the drug. This observation led us to hypothesize that immunotoxins elicit anti-tumor immunity that can be further potentiated by adding anti-CTLA-4 antibodies (aCTLA-4).

### Methods

To test our hypothesis, we constructed 66C14-M murine breast cancer cell line expressing human mesothelin on its cell surface. The cells were grown in BALB/c mice transgenic

for human mesothelin, because they were rejected by wild type mice. RG7787 or SS1P were injected directly into established tumors (average size >80 mm<sup>3</sup>) and aCTLA-4 was administered IP.

### Results

We found that the combination of aCTLA-4 with RG7787 or SS1P induced complete remissions in 23 out of 38 mice treated (60%) providing a significant survival benefit compared to mono-therapy (P < 0.001). No cures were obtained when aCTLA-4, RG7787, or SS1P were given separately. In addition, we found that responding mice treated with aCTLA-4 and SS1P had more abundant tumor-infiltrating CD8<sup>+</sup> T cells compared to mice treated with aCTLA-4 or SS1P alone (P < 0.05) and that the response was blocked when mice were treated with anti-CD8 antibodies. Furthermore, 22 out of the 23 surviving mice rejected an additional tumor challenge with the same number of 66C14-M or the parental cells (no human mesothelin) implanted 45 days after the mice were cured. These findings point to immune mediated tumor regression. To explore the mechanism responsible for the anti-tumor effect, we combined aCTLA-4 with a mutant RG7787 that is unable to kill 66C14-M cells and found that the survival of mice was not significantly better than that achieved with aCTLA-4 monotherapy. Some bacterial products activate the immune system by receptors that directly recognize microbe associated molecular patterns (MAMPs). However, our result indicates that MAMP recognition does not explain our findings.

### Conclusions

Combining intra-tumoral injection of immunotoxins with systemic administration of aCTLA-4 induced a high rate of immune mediated tumor regression. Our findings provide the first preclinical evidence to support use of this combination in patients.





## Combinations: Immunotherapy/Immunotherapy

Presenting author underlined; Primary author in italics

227

### Adjuvant effect of anti-PD-L1 in boosting HER2-targeted T cell adoptive immunotherapy

Leiming Xia<sup>1</sup>, Yang Xia<sup>1</sup>, Yangyang Hu<sup>1</sup>, Yi Wang<sup>2</sup>, Yangyi Bao<sup>2</sup>, Fu Dai<sup>2</sup>, Shiang Huang<sup>3</sup>, Elaine Hurt<sup>4</sup>, Robert E Hollingsworth<sup>4</sup>, Lawrence G Lum<sup>5</sup>, Alfred E Chang<sup>1</sup>, Max S Wicha<sup>6</sup>, Qiao Li<sup>7</sup>

<sup>1</sup>University of Michigan, Ann Arbor, MI, USA

<sup>2</sup>The No.1 People's Hospital of Hefei, Hefei, Anhui, People's Republic of China

<sup>3</sup>Union Hospital, Tongji Medical College, Huazhong University of Science and Technology, Wuhan, Hubei, People's Republic of China

<sup>4</sup>MedImmune Inc., Gaithersburg, MD, USA

<sup>5</sup>University of Virginia Cancer Center, Charlottesville, VA, USA

<sup>6</sup>University of Michigan Medical School, Ann Arbor, MI, USA

<sup>7</sup>University of Michigan Medical Center, Ann Arbor, MI, USA

#### Background

Adoptive immunotherapy utilizing anti-CD3 x anti-HER2 bispecific antibody (HER2Bi)-armed T cells benefited both HER2<sup>+</sup> patients and patients with 1 or 2<sup>+</sup> HER2 expression, ones that would be considered "HER2-negative" by classical criteria. We have also shown that the level of cancer stem cell (CSC) marker ALDH in HER2<sup>+</sup> breast cancer cells (ALDH<sup>high</sup>HER2<sup>+</sup>) is much higher than that in HER2<sup>-</sup> breast cancer cells (ALDH<sup>low</sup>HER2<sup>-</sup>), and that in luminal breast cancers that are considered HER2<sup>-</sup>, HER2 is actually selectively expressed in the ALDH<sup>high</sup> CSC population. These observations might account for the surprising result that HER2Bi-armed T cells, while intended to target HER2, seemed to benefit HER2<sup>-</sup> patients after adoptive transfer.

#### Methods

We tested the "mouse HER2" (*neu*) expression on ALDH<sup>high</sup> vs. ALDH<sup>low</sup> 4T1 cells (mouse TNBC). For mHER2 targeting in animal models, we generated anti-mouse HER2-CD3 bispecific (mHER2Bi) that binds to mouse HER2 and mouse CD3.

#### Results

HER2Bi-armed T cells used in the clinical trial killed ALDH<sup>high</sup> human breast CSCs isolated from MCF7 (HER2<sup>-</sup>) tumor significantly more than ALDH<sup>low</sup> MCF7 cells *in vitro*, while the same HER2Bi-armed T cells killed ALDH<sup>high</sup> human breast CSCs (ALDH<sup>high</sup>HER2<sup>+</sup>) isolated from BT474 (HER2<sup>+</sup>) tumor equally to ALDH<sup>low</sup> BT474 cells (ALDH<sup>low</sup>HER2<sup>+</sup>). We also found that mHER2 was selectively expressed in the ALDH<sup>high</sup> 4T1 CSC population. These results replicated our findings in human breast cancers that HER2 is selectively expressed on CSCs, even in HER2<sup>-</sup> murine tumors, such as 4T1. *In vitro*, the mHER2Bi-armed T cells killed ALDH<sup>high</sup> 4T1 CSCs significantly more than ALDH<sup>low</sup> 4T1 cells. *In vivo*, adoptive transfer of mHER2Bi-armed T cells for HER2-targeted therapy showed

antitumor effect in mHER2<sup>-</sup> 4T1-bearing host. Administration of anti-mouse PD-L1 during mHER2Bi-armed T cell adoptive transfer decreased metastases significantly more than the use of either strategy alone.

#### Conclusions

These studies have generated evidence providing proof of principle that due to the selective expression of HER2 on CSCs, HER2-targeted T cell therapy could benefit HER2<sup>-</sup> hosts as well as HER2<sup>+</sup> hosts via immune destruction of HER2<sup>+</sup> CSCs, and use of anti-PD-L1 could significantly boost the efficacy of HER2-targeted T cell therapy.

### 228 ★ Abstract Travel Award Recipient

#### Combining IL-6 blockade with novel targeted therapeutics in pancreatic cancer

Thomas Mace, Neil Makhijani, Erin Talbert, Gregory Young, Denis Guttridge, Darwin Conwell, Gregory B Lesinski

The Ohio State University, Columbus, OH, USA

#### Background

Pancreatic ductal adenocarcinoma (PDAC) is the fourth leading cause of cancer in America with few efficacious therapeutic options other than surgery. PDAC is characterized by dense and heterogeneous stroma that secretes elevated levels of the proinflammatory cytokine interleukin-6 (IL-6). Our laboratory has previously reported that higher IL-6 in PDAC patients is strongly associated with poor overall survival. Additionally, patients with pancreatic and gastrointestinal cancers have the highest incidence of cachexia. This syndrome, characterized by the loss of skeletal muscle and adipose tissue, cannot be reversed by nutritional intervention and is mediated in part by IL-6 signaling. Further, work completed by our group and others have also shown that IL-6 and other factors can promote cross-talk between the STAT3 and MEK pathways. Thus, we hypothesized that IL-6 blockade can be utilized to enhance the efficacy of novel immune or targeted therapeutics (anti-PD-L1 and cobimetinib) in pancreatic cancer.

#### Methods

*In vivo* efficacy studies were conducted with antibodies (Ab) blocking IL-6, in combination with checkpoint immunotherapy (anti-PD-L1) or MEK inhibition (cobimetinib). Experiments were conducted in mice bearing subcutaneous KPC-derived MT5 tumors; orthotopically injected KPC-luciferase expressing tumor cells in the pancreas; and Colon26 tumor bearing CD2F1 mice to determine effects on cancer cachexia.

#### Results

IL-6 blockade combined with anti-PD-L1 ( $p < 0.02$ ) or cobimetinib ( $p=0.007$ ) elicited anti-tumor efficacy in mice bearing subcutaneous KPC derived MT5 tumors, compared to



## Combinations: Immunotherapy/Immunotherapy

Presenting author underlined; *Primary author in italics*

vehicle controls. IL-6 blockade in combination with anti-PD-L1 antibodies limited tumor growth of orthotopic KPC-luciferase expressing tumor cells compared to isotype controls ( $p=0.05$ ). As a pancreatic cachexia model is not currently available, we tested IL-6 blockade in combination with cobimetinib on a classically accepted tumor cachexia model (CD2F1 mice bearing Colon26 tumors). Only mice treated with cobimetinib or the combination of IL-6 plus cobimetinib resulted in significant tumor inhibition compared to IL-6 alone or vehicle controls ( $p < 0.0001$ ). Furthermore, mice administered IL-6 alone or in combination with cobimetinib prevented tumor-induced body weight loss ( $p < 0.005$ ) and protected lean mass and hind limb muscles as compared to vehicle-treated mice ( $p < 0.05$ ).

### Conclusions

These pre-clinical results indicate that inhibition of IL-6 may affect the efficacy of novel targeted therapeutics on tumor progression, immunosuppression, and cachexia in pancreatic cancer.

### 229

#### **Distinct chemokines and chemokine receptors control the trafficking of effector and regulatory cells into melanoma tumors in the setting of combined PD-1 and CTLA-4 blockade**

Rodney JM Macedo Gonzales, Austin P Huffman, Ximi K Wang, Ran Reshef

Columbia Center for Translational Immunology, Columbia University Medical Center, New York, NY, New York, NY, USA

### Background

Pharmacologic blockade of the CTLA-4 and PD-1 immune checkpoint molecules is an effective approach for cancer immunotherapy especially in melanoma, but only a subset of patients respond. Trafficking of immune regulatory cells into the tumor microenvironment creates an immunosuppressive environment which dampens the anti-tumor response. Thus, identifying the mechanisms involved in the trafficking of effector and regulatory cells is critical for the development of strategies that increase effectiveness of checkpoint blockade. We aimed to determine which trafficking molecules are involved in anti-tumor responses by studying both human and murine melanoma.

### Methods

RNA sequencing data were obtained from 475 melanoma patients (The Cancer Genome Atlas database). Additionally, C57BL/6 mice were subcutaneously injected with 100,000 B16-F10 cells in the flank and sacrificed at day 14 for flow cytometry analysis. Anti-PD-1 + anti-CTLA-4 blocking antibodies or PBS were injected intraperitoneally at days 5, 8 and 11 after tumor inoculation.

### Results

Analysis of RNA-seq data showed that inflammatory chemokines (CCL2, CCL5, CXCL9, CXCL10) and their receptors (CCR2, CCR5, CXCR3) were overexpressed in human melanoma tumors. Interestingly, unsupervised clustering demonstrated that CCR2, CCR5 and CCL2 were associated with CD68 and CD14 genes while CXCR3, CCL5, CXCL9 and CXCL10 were associated with CD8A, CD8B and T-bet genes. Moreover, immunophenotyping of tumor-infiltrating CD45+ cells from B16-F10 tumor-bearing mice revealed higher levels of CCR2. Interestingly, monocytic myeloid-derived suppressor cells (M-MDSCs) and inflammatory dendritic cells had the highest expression of these receptors. When B16-F10 tumor-bearing mice were treated with anti-PD-1/anti-CTLA-4 antibodies, we observed a significant reduction of tumor size and increased levels of CD45+ cells ( $p < 0.05$ ), CD8+ T cells ( $p < 0.05$ ) and increased CD8/Treg ratio ( $p < 0.01$ ) in comparison to controls; however, the numbers of M-MDSC were not reduced. More importantly, CCR2 and CCR5 were still high within total CD45+ cells (26-30%) and M-MDSCs (54-71%) in both treated and control mice. Additionally, dual checkpoint blockade significantly increased the expression of CCR1 ( $p < 0.05$ ) and CXCR3 ( $p < 0.05$ ) in CD8+ T cells, without increasing levels of CCR2 and CCR5.

### Conclusions

Our data suggest that dual checkpoint blockade increases the trafficking of CD8+ T cells into the tumor using the CXCL9/CXCL10-CXCR3 axis but does not affect the CCL2-CCR2 and CCL5-CCR5 axis that are critical for M-MDSCs trafficking into the melanoma microenvironment. These results are important for the development of novel immunotherapy combinations that harness trafficking mechanisms to improve the efficacy of immunotherapies.

### 230

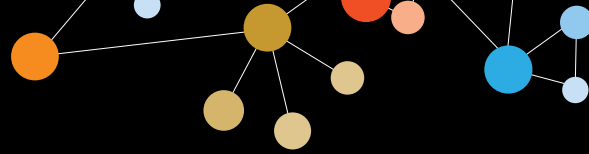
#### **Targeting tumor glutamine metabolism with CB-839 enhances the efficacy of immune checkpoint inhibitors**

Andy MacKinnon, Jason Chen, Matt Gross, Gisele Marguier, Peter Shwonek, Natalija Sotirovska, Susanne Steggerda, Francesco Parlati

Calithera Biosciences, South San Francisco, CA, USA

### Background

T cell activation and proliferation are metabolically demanding processes that require essential nutrients such as glucose and glutamine. Within the tumor microenvironment, competition between tumor cells and immune cells for limited nutrients can lead to poor T cell activation and suppression of an anti-tumor immune response. Engagement of immune checkpoints such as PD-1 further suppresses T cell activation. While therapeutic blockade of immune



## Combinations: Immunotherapy/Immunotherapy

Presenting author underlined; *Primary author in italics*

checkpoints may partially relieve T cell suppression, low nutrient availability in the tumor microenvironment is expected to limit an optimal immune response. CB-839 is a glutaminase inhibitor currently in phase I oncology trials. CB-839 blocks glutamine consumption by tumors leading to elevated glutamine levels in the tumor microenvironment. Based on the high demand of T cells for glutamine, we hypothesized that CB-839 might synergize with immune checkpoint inhibitors to relieve immune suppression and lead to enhanced anti-tumor immune responses.

### Methods

*Ex vivo* T cell activation was performed with anti-CD3/CD28 on CD3+ cells isolated from human PBMCs. Changes in mRNA expression after T cell activation was monitored by NanoString analysis. *In vivo* efficacy studies were conducted in syngeneic CT-26 or B16 tumor models.

### Results

T cell activation in the absence of glutamine inhibited cell proliferation and the expression of cell surface activation markers. Analysis of mRNA expression also showed suppression of normal activation markers and induction of T cell exhaustion markers including PD-1, CTLA-4 and BTLA, suggesting that T cell activation in the absence of glutamine may be sufficient to induce an exhausted phenotype. Previous work showed that CB-839 blocks glutamine consumption in tumors leading to reduced cell proliferation. Surprisingly, CB-839 had only minimal impact on T cell proliferation, highlighting differences in glutamine utilization pathways between tumor cells and T cells. In mouse tumor models, administration of CB-839 elevated tumor glutamine levels, consistent with inhibition of tumor glutaminase. Combination of CB-839 with anti PD-1 or anti PD-L1 in the syngeneic CT-26 colon model augmented tumor regressions relative to checkpoint inhibition alone. CB-839 also enhanced the anti-tumor activity of checkpoint inhibitors in the B16 melanoma model. Depletion of CD8+ T cells from tumor-bearing animals reversed the anti-tumor effects of the combination, confirming an immune-mediated mechanism of action.

### Conclusions

These data highlight a novel therapeutic approach to treat cancer by selectively targeting tumor metabolism as a means of enhancing the efficacy of checkpoint blockade. Our data provide a rationale for combining CB-839 with immune checkpoint inhibitors in the clinic.

## 231

### Arginase inhibitor CB-1158 alleviates immunosuppression and enhances anti-tumor responses as a single agent and in combination with other immunotherapies

Amani Makkouk, Mark K Bennett, Jason Chen, Ethan Emberley, Matt Gross, Tony Huang, Weiqun Li, Andy MacKinnon, Gisele Marguier, Silinda Neou, Alison Pan, Jing Zhang, Winter Zhang, *Francesco Parlati*

Calithera Biosciences, South San Francisco, CA, USA

### Background

T cells and natural killer (NK) cells require L-arginine for proliferation. Arginine depletion by arginase in the tumor microenvironment induces immunosuppression and is associated with tumor immune evasion. Arginase is expressed by myeloid-derived suppressor cells (MDSCs) and polymorphonuclear cells (PMNs), and its pharmacological inhibition is expected to restore arginine levels and relieve immunosuppression, leading to anti-tumor immune responses.

### Methods

We developed CB-1158, a potent and selective small molecule inhibitor of arginase ( $IC_{50}=98$  nM). The activity of CB-1158 was examined *ex vivo* using immune cells isolated from healthy volunteers or cancer patients, and *in vivo* using murine syngeneic tumor models. Arginase abundance in cancer patient plasma and in tumor tissue microarrays was also examined.

### Results

In a co-culture system of T cells with PMNs or MDSCs, CB-1158 reverses PMN- or MDSC-mediated immunosuppression by blocking arginine depletion, thereby allowing T cells to proliferate. T cells activated in the presence of PMN-conditioned media show suppressed production of cytokines involved in Th1-type adaptive immunity, and this effect is reversed by the addition of CB-1158. *In vivo*, CB-1158 has high oral bioavailability and is very well tolerated. In tumor-bearing mice, twice daily dosing of CB-1158 causes dose-dependent pharmacodynamic increases in plasma and tumor arginine levels associated with single agent anti-tumor efficacy in multiple syngeneic models. The anti-tumor efficacy of CB-1158 is abrogated in immunocompromised mice or via depletion of either CD8+ T cells or NK cells, confirming an immune-mediated mechanism of action. Moreover, CB-1158 enhances CD8+ T cell infiltration into tumors and increases expression of Th1 cytokines, T cell and NK cell activation markers, and interferon-inducible genes in the tumor. The immunomodulatory activity of CB-1158 supports the potential of its combination with other immunotherapies

## Combinations: Immunotherapy/Immunotherapy

Presenting author underlined; *Primary author in italics*

and/or standard-of-care therapies. CB-1158 enhances the anti-tumor efficacy of checkpoint inhibitors, including anti-PD-L1 and epacadostat in the B16F10 model. Moreover, CB-1158 enhances the anti-tumor efficacy of standard-of-care therapies such as chemotherapy. To assess the clinical potential of CB-1158, the abundance of arginase in tumors and plasma from cancer patients across multiple cancer histotypes was surveyed. Arginase-expressing PMN infiltrates are abundant in multiple tumor types. Plasma arginase levels are elevated in cancer patients compared to healthy controls, and are associated with decreased plasma arginine.

### Conclusions

These results support the clinical development of CB-1158, a first-in-class arginase inhibitor, as a novel immunomodulatory agent antagonizing myeloid-mediated immunosuppression. A phase I clinical trial testing the clinical activity of CB-1158 in cancer patients has been initiated.

232

### Revealing how adoptive T cell transfer into lymphodepleted host and checkpoint blockade therapy work together to treat blood cancers

Netonia Marshall, Thomas U Marron, Judith Agudo, Brian Brown, Joshua Brody

Icahn School of Medicine at Mount Sinai, New York, NY, USA

### Background

Blood cancers, with an estimated 160,000 new cases, account for nearly 10% of all cancer diagnoses and 9.4% of all cancer deaths this year in the United States. Unfortunately, despite therapeutic advances, the mortality rate still continues to rise. Thus, novel, mechanistically distinct therapies, such as immunotherapy, may have a significant impact particularly in addressing aggressive lymphoma subtypes such as those being modeled in our transplant-based approach. Two classes of immunotherapies that have had great success in treating a wide array of cancers are: checkpoint blockade (e.g., anti-CTLA-4 antibody-based treatments and anti-PD-1 antibody-based treatments) and adoptive T cell (e.g., TIL) transfer lymphocytes into lymphodepleted hosts.

### Methods

We have developed a novel therapy combining these approaches into 'checkpoint-blockade-primed immunotransplant' comprised of: treatment of tumor-bearing host with anti-CTLA-4 and/or anti-PD-1 antibodies, and splenocyte harvest and transfer to lymphodepleted recipient.

### Results

Our results show that this combined therapy results in superior anti-tumor immunity compared to either

individually as seen by increased production of IFN  $\gamma$  positive T cells. Treatment of both tumor-bearing donor and recipient with anti-PD-1 and anti-CTLA-4 antibodies induces cure of the majority of recipients, in a CD8, NK, and IFN $\gamma$ -dependent manner, despite the finding that antibody therapy alone (without transplantation and T cell transfer) induces minimal anti-tumor effect. Furthermore, we have demonstrated that T cells exposed to checkpoint blockade and transfer into the lymphopenic hosts demonstrate: greater *in vivo* serum levels of IL-15 and IL-7, higher *ex vivo* levels of IL-15R and IL-7 receptors expression on CD8s, *in vitro* STAT5 phosphorylation in response to common  $\gamma$ -chain cytokines, *in vivo* proliferation in response to exposure to cognate tumor antigen, and *in vitro* production of IFN $\gamma$  and TNF production in response to exposure to cognate tumor antigen.

### Conclusions

Ongoing studies will seek to assess the dependence of the above observations (cytokine production, proliferation, anti-tumor effect) on specific common  $\gamma$ -chain cytokines, the role of the lymphopenia in inducing T cell trafficking to tumor versus organs, and guide development of the immunotransplant model to optimize the amplification of anti-tumor immunity observed.

233

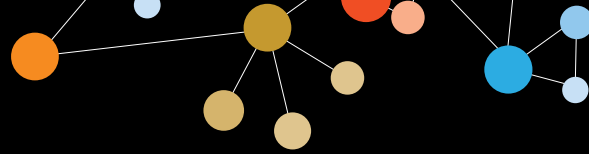
### Immunomodulatory cytokine blockade in combination with CTLA-4 blockade in murine models of pancreatic cancer

Christopher McQuinn, Thomas Mace, Matthew Farren, Hannah Komar, Reena Shakya, Gregory Young, Thomas Ludwug, Gregory B Lesinski

The Ohio State University, Columbus, OH, USA

### Background

Pancreatic cancer remains a significant challenge with 5 year survival rates of less than 7%. This devastating malignancy is expected to become the second leading cause of cancer death in the United States by 2030. Although effective in other malignancies, there has been a relative paucity of efficacy when immune checkpoint blockade has been applied in pancreatic cancer. We hypothesize this limited efficacy is due to local and systemic alterations in cytokine expression that shape the immune contexture in these patients. Although dysregulated cytokines represent attractive targets in pancreatic cancer, there are limited data to help prioritize among them for future translation. Prior studies from our group demonstrated that plasma interleukin-6 (IL-6), interleukin-10 (IL-10) and circulating CD8+CTLA-4+ cells were correlated with overall survival in a population of n=71 treatment naïve metastatic pancreatic cancer patients. We



## Combinations: Immunotherapy/Immunotherapy

Presenting author underlined; Primary author in italics

hypothesized that targeting IL-10 and IL-6 would augment the efficacy of antibodies targeting CTLA-4.

### Methods

*In vivo* efficacy of blocking antibodies against IL-6, IL-10, and CTLA-4 were evaluated in C57BL/6 mice bearing syngeneic, subcutaneous murine pancreatic tumor cells derived from *LSL-Kras<sup>G12D</sup>;LSL-p53<sup>R172H</sup>;Pdx1-Cr* and in a highly aggressive genetically engineered mouse model, harboring *Kras<sup>G12D</sup>; p53<sup>R172H</sup> and Brca2 mutation* (KPC-BRCA2). Relevant immune biomarkers were analyzed using flow cytometry or IHC, as appropriate.

### Results

*In vivo* studies demonstrated that combined blockade of IL-6 and CTLA-4 significantly decreased the rate of tumor growth in comparison to both isotype control ( $P = 0.0001$ ) and anti-CTLA-4 alone ( $P = 0.0207$ ). Treatment with antibody against IL-10, or IL-10 blockade in combination with anti-CTLA-4 slowed tumor growth in comparison to isotype control but were inferior to single agent anti-CTLA-4. FACS analysis of splenocytes from these mice revealed that combined IL-6 and CTLA-4 blockade increased the proportion of circulating CD4+ central memory cells (CD62L+CD44+). Blockade of IL-6 and CTLA-4 in combination, and as single agents, resulted in an increase in circulating Th1 cells while both isotype control and anti-IL-6 had significantly more naïve systemic T cells (CD4+/CD8+CD62L+CD44-). IHC analysis revealed increased infiltrating CD3+ cells throughout the tumor foci of the combination group in comparison to both single agents and isotype control (all  $P$ 's < 0.01). Ongoing analysis will further delineate the proportion and detailed phenotype of infiltrating and systemic immune cells.

### Conclusions

Antibodies targeting IL-6 but not IL-10 augment the efficacy of anti-CTLA-4 in murine models of pancreatic cancer, modulate T cell infiltration and immune biomarkers to promote Th1 immune responses.

### 234

#### Improvement of a therapeutic cancer vaccine in mice with the addition of a GITR-ligand fusion protein

Y Maurice Morillon<sup>1</sup>, Scott A Hammond<sup>2</sup>, Jeffrey Schlom<sup>1</sup>, John W Greiner<sup>1</sup>

<sup>1</sup>Laboratory of Tumor Immunology and Biology, Center for Cancer Research, National Cancer Institute, Bethesda, MD, USA

<sup>2</sup>MedImmune LLC, Gaithersburg, MD, USA

### Background

Breaking tolerance mechanisms to mount a durable adaptive immune response within tumors remains one

of the preeminent challenges of immuno-oncology. Immunosuppressive hurdles include: 1) suppression from immunoregulatory and tumor cells, 2) insufficient intratumoral “immune space” and survival signals, and 3) exhaustion of tumor specific effector T cells ( $T_{eff}$ ). GITR, an activating receptor belonging to the tumor necrosis factor receptor (TNFR) super family, is constitutively expressed on FoxP3+ regulatory T cells ( $T_{regs}$ ) and to a lesser extent on quiescent  $T_{eff}$ . Activation upregulates GITR on  $T_{eff}$  and  $T_{regs}$ , which however remains highest among  $T_{regs}$ . Thus, selectively targeting GITR can deliver activating signals to  $T_{eff}$  cells, while depleting high-GITR-expressing  $T_{regs}$ , and may improve efficacy of a therapeutic cancer vaccine.

### Methods

Recombinant poxviruses [modified vaccinia Ankara (rMVA-), fowlpox (rF-)] were engineered to express human *CEA* and murine costimulatory molecules, *B7.1*, *ICAM-1* and *LFA-3* (TRICOM); termed rMVA- or rF-*CEA*-TRICOM. A prime-boost strategy was utilized; the priming vaccine utilized rMVA-*CEA*-TRICOM while rF-*CEA*-TRICOM provided the boost. The diversified prime-boost vaccine regimen can break tolerance in transgenic mice expressing human *CEA*. GITR was targeted with a fusion protein (GITRL-FP) consisting of the extracellular domain of murine GITR-ligand molecularly fused to a trimerization domain and murine IgG2a-Fc. Murine colon adenocarcinoma cells expressing human *CEA* (MC32A) were implanted subcutaneously in CEA. Tg mice and treated with control IgG2a, GITRL-FP, rMVA/rF-*CEA*-TRICOM, or rMVA/rF-*CEA*-TRICOM + GITRL-FP.

### Results

Initial studies paired twice weekly dosing of GITRL-FP concurrent with MVA/rF-*CEA*-TRICOM and modest improvements in antitumor effects resulted. GITRL-FP targets GITR expressing cells, delivering activating signals, while the IgG2a-Fc depletes via Fc-mediated effector functions. Investigation into mechanism revealed depletion of  $T_{regs}$  and  $T_{eff}$ . To circumvent the problem of depleting vaccine induced  $T_{eff}$ , administration of GITRL-FP was switched to a single dose given 2 days prior to vaccine. The short half-life of the fusion protein allowed for temporal intratumoral depletion of both  $T_{regs}$  and  $T_{eff}$ . Single dose GITRL-FP abrogated the immunosuppressive constraints of  $T_{regs}$  and created a lymphopenic intratumoral T cell compartment. These events allowed for expansion of  $T_{eff}$  in response to MVA-*CEA*-TRICOM as shown by a 20% increase of proliferating intratumoral CD4+  $T_{eff}$  compared to GITRL-FP monotherapy, and a 2-fold increase in activated peripheral CD8+  $T_{eff}$ . Reduced tumor growth and improved survival was observed comparing combination to GITRL-FP monotherapy. Tumor-free mice were also protected against tumor rechallenge.



## Combinations: Immunotherapy/Immunotherapy

Presenting author underlined; Primary author in italics

### Conclusions

These data demonstrate the increased efficacy of utilizing targeted depletion of immunosuppression in combination with an immune boosting cancer vaccine.

### 235

#### Elucidating the role of CD47 in innate lymphoid cell-mediated tumor therapy

Pulak R. Nath<sup>1</sup>, Anthony L. Schwartz<sup>1</sup>, Dragan Maric<sup>2</sup>, David D. Roberts<sup>1</sup>

<sup>1</sup>National Cancer Institute, National Institutes of Health, Bethesda, MD, USA

<sup>2</sup>National Institute of Neurological Disorders and Stroke, National Institutes of Health, Bethesda, MD, USA

### Background

CD47 is a ubiquitous cell surface receptor that interacts with the secreted protein thrombospondin-1 and its counter-receptor SIRP $\alpha$  on phagocytes and antigen presenting cells (APCs). CD47 is highly expressed across many cancer types, hence, representing a potential target for therapeutic intervention. We recently reported a direct role for thrombospondin-1/CD47 signaling on cytotoxic T lymphocytes (CTL) to limit target tumor cell killing [1]. Many tumors are not sufficiently immunogenic to induce protective adaptive immunity. However, innate lymphoid cells (ILCs) may also play functional roles in tumor regression [2]. Here we evaluated the role of CD47 in NK and other ILCs homeostasis within the lymphoid organs as well as among tumor infiltrating lymphocytes.

### Methods

We analyzed tumor infiltration of NK and other ILCs following antisense suppression of CD47 alone or in combination with anti-CTLA-4 blockade. C57Bl/6 mice were injected with B16F10 melanoma in the hind limb, and once the tumors reached an average of 100 mm<sup>3</sup>, mice were treated with CD47-morpholino, anti-CTLA-4, or combined treatments.

### Results

Treatment of mice with CD47-morpholino increased the frequencies of splenic Lin<sup>-</sup>CD3<sup>-</sup>NK1.1<sup>+</sup> and Lin<sup>-</sup>CD3<sup>-</sup>CD127<sup>+</sup> populations. Studies using CD47-null mice further validated this result. We observed higher granzyme B and perforin mRNA expression in the CD3<sup>+</sup>CD4<sup>+</sup>CD8<sup>-</sup> cells compared to the CD8<sup>+</sup> cells from spleens of CD47-null mice. Image cytometric analysis revealed that these are mononuclear lymphocytes. These cells express higher eomes and T-bet, but lower Gata3 and Ror $\gamma$ t as compared to their CD4<sup>+</sup> counterparts, suggesting that they fall within the NK and ILC1 lineages. Indeed, lineage-depleted splenocytes from CD47-null mice showed higher frequencies of NK1.1<sup>+</sup> and CD127<sup>+</sup> cells compared to wildtype littermate controls. These cells infiltrated into

tumors of B16F10-bearing mice, and their numbers further increased following treatment with a combination of CD47-morpholino and anti-CTLA-4 antibody, which resulted in enhanced therapeutic benefits.

### Conclusions

Our data suggest that deficiency of CD47 in the tumor microenvironment or therapeutic blockade increases subtypes of ILCs with potent anti-tumor properties. The mechanism by which CD47 controls the homeostatic balance of ILCs or their development remains to be determined.

### References

- Soto-Pantoja DR, *et al*: **CD47 in the tumor microenvironment limits cooperation between antitumor T-cell immunity and radiotherapy**. *Cancer Res* 2014, **74**:6771–6783.
- Dadi S, *et al*: **Cancer immunosurveillance by tissue-resident innate lymphoid cells and innate-like T cells**. *Cell* 2016, **164**:365–377.

### 236

#### Restoration of antitumor effectiveness of PD-1 inhibition in immunotherapy-resistant “cold” tumors by combinatorial treatment enhancing the numbers of tumor-specific CTLs in tumor tissues

Nataša Obermajer<sup>1</sup>, David Bartlett<sup>1</sup>, Pawel Kalinski<sup>2</sup>

<sup>1</sup>Department of Surgery, University of Pittsburgh, Pittsburgh, PA, USA

<sup>2</sup>Department of Surgery; University of Pittsburgh Cancer Institute; Department of Infectious Diseases and Microbiology, University of Pittsburgh, Pittsburgh, PA, USA

### Background

Intratumoral accumulation of effector type-1 T cells (CTLs) is an independent prognostic factor of survival of patients with many cancer types and is required for the effectiveness of checkpoint blockade therapies.

### Methods

In this study, we have tested whether the enhancement of the numbers of tumor-infiltrating CTLs by DC vaccines together with combinatorial reprogramming of tumor-associated chemokines, can be used to convert the nominally checkpoint-resistant “cold” tumors into PD-1-sensitive ones.

### Results

In colorectal and ovarian cancer (transplantable MC38 and ID8 models) bearing mice, we observed only marginal therapeutic effect of PD-1 inhibition alone or combined with DC vaccine. However, combinatorial reprogramming of tumor-associated chemokines, using TLR3 ligand polyI:polyC<sub>12</sub>U, interferon- $\alpha$  and COX2 blockers, resulted in a striking increase



# Combinations: Immunotherapy/Immunotherapy

Presenting author underlined; Primary author in italics

in the numbers of tumor-infiltrating CTLs recognizing cancer-associated antigens and allowed for the conversion of these immunotherapy-resistant tumors into sensitive ones, resulting in high numbers of long-term surviving animals.

## Conclusions

This combinatorial DC-based vaccination approach may be used to induce specific immune cells against different tumor-relevant antigens and may be included as a component of anti-tumor therapeutic approaches that, by themselves do not induce new effector cells, nor promote their intratumoral accumulation.

## 237

### Immune activation by PEGylated human IL-10 (AM0010) and anti-tumor activity in renal cancer alone and in combination with anti-PD-1

Aung Naing<sup>1</sup>, Kyriakos P Papadopoulos<sup>2</sup>, Karen A Autio<sup>3</sup>, Deborah J Wong<sup>4</sup>, Manish Patel<sup>5</sup>, Gerald Falchook<sup>6</sup>, Shubham Pant<sup>7</sup>, Patrick A Ott<sup>8</sup>, Melinda Whiteside<sup>9</sup>, Amita Patnaik<sup>2</sup>, John Mumm<sup>9</sup>, Filip Janku<sup>1</sup>, Ivan Chan<sup>9</sup>, Todd Bauer<sup>10</sup>, Rivka Colen<sup>1</sup>, Peter VanVlasselaer<sup>9</sup>, Gail L Brown<sup>9</sup>, Nizar M Tannir<sup>1</sup>, Martin Oft<sup>9</sup>, Jeffrey Infante<sup>10</sup>

<sup>1</sup>University of Texas MD Anderson Cancer Center, Houston, TX, USA

<sup>2</sup>South Texas Accelerated Research Therapeutics, LLC, San Antonio, TX, USA

<sup>3</sup>Memorial Sloan Kettering Cancer Center, New York, NY, USA

<sup>4</sup>UCLA, Los Angeles, CA, USA

<sup>5</sup>Sarah Cannon Research Institute/Florida Cancer Specialists, Sarasota, FL, USA

<sup>6</sup>SCRI at HealthONE, Denver, CO, USA

<sup>7</sup>Oklahoma University, Oklahoma City, OK, USA

<sup>8</sup>Dana-Farber Cancer Institute, Boston, MA, USA

<sup>9</sup>ARMO BioSciences, Redwood City, CA, USA

<sup>10</sup>Sarah Cannon Research Institute, Nashville, TN, USA

## Background

IL-10 is regarded as an anti-inflammatory cytokine, but it is at least equally important for the cytotoxicity and proliferation of antigen activated CD8+ T cells. Activation of CD8+ T cells through the T cell receptor elevates IL-10 receptors and PD-1 on the cells. This provides the mechanistic rationale for combining AM0010 and anti-PD-1 for the treatment of cancer patients. A phase I clinical trial investigated the tolerability and anti-tumor activity of AM0010 alone and in combination with anti-PD-1 immune checkpoint inhibitors.

## Methods

Patients with advanced RCC were treated with AM0010 (daily SC) alone or in combination with pembrolizumab (q3wk IV) or nivolumab (q2wk IV). Tumor responses were monitored following irRC. Immune responses were measured by analysis

of serum cytokines, and the activation and clonality of T cells in peripheral blood mononuclear cells. Nineteen patients with RCC (15 evaluable), were treated with AM0010 alone (20 mg/kg). Eight patients were treated in combination with pembrolizumab (2mg/kg) and 15 patients with nivolumab (3mg/kg).

## Results

AM0010 alone or in combination with anti-PD-1 was tolerated well (observation periods exceeding 16 months). All TrAEs were transient and TrAEs leading to study discontinuation were not observed. There was no colitis, pneumonitis, or endocrine disruptions. G3/4 TrAEs in monotherapy included anemia (9), hypertriglyceridemia (3), thrombocytopenia (2), ALT/AST increase (2) and fatigue (2). AM0010 combination with anti-PD-1 did not increase TrAEs. Objective responses (PR/CR) were observed in 4 of 15 evaluable RCC patients in monotherapy (27%), in 4 of 8 patients in AM0010/pembrolizumab (50%). Progression-free survival (PFS) was 3 and 9.4 months, respectively. The AM0010/nivolumab cohort is currently in progress. AM0010 alone and also in combination with anti-PD-1 increased Th1 cytokines (IL-18, IFN $\gamma$ , TNF $\alpha$ ), CD8+ T cell associated effector molecules such as FasL and LymphotoxinB as well as cytokines stimulating T cell proliferation (IL-4, IL-7). As a result, the number and proliferation of activated, PD-1+ LAG-3+ CD8+ T cells in the blood of patients were increased on AM0010. In contrast, the proliferation of FoxP3+ Tregs and TGF $\beta$  was decreased. AM0010 alone or with anti-PD-1 induced oligoclonal expansion of T cell clones in the blood without affecting total lymphocyte counts. In particular, selected T cells clones previously not detected in the blood of patients before treatment were strongly expanded (*de novo* amplification).

## Conclusions

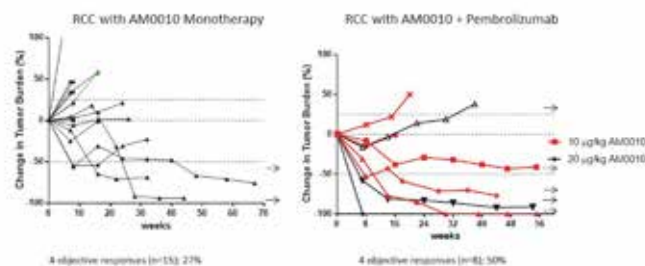
AM0010 alone or in combination with anti-PD-1 is well-tolerated. The clinical activity and the observed CD8+ T cell activation encourages the continued exploration of AM0010 in phase III studies.

## Trial Registration

ClinicalTrials.gov identifier NCT02009449.

Figure 1.

Anti-PD-1 Combination with AM0010 leads Increased and Accelerated Tumor Responses

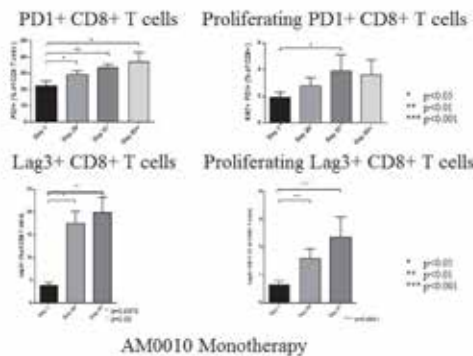


**Combinations: Immunotherapy/Immunotherapy**

Presenting author underlined; Primary author in italics

Figure 2.

AM0010 Increases PD1+ / LAG3+ CD8 T cell Proliferation In RCC Patients



238

**Initial experience administering BMS-986016, a monoclonal antibody that targets lymphocyte activation gene (LAG)-3, alone and in combination with nivolumab to patients with hematologic and solid malignancies**

Evan Lipson<sup>1</sup>, *Ajay Gopal*<sup>2</sup>, Sattva S Neelapu<sup>3</sup>, Philippe Armand<sup>4</sup>, Stephen Spurgeon<sup>5</sup>, John P Leonard<sup>6</sup>, F Stephen Hodi<sup>4</sup>, Rachel E Sanborn<sup>7</sup>, Ignacio Melero<sup>8</sup>, Thomas F Gajewski<sup>9</sup>, Matthew Maurer<sup>10</sup>, Serena Perna<sup>10</sup>, Andres A Gutierrez<sup>11</sup>, Raphael Clynes<sup>10</sup>, Priyam Mitra<sup>10</sup>, Satyendra Suryawanshi<sup>10</sup>, Douglas Gladstone<sup>1</sup>, Margaret K Callahan<sup>12</sup>

<sup>1</sup>Sidney Kimmel Comprehensive Cancer Center, Johns Hopkins University School of Medicine, Baltimore, MD, USA

<sup>2</sup>Seattle Cancer Care Alliance, University of Washington, Seattle, WA, USA

<sup>3</sup>University of Texas MD Anderson Cancer Center, Houston, TX, USA

<sup>4</sup>Dana-Farber Cancer Institute, Harvard University, Boston, MA, USA

<sup>5</sup>Center for Hematologic Malignancies, Oregon Health and Sciences University, Portland, OR, USA

<sup>6</sup>New York Presbyterian Hospital, Weill Cornell Medical College, New York, NY, USA

<sup>7</sup>Robert W. Franz Cancer Research Center, Earle A. Chiles Research Institute, Providence Cancer Center, Portland, Oregon, USA, Portland, OR, USA

<sup>8</sup>Center for Applied Medical Research (CIMA), University of Navarra, Pamplona, Navarra, Spain

<sup>9</sup>University of Chicago Medical Center, Chicago, IL, USA

<sup>10</sup>Bristol-Myers Squibb, Princeton, NJ, USA

<sup>11</sup>Bristol-Myers Squibb, Lawrence Township, NJ, USA

<sup>12</sup>Memorial Sloan Kettering Cancer Center, New York, NY, USA

**Background**

LAG-3 is a transmembrane receptor that negatively regulates T cell activation. Signaling through LAG-3 and other T cell

inhibitory receptors, including programmed death-1 (PD-1), can lead to T cell exhaustion and is a mechanism of immune escape for tumors. Preclinical data suggest that simultaneous blockade of LAG-3 and PD-1 may function synergistically to restore T cell activation and mediate tumor regressions. Here, we describe preliminary first-in-human phase I/IIa data for BMS-986016, a fully human IgG4 monoclonal antibody that targets LAG-3, alone and in combination with nivolumab (anti-PD-1) in patients with advanced B cell malignancies or solid tumors.

**Methods**

Sequential cohorts received BMS-986016 ± nivolumab every 14 days in 56-day cycles during dose escalation or expansion until disease progression, completion of 12 cycles, or prohibitive toxicity. Primary objectives included safety and tolerability.

**Results**

As of May 2016, 89 patients had received BMS-986016 alone (20 mg [n=8], 80 mg [n=13], 240 mg [n=24], or 800 mg [n=15]) or with nivolumab (BMS-986016/nivolumab; 20/80 mg [n=7], 20/240 mg [n=9], 80/240 mg [n=9], or 240/240 mg [n=4]). The pharmacokinetic characteristics of BMS-986016 were assessed across dose levels in patients treated with monotherapy and combination therapy. Anti-drug antibody assessments suggested low immunogenicity. Increases in peripheral blood T cell LAG-3 receptor occupancy (RO; 74-99%) were observed with escalating BMS-986016 dose and exposure. The maximum tolerated dose (MTD) was not reached with BMS-986016 monotherapy; evaluations to determine the MTD for the combination are ongoing. Infrequent and manageable treatment-related adverse events (TRAEs) were observed across monotherapy doses (Table 1), and included toxicities typically associated with immune checkpoint blocking agents. DLTs among patients receiving combination therapy included grade (G)3 mucositis, G4 ventricular fibrillation, G4 elevated lipase, and G4 myocarditis. Most TRAEs were grade 1-2. TRAEs leading to discontinuation of therapy were reported in 3% (BMS-986016) and 14% (BMS-986016 + nivolumab) of patients. There were no treatment-related deaths. Objective tumor regression was observed with LAG-3 monotherapy, and with combination therapy in PD-1-naïve patients and in patients with disease progression on nivolumab monotherapy.

**Conclusions**

BMS-986016 monotherapy was well tolerated at the dose levels tested. Emerging data characterizing the safety of the combination will be presented. BMS-986016 ± nivolumab demonstrated biological activity as evidenced by toxicities characteristic of immune checkpoint blockers and objective tumor regressions. These preliminary data support the

## Combinations: Immunotherapy/Immunotherapy

Presenting author underlined; Primary author in italics

ongoing evaluation of this combination in patients with solid tumors and hematologic malignancies.

### Trial Registration

ClinicalTrials.gov identifier NCT02061761 and NCT01968109.

**Table 1: TRAEs reported in > 2 patients or any TRAE ≥ grade 3 reported in patients treated with BMS-986016 ± nivolumab**

Table 1: TRAEs reported in > 2 patients or any TRAE ≥ grade 3 reported in patients treated with BMS-986016 ± nivolumab

	NCT01968109 (solid tumors)				NCT02061761 (B-cell malignancies)	
	BMS-986016 (n=22)		BMS-986016 + nivolumab (n=29)		BMS-986016 (N=38)	
Patients with a TRAE, n (%)	Any grade	Grade 3/4	Any grade	Grade 3/4	Any grade	Grade 3/4
Any	13 (59.1)	2 (9.1)	18 (62.1)	5 (17.2)	16 (42.1)	0
Fatigue	6 (27.3)	0	6 (20.7)	0	6 (15.8)	0
Nausea	2 (9.1)	0	3 (10.3)	0	1 (2.6)	0
Rash	1 (4.5)	0	1 (10.3)	0	2 (5.3)	0
Decreased appetite	3 (13.6)	0	1 (3.4)	0	1 (2.6)	0
Headache	2 (9.1)	0	1 (3.4)	0	2 (5.3)	0
Infusion-related reaction	1 (4.5)	0	2 (6.9)	0	2 (5.3)	0
Dry mouth	2 (9.1)	0	2 (6.9)	0	0	0
Amylase increased	1 (4.5)	0	2 (6.9)	1 (3.4)	0	0
Diarrhea	0	0	2 (6.9)	0	1 (2.6)	0
Hypothyroidism	0	0	2 (6.9)	0	1 (2.6)	0
Influenza-like illness	0	0	1 (3.4)	0	2 (5.3)	0
Lipase increased	1 (4.5)	1 (4.5)	2 (6.9)	1 (3.4)	0	0
Myalgia	2 (9.1)	0	1 (3.4)	0	0	0
Pruritus	2 (9.1)	0	1 (3.4)	0	0	0
Rash maculopapular	2 (9.1)	1 (4.5)	0	0	0	0
Dehydration	0	0	1 (3.4)	1 (3.4)	0	0
Dyspnea	1 (4.5)	0	1 (3.4)	1 (3.4)	0	0
Mucosal inflammation	0	0	1 (3.4)	1 (3.4)	0	0
Myocarditis	0	0	1 (3.4)	1 (3.4)	0	0
Ventricular fibrillation	0	0	1 (3.4)	1 (3.4)	0	0

239

### Clinical safety and efficacy assessment of the CD137 agonist urelumab alone and in combination with nivolumab in patients with hematologic and solid tumor malignancies

*Erminia Massarelli*<sup>1</sup>, Neil H Segal<sup>2</sup>, Vincent Ribrag<sup>3</sup>, Ignacio Melero<sup>4</sup>, Tara C Gangadhar<sup>5</sup>, Walter Urba<sup>6</sup>, Dirk Schadendorf<sup>7</sup>, Robert L Ferris<sup>8</sup>, Roch Houot<sup>9</sup>, Franck Morschhauser<sup>10</sup>, Theodore Logan<sup>11</sup>, Jason J Luke<sup>12</sup>, William Sharfman<sup>13</sup>, Fabrice Barlesi<sup>14</sup>, Patrick A Ott<sup>15</sup>, Laura Mansi<sup>16</sup>, Shivaani Kummur<sup>17</sup>, Gilles Salles<sup>18</sup>, Cecilia Carpio<sup>19</sup>, Roland Meier<sup>20</sup>, Suba Krishnan<sup>20</sup>, Dan McDonald<sup>20</sup>, Matthew Maurer<sup>20</sup>, Xuemin Gu<sup>20</sup>, Jaclyn Neely<sup>20</sup>, Satyendra Suryawanshi<sup>20</sup>, Ronald Levy<sup>17</sup>, Nikhil Khushalani<sup>21</sup>

<sup>1</sup>University of Texas MD Anderson Cancer Center, Houston, TX, USA

<sup>2</sup>Memorial Sloan Kettering Cancer Center, New York, NY, USA

<sup>3</sup>Institut Gustave Roussy, Villejuif, Ile-de-France, France

<sup>4</sup>Center for Applied Medical Research (CIMA), University of Navarra, Pamplona, Navarra, Spain

<sup>5</sup>University of Pennsylvania, Philadelphia, PA, USA

<sup>6</sup>Earle A. Chiles Research Institute, Providence Cancer Center, Portland, OR, USA

<sup>7</sup>Universitätsklinikum Essen, Essen, Nordrhein-Westfalen, Germany

<sup>8</sup>University of Pittsburgh, Pittsburgh, PA, USA

<sup>9</sup>CHU Rennes, Service Hématologie Clinique and INSERM 0203, Unité d'Investigation Clinique, Rennes, Bretagne, France

<sup>10</sup>Centre Hospitalier Régional Universitaire de Lille, Lille, Nord-Pas-de-Calais, France

<sup>11</sup>Simon Cancer Center, Indiana University, Indianapolis, IN, USA

<sup>12</sup>University of Chicago School of Medicine, Chicago, IL, USA

<sup>13</sup>Johns Hopkins University School of Medicine, Lutherville, MD, USA

<sup>14</sup>Multidisciplinary Oncology and Therapeutic Innovations, Hôpital Nord, Marseille, Provence-Alpes-Cote d'Azur, France

<sup>15</sup>Dana-Farber Cancer Institute, Boston, MA, USA

<sup>16</sup>Centre Hospitalier Régional Universitaire Hôpital Jean Minjoz, Besançon, Franche-Comte, France

<sup>17</sup>Stanford University School of Medicine, Stanford, CA, USA

<sup>18</sup>Hospices Civils de Lyon-Université de Lyon, Pierre Benite, Auvergne, France

<sup>19</sup>Hospital Universitari Vall d'Hebron, Universitat Autònoma de Barcelona, Barcelona, Catalonia, Spain

<sup>20</sup>Bristol-Myers Squibb, Princeton, NJ, USA

<sup>21</sup>H. Lee Moffitt Cancer Center, Tampa, FL, USA

## Combinations: Immunotherapy/Immunotherapy

Presenting author underlined; Primary author in italics

### Background

Urelumab is a fully human CD137 agonistic monoclonal antibody (mAb) that enhances T cell and natural killer (NK) cell antitumor activity in preclinical models. Nivolumab, a fully human programmed death-1 (PD-1) mAb that blocks the inhibitory function of the PD-1 receptor on T cells, has shown single-agent activity in many advanced malignancies. We hypothesized that the distinct, non-redundant mechanisms of these two mAbs could enhance antitumor activity without compromising safety. Here we report safety/tolerability, pharmacodynamics, and preliminary efficacy of urelumab and urelumab plus nivolumab combination therapy in patients with advanced malignancies.

### Methods

The monotherapy study evaluated urelumab in patients with advanced malignancies (0.1 or 0.3 mg/kg Q3W) or advanced non-Hodgkin lymphoma (8 mg Q3W or Q6W). The combination study evaluated urelumab (3 or 8 mg Q4W) plus nivolumab (3 mg/kg or 240 mg Q2W) in patients with advanced solid tumors or B cell lymphoma (dose escalation) or patients with diffuse large B cell lymphoma (DLBCL), melanoma, non-small cell lung cancer (NSCLC), or squamous cell carcinoma of the head and neck (SCCHN; cohort expansion). Based on preliminary safety/tolerability/pharmacokinetic assessments of urelumab, cohort expansion focused on flat doses of 8 mg.

### Results

Overall, patients who received urelumab monotherapy (N=123) experienced infrequent treatment-related serious AEs (7%) and treatment-related AEs (TRAEs) leading to discontinuation (5%; Table 1). In 104 patients treated with urelumab plus nivolumab (melanoma, n=40; NSCLC, n=20; SCCHN, n=22; DLBCL, n=22), the most frequent TRAE was fatigue (26%); grade 3/4 ALT/AST elevations (3%/3%) and TRAEs leading to discontinuation (7%) were infrequent. No treatment-related deaths were reported. Urelumab stimulated peripheral IFN- $\gamma$ -induced cytokine production; induction was greater with urelumab plus nivolumab. In most melanoma tumors evaluated, a trend toward increased T and NK cell number and expression of IFN- $\gamma$  and CXCL9 was observed upon treatment with the combination. Six patients with lymphoma treated with urelumab monotherapy had a partial (n=3) or complete (n=3) remission. Nine of 86 evaluable patients treated with the combination had partial responses (melanoma, n=8; SCCHN, n=1); no patients with NSCLC or DLBCL had confirmed responses at the interim analysis. Of 71 patients treated with urelumab plus nivolumab with RECIST/IWG assessments, 33 had reductions in tumor burden (Figure 1).

### Conclusions

Urelumab with or without nivolumab is safe/tolerable at flat and weight-based doses of 8 mg and 0.1 mg/kg. Although urelumab has demonstrated single-agent pharmacodynamic and antitumor activity in lymphoma, combination with nivolumab did not appear to provide significant additive/synergistic clinical benefit at the doses evaluated.

### Trial Registration

ClinicalTrials.gov identifier NCT01471210 and NCT02253992.

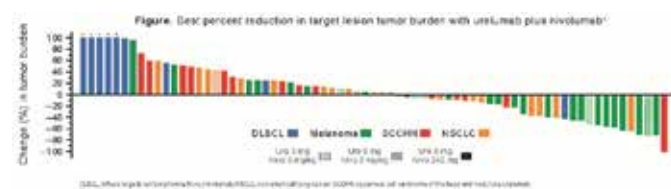
**Table 1. Treatment-related safety events**

	Urelumab monotherapy N=123	Urelumab + nivolumab N=104
Patients, n (%)		
Treatment-related AEs	65 (53)	65 (63)
Most frequent treatment-related AEs*		
Fatigue	18 (15)	27 (26)
AST increased	16 (13)	9 (9)
ALT increased	12 (10)	13 (13)
Treatment-related grade 3/4 AST elevation	4 (3)	3 (3)
Treatment-related grade 3/4 ALT elevation	3 (2)	3 (3)
Treatment-related serious AEs	9 (7)	10 (10)
Treatment-related AEs leading to discontinuation	6 (5)	7 (7)
Treatment-related deaths	0	0

AE, adverse event; ALT, alanine aminotransferase; AST, aspartate aminotransferase.

\* Treatment-related AEs occurring in  $\geq 10\%$  of all patients.

**Figure 1. Best percent reduction in target lesion tumor burden with urelumab plus nivolumab**



### 240

#### The effects of combination treatment of IMM-101, a heat-killed whole cell preparation of *Mycobacterium obuense* (NCTC 13365) with checkpoint inhibitors in pre-clinical models

*James Crooks*<sup>1</sup>, Sheila Brown<sup>1</sup>, Audrey Gauthier<sup>2</sup>, Marc Hillairet de Boisferon<sup>2</sup>, Andrew MacDonald<sup>1</sup>, Laura Rosa Brunet<sup>3</sup>

<sup>1</sup>MCCIR, University of Manchester, Manchester, England, UK

<sup>2</sup>Oncodesign, Dijon, Bourgogne, France

<sup>3</sup>Immodulon Therapeutics Ltd, Uxbridge, England, UK

### Background

While harnessing the power of the immune system to control cancer is becoming established as an effective way of treating patients, it has become increasingly clear that transformed





## Combinations: Immunotherapy/Immunotherapy

Presenting author underlined; *Primary author in italics*

cells exploit a number of mechanisms to escape such control. Hence, while the clinical use of checkpoint inhibitors (CPI) has yielded significant success, there is mounting evidence to suggest that combination treatment of CPI with immunomodulating therapies may further benefit cancer patients. Immodulon Therapeutics is developing IMM-101, an immunotherapeutic agent based on a heat-killed whole cell preparation of *Mycobacterium obuense* (NCTC 13365), which modulates systemic immune responses, as an adjunctive immunotherapy for cancer. Based on exposure data in over 300 patients, alone and in combination, IMM-101 is well-tolerated. Additionally, extended overall survival and progression-free survival were observed in IMAGE-1, a randomized open-label, phase II, first-line, proof of concept study (NCT01303172), in combination with gemcitabine in advanced pancreatic ductal adenocarcinoma.

### Methods

We found that *in vitro* exposure of IMM-101 primes *in vitro* generated murine dendritic cells (DC) and human monocyte-derived DC in a dose dependent manner and functionally affects DC by enhancing their ability to process and present antigen. Moreover, IMM-101 activated DC promote T cell secretion of IFN- $\gamma$  following re-stimulation of draining lymph node cell preparations, 7 days after adoptive transfer of IMM-101 primed DC into naïve recipient mice. We also investigated whether the effects of IMM-101 on innate and adaptive immune responses indeed improve on the therapeutic benefit of CPI treatment (anti-CTLA-4 or anti-PD-1) in two murine xenograft models using B16-F10, a mouse melanoma cell line, and EMT6, a mouse breast cell line.

### Results

We assessed effects on tumor burden and local and systemic immunological bias in treated mice. We report a significant benefit from combination treatment of CPI and IMM-101 on tumor burden. We also observed significant change to the CD8<sup>+</sup>/Treg ratio at the tumor site. We performed *in vitro* stimulation (antigenic as well as polyclonal) of immune cells present at the tumor site, in the draining lymph nodes and in the spleen. We report results at different time points over the course of the disease.

### Conclusions

On the basis of these promising results, formal clinical evaluation of IMM-101 in combination treatment with anti-PD-1 treatment is being undertaken (EudraCT identifier 2016-001459-28).

## 241

### **Intrathecal AAV9.trastuzumab for both tumor prophylaxis and treatment extends survival in a murine xenograft model of HER2+ human breast cancer brain metastasis**

William T Rothwell, Peter Bell, James M Wilson

University of Pennsylvania Perelman School of Medicine, Philadelphia, PA, USA

### Background

Breast cancer brain metastases (BCBM) occur in up to 14.3% of patients with human epidermal growth factor receptor 2 positive (HER2+) primary tumors [1]. Intravenous trastuzumab (anti-HER2 monoclonal antibody (mAb), Herceptin®) extends survival in patients with HER2+ systemic disease but does not cross the blood brain barrier (BBB) to treat HER2+ BCBM effectively [2]. Intrathecal (IT) trastuzumab can extend survival in patients with HER2+ BCBM [3] but requires regular IT infusions which carry risks and can compromise quality of life. Gene therapy offers a one-shot solution for mAb delivery across the BBB. Adeno-associated viral vectors, particularly serotype 9 (AAV9), can safely and efficiently deliver exogenous genes (transgenes) to central nervous system tissues after a single IT administration, resulting in constitutive, long-term expression of the transgene product [4].

### Methods

We characterize a xenograft model of HER2+ BCBM using BT474.M1 human ductal carcinoma cells injected stereotaxically into the brain parenchyma of Rag1<sup>-/-</sup> mice. AAV9.trastuzumab is delivered IT as tumor prophylaxis (at least 21 days before tumor administration) or as tumor treatment (3 days post tumor administration).

### Results

Median survival (MS) of Rag1<sup>-/-</sup> mice receiving IT AAV9.trastuzumab tumor prophylaxis (MS=111 days, n=7) is significantly greater after tumor administration than mice receiving vehicle (MS=48.5 days, n=8, p=0.0012\*), AAV9 expressing an irrelevant antibody (MS=54.5 days, n=10, p=0.0027\*), or AAV9 without a transgene (MS=50 days, n=4, p=0.0069\*). MS of mice bearing tumors treated with IT AAV9.trastuzumab (MS=82 days, n=6) is significantly greater than controls receiving vehicle (MS=61 days, n=7, p=0.002\*). \*Log-rank (Mantel-Cox) test.

### Conclusions

IT AAV9.trastuzumab as both tumor prophylaxis and treatment increases survival in a murine xenograft model of HER2+ BCBM, thus showing promise as HER2+ BCBM treatment and, more broadly, as a prophylactic measure for patients with HER2+ primary disease to extend survival in the case of BCBM.



## Combinations: Immunotherapy/Immunotherapy

Presenting author underlined; Primary author in italics

### References

1. Kennecke H, *et al*: **Metastatic behavior of breast cancer subtypes.** *J Clin Oncol* 2010, **28**:3271-3277.
2. Koo T, Kim I: **Brain metastasis in human epidermal growth factor receptor 2-positive breast cancer: from biology to treatment.** *Radiat Oncol J* 2016, **34**:1-9.
3. Zagouri F, Sargentanis T: **Intrathecal administration of trastuzumab for the treatment of meningeal carcinomatosis in HER2-positive metastatic breast cancer: a systematic review and pooled analysis.** *Breast Cancer Res* 2013, **139**:13-22.
4. Hinderer C, *et al*: **Widespread gene transfer in the central nervous system of cynomolgus macaques following delivery of AAV9 into the cisterna magna.** *Mol Ther Methods Clin Dev* 2014, **1**:14051.

### 242

#### Immunotherapy of head and neck squamous cell cancers with synthetic TLR agonists and checkpoint inhibitors in preclinical models

Fumi Sato-Kaneko<sup>1</sup>, Shiyin Yao<sup>1</sup>, Shannon S. Zhang<sup>2</sup>, Dennis A. Carson<sup>1</sup>, Cristina Guiducci<sup>2</sup>, Robert L. Coffman<sup>2</sup>, Kazutaka Kitauro<sup>3</sup>, Takaji Matsutani<sup>3</sup>, Ryuji Suzuki<sup>3</sup>, *Tomoko Hayashi*<sup>1</sup>, Ezra E.W. Cohen<sup>1</sup>

<sup>1</sup>Moores Cancer Center, University of California, San Diego, La Jolla, CA, USA

<sup>2</sup>Dynavax Technologies, Berkeley, CA, USA, Berkeley, CA, USA

<sup>3</sup>Repertoire Genesis Incorporation, Osaka, Japan, Ibaraki, Osaka, Japan

#### Background

Head and neck squamous cell cancers (HNSCC) constitute the sixth leading cancer by incidence worldwide. Though PD-1/PD-L1 blockade is effective in some patients, the majority do not benefit. We examined combination therapy with anti-PD-1 and synthetic agonists of toll-like receptors (TLR)7 and TLR9 in mouse models representing human papilloma virus (HPV)-positive and HPV-negative HNSCC, respectively. We hypothesized that the intratumoral treatment with TLR agonists could activate innate immune cells in the tumor microenvironment and enhance tumor specific adaptive immunity. Furthermore, this would be synergistic with checkpoint inhibitors that release negative signals on tumor infiltrating CD8<sup>+</sup> T cells.

#### Methods

Syngeneic tumor mouse models, SCC-7 cells (HPV-negative)/C3H background and MEER cells (HPV-positive)/C57BL/6 background, were used. Mice were implanted with tumor cells subcutaneously into opposite flanks. Treatments were started with intratumoral injections into only the right side

with TLR7 or TLR9 agonists with or without intraperitoneal injections of anti-PD-1 mAb. Lymphocytes were isolated from tumors and spleens on days 13 and 21 post tumor implantation, and were analyzed using flow cytometry. The T cell receptor (TCR) repertoire of CD8<sup>+</sup> T cells in the tumor and the spleen was evaluated by unbiased high throughput quantitative sequencing.

#### Results

In both HPV-negative and HPV-positive models, the combination therapies of intratumoral TLR7 or TLR9 agonists with anti-PD-1 suppressed tumor progression both at agonist-injected and uninjected sites (abscopal-like effect) (Figure 1). In the HPV-negative model, the combination treatment with TLR7 agonists and anti-PD-1 increased the M1/M2 ratio in CD11b<sup>+</sup>F4/80<sup>+</sup> tumor infiltrating macrophages (Figure 2). *Ex vivo* treatment with TLR7 agonist upregulated the expression of costimulatory molecules CD40, CD80, and decreased the expression level of CD206 (M2-macrophage marker). The combination therapy with TLR7 agonist increased the frequency of CD8<sup>+</sup> T cells in both sides of tumors and spleen. Elevated IFN $\gamma$ <sup>+</sup> activated T cell population was observed in mice treated with the TLR7 ligand and anti-PD-1 therapy (Figure 3). TCR repertoire analysis showed anti-PD-1 increased clonal expansion of splenic CD8<sup>+</sup> T cells (Figure 4).

#### Conclusions

The combination therapy with TLR agonists and anti-PD-1 suppressed progression of tumors in both injected and distant sites by two different mechanisms of action; clonal expansion of low frequency CD8<sup>+</sup> T cell population by anti-PD-1, and recruitment and activation of tumor specific T cells by intratumoral treatment with TLR ligands.

#### Acknowledgements

We thank Dr. John Lee in Sanford Research, who kindly provided us with HNC cells. This work was supported by the Fernanda and Ralph Whitworth Immunotherapy Foundation.

# Combinations: Immunotherapy/Immunotherapy

Presenting author underlined; Primary author in italics

**Figure 1. Therapeutic effect of intratumoral TLR7 and TLR9 agonist and anti-PD-1 in HPV negative HNC.**

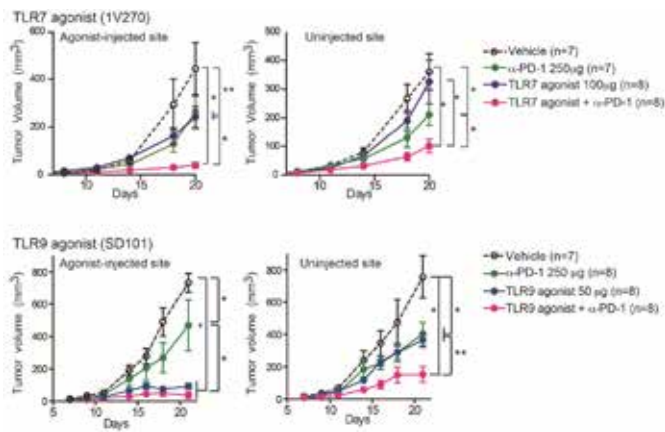


**Figure 2. Increased M1/M2 ratio by combination therapy with TLR7 agonist and anti-PD-1 in HPV negative HNC.**

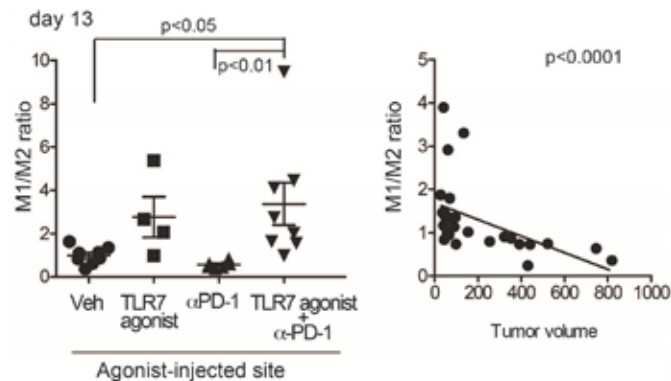


**Figure 3. Increased IFNγ+ activated CD8+ T cell population by combination therapy.**

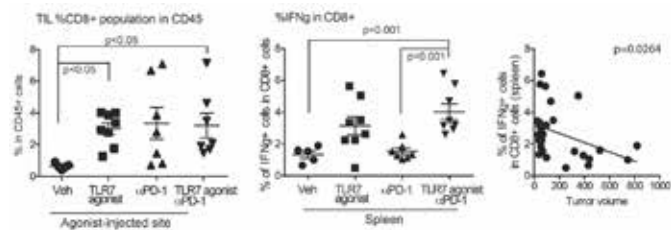
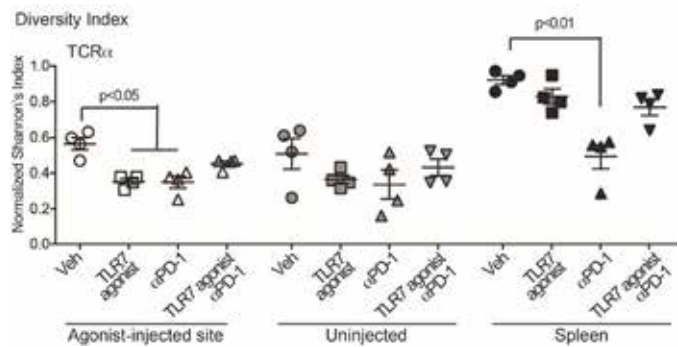


**Figure 4. Anti-PD-1 increased clonal expansion of splenic CD8+ T cells.**



## 243

### Modulating the intra-tumor immune balance through combinatorial blockade of CSF-1R and PD-L1 enhances anti-tumor efficacy

*David Schaer*<sup>1</sup>, Yanxia Li<sup>1</sup>, Julie Dobkin<sup>1</sup>, Michael Amatulli<sup>1</sup>, Gerald Hall<sup>1</sup>, Thompson Doman<sup>2</sup>, Jason Manro<sup>2</sup>, Frank Charles Dorsey<sup>2</sup>, Lillian Sams<sup>2</sup>, Rikke Holmgaard<sup>1</sup>, Krishnadatt Persaud<sup>1</sup>, Dale Ludwig<sup>1</sup>, David Surguladze<sup>1</sup>, John S Kauh<sup>3</sup>, Ruslan Novosiadly<sup>1</sup>, Michael Kalos<sup>1</sup>, Kyla Driscoll<sup>1</sup>

<sup>1</sup>Eli Lilly and Company, New York, NY, USA  
<sup>2</sup>Eli Lilly and Company, Indianapolis, IN, USA  
<sup>3</sup>Eli Lilly and Company, Bridgewater, NJ, USA

#### Background

Multiple mechanisms are involved in establishing an immunosuppressive tumor microenvironment. Although blockade of the PD-1/L1 axis alone has led to durable clinical responses in multiple malignancies, the majority of patients do not receive or maintain clinical benefit from monotherapy. Colony stimulating factor receptor 1 (CSF-1R) expressing tumor associated macrophages (TAMs) have been implicated as a poor prognostic factor in many cancers. TAMs and other suppressive myeloid cells may represent an additional suppressive axis present in many malignancies where PD-1/L1 blockade has shown some or little activity. CSF-1R has been implicated for maintaining TAM function and viability in tumor tissues, making it an attractive target to modulate TAM and possibly myeloid mediated suppression in cancer. As the CSF-1R Inhibitor LY3022855 has recently entered clinical testing in combination with PD-L1 blockade, it is important to understand how inhibiting two immune suppressive mechanisms will alter immune function to help guide rational clinical development.

#### Methods

To study and understand the immune modulating effects of CSF-1R inhibition, we developed an anti-mouse CSF-1R surrogate antibody CS7. CS7 blocks CSF-1 binding to CSF-

## Combinations: Immunotherapy/Immunotherapy

Presenting author underlined; Primary author in italics

1R and inhibits *in vitro* proliferation and differentiation of macrophages and depletes tissue resident macrophages *in vivo*.

### Results

Monotherapy treatment with CS7 causes intra-tumor depletion of ~50-60% of F4/80+ TAMs leading to a modest delay in tumor growth. This reduction was associated with an increased intra-tumor immune inflammation signature and reduced inhibitory metabolites, highlighting the role TAMs play suppressing the immune response inside the tumor microenvironment. Combining CSF-1R blockade with anti-PD-L1 enhances the control of tumor growth, displaying a late combinatorial effect leading to complete regressions in the majority of mice (~60%). Mice achieving complete regressions developed immunologic memory resisting rechallenge over 60 days after cessation of therapy. Intra-tumor gene expression analysis demonstrated a synergistic increase in T cell activation and reduction of immune suppression late in the response, correlating with the time point of increased efficacy. Effects of CS7 were dose-dependent, suggesting that while lower doses of CS7 are able to cause TAM depletion, modulation of the microenvironment requires more complete block of CSF-1R.

### Conclusions

Our results demonstrate that combination of CSF-1R blockade with PD-L1 checkpoint inhibition alters the tumor microenvironment in favor of enhanced immune activation. In addition, our data imply that the mechanism of CSF-1R blockade immunotherapy may extend beyond reduction of intra-tumor macrophages.

244

### A combination study of an intravenously delivered oncolytic virus, coxsackievirus A21 in combination with pembrolizumab in advanced cancer patients: phase Ib KEYNOTE 200 (STORM study)

Hardev Pandha<sup>1</sup>, Christy Ralph<sup>2</sup>, Kevin Harrington<sup>3</sup>, *Brendan Curti*<sup>4</sup>, Rachel E Sanborn<sup>5</sup>, Wallace Akerley<sup>6</sup>, Sumati Gupta<sup>6</sup>, Alan Melcher<sup>7</sup>, David Mansfield<sup>7</sup>, David R Kaufman<sup>8</sup>, Emmett Schmidt<sup>8</sup>, Mark Grose<sup>9</sup>, Bronwyn Davies<sup>9</sup>, Roberta Karpathy<sup>9</sup>, Darren Shafren<sup>9</sup>

<sup>1</sup>University of Surrey, Guildford, England, UK

<sup>2</sup>St James University Hospital, Leeds, England, UK

<sup>3</sup>Institute for Cancer Research, London, England, UK

<sup>4</sup>Providence Cancer Center, Portland, OR, USA

<sup>5</sup>Robert W. Franz Cancer Research Center, Earle A. Chiles Research Institute, Providence Cancer Center, Portland, Oregon, USA

<sup>6</sup>Huntsman Cancer Institute, Salt Lake City, UT, USA

<sup>7</sup>Institute for Cancer Research, London, England, UK

<sup>8</sup>Merck & Co., Inc., Kenilworth, NJ, USA

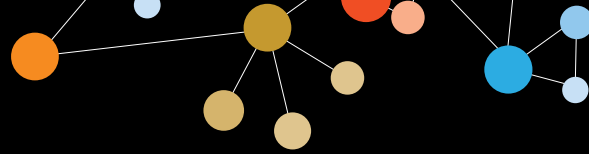
<sup>9</sup>Viralytics Ltd., Sydney, New South Wales, Australia

### Background

Coxsackievirus A21 (CVA21, CAVATAK) is a naturally-occurring ICAM-1 targeted oncolytic immunotherapeutic virus. Pembrolizumab is a human programmed death receptor-1 (PD-1) blocking antibody that has yielded significant solid tumor responses via reversal of tumor induced T cell suppression. Preclinical studies in immune-competent mouse models of non-small cell lung cancer (NSCLC) and melanoma confirmed that combinations of i.v. CVA21 + anti-PD-1 mAbs mediated significantly greater antitumor activity compared to use of either agent alone. We postulate that the combination of CVA21 + pembrolizumab may translate to a similar benefit in the clinic. We describe a phase Ib study assessing safety and efficacy of IV CVA21 ± pembrolizumab in advanced cancer patients (pts).

### Methods

The phase I STORM (systemic treatment of resistant malignancies; KEYNOTE 200) primary objectives are to assess dose-limiting toxicities (DLT) of CVA21 ± pembrolizumab. Secondary objectives are to assess ORR by irRECIST 1.1 criteria, PFS, and OS. Treatment Part A: pts were infused with CVA21 in 100 mL saline in Cohort 1 (n = 3), at a dose of  $1 \times 10^8$  TCID<sub>50</sub>, in Cohort 2 (n = 3) at a dose of  $3 \times 10^8$  TCID<sub>50</sub> and in Cohort 3 (n = 10) at a dose of  $1 \times 10^9$  TCID<sub>50</sub> on study days 1, 3, 5, 22 and Q3W for 6 additional infusions. Part A enrollment is complete. Treatment Part B: pts are infused with CVA21 in 100 mL saline + pembrolizumab. In Cohort 1 (n = 3), CVA21 is administered at a dose of  $1 \times 10^8$  TCID<sub>50</sub>, in



## Combinations: Immunotherapy/Immunotherapy

Presenting author underlined; Primary author in italics

Cohort 2 (n = 3) at a dose of  $3 \times 10^8$  TCID<sub>50</sub> and in Cohort 3 (n = ~80) at a dose of  $1 \times 10^9$  TCID<sub>50</sub> on study days 1, 3, 5, 8, 29, and Q3W for 6 additional infusions. Pembrolizumab is given in all cohorts at 200 mg IV Q3W from Day 8 for up to 2 years. Treatment with CVA21 ± pembrolizumab will continue until confirmed CR or PD (whichever comes first) per irRECIST 1.1 or DLT. Part B, Cohort 1 enrollment is complete.

### Results

IV delivery of CVA21 to all patients in Part A was generally well tolerated, with no Grade 3 or 4 product-related AE's.

### Conclusions

CVA21 tumor targeting in patients with melanoma, NSCLC, and bladder cancer patients in Part A Cohort 3 was confirmed by detection of CVA21 viral RNA in tumor biopsies at study Day 8.

### Trial Registration

ClinicalTrials.gov identifier NCT02043665.

### 245

#### Mutational status of p53 can influence its recognition by human T cells

Katerina Shamalov, Cyrille Cohen

Bar Ilan University, Ramat Gan, HaMerkaz, Iceland

### Background

p53 was reported to be an attractive immunotherapy target because it is mutated in approximately half of human cancers, resulting in its inactivation and often accumulation in tumor cells. Peptides derived from p53 are presented by class I MHC molecules and may act as tumor-associated epitopes which could be targeted by p53-specific T cells. Interestingly, it was recently shown that there is a lack of significant correlation between p53 expression levels in tumors and their recognition by p53-TCR transduced T cells.

### Methods

To better understand the influence of the mutational status of p53 on its presentation by the MHC system and on T cell anti-tumor reactivity, we generated several mutant p53 constructs and expressed them in HLA-A2+/p53- cells. Upon co-culture with p53-specific T cells, we measured the specific recognition of p53-expressing target cells by means of cytokine secretion, marker upregulation and cytotoxicity, and in parallel determined p53 expression levels by intracellular staining. We also examined the impact of mutant p53 expression on cell cycle dynamics and on the expression levels of the pro-apoptotic protein caspase-3.

### Results

Our results show that selected p53 mutations altering protein stability can modulate p53 presentation to T cells, leading

to a differential immune reactivity inversely correlated to measured p53 protein levels.

### Conclusions

Thus, p53 may behave differently than other classical tumor antigens and its mutational status should therefore be taken into account when elaborating immunotherapy treatments of cancer patients targeting p53.

### 246

#### Fc gamma receptor IV mediated depletion of tumor infiltrating regulatory T cells by anti-CTLA-4 antibody is promoted by TLR1/2 agonist and hence its efficacy in combination treatment of melanoma

Naveen Sharma, James Allison

University of Texas MD Anderson Cancer Center, Houston, TX, USA

### Background

Immune checkpoint blockade therapies have been successfully employed clinically to treat melanoma. Ipilimumab, which blocks inhibitory receptor CTLA-4 was one of the first checkpoint blockade therapies to get FDA approval for treating melanoma patients. Despite the effectiveness of these drugs, a significant number of cancer patients do not respond, and durable responses are only observed in a fraction of patients across tumor types. Therefore, combination therapies including checkpoint blockade antibodies are being studied to improve the outcome from immunotherapy treatment. Pattern recognition receptors like TLRs have been shown to have anti-tumor effects in various tumor models, through their effect on innate immunity.

### Methods

In this study, we set out to combine the innate immune arm like TLR ligand with the adaptive immune arm for treatment of melanoma in a mouse model. We identified TLR1/2 ligand Pam3CSK4 as innate immune system modulator to combine with anti-CTLA-4 antibody in this combination therapy. Mice were injected intradermal (i.d.) on the right flank with  $3 \times 10^5$  B16/F10 and considered day 0. Initial B16/F10 challenge was doubled to  $6 \times 10^5$  in experiments where mice would be sacrificed on day 14. Mice were then treated with intraperitoneal (i.p) injection of 100µg anti-CTLA-4 antibody and intratumoral injection with TLR1/2 ligand on every third after initial tumor challenge till day 12. The dose of anti-CTLA-4 antibody was doubled on day 3. In experiments where mice would be sacrificed on day 14, only two doses of anti-CTLA-4 antibody and TLR ligands were given on Day 9 and Day 12 after injection. These mice were either sacrificed on day 14 for obtaining lymphoid organs and tumors for phenotypic and functional analysis or tumor growth was analyzed.



## Combinations: Immunotherapy/Immunotherapy

Presenting author underlined; *Primary author in italics*

### Results

Our studies show that combining TLR1/2 ligand Pam3CSK4 with anti-CTLA-4 antibody decreases tumor burden and increases survival significantly, compared to anti-CTLA-4 antibody treatment alone. In our studies we found both CD4+ and CD8+ T cells to be important for this combination treatment efficacy. Most interestingly, we found that the mechanism of efficacy of combination treatment is due to an increased depletion of regulatory T cells modulated by enhanced FcγRIV expression on macrophages in combination therapy.

### Conclusions

Our findings suggest that combining TLR1/2 ligand with anti-CTLA-4 antibody will be an interesting prospect for treatment of cancer and it also suggest that TLR1/2 ligand modulate FcγRIV expression, which can be used to modulate the efficacy of other antibody-based immunomodulatory therapies.

### 247 Abstract Travel Award Recipient

#### **Immunostimulatory and oncolytic properties of rotavirus can overcome resistance to immune checkpoint blockade therapy**

Tala Shekarian<sup>1</sup>, Sandrine Valsesia-Wittmann<sup>2</sup>, Christophe Caux<sup>1</sup>, Aurelien Marabelle<sup>3</sup>

<sup>1</sup>Université Claude Bernard Lyon 1, Centre Leon Berard, Lyon, Rhone-Alpes, France

<sup>2</sup>Centre Leon Berard, Innovations in Immunotherapy Platform, Lyon, Rhone-Alpes, France

<sup>3</sup>Institut Goustave Roussy, Université Claude Bernard Lyon 1, Centre Leon Berard, Villejuif, Ile-de-France, France

### Background

Immune checkpoint targeted therapies against PD-1, PD-L1, and CTLA-4 are currently revolutionizing cancer care. However, a minority of patients generate objective tumor responses with these treatments. Therefore, new therapeutic interventions are needed to increase the immunogenicity of tumors in order to overcome the resistance to immune checkpoint blockade therapy. Pattern recognition receptors (PRR) such as toll-like receptor agonists have been shown to overcome resistance to immune checkpoint targeted therapy in pre-clinical models. Besides their intrinsic ability to stimulate PRR, the oncolytic properties of common viruses can be exploited also for the priming of anti-tumor immune responses. Hypothesis: Can anti-infectious vaccines be used as a source of PRR agonists and/or oncolytic viruses?

### Methods

We tested a TLR-Luc transgenic cell line for screening of the TLR agonist activity of anti-infectious vaccines. Cytotoxic activity induced by the vaccines was determined by SRB test

and IncuCyte imaging. Flow cytometry was performed to identify the type of cell death and to characterize different population of infiltrated immunity cells in the tumors. *In vivo* effect of immune checkpoints blockade were determined in monotherapy and in combination with the vaccines on tumor growth.

### Results

We confirmed that commercially available anti-infectious vaccines do have PRR agonist properties. Interestingly, we discovered that rotavirus vaccines also have oncolytic properties. These attenuated viruses can directly kill cancer cells with features of immunogenic cell death such as upregulation of calreticulin on dying cancer cells. Moreover, they have pro-inflammatory properties and can activate the NF-Kb pathway in a TLR and IRF3 independent manner. These *in vitro* biological properties translate into *in vivo* anti-tumor activity. Intra-tumoral rotavirus therapy has anti-tumor effects which are partly immune mediated as demonstrated by their activity in NSG xenograft models of human tumors. Interestingly, in immunocompetent syngeneic murine tumor models of neuroblastoma and lymphoma, intra-tumoral rotavirus therapy can overcome resistance and synergize with immune checkpoint targeted therapy. This therapeutic effect relied on specific modifications of tumor immune infiltrates and immune activation pathways. Intratumoral rotavirus vaccines was associated to an increase of leukocytes in the tumor microenvironment and upregulation of activation markers such as OX40/CD137 and CD86 on T cells and APC, respectively.

### Conclusions

Rotavirus vaccines are clinical grade products. Therefore, *in situ* immunization strategies with intra-tumoral attenuated rotavirus can be implemented quickly in the clinic. Intra-tumoral priming of the anti-tumor immunity with oncolytic and immunostimulatory rotavirus vaccines could be a feasible strategy to overcome resistance to anti-PD-1/anti-CTLA-4 therapy in patients with cancer.





## Combinations: Immunotherapy/Immunotherapy

Presenting author underlined; Primary author in italics

248

### **A phase I/II study of durvalumab alone or in combination with AXAL in recurrent/persistent or metastatic cervical or human papillomavirus (HPV)+ squamous cell cancer of the head and neck (SCCHN): preliminary phase I results**

Brian M Slomovitz<sup>1</sup>, Kathleen M Moore<sup>2</sup>, Hagop Youssoufian<sup>3</sup>, Marshall Posner<sup>4</sup>

<sup>1</sup>Sylvester Comprehensive Cancer Center / University of Miami, Miami, FL, USA

<sup>2</sup>Stephenson Oklahoma Cancer Center, Oklahoma City, OK, USA

<sup>3</sup>Advaxis Immunotherapies, Princeton, NJ, USA

<sup>4</sup>Icahn School of Medicine at Mount Sinai, Mount Sinai Medical Center, New York, NY, USA

#### **Background**

The success of immunotherapy for cervical cancer and HPV+ head and neck cancer may be enhanced by a combination of immune checkpoint blockade and tumor-selective vaccination. Axalimogene filolisbac (AXAL or ADXS11-001) is an irreversibly attenuated *Listeria monocytogenes*-listeriolysin O (*Lm*-LLO) immunotherapy bioengineered to secrete an HPV E7 tLLO fusion protein that induces HPV-specific cytotoxic T cells and reduces tumor-associated immune tolerance. Durvalumab is a selective, high-affinity human IgG1 mAb that blocks PD-L1 binding to PD-1 (IC<sub>50</sub> 0.1 nM) and CD80 (B7.1; IC<sub>50</sub> 0.04 nM). The PD-1/PD-L1 pathway is an important checkpoint used by tumor cells to inhibit antitumor responses. Preclinical mouse models demonstrate combination AXAL/anti-PD-1 treatment significantly reduces tumor growth and prolongs survival.

#### **Methods**

This is a phase I/II study (NCT02291055) of AXAL+durvalumab in patients (≥18 years) with either recurrent/metastatic cervical cancer or metastatic HPV+ SCCHN, who progressed on ≥1 platinum-based therapy. The primary objectives of the phase I, Part A dose escalation are to determine the safety/tolerability and establish the combination recommended phase II dose (RP2D) of AXAL (1×10<sup>9</sup> colony-forming units q4wk) and durvalumab (3mg/kg or 10mg/kg q2wk) following a 3+3 design. Part A includes a SCCHN expansion cohort (N=20) at the RP2D to evaluate efficacy. Part B will evaluate tumor response (RECIST and immune-related RECIST) of durvalumab monotherapy and AXAL+durvalumab combination therapy at the RP2D in recurrent/metastatic cervical cancer. Preliminary results of phase I dose escalation are reported.

#### **Results**

To date, 11 patients are enrolled in phase I (AXAL+durvalumab 3mg/kg: N=5; AXAL+durvalumab 10mg/kg: N=6); 91% had ECOG performance status 0, 73% had cervical cancer, of which 75% received prior bevacizumab. No dose-limiting toxicities have been observed. The following adverse events (AEs) were reported (3 vs. 10mg/kg): 100% vs. 83% of patients experienced AEs; 20% vs. 50% experienced SAEs; 60% vs. 50% experienced Grade 1 and Grade 2 treatment related AEs (TRAEs); Grade 3 TRAEs occurred in n=1 (rigors) and n=2 (rigors and neutropenia, respectively) patients. In the AXAL+durvalumab 3mg/kg cohort, 2 patients with cervical cancer obtained an objective response; 1 CR that is ongoing (9 months follow-up) and 1 PR with subsequent disease progression. Tumor assessments from the AXAL+durvalumab 10mg/kg cohort are not yet available. The RP2D was declared at durvalumab 10mg/kg q2wk + AXAL 1×10<sup>9</sup> colony-forming units q4wk.

#### **Conclusions**

The combination of AXAL/durvalumab appears safe and tolerable. Preliminary data indicate encouraging antitumor activity of the combination immunotherapy regimen.

#### **Trial Registration**

ClinicalTrials.gov identifier NCT02291055.

249

### **A specific 17-beta-hydroxywithanolide (LG-02) sensitizes cancer cells to apoptosis in response to TRAIL and toll-like receptor (TLR) ligands**

Poonam Tewary<sup>1</sup>, Alan D Brooks<sup>2</sup>, Ya-Ming Xu<sup>3</sup>, Kithsiri Wijeratne<sup>3</sup>, Leslie AA Gunatilaka<sup>4</sup>, Thomas J Sayers<sup>1</sup>

<sup>1</sup>CIP, Center for Cancer Research, BSP, Leidos Biomed Research Inc, National Cancer Institute-Frederick, Frederick, MD, USA

<sup>2</sup>CIP, Center for Cancer Research, Leidos Biomed Research Inc, National Cancer Institute-Frederick, Frederick, MD, USA

<sup>3</sup>University of Arizona, Southwest Center for Natural Products Research and Commercialization, Tucson, AZ, USA

<sup>4</sup>University of Arizona, Tucson, AZ, USA

#### **Background**

Despite many therapeutic successes, cancer is the second-most frequent cause of mortality in the United States. Strategies for cancer therapy aim to overcome excessive proliferation and avoidance of apoptosis. Therefore, methods of inducing apoptosis have become an important approach in the design of effective cancer therapies. Among these tumor necrosis factor-related apoptosis inducing ligand (TRAIL) has shown considerable promise as a nontoxic apoptotic inducer in cancer immunotherapy. However, many primary tumors are inherently resistant to TRAIL-mediated

## Combinations: Immunotherapy/Immunotherapy

*Presenting author underlined; Primary author in italics*

apoptosis and require additional sensitization. Therefore, there is an underlying interest in identifying agents that can be combined with TRAIL to improve its efficacy. Recent studies have also described a role of TLR3 signaling for initiating apoptosis in malignant cells and thus promote anticancer immune responses. We have previously shown that, withanolide E (WE), a 17 $\beta$ -hydroxywithanolide (17-BHW) and a natural product derived from the medicinal plant *Physalis peruviana* was capable of sensitizing tumor cells to TRAIL-mediated apoptosis by reducing cellular levels of the anti-apoptotic protein cFLIP.

### Methods

Encouraged by this, we screened a small library of 17-BHWs and have identified several that are more potent than WE for their ability to promote death ligand-mediated cancer cell death.

### Results

Among the 30 compounds tested, LG-02 was found to be 4-5 fold more potent than WE in sensitizing tumor cells to apoptotic signaling in response TRAIL as well as to the synthetic polynucleotide, poly(I:C), which is known to mimic anti-viral responses by activating TLR (toll-like receptor) signaling. Intra-tumor administration of LG-02 and poly(I:C) in a xenograft M14 melanoma model provided therapeutic benefit leading to complete tumor regression in 90% of the mice as compared to mice treated with vehicle or compounds alone. Molecular studies in melanoma cells demonstrated decreases not only in the anti-apoptotic cFLIP proteins but also in a number of IAPs including livin following LG-02 treatment. To date there are no withanolides reported to have this dual activity on reducing levels of different anti-apoptotic proteins.

### Conclusions

Thus, we hypothesized that 17-BHWs represent a unique NP scaffold, structural modification of which would lead to potent non-toxic sensitizers of apoptosis by TLR signaling that utilizes a downstream pathway similar to that of TNF death receptor signaling. Further studies with 17-BHWs could lead to the identification of novel and common therapeutic targets involved in apoptosis signaling in response to both TNF death receptor family members as well as TLR ligands.

### Acknowledgements

Funded by NCI Contract HHSN261200800001E.

## 250

### **Intratumoral administration of the TLR7/8 agonist MEDI9197 inhibits tumor growth and modulates the tumor microenvironment**

*John P Vasilakos*<sup>1</sup>, Tessa Alston<sup>1</sup>, Simon Dovedi<sup>2</sup>, James Elvecrog<sup>1</sup>, Iwen Grigsby<sup>1</sup>, Ronald Herbst<sup>3</sup>, Karen Johnson<sup>1</sup>, Craig Moeckly<sup>1</sup>, Stefanie Mullins<sup>2</sup>, Kristen Siebenaler<sup>1</sup>, Julius SternJohn<sup>1</sup>, Ashenafi Tilahun<sup>1</sup>, Mark A Tomai<sup>1</sup>, Katharina Vogel<sup>2</sup>, Robert W Wilkinson<sup>2</sup>

<sup>1</sup>M Company, St. Paul, MN, USA

<sup>2</sup>Medimmune, Cambridge, England, UK

<sup>3</sup>Medimmune, Gaithersburg, MD, USA

### Background

Toll-like receptor (TLR) agonists, such as the TLR7 agonist imiquimod, have been evaluated topically and systemically for cancer. Topical administration has shown antitumor activity against various cancers, such as melanoma, squamous cell carcinoma, and cutaneous breast cancer. However, systemic administration of TLR agonists in cancer patients has resulted in limited efficacy, in part due to cytokine-induced systemic adverse effects, which limits the therapeutic window. Therefore, a lipophilic imidazoquinoline, MEDI9197, was designed to be retained within the tumor following injection with the primary objective of directing immune activation to the tumor.

### Methods

The antitumor effects of intratumoral (IT) administered MEDI9197 were evaluated in 4 different mouse syngeneic subcutaneous implantation tumor models. Tumor and serum drug levels were quantified following IT administration. In addition, the tumor immune profile was assessed by qPCR, histology, and flow cytometry. Lastly, the antitumor effects of combination therapy using IT injected MEDI9197 in conjunction with CTLA-4 or PD-L1 antibodies were evaluated.

### Results

MEDI9197 is a human TLR7/8 agonist. Following IT administration, pharmacokinetic analysis shows that the drug is retained in the tumor, and very low levels of the drug are detected in the serum. MEDI9197 mediates antitumor activity (tumor growth inhibition and enhanced survival) in B16F10 luc, B16-OVA, 4T1, and CT-26 mouse tumor models. Administration of MEDI9197 by the IT route and by the SC route away from the tumor demonstrates that the antitumor effects of MEDI9197 require IT administration. IT dosed MEDI9197 modulates the local immune response characterized by an upregulation of genes involved in innate and adaptive immunity. IT dosed MEDI9197 induces tumor necrosis, leukocyte activation, and the formation of lymphoid aggregates evident by 7 days postdose. IT injected MEDI9197



## Combinations: Immunotherapy/Immunotherapy

Presenting author underlined; *Primary author in italics*

increases the number of tumor infiltrating CD8+ T cells, while concomitantly decreasing the number of tumor infiltrating CD4+ T cells. Moreover, MEDI9197 induces prolonged activation of tumor T cells and NK cells. Additionally, combination of MEDI9197 with CTLA-4 and PD-L1 antibodies enhances the efficacy observed in syngeneic mouse tumor models.

### Conclusions

The data presented shows IT administration of the TLR7/8 agonist MEDI9197 is retained in the tumor, modulates the tumor microenvironment in a manner consistent with an antitumor signature, and inhibits tumor growth in multiple mouse cancer models. Finally, the antitumor effects of MEDI9197 are further enhanced by combination therapy with checkpoint blockade therapies. MEDI9197 is currently being evaluated for safety and efficacy in human clinical trials (ClinicalTrials.gov Identifier: NCT02556463).

**251**

### Impact of intratumoral clonal heterogeneity on checkpoint inhibitor response

Eveline E Vietsch, *Anton Wellstein*

Georgetown University / Medical School / Lombardi Cancer Center, Washington, DC, USA

### Background

Cancer cells are subjected to evolutionary selection of clonal populations by changes in the microenvironment as well as their response to drug treatment. We wished to evaluate how this heterogeneity impacts efficacy of checkpoint inhibition.

### Methods

To understand the contribution of clonal subpopulations to the malignant progression and to the response to drugs, we established a model of tumor heterogeneity from six syngeneic, clonal primary cancer cells isolated from a mutant Kras/P53 mouse pancreatic cancer (KPC). The clones were characterized molecularly and tumors reconstituted from mixes of the clonal cell lines.

### Results

These clonal cells formed invasive and metastatic lesions when grafted into hosts. The original tumor and clonal cell lines harbored common mutations in 99 genes suggesting their common ancestry. Additional unique mutations in the clonal lines were used to identify and quantitate clones in heterogeneous cell pools. The clones showed different levels of MAP kinase signaling, unique morphologies, different growth rates *in vitro* and tumor growth rates in immune competent mice. Moreover, the sensitivity to ~200 anticancer drugs revealed an up to 25-fold varying *in vitro* sensitivity

of the clones to signal transduction inhibitors and cytotoxic drugs. To our surprise, drug sensitivity of individual clones when included in a heterogeneous cell population was strikingly different from their drug sensitivity when growing on their own. In particular, the sensitivity of clones to MEK or PI3K inhibition was not predictive of their sensitivity when grown in a pool with the other clones. Furthermore, the sensitivity of clones to an anti-PD-1 checkpoint inhibitor was distinct across the clonal cells growing in the heterogeneous mixture. Some clones were resistant and others highly sensitive to the checkpoint inhibition. We will discuss pathways and drivers of resistance in the different subpopulations.

### Conclusions

We conclude that malignant progression and selection of checkpoint inhibitor sensitive cancer cell subpopulations is impacted by the crosstalk between clonal cell populations present in heterogeneous tumors and the host environment.

**252**

### Beyond immune checkpoint: first-in-class antibody targeting soluble NKG2D ligand sMIC for cancer immunotherapy

Jennifer Wu, Jinyu Zhang, Fahmin Basher, Mark Rubinstein  
Medical University of South Carolina, Charleston, SC, USA

### Background

In response to oncogenic insult, human cells were induced to express a family of MHC I-chain related molecules A and B (MICA and MICB, generally termed MIC) on the surface which serve as the ligands for the activating immune receptor NKG2D expressed by all human NK, CD8 T, NKT, and subsets of gamma-delta T cells. Theoretically, engagement of NKG2D by tumor cell surface MIC is thought to signal and provoke the immune system to eliminate transformed cells. Clinically, almost all advanced tumors in cancer patients produce soluble MIC through proteolytic shedding mediated by metalloproteases, or by release in exosomes derived from the cell membrane. Tumor-derived sMIC is known to be highly immune suppressive and profoundly insults the immune system by downregulating receptor NKG2D expression on effector NK and T cells, driving the expansion of tumor-favoring myeloid suppressor cells, skewing macrophages into alternatively activated phenotypes, and perturbing NK cell peripheral maintenance. High levels of serum sMIC significantly correlate with advanced diseases of many types of cancer. These observations clearly endorse sMIC to be a cancer immune therapeutic target. However, due to mice lacking homologues to human MIC, this concept was not proven until our recent studies.

**Combinations: Immunotherapy/Immunotherapy**

Presenting author underlined; Primary author in italics

**Methods**

Using a “humanized” MIC-transgenic spontaneous mouse model which recapitulates the NKG2D-mediated onco-immune dynamics of human cancer patients, we addressed whether sMIC is a cancer immunotherapeutic target and whether antibody targeting sMIC synergizes with immune checkpoint blockade or adoptive T or NK cell therapy.

**Results**

We show that therapy with a first-in-field non-blocking antibody B10 that does not block the interaction of MIC with NKG2D revamps endogenous innate and antigen-specific CD8+ T cell responses and remodels immune reactive tumor microenvironment, by restoring NK cell hemostatic maintenance and function, enhancing CD8+ T cell infiltration to tumors and TCR clonality/diversity, modulating CD8+ T cells metabolic preferences, eliminating MDSCs and TAMS. Anti-sMIC stand-alone therapy resulted in effective debulking of primary tumors and eliminated metastasis. Using multiple pre-clinical animal models, we further demonstrate that antibody B10 neutralizing sMIC synergizes with CTLA-4 and PD-1/PD-L1 checkpoint blockade therapy and adoptive cell based therapy with no observed toxicity.

**Conclusions**

Our study has launched a new avenue of cancer immunotherapy which can be readily translated into clinical trials.

**High serum sMIC correlates with poor prognosis in cancer patients**

High serum sMIC correlates with poor prognosis in cancer patients

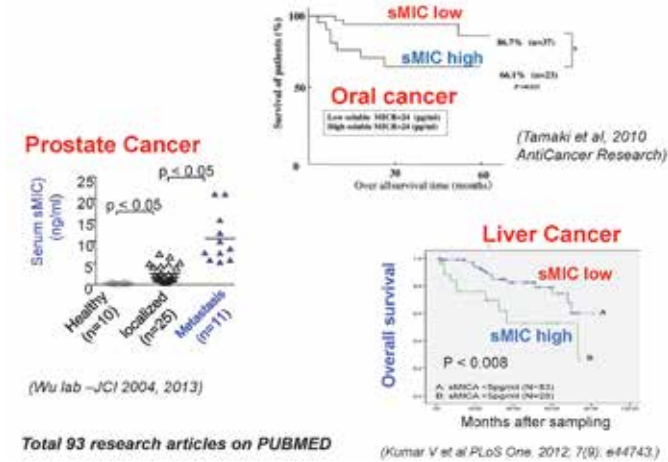


Figure 1. These are the examples in human cancer patients, prostate cancer, Oral cancer, and HBV-induced Liver cancer, where high levels of circulating sMIC correlates with advanced disease stages and poor survival.

**Pre-clinical proof-of-concept study: stand-alone therapy with CuraB-10 resulted in regression of primary tumors and eliminates metastasis in advanced “humanized” prostate tumor model**

Pre-clinical proof-of-concept study: stand-alone therapy with CuraB-10 resulted in regression of primary tumors and eliminates metastasis in advanced “humanized” prostate tumor model

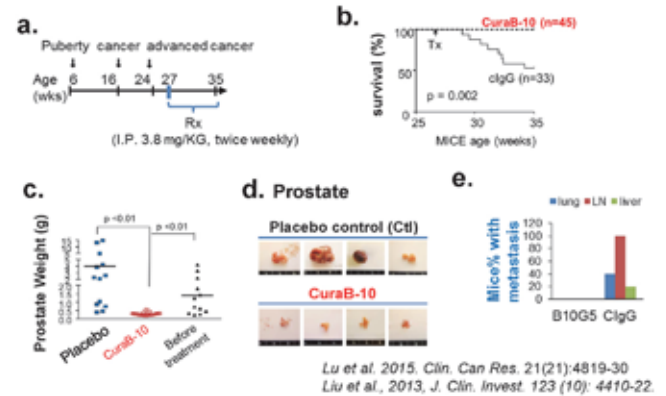


Figure 2. (a). Therapy of the clinically relevant spontaneous prostate tumor TRAMP/MICB model (Liu et al, 2013, JCI 123 (10) 4410 ) with CuraB10 (also called B10G5) or control IgG (placebo) at advanced stage via I.P. injection at the dose of 3.8 mg/KG body weight twice weekly for 8 weeks (b). Mice with CuraB-10 therapy all enjoyed longtime survived whereas mice in placebo group are succumbed to cancer (c). Prostate weight. Comparisons made between Placebo group and CuraB-10 group and between before and after treatment of CuraB-10. (d). Representative images of the prostate. Top showing large tumor burden. Bottom showing normal prostate size. (e). All mice in the control group developed metastasis whereas no metastasis was detected in animals received CuraB-10 therapy. In summary, the data demonstrate that CuraB-10 stand-alone therapy can effectively induce regression of primary tumors and eliminate metastasis.



## Combinations: Immunotherapy/Immunotherapy

Presenting author underlined; Primary author in italics

### CuraB-10 (B10G5) effectuates current checkpoint blockade cancer immunotherapy

### CuraB-10 (B10G5) effectuates current checkpoint blockade cancer immunotherapy

MODEL: Advanced (metastatic) spontaneous prostate cancer

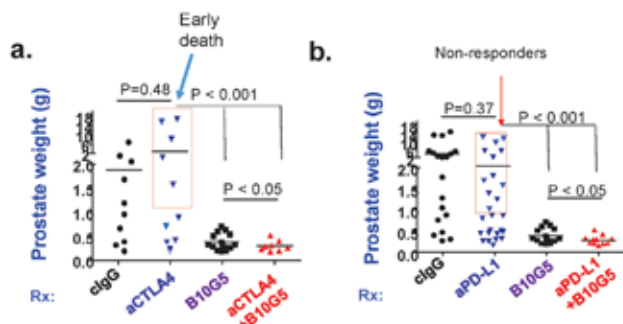


Figure 3. We further addressed the synergistic effect of CuraB-10 therapy with FDA approved checkpoint blockade therapy using the clinically relevant TRAMP/MIC spontaneous prostate tumor mouse model. Two points: 1) a percentage of TRAMP/MIC mice do not respond to checkpoint (CTLA4 or PD-1) blockade therapy, whereas all TRAMP/MIC mice are responsive to CuraB-10 therapy; also, a population of TRAMP/MICB animals died at 3-4 weeks of CTLA4 Rx alone. 2) CuraB-10 synergizes with checkpoint blockade (CTLA4 or PD-1) therapy when used in combination

### CuraB-10 augments the therapeutic effect of adoptive T cell therapy in non-lymph depleted host

### CuraB-10 augments the therapeutic effect of adoptive T cell therapy in non-lymph depleted host

Model: syngeneic transplantable melanoma

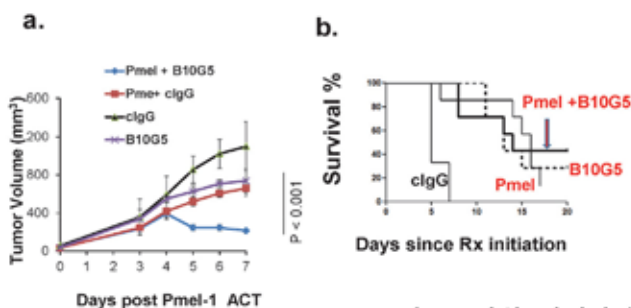


Figure 4. Because rodents do not express MIC, we engineered mouse melanoma B16 tumor cells to express sMIC (B16-sMIC). We implanted B16-sMIC into syngeneic host. When tumors grew to 50-100mm<sup>3</sup> in size, treatment starts. Four treatments were given: Adoptive transfer of melanoma antigen-specific Pmel CD8 T cells once, B10G5 (CuraB-10) twice 2 week Adoptive transfer of melanoma antigen-specific Pmel CD8 T cells once, control IgG (clgG) twice 2 week B10G5

alone 4) clgG alone Tumor growth curve demonstrating that treatment with B10G5 (CuraB-10) effectuates the effect of Pmel CD8 T therapy Survival curve. Tumor volume of 1000mm<sup>3</sup> was defined as survival end point. In one experiment, 2/7 animals received B10G5 and Pmel therapy had complete tumor regression. Note: currently Adoptive T cell transfer (ACT) requires prior-depletion of patient's immune cells with chemotherapy to be effective. With B10G5 therapy, not only lymph depletion is not required prior to ACT, but also ACT is more effective.

253

### Discovery and characterization of PF-06840003, a novel brain penetrant IDO1 inhibitor

*Martin Wythes*<sup>1</sup>, Stefano Crosignani<sup>2</sup>, Joseph Tumang<sup>1</sup>, Shilpa Alekar<sup>1</sup>, Patrick Bingham<sup>1</sup>, Sandra Cauwenberghs<sup>2</sup>, Jenny Chaplin<sup>1</sup>, Deepak Dalvie<sup>1</sup>, Sofie Denies<sup>2</sup>, Coraline De Maeseneire<sup>2</sup>, JunLi Feng<sup>1</sup>, Kim Frederix<sup>2</sup>, Samantha Greasley<sup>1</sup>, Jie Guo<sup>1</sup>, James Hardwick<sup>1</sup>, Stephen Kaiser<sup>1</sup>, Katti Jessen<sup>1</sup>, Erick Kindt<sup>1</sup>, Marie-Claire Letellier<sup>2</sup>, Wenlin Li<sup>1</sup>, Karen Maegley<sup>1</sup>, Reece Marillier<sup>2</sup>, Nichol Miller<sup>1</sup>, Brion Murray<sup>1</sup>, Romain Pirson<sup>2</sup>, Julie Preillon<sup>3</sup>, Virginie Rabolli<sup>2</sup>, Chad Ray<sup>1</sup>, Kevin Ryan<sup>1</sup>, Stephanie Scales<sup>1</sup>, Jay Srirangam<sup>1</sup>, Jim Solowiej<sup>1</sup>, Al Stewart<sup>1</sup>, Nicole Streiner<sup>1</sup>, Vince Torti<sup>1</sup>, Konstantinos Tsaparikos<sup>1</sup>, Xianxian Zheng<sup>1</sup>, Gregory Driessens<sup>2</sup>, Bruno Gomes<sup>2</sup>, Manfred Kraus<sup>1</sup>

<sup>1</sup>Pfizer, San Diego, CA, USA

<sup>2</sup>iTeos, 6041 Gosselies, Brussels Hoofdstedelijk Gewest, Belgium

<sup>3</sup>iTeos, Rue Auguste Piccard 48, Brussels Hoofdstedelijk Gewest, Belgium

### Background

Tumors use tryptophan-catabolizing enzymes such as indoleamine 2-3 dioxygenase (IDO1) to induce an immunosuppressive environment. IDO1 is induced in response to inflammatory stimuli and promotes immune tolerance, effector T cell anergy and enhanced Treg function. As such, IDO1 is a nexus for the induction of key immunosuppressive mechanisms and represents an important immunotherapeutic target in oncology.

### Methods

We have identified and characterized a new, selective, orally bioavailable IDO1 inhibitor, PF-06840003.

### Results

Key interactions of PF-06840003 with IDO1 will be presented, and rationalized using a novel X-ray crystal structure of PF-06840003 bound to human IDO1. In addition, binding studies with ferrous and ferric forms of human IDO1 have been performed. The results suggest that PF-06840003 is a tryptophan non-competitive, non-heme binding IDO1



## Combinations: Immunotherapy/Immunotherapy

Presenting author underlined; Primary author in italics

inhibitor. Key *in vitro* and *in vivo* pharmacology data, including combination studies with checkpoint inhibitors, and ADME data of PF-06840003 will be discussed. PF-06840003 shows a very favorable ADME profile (solubility, human hepatocyte stability, low *in vivo* clearance in preclinical species, high permeability, and high fraction absorbed in preclinical species) leading to favorable predicted human pharmacokinetic properties, including a predicted  $t_{1/2}$  of 19 hours.

### Conclusions

PF-06840003 is a selective IDO1 inhibitor with very favorable predicted human PK characteristics. Its prolonged projected human half-life should allow QD administration. CNS penetration suggests potential impact on brain metastases. Checkpoint antagonists against PD-L1 cause enhanced IDO1 expression and enhanced *in vivo* anti-tumor efficacy in combination with PF-06840003. These studies highlight the potential of PF-06840003 as a clinical candidate in Immuno-Oncology. A first in patient study for PF-06840003 in malignant gliomas is described at ClinicalTrials.gov (NCT02764151).

### 254

#### Enhanced anti-tumor effect of combination therapy with NHS-muLL-12 and anti-PD-L1 antibody (avelumab) in a preclinical cancer model

Chunxiao Xu<sup>1</sup>, Yanping Zhang<sup>2</sup>, Giorgio Kradjian<sup>2</sup>, Guozhong Qin<sup>2</sup>, Jin Qi<sup>2</sup>, Xiaomei Xu<sup>2</sup>, Bo Marelli<sup>2</sup>, Huakui Yu<sup>2</sup>, Wilson Guzman<sup>2</sup>, Rober Tighe<sup>2</sup>, Rachel Salazar<sup>2</sup>, Kin-Ming Lo<sup>2</sup>, Jessie English<sup>2</sup>, Laszlo Radvanyi<sup>2</sup>, Yan Lan<sup>2</sup>

<sup>1</sup>EMD Serono, Belmont, MA, USA

<sup>2</sup>EMD Serono, Billerica, MA, USA

### Background

Recent clinical studies have found that treatment with the immune checkpoint inhibitors anti-PD-1 or PD-L1 induce durable anti-tumor responses in some patients with advanced-stage cancers. However, many patients do not benefit from treatment because the induction, potency, and persistence of immune responses depend on a complex interplay between different immune cell populations. Thus, treatment with a combination of therapies that target distinct immune pathways may be a promising strategy to improve anti-tumor efficacy. NHS-IL-12 (MSB0010360N; M9241) is an investigational immunocytokine designed to target tumor necrotic regions as a method to deliver IL-12 into the tumor microenvironment. Avelumab\* (MSB0010718C) is a fully human anti-PD-L1 IgG1 monoclonal antibody designed to selectively bind to PD-L1 and competitively inhibit it from binding to PD-1, which has shown antitumor activity in various malignancies in clinical trials.

### Methods

In the pre-clinical studies described here, the anti-tumor efficacy of combination treatment with avelumab and the surrogate NHS-muLL-12 was investigated in an orthotopic EMT-6 breast cancer model.

### Results

Treatment with NHS-muLL-12 and avelumab generated an enhanced anti-tumor effect relative to either monotherapy. Most mice treated with the combination therapy had complete tumor regression and generated tumor-specific immune memory, as demonstrated by their protection against rechallenge with EMT-6 tumor cells and the significant induction of effector and memory T cells. The combination treatment dose-dependently stimulated cytotoxic NK and CD8+ T cell proliferation. NHS-muLL-12 treatment induced CD8+ T cell infiltration into the tumor microenvironment consistent with the induction of chemoattractants. Also, avelumab monotherapy reversed T cell immunosuppression and restored the function of exhausted CD8+ T cells in the tumor microenvironment.

### Conclusions

These preclinical findings indicate that the combination therapy with NHS-IL-12 and avelumab may provide a promising approach to treat patients with solid tumors. Asterisk (\*) indicates a proposed nonproprietary name.

### 255

#### Opposing effects of CTLA-4 and PD-1 blockade on follicular helper-like T cells with immunosuppressive functions

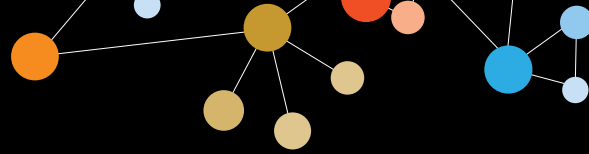
Roberta Zappasodi<sup>1</sup>, Sadna Budhu<sup>1</sup>, Matthew D Hellmann<sup>2</sup>, Michael Postow<sup>2</sup>, Yasin Senbabaoglu<sup>1</sup>, Billel Gasmi<sup>1</sup>, Hong Zhong<sup>1</sup>, Yanyun Li<sup>1</sup>, Cailian Liu<sup>1</sup>, Daniel Hirschhorn-Cymerman<sup>1</sup>, Jedd D Wolchok<sup>2</sup>, Taha Merghoub<sup>1</sup>

<sup>1</sup>Ludwig Collaborative Laboratory, Memorial Sloan Kettering Cancer Center, New York, NY, USA

<sup>2</sup>Department of Medicine, Memorial Sloan Kettering Cancer Center, New York, NY, USA

### Background

The mechanism underlying the improved anti-tumor activity of combined CTLA-4 and PD-1 blockade is not yet well understood. We reported that expansion of CD4<sup>+</sup>Foxp3<sup>-</sup> T cells expressing PD-1 (4PD-1<sup>hi</sup>) was associated with limited therapeutic improvement when a CTLA-4-blocking antibody was added to an anti-melanoma vaccine in B16-melanoma bearing mice. We went on to define functions and origin of 4PD-1<sup>hi</sup> to clarify the significance of their modulation by checkpoint blockade in mouse tumor models and cancer patients.



## Combinations: Immunotherapy/Immunotherapy

Presenting author underlined; *Primary author in italics*

### Methods

4PD-1<sup>hi</sup> frequency was monitored by flow cytometry. Their function was tested in standard *in vitro* suppression assays and 3D collagen-fibrin gel killing assays. RNAseq gene expression analyses were performed on a Proton sequencing system at the MSK Genomics Core Facility.

### Results

Circulating and intra-tumor 4PD-1<sup>hi</sup> frequencies positively correlated and both increased as a function of tumor burden in anti-CTLA-4-treated and naïve B16-bearing mice, suggesting a pro-tumor role of 4PD-1<sup>hi</sup>. Accordingly, the ratio between effector T cell (Teff) and 4PD-1<sup>hi</sup> inversely correlated with tumor size. 4PD-1<sup>hi</sup> from spleens and tumors of naïve and B16-bearing Foxp3-GFP-transgenic mice treated or not with CTLA-4 blockade suppressed Teff functions. RNAseq gene expression analysis revealed an enrichment of follicular helper T cell-(Tfh)-associated genes in 4PD-1<sup>hi</sup> in comparison with regulatory T cells (Tregs) and CD4<sup>+</sup>Foxp3<sup>+</sup>PD-1<sup>+</sup> T cells. We therefore immunized Foxp3-GFP transgenic mice with sheep red blood cells (sRBC) to boost development of Tfh and test their function *in vitro*. 4PD-1<sup>hi</sup> from sRBC-treated animals inhibited Teff more efficiently than those isolated from untreated mice. However, in contrast to Tregs and according to their Tfh-like phenotype, 4PD-1<sup>hi</sup> promoted activation and maturation of B cells *in vitro*. Moreover, concurrent PD-1 and CTLA-4 blockade, either alone or in combination with an anti-melanoma vaccine, prevented 4PD-1<sup>hi</sup> expansion and significantly improved anti-tumor responses in mice. In cancer patients, ipilimumab increased, whereas PD-1 blockade reduced, circulating 4PD-1<sup>hi</sup>. We took advantage of differential CD25 expression in 4PD-1<sup>hi</sup> and Tregs to isolate and compare these two cell subsets from healthy donors' peripheral blood as well as patients' tumors. Human 4PD-1<sup>hi</sup> inhibited Teff functions *in vitro* and expressed Tfh-associated markers, thus confirming our observations in mice.

### Conclusions

Our study describes T cell suppression functions of Tfh-like cells expanded by CTLA-4 blockade. Importantly, we show that these cells exist in healthy individuals and expand in the presence of tumor. We provide evidence that PD-1 blockade counteracts anti-CTLA-4-mediated 4PD-1<sup>hi</sup> induction, thus underscoring one of the mechanisms potentially responsible for the improved therapeutic activity of combination checkpoint blockade.

### Consent

Written informed consent was obtained from the patient for publication of this abstract and any accompanying images. A copy of the written consent is available for review by the Editor of this journal.

### 256

#### **WT1 peptide vaccine in Montanide or poly-ICLC triggers different immune responses in patients with myeloid leukemia**

Yuan Yuan Zha<sup>1</sup>, Gregory Malnassy<sup>2</sup>, Noreen Fulton<sup>2</sup>, Jae-Hyun Park<sup>2</sup>, Wendy Stock<sup>3</sup>, Yusuke Nakamura<sup>2</sup>, Thomas F Gajewski<sup>4</sup>, *Hongtao Liu*<sup>4</sup>

<sup>1</sup>University of Chicago, OSRF-HIM, Chicago, IL, USA

<sup>2</sup>University of Chicago, Chicago, IL, USA

<sup>3</sup>University of Chicago, Section of Hematology/Oncology, Chicago, IL, USA

<sup>4</sup>University of Chicago Medical Center, Chicago, IL, USA

#### **Background**

It has been well established that human T cells can recognize and destroy tumor cells. In solid tumors, it has been shown that peptide vaccine against tumor antigens can augment host anti-tumor immune response and achieve tumor control in some patients. WT1 is a defined leukemia-associated antigen, a transcription factor that over-expressed in AML, CML, ALL, and other tumors. WT1 is highly antigenic and is an attractive target for immunotherapy. However, the optimal strategy for vaccination to induce WT1-specific immune responses is not known.

#### **Methods**

In this pilot study, we randomized seven (4 males, 3 female ages 39 to 73) HLA-A02+ patients with myeloid leukemia in the minimal residual disease state to receive vaccination with WT1 126-134 peptide (RMFPNAPYL) in either Montanide or poly-ICLC (TLR3 agonist). Four patients were randomized to receive WT1 in Montanide and three were randomized to receive WT1 in poly-ICLC. The vaccine was administered every other week X 6 during the induction phase followed by monthly booster vaccinations X 6 months. Patients were monitored for disease and toxicity. Blood was collected to monitor WT1 transcript levels, antigen-specific CD8+ T cell responses, and TCR sequencing.

#### **Results**

After WT1 vaccination, three of four patients in the Montanide arm had decreased WT1 levels in circulation detected by qRT-PCR, and two of these demonstrated augmented WT1-specific CD8+ T cell responses detected by IFN- $\gamma$  ELISPOT assay. All three patients had TCR clonal enrichment after WT1 vaccination suggested by TCR alpha and beta CDR3 sequencing. In contrast, in the two patients on the poly-ICLC arm, no increase in WT1-specific CD8+ T cell responses was detected by IFN- $\gamma$  ELISPOT assay, and no clonal enrichment was detected by TCR alpha/beta sequencing. Interestingly, these two patients nonetheless demonstrated decreased WT1 transcript levels in circulation detected

## Combinations: Immunotherapy/Immunotherapy

Presenting author underlined; Primary author in italics

by qRT-PCR and remained in remission 3 years after the initiation of WT1 vaccination.

### Conclusions

Our results show that vaccination with WT1 peptide emulsified in Montanide is a superior vaccine strategy based on increased WT1-specific CD8+ T cell responses with TCR clonal and specific TCR beta CDR3 enrichment and decreased WT1 transcripts as a measure of minimal residual disease. The fact that vaccination with WT1 peptide in poly-ICLC nonetheless was associated with decreased WT1 transcripts suggests that a distinct immune activation mechanism might be occurring, for example an effect on dendritic cells of poly-ICLC alone.

257

### Combination of *Listeria*-based human papillomavirus (HPV) E7 cancer vaccine (AXAL) with CD137 agonist antibody provides an effective immunotherapy for HPV-positive tumors in a mouse model

*Xiaoming Ju*, Rachele Kosoff, Kimberly Ramos, Brandon Coder, Robert Petit, Michael Princiotta, Kyle Perry, Jun Zou

Advaxis Immunotherapies, Princeton, NJ, USA

### Background

HPV can cause cervical, anal, vulvar, vaginal, penile, and oropharyngeal cancers. AXAL is a genetically engineered *Listeria monocytogenes*-based therapeutic cancer vaccine currently in clinical trials for cervical (phase III), anal (phase II), and head and neck (phase I/II) cancers, either as monotherapy or in combination with checkpoint inhibitor (PD-1 or PD-L1) antibodies. To identify potentially synergistic immunotherapies, we evaluated AXAL ± antibodies for T cell co-inhibitory or co-stimulatory receptors (checkpoint inhibitors: CTLA-4, PD-1, TIM-3, LAG-3; co-stimulators: CD137, OX40, GITR, and CD40) in a mouse HPV-positive tumor model.

### Methods

C57BL/6 female mice and TC1 cells (C57BL/6 mouse lung epithelial cells co-transfected with HPV16 E6 and E7 and activated *Ras*) were obtained from Jackson Laboratories and ATCC, respectively. All antibodies were obtained from Bio X Cell. Mice were subcutaneously injected on the hind-leg flank with TC1 cells. AXAL ± the respective antibodies was injected intraperitoneally at  $5 \times 10^7$  colony-forming units/mouse weekly for 3 total doses. For combinations with superior performance, the tumor microenvironment (TME) was further evaluated using flow cytometry to immunophenotype the tumor-infiltrating lymphocytes (TILs), spleen, and tumor-draining lymph node.

### Results

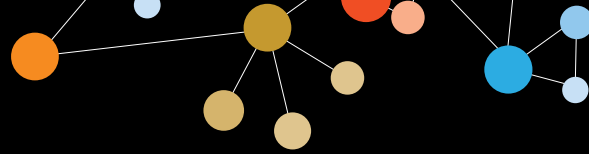
Among 8 antibodies tested in combination with AXAL, CD137 and CTLA-4 antibodies were the most effective for tumor growth inhibition, tumor regression, and survival. Consistent with prior reports that CD137 is expressed on natural killer, dendritic, and T cells, and can potentiate antitumor responses by altering the cellular makeup of the TME [1], immunophenotyping revealed increased TILs and CD8/Treg ratio, and decreased levels of highly immunosuppressive CD103-positive Tregs after CD137+AXAL treatment versus treatment with either agent alone. Additionally, increases were observed in PD-L1 expression on tumor cells and PD-1 expression on CD8-positive T cells. Mice with complete tumor regression after CD137+AXAL treatment (n=5) were subsequently rechallenged with TC1 cells. Two mice remained tumor free until study termination (an additional 6–7 weeks); the other 3 had delayed or slower tumor growth versus controls. CTLA-4+AXAL treatment resulted in complete tumor regression in 3 mice evaluated. These mice remained tumor free even after rechallenge.

### Conclusions

AXAL demonstrated strong anticancer activity in this preclinical model of HPV-positive cancer, especially in combination with CD137 and CTLA-4 antibodies. Moreover, these data suggest that addition of anti-PD-1 to anti-CD137+AXAL could be a potent triple combination therapy.

### References

1. Makkouk A, Chester C, Kohrt HE: **Rationale for anti-CD137 cancer immunotherapy.** *Eur J Cancer* 2016, **54**:112-119.



## Combinations: Immunotherapy/Standard of Care

Presenting author underlined; *Primary author in italics*

258

### **Tumor-resident T cells survive and mediate the antitumoral effects in a murine model of cancer therapy with localized ionizing radiation**

Ainhoa Arina<sup>1</sup>, Christian Fernandez<sup>1</sup>, Wenxin Zheng<sup>1</sup>, Michael A Beckett<sup>1</sup>, Helena J Mauceri<sup>1</sup>, Yang-Xin Fu<sup>2</sup>, Ralph R Weichselbaum<sup>1</sup>

<sup>1</sup>The University of Chicago, Chicago, IL, USA

<sup>2</sup>UT Southwestern, Dallas, TX, USA

#### **Background**

A role for T cells in the antitumor effects of radiation therapy is becoming increasingly clear [1]. Since lymphocytes are considered to be very sensitive to ionizing radiation (IR), and IR increases T cell infiltration of tumors, it is usually assumed that the newly infiltrating T cells mediate the therapeutic effects of IR. However, there is no clear data showing the contribution of tumor-resident vs. newly infiltrating T cells to the therapeutic effects of IR.

#### **Methods**

Longitudinal *in vivo* imaging of tumors using window chambers was performed as described [2]. “T cell reporter” mice were obtained by crossing CD4-Cre or Lck-cre mice with R26-stop-EYFP mice (Jackson).

#### **Results**

Panc02SIYCerulean cancer cells were injected s.c. into EYFP<sup>+</sup> T cell reporter mice bearing dorsal window chambers. When tumors were established (around day 21), mice received 800 cGy of whole-body irradiation (WBI) while their tumor was shielded. This procedure depleted most peripheral T cells while preserving tumor-resident EYFP<sup>+</sup> T cells. Following bone-marrow reconstitution with DsRed<sup>+</sup>Rag<sup>-/-</sup> cells, EGFP<sup>+</sup> 2C CD8<sup>+</sup> T cells specific for the SIY antigen were adoptively transferred, to distinguish newly infiltrating T cells. 3-4 days after 2C transfer, some mice received local IR as follows. 2 experiments using (i) 5 doses of 1.8 Gy each, 24 hours apart (fractionated IR model), and (ii) a single dose of 20 Gy (SBRT model) showed that a significant proportion of tumor-resident EYFP<sup>+</sup> T cells were still detected in the tumor and kept their motility even after 20 Gy of IR, for up to 2 weeks. 2C-EGFP<sup>+</sup> T cells infiltrated IR-treated tumors with some delay, but eventually reached high numbers in IR-treated and untreated tumors. Treating MC38 tumor-bearing mice with increasing doses of WBI (1-10 Gy) showed that tumor-resident T cells were more resistant to IR than circulating T cells. Experiments treating MC38-bearing animals with 20 Gy local IR and systemic sphingosine 1-phosphate receptor agonist FTY720, suggest that tumor-resident T cells might suffice for the antitumoral effects of single high-dose IR.

#### **Conclusions**

Tumor-resident T cells show preferential survival to IR compared to circulating T cells and can contribute to the therapeutic effects of radiotherapy.

#### **References**

1. Burnette B, Fu YX, Weichselbaum RR: **The confluence of radiotherapy and immunotherapy.** *Front Oncol* 2012, **2**:143.
2. Schietinger A, Arina A, *et al*: **Longitudinal confocal microscopy imaging of solid tumor destruction following adoptive T cell transfer.** *Oncoimmunology* 2013, **2**:e26677.

259

### **Multi-kinase inhibitors for the treatment of mRCC: implications for combined therapy with AGS-003, an autologous dendritic cell immunotherapy**

Mark DeBenedette, Whitney Lewis, Alicia Gamble, Charles Nicolette

Argos Therapeutics, Durham, NC, USA

#### **Background**

AGS-003, is an autologous dendritic cell (DC) immunotherapy consisting of matured DCs co-electroporated with amplified autologous tumor RNA and CD40L RNA. AGS-003, is being evaluated in the pivotal ADAPT phase III clinical trial for the treatment of metastatic renal cell carcinoma (mRCC) in combination with standard-of-care, based on a phase II clinical trial suggesting that response combination of sunitinib+AGS-003 was greater than sunitinib alone. The standard-of-care tyrosine kinase inhibitors including sunitinib, sorafenib, axitinib, pazopanib, cabozantinib and tivozanib, and the mTOR inhibitors, everolimus and temsirolimus, are anti-angiogenic therapeutics targeting signaling pathways implicated in the progression of RCC. However, these same signaling pathways are essential for the activation of antigen-specific T cell responses. Combining kinase inhibitor therapy with an active immunotherapeutic, such as AGS-003, may be ineffective, if kinase inhibitor therapy impedes the induction of CTL responses *in vivo*, which is the proposed mechanism of action (MOA) of AGS-003. Therefore, it was of interest to test these combinations *in vitro* with DCs representative of AGS-003 to observe the effects of combination therapy on antigen-specific CTL proliferation and CTL functional responses.

#### **Methods**

DCs derived from normal donor monocytes were co-electroporated with MART-1 RNA and CD40L RNA to represent AGS-003 DC products. *In vitro* co-cultures were set up with autologous CD8<sup>+</sup> T cells and MART-1/CD40L-DCs in the presence of various concentrations of the kinase inhibitors. Kinase inhibitor concentrations were chosen to



## Combinations: Immunotherapy/Standard of Care

*Presenting author underlined; Primary author in italics*

represent steady-state concentrations reported in patients receiving active therapy. Subsequent expansion of MART-1 specific CTLs and multi-functional responses were mapped using multi-color flow cytometry.

### Results

Our *in vitro* analysis demonstrated that sunitinib, axitinib, cabozantinib, tivozanib, everolimus and temsirolimus did not impact the priming nor proliferation of MART-1-specific CTL responses. Furthermore, these kinase inhibitors did not impact multi-functionality of CD28<sup>+</sup>/CD45RA<sup>+</sup> effector/memory CTL. However, sorafenib, when present in the CTL/DC co-cultures, did significantly impair anti-MART-1-specific CTL expansion and CTL multi-functionality.

### Conclusions

Autologous DCs co-electroporated with MART-1 RNA/CD40L RNA exhibit a similar MOA *in vitro* to AGS-003 administered *in vivo*, whereby both DC preparations induce antigen-specific multi-functional CTLs. Understanding the MOA of AGS-003 *in vitro*, allows for the testing of a broad range of potential combination therapies to provide feasibility data to support clinical trials of combination therapy for mRCC. Data provided show that most, but not all, kinase inhibitors are compatible with the MOA of AGS-003, the induction of effector/memory CTL responses, and that each therapeutic agent warrants testing.

### Trial Registration

ClinicalTrials.gov identifier NCT01582672.

260

### Multiple tumor antigen-activated T cell therapy elicits individual and dynamic T cell responses in patients with hepatocellular carcinoma

Yanyan Han<sup>1</sup>, Yeting Wu<sup>2</sup>, Chou Yang<sup>2</sup>, Jing Huang<sup>2</sup>, Dongyun Wu<sup>3</sup>, Jin Li<sup>3</sup>, Xiaoling Liang<sup>1</sup>, Xiangjun Zhou<sup>3</sup>, Jinlin Hou<sup>2</sup>

<sup>1</sup>R&D Department, HRYZ Biotech Co., Shenzhen, Guangdong, People's Republic of China

<sup>2</sup>Department of Infectious Diseases and Hepatology Unit, Nanfang Hospital, Guangzhou, Guangdong, People's Republic of China

<sup>3</sup>HRYZ Biotech Co., Shenzhen, Guangdong, People's Republic of China

### Background

We have previously reported that the immunotherapy with multiple tumor antigens activated autologous T cells (MASCT) was a safe treatment, which may improve the immunologic function and clinical outcome of the patients with hepatocellular carcinoma (HCC). In this study, we investigated the dynamics of MASCT-induced immune responses and

demonstrated the mechanism and advantages of using multiple tumor antigens.

### Methods

13 patients with stage B stage (BCLC) were treated with MASCT for three courses after tumor resection. During each course, the patients received two subcutaneous injections of mature dendritic cells (mDCs) pulsed with a peptide pool of multiple tumor antigens, and three i.v. injections of autologous T cells activated by mDCs described above. Each course lasted 14-15 weeks.

### Results

After repeated treatment of MASCT, the frequency of regulatory T cells in the patients' PBMCs was significantly decreased, while antigen peptide pool-triggered T cell proliferation and IFN $\gamma$ -production were significantly enhanced in the patients' PBMCs. Moreover, the specific immune responses of T cells against each kind of tumor antigen peptide in the pool were also measured by IFN $\gamma$  ELISPOT assay. These specific immune responses could be detected in 11 out of 13 patients' PBMCs but with individual and dynamic patterns during the treatments of MASCT. After 1 course of treatment, the best patient has specific immune responses against 9 tumor antigens out of 14 in the pool, and the worst patient has responses against 2 tumor antigens. These numbers have increased to 11 and 3 after the second course. The most immunogenic tumor antigens are survivin (7/13), cyclin D1 (CCND1, 6/13), carcinoembryonic antigen (CEA, 5/13), and HBV DNA polymerase (5/13). There were 7 patients left without progression 1 year after the immunotherapy initiation. And, the specific immune responses detected in these patients' PBMCs were significantly stronger than that in the patients with progression.

### Conclusions

Our study demonstrates that individual and dynamic tumor antigen-specific T cell responses can be induced in HCC patients after repeated treatments of MASCT, providing evidence to show the advantage of using multiple tumor antigens in immunotherapy instead of single antigen. In addition, these specific immune responses may correlate with the clinical outcomes.





## Combinations: Immunotherapy/Standard of Care

Presenting author underlined; Primary author in italics

261

### **Live, attenuated, double-deleted *Listeria monocytogenes* expressing mesothelin (CRS-207) with immunomodulatory doses of cyclophosphamide, combined with chemotherapy as treatment for malignant pleural mesothelioma (MPM)**

Raffit Hassan<sup>1</sup>, Thierry Jahan<sup>2</sup>, Scott J Antonia<sup>3</sup>, Hedy L Kindler<sup>4</sup>, Evan W Alley<sup>5</sup>, Somayah Honarmand<sup>6</sup>, Weiqun Liu<sup>6</sup>, Meredith L Leong<sup>6</sup>, Chan C Whiting<sup>6</sup>, Nitya Nair<sup>6</sup>, Amanda Enstrom<sup>6</sup>, Edward E Lemmens<sup>6</sup>, Takahiro Tsujikawa<sup>7</sup>, Sushil Kumar<sup>7</sup>, Lisa M Coussens<sup>7</sup>, Aimee L Murphy<sup>6</sup>, Dirk G Brockstedt<sup>6</sup>

<sup>1</sup>Thoracic and GI Oncology Branch, National Cancer Institute, Bethesda, MD, USA

<sup>2</sup>Department of Medicine, Division of Hematology Oncology, UCSF, San Francisco, CA, USA

<sup>3</sup>H. Lee Moffitt Cancer Center, Tampa, FL, USA

<sup>4</sup>Gastrointestinal Oncology and Mesothelioma Programs, Section of Hematology/Oncology, University of Chicago, Chicago, IL, USA

<sup>5</sup>Penn Prebyterian Medical Center, University of Pennsylvania, Philadelphia, PA, USA

<sup>6</sup>Aduro Biotech, Inc., Berkeley, CA, USA

<sup>7</sup>Oregon Health & Science University, Portland, OR, USA

#### **Background**

CRS-207 is live, attenuated, double-deleted *Listeria monocytogenes* (LADD) engineered to express mesothelin, a tumor-associated antigen over-expressed in several cancers, including MPM, an aggressive treatment-refractory disease with poor prognosis. CRS-207 activates innate and adaptive immunity and may act synergistically with chemotherapy to increase the susceptibility of the tumor microenvironment to immune-mediated killing. CRS-207 in combination with standard of care (SOC) pemetrexed/cisplatin demonstrated clinical activity in a phase Ib study. Low-dose cyclophosphamide (Cy) has been shown to decrease regulatory T cells and enhance vaccine-induced responses. Preclinical data demonstrate CRS-207 with low-dose Cy improves survival in a murine lung metastasis model.

#### **Methods**

60 patients were enrolled into 2 cohorts in this phase Ib study. Eligibility required unresectable, untreated MPM, ECOG 0 or 1, and adequate organ function. Patients in Cohort 1 received 2 CRS-207 2 weeks apart, 6 cycles pemetrexed/cisplatin 3 weeks apart, followed by 2 CRS-207 3 weeks apart. Clinically stable patients continued CRS-207 every 8 weeks. Patients in Cohort 2 received Cy (200 mg/m<sup>2</sup>) 1 day prior to each CRS-207. Safety, immunogenicity, tumor responses, survival and tumor markers were assessed.

#### **Results**

22 patients were enrolled into the Cy/CRS-207 cohort of this study; 77% male, median age 70. The most common Cy/CRS-207 related adverse events (AEs) were grades 1/2 fever, chills, hypotension and nausea/vomiting, with no treatment-related serious AEs or deaths. As of August 2016, of 22 evaluable patients receiving Cy/CRS-207 + chemotherapy, 86% (19/22) had disease control with 11 (50%) whose best overall response was partial response (PR) and 8 (36%) had stable disease. Tumor shrinkage was observed in 8/22 (36%) patients including 3 PR after 2 doses of Cy/CRS-207 prior to chemotherapy initiation. Comprehensive immune profiling including multidimensional immunohistochemistry (IHC) analyses will be presented.

#### **Conclusions**

Addition of immune-modulating doses of Cy to a regimen of CRS-207 and SOC chemotherapy appears to be well-tolerated with no increase in toxicity compared to those receiving CRS-207 alone with chemotherapy. Preliminary results show signs of tumor activity following 2 doses of Cy/CRS-207 prior to chemotherapy (36% tumor shrinkage) and the combination with chemotherapy resulted in 86% disease control and 50% response rate compared to published response rates of 20-41% with chemotherapy alone. Immune analyses and further follow-up are warranted to evaluate the Cy/CRS-207 + chemotherapy regimen as a treatment for MPM.

#### **Trial Registration**

ClinicalTrials.gov identifier NCT01675765.

## Combinations: Immunotherapy/Standard of Care

Presenting author underlined; Primary author in italics

262

### **Phase Ib trial of RActive® cancer vaccine BI1361849 (CV9202) and local radiotherapy in stage IV non-small cell lung cancer (NSCLC) patients with disease control after 1st-line therapy: updated clinical results and immune responses**

Sven D Koch<sup>1</sup>, Martin Sebastian<sup>2</sup>, Christian Weiss<sup>3</sup>, Martin Früh<sup>4</sup>, Miklos Pless<sup>5</sup>, Richard Cathomas<sup>6</sup>, Wolfgang Hilbe<sup>7</sup>, Georg Pall<sup>8</sup>, Thomas Wehler<sup>9</sup>, Jürgen Alt<sup>9</sup>, Helge Bischoff<sup>10</sup>, Michael Geissler<sup>11</sup>, Frank Griesinger<sup>12</sup>, Jens Kollmeier<sup>13</sup>, Alexandros Papachristofilou<sup>14</sup>, Fatma Doener<sup>1</sup>, Mariola Fotin-Mleczek<sup>1</sup>, Madeleine Hipp<sup>1</sup>, Henoch S Hong<sup>1</sup>, Karl-Josef Kallen<sup>1</sup>, Ute Klinkhardt<sup>15</sup>, Claudia Stosnach<sup>15</sup>, Birgit Scheel<sup>1</sup>, Andreas Schroeder<sup>15</sup>, Tobias Seibel<sup>15</sup>, Ulrike Gnad-Vogt<sup>15</sup>, Alfred Zippelius<sup>14</sup>

<sup>1</sup>CureVac AG, Tübingen, Baden-Württemberg, Germany

<sup>2</sup>University Hospital Frankfurt, Medical Clinic II, Goethe University, Frankfurt, Hessen, Germany

<sup>3</sup>Klinikum Darmstadt GmbH, Darmstadt, Hessen, Germany

<sup>4</sup>Kantonsspital St. Gallen, St. Gallen, Switzerland

<sup>5</sup>Kantonsspital Winterthur, Winterthur, Zurich, Switzerland

<sup>6</sup>Kantonsspital Graubünden, Chur, Graubünden, Switzerland

<sup>7</sup>Wilhelminenspital Wien, Wien, Austria

<sup>8</sup>Fachkliniken Wangen, Wangen (Allgäu), Baden-Württemberg, Germany

<sup>9</sup>J. Gutenberg University Hospital Mainz, Mainz, Rheinland-Pfalz, Germany

<sup>10</sup>Thoraxklinik Heidelberg gGmbH, Heidelberg, Baden-Württemberg, Germany

<sup>11</sup>Klinikum Esslingen GmbH, Esslingen, Baden-Württemberg, Germany

<sup>12</sup>Pius Hospital Oldenburg, Oldenburg, Niedersachsen, Germany

<sup>13</sup>Heckeshorn Lung Clinic, Berlin, Germany

<sup>14</sup>University Hospital Basel, Basel-Stadt, Switzerland

<sup>15</sup>CureVac AG, Frankfurt am Main, Hessen, Germany

#### **Background**

Preclinical studies demonstrated that local radiotherapy (RT) acts synergistically with RActive® mRNA vaccines to enhance anti-tumor effects and increase tumor-infiltrating lymphocytes. BI1361849 is a therapeutic vaccine comprising optimized mRNA constituents encoding six NSCLC-associated antigens. Interim data of a phase Ib study, employing local RT to increase the immune mediated tumor control by BI1361849, have been previously published [1]. Here we report results of immune response analyses as well as updated safety and efficacy data.

#### **Methods**

26 patients (pts) with stage IV NSCLC were enrolled in three cohorts based on histological and molecular NSCLC subtypes (squamous and non-squamous cell with/without activating EGFR mutations). Pts received two vaccinations with BI1361849 before local RT to a single tumor lesion was administered in four consecutive daily fractions of 5 GY. Vaccination was continued until start of subsequent anti-cancer therapy. Maintenance pemetrexed (mP) and EGFR-TKIs were allowed where indicated. Cellular and humoral immune responses were measured *ex vivo* by multifunctional intracellular cytokine staining, IFN-g ELISpot, and ELISA in pre- and post-treatment blood samples. The induction of humoral immune responses against 27 lung cancer antigens not encoded by the vaccine was measured by antibody array.

#### **Results**

26 pts were enrolled. 15 pts received mP, two received EGFR TKIs. Most frequent AEs were mild to moderate injection-site reactions and flu-like symptoms. No BI1361849-related SAEs were reported. Based on preliminary data following up to 110 weeks of exposure, one confirmed PR was observed in a pt on mP, 13 pts (52%) experienced SD (8 pts on mP, 2 pts on EGFR-TKI and 3 pts without concomitant maintenance treatment, associated with 15% tumor shrinkage outside the radiation field in one of them). 25 pts were available for immune response analysis. Preliminary data indicate that BI1361849 was capable of eliciting antigen-specific immune responses in of the majority of the patients including cellular and humoral immune responses. Moreover all encoded antigens were immunogenic and responses against multiple antigens were observed. Treatment induced immune responses against other lung cancer antigens were detected in several patients.

#### **Conclusions**

BI1361849 can be safely combined with local RT and mP treatment. Shrinkage of non-irradiated lesions and prolonged disease stabilization was observed in a subset of pts, mainly in combination with mP. Data indicate immunogenicity of BI1361849. Analyses of cellular and humoral immune responses will be updated, as well as updated clinical data.

#### **References**

1. *J Clin Oncol* 2016, **34**(supl):Abstr e20627.



## Combinations: Immunotherapy/Standard of Care

Presenting author underlined; *Primary author in italics*

263

### **Overcoming resistance to tyrosine kinase inhibitor by natural killer (NK) cells in non-small cell lung cancer (NSCLC) cells**

Ha-Ram Park<sup>1</sup>, Yong-Oon Ahn<sup>1</sup>, Tae Min Kim<sup>2</sup>, Soyeon Kim<sup>1</sup>, Seulki Kim<sup>1</sup>, Yu Soo Lee<sup>1</sup>, Bhumsuk Keam<sup>2</sup>, Dong-Wan Kim<sup>2</sup>, Dae Seog Heo<sup>2</sup>

<sup>1</sup>SNU Cancer Research Institute, Seoul, Republic of Korea

<sup>2</sup>Seoul National University Hospital, SNU Cancer Research Institute, Seoul, Republic of Korea

#### **Background**

Receptor tyrosine kinase signals are altered in NSCLC and tyrosine kinase inhibitors (TKIs) have been used to treat NSCLC harboring driver mutations (e.g. ALK fusion and EGFR). Although TKIs are sensitive to NSCLC with driver mutations, acquired resistance to TKIs is inevitable by various mechanisms including gatekeeper mutation and alternative pathway activation. Considering immunotherapy is one of the main strategies that override drug resistance and cancer stemness, we evaluated an immunologic strategy to overcome acquired resistance to TKIs using NK cells in NSCLC.

#### **Methods**

TKI-resistant NSCLC cell lines (H3122CR1, H3122LR1, H3122CR1LR1, EBC-R1, EBC-R2, PC-9GR, and PC-9ER) were established from NCI-H3122 (*EML4-ALK* fusion), EBC-1 (*MET* amplification), and PC-9 (*EGFR* exon 19 deletion) after continuous exposure to crizotinib, ceritinib, capmatinib, gefitinib, and erlotinib. NK cytotoxicity and antibody-dependent cell-mediated cytotoxicity (ADCC) using anti-EGFR monoclonal antibody (mAb) cetuximab were measured using 'off-the-shelf' NK92-CD16 cell line as effectors and detected by <sup>51</sup>chromium-release assay. Expression of the ligands for NK cell receptors and total EGFR were analyzed by flow cytometry.

#### **Results**

Most of TKI-resistant NSCLC cell lines were more susceptible to NK92-CD16 cells compared with their parental cell lines. The percentage of cytotoxicity was determined to be 0.2% in H3122 and 13.4%, 30.2% and 39.1% in TKI-resistant H3122 group with an effector:target ratio of 30:1. (PC-9: 18.2% vs. 38.8% vs. 24.8%). The expression of ICAM-1, which is a ligand for LFA-1 in NK cells, is higher in TKI-resistant NSCLC cells than in parental cells. When we blocked ICAM1-CD11a interaction during a cytotoxic assay, the cytotoxicity was decreased about 10%. Cetuximab-mediated ADCC was higher in resistant cells due to the increased expression level of total EGFR in resistant cells.

#### **Conclusions**

TKI-resistant NSCLC cells are more sensitive to NK92 cell-mediated cytotoxicity that is partially dependent on up-regulation of ICAM-1 via an immunological synapse. In addition, cetuximab, an EGFR-targeting mAb, significantly increases NK cell cytotoxicity in TKI-resistant NSCLC cells. Taken together, NK-cell based immunotherapy with cetuximab might be feasible to treat NSCLC patients with acquired resistance to TKIs.

264

### **Intralesional injection with Rose Bengal and systemic chemotherapy induces anti-tumor immunity in a murine model of pancreatic cancer**

Shari Pilon-Thomas, Amy Weber, Jennifer Morse, Krithika Kodumudi, Hao Liu, John Mullinax, *Amod A Sarnaik*

H. Lee Moffitt Cancer Center, Tampa, FL, USA

#### **Background**

Rose Bengal is a xanthene dye that has been utilized for liver function studies and is currently used topically in ophthalmology. Intralesional (IL) Rose Bengal (PV-10) has been shown in murine models and melanoma clinical trials to induce regression of treated melanoma lesions and uninjected bystander lesions. This study was undertaken to measure whether IL PV-10 can induce systemic anti-tumor effects alone or in combination with gemcitabine (Gem) therapy in a murine model of pancreatic cancer.

#### **Methods**

C57BL/6 mice received Panc02 pancreatic tumor cells subcutaneously (SC) on one flank to establish a single tumor. On day 7, tumor was treated with IL PV-10. Control mice received IL phosphate buffered saline (PBS). Tumor growth was measured. Splenic T cells were collected and co-cultured with Panc02 or irrelevant B16 cells. Supernatants were collected to measure Panc02-specific T cell responses by IFN-gamma ELISA. To measure the effect of IL PV-10 on the growth of an untreated, bystander tumor, mice received Panc02 cells in bilateral flanks. The resulting right tumor was injected IL with PV-10 or PBS. Tumor sizes were measured for both the right (treated) and left (untreated/bystander) tumors. To determine the efficacy of combination therapy with IL PV-10 and systemic Gem, mice bearing a single or bilateral Panc02 tumors were treated with PV-10 alone or in combination with Gem. Mice received 60 mg/kg Gem intraperitoneally (IP) twice per week.

#### **Results**

C57BL/6 mice bearing Panc02 tumors treated with IL PV-10 had significantly smaller tumors than mice treated with PBS ( $p < 0.001$ ). A significant increase in the IFN-gamma production in response to Panc02 was measured in the

## Combinations: Immunotherapy/Standard of Care

Presenting author underlined; Primary author in italics

splenocytes of mice treated with PV-10 as compared to mice treated with PBS ( $p < 0.05$ ). Mice with bilateral tumors had a significant regression of tumors injected IL with PV-10 and there was a reduction in the untreated (bystander) flank Panc02 tumor ( $p < 0.01$ ). Gem therapy in combination with IL PV-10 injection led to enhanced tumor regression ( $p < 0.05$ ) compared to IL PV-10 or Gem alone in both a single tumor model and a bilateral tumor model.

### Conclusions

Regression of untreated pancreatic tumors by IL injection of PV-10 in concomitant tumor supports the induction of a systemic anti-tumor response. Addition of Gem chemotherapy enhances the effects of IL PV-10 therapy. Given that patients with metastatic pancreatic cancer have a dismal prognosis, combination therapy of IL PV-10 combined with Gem may benefit patients with metastatic pancreatic cancer.

### 265 Abstract Travel Award Recipient

#### Multi-institution evaluation of outcomes following radiation and PD-1 inhibition

Luke Pike<sup>1</sup>, Andrew Bang<sup>2</sup>, Patrick A. Ott<sup>3</sup>, Tracy Balboni<sup>1</sup>, Allison Taylor<sup>1</sup>, Alexander Spektor<sup>1</sup>, Tyler Wilhite<sup>1</sup>, Monica Krishnan<sup>1</sup>, Daniel Cagney<sup>1</sup>, Brian Alexander<sup>1</sup>, Ayal Aizer<sup>1</sup>, Elizabeth Buchbinder<sup>1</sup>, Mark Awad<sup>1</sup>, Leena Ghandi<sup>1</sup>, F Stephen Hodi<sup>3</sup>, Jonathan Schoenfeld<sup>1</sup>

<sup>1</sup>Brigham and Women's / Dana-Farber Cancer Center, Harvard University, Boston, MA, USA

<sup>2</sup>Harvard Radiation Oncology Program, Boston, MA, USA

<sup>3</sup>Dana-Farber Cancer Institute, Harvard University, Boston, MA, USA

### Background

Preclinical models suggest radiation may synergize with immunotherapy; for instance, increased responses and prolonged survival have been observed in mice treated with radiation and either PD-1 inhibition or combined CTLA-4/PD-1 blockade. We previously observed that radiation was associated with favorable responses in melanoma patients treated with ipilimumab [1]. However, clinical data are lacking in regards to combining radiation with PD-1 inhibitors with or without CTLA-4 blockade.

### Methods

We conducted an IRB-approved retrospective multi-institution analysis of patients with metastatic melanoma, non-small cell lung cancer (NSCLC), and renal cell carcinoma (RCC) treated at 6 centers with palliative radiation and PD-1 inhibitors, either before, after, or concurrent with radiation.

### Results

137 patients (NSCLC, n=79; melanoma, n=48; RCC, n=10) received 279 courses of radiation (median 2, range 1-6) and

a median of 4 PD-1 inhibitor cycles (range 1-66). Sixteen patients received concurrent PD-1/CTLA-4 blockade. Sites irradiated included the brain (n=144), spine (n=40), lungs (n=38), pelvis (n=20), and other (n=32); these sites, and the use of WBRT/SRS were balanced before versus after the start of PD-1 therapy. Median survival following start of anti-PD-1 therapy was 192, 394, and 121 days in patients with NSCLC, melanoma, and RCC, respectively. On multivariate analyses adjusting for histology, targetable mutations and concurrent PD-1/CTLA-4 inhibition, there was a significant association between radiation administered following the start of PD-1 directed treatment and improved survival (HR 0.59,  $p=0.02$ ). There was a significant interaction between the impact of concurrent PD-1/CTLA-4 checkpoint blockade and subsequent radiation on survival ( $p=0.03$  for interaction, HR for radiation = 0.28). One-year survival was 71% in patients treated with radiation following PD-1/CTLA-4 blockade, and 4/8 of these patients continued to receive PD-1 therapy after radiation. In all patients, median survival from first course of brain-directed radiation was 634 days.

### Conclusions

In this multi-institution retrospective analysis, targeted radiotherapy administered following PD-1 blockade was associated with increased survival. Although this finding is retrospective and therefore subject to bias, particularly striking is survival observed following brain-directed radiation and in patients treated with concurrent CTLA-4/PD-1 blockade. These data suggest select use of radiation in patients treated with anti-PD-1 therapy may allow for continuation of effective systemic immunotherapy that could augment long-term survival.

### References

1. Chandra RA, Wilhite TJ, Balboni TA, *et al*: **A systematic evaluation of abscopal responses following radiotherapy in patients with metastatic melanoma treated with ipilimumab.** *Oncoimmunology* 2015, **4(11)**:e1046028.

### 266

#### Combined blockade of CTLA-4 and CD47 with tumor irradiation extends survival in melanoma

Anthony L Schwartz<sup>1</sup>, Pulak R Nath<sup>1</sup>, Elizabeth Lessey-Morillon<sup>1</sup>, Lisa Ridnour<sup>2</sup>, David D Roberts<sup>3</sup>

<sup>1</sup>National Cancer Institute, Bethesda, MD, USA

<sup>2</sup>National Cancer Institute, Frederick, MD, USA

<sup>3</sup>Department of Pathology, National Cancer Institute, Bethesda, MD, USA

### Background

Irradiation (IR) combined with chemotherapy is the post-surgical standard of care treatment for melanoma, but metastasis still results in high mortality rates. Recently,



## Combinations: Immunotherapy/Standard of Care

Presenting author underlined; Primary author in italics

immune checkpoint inhibitors such as antibodies targeting cytotoxic T lymphocyte antigen-4 (CTLA-4) have proven effective for immunotherapy of melanoma. CTLA-4 is up-regulated post-T cell activation, and antibody blockade enhances tumor responses in immunocompetent rodents and humans. Ongoing trials suggest that combinations of immune checkpoint inhibitors are more efficacious than single agents, but tumors in many patients remain resistant. Our laboratory is investigating CD47 blockade for the treatment of cancer in several immune competent mouse models. CD47 expression is frequently elevated in cancers and serves as an inhibitory receptor for thrombospondin-1 on immune cells in the tumor stroma. CD47 blockade on CD8+ T cells or tumor cells significantly enhances immune-targeted tumor cell killing post-irradiation compared to irradiation alone. Here we explore the potential for CD47 blockade to improve the response rates to anti-CTLA-4 therapy alone or in combination with irradiation using a syngeneic mouse melanoma model.

### Methods

C57BL/6 mice were inoculated with  $1 \times 10^6$  B16F10 melanoma cells into the right hind limb and treated with local 10Gy irradiation combined with CTLA-4 blocking antibody, CD47 translational blocking morpholino, or the combination of CTLA-4 antibody and CD47 morpholino. Subjects were humanely euthanized, and tumors were analyzed using qPCR to evaluate granzyme B and FOXP3 mRNA expression. Tumors were sectioned and subjected to H&E and anti-CD8 staining.

### Results

In non-irradiated tumors, histology revealed minimal tumor necrosis, while all irradiated groups showed increased necrosis. Tumor IR in combination with CTLA-4 or CD47 increased immune cell infiltration. However, the combination of irradiation with CTLA-4 and CD47 showed widespread tumor necrosis encompassing the entire field. All groups treated with the CD47 morpholino also exhibited focal hemorrhage, which was more extensive when combined with CTLA-4. FOXP3 mRNA expression showed a two-fold increase in CD47/CTLA-4-treated mice, which further increased to 4-fold when administered with IR. Granzyme B mRNA expression increased 3.5 fold with the CTLA-4/CD47/IR combination. Overall survival in IR/CTLA-4 was ~50% while the combination of IR/CTLA-4/CD47 blockade was 75% at 50 days.

### Conclusions

The results described herein suggest that IR in combination with CTLA-4 and CD47 checkpoint blockade can provide a survival benefit by activating beneficial adaptive immune signaling pathways.

267

### Assessing the potential for enhanced antibody-dependent cell-mediated cytotoxicity (ADCC) by combining the CD137 antibody urelumab with rituximab or cetuximab in patients with refractory lymphoma or select advanced solid tumors

*Neil H Segal<sup>1</sup>*, Manish Sharma<sup>2</sup>, Dung T Le<sup>3</sup>, Patrick A Ott<sup>4</sup>, Robert L Ferris<sup>5</sup>, Andrew D Zelenetz<sup>1</sup>, Sattva S Neelapu<sup>6</sup>, Ronald Levy<sup>7</sup>, Izidore S Lossos<sup>8</sup>, Caron Jacobson<sup>4</sup>, Radhakrishnan Ramchandren<sup>9</sup>, John Godwin<sup>10</sup>, A Dimitrios Colevas<sup>7</sup>, Roland Meier<sup>11</sup>, Suba Krishnan<sup>11</sup>, Xuemin Gu<sup>11</sup>, Jaclyn Neely<sup>11</sup>, Satyendra Suryawanshi<sup>11</sup>, John Timmerman<sup>12</sup>

<sup>1</sup>Memorial Sloan Kettering Cancer Center, New York, NY, USA

<sup>2</sup>University of Chicago Medicine, Chicago, IL, USA

<sup>3</sup>Sidney Kimmel Comprehensive Cancer Center at Johns Hopkins University, Baltimore, MD, USA

<sup>4</sup>Dana-Farber Cancer Institute, Boston, MA, USA

<sup>5</sup>University of Pittsburgh, Pittsburgh, PA, USA

<sup>6</sup>University of Texas MD Anderson Cancer Center, Houston, TX, USA

<sup>7</sup>Stanford University School of Medicine, Stanford, CA, USA

<sup>8</sup>University of Miami Miller School of Medicine, Sylvester Comprehensive Cancer Center, Miami, FL, USA

<sup>9</sup>Karmanos Cancer Institute, Detroit, MI, USA

<sup>10</sup>Earle A. Childs Research Institute, Providence Cancer Center, Portland, OR, USA

<sup>11</sup>Bristol-Myers Squibb, Princeton, NJ, USA

<sup>12</sup>UCLA Medical Center, Los Angeles, CA, USA

### Background

Urelumab, a fully human CD137 agonistic monoclonal antibody (mAb) with single-agent pharmacodynamic and clinical activity in patients with lymphoma, has potential to enhance cytotoxic activity of natural killer (NK) cells when combined with antibody-based targeted therapies. The potential of urelumab to enhance ADCC/phagocytosis and thus improve efficacy was evaluated in phase Ib studies of urelumab combined with rituximab (anti-CD20 mAb) in patients with refractory B cell non-Hodgkin lymphoma or cetuximab (anti-EGFR mAb) in patients with refractory colorectal cancer (CRC) or squamous cell carcinoma of the head and neck. Here we report safety/tolerability, pharmacokinetics, pharmacodynamics, and preliminary clinical efficacy results from these trials.

### Methods

During escalation in NCT01775631, patients with relapsed/refractory B-NHL received urelumab at 0.1 or 0.3 mg/kg or a flat dose of 8 mg (equivalent to 0.1 mg/kg in an 80-kg patient; initiated based on available pharmacokinetic and safety data) Q3W plus rituximab 375 mg/m<sup>2</sup> QW (4 doses);



## Combinations: Immunotherapy/Standard of Care

Presenting author underlined; Primary author in italics

during expansion, patients with relapsed/refractory diffuse large B cell lymphoma (DLBCL) or follicular lymphoma (FL) were treated with urelumab 8 mg plus rituximab. The NCT02110082 study evaluated urelumab (0.1 mg/kg or 8 mg Q3W) plus cetuximab (400 mg/m<sup>2</sup> on week 1 and 250 mg/m<sup>2</sup> Q1W thereafter) in patients with metastatic CRC or SCCHN. Primary endpoints were safety/tolerability.

### Results

Treated patients included those with DLBCL (n=29), FL (n=17), CRC (n=47), and SCCHN (n=19). Overall, 2–3% of patients discontinued due to treatment-related AEs, and one patient experienced a grade 3/4 ALT elevation (Table 1). One patient who received urelumab plus rituximab experienced treatment-related sepsis and died. Apparent increases in IFN $\gamma$ -induced cytokines were observed, and activated/proliferating CD8+ cells and cytotoxic NK cells appeared to increase in the periphery after 1 week of treatment with either regimen; however, in most tumors, the increase in CD8+ and NK cells was not observed. Overall response rates (ORRs) with urelumab plus rituximab were 10% (3/29) in DLBCL and 35% (6/17) in FL (Table 2). There were no confirmed responses with urelumab plus cetuximab in patients with CRC or SCCHN.

### Conclusions

Urelumab is safe and well tolerated in combination with rituximab or cetuximab at doses of 0.1 mg/kg or 8 mg, with minimal evidence of liver toxicity. Although pharmacodynamic activity was observed in peripheral blood samples, urelumab with rituximab or cetuximab did not demonstrate substantial enhancement of clinical responses or lead to intratumoral immune modulation in these tumor settings.

### Trial Registration

ClinicalTrials.gov identifier NCT01775631 and NCT02110082.

**Table 1. Treatment-related safety events**

	Urelumab + rituximab N=46				Urelumab + cetuximab N=66		
	0.1 mg/kg n=17	0.3 mg/kg n=6	8 mg n=23	Total N=46	0.1 mg/kg n=3	8 mg n=63	Total N=66
Treatment-related AEs	13 (76)	4 (67)	16 (70)	33 (72)	1 (300)	56 (89)	59 (89)
Treatment-related grade 3/4 ALT elevation	0	0	1 (4)	1 (2)	0	0	0
Treatment-related serious AEs	0	1 (17) <sup>a</sup>	1 (4)	2 (4)	0	2 (3)	2 (3)
Treatment-related AEs leading to discontinuation	0	1 (17) <sup>a</sup>	0	1 (2)	0	2 (3)	2 (3)
Treatment-related deaths	0	1 (17) <sup>a</sup>	0	1 (2)	0	0	0

AE, adverse event; ALT, alanine aminotransferase.

<sup>a</sup> One patient treated with urelumab 0.3 mg/kg plus rituximab experienced a treatment-related serious AE of sepsis, discontinued therapy at week 4, and died.

**Table 2. Efficacy of urelumab plus rituximab or urelumab plus cetuximab**

Parameter <sup>b</sup>	Urelumab + rituximab N=46 <sup>a</sup>	
	DLBCL n=29	FL n=17
Best overall response, n (%)		
CR	2 (7)	2 (12)
PR	1 (3)	4 (24)
SD	4 (14)	6 (35)
PD	19 (66)	3 (18)
Unable to determine/other	3 (10)	2 (12)
Confirmed ORR, n (%)	3 (10)	6 (35)
Confirmed DCR, n (%)	7 (24)	12 (71)
Parameter <sup>c</sup>	Urelumab + cetuximab N=66 <sup>a</sup>	
	CRC n=47	SCCHN n=19
Best overall response, n (%)		
CR	0	0
PR	0	0
SD	17 (36)	12 (63)
PD	22 (47)	4 (21)
Unable to determine	8 (17)	3 (16)
Confirmed ORR, n (%)	0	0
Confirmed DCR, n (%)	17 (36)	12 (63)

CR, complete response/remission; DCR, disease control rate (CR + PR + SD); ORR, overall response rate (CR + PR); PD, progressive disease; PR, partial response/remission; SD, stable disease.

<sup>a</sup> Includes evaluable patients; <sup>b</sup> Assessed by IWG criteria; <sup>c</sup> Assessed by RECIST v.1.1.

### 268 Abstract Travel Award Recipient

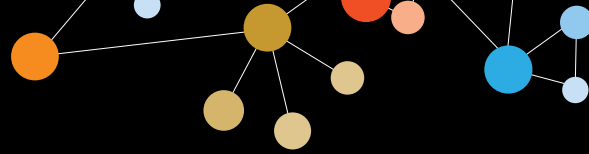
#### ATM is essential for the radiation-induced upregulation of the immunosuppressive cytokine actin-A by breast cancer cells

*Claire I Vanpouille-Box*, Silvia C Formenti, Sandra Demaria

Weill Cornell Medicine, Department of Radiation Oncology, New York, NY, USA

#### Background

Actin A (actA) is a member of the transforming growth factor beta (TGF $\beta$ ) superfamily. Recent evidence suggests that actA may facilitate tumorigenesis in part by suppressing immunity in the tumor microenvironment [1]. Treatment-induced DNA double-strand breaks (DSBs) induce actA mRNA and protein [2]. The ataxia telangiectasia-mutated (ATM) kinase is activated at DNA DSBs caused by genotoxic agents such as radiotherapy (RT) and is critical for DNA repair. Here we tested the hypothesis that induction of actA by RT limits RT-induced activation of anti-tumor immunity.



## Combinations: Immunotherapy/Standard of Care

Presenting author underlined; Primary author in italics

### Methods

To test this hypothesis, 4T1 mammary carcinoma cells were engineered to express a doxycycline (dox) inducible shRNA silencing inhibin A (*Inhba*, gene encoding for actA) (4T1<sup>shInhba</sup>). 4T1<sup>shInhba</sup> or its non-silencing control (4T1<sup>shNS</sup>) were exposed to ionizing radiations to determine *Inhba* gene expression by RT-qPCR as well as secretion of actA by ELISA. To determine if ATM controls the expression of actA, derivatives with inducible knockdown of ATM were also generated (4T1<sup>shATM</sup>). 4T1<sup>shInhba</sup>, 4T1<sup>shATM</sup> and 4T1<sup>shNS</sup> were injected s.c. in syngeneic BALB/c mice on day 0. Knockdown of *ATM* and *Inhba* genes was induced by dox at day 8. Tumors were irradiated with 6 Gy repeated on days 13, 14, 15, 16 and 17. Mice were monitored and euthanized at day 22 and day 28 for evaluation of immune cells infiltration into the tumor.

### Results

RT upregulated actA expression and secretion by 4T1 cells. Secreted actA promoted CD4+ T cells conversion into regulatory T (Tregs) cells. *In vitro*, knockdown of ATM abolished both *Inhba* gene expression and actA secretion by tumor cells after RT. *In vivo*, this resulted in reduced Tregs infiltration in irradiated tumors, and increased activation of intra-tumoral CD8+ T cells. 4T1<sup>shInhba</sup> and 4T1<sup>shATM</sup> tumors showed an increased response to RT compared to 4T1<sup>shNS</sup> tumors.

### Conclusions

These data suggest that ATM plays a critical role in RT-induced actA secretion, which promotes an immunosuppressive environment in the irradiated tumor. Inhibition of ATM may increase tumor radiosensitivity and at the same time enhance *in situ* vaccination by radiation by hindering Treg generation.

### Acknowledgements

Supported by DOD BCRP post-doctoral fellowship W81XWH-13-1-0012.

### References

1. Loomans HA, *et al*: *Cancers (Basel)* 2014.
2. Fordyce C, *et al*: *Cancer Prev Res* 2010.

### 269

#### Adenosine regulates tumor response to radiation by hindering recruitment and activation of CD103+ DCs

Erik Wennerberg<sup>1</sup>, Aranzazu Mediero<sup>2</sup>, Bruce N Cronstein<sup>2</sup>, Silvia C Formenti<sup>3</sup>, Sandra Demaria<sup>3</sup>

<sup>1</sup>Weill Cornell Medical College, New York, NY, USA

<sup>2</sup>New York University Langone Medical Center, New York, NY, USA

<sup>3</sup> Department of Radiation Oncology, Weill Cornell Medicine, New York, NY, USA

### Background

Preclinical data and clinical observations support the concept that localized radiation therapy (RT) can be a powerful adjuvant to immunotherapeutic strategies by triggering *de novo* anti-tumor immune responses to poorly immunogenic tumors. We have previously shown that radiation induces the release of ATP in a dose-dependent manner [1]. ATP enhances recruitment and activation of dendritic cells (DCs), including CD103+ DCs recently identified as the key DC subset responsible for cross-presentation of tumor-derived antigens to CD8+ T cells. To determine whether rapid conversion of ATP to immunosuppressive adenosine could contribute to the limited ability of high dose RT to activate anti-tumor immunity we inhibited the rate-limiting CD73 ectonucleotidase.

### Methods

Wild type (WT) or *BATF3*<sup>-/-</sup> mice (ablated development of CD8a+/CD103+ DCs) were inoculated s.c. with the poorly immunogenic breast cancer cell line TSA on day 0 and assigned to treatment with: (1) control Ab; (2) anti-CD73 (TY/23 Ab); (3) RT (20 Gy); (4) RT + TY/23. TY/23 (200 µg) was administered i.p. on day 11, 14, 17 and 20. RT was given locally to the tumor as single 20 Gy dose on day 12. On day 18, some tumors were harvested for flow cytometry analysis of DCs and T cells. Mice were monitored for tumor progression by caliper measurements.

### Results

In RT-treated mice, blockade of ADO generation by anti-CD73 resulted in increased infiltration of CD103+DCs (8.9±2.6% of DCs in RT+TY/23 v. 3.5±2.8% of DCs in RT) expressing elevated levels of activation markers CD40 and CD86 compared to mice treated with RT alone. This change was associated with improved CD8+T cell/Tregs ratio (5±2.8 in RT+TY/23 v. 0.8±0.2 in RT). Importantly, CD73 blockade had no effect by itself but improved significantly radiation-induced tumor control (tumor volume on day 57 post inoculation: 385±525 mm<sup>3</sup> in RT+TY/23 v. 1036±727 mm<sup>3</sup> in RT). Consistent with the hypothesis that CD103+ DC are essential for anti-tumor

## Combinations: Immunotherapy/Standard of Care

Presenting author underlined; *Primary author in italics*

responses, the therapeutic effect of RT+CD73 blockade was abrogated in BATF3<sup>-/-</sup> mice.

### Conclusions

Our data indicate a key role of adenosine generated in the irradiated tumor in hindering development of anti-tumor immune responses and identify, as a mechanism of this effect, the inhibition of CD103+ DCs. Blockade of adenosine generation is a promising strategy to enhance radiation-induced anti-tumor immunity.

### References

1. Golden EB, Frances D, Pellicciotta I, Demaria S, Helen Barcellos-Hoff M, Formenti SC: **Radiation fosters dose-dependent and chemotherapy-induced immunogenic cell death**. *Oncoimmunology* 2014, **3**:e28518.

## Diet, Exercise and/or Stress and Impact on the Immune System

*Presenting author underlined; Primary author in italics*

270

### **$\beta$ -adrenergic signaling induced by cool housing temperatures mediates immune suppression and impairs the efficacy of anti-PD-1 checkpoint blockade immunotherapy in laboratory mice**

Mark Bucsek, Guanxi Qiao, Cameron MacDonald, Bonnie Hylander, Elizabeth Repasky

Roswell Park Cancer Institute, Buffalo, NY, USA

#### **Background**

Recent work from our laboratory has shown that anti-tumor immunity is suppressed in mice housed at standard temperatures (ST; 22°C) which could be reversed by housing mice at warmer, thermoneutral temperatures (TT; 30°C) [1]. However, the mechanisms causing this impairment at ST remain unclear. Cold stress is mediated specifically by activation of the sympathetic nervous system and the release of norepinephrine (NE), which is highly suppressive when signaling through  $\beta$ -adrenergic receptors ( $\beta$ -ARs) on immune cells. We found that NE levels are significantly elevated in tumor-bearing mice housed at ST compared to TT, which led us to hypothesize that chronic stress induced by cool housing temperatures increases  $\beta$ -AR signaling that dampens the anti-tumor immune response and the efficacy of immune modulating therapies.

#### **Methods**

We used both physiologic (housing temperature; ST and TT) and pharmacologic blockade ( $\beta$ -blockers) to modulate  $\beta$ -AR signaling levels in immune-competent and SCID mice bearing 4T1 or B16-OVA tumors. Flow cytometry was used for immune cell analysis. Anti-PD-1 checkpoint blockade was given in 6, 200 $\mu$ g doses (Days 0, 2, 4, 6, 9, and 12) starting the day after tumors became detectable.

#### **Results**

We found that the addition of  $\beta$ -blockade significantly delayed 4T1 and B16-OVA tumor growth in mice housed at ST, recapitulating the slower tumor growth observed in mice housed at TT. However,  $\beta$ -blockade had no impact on tumor growth in SCID mice at ST or TT indicating dependence on the adaptive immune system. Analysis of 4T1 and B16-OVA tumors from immune-competent mice showed increased IFN- $\gamma$  expression in both CD4+ and CD8+ T cells in mice treated with  $\beta$ -blockade indicating a more robust anti-tumor immune response. Lastly, we investigated the impact of  $\beta$ -AR signaling on anti-PD-1 checkpoint blockade efficacy and found that reducing  $\beta$ -AR signaling by both physiologic (TT) and pharmacologic ( $\beta$ -blockade) strategies improved responses in both tumor models. Further analysis of 4T1 tumors from mice treated with  $\beta$ -blockade and anti-

PD-1 showed an increase in IFN- $\gamma$ , producing CD8+ T cells compared to either  $\beta$ -blockade or anti-PD-1 alone.

#### **Conclusions**

Taken together, these data indicate that elevated  $\beta$ -AR stress signaling caused by cool housing temperatures impairs anti-tumor immunity and the response of tumors to anti-PD-1 checkpoint blockade.

#### **Acknowledgements**

Supported by: The Peter T. Rowley Breast Cancer Research Grant, The Harry J. Lloyd Charitable Trust, the Roswell Park Alliance Foundation, and 5T32CA085183-12.

#### **References**

1. Kokolus K, *et al*: **Baseline tumor growth and immune control in laboratory mice are significantly influenced by subthermoneutral housing temperature.** *PNAS* 2013, **110**:20176-20181.

271

### **The influence of exercise and fitness on the composition of leukocytes in peripheral blood; implications for cancer immunotherapy**

Michael P Gustafson, AriCeli DiCostanzo, Courtney Wheatley, Chul-Ho Kim, Svetlana Bornschlegl, Dennis A Gastineau, Bruce D Johnson, Allan B Dietz

Mayo Clinic, Rochester, MN, USA

#### **Background**

Exercise immunology has become a growing field in the past 20 years, with an emphasis on understanding how different forms of exercise affect immune function. Overexertion may lead to suppressed immune function whereas moderate exercise may improve immunity. The improvement of immune function through exercise may benefit cancer patients receiving immunotherapy. To begin to test this hypothesis, we investigated the effects of acute and endurance exercise on the composition of peripheral blood leukocytes over time in a healthy male population of varying fitness.

#### **Methods**

Fifteen males participated in two cycling bouts; a short incremental exercise test to exhaustion on one visit and a 45 minute endurance exercise test (cycling at 60% maximum workload) on the second visit. Lean body mass (LBM) and percent body fat (%BF) were calculated from DEXA (Dual-energy X-ray absorptiometry) scan on study visit 1. Flow-volume curves (FVC) were also collected on visit 1 with the average of 3 attempts within 150mL of each other. Blood was collected at pre-exercise, immediately post-exercise, 3 hours post-exercise, and 24 hours post-exercise. Leukocytes were measured by multi-parameter flow cytometry of more than 50 immunophenotypes for each collection sample.

## Diet, Exercise and/or Stress and Impact on the Immune System

Presenting author underlined; *Primary author in italics*

### Results

We found a differential induction of leukocytosis dependent on exercise intensity and duration. Cytotoxic natural killer cells demonstrated the greatest increase (average of 5.6 fold) immediately post-maximal exercise whereas CD15<sup>+</sup> granulocytes demonstrated the largest increase at 3 hours post-maximal exercise (1.6 fold). The longer, less intense endurance exercise resulted in an attenuated leukocytosis. Induction of leukocytosis did not differ in our limited study of active (n=10) and sedentary (n=5) subjects to exercise although we found that in baseline samples, sedentary individuals had elevated percentages of CD45RO<sup>+</sup> memory CD4<sup>+</sup> T cells and elevated proportions of CD4<sup>+</sup> T cells expressing the negative immune regulator programmed death-1 (PD-1). Finally, we identified several leukocytes whose presence correlated with obesity related fitness parameters.

### Conclusions

Taken together, our data suggests pre-existing compositional differences of leukocytes based on fitness and rapid and specific accumulation of leukocytes subsets into the blood dependent on the intensity and duration of to exercise.

### References

1. Gustafson MP, Lin Y, Maas ML, Van Keulen VP, Johnson P, Peikert T, *et al*: **A method for identification and analysis of non-overlapping myeloid immunophenotypes in humans.** *PLoS One* 2015, **10(3)**:e0121546.

### 272

#### **Blockade of $\beta$ -adrenergic receptor signaling enhances anti-tumor immunity while increasing the sensitivity of tumor cells to radiation therapy**

Cameron MacDonald, Mark Bucsek, Guanxi Qiao, Bonnie Hylander, Elizabeth Repasky

Roswell Park Cancer Institute, Buffalo, NY, USA

### Background

Radiation therapy has evolved into an effective treatment for many cancers because of its ability to kill tumor cells and stimulate anti-tumor immunity, but radioresistance remains a major obstacle in cancer treatment. Recent studies indicate that norepinephrine (NE) released from sympathetic nerves suppresses immune cells and promotes tumor cell survival via  $\beta$ -adrenergic receptor ( $\beta$ -AR) activation. Work from our laboratory has shown that the cool housing temperature of laboratory mice is a significant source of cold stress which stimulates NE release. Moreover, we showed that  $\beta$ -AR signaling in mouse tumor models enhanced chemotherapeutic resistance, and treatment with  $\beta$ -AR antagonists ( $\beta$ -blockers) reversed this effect [1]. This finding led us to hypothesize that  $\beta$ -AR signaling promotes

radioresistance in tumor cells but suppresses the anti-tumor immune response.

### Methods

*In vitro*, we used Pan02 (abundant  $\beta$ -AR expression) and 4T1 tumor cells (no  $\beta$ -AR expression). We treated cells with the pan- $\beta$ -agonist, isoproterenol, and performed clonogenic assays examining survival at various radiation doses (0-8 Gy). *In vivo*, we implanted CT26.CL25 tumor cells subcutaneously into the leg of immunodeficient SCID mice and immune-competent BALB/c mice. When tumors became palpable, mice were randomized to receive daily  $\beta$ -blocker or PBS injections followed by radiation (6 Gy) 3 days later. Flow cytometry was used to analyze immune cells within tumors.

### Results

*In vitro*, isoproterenol treatment significantly increased the survival of radiated Pan02 cells compared with controls but had no impact on radiated 4T1 tumor cells suggesting that  $\beta$ -AR signaling enhances radioresistance. *In vivo*, radiation alone moderately slowed tumor growth in SCID mice. However, combining  $\beta$ -blockade with radiation significantly enhanced the effect of radiation, indicating that  $\beta$ -blockade was sensitizing tumor cells to radiation. Lastly, we repeated this experiment in immune-competent BALB/c mice and again observed a significant reduction of tumor growth in mice receiving  $\beta$ -blockade and radiation compared to radiation alone. To determine if  $\beta$ -blockade was enhancing anti-tumor immunity in radiated mice, we analyzed tumors using flow cytometry and observed a significant increase in CD4<sup>+</sup> and CD8<sup>+</sup> T cells expressing IFN- $\gamma$  and granzyme B in the group receiving  $\beta$ -blockade and radiation compared to those receiving radiation alone, indicating that  $\beta$ -blockade was also stimulating anti-tumor immunity.

### Conclusions

Taken together, this data suggests that  $\beta$ -AR blockade decreases tumor cell radioresistance while simultaneously bolstering anti-tumor immunity.

### Acknowledgements

Supported by: The Roswell Park Alliance Foundation.

### References

1. Eng J, *et al*: **Housing temperature-induced stress drives therapeutic resistance in murine tumour models through  $\beta$ 2-adrenergic receptor activation.** *Nat Commun* 2015, **6**:6426.





## Diet, Exercise and/or Stress and Impact on the Immune System

Presenting author underlined; *Primary author in italics*

273

### **The dual administration of immunotherapy is enhanced by activity-induced weight maintenance in the 4T1.2 mammary tumor model**

William J Turbitt, Yitong Xu, Andrea Mastro, *Connie J Rogers*  
Pennsylvania State University, University Park, PA, USA

#### **Background**

Lifestyle factors (e.g., body weight, physical activity) can impact breast cancer risk and response to therapy. Changes in metabolic, inflammatory, and immune mediators are possible factors underlying this relationship. Few studies have examined the effect of body weight and activity on the efficacy of immunomodulatory or immunotherapeutic strategies. Thus, the goal of the current study was to determine if preventing weight gain (via activity and diet) could delay primary tumor growth and metastatic progression in tumor-bearing mice and determine if there were any additive effects of weight maintenance and the dual administration of an allogeneic whole tumor cell vaccine and PD-1 checkpoint blockade on the aforementioned outcomes.

#### **Methods**

Female BALB/c mice were randomized to sedentary, weight gain (WG) or exercising, weight maintenance (WM) groups (n=20-24/group). After 8 weeks, all mice were orthotopically injected with  $5 \times 10^4$  luciferase-transfected 4T1.2 cells into the fourth mammary fat pad and continued on their intervention for 35 days. After injection, mice were further randomized into vaccination (n=9-12/group) or vehicle control (n=11-12/group) groups and administered irradiated 4T1.2 cells (VAX) or vehicle (VEH) control at day 7, 14, 21, and 28 post-tumor injection. Current studies are investigating if the dual administration of VAX plus PD-1 checkpoint blockade (10 mg/kg/mouse) is enhanced in WM tumor-bearing mice.

#### **Results**

All WM groups weighed significantly less than WG groups over the course of the study ( $p < 0.0001$ ). There was a significant effect of both WM and VAX alone on primary tumor growth ( $p < 0.0001$ ) and splenic IFN $\gamma$  production ( $p=0.010$ ) and an additive effect of WM+VAX on primary tumor growth ( $p < 0.05$ ), metastatic burden in lung ( $p=0.0267$ ) and heart ( $p=0.0492$ ), and the accumulation of splenic MDSCs ( $p=0.021$ ). A pilot study showed an additive effect of the dual administration of VAX and anti-PD-1 in WG mice; however, experiments investigating the dual administration of VAX and PD-1 checkpoint blockade in WM cohorts are currently underway.

#### **Conclusions**

These results demonstrate that activity-induced weight maintenance in combination with an allogeneic whole tumor

cell vaccine is highly effective at delaying primary tumor growth and metastases, and reducing splenic MDSC levels in this metastatic model. Interventions that maintain body weight may yield significant additive benefit in multimodal immunotherapy treatment strategies.

#### **Acknowledgements**

This work is supported by NIH grant R21 CA209144.

274

### **Multi-species assessment of the impact of aging and obesity on T cell exhaustion**

Sita Withers<sup>1</sup>, Ziming Wang<sup>1</sup>, Lam T Khuat<sup>1</sup>, Cordelia Dunai<sup>1</sup>, Bruce R Blazar<sup>2</sup>, Dan Longo<sup>3</sup>, Robert Rebhun<sup>1</sup>, Steven K Grossenbacher<sup>1</sup>, Arta Monjazeb<sup>1</sup>, William J Murphy<sup>1</sup>

<sup>1</sup>University of California, Davis, Sacramento, CA, USA

<sup>2</sup>University of Minnesota, Minneapolis, MN, USA

<sup>3</sup>Dana-Farber Cancer Institute, Boston, MA, USA

#### **Background**

Reinvigorating exhausted T lymphocytes with immune checkpoint inhibitors has proved to be a particularly successful strategy for the treatment of cancer. There remains however, a great deal of variability in response and toxicity between patients. Our previous murine studies revealed that obesity and age significantly enhanced toxicity to stimulatory immunotherapy as a consequence of their resting pro-inflammatory state. Here, we characterize the resting exhaustion phenotype and functional characteristics of T lymphocytes in obese and aged individuals, within a range of species, in order to understand the differential impact checkpoint inhibition might have on these populations.

#### **Methods**

Diet induced obese (DIO) mice within various age groups were fed a high fat diet long-term prior to analysis of splenocytes. Peripheral blood was collected from non-human primates (NHP) and laboratory beagles stratified into lean and obese groups based on weight and body condition score, respectively. Flow cytometry was used to quantify relative expression of T cell exhaustion markers, in addition to assessing T cell function as determined by intracellular cytokine expression and Ki67 positivity.

#### **Results**

We observed elevated PD-1 expression in CD4+ and CD8+ T cells in  $\geq 12$ -month-old (mo) mice compared to 7mo mice. This coincided with altered expression of TNF- $\alpha$  and IFN- $\gamma$  expression, and decreased proliferation following stimulation. Interestingly, PD-1 expression, proportions of naïve and effector memory cells, cytokine expression levels and proliferative responses of T cells from lean 13mo mice

## **Diet, Exercise and/or Stress and Impact on the Immune System**

Presenting author underlined; *Primary author in italics*

were similar to that of 7mo mice. Conversely, T cells from DIO 13mo mice appeared similar to 24mo mice in that they were phenotypically and functionally more exhausted. In NHPs, while PD-1 expression did not differ between small numbers of lean and obese animals, a trend towards decreased proliferation in CD4+ memory T cells of obese animals was observed. Similarly, decreased mitogen responses in T cells from obese dogs were also noted.

### **Conclusions**

Both aging and obesity appear to impact PD-1 expression and T cell function. Data from dogs and NHPs suggest these findings may be consistent across species. Ultimately, these data add to our understanding of T cell function in differing physiologic states, and may provide the foundation for predicting toxicity and response to checkpoint inhibitors.



## Immune Metabolism

Presenting author underlined; *Primary author in italics*

275

### **Disruption of the L-arginine balance in the tumor microenvironment with a recombinant human arginase 1 (AEB1102) sensitizes cancer to immunotherapy**

Scott Rowlinson, Giulia Agnello, Susan Alters, David Lowe

Aeglea BioTherapeutics, Austin, TX, USA

#### **Background**

Human arginase I (hArgI) is a  $Mn^{2+}$ -dependent enzyme that displays low activity and low stability in serum. Myeloid-derived suppressor cells (MDSC) express human arginase I (hArgI) and nitric-oxide synthase (NOS), which control the availability of L-arginine in the tumor microenvironment and in turn regulate the function of T cells. Depletion of L-arginine by MDSC has been correlated to impairment of T cell anti-tumor function and tumor evasion of host immunity. Analysis of the expression of enzymes of the L-arginine biosynthetic pathway in peripheral blood mononuclear cells, bone marrow mononuclear cells and  $CD34^+$  cells showed low levels of ornithine transcarbamylase (OTC) and argininosuccinate synthase (ASS), suggestive of dependence of these cells on exogenous/extracellular L-arginine for physiological function. As a result, long term depletion of L-arginine may negatively impact the MDSC population and therefore enhance immune regulation of tumor growth. This hypothesis was tested using a recombinant hArgI (AEB1102), developed by replacement of the  $Mn^{2+}$  natural cofactor with  $Co^{2+}$  which results in significantly improved catalytic activity and serum stability as compared to endogenous hArgI.

#### **Methods**

Administration of AEB1102 results in chronic depletion of L-arginine in serum to levels below  $1 \mu M$ . The murine CT26 colon-cancer model was dosed with AEB1102 alone and in combination with anti-PD-L1 and anti-PD-1 monoclonal antibodies (mAbs).

#### **Results**

*In vivo* treatment of CT26 mice with AEB1102 monotherapy resulted in an increased life span (ILS) (46%,  $p < 0.001$ ) as compared to the untreated control group, whereas standard monotherapy using immunomodulatory antibodies that target PD-1 and PD-L1 resulted in a 0% ( $p = 0.5$ ) and 29% ( $p = 0.002$ ) ILS respectively. Of significance, combination therapy of AEB1102 with anti-PD-1 (ILS 67%,  $p < 0.001$ ) or PD-L1 (ILS 67%,  $p < 0.001$ ) mAbs resulted in additive and synergistic anti-tumor effect compared to AEB1102 alone and immunotherapy alone.

#### **Conclusions**

Collectively these results demonstrate that disrupting the L-arginine physiological balance in the tumor microenvironment inhibits tumor growth and further

sensitizes the tumor to immunotherapy. AEB1102 is currently in phase I (monotherapy) clinical trials. These data open the possibility of clinical combination of AEB1102 with anti-PD-1 and anti-PD-L1 mAbs to further improve outcomes in cancer patients.

276

### **NAD-Sirt1 axis is central to the unique immunometabolic phenotype of Th1/17 hybrid cells in regulating its enhanced anti-tumor potential**

Shilpak Chatterjee<sup>1</sup>, Anusara Daenthanasanmak<sup>1</sup>, Paramita Chakraborty<sup>1</sup>, Kyle Toth<sup>1</sup>, Megan Meek<sup>1</sup>, Elizabeth Garrett-Mayer<sup>1</sup>, Michael Nishimura<sup>2</sup>, Chrystal Paulos<sup>1</sup>, Craig Beeson<sup>1</sup>, Xuezhong Yu<sup>1</sup>, *Shikhar Mehrotra*<sup>1</sup>

<sup>1</sup>MUSC, Charleston, SC, USA

<sup>2</sup>Loyola Cancer Center, Maywood, IL, USA

#### **Background**

Th17 cells hold promise for immunotherapy of cancer [1]. While the anti-tumor potential of Th17 cells primarily depends upon  $IFN-\gamma$  secretion and persistence [1], a long-term tumor control has still remained elusive. Given that both the “effector” and “stemness like” features are prerequisites for T cells to mount durable anti-tumor responses, we hypothesized that combining the culture conditions of Th1 (effector) and Th17 (stemness like) cells could generate hybrid Th1/17 cells with improved anti-tumor properties.

#### **Methods**

Melanoma epitope tyrosinase reactive  $CD4^+$  T cells obtained from h3T TCR transgenic mice were differentiated *ex vivo* to Th1, Th17, and Th1/17 cells before adoptive transfer ( $0.25 \times 10^6$  cells/animal i.v.) to C57BL/6 recipient animals with subcutaneously established B16 melanoma. Quantitative PCR (q-PCR), flow cytometry, and metabolomic analyses were used to evaluate the expression of various metabolism and stemness associated genes as well as protein expression in the T cells. To compare the metabolic commitment between different subsets (Th1, Th17 and Th1/17), real time metabolic flux analyzer (Seahorse Biosciences, USA) and radioactive tracer studies were used.

#### **Results**

The combined culture conditions of Th1 and Th17 generates hybrid Th1/17 cells with a  $IFN-\gamma^{hi}$ ,  $IL17^{hi}$ ,  $GM-CSF^{hi}$ ,  $CD107a^{hi}$ ,  $T-bet^{hi}$ , Granzyme  $B^{hi}$ ,  $IL23R^{hi}$ ,  $IL22^{hi}$ ,  $Bcl6^{hi}$ ,  $Tcf7^{hi}$  signature. These hybrid Th1/17 cells exhibit enhanced tumor control in subcutaneous and lung metastasis models of murine melanoma. A hypothesis generating transcriptional, metabolic, and proteomic profiling, followed by confirmatory experiments established that the enhanced anti-tumor properties were attributed to increased NAD<sup>+</sup> mediated

## Immune Metabolism

Presenting author underlined; Primary author in italics

activity of histone deacetylase Sirt1 in hybrid Th1/17 cells. Inhibition of NAD<sup>+</sup> and Sirt1 activity either pharmacologically or by genetic ablation (Sirt1-KO T cells) led to loss of stable anti-tumor control. Importantly, anti-tumor T cells or tumor infiltrating lymphocytes programmed in the presence of exogenous NAD<sup>+</sup> also led to the similar metabolic phenotype and improved anti-tumor control.

### Conclusions

The present study discloses that metabolic status plays an important role in dictating the anti-tumor response of the T cells. Combining the culture conditions of Th1 and Th17 cells renders hybrid Th1/17 cells with a unique immune-metabolic feature that enables them to orchestrate distinct transcriptional programs leading to highly effector and stem-like T cells.

### References

1. Muranski P, Boni A, Antony PA, *et al*: **Tumor-specific Th17-polarized cells eradicate large established melanoma.** *Blood* 2008, **112**:362-373.

277

### The Wnt5a-beta-catenin pathway triggers a metabolic switch that drives indoleamine 2,3-dioxygenase activity and dendritic cell tolerization in the melanoma microenvironment: optimizing checkpoint inhibitor immunotherapy

*Fei Zhao*<sup>1</sup>, Kathy Evans<sup>1</sup>, Christine Xiao<sup>1</sup>, Alisha Holtzhausen<sup>2</sup>, Brent A. Hanks<sup>1</sup>

<sup>1</sup>Duke University Medical Center, Durham, NC, USA

<sup>2</sup>Lineberger Comprehensive Cancer Center, University of North Carolina, Chapel Hill, NC, USA

### Background

Despite recent advances, many cancers remain refractory to available immunotherapies by developing various strategies to evade the immune system. Emerging evidence indicates that the tolerization of local dendritic cells (DCs) within the tumor microenvironment plays a critical role in immune evasion. The role of metabolic re-programming in DC tolerization remains poorly characterized and the mechanisms by which cancers may utilize these pathways to promote the establishment of an immunotolerant microenvironment have not been described.

### Methods

We investigated the role of the Wnt-beta-catenin pathway in the metabolic reprogramming of melanoma-derived DCs using real-time metabolic flux analysis. The impact of DC metabolic re-programming on the enzymatic activity of indoleamine 2,3-dioxygenase (IDO) was analyzed by HPLC while protoporphyrin IX (PpIX) levels were quantified by

flow cytometry. The role of DC fatty acid oxidation (FAO) on regulatory T cell (Treg) generation was investigated using pharmacologic and genetic approaches. The impact of FAO inhibition on anti-tumor immune responses to anti-PD-1 antibody therapy were investigated in a transgenic melanoma model.

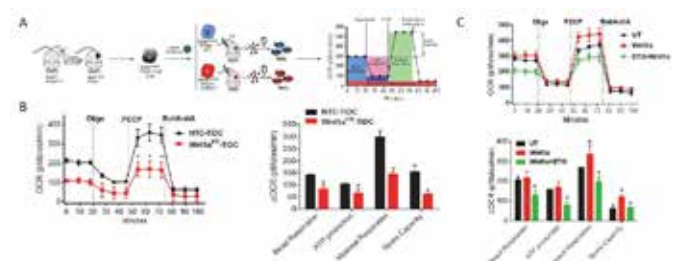
### Results

We show that the Wnt5a-beta-catenin-PPAR $\gamma$  pathway shifts DCs from glycolysis to FAO in the melanoma microenvironment in a manner dependent upon induction of the mitochondrial fatty acid transporter, CPT1A (Figure 1). This metabolic shift promotes DC tolerization by 1) elevating DC levels of the PpIX prosthetic group of IDO, resulting in the enhanced activity of this enzyme (Figure 2) and 2) potentially suppressing DC-expression of IL-6 and IL-12, both culminating in the generation of Tregs both *in vitro* and *in vivo* (Figure 3). Genetic silencing and the pharmacologic inhibition of CPT1A potentially enhances the ability of DCs to stimulate effector T cell responses. Indeed, genetic silencing of melanoma-expressed Wnt5a significantly promotes T cell tumor infiltration and augments PD-L1 expression in this melanoma model. Consistent with these findings, we further show FAO inhibition to enhance the efficacy of anti-PD-1 therapy while augmenting melanoma antigen-specific T cell responses (Figure 4).

### Conclusions

Our findings implicate the Wnt5a-beta-catenin-PPAR $\gamma$ -CPT1A paracrine signaling axis as a driver of DC FAO and functional DC tolerization in the melanoma microenvironment and connect this pathway with the promotion of a “non-inflamed” phenotype in melanoma. This work describes a novel association between DC metabolism and the regulation of IDO enzymatic activity and suggests that this pathway may be a potent pharmacological target for increasing the responsiveness of “non-inflamed” tumors to anti-PD-1 antibody immunotherapy.

**Figure 1**

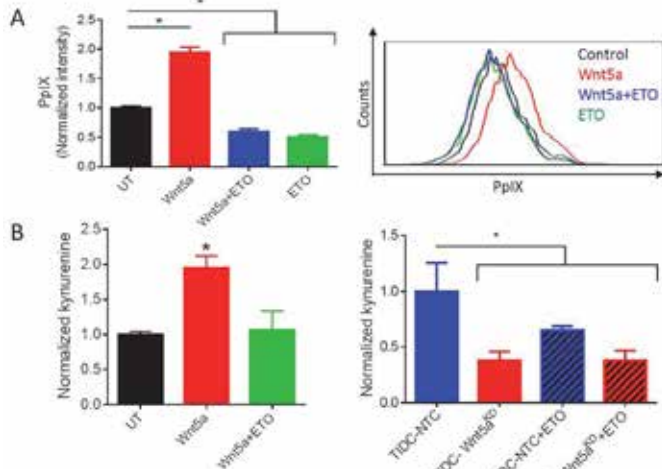


Wnt5a Promotes DC FAO in the Melanoma Microenvironment. A. Schematic of tumor-infiltrating DC (TIDC) metabolic analysis. B. Melanoma-derived Wnt5a promotes TIDC OXPPOS. C. Wnt5a promotes DC FAO

# Immune Metabolism

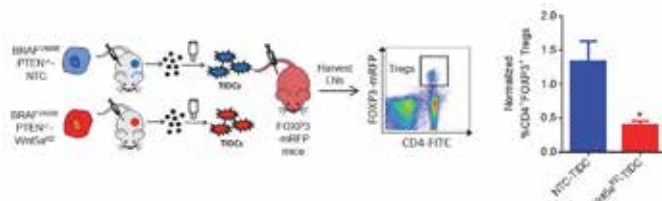
Presenting author underlined; Primary author in italics

**Figure 2**



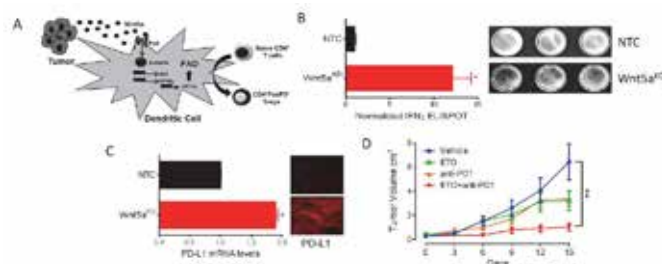
Wnt5a-induced FAO Promotes DC Synthesis of PpIX and Enhances IDO Enzyme Activity. A. Wnt5a stimulates DC PpIX synthesis. B,C. Wnt5a promotes DC IDO activity in a FAO-dependent manner both *in vitro* and *in vivo*.

**Figure 3**



Wnt5a-induced DC OXPHOS Promotes Treg Generation in the Melanoma Microenvironment. Melanoma-derived Wnt5a conditions DCs to promote Treg generation *in vivo*.

**Figure 4**



Inhibition Wnt5a-DC FAO Enhances Melanoma PD-L1 Expression and Augments anti-PD-1 antibody Efficacy. A. Schematic of Wnt5a paracrine signaling pathway. B,C. Genetic silencing of Wnt5a in melanoma promotes T cell infiltration and PD-L1 upregulation. D. Inhibition of CPT1A/FAO synergizes with anti-PD-1 antibody therapy in melanoma.

**278**

## Metformin treatment synergizes with PD-1 blockade therapy by reducing tumor hypoxia

Nicole Scharping<sup>1</sup>, Ashley V Menk<sup>2</sup>, Ryan Whetstone<sup>1</sup>, Xue Zeng<sup>1</sup>, Greg M Delgoffe<sup>1</sup>

<sup>1</sup>University of Pittsburgh, Pittsburgh, PA, USA

<sup>2</sup>University of Pittsburgh Cancer Institute, Pittsburgh, PA, USA

### Background

Tumors create a suppressive microenvironment that prevents antitumor immunity through a number of mechanisms like recruitment of regulatory T cells or through ligation of co-inhibitory molecules such as PD-1. PD-1 blockade therapy has become a major success in cancer treatment; however, most patients fail to respond to anti-PD-1 therapy. It has become clear in recent years that the lack of nutrients and oxygen in the tumor microenvironment may also play an immunosuppressive role. Since T cell effector function is dependent on these nutrients to produce the energy needed, we hypothesized that changing this environment would improve the efficacy of immunotherapy.

### Methods

B16 and MC38 were injected into mice and were treated when tumors were palpable with either 0.2 mg anti-PD-1 or hamster IgG isotype control, injected every 4 days intraperitoneally, and 50 mg/kg metformin or PBS, injected every 2 days intraperitoneally. CD8<sup>+</sup> T cells were isolated from lymph nodes and tumors and tested for hypoxia and cytokine production by flow cytometry and metabolic function with Seahorse XFe96 Bioanalyzer. Similar analysis was done *in vitro* with B16, MC38, and SIINFEKL stimulated OT-1 cells harvested from spleen and lymph nodes of mice.

### Results

We show that B16, a melanoma resistant to PD-1 therapy, and MC38, a colon adenocarcinoma partially sensitive to PD-1 blockade, consume different amounts of oxygen and as a result, produce distinct hypoxic environments *in vivo*. The amount of hypoxia in the tumor microenvironment can be reduced by treating mice with metformin, a type II diabetes drug that inhibits mitochondrial complex I, which we show acts directly on the tumor cells to inhibit their oxygen consumption. As hypoxia can inhibit T cell responses *in vivo*, we hypothesized that metformin-induced mitigation of tumor hypoxia might improve immunotherapeutic responses. We also show that pairing metformin with PD-1 blockade therapy results in substantially improved antitumor immunity and tumor clearance, even in PD-1 insensitive tumor models.

### Conclusions

Our data suggest that the degree of tumor hypoxia, partially a result of the degree of cancer cell metabolic deregulation,



## Immune Metabolism

Presenting author underlined; *Primary author in italics*

may determine whether T cells have a permissive microenvironment for effective immunotherapy. More importantly, our results suggest that metabolic remodeling of the tumor microenvironment may help patients better respond to immunotherapy.

**279**

### Tumor-derived alpha-fetoprotein (tAFP) inhibits dendritic cell metabolism

Patricia M Santos<sup>1</sup>, Ashley V Menk<sup>1</sup>, Jian Shi<sup>1</sup>, Greg M Delgoffe<sup>2</sup>, Lisa H Butterfield<sup>1</sup>

<sup>1</sup>University of Pittsburgh Cancer Institute, Pittsburgh, PA, USA

<sup>2</sup>University of Pittsburgh, Pittsburgh, PA, USA

#### Background

Previous studies have proposed an immune suppressive role for alpha-fetoprotein (AFP), an oncofetal antigen expressed by over 50% of hepatocellular carcinomas (HCC). AFP-L3 is the major isoform present in the serum of HCC patients and is associated with poor patient prognosis. While tumor-derived AFP (tAFP) contains >80% of AFP-L3, cord blood serum-derived AFP (nAFP) contains less than 5% of AFP-L3. Our previous work shows that monocytes, cultured in the presence of AFP (in particular tAFP), differentiated into dendritic cells (DC), retained a monocyte-like morphology, had decreased expression of DC maturation markers, and exhibited limited production of inflammatory cytokines and chemokines. Importantly, monocyte-derived DC cultured in the presence of tAFP failed to stimulate antigen-specific T cell responses. In this study, we examined the effect of AFP on DC cellular metabolism.

#### Methods

Monocytes were isolated from healthy donor peripheral blood mononuclear cells and cultured for 5 days with IL-4 and GM-CSF in the presence or absence of 10 µg/mL ovalbumin (OVA), nAFP or tAFP (n=3-5 HD per experiment). DC were collected and tested for 1) mitochondria levels and function (flow cytometry), 2) metabolic function by seahorse extracellular flux analyzer, and 3) expression of oxidative phosphorylation (OXPHOS)-related proteins, including electron transport chain proteins, and PGC1α levels (western blot and flow cytometry).

#### Results

DC cultured in the presence of nAFP and tAFP, had reduced mitochondrial mass and mitochondrial activity compared to OVA-DC. This was confirmed by a reduction in the basal oxygen consumption rate (OCR) in nAFP-DC and a more severe reduction in basal OCR in tAFP-DC. We also show that while mitochondrial metabolism is affected, glycolysis of DCs was not affected. Our data suggest that the changes observed in DC metabolism occur within 24 hours of

AFP exposure and that tAFP inhibition of mitochondrial metabolism leads to a transient compensatory increase in glycolysis in the first 24-48 hours. We also show differences in the expression of mitochondrial electron transport proteins responsible for OXPHOS in DC exposed to nAFP and tAFP. Lastly, we show that there is reduced expression of a key mitochondrial regulator, PGC1α, in nAFP and tAFP-DC.

#### Conclusions

Collectively, these data show profound negative effects of AFP, specifically tAFP on mitochondrial metabolism. These novel findings elucidate a key mechanism of immune suppression in HCC and may lead to new therapeutic approaches to reverse tAFP effects.

### 280 Presidential Travel Award Recipient

#### Mitochondrial biogenesis is repressed in tumor-infiltrating CD8+ T cells resulting in metabolic insufficiency and T cell dysfunction

Nicole Scharping<sup>1</sup>, Ashley V Menk<sup>2</sup>, Rebecca Moreci<sup>2</sup>, Ryan Whetstone<sup>1</sup>, Rebekah Dadey<sup>1</sup>, Simon Watkins<sup>1</sup>, Robert Ferris<sup>1</sup>, Greg M Delgoffe<sup>1</sup>

<sup>1</sup>University of Pittsburgh, Pittsburgh, PA, USA

<sup>2</sup>University of Pittsburgh Cancer Institute, Pittsburgh, PA, USA

#### Background

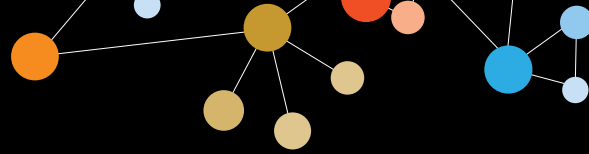
CD8<sup>+</sup> tumor-infiltrating T lymphocytes (CD8<sup>+</sup> TIL) in the tumor microenvironment (TME) are unable to effectively control their tumor targets due to a variety of immunosuppressive mechanisms, including direct tumor cell-T cell inhibition and soluble immunosuppressive factors. This allows cancer to progress unchecked as T cells are rendered functionally inert. Recently, poor metabolite availability in the TME has been identified as an additional suppressive mechanism exploited by bioenergetically-dysregulated tumors. Because T cell activation also has robust metabolic demands, we hypothesized that CD8<sup>+</sup> TIL dysfunction was a result of metabolic insufficiency.

#### Methods

Metabolic capacity was measured at the single cell level by 2NBDG and MitoTracker FM. Metabolic output was measured by Seahorse extracellular flux analysis. T cell reprogramming was performed by retroviral transduction on OVA-specific transgenic T cells *in vitro* before adoptive transfer into B16<sup>OVA</sup> bearing mice.

#### Results

We found CD8<sup>+</sup> TIL are characterized by dramatic loss of mitochondrial mass in B16, MC38, and LLC implantable mouse tumors and human CD8<sup>+</sup> TIL, which correlates with upregulation of co-inhibitory checkpoint molecules PD-1 and Tim-3. CD8<sup>+</sup> TIL mitochondrial mass loss is caused



## Immune Metabolism

Presenting author underlined; Primary author in italics

by decreased mitochondrial biogenesis, due in part to repression of the transcriptional co-activator PGC1 $\alpha$  resulting from chronic Akt signaling. Surprisingly, anti-PD-1 therapy had no effect on increasing PGC1 $\alpha$  or mitochondrial mass in CD8<sup>+</sup> TIL. We then asked whether improving CD8<sup>+</sup> TIL metabolism genetically might result in enhanced effector function, so we reprogrammed tumor-specific CD8<sup>+</sup> T cells to upregulate mitochondrial biogenesis prior to adoptive cell therapy. We found increased mitochondrial mass, restored cytotoxic functionality, and dramatically improved tumor regression in mice with reprogrammed CD8<sup>+</sup> TIL. To better understand why mitochondrial loss causes T cell dysfunction, we are exploring the importance of mitochondria for T cell functionality, including ATP and nucleotide production, calcium buffering, and ROS production.

### Conclusions

Our data support a model in which chronically-activated CD8<sup>+</sup> TIL are unable to metabolically support their effector functions. By understanding these metabolic insufficiencies, we can both better understand T cell dysfunction and design metabolic modulation strategies to improve cancer immunotherapy.

281

### Treg cells utilize lactic acid to fuel immune suppression in the tumor microenvironment

Ryan Whetstone<sup>1</sup>, Ashley V Menk<sup>2</sup>, Nicole Scharping<sup>1</sup>, Greg Delgoffe<sup>1</sup>

<sup>1</sup>University of Pittsburgh, Pittsburgh, PA, USA

<sup>2</sup>University of Pittsburgh Cancer Institute, Pittsburgh, PA, USA

### Background

The suppressive function of regulatory T (Treg) cells contributes significantly to the failure of cytotoxic T cells to eliminate cancer cells in the tumor microenvironment (TME). Within the TME, Treg cells retain their metabolic capacity as well as proliferative and suppressive functions, while conventional, effector T cells suffer reduced metabolic capacity in the energy substrate dearth environment. Thus, in the metabolically distinct TME, Treg cells may be bioenergetically supported by factors distinct from those that support conventional T cells. Lactic acid, a product of tumor glycolytic metabolism that is abundant in the TME has long been known to be immunosuppressive. We hypothesize that Treg cells in the TME utilize alternative metabolic substrates, particularly lactic acid, that allows them to maintain a significant level of suppression.

### Methods

To test our hypothesis we employed lactic acid treatment of conventional and regulatory T cells, as well as generating a mouse line in which *Slc16a1*, encoding a lactate transporter,

can be specifically deleted in Treg cells, constitutively or in a tamoxifen-induced manner. We also employed <sup>13</sup>C-labeled lactic acid coupled to mass spectrometric analysis.

### Results

Intratumoral Treg cells are highly proliferative in the tumor microenvironment. Lactic acid treatment of freshly isolated lymph node Treg cells supports enhanced proliferation, in striking contrast to the suppressive effects on conventional T cells. Intratumoral Treg cells upregulate monocarboxylate transporters (MCT 1, encoded by *Slc16a1* and MCT2, encoded by *Slc16a7*) which actively transport short chain carbons, including lactic acid, both into and out of cells. We found that MCT1 null Treg cells have a diminished suppressive capacity compared to MCT1 competent Treg cells. We also found that the pharmacologic inhibition of lactate metabolism in tumor-bearing animals results in dramatically decreased intratumoral Treg cell proliferation. Our ongoing studies seek to determine specifically how lactic acid is utilized by intratumoral Treg cells.

### Conclusions

Our data strongly support a model in which tumor cells evade the immune response, in part, by metabolically supporting immunosuppressive populations. Targeting MCT1 in Treg cells and diminishing immune suppression may be an appealing target for therapeutic intervention, especially while combining MCT1 inhibition with a therapy that reestablishes cytotoxic T cell functions, such as anti-PD-1 checkpoint blockade.

## Immune-related Adverse Event Management: Evidence Based Strategies and Clinical Care

*Presenting author underlined; Primary author in italics*

282

### Management of immune-mediated diarrhea and the impact of infliximab on outcome

Alfonso Cortés Salgado<sup>1</sup>, Meghan Campo<sup>2</sup>, Anita Giobbie-Hurder<sup>3</sup>, Ainara Soria<sup>1</sup>, Donald P Lawrence<sup>2</sup>, Javier Cortés<sup>1</sup>, Ryan J Sullivan<sup>2</sup>

<sup>1</sup>Medical Oncology Department, Hospital Universitario Ramón y Cajal, Madrid, Madrid, Spain

<sup>2</sup>Medical Oncology Department, Massachusetts General Hospital, Boston, MA, USA

<sup>3</sup>Department of Biostatistics & Computational Biology, Boston, MA, USA

#### Background

With the increasing use of immune checkpoint inhibitors (ICI), the recognition and prompt effective treatment of immune related adverse effects (irAEs), such as immune-mediated diarrhea (IMD) is crucial. IMD is commonly managed with steroid treatment and in severe cases, the TNF-alpha inhibitor infliximab (INF) however little is known on the impact INF has on patient outcomes.

#### Methods

We retrospectively reviewed 46 patients treated with iCI (anti-CTLA-4, anti-PD-1 or combination therapy) at Massachusetts General Hospital between 2008 and 2015 who developed grade 3-4 IMD with 96% of cases confirmed on colonoscopy. The primary aim was to characterize patients who received intravenous INF 5mg/kg (up to 3 doses) compared to those who did not and evaluate for impact of INF on outcomes. Kaplan-Meier and extended Cox regression were used to calculate OS and PFS.

#### Results

Of the 46 patients who developed IMD, 60.9% were treated with CTLA-4 inhibitor monotherapy, 30.4% with combination CTLA-4/PD-1 inhibition and 8.7% with anti-PD-1 therapy alone. Median follow-up measured after the first dose of treatment causing diarrhea was 20.5 months (95% CI: 13.0-25.1 months). Of the 46 patients, 2 (4.4%) had neither steroids nor INF. Of the remaining 44, 17 (37%) had both steroids and INF and 27 (59%) had steroids alone. Of the 27 patients treated with steroids alone, 26 improved to grade 1 or better; median time of 25 days. For the 17 patients treated with steroids followed by INF, the median time on steroids prior to INF was 24 days; median time from start of symptoms to grade-1 resolution was 68 days. Of the 17 patients who received INF, 53% required 1 dose, 35% two doses, and 12% three doses. When stratified by ECOG PS and adjusted for comorbidities, INF therapy was a significant predictor of PFS with a 76% reduction compared with

patients who had not yet started or never received the drug (HR: 0.24, 95% CI: 0.1-0.8, p=0.02). Treatment with INF was not a predictor of OS (HR: 0.97, 95% CI: 0.3-3.7, p=0.97).

#### Conclusions

Development of IMD is a common ir-AEs. The lag between development of IMD and the administration of INF in our study renders it difficult to determine if INF significantly shortens symptom duration however our data demonstrate the significance of INF use on PFS. Though this finding requires further validation in a larger patient cohort it does bolster the hypothesis that severe ir-AE, necessitating stronger immune suppression, may correlate with treatment efficacy.

283

### Transaminitis on PD-1/L1 inhibitors; the difficulties in distinguishing among progression, tumor flare and autoimmune hepatitis

Misako Nagasaka, Ammar Sukari

Karmanos Cancer Institute, Detroit, MI, USA

#### Background

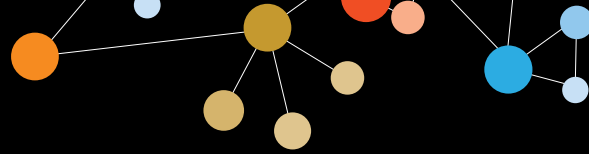
Autoimmune hepatitis is a well-documented rare but serious immune related event known to occur with anti PD-1/L1 inhibition and may mimic progression or tumor flare.

#### Methods

We evaluated three patients with liver metastasis who developed transaminitis with anti-PD-1/L1 inhibitors using CTCAE ver4.0 and RECIST ver1.1.

#### Results

Case 1: A 36 year old man with nasopharyngeal carcinoma with liver metastasis developed grade 2 transaminitis and RUQ pain after 2 doses of nivolumab. Ultrasound revealed stable liver metastasis but with hepatomegaly and new ascites. Nivolumab was discontinued and switched to taxol. His hepatomegaly and ascites resolved. Case 2: A 35 year old woman with nasopharyngeal carcinoma with liver metastasis developed grade 1 transaminitis after 3 doses of nivolumab. Progression of liver metastasis was seen on CT scan. Case 3: A 69 year old man with oropharyngeal cancer with liver metastasis was placed on a clinical trial utilizing tremelimumab and MEDI4736. He had grade 1 transaminitis with stable disease on CT scan post 4 cycles. He continued on MEDI4736, developed grade 2 transaminitis and CT scan showed progression of liver metastasis. He was switched to carboplatin/ 5FU with weekly cetuximab and his liver enzymes normalized soon after. These observations raise the issue of the difficulties in distinguishing autoimmune hepatitis vs tumor progression vs tumor flare in patients with



## Immune-related Adverse Event Management: Evidence Based Strategies and Clinical Care

Presenting author underlined; *Primary author in italics*

liver metastasis on PD-1/L1 inhibitors. Case 1 appears to have had autoimmune hepatitis, whereas others had progression. Drug-related hepatitis is seen in 1% to 2% of patients on checkpoint inhibitors. Grade 3/4 transaminitis may require high-dose corticosteroids [1]. Toxicities with PD-1/L1 antibodies may also vary with the histology. For example, in NSCLC patients receiving nivolumab, pneumonitis was observed in 6% [2] whereas only 1.9% of melanoma patients had pneumonitis [3]. Similarly, liver metastasis patients on PD-1/L1 therapy may be more prone to autoimmune hepatitis.

### Conclusions

Close monitoring of the liver enzymes as well as careful assessment of liver are imperative while we await further “big data” on better consensus to evaluate transaminitis following checkpoint inhibitors in patients with liver metastasis.

### References

1. Weber JS, *et al*: **Toxicities of Immunotherapy for the Practitioner**. *J Clin Oncol* 2015, **33**:2092-2099.
2. Brahmer J, *et al*: **Nivolumab versus Docetaxel in Advanced Squamous-Cell Non–Small-Cell Lung Cancer**. *N Engl J Med* 2015, **373**:123-135.
3. Weber JS, *et al*: **Nivolumab versus chemotherapy in patients with advanced melanoma who progressed after anti-CTLA-4 treatment (CheckMate037): a randomised, controlled, open-label, phase 3 trial**. *Lancet Oncol* 2015, **16**:375-384.

### Consent

Informed consent was obtained from the patients.

## Immunogenomics and Oncogenetics

Presenting author underlined; Primary author in italics

284

### Cognate pairing of human T cell receptor alpha and beta V-regions from single cells

Miranda Byrne-Steele, Wenjing Pan, Xiaohong Hou, Brittany Brown, Mary Eisenhower, Jian Han

iRepertoire, Inc., Huntsville, AL, USA

#### Background

Immune repertoire amplification of T cell receptors (TCR) coupled to next-generation sequencing (NGS) provides detailed sequence-level insight into the immune system. However, information related to the cognate pairing of TCR alpha and beta chains is lost once RNA extraction is performed on the bulk sample. We describe a sensitive method that allows for the amplification of both human TCR alpha and beta chains from single cells using amplicon-rescue-multiplex-PCR in the same reaction tube.

#### Methods

During the first round of PCR, reverse transcription and PCR is performed with nested, multiplex primers covering both the alpha and beta locus with communal forward and reverse binding sites included on the 5' end of the inside primers. Included on the C-region gene primer is an in-line 6 nucleotide barcode, which serves as a plate identifier so that multiple 96-well (or 384-well) plates may be multiplexed in the same sequencing flow cell. After RT-PCR1, the first round PCR1 products are rescued using SPRI beads. A second PCR is performed with dual-indexed primers that complete the sequencing adaptors introduced during PCR1 and provide plate positional information for the sequenced products. Libraries from multiple plates may be pooled together on the same MiSeq flow cell and sequenced directly using a 500 or 600 cycle kit (250 paired-end read). An iPair GUI was also developed to enhance visualization of paired-receptors on the plate and to aid with identification of "interesting" pairs that warrant further investigation.

#### Results

This method was utilized in the analysis of a breast cancer patient's peripheral CD4+ lymphocytes as part of a longitudinal study of the immune repertoire pre- and post-treatment. Under optimal conditions, the amplification success rate is greater than 90%, with successfully identified pairs as high as 60% of those amplified. In the described experiments, bulk sequencing of each chain was also performed on RNA from remaining cells, and the observed single cell alpha and beta chains are typically represented in the top 1 and 5% of the most frequent clones from the bulk sample, respectively.

#### Conclusions

We have developed an extremely sensitive method for the identification of cognate pairs from single cells in the same reaction tube. Future work involves the characterization of single cells for gene products beyond the variable gene region of TCRs, allowing for a more complete characterization of the cellular landscape. With the rise of immunological-based treatments for cancer, this type of technology holds promise for uncovering TCR cognate pairs of therapeutic significance.

### 285 Abstract Travel Award Recipient

#### Defining molecular mechanisms of resistance to tumor immunity

Natalie Collins<sup>1</sup>, Robert Manguso<sup>1</sup>, Hans Pope<sup>1</sup>, Yashaswi Shrestha<sup>2</sup>, Jesse Boehm<sup>2</sup>, W Nicholas Haining<sup>1</sup>

<sup>1</sup>Dana-Farber Cancer Institute, Boston, MA, USA

<sup>2</sup>Broad Institute, Cambridge, MA, USA

#### Background

Recent success of immune checkpoint blockade solidifies the importance of the immune system in the defense against cancer. The clinical impact of the immune response is, however, very heterogeneous, with some patients achieving dramatic responses while others fail to respond. Known genomic correlates of response to immunotherapy are not perfectly predictive of clinical outcome, supporting the existence of unknown mechanisms of resistance. We hypothesize somatic mutations account for heterogeneity in the spontaneous immune response and response to immunotherapy. We have undertaken a systematic *in vivo* screen to identify novel mechanisms of resistance to tumor immunity in order to define a comprehensive set of therapeutic targets and provide biomarkers of sensitivity to immunotherapeutic strategies.

#### Methods

Mouse tumor cell lines (MC38 colon carcinoma, B16 melanoma) were engineered to express a library of barcoded open reading frames (ORFs) mutagenized to encode cancer-associated somatic mutations from the Pan-Cancer analysis within The Cancer Genome Atlas (TCGA) [1]. These cell lines form tumors when implanted subcutaneously in immunocompetent animals. Tumor-bearing animals were then subjected to immunotherapy with either therapeutic vaccination or anti-PD-1 checkpoint blockade. Barcode relative representation was measured by next generation sequencing at the time of tumor implantation and at tumor harvest post-immunotherapy. Barcoded mutant ORFs that confer immune resistance increased in representation under immune pressure in comparison to untreated or immunodeficient animals.



## Immunogenomics and Oncogenetics

Presenting author underlined; Primary author in italics

### Results

A mutation in Phospho-Inositol 3 Kinase (PI3K), PIK3CA c.3140A>G, consistently increased in representation in both B16 and MC38 immunotherapy-treated tumors but not in immunodeficient animals. This suggests that activity of this mutant allele conferred selective growth advantage in the setting of tumor immunity. This mutation encodes a constitutively active catalytic domain of PI3K, PIK3CA H1047R. MC38 tumors homogeneously expressing PIK3CA H1047R and implanted into wild type mice failed to respond to anti-PD-1 therapy, while tumors expressing a control gene regressed after treatment with anti-PD-1. Pharmacologic PI3K inhibition resensitized tumors to treatment with anti-PD-1. PD-1-treated PIK3CA H1047R tumors had fewer infiltrating CD8<sup>+</sup> T cells as measured by immunohistochemistry and flow cytometry of tumor infiltrating lymphocytes.

### Conclusions

PI3K has, in addition to its well-described oncogenic role, a role in tumor immune evasion. As such, activating mutations in PI3K may be useful as a predictor of poor response to immunotherapy. Importantly, these findings also provide a rationale for therapeutic combination trials of immune checkpoint blockade and PI3K inhibition.

### References

1. Kandoth C, *et al*: **Mutational landscape and significance across 12 major cancer types.** *Nature* 2013, **502**:333-339.

### 286

#### **A germline polymorphism associated with the T cell-inflamed tumor microenvironment in metastatic melanoma**

*Kyle R Cron*<sup>1</sup>, Ayelet Sivan<sup>1</sup>, Keston Aquino-Michaels<sup>1</sup>, Thomas F Gajewski<sup>2</sup>

<sup>1</sup>University of Chicago, Chicago, IL, USA

<sup>2</sup>University of Chicago Medical Center, Chicago, IL, USA

### Background

Baseline tumor infiltration with CD8<sup>+</sup> T cells and an associated chemokine/interferon gene signature are correlated with a favorable clinical outcome to immunotherapies. Recent work has indicated that differential presence of this phenotype can be influenced by specific oncogene pathways activated within the tumor cells, and also by host commensal microbiota. However, germline polymorphisms among the patient population also could influence the degree of the natural immune response against a tumor.

### Methods

To investigate this possibility, TCGA RNAseq data were used to analyze the degree of expression of a predetermined T

cell gene signature, and germline SNP data from the same patients were utilized to perform a GWAS against the gene signature as a phenotype. The top hit, a minor allele of SNP rs1483185, was significantly associated with increased T cell gene expression in the tumor ( $p = 8.812e^{-08}$ ). Interrogation using the GTEX database revealed lower gene expression in association with this SNP, arguing for a loss-of-function phenotype. To explore this concept mechanistically, gene-targeted mice were utilized lacking this gene. To focus gene deletion on hematopoietic cells, bone marrow (BM) chimeras were utilized.

### Results

Mice reconstituted with knockout BM grew B16.SIY tumors more slowly and had higher numbers of SIY<sup>+</sup> CD8<sup>+</sup> T cells in both the tumor infiltrating lymphocyte fraction as well as the spleen compared to WT engrafted mice. Additionally, 80% of splenic SIY<sup>+</sup> CD8<sup>+</sup> T cells had an activated CD44<sup>+</sup> CD62L<sup>-</sup> phenotype in knockout recipients versus 40% in WT recipients. The TIL populations from KO recipients also showed higher expression of surface molecules indicating antigen experience, as well as expression of PD-1, Lag3, and 4-1BB indicating antigen-specificity. Mechanistically, T cells from KO mice showed no obvious increase in activation potential. However, a significant increase in CD11c<sup>+</sup> CD8<sup>+</sup> dendritic cells was observed in KO BM recipients, suggesting a possible effect at the level of APCs.

### Conclusions

Together, our results have identified a functionally relevant SNP that can lead to improved spontaneous anti-tumor immunity. The development of pharmacologic approaches to phenocopy this loss of function genetic phenotype may be attractive to pursue as a cancer therapeutic.

### 287

#### **Graphene oxide and amino functionalized graphene characterization for immunotherapy applications using new high-throughput analysis**

*Marco Orecchioni*<sup>1</sup>, Davide Bedognetti<sup>2</sup>, Wouter Hendrickx<sup>2</sup>, Claudia Fuoco<sup>3</sup>, Filomena Spada<sup>3</sup>, Francesco Sgarrella<sup>1</sup>, Gianni Cesareni<sup>3</sup>, Francesco Marincola<sup>4</sup>, Kostas Kostarelos<sup>5</sup>, Alberto Bianco<sup>6</sup>, Lucia Delogu<sup>1</sup>

<sup>1</sup>University of Sassari, Sassari, Sardegna, Italy

<sup>2</sup>Sidra Medical and Research Center, Doha, Ad Dawhah, Qatar

<sup>3</sup>University of Roma Tor Vergata, Roma, Lazio, Italy

<sup>4</sup>Research Branch, Sidra Medical and Research Center, Doha, Ad Dawhah, Qatar

<sup>5</sup>Faculty of Medical & Human Sciences, University of Manchester, Manchester, England, UK

<sup>6</sup>CNRS, Institute de Biologie Moléculaire et Cellulaire, Strasbourg, Alsace, France

## Immunogenomics and Oncogenetics

Presenting author underlined; Primary author in italics

### Background

There is an enormous interest in exploring the potentialities of novel nanomaterials such as graphene and its derivatives in biomedical applications [1]. The understanding of the biomolecular interactions of graphene nanomaterials with human cells is critical for their implementation as diagnostic or therapeutic agents [1]. In this context the immune modulation mediated by graphene oxide (GO) or nanomaterials in general could be interesting also in immunotherapy applications. Indeed nanotechnology can enhance the efficacy of immunostimulatory small molecules and biologics by altering their co-localization, biodistribution, and release kinetics [2]. The impact exerted by graphene and GO exposure on the immune system is still unknown.

### Methods

Here, we propose an integrative analytical pipeline encompassing molecular and cellular characterization of the impact of graphene nanomaterials on immune cells. For the first time in the context of nanotechnology, we employed single cell mass cytometry to deconvolute the effect of GO flakes (between 1-2 graphene layers) functionalized by us through the addition of 1,3 dipolar-cycloaddition of amino groups (GONH<sub>2</sub>) on 15 immune cell populations looking at 30 markers at single-cell level. We then used whole transcriptomic analysis for further functional molecular characterization.

### Results

Intriguingly functionalization is able to increase the biocompatibility of GO in all the sub-population analyzed (Figure 1). GONH<sub>2</sub> was found to be a potent immune-activator of monocytes and dendritic cells. This effect was confirmed and explained by the transcriptomic analysis. Notably, GO mainly modulated cell metabolism. GONH<sub>2</sub> instead did not have an impact on the cell metabolism. Rather, they induce, in both monocytes and T cells, the activation of immunomodulatory pathways mainly related with innate and adaptive system and centered on interferon (IFN) signaling (Figure 2). Immune activations resulted in increased expression of the T helper 1 chemokines (i.e., CXCR3 and CCR5 ligands), critical for the development of an effective anti-tumor immune response [3].

### Conclusions

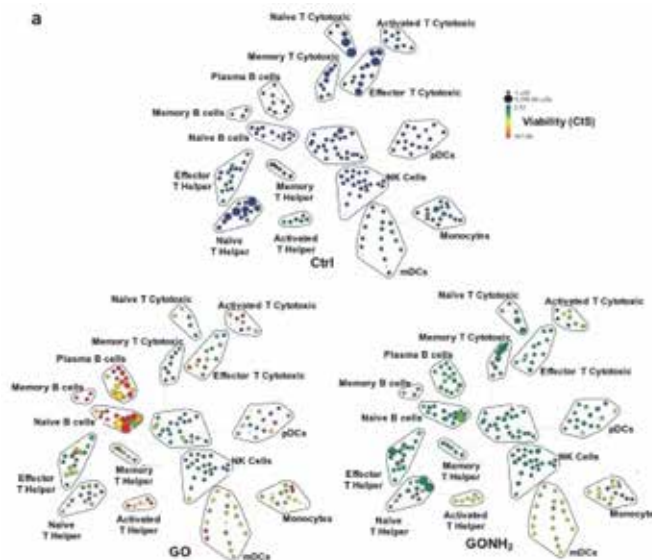
These idiosyncratic immune-modulatory properties of GONH<sub>2</sub> represent the proof of principle to develop new nanoscale platforms in medicine as novel immunotherapeutic tools.

### References

1. Orecchioni M, Bedognetti D, Sgarrella F, Marincola FM, Bianco A, Delogu LG: **Impact of carbon nanotubes and graphene on immune cells.** *J Transl Med* 2014, **12**:138.

2. Goldberg MS: **Immunoengineering: How nanotechnology can enhance cancer immunotherapy.** *Cell* 2015, **161**(2):201-204. 3. Galon J, Angell HK, Bedognetti D, Marincola FM: **The continuum of cancer immunosurveillance: prognostic, predictive, and mechanistic signatures.** *Immunity* 2013, **39**:11-26.

**Figure 1. Viability analysis with single cell mass cytometry.**

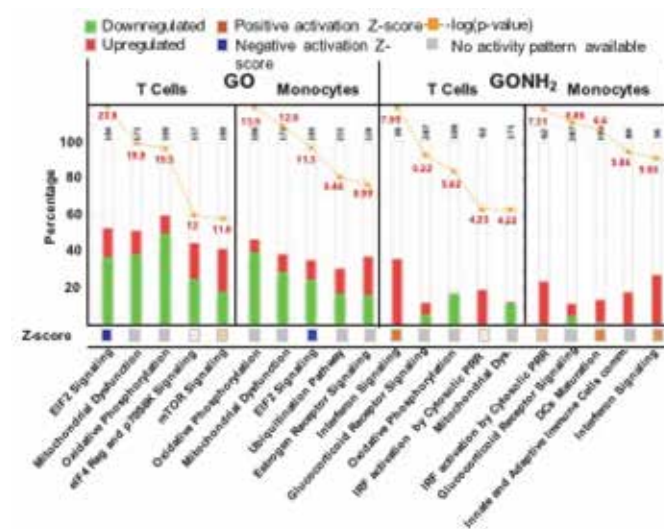


The SPADE tree plot was constructed by using 17 cell-surface antigens in treated and untreated healthy human PBMCs. The size of each circle in the tree indicates relative frequency of cells that fall within the 17-dimensional confines of the node boundaries. Node color is scaled to the median intensity of marker expression of the cells within each node, expressed as a percentage of the maximum value in the data set (CIS is shown).

# Immunogenomics and Oncogenetics

Presenting author underlined; Primary author in italics

**Fig 2. Microarray analysis**



Top 5 first canonical pathways ranking according to significance level [Fisher exact test es log (p-value) reported in red] modulated by the GO and GONH2 in T cell (Jurkat cell lines) and monocytes (THP1 cell lines) cell lines identified using Ingenuity Pathway Analysis (IPA). The Z-score of each pathway is expressed under each column.

288

## Curated GEO dataset collection for discovery and validation of breast cancer immune phenotypes

*Wouter Hendrickx*<sup>1</sup>, *Jessica Roelands*<sup>1</sup>, *Sabri Boughorbel*<sup>1</sup>, *Julie Decock*<sup>2</sup>, *Scott Presnell*<sup>3</sup>, *Ena Wang*<sup>5</sup>, *Franco M Marincola*<sup>1</sup>, *Peter Kuppen*<sup>4</sup>, *Michele Ceccarelli*<sup>5</sup>, *Darawan Rinchai*<sup>1</sup>, *Damien Chaussabel*<sup>1</sup>, *Lance Miller*<sup>6</sup>, *Davide Bedognetti*<sup>1</sup>

<sup>1</sup>Sidra Medical and Research Center, Doha, Ad Dawhah, Qatar

<sup>2</sup>Qatar Biomedical Research Institute (QBRI), Doha, Ar Rayyan, Qatar

<sup>3</sup>Benaroya Research Institute, Seattle, WA, USA

<sup>4</sup>Leiden University Medical Center, Leiden, Zuid-Holland, Netherlands

<sup>5</sup>Qatar Computing Research Institute, Doha, Ad Dawhah, Qatar

<sup>6</sup>Wake Forest School of Medicine, Winston-Salem, NC, USA

### Background

Sharing of -omics data has become the default modus operandi in recent years, with many funding sources and journals requiring authors to deposit their data in public repositories. This has led to a wealth of available datasets for *in silico* analysis or validation of new findings. To date, over 65,000 studies were deposited in the NCBI Gene Expression Omnibus (GEO) of which more than 1200 relate to breast cancer. However, these repositories are accompanied

with minimal analysis and/or limited built-in visualization features in addition, offline analysis is relying on elevated bio-informatics skills. In order to make these datasets more accessible and interactive, we developed a web application called gene expression browser or GXB [1].

### Methods

As a pilot project, we uploaded the GEO datasets we recently used to validate breast cancer immune subtypes to the GXB application and annotated the datasets collating data from the GEO database entries, the matching publications and added our own immune gene clustering assignments [2, 3].

### Results

A total of 2178 samples were imported as part of 14 GEO datasets, 1728 of which were used in our validation set. One dataset (GSE9151) was deposited in GEO in an incompatible format and had to be reprocessed from the raw CELL files into a normalized expression matrix. Adding group sets for clinical features, immunological gene clusters and generating matching gene rank lists will allow the users to quickly visualize differentially expressed genes. The addition of extra overlay data will enable the user to investigate correlations between phenotypic features. An example of the visualizations available in this application is demonstrated in Figure 1.

### Conclusions

The web application and the data set collection presented here demonstrate how data that is now secluded from many scientists can be made available in a more comprehensive and visually compelling environment. This approach will contribute to more effective data sharing and increased reproducibility of downstream bioinformatics pipelines.

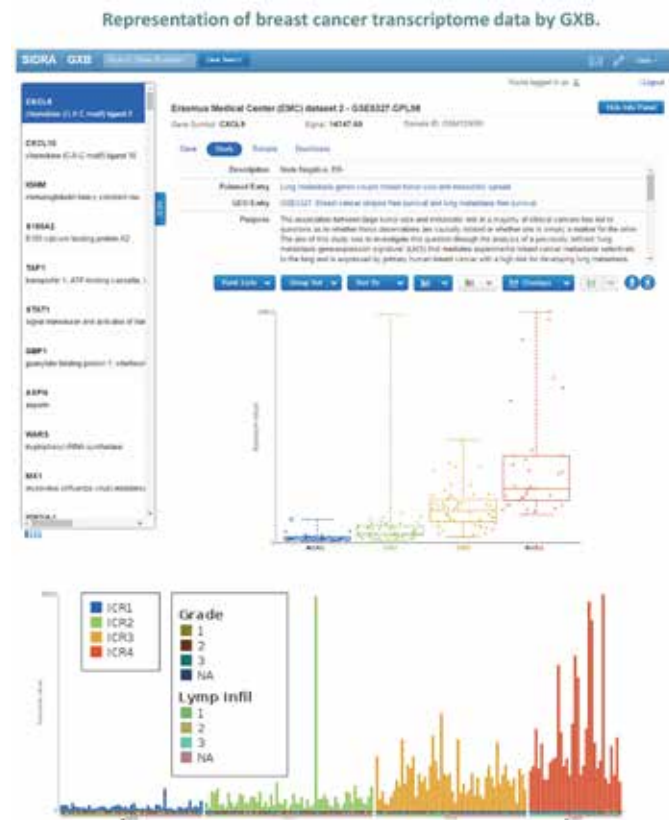
### References

1. Speake C, *et al*: **An interactive web application for the dissemination of human systems immunology data.** *J Transl Med* 2015, **13**:196.
2. Miller LD, *et al*: **Immunogenic subtypes of breast cancer delineated by gene classifiers of immune responsiveness.** *Cancer Immunol Res* 2016, **4**(7):600-610.
3. <http://breastcancer.gxbsidra.org/dm3/geneBrowser/list>
4. Simeone I, *et al*: **Toward the identification of genetic determinants of breast cancer immune responsiveness.** *J Immunother Cancer* 2015, **3**(Suppl 1):P1.

## Immunogenomics and Oncogenetics

Presenting author underlined; Primary author in italics

**Figure 1. Representation of breast cancer transcriptome data by GXB**



Example of CXCL9 gene expression visualization either by annotated bar chart or box-plot.

289

### Identifying patient-specific neopeptides for vaccine immunotherapy reveals rarely shared recurrent neopeptides

Andrew Nguyen<sup>1</sup>, J Zachary Sanborn<sup>2</sup>, Charles Vaske<sup>2</sup>, Shahrooz Rabizadeh<sup>2</sup>, Kayvan Niazi<sup>2</sup>, Steven Benz<sup>2</sup>

<sup>1</sup>NantOmics, San Jose, CA, USA

<sup>2</sup>NantOmics, Santa Cruz, CA, USA

#### Background

Targeted therapies for breast cancers such as trastuzumab and everolimus have durable clinical benefits for patients that express the relevant biomarkers (HER2 and mTOR respectively). Triple negative breast cancer patients lack these biomarkers and are left with few options. Recent advances in immunotherapy agents against PD-1/CTLA-4 for patients with melanoma have yielded amazing clinical benefits for a subset of patients and may have similar results in breast cancer patients, but again the vast majority of patients still undergo disease progression. We analyzed whole genome sequencing

and RNA sequencing data from The Cancer Genome Atlas (TCGA) to identify neopeptides across all cancer patients that could be used to develop next-generation, patient-specific cancer immunotherapies. Neopeptides are tumor-specific markers that arise from mutations acquired from cancer and may represent a path to targeted therapies.

#### Methods

We analyzed 750 cancer patients from TCGA, containing a mixture of 23 different cancer classifications. These cancer patient samples were selected by the availability of whole genome sequencing (WGS) data, RNA-sequencing data as well as clinical outcome data.

#### Results

We identified an average of 680 potential neopeptides per patient based solely on WGS data. To further refine and select high quality neopeptides we restricted these neopeptides based on gene expression yielding an average of 304 expressed neopeptides per patient. We predicted each patient's HLA typing using only omics data, which we then used to predict HLA-expressed neopeptide binding analysis resulting in an average of 11 high-quality tumor specific neopeptides per patient. We identified few recurrent neopeptides that were bound and expressed, indicating the need for a personalized medicine approach.

#### Conclusions

Within the TCGA dataset, the majority of neopeptides among patients with breast cancer were unique to each patient. Rarely within subsets of breast cancers such as HER2+, do we identify neopeptides that are shared between patients. For cancer patients who do not respond to targeted therapies, high-throughput identification of neopeptides could serve as the basis for the development of next-generation, patient-specific immunotherapies.

290

### A genome-scale CRISPR screen to identify essential genes for T cell based cancer therapies

Shashank Patel, Nicholas Restifo

National Cancer Institute, Bethesda, MD, USA

#### Background

In responding to immune selection pressure mediated by T cells, somatic mutations can function in a bi-directional manner. On one hand, somatic mutations give rise to neoantigens capable of eliciting potent T cell responses. On the other hand, loss-of-function mutations or downregulation of gene expression in the tumor cell can also contribute to an immune evasion against T cells. Limited evidence exists on which gene perturbations in human cancer can directly or indirectly impair T cell mediated cytotoxicity.



# Immunogenomics and Oncogenetics

Presenting author underlined; Primary author in italics

## Methods

To identify the genes essential in tumors to elicit a T cell-mediated cytolytic response, we developed a 'two cell-type' (2CT) CRISPR assay system consisting of human T cells as effectors and tumor cells as targets. We combined CRISPR-Cas9 screen datasets with TCGA gene expression datasets from >10,000 patient biopsies to study the patterns of immune sensitivity in human cancers.

## Results

Using the 2CT genome-scale perturbation screen in melanoma cells, we identified and validated multiple genes whose loss impaired the effector function of T cells. Moreover, we uncover a group of core genes from these screens that correlates with cytolytic activity across the majority of the cancer types, reflecting context independence of these genes in the modulation of inherent T cell responses in multiple cancers. This dataset can be utilized to stratify patients for T cell based immunotherapies, and also for studying emergence of novel immune escape mechanisms.

## Conclusions

This study demonstrates the broad applicability of 2CT CRISPR screens to study the interaction of cancer cells with immune cells and identify novel therapeutic targets for cellular therapies.

## 291

### A non-invasive approach to assess tumor mutation load for treatment with cancer immunotherapy

*James White*, Sam Angiuoli, Mark Sausen, Sian Jones, Maria Sevdali, John Simmons, Victor Velculescu, Luis Diaz, [Theresa Zhang](#)

Personal Genome Diagnostics, Baltimore, MD, USA

## Background

Checkpoint inhibitors yield a significant clinical benefit for a subset of cancer patients. Given the high cost of these therapies and the time required to determine whether a therapy is efficacious, tests that can identify patients who are most likely to benefit are urgently needed. Supported by a strong biological rationale, tumor mutational load has emerged as a robust determinant of clinical benefit for multiple checkpoint inhibitors in multiple cancer types. However, existing approaches for assessment of tumor mutational load are expensive and rely on tumor specimens that are not readily available or may yield insufficient material for mutational load analyses.

## Methods

We initiated the development of MutatorDetect, a plasma-based, non-invasive, cost effective method that can accurately identify late stage cancer patients whose tumors

have high mutational load, regardless of the availability of tumor specimens. Previously, we have successfully developed an ultrasensitive platform for mutation detection using hybrid capture methodology and next generation sequencing. The platform is able to interrogate large exonic regions and detect cancer mutations from circulating cell free tumor DNA (ctDNA) in plasma with high sensitivity and specificity.

## Results

We are currently implementing MutatorDetect using this platform and will present preliminary analytical and clinical validation data.

## Conclusions

Further studies are warranted to examine MutatorDetect's performance in assessing tumor mutational load in large cohorts of late stage cancer patients and identifying patients who are likely to respond to checkpoint inhibitors.

## 292

### Profiling abscopal regression in a pediatric fibrosarcoma with a novel EML4-NTRK3 fusion using immunogenomics and high-dimensional histopathology

[Jennifer S Sims](#)<sup>1</sup>, Sunjay M Barton<sup>1</sup>, Robyn Gartrell<sup>1</sup>, Angela Kadenhe-Chiweshe<sup>1</sup>, Filemon Dela Cruz<sup>1</sup>, Andrew T Turk<sup>1</sup>, Yan Lu<sup>1</sup>, Christopher F Mazzeo<sup>2</sup>, Andrew L Kung<sup>1</sup>, Jeffrey N Bruce<sup>1</sup>, Yvonne M Saenger<sup>3</sup>, Darrell J Yamashiro<sup>1</sup>, *Eileen P Connolly*<sup>1</sup>

<sup>1</sup>Columbia University Medical Center, New York, NY, USA

<sup>2</sup>Fordham University, New York, NY, USA

<sup>3</sup>New York Presbyterian/Columbia University Medical Center, New York, NY, USA

## Background

The abscopal effect, or simultaneous tumor regression at multiple sites, is believed to result from the migration of T cells activated at the primary site to the distal sites. We have studied the case of a 1-year-old boy with congenital fibrosarcoma (forearm) bearing a novel EML4-NTRK3 fusion [1] who developed lung tumors 6 months after resection of the initial tumor. He received fractionated radiation therapy (RT) to the right lung only, but experienced complete regression of both right and left lung tumors.

## Methods

Using whole exome sequencing (WES), high-throughput sequencing of peripheral and infiltrating T cell receptor repertoires (TCRseq), and multiplex immunohistochemistry (mIHC) using MANTRA (for biomarkers DAPI, CD3, CD4, CD8, CD68, HLA-DR, and Ki67), we investigated the relationship between tumor progression and metastasis, the pre- and post-treatment microenvironment, and the co-evolution of the tumor-infiltrating immune cell populations in this patient.



## Immunogenomics and Oncogenetics

Presenting author underlined; *Primary author in italics*

### Results

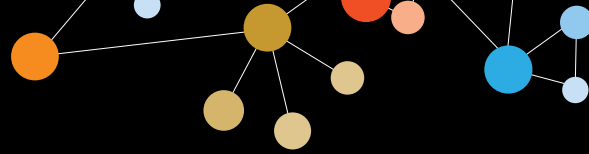
Comparative WES of the initial fibrosarcoma and subsequent lung tumors identified the same EML4-NTRK3 fusion, validating their metastatic relationship, as well as the evolution of additional coding mutations upon recurrence. By both traditional and multiplex immunohistochemistry, the primary fibrosarcoma and pre-radiotherapy lung tumor were infiltrated by a very low density of CD4+ and CD8+ T cells. This infiltration was markedly increased (both CD4+ and CD8+ T cells) post-radiotherapy, particularly in the non-irradiated lung lesion, which is consistent with the model that abscopal regression depends on infiltration by trans-acting anti-tumor T cells. TCRseq of the TIL populations revealed little similarity between those of the primary fibrosarcoma and the lung lesions. However, the TCR repertoires of the irradiated and non-irradiated sites following radiotherapy showed substantial similarity, sharing a larger percentage of CDR3 sequences with one another (6.7% of combined total) than with the primary tumor ( $\leq 0.6\%$  combined total) or the pre-radiotherapy lung tumor ( $\leq 1.6\%$  combined total). Furthermore, the breadth of the TIL repertoire and its binding-associated divergence from the peripheral blood was greatest in the irradiated lung tumor following radiotherapy, suggesting a direct link between the evolution of trans-acting immunity and antigen-driven immunogenicity at that site.

### Conclusions

Our results, particularly anti-tumor T cell specificities shared inside and outside of the radiation field, offer key insights into the mechanisms underlying abscopal tumor regression, which may in turn be targeted for enhancement through immunotherapy.

### References

1. Tannenbaum-Dvir S, *et al*: **Characterization of a novel fusion gene EML4-NTRK3 in a case of recurrent congenital fibrosarcoma.** *Cold Spring Harb Mol Case Stud* 2015, **1(1)**:a000471.



## Inflammation, Innate Immunity, and the Microbiome

Presenting author underlined; *Primary author in italics*

293

### **Cyclic dinucleotides activating STING are a safe and effective treatment for premalignant tumors**

Jason Baird<sup>1</sup>, Marka Crittenden<sup>2</sup>, David Friedman<sup>1</sup>, Hong Xiao<sup>3</sup>, Rom Leidner<sup>1</sup>, Bryan Bell<sup>1</sup>, Kristina Young<sup>2</sup>, Michael Gough<sup>2</sup>

<sup>1</sup>Earle A. Chiles Research Institute, Robert W. Franz Cancer Center, Providence Portland Medical Center, Portland, OR, USA

<sup>2</sup>Earle A. Chile Research Institute, Portland, OR, USA

<sup>3</sup>Providence Portland Medical Center, Portland, OR, USA

#### **Background**

As our ability to detect cancer improves, there is an opportunity to treat early tumors before they become invasive and metastatic. Most cancers are known to exhibit a premalignant state, where an expanded population of mutated cells disrupts normal tissue organization. This premalignant state can exist for years and may remain, resolve, or progress into invasive cancer. Cancer screening programs, for example those based around the Pap smear for cervical carcinoma, aim to identify these abnormal cells for intervention before further malignant transformation. HPV+ tumors represent a large proportion of anal, vulvar, vaginal, cervical, and head and neck carcinomas. Vaccination against human papilloma virus (HPV) can prevent HPV infection and thus prevent HPV-associated malignancies. However, once tumors develop, vaccination against the virus does not impact tumor progression. Current therapies for a positive pap smear include excision of the abnormal region, or ablation by freezing or lasers. Immunotherapies, including interferon alpha and imiquimod have been added to excisional therapies to decrease the rate of recurrence; however, in randomized clinical trials it was found that neither approach impacts the rate of recurrence of cervical dysplasia.

#### **Methods**

In the transgenic mouse model carrying the mutant tumor-driving genes Kras(G12D) and p53(R172H) that are controlled by expression of Cre under a pancreas-specific promoter, this results in progressive carcinogenesis through pancreatic intraepithelial neoplasia to pancreatic ductal adenocarcinoma. In addition, due to leaky expression of Cre, at variable penetrance these mice spontaneously develop papilloma of the face and vulva. In these mice the normal skin undergoes epidermal thickening that closely resembles HPV-associated papilloma in humans. Since innate immune molecules, such as interferon alpha, and innate stimuli, such as imiquimod, have shown efficacy but failed in randomized studies, there is a need for novel approaches to treat premalignant disease and this mouse model represents a novel model system to test new therapies.

#### **Results**

Recently, we and others have demonstrated that novel agents that activate the STimulator of INterferon Genes (STING) are strong inducers of type I IFN and TNF $\alpha$  and can cause rapid regression of a range of advanced tumors. For these reasons, we tested the effect of STING ligands on papilloma in mice.

#### **Conclusions**

We tested the effect of STING ligands on papilloma in mice. Treatment with STING ligands causes rapid regression of spontaneous murine papilloma, and may represent an advance in treatment of virus-associated and premalignant diseases.

294

### **Inflammatory activation via PKC-Syk pathway in macrophages lacking CD47-SIRP $\alpha$ restraint initiates potent phagocytosis toward cancer**

Zhen Bian, Koby Kidder, Yuan Liu

Georgia State University, Atlanta, GA, USA

#### **Background**

The CD47-SIRP $\alpha$  interaction serves as the critical self-recognition mechanism in macrophage phagocytosis toward self-cells through inhibitory signaling via SIRP $\alpha$  cytoplasmic ITIMs and tyrosine phosphatase SHP-1/2. This signaling axis, thus, prevents macrophage phagocytosis toward cancer cells, which exploit this mechanism by upregulating expression of CD47 to evade immunological eradication. Despite this mechanism being suggestively imperative, deficiency of CD47-SIRP $\alpha$  does not manifest enhanced macrophage phagocytosis toward self- or cancer cells. Therefore, this phenomenon suggests that the CD47-SIRP $\alpha$  mechanism alone provides little insight necessary to explain when macrophages would target self- or cancer cells, which bear no 'eat-me' signal and thus do not activate macrophage phagocytosis.

#### **Methods**

Establishment of SIRP $\alpha$ <sup>-/-</sup> mice. *Ex vivo* and *in vivo* determination of macrophage phagocytosis toward self- and cancer cells (i.e., B16 melanoma, MC38 colon cancer, LLC lung cancer and EL4 lymphoma). Identification of signaling mechanisms that activate macrophage phagocytosis toward self-cells.

#### **Results**

Mice depleted of SIRP $\alpha$  display activated macrophage phagocytosis toward self-RBC or engrafted B16 and LLC tumors under inflammatory conditions and/or treatment by LPS/IL-17. *Ex vivo* phagocytosis assays demonstrate that macrophages from SIRP $\alpha$ <sup>-/-</sup> or CD47<sup>-/-</sup>, and even WT

## Inflammation, Innate Immunity, and the Microbiome

Presenting author underlined; *Primary author in italics*

mice, are generally incompetent to attack self-cells albeit aggressive toward bacteria, fungi, apoptotic cells and immune complexes. Treatment of macrophages with IL-17, LPS, IL-6, IL-1 $\beta$  or TNF $\alpha$ , but not IFN $\gamma$ , markedly initiates potent phagocytosis toward self which leads to macrophage-mediated eradication of B16, LLC, MC38, and EL4 cancer cells, providing an absence of the CD47-SIRP $\alpha$  restraint. Capitalizing on cytokine/LPS-activated SIRP $\alpha$ <sup>-/-</sup> macrophages targeting CD47-expressing cells, we enlist these macrophages against B16 melanoma and demonstrate complete elimination of lung metastases in SIRP $\alpha$ <sup>-/-</sup> mice and in WT mice into which SIRP $\alpha$ <sup>-/-</sup> macrophage-induced cancer immunity has been adoptively transferred. Mechanistic studies suggest that a PKC-Syk-mediated signaling pathway, to which IL-10 conversely inhibits, is required for activating macrophages toward cancer cells.

### Conclusions

These findings demonstrate for the first time that macrophage phagocytosis toward cancer requires activation by inflammatory cytokines/factors that stimulate the PKC-Syk pathway. The ramifications to arise from the combination of both phagocytic activation and perturbation of the CD47-SIRP $\alpha$  interaction would lead to the eradication of cancer, especially toward those which therapeutic antibodies are yet unavailable. (*The work is currently in press for publishing in PNAS.*)

295

### Anti-leukemia immunity following STING agonist therapy requires a type I interferon-independent mechanism

Emily Curran<sup>1</sup>, Xiufen Chen<sup>2</sup>, Leticia P Corrales<sup>1</sup>, Justin Kline<sup>3</sup>

<sup>1</sup>University of Chicago, Chicago, IL, USA

<sup>2</sup>Department of Medicine, University of Chicago, Chicago, IL, USA

<sup>3</sup>Committee on Immunology and Department of Medicine, University of Chicago, Chicago, IL, USA

### Background

The Stimulator of Interferon Genes (STING) pathway has been implicated as a major mechanism by which the host innate immune system “senses” cancer. STING pathway activation leads to the production of several downstream cytokines, most notably type I interferon (IFN), which is essential for bridging innate and adaptive immune responses against solid tumors. Administration of STING agonists induces broad immunity against transplanted solid malignancies in a type I IFN-dependent manner. We have recently demonstrated potent efficacy of systemic STING agonist therapy in murine AML models. Unlike the activity of STING agonists in solid tumor models, we observed a major type I IFN-independent effect in mice with AML, leading us to hypothesize that other

cytokines may be important for the effectiveness of STING agonist therapy in mice with systemic leukemia.

### Methods

C1498 AML cells engineered to express the model SIY peptide antigen (C1498.SIY) were inoculated intravenously into syngeneic C57BL/6 or *Ifnar*<sup>-/-</sup> mice and mice were treated with the selective murine STING agonist, DMXAA (5,6-dimethylxanthenone-4-acetic acid), or vehicle control.

### Results

Surprisingly, SIY/K<sup>b</sup> pentamer and intracellular cytokine staining followed by flow cytometric analysis revealed a similarly marked expansion of functional SIY-reactive CD8<sup>+</sup> T cells in both wildtype and *Ifnar*<sup>-/-</sup> mice. Survival following DMXAA treatment was significantly prolonged in wild-type, and to a lesser extent, in *Ifnar*<sup>-/-</sup> mice, suggesting that other downstream cytokines, such as TNF- $\alpha$  or IL-6 may partially mediate STING-dependent immune effects in leukemia-bearing hosts. For example, STING pathway activation led to significantly increased TNF- $\alpha$  levels in both wildtype and *Ifnar*<sup>-/-</sup> mice (3-fold and 6-fold, respectively). Based on the known inflammatory and immune-activating properties of TNF- $\alpha$ , we speculate that it may also be contributing to the positive effects of STING activation in leukemia.

### Conclusions

Collectively, our data demonstrate that STING-mediated enhancement of anti-leukemia immunity are at least partially independent of type I IFN. In addition to type I IFN, other cytokines/pathways appear to be required to mediate the powerful immunotherapeutic effect of STING agonists in AML. TNF- $\alpha$  is significantly increased following STING activation and may be mediating these effects, but further investigation is needed. Finally, these results imply that the mechanisms by which STING activation mediates anti-cancer effects may differ considerably between solid and hematologic malignancies.

296

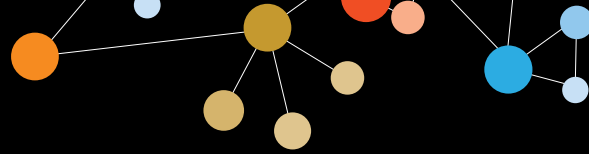
### Opposing roles of natural killer cell subsets in a mouse model of acute myeloid leukemia and hematopoietic stem cell transplant

Cordelia Dunaj, Ethan G Aguilar, Lam T Khuat, William J Murphy

University of California, Davis, Sacramento, CA, USA

### Background

Natural killer (NK) cells are lymphocytes that bridge innate and adaptive immune responses. The activity of NK cells is controlled by the integration of activating and inhibitory signals. NK cells can be divided into subsets termed licensed and unlicensed based on the expression of inhibitory



## Inflammation, Innate Immunity, and the Microbiome

Presenting author underlined; *Primary author in italics*

receptors with varying affinity for MHC class I molecules. In general, licensed NK cells have higher cytotoxic potential than unlicensed NK cells. Hematopoietic stem cell transplant (HSCT) is a treatment for a number of hematological malignancies, including acute myeloid leukemia (AML). Patients who are not eligible to receive intensive cytoreductive therapy, are at risk for primary refractory disease, or are experiencing relapse, are all candidates for HSCT. NK cells are the first lymphocytes to recover post-HSCT and have been shown to be critical for an anti-leukemia response. Here we investigate the contribution of NK cell subsets to anti-leukemia responses in the context of a mouse model of HSCT.

### Methods

C1498 acute myelogenous leukemia cells were administered to control mice and mice that received total body irradiation followed by syngeneic HSCT. Monoclonal antibodies were used to deplete the licensed or unlicensed NK cell subsets (anti-Ly49C/I and anti-Ly49G2, respectively). Survival was monitored continuously and immune reconstitution was characterized by flow cytometry on days 17 and 24 post-C1498 administration.

### Results

Control mice with intact immune systems survived with AML longer than HSCT mice. In control mice, the depletion of licensed or unlicensed NK cells did not significantly affect survival time. However, in HSCT mice, the depletion of the unlicensed NK cell subset resulted in statistically significant prolonged survival when compared to licensed-depleted and non-depleted controls, suggesting an antagonistic role for unlicensed NK cells in combating AML post-HSCT. Immune phenotyping showed that unlicensed depletion led to increased numbers of the licensed population post-HSCT, without the same reciprocal expansion of unlicensed NK cells with licensed depletion.

### Conclusions

Unlicensed NK cells limit the expansion of licensed NK cell post-HSCT, which has a detrimental effect on survival after C1498 challenge. NK cell subsets have non-overlapping roles, with the licensed playing the dominant anti-leukemia role post-HSCT, and the unlicensed negatively regulating the response of the licensed. Modulation of these opposing roles may be advantageous for clinical use of HSCT and NK cell therapies.

297

### **Harnessing tumor associated macrophages with a novel compound to enhance chemotherapy and checkpoint blockade in breast cancer**

Jennifer Guerriero<sup>1</sup>, Alaba Sotayo<sup>1</sup>, Holly Ponichtera<sup>2</sup>, Alexandra Pourzia<sup>1</sup>, Sara Schad<sup>1</sup>, Ruben Carrasco<sup>1</sup>, Suzan Lazo<sup>1</sup>, Roderick Bronson<sup>3</sup>, Anthony Letai<sup>1</sup>

<sup>1</sup>Dana-Farber Cancer Institute, Boston, MA, USA

<sup>2</sup>Evelo Biosciences, Cambridge, MA, USA

<sup>3</sup>Harvard Medical School, Boston, MA, USA

### Background

The breast tumor environment is complex and includes both neoplastic and immune cells. The most abundant immune cell population within breast tumors is tumor associated macrophages (TAMs). Macrophages have the ability to polarize into either M1 cells, which have potent anti-tumor capabilities, or M2 macrophages which promote tumor progression by stimulating tumor vasculature, invasion, metastasis, and can enhance tumor resistance to chemotherapy. Generally TAMs in breast tumors are considered M2 macrophages and a high tumor density of TAMs clinically correlates to both overall worse prognosis and increased metastasis. Several therapeutic strategies exist to modulate TAMs clinically, focusing on depleting or inhibiting TAMs. However, macrophage are required for optimal tumor regression in response to both chemotherapy and immunotherapy. Their embedded location and their untapped potential provide impetus to the discovery of strategies to turn them against tumors and to harness for cancer therapy. Therefore here, we describe a novel method to polarize pro-tumor macrophages to an anti-tumor phenotype.

### Methods

We recently reported that a first in class selective class IIa HDAC inhibitor (TMP195) influenced human monocyte responses to colony stimulating factors CSF-1 and CSF-2 *in vitro*. Here, we utilize a macrophage-dependent autochthonous mouse model of breast cancer to demonstrate that *in vivo* TMP195 treatment alters the tumor microenvironment and reduces tumor burden and pulmonary metastases through macrophage modulation.

### Results

TMP195 induces recruitment and differentiation of highly phagocytic and stimulatory macrophages within tumors. Furthermore, combining TMP195 with chemotherapy regimens or T cell checkpoint blockade in this model significantly enhances the durability of tumor reduction.

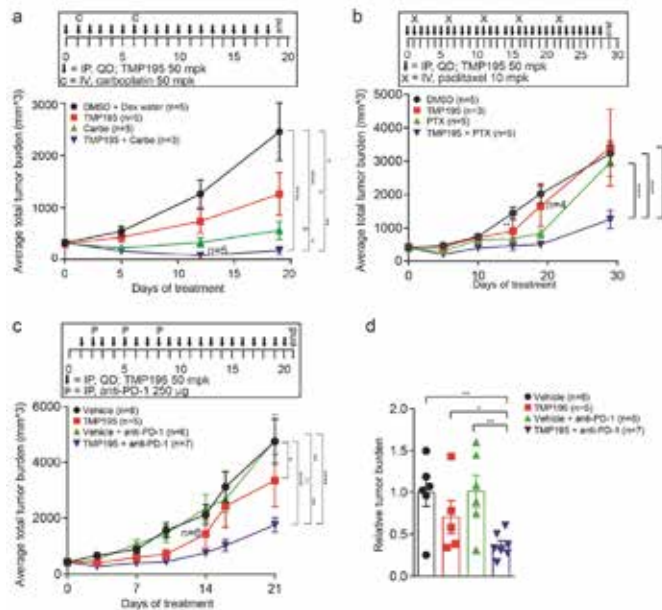
## Inflammation, Innate Immunity, and the Microbiome

Presenting author underlined; Primary author in italics

### Conclusions

These data introduce class IIa HDAC inhibition as a novel means to harness the anti-tumor potential of macrophages to enhance cancer therapy.

Figure 1.



298

### Interferon production and immunity elicited by a constitutively active form of interferon-beta promoter stimulator-1 (IPS-1)

Richard S Kornbluth<sup>1</sup>, Sachin Gupta<sup>2</sup>, James Termini<sup>2</sup>, Elizabeth Guirado<sup>2</sup>, *Geoffrey W Stone*<sup>2</sup>

<sup>1</sup>Receptome, LLC, La Jolla, CA, USA

<sup>2</sup>Miller School of Medicine, University of Miami, Miami, FL, USA

#### Background

Type I interferon (IFN) promotes the activity of anti-tumor CD8+ T cells. IFN induced by intratumoral injections of stimulator of interferon genes (STING) activators has shown remarkable efficacy as a “gas pedal” when combined with PD-1/PD-L1 checkpoint blockade in mouse models. Like STING, IPS-1 (also called MAVS, Cardif, or VISA) can lead to strong IFN production. IPS-1 is normally activated by viral RNAs bound to RIG-I which in turn modifies IPS-1 so that it clusters onto the surface of mitochondrial membranes. To circumvent the need for RIG-I, this study fused IPS-1 with the membrane clustering, N-terminal region of EBV latent membrane protein 1 (LMP1).

#### Methods

The N-terminus of the Epstein-Barr virus (EBV) LMP1 protein contains 6 transmembrane domains that self-associate and cluster in membranes. Genetically fusing this N-terminal region to IPS-1 forms LMP1-IPS-1 which is a constitutively activated form of IPS-1. The resulting nucleic acid sequence was tested either as mRNA, plasmid DNA, or by viral delivery using adenovirus 5 (Ad5) (Ad5-LMP1-IPS-1).

#### Results

Human dendritic cells transduced with Ad5-LMP1-IPS-1 upregulated CD80 and CD86 and produced large amounts of IL-12 and TNF. 293 cells transfected with LMP1-IPS-1 plasmid DNA produced high levels of IFN- $\alpha$ , IFN- $\beta$ , and chemokines. By microarray analysis, mRNAs for IFN-associated genes were strongly upregulated. *In vivo*, mice vaccinated with Ad5-LMP1-IPS-1 plus Ad5 expressing HIV Gag were completely protected from vaccinia-Gag challenge virus.

#### Conclusions

LMP1-IPS-1 shares similar activities with activated STING. Whereas STING activators are small molecules, LMP1-IPS-1 is constitutively active and its nucleic acid sequence can be used as mRNA, plasmid DNA, part of a viral vector, or the payload of an “armed” oncolytic virus.

#### Acknowledgements

Supported by NIH grant R21AI093294 and Florida Dept. Health Technology Transfer Feasibility Award 4KF03.

#### References

- Gupta S, Termini JM, Issac B, Guirado E, Stone GW: **Constitutively Active MAVS Inhibits HIV-1 Replication via Type I Interferon Secretion and Induction of HIV-1 Restriction Factors.** *PLoS ONE* 2016, **11(2)**:e0148929.

299

### Modulation of Fc $\gamma$ receptor function by HLA-G

Christina Meyer<sup>1</sup>, Laura Helming<sup>2</sup>, Joseph Tumang<sup>3</sup>, Nicholas Wilson<sup>4</sup>, Robert Hofmeister<sup>5</sup>, Laszlo Radvanyi<sup>1</sup>

<sup>1</sup>EMD Serono, Billerica, MA, USA

<sup>2</sup>Merck KGaA, Darmstadt, Hessen, Germany

<sup>3</sup>Compass Therapeutics, Cambridge, MA, USA

<sup>4</sup>Agenus Inc., Lexington, MA, USA

<sup>5</sup>TCR2 Therapeutics, Cambridge, MA, USA

#### Background

HLA-G is a non-classical major histocompatibility complex (MHC) molecule expressed at the fetal maternal interface and in tumors, where it exerts immunomodulatory effects. These immunosuppressive effects are mediated through interactions of HLA-G with its receptors, ILT2 and ILT4, which are expressed primarily on cells of the myeloid lineage. To further understand the effect of tumor HLA-G expression on





## Inflammation, Innate Immunity, and the Microbiome

Presenting author underlined; *Primary author in italics*

myeloid immune suppression, we investigated the effect of HLA-G on Fcγ receptor signaling—a myeloid effector function which has important implications in the immune response to tumors and the effect of antibody-based therapeutics.

### Methods

Using an inducible HLA-G-expressing tumor cell line and tumor-specific antibody, we examined Fcγ receptor effector functions in a human monocyte-like cell line as well as in primary human monocytes and macrophages.

### Results

We found that HLA-G inhibits signaling downstream of FcγR activation in a monocytic cell line and in primary monocytes. Furthermore, HLA-G expression on tumor target cells results in inhibition of antibody-dependent phagocytosis by macrophages as well as decreased FcγR-induced production of inflammatory cytokines. These effects were dependent on HLA-G interaction with its receptors, ILT2 and ILT4.

### Conclusions

Our findings suggest a role for HLA-G in promoting tumor immune escape, as well as a novel mechanism for HLA-G-mediated inhibition of antibody-based tumor cell phagocytosis by macrophages.

### 300 Presidential Travel Award Recipient

#### Intestinal microbiota and relapse after hematopoietic-cell transplantation

Jonathan Peled, Sean Devlin, Anna Staffas, Melissa Lumish, Kori Porosnicu Rodriguez, Katya Ahr, Miguel Perales, Sergio Giralt, Ying Taur, Eric Pamer, Marcel R. M. van den Brink, Robert Jenq

Memorial Sloan Kettering Cancer Center, New York, NY, USA

#### Background

The major causes of mortality after allogeneic hematopoietic-cell transplantation (allo-HCT) are relapse, graft-versus-host disease (GVHD), and infection. We have previously reported that alterations in the intestinal flora are associated with GVHD, bacteremia, and reduced overall survival after allo-HCT. As intestinal bacteria are potent modulators of systemic immune responses including antitumor effects triggered by checkpoint blockade, we hypothesized that components of the intestinal flora could be associated with relapse after allo-HCT.

#### Methods

The intestinal microbiota of 541 patients admitted for allo-HCT was profiled by means of 16S ribosomal sequencing of prospectively collected stool samples. We hypothesized that evolutionarily related species exhibit functional similarities, and we therefore defined clusters of related operational taxonomic units (cOTUs) to evaluate for associations with

clinical outcomes. To group OTUs by evolutionary distances, a phylogenetic tree was empirically constructed from a sequence alignment of all OTUs identified in the whole cohort (Figure 1). We examined the relationship between abundance of microbiota species or groups of related species and relapse/progression of disease during two years of follow-up after allo-HCT using cause-specific Cox proportional hazards in a retrospective discovery-validation study (Figure 2).

#### Results

The intestinal presence of a group comprised mostly of *Eubacterium limosum* in the validation set was associated with less relapse/progression of disease (HR 0.52, CI 0.31–0.87,  $p = 0.01$ , Figure 3). The two-year cumulative incidence of relapse/progression among patients with and without this group of bacteria was 33.8% and 19.8%, respectively. The relative abundance of this group was also associated with less relapse/progression of disease (HR 0.82, CI 0.71–0.95,  $p = 0.009$ ). These associations remained significant in multivariate models and were strongest among recipients of T cell-replete allografts.

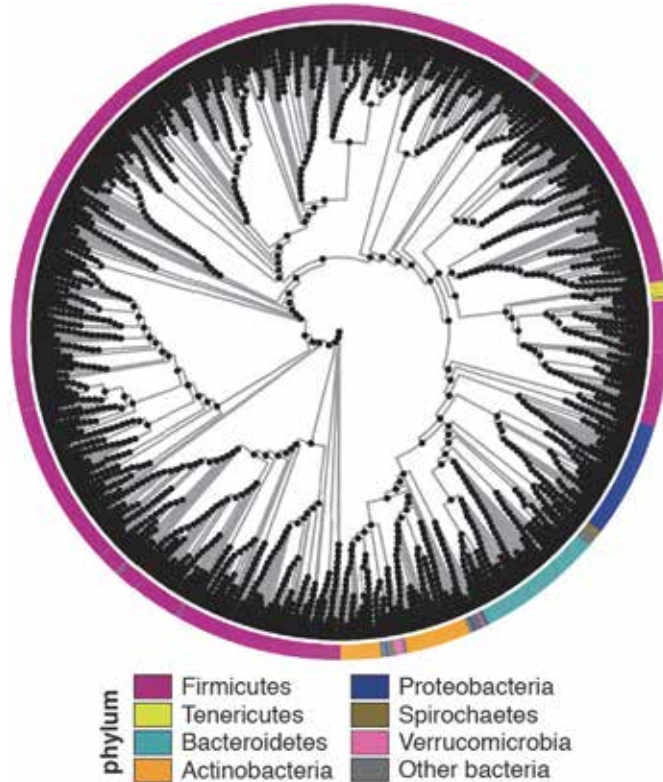
#### Conclusions

We found associations between the abundance of a group of bacteria in the intestinal flora and relapse/progression of disease after allo-HCT. These might serve as potential biomarkers or therapeutic targets to prevent relapse and improve survival after allo-HCT.

## Inflammation, Innate Immunity, and the Microbiome

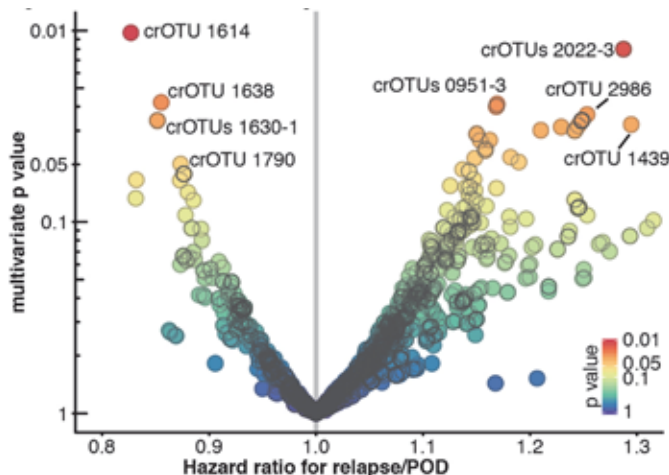
Presenting author underlined; Primary author in *italics*

**Figure 1. Phylogenetic tree of OTUs and clusters of related operational taxonomic units (crOTUs)**



Each black point is a crOTU. Phylum is color coded along the circumference. Members of the same phyla were largely grouped together, indicating that the tree was broadly concordant with standard taxonomy.

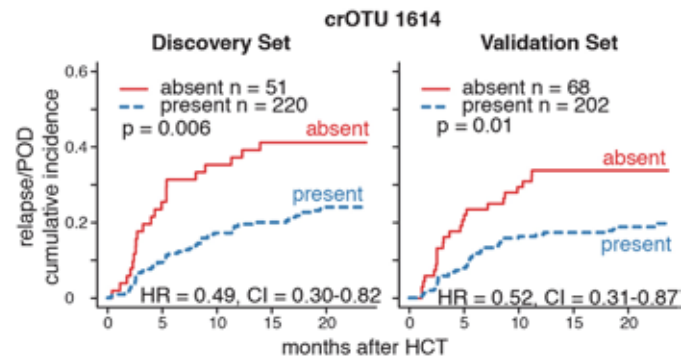
**Figure 2. Multivariate screening of microbial features for association with relapse**



Volcano plot of multivariate p values of crOTUs against the multivariate hazard ratios for relapse/progression of disease

in the discovery set. crOTUs are color coded by p value. Multivariate adjustment was performed for Disease Risk Index score, graft source, and conditioning intensity. The most abundant species in each of the labeled crOTUs are 1614: *Eubacterium limosum*. 2022-3: *Streptococcus sinensis*. 1638: *Eubacterium limosum*. 1630-1: *Eubacterium limosum*. 1790: *Parvimonas micra*. 0951-3: *Leptotrichia hongkongensis*. 2986: *Flavonifractor plautii*. 1439: *Actinomyces odontolyticus*.

**Figure 3. crOTU 1614, which includes members of family Eubacteriaceae is associated with decreased relapse after allo-HCT**



Cumulative incidence of relapse/POD in the discovery (n = 271) and validation (n = 270) sets stratified by presence or absence of crOTU 1614.

### 301

#### Melanoma cells upregulate innate immune genes in response to CTL attack

*Natalie J Neubert*<sup>1</sup>, *Laure Tillé*<sup>1</sup>, *David Barras*<sup>2</sup>, *Charlotte Sonesson*<sup>2</sup>, *Petra Baumgaertner*<sup>1</sup>, *Donata Rimoldi*<sup>1</sup>, *David Gfeller*<sup>1</sup>, *Mauro Delorenzi*<sup>2</sup>, *Silvia A Fuertes Marraco*<sup>1</sup>, *Daniel E Speiser*<sup>1</sup>

<sup>1</sup>University of Lausanne, Ludwig Cancer Research, Epalinges, Vaud, Switzerland

<sup>2</sup>SIB Swiss Institute of Bioinformatics, Lausanne, Vaud, Switzerland

#### Background

T cell-based immunotherapies have brought great progress for cancer patients. However, very little is known about the cancer cell response to cytotoxic T lymphocyte (CTL) attack.

#### Methods

We studied the dynamic T cell-cancer cell interplay. Low passage melanoma cell lines were cultured with MelanA/MART1-specific CD8+ T cells and characterized using differential gene expression analysis and flow cytometry. Specific gene products were investigated by immunohistochemistry and results were interpreted based



## Inflammation, Innate Immunity, and the Microbiome

Presenting author underlined; *Primary author in italics*

on the literature including single cell data from melanoma patients.

### Results

As expected, significant fractions of melanoma cells died in presence of melanoma-specific CD8+ T cells. However, still many melanoma cells persisted for up to three days of co-culture. Characterization of the surviving melanoma cells revealed increased mRNA levels of genes associated with an antimicrobial immune response: *DDX58*, *TLR3*, *AIM2*, *MyD88*, *NFKB*, *IFITM3*, and *ISG15* after co-culture. Upregulation of these genes is known to enhance innate immune responses. DDX58 (also RIG-I) and TLR3 sense intracellular viral RNA, and AIM2 recognizes cytosolic double-stranded DNA. MyD88 acts as an adaptor downstream of TLRs and signals to NFκB. IFITM3, a transmembrane protein, inhibits viral entry into its host and ISG15 has multiple anti-viral roles including induction of NK cell proliferation. These and further gene and protein expression changes were dependent on antigen-specific interaction of CTLs with melanoma cells and were mediated by IFNγ and TNFα, two cytokines secreted by CTLs upon antigen recognition.

### Conclusions

So far, mainly immunosuppressive mechanisms of cancer cells upon exposure to CTLs have been described, such as increased expression of IDO1 and the inhibitory receptor ligand PD-L1. Here we show that in addition to these immunosuppressive mechanisms, melanoma cells respond to melanoma-specific CTLs with a cytokine-driven upregulation of genes involved in the innate immune response, likely also supporting the T cell responses. Moreover, melanoma cells upregulate further immune genes which we will discuss at the congress. Our findings may play a role in immunotherapy, and might explain why immune reactions in cancer patients are often promoting both pro- and anti-tumor immune mechanisms.

### Acknowledgements

We thank J. Joyce, T. Petrova, M. De Palma, and R. Debets for discussions and advice, A. Wilson, C. Fumey, S. Winkler, T. Pillonel, N. Montandon and K. Mühlethaler for technical help, and B. van den Eynde for IDO-specific antibody.

**Not Listed/Other**

Presenting author underlined; *Primary author in italics*

**302****Identification of T cell receptors targeting the intestinal self-antigen and colorectal cancer target GUCY2C by next-generation sequencing**

Tara S Abraham, Bo Xiang, Michael S Magee, Scott A Waldman, Adam E Snook

Thomas Jefferson University, Philadelphia, PA, USA

**Background**

Identifying T cell receptors (TCRs) targeting self-antigens may provide opportunities for effective cancer therapy employing adoptive T cell therapy. However, the enormous diversity of TCRs and low abundance of antigen-specific clones make identification of individual TCRs difficult. Moreover, tolerance further limits self-reactive TCR abundance and affinity.

**Methods**

Here, we define a process to identify TCRs from CD4<sup>+</sup> T cells recognizing the intestinal self-antigen GUCY2C, an emerging target in colorectal cancer immunotherapy. GUCY2C-specific CD4<sup>+</sup> T cells were identified and purified from GUCY2C-immunized mice. Next-generation sequencing of TCR transcripts quantified individual TCRs, permitting synthesis and assembly of TCR constructs that were engineered into CD4<sup>+</sup> T cells.

**Results**

GUCY2C recognition by engineered CD4<sup>+</sup> T cells *in vitro* confirmed TCR specificity and activity. Further, TCR constructs were engineered into purified mouse hematopoietic stem cells (HSCs) *ex vivo*, which were adoptively transferred to HSC-depleted recipient mice. These engineered HSCs gave rise to naïve T cells expressing GUCY2C-specific TCR transgenes, allowing us to validate our *in vitro* findings of GUCY2C recognition following GUCY2C vaccination.

**Conclusions**

This transgenic TCR model system can be employed to define tolerance mechanisms restricting GUCY2C-specific immunotherapy, facilitating 2<sup>nd</sup>-generation GUCY2C vaccine design. Moreover, this approach to identify and validate self-antigen specific TCRs may be employed for cancer immunotherapies, accelerating therapeutic discovery.

**303****Clinical significance of immune-related factors on systemic trafficking of bone marrow-derived stem cells in patients with different types of gastric neoplasms**

Wojciech Blogowski<sup>1</sup>, Ewa Zuba-Surma<sup>2</sup>, Marta Budkowska<sup>3</sup>, Daria Salata<sup>3</sup>, Barbara Dolegowska<sup>4</sup>, Teresa Starzynska<sup>5</sup>

<sup>1</sup>Department of Internal Medicine, University of Zielona Gora, Zielona Gora, Lubuskie, Poland

<sup>2</sup>Department of Medical Biotechnology, Jagiellonian University, Krakow, Poland, Krakow, Malopolskie, Poland

<sup>3</sup>Department of Medical Analytics, Pomeranian Medical University, Szczecin, Zachodniopomorskie, Poland

<sup>4</sup>Department of Microbiology and Immune Diagnostics, Pomeranian Medical University, Szczecin, Zachodniopomorskie, Poland

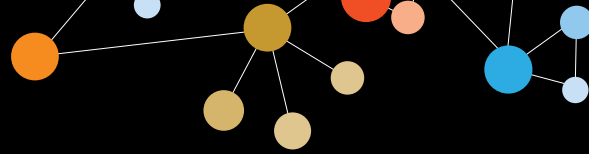
<sup>5</sup>Department of Gastroenterology, Pomeranian Medical University, Szczecin, Poland, Szczecin, Zachodniopomorskie, Poland

**Background**

Gastric neoplasms constitute some of the most commonly occurring and heterogenic tumors, which are associated with a high percentage of mortality among affected individuals. While the most common is gastric cancer, within the gastric tissue, several other types of malignancy may arise, including lymphomas, gastrointestinal stromal tumors, and neuroendocrine neoplasms, which offer much more favorable prognosis. Recently there has been an increased interest in the potential role of bone marrow-derived stem cells (BMSCs) in the development/progression of malignancies in humans. However, currently very little is known about BMSC homeostasis in patients with different types of gastric neoplasms. Therefore, in this study, we wanted to comprehensively examine and compare the peripheral trafficking of different populations of BMSCs in these patients, as well as to (at least preliminarily) elucidate the immune-related substances that might be associated with this phenomenon.

**Methods**

Using FACS analysis supported by ImageStream technique verification, various populations of BMSCs, such as Lin-CD45-CD133+CXCR4+ very small embryonic/epiblast-like stem cells (VSELs), CD45-STRO-1+CD105+ mesenchymal stem cells (MSCs), Lin-CD45+CD133+ hematopoietic stem/progenitor cells (HSPCs), and CD34+/KDR+/CD31+/CD45- endothelial progenitor cells (EPCs), were enumerated and sorted from the peripheral blood samples collected from patients with gastric cancer (n=25) other gastric tumors (GISTs, NENs, lymphomas; n=15) and control individuals (n=20). Plasma levels of stromal-derived factor-1 (SDF-1), complement-



## Not Listed/Other

Presenting author underlined; *Primary author in italics*

derived anaphylatoxins/molecules (C3a, C5a, C5b-9), cytokines (IL-1, IL-6, IL-8, IL-10, IL-17, IL-23, TNF $\alpha$ ), growth factors (HGF, FGF, IGF-1) and immunomodulatory bioactive lipids (sphingosine-1-phosphate-S1P and lipoxin A4) were measured using ELISA.

### Results

Significantly lower numbers of circulating HSPCs and intensified peripheral trafficking of both VSEs and MSCs was observed in patients with gastric cancer but not in those with other types of gastric tumors. The abnormal balance in the peripheral trafficking of BMSCs in patients with gastric cancer was neither associated with the clinical stage of the disease nor with the systemic levels of SDF-1, which were comparable between all analyzed groups. In patients with gastric cancer, significantly increased levels of C5b-9, interleukins (IL-6, IL-8, IL-23), HGF and bioactive lipids (S1P, lipoxin A4) were strongly associated with observed phenomenon of intensified circulation of VSEs and MSCs.

### Conclusions

Abnormal peripheral trafficking of BMSCs occurs in patients with gastric cancer and is specific only for this group of patients suffering from gastric tumors. Selected interleukins, complement cascade-derived molecules, growth factors and bioactive lipids, but not SDF-1, seem to be significant players associated with this phenomenon in humans.

### Acknowledgements

Study financed from POIG.01.01.02-00-109/09 and IP2014003273.

304

### Quantification of natural killer cell-mediated cytotoxicity using Celigo imaging cytometry

Leo Chan<sup>1</sup>, Srinivas Somanchi<sup>2</sup>, Kelsey McCulley<sup>1</sup>, Dean Lee<sup>3</sup>

<sup>1</sup>Nexcelom Bioscience, Lawrence, MA, USA

<sup>2</sup>University of Texas MD Anderson Cancer Center, Houston, TX, USA

<sup>3</sup>Nexcelom Bioscience, Houston, MA, USA

### Background

Cytotoxicity assays play a central role in studying the function of immune effector cells such as cytotoxic T lymphocytes (CTL) and natural killer (NK) cells. Traditionally, cytotoxicity assays have been performed using <sup>51</sup>chromium (<sup>51</sup>Cr) and calcein release assays. The assays involve labeling tumor cells (target) with radioisotope or fluorescent dyes, when the target cells are subjected to cytolysis by CTLs or NK cells (effector), they release the entrapped labels into the media upon lysis. The amount of labels in the media is measured to determine the level of cytotoxicity the effectors have induced. These traditional methods may generate

inconsistent results due to low sensitivity caused by poor loading efficiency and high spontaneous release of the reagents.

### Methods

In this work, we demonstrate a novel cytotoxicity assay using the Celigo imaging cytometry method. Utilizing imaging cytometry, direct cell counting of live fluorescent target cells can be performed, which is a direct method for assessment of cytotoxicity. Human NK cells from one healthy donor were used as effectors, and K562 (suspension) and IMR32 (adherent) were used as the target cells. Both target cells were first stained with calcein AM, and seeded at 10,000 cells/well in a standard 96-well microplate. The donor NK cells were then added to each well at effector-to-target (E:T) ratios 10:1, 5:1, 2.5:1, 1.25:1, 0.625:1, and 0.3125:1. The 96 well plate was then scanned and analyzed using Celigo imaging cytometer at t = 1, 2, 3, and 4 h to measure the % lysis of target cells.

### Results

The results showed increasing % lysis as incubation time and E:T ratio increased. For the E:T ratios at 10:1, 5:1, 2.5:1, 1.25:1, 0.625:1, and 0.3125:1, the % lysis were 99, 93, 75, 52, 30, and 7%, respectively for IMR32. The K562 cells showed similar % lysis results. In addition, the change in % lysis over time was monitored for both cell types, showing increasing % lysis from 1 to 4 hours.

### Conclusions

The proposed Celigo imaging cytometry is an accurate and simple method for direct quantification of NK cell-mediated cytotoxicity, which can be an attractive method for both academic and clinical research. In addition, plate-based image cytometry enables high-throughput screening platform for more efficient identification of potential antibody drug candidates.

### Figure 1. E:T Ratio dependent cytotoxicity fluorescent images



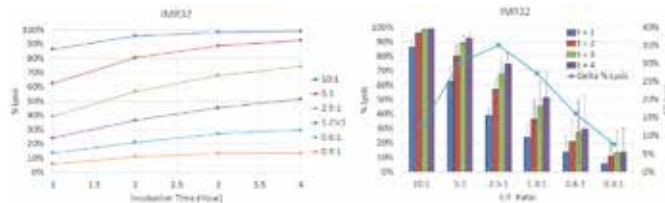
The calcein AM fluorescent images are the K562 Target cells at t = 4 hours, showing decrease in calcein AM positive Target cells as E:T ratio increased. The IMR32 images were similar.



## Not Listed/Other

Presenting author underlined; Primary author in italics

**Figure 2. Time course and dose dependent cytotoxicity results**



The time course results showed increase in % lysis from 1 to 4 hours. The dose response graphs showed increasing % lysis as E:T ratio increased.

**305**

### **The HLA-associated phosphoproteome as a new target for immunotherapy against hepatocellular carcinoma**

Nico Buettner<sup>1</sup>, Feng Shi<sup>2</sup>, Paisley T Myers<sup>3</sup>, Stuart Curbishley<sup>4</sup>, Sarah A Penny<sup>4</sup>, Lora Steadman<sup>4</sup>, David Millar<sup>2</sup>, Ellen Speers<sup>3</sup>, Nicola Ruth<sup>4</sup>, Gabriel Wong<sup>4</sup>, Robert Thimme<sup>1</sup>, David Adams<sup>4</sup>, Mark Cobbold<sup>2</sup>

<sup>1</sup>Universitätsklinikum Freiburg, Freiburg, Germany

<sup>2</sup>Massachusetts General Hospital Cancer Center, Boston, MA, USA

<sup>3</sup>University of Virginia, Charlottesville, VA, USA

<sup>4</sup>University of Birmingham, Birmingham, England, UK

#### **Background**

Hepatocellular carcinoma (HCC) is the sixth most common cancer with a growing incidence and mortality. Since HCC is believed to be immunogenic, immunotherapy is considered a promising new treatment modality. The identification of novel and specific tumor-associated antigens provides the basis for the development of an efficient immunotherapy. However, only very few HCC-specific tumor antigens have been characterized so far and post-translational modified peptides have been completely overlooked in the past. Dysregulation of signaling pathways in cancers leads to aberrant and augmented protein phosphorylation and in such way modified proteins can be degraded to generate cancer-specific phosphopeptides. These are presented by MHC class I molecules and recognized by T cells. The aim of this study was to identify HCC-associated, MHC class I-bound phosphopeptides (MHC-I-pP) and to assess immunity against this novel class of antigens in patients with chronic liver disease and HCC.

#### **Methods**

For identification, tissues were lysed and MHC class-I complexes affinity purified. The bound phosphopeptides were eluted, enriched and characterized using mass spectrometry. We compared MHC class I-bound phosphopeptides (MHC-I-pP) found on healthy, cirrhotic

liver tissue and HCC from patients undergoing liver transplantation. To assess immunity PBMCs, intrahepatic lymphocytes (IHLs) and tumor-infiltrating lymphocytes (TILs) were extracted from healthy donors, patients with chronic liver disease and HCC, and analyzed using multiplexed intracellular cytokine staining. Additionally, MHC-I-pP-specific CD8+ T cells from IHLs and TILs were expanded in a large scale using a rapid expansion protocol with anti-CD3, IL-2 and irradiated feeder cells.

#### **Results**

So far we have identified over 300 HCC-associated MHC-I-pP presented by various HLA molecules. Many of the novel identified MHC-I-pP were derived from proteins, which can be directly linked to important cancer-associated signaling-pathways. More MHC-I-pP were displayed in a greater diversity during the course of liver disease from non-cirrhotic liver to precancerous liver cirrhosis and up to HCC. CD8+ T cell responses were found regularly in patients with early chronic liver disease and were much rarer in patients with end-stage liver cirrhosis and after HCC formation.

#### **Conclusions**

Immune responses against these novel tumor-antigens were comparable in quantity and quality to those seen against viral control epitopes. Our results therefore suggest that MHC-I-pP may be the target of cancer immune surveillance in liver disease. Furthermore, a directed expansion of MHC-I-pP-specific CD8+ T cells was possible in a large scale for a possible application in adoptive T cell therapy. Therefore, MHC class-I bound phosphopeptides represent an attractive novel target for future cancer immunotherapies.

**306**

### **Cancer testis antigens, immunotherapeutic target antigens in triple negative breast cancer**

Remy Thomas<sup>1</sup>, Wouter Hendrickx<sup>2</sup>, Mariam Al-Muftah<sup>1</sup>, Julie Decock<sup>1</sup>

<sup>1</sup>Qatar Biomedical Research Institute (QBRI), Doha, Ar Rayyan, Qatar

<sup>2</sup>Sidra Medical and Research Center, Doha, Ad Dawhah, Qatar

#### **Background**

Cancer testis antigens (CTA) represent one type of tumor antigen that can elicit strong immune responses thanks to their restricted expression in normal germ cells and tumor cells. Upregulated expression has been observed in various cancer types including melanoma, bladder, lung, ovarian, and hepatocellular carcinomas. NY-ESO-1 has emerged as a promising target as it is highly immunogenic and associated with poor clinical outcome [1, 2]. Reports on CTA expression in breast cancer are inconclusive and sparse data is available on triple negative breast cancer (TNBC).

## Not Listed/Other

Presenting author underlined; *Primary author in italics*

### Methods

Using a bioinformatics approach, we investigated the expression of CTAs that are transcriptionally silent in normal non-germline tissues [3] in both human TNBC cell lines and specimens. Gene and protein analyses were performed *in vitro* to evaluate our *in silico* findings, and functional assays were conducted for 3 CTAs.

### Results

We mined the TCGA and NCBI GEO repositories for CTA expression in TNBC and found a consensus moderate expression of DKKL1, LDHC, MAGE-A3, PIWIL2, PLAC1, PRAME, PRSS50 and TSGA10 in cell lines and tumor specimens. Interestingly, NY-ESO-1 expression was not found to be upregulated in triple negative breast cancer. Expression profiling of 9 human TNBC cell lines, encompassing all 6 TNBC subtypes, confirmed LDHC, MAGE-A3 and PRAME to be good candidate targets. Their cellular localization, determined by immunocytochemistry, indicates that redirected, rather than chimeric antigen receptor (CAR)-modified T cells, should be developed as tools for adoptive T cell therapy. We are currently identifying the immunogenic peptides to be used for T cell engineering. Furthermore, we are conducting functional assays to determine the role of LDHC, PRAME and MAGE-A3 in TNBC development and progression, in particular in cell metabolism, proliferation, apoptosis, migration and invasion.

### Conclusions

We found a number of cancer testis antigens to be expressed at moderate to high levels in triple negative breast cancer. Our preliminary findings suggest that LHDC, MAGE-A3 and PRAME could be good targets for adoptive T cell therapy of TNBC.

### References

1. Gnjatic S, Nishikawa H, Jungbluth AA *et al*: **NY-ESO-1: review of an immunogenic tumor antigen**. *Adv Cancer Res* 2006, **95**:1-30.
2. Svobodová S, Browning J, MacGregor D, *et al*: **Cancer-testis antigen expression in primary cutaneous melanoma has independent prognostic value comparable to that of Breslow thickness, ulceration and mitotic rate**. *Eur J Cancer* 2011, **47(3)**:460-469.
3. Rooney MS, Shukla SA, Wu CJ, *et al*: **Molecular and genetic properties of tumors associated with local immune cytolytic activity**. *Cell* 2015, **160(1-2)**:48-61.

### 307

#### Overall survival and outcomes of patients treated with high dose IL-2 from the PROCLAIM registry

Michael KK Wong<sup>1</sup>, Michael Morse<sup>2</sup>, David F McDermott<sup>3</sup>, Joseph I Clark<sup>4</sup>, Howard L Kaufman<sup>5</sup>, Gregory A Daniels<sup>6</sup>, Hong Hua<sup>7</sup>, Tharak Rao<sup>7</sup>, Janice P Dutcher<sup>8</sup>

<sup>1</sup>University of Texas MD Anderson Cancer Center, Houston, TX, USA

<sup>2</sup>Duke University Medical Center, Durham, NC, USA

<sup>3</sup>Beth Israel Deaconess Medical Center, Boston, MA, USA

<sup>4</sup>Loyola University Medical Center, Maywood, IL, USA

<sup>5</sup>Rutgers Cancer Institute of New Jersey, New Brunswick, NJ, USA

<sup>6</sup>UC San Diego Moores Cancer Center, La Jolla, CA, USA

<sup>7</sup>Prometheus Laboratories Inc., San Diego, CA, USA

<sup>8</sup>Cancer Research Foundation, Chappaqua, NY, USA

#### Background

High dose IL-2 (HD IL-2) can provide durable responses in patients with metastatic melanoma (mM) and metastatic renal cell carcinoma (mRCC). PROCLAIM<sup>SM</sup> [<http://www.proclaimregistry.com>] is an IL-2 registry that captures real-world patient population survival and outcomes. Herein, we report on patient experience sequencing HD IL-2 with immune checkpoint blockade (ICB) and/or targeted therapy (TT) in mM and mRCC.

#### Methods

Patients were prospectively enrolled into the registry as of 2011 and must have received at least one dose of HD IL-2. Statistics and survival analysis were performed on datasets as of December 17, 2015.

#### Results

The mOS for mM patients (n=337) was 19.4 months, with a median follow-up (mFU) of 22 months. The overall response rate (ORR) for 323 patients with available data was 13.9%. The mOS for those with complete response (CR, n=10) and partial response (PR, n=35) was not reached (NR). The mOS for patients experiencing stable disease (SD, n=92) and progressive disease (PD, n=186) was 29.3 and 12.2 months, respectively. The mOS for all mRCC patients (n=412) was NR, with a mFU of 21 months. The ORR for the 382 patients with available data was 17.8%. For patients with CR (n=14), PR (n=53), or SD (n=146) mOS was NR while in patients with PD (n=169), mOS was 17 months. In mM, two groups were further analyzed; HD IL-2 followed by ipilimumab alone (IL-2 then IPI), and HD IL-2 followed by PD-1/PD-L1 inhibitors with or without ipilimumab (IL-2 then aPD-1 ± IPI, Table 1). In mRCC, survival based on TT or ICB after HD IL-2 was analyzed (Table 2). Survival of patients receiving HD IL-2 as first line with no post therapy was also determined (Table 2).

## Not Listed/Other

Presenting author underlined; Primary author in italics

### Conclusions

This analysis of the national IL-2 registry suggests that HD IL-2 continues to be a valuable treatment option for eligible mM and mRCC patients. Attainment of SD is clinically relevant and contributes to HD IL-2's survival benefit. Support for investigation of HD IL-2 in combination or sequence with ICB is warranted.

### Trial Registration

ClinicalTrials.gov identifier NCT01415167.

**Table 1.**

Groups based on therapies after IL 2	Metastatic Melanoma	
	IL-2 then IPI	IL-2 then aPD-1±IPI
n	81	56
mOS (months)	15.8	28.7
1-,2-,3-year survival (%)	64,28,18	96,66,35

**Table 2.**

Groups based on therapies after IL 2	mRCC				
	TT	TT & ICB	ICB	No TT or ICB	IL-2 first line (no prior or post therapy)
n	190	14	12	196	149
mOS (months)	35.5	NR	NR	NR	NR
1-,2-,3-year survival (%)	81,63,49	100,81,81	90,79,79	76,65,65	82,72,72

308

### Tetrahydrouridine and decitabine combination for p53-independent cyto-reduction and immune-priming of NSCLC *in vivo*

Kai Kang<sup>1</sup>, Yogen Sauntharajah<sup>2</sup>, Vamsidhar Velcheti<sup>2</sup>

<sup>1</sup>Taussig Cancer Institute, Cleveland Clinic, Cleveland, OH, USA

<sup>2</sup>Cleveland Clinic, Cleveland, OH, USA

### Background

Even if a cancer is immune recognized, it may evade immune attack using immune checkpoint. Such immune-recognized cancers are vulnerable to immune checkpoint inhibitors (e.g., anti-PD-1). Unfortunately, the response rate of non-small cell lung cancer to nivolumab is only ~20%. One important approach to improve immune checkpoint blockade is to increase the rate at which NSCLC is immune-recognized in the first place. A major way in which cancers escape immune recognition is by epigenetic silencing

of neo-antigens. A central epigenetic protein mediating such silencing is DNA methyl-transferase 1 (DNMT1), and DNMT1 has been validated as a molecular target to increase NSCLC immune-recognition. Moreover, DNMT1-depletion cyto-reduces cancers directly by increasing expression of epithelial-differentiation genes that directly antagonize MYC, to produce p53-independent cell cycle exits that spare immune-effectors. Decitabine (Dec) depletes DNMT1 and can potentially translate this science; however, Dec has a very brief plasma  $t_{1/2}$  *in vivo*. Therefore, we combined an inhibitor of CDA, tetrahydrouridine (THU), with reduced doses of Dec, with the objective that depletes DNMT1 while avoiding a high Cmax that causes off-target cytotoxicity.

### Methods

C57/BL6 mice were inoculated with LL3 cells by tail vein. Mice (n=15) randomized into 3 groups were treated with PBS, Dec (0.2 mg/kg s.c. 3X/wk), or THU-Dec (10/0.1 mg/kg s.c. 3X/wk). Peripheral blood was collected to detect MDSC and T lymphocytes. Survival time was recorded. At sacrifice, tumor samples were examined by flow cytometry, H&E staining, Western blot and QRT-PCR.

### Results

Survival time significantly increased with THU-Dec (62) > Dec (50) > vehicle (37) (median survival days) (Figure 1a). Tumor DNMT1 and MYC protein decreased to a substantially greater extent with THU-Dec than with Dec alone, concurrent with substantial increase in p27 (Figure 1b). THU-Dec preserved peripheral blood counts including absolute lymphocyte counts (Figure 1c), while substantially decreasing the numbers of MDSC (Figure 1d). THU-Dec also significantly increased expression of immunotherapy antigenic targets MAGE-A1 and MAGE-A3 to a greater extent than Dec ( $p < 0.01$ ) (Figure 1e). THU-Dec treatment also decreased regulatory T cells in blood and tumor, and increased the release of INF $\gamma$  and expression of PD-L1 in tumor cells, compared to Dec alone or PBS (Figure 1f).

### Conclusions

Addition of THU to Dec, to address pharmacologic limitations of Dec alone, improved immune-priming and induced p53-independent cell cycle exits in NSCLC *in vivo*. There is scientific and pharmacologic rationale to combine THU-Dec with nivolumab in the clinical trial NCT02664181.

## Not Listed/Other

Presenting author underlined; Primary author in italics

**Figure 1. THU-Dec directly cytoreduced lung cancer in vivo by p53-independent mechanisms while preserving immune-effectors and increasing antigen presentation.**

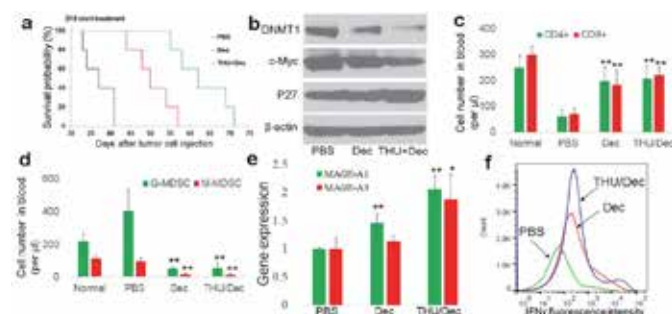


**Figure 1:** THU-Dec directly cytoreduced lung cancer in vivo by p53-independent mechanisms while preserving immune-effectors and increasing antigen presentation. C57/BL6 mice were inoculated via tail vein with LL3 lung cancer cells. **a)** Survival time. **b)** Protein expression in tumor. **c)** Absolute numbers of CD4/8 T cells in peripheral blood after 2 weeks of treatment. **d)** Absolute numbers of MDSC in blood after 2 weeks of treatment. **e)** Cancer testis antigen expression in tumor. **f)** Intracellular IFN $\gamma$  expression in tumor. Data were expression as mean  $\pm$  SD. \* $p < 0.05$ , \*\* $p < 0.01$  vs PBS group.

C57/BL6 mice were inoculated via tail vein with LL3 lung cancer cells. **a)** Survival time; **b)** Protein expression in tumor; **c)** Absolute numbers of CD4/8 T cells in peripheral blood after 2 weeks of treatment; **d)** Absolute numbers of MDSC in blood after 2 weeks of treatment; **e)** Cancer testis antigen expression in tumor; **f)** Intracellular IFN $\gamma$  expression in tumor. Data were expression as mean  $\pm$  SD. \* $p < 0.05$ , \*\* $p < 0.01$  vs PBS group.

**309**

### **Umbelliferon- $\alpha$ -D-glucopyranosyl-(2I $\rightarrow$ 1II)- $\alpha$ -D-glucopyranoside: a potential candidate affords chemoprevention against chemically-induced carcinogenesis through attenuating nuclear factor- $\kappa$ B**

Vikas Kumar<sup>1</sup>, Firoz Anwar<sup>2</sup>, Amita Verma<sup>1</sup>

<sup>1</sup>Sam Higginbotham Institute of Agriculture, Technology & Sciences, Allahabad, Uttar Pradesh, India

<sup>2</sup>King Abdulaziz University, Jeddah, Afghanistan

#### **Background**

The liver is the principal metabolizing site of the body, which is commonly prone to damage through various toxicants. Diethylnitrosamine (DEN) is a potent hepatocarcinogen and hepatotoxin, which is well known for modulating the inflammatory cytokines and oxidative stress in the liver. The plants are the rich source of umbelliferone, which are the secondary metabolites widely distributed in various species of fruits, vegetables, tea, spices and widely consumed by humans worldwide. The aim of the current investigation was to exemplify the effect of umbelliferon- $\alpha$ -D-glucopyranosyl-(2I $\rightarrow$ 1II)- $\alpha$ -D-glucopyranoside (UFD) on tissue protection, chronic hepatic inflammation and oxidative stress induced by DEN.

#### **Methods**

The rats were subjected to hepatic carcinogenesis by treating with a single intraperitoneally injection of DEN (200 mg/kg). The rats were euthanized at the end of the experiment and livers were microscopically scrutinizing. Biomarker of oxidative stress (lipid peroxides, reduced glutathione and conjugated dienes), liver enzyme parameters and nonenzyme liver parameters were also examined. The liver tissue was also invested for the existence of proinflammatory cytokines, including IL-1 $\beta$ , IL-6 and TNF- $\alpha$ .

#### **Results**

The results clearly demonstrated the UFD dose-dependently inhibited those as mentioned earlier elevated oxidative stress parameters, liver and non-liver parameters dose dependently. Our result revealed the essential repression of the inflammation cascade through modulation of nuclear factor-kappa B (NF- $\kappa$ B) signaling pathway may characterize a novel mechanism of action hepatic tumor inhibitory effect of UFD against experimental toxicant-induced hepatocarcinogenesis.

#### **Conclusions**

It is evident from the present study that UFD inhibits the DEN-initiated hepatocarcinogenesis in rats through proinflammatory cytokines via the anti-inflammatory mechanism.

#### **Acknowledgements**

The authors acknowledge the Department of Pharmaceutical Sciences, Faculty of Health Sciences, SHIATS.

#### **References**

1. Kumar V, Khan R, Kazmi I, Afzal M, Al-Abbasi FA, Anwar F: **Fixed dose combination therapy loperamide and niacin ameliorates diethylnitrosamine-induced liver carcinogenesis in albino wistar rats.** *RSC Advances* 2015, **5**:67996-68002.
2. Kumar V, Anwar F, Sethi N, Al-Abbasi FA: **Umbelliferone  $\beta$ -D-galactopyranoside inhibits chemically induced renal carcinogenesis via alteration of oxidative stress, hyperproliferation and inflammation: possible role of NF- $\kappa$ B.** *Toxicol Res* 2015.



## Not Listed/Other

Presenting author underlined; Primary author in italics

310

**Novel and shared neoantigen derived from histone 3 variant H3.3 K27M mutation – characterization of the epitope and cloning of a specific T cell receptor for glioma T cell therapy**

Zinal Chheda<sup>1</sup>, Gary Kohanbash<sup>1</sup>, John Sidney<sup>2</sup>, Kaori Okada<sup>1</sup>, Shruti Shrivastav<sup>1</sup>, Diego A Carrera<sup>1</sup>, Shuming Liu<sup>1</sup>, Naznin Jahan<sup>1</sup>, Sabine Mueller<sup>1</sup>, Ian F Pollack<sup>3</sup>, Angel M Carcaboso<sup>4</sup>, Alessandro Sette<sup>2</sup>, Yafei Hou<sup>1</sup>, Hideho Okada<sup>1</sup>

<sup>1</sup>University of California, San Francisco, San Francisco, CA, USA

<sup>2</sup>La Jolla Institute for Allergy and Immunology, La Jolla, CA, USA

<sup>3</sup>University of Pittsburgh, Pittsburgh, PA, USA

<sup>4</sup>Hospital Sant Joan de Déu Barcelona, Barcelona, Spain

**Background**

Brain tumors are the leading cause of cancer-related mortality and morbidity in children. Recent genetic studies have revealed that malignant gliomas in children and young adults often show shared missense mutations in the gene encoding the replication-independent histone 3 variant H3.3 [1]. Approximately 70% of midline gliomas, such as DIPG, harbor the amino-acid substitution from lysine (K) to methionine (M) at the position 27 of H3.3 (the H3.3 K27M mutation hereafter). The K27M mutation in DIPG is universally associated with shorter survival compared with patients with non-mutated H3.3.

**Methods**

We evaluated whether the H3.3 K27M mutation can induce specific cytotoxic T lymphocyte (CTL) responses in human leukocyte antigen (HLA)-A2+ CD8+ T cells as a neoantigen epitope. Competitive binding inhibition assays were performed for evaluation of affinity of synthetic peptides to HLA-A2.  $\alpha$ - and  $\beta$ -chain cDNAs from a high-affinity T cell receptor (TCR) were cloned by amplification of cDNA Ends-PCR (RACE-PCR).

**Results**

*In vitro* stimulation of HLA-A2+ donor-derived CD8+ T cells with a synthetic peptide encompassing the H3.3 K27M mutation (the H3.3.K27M epitope hereafter) induced CTL lines which recognized not only the synthetic H3.3.K27M epitope peptide loaded on T2 cells but also lysed HLA-A2+ DIPG cell lines which endogenously harbor the H3.3.K27M mutation. On the other hand, CTL lines did not react to HLA-A2+, H3.3 K27M mutation-negative cells or HLA-A2-negative, H3.3 K27M mutation+ cells. The H3.3.K27M epitope peptide, but not the non-mutant counterpart, indicated an excellent affinity (Kd 151 nM) to HLA-A2. Furthermore, CTL clones with high and specific affinities to HLA-A2-H3.3.K27M-

tetramer were successfully obtained, and both retroviral and lentiviral vectors have been created to encode  $\alpha$ - and  $\beta$ -chain cDNAs from a high-affinity TCR. Human T cells transduced with the lentiviral or retroviral TCR demonstrated antigen-specific reactivity. Furthermore, critically important for safety of clinical application, alanine scanning demonstrated that the key amino-acid sequence motif in the epitope for the TCR reactivity is not shared by any known human protein.

**Conclusions**

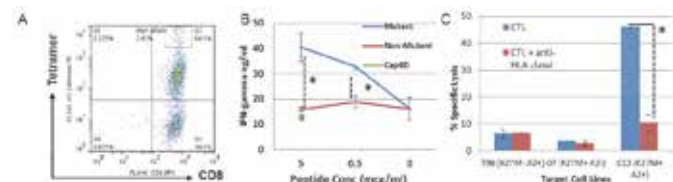
These data provide us with a strong basis for developing peptide-based vaccines as well as adoptive transfer therapy using autologous T cells transduced with the TCR.

**Acknowledgements**

This study is supported by the NIH/NINDS (1R01NS096954), V Foundation and Parker Institution for Cancer Immunotherapy.

**References**

- Schwartzentruber J, Korshunov A, Liu XY, Jones DT, Pfaff E, Jacob K, *et al*: **Driver mutations in histone H3.3 and chromatin remodelling genes in paediatric glioblastoma.** *Nature* 2012, **482**:226-31.

**Figure 1. HLA-A2.1+ donor-derived CTLs specifically recognize HLA-A2.1+ K27M+ glioma cells in an HLA-class I-dependent manner**

Peripheral blood mononuclear cells from an HLA-A2.1+ donor were stimulated *in vitro* with the H3.3.K27M peptide and evaluated for their reactivity against: (A) HLA-A2.1/H3.3.K27M-specific tetramer and anti-CD8 mAb, and (B) T2 cells pulsed with the mutant or non-mutated H3.3 peptide by IFN- $\gamma$  ELISA. In (A), among the CD8+tetramer+ population (64.1% of total lymphocyte-gated cells), there is a tetramer<sup>high</sup> subpopulation (2.4% of total lymphocyte-gated cells), some of which were used as CTL clones (Aim 2). In (B), the Cap1-6D peptide (tested at 5mcg/ml only) is a high avidity HLA-A2.1-binding epitope derived from CEA1 used as an irrelevant negative control. (C) The CTL line was evaluated for cytotoxicity against glioma cell lines T98 (HLA-A2.1+but K27M-negative), HSJD-DIPG-07 (HLA-A2.1-negative but K27M+), and HSJD-DIPG-13 (HLA-A2.1+ and K27M+) lines. CFSE-labeled target cells (10e4/well) were incubated with CTLs at the E/T ratio of 25 for 4 hours. To block the CTL cytotoxicity, anti-HLA-ABC 10 $\mu$ g/ml was added to one group. At the end of incubation, 7-AAD was added into each well and incubated for 10 minutes on ice. The samples were

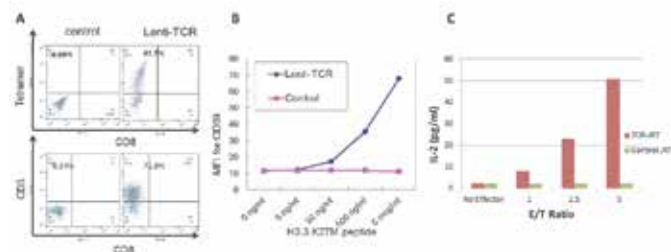


## Not Listed/Other

Presenting author underlined; Primary author in italics

analyzed by flow cytometry, and the killed target cells were identified as CFSE+ and 7-AAD+ cells. The cytotoxicity was calculated as the percentage of CFSE+ and 7-ADD+ cells in total HLA-A2+ CFSE+ cells (\*p<0.05 by Wilcoxon rank-sum tests).

**Figure 2. Evaluation of H3.3.K27M-specific TCR**



(A) J.RT-T3.5 cells were transduced with lentiviral vector encoding the TCR  $\alpha$ - or  $\beta$ -chains derived from H3.3.K27M-specific CTL clone IH5 (J.RT-T3.5-TCR). The J.RT-T3.5-TCR or control non-transduced J.RT-T3.5 cells were evaluated for the surface TCR expression using PE-labeled HLA-A\*0201/H3.3.K27M tetramer (upper panel) or PE-labeled anti-CD3 mAb (upper and lower panels). Since J.RT-T3.5 cells are CD4+ and CD8-negative, tetramer+ CD8-negative cells are ones expressing the transgene-derived TCR. CD3-upregulation indicates activation of cells. (B) J.RT-T3.5-TCR, but not control J.RT-T3.5 cells, upregulate CD69 expression upon recognition of the H3.3 K27M peptide loaded on T2 cells. (C) DIPG 13 cells [HLA-A\*0201+ (albeit dim), K27M mutation+] were incubated with J.RT-T3.5-TCR or control J.RT-T3.5 cells. IL-2 secretion in the culture media was assayed by specific ELISA.

**Figure 3. Efficient expression of transgene TCR on human PBMC-derived T cells**

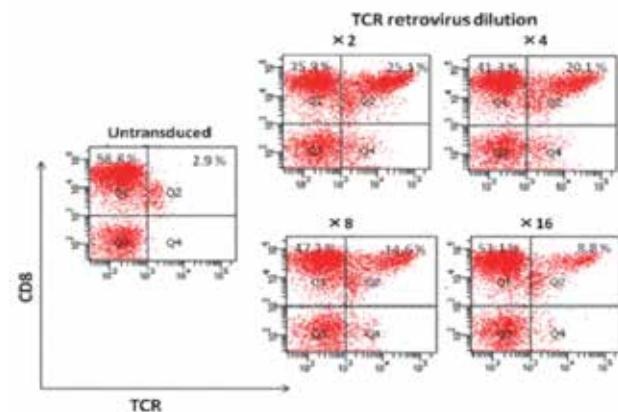
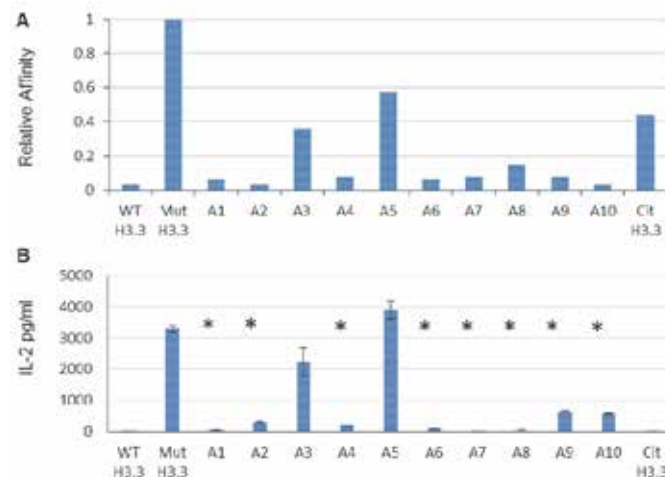


**Figure 3. Detection of TCR on transduced T cells.**

Human PBMC-derived T cells were transduced with serially diluted preparation of the retroviral vector encoding

H3.3.K27M-specific TCR and evaluated by HLA-A2-H3.3.K27M-specific tetramer and anti-CD8 monoclonal antibody.

**Figure 4. Alanine scanning to determine the key immunogenic AA residues of the H3.3.K27M epitope**



(A) Relative HLA-A\*0201-binding affinity of each peptide to that of H3.3.K27M (26-35) was determined by cell-free binding assay. (B) J.RT-T3.5 cells were transduced with lentiviral vector encoding the H3.3.K27M-specific TCR and evaluated for the recognition of each peptide loaded on T2 cells by production of IL-2. Each group was assayed as triplicate \*p<0.05 by Student-t compared with the mutant H3.3. In addition to 10 synthetic peptides each containing the substitution with alanine (A1-A10), we also evaluated synthetic peptides designed for citrullinated H3.3. K27M epitope (Cit H3.3; i.e., the first AA of the H3.3.K27M epitope is replaced by citrulline).

### 311

#### The fucosylation inhibitor 2-fluorofucose exhibits anti-tumor activity and modulates immune cell activity both in vitro and in vivo

Jessica J Field, Weiping Zeng, Vincent FS Shih, Che-Leung Law, Peter D Senter, Shyra J Gardai, *Nicole M Okeley*

Seattle Genetics, Inc., Bothell, WA, USA

#### Background

2-Fluorofucose (2FF) is a small molecule inhibitor of glycoprotein fucosylation. 2FF-mediated afucosylation of cancer cells results in reduced adhesive properties. Furthermore, T cells treated with 2FF during expansion show increased T cell receptor (TCR) signaling, enhanced maturation of autologous dendritic cells (DCs), and reduced regulatory T cell numbers, demonstrating modulation of immune activity [1]. 2FF has shown promising *in vivo* anti-tumor activity, both alone and in combination with a cancer

## Not Listed/Other

Presenting author underlined; *Primary author in italics*

vaccine, which appears to be dependent on immune cell activity. Specifically, 2FF elicits growth delay in the generally refractory 4T1 murine breast cancer model, whereas this effect is lost when the 4T1 model is run in immunodeficient NSG mice.

### Methods

To further understand the immune modulatory activity of 2FF, tumor infiltrating immune cells in 4T1 tumors were counted and profiled using multi-color flow cytometry. Additionally, antigen recall function of CMV reactive T cells expanded with 2FF was assessed by culturing T cells and autologous DCs with CMV peptides and monitoring IFN $\gamma$  and IL-12p70 production. We also used this model to investigate the combinatorial activity of 2FF treated T cells with anti-PD-1 antibodies.

### Results

2FF treatment in the 4T1 murine model reduced the number of regulatory T cells and increased activated DCs. These DCs showed a mild increase in the maturation markers CD83, CD86, and MHCII. The effects observed *in vivo* recapitulate our *in vitro* observations with human T cells and T cell/DC co-cultures, and demonstrate the translation of 2FF immune modulatory activity from *in vitro* to *in vivo*. Since 2FF reduces the regulatory T cell population, an effect seen with anti-CTLA-4 antibodies, we postulated that PD-1 checkpoint blockade antibodies would enhance 2FF-treated T cell function. T cells treated with 2FF during expansion showed increased CMV antigen specific response, while co-cultures that contained both 2FF-treated T cells and anti-PD-1 antibody showed increased levels of production of IFN $\gamma$  and IL-12p70 above those seen with either single agent alone. These data suggest that co-treatment with 2FF and anti-PD-1 antibody can lead to increased antigen specific T cell activation *in vitro*.

### Conclusions

Overall, we conclude that 2FF may promote a more active tumor immune microenvironment, providing a better opportunity for an effective host anti-tumor immune response alone or in combination with checkpoint blockade. A first-in-human phase I clinical trial evaluating 2FF in advanced solid tumors is planned.

### References

1. Field JJ, *et al*: **Understanding the mechanism of 2FF-induced immune modulation [abstract]**. *Proc Am Assoc Cancer Res* 2016, **76(14 Suppl)**: Abstract 4005.

## 312

### Phosphopeptides as novel tumor antigens in colorectal cancer

*Sarah A Penny*<sup>1</sup>, Jennifer G Abelin<sup>2</sup>, Abu Z Saeed<sup>1</sup>, Stacy A Malaker<sup>3</sup>, Paisley T Myers<sup>2</sup>, Jeffrey Shabanowitz<sup>2</sup>, Stephen T Ward<sup>1</sup>, Donald F Hunt<sup>2</sup>, Mark Cobbold<sup>4</sup>

<sup>1</sup>University of Birmingham, Birmingham, England, UK

<sup>2</sup>University of Virginia, Charlottesville, VA, USA

<sup>3</sup>Stanford University, Stanford, CA, USA

<sup>4</sup>Massachusetts General Hospital Cancer Center, Boston, MA, USA

### Background

There is a pressing need for novel immunotherapeutic targets in colorectal cancer (CRC). Memory CD8+ T cell infiltration is now well established as a key prognostic indicator in CRC, and it is known that these tumor infiltrating lymphocytes (TILs) are specifically targeting and killing tumor cells. However, the antigens that these TILs target have not previously been determined. This has limited the use of immunotherapies in CRC, despite their efficacy in other cancer types. Recently, phosphopeptides have emerged as strong candidates for tumor-specific antigens, since dysregulation of signaling in cancers leads to aberrant protein phosphorylation. Here, we identify CRC-associated phosphopeptides and assess the tumor-resident immunity against these novel posttranslationally modified tumor antigens.

### Methods

We compared tumor and healthy tissue from CRC patients, to identify tumor-specific MHC class I associated phosphopeptides. Phosphopeptides were enriched using immobilized metal affinity chromatography, and characterized using mass spectrometry. TILs, from the same tumors, were extracted and expanded, and their responses to the phosphopeptides assessed using multiplexed intracellular cytokine staining. Cytolytic activity was observed by staining for surface mobilization of CD107a. Healthy donor responses were quantified using interferon- $\gamma$  ELISpot and functionality assessed using a europium release killing assay.

### Results

We have identified 133 tumor-associated MHC class I phosphopeptides from CRC, with different HLA-restrictions. There were, on average, 3.1 times more different phosphopeptides identified on primary cancers than healthy tissues, at 6.9-fold higher levels. 35% of these can be attributed to signaling events in well-defined cancer pathways and are therefore markers of malignancy. Through analysis of TIL's cytokine responses to these phosphopeptides, we have established that they are playing a key role in tumor-resident immunity. There were multifunctional TILs present



## Not Listed/Other

Presenting author underlined; *Primary author in italics*

in primary and metastatic tumors that recognized and killed in response to these phosphopeptides. Up to 0.7% of expanded TILs targeted each phosphopeptide, comparable with responses seen to viral epitopes. Immunity to these tumor-associated phosphopeptides represents a biological strategy for distinguishing tumor from healthy tissue. Furthermore, we have shown that healthy donors have pre-existing, memory T cell responses to many (58%) of these CRC-associated phosphopeptides. These phosphopeptide-specific T cells are readily expanded *ex vivo* and kill CRC cell lines. Thus, MHC class I associated phosphopeptides are ideal immunotherapeutic targets, as immunity must spare healthy tissue.

### Conclusions

The identification of this novel class of MHC class I antigens in CRC offers new hope for the future of immunotherapy in this malignancy.

313

### **Rapid and durable complete response to atezolizumab (anti-PD-L1), with sloughing of tumor tissue through urethra, in metastatic chemotherapy-resistant urothelial cancer (UC)**

*Pam Profusek*, Laura Wood, Dale Shepard, Petros Grivas  
Cleveland Clinic, Cleveland, OH, USA

### Background

Metastatic UC is usually fatal causing significant morbidity. Atezolizumab, an anti-PD-L1 checkpoint inhibitor, is FDA-approved for locally advanced or metastatic UC after progression on/after platinum-containing chemotherapy based on results of the IMVigor 210 trial.

### Methods

We present a trial patient with unique sloughing of tumor tissue, outstanding treatment response and tolerance.

### Results

A 76 year old man was diagnosed with high grade muscle-invasive UC of the bladder in April 2013. Patient completed 3 cycles of 'neoadjuvant' gemcitabine/cisplatin but had progression, he then received 6 cycles of docetaxel & investigational agent with progression, followed by 2 cycles of a targeted therapy on a phase I trial also with progression. Patient was then screened for the cohort 2 of the IMVigor210 trial evaluating the use of atezolizumab, 1200 mg every 21 days, in platinum-pretreated advanced UC. Screening CT showed the bladder lumen replaced by multiple masses and a left peri-aortic node 1.1 cm without other clear evidence of metastasis. Patient was experiencing fatigue, and hourly urgent urination with detrimental effect on his sleep, and overall quality of life (ECOG PS 1, normal GFR, Hgb 10.2 on

Cycle 1 Day 1(C1D1). Tumor tissue analysis showed high PD-L1 expression in both tumor-infiltrating immune cells (IC2) and tumor cells (TC2), TCGA subtype IV (Basal), and a high mutational load of 18.02 Mut/MB (compared to IMVigor210, Cohort 2 median of 8.11 Mut/MB). At C2D1 visit, he already had major clinical benefit with symptomatic improvement and sloughing of tumor tissue that passed through the urethra; the latter underwent pathology review and showed necrotic debris with highly atypical cells suspicious for carcinoma. Ten days later he presented to the ED due to difficulty voiding; cystoscopy was performed to remove necrotic tissue passing through urethra. Scans at C3D1 demonstrated great response with 83% tumor reduction, he continued to have very good quality of life. Scans at C10D1 showed that the bladder mass was no longer measurable and the lymph node was stable. Patient continues on trial without notable adverse events (has asymptomatic atrial fibrillation that was deemed possibly related to therapy) and has received 35 cycles. Patient remains very active, riding his bike most days of the week, denies urinary issues, has ECOG PS 0, with durable complete response on scans.

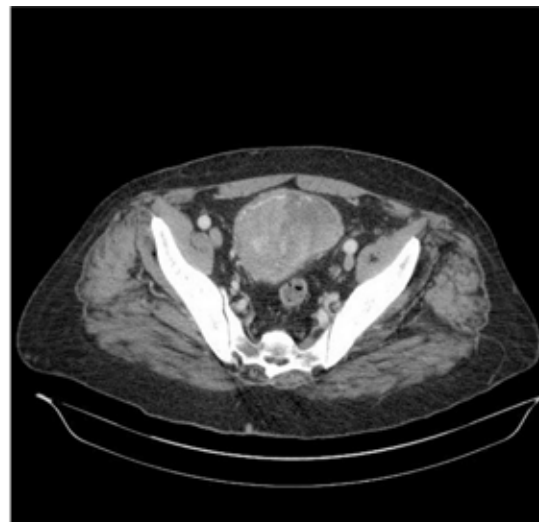
### Conclusions

Atezolizumab can produce rapid and durable responses in advanced platinum-resistant urothelial cancer and represents a new treatment option. Several clinical trials are ongoing.

### Trial Registration

ClinicalTrials.gov identifier NCT02108652.

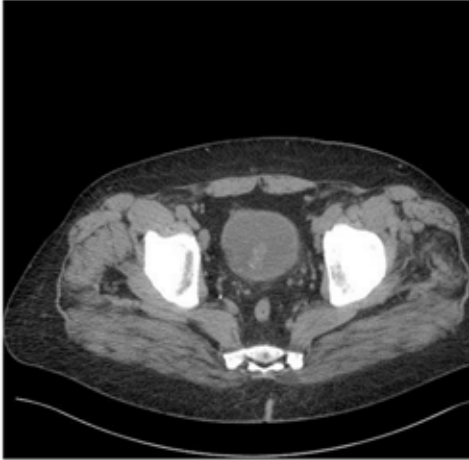
### Figure 1. Bladder CT - Baseline



Pre-dose

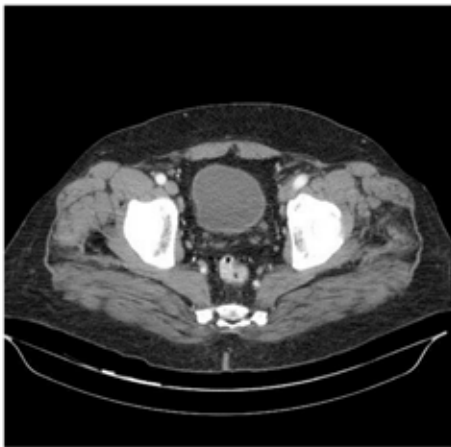
**Not Listed/Other**

Presenting author underlined; Primary author in italics

**Figure 2. Bladder CT - 9 Weeks of Therapy**

MPDL3280A –atezolizumab (anti-PDL1) 6 weeks treatment

83% Reduction

**Figure 3. Bladder CT - 9 Months of Therapy**

MPDL3280A 9 months of therapy

Complete Response

**314**

**Preclinical immunological and anti-tumor data of the new enantiomeric TLR9 agonist EnanDIM**

*Kerstin Kapp*<sup>1</sup>, *Barbara Volz*<sup>1</sup>, *Detlef Oswald*<sup>1</sup>, *Burghardt Wittig*<sup>2</sup>, *Manuel Schmidt*<sup>1</sup>

<sup>1</sup>Mologen AG, Berlin, Germany

<sup>2</sup>Foundation Institute Molecular Biology and Bioinformatics, Freie Universitaet Berlin, Berlin, Germany

**Background**

TLR9 agonists have shown anti-tumor effects, modulating the immune system via cellular and humoral responses. Two different families of DNA molecules containing non-methylated CG-motifs for TLR9 activation have been established so far: i) Dumbbell-shaped dSLIM<sup>®</sup> molecules protected against exonucleolytic degradation by their covalently-closed, natural phosphodiester (PO) backbone and ii) single-stranded, oligodeoxynucleotides (CpG-ODN) in most cases chemically-stabilized by phosphorothioates (PTO) in their phosphate moieties. However, PTO modifications produce off-target effects in immune cell populations and result in unfavorable risk-to-benefit ratios.

**Methods**

A novel family of TLR9 agonists avoids the off-target effects of PTO-modified CpG-ODN: linear single-stranded ODN synthesized using L-deoxyribonucleotides (natural enantiomers of D-deoxyribonucleotides) at their 3'-ends - EnanDIM<sup>®</sup>. The vast majority of deoxyribose in organisms consists of D-deoxyribose, thus co-evolved nucleases are blind for L-deoxyribose - thereby leaving L-protected ODN intact. We selected nucleotide sequences of EnanDIM<sup>®</sup> using high secretion of IFN-alpha and IP-10 from human peripheral blood mononuclear cells as marker. We employed a maximum feasible dose (MFD) approach: Mice received subcutaneous injection of single doses of 10 to 50 mg EnanDIM<sup>®</sup> to evaluate their acute toxicity and immunomodulatory properties. A pilot study was used to investigate the anti-tumor effect of EnanDIM<sup>®</sup> in a CT26 tumor model.

**Results**

EnanDIM581 and EnanDIM532 were selected due to their pronounced activation of immune cells (e.g. monocytes, NK cells and pDC) and their prominent induction of IFN-alpha and IP-10 secretion *in vitro*. EnanDIM744, an EnanDIM581 variant with additional 5'-end L-nucleotide protection, was also used for MFD studies. Safety assessments throughout the study revealed no signs of toxicity despite the extremely high doses (300 to 1700 mg/kg). A gross necropsy consisting of a macroscopic organ evaluation at day 15 also revealed no abnormalities. Dose-dependent increase of IP-10 levels in serum was observed between 6 and 24 hours after injection but none after 15 days, confirming that L-nucleotides in EnanDIM<sup>®</sup> do not alter the kinetic profile known from other TLR9 agonists. First data from the CT26 tumor model showed that EnanDIM532 reduces tumor growth and prolongs survival of mice.

**Conclusions**

EnanDIM<sup>®</sup>, a new family of TLR9 agonists, broadly activates the immune system. Even maximal feasible doses of EnanDIM<sup>®</sup> resulted in no signs of toxicity, whereas a reduction of tumor growth was observed in a murine CT26 tumor





## Not Listed/Other

Presenting author underlined; *Primary author in italics*

model. Therefore EnanDIM<sup>®</sup> compounds have the potential for clinical development as immune surveillance reactivators in the treatment of cancer.

**315**

### **Loading of recycling MHC class I molecules with antibody-delivered viral peptides leads to efficient CD8+ T cell-mediated tumor cell killing**

Julian P Sefrin, Lars Hillringhaus, Valeria Lifke, Alexander Lifke  
Roche Diagnostics GmbH, Penzberg, Bayern, Germany

#### **Background**

In the past, antigen-armed antibodies have been used in cancer immunotherapy. Recently, Yu et al.[1] efficiently delivered Epstein-Barr virus (EBV) antigens to lymphoma cells by targeting B cell surface receptors. However, they only obtained CD4<sup>+</sup> T cell activation, as externally introduced proteins enter the MHC class II antigen processing pathway. Here, we generated antibody-targeted pathogen-derived peptides (ATPPs), which deliver and release mature, virus-derived MHC class I peptides in an endosomal compartment where MHC is loaded with peptide, thereby triggering CD8<sup>+</sup> T cell activation and tumor cell killing.

#### **Methods**

We generated antigen-armed antibodies called ATPPs, by coupling virus-derived MHC class I peptides to tumor-associated antigen-specific antibodies. Fluorescence resonance energy transfer (FRET) was performed to demonstrate the supposed mode of action. T cell activation and tumor cell killing was assessed by quantification of interferon-gamma or lactate dehydrogenase (LDH) release. Human PBMCs or expanded peptide-specific T cells were used as effector cells for *in vitro* functionality assays and *in vivo* efficacy in MDA-MB231 breast cancer subcutaneous xenograft model.

#### **Results**

FRET imaging revealed that after ATPP binding to the antigen and subsequent internalization, the peptides are released in an early endosomal compartment and loaded onto recycling MHC class I complexes. MHC-peptide complexes are subsequently presented on the tumor cell surface and mediate activation of peptide-specific CD8<sup>+</sup> T cells. Treatment of various tumor types resulted in efficient activation of peptide-specific CD8<sup>+</sup> memory T cells and subsequent lysis of target cells *in vitro*. Similar results were obtained when targeting different tumor antigens or using various peptides with differing HLA-restrictions. Intriguingly, a 7200-fold higher amount of free peptide versus ATPP was required for comparable T cell activation. Using an elongated peptide that would require antigen processing for MHC class I binding revealed that the MHC class I antigen processing machinery

is not involved. Importantly, PBMCs, where only 0.5% of CD8<sup>+</sup> T cells were antigen specific, mediated significant tumor cell lysis at an E:T cell ratio of 1:10. ATPP activated peptide specific CD8<sup>+</sup> T cells induced tumor growth inhibition *in vivo*.

#### **Conclusions**

Our results demonstrate potent ATPP-mediated anti-tumor efficacy, independently of the MHC class I antigen processing machinery, by loading tumor cells with viral peptide antigens and redirecting virus-specific cytotoxic T cells against cancer.

#### **References**

1. Yu X, *et al*: **Antigen-armed antibodies targeting B lymphoma cells effectively activate antigen-specific CD4+ T cells**. Blood 2015, **125**:1601–1610.

**316**

### **Treatment of tumor cells with mirvetuximab soravtansine, a FR $\alpha$ -targeting antibody-drug conjugate (ADC), activates monocytes through Fc-Fc $\gamma$ RIII interaction and immunogenic cell death**

Anna Skaletskaya, Jose Ponte, Thomas Chittenden, Yulius Setiady

ImmunoGen, Inc., Waltham, MA, USA

#### **Background**

Mirvetuximab soravtansine (IMGN853) is an ADC, comprising a humanized FR $\alpha$ -binding M9346A antibody linked to the tubulin-disrupting maytansinoid, DM4. IMGN853 binds to FR $\alpha$  on cancer cells and is internalized; DM4 is released through enzymatic degradation of the antibody and linker cleavage, resulting in disruption of cell division and cell death. IMGN853 shows promising single-agent activity and a favorable safety profile in FR $\alpha$ -positive ovarian cancer patients in a phase I study. IMGN853 is entering FORWARD I, a phase III monotherapy study and is also being evaluated in combination with other agents including pembrolizumab in a phase Ib/II study, FORWARD II. Here we have explored potential mechanism(s) whereby IMGN853 can show enhanced activity in combination with a checkpoint inhibitor. Specifically, we report pre-clinical studies that examine the impact of IMGN853 treatment of tumor cells on human monocytes *in vitro*.

#### **Methods**

Peripheral blood mononuclear cells (PBMC) from normal donors were incubated with FR $\alpha$ -expressing KB tumor cells in the presence of test articles for two days. PBMC were then analyzed for activation marker expression by flow cytometry. The level of immunogenic cell death markers were evaluated by flow cytometry or ELISA to examine the direct impact of IMGN853 on KB cells.



## Not Listed/Other

Presenting author underlined; *Primary author in italics*

### Results

IMGN853 treatment of PBMC did not affect monocytes. Incubation of PBMC with KB cells decreased the CD86+ monocytes from ~30% to ~10%, and addition of DM4, the free payload of IMGN853, reversed the CD86 expression to basal levels. Intriguingly, addition of IMGN853, but not non-targeting ADC, increased the activated monocytes to ~80%. Similar results were obtained with isolated CD14+ monocytes, indicating that the monocyte activation is independent of other types of peripheral blood cells. Additionally, comparable increases in monocyte activation were observed in co-cultures of monocytes and KB cells treated with a mixture of M9346A and DM4, and not with M9346A or DM4 alone, suggesting both components of the ADC are necessary. Furthermore, a variant of IMGN853 with a point mutation that abrogates the FcγR binding only produced the same degree of monocyte activation as DM4 treatment, suggesting the significance of Fc/FcγR interaction. Finally, treatment of KB cells with IMGN853 increased calreticulin, ATP and HMGB1, three immunogenic cell death markers which can activate monocytes.

### Conclusions

Treatment of FRα-expressing KB cells with IMGN853 induces activation of co-cultured monocytes through Fc/FcγR interaction and upregulation of immunogenic cell death markers. These data provides a rationale for the clinical evaluation of IMGN853 and a checkpoint inhibitor.

### Trial Registration

ClinicalTrials.gov identifier NCT01609556, NCT02631876, and NCT02606305.

317

### **CovIsoLink, a new enzymatic conjugation for the development of innovative antibody drug conjugates**

Sandrine Valsesia-Wittmann<sup>1</sup>, Eva Sivado<sup>1</sup>, Vincent Thomas<sup>2</sup>, Meddy El Alaoui<sup>1</sup>, Sébastien Papot<sup>3</sup>, Charles Dumontet<sup>4</sup>, Mike Dyson<sup>5</sup>, John McCafferty<sup>5</sup>, Said El Alaoui<sup>2</sup>

<sup>1</sup>Centre Léon Bérard, innovations in immunotherapy platform, Lyon, Rhone-Alpes, France

<sup>2</sup>Covalab, Villeurbanne, Rhone-Alpes, France

<sup>3</sup>IC2MP, Poitiers, Limousin, France

<sup>4</sup>CRCL, Lyon, Rhone-Alpes, France

<sup>5</sup>IONTAS, Cambridge, England, UK

### Background

Monoclonal antibodies coupled to highly toxic agents or ADC (antibody-drug conjugate) are becoming a significant component of anticancer treatment. Currently approved immunoconjugates are heterogeneous in terms of degree of substitution, which is suboptimal both in terms of antitumor efficacy and risk of toxicity. The aim of this project is to bring

the *in vivo* proof of concept of a novel immunoconjugate technology using a unique enzymatic coupling of the payload on a substrate for an enzyme site inserted in the antibody core. These enzyme substrates are small unnatural and innovative peptide (patent pending). The major advantage of this method named CovIsoLink™ is to obtain a homogenous immunoconjugate with uniform stoichiometry by controlling: (a) the location of coupling sites on the antibody without affecting its immunoreactivity and (b) the number of molecules coupled per molecule of antibody by controlling the coupling drug antibody ratio (DAR) and consequently the toxicity and efficacy of therapeutic molecules.

### Methods

Using an in house peptide library, and the transglutaminase colorimetric assay, we identified selected tag peptides that were recognized as glutamine donor substrates with improved affinity compared with the known peptides (such as ZQG, LLQG, etc.). As a proof-of-concept, we compare our CovIsoLink immunoconjugates with Kadcyła® (targeting HER2) recently approved.

### Results

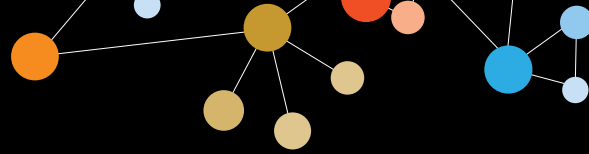
We developed and characterized different recombinant anti Her2 IgG1 mAb carrying optimized enzymatic substrate (tag) by genetic insertion in the coding sequence of mAb. We then evaluate the best linkers and conformation to incorporate different compounds through bacterial transglutaminase (mTG) enzymatic reaction. We set up experimental conditions, production, purification, HPLC/MS analysis and control of the immunoreactivity of CovIsoLink™ Her2-ADC. Using mTG, we obtained site specific conjugation of different modified drugs with optimized linker on the antiHer2 IgG1 antibody. By HIC analysis, we validated a specific and reproducible DAR reaching DAR2 depending on drugs and experimental conditions. *In vitro* and *In vivo* characterization and dose response studies of CovIsoLink-ADC specificity and reactivity are currently performed in Her2 positive models by comparison with Kadcyła (T-DM1).

### Conclusions

This technology is potentially applicable to a large variety of antitumor (or anti-stromal) antibodies since it is neither limited by the specificity of antigen targeted by the antibody nor by drugs that can be engrafted. Site specific conjugation will allow to remove barriers for the use of molecules that are too toxic in systemic injection or to enhance the efficacy of antibodies with low anti-tumor activity.

### Acknowledgements

Metropole Grand Lyon for funding.



## Not Listed/Other

Presenting author underlined; *Primary author in italics*

318

### **Efficacy of variable dose of gallic acid to combat chemically induced hepatocarcinogenesis by altering the hepatic proinflammatory cytokines and oxidative stress**

Amita Verma, Vikas Kumar

Sam Higginbotham Institute of Agriculture, Technology & Sciences, Allahabad, Uttar Pradesh, India

#### **Background**

Hepatocellular carcinoma (HCC), a hypervascular tumor, one of the most cancers worldwide, it causes the cancer related mortality. Hepatic inflammation and oxidative stress plays an important role in the development of HCC, which occur due to viral infections, environmental carcinogens, dietary carcinogens as well as alcohol abuses. We have found that gallic acid, a dietary flavonoids present in various plants avoid diethyl nitrosamine (DENA) induced hepatic carcinoma in experimental rats through inhibit the oxidative stress and repression of inflammation. The aim of the present study to investigate the chemoprotective effect of gallic acid on hepatic cytokines in the DENA induced carcinogenesis rats.

#### **Methods**

DENA (200 mg/kg) used for the induction of HCC in the Wistar rats. The DENA treated rats were divided into different groups and received the doses of gallic acid (25, 50 and 100 mg/kg) for 22 weeks different biochemical alpha feto-protein (AFP), serum glutamate oxaloacetate transaminase (SGOT), serum glutamate pyruvate transaminase (SGPT), alkaline phosphatase (ALP); hematological parameters viz., red blood cells (RBC), white blood cells (WBC), hemoglobin (Hb), erythrocytes sedimentation rate (ESR); antioxidant markers viz., lipid peroxidation (LPO), superoxide dismutase (SOD), catalase (CAT), reduced glutathione (GSH); inflammatory mediators viz., tumor necrosis factor- $\alpha$  (TNF- $\alpha$ ), interleukin-6 (IL-6) and interleukin-1 $\alpha$  (IL-1 $\alpha$ ) were estimated.

#### **Results**

DENA induced rats received the different doses of the gallic acid at dose dependent manner until 22 weeks. The hepatic serum, antioxidant markers and hematological parameters significantly ( $P < 0.001$ ) altered at effective dose dependent manner. The level of proinflammatory cytokines viz., TNF- $\alpha$ , IL-6 and IL-1 $\alpha$  significantly altered by the gallic acid at dose dependent manner. The histopathology study showed from the test group exhibited almost normal architecture as compared to HCC control rats.

#### **Conclusions**

It can be concluded that gallic acid mediated chemoprotective effect of DENA induced hepatocarcinogenesis is related to alteration of oxidative stress as well as proinflammatory cytokines.

#### **References**

1. Kumar V: **Effect of  $\alpha$ -magostin on nitrosamine induced hepatic carcinogenicity in neonatal pups.** *Ann Oncol* 2015, **26 (suppl\_9)**:1-7.
2. Anwar, *et al*: **Anticancer effect of rosiglitazone in rats treated with Nnitrosodiethylamine via inhibition of DNA synthesis: an implication for hepatocellular carcinoma.** *RSC Adv* 2015, **5**:68385.
3. Kumar, *et al*: **Fixed dose combination therapy loperamide and niacin ameliorates diethylnitrosamine-induced liver carcinogenesis in albino wistar rats.** *RSC Advances* 2015, **5**:67996-68002.

## Oncolytic Viruses

Presenting author underlined; *Primary author in italics*

319

### Phase I/II CANON study: oncolytic immunotherapy for the treatment of non-muscle invasive bladder (NMIBC) cancer using intravesical Coxsackievirus A21

Nicola Annelis<sup>1</sup>, Hardev Pandha<sup>1</sup>, Guy Simpson<sup>1</sup>, Hugh Mostafid<sup>2</sup>, Kevin Harrington<sup>3</sup>, Alan Melcher<sup>4</sup>, Mark Grose<sup>5</sup>, Bronwyn Davies<sup>5</sup>, Gough Au<sup>5</sup>, Roberta Karpathy<sup>5</sup>, Darren Shafren<sup>5</sup>

<sup>1</sup>University of Surrey, Guildford, England, UK

<sup>2</sup>Royal Surrey County Hospital, Guildford, England, UK

<sup>3</sup>Institute for Cancer Research, London, England, UK

<sup>4</sup>The Institute for Cancer Research, London, England, UK

<sup>5</sup>Viralitics, Inc., Sydney, New South Wales, Australia

#### Background

As a clinical setting in which local live biological therapy is already well established, non-muscle invasive bladder cancer (NMIBC) presents intriguing opportunities for oncolytic virotherapy. Coxsackievirus A21 (CVA21, CAVATAK™) is a novel intercellular adhesion molecule-1 (ICAM-1)-targeted immunotherapeutic virus which exerts potent oncolytic activity against NMIBC cell lines and *ex-vivo* human bladder tumour. CVA21 in combination with low doses of Mitomycin C enhances CVA21 viral replication and oncolysis by increasing surface expression levels of ICAM-1.

#### Methods

A two stage Phase I/II study (CANON) was initiated to study the tolerance of escalating intravesicular (IV) doses of CVA21 administered alone or in combination with MitomycinC (10mg) in 16 first-line NMIBC cancer patients prior to TURBT surgery. Cystoscopy photography was performed before and after treatment. Tissues were analysed for CVA21 replication, apoptosis, changes in immune cell infiltrates (multi-spectral imaging) and immune-checkpoint molecules.

#### Results

IV administration of CAVATAK was well tolerated with no adverse events. Anti-cancer activity including viral induced tumour inflammation was demonstrated by serial cystoscopy including a complete response observed in one of 3 patients in the highest dose monotherapy cohort. Tumour targeting by CVA21 was shown by detection of secondary viral load peaks in the urine and by immunohistochemical analysis of TURBT tissue displaying tumour-specific viral replication and apoptotic cell death. Nanostring analysis revealed an upregulation of interferon-response and immune checkpoint inhibitory genes in CVA21-treated tissues compared to untreated historical controls. Notable changes in immune cell infiltrates and expression of PD-L1 within the CVA21-treated NMIBC tissue were also observed. Increased urinary levels

of the chemokine, HMGB1, was observed in six of eleven patients following exposure to CVA21.

#### Conclusions

The utility of CVA21 as a potent immunotherapeutic agent has been demonstrated by the observed tumour targeting and viral replication. Upregulation of checkpoint molecules following CVA21 exposure may also allow potential sequential combination therapies with checkpoint targeting.

320

### The oncolytic effect of talimogene laherparepvec (T-VEC) can be augmented by MEK inhibition in melanoma cell lines

Praveen K Bommarreddy<sup>1</sup>, Howard L Kaufman<sup>2</sup>, Andrew Zloza<sup>2</sup>, Frederick Kohlhapp<sup>1</sup>, Ann W Silk<sup>1</sup>, Sachin Jhavar<sup>1</sup>, Tomas Paneque<sup>3</sup>

<sup>1</sup>Rutgers University, New Brunswick, NJ, USA

<sup>2</sup>Rutgers Cancer Institute of New Jersey, New Brunswick, NJ, USA

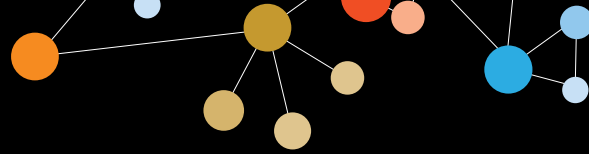
<sup>3</sup>Rutgers Robert Wood Johnson Medical School, Somerset, NJ, USA

#### Background

Talimogene laherparepvec (T-VEC) is an engineered oncolytic herpes simplex virus, type 1 (HSV-1) encoding GM-CSF that has been approved for treating melanoma. Oncolytic viruses may preferentially replicate in cancer cells due to defects in oncogenic signaling pathways that promote cell survival and allow time for more complete viral replication and assembly by suppressing apoptotic machinery including double-stranded RNA-dependent protein kinase (PKR). It is thought that the MAPK pathway interacts with PKR, but the mechanism is poorly understood. Since the MAPK pathway is frequently mutated in melanoma cells, we sought to determine if mutations in BRAF or NRAS might enhance T-VEC-mediated oncolysis. We further sought to determine if BRAF or MEK inhibition might influence the oncolytic potential of the virus.

#### Methods

Melanoma cell lines were selected for BRAF, NRAS, and other mutations for evaluation. The cells were plated in 96 well plates (10<sup>4</sup> cells/well) and treated with a range of T-VEC doses (MOI of 1-0.001). Cell viability was assessed by the AlamarBlue assay. After establishing baseline viability results, cells were concurrently treated with T-VEC and MEK inhibitors (trametinib or PD0325901 at doses 100nM-1nM) or BRAF inhibitor (vemurafenib, 100nM-1nM) and cell viability determined by AlamarBlue assay. For *in vivo* viral propagation, NSG mice were challenged with SK-MEL-28 (5x10<sup>6</sup>) at day 0. Mice were treated with T-VEC (3x10<sup>6</sup> PFU) and/or trametinib (0.3 mg/kg) on day 10 and day 12. Tumors



## Oncolytic Viruses

Presenting author underlined; Primary author in italics

were harvested (day 17) and viral load was determined by immunoblotting for HSV-1 glycoprotein D. Statistical comparisons between treatment groups were determined using the Student's t test with  $P < 0.05$  being considered statistically significant.

### Results

All cell lines were highly susceptible to lysis by T-VEC although this effect was reduced when the MOI was decreased to 0.001 for most cells. There was no correlation between BRAF or NRAS mutation status and cell viability at tested doses. There was also no effect of vemurafenib on cell viability following T-VEC infection. However, treatment with the combination of T-VEC and trametinib significantly increased cancer cell death ( $P < 0.01$ ). A similar effect was seen with a second MEK inhibitor (PD0325901;  $P < 0.001$ ).

### Conclusions

The combination of T-VEC with MEK inhibition resulted in enhanced *in vitro* tumor cell killing and viral propagation. Combining MEK inhibitors with T-VEC represents an attractive therapeutic option and further studies are needed to understand if oncolytic viruses *in vivo* might limit resistance to MEK inhibition.

### 321

#### **Oncolytic herpes simplex virus, type 1 (HSV-1) encoding GM-CSF induces HSV-1 glycoprotein B-specific T cell responses that traffic to injected and un-injected melanoma tumors**

Praveen K Bommarreddy<sup>1</sup>, Frederick Kohlhapp<sup>1</sup>, Jenna Newman<sup>1</sup>, Pedro Beltran, Andrew Zloza<sup>2</sup>, Howard L Kaufman<sup>2</sup>

<sup>1</sup>Rutgers University, New Brunswick, NJ, USA

<sup>2</sup>Rutgers Cancer Institute of New Jersey, New Brunswick, NJ, USA

### Background

The first oncolytic virus using an attenuated oncolytic herpes simplex virus, type 1 (HSV-1) encoding GM-CSF, called talimogene laherparepevec (T-VEC) has been approved for the treatment of accessible and unresectable melanoma. T-VEC enters tumor cells through Nectin cell surface receptors and results in cell lysis and induction of anti-tumor immunity. We previously identified MART-1-specific CD8+ effector T cells within the tumor microenvironment of T-VEC-treated lesions but the contribution of viral-specific T cell responses to the anti-tumor activity following T-VEC treatment has not been reported. To determine if there might be a role for HSV-1-specific T cells, we developed a murine-adapted model in which the complete T-VEC backbone was used with the substitution of murine GM-CSF (mTVEC) in place of the human gene. We hypothesized that anti-viral T cell responses might contribute to the anti-tumor activity.

### Methods

C57/BL6 mice were challenged with B16-nectin ( $10^5$ ) tumor cells on the right and left flank (day 0). mTVEC ( $3 \times 10^6$  PFU) was injected into the right flank tumor (day 7). Tumor growth was monitored every 2-3 days by caliper measurement. Tumors were harvested at various times and analyzed by flow cytometry for NK cells, antigen-presenting cells, T cells, and activation markers. Antigen specificity was determined using gp100 and HSV-1 glycoprotein B tetramers. Statistics were determined using the Student's t test with  $P < 0.05$  being considered statistically significant.

### Results

mTVEC resulted in significant regression of injected, right flank tumors with minimal effects on the growth of un-injected, left flank tumors ( $P < 0.0001$ ). We observed a significant increase in tumor immune infiltration into the injected lesion, with a lower number of immune cells in the un-injected sites ( $P < 0.01$ ). The pattern and the timing of immune infiltration mimicked that of acute viral infection with an initial infiltration of NK cells and antigen-presenting cells followed by infiltration of HSV-1 gB-specific CD8+ T cells that peaked at day 7 post injection. Additionally, we observed that HSV-1-specific CD8+ T cells trafficked to un-injected lesions. In this model, gp100 T cell responses were not detected.

### Conclusions

Our data indicate that oncolytic HSV-1-GM-CSF mediates anti-tumor therapeutic responses in a mouse model of melanoma, treatment induces a typical anti-viral innate and adaptive immune response, and HSV-1-specific T cells can be generated and traffic to both injected and un-injected tumors. These data suggest that anti-viral T cell responses may contribute to the anti-tumor effects of HSV-1-based oncolytic virus immunotherapy.

### 322

#### **A CD47-blocking oncolytic vaccinia virus for cancer therapy**

Felicia Cao, Bang-Xing Hong, Tania Rodriguez-Cruz, Xiao-Tong Song, Stephen Gottschalk

Center for Cell and Gene Therapy, Texas Children's Hospital, Houston Methodist, Baylor College of Medicine, Houston, TX, USA

### Background

Oncolytic vaccinia viruses (VV) have shown antitumor activity in early phase clinical studies but few patients have been cured, likely due to the inability of VVs to kill all tumor cells. Tumor-associated macrophages (TAMs) are key in creating an immunosuppressive tumor microenvironment. However, recent studies have shown that the phagocytic capacity of

## Oncolytic Viruses

Presenting author underlined; Primary author in italics

TAMs can be harnessed to induce antitumor responses by blocking CD47 and providing a phagocytosis signal using a chimeric molecule composed of the high-affinity ectodomain of SIRP $\alpha$  fused to IgG4 Fc (SIRP $\alpha$ -Fc). We propose to adapt this approach to oncolytic VVs and hypothesize that an oncolytic VV genetically modified to express SIRP $\alpha$ -Fc (SIRP $\alpha$ -Fc-VV) has enhanced antitumor activity.

### Methods

To initially evaluate our strategy we genetically modified CD47+ tumor cells (OV10.315, MC38, Raji) with lentiviral vectors encoding SIRP $\alpha$  or SIRP $\alpha$ -Fc.

### Results

*In vitro*, OV10.315.SIRP $\alpha$ -Fc cells were readily phagocytosed by M1 and M2 macrophages in comparison to OV10.315.SIRP $\alpha$  and non-transduced (NT) OV10.315 cells ( $p < 0.05$ ). *In vivo*, Raji.SIRP $\alpha$ -Fc cells had decreased tumorigenicity in comparison to Raji.SIRP $\alpha$  and NT Raji cells post IV injection in NSG mice resulting in a significant survival advantage ( $p < 0.05$ ). 4/5 C57BL/6 mice rejected MC38.SIRP $\alpha$  and MC38.SIRP $\alpha$ -Fc cells post SC injection in contrast to 0/4 NT MC38 cells ( $p < 0.05$ ). Having established that SIRP $\alpha$ -Fc expression in tumor cells has the desired therapeutic effect, we generated VVs encoding either SIRP $\alpha$  or SIRP $\alpha$ -Fc (SIRP $\alpha$ -VV or SIRP $\alpha$ -Fc-VV). *In vitro*, both SIRP $\alpha$ -VV and SIRP $\alpha$ -Fc-VV had similar oncolytic activity compared to parental VV (VSC20). The expression and secretion of SIRP $\alpha$  and SIRP $\alpha$ -Fc was confirmed by FACS analysis. In co-culture assays, only SIRP $\alpha$ -Fc-VV was able to induce M1 and M2 macrophage killing. Based on our encouraging *in vitro* experiments, we have initiated *in vivo* studies to test the safety and efficacy of SIRP $\alpha$ -Fc-VV in the MC38 C57BL/6 model.

### Conclusions

We demonstrate here that tumor cells secreting SIRP $\alpha$ -Fc are readily phagocytosed by M1 and M2 macrophages and have reduced tumorigenicity in xenograft and immune competent animal models. In addition, SIRP $\alpha$ -Fc-VVs readily infect tumor cells and induce phagocytosis by macrophages. Thus, arming oncolytic viruses such as VVs with SIRP $\alpha$ -Fc has the potential to improve their antitumor activity.

323

### Selective activation of innate immune responses by the Ad11/Ad3 chimeric oncolytic group B adenovirus enadenotucirev

Hugo Calderon<sup>1</sup>, Sam Illingworth<sup>1</sup>, Alice Brown<sup>1</sup>, Kerry Fisher<sup>1</sup>, Len Seymour<sup>2</sup>, Brian Champion<sup>1</sup>

<sup>1</sup>PsiOxus Therapeutics Ltd, Abingdon, England, UK

<sup>2</sup>Oxford University, Oxford, England, UK

### Background

Oncolytic viruses (OVs) are characterized by their ability to selectively infect and kill tumor cells. More recently they have been exploited for their capacity to be encoded with, and locally deliver, a variety of payloads including immunotherapeutic transgenes to enhance immune responses against the tumor. Viral properties of OVs may also be able to engage the innate immune system and thus influence the suppressive nature of the tumor microenvironment. A better understanding of these interactions may help guide both the rational design of 'armed' viruses as well as the design of strategies for combining with other immunotherapies. Enadenotucirev (EnAd) is a chimeric Ad11/Ad3 group B oncolytic adenovirus under development for the systemic treatment of metastatic carcinomas. Unlike the group C virus Ad5, EnAd does not bind to cells via the CAR receptor but instead uses CD46 which is expressed by innate immune cells.

### Methods

We have been evaluating the effect of EnAd on innate immune responses using *in vitro* immature human monocyte-derived dendritic cells (DC) as a model suppressive phenotype APC.

### Results

EnAd induced up-regulation of surface activation markers and induced the production of pro-inflammatory cytokines. Further mechanistic experiments, comparing the effects of EnAd to those of Ad5 indicated that the activation was selective for EnAd, was particle-mediated and dependent on CD46 binding. In order to understand the functional implications downstream of these interactions, T cell activation and phenotype was assessed using an allogeneic mixed lymphocyte reaction approach. EnAd-treated DCs selectively stimulated stronger T cell responses, including enhanced IFN $\gamma$  production. The data supports EnAd as a good candidate OV for steering the response of T cells activated within the tumor towards a Th1 phenotype for enhanced effector responses.

### Conclusions

Thus, as well as its potent oncolytic properties, EnAd particles may also function in the tumor microenvironment to help drive functional adaptive immune responses by inducing pro-inflammatory phenotype APCs, which should also synergize effectively with other immunotherapy strategies.





## Oncolytic Viruses

Presenting author underlined; Primary author in italics

324

### **CD40L-armed oncolytic LOAd viruses control growth of CD40+ T24 bladder cancer via both oncolysis and CD40-mediated apoptosis**

Emma Eriksson<sup>1</sup>, Jessica Wenhe<sup>1</sup>, Ann-Charlotte Hellström<sup>1</sup>, Gabriella Paul-Wetterberg<sup>1</sup>, Angelica Loskog<sup>2</sup>

<sup>1</sup>Uppsala University, Uppsala, Sweden

<sup>2</sup>Uppsala University, Lokon Pharma AB, Uppsala, Sweden

#### **Background**

CD40-CD40L signaling is a powerful pathway that can be used in cancer immunotherapy. CD40 stimulation of immune cells drives a Th1 anti-tumor response but CD40 stimulation on tumor cells can lead to enhanced tumor cell apoptosis. This is due to the up-regulation of FASL, tumor necrosis factor alpha (TNF $\alpha$ ), and TNF-related apoptosis-inducing ligand (TRAIL) on tumor cells after CD40-CD40L interaction. Also, CD40 signaling in tumor cells can induce activation of caspases through the binding of TRAF 2. LOAd viruses are oncolytic adenoviruses that encode a trimerized form of CD40L (TMZ-CD40L) alone (LOAd700) or in combination with 4-1BBL (LOAd703). In the current study, the role of CD40L on CD40+ tumor cells has been elucidated.

#### **Methods**

The cell viability post virus infection of CD40+ T24 tumor cells was investigated *in vitro* by MTS assay. To further investigate the cell death induced by CD40L signaling apart from oncolysis due to LOAd virus infection, monocyte-derived dendritic cells were infected with LOAd(-) and LOAd700 and then co-cultured with T24 cells. Apoptosis induction was investigated at 48 hours post co-culture initiation by flow cytometry for Annexin V and 7-AAD. In a T24 xenograft model using Nu/Nu immunodeficient mice, LOAd viruses expressing human TMZ-CD40L that does not cross-react to murine CD40 was used (6x) to evaluate *in vivo* efficacy. LOAd(-) was used as a control of growth control by oncolysis and PBS-treated controls determined normal growth rate.

#### **Results**

The LOAd viruses induced oncolysis of the CD40+ urinary bladder cancer T24 cell line independently of transgene expression. However, infected T24 showed a significant decrease in cell viability after infection with TMZ-CD40L-expressing LOAd700 compared to LOAd(-). Co-culture of LOAd-infected dendritic cells expressing TMZ-CD40L or not with T24 led to an increased induction of apoptosis when co-cultured with dendritic cells expressing TMZ-CD40L. *In vivo*, both LOAd(-) and LOAd703 treatment led to a decreased tumor growth compared to PBS-treated animals. When TMZ-CD40L was expressed (e.g. LOAd703), tumor control was faster and at end point, only 1/5 animals had tumor growth

compared to 3/5 in the LOAd(-)-treated group, demonstrating the additional growth control by CD40-induced tumor cell death. Models with CD40- tumor cells (Panc01, H727, SKOV3) responded similarly to control virus and virus expressing TMZ-CD40L.

#### **Conclusions**

Oncolytic viruses encoding TMZ-CD40L have an increased killing capacity via CD40L-mediated killing of CD40+ tumor cells.

325

### **A novel oncolytic adenovirus expressing immunostimulatory genes that promotes an anti-tumor response**

Emma Eriksson<sup>1</sup>, Ioanna Milenova<sup>2</sup>, Jessica Wenhe<sup>1</sup>, Magnus Ståhle<sup>1</sup>, Justyna Jarblad-Leja<sup>3</sup>, Gustav Ullenhag<sup>4</sup>, Anna Dimberg<sup>1</sup>, Rafael Moreno<sup>5</sup>, Ramon Alemany<sup>5</sup>, Angelica Loskog<sup>6</sup>

<sup>1</sup>Uppsala University, Uppsala, Sweden

<sup>2</sup>Uppsala University, Amsterdam, Netherlands

<sup>3</sup>Uppsala University, Immuneed AB, Uppsala, Sweden

<sup>4</sup>Uppsala University, Uppsala University Hospital, Uppsala, Sweden

<sup>5</sup>Institut Catalá d'Oncologia, Barcelona, Spain

<sup>6</sup>Uppsala University, Lokon Pharma AB, Uppsala, Sweden

#### **Background**

Immunotherapies aim to break the tolerance of immune cells seen in cancer patients and redirect the response from a pro-tumor to an anti-tumor response. There are many ways to achieve anti-tumor immunity, for example by stimulation of immunostimulatory pathways. CD40L interactions with its receptor CD40 on dendritic cells leads to maturation of these cells and polarization towards a Th1 response. CD40L can also reduce the level of myeloid suppressor cells and M2 macrophages as well as induce apoptosis in CD40 positive tumor cells. 4-1BB ligand (4-1BBL) interactions with its receptor 4-1BB on T cells leads to activation and survival of the cells and can expand memory T cells. Herein, we present an oncolytic adenovirus with a CMV-driven transgene cassette containing the human transgenes for a trimerized, membrane-bound CD40 ligand (TMZ-CD40L) and the full length 4-1BBL.

#### **Methods**

Pancreatic cell lines and exocrine cells from healthy donors were infected with LOAd703 and analyzed for cell death 48 and 72 hours post-infection with MTS-assay. Immunodeficient mice with established human Panc01 tumors were treated twice a week for three weeks and evaluated for tumor size. Both the *in vitro* and *in vivo* experiments were repeated in combination with gemcitabine. Dendritic cells were infected

## Oncolytic Viruses

Presenting author underlined; *Primary author in italics*

with the virus and evaluated by flow cytometry and ProSeek. The dendritic cells were also pulsed with CMV peptides and co-cultured with autologous CD14<sup>-</sup> cells to investigate the expansion of CMV<sup>+</sup> T cells by flow cytometry.

### Results

LOAd703 decreased the viability of pancreatic tumor cells at both 48 hours and 72 hours as compared to cells infected with a non-replication competent virus but spared healthy exocrine cells. Mice treated with LOAd703 had a decreased tumor burden compared to PBS treated animals. LOAd703 could be successfully combined with gemcitabine without any negative effects on oncolysis both *in vitro* and *in vivo*. Dendritic cells infected with LOAd703 showed a mature phenotype with expression of CD83, CD86, and secretion of cytokines, chemokines including IL12p70 and IFN $\gamma$ . The dendritic cells were also functional and could expand antigen-specific CMV<sup>+</sup> T cells and NK cells.

### Conclusions

In conclusion, LOAd703 is a novel oncolytic virus that targets both the tumor with oncolysis and the immune system with Th1 type response from dendritic cells and an expansion of antigen-specific T cells. The next step is to bring the virus from the lab bench to the bedside in a clinical trial to elucidate its effect in pancreatic cancer (NCT02705196).

326

### **An oncolytic virus targeting tumor cell survival, desmoplasia and immune activation in pancreatic cancer**

Emma Eriksson<sup>1</sup>, Ioanna Milenova<sup>2</sup>, Rafael Moreno<sup>3</sup>, Ramon Alemany<sup>3</sup>, Angelica Loskog<sup>4</sup>

<sup>1</sup>Uppsala University, Uppsala, Sweden

<sup>2</sup>Uppsala University, Amsterdam, Netherlands

<sup>3</sup>Institut Catalá d'Oncologia, Barcelona, Spain

<sup>4</sup>Uppsala University, Lokon Pharma AB, Uppsala, Sweden

### Background

The tumor microenvironment supports the tumor cells. In pancreatic cancer, stellate cells, immune cells and extracellular matrix compose the majority of the lesions and create a condition referred to as desmoplasia. IL6 drives STAT3 activation leading to transforming growth factor (TGF) beta and collagen type 1 production. TGF beta also promotes immunosuppression by inhibition of T cells and expansion of T regulatory cells (Tregs). Hence, IL6, which is overexpressed in pancreatic cancer, is one of the regulators of desmoplasia. Further, IL6 is associated to poor prognosis of pancreatic cancer. In order to target both IL6 and induce immune activation, the oncolytic adenovirus LOAd713 was developed. It is double-armed with an anti-IL6 receptor antibody single chain fragment (aIL6R scFv) aiming to disrupt IL6 signaling

and a trimerized membrane-bound CD40 ligand (TMZ-CD40L) that drives Th1 immunity.

### Methods

LOAd713 is an Ad5/35 virus that replicates only in cells with a dysfunctional retinoblastoma pathway (E1Adelta24). Further, the serotype 5 fiber was changed to a serotype 35 fiber to target CD46 expressed by most tumors. A CMV-driven transgene cassette with the transgenes for TMZ-CD40L and aIL6R scFv was added into the genome. The activity of LOAd713 was evaluated by 1) infecting pancreatic tumor cell lines and evaluating their viability in a MTS cytotoxicity assays (oncolysis), 2) by infecting human dendritic cells (DC) and performing phenotypic assays by flow cytometry, cytokine arrays and lymphocyte stimulation assays (immune activation), and 3) by infecting pancreatic stellate cells and investigating biological changes in a proteomic analysis (ProSeek).

### Results

LOAd713 had oncolytic capacity in a panel of pancreatic cancer cell lines as shown by the viability analysis post infection while pancreatic stellate cells infected with LOAd713 did not lose viability. However, LOAd713 significantly decreased the expression of hepatocyte growth factor (HGF), TGF beta, fibroblast growth factor-5 (FGF-5) and collagen type I, all connected to stellate cell function and desmoplasia. Nevertheless, LOAd713-infected stellate cells increased their expression of IL1 alpha, IL6, IL8, CXCL10 and CCL20, which may both promote angiogenesis and attract lymphocytes. LOAd713-infected DCs showed an increased level of maturation markers such as CD83 and IL12 as shown by flow cytometry and luminex methodology, and such DCs could expand antigen-specific T cells.

### Conclusions

LOAd713 is an oncolytic adenovirus aiming to interrupt the IL6/IL6R pathway resulting in reduced factors that drive desmoplasia. Further, via TMZ-CD40L, LOAd713 can activate DCs to drive lymphocyte responses.

327

### **Radiation therapy augments the effect of talimogene laherparepvec (T-VEC) on melanoma cell viability**

Sachin Jhawar<sup>1</sup>, Sharad Goyal<sup>2</sup>, Praveen K Bommareddy<sup>1</sup>, Tomas Paneque<sup>3</sup>, Howard L Kaufman<sup>2</sup>, Andrew Zloza<sup>2</sup>

<sup>1</sup>Rutgers University, New Brunswick, NJ, USA

<sup>2</sup>Rutgers Cancer Institute of New Jersey, New Brunswick, NJ, USA

<sup>3</sup>Rutgers Robert Wood Johnson Medical School, Somerset, NJ, USA



## Oncolytic Viruses

Presenting author underlined; *Primary author in italics*

### Background

The oncolytic herpes virus talimogene laherparepvec (T-VEC), engineered to express GM-CSF, is the first oncolytic virus approved for treatment of cancer in the US. T-VEC treatment increases median overall survival (OS) in patients with locally advanced and metastatic melanoma; however, a majority of treated patients still progress on this therapy. Radiation therapy (RT) in combination with immunotherapies has been shown to improve response rates in melanoma (compared to either modality alone) and may exhibit different cytotoxic and immunoregulatory effects on tumors than T-VEC. Therefore, we hypothesized that combination RT and T-VEC may represent a potentially synergistic therapeutic approach and investigated the effect of this combination.

### Methods

Human melanoma cell lines cultured in 96-well plates (7x10<sup>3</sup> cells per well) were treated in triplicate with RT (0, 4, or 8 Gy) delivered via the Gammacell 40 exactor. Twelve hours later the cells were further treated with T-VEC (0, 0.01, 0.1, and 1 MOI) for 60 hours. The effects of RT and T-VEC were determined by AlamarBlue cell viability assay performed 72 hours after initial treatment. A P value < 0.05 obtained using the Student's t test was considered to denote a statistically significant difference between groups.

### Results

Treatment of UACC62 melanoma cells with T-VEC (1 MOI) alone resulted in a 12% decrease in cell viability compared to no treatment (P < 0.013), while treatment with RT (8 Gy) did not result in a significant decrease (2.1%, P=0.42). However, combination RT (8 Gy) and TVEC (1 MOI) resulted in a significant decrease in cell viability (21%, P < 0.001) compared with no treatment. This likewise represented a significant decrease compared to RT alone (p=0.0028) or T-VEC alone (p=0.0389). Similar findings were noted in experiments utilizing other melanoma cell lines.

### Conclusions

Treatment with combination RT and T-VEC results in an *in vitro* decrease in melanoma cell viability. Further studies are needed to understand the mechanism underlying the reported synergy, the effect of radiation on viral propagation, the effect of viral replication on radiation sensitivity, and whether this approach can be used in patients resistant to either modality alone or to other single and combination immunotherapies. Studies assessing this combination therapy in other solid tumors and in pre-clinical *in vivo* immune-competent autologous double-humanized mouse models are currently underway.

### 328

#### Interim results of the CAPRA clinical trial: CAVATAK and pemrolizumab in advanced melanoma

Howard L Kaufman<sup>1</sup>, Ann Silk<sup>1</sup>, Janice Mehnert<sup>1</sup>, Nashat Gabrail<sup>2</sup>, Jennifer Bryan<sup>1</sup>, Daniel Medina<sup>1</sup>, Praveen K Bommareddy<sup>1</sup>, Darren Shafren<sup>3</sup>, Mark Grose<sup>3</sup>, Andrew Zloza<sup>1</sup>

<sup>1</sup>Rutgers Cancer Institute of New Jersey, New Brunswick, NJ, USA

<sup>2</sup>Gabrail Cancer Center, Canton, OH, USA

<sup>3</sup>Viralytics Limited, Sydney, New South Wales, Australia

### Background

CAVATAKä is a novel bio-selected oncolytic, immunotherapeutic Coxsackievirus A21 (CVA21) strain. Intratumoral (i.t.) CAVATAKä injection can induce selective tumor-cell infection, immune-cell infiltration, g-INF response gene up-regulation, increased PD-L1 expression, tumor cell lysis and systemic immune responses. Preclinical studies in an immune-competent mouse model of melanoma have revealed that combinations of i.t. CVA21 and anti-PD-1 blockade mediate significantly greater antitumor activity compared to use of either agent alone. The presented clinical trial evaluates combination CAVATAKä and pembrolizumab based on increased expression of PD-L1 following virus administration and higher response rates of pembrolizumab in patients with increased tumor PD-L1.

### Methods

This is a phase I trial of i.t. CVA21 and pembrolizumab for treated or untreated unresectable Stage IIIC-IVM1c melanoma. Patients receive up to 3 x 10<sup>8</sup> TCID<sub>50</sub> CVA21 i.t. on days 1,3,5,8 and 22, and then every 3w for up to 19 injections. Patients also receive pembrolizumab (2mg/kg) i.v. every 3w starting day 8. The primary endpoint is safety/tolerability by incidence of dose-limiting toxicity. Secondary endpoints include response rate, immune-related progression-free survival at 12m, PFS hazard ratio, 1y and overall survival. In addition, quality-of-life, time to initial response, durable response rate, changes in melanoma-specific T cells, PD-L1 expression and Th1/Th2 gene expression profiles, will be determined. Safety will be assessed using NCI CTCAE. Response will utilize Simon's two-stage design. In the first stage, 12 subjects will be accrued. If 2 or fewer responses occur within 12m of starting treatment, the study will be stopped due to futility of treatment. Otherwise, 18 additional subjects will be accrued.

### Results

To-date, 10 subjects have been enrolled with one patient leaving the study with PD and another patient with a non-treatment-related adverse event. Overall, adverse events have generally been low-grade constitutional symptoms

## Oncolytic Viruses

Presenting author underlined; *Primary author in italics*

related to CVA21 and standard pembrolizumab-related side effects. Preliminary observations have revealed reduction in a number of injected and non-injected lesions, with a number of patients displaying evidence of post-injection systemic exposure to CVA21.

### Conclusions

At present combination CVA21 and pembrolizumab appears to be generally safe and well-tolerated in an interim analysis of patients with advanced melanoma. Early analysis identified reductions in a number of injected and non-injected lesions and we look forward to evaluating a more mature overall response data set. Combination CVA21 and pembrolizumab may represent a new approach for the treatment of advanced melanoma.

### Acknowledgements

We would like to acknowledge the patients and families that participated in the clinical trial.

### 329

#### Gene transfer of cytosine deaminase with Toca 511 and subsequent treatment with 5-fluorocytosine induces anti-tumor immunity

Leah Mitchell, Kader Yagiz, Fernando Lopez, Daniel Mendoza, Anthony Munday, Harry Gruber, Douglas Jolly

Tocagen Inc., San Diego, CA, USA

### Background

Toca 511 (vocimagene amiretrorepvec) is a gene therapy which utilizes a gamma retroviral replicating vector encoding cytosine deaminase to selectively infect cancer cells. When used in combination with the prodrug, 5-fluorocytosine (5-FC), Toca 511 and 5-FC kill tumor cells by local production of 5-fluorouracil (5-FU), and induce a local immunotherapeutic effect that results in long-term survival after cessation of 5-FC treatment. The work described herein identifies the immune cell populations that change over time following administration of 5-FC as well as the role of T cells in long-term anti-tumor immune memory.

### Methods

A mouse glioma cell line, Tu-2449SC (2% pretransduced with Toca 511) was injected subcutaneously in B6C3F1 mice. 5-FC (500mg/kg, IP, SID) or PBS treatment was initiated once tumors were palpable, for 5 consecutive days followed by 2 days off drug. This treatment cycle was continued for the duration of the study. At 3, 6, 9, and 14 days after 5-FC start, tumors were harvested for immunophenotyping.

### Results

Tumor burden was significantly reduced within 14 days of treatment in mice that received 5-FC vs. PBS control. By day 6 post 5-FC treatment initiation, tumor associated

macrophages (TAM), myeloid derived suppressor cells (MDSC), and monocyte populations were significantly reduced in treated tumors compared to PBS controls. This myeloid cell depletion effect correlates with previous work by others [1] using systemic 5-FU but was complemented by an attractive pharmacokinetic profile with high levels of 5-FU in tumor tissue and undetectable levels of 5-FU in the plasma, thus avoiding systemic myelotoxicity. At 14 days post 5-FC treatment start, TAM and MDSC remained reduced in tumors of treated animals, and both CD4+ and CD8+ T cells were significantly increased. Additionally we noted that treatment with 5-FC induced high expression of IFN $\gamma$  in CD8+ T cells and polarized CD4+ T helper cells away from Th2 and Th17 differentiation pathways. Tumors were completely cleared from greater than 50% of animals treated with 5-FC and such animals resisted subsequent rechallenge at a distant site with the virus-free parental cell line. Further, adoptive transfer of splenocytes from these cured and now immunized animals led to clearance of established, orthotopic Tu-2449 tumors in recipient naïve animals as long as the donor cell transfer contained T cells.

### Conclusions

Toca 511 + 5-FC treatment results in reduced tumor burden and creates a tumor microenvironment that is more permissive to immune activation and ultimately establishment of anti-tumor immune response.

### References

1. Vincent J, Mignot G, Chalmin F, Ladoire S, Bruchard M, Chevriaux A, *et al*: **5-Fluorouracil selectively kills tumor-associated myeloid-derived suppressor cells resulting in enhanced T cell-dependent antitumor immunity.** *Cancer Res* 2010, **70(8)**:3052-3061.

### 330

#### T-Stealth™ technology mitigates antagonism between oncolytic viruses and the immune system through viral evasion of anti-viral T cells

Steven Fuhrmann<sup>1</sup>, Sasa Radoja<sup>1</sup>, Wei Tan<sup>1</sup>, Aldo Pourchet<sup>2</sup>, Alan Frey<sup>2</sup>, Ian Mohr<sup>2</sup>, Matthew Mulvey<sup>1</sup>

<sup>1</sup>BeneVir Biopharm, Inc., Gaithersburg, MD, USA

<sup>2</sup>New York University Langone School of Medicine, New York, NY, USA

### Background

The immune system is both friend and foe to oncolytic viruses (OV). It is a friend because OV rely on anti-tumor cytotoxic T lymphocytes (CTL) for a major component of their clinical efficacy. It is a foe because CTL that recognize viral antigens can kill infected cells. This blocks viral spread by terminating *in situ* viral progeny production. In this way, anti-viral CTL limit the number of virally killed cancer cells





## Oncolytic Viruses

Presenting author underlined; Primary author in italics

and blunt induction of tumor neo-antigen CTL necessary for achieving durable patient responses. BeneVir's T-Stealth™ OV arming technology blocks display of viral antigens on the surface of infected cells. This promotes viral spread and persistence in the tumor microenvironment because it renders infected tumor cells invisible to anti-viral CTL. By evading anti-viral CTL, T-Stealth™ armed OV kill more cancer cells in the context of an inflamed tumor microenvironment resulting in enhanced induction of anti-tumor CTL. T-Stealth™ armed OV are designed to combine especially well with immune checkpoint inhibitors (ICI). This is because ICI facilitate both anti-tumor as well as anti-viral CTL effector function in the tumor microenvironment and exacerbate the friend vs. foe dynamic between OV and the immune system.

### Methods

We generated an attenuated, replication competent HSV-1 OV encoding T-Stealth™ technology as well as viruses that do not encode T-Stealth™ technology or encode murine GM-CSF. These viruses were tested for their ability to control the growth of both virally infected as well as uninfected tumors in multiple syngeneic murine tumor models.

### Results

Compared to control viruses that do not encode T-Stealth™ technology or express murine GM-CSF, the T-Stealth™ armed OV persisted longer in the tumor microenvironment and enhanced the generation of anti-tumor CTL. Simultaneous treatment of mice with the T-Stealth™ armed HSV-1 and ICI against PD-1 and CTLA-4 yielded synergistic results in an aggressive bi-lateral murine tumor model. Detailed analysis of lymphocytes in untreated distant tumors revealed that the T-Stealth™ armed HSV-1 induces greater infiltration of CD8+ CTL and significantly increases TCR diversity.

### Conclusions

T-Stealth™ technology allows OV to resist premature clearance by anti-viral CTL. Because ICI enhance the ability of anti-viral CTL to clear OV from the tumor microenvironment, T-Stealth™ armed OV hold great promise for synergism with ICI in simultaneous combination regimens. The first T-Stealth™ armed OV is currently undergoing cGMP manufacturing and a phase I trial in solid tumors will commence in late 2017.

331

### **PeptiCRAd: an innovative oncolytic vaccine platform to tilt immune response from virus to tumor**

*Tuuli Ranki*<sup>1</sup>, *Sari Pesonen*<sup>1</sup>, *Cristian Capasso*<sup>2</sup>, *Erkko Ylösmäki*<sup>2</sup>, *Vincenzo Cerullo*<sup>2</sup>

<sup>1</sup>PeptiCRAd Oy, Helsinki, Uusimaa, Finland

<sup>2</sup>University of Helsinki, Helsinki, Uusimaa, Finland

### Background

Several strategies are being evaluated to activate the anti-tumor immunity for combinations with checkpoint blockade. Among these agents, viruses are promising for their natural immunogenicity and the interferon gamma response they induce. Many different viruses are being tested in the clinic as tumor vaccinations, and preliminary clinical data suggests that a local virus vaccination can induce a cellular anti-tumor response. However, virus-induced anti-tumor responses seem to be a rare exception, likely due to the initial host response to the virus overwhelming the initiation of any meaningful responses directed against tumor. Means to divert the immune response from virus towards tumor are needed to fully exploit the potential of viruses to activate clinically relevant anti-tumor immunity.

### Methods

PeptiCRAd is an oncolytic adenovirus vaccine platform where MHC I-restricted immunogenic tumor peptides, that have been modified to become positively charged, are adsorbed onto the negatively charged viral capsid via electrostatic interactions. We used the classical proof-of-concept SIINFEKL peptide (the chicken ovalbumin model) as well as clinically relevant human melanoma peptides complexed with an oncolytic adenovirus, and analyzed the characteristics and efficacy of our approach in different *in vitro* and immunocompetent *in vivo* models of murine and human melanoma.

### Results

Our results clearly show that PeptiCRAd is superior to oncolytic virus or peptide vaccinations. Importantly, the adsorption of peptides to the virus capsid is crucial, as virus in combination with non-complexed peptides was significantly less effective than PeptiCRAd. Treatment with PeptiCRAd resulted in clear growth reduction both in treated and distant tumors in aggressive immunocompetent melanoma tumor model. With PeptiCRAd approach the peptides were efficiently cross-presented in an MHC I restricted manner and both the frequency of dendritic cells cross-presenting the PeptiCRAd peptides and the frequency of peptide-specific CD8+ T cells were clearly elevated in PeptiCRAd treated animals compared to virus alone or virus with non-complexed peptide.

### Conclusions

PeptiCRAd is a novel oncolytic vaccine platform which innovatively combines adjuvant (virus) and tumor epitopes to enable a robust anti-tumor immune response. This simple strategy rapidly and cost-efficiently adapts to different tumors and antigens without the need to manipulate the viral backbone. A phase I/II clinical trial is currently under preparation.



## Oncolytic Viruses

Presenting author underlined; *Primary author in italics*

332

### **Pre-existing immunity to oncolytic virus potentiates its therapeutic efficacy.**

Jacob Ricca<sup>1</sup>, Taha Merghoub<sup>2</sup>, Jedd D Wolchok<sup>3</sup>, Dmitriy Zamarin<sup>1</sup>

<sup>1</sup>Memorial Sloan Kettering Cancer Center, New York, NY, USA

<sup>2</sup>Ludwig Collaborative Laboratory, Memorial Sloan Kettering Cancer Center, New York, NY, USA

<sup>3</sup>Department of Medicine, Memorial Sloan Kettering Cancer Center, New York, NY, USA

#### **Background**

Despite the significant promise of oncolytic viral (OV) therapy in preclinical models, clinical efficacy of systemically-administered viruses has proven to be modest. One major limitation of the systemic OV therapy is neutralization of the virus by pre-existing immunity, or development of neutralizing antibodies shortly after therapy initiation, which limit viral delivery to tumor sites. Recently, we and others have demonstrated that intratumoral therapy with OV can lead to systemic anti-tumor immunity and abscopal effects, and several clinical trials are currently exploring intratumorally administered OVs in patients. The effect of pre-existing anti-viral immunity or the development of new anti-viral immunity on the anti-tumor efficacy, however, is not well defined.

#### **Methods**

Using oncolytic Newcastle Disease Virus (NDV) as a model, we explored the effect of pre-existing immunity to the virus on its therapeutic efficacy using syngeneic B16-F10 melanoma and MB49 bladder carcinoma models.

#### **Results**

BL6 mice were immunized with NDV and subsequently implanted with B16 or MB49 murine cancer cells. Immunized and naïve tumor-bearing mice were treated intratumorally with NDV. As expected, pre-immunized animals demonstrated decreased levels of NDV replication. Surprisingly, pre-existing immunity to the virus did not decrease the antitumor efficacy and led to superior tumor clearance and long-term animal survival. Analysis of tumor-infiltrating lymphocytes from the treated animals demonstrated marked increase in infiltration with CD8+ and CD4+FOXP3- cells, and significant decrease in CD4+FOXP3+ cells, an effect that was significantly more pronounced in the pre-immunized animals. This was observed in both virus-injected and contralateral flank tumors, in absence of viral spread to distant tumor sites. Concurrent adoptive transfer of luciferase-tagged tumor-specific Trp-1 lymphocytes demonstrated increased intratumoral accumulation of Trp-1 cells in pre-immunized mice. Furthermore, lymphocytes

isolated from tumors of NDV-treated pre-immunized mice produced more IFN $\gamma$  than those of NDV-treated naïve mice when cultured with tumor cells *in vitro*, suggestive of antigen spreading. Finally, in an animal model of recurrent cancer after "cure" with NDV, re-treatment with NDV resulted in regression of tumors and long-term animal survival, an effect accompanied by significant increase in tumor-infiltrating immune cells.

#### **Conclusions**

Our findings demonstrate that pre-existing immunity to OVs might not deter, and even augment the efficacy of intratumoral OV therapy, which is likely mediated by enhanced tumor-specific immune response. This is a clinically-relevant question, which suggests that prior anti-viral immunity should not be a deterrent to OV therapy with locoregional administration, though it remains to be demonstrated whether such findings would translate to other oncolytic viruses.

333

### **A phase II multicenter trial to evaluate efficacy and safety of HF10 oncolytic virus immunotherapy and ipilimumab in patients with unresectable or metastatic melanoma**

Robert HI Andtbacka<sup>1</sup>, Merrick Ross<sup>2</sup>, Sanjiv Agarwala<sup>3</sup>, Kenneth Grossmann<sup>1</sup>, Matthew Taylor<sup>4</sup>, John Vetto<sup>5</sup>, Rogerio Neves<sup>6</sup>, Adil Daud<sup>7</sup>, Hung Khong<sup>1</sup>, Stephanie M Meek<sup>8</sup>, Richard Ungerleider<sup>9</sup>, Scott Welden<sup>9</sup>, Maki Tanaka<sup>10</sup>, Matthew Williams<sup>11</sup>

<sup>1</sup>University of Utah, Huntsman Cancer Institute, Salt Lake City, UT, USA

<sup>2</sup>University of Texas MD Anderson Cancer Center, Houston, TX, USA

<sup>3</sup>St. Luke's Hospital, Easton, PA, USA

<sup>4</sup>Oregon Health & Science University, Portland, OR, USA

<sup>5</sup>Knight Cancer Institute, Oregon Health and Science University, Portland, OR, USA

<sup>6</sup>Pennsylvania State University, Hershey Cancer Institute, Hershey, PA, USA

<sup>7</sup>UCSF Helen Diller Family Comprehensive Cancer Center, San Francisco, CA, USA

<sup>8</sup>University of Utah School of Medicine, Salt Lake City, UT, USA

<sup>9</sup>Theradex, Princeton, NJ, USA

<sup>10</sup>Takara Bio, Inc., Otsu Shiga, Japan

<sup>11</sup>University of Utah, Salt Lake City, UT, USA

#### **Background**

HF10, an attenuated, replication-competent mutant strain of herpes simplex virus type 1 (HSV1), is a promising new oncolytic viral immunotherapy. HF10 (intratumoral injection) shows activity in injected lesions and uninjected metastatic

## Oncolytic Viruses

*Presenting author underlined; Primary author in italics*

lesions. An ongoing phase II study in melanoma patients (pts) is assessing whether the combination of HF10 and the immune checkpoint inhibitor ipilimumab (ipi) enhances the antitumor effect of HF10.

### Methods

Ipi naïve pts with stage IIIB, IIIC or IV unresectable melanoma were enrolled. HF10 was administered intratumorally into single or multiple tumors ( $1 \times 10^7$  TCID<sub>50</sub>/mL, up to 5 mL/dose); 4 injections qwk; then up to 15 injections q3wk. Ipi was administered intravenously (3 mg/kg), q3wk for 4 doses. Tumor responses (irRC) were assessed at 12, 18, 24, 36, and 48wks. Best Overall Response Rate (BORR) was determined at 24wks. Serial peripheral blood and tumor biopsies were obtained and analyzed for changes in cytokines, immune profile and tumor microenvironment. Herein we present the safety, efficacy, and preliminary correlative study results.

### Results

In total, 46 pts were enrolled, of which 20% were stage IIIB, 43% stage IIIC, and 37% stage IV melanoma. Most HF10-related adverse events (AEs) were  $\leq$ G2, similar to HF10 monotherapy. No DLTs were reported; 3 G4 AEs reported, all not treatment related. 30.4% had G3 AEs. HF10-related G3 AEs (n=3) were left groin pain, thromboembolic event, lymphedema, hypoglycemia, and diarrhea. Of 44 efficacy evaluable pts, preliminary BORR at 24 wks was 42% and overall study BORR including those after 24 wks was 50% (20% CR, 30% PR) with a disease control rate of 68%. Of 15 evaluable stage IV pts, 8 (53%) pts were responders. In 24 treatment naïve pts BORR was 58% (21% CR, 37% PR) and in 20 pts who had failed  $\geq$ 1 therapies, BORR was 40% (20% CR, 20% PR). Preliminary serial peripheral blood analyses demonstrated in 75% of responders a sustained  $\geq$ 2 fold induction of the Th1 cytokines IFN-gamma and/or TNF-alpha compared to baseline at day 0. In contrast, 12% of non-responders demonstrated similar induction. Future efforts will focus on comprehensive statistical analysis of T cell cytokine induction in response to treatment, correlated to disease outcome.

### Conclusions

Combination HF10 and ipi treatment is safe and well tolerated, with promising responses in both treatment naïve and treatment failure pts. Peripheral blood Th1 cytokine upregulation may be a potential marker for response in HF10+ipi treatment.

334

### Phase II CALM extension study: intratumoral CAVATAK™ increases immune-cell infiltrates and up-regulates immune-checkpoint molecules in the microenvironment of lesions from advanced melanoma patients

Robert HI Andtbacka<sup>1</sup>, Brendan Curti<sup>2</sup>, Sigrun Hallmeyer<sup>3</sup>, Bernard Fox<sup>4</sup>, Zipei Feng<sup>2</sup>, Christopher Paustian<sup>2</sup>, Carlo Bifulco<sup>4</sup>, Mark Grose<sup>6</sup>, Darren Shafren<sup>6</sup>

<sup>1</sup>University of Utah, Huntsman Cancer Institute, Salt Lake City, UT, USA

<sup>2</sup>Providence Cancer Center, Portland, OR, USA

<sup>3</sup>Oncology Specialists, Chicago, IL, USA

<sup>4</sup>Robert W. Franz Cancer Research Center, Earle A. Chiles Research Institute, Providence Cancer Center, Portland, OR, USA

<sup>6</sup>Viralytics Limited, Sydney, New South Wales, Australia

### Background

CAVATAK™, an oncolytic immunotherapy, is a bio-selected strain of Coxsackievirus A21. Intratumoral (IT) injection of CAVATAK can induce preferential tumor cell infection, cell lysis and enhancement of a systemic anti-tumor immune response. The phase II CALM study investigated the efficacy and safety of IT CAVATAK in 57 patients (pts) with advanced melanoma resulting in a confirmed ORR of 28.1% and DRR (>6 mths) of 21.1%. Presented is an extension study aimed at understanding the impact of CAVATAK on immune cell infiltrates and immune checkpoint molecules within the tumor-microenvironment (TME) of treated lesions from advanced melanoma pts referenced to tumor response.

### Methods

In the CALM extension study a cohort of 13 advanced melanoma pts received up to  $3 \times 10^8$  TCID<sub>50</sub> CAVATAK IT on study days 1, 3, 5, and 8 and then every three weeks for a further 6 injections. Sequential tumor biopsies of injected lesions (study days 1 and 8) from 9 pts were monitored for evidence of viral-induced changes to immune cell infiltrates and checkpoint molecules being referenced to tumor response.

### Results

Of the 9 pts evaluable for tissue response assessment in this study, CAVATAK-treated lesions from 6 pts displayed disease control (CR, PR or SD), while injected lesions from 3 pts exhibited disease progression. Multi-spectral immunohistochemistry imaging revealed elevated levels of immune cell infiltrates within the TME of lesions displaying disease control (DC) compared to progressing lesions, in particular elevated levels of CD8+ cells and PD-L1+ cells. NanoString® RNA analysis of pre- and post-treatment biopsy samples identified significant increases in the levels

## Oncolytic Viruses

Presenting author underlined; *Primary author in italics*

of immune checkpoint molecules, including PD-L1, CTLA-4, IDO, TIM-3 and LAG-3 in lesions exhibiting DC compared to progressing lesions. A similar differential pattern was observed with respect to a number of immune modulation elements, including interferon-induced and viral RNA response genes. Of notable interest was the preferential up-regulation in DC lesions of CD122 (a component of the IL-2 receptor complex), which is postulated to be a potential prognostic marker for anti-tumor activity by anti-CTLA-4 blockade strategies. In addition, CAVATAK treatment initiated the reconstitution of immune cell infiltrates in a number of lesions from pts failing previous immune-checkpoint blockade or other immunotherapies.

### Conclusions

The changes in TME induced by CAVATAK support combination therapy with T cell checkpoints, especially anti-CTLA-4. There is an ongoing phase Ib study of CAVATAK + ipilimumab showing higher ORR than anticipated with either agent alone supporting the continued study of the combination.

335

### **A fully serotype 3 oncolytic adenovirus coding for CD40L as an enabler of dendritic cell therapy**

Sadia Zafar<sup>1</sup>, Suvi Parviainen<sup>1</sup>, Mikko Siurala<sup>1</sup>, Otto Hemminki<sup>1</sup>, Riikka Havunen<sup>1</sup>, Siri Tähtinen<sup>1</sup>, Simona Bramante<sup>1</sup>, Lotta Vassilev<sup>1</sup>, Hongjie Wang<sup>3</sup>, Andre Lieber<sup>3</sup>, Silvio Hemmi<sup>4</sup>, Tanja de Gruij<sup>5</sup>, Anna Kanerva<sup>1</sup>, Akseli Hemminki<sup>1</sup>

<sup>1</sup>University of Helsinki, Helsinki, Uusimaa, Finland

<sup>3</sup>University of Washington, Seattle, WA, USA

<sup>4</sup>University of Zurich, Zurich, Switzerland

<sup>5</sup>VU University Medical Center, Amsterdam, Netherlands

### Background

Dendritic cell (DC) therapy is currently considered as a promising cancer immunotherapy. Dendritic cells are considered as principal initiators of the immune system. However, tumor induced immunosuppression impairs the biological function of DCs. Therefore, clinical outcomes with DC therapy have often been disappointing. Interestingly, oncolytic adenoviruses have good safety profile in humans. They have been shown to activate immune responses by triggering danger signals at the tumor site and enhancing the release of tumor-specific antigens.

### Methods

To achieve optimal activation of the transferred dendritic cells, we armed adenoviruses with CD40 ligand (CD40L), best known for its capacity to initiate multifaceted signals in dendritic cells, leading to the activation of cytotoxic T cells. Therefore, we constructed a novel virus Ad3-hTERT-

CMV-hCD40L which features Ad3 for enhanced tumor transduction, human telomerase reverse transcriptase (hTERT) promoter for enhancing tumor selectivity and CD40L, a potent stimulator of dendritic cells and to increase antitumor efficacy. The viral particles are produced in 293 cells using a standard calcium phosphate method. Then, HeLa cells were infected with the cell lysate containing Ad3-GFP virus for further virus propagation. The functionality of the viruses is studied by infecting different cell lines with different amount of viral particles and measuring the proportion of surviving cells with MTS assay. To deeply dissect if CD40L encoding adenovirus can modulate the tumor microenvironment, we generated a murine version of the virus (Ad5/3-CMV-mCD40L).

### Results

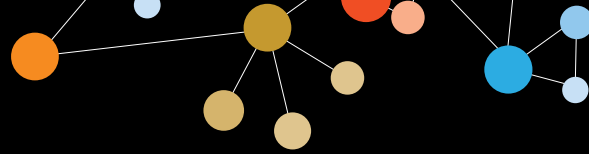
The major obstacle with oncolytic adenoviruses is suboptimal systemic delivery, which is circumvented by using a fully Ad3 platform. As human [1] and our animal data have shown, the ability of Ad3 to successfully reach tumors is through the intravenous route. In syngeneic studies in immunocompetent model, DC therapy in combination with Ad5/3-CMV-mCD40L showed potent antitumor activity and triggered significant antitumor immune responses. The improved therapeutic effect by the adenovirus expressing CD40L and DCs combination treatment correlated with increased numbers of tumor infiltrating lymphocytes, induction of the T helper type 1 cytokines IFN-gamma, RANTES, and TNF-alpha and the reduction of immunosuppression in the tumor stroma.

### Conclusions

Our findings support the development of clinical trials where dendritic cell therapy is enhanced with oncolytic adenovirus.

### References

1. Hemminki O, Diaconu I, Cerullo V, *et al*: **Ad3-hTERT-E1A, a Fully Serotype 3 oncolytic adenovirus, in patients with chemotherapy refractory cancer.** *Mol Ther* 2012, **20**:1821–1830.



## Promoting and Measuring Antitumor Immunity

Presenting author underlined; Primary author in italics

336

### **A multi-color natural killer-cell mediated cytotoxicity detection using fluorescence and direct cell imaging**

Tameem Ansari, Srividya Sundararaman, Diana Roen, Paul Lehmann

Cellular Technology Ltd, Shaker Hts, OH, USA

#### **Background**

The most essential role of effector immune cells such as CD8+ cells and natural killer (NK) cells is to identify and lyse target cells. NK cell - and antibody dependent cell cytotoxicity (ADCC) - has traditionally been assessed by the release of radioactive chromium from target cells following lysis. These assays are laborious and require substantial quantities of patient blood to detect minor changes in cell lysis. We have previously developed an assay that can visualize individual target cells to detect cytolytic activity within a high signal to noise range, without involving radioactivity, via high-throughput imaging. In order to further reduce the amount of cell material required and detect the effect of NK cells on different target cell lines, we have now developed a multi-color cytotoxicity detection assay.

#### **Methods**

The assay we developed images individual fluorescence-labeled target cells. K562, A549 and T2 tumor cells were used as targets, and peripheral blood mononuclear cells (PBMC) as effector cells. When performing the assay in 96 well format, the PBMC were plated in serial dilution between 500,000 and 7,500 cells per well with 5,000 target cells per well. Four hours later, the number of viable tumor cells was quantitated using a fluorescence capable ImmunoSpot® Analyzer or the radioactivity released was measured. For multi-color analysis, we stained three different cancer cell lines (one of which had intact MHC receptors) with three different dyes and incubated them in the same well with effector to target ratios that match one cell line per well.

#### **Results**

The target cell visualization and chromium release assay in a 96-well format required the same number of cells and the results were comparable to each other. While, expectedly, percentage of killing for different donors was highly variable, the assay was highly reproducible for cryopreserved samples between multiple days and when performed by multiple researchers. The results obtained via multi-color assessment show that we can simultaneously detect the cytolytic effect of NK cells on three different target cell types using only a third of the effector cells as previously required. Also, the data show that control target cells with MHC receptors are not susceptible to NK killing.

#### **Conclusions**

We have demonstrated the feasibility of assessing NK function in a non-radioactive, high-throughput capable system which will benefit clinical immune monitoring. The multi-color analysis should be of particular value when access to PBMC is limited, such as in pediatric, geriatric, and immune deficient populations.

337

### **Intratumoral injection of INT230-6 induces protective T cell immunity**

Anja C Bloom<sup>1</sup>, Lewis H Bender<sup>2</sup>, Ian B Walters<sup>2</sup>, Masaki Terabe<sup>1</sup>, Jay A Berzofsky<sup>1</sup>

<sup>1</sup>National Cancer Institute, Bethesda, MD, USA

<sup>2</sup>Intensity Therapeutics, Inc., Westport, CT, USA

#### **Background**

Standard care for many types of cancer involves systemic administration of cytotoxic agents. This may result in low drug concentration at tumor sites, which limits cell killing. More recently it has been shown that cytotoxic formulations designed for intratumoral delivery improve drug efficacy presumably by increasing drug concentration at the tumor site. Furthermore, it has been revealed that the mechanisms of anticancer agents extend beyond direct tumor cell lysis. One major aspect is that cell death often induces an immune response. Different types of cell death such as necrosis and autophagy induced by cytotoxic agents trigger immune responses with varying degrees of inflammation and involving different types of immune cells. The ideal immune responses that may give maximum benefit to patients would be strong and long lasting anti-tumor T cell responses.

#### **Methods**

In this study, a novel tissue and cell diffusive cytotoxic formulation, INT230-6, was administered intratumorally over 5 sequential days into subcutaneous 300mm<sup>3</sup> murine Colon26 tumors.

#### **Results**

Treatment resulted in regression from baseline of 100% of the tumors and up to 80% complete response (CR). We then sought to analyze the T cell responses in the protection induced by INT230-6. Mice with CR were protected from re-challenge either by subcutaneous or intravenous re-inoculation of the Colon26. The protection was abrogated by CD4/CD8 double depletion prior to the re-challenge, indicating that immunological memory was induced. Colon26 tumors express the endogenous retroviral protein gp70 containing the AH-1 CTL epitope. AH-1-specific CD8+ T cells were detected *ex vivo* in systemic organs such as spleens and peripheral blood of a subset of mice with CR, confirming



## Promoting and Measuring Antitumor Immunity

Presenting author underlined; Primary author in italics

induction of CD8+ T cell specific responses to tumor cells upon INT230-6 treatment.

### Conclusions

Hence, INT230-6 given locally to treat tumors induces tumor specific protective T cell immunity.

### 338 ★ Abstract Travel Award Recipient

#### Fluorine-19 nuclear magnetic resonance (NMR) to track and quantify human transgenic T cell biodistribution in murine studies of glioblastoma immunotherapy

Fanny Chapelin<sup>1</sup>, Hideho Okada<sup>2</sup>, Eric T Ahrens<sup>1</sup>

<sup>1</sup>University of California, San Diego, La Jolla, CA, USA

<sup>2</sup>University of California, San Francisco, San Francisco, CA, USA

### Background

Glioblastoma multiforme (GBM) is the most common brain cancer for which classical treatment options remain limited. Recent advances in immunotherapy for other cancers hold great promise for the treatment of GBM. To uncover the mechanisms of such therapies, it is critical to develop tools to quantitatively assay T cell biodistribution and survival after delivery to correlate with putative therapeutic effects. In this study, we used a new probe technology to quantify T cell therapy distribution in intact tissue samples and correlated the results to tumor growth.

### Methods

Human PBMC-isolated T cells were transduced with a chimeric antigen receptor (CAR) lentiviral vector to express a surface antibody against EGFRvIII, a common receptor in GBM. We compared CAR T cells efficacy and biodistribution to those of naïve T cells. CAR-T cells and naïve T cells were intracellularly labeled with a perfluorocarbon (PFC) emulsion *ex vivo* and injected intravenously in SCID mice bearing bilateral subcutaneous human U87 tumors engineered to express EGFRvIII. Tumor growth was monitored over 7 days with bioluminescence imaging and caliper measurements. Intact organs were then harvested for fluorine-19 NMR measurements to quantify the fluorine content and apparent cell count, followed by processing for histological validation.

### Results

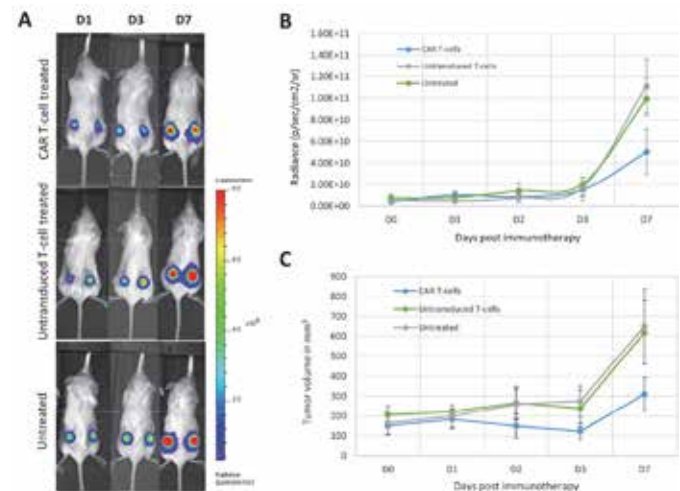
Longitudinal bioluminescence acquisitions and tumor measurements showed considerable tumor regression 7 days after CAR treatment with a radiance average of  $5.02 \times 10^{10}$  photons/sec/cm<sup>2</sup>/sr, which was twice lower than the luminescence measured for both naïve T cell treated and untreated groups ( $p=0.0001$ , Figure 1). NMR measurements in whole organs at days 2 and 7 showed strong signal in the liver, lungs, lymph nodes and tail (injection site) but modest signal in the spleen and tumors in both groups (Figure 2). We

were able to detect as low as 20,000 CAR T cells homing to the tumors but did not find any naïve T cells in the tumors. On average, the liver in naïve T cell recipients had twice the fluorine signal compared to CAR T cells. The liver signals likely represent the dead T cell fraction. We were also able to visualize failure of therapy delivery in a few animals where most of the cells remained in the lungs days after therapy injection.

### Conclusions

To conclude, <sup>19</sup>F NMR analysis, in conjunction with bioluminescence imaging, may accelerate the timeline to evaluate new immunotherapeutic cell candidates by providing a rapid and straight-forward method to determine therapy efficacy, cell biodistribution and fate in preclinical studies. We are currently performing *in vivo* <sup>19</sup>F MRI studies using the PFC technology.

**Figure 1. Immunotherapy impact on tumor growth in vivo.**



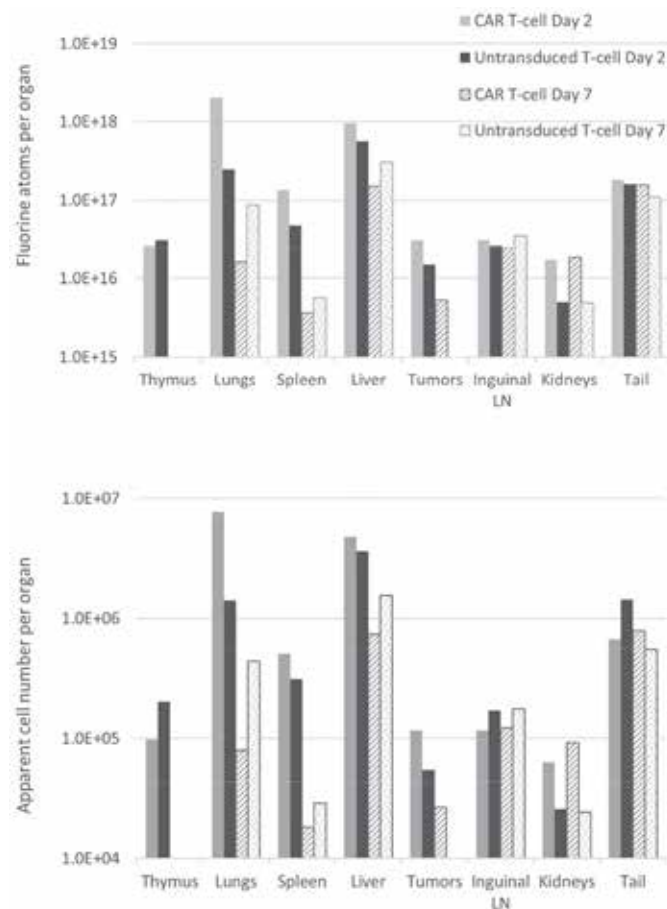
A. Representative BLI images at day 1, 3 and 7 after immunotherapy for all 3 groups. Signals are expressed in radiance (p/sec/cm<sup>2</sup>/sr) B. Time course of bioluminescence intensity in treated and untreated groups. CAR-T cell treated animals display a radiance half as high as untransduced-T cell treated animals or untreated animals. C. Corresponding tumor volumes show 50% reduction in tumor growth for the CAR-T cell treated group ( $p=0.0001$ ) and no significant difference between untransduced T cell treated and untreated groups ( $p=0.38$ ).



## Promoting and Measuring Antitumor Immunity

Presenting author underlined; Primary author in italics

**Figure 2. Biodistribution quantification of fixed tissue samples by  $^{19}\text{F}$  NMR at 2 days and 7 days post treatment.**



$^{19}\text{F}$  NMR measurements of organ biodistribution of the PFC-labeled CAR-T cells and untransduced T cells show strong liver, lungs, lymph node, and tail signal but modest signal in the spleen and tumors in both groups. Data is presented as the average fluorine atom content per organ (top) and the corresponding apparent cell number (bottom). These measurements do not account for cell division, thus referred to as “apparent cell number”. The tail signal represents mis-injection.

339

### Immune profiling of an elite responder following checkpoint inhibitor therapy reveals functional anti-tumor antibodies within expanded IgG lineages

Jeff DeFalco<sup>1</sup>, Michael Harbell<sup>1</sup>, Amy Manning-Bog<sup>1</sup>, Alexander Scholz<sup>1</sup>, Danhui Zhang<sup>1</sup>, Gilson Baia<sup>1</sup>, Yann Chong Tan<sup>1</sup>, Jeremy Sokolove<sup>2</sup>, Dongkyoon Kim<sup>1</sup>, Kevin Williamson<sup>1</sup>, Xiaomu Chen<sup>1</sup>, Jillian Colrain<sup>1</sup>, Gregg Espiritu Santo<sup>1</sup>, Ngan Nguyen<sup>1</sup>, Wayne Volkmuth<sup>1</sup>, Norman Greenberg<sup>1</sup>, William Robinson<sup>2</sup>, *Daniel Emerling<sup>1</sup>*

<sup>1</sup>Atreca, Redwood City, CA, USA

<sup>2</sup>Stanford University School of Medicine, Stanford, CA, USA

#### Background

Anti-tumor antibodies can contribute to effective patient immune responses to cancer, yet we do not fully understand their characteristics or mechanisms of action. To better elucidate the nature and significance of such antibodies we sequenced over 2500 blood plasmablasts (activated B cells) of a patient (DID-08291) with stage IV melanoma during a period of stable disease and characterized activities of resultant monoclonal antibodies.

#### Methods

Patient plasmablasts were collected and antibody sequences obtained from single cells using Atreca’s Immune Repertoire Capture™ (IRC™) technology. IRC™ incorporates complex DNA barcodes with reverse transcription, PCR and next generation sequencing to provide nearly error-free, full-length variable regions of natively paired immunoglobulin heavy and light chain genes. Sequences obtained through IRC™ can subsequently be used to synthesize and express recombinant antibodies for *in vitro* and *in vivo* testing.

#### Results

The IRC™ analysis of two sequential samples, collected 3 months apart while the patient was undergoing ipilimumab therapy, revealed extensive diversity of germline gene usage, CDR lengths, and levels of somatic hypermutation (SHM) across individual B cells. Over 1400 putative clonal antibody families were identified by grouping sequences based on immunoglobulin gene usage and other sequence features. Of these families, over 400 showed evidence of clonal expansion and/or were observed at both blood collection time points. Full length natively paired variable regions were subsequently expressed from IRC™ sequences representing both large and small putative families to generate recombinant antibodies. Multiple antibodies were found to exhibit binding to the surface of cancer cells and were further characterized for their ability to mediate *in vitro* cancer cell killing through various mechanisms including ADCC, ADC, and/or ADCP. Protein arrays are being used to

## Promoting and Measuring Antitumor Immunity

Presenting author underlined; *Primary author in italics*

identify the targets of these antibodies, while tumor growth inhibition/regression studies in syngeneic mouse models are underway to better understand the antibodies therapeutic capabilities when delivered alone or in combination with other immunotherapies.

### Conclusions

These results illustrate that naturally occurring patient antibodies have anti-tumor activity and support their further development as novel immunotherapeutics.

**340**

### Cytokine profile of sipuleucel-T in differentiating reactivation of latent immunity from de novo immune responses

Charles G Drake<sup>1</sup>, Daniel P Petrylak<sup>2</sup>, Emmanuel S Antonarakis<sup>3</sup>, Adam S Kibel<sup>4</sup>, Nancy N Chang<sup>5</sup>, Tuyen Vu<sup>5</sup>, Dwayne Campogan<sup>5</sup>, Heather Haynes<sup>5</sup>, James B Trager<sup>5</sup>, Nadeem A Sheikh<sup>5</sup>, David I Quinn<sup>6</sup>

<sup>1</sup>Johns Hopkins Sidney Kimmel Comprehensive Cancer Center, Baltimore, MD, USA

<sup>2</sup>Yale Cancer Center, New Haven, CT, USA

<sup>3</sup>Urologic Surgery, Brigham and Women's Hospital, Harvard University, Boston, MA, USA

<sup>4</sup>Dendreon Pharmaceuticals, Inc., Seattle, WA, USA

<sup>5</sup>Norris Comprehensive Cancer Center, University of Southern California, Los Angeles, CA, USA

### Background

Sipuleucel-T is an autologous cellular immunotherapy approved by the FDA for treatment of asymptomatic or minimally symptomatic metastatic castration-resistant prostate cancer (mCRPC)[1]; it is manufactured from autologous peripheral blood mononuclear cells (PBMCs) cultured with the immunogen PA2024, a fusion of prostatic acid phosphatase (PAP) conjugated to granulocyte macrophage colony-stimulating factor. Antibody and T cell responses to PA2024 and/or PAP correlate with improved overall survival in sipuleucel-T-treated mCRPC patients [2]. To better understand sipuleucel-T-induced T cell responses, we assessed CD4+ and CD8+ T cells for proliferation, intracellular cytokine production, and cytokine release after PA2024 or PAP stimulation.

### Methods

PBMCs were obtained from sipuleucel-T-treated mCRPC patients (STRIDE) and nonmetastatic, biochemically recurrent, hormone-sensitive PC patients (STAND). Samples were collected at baseline through month 6 post-sipuleucel-T. PBMCs were cultured in vitro and stimulated with either PA2024 or PAP. CD4+ and CD8+ T cells were assessed (n=19) for proliferation and for intracellular IL-2 and IFN-γ. The cytokine profile was confirmed in supernatant

with a meso scale discovery assay. p<0.10 was statistically significant

### Results

Compared with baseline, PA2024-specific proliferating CD4+ and CD8+ T cells had increased intracellular IL-2 and IFN-γ at week 6 and month 6 with a similar trend for PAP-specific proliferating T cells (Table 1). Compared with unstimulated controls, a significant >2-fold increase in PA2024-stimulated IL-2 and IFN-γ in supernatant was observed at wk 6 and mo 6 over baseline (p<0.001). PAP-stimulated IL-2 and IFN-γ supernatant levels increased over baseline and was significantly elevated for IFN-γ at wk 6 (p<0.10).

### Conclusions

Sipuleucel-T therapy generated a de novo PA2024-specific T cell response, as indicated by the cytokine release profile. The PAP-stimulated cytokine profile suggests that pre-existing immunity with terminally differentiated T cells are expanded. Thus, sipuleucel-T reactivated an anti-PAP response in memory T cells, thereby overcoming immunosuppressive mechanisms in PC.

### Acknowledgements

Medical writing services provided by Brian R. Haas, PhD, were funded by Dendreon Pharmaceuticals, Inc.

### Trial Registration

NCT01431391 and NCT01981122

### References

1. PROVENGE® (sipuleucel-T) prescribing information [Internet]. Seattle: Dendreon Corporation; c2014 [last revision 2014 October; cited 2016 April 21]. Available from: <http://www.valeant.com/Portals/25/Pdf/PI/Provenge-PI.pdf>.
2. Sheikh, *et al*: *Cancer Immunol Immunother* 2013; **62**:137-147.

Table 1. Elevation in intracellular cytokine levels

	CD4 T cell		CD8 T cell		
	Wk 6	Mo 6	Wk 6	Mo 6	
PA2024	IL-2	p<0.001	p<0.001	p<0.05	p<0.01
	IFN-γ	p<0.001	p<0.05	p<0.10	p<0.05
PAP	IL-2	p<0.001	ns	p<0.05	ns
	IFN-γ	p<0.05	ns	p<0.05	ns

ns = not significant



# Promoting and Measuring Antitumor Immunity

Presenting author underlined; Primary author in italics

341

## Immunoscore® Colon analytical performance

Luciana Batista<sup>1</sup>, Florence Marliot<sup>2</sup>, Angela Vasaturo<sup>3</sup>, Sabrina Carpentier<sup>4</sup>, Cécile Poggionovo<sup>1</sup>, Véronique Frayssinet<sup>1</sup>, Jacques Fieschi<sup>1</sup>, Marc Van den Eynde<sup>5</sup>, Franck Pagès<sup>6</sup>, Jérôme Galon<sup>3</sup>, Fabienne Hermitte<sup>1</sup>

- <sup>1</sup>HalioDx, Marseille, Provence-Alpes-Cote d’Azur, France
- <sup>2</sup>Université Paris Descartes, APHP, Paris, Ile-de-France, France
- <sup>3</sup>INSERM, Paris, Ile-de-France, France
- <sup>4</sup>MI-mAbs, Marseille, Provence-Alpes-Cote d’Azur, France
- <sup>5</sup>Université Catholique de Louvain, Brussels, Belgium
- <sup>6</sup>APHP, Paris, Ile-de-France, France

### Background

The Immunoscore® was validated as a powerful prognostic marker in colon cancer in a study conducted by the Immunoscore® worldwide consortium, led by the Society for Immunotherapy of Cancer (SITC) involving 23 pathology centers from 17 countries, and including more than 3800 patients. HalioDx has developed a standardized version of the test that was used in this study. Here we show the concordance with the research version and present the main analytical performances of the system.

### Methods

For each colon tumor block, 2 slides are stained using an automated IHC staining instrument: one with CD3 and one with CD8. Digital images of stained slides are obtained using a whole slide scanner, and analyzed by a software program (Immunoscore® Analyzer, HalioDx). The Immunoscore® Analyzer automatically processes images for tissue detection (core of the tumor, CT and invasive margin, IM). Densities of positive lymphocytes in the CT and IM are reported. For each marker and each zone, densities distributions have been established in the SITC study training set. The Immunoscore® is reported in 5 categories from 0 to 4, or as IS High (IS3 and IS4), Low (IS0 and IS1) & intermediate (IS2). Precision of HalioDx Immunoscore® Colon assay in terms of repeatability and reproducibility was evaluated using commercial FFPE colon cancer blocks, with 152 independent stainings from 4 samples, corresponding to 62 CD3 and CD8 pairs. Intra-block and inter-block variability were assessed from 8 additional blocks. Accuracy based on inter-laboratory concordance was determined using 119 samples. The European Hospital Georges Pompidou (HEGP - center of reference for the SITC study) workflow was used as reference.

### Results

The inter-instrument, inter-lot and inter-operator/-reader precision in terms of cell density (cells/mm<sup>2</sup>) CV were below 12%, 22% and 18%, respectively. Only 1 change in

Immunoscore® category (out of 62 IS assessments) was observed, from IS1 to IS0. The equivalency between HalioDx and HEGP workflows was assessed in terms of cell densities. Deeming regression slopes were not significantly different from 1 for both CD3 and CD8 antibodies. Pearson correlation coefficients were above 0.89. The concordance table is provided in Table 1, corresponding to a weighted Cohen’s kappa coefficient of 0.88.

### Conclusions

The Immunoscore® Colon is a robust, easy-to-use and accurate assay. It is the first standardized immune-based assay for the classification of cancer.

### References

1. Galon J, et al: *J Pathol* 2014, **232(2)**:199-209.
2. Galon J, et al: *JCO* 2016, **34(15\_suppl)**:3500.

Table 1

		Reference (HEGP)				
		IS0	IS1	IS2	IS3	IS4
HalioDx	IS0	11	5	0	0	0
	IS1	4	16	5	0	0
	IS2	0	2	52	5	0
	IS3	0	0	2	15	1
	IS4	0	0	0	0	1

342

## NKTR-255: an IL-15-based therapeutic with optimized biological activity and anti-tumor efficacy

Peter Kirk<sup>1</sup>, Murali Addepalli<sup>1</sup>, Thomas Chang<sup>1</sup>, Ping Zhang<sup>1</sup>, Marina Konakova<sup>1</sup>, Katsunobu Hagihara<sup>2</sup>, Steven Pai<sup>3</sup>, Laurie VanderVeen<sup>1</sup>, Palakshi Obalapur<sup>1</sup>, Peiwen Kuo<sup>1</sup>, Phi Quach<sup>1</sup>, Lawrence Fong<sup>3</sup>, Deborah H Charych<sup>1</sup>, Jonathan Zalevsky<sup>1</sup>

- <sup>1</sup>Nektar Therapeutics, San Francisco, CA, USA
- <sup>2</sup>University of California, San Francisco School of Medicine, San Francisco, CA, USA
- <sup>3</sup>Hellen Diller Family Comprehensive Cancer Center, San Francisco, CA, USA

### Background

Interleukin-15 has been identified as a promising candidate for use as an immuno-oncology therapeutic, but the native cytokine has poor drug-like properties. NKTR-255 is a novel immunotherapeutic agent consisting of polymer-engineered IL-15 designed to optimally engage the IL-15 receptor complex and provide durable pathway activation *in vivo*. Here

## Promoting and Measuring Antitumor Immunity

Presenting author underlined; *Primary author in italics*

we show that NKTR-255 has greatly improved plasma and tumor exposure relative to IL-15, induces NK and CD8+ T cell activation and proliferation, and has single-agent efficacy in syngeneic tumor models.

### Methods

Binding kinetics and affinity of NKTR-255 for IL-15R $\alpha$  were measured by surface plasmon resonance using immobilized IL-15R $\alpha$ . Cell-based potency was determined by treating CTLL-2 cells with NKTR-255 at a range of concentrations and measuring phosphorylation of STAT5 in cell lysate by immunoassay. Pharmacokinetic analysis was performed following single-dose intra-venous administration of IL-15 and NKTR-255 in normal mice and in mice bearing sub-cutaneous B16F10 and CT-26 tumors, with analytes quantified in tumor and plasma by ELISA. Immunophenotyping studies were performed by flow cytometry on lymphocytes from peripheral blood of NKTR-255-treated and IL-15-treated normal mice and from spleen, tumor and draining lymph node of treated mice carrying sub-cutaneous TRAMP-C2 tumors. Efficacy was determined by measuring tumor volume of sub-cutaneous TRAMP-C2 and CT-26, with q5dx3 treatment with NKTR-255.

### Results

NKTR-255 binds to IL-15R $\alpha$ , and induces STAT5 phosphorylation in CTLL-2 cells with sub-nanomolar EC<sub>50</sub>. Following intravenous administration, NKTR-255 demonstrates a greatly reduced clearance rate compared to IL-15, with plasma t<sub>1/2</sub> of 22-26h versus <1h for IL-15. Tumor exposure of NKTR-255 was 50-fold greater than IL-15 in B16F10-bearing C57/Bl6 mice and 110-fold greater in CT-26-bearing Balb/c mice. Immunophenotyping studies in normal mice showed an induction of Ki-67 and CD122 expression in NK cells, indicating proliferation and activation. In tumor-bearing mice, NKTR-255 treatment resulted in an increased CD8:CD4 and CD8:Treg ratio in tumor and spleen, and an increased frequency of CD8<sup>+</sup>TNF<sup>+</sup>IFN $\gamma$ <sup>+</sup> T cells. Tumor growth inhibition was observed in both CT-26 and TRAMP-C2 models.

### Conclusions

NKTR-255 treatment results in sustained IL-15 activity which induces CD8+ T cell and NK cell activation and proliferation, and produces long-lived immunophenotypic changes in tumor-bearing mice. The design of NKTR-255 enables a potential drug-like therapeutic strategy for accessing IL-15-based immunotherapy.

343

### Anti-tumor activity of NKTR-214; a CD122-biased agonist that promotes immune cell activation in the tumor microenvironment and lymphoid tissues

John L Langowski, Murali Addepalli, Yolanda Kirksey, Ravi Nutakki, Shalini Kolarkar, Rhoneil Pena, Ute Hoch, Jonathan Zalevsky, Stephen K Doberstein, *Deborah H Charych*

Nektar Therapeutics, San Francisco, CA, USA

### Background

NKTR-214 is a novel agonist of the IL-2 pathway that provides a sustained and biased activation signal to the heterodimeric IL-2R complex (IL-2R $\beta\gamma$ ). Here we examine its biological activity, pharmacodynamic effects and mechanism of action in a murine tumor model.

### Methods

To determine efficacy, mice bearing established subcutaneous B16F10 melanoma tumors were treated with NKTR-214 (q9dx3) or aldesleukin (qdx5, two cycles). For mechanistic studies, mice were treated once with NKTR-214 or with five daily administrations of aldesleukin. Splenic or tumor-infiltrating lymphocytes (TIL) were assessed by flow cytometry and gene expression analysis was conducted by RNA-Seq 5, 7, and 10 days after treatment initiation. To assess the relative contribution of tumor-resident or migrating lymphocytes to efficacy, the sphingosine-1-phosphate receptor modulator FTY720 was administered daily alone or in combination with NKTR-214.

### Results

In the aggressive B16F10 model, vehicle-treated tumors grew to the volume endpoint 8 days after initiation, with a tumor volume quadrupling time (TVQT) of 5 days. NKTR-214 showed better efficacy than aldesleukin (TVQT 16.7 versus 10 days). FTY720 significantly decreased blood lymphocytes and when added to treatment, efficacy with NKTR-214 was reduced by 39% but not completely abrogated. Analysis of TIL demonstrated that both NKTR-214 and aldesleukin led to an increase in activated NK cells. However, NKTR-214 administration led to significant and sustained increases in total and memory CD8+ T cells, while the effects from aldesleukin were transient. NKTR-214 also reduced the percentage of intratumoral Tregs at every time point, while aldesleukin had little effect on this parameter. Consequently, NKTR-214 increased the average CD8+ T cell/Treg ratio to >400, which surpassed that achieved by aldesleukin. Immune cell changes in the spleen followed a similar pattern, however with a lesser magnitude. In addition to changes in cell number, NKTR-214 treatment also induced modulation of immune gene expression networks directly in the tumor microenvironment.





## Promoting and Measuring Antitumor Immunity

*Presenting author underlined; Primary author in italics*

### Conclusions

Efficacy generated by the sustained and biased signaling of the IL-2 pathway with NKTR-214 cannot be achieved even with multiple daily administrations of aldesleukin. Furthermore, the profound changes in tumor-infiltrating lymphocytes associated with the anti-tumor activity of NKTR-214 arise from T cells stimulated in both the tumor microenvironment and the lymphoid tissues. NKTR-214 is currently being evaluated in a in an ongoing single-agent phase I/II clinical trial to assess safety, efficacy, pharmacokinetics and immune changes in the tumor microenvironment.

**344**

### Nanosecond pulsed electric field treatment of murine melanomas initiates an immune response and inhibits metastasis

John Cha, Zach Mallon, Myra Perez, Amanda McDaniel, Snjezana Anand, Darrin Uecker, Richard Nuccitelli

Pulse Biosciences, Burlingame, CA, USA

### Background

Nano-Pulse Electro-Signaling (NPES) is a non-thermal, localized application of ultrashort electrical pulses in the nanosecond range that can trigger immunogenic cell death in treated tumors. We have demonstrated previously that the application of 2000 pulses 100 ns long and, 30 kV/cm in amplitude completely ablates the treated tumor within 3 weeks via apoptosis and initiates an immune response that inhibits secondary tumor growth [1]. We wanted to determine if this primary tumor treatment also inhibits metastasis by injecting live tumor cells into the tail vein and counting the number of lung metastases 3 weeks later.

### Methods

14 female B6/J albino mice were given intradermal injections of 500,000 B16-GFP cells in 15uL HBSS. Upon reaching 5mm in their largest dimension as visualized by epifluorescence, 6 mice had their tumors resected surgically, and the tumors in 8 mice were treated with 2000 pulses of 100 ns and 53kV/cm. Four weeks after resection or NPES treatment, both the six surgically resected mice and four NPES-treated mice were injected with 200,000 B16-GFP cells into the lateral tail vein. 4 NPES treated mice were not challenged as negative controls. Lung metastases were counted 3 weeks later by epifluorescence imaging.

### Results

Three weeks after intravenous injection with 200,000 B16-GFP melanoma cells, mice with surgical resection of the primary tumor averaged 17 lung metastases/mouse. Mice with NPES ablation of the primary tumor averaged 3.3 lung metastases/mouse from intravenous challenge. Mice

with NPES ablation of the primary tumor and no challenge exhibited no lung metastases.

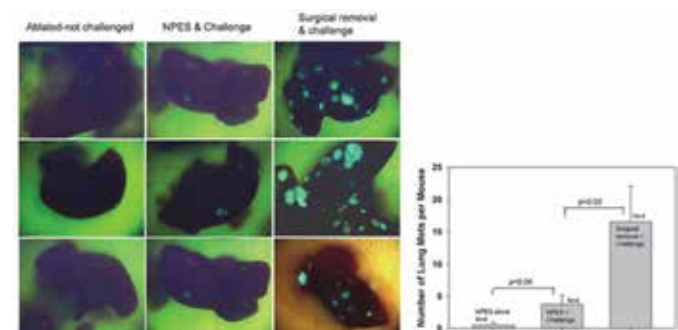
### Conclusions

Immunogenic cell death caused by NPES treatment of primary tumors stimulates anti-tumor immunity to a subsequent challenge with intravenous B16-GFP cells, extending the vaccination effect beyond solid secondary malignancies to circulating cancer cells.

### References

1. Nuccitelli R, Tran K, Lui K, Huynh J, Athos B, Kreis M, Nuccitelli P, De Fabo EC: **Non-thermal nanoelectroablation of UV-Induced murine melanomas stimulates an immune response.** *Pigment Cell Melanoma Res* 2012, **25**:618-629.

**Figure 1. NPES treatment of primary tumor inhibits lung metastases**



B16-GFP cell metastasis is greatly inhibited in mice whose primary tumor was treated with NPES

**345**

### Nanosecond pulsed electric field treatment of tumor cell lines triggers immunogenic cell death (ICD)

Amanda McDaniel, Snjezana Anand, John Cha, Darrin Uecker, Richard Nuccitelli

Pulse Biosciences, Burlingame, CA, USA

### Background

Nano-Pulse Electro-Signaling (NPES) is a non-thermal, localized application of ultrashort electrical pulses in the nanosecond range that can trigger immunogenic cell death in treated tumors. We have demonstrated previously that the application of 400 pulses 100 ns long and, 30 kV/cm in amplitude completely ablates treated orthotopic rat liver tumors within 2 weeks via apoptosis and initiates an immune response that inhibits secondary tumor growth in a CD8-dependent manner [1]. Here we determine if NPES treatment results in the expression of three damage-associated molecular patterns (DAMPs) that play significant roles in immune signaling.



## Promoting and Measuring Antitumor Immunity

Presenting author underlined; Primary author in italics

### Methods

We treated three separate cancer cell lines (MCA205, McA-RH7777, Jurkat E6-1) with NPES. One million cells were suspended in 800 µl media and treated in a 4mm electroporation cuvette. Five total treatments were delivered ranging in energy from 5-50 J/mL. The pulse parameters were fixed (15 kV/cm, 100 ns, 2 pps) and energy delivery was controlled by varying the pulse number. 500,000 cells from each treatment group and untreated cells were seeded into a 24-well plate and incubated at 37°C for 24-hours. Cell culture supernatants were collected to measure levels of HMGB1 and ATP. Cells were also harvested and the expression levels of cell surface calreticulin were determined using flow cytometry.

### Results

NPES induced all three markers of ICD in an energy-dependent manner. HMGB1 release and calreticulin expression increased with treatment energy in all three cell lines. Extracellular ATP followed a different pattern, showing a bell-shaped response that peaked at 15 J/mL followed by a drop off at 25 J/mL in both the MCA-205 and McA-RH7777 cell lines. ATP levels in the Jurkat cells remained low across all conditions.

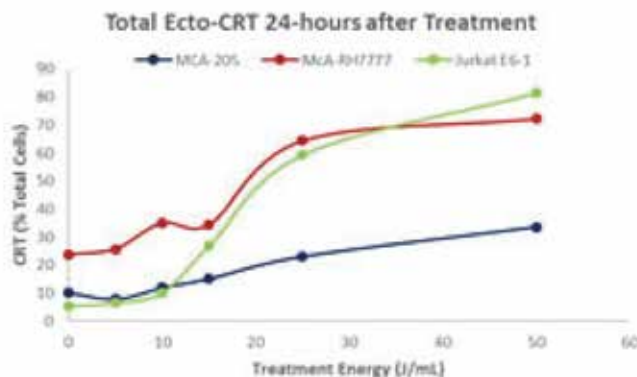
### Conclusions

We have demonstrated that three key markers of ICD can be induced by treating tumor cells with NPES. This can explain why we see a vaccine-like effect after *in vivo* NPES treatment, inhibiting secondary tumor growth after subsequent challenges with tumor cells.

### References

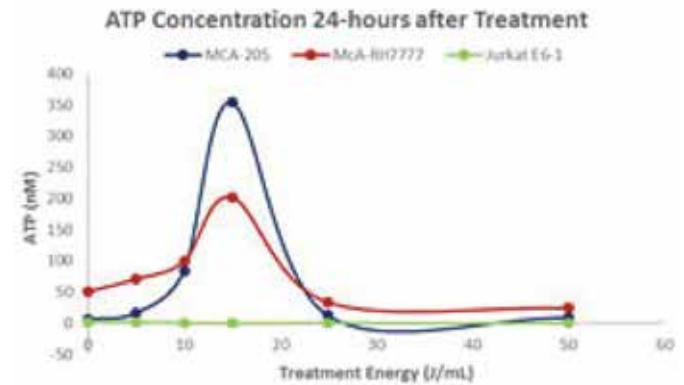
1. Nuccitelli R, Berridge JC, Mallon Z, Kreis M, Athos B, Nuccitelli P: **Nanoelectroablation of murine tumors triggers a CD8-dependent inhibition of secondary tumor growth.** *PLoS One* 2015, **10**: e0134364.

Figure 1. Ecto-Calreticulin 24 h



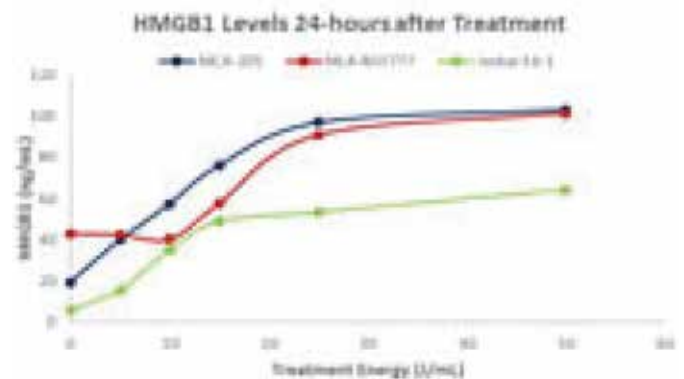
Ecto-calreticulin on NPES-treated cells 24 h after treatment

Figure 2. ATP secreted at 24 h



ATP concentration outside cells 24 h after treatment

Figure 3. HMGB1 secretion 24 h after treatment



HMGB1 is secreted 24 h post treatment at all energies

346

### Monitoring the changes in tumor-specific TILs during immunotherapy

*Nataša Obermajer*<sup>1</sup>, Julie Urban<sup>2</sup>, Eva Wieckowski<sup>2</sup>, Ravikumar Muthuswamy<sup>2</sup>, Roshni Ravindranathan<sup>2</sup>, David Bartlett<sup>1</sup>, Pawel Kalinski<sup>3</sup>

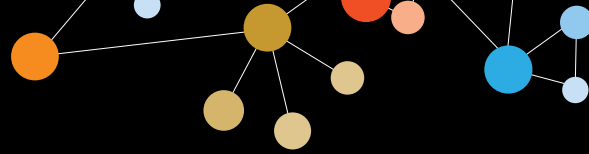
<sup>1</sup>Department of Surgery, University of Pittsburgh, Pittsburgh, PA, USA

<sup>2</sup>University of Pittsburgh, Pittsburgh, PA, USA

<sup>3</sup>Department of Surgery; University of Pittsburgh Cancer Institute; Department of Infectious Diseases and Microbiology, University of Pittsburgh, Pittsburgh, PA, USA

### Background

The development of novel immunotherapeutic approaches need to consider two critical aspects of anti-tumor immunity: generation of high-magnitude effector and memory T cell responses (i.e. cytotoxic CD8+ T, CTLs) and the means



## Promoting and Measuring Antitumor Immunity

*Presenting author underlined; Primary author in italics*

to facilitate effective infiltration of CTLs into the tumor microenvironment.

### Methods

Here we use a novel protocol of evaluating the changing numbers of tumor-specific T cells within tumors of mice receiving different forms of immunotherapy, and strategies to increase numbers of specific CTLs in murine tumors.

### Results

We report separate requirements for the induction of tumor-specific T cells in the spleen and lymph nodes versus the tumor tissues in the course of combinatorial immunotherapies involving a specialized dendritic cell (DC) vaccine, with augmented ability to enhance systemic numbers of tumor-specific effector CTLs, and the combinatorial strategy to promote the homing of the vaccination-induced CTLs to tumors.

### Conclusions

In contrast to commonly used tumor models involving highly-immunogenic model antigens, our approach allows for the assessment of local immune responses to more clinically relevant, weakly-immunogenic non-manipulated cancers, facilitating the development and preclinical evaluation of new immunotherapies.

**347**

### **Bortezomib enhances expression of effector molecules in anti-tumor CD8+ lymphocytes by modulating Notch-NFκB-miR-155 crosstalk**

*Ariana N Renrick*<sup>1</sup>, Menaka Thounaojam<sup>2</sup>, Portia Thomas<sup>1</sup>, Samuel Pellom<sup>1</sup>, Anil Shanker<sup>3</sup>

<sup>1</sup>Meharry Medical College, Nashville, TN, USA

<sup>2</sup>Medical College of Georgia, Augusta, GA, USA

<sup>3</sup>Meharry Medical College School of Medicine, Nashville, TN, USA

### Background

The immunosuppressive tumor microenvironment disturbs immune regulatory networks and takes over host antitumor immune responses. We have previously reported that tumor interferes with host hematopoietic Notch system, which could result in the inadequate induction of antitumor immunity. Interestingly, we found that tumor-induced decrease in immune Notch could be restored by the FDA-approved proteasome inhibitor bortezomib, which also sensitizes tumors to death signals. We are also elucidating components of microRNA regulation affecting NICD-NFκB crosstalk.

### Methods

WT Balb/c mice (Harlan) will be used in four different groups with 3 mice per group. The treatment groups are as follows: saline alone, bortezomib alone, tumor (4T1 breast tumor

cells 2x10<sup>6</sup>) alone, or tumor + bortezomib administration. Tumor-bearing mice will be injected sub-cutaneously with the tumor cells. We will then allow for the solid tumor to establish in the mice, which takes approximately 14 days. The tumors should be approximately 125 mm<sup>3</sup>. After the establishment of tumor, the mice will be injected with 1mg/kg body weight of bortezomib intra-venously. After 4 hours, the mice will be sacrificed and the spleen and lymph nodes will be harvested and CD8<sup>+</sup> T cells will be purified. Analysis of T cell activation markers, Notch signaling markers, T cell effector molecules and miR-155 expression will be analyzed by flow cytometry and RT-qPCR.

### Results

Bortezomib administration modulates Notch system in CD8<sup>+</sup> T cells isolated from tumor-bearing mice. Bortezomib improves cytolytic T lymphocyte function. Bortezomib abrogates the negative effect of g-secretase inhibitor (GSI) on T cell effector molecules. Bortezomib abrogates GSI effect and stimulates Notch genes via NICD cleavage and/or NFκB activation. Bortezomib intersects with both canonical (NICD) and non-canonical (NFκB) pathway. Bortezomib upregulates miR-155 expression in the presence of tumor. miR-155 expression is suppressed in T cells when Notch signaling is inhibited by GSI. Notch target gene expression is suppressed when miR-155 is inhibited.

### Conclusions

Bortezomib modulates Notch signaling at both the Notch receptor and target gene level, thereby improving the expression of T cell effector molecules in tumor-bearing mice. Bortezomib presents the opportunity to sensitize tumors to cell death, while simultaneously improving CD8<sup>+</sup> T cell function via NICD and NFκB activation leading to effective antitumor immune function. Bortezomib has the ability to increase miR-155 expression even when Notch signaling is blocked by GSI, suggesting an interplay between Notch and miR-155 affecting expression of T cell effector molecules.

**348**

### **Bortezomib improves adoptive T cell immunotherapy in solid tumors**

*Samuel Pellom*<sup>1</sup>, Menaka Thounaojam<sup>2</sup>, Duafalia Dudimah<sup>3</sup>, Alan Brooks<sup>4</sup>, Thomas J. Sayers<sup>5</sup>, *Anil Shanker*<sup>3</sup>

<sup>1</sup>Meharry Medical College, Nashville, TN, USA

<sup>2</sup>Medical College of Georgia, Augusta, GA, USA

<sup>3</sup>Meharry Medical College School of Medicine, Nashville, TN, USA

<sup>4</sup>National Cancer Institute-Frederick, Frederick, MD, USA

<sup>5</sup>CIP, Center for Cancer Research, BSP, Leidos Biomed Research Inc, National Cancer Institute-Frederick, Frederick, MD, USA

## Promoting and Measuring Antitumor Immunity

*Presenting author underlined; Primary author in italics*

### Background

Tumor-induced immune suppression is a hallmark feature of tumor growth, which is responsible for the blockade of host antitumor immunity and poor efficacy of anti-cancer immunotherapy. Therefore, restoration of the antitumor immune response is a cornerstone of therapeutic interventions aimed to control tumor growth. The therapeutic proteasome inhibitor bortezomib sensitizes solid tumors to apoptosis in response to TNF-family death ligands.

### Methods

We investigated the effects of bortezomib on T cell responses in immunotherapy models involving low-avidity antigens. We also investigated the potential of bortezomib in modulating the antitumor immune response in solid tumor mouse models.

### Results

Bortezomib did not decrease MHC class I/II-associated antigen presentation to cognate T cells. Rather, bortezomib stabilized the expression of T cell receptor CD3 $\zeta$  and IL2 receptor- $\alpha$ , while maintaining IFN $\gamma$  secretion to improve FasL-mediated tumor lysis. Notably, bortezomib increased tumor cell surface expression of Fas in mice as well as human melanoma tissue from a responsive patient. In renal tumor-bearing immunodeficient Rag2<sup>-/-</sup> mice, bortezomib treatment after adoptive T cell immunotherapy reduced lung metastases and enhanced host survival. We observed that bortezomib treatment also resulted in increased CD8<sup>+</sup> T lymphocyte IFN $\gamma$  secretion and expression of effector molecules, perforin and granzyme B, as well as the T-box transcription factor eomesodermin in tumor-bearing mice. Moreover, bortezomib promoted CD8<sup>+</sup> T cell nuclear factor- $\kappa$ B (NF $\kappa$ B) activity by increasing the total and phosphorylated levels of the I $\kappa$ B kinase and I $\kappa$ B $\alpha$  as well as the cytoplasmic and nuclear levels of phosphorylated p65. In addition, Bzb treatment increased the levels of immunostimulatory interleukins IL-2, IL-12, IL-15, and increased phosphorylation of STAT3/5. Along with these immunostimulatory effects, bortezomib administration reduced number of pulmonary tumor nodules in 4T1.2HA tumor-bearing mice.

### Conclusions

These findings provide novel insights on using bortezomib not only as an agent to sensitize tumors to cell death but also to enhance antitumor T cell function, provide lymphocyte-stimulatory effects, and help in modulating lymphocyte-stimulatory cytokine signaling, thereby overcoming immunosuppressive actions of tumor on antitumor T cell functions.

349

### Mechanisms of chitosan/IL-12 immunotherapy for the treatment of bladder cancer

*Sean G Smith*<sup>1</sup>, Khue Nguyen<sup>2</sup>, Sruthi Ravindranathan<sup>3</sup>, Bhanu Koppolu<sup>1</sup>, David Zaharoff<sup>1</sup>

<sup>1</sup>Joint Department of Biomedical Engineering, North Carolina State University and the University of North Carolina, Raleigh, NC, Cary, NC, USA

<sup>2</sup>Cell and Molecular Biology, University of Arkansas, Fayetteville, AR, USA

<sup>3</sup>Biomedical Engineering, University of Arkansas, Fayetteville, AR, USA

### Background

Bladder cancer afflicts 430,000 people every year globally and is plagued by recurrence rates as high as 50%. One way to mitigate the risk of recurrence is by engaging adaptive immunity. Our group has been able to direct adaptive immunity via intravesical treatment with CS/IL-12, a coformulation of interleukin(IL)-12 and the biopolymer chitosan. Four twice-weekly administrations of CS/IL-12 routinely eliminate more than 90% of orthotopic bladder tumors in mice while providing systemic protection from recurrence and rechallenge for the duration of the lifespan of treated mice. The purpose of this study is to gain insights into the mechanisms underlying both the initial elimination and later rejection of bladder tumors by exploring the importance of the number of administrations, lymphocyte subtypes, and the immune cell infiltration throughout and following treatment.

### Methods

Female C57BL/6J mice were implanted orthotopically with 75,000 MB49 bladder cancer cells. Beginning 7 days after implantation, mice were treated intravesically 2x/week for two weeks with CS/IL-12 (1  $\mu$ g). The importance of the number of treatments was investigated by monitoring survival while varying the treatment number. The role of lymphocyte subtypes was investigated by monitoring survival after depleting CD4<sup>+</sup>, CD8<sup>+</sup>, or NK1.1<sup>+</sup> cells prior to and throughout treatment or rechallenge. Cellular responses 24 hours after each treatment were measured in the bladder, bladder draining lymph nodes (BDLNs), and the spleen via flow cytometry.

### Results

Varying the number of treatments revealed that a single administration significantly extended survival beyond saline with 4/10, 2/8, 6/9, and 7/8 mice surviving long term after 1, 2, 3, or 4 applications respectively. Depletion studies showed a dependence on CD8<sup>+</sup> T cells for tumor elimination (Figure 1a) and on CD4<sup>+</sup> T cells for rejection of subsequent tumor

## Promoting and Measuring Antitumor Immunity

Presenting author underlined; Primary author in italics

rechallenge (Figure 1b). Flow cytometry revealed fluctuations in the immune-cell populations over the course of treatment (Figure 2). The first treatment was characterized by a 54% increase of macrophages in the bladder and a 56% increase in the CD8:Regulatory T cell ratio in the BDLNs. By the third treatment there was an influx of CD4+ and CD8+ T cells in the bladder as well as increased CD8+ T cells in the BDLNs.

### Conclusions

Even a single administration of CS/IL-12 eliminates established tumors, though higher rates of survival were possible with 3 or 4 treatments. The initial response is inflammatory and driven by macrophage infiltration and CD8+ T cells while the memory responses is directed by CD4+ T cells.

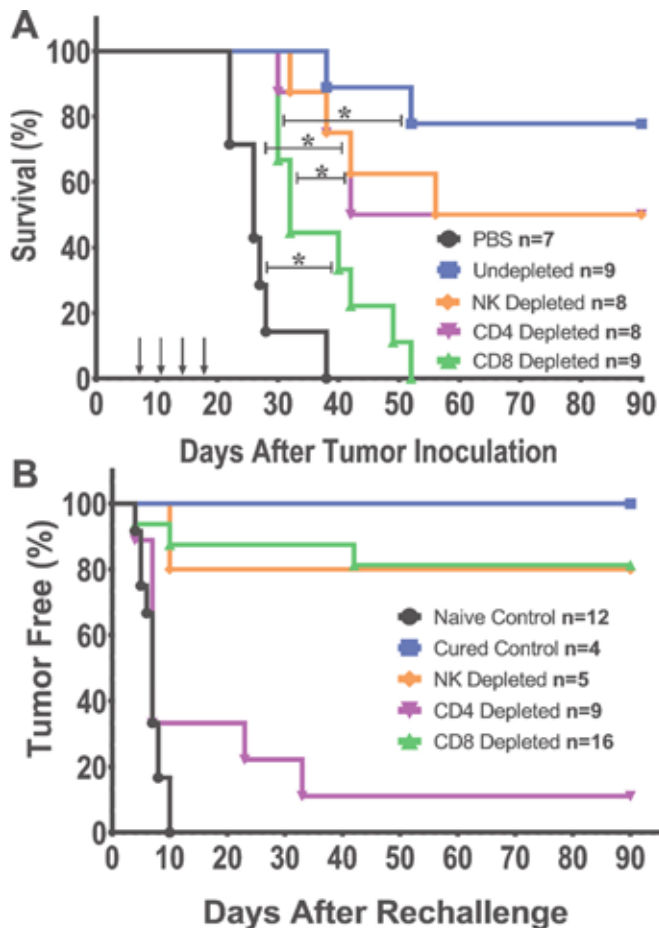


Figure 1: Depletion studies reveal role of T cell subtypes. Mice were depleted of NK1.1+, CD4+, or CD8+ cells either throughout treatment with CS/IL-12 (A) or rechallenge at a distant site (B). Significant differences ( $P < 0.05$ ) in median survival by the Log-Rank test are indicated by \*.

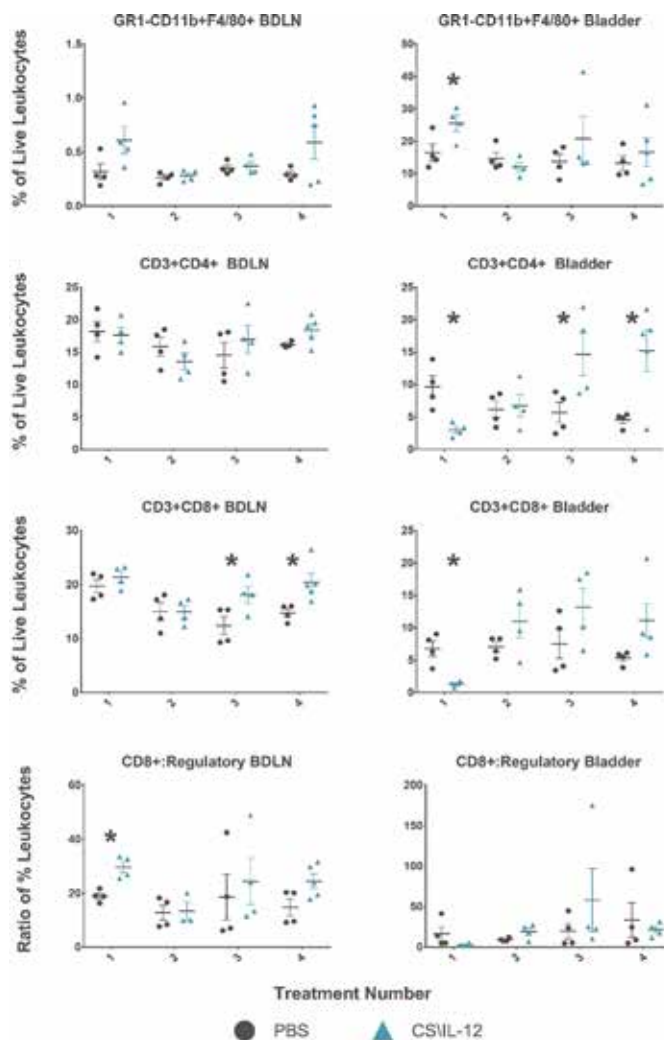


Figure 2: Immune infiltrates after each treatment. Bladder tumor tissues and bladder draining lymph nodes (BDLNs) were dissociated and analyzed via flow cytometry 24 hours after intravesical treatment with either PBS or CS/IL-12. Regulatory T cells were defined as CD3+CD4+CD25+FoxP3+. Each symbol represents an individual mouse. Significant differences ( $P < 0.05$ ) by T-tests are indicated by \*.

### 350

#### Extracellular vesicles as carriers for the delivery of immunotherapeutic oligonucleotides

Yu-Lin Su<sup>1</sup>, Tomasz Adamus<sup>2</sup>, Qifang Zhang<sup>2</sup>, Sergey Nechaev<sup>2</sup>, Marcin Kortylewski<sup>2</sup>

<sup>1</sup>Beckman Research Institute / City of Hope, Monrovia, CA, USA

<sup>2</sup>City of Hope, Duarte, CA, USA



## Promoting and Measuring Antitumor Immunity

*Presenting author underlined; Primary author in italics*

### Background

While oligonucleotide therapeutics (ONTs) allow for targeting of currently undruggable molecular targets, such as oncogenic/tolerogenic STAT3, their delivery to target cells remains major obstacle limiting clinical application. We previously developed a strategy for delivery of STAT3 siRNA, decoy DNA or antisense ONTs to certain immune and cancer cells as conjugates with TLR9 ligand, CpG oligonucleotide. The CpG-STAT3 inhibitors (CSIs) proved effective in systemic administration against mouse models of leukemia. To further improve conjugate nuclease resistance, circulatory half-life and thereby penetration to distant organs or solid tumors, we developed a method for encapsulation of CSIs in extracellular vesicles (EVs).

### Methods

We tested several types of immune and cancer cells, such as human and mouse macrophages (RAW264.7), leukemia (MV4-11) and prostate cancer cells (DU145, PC3, TRAMP-C2), for their ability to spontaneously encapsulate CSIs into EVs following the ONT uptake. The loaded EVs were then isolated by a standard ultracentrifugation and characterized as for the vesicle size, concentration (Nanosight) as well as loading efficiency (fluorescent assay/FACS). The biodistribution of EV-encapsulated and fluorescently labeled CpG-siRNA<sup>Cy3</sup> was assessed after intravenous injections into mice.

### Results

Cells were incubated with various concentrations of CSIs in EV-free medium for 72h resulting in the near complete penetration of target cells. The EVs were isolated from supernatants collected from donor cells and further characterized. We found that ~20-40% isolated EVs were loaded with CSIs. The EVs had an average diameter of 100-150nm depending on donor cell type. For majority of tested cells, concentration of EVs increased following treatment using CSIs which suggests a potential positive effect of TLR9 signaling on EV secretion. The EV/CSIs were internalized mainly through scavenger receptor-mediated endocytosis and not by a fusion with target cell membrane as verified using confocal microscopy. Importantly, the encapsulation of CpG-STAT3siRNA did not prevent target gene silencing or TLR-dependent NF- $\kappa$ B activation. Systemic injection of EV-encapsulated CpG-STAT3siRNA into mice improved the biodistribution of oligonucleotides especially to myeloid cells in bone marrow and other organs.

### Conclusions

We demonstrate the feasibility of using EV-encapsulated CSIs for improving systemic delivery of immunostimulatory ONTs to TLR9+ immune and cancer cells. Our further studies will verify whether EV/CSIs will allow for improved penetration of solid tumors and their distant metastases.

### 351

#### Deep profiling of tumor infiltrating immune subsets by mass cytometry

*Spencer Wei*, James Allison

University of Texas MD Anderson Cancer Center, Houston, TX, USA

### Background

Checkpoint blockade is able to elicit durable responses in a fraction of cancer patients. However, what factors define responsiveness to checkpoint blockade therapy remain to be elucidated [1, 2]. Tumor cell intrinsic properties and the host immune response co-define responsiveness to checkpoint blockade. We sought to identify facets of the host immune response that are regulated by and functionally important for the efficacy of checkpoint blockade.

### Methods

To accomplish this we utilized mass cytometry to comprehensively profile changes in tumor immune infiltrates following checkpoint blockade. This approach allows for the interrogation of greater than 40 analytes at single cell resolution [3]. We subsequently analyzed mass cytometry data using clustering and dimension reduction algorithms to identify and visualize infiltrating immune populations in an unsupervised manner.

### Results

Using this approach we analyzed B16BL6 murine melanoma tumors in mice treated with anti-CTLA-4, anti-PD-1, or control antibody. More than 20 distinct tumor infiltrating immune cell populations were identified. Notably, multiple sub-populations within canonical immune compartments were identified as individual clusters. This suggests that this approach can capture, to an extent, the complexity of tumor immune infiltrates. Using these clusters to categorize immune infiltrates, we identified cell types responsive to checkpoint blockade. Of particular interest, we were able to survey the diversity within the T cell compartment and assess the influence of checkpoint blockade on the frequencies of distinct T cell populations. Broadly, both checkpoint blockade responsive and non-responsive immune clusters were identified, including those that expanded and contracted following treatment (n=6 to 7 per group; p < 0.05).

### Conclusions

These results indicate that deep profiling of tumor immune infiltrates using mass cytometry can identify biologically relevant populations in a comprehensive and unsupervised manner. These data support our understanding that CTLA-4 and PD-1 regulate T cell activity through distinct mechanisms. Further investigation into the identity and functional requirement of the identified subsets is required





## Promoting and Measuring Antitumor Immunity

Presenting author underlined; *Primary author in italics*

and will help to further elucidate the mechanism of action of individual checkpoint blockade therapies.

### Acknowledgements

We acknowledge the MDACC core facility NCI Support Grant P30CA16672.

### References

1. Sharma P, Allison JP: **The future of immune checkpoint therapy**. *Science* 2015, **348**:56-61.
2. Topalian SL, Drake CG, Pardoll DM; **Immune checkpoint blockade: a common denominator approach to cancer therapy**. *Cancer Cell* 2015, **27**:450-461.
3. Tanner SD, Baranov VI, Ornatsky OI, Bandura DR, George TC. **An introduction to mass cytometry: fundamentals and applications**. *Cell* 2013, **62**:955-965.

## Survivorship Issues Related to Immunotherapy

Presenting author underlined; Primary author in italics

352

### Neutrophil count predicts survival in patients on ipilimumab with radiation

Clark Anderson, Chad Tang, Jonathan Schoenhals, Efrosini Tsouko, John Heymach, Patricia de Groot, Joe Chang, Kenneth R Hess, Adi Diab, Padmanee Sharma, James Allison, Aung Naing, David Hong, James Welsh

University of Texas MD Anderson Cancer Center, Houston, TX, USA

#### Background

Neutrophils can have immunosuppressive effects, and the neutrophil-to-lymphocyte ratio (NLR) is a negative prognostic marker in some cancers. We analyzed whether immune cells can predict outcome in patients enrolled in an ongoing clinical trial of radiation plus ipilimumab (NCT 02239900). We hypothesized that patients with greater absolute lymphocyte counts (ALC) or decreased neutrophil counts (NC) will have increased survival.

#### Methods

Data were available from 74 patients. Blood samples for NC and ALC were collected at baseline, at the end of treatment, and immediately before every cycle of ipilimumab. Tumor size was measured by CT scan at baseline, between cycles 2 and 3 of ipilimumab, and every 1-3 months thereafter and response was classified by the immune response criteria (ir-RC). Information on body weight was extracted starting 6 months before treatment through the end of treatment. Continuous and discrete variables were analyzed with Spearman correlations and Fisher's exact test. Overall survival was compared via log-rank test and hazard ratios obtained by Cox proportional analysis. Commonly reported cut-points used were 5 for NLR and  $5 \times 10^9/L$  for NC. Associations were considered significant at  $p < 0.05$ ; all tests were two-sided.

#### Results

Baseline NC correlated with tumor growth ( $\rho=0.312$ ,  $p=0.0069$ ). High baseline NC ( $>5 \times 10^9/L$ ) was a significant risk factor for progressive disease (odds ratio=4.83,  $p=0.0034$ ); 9 out of 28 patients with high baseline NC had a best response of stable disease or partial response versus 32 out of the 46 patients with low baseline NC. Baseline NC predicted survival (HR=3.108,  $p=0.0006$ ), as did baseline NLR (HR=2.570,  $p=0.0049$ ). NC at the time of the second ipilimumab administration predicted survival more strongly than did NC at baseline (HR=4.598,  $p < 0.0001$ ). Both end-of-treatment NC and NLR were associated with survival (NC: HR=4.881,  $p < 0.0001$ ; NLR: HR=5.055,  $p < 0.0001$ ). Weight loss correlated with an increase in tumor growth ( $\rho=0.26$ ,  $p=0.025$ ), a decrease in ALC ( $\rho=-0.34$ ,  $p=0.0031$ ), and an increase in NC ( $\rho=0.394$ ,  $p=0.0022$ ).

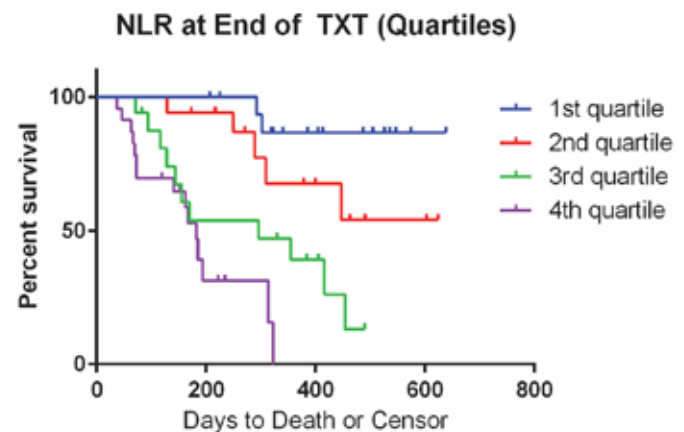
#### Conclusions

Our findings suggest that having high NC or NLR is a strong negative prognostic indicator in cancer patients receiving radiation with immunotherapy. These outcomes may reflect neutrophils antagonizing the effects of ipilimumab by suppressing lymphocyte proliferation or exacerbating cachexia.

#### Trial Registration

ClinicalTrials.gov identifier NCT02239900.

Figure 1. NLR at end of TXT (Quartiles)



353

### Incidence and outcomes of central nervous system metastasis in metastatic melanoma patients treated with anti-PD-1 therapy

Gustavo Schvartzman, Roland Bassett, Jennifer L McQuade, Lauren E Haydu, Michael A Davies, Hussein Tawbi, Isabella Glitza

University of Texas MD Anderson Cancer Center, Houston, TX, USA

#### Background

Central nervous system (CNS) metastasis are common in patients with metastatic melanoma (MM) and represent a frequent site of treatment failure with current therapies. However, little is known about the incidence, characteristics and outcomes of CNS metastasis in MM patients treated with anti-programmed death-1 (PD-1) and in conjunction with more intensive local CNS treatment strategies.

#### Methods

Under an IRB-approved protocol, outcomes of MM patients treated with anti-PD-1 at The University of Texas MD Anderson Cancer Center from January 2012 to February 2016 were reviewed. The association between development of CNS metastasis and overall survival (OS) was assessed using



## Survivorship Issues Related to Immunotherapy

Presenting author underlined; *Primary author in italics*

Cox regression analysis with time to CNS metastasis treated as a time-varying covariate.

### Results

We identified 264 MM patients who received anti-PD-1 treatment, including 74 (28%) who had CNS metastasis prior to the first dose of anti-PD-1. With a median follow-up of 10.4 months (range 0-51.6) from the start of this therapy, 37 (19% of patients without prior CNS metastasis) developed CNS metastasis after the initiation of anti-PD-1. Of those, 27 patients were diagnosed with CNS metastasis during anti-PD-1 or within 90 days of treatment discontinuation, and 10 patients were diagnosed with CNS mets >90 days after last anti-PD-1 dose. The majority of these patients were male (62%), their mean age at new CNS metastasis was 62 years (range 31-86), and most patients had a history of cutaneous primary (59%). Of the 26 patients who were tested for mutations, BRAF was identified in 8 (22%, V600E in 6 patients, V600K in 2 patients), NRAS in 5 (14%) and KIT in 6 (16%). 86% received at least one CNS directed treatment approach. 62% were treated with stereotactic radiosurgery, 11% received whole-brain radiation and 30% underwent surgery. Median OS from start of anti-PD-1 was 34 months (range 0-51.6 months) for the whole anti-PD-1 treatment cohort. Development of CNS metastasis while on anti-PD-1 therapy was strongly significantly associated with death (HR 3.39, 95% CI 2.06, 5.59,  $p < .0001$ ).

### Conclusions

To our knowledge, this is the first report describing the incidence of CNS metastasis as an initial site of disease progression in MM patients treated with anti-PD-1 and associated with worse OS, despite additional CNS directed therapy.

## Therapeutic Cancer Vaccines

*Presenting author underlined; Primary author in italics*

354

### **Heterologous boosts with an adenoviral vector following a dendritic cell-tropic ZVex® prime generates robust antigen-specific T cell responses and enhanced anti-tumor protection**

*Tina C Albershardt*, Andrea J Parsons, Jardin Leleux, Rebecca S Reeves, Jan ter Meulen, Peter Berglund

Immune Design, Seattle, WA, USA

#### **Background**

Effective immunization regimens generally require more than one administration, often in the form of prime-boosts. ZVex is an integration-deficient lentiviral vector platform, pseudotyped with a modified Sindbis virus envelope protein to deliver tumor-associated antigens (TAAs) to human dendritic cells (DCs) for optimal priming of TAA-specific CD8+ T cells. We have previously reported that mice immunized once or repeatedly with ZVex/TAA developed strong, dose-dependent, multifunctional, and TAA-specific cytotoxic T cells that critically controlled tumor growth. Here, we show that priming with ZVex/TAA and boosting with adenoviral vector (Ad5) encoding the same antigen strongly increased frequency of TAA-specific T cells and improved anti-tumor efficacy.

#### **Methods**

To evaluate immunogenicity of ZVex and Ad5 expressing human NY-ESO-1 and murine TRP-1, BALB/c or C57BL/6 female mice were immunized with ZVex/TAA or Ad5/TAA twice, 21 days apart. Splenic T cell responses were assessed 14 days post-last immunization via intracellular cytokine staining. To evaluate therapeutic efficacy of immunization regimens, two murine tumor models were used: 1) a B16 melanoma model, where tumor cells were inoculated in the flank and measured 2-3 per week; and 2) a metastatic CT26 colon carcinoma model expressing human NY-ESO-1, where tumor cells were inoculated intravenously, and lung nodules were enumerated 17-19 days post-tumor inoculation.

#### **Results**

Repeated ZVex/TAA administration (homologous prime-boost) in mice maintained the frequency of TAA-specific CD8+ T cells at peak levels. While repeat-dose compared to single-dose regimen did not improve anti-tumor control in the CT26 lung metastasis model, it delayed tumor growth in the B16 tumor model, suggesting that homologous prime-boost can be efficacious against selected tumor types. Compared to mice immunized repeatedly with ZVex/TAA, mice primed with ZVex/TAA and boosted with Ad5/TAA (heterologous prime-boost) generated 10-fold increase in frequency of TAA-specific CD8+ T cells capable of producing IFN $\gamma$ , TNF, and/or IL-2. Tumor-bearing mice that received

heterologous prime-boost regimen exhibited slower tumor growth or developed fewer metastatic lung nodules than animals that received a homologous regimen. These results demonstrate that a heterologous prime-boost strategy can be used to generate more TAA-specific T cells, leading to more efficacious anti-tumor control.

#### **Conclusions**

ZVex is a DC-tropic vector platform that efficiently primes robust antigen-specific CD8+ T cell responses that alone can effectively control tumor growth. Heterologous prime-boost regimens, where adenoviral vectors or other modalities are used as booster immunizations, provide exciting opportunities to further enhance this unique DC-tropic gene delivery platform, by further increasing T cell effectors and anti-tumor efficacy.

355

### **Characteristics of adjuvants for therapeutic cancer vaccines**

*Stephane Ascarateil*<sup>1</sup>, Marie Eve Koziol<sup>2</sup>

<sup>1</sup>Seppic, Puteaux, Ile-de-France, France

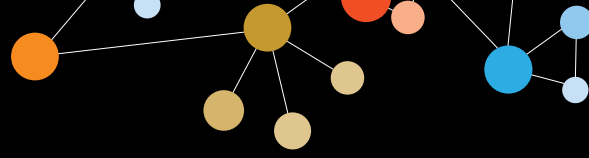
<sup>2</sup>Seppic Inc., Fairfield, NJ, USA

#### **Background**

Therapeutic cancer vaccines are an interesting alternative to treat cancer by active immunotherapy. The use of small, highly defined antigens or over-expressed self-antigens is generally linked with weak and too brief immune responses. In order to improve the immune response induced, antigens may be associated with enhancers such as adjuvants. Water-in-oil (W/O) emulsions represent an interesting option for immunotherapy vaccines where potent adjuvants are required. These emulsions, based on Montanide™ ISA 51VG adjuvant, have been successfully used to increase the biological efficacy and immunogenicity of human therapeutic peptides vaccines. Some of the mechanisms of action that allow this potent and prolonged stimulation are brought forward.

#### **Methods**

Cellular activation mechanisms: 5 C57BL/6 mice per group were vaccinated subcutaneously with 25 $\mu$ g of nucleoprotein (NP) alone or with the Montanide™ ISA 51 VG at weeks 0 and 3. At week 5, splenocytes are sampled. T cells are put in culture for 48h and restimulated with NP antigen. IFN $\gamma$  response is followed by ELISpot. Cytokine secretions into the medium (supernatant) (TNF $\alpha$ , IL-2, IFN $\gamma$ ) were measured by ELISA. Distinct populations of memory CD8+ T cells were evaluated by flow cytometric analysis.



# Therapeutic Cancer Vaccines

Presenting author underlined; Primary author in italics

## Results

Mice immunized with NP associated with the Montanide™ ISA 51 VG elicited an increase in anti-NP T cells, CD4+ and CD8+ T cell responses. We observe a significant increase of IFN $\gamma$  response in the group vaccinated with adjuvant. Response from total splenocytes is increased 6 times, 5 times for CD4+ population and more than 4 times for CD8+ T cell population. Mice immunized with the NP associated to the Montanide™ ISA 51 VG showed an increase in TNF $\alpha$ , IL-2, and IFN $\gamma$  cytokine secretion. Mice immunized with NP antigen associated with the Montanide™ ISA 51 VG elicited a higher amount of effector memory T lymphocytes and central memory T lymphocytes. The higher amount of CD44+ CD62L+ (T<sub>CM</sub> sub-population) in mice immunized with NP associated to Montanide™ ISA 51 VG showed an increased engraftment and persistence of T cells.

## Conclusions

Vaccines based on Montanide™ ISA 51 VG are strong inducers of danger signals through an enhancement of interaction between antigen and dendritic cells. They induce an important IFN $\gamma$  TH1 polarized response, and potent CD8+ T cell response. Montanide™ ISA 51 VG is an interesting candidate in therapeutic cancer vaccines. Moreover it has been safely administered to almost 20,000 patients in 258 clinical trials, some of them being included in vaccination schedules involving repeated doses over several years.

Figure 1. W/O emulsion structure and mechanism of immune stimulation

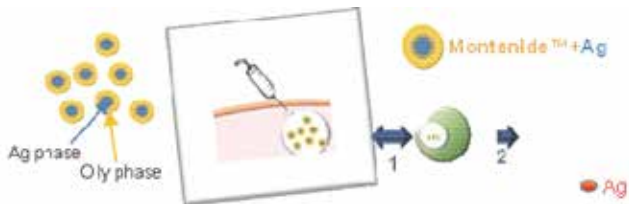


Fig 1: W/O emulsion structure and mechanism of immune stimulation

Figure 2. Cytotoxic T Lymphocytes response following vaccination based on Montanide™ ISA 51 VG

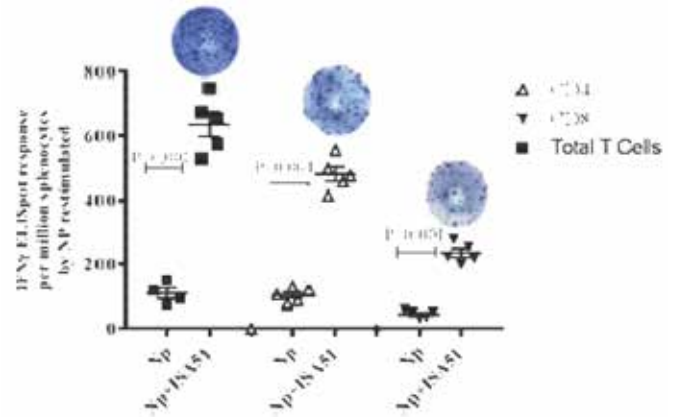


Figure 3. TNF $\alpha$ , IL-2, IFN $\gamma$  secretion after in vitro T cells NP restimulation

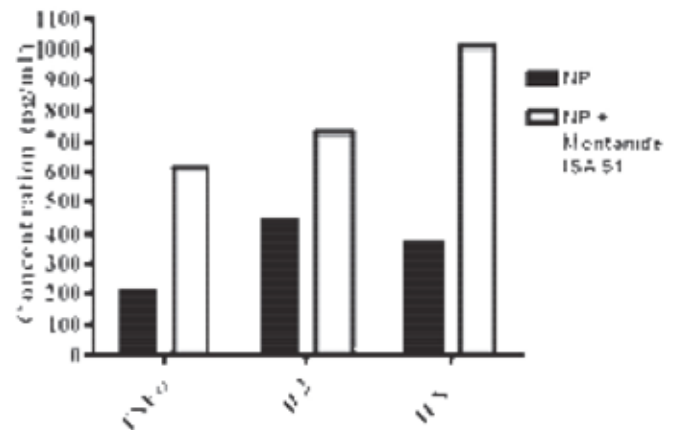
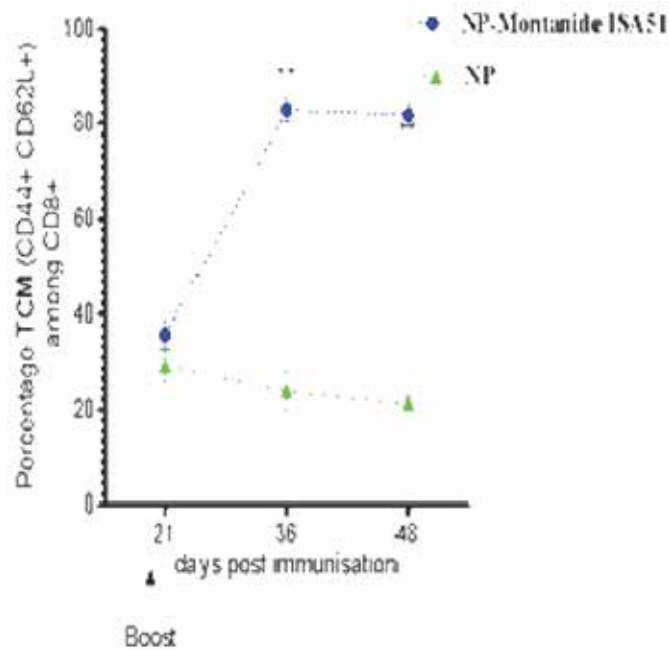


Figure 4. TCM (CD44+ CD62L+) sub-population of CD8+ cells in mice vaccinated with or without Montanide™ ISA 51 VG



## Therapeutic Cancer Vaccines

Presenting author underlined; Primary author in italics



356

### Glycosylated and methylated peptides as neoantigens in leukemia

Sarah A Penny<sup>1</sup>, Stacy A Malaker<sup>2</sup>, Lora Steadman<sup>1</sup>, Paisley T Myers<sup>3</sup>, Dina Bai<sup>3</sup>, Jeffrey Shabanowitz<sup>3</sup>, Donald F Hunt<sup>3</sup>, Mark Cobbold<sup>4</sup>

<sup>1</sup>University of Birmingham, Birmingham, England, UK

<sup>2</sup>Stanford University, Stanford, CA, USA

<sup>3</sup>University of Virginia, Charlottesville, VA, USA

<sup>4</sup>Massachusetts General Hospital Cancer Center, Boston, MA, USA

#### Background

Recent advances have highlighted the importance of the immune response in the fight against cancers. In many cancers, these responses are thought to target mutated peptides; however, leukemia has been shown to have a lower mutational load than many cancers, despite being highly immunogenic. Thus, leukemia-specific antigens may derive from the posttranslational modifications (PTMs) associated with aberrant signaling. Previously, phosphorylated peptides have been identified as potent cancer antigens; here, we identify several peptides with O-linked  $\beta$ -N-acetylglucosamine (O-GlcNAc) modifications, with some that also contain methylated arginine residues. O-GlcNAc is a PTM that modulates cellular functions through extensive cross-talk with the signaling cascades also regulated by phosphorylation. Thus, O-GlcNAcylated peptides may represent cancer-specific neoantigens.

#### Methods

We eluted MHC class-I associated peptides from leukemia patient samples to identify O-GlcNAcylated antigens, using enrichment coupled with high-resolution mass spectrometry. Healthy donor immune responses were assessed using IFN $\gamma$  ELISpot and multiplexed intracellular cytokine staining. Functionality was assessed using a europium-release killing assay.

#### Results

We have identified 36 MHC class I associated O-GlcNAc neoantigens from primary leukemia samples, the first tumor antigens containing this PTM. A subset of these neoantigens is linked to key cancer pathways, including the mitogen activated protein kinase (MAPK) and retinoblastoma (RB1) pathways, and these peptides were shared across all of the patient samples tested. 71% (5/7) of the HLA-B\*0702 O-GlcNAcylated neoantigens tested were immunogenic, with 100% (5/5) of healthy donors having multifunctional memory CD8+ T cell responses to them. Cells targeting these neoantigens were shown to degranulate. This multifunctionality and degranulation in response to antigen indicated that O-GlcNAc-specific T cells may kill. Indeed, an O-GlcNAc-specific T cell line was grown and these cells specifically killed autologous cells pulsed with the modified peptide, but not the equivalent unmodified peptide ( $p=0.015$ ). T cell responses were also identified that specifically targeted the methylated arginine in the peptide with the O-GlcNAc modification.

#### Conclusions

O-GlcNAcylated neoantigens derive from aberrations in key cancer pathways, are shared across patients and are immunogenic. CD8+ T cells targeting these O-GlcNAcylated neoantigens specifically recognize and kill only the PTM antigen. Therefore, these O-GlcNAcylated neoantigens provide logical targets for cancer immunotherapy.

357

### Intratumoral delivery of modified vaccinia virus Ankara expressing human Flt3L as cancer immunotherapy

Peihong Dai<sup>1</sup>, Weiyi Wang<sup>1</sup>, Ning Yang<sup>1</sup>, Stewart Shuman<sup>1</sup>, Taha Merghoub<sup>2</sup>, Jedd D Wolchok<sup>3</sup>, Liang Deng<sup>3</sup>

<sup>1</sup>Memorial Sloan Kettering Cancer Center, New York, NY, USA

<sup>2</sup>Ludwig Collaborative Laboratory, Memorial Sloan Kettering Cancer Center, New York, NY, USA

<sup>3</sup>Department of Medicine, Memorial Sloan Kettering Cancer Center, New York, NY, USA

#### Background

Modified vaccinia virus Ankara (MVA) is a highly attenuated vaccinia strain that is an important vaccine vector for infectious diseases and cancers. MVA has a 31-kb deletion of

## Therapeutic Cancer Vaccines

Presenting author underlined; Primary author in italics

the parental vaccinia genome and was shown to be safe for human use during smallpox vaccination. The investigation of MVA as cancer therapeutics has so far been limited to its use as a vaccine vector to express tumor antigens. We hypothesize that intratumoral delivery of recombinant MVA $\Delta$ E3L (with deletion of vaccinia virulence factor E3) expressing human flt3L (Fms-like tyrosine kinase 3 ligand) would provide *in situ* therapeutic vaccine effects. Flt3L plays a critical role in the development of DC subsets, including CD103<sup>+</sup>/CD8 $\alpha$ <sup>+</sup> DCs, which are critical for cross-presentation of tumor antigens.

### Methods

We compared the immune responses of B16-F10 murine melanoma cells and MC38 murine colon adenocarcinoma cells as well as dendritic cells to either MVA or MVA $\Delta$ E3L infection. We compared the efficacy of intratumoral delivery of MVA vs. MVA $\Delta$ E3L in two syngeneic bilateral tumor implantation models. We also generated recombinant MVA $\Delta$ E3L-TK-hFlt3L through homologous recombination at the thymidine kinase (TK) locus. We compared the efficacies of intratumoral delivery of MVA $\Delta$ E3L-TK-hFlt3L vs. MVA $\Delta$ E3L in bilateral tumor implantation models.

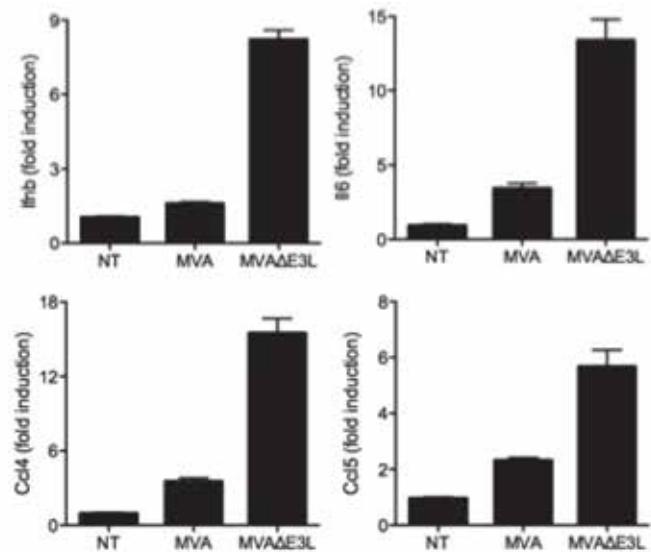
### Results

We found that MVA $\Delta$ E3L infection of B16-F10 and MC38 induces higher levels of IFN- $\beta$ , IL-6, CCL4 and CCL5 than MVA. MVA $\Delta$ E3L-induction of type I IFN in cDCs is mainly dependent on the cGAS/STING pathway. Intratumoral injection of MVA $\Delta$ E3L is more efficacious than MVA in tumor eradication and extension of survival in bilateral tumor implantation models, which correlates with stronger induction of activated CD8<sup>+</sup> and CD4<sup>+</sup> effector T cells in both injected and non-injected tumors from MVA $\Delta$ E3L-treated mice compared with MVA-treated mice. Furthermore, intratumoral injection of MVA $\Delta$ E3L-TK-hFlt3L exerts stronger anti-tumor effects than MVA $\Delta$ E3L in a murine melanoma bilateral implantation model. B16-F10-tumor bearing mice successfully treated with MVA $\Delta$ E3L-TK-hFlt3L also rejected a lethal dose of MC38 challenge.

### Conclusions

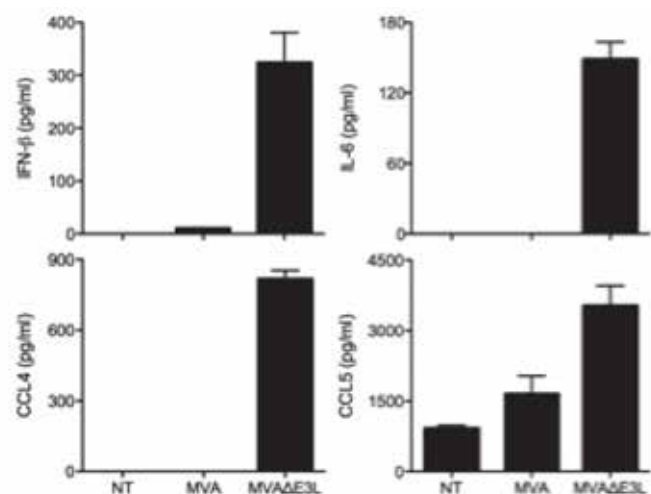
Our results show that intratumoral injection of MVA or MVA $\Delta$ E3L leads to alteration of tumor immune suppressive microenvironment, which facilitates tumor antigen presentation, recruitment and activation of anti-tumor CD8<sup>+</sup> and CD4<sup>+</sup> T cells. MVA $\Delta$ E3L is a stronger immune activator than MVA. Intratumoral delivery of MVA $\Delta$ E3L-TK-hFlt3L is more efficacious than MVA $\Delta$ E3L. Current studies focuses on tumor infiltrating immune cells including CD103<sup>+</sup> DCs and CD8<sup>+</sup> cytotoxic T cells in MVA $\Delta$ E3L-TK-hFlt3L vs. MVA $\Delta$ E3L-treated mice.

**Figure 1. MVA $\Delta$ E3L infection of B16-F10 cells induces higher levels of Ifnb, Il6, Ccl4 and Ccl5 than MVA**



B16-F10 melanoma cells (1 x 10<sup>6</sup>) were infected with MVA, and MVA $\Delta$ E3L viruses at a MOI of 10. Cells were collected at 6 h post infection. Real-time PCR was performed to analyze gene expression.

**Figure 2. MVA $\Delta$ E3L infection of MC38 cells induces higher levels of IFN and proinflammatory cytokines and chemokines than MVA**

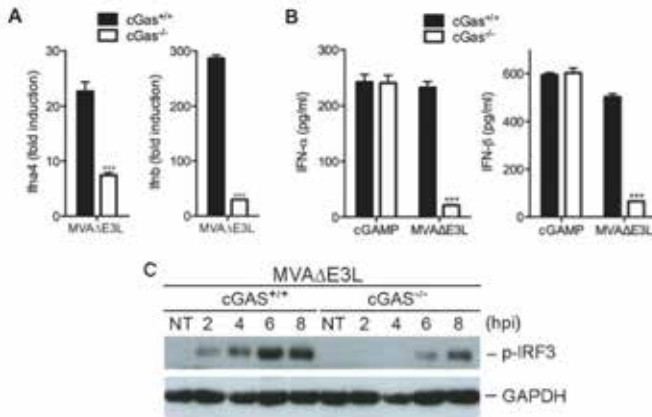


MC38 colon cancer cells (1 x 10<sup>6</sup>) were infected with MVA, and MVA $\Delta$ E3L viruses at a MOI of 10. Supernatants were collected at 22 h post infection. The levels of cytokines were determined by ELISA.

**Therapeutic Cancer Vaccines**

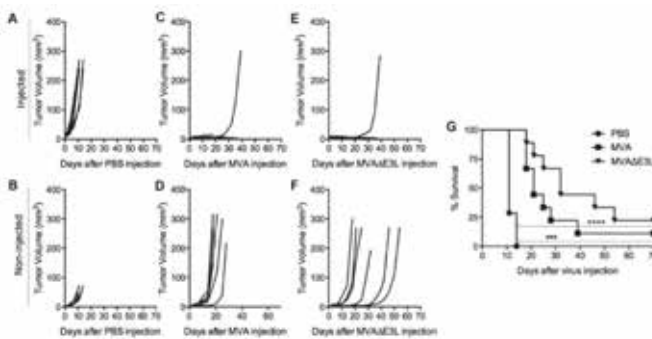
Presenting author underlined; Primary author in italics

**Figure 3. Innate immune sensing of MVAΔE3L virus in cDCs**



Shown here is a series of bar graphs showing that cGAS is required for the induction of type I IFN by MVAΔE3L in cDCs. (A) Bar graphs showing mRNA levels of IFNA4 and IFNB in cGAS+/+ and cGAS-/- cDCs infected with MVAΔE3L. (B) Bar graphs showing IFN-α and IFN-β secretion levels in cGAS+/+ and cGAS-/- cDCs infected with MVAΔE3L or treated with cGAMP, an agonist for STING. (C) A scanned image of an immunoblot showing protein levels of p-IRF3 and GAPDH in cGAS+/+ and cGAS-/- cDCs infected with MVAΔE3L.

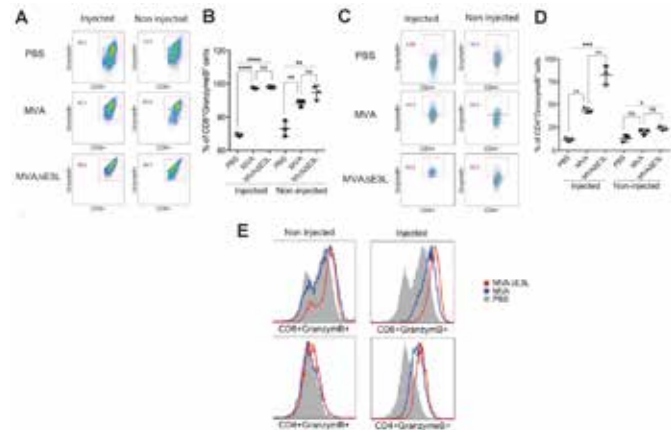
**Figure 4. Intratumoral injection of MVAΔE3L or MVA is effective in a B16-F10 bilateral implantation model**



B16-F10 bilateral tumor implantation model was used to assess the anti-tumor efficacy of MVAΔE3L vs MVA. Briefly, B16-F10 melanoma cells were implanted intradermally to the left and right flanks of C57B/6 mice (5 x 10<sup>5</sup> to the right flank and 1 x 10<sup>5</sup> to the left flank). 8 days after tumor implantation, the larger tumors on the right flank were intratumorally injected with 2 x 10<sup>7</sup> pfu of MVA or an equivalent amount of MVAΔE3L. The tumor sizes were measured and the tumors were re-injected twice a week. The survival of mice was monitored. Graphs of injected (A, C, E) and non-injected (B, D, F) tumor volume plotted against time (days) after PBS, MVA, or MVAΔE3L injection respectively. G is a Kaplan-Meier survival curve of tumor-bearing mice

(B16-F10 cells) injected with PBS (filled circles), MVA (filled squares), or MVAΔE3L (filled triangles). \*\*\*\*, p < 0.0001 (MVAΔE3L vs. PBS group); \*\*\*, p < 0.001 (MVA vs. PBS group).

**Figure 5. Intratumoral injection of MVAΔE3L and MVA induces activating TILs in injected and non-injected tumors**

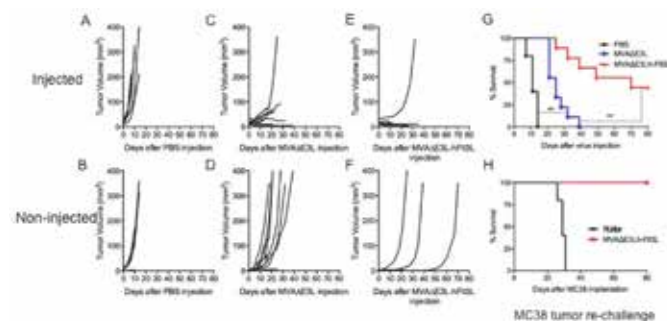


B16-F10 melanoma cells were implanted intradermally to the left and right flanks of C57B/6 mice (5 x 10<sup>5</sup> to the right flank and 2.5 x 10<sup>5</sup> to the left flank). 7 days after tumor implantation, the larger tumors on the right flank were intratumorally injected with 2 x 10<sup>7</sup> pfu of MVA or an equivalent amount of MVAΔE3L, repeated three days later. Both injected and non-injected tumors were harvested at 3 days post the second injection, and TILs were analyzed by FACS. Shown here is a series of graphical representations of data showing that intratumoral injection of MVA or MVAΔE3L induces activated effector CD8+ and CD4+ T cells in both injected and non-injected tumors in a murine B16-F10 melanoma bilateral implantation model. (A) Dot-plots of flow cytometric analysis of CD8+ cells expressing granzyme B+. (B) %CD8+ granzyme B+ T cells in both injected and non-injected tumors treated with PBS, MVA or MVAΔE3L. (C) Dot-plots of flow cytometric analysis of CD4+ cells expressing granzyme B+. (D) %CD4+ granzyme B+ T cells in both injected and non-injected tumors treated with PBS, MVA or MVAΔE3L. (\*, p < 0.05; \*\*, p < 0.01; \*\*\*, p < 0.001; \*\*\*\*, p < 0.0001). (E) Histogram of CD8+ granzyme B+ and CD4+ granzyme B+ TILs in both injected and non-injected tumors treated with PBS, MVA or MVAΔE3L.

## Therapeutic Cancer Vaccines

Presenting author underlined; Primary author in italics

**Figure 6. MVAΔE3L-hFlt3L is more efficacious than MVAΔE3L**



Shown here are tumor volumes of injected (A, C and E) and non-injected tumors (B, D, and F). (G) A Kaplan-Meier survival curve of tumor-bearing mice (B16-F10 cells) injected with PBS (filled circles), MVAΔE3L (filled squares), or MVAΔE3L-hFlt3L (filled triangles). \*\*,  $p < 0.01$  (MVAΔE3L vs. PBS group); \*\*,  $p < 0.01$  (MVAΔE3L-hFlt3L vs. MVAΔE3L group). (H) A Kaplan-Meier survival curve of tumor-bearing mice (B16-F10 cells) successfully treated with MVAΔE3L-hFlt3L vs naive mice challenged with a lethal dose of MC38 cells intradermally ( $1 \times 10^5$ ).

### 358

#### A pilot study of the immunogenicity of a 9-peptide breast cancer vaccine plus poly-ICLC in stage IB-IIIa breast cancer

Patrick Dillon<sup>1</sup>, Gina Petroni<sup>1</sup>, David Brenin<sup>1</sup>, Kim Bullock<sup>1</sup>, Walter Olson<sup>1</sup>, Mark E Smolkin<sup>2</sup>, Kelly Smith<sup>1</sup>, Carmel Nail<sup>1</sup>, Craig L Slingsluff Jr<sup>3</sup>

<sup>1</sup>University of Virginia, Charlottesville, VA, USA

<sup>2</sup>Department of Public Health Sciences, University of Virginia, Charlottesville, VA, USA

<sup>3</sup>Division of Surgical Oncology, University of Virginia, Charlottesville, VA, USA

#### Background

Breast cancer remains a leading cause of cancer death worldwide. Effective adjuvant therapy exists, but there is evidence that immunotherapy may play a significant role in the eradication of residual disease. Peptide vaccines require adjuvants to achieve durable immune memory. Toll-like receptor agonists and help peptides are two recently optimized adjuvants which are investigated in this trial.

#### Methods

A vaccine consisting of nine-class I MHC-restricted breast cancer-associated peptides was combined with a TLR3, poly-ICLC) along with a helper peptide from tetanus toxoid. The peptides used in the study are encoded by the genes: MAGE-A1, -A3, -A10, CEA, NY-ESO-1, and HER2. The peptides lack tumor-specific mutations. The vaccine was given on days

1, 8, 15, 36, 57, 78 and response was assessed by both direct and stimulated ELISpot. Eleven patients with breast cancer were treated. Five of the patients had estrogen receptor positive disease. None were HER2 amplified.

#### Results

The vaccine was well tolerated with no grade 3 nor dose limiting toxicities. Mild injection site reactions and flu-like symptoms were reported in most patients. The most common toxicities were injection site reaction/induration and fatigue, which were experienced by 100% and 91% of participants, respectively. The stimulated ELISpot detected T cell responses in four out of eleven patients. None were detectable in a direct ELISpot assay. Another two patients had borderline immune responses and four had immune response extending 30 days beyond the end of the vaccination series. No difference in immune response was observed between patients receiving endocrine therapy and those not receiving endocrine therapy. The peptides from CEA and MAGE-A1 were immunogenic.

#### Conclusions

The administration of a peptide vaccine in the adjuvant breast cancer setting was safe and feasible. An adjuvant poly-IC plus helper peptide mixture provided modest immune stimulation and should be further optimized for use with peptide vaccines.

#### Trial Registration

ClinicalTrials.gov identifier NCT01532960.

### 359

#### NKTR-214, an engineered cytokine, synergizes and improves efficacy of anti-cancer vaccination in the treatment of established murine melanoma tumors

Meenu Sharma<sup>1</sup>, Faisal Fa'ak<sup>2</sup>, Louise Janssen<sup>1</sup>, Hiep Khong<sup>1</sup>, Zhilan Xiao<sup>1</sup>, Yared Hailemichael<sup>2</sup>, Manisha Singh<sup>1</sup>, Christina Vianden<sup>1</sup>, Adi Diab<sup>1</sup>, Jonathan Zalevsky<sup>3</sup>, Ute Hoch<sup>3</sup>, Willem W Overwijk<sup>1</sup>

<sup>1</sup>University of Texas MD Anderson Cancer Center, Houston, TX, USA

<sup>2</sup>Department of Melanoma Medical Oncology, University of Texas MD Anderson Cancer Center, Houston, TX, USA

<sup>3</sup>Nektar Therapeutics, San Francisco, CA, USA

#### Background

IL-2 has been used as effective immunotherapy in metastatic renal cell carcinoma and melanoma, and may synergize with other cancer immunotherapies. However, toxicities associated with high dose IL-2 treatment limited its further use in anti-cancer therapies. NKTR-214, which is an engineered IL-2 cytokine, was designed to provide a non-toxic, stable and more efficient alternative to IL-2. NKTR-214 provides



## Therapeutic Cancer Vaccines

Presenting author underlined; *Primary author in italics*

sustained activation of the IL-2 pathway through controlled release of active CD122-biased (IL-2R $\beta$ ) cytokines. Prior preclinical studies demonstrated that NKTR-214 can expand tumor-infiltrating lymphocyte populations resulting in marked tumor growth suppression as single-agent and in combination with checkpoint inhibitors. In this pre-clinical study, we investigated whether NKTR-214 can promote expansion and function of vaccination-induced, tumor specific effector CD8+ T cells using the murine B16 melanoma model. We also studied how NKTR-214 impacts the localization of effector CD8+ T cells and Tregs to tumor and spleen.

### Methods

To understand the effect of NKTR-214 on antigen-specific CD8+ T cells, we adoptively transferred naïve gp100-specific TCR transgenic pmel-1 CD8+ T cells into mice bearing established subcutaneous B16 tumors, followed by vaccination (gp100 peptide + anti-CD40 mAb + TLR-7 agonist) alone or in combination with NKTR-214 or IL-2. Mice then received NKTR-214 or IL-2 every 8 days. Tumor growth, survival and T cell response in blood was monitored, and localization of effector pmel-1 CD8+ T cells and CD4+ Foxp3+ Tregs in tumor and spleen were analyzed.

### Results

NKTR-214 efficiently synergized with vaccination, potently suppressing tumor growth and improving survival of mice compared to vaccination with IL-2. NKTR-214 enhanced pmel-1 CD8+ T cell numbers and decreased numbers of immune-suppressive Tregs in tumor. NKTR-214 was able to stably maintain a high ratio of pmel-1 CD8+ T cells over Tregs in tumor for >30 days. Despite the induction of very strong CD8+ T cell responses and anti-tumor activity, no gross toxicity was observed.

### Conclusions

NKTR-214 synergizes with vaccination by supporting the survival, maintenance and tumor infiltration of effector CD8+ T cells without promoting the intratumoral accumulation of immune-suppressive Tregs. These preclinical results establish that NKTR-214 is highly effective in increasing CD8+ effector T cell responses with potent anti-tumor activity.

### 360

#### **A tumor mitochondria vaccine protects against experimental renal cell carcinoma**

Andrea Facciabene, *Pierini Stefano*, Fang Chongyung, Stavros Rafail

University of Pennsylvania, Philadelphia, PA, USA

### Background

Mitochondria provide energy for cells via oxidative phosphorylation. Reactive oxygen species, a byproduct of this

mitochondrial respiration, can damage mitochondrial DNA (mtDNA), and somatic mtDNA mutations have been found in all colorectal, ovarian, breast, urinary bladder, kidney, lung, and pancreatic tumors studied. The resulting altered mitochondrial proteins or tumor-associated mitochondrial antigens (TAMAs) are potentially immunogenic, suggesting that they may be targetable antigens for cancer immunotherapy.

### Methods

We generated a cellular tumor vaccine by pulsing dendritic cells with enriched mitochondrial proteins from RENCA cells.

### Results

Our dendritic cell-based RENCA mitochondrial lysate vaccine elicited a cytotoxic T cell response *in vivo* and conferred durable protection against challenge with RENCA cells when used in a prophylactic or therapeutic setting. By sequencing mtDNA from RENCA cells, we identified two mutated molecules: COX1 and ND5. Peptide vaccines generated from mitochondrial-encoded COX1 but not from ND5 had therapeutic properties similar to RENCA mitochondrial protein preparation.

### Conclusions

Our results demonstrated that TAMAs can elicit effective antitumor immune responses, potentially providing a new immunotherapeutic strategy to treat cancer.

### 361

#### **Integrin activator 7HP349 enhances anti-CTLA-4 antibody-based cancer therapy**

Yared Hailemichael<sup>1</sup>, Michael Nielsen<sup>1</sup>, Faisal Fa'ak<sup>1</sup>, Peter Vanderslice<sup>2</sup>, Darren G Woodside<sup>3</sup>, Robert V Market<sup>6</sup>, Ronald J Biediger<sup>6</sup>, Upendra K Marathi<sup>4</sup>, Willem W Overwijk<sup>1</sup>

<sup>1</sup>Department of Melanoma Medical Oncology, University of Texas MD Anderson Cancer Center, Houston, TX, USA

<sup>2</sup>Texas Heart Institute, Houston, TX, USA

<sup>3</sup>Department of Molecular Cardiology, Texas Heart Institute, Houston, TX, USA

<sup>4</sup>7 Hills Pharma LLC, Houston, TX, USA

### Background

Checkpoint blockade therapy has therapeutic benefit in several human cancers [1], but in many patients, checkpoint blockade-induced T cells do not infiltrate tumors [2,3], preventing clinical benefit. One mechanism of intratumoral T cell accumulation is through the activity of the integrins very late antigen-4 (VLA-4) and lymphocyte function-associated antigen-1 (LFA-1) on activated T cells. We evaluated the effect of an integrin agonist, 7HP349, on promoting intratumoral T cell accumulation to potentiate CTLA-4 checkpoint blockade-induced anti-tumor activity.





## Therapeutic Cancer Vaccines

Presenting author underlined; *Primary author in italics*

### Methods

To evaluate the effect of 7HP349 in promoting checkpoint blockade-induced anti-tumor immunity, we combined it with anti-CTLA-4 therapy in the standard treatment model of established subcutaneous B16 melanoma [4].

### Results

CTLA-4 checkpoint blockade enhanced vascular cell adhesion molecule-1 (VCAM-1) and intercellular cell adhesion molecule-1 (ICAM-1) expression on tumor vasculature consequently resulting in increased intratumoral accumulation of CD8<sup>lo</sup>CD11a<sup>hi</sup>CD44<sup>hi</sup> effector T cells (Teff) and inflammatory monocytes (iMO) and granulocytes (Gran). ICAM-1 antibody blockade or genetic ablation caused reduced accumulation of Teff and tumor control. Intratumoral administration of 7HP349 enhanced CD8+ T cell accumulation and tumor control compared to mice treated with anti-CTLA-4 monotherapy or with vehicle control ( $P < 0.01$ ). Mice treated with anti-CTLA-4 and 7HP349 showed increased depigmentation (vitiligo) suggesting immunity to melanocyte differentiation antigens. Therapeutic efficacy was also observed after systemic administration of 7HP349 in combination with anti-CTLA-4 therapy, resulting in (80%) tumor-free survival compared to anti-CTLA-4 monotherapy (33%) ( $P < 0.01$ ).

### Conclusions

Activation of integrin cell adhesion molecules with 7HP349 is a promising approach to enhance the anti-cancer activity of checkpoint blockade therapy with antibodies against CTLA-4, and possibly other checkpoint molecules such as PD-1 and PD-L1.

### References

1. Sharma P, Allison JP: **Immune checkpoint targeting in cancer therapy: toward combination strategies with curative potential.** *Cell* 2015, **161**, 205-214.
2. Gajewski TF: **The Next Hurdle in Cancer Immunotherapy: Overcoming the Non-T-Cell-Inflamed Tumor Microenvironment.** *Sem Oncol* 2015, **42**:663-671.
3. Peske JD, Woods AB, Engelhard VH: **Control of CD8 T-Cell Infiltration into Tumors by Vasculature and Microenvironment.** *Adv Cancer Res* 2015, **128**:263-307.
4. van Elsas A, *et al*: **Elucidating the autoimmune and antitumor effector mechanisms of a treatment based on cytotoxic T lymphocyte antigen-4 blockade in combination with a B16 melanoma vaccine: comparison of prophylaxis and therapy.** *J Exp Med* 2001, **194**:481-489.

### 362

## **Intramuscular anti-HER2 antibody gene transfer as an alternative to conventional antibody protein therapy: a pre-clinical proof of concept study in breast cancer**

Kevin Hollevoet, Nick Geukens, Paul Declerck

KU Leuven, Leuven, Vlaams-Brabant, Belgium

### Background

Monoclonal antibodies (mAbs) are taking the field of cancer immunotherapy by storm. Despite their growing use, a broader accessibility and implementation is hampered by dismal pharmaco-economics, the practicalities and patient discomfort associated with frequent and long-term high-dose mAb administration, and the often limited therapeutic effect as single agent. To address these issues, the laboratory focuses on the development of a therapeutic DNA platform for non-viral antibody gene transfer. After administration of vectors that carry the encoding mAb sequences, this approach enables the site of delivery (e.g., muscle or tumor) to produce mAbs *in vivo* followed by secretion into circulation for a prolonged period of time. *In vivo* mAb expression presents a labor- and cost-effective alternative to the conventional production, purification and parenteral delivery of mAb proteins. The less frequent administrations and gradual *in vivo* mAb production and buildup are anticipated to improve patient comfort and safety. Also, by making mAb therapy more affordable, more effective combinations could be implemented more easily.

### Methods

This study aims to demonstrate the feasibility of intramuscular mAb gene electrotransfer in mice using the well-characterized trastuzumab or its murine precursor 4D5 encoded in plasmid DNA (pDNA). Following intramuscular pDNA injection and electroporation, mAb plasma levels were measured with ELISA using HER2-coated plates. *In vivo* therapeutic efficacy of mAb gene transfer was evaluated in a BT474 breast cancer mouse model.

### Results

Following intramuscular electrotransfer of the encoding pDNA in BALB/c mice, trastuzumab was found at microgram per milliliter concentrations in plasma. In this immune competent strain, however, detection was lost 10 days after pDNA delivery, because of an immune response against the humanized trastuzumab. This was overcome by delivery of trastuzumab pDNA in immune compromised mice (RAG2<sup>-/-</sup>/γC<sup>-/-</sup> and athymic nude mice) or by delivery of 4D5 pDNA, thus matching the mAb sequence with the host species. Both approaches resulted in continued mAb expression at microgram per milliliter concentrations for at least 6 months, the duration of the follow-up. mAb plasma

## Therapeutic Cancer Vaccines

*Presenting author underlined; Primary author in italics*

concentration could be adjusted by adapting the pDNA dose or administering additional pDNA doses. In a BT474 xenograft mouse model, intramuscular electrotransfer of 4D5 pDNA induced significant anti-tumor responses compared to the untreated control group.

### Conclusions

This study achieved proof of concept for prolonged and therapeutically relevant *in vivo* mAb expression in mice using anti-HER2 mAbs as demonstrator. Ongoing work focuses on expanding the DNA platform to immunomodulatory mAb combinations and bridging the gap towards clinical application.

**363**

### Direct identification of neopeptides in tumor tissue

Nathalie Joly, Laura McIntosh, *Eustache Paramithiotis*

Caprion Biosciences Inc., Montreal, PQ, Canada

#### Background

Antigen presentation by MHC is central to the development of adaptive immunity. While traditional modeling approaches yield large numbers of candidates and high attrition rates, direct identification of naturally-processed peptides by mass spectrometry can significantly streamline the neo-epitope identification.

#### Methods

To demonstrate the feasibility and advantages of this approach, a pilot study was conducted in clear cell renal cell carcinoma. MHC I-peptide complexes were isolated from tumor and matched adjacent normal tissue from treatment-naïve patients with the same tumor grade but heterogeneous HLA haplotypes. Peptides were eluted from the complexes using mild acid and were analyzed by mass spectrometry and their expression was compared to matched adjacent tissue.

#### Results

Results demonstrated effective enrichment and detection of MHC-associated peptides, with identification of an average of over 6800 peptides per sample and characteristics appropriate for peptides presented by MHC I. Differential expression analysis indicated that approximately 13% of identified peptides were substantially overexpressed (> 3-fold) in the tumor tissue, with approximately 3.5% uniquely presented in tumors. In many cases multiple HLA allele-specific peptides derived from the same tumor-presented protein were identified, thereby increasing coverage across different haplotypes. A relatively small number of modified peptides presented only by the tumor were identified, consistent with the low mutational load of clear cell renal cell carcinoma. Most of these peptides appeared to be derived from protein fusions (37%), single amino acid

substitutions (25%) and frameshift mutations (19%), with a lower contribution from splicing variants (6%) and post-translational modifications (9%). Pathway analysis showed significant over-representation of proteins associated with hypoxia and angiogenesis, two processes previously reported to change in clear cell renal carcinoma.

### Conclusions

Thus tumor-associated antigen presentation reflected protein expression changes previously reported in renal cell carcinoma, and identified multiple novel candidates. Direct identification of naturally processed peptides generated a small but high quality list of candidates for further investigation.

**364**

### Intratumorally injected pro-inflammatory allogeneic dendritic cells as immune enhancers - a phase I/II study in patients with advanced hepatocellular carcinoma

*Magnus Rizell*<sup>1</sup>, Malin Sternby<sup>1</sup>, Bengt Andersson<sup>2</sup>, Alex Karlsson-Parra<sup>3</sup>

<sup>1</sup>Transplant Institute, Sahlgrenska Academy at University of Gothenburg, Gothenburg, Sweden

<sup>2</sup>Department of Clinical Immunology, Gothenburg University, Gothenburg, Sweden

<sup>3</sup>Department of Immunology, Genetics and Pathology, Uppsala University, Uppsala, Sweden

#### Background

Accumulating pre-clinical data indicate that the efficient induction of antigen-specific cytotoxic T cells characterizing viral infections is caused by cross-priming where initially infected DCs act as a pure adjuvant, not as antigen presenting cells, producing inflammatory factors that recruit and activate non-infected "bystander" DCs. Accordingly, we have developed a cellular adjuvant consisting of pro-inflammatory monocyte-derived allogeneic DCs producing high levels of DC-recruiting and DC-maturing factors in a sustained fashion.

#### Methods

Eleven patients with advanced hepatocellular carcinoma (HCC) were included in a phase I/II study. Vaccine cells (INTUVAX) were produced from a leukapheresis-product collected from one healthy blood donor and subsequently deep-frozen. Three doses of vaccine cells (10-20 million cells/dose) were injected intratumorally. Using mixes of overlapping peptides for alpha fetoprotein (AFP) and human telomerase reverse transcriptase (hTERT) spanning the entire protein sequence, CD8+ T cell responses could be evaluated, regardless of the patient's HLA-type.



## Therapeutic Cancer Vaccines

*Presenting author underlined; Primary author in italics*

### Results

Nine out of 11 patients received all 3 vaccine doses. Six of these 9 patients had received prior first-line systemic treatment with sorafenib while 3 patients were naive to systemic treatment. INTUVAX was generally well tolerated but two severe adverse events, both fever episodes, were reported as drug-related. Among the 9 fully treated patients, 6 patients exhibited an increase of AFP and/or hTERT specific and IFN-gamma producing CD8+ T cells 1 week after the third vaccine dose as compared to pre-vaccination levels. Median overall survival (mOS) for the fully treated patient subgroup given INTUVAX as second-line systemic treatment (n=6) is still not reached but is currently (8AUG2016) 8.2 months while mOS for the three patients receiving INTUVAX as first-line systemic treatment was 11.7 months. These data compare favorably with historical data. Notably, two out of three patients who did not respond with an increase in tumor-specific T cells died within 5 months after the first INTUVAX dose.

### Conclusions

Our findings indicate that intratumoral administration of proinflammatory allogeneic DCs induces a CTL-mediated systemic anti-tumor response in a majority of HCC patients that this response correlate to prolonged survival.

### Trial Registration

ClinicalTrials.gov identifier NCT01974661.

### 365

## Nanodisc neoantigen vaccination combined with immune checkpoint blockade efficiently eliminates established tumors

Rui Kuai, Lukasz Ochyl, Anna Schwendeman, James Moon

University of Michigan, Ann Arbor, MI, USA

### Background

With the rapid development of next-generation DNA/RNA sequencing technology, patient-specific tumor neo-antigens can now be identified, potentially ushering in the new era of personalized cancer vaccines. Peptide vaccines, known for ease of manufacturing, quality control and human safety, can be easily applied for neo-antigen-based immunotherapy. However, peptide-based cancer vaccines have shown limited therapeutic efficacy in humans, partially due to inefficient co-delivery of antigen (Ag) and adjuvants to lymphoid tissues as well as T cell dysfunction and deletion.

### Methods

Here we report that synthetic high density lipoprotein (sHDL) nanodiscs, with an established clinical manufacturing procedure and excellent safety profiles in humans, can be simply mixed with Ag peptides and adjuvants, producing

homogeneous, stable, and ultrasmall (~10 nm in diameter) nanodiscs in less than 2 hrs for personalized neo-antigen vaccination.

### Results

Nanodiscs efficiently co-delivered Ag and CpG, a Toll-like receptor-9 agonist, to draining lymph nodes and promoted strong and durable Ag presentation on antigen-presenting cells. Strikingly, nanodiscs elicited up to 47-fold greater frequency of tumor neoantigen-specific CD8+ T lymphocytes (CTLs) than soluble vaccines and even 31-fold greater than arguably the strongest CTL adjuvant in clinical trials (i.e., CpG in Montanide). Moreover, in mice bearing MC-38 colon tumors, therapeutic sHDL vaccination led to significantly enhanced IFN- $\gamma$ <sup>+</sup>TNF- $\alpha$ <sup>+</sup> Ag-specific CTL responses that substantially inhibited tumor growth and extended animal survival, compared with soluble vaccines ( $p < 0.01$ ). When nanodisc vaccination was combined with the immune checkpoint inhibitor, anti-PD-1 ( $\alpha$ -PD-1), ~88% of MC-38 tumor-bearing mice were cured, whereas the soluble peptide+CpG vaccine combined with  $\alpha$ -PD-1 therapy cured only 25% mice. Those cured mice were completely protected against MC-38 cell re-challenge administered on day 70, indicating resistance to tumor relapse. To treat a more aggressive B16F10 melanoma model, multiple MHC class I and class II epitopes were loaded in nanodiscs. Vaccination with multi-epitope nanodiscs generated ~30% tumor antigen-specific, IFN- $\gamma$ <sup>+</sup> CD8+ and CD4+ T cells in peripheral blood, whereas only ~2% response was observed for the soluble vaccine or Ag+CpG+Montanide group. More strikingly, when multi-epitope nanodisc vaccination was combined with  $\alpha$ -PD-1/ $\alpha$ -CTLA-4 therapy, ~90% B16F10 tumor-bearing mice were cured, whereas only ~38% rate of tumor regression was observed in animals treated with the soluble peptide vaccine plus  $\alpha$ -PD-1/ $\alpha$ -CTLA-4 therapy.

### Conclusions

Overall, our approach offers a powerful and convenient platform technology for patient-tailored cancer vaccines, which in combination with the immune checkpoint inhibitor can efficiently eliminate established tumors and prevent relapse.

## Therapeutic Cancer Vaccines

Presenting author underlined; Primary author in italics

366

### Development of personalized, live, attenuated double-deleted *Listeria monocytogenes* (pLADD) immunotherapy targeting tumor-specific neoantigens to treat cancer

*Weiwen Deng*, Thomas E Hudson, Edward E Lemmens, Bill Hanson, Chris S Rae, Joel Burrill, Justin Skoble, George Katibah, Aimee L Murphy, Michele deVries, Dirk G Brockstedt, Meredith L Leong, Peter Lauer, Thomas W Dubensky, Chan C Whiting

Aduro Biotech, Inc., Berkeley, CA, USA

#### Background

Clinical success of checkpoint inhibitors, dendritic cell-based therapies and adoptive T cell transfer studies highlight the importance of tumor-specific neoantigens as critical targets for effective immunotherapy [1, 2]. Advances in genome sequencing and predictive epitope binding algorithms provide an unprecedented opportunity to develop highly personalized immunotherapeutics [3]. Aduro is developing personalized therapy (pLADD) based on the live, attenuated double-deleted *Listeria monocytogenes* (LADD) platform which has been administered to over 300 cancer patients with an acceptable safety profile.

#### Methods

Tumor-bearing C57BL/6 mice were treated with pLADD-MC38 and anti-PD-1. MC38 mutated epitopes [4] were expressed as a synthetic neoantigen protein from the *Listeria* chromosome. Tumor growth was monitored; immune responses measured by IFN $\gamma$  ELISpot.

#### Results

We constructed a pLADD strain expressing tumor-specific neoepitopes from murine MC38 tumor cells (pLADD-MC38). Administration of pLADD-MC38 in mice induces cellular immune responses against encoded neoepitopes but not against native sequences. Moreover, we also showed synergistic anti-tumor efficacy of pLADD-MC38 and anti-PD-1. To effectively translate pLADD into the clinic, we have established an accelerated, small-scale LADD manufacturing process.

#### Conclusions

pLADD is an attractive immunotherapy approach to target multiple tumor-specific neoantigens using the LADD platform to take advantage of rapid construction, manufacture, and release, an established clinical safety profile with repeated administration, and induction of innate and adaptive immunity and favorable tumor microenvironment changes. The FDA has cleared an IND for a phase I trial to evaluate safety and immunogenicity of pLADD in subjects with advanced gastrointestinal cancers, and its progress will be discussed.

#### References

1. Carreno BM, Magrini V, Becker-Hapak M, Kaabinejadian S, Hundal J, Petti AA, *et al*: **A dendritic cell vaccine increases the breadth and diversity of melanoma neoantigen-specific T cells.** *Cancer Immunother* 2015, **348**:803-808.
2. Tran E, Turcotte S, Gros A, Robbins PF, Lu YC, Dudley ME, *et al*: **Cancer immunotherapy based on mutation-specific CD4+ T cells in a patient with epithelial cancer.** *Science* 2014, **344**:641-645.
3. Schumacher TN, Schreiber RD: **Neoantigens in cancer immunotherapy.** *Science* 2015, **348**:69-73.
4. Yadav M, Jhunjhunwala S, Phung QT, Lupardus P, Tanguay J, Bumbaca S, *et al*: **Predicting immunogenic tumour mutations by combining mass spectrometry and exome sequencing.** *Nature* 2014, **515**:572-576.

367

### Therapeutic efficacy of cancer stem cell-vaccine in the PD-1/PD-L1 blockade

*Xin Chen*<sup>1</sup>, Yangyang Hu<sup>2</sup>, Yang Xia<sup>2</sup>, Li Zhou<sup>1</sup>, Yangyi Bao<sup>3</sup>, Shiang Huang<sup>4</sup>, Xiubao Ren<sup>5</sup>, Elaine Hurt<sup>6</sup>, Robert E Hollingsworth<sup>6</sup>, Alfred E Chang<sup>2</sup>, Max S Wicha<sup>7</sup>, Qiao Li<sup>8</sup>

<sup>1</sup>University of Michigan Cancer Center, Ann Arbor, MI, USA

<sup>2</sup>University of Michigan, Ann Arbor, MI, USA

<sup>3</sup>The Third Affiliated Hospital of Anhui Medical University, Hefei, Anhui, People's Republic of China

<sup>4</sup>Union Hospital, Tongji Medical College, Huazhong University of Science and Technology, Wuhan, Hubei, People's Republic of China

<sup>5</sup>Tianjin University Cancer Institute and Hospital, Tianjin, Hebei, People's Republic of China

<sup>6</sup>MedImmune Inc., Gaithersburg, MD, USA

<sup>7</sup>University of Michigan Medical School, Ann Arbor, MI, USA

<sup>8</sup>University of Michigan Medical Center, 1150 W. Medical Center Dr., MI, USA

#### Background

We have previously reported the development of a strategy to target the cancer stem cell (CSC) populations in melanoma and squamous cell carcinoma using CSC lysate-pulsed dendritic cells (DCs). Using mouse models we demonstrated that DCs pulsed with CSCs enriched by virtue of their expression of the CSC marker ALDH (termed CSC-DC) significantly inhibited tumor growth. However, CSC-DC vaccine therapy alone may not be sufficient to overcome the immunosuppressive components of the tumor microenvironment. CSC-mediated suppression of T cells has been reported in a process involving the PD-L1/PD-1 axis. Immunologically targeting CSCs while simultaneously blocking PD-L1/PD-1-mediated immune suppression





## Therapeutic Cancer Vaccines

Presenting author underlined; *Primary author in italics*

may significantly enhance the outcome of current immunotherapies of cancer.

### Methods

To test this hypothesis, we investigated the effect of using anti-PD-L1 to block immunosuppression during the CSC-DC vaccination to augment the therapeutic efficacy of using each regimen alone. We used the 4T1 cell line, a mammary carcinoma syngeneic to BALB/c mice, and found that 4T1 tumors contain approx. 6-10% ALDEFLUOR<sup>+</sup>/ALDH<sup>high</sup> cells, and that these cells are enriched for tumor initiating capacity compared to bulk or ALDEFLUOR<sup>-</sup>/ALDH<sup>low</sup> cells. Inoculating 4T1 cells into the mammary fat pad induces the development of spontaneous pulmonary metastases.

### Results

ALDH<sup>high</sup> 4T1 CSCs expressed PD-L1. 4T1 ALDH<sup>high</sup> CSC-DC vaccine + anti-PD-L1 administration significantly reduced pulmonary metastases and prolonged survival compared with 4T1 ALDH<sup>high</sup> CSC-DC vaccine or anti-PD-L1 administration alone. Anti-PD-L1 administration increased systemic anti-4T1 CSC immunity induced by CSC-DC vaccine. This is evident by the increased production of total IgG in the serum samples collected from the 4T1-bearing animals subjected to 4T1 CSC-DC vaccination with anti-PD-L1 administration. The CSC-reactivity/specificity of the immune sera was demonstrated by their specific binding to the ALDH<sup>high</sup> vs. ALDH<sup>low</sup> 4T1 cells in flow cytometry. Importantly, the immunological consequence of such binding was Ab-mediated ALDH<sup>high</sup> 4T1 CSC lysis via complement dependent cytotoxicity. In addition, CTLs generated from the splenocytes harvested from the hosts subjected to 4T1 CSC-DC vaccination with anti-PD-L1 administration killed ALDH<sup>high</sup> 4T1 CSCs significantly more than ALDH<sup>low</sup> 4T1 cells.

### Conclusions

These results are supportive of the conclusion that administration of anti-PD-L1 could significantly boost the therapeutic efficacy of the CSC-DC vaccine, and that this effect was due to both antibody and T cell-mediated anti-CSC immunity.

368

### Immunotherapy with INO-3112 (plasmids encoding HPV16 and HPV18 E6/E7 antigens and IL-12) induces immune responses in peripheral blood and tumor tissue in patients with HPV associated head and neck squamous cell carcinoma (HNSCCa)

Charu Aggarwal<sup>1</sup>, Drishty Mangrolia<sup>2</sup>, Roger Cohen<sup>1</sup>, Gregory Weinstein<sup>3</sup>, Matthew Morrow<sup>2</sup>, Joshua Bauml<sup>1</sup>, Kim Kravnyak<sup>2</sup>, Jean Boyer<sup>4</sup>, Jian Yan<sup>2</sup>, Jessica Lee<sup>2</sup>, Laurent Humeau<sup>4</sup>, Sandra Oyola<sup>2</sup>, Susan Duff<sup>2</sup>, David Weiner<sup>5</sup>, Zane Yang<sup>2</sup>, Mark Bagarazzi<sup>2</sup>

<sup>1</sup>University of Pennsylvania, Philadelphia, PA, USA

<sup>2</sup>Inovio Pharmaceuticals, Plymouth Meeting, PA, USA

<sup>3</sup>Inovio Pharmaceuticals, Philadelphia, PA, USA

<sup>4</sup>Inovio Pharmaceuticals, San Diego, CA, USA

<sup>5</sup>The Wistar Institute, Philadelphia, PA, USA

### Background

We have previously reported interim results of safety and immunogenicity of the INO-3112 in subjects with HPV-associated HNSCCa. INO-3112 was shown to be safe and immunogenic, inducing HPV-specific CD8<sup>+</sup> T cell responses [1].

### Methods

Subjects were enrolled into two cohorts. Cohort 1 received INO-3112 pre- and post-surgery. Cohort 2 received INO-3112 after completion of cisplatin based chemoradiation. Here, we report immune responses post immunotherapy in peripheral blood and tumor tissue obtained from surgery for Cohort 1 subjects. Tumor samples were stained with immunohistochemistry techniques for CD8 and FoxP3. In addition, ELISpot analysis was used to determine the number of cells capable of secreting IFN- $\gamma$  in response to HPV antigen stimulation.

### Results

As of August 1 2016, accrual has been completed with 22 enrolled subjects. Cohort 1: n=6, Cohort 2: n=16, 20 males, median age 57.5 years; base of tongue cancer=10, tonsil cancer=12; never smoker=10. Six subjects in Cohort 1 received at least one dose of INO-3112 on average 14 days (range 7 to 28 days) prior to definitive surgery. Paired pre- and post-INO-3112 therapy tumor samples were available for five of the 6 subjects. CD8 positive T cell counts increased in tumor tissue in 2 subjects, average 160.6% increase (range 61.7% to 259.4%) from baseline. FoxP3 positive cell counts decreased in tumor tissue in 3 subjects, average 48% decrease (range 44% to 53%). Four of the 5 subjects showed increased CD8:FoxP3 ratio post INO-3112, average 60.3% increase (range 1.4% to 209.3%). Five of 6 subjects had peripheral blood available for analysis of peripheral



## Therapeutic Cancer Vaccines

*Presenting author underlined; Primary author in italics*

HPV-specific T cell responses by IFN- $\gamma$  ELISpot. Four subjects exhibited an increase in ELISpot response magnitude post INO-3112 compared to baseline (range 30.00 to 158.33 SFU). Two subjects with increase in CD8 positive cells in tumor tissue demonstrated the highest increase in ELISpot response (108.33 and 158.33 SFU, respectively). Four of 6 subjects remain progression-free; median PFS of 17 months (range 12 to 23 months) to date. One subject withdrew consent after surgery. One subject demonstrated only marginal increases in ELISpot response magnitude to HPV 16 (3.33 to 16.67 SFU) and no increase in CD8/FoxP3 ratio (0.95 to 0.60) in tumor tissue post INO-3112 developed progressive disease (11 months post INO-3112).

### Conclusions

These results demonstrate that INO-3112 DNA-based immunotherapy can induce detectable immune responses in peripheral blood and tumor tissue in subjects with HPV associated HNSCCa.

### Trial Registration

ClinicalTrials.gov identifier NCT02163057.

### References

1. *J Immunother Cancer* 2015, **3**(Suppl 2):426.

### 369

#### **DNA vaccine with pembrolizumab elicits anti-tumor responses in patients with metastatic, castration-resistant prostate cancer (mCRPC)**

Douglas G McNeel<sup>1</sup>, Jens Eickhoff<sup>2</sup>, Robert Jeraj<sup>2</sup>, Mary Jane Staab<sup>1</sup>, Jane Straus<sup>1</sup>, Brian Rekoske<sup>2</sup>, Glenn Liu<sup>1</sup>

<sup>1</sup>University of Wisconsin Carbone Cancer Center, Madison, WI, USA

<sup>2</sup>University of Wisconsin, Madison, WI, USA

### Background

In our evaluation of anti-tumor DNA vaccines as treatments for prostate cancer, we have recently shown in murine models that, depending on the duration of antigen expression encoded by the DNA and the strength of MHC:TCR affinity of CD8+ T cells elicited with vaccination, these T cells express higher levels of PD-1 or LAG-3 [1]. Blockade of these regulatory mechanisms at the time of T cell activation with vaccine produced anti-tumor responses *in vivo*. Similarly, we have recently found that patients with prostate cancer previously immunized with a DNA vaccine develop PD-1-regulated T cells [2]. These findings suggested that combined PD-1 blockade with vaccination should elicit superior anti-tumor responses in patients with prostate cancer.

### Methods

A clinical trial was designed to evaluate the immunological and clinical efficacy of a DNA vaccine encoding PAP (pTVG-

HP) when delivered in combination or in sequence with pembrolizumab, in patients with mCRPC. Serial biopsies, blood draws, and exploratory FLT PET/CT imaging are being conducted for correlative analyses.

### Results

While trial accrual continues, 1 of 14 subjects has experienced a grade 3 adverse event. There have been no grade 4 events. 4 of 6 patients treated with the combination have experienced serum PSA declines, and 3 of 6 have experienced decreases in tumor volume by radiographic imaging at 12 weeks, including one partial response. Expansion of PAP-specific Th1-biased T cells has been detected in peripheral blood samples. Exploratory FLT PET/CT imaging has demonstrated proliferative responses in metastatic lesions and in vaccine-draining lymph nodes.

### Conclusions

PD-1 pathway inhibitors have demonstrated little clinical activity to date when used as single agents for treating prostate cancer. Our findings suggest that combining this blockade with tumor-targeted T cell activation by a DNA vaccine is safe and can augment tumor-specific T cells, detectable within the peripheral blood and by imaging, and result in objective changes. We are currently exploring expansion of this trial to treat over an extended period of time and in an earlier stage of disease.

### Acknowledgements

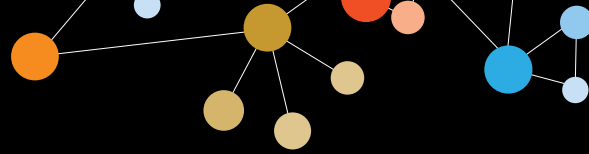
Funding from 2014 Movember Prostate Cancer Foundation Challenge Award and Madison Vaccines, Inc.

### Trial Registration

ClinicalTrials.gov identifier NCT02499835.

### References

1. Rekoske BT, Smith HA, Olson BM, Maricque BB, McNeel DG: **PD-1 or PD-L1 blockade restores antitumor efficacy following SSX2 epitope-modified DNA vaccine immunization.** *Cancer Immunol Res* 2015, **3**:946-955.2. Rekoske BT, Olson BM, McNeel DG: **Anti-tumor vaccination of prostate cancer patients elicits PD-1/PD-L1 regulated antigen-specific immune responses.** *Oncoimmunology* 2016, **5**:e1165377.



## Therapeutic Cancer Vaccines

Presenting author underlined; Primary author in italics

370

### A multi-peptide vaccine plus toll-like receptor (TLR) agonists LPS or polyI:CLC in combination with incomplete Freund's adjuvant (IFA) in melanoma patients

Marit Melssen<sup>1</sup>, Gina Petroni<sup>1</sup>, William Grosh<sup>1</sup>, Nikole Varhegyi<sup>1</sup>, Kim Bullock<sup>1</sup>, Mark Smolkin<sup>1</sup>, Kelly Smith<sup>1</sup>, Nadejda Galeassi<sup>1</sup>, Donna H Deacon<sup>2</sup>, Elizabeth Gaughan<sup>1</sup>, Craig L Slingluff Jr<sup>3</sup>

<sup>1</sup>University of Virginia, Charlottesville, VA, USA

<sup>2</sup>Department of Surgery, University of Virginia, Charlottesville, VA, USA

<sup>3</sup>Division of Surgical Oncology, University of Virginia, Charlottesville, VA, USA

#### Background

Adjuvants for cancer vaccines have not been optimized. In a murine model, vaccines with IFA may deplete circulating T cells, but vaccination with TLR agonists plus CD40 antibody induces strong, durable CD8 responses. An alternate approach to ligating CD40 is to activate CD4+ T cells, to upregulate CD40L. The present study tests safety and immunogenicity of vaccination with 12 Class I MHC-restricted melanoma peptides (12MP) to activate CD8+ T cells and a tetanus toxoid peptide (Tet) to activate CD4+ T cells, plus either of two TLR agonists, with or without IFA. We hypothesized that vaccines with TLR3 agonist polyI:CLC or TLR4 agonist lipopolysaccharide (LPS) would be safe and would induce stronger and more durable T cell responses than when IFA was included.

#### Methods

Participants with resected stage IIB-IV melanoma were randomly assigned 2:1 to cohort 1 (LPS dose-escalation, n=33) or cohort 2 (polyI:CLC 1 mg, n=18). Each cohort included 3 subgroups (a-c), receiving 12MP+Tet+TLR agonist (a) without IFA, (b) plus IFA in the first vaccine only (V1), or (c) plus IFA in all six vaccines (V6). Toxicities were recorded (CTCAE v4). T cell responses were measured with IFN $\gamma$  ELISpot either *ex vivo*, or 14 days after *in vitro* stimulation (IVS).

#### Results

There were no DLTs in Cohort 1 (LPS) but two in cohort 2 (1 of 6, subgroups 2b and 2c). CD8+ T cell responses to 12MP were detected *ex vivo* in 43%, 67%, 50%, and 29% of patients in Cohort 1 with 25, 100, 400, and 1600 EU LPS, respectively, and in 56% of patients in Cohort 2. Responses to 12MP were detected *ex vivo* in 18%, 50%, and 78% for subgroups (a)-(c), respectively (Figure). Responses were more durable and of highest magnitude for IFA V6. IVS CD8 responses and *ex vivo* CD4 responses were also improved with addition of IFA.

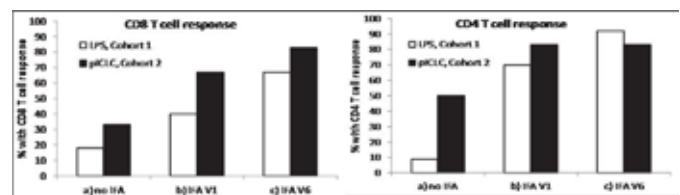
#### Conclusions

LPS is a safe and effective vaccine adjuvant when combined with IFA; the optimal biologic dose may be 100-400 EU. All regimens were deemed safe. Despite recent concerns about IFA, this study demonstrates that in humans, IFA enhanced magnitude and durability of T cell responses to peptide vaccines when added to TLR agonists. Thus, combination strategies with IFA and LPS and/or pI:CLC offer promise for next generation vaccines.

#### Trial Registration

ClinicalTrials.gov identifier NCT0158535.

Figure 1.



371

### Long-term follow-up of Vigil (DNA engineered bi-shRNA furin GMCSF plasmid/autologous tumor) in recurrent metastatic Ewing's sarcoma (EWS)

Maurizio Ghisoli<sup>1</sup>, Minal Barve<sup>1</sup>, Robert Mennel<sup>2</sup>, Gladice Wallraven<sup>3</sup>, Luisa Manning<sup>4</sup>, Neil Senzer<sup>5</sup>, *John Nemunaitis*<sup>5</sup>

<sup>1</sup>Mary Crowley Cancer Research Centers, Texas Oncology, P.A., Dallas, TX, USA

<sup>2</sup>Texas Oncology, P.A., Baylor University Medical Center, Dallas, TX, USA

<sup>3</sup>Gradalis, Inc., Carrollton, TX, USA

<sup>4</sup>Gradalis, Inc., Dallas, TX, USA

<sup>5</sup>Mary Crowley Cancer Research Centers, Gradalis, Inc., Dallas, TX, USA

#### Background

EWS is an aggressive, rare (10 cases per million 10-19 year old children) pediatric cancer of bone and, less frequently, extraskelatal sites. Although first-line intensive chemotherapy has been effective in localized disease, it is less so in metastatic disease and poorly effective in patients with progressive or recurrent disease. Patients relapsing within 2 years of diagnosis, which occurs in 72% of the patients, have a 2-year survival of 7%. The outcome for refractory and third-line patients is even worse.

#### Methods

We recently completed a 3-year follow-up of a prospective, non-randomized study of Vigil vaccine ( $1 \times 10^6$  -  $1 \times 10^7$  cells/ID injection 1x/mo) in recurrent/refractory EWS patients (n=16) and compared results to a contemporaneous group (n=14) not treated with Vigil (Table 1).

## Therapeutic Cancer Vaccines

Presenting author underlined; Primary author in italics

### Results

Results suggest survival benefit without evidence of Vigil related toxicity (no  $\geq$  grade 3). Specifically, we observed 1-year actual survival of 73% for Vigil treated patients compared to 23% in those not treated and a 17.2 month improvement in overall survival (Figure 1).

### Conclusions

In conclusion, Vigil appears to confer a survival advantage and enhanced therapeutic index in advanced EWS. A randomized multi-site study comparing Vigil vs. gemcitabine/Taxotere in third-line metastatic EWS has been initiated to see if these exploratory data can be confirmed (n=62, HR 0.387).

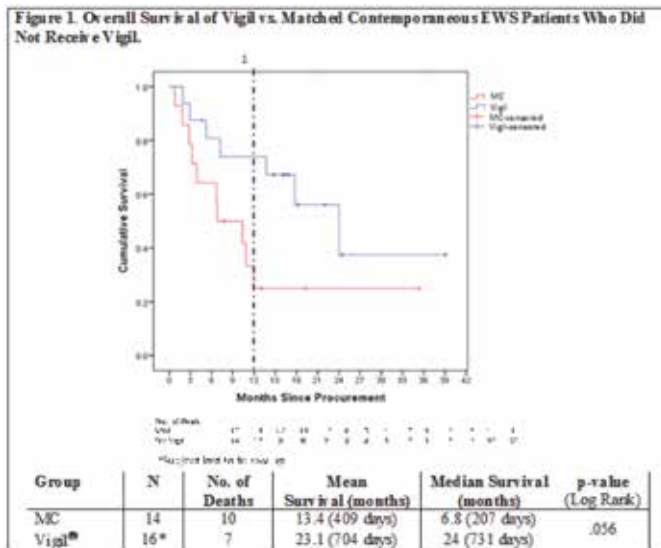
Table 1.

Table 1. Ewing's Sarcoma Phase I Demographics

	Vigil*	Matched Comparator (MC)*
Tumor Location Harvest (Lung/Soft Tissue/Other)	13/0/3	11/2/1
Sex (M/F)	12/4	7/7
Age median (range)	19 (59-12)	17 (30-12)
Performance (ECOG 0, 1)	16	14
Ethnicity (Caucasian/Other)	13/3	12/2
Prior Systemic Tx (Frontline/2nd-3rd)	1/5/10	3/4/7
General Surgery Harvest (Yes/No)	16/0	14/0

\* 3 insufficient viable tumor cells, 6 contaminants, 5 sought other management

Figure 1.



372

### Vaccination of advanced or relapsed prostate cancer patients with WT1 peptide-pulsed dendritic cells induces immunological and clinical responses

Masahiro Ogasawara, Shuichi Ota

Sapporo Hokuyu Hospital, Sapporo, Hokkaido, Japan

### Background

Survival of patients with advanced prostate cancer is significantly less than patients with early stage. Immunotherapy is a promising approach for the treatment of patients in advanced stage. In the current study, we have evaluated the clinical and immunological responses in patients with advanced or relapsed prostate cancer who received Wilms' tumor 1 (WT1) peptide-pulsed dendritic cell (DC) vaccination in combination with a toll-like receptor (TLR) 4 agonist, OK432.

### Methods

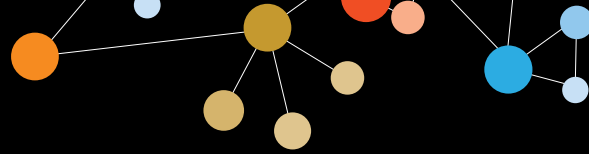
Twelve patients aged 57-82 years were enrolled in the present study. Autologous DCs were generated by culturing adherent mononuclear cells with interleukin-4 and granulocyte-macrophage colony stimulating factor. DCs were then loaded with synthetic peptides derived from WT1 following maturation by prostaglandin E<sub>2</sub> and OK432. DCs and OK432 were administered intradermally every 2 weeks for 7 times. Induction of vaccine-induced T cell responses was evaluated using a HLA-tetramer assay, an intracellular cytokine staining assay and a flow cytometry analysis.

### Results

The treatment was well tolerated and none of the patients experienced more than grade 2 adverse events. Of 12 patients, 7 had stable disease (SD) and 5 had disease progression after one course of vaccination. Survival of patients achieving SD after DC vaccination (responder) was longer than those who did not respond to the treatment (non-responder) (median duration of survival; 48 vs 10 months). Increase in positivity of WT1-specific CD8<sup>+</sup> T cells was observed in both responders and non-responders after one course of vaccination. However, increment in positivity was marked in responders in comparison with non-responders; 53.5 and 2.1 fold in responders and non-responders, respectively. Similarly, intracellular IFN $\gamma$  staining assay showed that marked increase in WT1 specific IFN $\gamma$ -producing CD8<sup>+</sup> T cells in responders compared with non-responders (68.2 vs 3.9 fold increase). Decrease in the absolute number of regulatory T cells (Tregs) or myeloid-derived suppressor cells (MDSCs) was observed in responders after vaccination. While the reduction in the absolute number of Tregs and monocytic MDSCs was moderate (9.0% and 13.5%, respectively), marked reduction in the absolute number of granulocytic MDSCs (61.0%) was observed, indicating that DC vaccination may contribute to the reversal of immunosuppression by these cells.

### Conclusions

DC vaccine-based immunotherapy combined with a TLR agonist was demonstrated to be safe and elicit both innate and acquired cellular immune responses correlated with clinical effects. These results suggest that DC vaccination



## Therapeutic Cancer Vaccines

Presenting author underlined; *Primary author in italics*

might be a promising novel strategy for the treatment of patients with advanced or relapsed prostate cancer.

**373**

### **Phase Ib trial of two folate binding protein peptide booster vaccines (E39 and J65) in breast and ovarian cancer patients**

Kaitlin M Peace<sup>1</sup>, Diane F Hale<sup>1</sup>, Timothy J Vreeland<sup>2</sup>, Doreen O Jackson<sup>1</sup>, John S Berry<sup>3</sup>, Alfred F Trappey<sup>1</sup>, Garth S Herbert<sup>1</sup>, Guy T Clifton<sup>1</sup>, Mark O Hardin<sup>4</sup>, Anne Toms<sup>5</sup>, Na Qiao<sup>5</sup>, Jennifer Litton<sup>5</sup>, George E Peoples<sup>6</sup>, *Elizabeth A Mittendorf*<sup>5</sup>

<sup>1</sup>Brooke Army Medical Center, San Antonio, TX, USA

<sup>2</sup>Womack Army Medical Center, Fayetteville, NC, USA

<sup>3</sup>Department of Colon and Rectal Surgery, Washington University, St Louis, MO, USA

<sup>4</sup>Madigan Army Medical Center, Tacoma, WA, USA

<sup>5</sup>University of Texas MD Anderson Cancer Center, Houston, TX, USA

<sup>6</sup>Cancer Vaccine Development Program, San Antonio, TX, USA

#### **Background**

Folate binding protein (FBP) is over-expressed in multiple cancers. An immunogenic peptide (E39) and an attenuated version (J65) have been shown to stimulate cytotoxic T lymphocytes (CTLs) to recognize and destroy FBP-expressing cancer cells. In addition, previous trials have shown that boosting vaccinations helps maintain long-lasting immunity, though attenuated peptides may be a better choice for boosting due to antigen-induced cell death (AICD) of CTLs after over-stimulation. Here, we report peptide-specific immune response to E39 and J65 after different combinations of vaccination and boosting.

#### **Methods**

This is a prospective, randomized, non-blinded, single-center phase Ib trial. Patients with breast or ovarian cancer rendered disease-free after standard-of-care therapy were enrolled. HLA-A2+ patients were stratified (breast versus ovarian), and for the primary vaccine series (PVS) received either six inoculations with E39, three E39, then three J65 or three J65, then three E39. *Ex vivo* immunologic recognition of E39 was assessed by clonal expansion of cytotoxic T lymphocytes (CTL) and *in vivo* response by delayed-type hypersensitivity (DTH). The 6-month post-PVS immunologic data was used to assess patients for significant residual immunity (SRI), defined as  $\geq 2$ -fold increase from pre-PVS in E39-specific CD8+T cells. Patients were sorted into two groups: with SRI (SRI) and without (nSRI). Patients within each group were randomized to one booster of either J65/E39 resulting in four groups: SRI receiving E39 (SRI-E39), SRI receiving J65 (SRI-J65), nSRI receiving E39 (nSRI-E39), nSRI receiving J65 (nSRI-J65). Immunologic data was gathered at

1- and 6-months post-booster. This immunologic data was then analyzed.

#### **Results**

28 patients were randomized to booster arms (SRI-E39:n=9; SRI-J65:n=7; nSRI-E39:n=7; nSRI-J65:n=5). There were no clinicopathologic differences between groups. All related adverse events were grade 1-2. When comparing DTH pre-booster and at 1 and 6-months post-booster there were no significant differences between SRI vs nSRI ( $p=0.350$ ,  $p=0.276$ ,  $p=0.133$ , respectively), E39 vs. J65 ( $p=0.270$ ,  $p=0.329$ ,  $p=0.228$ ), nor between all four groups ( $p=0.394$ ,  $p=0.555$ ,  $p=0.191$ ). Comparing delta-CTL from pre- and 6-months post-booster, regardless of SRI, patients boosted with J65 had increased CTL (+0.02) while those boosted with E39 had decreased CTL (-0.07,  $p=0.077$ ). There was no difference comparing delta-DTH between groups ( $p=0.927$ ).

#### **Conclusions**

Both E39 and J65 are safe, well tolerated boosters. Though numbers were small, patients boosted with the attenuated peptide did appear to have increased CTL response to boosting regardless of SRI after the PVS. This is consistent with the theoretical advantage of boosting with an attenuated peptide, which has a maintained E39 specific immunity.

#### **Trial Registration**

ClinicalTrials.gov identifier NCT02019524.

**374**

### **Genome-scale neoantigen screening using ATLAS™ prioritizes candidates for immunotherapy in a non-small cell lung cancer patient**

*Lila Ghamsari*<sup>1</sup>, Emilio Flano<sup>1</sup>, Judy Jacques<sup>1</sup>, Biao Liu<sup>1</sup>, Jonathan Havel<sup>2</sup>, Vladimir Makarov<sup>2</sup>, Taha Merghoub<sup>3</sup>, Jedd D Wolchok<sup>4</sup>, Matthew D Hellmann<sup>4</sup>, Timothy A Chan<sup>2</sup>, Jessica B Flechtner<sup>1</sup>

<sup>1</sup>Genocea Biosciences, Cambridge, MA, USA

<sup>2</sup>Memorial Sloan Kettering Cancer Center, New York, NY, USA

<sup>3</sup>Ludwig Collaborative Laboratory, Memorial Sloan Kettering Cancer Center, New York, NY, USA

<sup>4</sup>Department of Medicine, Memorial Sloan Kettering Cancer Center, New York, NY, USA

#### **Background**

Despite the unprecedented efficacy of checkpoint inhibitor (CPI) therapy in treating some cancers, the majority of patients fail to respond. Several lines of evidence support that the mutational burden of the tumor influences the outcome of CPI therapies. Capitalizing on neoantigens derived from non-synonymous somatic mutations may be a good strategy for therapeutic immunization. Current approaches



## Therapeutic Cancer Vaccines

Presenting author underlined; *Primary author in italics*

to neoantigen prioritization involve mutanome sequencing, *in silico* epitope prediction algorithms, and experimental validation of cancer neoepitopes. We sought to circumvent some of the limitations of prediction algorithms by prioritizing neoantigens empirically using ATLAS™, a technology developed to screen T cell responses from any subject against their entire complement of potential neoantigens.

### Methods

Exome sequences were obtained from peripheral blood mononuclear cells (PBMC) and tumor biopsies from a non-small cell lung cancer patient who had been successfully treated with pembrolizumab. The tumor exome was sequenced and somatic mutations identified. Individual DNA sequences (399 nucleotides) spanning each mutation site were built, cloned and expressed in *E. coli* co-expressing listeriolysin O. Polypeptide expression was validated using a surrogate T cell assay or by Western blotting. Frozen PBMCs, collected pre- and post-therapy, were used to derive dendritic cells (MDDC), and CD8<sup>+</sup> T cells were enriched and expanded using microbeads. The *E. coli* clones were pulsed onto MDDC in an ordered array, then co-cultured with CD8<sup>+</sup> T cells overnight. T cell activation was detected by analyzing cytokines in supernatants. Antigens were identified as clones that induced a cytokine response that exceeded 3 standard deviations of the mean of ten negative controls, then their identities compared with T cell epitopes predicted using previously described algorithms.

### Results

Peripheral CD8<sup>+</sup> T cells, screened against 100 mutated polypeptides derived from the patient's tumor, were responsive to five neoantigens prior to CPI intervention and seven post-treatment. One was identified as a T cell target both pre- and post-CPI therapy. Five neoantigens did not contain epitopes predicted by *in silico* methods.

### Conclusions

These data represent evidence that multiple patient-specific neoantigens can be identified through functional evidence of T cell response from peripheral blood without epitope prediction. By profiling natural and CPI-enhanced immunity to neoantigens, a broad catalog of T cell targets can be identified for development of immunotherapies that engage T cells against cancer to improve outcomes for patients for whom current therapies are insufficient.

**375**

### Targeting tumor vasculature with a DNA vaccine against endosialin (TEM1 or CD248)

Pierini Stefano, *Andrea Facciabene*, John Facciponte, Stefano Ugel, Francesco De Sanctis, George Coukos

University of Pennsylvania, Philadelphia, PA, USA

### Background

Tumor endothelial marker 1 (TEM1; also known as endosialin or CD248) is a protein found on tumor vasculature and in tumor stroma.

### Methods

Here, we tested whether TEM1 has potential as a therapeutic target for cancer immunotherapy by immunizing immunocompetent mice with Tem1 cDNA fused to the minimal domain of the C fragment of tetanus toxoid (referred to herein as Tem1-TT vaccine).

### Results

Tem1-TT vaccination elicited CD8<sup>+</sup> and/or CD4<sup>+</sup> T cell responses against immunodominant TEM1 protein sequences. Prophylactic immunization of animals with Tem1-TT prevented or delayed tumor formation in several murine tumor models. Therapeutic vaccination of tumor-bearing mice reduced tumor vascularity, increased infiltration of CD3<sup>+</sup> T cells into the tumor, and controlled progression of established tumors. Tem1-TT vaccination also elicited CD8<sup>+</sup> cytotoxic T cell responses against murine tumor-specific antigens. Effective Tem1-TT vaccination did not affect angiogenesis-dependent physiological processes, including wound healing and reproduction.

### Conclusions

Based on these data and the widespread expression of TEM1 on the vasculature of different tumor types, we conclude that targeting TEM1 has therapeutic potential in cancer immunotherapy.

**376**

### Hafnium oxide nanoparticle, a radiation enhancer for in situ cancer vaccine

Sébastien Paris<sup>1</sup>, Agnes Pottier<sup>1</sup>, Laurent Levy<sup>1</sup>, Bo Lu<sup>2</sup>

<sup>1</sup>Nanobiotix, Paris, Ile-de-France, France

<sup>2</sup>Thomas Jefferson University, Philadelphia, PA, USA

### Background

Effective immunotherapy requires optimal combination of immunotherapeutic agents to build a robust immune response against cancer. In this framework, radiotherapy has proven its ability to induce immunogenic cell death (ICD), showing a promising potential for successful combination. Hafnium oxide (HfO<sub>2</sub>) nanoparticles, undergoing clinical trials for enhancing radiotherapy, was designed as high electron density material at the nanoscale to enhance the absorption of radiation delivered within tumors. The nanoparticles are taken up by cancer cells and, when exposed to radiotherapy, locally increase the radiation dose deposit, triggering more cancer cells death when compared to radiotherapy alone (Figure 1).



# Therapeutic Cancer Vaccines

Presenting author underlined; Primary author in italics

## Methods

Generation of ICD components – namely calreticulin (CALR) surface exposure, release of high mobility group box 1 (HMGB1) protein and liberation of adenosine-5'-triphosphate (ATP) – were examined on human cancer cell lines across human cancer types, 24- to 96-hrs post-treatment with HfO<sub>2</sub> nanoparticles and exposure to irradiation (from 4Gy to 15 Gy). CT 26 (murine colorectal cancer cells) treated with or without HfO<sub>2</sub> nanoparticles were exposed to irradiation (6Gy). Irradiated cells (1.10<sup>6</sup>) were inoculated subcutaneously into the flank of BALB/c mice (vaccination phase). Seven days after, mice were challenged with live CT 26 tumor cells (3.10<sup>5</sup>) (challenge phase). The host immune response against these cells was evaluated by the apparition of at least one tumor (vaccination or challenge site).

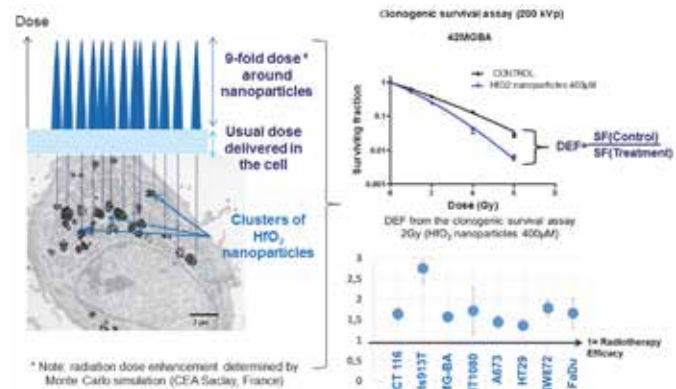
## Results

*In vitro*, human cancer cell lines treated with HfO<sub>2</sub> nanoparticles exposed to irradiation enhanced the quantity of ICD (more than 25%) when compared to irradiation alone. Interestingly, in tested human cell lines HCT116 (radiosensitive colorectal cancer) and 42MGBA (radioresistant glioblastoma), the generation of HMGB1 from cells treated with HfO<sub>2</sub> nanoparticles and exposed to 4Gy and 10Gy respectively, was superior to the generation of ICD from cells treated with 6Gy and 15Gy alone respectively. *In vivo*, the percentage of mice protected against live CT 26 challenge was markedly increased for mice vaccinated with cells treated with HfO<sub>2</sub> nanoparticles exposed to 6Gy versus 6Gy alone (66% vs 33% respectively).

## Conclusions

HfO<sub>2</sub> nanoparticles exposed to irradiation enhanced cancer cells destruction and ICD compared to irradiation alone, suggesting a strong potential for transforming tumor into an effective *in situ* vaccine. They may contribute to transform “cold” tumor into “hot” tumor and effectively be combined with most of the immunotherapeutic agents across oncology.

Figure 1.



HfO<sub>2</sub> nanoparticles: same mode of action than radiotherapy, but amplified.

## 377

### 5T4 oncofetal protein – an old antigen for a novel prostate cancer vaccine

*Federica Cappuccini*<sup>1</sup>, *Emily Pollock*<sup>1</sup>, *Richard Bryant*<sup>2</sup>, *Freddie Hamdy*<sup>2</sup>, *Adrian Hill*<sup>1</sup>, *Irina Redchenko*<sup>1</sup>

<sup>1</sup>The Jenner Institute/University of Oxford, Oxford, England, UK

<sup>2</sup>Nuffield Department of Surgical Sciences/University of Oxford, Oxford, England, UK

## Background

Prostate cancer is the cancer type for which the first therapeutic vaccine was approved by the FDA. Sipuleucel-T is a personalized cell based immunotherapy that costs \$93,000 per patient and prolongs life for 4.1 months. Another most clinically advanced prostate cancer vaccine, ProstVac-VF, is based on the two replication competent viral vectors, vaccinia and fowlpox. A global phase III trial of this vaccine has completed enrollment and the results are eagerly awaited by the scientific community. Both Sipuleucel-T and ProstVac-VF were shown to induce cellular immune responses but the responses were of relatively low magnitude, which could be an underlying cause of the modest clinical benefit.

## Methods

We set out to evaluate an alternative viral based vaccination approach as a novel prostate cancer immunotherapy. The scientific rationale for this endeavor has been underpinned by numerous studies conducted at the Jenner Institute research laboratories over the past decade. They have demonstrated that a prime boost vaccination regime based on two replication deficient viruses - the simian adenovirus and modified vaccinia Ankara virus, MVA, is the most potent

## Therapeutic Cancer Vaccines

Presenting author underlined; *Primary author in italics*

strategy for induction of strong, poly-functional, durable and protective cellular immune responses in infectious disease setting. To test this vaccination platform in cancer settings, simian adenovirus, ChAdOx1, and MVA were engineered to express 5T4 - the tumor-associated antigen that has been previously targeted clinically by homologous vaccinations in a number of tumor types including colorectal, renal and prostate cancer.

### Results

Following ChAdOx1.5T4-MVA.5T4 vaccination, the mice mounted strong T cell responses against 5T4 and were completely protected against subsequent tumor challenge with the syngeneic B16 melanoma cell line expressing 5T4. The vaccine was also protective in therapeutic settings delaying progression of already established tumors in vaccinated mice. The ChAd-MVA vaccination platform significantly outperformed 5T4 targeting homologous vaccinations previously tested by other researchers in terms of both immunogenicity and efficacy. Strikingly, a combination of ChAd-MVA vaccine with anti-PD-1 mAb resulted in 80% of mice remaining tumor-free while all the control animals succumbed to tumors in this highly aggressive cancer model.

### Conclusions

Our preclinical data have supported further clinical development of the novel prostate cancer vaccine. Recruitment is currently underway in the UK to test ChAdOx1.5T4-MVA.5T4 vaccination regime in a first-in-human “window” trial in low and intermediate risk prostate cancer patients. Preliminary immunogenicity and efficacy data are expected later on this year.

### Acknowledgements

This work was supported by the European Union’s Seventh Framework Programme under Grant Agreement No. 602705.

### Trial Registration

ClinicalTrials.gov identifier NCT02390063.

378

### Peptide vaccines/IL2 complex combination expands high quality endogenous T cell responses that eradicate tumors

Hussein Sultan, Takumi Kumai, Valentyna Fesenkova, Esteban Celis

Augusta University, Georgia Cancer Center, Augusta, GA, USA

### Background

Cancer vaccines, that generate tumor-reactive cytotoxic T lymphocyte (TR-CTL) responses are promising approach in cancer treatment. Unfortunately, most cancer vaccines induce suboptimal CTL responses (both in the quality and

quantity), which are not sufficient to eradicate established tumors. In contrast, CTL adoptive cell therapy (ACT) has shown in many instances great therapeutic success but this therapy is not cost effective and remains technically challenging. We hypothesize that expansion of high quality endogenous TR-CTLs using peptide vaccines will circumvent the technical difficulties of ACT and boost the antitumor efficacy in a cost effective manner.

### Methods

Our lab developed a novel vaccination strategy using peptides from tumor-associated antigens and poly-IC (BiVax), which showed promising antitumor effects [1]. Mice were injected with BiVax (120 µg of peptide and 50µg of Poly-IC) on day 0 and 12. Mouse IL-2cx<sub>CD25<sup>+</sup></sub>, IL-2cx<sub>CD122<sup>+</sup></sub>, or IL-2Fc (20 µg/mouse) was injected intraperitoneally on day 12, 14, and 16. In some mice, cytokines were injected on day 1 to 4.

### Results

In this study, we further improved the efficacy of BiVax by utilizing IL-2/anti-IL-2 antibody complexes (IL-2cx). The combination of BiVax with IL-2cx (BiVax<sub>IL-2cx</sub>) induced a robust amount of endogenous TR-CTLs (~40 million TR-CTLs/spleen) in a peptide dose-dependent manner. These cells were able to recognize tumor *in vitro* as shown by ELISPOT assay. Moreover, BiVax<sub>IL-2cx</sub>-expanded TR-CTLs were able to significantly delay B16F10 melanoma growth, enhance the survival of the tumor bearing mice, and eradicate tumors in 20% of mice. The timing for IL-2cx administration was critical, thus the activation of T cells by peptide vaccines before cytokine administration was crucial to expand the TR-CTLs.

### Conclusions

In conclusion, our data showed that peptide vaccines have the ability to expand huge number of TR-CTLs with good quality that able to control and in some instances eradicate aggressive tumors. Moreover, the adjuvant and its timing of administration are critical in expanding the TR-CTLs by peptide vaccines. Finally, our findings may pave the way for the development of promising immunologic approach for cancer treatment, which may circumvent lymphodepletion in ACT therapy and enhance the checkpoint blockade inhibitors treatment.

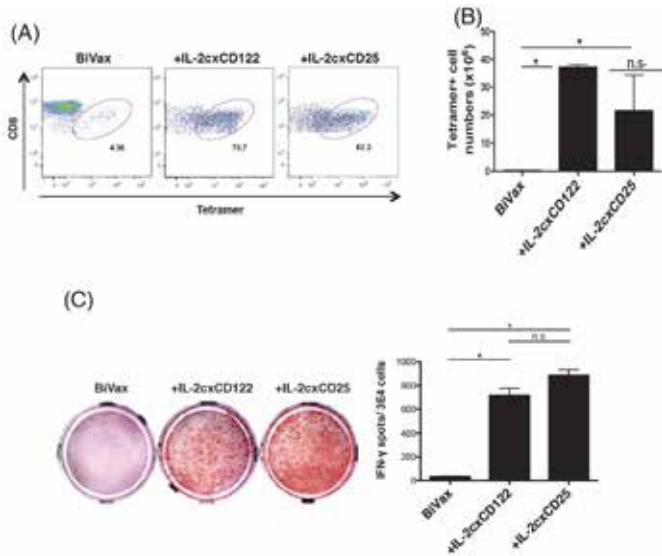
### References

1. Cho HI, Barrios K, Lee YR, Linowski AK, Celis E: **BiVax: a peptide/poly-IC subunit vaccine that mimics an acute infection elicits vast and effective anti-tumor CD8 T-cell responses.** *Cancer Immunol Immunother.* 2013, **62(4)**:787-799.

# Therapeutic Cancer Vaccines

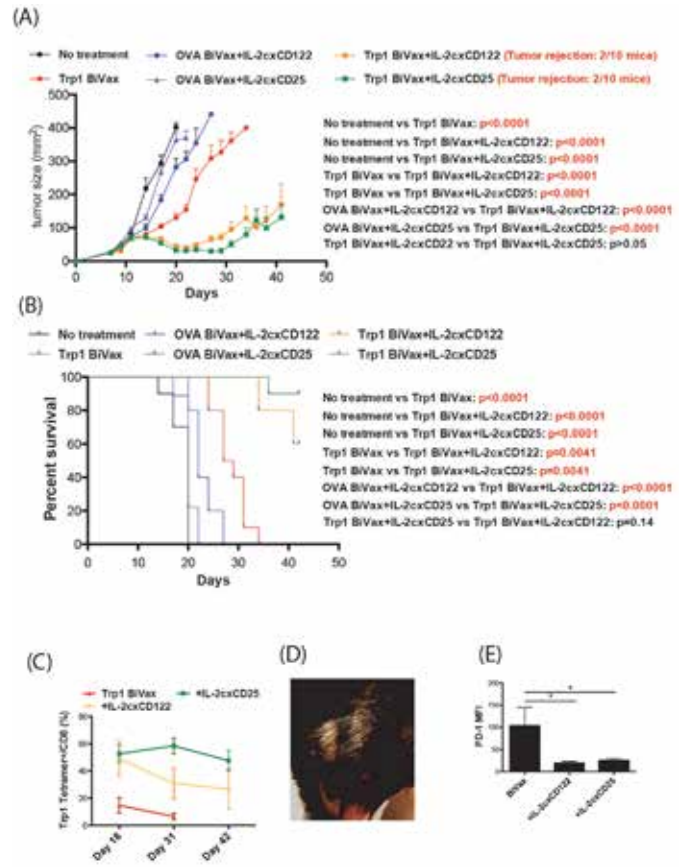
Presenting author underlined; Primary author in italics

**Figure 1.** The combination of BiVax with IL-2cx induced a robust amount of endogenous TR-CTLs



(A) C57BL/6 mice were immunized with BiVax on day 0 and 12. IL-2 complexCD122 or IL-2 complexCD25 was administered on day 12, 14, and 16 in the indicated group. The percentage of (TAPDNLGYM) Trp1-tetramer+ cells in blood CD8+ T cells was examined on day 19 (boost). Images of the representative results on day 19 are shown. (B) On day 19, the number of Trp1-tetramer+ cells in spleen was examined. (C) Purified CD8+ T cells from vaccinated mice were used in ELISpot assay. T cells were cultured with B16F10 melanoma cells for overnight. Results are presented as mean  $\pm$  SD. (\* $p < 0.05$ , n.s.: not significant)

**Figure 2.** The therapeutic effects of IL-2 complex with peptide vaccine.

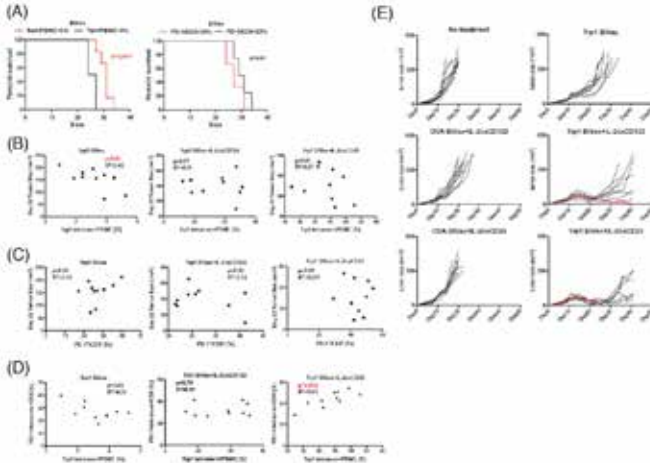


(A-E) C57BL/6 mice were inoculated with B16F10 melanoma cells ( $5 \times 10^5$  cells/mouse). After 7 days, mice received BiVax twice (day 7 and 12). IL-2 complexCD122 or IL-2 complexCD25 was administered on day 12, 14, and 16. (A) The mean sizes of tumor and (B) the overall survival of tumor-bearing mice are depicted. (C) The percentage of Trp1-tetramer+ cells in CD8+ T cells was examined on day 18 and 31. (D) The representative image of vitiligo at the tumor-inoculated lesion in the mouse, which received BiVax and IL-2 complexCD25 (day 30). (E) The expression of PD-1 on Trp1-tetramer+ CD8+ T cells was assessed on day 31. Results are presented as mean  $\pm$  SD. (\* $p < 0.05$ , n.s.: not significant)

**Therapeutic Cancer Vaccines**

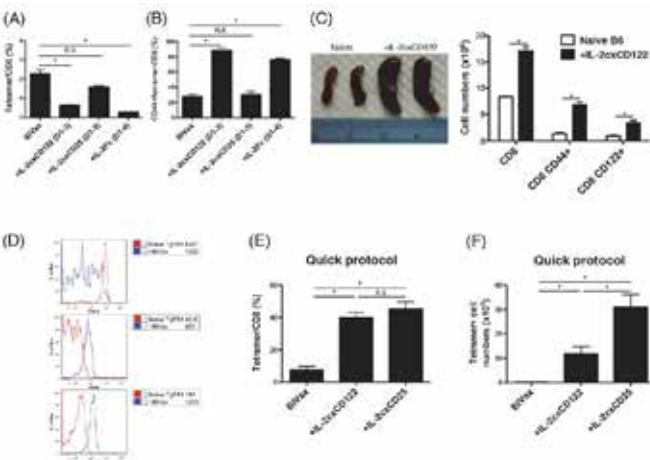
Presenting author underlined; Primary author in italics

**Figure 3. The antitumor effects of BiVax correlate with the percentage of Trp1-tetramer positive CD8+ T cells.**



C57BL/6 mice were inoculated with B16F10 melanoma cells ( $5 \times 10^5$  cells/mouse). After 7 days, mice received BiVax twice on day 7 and 12 and IL-2 complexCD122 or IL-2 complexCD25 was administered on day 12, 14, and 16. (A) The percentage survival of Trp1-BiVax-received mice. (B) The Pearson correlation analysis of the tumor size (day 22) and the percentage of Trp1-tetramer+ cells in PBMC. (C) The Pearson correlation analysis of the tumor size (day 22) and the percentage of PD-1+ cells in PBMC. (D) The Pearson correlation analysis of the percentage of Trp1-tetramer+ cells and the percentage of PD-1+ cells in PBMC. (E) The sizes of individual tumor are demonstrated.

**Figure 4. Proper timing of IL-2 complex administration is necessary to induce CD8+ T cell responses.**



(A) C57BL/6 mice were injected with BiVax on day 0 combined with IL-2 complexCD122 (day 1, 2, and 3), IL-2 complexCD25 (day 1, 2, and 3) or IL-2Fc (day 1 to 4). The percentage of tetramer+ cells in CD8+ T cell or (B) CD44+ T

cells in Trp1-tetramer- CD8+ T cells was examined in blood on day 7. (C) C57BL/6 mice received IL-2 complexCD122 on day 0, 2, and 4 and the number of CD44+ or CD122+ cells in spleen was examined on day 7. The picture of spleen after the treatment is shown. (D) C57BL/6 mice received TgTR1 cells (2000 cells/ mouse) and BiVax. After 7 days, the expression of blood CD62L, CD44, and CD122 on activated TgTR1 cells were compared to naïve TgTR1 cells. (E) C57BL/6 mice were injected with BiVax on day 0 and 5. IL-2 complexCD122 or IL-2 complexCD25 was administered on day 5, 7, and 9. The percentages of tetramer+ cells in blood CD8+ T cells and (F) the numbers of tetramer+ cells in spleen on day 12 are shown. Results are presented as mean  $\pm$  SD. (\* $p < 0.05$ , n.s.: not significant)

**379**

**Identification and characterization of agonist human cytotoxic T cell epitopes of the human papillomavirus type 16 (HPV-16) E6/E7**

*Kwong Tsang*<sup>1</sup>, Massimo Fantini<sup>1</sup>, Ingrid Fernando<sup>1</sup>, Claudia Palena<sup>1</sup>, Justin M David<sup>1</sup>, James Hodge<sup>1</sup>, Elizabeth Gabitzsch<sup>2</sup>, Frank Jones<sup>2</sup>, James L Gulley<sup>3</sup>, Jeffrey Schlom<sup>4</sup>

<sup>1</sup>Laboratory of Tumor Immunology and Biology, National Cancer Institute, National Institutes of Health, Bethesda, MD, USA

<sup>2</sup>Etubics Corporation, Seattle, WA, USA

<sup>3</sup>Genitourinary Malignancies Branch, Center for Cancer Research, National Cancer Institute, National Institutes of Health, Bethesda, MD, USA

<sup>4</sup>Center for Cancer Research, National Cancer Institute, National Institutes of Health, Bethesda, MD, USA

**Background**

Human papillomavirus (HPV) type 16 is associated with the etiology of cervical cancer, head and neck squamous cell carcinoma (HNSCC), and many other HPV-associated tumors. Current HPV-16 vaccines utilize viral coat proteins or virus-like particles with HPV-16 late gene products. Many HNSCC express early E6/E7 rather than late viral genes such as the viral coat proteins. Thus, vaccines that use late viral proteins may not be effective in treating established tumors. E6/E7, the early proteins of HPV-16, have a transforming capacity. They interfere with cell-cycle control of infected cells and are essential for maintaining the transformed state. An immune-based therapeutic vaccine that targets E6/E7 may prove more effective than a late viral protein vaccine. Identifying and characterizing MHC class I-restricted immunogenic peptides derived from E6/E7 proteins is essential for designing and developing vaccines to treat HPV-16-induced carcinomas, and for monitoring clinical trials and immunotherapeutic approaches for the treatment of these tumors.





## Therapeutic Cancer Vaccines

Presenting author underlined; *Primary author in italics*

### Methods

We report here the development of immunogenic HLA-A\*0201-restricted 9-mer epitopes and agonist epitopes of E6 and E7. We selected two E6- and one E7-derived peptide epitope and the corresponding agonist epitopes with high affinities for HLA-A\*0201 molecules. The immunogenicity of these six peptides was evaluated by their ability to activate T cell lines generated from human dendritic cells infected with the Ad5 [E1-, E2b-]-E6 Δ/E7Δ vector and normal human peripheral blood mononuclear cells (PBMC). The Ad5 [E1-, E2b-]-E6 Δ/E7Δ vector contains mutations that render E6/E7 nononcogenic, while preserving antigenicity.

### Results

Our results show that these peptide-pulsed dendritic cells, as well as Ad5 [E1-, E2b-]-E6 Δ/E7Δ vector-infected dendritic cells, can activate T cell lines generated from human dendritic cells infected with the Ad5 [E1-, E2b-]-E6 Δ/E7Δ vector. Compared to native peptides, the agonist peptides more efficiently (1) enhanced the production of IFN-γ by peptide-activated human T cells and (2) lysed human tumor cells expressing HPV in an MHC-restricted manner. These agonist peptides are highly immunogenic.

### Conclusions

These studies provide a rationale for the incorporation of these agonist epitopes into therapeutic vaccine platforms and for the *ex vivo* generation of HPV-specific human T cells.

**380**

### **Liposome-encapsulated doxorubicin is a promising adjuvant to increase the efficacy of mTERT DNA-vaccine**

Mireia Uribe Herranz, Stavros Rafail, Stefano Ugel, John Facciponte, Pierini Stefano, *Andrea Facciabene*

University of Pennsylvania, Philadelphia, PA, USA

### Background

Challenging the notion that chemotherapy negatively modulates the immune system of tumor-bearing hosts, recent evidence on the contrary indicates that some cytotoxic drugs control tumor growth in part by facilitating an anti-tumor immune response. The precise mechanism(s) that controls this phenomenon have not been elucidated. Chemotherapy, especially at low doses, may modify the host's immune system by either augmenting antigen-specific effector cells by rendering tumor cells immunogenic or eliminating immune-suppressive cell populations that limit the anti-tumor immune effect. Doxil (pegylated liposomal doxorubicin) possesses specific immunomodulatory properties such as inducing immunogenic tumor cell apoptosis.

### Methods

Mice were injected intraperitoneally (i.p.) with  $5 \times 10^6$  ID8 cells. For chemotherapeutic treatment, mice received a single i.p. injection of either 50 mg/m<sup>2</sup> of Doxil (doxorubicin HCl liposome injection) or 50 mg/m<sup>2</sup> of doxorubicin. DNA immunization (mTERT-LTB) was performed according to commonly used protocols: 50 micrograms of plasmid DNA was injected into mice quadriceps and then electroporation was carried out with a BTX electroporator intramuscularly at the injection site. For natural killer (NK) cell depletion, tumor-free and ID8 tumor-bearing mice were treated with anti-asialo GM1.

### Results

Here, we characterize how Doxil treatment is able to improve both the tumor-free and tumor-bearing host immune system by expanding NK cell populations after 5 days from the time of drug administration. Moreover, NK cells isolated from Doxil-treated mice produce greater amounts of interferon (IFN)-γ compared to isolated NK cells from untreated mice, promoting selective Th-1 polarization of naïve CD4+ T cells. These immune modifications mediated by chemotherapy ameliorates the capability of a DNA-vaccine to select and expand an antigen-specific CD8+ T cell population. This synergistic effect between chemotherapy and vaccination was completely mediated by NK cell expansion; in fact, the *in vivo* depletion of this cell subset totally abrogated the Doxil immune adjuvant activity. We combined Doxil with a DNA-vaccine encoding mouse telomerase reverse transcriptase (TERT).

### Conclusions

TERT is an attractive target antigen for cancer vaccine because its expression is reactivated in tumors of different histology such as ovarian cancer. We verified different vaccination schedules in ID8 ovarian tumor-bearing mice and only combinations that resulted in significant tumor growth inhibition were related to a specific anti-TERT CD8+ T cell response. This data demonstrates "chemo-immune adjuvancy" of a conventional drug and highlights the importance to define the precise time window between treatments to improve their therapeutic synergism.

**381**

### **Efficient design method for pan-HLA multi-valent cancer vaccine**

Hiroshi Wada, Atsushi Shimizu, Toshihiro Osada, Satoshi Fukaya, Eiji Sasaki

Taiho Pharmaceutical Co., Ltd, Tsukuba, Ibaraki, Japan

### Background

Recently, a lot of tumor antigen peptides are examined for clinical applications. The treatment strategy using multiple



## Therapeutic Cancer Vaccines

*Presenting author underlined; Primary author in italics*

peptides is expected to achieve better outcomes than single peptide treatment in terms of HLA restriction. In addition, many advantages administering the synthetic long peptides (SLPs) are reported. Based on this information, and aiming for improvement of popularity coverage, we planned to design SLP vaccines containing multiple cytotoxic T lymphocyte (CTL) epitopes which are restricted HLA-A2, A24, A3 supertype, respectively. However, there are few screening strategies to confirm whether designed SLP vaccines could induce all epitopes specific-CTLs in humans except confirmations using human PBMCs or expensive HLA-expressing mice. In order to improve this issue, we performed the following screening procedures.

### Methods

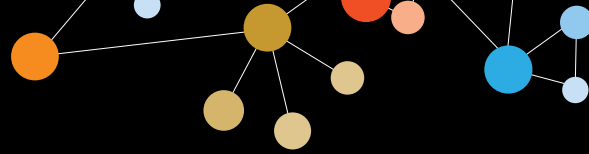
Murine-immunoproteasome digestion assay was conducted as follows. Briefly, SLPs were dissolved with buffer and incubated with murine i20s immunoproteasome for 1h, 2h and 4h. Then, digested peptides were separated using an UPLC system, and the eluent was analyzed by mass spectrometry. The sequences of the digested peptides were assigned based on the results of their m/z. Finally, the “digestion maps” were drawn by rearranging digested peptides fragments from N-terminal. In order to compare the digestion maps to the peptide specific CTL induction, the SLPs were administered to HLA-A knock-in mice and the CTL induction was analyzed using IFN- $\gamma$  ELISPOT assay.

### Results

We applied 4 SLPs to the murine-immunoproteasome digestion assay. Immunoproteasomal degradations were observed in all SLPs and they were time-dependent. In this study, we focused on the generations of intact epitopes, Arg added epitopes, and Arg-Arg added epitopes to the N-terminus at any time points because proteasomal digestion of exact C-terminus of CTL epitope is known to be an essential process for the antigen presentation. Regarding this criteria, 8 epitopes were determined as a “living epitope,” which would be able to induce specific CTLs, but 4 epitopes were determined as a “dead epitope”. Compared with the IFN- $\gamma$  ELISPOT assay, the results of murine-immunoproteasome digestion assay were substantially matched the results of CTL induction (11 of 12 epitopes: 91.7%).

### Conclusions

Murine-immunoproteasome digestion assay could predict the CTL induction with a high degree of accuracy. We concluded that murine-immunoproteasome digestion assay strategy could be a prognostic approach for IFN- $\gamma$  ELISPOT assay using an HLA-expressing mice model. In addition, our results suggested that the positions of each epitope peptide are important for the design of SLP vaccines. Murine-immunoproteasome digestion assay is very useful to develop “suitable” multi-valent SLP vaccines.



## Tumor Microenvironment

Presenting author underlined; Primary author in italics

382

WITHDRAWN

383

### **IL-10 blockade sensitizes ovarian cancer to anti-PD-1 antibody therapy by editing tumor-associated leukocyte populations**

*Dallas B Flies*<sup>1</sup>, Tomoe Higuchi<sup>2</sup>, Wojciech Ornatowski<sup>3</sup>, Jaryse Harris<sup>4</sup>, Sarah F Adams<sup>3</sup>

<sup>1</sup>NextCure, Beltsville, MD, USA

<sup>2</sup>University of New Mexico Comprehensive Cancer Center, Beltsville, MD, USA

<sup>3</sup>University of New Mexico Comprehensive Cancer Center, Albuquerque, NM, USA

<sup>4</sup>University of New Mexico, Albuquerque, NM, USA

#### Background

Our recent results demonstrate that the ovarian tumor environment is characterized by local T cell exhaustion and high levels of immunosuppressive cytokines, including interleukin (IL)-10 [1]. We hypothesized that IL-10 blockade would synergize with immune checkpoint antibodies to promote tumor clearance in ovarian cancer.

#### Methods

Dendritic cells (DC) in mice treated with 300ug of an IL-10 receptor antibody (IL-10Rab) were analyzed in two murine tumor models [2, 3]. In the implantable ID8ova model, mice were treated 7 and 14 days after tumor challenge; MISIIRTag mice were treated at 14 weeks of age. Immune checkpoint antibody treatment was evaluated in wildtype or IL10-knockout (IL10KO) mice treated with 500ug of anti-PD-1 antibody on days 17 and 21 after ID8ova tumor challenge (n=5/group). Survival was measured from tumor challenge until mice reached 30g due to ascites accumulation.

#### Results

In both models, IL-10Rab treatment increased stimulatory CD103+ DC (18% to 30% in ID8ova; 5% to 45% in MISIIRTag), and decreased suppressive Lair1+ DC in the peritoneal tumor environment and in primary ovarian tumors [1]. This was associated with an increase in CD8+ T cells and a decrease in regulatory FoxP3+ CD4+ T cells (45% to 30%). The proportion of CD4+ and CD8+ T cells producing interferon-gamma also increased (12% to 28%). Long-term survival was observed in 100% of IL10KO mice treated with PD-1 antibody but treatment did not improve survival in wild-type controls.

#### Conclusions

These results demonstrate an enrichment of stimulatory CD103+ DC in the tumor microenvironment with IL-10R blockade, associated with evidence of increased T cell effector capacity and a reduction in suppressive Treg. This

was associated with a significant survival benefit in IL10KO mice receiving anti-PD-1 antibody. These data support combining IL-10Rab with immune checkpoint antibodies for the treatment of ovarian cancer.

#### References

1. Flies DB, Higuchi T, Harris JC, Jha V, Gimotty PA, Adams SF: **Immune checkpoint blockade reveals the stimulatory capacity of tumor-associated CD103+ dendritic cells in late-stage ovarian cancer.** *Oncoimmunology* In press: <http://www.tandfonline.com/doi/full/10.1080/2162402X.2016.1185583>.

2. Roby KF, Taylor CC, Sweetwood JP, Cheng Y, Pace JL, Tawfik O, *et al*: **Development of a syngeneic mouse model for events related to ovarian cancer.** *Carcinogenesis* 2000, **21**:585-591.

3. Connolly DC, Bao R, Nikitin AY, Stephens KC, Poole TW, Hua X, *et al*: **Female mice chimeric for expression of the simian virus 40 TAG under control of the MISIIR promoter develop epithelial ovarian cancer.** *Cancer Res* 2003, **63**:1389-1397.

384

### **Axl tyrosine kinase is a key mediator of immunologic resistance after radiation therapy**

*Todd Aquilera*<sup>1</sup>, Marjan Rafat<sup>1</sup>, Laura Castellini<sup>1</sup>, Hussein Shehade<sup>1</sup>, Mihalis Kariolis<sup>1</sup>, Dadi Jang<sup>1</sup>, Rie vonEbyen<sup>1</sup>, Edward Graves<sup>1</sup>, Lesley Ellies<sup>2</sup>, Erinn Rankin<sup>1</sup>, Albert Koong<sup>1</sup>, Amato Giaccia<sup>1</sup>

<sup>1</sup>Stanford Department of Radiation Oncology, Stanford University School of Medicine, Stanford, CA, USA

<sup>2</sup>Department of Pathology, University of California, San Diego, La Jolla, CA, USA

#### Background

Hypofractionated high dose ionizing radiation (RT) can enhance antitumor immune responses in many cancers. In some cases the combination of RT and checkpoint immunotherapy suppress adaptive resistance leading to a greater immunologic effect. However, many tumors are unresponsive to the combination making it important to understand factors that render tumors immunologically inactive. We previously described immunologically responsive (Py117) and unresponsive (Py8119) syngeneic tumors from the PyMT mammary carcinoma model and used these tumors to determine new targets to reverse T cell exclusion.

#### Methods

A reverse phase protein array was used to study differences between the Py117 and Py8119 tumors. The CRISPR/Cas9 technology was used to knockout Axl, a TAM family tyrosine kinase. We confirmed signal abrogation with the loss of Axl through western blot, measured the intrinsic radiosensitivity

## Tumor Microenvironment

Presenting author underlined; Primary author in italics

by clonogenic survival, determined cellular proliferation, evaluated growth in 3D tissue culture, implanted tumors to determine radiosensitivity in mice, and evaluated the response in immunodeficient mice. Given the presence of an immunologic phenotype we measured the impact of Axl on antigen presentation and cytokine production. Lastly, we defined the antitumor immune response by dissociating tumors then immunophenotyping infiltrates, evaluating T cell function, and tumor cell responses. Lastly, we combined radiation, PD-1, and CTLA-4 therapy to demonstrate that loss of Axl sensitizes tumors to immunotherapy.

### Results

Through a RPPA, we identified differences in Axl expression a protein associated with the epithelial to mesenchymal transition (EMT). Then we knocked out Axl, which revealed no changes in proliferation or intrinsic radiosensitivity but altered the EMT phenotype, resulted in greater tumor latency and enhanced radiosensitivity after 20 Gy in mice. Key features of the Axl knockouts were enhanced MHC1 expression and decreased myeloid promoting cytokines and chemokines. The radiation response was decreased in mice carrying Axl knockout tumors suggesting the importance of the immune response. Profiling the tumor microenvironment revealed greater immune infiltrates in Axl knockout tumors and greater CD8+ T cells at baseline. Ten days after radiation there was increased CD8 and CD4+ T cells and decreased macrophages. T cells remained functional but adaptive immune resistance was supported by increased PD-L1 and FoxP3+ T regs in Axl deficient tumors. We hypothesized and confirmed that a greater radiation response was obtained with PD-1 and CTLA-4 inhibition in Axl deficient tumors.

### Conclusions

These data suggest that Axl may not only mediate invasion and metastasis but can influence immunosurveillance and response to therapy by suppressing an antitumor immune response.

385

### Impact of immune selection pressure on epithelial cell signaling pathway activation in a syngeneic pancreatic cancer model

Reham Ajina<sup>1</sup>, Shangzi Wang<sup>1</sup>, Jill Smith<sup>1</sup>, Mariaelena Pierobon<sup>1</sup>, Sandra Jablonski<sup>1</sup>, Emanuel Petricoin III<sup>2</sup>, Louis M Weiner<sup>1</sup>

<sup>1</sup>Georgetown Lombardi Comprehensive Cancer Center, Washington, DC, USA

<sup>2</sup>George Mason University, Manassas, VA, USA

### Background

Pancreatic ductal adenocarcinoma (PDAC) is the fourth leading cause of cancer death in the United States [1].

PDAC is characterized by oncogenic *KRAS* mutations and resistance to chemotherapy and immunotherapy [2]. Epidermal growth factor receptor (EGFR) is required for *KRAS*-induced pancreatic tumorigenesis [3]. Although EGFR network activation represents a possible therapy target in PDAC, the anti-EGFR small molecule erlotinib has minimal therapeutic activity [4]. Accumulating evidence suggests that the immune system plays an important but complex role in the development and progression of PDAC [2]. Accordingly, we explored the effect of immune selection pressure on EGFR and related signaling pathways using syngeneic Panc02 pancreatic cancer models.

### Methods

1 X10<sup>6</sup> Panc02 cells were injected subcutaneously in immunocompetent B6.CB17 (WT) and immunodeficient B6.CB17-Prkdc<sup>scid</sup>/SzJ (SCID) mice (16mice/group). One cm<sup>3</sup> tumors were harvested and processed for reverse phase protein array (RPPA) of 125 proteins (18 total proteins, 107 phosphorylated species) to evaluate protein signaling networks. Due to tumor invasiveness it was not possible to perform laser capture microdissection on the specimens. Statistical analysis included Wilcoxon test, Student's t-test and principal component analysis (PCA) to identify significant hits. Pathways Studio was then used to identify selectively activated signaling pathways.

### Results

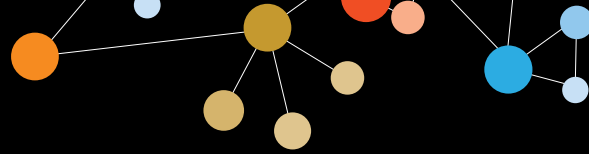
As expected, Panc02 tumors grow more slowly in immunocompetent as opposed to syngeneic immunodeficient mice. Interestingly, PCA of the RPPA data demonstrated a significant difference in cellular protein activity between Panc02 tumors engrafted in the two groups of mice. 32.8% (41/125) of proteins tested by RPPA were statistically significantly activated in immunocompetent mice as opposed to immunodeficient mice. Pathway analysis of these activated hits revealed selective activation of EGFR, ERK/MAPK, JAK/STAT, AMPK and TGFβ/Smad signaling pathways in immunocompetent mice.

### Conclusions

Immune selection pressure in syngeneic Panc02 pancreatic cancer models selectively activates multiple, related signaling pathways. These observations lay important groundwork for understanding and therapeutically exploiting the interplay of host immunity and tumor cell signaling.

### References

1. Siegel RL, Miller KD, Jemal A: **Cancer statistics, 2016**. *CA Cancer J Clin* 2016, **66(1)**:7–30.
2. Brunet LR, Hagemann T, Andrew G, Mudan S, Marabelle A: **Have lessons from past failures brought us closer to the success of immunotherapy in metastatic pancreatic cancer?** *Oncoimmunology* 2016, **5(4)**:e1112942.



## Tumor Microenvironment

*Presenting author underlined; Primary author in italics*

3. Ardito CM, Grüner BM, Takeuchi KK, Lubeseder-Martellato C, Teichmann N, Mazur PK, *et al*: **EGF receptor is required for KRAS-induced pancreatic tumorigenesis.** *Cancer Cell* 2012, **22(3)**:304–317.

4. Kelley RK, Ko AH: **Erlotinib in the treatment of advanced pancreatic cancer.** *Biologics* 2008, **2(1)**:83–95.

**386**

### **Immune cell spatial analysis on FoxP3 and CD8 positive IHC stained T cells within the tumor microenvironment**

Lozcan Sherry, John Waller, Mark Anderson, Alison Bigley

OracleBio, Newhouse, Scotland, UK

#### **Background**

The presence of T cells in the tumor microenvironment and their potential impact on prognosis has been investigated over many years. One implication has been that the presence of CD8 (cytotoxic T cell marker), as well as a high CD8/FoxP3 ratio, indicates a positive effect on patient survival. The forkhead box p3 (FoxP3) regulatory T cell (Tregs) marker has been utilized to investigate how Tregs function in suppressing immune response, in particular their influence on other T cells [1]. Therefore, understanding suppressive mechanisms and interactions between T cell subsets, by exploring spatial interactions, will inevitably provide evidence in support of the development of drugs for effective control of immune responses via Tregs. Using recent developments in histology image analysis techniques, we aimed to quantify CD8 and FoxP3 immune cell relationships in terms of cell infiltrations and cell-cell proximities within the tumor tissue microenvironment.

#### **Methods**

Tumor tissue was immunohistochemically (IHC) dual labelled for FoxP3 (brown nuclear chromogen) and CD8 (red membrane chromogen). Image analysis was performed within manually annotated regions of interest (ROI) using Indica Labs Halo™ software. Cellular analysis settings and thresholds were established to identify and count FoxP3, CD8, and dual labelled cells. 50µm margin bands were generated around interface ROI into the active stroma region and out to tumor regions. Application of spatial analysis was performed using cytonuclear analyzed object data outputs to quantify infiltration analysis (number of cells per 50µm margin band around defined interfaces) and proximity analysis (measure distances between defined cell populations within <50µm range, using 5µm bins).

#### **Results**

Tumor/stroma interface quantification indicated higher FoxP3 to CD8 ratios 100µm inside the tumor boundary when compared to adjacent active stromal regions, 100µm outside

the tumor. This difference in cell number was also reflected in cell proximity values with shorter FoxP3 to CD8 cell distances in the stroma compared to tumor.

#### **Conclusions**

These example data highlight the benefits of utilizing tissue-based whole slide image analysis to characterize therapeutic activity using spatial correlations within the tumor microenvironment, which provides distinct advantages over flow cytometry-based approaches where critical information on spatial cellular context is lost.

#### **References**

1. Sakaguchi S, Wing K, Onishi Y, Prieto-Martin P and Yamaguchi: **Regulatory T cells: how do they suppress immune responses?** *Int Immunol* 2009, **21(10)**:1105-1111.

**387**

### **A CD122-biased agonist increases CD8+T Cells and natural killer cells in the tumor microenvironment; making cold tumors hot with NKTR-214**

*Chantale Bernatchez*<sup>1</sup>, Cara Haymaker<sup>1</sup>, Nizar M Tannir<sup>1</sup>, Harriet Kluger<sup>2</sup>, Michael Tetzlaff<sup>1</sup>, Natalie Jackson<sup>1</sup>, Ivan Gergel<sup>3</sup>, Mary Tagliaferri<sup>3</sup>, Jonathan Zalevsky<sup>3</sup>, Ute Hoch<sup>3</sup>, Patrick Hwu<sup>1</sup>, Mario Snzol<sup>2</sup>, Michael Hurwitz<sup>2</sup>, Adi Diab<sup>1</sup>

<sup>1</sup>University of Texas MD Anderson Cancer Center, Houston, TX, USA

<sup>2</sup>Yale Medical Oncology, New Haven, CT, USA

<sup>3</sup>Nektar Therapeutics, San Francisco, CA, USA

#### **Background**

Abundance and functional quality of tumor-infiltrating lymphocytes are positively linked with tumor response and improved survival with checkpoint inhibitors. NKTR-214 provides sustained activation of the IL-2 pathway through controlled release of active CD122-biased (IL-2Rβγ) cytokines. Preclinical models demonstrated NKTR-214 preferentially expands effector CD8+T cells and NK cells within the tumor resulting in marked tumor growth suppression as single-agent and in combination with checkpoint inhibitors. A phase I/II trial was initiated to evaluate NKTR-214 safety and efficacy and to assess immune changes in the tumor microenvironment.

#### **Methods**

This is an ongoing dose-escalation and dose-expansion study of NKTR-214 in patients with locally advanced or metastatic solid tumors with a standard 3+3 design. Extensive blood and tumor tissue samples have been collected to measure immune activation using immunophenotyping including flow cytometry, immunohistochemistry (IHC), T cell clonality and gene expression analyses. Safety, pharmacokinetics and preliminary anti-tumor activity of NKTR-214 are being

## Tumor Microenvironment

Presenting author underlined; *Primary author in italics*

evaluated. NKTR-214 is administered IV q2-q3 weeks in an outpatient setting with initial dosing at 0.003 mg/kg.

### Results

As of August 2, 2016, 18 patients who received prior standard of care were enrolled (RCC [n=12], MEL [n=4], CRC [n=1]; UBC [n=1]). 7/12 (58%) patients had stable disease at initial 6 or 8-week scan with 9 patients still on treatment. Outpatient treatment with NKTR-214 was well tolerated and the MTD has not been reached. One patient experienced DLTs (Grade 3 syncope and hypotension) at 0.012 mg/kg. No immune-related AEs or capillary leak syndrome were observed at any dose. No drug-related AEs led to study discontinuation. 9/18 patients had serial tumor biopsies (pre and post-dose) evaluable. In 6/9 patients, flow cytometry enumeration and/or IHC revealed an up to 10-fold increase from baseline in CD8+T cells and NK cells in the tumor microenvironment, with minimal changes to Tregs. Most of the infiltrating CD8+T cells were newly proliferative (Ki67+) and cell-surface PD-1 expression was increased up to 2-fold. Analyses of blood samples showed concordant increases in Ki67+ immune cells, PD-1+ CD8+T cells, and NK cells 8 days after a single dose of NKTR-214. The study continues to enroll patients.

### Conclusions

NKTR-214 results in substantial increases in both CD8+T cells and NK cells in the tumor microenvironment with a favorable outpatient safety profile. These data support continued evaluation of NKTR-214 and the potential advantages of combining NKTR-214 with a variety of immunotherapeutic agents including checkpoint inhibitors. Updated data will be presented.

### Trial Registration

ClinicalTrials.gov identifier NCT02869295.

388

### NF- $\kappa$ B p50 promotes the suppressive M2 phenotype of tumor-associated macrophages in a mouse model of glioma

Theresa Barberi, Allison Martin, Rahul Suresh, David Barakat, Sarah Harris-Bookman, Charles Drake, Alan Friedman

Johns Hopkins University, Baltimore, MD, USA

### Background

Glioblastoma multiforme (GBM) brain tumors are nearly uniformly fatal. The GBM microenvironment includes abundant tumor-associated macrophages (TAMs) that predominantly assume a pro-tumor "M2" phenotype rather than a pro-inflammatory "M1" phenotype. The inhibitory p50 subunit of the NF- $\kappa$ B transcription factor exhibits markedly increased nuclear expression in TAMs and M2-polarized macrophages, and p50 knockdown/deletion suppresses

expression of M2-associated factors [1, 2]. We hypothesize that absence of p50 will convert TAMs to an M1 phenotype that will reduce glioma growth and prolong survival.

### Methods

GL261-Luc cells were intracranially implanted into mice. Tumor growth was monitored by IVIS imaging. Brains were removed 13-16 days after implantation for flow cytometry (FC) or RT-qPCR analysis. Depleting antibodies were administered by i.p. injection; clodronate by tail vein injection. Naïve T cells were enriched from spleens, skewed *in vitro* with cytokines and blocking antibodies, expanded in IL-2, then stimulated with PMA/ionomycin. Cells were assessed for Th or Tc1 skewing by FC or ELISA.

### Results

p50(-/-) mice exhibit significantly slower GL261-Luc tumor growth and prolonged survival. p50(-/-) tumor CD11b+ myeloid cells express increased M1-associated and decreased M2-associated mRNAs relative to WT mice. FC indicates glioma-bearing p50(-/-) brains contain fewer TAMs expressing the M2 marker CD206/MRC1, as well as fewer Tregs, increased IFN $\gamma$ -producing CD4+ T cells, and increased granzyme B+ CD8+ T cells. Transplant of p50(-/-) bone marrow into lethally-irradiated WT recipients confers a significant survival advantage upon tumor inoculation. Clodronate-mediated macrophage depletion decreases survival of tumor-bearing p50(-/-) mice but has no effect on WT mice. Depletion of CD4+ T cells markedly reduces survival in tumor-bearing p50(-/-) mice whereas depletion of CD8+ T cells has no effect. We observe no intrinsic defect in the ability of p50(-/-) naïve splenic CD4+ T cells to differentiate into Tregs, Th1, Th17, or Th2 subsets; however, p50(-/-) naïve splenic CD8+ T cells exhibit enhanced ability to produce IFN $\gamma$ , TNF $\alpha$ , and granzyme B.

### Conclusions

NF- $\kappa$ B p50 is an important modulator of the suppressive immune phenotype in GBM. Both TAM and T cells are more activated and less tumor-permissive when p50 is absent. Targeted deletion of p50 from TAMs and/or T cells may serve as a viable therapeutic for patients with GBM.

### References

1. Sacconi A, *et al*: **p50 nuclear factor- $\kappa$ B overexpression in tumor-associated macrophages inhibits M1 inflammatory responses and antitumor resistance**. *Cancer Res* 2006, **66(23)**:11432-11440.
2. Porta C, *et al*: **Tolerance and M2 (alternative) macrophage polarization are related processes orchestrated by p50 nuclear factor  $\kappa$ B**. *Proc Natl Acad Sci* 2009, **106(35)**:14978-14983.





## Tumor Microenvironment

Presenting author underlined; Primary author in italics

389

### The differentiation of Th17-into-Treg cells in the tumor microenvironment reveals novel targets in cancer immunotherapy

Sara Berkey<sup>1</sup>, Stephanie Downs-Canner<sup>1</sup>, Greg M DelGoffe<sup>2</sup>, Robert P Edwards<sup>2</sup>, Tyler Curiel<sup>3</sup>, Kunle Odunsi<sup>4</sup>, David Bartlett<sup>1</sup>, *Nataša Obermajer*<sup>1</sup>

<sup>1</sup>Department of Surgery, University of Pittsburgh, Pittsburgh, PA, USA

<sup>2</sup>University of Pittsburgh, Pittsburgh, PA, USA

<sup>3</sup>University of Texas Health Science Center at San Antonio, San Antonio, TX, USA

<sup>4</sup>Roswell Park Cancer Institute, Buffalo, NY, USA

#### Background

Th17 and regulatory T (T<sub>reg</sub>) cells are integral in maintaining immune homeostasis and the Th17-T<sub>reg</sub> balance is associated with the inflammatory immunosuppression observed in cancer. Expansion of T<sub>reg</sub> cells within the tumor is a known barrier to successful cancer immunotherapy. Because of this, T<sub>reg</sub> cell regulation has become a popular interest for new therapeutic modalities. However, current approaches designed to deplete T<sub>reg</sub> cells are only variably effective and urge for novel strategies to specifically target the suppressive function of intratumoral T<sub>reg</sub> cells.

#### Methods

We have used IL17 (*Il17a*<sup>Cre</sup>*Rosa26*<sup>eYFP</sup>) and T<sub>reg</sub> (B6.129(Cg)-*Foxp3*<sup>tm3(DTR/GFP)Ayr</sup>) reporter mice to study Th17 cell plasticity and Th17-into-T<sub>reg</sub> cell transdifferentiation as a novel tumor-associated phenomenon supporting immunosuppressive microenvironment in tumor-bearing mice.

#### Results

We demonstrate that in addition to natural (n)T<sub>reg</sub> and induced (i)T<sub>reg</sub> cells developed from naïve precursors, Th17 cells are a novel source of tumor-induced forkhead box P3 (Foxp3<sup>+</sup>) cells by progressive direct conversion into immunosuppressive IL17A<sup>+</sup>Foxp3<sup>+</sup> and ex-Th17 Foxp3<sup>+</sup> cells. Transcriptome analysis of the Th17-T<sub>reg</sub> plastic subsets reveals upregulation of 119 genes in the IL17A<sup>+</sup>Foxp3<sup>+</sup> cells compared to IL17A<sup>+</sup>Foxp3<sup>neg</sup> Th17 cells (Th17-T<sub>reg</sub> plasticity markers). Seven of these plasticity markers identified by transcriptome analysis were confirmed by flow cytometry of plastic IL17<sup>+</sup>Foxp3<sup>+</sup> cells. The immunometabolism of the plastic IL17A<sup>+</sup>Foxp3<sup>+</sup> subset revealed an additional level of complexity in controlling the immune function of CD4<sup>+</sup> T cells and to modulate (trans) differentiation of Th cells, which thereby control their ultimate function and role in diverse environments.

#### Conclusions

Tumor-associated Th17-into-Foxp3<sup>+</sup> T cell transdifferentiation helps to reconcile the contradictory observations about

the role of Th17 cells in tumor immune surveillance, and demonstrates an alternative source for IL17<sup>+</sup>Foxp3<sup>+</sup> and IL17<sup>neg</sup>Foxp3<sup>+</sup> T cells in tumors. Further, this newly identified tumor-associated phenomenon warrants strategies to manipulate the Th17-T<sub>reg</sub> cell plasticity in cancer and identifies novel IL17/T<sub>reg</sub>-associated targets that might be amenable for therapeutic interventions to enhance antitumor immunity.

### 390 Abstract Travel Award Recipient

#### Antigen-presenting tumor B cells associate with the phenotype of CD4+ tumor infiltrating T cells in non-small cell lung cancer patients

Tullia C Bruno<sup>1</sup>, Brandon Moore<sup>2</sup>, Olivia Squalls<sup>2</sup>, Peggy Ebner<sup>2</sup>, Katherine Waugh<sup>2</sup>, John Mitchell<sup>3</sup>, Wilbur Franklin<sup>4</sup>, Daniel Merrick<sup>4</sup>, Martin McCarter<sup>5</sup>, Brent Palmer<sup>6</sup>, Jeffrey Kern<sup>7</sup>, Dario Vignali<sup>8</sup>, Jill Slansky<sup>2</sup>

<sup>1</sup>Department of Immunology, University of Pittsburgh, Pittsburgh, PA, USA

<sup>2</sup>Department of Immunology and Microbiology, University of Colorado, Aurora, CO, USA

<sup>3</sup>Department of Cardiothoracic Surgery, University of Colorado, Aurora, CO, USA

<sup>4</sup>Department of Pathology, University of Colorado, Aurora, CO, USA

<sup>5</sup>Department of Surgery, University of Colorado, Aurora, CO, USA

<sup>6</sup>Department of Medicine, University of Colorado, Aurora, CO, USA

<sup>7</sup>National Jewish Health, Denver, CO, USA

<sup>8</sup>University of Pittsburgh, Pittsburgh, PA, USA

#### Background

Despite improvements in surgical techniques and combined chemo- and immunotherapies, the 5-year survival rate for all stages of non-small cell lung cancer (NSCLC) is only 18%. The focus of immunotherapy has been on subsets of CD8<sup>+</sup> and CD4<sup>+</sup> tumor infiltrating lymphocytes (TILs). However, tumor infiltrating B cells (TIL-Bs) have been reported in tertiary lymphoid structures (TLS) with CD4<sup>+</sup> TILs, both positively correlating with patient survival. TIL-B function in the tumor microenvironment (TME) has been understudied with no focus on their role as antigen presenting cells (APCs). We hypothesized that TIL-Bs help generate potent, long-term immune responses against cancer by presenting tumor antigens to CD4<sup>+</sup> TILs.

#### Methods

All studies were completed on freshly collected, un-manipulated primary human B cells from tumor and tumor adjacent lung tissue. We analyzed the number and phenotype of TIL-Bs via flow cytometry and

## Tumor Microenvironment

Presenting author underlined; *Primary author in italics*

immunofluorescence. We generated a specific antigen presentation assay *in vitro* to assay APC function.

### Results

We observed that the total number of B cells at the site of the tumor versus the tumor-adjacent tissue was increased compared to other immune subsets. Further, we found three types of CD4+ TIL responses when TIL-Bs presented autologous tumor antigens. There were activated responder CD4+ TILs that proliferated when combined with TIL-Bs alone, which indicates stimulation with endogenous tumor antigens. There were antigen-associated responders that required exogenous autologous tumor lysate to elicit a CD4+ TIL response, and there were patient CD4+ TILs that did not respond to antigen presentation by TIL-Bs. Within the activated and antigen-associated responders, the TIL-B phenotype associated with the CD4+ TIL phenotype; if the TIL-Bs were activated (CD69+CD27+CD21+), the CD4+ TILs were T helper (anti-tumor) CD4+ T cells and if the TIL-Bs were exhausted (CD69-CD27-CD21-), the CD4+ TILs were T regulatory cells (pro-tumor). These data suggest that TIL-Bs affect the phenotype and function of CD4+ TILs in NSCLC patient tumors.

### Conclusions

In conclusion, TIL-Bs are increased in NSCLC primary tumors and they can present antigen to and associate with CD4+ TILs in the tumor microenvironment. Determining if TIL-Bs are activated or exhausted in NSCLC patients will determine the extent of their anti-tumor function. Ultimately, results from this study will help predict how to target TIL-B functions in future immunotherapies for NSCLC patients.

### Acknowledgements

T32 grant AI007505, the American Cancer Society grant RSG LIB-114645, Cancer League of Colorado, The University of Colorado Lung Cancer SPORE Career Development Award 5P50CA058187-20, and CCSG CA 046934, and CCTSI UL1 TR 001082.

391

### **Imprime PGG, a novel pathogen associated molecular pattern (PAMP) treatment elicits M1-like transcriptional profile from bone marrow-derived macrophages and tumor associated macrophages (TAMs)**

*Anissa SH Chan, Xiaohong Qiu, Kathryn Fraser, Adria Jonas, Nadine Ottoson, Keith Gordon, Takashi O Kangas, Steven Leonardo, Kathleen Ertelt, Richard Walsh, Mark Uhlik, Jeremy Graff, Nandita Bose*

Biothera Pharmaceuticals Inc., Eagan, MN, USA

### Background

The success of cancer immunotherapy is often limited by multiple mechanisms of tumor-induced immunosuppression; M2-like TAMs being one of the critical mediators of immunosuppression. Imprime PGG (Imprime), an intravenously administered soluble yeast  $\beta$ -1,3/1,6 glucan is being clinically developed in combination with tumor-targeting antibodies, anti-angiogenics, and checkpoint inhibitors. Imprime has shown promising results in two randomized phase II studies in non-small cell lung cancer (NSCLC). Imprime acts mechanistically as a PAMP enlisting innate immune functions including cytotoxic effector mechanisms, reversal of immunosuppression and cross-talk with the adaptive immune system. With respect to immunosuppression, Imprime has been shown to repolarize M2 macrophages to an anti-tumor M1-like orientation in human *ex vivo* studies [1]. The objective of this study was to expand on this finding in an *in vivo* setting.

### Methods

Imprime's M1-polarization effect was evaluated in tumor-free mice, and xenograft and syngeneic tumor models. Bone marrow-derived macrophages (BMDM) prepared from Imprime- or vehicle-treated tumor-free mice were evaluated by qRT-PCR. Imprime was tested in combination with an anti-angiogenic agent, DC101 ( $\alpha$ -VEGFR2 Mab) in H441 NSCLC xenograft model in athymic nude mice, and in combination with anti-TRP1 tumor-targeting antibody TA-99 in B16 experimental lung metastases model. Immunohistochemistry of FFPE tumor tissue or lung tissue were evaluated.

### Results

qRT-PCR analyses of Imprime-treated BMDM from tumor-free mice revealed an increase in M1 markers (iNOS, PD-L1, IL-12b, TNF- $\alpha$ , CXCL9, CXCL10, and CXCL11) with a coincident decrease in M2 markers (CD206, YM-1, Fizz1, and CCL17). Imprime's M1-polarization effect was also observed in H441 NSCLC tumor model where Imprime treatment alone upregulated M1-like genes in TAMs as well as significantly suppressed tumor growth when combined with DC101, an agent that also modulates tumor microenvironment. Imprime-mediated M1-polarization was also observed in the B16 experimental lung metastasis model where the combination of Imprime with TA-99 significantly reduced both the number and size of B16 lung metastases. Immunohistochemistry analysis showed an increase in the number of tumor-infiltrating CD11b+ cells with an M1 phenotype evidenced by increase in iNOS expression.

### Conclusions

Collectively, these data indicate that Imprime, by reorienting the M2 macrophages to an M1-like polarization state can remold the suppressive tumor microenvironment to be more sensitive to other immunotherapeutic modalities.

## Tumor Microenvironment

Presenting author underlined; Primary author in italics

### References

1. Chan A, Qui X, Jonas AB, Patchen ML, Bose N: **Imprime PGG, a yeast  $\beta$ -glucan immunomodulator, has the potential to repolarize human monocyte-derived M2 macrophages to M1 phenotype.** *JITC* 2014, **2(Suppl 3)**:191.

### 392

#### **Integrated genomics approach of modeling tumors to assess their sensitivity to immune-mediated elimination**

Ravi Gupta, Nitin Mandloi, Kiran Paul, Ashwini Patil, Rekha Sathian, Aparna Mohan, Malini Manoharan, Amitabha Chaudhuri

MedGenome Inc., Foster City, CA, USA

#### **Background**

The somatic mutation burden, together with the immunoregulatory processes active in the tumor microenvironment, can provide powerful predictive biomarkers to facilitate the clinical translation of checkpoint control modulators and therapeutic vaccines. The molecular determinants of a productive anti-tumor immune response is multifactorial, shows significant intersubject variability and is influenced by host genetic and environmental factors. To investigate this complex interaction between the epithelial, stromal and the immune compartments, an unbiased NGS approach is a powerful method that can complement other conventional techniques, such as immunohistochemistry and cell sorting.

#### **Methods**

In this study, we have used our proprietary integrated NGS-based immuno-genomics platform OncoPept™, to analyze the TCGA somatic mutation and gene expression data and produced novel biological insights of therapeutic relevance. The combined expression of genes present in a signature was used to calculate an expression score that captured the relative abundance of specific cell types within the tumor. We also analyzed 9345 tumors from 33 cancers for T cell neo-epitope burden using our proprietary neo-epitope prioritization pipeline and combined the abundance of T cell neo-epitopes with the infiltration of specific immune cell types present in the tumor microenvironment to examine potential relationship between these two separate biological events.

#### **Results**

Our signature-based analysis of immune cell abundance identified core signaling pathways associated with high CD8+ T cell infiltration. These core pathways are enriched across many different cancers. Components from these core pathways can be combined with other immune cell markers to create a comprehensive response signature to select patients for treatment with checkpoint control modulators.

Several recent studies have highlighted the significance of T cell neo-epitopes in enhancing the therapeutic benefit of cancer immunotherapy drugs, specifically in tumors with low mutation burden. We assessed the T cell neo-epitope burden using our neo-epitope prioritization pipeline and observed that in some cancers the neo-epitope load is associated with higher inflammation, higher CD8+ T cell infiltration, IFN-g signaling and high PD-1 and PD-L1 level providing a basis for superior clinical response.

#### **Conclusions**

In conclusion, our analysis supports the idea that application of NGS in a clinical setting has the potential to generate deep biological insights of the tumor and its microenvironment to enable cancer immunotherapy treatment effective and personalized.

### 393

#### **Classification of gastric cancer based on tumor microenvironment expression of PD-L1 and CD8+ T cell infiltration**

Yu Chen, Jing Lin, Yun-bin Ye, Chun-wei Xu, Gang Chen, Zeng-qing Guo

Fujian Provincial Cancer Hospital, Fuzhou, Fujian, People's Republic of China

#### **Background**

Previous data has shown that a positive response to immunotherapy usually relies on active interactions between tumor cells and immunomodulators inside the tumor microenvironment (TME). The aim of this study was to classify gastric cancer subsets based on the TME immune status according to the expression of PD-L1 and infiltration of CD8+ T cells.

#### **Methods**

186 gastric cancer patients with a curative D2 gastrectomy were enrolled (Table 1). PD-L1 and CD8+ T cell status were evaluated with immunohistochemistry using specific antibodies (SP142, SP16). The samples were classified into four TME immune types and associated with different clinicopathological features and outcomes.

#### **Results**

Among 186 samples, there was positive PD-L1 expression (TC1/2/3 or IC1/2/3) in 60.3% (112/186) of patients (Figure 1A). A significant correlation between the PD-L1 expression and the intensity of CD8+ T cell infiltration ( $p=0.000$ , Figure 1B) was found. According to the immune-related classification, the TME was divided into both PD-L1+ and CD8+ T cell positive (type I), both PD-L1 and CD8+ T cell negative (type II), PD-L1 positive but CD8+ T cell negative (type III), and PD-L1 negative but CD8+ T cell positive (type



**Tumor Microenvironment**

*Presenting author underlined; Primary author in italics*

IV). Types I, II, III, IV were 60.3%, 11.8%, 0%, and 27.9%, respectively (Figure 1C, Figure 2, Table 2). The expression of STAT3, and pSTAT3, rather than STAT1 and pSTAT1, was significantly correlated with the CD8+ T cell infiltration, and PD-L1 status (Figure 3, Figure 4). CD8+ T cell infiltration was significantly associated with disease-free survival (DFS) and overall survival (OS) ( $p=0.003$  and  $p=0.001$ , Table 3, Table 4, Figure 5A). The DFS and OS of patients with immune type II tumors was significantly worse compared to immune types I and IV; there was no significant difference in DFS and OS between type I and IV (type I vs. type II,  $p=0.015$ ,  $p=0.003$ ; type IV vs. type II,  $p=0.017$ ,  $p=0.005$ ; type I vs. type IV,  $p=0.806$ ,  $p=0.808$ ; Figure 5C). The hazard ratios of DFS and OS numerically favored type I and type IV compared with type II across most subgroups (Figure 6).

**Conclusions**

This is the first reported stratification of TME based on PD-L1 expression and CD8+ T cell infiltration in gastric cancer. The PD-L1 expression was significantly correlated with the CD8+ T cell infiltration. Immune type III was absent, and type II patients have a worst prognosis compared with type I and IV patients. Our results may be useful for the development of clinical treatments for the blockade of immune checkpoints.

Figure 1.

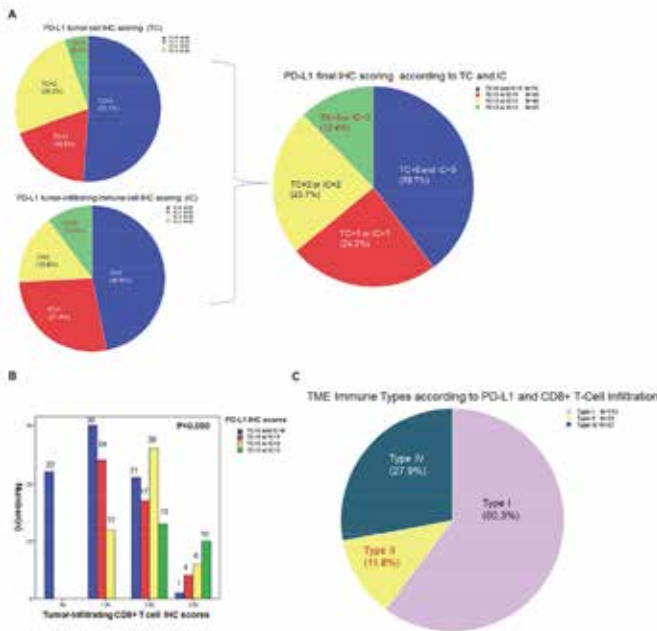


Fig.1 (A) Distribution (%) of 186 patients with gastric cancer according to the expression of PD-L1 on tumor cells (TC) and tumor-infiltrating immune cells (IC). (B) PD-L1 expression by tumor cells (TC) and tumor-infiltrating immune cells (IC) is reduced with fewer infiltrating CD8+ T cells. (C) Distribution (%) of tumor microenvironment immune type based on the

presence of tumor-infiltrating CD8+ T cells and PD-L1 status. Tumor-infiltrating CD8+ T cell IHC score=1-3 were considered positive. PD-L1 in tumor samples by TC1/2/3 or IC1/2/3 was considered positive.

Figure 2.

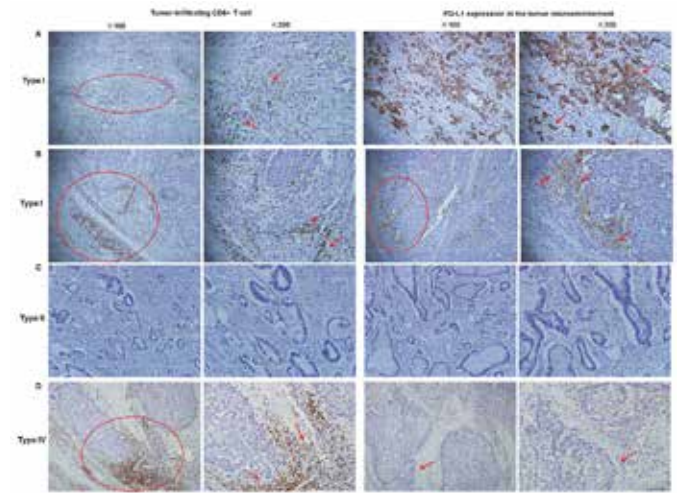


Fig.2 Representative images of immunohistochemistry (IHC) staining for tumor-infiltrating CD8+ T cells and PD-L1 status from the 186 patients with gastric cancer. (A) Type I, adaptive immune resistance. More than 50% of the tumor cells (TC=3) demonstrated cell membrane PD-L1 expression with a “severe” grade of CD8+ T cell infiltration. (B) Type I, adaptive immune resistance. About 1-3% of the tumor cells (TC=1) and 3-5% tumor-infiltrating immune cells (IC=1) in the invasive tumor margin demonstrated cell membrane PD-L1 expression with a “moderate” grade of CD8+ T cell infiltration. (C) Type II, immune ignorance. PD-L1 negative (TC=0 and IC=0) with no CD8+ T cell infiltration. (D) Type IV, other suppressor. PD-L1 negative (TC=0 and IC=0) with a “severe” grade of CD8+ T cell infiltration.

Figure 3.

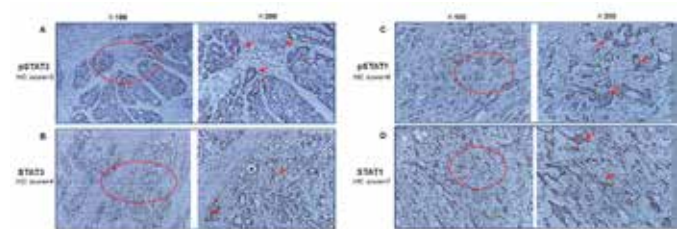


Figure 3 Representative images of IHC staining for STAT3, pSTAT3, STAT1, and pSTAT1 from the 186 patients with gastric cancer. (A) pSTAT3 positive cells with nuclear staining in the invasive tumor margin, IHC score=3. (B) STAT3 positive cells with cytoplasmic staining in tumor foci and in the invasive tumor margin, IHC score=4. (C) pSTAT1 positive nuclear

# Tumor Microenvironment

Presenting author underlined; Primary author in italics

staining in tumor cells and partly in stroma lymphocyte, IHC score=6. (D) STAT1 positive cytoplasmic staining in tumor cells and partly in stroma lymphocyte, IHC score=7.

Figure 4.

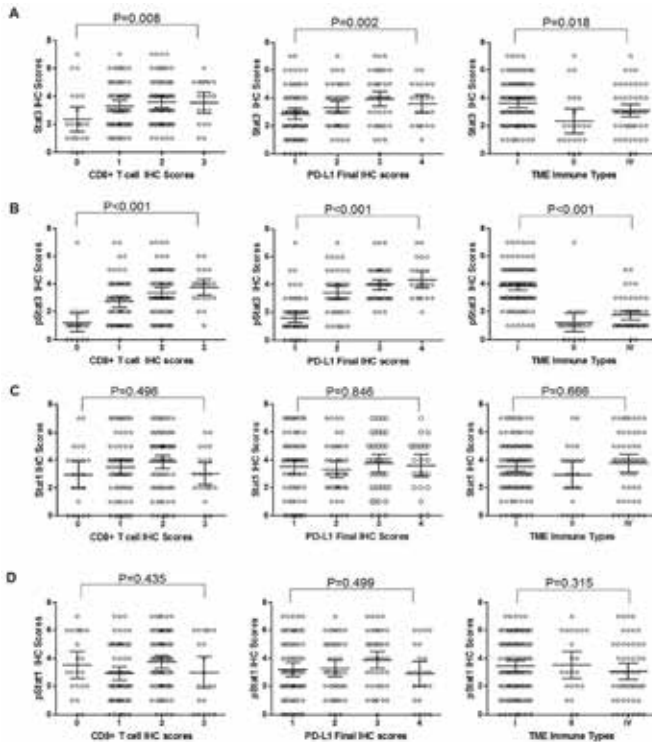


Figure 4 Relation between immunohistochemical staining for STAT3 (A), pSTAT3 (B), STAT1 (C), and pSTAT1 (D) in 186 tumor specimens and tumor-infiltrating CD8+ T cell, PD-L1 status and TME immune type.

Figure 5.

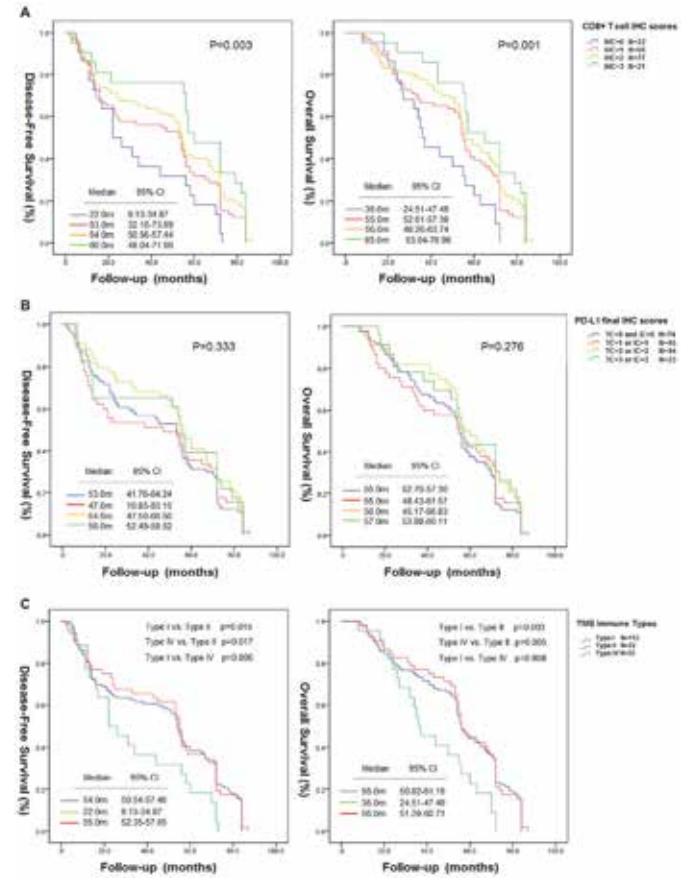


Figure 5 Kaplan-Meier survival curves for Disease-Free-Survival (DFS) and Overall Survival (OS) in 186 patients according to tumor-infiltrating CD8+ T cells, PD-L1 status and TME immune type. (A) DFS and OS associations with four grades of tumor-infiltrating CD8+ T cells. (B) DFS and OS associations with PD-L1 expression by the TC and IC. (C) DFS and OS associations with TME immune type.

Figure 6.

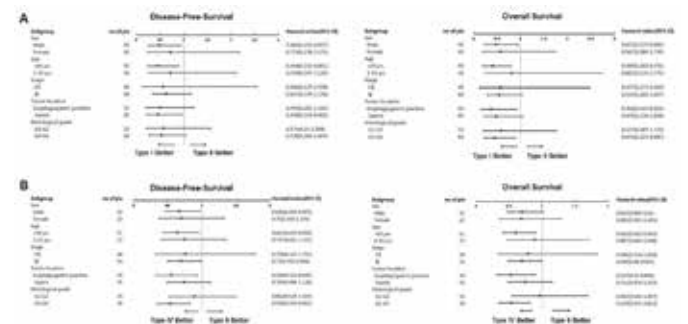


Figure 6 Prespecified subgroup analysis of Disease-Free-Survival and Overall Survival, according to the TME immune type.



## Tumor Microenvironment

Presenting author underlined; Primary author in italics

**Table 1: Baseline characteristics (N=186)**

Characteristics	Total (n=186)
Age	mean=59.5(27-79)
	<65 127(68.3%)
	≥65 59(31.7%)
Sex	Male 128(68.8%)
	Female 58(31.2%)
Histological grade	G1-G2 78(41.9%)
	G3-G4 108(58.1%)
Stage	I 18(9.7%)
	II 43(23.1%)
	III 125(67.2%)
Tumor location	Esophagogastric junction 70(37.6%)
	Gastric 116(62.4%)

**Table 2: Correlation of Tumor-infiltrating CD8+ T cells, PD-L1 status, and TME Immune Types with Clinicopathologic Features in 186 patients.**

Characteristics	Tumor-infiltrating CD8+ T cells					PD-L1 status		TME Immune Types			
	IHC=0	IHC=1	IHC=2	IHC=3	P-value	TC=0 and IC=0	TC=1 or IC=1	TC=2 or IC=2	TC=3	IC=3	P-value
Sex	106	18	31	31	0.014	11	76	0.108	76	36	0.001
Age	71	21	22	14	0.001	11	38	0.001	38	14	0.001
Stage	45	17	42	21	0.001	11	76	0.001	76	36	0.001
Histological grade	35	13	22	8	0.001	11	38	0.001	38	14	0.001
Tumor location	102	18	28	12	0.001	11	38	0.001	38	14	0.001

**Table 3: Univariate analysis of clinicopathologic prognostic factors for survival in 186 patients.**

Variable	n	m DFS	p-value	m OS	p-value
Sex					
Male	127	53.0	0.335	54	0.225
Female	59	57.0		63.0	
Age					
<65	128	55.0	0.196	56.0	0.259
≥65	58	43.0		54.0	
Histological grade					
G1-G2	78	55.0	0.375	57.0	0.452
G3-G4	108	53.0		55.0	
Stage					
I	18	72.0	0.024	72.0	0.040
II	43	55.0		64.0	
III	125	34.0		54.0	
Tumor location					
EGJ	70	43.0	0.123	54.0	0.136
Gastric	116	56.0		57.0	
CD8+ T-cells					
IHC=0	22	22.0	0.003	36.0	0.001
IHC=1	66	53.0		55.0	
IHC=2	77	54.0		56.0	
IHC=3	21	60.0		65.0	
PD-L1 status					
TC=0 and IC=0	74	53.0	0.333	55.0	0.276
TC=1 or IC=1	45	47.0		55.0	
TC=2 or IC=2	44	54.0		56.0	
TC=3 or IC=3	23	56.0		57.0	

**Table 4: Multivariate analysis of prognostic factors for survival in 186 patients.**

Variable	DFS			OS		
	P value	Hazard ratio	95%CI	P value	Hazard ratio	95%CI
CD8+ T-cells	0.006	0.779	0.652-0.930	0.013	0.747	0.593-0.941
Stage	0.033	1.289	1.020-1.628	0.042	1.277	1.009-1.616
TME Immune Types	0.095	0.853	0.707-1.028	0.108	0.859	0.714-1.034
PD-L1	0.420	0.896	0.686-1.170	0.452	0.903	0.692-1.178

### 394

## Molecular profiling of tumor microenvironment for biomarker discovery

*Andrey Komarov*, Alex Chenchik, Michael Makhanov, Costa Frangou

Cellecta, Inc., Mountain View, CA, USA

### Background

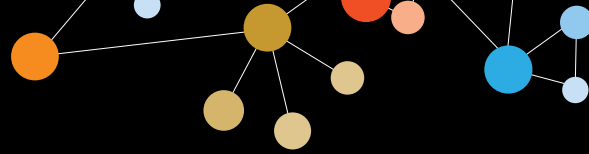
Human carcinomas consist of a complex mixture of neoplastic epithelial cells, endothelial cells, fibroblasts, myofibroblasts, and immune cells, which collectively form the tumor stroma. The presence of stromal cell types within carcinomas is a powerful component of the biology of a tumor through its ability to have profound influences on cancer progression, metastasis, and drug resistance. Correspondingly, the clinical importance of tumor immune infiltrates is now recognized as an emerging area of triple-negative breast cancer (TNBC) research, where increased immune infiltrate predicts both responses to chemotherapy and improved survival. Quantitative molecular profiles of tumor-associated normal cells may provide valuable insights into tumor biology and facilitate the discovery of new biomarkers and therapeutic targets.

### Methods

To this end, we have developed GeneNet™, a genome-wide targeted RNA expression assay that profiles ~19,000 genes using multiplex RT-PCR followed by NGS. The GeneNet 19K assay provides comprehensive cellular composition analysis of tumor stroma and allows human hematopoietic cell phenotypes, including naïve and memory B cells, seven T cell types, dendritic cells, plasma cells, natural killer (NK) cells and myeloid subsets to be distinguished. The developed targeted RNA expression platform profiles in 10<sup>5</sup>-fold dynamic range the complete set of genes involved in checkpoint blockade and immunotherapy biomarkers, immune cell activation, and canonical immune pathway genes for both innate adaptive and humoral immune responses.

### Results

Proof-of-principle studies demonstrate the assay's unparalleled specificity and sensitivity resulting in unique detection of low abundance mRNA transcripts as well as an improved cost-effectiveness for high-throughput clinical applications.



## Tumor Microenvironment

Presenting author underlined; *Primary author in italics*

### Conclusions

In this study, we present a molecular assay that unambiguously characterizes the cellular composition of the tumor microenvironment and determines the activation status of infiltrating immune cells in primary tumor tissues from TNBC patients.

**395**

### **A fully-automated staining assay for probing the tumor microenvironment using fluorescent multiplex immunohistochemistry**

Yi Zheng, Carla Coltharp, Darryn Unfricht, Ryan Dilworth, Leticia Fridman, Linying Liu, Milind Rajopadhye, Peter Miller PerkinElmer, Hopkinton, MA, USA

### Background

In recent years, cancer immunotherapy research has increasingly leveraged knowledge about the tumor microenvironment for the development of novel therapeutics and targets. Advancing our current understanding of the tumor microenvironment will involve continued characterization of the interactions that occur among immune cells and cancer cells that reside within the tumor and its periphery. Fluorescent multiplex immunohistochemistry (mIHC) assays are uniquely suited to characterizing and quantifying these complex interactions *in situ*. In response, we commercialized manual Opal™ mIHC and Opal™ cancer immunology staining kits that are optimized for multispectral imaging. Here we describe a robust, fully-automated 7-color mIHC procedure that streamlines Opal™ staining. We coupled this automated staining procedure with a multispectral imaging system for simultaneous detection of up to 6 tissue biomarkers plus nuclear counterstain, providing the ability to visualize interactions between specific immune and cancer cells within the context of the tumor microenvironment.

### Methods

Formalin-fixed paraffin-embedded samples of primary tumors were immunostained using Opal™ reagent kits on a fully automated Leica BOND RX™ stainer, imaged with a Vectra 3.0® automated imaging system, and analyzed with inForm® software. Equivalent assays using manual staining protocols were also performed for comparison.

### Results

We developed a fully-automated staining protocol and assessed its robustness with respect to fluorescence signal degradation, impact on antigen epitope availability, influence on tissue morphology, and potential cross-labeling due to incomplete inactivation between staining steps. We observed minimal degradation of fluorescence signal, epitope availability, or tissue morphology throughout the automated

staining process. We achieved comparable signal contrast and cross-talk levels to those obtained with manual protocols while substantially reducing hands-on time.

### Conclusions

The fully-automated staining assay that we developed for Opal™ 7-color mIHC is a robust method to increase the throughput of multiplex tissue staining.

**396**

### **EGFR/JAK2 inhibition downregulates immunosuppressive cytokine secretion in head and neck cancer**

Fernando Concha-Benavente, Julie Bauman, Sumita Trivedi, Raghendra Srivastava, James Ohr, Dwight Heron, Uma Duvvuri, Seungwon Kim, William Gooding, Robert L Ferris University of Pittsburgh, Pittsburgh, PA, USA

### Background

The EGFR, which is overexpressed in more than 90% of head and neck cancers (HNC), activates the Janus kinase 2 (JAK2)/signal transducer and activator of transcription 3 (STAT3) pathway leading to carcinogenesis. STAT3 plays a major role in promoting tumor immune escape, including production of immunosuppressive cytokines such as vascular endothelial growth factor (VEGF), IL-6, IL-10 and TGFβ, which in turn activate STAT3 in tumor-associated suppressive immune cells, providing a feed forward mechanism to ensure a STAT3-dominated microenvironment. Cetuximab, a specific EGFR blocking mAb, downregulates EGFR-mediated STAT3 activation; however, other STAT3 activating pathways exist. The IL-6 receptor (IL-6R) constitutes a major EGFR-independent STAT3 activating pathway in HNC. Given that JAK2 is common signaling molecule to both EGFR and IL-6R pathways we hypothesized that combined EGFR and JAK2 inhibition may downregulate STAT3-dependent production of immunosuppressive cytokines.

### Methods

mRNA expression for the cytokines analyzed in this study was accessed and downloaded from the cancer genome atlas (TCGA) repository. Protein concentration of cytokines in plasma from head and neck cancer patients enrolled in cetuximab single agent on a neoadjuvant trial (UPCI #08-013, NCT #01218048) were determined by ELISA. Data analysis was done using Graphpad v6.0.

### Results

Herein we show that tumors of HNC patients annotated in The Cancer Genome Atlas (TCGA) express higher immunosuppressive cytokines including TGFβ, IL-10, VEGFA and IDO than control tissues and have lower expression of inflammatory cytokines such as IL-12A and IL-17A,

## Tumor Microenvironment

Presenting author underlined; Primary author in italics

confirming the view of a dominant immunosuppressive tumor microenvironment that prevents proper immune effector cell activation. In addition, EGFR and JAK2 inhibition downregulate STAT3 activation and secretion of these immunosuppressive STAT3-dependent cytokines *in vitro*, providing evidence that supports targeting the EGFR/JAK2/STAT3 mediated suppressive tumor microenvironment.

### Conclusions

Importantly, our findings are clinically relevant since HNC patients that were treated with cetuximab single agent on a neoadjuvant trial (UPCI #08-013, NCT #01218048) who are resistant to cetuximab therapy have significantly higher TGF $\beta$  concentration and a lower immunostimulatory cytokine profile in plasma, which endorses the use of combined therapy in those patients where EGFR blockade is not sufficient to reverse production of immunosuppressive cytokines and chemokines that feed the tolerant cellular network in the tumor microenvironment.

### Trial Registration

ClinicalTrials.gov identifier NCT01218048.

**397**

### Direct oncogene-targeted cancer killing and selective tumor Treg killing through the TNFR2 receptor via dominant antibody antagonists

Heather Torrey<sup>1</sup>, Toshi Mera, Yoshiaki Okubo, Eva Vanamee, Rosemary Foster, Denise Faustman

Massachusetts General Hospital/Harvard Medical, Boston, MA, USA

### Background

A major barrier to cancer immunotherapy is lack of selective inhibitors of the regulatory T cells (Tregs) in the cancer microenvironment. New methods to directly kill tumors through novel surface oncogenes are also desirable. Tumor necrosis factor receptor 2 (TNFR2) is a target protein with restricted expression on the most potent tumor-infiltrating Tregs. On human tumors, it is a newly-discovered and broadly-expressed human oncogene.

### Methods

We characterized the expression and the functional effects of the newly-created TNFR2 antibody antagonists on the tumor infiltrating Tregs of ovarian ascites compared to Tregs of peripheral blood from patients with ovarian cancer and healthy controls. We also investigated if well-known ovarian tumor cells lines express the TNFR2 oncogene and the effects of the TNFR2 antagonistic antibody on direct cancer killing.

### Results

TNFR2 antagonists inhibited Treg proliferation with exponential potency and selectivity for the tumor

microenvironment Tregs. Furthermore, common ovarian cancer cell lines such as OVCAR3 express the TNFR2 oncogene and were rapidly and completely killed by TNFR2 antagonistic antibodies, even at low concentrations.

### Conclusions

Dominant TNFR2 antagonists demonstrate tumor-specific Treg depletion with heightened specificity for the tumor microenvironment over the Tregs of peripheral blood. Blocking TNFR2 signaling with antagonist antibodies also creates a novel tool to directly eliminate ovarian tumors expressing the TNFR2 oncogene.

**398**

### WITHDRAWN

**399**

### Induction of potent and durable anti-tumor immunity by intratumoral injection of STING-activating synthetic cyclic dinucleotides

Laura Hix Glickman<sup>1</sup>, David B Kanne<sup>1</sup>, Kelsey S Gauthier<sup>1</sup>, Anthony L Desbien<sup>1</sup>, Brian Francica<sup>2</sup>, George Katibah<sup>1</sup>, Leticia P Corrales<sup>3</sup>, Justin L Leong<sup>1</sup>, Leonard Sung<sup>1</sup>, Ken Metchette<sup>1</sup>, Shailaja Kasibhatla<sup>4</sup>, Anne Marie Pferdekamper<sup>4</sup>, Lianxing Zheng<sup>5</sup>, Charles Cho<sup>4</sup>, Yan Feng<sup>5</sup>, Jeffery M McKenna<sup>5</sup>, John Tallarico<sup>5</sup>, Steven Bender<sup>4</sup>, Chudi Ndubaku<sup>1</sup>, Sarah M McWhirter<sup>1</sup>, Charles G Drake<sup>6</sup>, Thomas F Gajewski<sup>7</sup>, Thomas W Dubensky<sup>1</sup>

<sup>1</sup>Aduro Biotech, Berkeley, CA, USA

<sup>2</sup>Johns Hopkins University School of Medicine, Baltimore, MD, USA

<sup>3</sup>The University of Chicago, Chicago, IL, USA

<sup>4</sup>Genomics Institute of the Novartis Research Foundation (GNF), San Diego, CA, USA

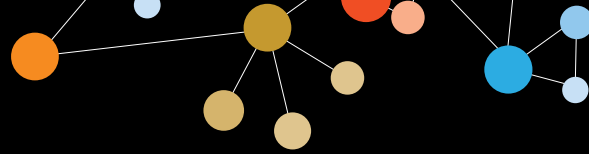
<sup>5</sup>Novartis Institutes for BioMedical Research, Inc., Cambridge, MA, USA

<sup>6</sup>Johns Hopkins University Cancer Center, Baltimore, MD, USA

<sup>7</sup>University of Chicago Medical Center, Chicago, IL, USA

### Background

In human melanoma, spontaneous T cell infiltration into the tumor microenvironment (TME) is correlated with a type I interferon (IFN) transcriptional signature. Induction of IFN- $\beta$  in this context is dependent upon activation of stimulator of interferon genes (STING), a critical component of the cytosolic DNA sensing pathway of the innate immune system. STING is activated by binding of cyclic dinucleotides (CDNs) produced by an intracellular enzyme, cGAS, in response to the presence of cytosolic pathogen or tumor-derived DNA. STING induction of IFN within the TME leads to the priming and activation of tumor antigen-specific CD8<sup>+</sup> T cell immunity. We hypothesized that direct activation of STING in the TME



## Tumor Microenvironment

Presenting author underlined; *Primary author in italics*

by intratumoral (IT) injection of synthetic CDNs would induce potent anti-tumor immunity against a broad repertoire of an individual's tumor antigenic milieu.

### Methods

Through screening a panel of synthetic CDNs, we selected ADU-S100 (MIW815) for clinical development for its ability to broadly and potently activate all human STING alleles, elicit profound tumor regression of injected and distal lesions in aggressive mouse tumor models, and promote durable anti-tumor immunity.

### Results

A bell-shaped ADU-S100 dose response curve was found to delineate regression of injected tumor, induction of tumor-specific CD8<sup>+</sup> T cell immunity, and protection against autologous tumor challenge. *In vivo* mechanistic studies demonstrate that STING-mediated anti-tumor immunity is due in part to an acute pro-inflammatory TNF- $\alpha$ -mediated cytokine response, as well as a tumor-specific CD8<sup>+</sup> T cell response. Studies in chimeric wild-type and STING<sup>-/-</sup> mice showed that while STING signaling in the tumor stromal compartment contributes to acute tumor rejection, STING signaling in the hematopoietic compartment is required for induction of CD8<sup>+</sup> T cell mediated anti-tumor immunity. Anti-tumor efficacy is enhanced by combination with immune checkpoint inhibitors, including  $\alpha$ -PD-1 and  $\alpha$ -CTLA-4, informing future clinical development.

### Conclusions

The ability to elicit innate and T cell-mediated anti-tumor immunity via activation of STING in the TME demonstrates that CDNs have high translational potential for the treatment of patients with advanced/metastatic solid tumors. To this end, a phase I clinical study is in progress to evaluate the safety and tolerability and possible anti-tumor effects in subjects with cutaneously-accessible non UV-induced and UV-induced malignancies or lymphomas given repeated IT doses of ADU-S100.

### Trial Registration

ClinicalTrials.gov identifier NCT02675439.

### Consent

Written informed consent was obtained from the patient for publication of this abstract and any accompanying images. A copy of the written consent is available for review by the editor of this journal.

400

## Modulation of NK cell exhaustion in metastatic melanoma tumors

Elena Gonzalez Gugel<sup>1</sup>, Charles JM Bell<sup>2</sup>, Adiel Munk<sup>1</sup>, Luciana Muniz<sup>1</sup>, Nina Bhardwaj<sup>1</sup>

<sup>1</sup>Tish Cancer Institute, Icahn School of Medicine at Mount Sinai, New York, NY, USA

<sup>2</sup>Murray Edwards College and School of Clinical Medicine, University of Cambridge, Cambridge, England, UK

### Background

Interventions such as checkpoint blockade have made a high impact in melanoma treatment, but a significant number of patients fail to respond or become resistant to therapy [1]. The tumor microenvironment in malignant melanoma promotes NK cell exhaustion, a state characterized by i) up-regulation of inhibitory receptors (TIM-3, KIRB1 and KIRNKAT2), ii) down-regulation of activating receptors (NKG2D and NKp46), IL-2R and transcription factors (T-bet and Eomes) and iii) loss of IFN-g production, proliferation and cytotoxicity. Interestingly, this exhaustion can be partially reversed by checkpoint blockade of Tim-3 [2]. Most strikingly, however, we also found that patients who have a clinical response to Ipilimumab treatment spontaneously restored their NK cell function, despite the fact that these cells express little or no CTLA-4 (or PD-1 or PDL-1) [3]. Here we investigate further aspects of NK cell exhaustion in human and animal models of melanoma.

### Methods

Our results show that NK cells from human melanoma donors (MDs) are exhausted – a phenotype which is characterized by reduction of: (i) cytotoxicity (ii) IFN- $\gamma$  production and (iii) proliferation. In addition we show that NK cells from healthy donors (HDs) cultured with IL-2 increase expression levels of epigenetic modification indicators (HIST1H1C, HIST1H4I, ZNF286B, HIST2H2BE) whereas IL-2/IL-12 stimulated NK cells up regulated mRNA encoding cytokines (IFN- $\gamma$ , IL-1 $\beta$ , IL-6 and TNF) and chemokines (CCL3, CXCL1, CXCL3), as well as the expression of different activating and inhibitory NK cells receptors. This is consistent with an activation phenotype that is deficient in MDs samples. We are also able to demonstrate that NK cells can become exhausted *in vitro* through a pathway driven by Ceacam-1 and found evidence of NK cell exhaustion in a B16BL6 melanoma model.

### Results

The methodology used on this study included assays such as Mass cytometry measurement (CyTOF), Flow cytometry, Poly (A) RNAseq, Quantitative RT-PCR, Western Blot and tumor melanoma mice model.



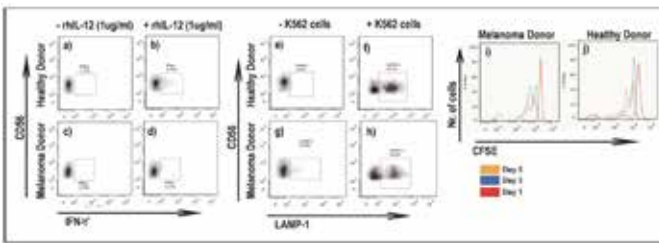
**Tumor Microenvironment**

Presenting author underlined; Primary author in italics

**Conclusions**

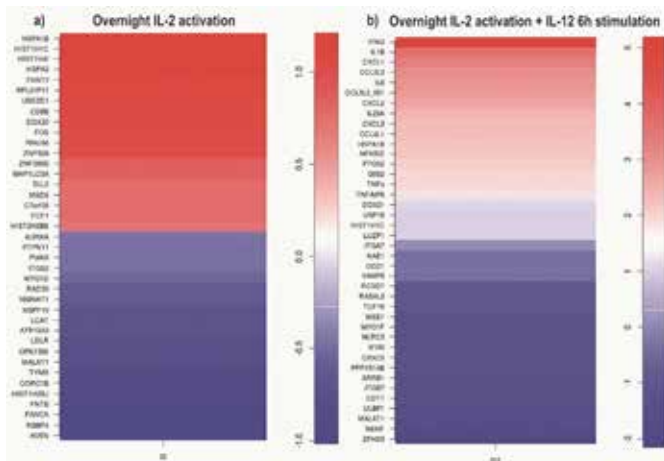
We hypothesize that NK cell exhaustion becomes evident as melanomas progress in human and mouse models possibly driven by specific ligands within the tumor microenvironment. Fully appreciating the factors and immune suppressive mechanisms that contribute towards NK cell exhaustion in these patients will impact the development of drugs that facilitate effective anti-tumor immune responses.

**Figure 1. Features of exhaustion were detected on NK cells isolated from fresh melanoma donor (MD) blood**



NK cells from MD show reduced cytotoxicity capacity (expression of LAMP-1/CD107a in response to co-culture with K562 cells), IFN-γ production in response to IL-12, and proliferation after IL-2 stimulation, compared with NK cells isolated from fresh healthy donor (HD) blood. These reduced functional properties are consistent with the concept that advanced disease is progressively associated with systemic immune suppression.

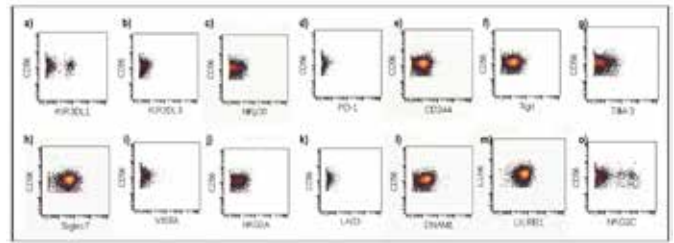
**Figure 2. Transcriptome analysis in NK cells**



Purified NK cells from HD were isolated and transcriptome analysis was performed under two different conditions a) IL-2 stimulated NK cells that showed evidence of priming through epigenetic modification indicators (HIST1H1C, HIST1H4I, ZNF286B, HIST2H2BE); b) IL-2/IL-12 stimulated NK cells that up-regulated mRNA encoding cytokines (IFN-γ, IL-1β, IL-6 and TNF) and chemokines (CCL3, CXCL1, CXCL3) consistent with an activation phenotype. This approach will be useful to

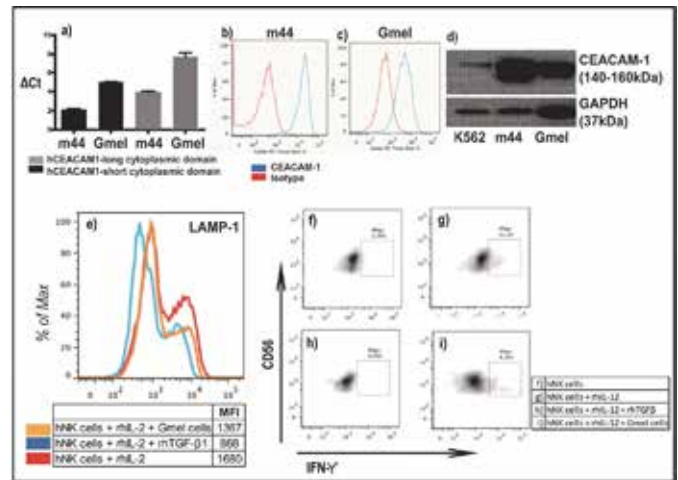
show which pathways and genes are modulated during NK cell exhaustion when the analysis will be repeated in NK cells from MD as represented in Figure 1.

**Figure 3. NK cell Phenotype analysis by CyTOF**



Purified NK cells from HD were isolated and stained with a cocktail antibody containing a complete panel of 33 activating and inhibitory NK cell receptors including checkpoint molecules such as Tim-3, PD-1, DNAM-1, VISTA, LAG-3, TIGIT and Siglec-7 among others, as represented in this figure. This approach will be useful to determine the distribution of inhibitory receptors that impact NK cell exhaustion when the analysis will be repeated in NK cells from MD as represented in Figure 1.

**Figure 4. In vitro NK cell exhaustion**



CEACAM-1 was recently discovered as a necessary co-receptor and ligand of Tim-3 on T cells [4] functioning both in cis and in trans to potentiate the inhibitory activity of Tim-3. Up regulated in primary melanoma, it is associated with poor prognosis for survival and increased invasive behavior [5]. CEACAM-1 also increases on IL-2 activated CD56hi NK cells [6] and functions to inhibit cytolytic activity after exposure to CEACAM-1-bearing tumor cells [7]. Here we first show high expression of short cytoplasmic Ceacam-1 isoform in the human melanoma cell lines m44 and Gmel. Interestingly, we found that similar to TGFβ exposed NK cells, Gmel co-cultured NK cells also displayed clear signals of exhaustion

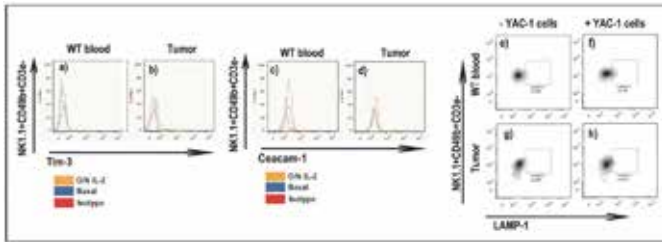


## Tumor Microenvironment

Presenting author underlined; Primary author in italics

such as significant loss of cytotoxic activity and reduced IFN- $\gamma$  production following IL-12 stimulation. Indicating the ability of tumors to suppress NK cells driven anti-tumor activity. This approach will be useful for gaining insight into mechanisms of NK cell exhaustion induced by melanoma cells.

### NK cell exhaustion in murine melanoma model



Here we show how NK cells from B16BL6 tumor bearing mice became dysfunctional in progressive melanoma. NK cells expressed high levels of Tim-3 and Ceacam-1 when isolated from B16BL6 tumors compared with C57BL/6J non-tumor mice blood after IL-2 overnight stimulation. In addition, NK cells from tumors showed reduced cytotoxicity against YAC-1 target cells compared with NK cells from blood WT non-tumor bearing mice. These findings of dysfunctional activity are consistent with data obtained in human melanoma patients.

### 401

### Stromal fibroblasts promote Wnt5a expression and suppress responses to anti-PD-1 antibody therapy in an autochthonous melanoma model

*Fei Zhao*<sup>1</sup>, *Kathy Evans*<sup>1</sup>, *Christine Xiao*<sup>1</sup>, *Alisha Holtzhausen*<sup>2</sup>, *Brent A Hanks*<sup>1</sup>

<sup>1</sup>Duke University Medical Center, Durham, NC, USA

<sup>2</sup>Lineberger Comprehensive Cancer Center, University of North Carolina, Chapel Hill, NC, USA

### Background

TGF- $\beta$  is a multifunctional cytokine that suppresses many facets of cellular immunity. These immunosuppressive properties have led to the development of immunotherapy regimens to evaluate the ability of type I TGF- $\beta$  receptor (TBRI) inhibitors to augment the efficacy of checkpoint inhibition. The TGF- $\beta$  cytokine also plays a role in cellular homeostasis and suppresses fibroblast expansion while promoting melanoma expression of Wnt5a, a ligand previously associated with resistance to anti-PD-1 antibody therapy in melanoma.

### Methods

Using the BRAF<sup>V600E</sup>PTEN<sup>-/-</sup> transgenic melanoma model, we investigated the impact of TBRI inhibition on anti-CTLA-4 antibody and anti-PD-1 antibody immunotherapy. Primary/

metastatic tumor progression was correlated with the generation of anti-tumor immunity. Immunohistochemistry/flow cytometry was performed to assess the effect of TBRI inhibition on the tumor stroma. Melanoma and melanoma-associated fibroblast (MAF) lines were generated and utilized in co-transplant assays to examine the influence of MAFs on anti-PD-1 antibody therapy. Melanoma-MAF transwell assays were performed to investigate the underlying mechanism of anti-PD-1 antibody resistance.

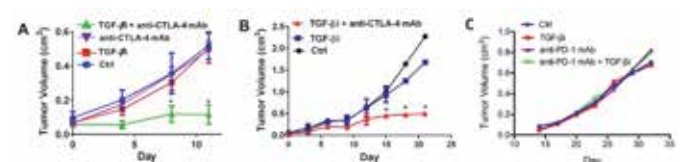
### Results

TBRI inhibition synergistically enhances anti-CTLA-4 antibody immunotherapy in the BRAF<sup>V600E</sup>PTEN<sup>-/-</sup> transgenic melanoma model but fails to augment anti-PD-1 antibody therapy in this same model (Figure 1). Immunohistochemistry and flow cytometry of TBRI-treated melanomas reveals an expansion of the MAF population while *in vitro* experiments show TBRI inhibition to enhance fibroblast proliferation (Figure 2). TBRI inhibition augments anti-PD-1 antibody therapy in a stromal-poor BRAF<sup>V600E</sup>PTEN<sup>-/-</sup> transplant tumor model while the co-transplantation of a BRAF<sup>V600E</sup>PTEN<sup>-/-</sup> melanoma-derived MAF cell line reverses this effect (Figure 3). MAFs were found to express high levels of TGF- $\beta$  which correlates with melanoma expression of Wnt5a in resected melanoma tissues. Melanoma-MAF co-cultures revealed that TBRI-treated MAFs promote melanoma expression of Wnt5a and suppress PD-L1 expression both *in vitro* and *in vivo* (Figure 4). Silencing of Wnt5a expression by the BRAF<sup>V600E</sup>PTEN<sup>-/-</sup> melanoma model enhances PD-L1 expression and eliminates the impact of MAFs on responses to anti-PD-1 antibody therapy.

### Conclusions

This work illustrates the importance of the tumor stroma on the efficacy of anti-PD-1 antibody therapy and that pharmacologic modulation of the melanoma microenvironment can have significant effects on anti-PD-1 antibody therapy outcomes. TGF- $\beta$ -mediated upregulation of Wnt5a represents an important paracrine signaling pathway that can impact checkpoint inhibitor efficacy in the melanoma microenvironment. TBRI inhibition should be further evaluated in combination with anti-CTLA-4 antibody therapy and Wnt signaling blockade represents a promising approach for augmenting anti-PD-1 antibody therapy in future clinical trials.

Figure 1.

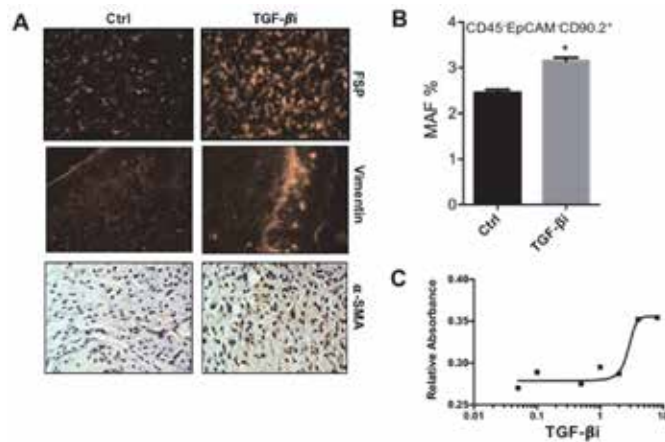


**Tumor Microenvironment**

*Presenting author underlined; Primary author in italics*

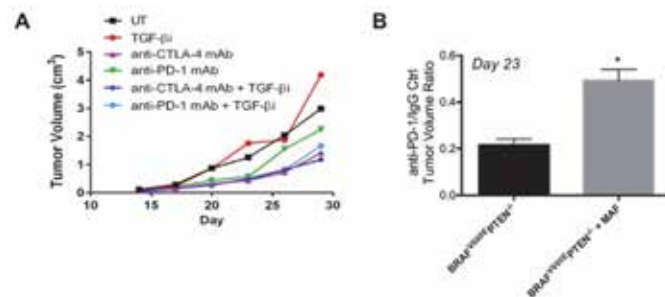
TBRI inhibition augments anti-CTLA-4 antibody but not anti-PD-1 antibody immunotherapy in the BRAF(V600E)-PTEN<sup>-/-</sup> transgenic melanoma model. A. Assay 1. Short duration combination TGFβi (TGF-beta inhibitor)-anti-CTLA-4 antibody therapy. B. Assay 2. Longer duration TGFβi-anti-CTLA-4 antibody therapy. C. Combination TGFβi-anti-PD-1 antibody therapy.

**Figure 2.**



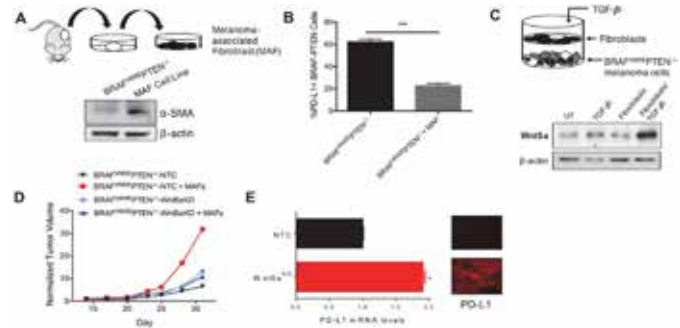
TBRI Inhibition Induces Melanoma-associated Fibroblast (MAF) Expansion. A. Immunofluorescence and immunohistochemical analysis of MAF markers in resected BRAF(V600E)PTEN<sup>-/-</sup> tumors treated with vehicle ctrl vs TGFβi. B. Flow cytometry quantitation of MAFs based on the CD45, EpCAM, and CD90.2 surface markers. C. TGFβi promotes MAF proliferation in culture.

**Figure 3.**



TBRI Inhibition Augments anti-PD-1 Antibody Therapy in a Stroma-poor BRAF(V600E)-PTEN<sup>-/-</sup> Transplant Model of Melanoma that is Reversed with MAF Co-Transplantation. A. Anti-PD-1 and Anti-CTLA-4 antibody therapy in combination with TGFβi in a cell line-derived transplant model of BRAF(V600E)PTEN<sup>-/-</sup> melanoma. B. Co-transplantation of MAFs with the BRAF(V600E)PTEN<sup>-/-</sup> melanoma cell line suppresses the efficacy of anti-PD-1 antibody therapy.

**Figure 4.**



MAFs Suppress PD-L1 Expression and Promote Melanoma Progression in a Wnt5a-dependent Manner. A. Generation of MAFs from resected BRAF(V600E)PTEN<sup>-/-</sup> melanoma tissues. B. Transwell cultures of MAFs and BRAF(V600E)PTEN<sup>-/-</sup> melanoma cells followed by PD-L1 flow cytometry. C. Transwell culture of MAFs and BRAF(V600E)PTEN<sup>-/-</sup> melanoma cells +/- TGFβi followed by Wnt5a Western blot analysis. D. Primary tumor growth of co-transplanted MAFs with control BRAF(V600E)PTEN<sup>-/-</sup> melanoma cells (NTC) vs Wnt5a-silenced BRAF(V600E)PTEN<sup>-/-</sup> melanoma cells (Wnt5aKD). E. qrt-PCR and immunofluorescence of PD-L1 expression by BRAF(V600E)PTEN<sup>-/-</sup>-NTC melanomas vs BRAF(V600E)PTEN<sup>-/-</sup>-Wnt5aKD melanomas.

**402**

**Inhibitors of B cell activation reduce tumor growth and attenuate pro-tumorigenic phenotype of tumor immune infiltrates in a syngeneic mouse model of ovarian cancer**

*Nathalie Scholler*<sup>1</sup>, Catherine Yin<sup>1</sup>, Pien Van der Meijs<sup>2</sup>, Andrew M Prantner<sup>3</sup>, Cecile M Krejsa<sup>4</sup>, Leia Smith<sup>4</sup>, Brian Johnson<sup>5</sup>, Daniel Branstetter<sup>6</sup>, Paul L Stein<sup>1</sup>

<sup>1</sup>Stanford Research Institute, Menlo Park, CA, USA

<sup>2</sup>Rijksuniversiteit Groningen, Groningen, Amsterdam, Netherlands

<sup>3</sup>University of Pennsylvania, Philadelphia, PA, USA

<sup>4</sup>Acerta Pharma, Bellevue, WA, USA

<sup>5</sup>University of Washington, Seattle, WA, USA

<sup>6</sup>Cynosure Clinical Research LLC, North Bend, WA, USA

**Background**

Recent findings support a pro-tumorigenic role for regulatory B cells [1]. B cell signaling is dependent on Bruton's tyrosine kinase (BTK) and phosphoinositide 3-kinase delta (PI3Kδ) activity. Acalabrutinib is a highly selective, potent BTK inhibitor in clinical development for treatment of hematologic malignancies, solid tumors, and autoimmune diseases; ACP-319 is a selective inhibitor of PI3Kδ. We hypothesized that these agents, which inhibit B cell activation and alter myeloid cell signaling, might improve antitumor



## Tumor Microenvironment

Presenting author underlined; *Primary author in italics*

responses with checkpoint inhibition (anti-PD-L1 mAb) for tumors containing regulatory B cell infiltrates.

### Methods

To assess regulatory B cells in the syngeneic ID8 ovarian tumor model, we adoptively transferred IL-10/GFP reporter B cells into mice deficient for functional B cells ( $\mu$ MT) then orthotopically implanted the mice with ID8 cells; GFP expression was analyzed by histology. Next, C57BL/6 mice orthotopically implanted with luciferase-transduced ID8 cells were treated with acalabrutinib +/- ACP-319 in combination with anti-PD-L1. Both oral agents were dosed 15 mg/kg twice daily; anti-PD-L1 (10F.9G2) was dosed intraperitoneally 200  $\mu$ g every 3 days. Tumor growth was monitored by *in vivo* bioluminescence imaging and *ex vivo* caliper measurements of ovaries and fallopian tubes. Tumor-immune infiltrates were characterized by flow cytometry (peritoneal lavages) and histologic analysis (tumor sections).

### Results

In  $\mu$ MT mice reconstituted with IL-10/GFP, many tumor-infiltrating cells expressed GFP, consistent with a regulatory B cell phenotype in the ID8 tumor microenvironment, whereas GFP expression was not observed in paired spleens. Significant tumor growth reductions (>50%) were observed in mice treated for 10 weeks with acalabrutinib ( $p=0.027$ ), acalabrutinib + anti-PD-L1 ( $p=0.037$ ), acalabrutinib/ACP-319 ( $p=0.012$ ) or acalabrutinib/ACP-319 + anti-PD-L1 ( $p=0.036$ ), but not with anti-PD-L1 alone ( $p=0.104$ ), compared with vehicle-treated controls. All anti-PD-L1 groups had increased CD8+ T cells in peritoneal lavages. Acalabrutinib/ACP-319 treatment decreased B cells in peritoneal lavages by 70% compared with vehicle, and acalabrutinib synergized with anti-PD-L1 to decrease PD-L1+ macrophages in bone marrow (90%). In mice treated with acalabrutinib/ACP-319 + anti-PD-L1, histology scores were significantly higher ( $p\leq 0.031$ ) for immune infiltrates and fibrosis, compared with controls. Tumor-infiltrating B cells, macrophages, T cells, and FoxP3-positive cells were decreased in the acalabrutinib/ACP-319 group. Treatment with acalabrutinib/ACP-319 + anti-PD-L1 increased tumor-infiltrating CD8+ T cells ( $p=0.026$ ).

### Conclusions

These results suggest that inhibition of BTK and PI3K $\delta$  targets both regulatory B cell subsets and myeloid cells in the tumor microenvironment. Combined with anti-PD-L1, acalabrutinib alone or with ACP-319 promotes an anti-tumor response against ovarian cancer.

### References

1. Gunderson: **BTK-Dependent Immune Cell Cross-talk Drives Pancreas Cancer**. *Cancer Discov* 2016, **6**(3): 270-285.

403

### Use of experimental tumor model to characterize the effects of small-molecule CD73 inhibitors on tumor biology and immune infiltrate

Juan C Jaen, Joanne BL Tan, Ada Chen, Yu Chen, Timothy Park, Jay P Powers, Holly Sexton, Guifen Xu, Steve W Young, Ulrike Schindler

Arcus Biosciences, Hayward, CA, USA

### Background

High levels of extracellular ATP (eATP) have been documented in many solid tumors. eATP, which enhances activation of antigen-presenting cells, is efficiently hydrolyzed to adenosine by extra-cellular CD39 (ATP $\rightarrow$ AMP) and CD73 (AMP $\rightarrow$ adenosine). Adenosine is a potent inhibitor of T cell and NK activation. Thus, CD73 has drawn interest as a next-generation immune-oncology target. We describe the CT26 tumor model to characterize the effects of CD73 inhibition on tumor biology and plasma AMP/adenosine levels as markers of systemic CD73 inhibition.

### Methods

Human PBMC and mouse spleen/blood/tumor leukocytes were isolated using standard methods. Cell markers were quantified by flow cytometry. Therapeutic treatment of subcutaneous (106 cells) CT26 tumors was initiated at volumes  $\sim$ 100 mm<sup>3</sup>; Cohorts: vehicle + isotype control; CD73; A000830 + isotype control; vehicle +  $\alpha$ -PD-1; A000830 +  $\alpha$ -PD-1).

### Results

CD73 expression was high in all subsets of human blood CD8+ T cells, B cells, and Treg, but not Treg-depleted CD4+ T cells. CD39 was broadly expressed on lymphoid and myeloid cells, with highest levels on effector Treg, monocytes, neutrophils, B cells, and activated CD8+ T cells. CD73 expression was higher on C57BL/6 than Balb/c mouse spleen and blood T cells (all subsets). On B and NK cells, CD73 expression was similar between both mouse strains. In Balb/c mice carrying CT26 tumors, CD73 expression in TILs was limited to T cells and MDSC; CD73 expression was increased on CD8+ TIL relative to splenic CD8+ T cells from tumor-bearing mice, and both were higher than in normal splenic CD8+ T cells. Human blood CD8+ T cells exhibit robust CD39 and CD73 activity, which can be blocked by CD39 and CD73 inhibitors, respectively. Mouse spleen CD8+ T cells also showed a lower but detectable level of CD39 and CD73 activity. Plasma AMP:adenosine ratios were  $\sim$ 15X higher in CD73 KO than in gender- and age-matched WT mice. Similarly, plasma AMP:adenosine ratios were increased in WT mice dosed with a CD73 inhibitor. Administration of a novel small-molecule CD73 inhibitor (A000830) to CT26 tumor-bearing mice resulted in significant reduction in tumor

## Tumor Microenvironment

Presenting author underlined; Primary author in italics

volume, with an even larger effect observed in combination with  $\alpha$ -PD-1. Co-administration of A000830 with  $\alpha$ -PD-1 antibody increased the number of TIL relative to control or single-treatment tumors.

### Conclusions

Syngeneic CT26 colon tumors provide an excellent model to assess the effects of CD73 inhibition on tumor growth and immune infiltration. Plasma levels of AMP/adenosine provide a simple way of monitoring systemic CD73 inhibition.

404

### CD8 $\alpha$ <sup>+</sup> dendritic cells regulate leukemia antigen-specific CD8<sup>+</sup> T cell tolerance

Douglas Kline<sup>1</sup>, Xiufen Chen<sup>2</sup>, Dominick Fosco<sup>2</sup>, Justin Kline<sup>3</sup>

<sup>1</sup>Committee on Immunology, University of Chicago, Chicago, IL, USA

<sup>2</sup>Department of Medicine, University of Chicago, Chicago, IL, USA

<sup>3</sup>Committee on Immunology and Department of Medicine, University of Chicago, Chicago, IL, USA

### Background

*Batf3*-lineage CD8 $\alpha$ <sup>+</sup> and CD103<sup>+</sup> dendritic cells (DCs) are required for the spontaneous priming of CD8<sup>+</sup> T cells against solid tumors. In contrast, the APCs that regulate immune responses against hematological malignancies have not been characterized. Syngeneic transplantable and genetically-engineered acute myeloid leukemia (AML) models associated with a dense CD8<sup>+</sup> T cell tolerant state were employed to identify the APCs responsible for inducing T cell tolerance *in vivo*.

### Methods

Transplantable C1498 and genetically-engineered *Mx1-Cre* x LSL<sup>*AML1-ETO*<sup>+/+</sup></sup> x *FLT3*<sup>*ITD/ITD*</sup> x *R26-LSL*<sup>*SIV*<sup>+/+</sup></sup> (MAFFS) AML models were employed to characterize APCs involved in generating leukemia-specific CD8<sup>+</sup> T cell tolerance.

### Results

Following systemic introduction of viable, CellTrace violet-labeled AML cells, leukemia cell-derived fluorescence was observed exclusively within splenic CD8 $\alpha$ <sup>+</sup> DCs, whereas uptake of proteins from dead AML cells was mediated by CD11b<sup>+</sup> macrophages. CD8 $\alpha$ <sup>+</sup> DCs were also uniquely capable of cross-presenting leukemia antigens to CD8<sup>+</sup> T cells directly *ex vivo*. Interestingly, antigen encounter by leukemia-specific CD8<sup>+</sup> T cells was severely reduced in *Batf3*<sup>-/-</sup> mice, indicating that CD8 $\alpha$ <sup>+</sup> DCs mediate T cell recognition of leukemia antigens, and that their absence is associated with immunological ignorance of AML antigens. Moreover, leukemia-specific CD8<sup>+</sup> T cells in wildtype AML-bearing mice failed to respond following vaccination with the tolerizing

antigen, while those in leukemia-bearing *Batf3*<sup>-/-</sup> mice expanded vigorously, demonstrating that CD8 $\alpha$ <sup>+</sup> DCs induce leukemia-specific tolerance *in vivo*. Activation of CD8 $\alpha$ <sup>+</sup> DCs with the TLR-3 agonist, poly(I:C) restored functional anti-leukemia T cell responses and protected mice from disease progression in a *Batf3*-dependent manner. RNA-seq analysis of "tolerogenic" versus "naive" CD8 $\alpha$ <sup>+</sup> DCs from leukemia-bearing mice revealed ~200 differentially expressed genes in the former, suggesting that tolerance induction by CD8 $\alpha$ <sup>+</sup> DCs is an active process.

### Conclusions

Our data support a growing body of evidence that has defined a prominent role for *Batf3*-dependent DCs in regulating anti-cancer immune responses. *Batf3*-lineage DCs generate functional CD8<sup>+</sup> T cell responses against solid tumors, but actively and exclusively induce CD8<sup>+</sup> T cell tolerance to systemic leukemia, indicating that the same DC lineage can imprint disparate T cell fates in mice with solid versus hematopoietic malignancies, and suggesting that environmental cues perceived by CD8 $\alpha$ <sup>+</sup> DCs may dictate their ability to activate or tolerize cancer-specific CD8<sup>+</sup> T cells. These results highlight stark differences in the regulation of anti-cancer immunity in hosts with solid versus hematological malignancies.

405

### WISP1 stimulates melanoma cell invasion by promoting epithelial-mesenchymal transition (EMT) through both autocrine and paracrine signaling

Wentao Deng, David John Klinke

West Virginia University, Morgantown, WV, USA

### Background

A dire prognosis is associated with the metastasis of human melanoma. Melanoma invasion and metastasis is coordinated by soluble signals present within the tumor microenvironment. One soluble signal is WNT1 inducible signaling pathway protein 1 (WISP1), a secreted matricellular protein that is elevated in a variety of cancers. Functionally, *Wisp1* is secreted in response to disruption of adherens junctions [1], such as occurs during invasion, but also represses anti-tumor immunity through a paracrine mechanism [2]. Here, our goal was to parse autocrine, that is the impact on intrinsic tumor cell behavior, from paracrine, that is a mediator of intercellular communication, effects of WISP1 on tumor growth.

### Methods

*Wisp1* in mouse melanoma B16 cells was knocked out using the CRISPR/Cas9 system to evaluate its role in melanoma progression and metastasis using *in vitro* and *in vivo* assays. We also knocked out or over-expressed *Wisp1* in mouse





## Tumor Microenvironment

Presenting author underlined; Primary author in italics

fibroblasts to compare the autocrine and paracrine effects on *in vitro* tumor cell invasion assays using fibroblast conditioned medium.

### Results

*In vitro*, Wisp1 disruption increased tumor cell proliferation and anchorage-independent growth but repressed its wound healing, migration and invasion. *In vivo*, B16 cells without Wisp1 exhibited a lower propensity for spontaneous metastasis to the lung. With Wisp1 knockout, certain epithelial–mesenchymal transition (EMT) markers were down-regulated. This suppression could be partially rescued by supplementation of Wisp1, suggesting an autocrine mechanism of Wisp1 for EMT gene activation and enhanced tumor invasion. Further work with multiple metastatic melanoma lines using conditional medium from mouse fibroblast NIH3T3 cells with Wisp1 knockout or over-expression also supported a paracrine scenario in which fibroblast-secreted Wisp1 promotes tumor invasion. Wisp1 from fibroblasts activated both Akt and MEK/ERK signaling, repressed E-cadherin, and upregulated certain EMT genes. Kinase inhibition confirmed the importance of both pathways for EMT gene regulation.

### Conclusions

Collectively, the results support a pleiotropic regulation of melanoma invasion and metastasis by WISP1 through directly induction of EMT in tumor cells and indirect promotion of tumor invasion by fibroblasts within the tumor microenvironment.

### References

1. Klinke DJ, Horvath N, Cuppett V, Wu Y, Deng W, Kanj R: **Interlocked positive and negative feedback network motifs regulate  $\beta$ -catenin activity in the adherens junction pathway.** *Mol Biol Cell* 2015, **26**:4135-4148.
2. Kulkarni YM, Chambers E, McGray AJR, Ware JS, Bramson JL, Klinke DJ: **A quantitative systems approach to identify paracrine mechanisms that locally suppress immune response to Interleukin-12 in the B16 melanoma model.** *Integr Biol (Camb)* 2012, **4**:925-936.

406

### **Jak/STAT signaling as a mediator of immune suppression from pancreatic stellate cells in vitro and caerulein-induced pancreatitis in vivo**

Hannah M Komar<sup>1</sup>, Thomas Mace<sup>1</sup>, Gregory Serpa<sup>1</sup>, Omar Elnaggar<sup>1</sup>, Darwin Conwell<sup>1</sup>, Philip Hart<sup>2</sup>, Carl Schmidt<sup>2</sup>, Mary Dillhoff<sup>2</sup>, Ming Jin<sup>2</sup>, Michael C Ostrowski<sup>1</sup>, Gregory B Lesinski<sup>1</sup>

<sup>1</sup>The Ohio State University, Columbus, OH, USA

<sup>2</sup>The Ohio State University Wexner Medical Center, Columbus, OH, USA

### Background

Pancreatic stellate cells (PSC) are implicated in the pathogenesis of pancreatic ductal adenocarcinoma (PDAC) and chronic pancreatitis (CP). These cells orchestrate fibrosis and contribute to immune suppression in the PDAC microenvironment. As such, PSC may facilitate resistance to immunotherapy. Soluble factors from these cells can activate inflammatory Jak/STAT and MAPK signaling in an autocrine and paracrine manner. We hypothesized that inhibiting the Jak/STAT or MAPK pathways may limit features of inflammation and immune suppression in the diseased pancreas.

### Methods

*In vitro* studies utilized immortalized PSC lines, and primary PSC from patients with CP and PDAC. Cytokine/chemokine expression was analyzed in supernatants via multiplex immunoassay. PSC supernatants were utilized to generate functionally suppressive MDSC *in vitro*. PSC were treated with ruxolitinib (Jak1/2 inhibitor), or MEK162 (MEK inhibitor) purchased commercially. Cell viability was assessed via MTT assay. Immunoblot analysis was utilized to evaluate the effect of inhibitors on STAT3, MAPK, and apoptotic pathways. To model pancreatic inflammation, we used the well-characterized *in vivo* model of caerulein-induced pancreatitis. This involved 6 hourly intraperitoneal injections of 50 $\mu$ g/kg caerulein 3 days/week for 5 weeks. During the final week of caerulein, mice received oral gavage of ruxolitinib at 90mg/kg 2X/day. Pancreata from these mice were stained for H&E, Masson's Trichrome, and  $\alpha$ SMA.

### Results

All PSC displayed constitutive activation of Jak/STAT and MAPK pathways. PSC supernatants contained robust levels of soluble factors including MCP-1, IL-6, and VEGF (up to 31,000, 19,000, and 800 pg/mL, respectively). Culture of PBMC from healthy human donors with PSC supernatants promoted differentiation of MDSC (CD33<sup>+</sup>CD11b<sup>+</sup>HLADR<sup>lo</sup>) that functionally suppressed proliferation of autologous, CD3/CD28-stimulated T cells. This effect was blocked by adding IL-6 neutralizing antibody or STAT3 inhibitor to culture media, indicating a role for IL-6/STAT3 signaling in PSC-derived immune suppression. Treatment of PSC with ruxolitinib reduced STAT3 phosphorylation, decreased growth (40% growth after 72 hours) but did not induce apoptosis. Instead, PSC exhibited a dose-dependent decrease in  $\alpha$ SMA, a marker of PSC activation. In contrast, treatment with MEK162 had no effect on growth or activation. In a murine model of caerulein-induced inflammation and pancreatitis, short-term ruxolitinib treatment resulted in significantly less acinar loss and fibrosis.



## Tumor Microenvironment

Presenting author underlined; Primary author in italics

### Conclusions

These data suggest that the Jak/STAT pathway promotes immune suppressive features via stellate cells in the pancreatic microenvironment. These findings support future studies whereby Jak/STAT inhibition may reduce desmoplasia and augment the response to immunotherapy.

407

### Role of STAT1 induced CXCL10 in tumor progression and the immune microenvironment of high-grade grade serous ovarian cancer

Madhuri Koti, Katrina Au, Nichole Peterson, Peter Truesdell, Gillian Reid-Schachter, Charles Graham, Andrew Craig, Julie-Ann Francis

Queen's University, Kingston, ON, Canada

### Background

We previously reported the presence of a STAT1 associated distinct T helper type I tumor immune microenvironment (TME) associated with chemotherapy response in high-grade serous ovarian cancer in a cohort of chemotherapy naïve tumors from 734 patients. We also demonstrated that STAT1 enhanced the prognostic relevance of cytotoxic tumor infiltrating T lymphocytes. The current study was performed with an aim to elucidate the role of STAT1 induced CXCL10 in HGSC tumor immune microenvironment in the established ID8 mouse model of HGSC.

### Methods

ID8 mouse ovarian cancer cells were transduced with lentiviral constructs to overexpress CXCL10. *In vitro* cell proliferation and migration assays were performed to determine cancer cell intrinsic effects of increased CXCL10 expression. For *in vivo* studies, the CXCL10 overexpressing and control ID8 cells were implanted via intra-peritoneal injection into immunocompetent C57BL/6 mice. Ascites samples collected at each endpoint were subjected to multiplex cytokine analysis using a mouse 31-plex assay. RNA isolated from tumor tissues was subjected to immune transcriptome profiling using the NanoString mouse pan cancer immune profiling panel consisting of over 500 immune and 40 reference genes. The effect of CXCL10 on the tumor vasculature of HGSC TME was evaluated by CD31 immunofluorescence staining.

### Results

A significant decrease in tumor progression and metastatic tumor nodule formation in mice injected with ID8 CXCL10 overexpressing cells compared to those with ID8 vector control cells was observed. Multiplex cytokine analysis of malignant ascites showed differential expression of IL-6, VEGF and CXCL9 between the two groups. CD31 endothelial cell marker staining showed differences in tumor vasculature

between the two groups. Immune transcriptomic profiling of tumors from both groups identified distinct expression profiles in genes associated with cytokines, chemokines, interferons, T cell function and apoptosis between the two groups.

### Conclusions

Our findings provide evidence that the differential expression of CXCL10 in HGSC tumors potentially contributes to altering tumor progression and associated tumor immune microenvironment. Findings from this study provide the basis for future studies aimed at understanding mechanisms underlying differential tumor STAT1 and CXCL10 expression and its role in pre-existing tumor immunologic diversity and aid in design of novel immunomodulatory therapies in HGSC.

### Acknowledgements

Funding for the study was provided by the Cancer Research Society.

408

### Pre-implantation factor (PIF) – blocks proliferation and enhances tumor footprint in cultured human metastatic melanoma lymph nodes – translational aspects

Beatrix Kotlan<sup>1</sup>, Timea Balatoni<sup>1</sup>, Emil Farkas<sup>1</sup>, Laszlo Toth<sup>1</sup>, Mihaly Ujhelyi<sup>1</sup>, Akos Savolt<sup>1</sup>, Zoltan Doleschall<sup>1</sup>, Szabolcs Horvath<sup>1</sup>, Klara Eles<sup>1</sup>, Judit Olasz<sup>1</sup>, Orsolya Csuka<sup>1</sup>, Miklos Kasler<sup>1</sup>, Gabriella Liszky<sup>1</sup>, Eytan Barnea<sup>2</sup>

<sup>1</sup>National Institute of Oncology, Budapest, Hungary

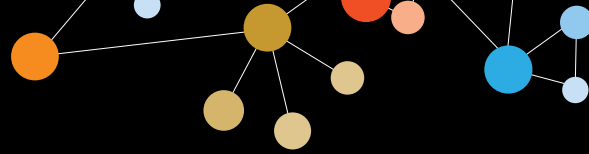
<sup>2</sup>BioIncept, Cherry Hill, NJ, USA

### Background

Embryonic and cancer cell phenotypes share common features. Whereas during embryogenesis proliferation/differentiation is regulated, in cancer altered programming leads to invasion and immortality. Our premise is that embryo-derived, immune-regulatory PIF regulates this process. Synthetic PIF peptide transposes endogenous regulatory features in clinically-relevant models and is in FDA fast track clinical trial for autoimmune disease (NCT02239562). Having shown that PIF reduces metastatic melanoma (NSG/H199 model), human melanoma cultures were examined, towards its translation to therapeutic use.

### Methods

Following ethical committee approval (ETT TUKEB 1642-02/2010), minor tissue samples from surgically removed lymph nodes of patients with metastatic melanoma were investigated. Effect on proliferation was examined in cell cultures with or without PIF and further analyzed by molecular and immunological assays.



## Tumor Microenvironment

Presenting author underlined; Primary author in italics

### Results

PIF treatment (250 nm) delayed tumor outgrowth in a time-dependent manner in the 8 investigated cultures. Importantly, PIF increased the expression of disialylated glycosphingolipid tumor associated antigens in melanoma cells in the majority of the tested cases, as evidenced by immunofluorescence FACS cell sorting and confocal laser microscopy (enhanced footprint). Assessment of PIF effect on tumor associated changes in gene expression is ongoing.

### Conclusions

PIF reduces proliferation and may directly or indirectly promote glycosphingolipid-type tumor associated antigen expression. By this enhanced tumor footprint visibility, PIF may help trigger immune-improved anticancer response. Overall, PIF use for tumor targeting and improved antigen expression may facilitate cancer treatment.

### Acknowledgements

HJLCT Melanoma Research Award 2010, Fulbright Research Grant No: 1214104/2014, BioIncept LLC sPIF (proprietary).

### References

1. Perry JK, Lins RJ, Lobie PE, Mitchell MD: **Regulation of invasive growth: similar epigenetic mechanisms underpin tumour progression and implantation in human pregnancy.** *Clin Sci* 2009, **118**:451- 457.
2. Shainer R, Almogi-Hazan O, Berger A, *et al*: **PIF Provides Comprehensive Protection against Radiation Induced Pathologies.** *Oncotarget* 2016, DOI:10.18632/oncotarget.10635.
3. Kotlan B, Liskay G, Blank M, Csuka O, Balatoni T, Toth L, *et al*: **The novel panel assay to define tumor-associated antigen-binding antibodies in patients with metastatic melanomas may have diagnostic value.** *Immunol Res* 2015, **61**:11–23.
4. Mueller M, Zhou J, Yang L, Gao Y, Wu F, Schoeberlein A, *et al*: **Preimplantation Factor Promotes Neuroprotection by Targeting microRNA Let-7.** *Proc Natl Acad Sci USA* 2014, **111**(38):13882-13887.

## 409

### PD-L1 expressing myeloid cells limit response to CSF-1R targeted therapy

Sushil Kumar<sup>1</sup>, Takahiro Tsujikawa<sup>1</sup>, Collin Blakely<sup>2</sup>, Patrick Flynn<sup>1</sup>, Reid Goodman<sup>1</sup>, Raphael Bueno<sup>3</sup>, David Sugarbaker<sup>4</sup>, David Jablons<sup>5</sup>, V Courtney Broaddus<sup>2</sup>, Brian West<sup>6</sup>, Lisa M Coussens<sup>1</sup>

<sup>1</sup>Oregon Health & Science University, Portland, OR, USA

<sup>2</sup>University of California, San Francisco School of Medicine, San Francisco, CA, USA

<sup>3</sup>Brigham and Women's Hospital, Boston, MA, USA

<sup>4</sup>Baylor Clinic, Houston, TX, USA

<sup>5</sup>UCSF Helen Diller Family Comprehensive Cancer Center, San Francisco, CA, USA

<sup>6</sup>Plexxikon Inc., Berkeley, CA, USA

### Background

Malignant mesothelioma (MM) is an inflammation-associated cancer that is markedly resistant to “standard-of-care” chemotherapy with extremely poor prognosis.

### Methods

We utilized MM patient biopsies and an immunocompetent MM mouse model to investigate the role of tumor-infiltrating leukocytes in regulating response to therapy.

### Results

We report herein that chemotherapy leads to increased frequency of colony stimulating factor-1 receptor (CSF-1R)<sup>+</sup> macrophages in human MM, as well as in an immunocompetent mouse model of MM. While therapeutic blockade of CSF-1R instigated activation of CD8<sup>+</sup> T cells in primary tumors resulting in ~50% decreased primary tumor burden, combined therapy did not improve animal survival as therapy failed to reduce pulmonary metastasis. To investigate mechanisms underlying the tissue-specific response to combined chemo/CSF1R inhibition, we identified programmed death ligand 1 (PD-L1) as an abundant immune checkpoint molecule expressed by alveolar macrophages in lung metastases. Based on this, we hypothesized that combination blockade of PD-L1 with CSF-1R would improve survival by driving CD8<sup>+</sup> T cell activation and cytotoxicity in both primary and metastatic tumors thereby extending survival and improving outcome. Indeed, combination therapy using CSF-1R/PD-L1 inhibitors enhanced activated CD8<sup>+</sup> T cell frequency and further reduced tumor burden at both primary and metastatic sites resulting in increased animal survival. Activated CD8<sup>+</sup> T cells, in both primary and metastatic tumors, exhibited biomarkers of “reinvigoration” marked by co-expression of Ki-67 with PD-1 and EOMES. CD8<sup>+</sup> T cells were essential for therapeutic benefit of CSF-1R/PD-L1 combination therapy since their depletion subverted therapy response.

## Tumor Microenvironment

Presenting author underlined; Primary author in italics

### Conclusions

Tissue-specific tumor niches pose distinct requirements for generating adaptive immune responses and/or perturbing/abrogating tumor growth. Results from these studies highlight a rationale for combination therapy where individual constituents target different immunosuppressive microenvironments to impact BOTH primary tumor responses as well as thwarting secondary tumor growth.

### Acknowledgements

SK acknowledges support from the OHSU Knight Cancer institute and Collins Medical Trust. LMC acknowledges support from the NIH/NCI, DOD BCRP Era of Hope Scholar Expansion Award, Susan G. Komen Foundation, Stand Up To Cancer – Lustgarten Foundation Pancreatic Cancer Convergence Dream Team Translational Research Grant, Breast Cancer Research Foundation, and the Brenden-Colson Center for Pancreatic Health.

### 410

#### CD56+ cell infiltration correlates with a worse prognosis in cholangiocarcinoma

Paul R Kunk<sup>1</sup>, Joseph M Obeid<sup>1</sup>, Kevin Winters<sup>1</sup>, Patcharin Pramoonjago<sup>1</sup>, Mark E Smolkin<sup>2</sup>, Edward B Stelow<sup>1</sup>, Todd W Bauer<sup>1</sup>, Craig L Slingluff Jr<sup>3</sup>, Osama E Rahma<sup>4</sup>

<sup>1</sup>University of Virginia, Charlottesville, VA, USA

<sup>2</sup>Department of Public Health Sciences, University of Virginia, Charlottesville, VA, USA

<sup>3</sup>Division of Surgical Oncology, University of Virginia, Charlottesville, VA, USA

<sup>4</sup>Dana Farber Cancer Institute/Harvard University, Boston, MA, USA

### Background

Cholangiocarcinoma (CC) is an uncommon malignancy increasing in incidence and characterized by rapid progression. The tumor immune microenvironment (TME) has been extensively studied in a variety of cancers, but characterization of the CC TME is not well understood. We aimed to perform a comprehensive analysis of the TME of CC in order to identify new potential immunotherapy targets.

### Methods

A retrospective analysis was conducted of CC tumor samples at the University of Virginia from 2000-2014. Tissue microarrays (TMAs) were constructed of 3-4 cores from each tumor and were stained by immunohistochemistry (IHC) for a number of immune cells and markers of immune activation or inhibition (17 total). These were grouped into a positive effector signal (CD4, CD8, CD14, CD40, CD45, CD45RO, CD56, CD68, CD69, CD83, granzyme, and OX40) and a negative suppressor signal (FoxP3, CD163, TIM3, LAG3, and IDO). TMAs were scanned using the Leica SCN400 and was

analyzed using the Digital Image Hub software. Stain intensity thresholds for determining positive cells were determined by two users and recorded as an average of all cores from each tumor. Correlation with overall survival was assessed using Cox-proportional hazard with p-values < 0.05 being considered as statistically significant.

### Results

Ninety-nine CC tumors were available for analysis. Median age was 68 years old with 26 intrahepatic, 37 hilar and 36 distal CC. In univariate analysis, increasing CD56<sup>+</sup> (HR: 1.75; CI: 1.24-2.46), p+ (HR: 1.07; CI: 1.02-1.12, p=0.007) infiltrations significantly correlated with worse survival. CD163<sup>+</sup> infiltration trended towards a significant decrease in survival (HR: 1.19; CI: 0.9-1.43, p=0.06) while CD40<sup>+</sup> infiltration trended towards a significant increase in survival (HR: 0.66; CI: 0.42-1.05, p=0.08).

### Conclusions

CD56<sup>+</sup> cell infiltration into cholangiocarcinoma correlates with a worse prognosis. Further studies including a multivariate analysis and multicolored IHC are planned to better understand to the role of CD56<sup>+</sup> cells in CC.

### 411

#### Defining the immune microenvironment in patients with acute myeloid leukemia

Adam Lamble<sup>1</sup>, Yoko Kosaka<sup>1</sup>, Fei Huang<sup>2</sup>, Kate A Saser<sup>2</sup>, Homer Adams<sup>2</sup>, Christina E Tognon<sup>1</sup>, Ted Laderas<sup>1</sup>, Shannon McWeeney<sup>1</sup>, Marc Loriaux<sup>1</sup>, Jeffery W Tyner<sup>1</sup>, Brian J Druker<sup>3</sup>, Evan F Lind<sup>1</sup>

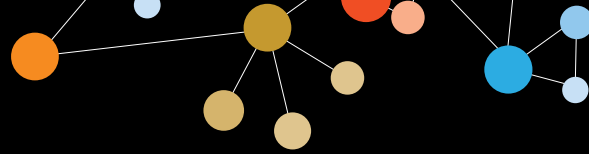
<sup>1</sup>Oregon Health & Science University, Portland, OR, USA

<sup>2</sup>Janssen Pharmaceutical R&D, Spring House, PA, USA

<sup>3</sup>Knight Cancer Institute/ Howard Hughes Medical Institute, Portland, OR, USA

### Background

The aim of our project is to identify the phenotypic and functional status of immune cells in the bone marrow of patients with acute myeloid leukemia (AML). The goal of the immunophenotyping is to identify the relevant myeloid and lymphoid cell subsets present in the marrow of patients with AML, understand their differentiation and activation status, and to quantify the density of immune modifiers on cells of interest. The goal of the functional assays is to further define the status of T cells in the AML microenvironment by evaluating the responsiveness of these cells to stimulation. Additionally, these studies assess the impact of costimulatory or immune checkpoint inhibitors on the proliferative and cytokine production capacity of T cells, as well as tumor cells, resident in AML bone marrow.



## Tumor Microenvironment

Presenting author underlined; Primary author in italics

### Methods

Immunophenotyping was performed using mass cytometry (CyTOF). Primary AML bone marrow samples were stained with four distinct antibody panels to identify the status of over 70 cell surface and intracellular proteins and cytokines. Functional assays measured both the proliferative capacity and cytokine production profile of AML bone marrow T cells in response to CD3 stimulation in the context of the tumor microenvironment. Analysis of the changes to the baseline T cell functional profile in the presence of various checkpoint inhibitors and immune stimulatory antibodies was measured.

### Results

Our initial studies have begun to identify the major myeloid and lymphoid subsets present in the marrow of patients with AML with a focus on the detailed description of T cell subsets and activation status. We have identified the cellular expression of various immune checkpoint proteins and inhibitory cytokines on both myeloid and lymphoid cellular subsets. The functional studies have identified a subset of AML patient samples where T cells are impaired in their ability to proliferate in response to CD3 ligation. We have found differential effects of several immune checkpoint inhibitor antibodies on T cell proliferation and cytokine production.

### Conclusions

These results provide the beginning of a functional and phenotypic description of the immune status in the marrow of patients with AML. We have identified potential immune targets in AML. This is a report of initial findings of our study; accrual of patient samples is ongoing to expand the power of our observations.

412

### **Tim-3+CD4+CD25hiFOXP3+ regulatory T cells underlies enhanced suppressive function in HNSCC patients**

Zhuqing Liu<sup>1</sup>, Shanhong Lu<sup>1</sup>, Lawrence P Kane<sup>2</sup>, Robert L Ferris<sup>3</sup>

<sup>1</sup>University of Pittsburgh Medical Center, Hillman Cancer Center, Pittsburgh, PA, USA

<sup>2</sup>Department of Immunology, University of Pittsburgh, Pittsburgh, PA, USA

<sup>3</sup>University of Pittsburgh, Pittsburgh, PA, USA

### Background

Regulatory T (Treg) cells are essential for maintenance of immune homeostasis, and are important suppressive cells among tumor infiltrating lymphocytes (TIL). Tim-3 was first identified on Th1 T cells as a negative regulator of type 1 immunity. Tim-3 can also be expressed by some Tregs, but the functional status of human Tregs expressing Tim-3 remains unclear.

### Methods

Treg were sorted from fresh HNSCC TIL based on Tim-3 expression. Gene expression profiling and NanoString RNA analysis were used to compare differences between these populations. Functional and phenotypic features of Tim-3<sup>+</sup> and Tim-3<sup>-</sup> Treg in freshly isolated HNSCC patient TILs were tested by multi-color flow cytometry.

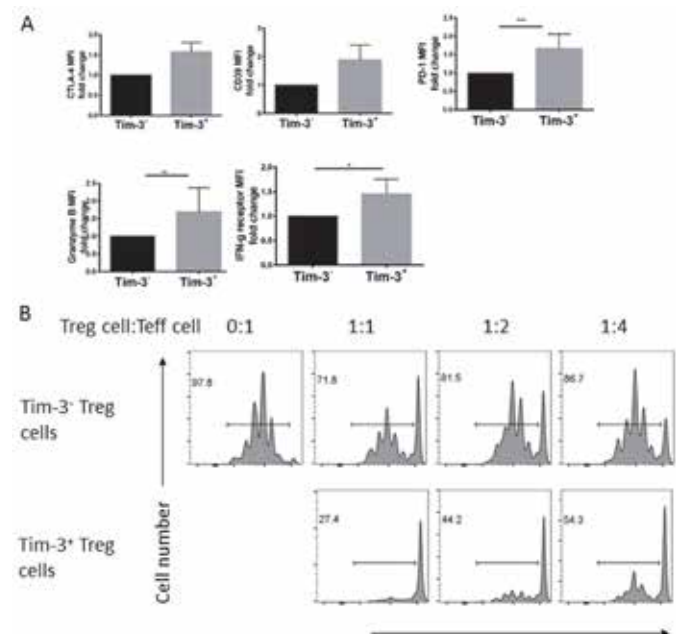
### Results

Tim-3<sup>+</sup> Treg from human HNSCC TIL display a more effector-like phenotype, based on gene expression profiling and NanoString analysis. Compared with Tim-3<sup>-</sup> Treg, Tim-3<sup>+</sup> Treg exhibited more robust expression of CD39, CTLA-4, PD-1, granzyme B, IFN- $\gamma$  receptor and IFN- $\gamma$  by flow cytometry. Despite this phenotype, Tim-3<sup>+</sup> TIL Treg displayed a greater capacity for inhibiting naïve CD8<sup>+</sup> T cell proliferation and subsequent cytokine production than Tim-3<sup>-</sup> Treg. In addition, suppression mediated by Tim-3<sup>+</sup> Treg was partially reversed by exogenous IFN-g treatment.

### Conclusions

Tim-3 expression on HNSCC TIL Treg cells identifies a phenotypically and functionally distinct population of cells that is highly effective in inhibiting T cell proliferation and cytokine production. Induction of IFN-g by successful immunotherapy may overcome suppressive features of this Treg population. Anti-Tim-3 directed therapies may yield immunotherapeutic benefits.

Figure 1.



\* p<0.05, \*\* p<0.01, \*\*\* p<0.001 Data expressed as mean  $\pm$  standard deviation (SD).

## Tumor Microenvironment

Presenting author underlined; Primary author in italics

413

### PD-1+/OX40+ Tregs in head and neck squamous cell cancer suppress responder T cell responses

Zhuqing Liu<sup>1</sup>, Gulidanna Shayan<sup>1</sup>, Shanhong Lu<sup>1</sup>, Robert L Ferris<sup>2</sup>

<sup>1</sup>University of Pittsburgh Medical Center, Hillman Cancer Center, Pittsburgh, PA, USA

<sup>2</sup>University of Pittsburgh, Pittsburgh, PA, USA

#### Background

FOXP3<sup>+</sup> regulatory T cells (Tregs) are central for the maintenance of self-tolerance and are important suppressive components in the tumor microenvironment. The aim of this study was to investigate the phenotypic and functional characteristics of tumor infiltrating lymphocytes (TIL) with multiple immune checkpoint receptor expression, including PD-1 and OX40, directly from head and neck squamous carcinoma (HNSCC) tumors.

#### Methods

Lymphocytes were extracted from freshly excised HNSCC tumors and matched peripheral blood. Flow cytometry was conducted using HNSCC lymphocytes and *in vitro* functional assays were performed using sorted TIL or circulating T cells.

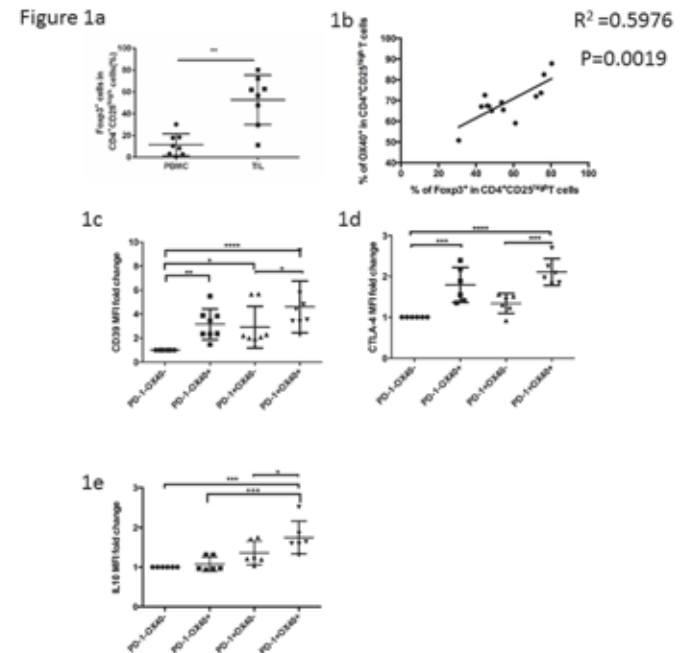
#### Results

CD4<sup>+</sup>CD25<sup>hi</sup>FOXP3<sup>+</sup> Tregs were more frequent in HNSCC TIL vs PBL (52.7% vs 11.5% of CD4<sup>+</sup>CD25<sup>hi</sup> immune infiltrate, n=10) (Figure 1a). HNSCC Tregs expressed significantly higher levels of OX40 (70.8% of FOXP3<sup>+</sup> cell population, n=10 tumors) and PD-1 (26.6%, n=9) than Tregs from peripheral blood (p=0.01). We found a significant positive correlation (p+CD25<sup>high</sup>) (Figure 1b). Double-positive (PD-1<sup>+</sup>OX40<sup>+</sup>) TIL Tregs had a more suppressive phenotype than single-positive (PD-1<sup>+</sup> or OX40<sup>+</sup>) TIL Tregs (Figure 1c, 1d), including the ability to proliferate and to express IL-10 and TGF- $\beta$ -associated LAP (Figure 1e). Double-positive (PD-1<sup>+</sup>OX40<sup>+</sup>) TIL Tregs also significantly inhibited effector T cells. Triggering OX40 with the an agonistic mAb (MEDI0562) overcame the suppression exerted by Tregs, leading to increased effector CD4<sup>+</sup> or CD8<sup>+</sup> T cell proliferation.

#### Conclusions

These findings contribute to ongoing efforts to improve PD-1 or OX40-based immunotherapy in HNSCC patients, and suggest that dual targeting of these pathways may reverse suppressive function of Tregs in the clinic.

Figure 1.



\* p<0.05, \*\* p<0.01, \*\*\* p<0.001, \*\*\*\* p<0.0001 Data expressed as mean  $\pm$  standard deviation (SD).

414

### Lymphatic vessels as biomarkers of in situ immunity in melanoma

Julia Femel, Takahiro Tsujikawa, Ryan Lane, Jamie Booth, Amanda W Lund

Oregon Health & Science University, Portland, OR, USA

#### Background

Lymphatic vessel remodeling is correlated with melanoma progression and lymph node metastasis. While lymphatic vessels provide an important route for disseminating tumor cells, their role in responding to immunological challenge has yet to be appreciated with respect to tumor progression. We recently published that in the absence of dermal lymphatic vessels, the tumor microenvironment of murine melanoma remains completely uninfamed and fails to induce a robust T cell response. Consistently, in an analysis of human cutaneous metastatic melanoma (TCGA), we identified positive correlations between lymphatic endothelial cell gene expression and immune genes suggesting a relationship between lymphatic vessel remodeling and local immunity. We therefore hypothesize that lymphatic vessels are a biomarker of *in situ* immune responsiveness and response to therapy.

#### Methods

In this work, we present the simultaneous evaluation of immune and vascular components in human primary





## Tumor Microenvironment

Presenting author underlined; *Primary author in italics*

melanoma samples using a multiplex-immunohistochemistry-based approach. We have optimized a staining panel for simultaneous detection of 10 biomarkers (S-100, CD8a, CD68, CD31, D2-40, Lyve1, Prox1, FasL, PD-L1, PD-1) within a single FFPE section. Tissue regions that include tumor/stroma borders and show high CD8<sup>+</sup> T cell infiltrates are selected for analysis, followed by tissue segmentation and automated detection of cell populations within intra-tumoral regions and stroma. We have identified a cohort of 18 human primary cutaneous melanomas with clinical annotation for protocol optimization and validation of hypotheses.

### Results

Multiplexed immunohistochemistry of the validation cohort has identified poorly inflamed and inflamed primary melanomas. Interestingly, those tumors with enhanced hematopoietic infiltrate (CD68 and CD8) also appear to demonstrate increased vasculature, both blood and lymphatic. Preliminary data demonstrates that lymphatic vessels, blood vessels and CD8<sup>+</sup> T cells are enriched in stroma, while CD68<sup>+</sup> cells are homogeneously distributed throughout tissue. Furthermore, blood and lymphatic endothelial cells are positively correlated in stroma as are, interestingly, intratumoral CD8<sup>+</sup> T cells and stromal lymphatic vessels.

### Conclusions

Intratumoral CD8<sup>+</sup> T cells are predictive of survival. Lymphatic vessels, however, are required for transport of antigen-bearing cells to lymph nodes for induction of adaptive immunity and as such may be a prerequisite to antigen-specific T cell infiltrates and the *in situ* anti-tumor response. Our data, across multiple model systems, provides strong experimental evidence to indicate that the lymphatic vasculature is an important, active component of the anti-tumor immune response. Furthermore, lymphatic remodeling and local dysfunction may represent a biomarker to stratify patient response and survival for effective clinical immunotherapy.

415

### **CD103 and CD49a expression on melanoma-derived tumor infiltrating lymphocytes depend on location and a small fraction expresses memory T cell markers**

Marit Melssen<sup>1</sup>, Anthony Rodriguez<sup>1</sup>, Craig L Slingluff Jr<sup>2</sup>, Victor H Engelhard<sup>1</sup>

<sup>1</sup>University of Virginia, Charlottesville, VA, USA

<sup>2</sup>Division of Surgical Oncology, University of Virginia, Charlottesville, VA, USA

### Background

Tissue resident memory (TRM) cells are found in certain peripheral tissues long after resolution of infections that generate them. TRM formation is induced by TGFβ and has

been associated with upregulation of CD103 and CD49a. Interaction of CD103 and CD49a with their respective ligands is thought to allow long term persistence of TRM cells in peripheral tissues. In melanoma patients, increased expression of CD103 and CD49a has been observed on tumor infiltrating lymphocytes (TIL) compared to PBMCs. These phenotypic similarities suggest that a subset of TIL might function as TRM. However, the impact of continuous antigen presentation and/or differential TGFβ expression levels on this property of TIL is currently unknown.

### Methods

For *in vivo* tumor studies C57BL/6 mice were injected with 4x10<sup>5</sup> B16-OVA or B16-F1-shTGFβ/shNEG cells, either subcutaneous or intraperitoneal. Tumors were grown for 14 days, harvested, processed in single cell suspensions and stained for multicolor flow cytometry. Human tumors were recovered from frozen single cell suspensions, counted and stained for multicolor flow cytometry. For *in vitro* studies, bulk splenocytes (OT-1 mice) or PBMC (human normal donor) were cultured for 2-7 days in presence of CD3 and CD28 stimulating antibodies and/or 5 ng/ml recombinant TGFβ.

### Results

Here, we demonstrate that, in murine B16-OVA and human melanoma tumors, CD8<sup>+</sup> TIL co-express CD49a and CD103. Additionally, relative expression of CD49a and CD103 differs on TIL in subcutaneous versus intraperitoneal murine tumors, as well as between skin and small bowel human melanoma metastases. Furthermore, we identified a small subset of CD103<sup>pos</sup> CD8<sup>+</sup> TIL that express CD127 and CD69. However, the majority of CD103<sup>pos</sup> CD8<sup>+</sup> TIL express no CD127. Lastly, we show that, despite established knowledge on the induction of CD103 expression by TGFβ, secretion of this cytokine by tumor cells is not required for CD103 expression.

### Conclusions

Our data indicate that the capacity of T cells to persist in tumors potentially changes based on tumor location, which may be dependent on TGFβ levels. Furthermore, we showed that a small subset of CD103<sup>pos</sup> CD8<sup>+</sup> TIL appear to be authentic TRM, however the majority may be either terminal effectors or inactive, potentially anergic/exhausted, TIL. Taken together, our results raise important questions about the role of CD103 on non-TRM-like TIL and the importance of TGFβ in the establishment of these TIL.

## Tumor Microenvironment

Presenting author underlined; Primary author in italics

### 416 Abstract Travel Award Recipient

#### Cancer promotion and immune tolerance via cancer cell - intrinsic surface expression of GARP

Alessandra Metelli, Bill X Wu, Caroline W Fugle, Rachidi Saleh, Shaoli Sun, Jennifer Wu, Bei Liu, Zihai Li

Medical University of South Carolina, Charleston, SC, USA

#### Background

The role of TGF- $\beta$  in oncogenesis and immune evasion is well recognized [1]. Membrane Latent TGF- $\beta$  is highly expressed on the surface of regulatory T cells and platelets by binding its receptor Glycoprotein-A Repeats Predominant Protein (GARP). Several lines of evidence suggest that GARP enhances the conversion of the membrane Latent TGF- $\beta$  in its active form [2].

#### Methods

We performed an immunohistochemistry evaluation of human breast, prostate, colon, prostate, head and neck cancer tissue microarrays and correlation with disease stage and survival. Analysis of human serum was performed by ELISA. GARP function in metastatic and non-metastatic breast cancer was evaluated by preclinical models where GARP expression was either enforced or knocked down. Therapeutic role of anti-GARP antibody was assessed using metastatic 4T1 breast cancer model.

#### Results

We herein report that GARP is aberrantly expressed by human cancers, including colon, prostate, head and neck, and breast cancer, in addition to a well-characterized murine prostate cancer model. Importantly, expression of GARP inversely correlates with overall survival. We also identified the presence of soluble GARP in prostate cancer patients and observed that the concentration of soluble GARP is higher in cancer patients compared to healthy controls. Through genetic strategies, we found that GARP expression in multiple animal tumor models increases the bioavailability of active TGF- $\beta$ , promoted regulatory T lymphocytes in tumor environment, favored the immune evasion of cancer cells, and contributed to the formation of secondary tumors. Finally, we tested a panel of anti-GARP antibodies, alone and in combination with cyclophosphamide, in a mouse model of mammary carcinoma, and we found that they have significant anti-tumor activity especially by inhibiting the formation of lung metastasis.

#### Conclusions

We conclude that GARP is expressed on several human cancers, and its expression correlates with poor prognosis. Mechanistically, GARP increases the availability of active TGF- $\beta$  that promotes an immune tolerant tumor environment. Based on these observations, we propose

GARP-TGF- $\beta$  as a novel oncogenic axis that can be exploited for diagnosis, prognosis and treatment of cancer.

#### References

1. Derynck R, Akhurst RJ, Balmain A: **TGF-beta signaling in tumor suppression and cancer progression.** *Nat Genet* 2001, **29**:117-129.
2. Tran DQ, *et al*: **GARP (LRRC32) is essential for the surface expression of latent TGF-beta on platelets and activated FOXP3+ regulatory T cells.** *PNAS* 2009, **106**:13445-13450.

### 417

#### Concomitant immune tolerance in mice with tumors at two sites exhibits reciprocal tumor specificity and requires regulatory T cells

Zachary S Morris<sup>1</sup>, Emily I Guy<sup>1</sup>, Clinton Heinze<sup>1</sup>, Jasdeep Kler<sup>1</sup>, Monica M Gressett<sup>1</sup>, Lauryn R Werner<sup>1</sup>, Stephen D Gillies<sup>2</sup>, Alan J Korman<sup>3</sup>, Hans Loibner<sup>4</sup>, Jacquelyn A Hank<sup>1</sup>, Alexander L Rakhmilevich<sup>1</sup>, Paul M Harari<sup>1</sup>, Paul M Sondel<sup>1</sup>

<sup>1</sup>University of Wisconsin School of Medicine and Public Health, Madison, WI, USA

<sup>2</sup>Provenance Biopharmaceuticals Corp., Carlisle, MA, USA

<sup>3</sup>Bristol-Myers Squibb, Princeton, NJ, USA

<sup>4</sup>Apeiron Biologics, Vienna, Austria

#### Background

We reported a cooperative interaction between local radiation (RT) and intratumoral (IT) injection of hu14.18-IL2 immunocytokine (IC, anti-GD2 antibody linked to IL2) in mice bearing a single subcutaneous tumor, resulting in 71% complete regression [1]. However, when two tumors of the same type are present and one is treated with RT and IT-IC, the enhanced response is not seen. The non-treated tumor induces a systemic suppressive effect on the efficacy of RT and IT-IC. We hypothesize that this "concomitant immune tolerance" is a tumor-specific effect of regulatory T cells (Tregs).

#### Methods

C57BL/6 mice were implanted with one or two syngeneic B78(GD2+) melanomas or Panc02(GD2- & GD2+ subclones) pancreatic tumors. Five weeks later, mice were treated at one tumor site with single fraction (12 Gy) RT followed by IT-IC or IT-control IgG (50 $\mu$ g days 6-10 after RT). C57BL/6 DEREG mice were used to test the necessity of Tregs for concomitant immune tolerance by specific depletion using intraperitoneal injection of diphtheria toxin. Tumor volumes were measured and mixed-effect-models were used to estimate and compare the tumor growth curves.

#### Results

In mice bearing single B78(GD2+) or Panc02(GD2+) tumors, combined treatment with RT and IT-IC resulted in markedly

## Tumor Microenvironment

Presenting author underlined; *Primary author in italics*

improved tumor response compared to single modality treatments. In contrast, in mice bearing two B78 tumors or two Panc02 tumors, treatment with RT and IT-IC to the GD2+ tumor did not improve tumor response compared to RT alone. This effect was tumor-specific and was not observed in mice bearing a treated B78 tumor and an untreated distant Panc02(GD2-) tumor or those bearing a treated Panc02(GD2+) tumor and an untreated distant B78(GD2+) tumor. In these mice with two histologically distinct types of tumors, response of the treated tumor to combined RT and IT-IC was similar to that observed in mice bearing a single tumor treated with RT and IT-IC. In mice bearing two B78 tumors, one treated with RT and IT-IC, depletion of Tregs (in DEREG mice or by anti-CTLA-4 IgG2a mAb in C57Bl/6 mice) facilitated a response at the treated tumor comparable to that observed with RT and IT-IC in mice bearing a single B78 tumor.

### Conclusions

Our findings suggest that concomitant immune tolerance is a tumor-specific, Treg-dependent, suppressive effect of distant, untreated tumors on the anti-tumor efficacy of RT and IT-IC treatment of a separate tumor.

### References

1. Morris ZS, *et al*: **In situ tumor vaccination by combining local radiation and tumor-specific antibody**. *Cancer Res* 2016, **76**:3929-3941.

418

### Local but not distant viral infection improves cancer outcomes: implications for cancer immunotherapy

Jenna Newman<sup>1</sup>, Andrew Zloza<sup>2</sup>, Erica Huelsmann<sup>3</sup>, Joseph Brucek<sup>3</sup>, Howard L Kaufman<sup>2</sup>

<sup>1</sup>Rutgers University, New Brunswick, NJ, USA

<sup>2</sup>Rutgers Cancer Institute of New Jersey, New Brunswick, NJ, USA

<sup>3</sup>Rush University, Chicago, IL, USA

### Background

Patients with cancer are at increased risk of infections; however, there is a paucity of information available regarding the effects of concomitant local or distant non-oncogenic infection on cancer and response to therapy. Further, studies interrogating the antigen-specificity of tumor-infiltrating T cells have demonstrated the existence of CD8+ T cells within the tumor that are not specific to the antigens expressed by the tumor. A portion of these CD8+ T cells are specific to antigens expressed by pathogens to which patients are commonly exposed. However, how such cells effect tumor growth is not well understood.

### Methods

Therefore, we challenged C57Bl/6 mice with B16-F10 (10<sup>5</sup>) tumor cells via intradermal injection of the right flank (for tumor growth distal to the infection) or via intravenous injection (for tumor growth local [within the lung] to the infection). B6 mice were infected with influenza (A/H1N1/PR8) expressing OVA<sub>257-264</sub> (FLU-OVA; 10,000 pfu; intranasal administration). Every 2-3 days tumor growth was monitored by caliper measurement and influenza infection was monitored by body weight measurement. Tumors were harvested at various times and analyzed by flow cytometry for OVA-specific CD8+ T cells (representing influenza-specific cells) using tetramer staining. Statistics were determined using the Student's t test and comparisons with P < 0.05 were considered statistically significant.

### Results

Infection of the lung with FLU-OVA expectedly lead to the expansion of CD8+ T cells specific for OVA<sub>257-264</sub> in the lung. Unexpectedly, such infection likewise led to the distal accumulation of OVA<sub>257-264</sub>-specific T cells (up to 23% of all CD8+ T cells; P < 0.01) in the tumor microenvironment (skin of the flank) and accelerated of tumor growth (P < 0.001). Importantly, in the context of B16 melanoma in the lung, infection of the lung with FLU-OVA resulted in reduced B16 melanoma foci compared to no infection (38% reduction; P < 0.01). Melanoma foci were further reduced (81%) in the lung with combination FLU-OVA and PD-1 blocking antibody (P < 0.01).

### Conclusions

Infection local to the tumor site (lung infection in the context of lung melanoma) but not distal to the site (lung infection in the context of skin melanoma) improves cancer outcome. This finding may have implications for viral infections used as immunotherapeutic strategies (including oncolytic viruses), which may demonstrate maximum efficacy when administered local to the tumor and when offsite distant infection is minimized. Further studies utilizing the engagement of pathogen-specific CD8+ T cells in the tumor microenvironment as a novel immunotherapeutic approach are currently underway.

## Tumor Microenvironment

Presenting author underlined; Primary author in italics

419

### **“Enriched-in-renal-carcinoma dendritic cells” (ercDCs) are unique macrophages with a gene signature indicative of immune escape**

*Dorothee Brech*<sup>1</sup>, Tobias Straub<sup>2</sup>, Martin Irmiler<sup>3</sup>, Johannes Beckers<sup>3</sup>, Florian Buettner<sup>4</sup>, Elke Schaeffeler<sup>4</sup>, Matthias Schwab<sup>5</sup>, Elfriede Noessner<sup>6</sup>

<sup>1</sup>Helmholtz Zentrum München, Immunoanalytics-Tissue Control of Immunocytes, Munich, Bayern, Germany

<sup>2</sup>Bioinformatics Core Unit, Biomedical Center, Ludwig-Maximilians-University, Planegg-Martinsried Munich, Bayern, Germany

<sup>3</sup>Helmholtz Zentrum München, Institute of Experimental Genetics, Neuherberg, Bayern, Germany

<sup>4</sup>Dr. Margarete Fischer-Bosch-Institute of Clinical Pharmacology, Stuttgart, Baden-Wuerttemberg, Germany

<sup>5</sup>Dr. Margarete Fischer-Bosch-Institute of Clinical Pharmacology, Stuttgart, University of Tuebingen; Department of Clinical Pharmacology, University Hospital Tuebingen,, Stuttgart, Baden-Wuerttemberg, Germany

<sup>6</sup>Helmholtz Zentrum München, Immunoanalytics-Tissue Control of Immunocytes, Munich, Bayern, Germany

#### **Background**

Clear cell renal cell carcinoma (ccRCC) is considered immunosensitive and tumors typically show a strong immune cell infiltrate. Yet, tumor control is not achieved. Previously, we have described that infiltrating CD8<sup>+</sup> T effector cells and NK cells are unresponsive to stimulation with a signature of anergy and cell cycle arrest [1, 2]. These features were caused by the tumor microenvironment as they were not observed in cells from non-tumor kidney (NKC). Many T cells in the tumor tissue were in close contact with CD209<sup>+</sup> myeloid cells, which is suggestive of intense intercellular communication. Further analysis revealed unusual co-expression of DC and macrophage markers. Those unusual cells were highly enriched in tumor tissue compared to non-tumor kidney cortex (NKC), thus they were referred to as “enriched-in-renal-carcinoma DCs” (ercDCs) [3]. For a deeper understanding of the role which this unusual myeloid subset might play and to potentially identify targets for therapeutic intervention we conducted genome-wide transcriptional profiling of sorted ercDCs.

#### **Methods**

*In situ* analysis using triple-marker immunofluorescence with confocal microscopy; *ex vivo* analysis using polychromatic flow cytometry; cell sorting from ccRCC tissue suspensions and blood; *in vitro* generation of reference myeloid subsets; transcriptional profiling using Affymetrix microarrays; bioinformatics using data from sorted cells and publicly

available repositories, including The Cancer Genome Atlas (TCGA; <http://cancergenome.nih.gov/>).

#### **Results**

ErcDCs were found to strongly express macrophage core genes, macrophage-associated transcription factors and growth factor receptors. They combined characteristics of M1- and M2-macrophages and exhibited a pro-angiogenic and invasive gene expression profile. A unique transcriptional signature could be identified that distinguished ercDCs from all other analyzed myeloid subsets except inflammatory macrophages from ascites of ovarian cancer. Applying the gene signature to TCGA ccRCC expression data (RNA Seq) revealed a significant association between a high ercDC score and advanced tumor grade and shorter patient survival. The gene expression profile contains targets with promise for repolarization of ercDCs into an immunocompetent cell type.

#### **Conclusions**

The transcriptional profile of ercDCs identified them as a unique myeloid subset within the macrophage spectrum. A high ercDC score is associated with poor patient survival. The gene expression profile contains promising targets for intervention.

#### **Acknowledgements**

We appreciate the cooperation with clinicians and pathologists, and express our gratitude to all patients for their tissue donation.

#### **References**

1. Prinz P, *et al*: *J Immunol* 2012, **188**(12):5990-6000.
2. Prinz P, *et al*: *Int J Cancer* 2014, **135**(8):1832-1841.
3. Figel A-M, Brech D, *et al*: *Am J Pathol* 2011, **179**(1):436-451.

420

### **Nano-Pulse Electro-Signaling treatment of murine tumors significantly reduces the percentage of regulatory T cells in the treated tumor**

Snjezana Anand, Amanda McDaniel, John Cha, Darrin Uecker, Richard Nuccitelli

Pulse Biosciences, Burlingame, CA, USA

#### **Background**

Nano-Pulse Electro-Signaling (NPES) refers to the application of ultrashort electric pulses in the nanosecond range and can be used to initiate a variety of cellular responses. This physical treatment is drug-free, non-thermal and highly localized between electrodes. We have previously found that murine cells and tumors exposed to the appropriate NPES can be stimulated to undergo immunogenic apoptosis. When these mice are injected with a challenge secondary



## Tumor Microenvironment

Presenting author underlined; Primary author in italics

tumor they reject that tumor in a CD8-dependent manner. In addition, we can vaccinate a mouse against specific tumors with a sub-dermal injection of NPES-treated tumor cells [1]. We are using flow cytometry to examine changes in the T cell population in the primary and challenge tumor microenvironment before and after NPES treatment.

### Methods

Murine MCA205 fibrosarcoma cells were injected subdermally into syngeneic B6 mice to form a tumor. Once the tumor reached a diameter of 5 mm, we treated it *in vivo* with NPES (1300 pulses, 300 ns, 30 kV/cm). Some of these tumors were removed surgically and dissociated into single cells for analysis by flow cytometry. Others were allowed to undergo apoptosis and three weeks later a challenge tumor was injected into the contralateral flank of the mouse. 2 weeks later, those mice were sacrificed and their spleens and lymph nodes were removed and dissociated for flow cytometry analysis.

### Results

Tumor treatment by NPES results in a significant reduction in both Tregs and CD8+ T cells within the tumor (Figure 1). In contrast, the spleen and lymph nodes of the treated mice had slightly higher levels of Treg and CD8+ T cells than those with untreated tumors. Ongoing flow cytometry studies of the changes in the secondary challenge tumors will be also be presented.

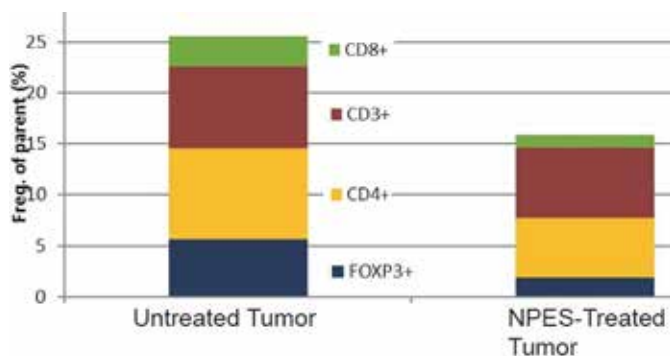
### Conclusions

We conclude that NPES treatment reduces the number of regulatory T cells in the treated primary tumor and are currently examining the changes in the T cell population in challenge tumors.

### References

1. Nuccitelli R, Berridge JC, Mallon Z, Kreis M, Athos B, Nuccitelli P: **Nanoelectroablation of Murine Tumors Triggers a CD8-Dependent Inhibition of Secondary Tumor Growth.** *PLoS One* 2015, **10(7)**:e0134364.

**Figure 1. T cell population in NPES-treated and untreated tumors**



There is a 50% reduction in Tregs in tumors treated with NPES.

### 421

## Targeting colony stimulating factor-1 receptor (CSF-1R) with SNDX-6352, a novel anti-CSF-1R targeted antibody

Peter Ordentlich<sup>1</sup>, Alison Wolfreys<sup>2</sup>, Andre Da Costa<sup>3</sup>, John Silva<sup>2</sup>, Andrea Crosby<sup>2</sup>, Ludovicus Staelens<sup>3</sup>, Graham Craggs<sup>2</sup>, Annick Cauvin<sup>3</sup>, Sean Mason<sup>2</sup>

<sup>1</sup>Syndax Pharmaceuticals, Inc., Waltham, MA, USA

<sup>2</sup>UCB Biopharma, Slough, England, UK

<sup>3</sup>UCB Biopharma, Braine-l'Alleud, Brabant Wallon, Belgium

### Background

CSF-1R is expressed on immunosuppressive tumor associated macrophages (TAMs) that accumulate within the tumor microenvironment. High levels of TAMs correlate with poor prognosis for certain cancers and inhibition of TAMs can enhance anti-tumor immune responses. SNDX-6352 is a humanized IgG4 monoclonal antibody with high affinity against CSF-1R under investigation for the treatment of neoplastic diseases.

### Methods

*In vitro* binding studies, functional cell based assays, and mouse tumor models were utilized to characterize SNDX-6352 and a surrogate rodent antibody, Ab535. Reported toxicology and pharmacodynamics studies for SNDX-6352 were in cynomolgus monkeys.

### Results

SNDX-6352 binds to human CSF-1R (KD 4-8pM, Fc-tagged construct) and cross reacts with cynomolgus monkey CSF-1R but not rodent CSF-1R. SNDX-6352 has been shown to inhibit both CSF-1 (IC<sub>50</sub> 270pM) and IL-34 (IC<sub>50</sub> 100pM) induced MCP-1 release from human monocytes) and the viability of macrophages during tCSF-1-mediated differentiation process *in vitro* (IC<sub>50</sub> 455pM). A dual ligand blocking surrogate rodent antibody, Ab535, was generated for preclinical studies in mice and shown to inhibit tumor growth in colon (MC38), breast (MCF-7, MDA-MB-231) and prostate (PC-3) cancer models and enhance immune checkpoint blockade in the MC38 model. A 13-week toxicology study in cynomolgus monkeys indicated that weekly intravenous administration of SNDX-6352 at 10, 30, and 100 mg/kg was well tolerated. Swelling around the eyes was observed at the mid and high dose groups, occurring from Day 85 onward and may be related to CSF-1R pharmacology, as it has been observed with other anti-CSF-1R molecules, including in clinical trials at supra-therapeutic doses. Other changes were also all related to the mode of action of SNDX-6352. Clinical pathology changes included dose-related increases in aspartate transferase, alanine transferase and glutamate dehydrogenase levels



## Tumor Microenvironment

Presenting author underlined; Primary author in italics

correlating with SNDX-6352 exposure but not translating into histopathological liver changes. These changes resulted from pharmacological inhibition of CSF-1R on Kupffer cells within the liver, which are involved in the clearance of these hepatic enzymes and as such, considered to be non-adverse. Dose-related increases in CSF-1 plasma concentration and decreases in non-classical (CD14+CD16+) monocytes and markers of bone formation and resorption were observed during the treatment phase and were rapidly reversible upon SNDX-6352 clearance. Changes in bone markers were not associated with histological changes or changes in bone densitometry in the context of this study. Upon SNDX-6352 clearance, all parameters rapidly returned to control values.

### Conclusions

SNDX-6352 is a novel, high affinity humanized IgG4 anti-CSF-1R antibody available for initiation of first-in-human studies.

422

### Neuropilin-1-deficient regulatory T cell-derived interferon- $\gamma$ drives infectious instability and tumor clearance

Abigail Overacre<sup>1</sup>, Maria Chikina<sup>1</sup>, Erin Brunazzi<sup>1</sup>, Gulidanna Shayan<sup>2</sup>, William Horne<sup>1</sup>, Jay Kolls<sup>1</sup>, Robert L Ferris<sup>1</sup>, Greg M. Delgoffe<sup>1</sup>, Tullia C Bruno<sup>3</sup>, Creg Workman<sup>1</sup>, Dario Vignali<sup>1</sup>

<sup>1</sup>University of Pittsburgh, Pittsburgh, PA, USA

<sup>2</sup>Tsinghua University, Pittsburgh, PA, USA

<sup>3</sup>University of Pittsburgh/Department of Immunology, Pittsburgh, PA, USA

### Background

Regulatory T cells ( $T_{regs}$ ) play an integral role in maintaining immune homeostasis; however, they are detrimental in cancer through suppression of the anti-tumor immune response. Therefore, identifying  $T_{reg}$  targets that are specifically required in the tumor microenvironment is warranted. We have previously shown that the Neuropilin-1 (Nrp1) pathway is required for functional stability of intratumoral  $T_{regs}$  but remains disposable in maintaining peripheral immune homeostasis. However, 1) the mechanisms that drive  $T_{reg}$  functional instability, 2) the fate and impact of functionally unstable Nrp1-deficient (Nrp1<sup>-/-</sup>)  $T_{regs}$  on the tumor microenvironment and 3) how NRP1 affects function in human  $T_{regs}$  remain unknown.

### Methods

In order to further understand the role of Nrp1<sup>-/-</sup>  $T_{regs}$  in cancer, we injected B16.F10 melanoma into Nrp1<sup>L/L</sup>Foxp3<sup>Cre-YFP/DTR-GFP</sup> cellular heterozygous mice comprised of 50% WT  $T_{regs}$  and 50% Nrp1<sup>-/-</sup>  $T_{regs}$ . Using these mice, we performed whole transcriptome sequencing to determine global transcriptomic changes. Once identified, differentially regulated pathways were tested both *ex vivo* through functional assays and *in*

*vivo* with  $T_{reg}$  transfers into Foxp3<sup>-/-</sup> mice. Lastly, we obtained head and neck squamous cell carcinoma and metastatic melanoma samples to determine the abundance and function of NRP1 on human  $T_{regs}$ .

### Results

Using Nrp1<sup>L/L</sup>Foxp3<sup>Cre-YFP/DTR-GFP</sup> mice, we found that intratumoral Nrp1<sup>-/-</sup>  $T_{regs}$  produce interferon- $\gamma$  (IFN $\gamma$ ), driving the functional destabilization of surrounding WT  $T_{regs}$  which in turn boosts antitumor immunity and facilitates tumor clearance. Furthermore, we have shown that NRP1 is expressed on a proportion of TIL  $T_{regs}$  in head and neck cancer as well as metastatic melanoma and that the IFN $\gamma$  pathway is likely conserved in human  $T_{regs}$ . In addition, human TIL  $T_{regs}$  pre-treated with IFN $\gamma$  show significantly reduced suppressive function in comparison to those without pre-treatment.

### Conclusions

Overall, we have shown that Nrp1 is required for functional stability of intratumoral  $T_{regs}$ , and in its absence, there is an alteration in the tumor microenvironment, leading to an enhanced anti-tumor immune response. These studies uncover a novel potential target for cancer immunotherapies that preserves peripheral immune health. This is of clinical interest, given that NRP1 is expressed on select  $T_{regs}$  in human melanoma and head and neck cancer and that NRP1<sup>+</sup>  $T_{regs}$  show a suppressive advantage over NRP1<sup>-</sup>  $T_{regs}$ .

423

### Anti-CD47 monoclonal antibody SRF231 is a potent inducer of macrophage-mediated tumor cell phagocytosis and has anti-tumor activity in preclinical models

Alison M Paterson, Andrew C Lake, Caroline M Armet, Rachel W O'Connor, Jonathan A Hill, Emmanuel Normant, Ammar Adam, Detlev M Biniszkiwicz, Scott C Chappel, Vito J Palombella, Pamela M Holland

Surface Oncology, Cambridge, MA, USA

### Background

CD47 has been identified as a tumor antigen on human ovarian cancer cells and is expressed on multiple tumor types. CD47 negatively regulates phagocytosis by interacting with signal regulatory protein alpha (SIRP $\alpha$ ), an inhibitory protein expressed on macrophages. High expression of CD47 on tumors contributes to tumor immune evasion by blocking phagocytic uptake. Agents that block the CD47-SIRP $\alpha$  interaction are promising therapeutics in that they restore phagocytic uptake of CD47<sup>+</sup> tumor cells *in vitro* and attenuate tumor growth *in vivo*. Here we characterize SRF231, one of a panel of fully human CD47 antibodies, and demonstrate that it displays the desired criteria for development as a therapeutic.



## Tumor Microenvironment

Presenting author underlined; Primary author in italics

### Methods

Anti-CD47 antibodies were generated using transgenic mice carrying human V regions and SRF231 was subsequently engineered as several Fc-region variants. *In vitro* phagocytosis assays were performed using primary human macrophages differentiated from peripheral blood-derived monocytes. Phagocytosis was measured by flow cytometric analysis of CFSE-labeled target cells after incubation with CD14<sup>+</sup> macrophages. For *in vivo* studies, SCID mice were injected subcutaneously with tumor cells and treated with the indicated antibodies.

### Results

SRF231 binds with high affinity to human CD47 and is a potent blocker of the CD47-SIRP $\alpha$  interaction. SRF231 enhances phagocytic uptake of primary tumor cells and tumor cell lines *in vitro*, and does so irrespective of macrophage polarization. SRF231-mediated tumor cell phagocytosis is also enhanced in the presence of opsonizing antibodies. Importantly, since loss of CD47 expression serves as a marker of aged/damaged red blood cells (RBC) and promotes their phagocytic clearance, SRF231 does not enhance phagocytosis or induce hemagglutination of human or cynomolgus RBC, despite binding to these cells. To better understand the relative contribution of Fc receptor (FcR) interactions on SRF231 mediated activity, we generated and characterized SRF231 isotypes both with and without effector function. Potency in the phagocytosis assay is mildly decreased in isotypes with lower or no ability to bind FcR. In a tumor xenograft model, antibodies display isotype-specific differences in anti-tumor activity despite having equivalent systemic exposures.

### Conclusions

SRF231 binds with high affinity to CD47 and potently disrupts the CD47-SIRP $\alpha$  interaction. SRF231 is unique in its ability to promote robust tumor cell phagocytosis without inducing RBC phagocytosis or hemagglutination. In addition, SRF231 shows potent *in vivo* anti-tumor efficacy in preclinical models either as monotherapy or in combination settings. SRF231 is currently in IND-enabling studies and is expected to enter clinical trials in 2017.

424

### Selective small molecule inhibitors of CD73 promote human CD8+ T cell activation and positively impact tumor growth and immune parameters in experimental tumor models

Jay P Powers, Annette Becker, Ada Chen, Manmohan R Leleti, Eric Newcomb, Holly Sexton, Ulrike Schindler, Joanne BL Tan, Steve W Young, Juan C Jaen

Arcus Biosciences, Hayward, CA, USA

### Background

In the tumor micro-environment extracellular ATP is sequentially hydrolyzed to adenosine by the ecto-nucleotidases CD39 (ATP $\rightarrow$ AMP) and CD73 (AMP $\rightarrow$ adenosine). Adenosine is a potent inhibitor of T cell activation, resulting in an immunosuppressed phenotype, and thus inhibition of CD73 has recently generated much interest in immuno-oncology. We present here novel, selective, and highly potent small molecule inhibitors of CD73.

### Methods

CD73 inhibitor *in vitro* potency was assessed by measuring the hydrolysis of AMP to adenosine in the presence of varying amounts of inhibitors in endogenously expressing (hCD73/SKOV-3; mCD73/E771) and stably over-expressing (hCD73/CHO; hCD39/CHO) cells. Selectivity was assessed in transiently expressing CHO cells (mCD73, NTPDase2, NTPDase3, and NTPDase8). Activity in a CD8<sup>+</sup> T cell functional assay was assessed in human and mouse CD8<sup>+</sup> T cells which were pretreated with inhibitor, buffer control, or CD73-inactive control followed by stimulation (3 days; CD3/CD28  $\pm$  50 mM AMP). Cell activation, proliferation, and effector function were quantified by flow cytometry. CD73 inhibition in a tumor setting was assessed in a subcutaneous CT26 tumor model in Balb/c mice. Treatment was initiated when tumor volumes reached  $\sim$ 100 mm<sup>3</sup> and mice were divided into four cohorts (vehicle control + isotype control, CD73 inhibitor A000830 + isotype control, vehicle control + anti-PD-1 Ab, and A000830 + anti-PD-1 Ab).

### Results

A000830 and A001190 are representative members of a series of potent and selective inhibitors of CD73 (hCD73/CHO IC<sub>50</sub> = 1 nM and 0.03 nM respectively). A000830 and A001190 potently blocked the conversion of AMP to adenosine in human CD8<sup>+</sup> T cells (IC<sub>50</sub> = 0.2 and 0.008 nM respectively) and robustly reversed adenosine-mediated inhibition of proliferation, CD25 expression, and IFN- $\gamma$  and granzyme B production in human CD8<sup>+</sup> T cells. The compounds are highly selective (>10,000-fold) against related ecto-nucleotidases (CD39, NTPDases2/3/8) as well as a large panel of unrelated targets. *In vivo*, A000830 was well tolerated in mice at plasma concentrations sustained well over IC<sub>90</sub> (21 days). Therapeutic dosing of A000830 in mice in combination with an anti-PD-1 antibody resulted in robust inhibition of CT26 tumor growth, greater than either treatment alone.

### Conclusions

We have designed a series of potent and selective small molecule inhibitors of mouse and human CD73 exemplified by A000830 and A001190. These inhibitors block the generation of adenosine from AMP, reverse adenosine-mediated inhibition of human and mouse T cell activation,

## Tumor Microenvironment

Presenting author underlined; Primary author in italics

and demonstrate promising anti-tumor activity when dosed in combination with PD-1 blockade.

425

### Observation of immunobiology landscape in mucosal melanoma

Suthee Rapisuwon<sup>1</sup>, Arash Radfar<sup>2</sup>, Kellie Gardner<sup>3</sup>, Geoffrey Gibney<sup>3</sup>, Michael Atkins<sup>3</sup>

<sup>1</sup>Georgetown Lombardi Comprehensive Cancer Center, Washington, DC, USA

<sup>2</sup>Washington Hospital Center, Washington, DC, USA

<sup>3</sup>Lombardi Comprehensive Cancer Center, Washington, DC, USA

#### Background

Both increased number of pre-treatment CD8+ T lymphocytes and PD-L1 expression at the invasive tumor margin of advanced cutaneous melanoma metastases predicted improved treatment outcome in patients receiving single agent therapy with the PD-1 inhibitor, pembrolizumab [1, 2]. Association between CD8+ T cell numbers or PD-L1 expression and response to combined immune-checkpoint blockade in mucosal melanoma has not been established.

#### Methods

Four cases of advanced mucosal melanoma were each stained with antibodies against CD8, and PD-L1 (SP-142; rabbit monoclonal antibody, Spring Bioscience). A pan-melanoma (HMB-45, MART-1, and tyrosinase), mouse monoclonal antibody (Biocare) was used to identify the tumor area and margins. The pathologist was blinded to the diagnosis and clinical information. Intensity of immunostaining was measured with average optical density (OD). CD8+ T cells and PD-L1 cells density were measured using ImageJ with semi-automated Nuclei Segmentation-IHC Tool Box plugin developed by Shu, et al. [3].

#### Results

The breakdown of PD-L1 and CD8 immunohistochemistry (IHC) from three anorectal melanoma and one paranasal melanoma are described in Table 1. Tumor PD-L1 staining was negative in all tumors measured. CD8+ T cells are non-brisk in all tumors measured. There is a discrepancy in density of total CD8+ T cells. CD8+ T cells at the invasive margin are scarce.

#### Conclusions

This preliminary data is unable to demonstrate any definitive pattern of CD8+ T cells or PD-L1 expression in a small case series of mucosal melanoma. To further address the immunobiology of mucosal melanoma and its microenvironment, the Melanoma Research Foundation Breakthrough Consortium, is conducting, "A Study to

Estimate the Anti-tumor Activity and Identify Potential Predictors of Response in Patients with Advanced Mucosal or Acral Lentiginous Melanoma Receiving Standard Nivolumab in Combination with Ipilimumab Followed by Nivolumab Monotherapy." The study will assess whether pre-existing immune cell infiltrates and PD-L1-expressing cells at the invasive tumor margin correlate with clinical response to combination checkpoint blockade in these uncommon melanoma subtypes.

#### References

- Messina JL, Fenstermacher DA, Eschrich S, Qu X, Berglund AE, Lloyd MC, *et al*: **12-Chemokine gene signature identifies lymph node-like structures in melanoma: potential for patient selection for immunotherapy?** *Sci Rep* 2012, **2**:765.
- Tumeh PC, Harview CL, Yearley JH, Shintaku IP, Taylor EJ, Robert L, *et al*: **PD-1 blockade induces responses by inhibiting adaptive immune resistance.** *Nature* 2014, **515(7528)**:568-571.
- Shu J, Fu H, Qiu G, Kaye P, Ilyas M: **Segmenting overlapping cell nuclei in digital histopathology images.** *Conf Proc IEEE Eng Med Biol Soc* 2013, **2013**:5445-5448.

Table 1.

Case(s)	Subtype	PD-L1		CD8+TILs		Treatment	BOR/DOR(months)
		Density (per mm <sup>2</sup> )	Intensity (0-3)	Density (per mm <sup>2</sup> )	Intensity (0-3)		
1	Anorectal	0	0	20	1+	Ipi→Nivo	PR/ 8,12
2	Anorectal	0	0	210	1+	Ipi	SD / 12
3	Anorectal	0	0	18	0-1	Ipi→PD→Nivo	PD / 0,0
4	Paranasal	0	0	102	1+	Carbo/Taxol	PD/ 0

Discrepancy of CD8+TILs in mucosal melanoma (BOR: Best Overall Response, DOR: Duration of Response)

426

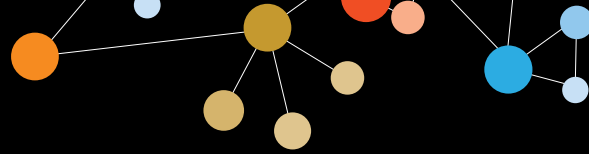
### Leukocyte chemoattractant chemerin upregulates PTEN activity in human tumors via CMKLR1

Keith R Rennie, Robert Crowder, Ping Wang, Russell K Pachynski

Washington University School of Medicine in St. Louis, St. Louis, MO, USA

#### Background

The balance between anti-tumor effector and immunosuppressive immune cells in the tumor microenvironment (TME) is a key determinant of response to cancer treatment. Phosphatase and tensin homolog (PTEN) modulation can directly affect T cell mediated immunotherapies. Specifically, the loss of PTEN has been shown to promote resistance to this type of immunotherapy, supporting the significance of this oncogenic pathway in immunotherapy responses and suggesting upregulation of PTEN activity may have a favorable impact. Chemerin (*RARRES2*; retinoic acid receptor responder 2) is a recently



## Tumor Microenvironment

Presenting author underlined; *Primary author in italics*

identified endogenous leukocyte chemoattractant shown to recruit innate immune cells. Previous studies in mouse tumor models suggest that chemerin is a tumor suppressive chemoattractant cytokine, capable of recruiting immune effector cells into the TME. *RARRES2* is commonly downregulated across multiple tumor types compared to normal tissue counterparts in microarray studies. Several methylome-wide studies in various tumor types have identified *RARRES2* as one of the most hypermethylated genes, potentially leading to decreased chemerin expression. Therefore, we hypothesized that augmentation of chemerin in the TME might inhibit tumor progression and activity.

### Methods

To test this, we exposed human cancer cell lines to exogenous chemerin *in vitro*.

### Results

Surprisingly, we found recombinant chemerin was able to upregulate PTEN expression, a key cell survival and proliferation checkpoint. Specifically, mRNA and protein analyses show a significant upregulation of PTEN after 48 hour chemerin exposure, without significant changes in tumor cell proliferation or apoptosis. Additionally, we found that treatment with chemerin was also able to significantly decrease tumor cell migration. Using siRNA, we found that knockdown of CMKLR1 – the main chemerin receptor that mediates leukocyte chemotaxis – abrogated chemerin-induced upregulation of PTEN, suggesting chemerin's effect on PTEN expression in tumor cells is mediated through this G-protein coupled receptor. These studies help delineate the role of chemerin/*RARRES2* suppression within the tumor microenvironment, and elucidate a novel chemerin-PTEN pathway that may have implications on tumor progression and migration. Importantly, these effects of chemerin are independent of its ability to recruit leukocytes into the TME, suggesting chemerin has multiple mechanisms of anti-tumor action.

### Conclusions

Overall, our studies show a novel finding that chemerin augments PTEN activity via CMKLR1. Thus, chemerin-driven increased PTEN expression and activity may help facilitate improved immunotherapy, not only by recruiting immune effector cells into, but also by augmenting PTEN expression within the TME. Future experimental studies will focus on the chemerin-driven upregulation of PTEN activity and its effects on immunotherapy strategies.

427

### Regulation of IL-15 in the tumor microenvironment by the STING pathway

Rosa M Santana Carrero<sup>1</sup>, Sarai Rivas<sup>2</sup>, Figen Beceren-Braun<sup>2</sup>, Scott Anthony<sup>3</sup>, Kimberly S Schluns<sup>2</sup>

<sup>1</sup>The University of Texas Graduate School of Biomedical Sciences at Houston, Houston, TX, USA

<sup>2</sup>Department of Immunology, University of Texas MD Anderson Cancer Center, Houston, TX, USA

<sup>3</sup>Department of Microbiology, University of Iowa, Iowa City, IA

### Background

Expression of IL-15 within the tumor correlates with increased tumor infiltrating T cells, decreased metastasis and increased patient survival [1]. Unfortunately, the regulation of IL-15 within the tumor microenvironment is not clear. In our recent study we showed that agonists of the Stimulator of Interferon Genes (STING) pathway are potent inducers of soluble IL-15 complexes (sIL-15c) *in vivo* [2]. Since the STING pathway is important for regulation of type I interferons (IFNs) in tumors, we set out to determine if sIL-15c are produced in the tumor microenvironment and are regulated by STING signaling.

### Methods

C57BL/6, IL-15Ra<sup>-/-</sup>, IFNAR1<sup>-/-</sup> and Tmem173<sup>-/-</sup> mice were challenged with 300,000 B16-F10 melanoma cells by s.c. injection. Tumors of various sizes were isolated and sIL-15c were measured in homogenates from tumors and spleens using ELISAs. For stimulation of STING pathway, mice were administered c-di-GMP (25ug/mouse) via intratumoral injection every three days. To measure proliferation, OT-I CD8<sup>+</sup> T cells were CFSE labelled and adoptively transferred into wild-type and IL-15Ra<sup>-/-</sup> mice. Tumors, spleens and tumor-draining lymph nodes were processed and stained for analysis via flow cytometry.

### Results

Levels of sIL-15c were high in homogenates from small tumors and low in larger tumors, but were absent in homogenates from IL-15Ra<sup>-/-</sup> mice indicating sIL-15c were produced by the tumor stroma. Tumors isolated from IFNAR1<sup>-/-</sup> mice contained decreased levels of sIL-15c, but interestingly, those isolated from mice with a defective STING pathway had normal levels of sIL-15c suggesting that type I IFN-dependent, but STING-independent pathway was required for intratumoral IL-15 regulation. Nonetheless, intratumoral delivery of STING agonists enhanced production of sIL-15c in B16 tumors. Whereas treatment of tumors with STING agonists promoted tumor regression and enhanced proliferation of tumor-specific CD8<sup>+</sup> T cells, these effects were severely blunted in IL-15Ra<sup>-/-</sup> mice.



## Tumor Microenvironment

Presenting author underlined; Primary author in italics

### Conclusions

These findings indicate that IL-15 is a critical factor mediating the anti-tumor responses induced by STING signaling.

### References

1. Mlecnik B, Bindea G, Angell HK, Sasso MS, Obenauf AC, Fredriksen T, *et al*: **Functional network pipeline reveals genetic determinants associated with in situ lymphocyte proliferation and survival of cancer patients.** *Sci Transl Med* 2014, **6**:228ra37.
2. Anthony SM, Howard ME, Hailemichael Y, Overwijk WW, Schluns KS: **Soluble interleukin-15 complexes are generated in vivo by type I interferon dependent and independent pathways.** *PLoS One* 2015, **10**:e0120274.

428

### Regulatory T cell derived inhibitory cytokines IL35 and IL10 promote T cell dysfunction in the tumor microenvironment

Deepali Sawant, Maria Chikina, Hiroshi Yano, Creg Workman, Dario Vignali

University of Pittsburgh, Pittsburgh, PA, USA

### Background

Regulatory T cells ( $T_{reg}$ ) are a specialized suppressive CD4<sup>+</sup> T cell sub-population capable of restricting deleterious immune responses to self and foreign antigens that underlie autoimmune and chronic inflammation. Conversely,  $T_{reg}$  block beneficial anti-tumor immune responses and thereby pose severe impediment to effective tumor immunotherapies. Although  $T_{reg}$  depletion reduces tumor burden, the ensuing autoimmune sequelae limits its utility in the clinic. Thus targeted approaches limiting  $T_{reg}$  cell activity specific to the tumor microenvironment are warranted. One of the major mechanism by which  $T_{reg}$  exert their suppressive effects is via secretion of inhibitory cytokines. However, the physiological relevance of this mode of suppression to the tumor microenvironment remains largely unclear.

### Methods

To interrogate the role of the two predominant  $T_{reg}$  suppressive cytokines, IL35 and IL10, in the tumor setting, we injected B16F10 tumors intradermally into *Foxp3*<sup>Cre-YFP</sup> mice bearing reporters for IL35 and IL10 (*Foxp3*<sup>Cre-YFP</sup>.*Ebi3*<sup>tdTom</sup>.*IL10*<sup>GFP</sup>). This enabled tracking of  $T_{reg}$  expressing/co-expressing IL35 and IL10 in the tumor microenvironment. We also performed tumor experiments in mice bearing IL35-deficient  $T_{reg}$  (*Foxp3*<sup>Cre-YFP</sup>.*Ebi3*<sup>L/L</sup>) and IL10-deficient  $T_{reg}$  (*Foxp3*<sup>Cre-YFP</sup>.*IL10*<sup>L/L</sup>) to assess the impact of  $T_{reg}$ -specific deletion of the two suppressive cytokines on tumor growth and CD8<sup>+</sup> T cell effector function.

### Results

Preliminary studies using the dual cytokine reporter mice reveal distinct populations of  $T_{reg}$  expressing IL35 and IL10 in the B16 tumor microenvironment, with a preferential enrichment of IL35<sup>+</sup>  $T_{reg}$  and little to no co-expression of the two cytokines on  $T_{reg}$ . Reduced tumor burden was noted in both *Foxp3*<sup>Cre-YFP</sup>.*Ebi3*<sup>L/L</sup> and *Foxp3*<sup>Cre-YFP</sup>.*IL10*<sup>L/L</sup> mice. Interestingly, this was associated with a significant loss of multiple inhibitory receptors (IRs) on CD8<sup>+</sup> T cells in both floxed environments. These findings suggest a potential role for the  $T_{reg}$ -derived inhibitory cytokines in inducing multi-IR<sup>+</sup> exhausted state on CD8<sup>+</sup> T cells in tumors.

### Conclusions

The dramatic loss of IR<sup>+</sup> T cells in mice bearing IL35 and IL10-deficient  $T_{reg}$  highlights the possibility of targeting these inhibitory cytokines to limit T cell exhaustion in tumors. Our study uncovers a novel mechanism of  $T_{reg}$  suppression within the tumor microenvironment wherein  $T_{reg}$ -derived inhibitory cytokines induce a state of dysfunction on the effector T cells thereby contributing to tumor immune evasion.

429

### Human melanomas and ovarian cancers overexpressing mechanical barrier molecule genes lack immune signatures and have increased patient mortality risk

*Elise Salerno*<sup>1</sup>, Davide Bedognetti<sup>2</sup>, *Ileana Mauldin*<sup>3</sup>, Donna Deacon<sup>3</sup>, Sofia Shea<sup>4</sup>, Joel Pinczewski<sup>5</sup>, Joseph M Obeid<sup>6</sup>, George Coukos<sup>7</sup>, Ena Wang<sup>2</sup>, Thomas Gajewski<sup>8</sup>, Franco M Marincola<sup>2</sup>, Craig L Slingluff Jr<sup>3</sup>

<sup>1</sup>University of Alabama, Birmingham, AL, USA

<sup>2</sup>Sidra Medical and Research Center, Doha, Ad Dawhah, Qatar

<sup>3</sup>University of Virginia, Charlottesville, VA, USA

<sup>4</sup>Hunter Holmes McGuire Veterans Administration Medical Center, Richmond, VA, USA

<sup>5</sup>Dorevitch Pathology, Heidelberg West, Victoria, Australia

<sup>6</sup>Department of Surgery, University of Virginia, Charlottesville, VA, USA

<sup>7</sup>Ludwig Institute for Cancer Research, Epalinges, Vaud, Switzerland

<sup>8</sup>The University of Chicago, Chicago, IL, USA

### Background

Immune signatures of T cell infiltration for melanoma and ovarian cancer are associated with improved survival. Mechanisms enabling and regulating T cell infiltration in the tumor microenvironment are being elucidated. We hypothesized that genes overexpressed in tumors without T cell infiltration may limit T cell infiltration and have prognostic implications.



## Tumor Microenvironment

Presenting author underlined; Primary author in italics

### Methods

Gene expression profiling of 44 human melanoma metastases had previously identified subsets with or without Th1 immune signatures. We identified genes overexpressed five-fold or more in tumors lacking immune signatures, at a significance level of  $p < 0.01$ . These findings were further validated in gene expression data from melanoma metastases and ovarian cancers. To assess associations with survival, RNAseq data and patient survival data from The Cancer Genome Atlas (TCGA) were assessed with Kaplan-Meier curves, and log-rank tests.

### Results

We identified 8 genes overexpressed in human melanomas and ovarian cancers lacking Th1 immune signatures, and which encode molecules with mechanical barrier function in normal tissues: filaggrin (FLG), tumor-associated calcium signal transducer 2 (TACSTD2), and 6 desmosomal proteins (DST, DSC3, DSP, PPL, PKP3, and JUP). This association was validated in another 114 melanoma metastases, where DST expression alone was sufficient to identify melanomas without immune signatures, while FLG and the other 6 putative barrier molecules were overexpressed in a different subset of melanomas lacking immune signatures. Similar associations were identified in a set of 186 ovarian cancers. RNA-seq data from 471 melanomas and 307 ovarian cancers in the TCGA further supported these findings and also revealed that overexpression of barrier molecules was largely independent of  $\beta$ -catenin/WNT and endothelin receptor B gene expression. Overexpression of barrier molecules was associated with early patient mortality for melanoma ( $p = 0.0002$ ) and ovarian cancer ( $p < 0.01$ ). This was true for FLG for melanoma ( $p = 0.012$ ) and ovarian cancer ( $p = 0.006$ ), whereas DST overexpression was negatively associated with CD8 gene expression, but not with patient survival.

### Conclusions

Overexpression of FLG or DST identifies 2 distinct patient populations with low immune cell infiltration in melanoma and ovarian cancers, but with different prognostic implications for each. These data raise the possibility that molecules with mechanical barrier function in skin and other tissues may be used by cancer cells to protect them from immune cell infiltration and immune-mediated destruction.

### Acknowledgements

Gene expression data from melanoma metastases were provided by Steven A Rosenberg (NCI). Some results here are based upon data generated by the TCGA Research Network: <http://cancergenome.nih.gov> (Cerami, *et al.*, PMID 22588877; Gao J, *et al.*, PMID 23550210).

### 430 Abstract Travel Award Recipient

#### Direct visualization of tumor immune evasion against CD8+ effector T cells using intravital microscopy

Stefani Spranger<sup>1</sup>, Brendan Horton<sup>1</sup>, Thomas F Gajewski<sup>2</sup>

<sup>1</sup>Department of Pathology, The University of Chicago, Chicago, IL, USA

<sup>2</sup>University of Chicago Medical Center, Chicago, IL, USA

#### Background

CD8<sup>+</sup> T cell infiltration into the tumor microenvironment appears to be correlative for clinical response to checkpoint blockade immunotherapy. Understanding the molecular mechanisms which cause lack of T cell infiltration will be instrumental for the development of novel treatment combinations to expand clinical efficacy. Recent studies have demonstrated that tumor cell-intrinsic signaling pathways, including the Wnt/ $\beta$ -catenin pathway, result in a lack of T cell infiltration in patients and genetically engineered mouse (GEM) models. Mechanistically, activation of the Wnt/ $\beta$ -catenin signaling pathway in the primary tumor mediates inhibition of priming of tumor-antigen-specific T cells through failed recruitment of Batf3-lineage DCs. However, it was not clear whether activation of a tumor cell-intrinsic signaling pathway could also mediate secondary resistance in the presence of a systemic anti-tumor immune response. In addition, it was not known whether adoptive T cell transfer would be a potential therapeutic option for non-T cell inflamed tumors.

#### Methods

To address those questions we used GEMs for murine melanoma with or without activation of the Wnt/ $\beta$ -catenin signaling pathway and engineered to express the model antigen SIY (SIYRYGL).

#### Results

By using these GEMs we now show that tumor cell-intrinsic activation of  $\beta$ -catenin was capable to mediate secondary resistance by excluding effector T cell from the tumor microenvironment. Effector T cell infiltration in  $\beta$ -catenin negative tumors was further associated with the emergence of immuno-edited tumor escape variants, which were never observed in  $\beta$ -catenin positive non-T cell inflamed tumors. Consistently, adoptive T cell transfer of antigen-specific T cells failed to provide therapeutic benefit in tumors with activated  $\beta$ -catenin signaling. Using intravital-microscopy we found that, while effector T cells in  $\beta$ -catenin negative tumors made direct tumor cell contact and showed a dynamic and directed migratory behavior, the few effector T cells found in  $\beta$ -catenin positive tumor failed to engage close contact with tumor cells and were immobile within areas having the appearance of stroma. Mechanistically, we identified a lack of expression of

## Tumor Microenvironment

Presenting author underlined; *Primary author in italics*

the chemokines CXCL9 and CXCL10 in tumor with activated b-catenin signaling, which are normally produced by CD103<sup>+</sup> Batf3-driven DCs.

### Conclusions

Our data support the notion that CD103<sup>+</sup> dendritic cells within the tumor microenvironment are essential for effector CD8<sup>+</sup> T cell recruitment and mobility. Strategies to promote CD103<sup>+</sup> dendritic cell accumulation and activation within the tumor microenvironment could be essential for expanding efficacy to checkpoint blockade immunotherapy.

431

### Inhibition of matrix metalloproteinases by cysteamine regulates tumor invasion and metastasis in mouse models of human ovarian cancer

Akiko Suzuki, Pamela Leland, Bharat H Joshi, *Raj K Puri*

Center for Biologics Evaluation and Research, Food and Drug Administration, Silver Spring, MD, USA

### Background

Previously, we have reported that cysteamine, an anti-oxidant aminothioliol, inhibited the tumor invasion *in vitro* and metastasis of pancreatic cancer *in vivo* in mouse models of human pancreatic cancer. We have also shown that subcutaneous cysteamine treatment improves the survival of mice bearing orthotopically transplanted pancreatic tumors. Herein, we examined whether cysteamine can inhibit invasion and metastasis of other human cancers.

### Methods

We examined cysteamine's anti-invasion effects in 6 human ovarian cancer cell lines by a matrigel invasion assay. To study the mechanism of action, we evaluated the cytotoxic activity of cysteamine *in vitro* and measured the effect of cysteamine on matrix metalloproteinases (MMP), which are known to be involved in metastasis. We examined the anti-metastatic effect of cysteamine in two orthotopic murine models of human ovarian cancer by monitoring peritoneal metastases. A2780 and IGROV-1 ovarian cancer cells were surgically implanted orthotopically in the ovary followed by monitoring tumor growth and peritoneal metastasis using a high-resolution ultrasound system. Four days after tumor implantation, increasing doses of cysteamine (0, 100, or 250 mg/kg/day) were subcutaneously injected twice a day until the end of the experiment.

### Results

We observed that cysteamine inhibited cell invasion *in vitro* in a concentration-dependent manner. Similar to invasion, MMP activity was inhibited by cysteamine in a concentration-dependent manner. We next examined the anti-metastatic effect of cysteamine on peritoneal metastasis

in two orthotopic murine models of human ovarian cancer. Cysteamine significantly decreased the number of metastases and total weight of metastatic lesions in these mice ( $p < 0.01$  in A2780 and  $p < 0.05$  in IGROV-1 xenografts compared to untreated control mice), while the primary tumor volumes and weights were not changed. We did not observe any symptoms of general toxicity (such as general appearance, body weight, or mortality) in animals treated at the highest dose of cysteamine. Similar to the *in vitro* results, MMP activity was significantly decreased in primary tumors in both A2780 & IGROV-1 xenograft models treated with cysteamine ( $p < 0.05$ ). Tumor growth was also monitored weekly by ultrasound volumetric analyses. We observed that tumor volumes measured by ultrasound imaging correlated positively with the *ex vivo* tumor weight measurements following dissection of the primary tumor at the end of experiment (Spearman  $r = 0.7870$  in A2780 and  $0.9800$  in IGROV-1 xenografts).

### Conclusions

Based on these results, we conclude that cysteamine may be a useful therapeutic option for ovarian cancer as a mono- or combination-therapy with other anti-cancer agents such as cancer vaccines and immunotherapy.

### 432 Abstract Travel Award Recipient

### Validation of FGFR3 activation in non-T cell-inflamed bladder cancer

Randy F Sweis<sup>1</sup>, Riyue Bao<sup>1</sup>, Jason Luke<sup>1</sup>, Thomas F Gajewski<sup>2</sup>

<sup>1</sup>University of Chicago, Chicago, IL, USA

<sup>2</sup>University of Chicago Medical Center, Chicago, IL, USA

### Background

Immune checkpoint therapy recently led to the first regulatory approval in metastatic bladder cancer in well over a decade. Despite remarkable responses observed in some patients, the objective response rate remains 15%. We recently reported a characterization of bladder cancers lacking a T cell-inflamed tumor microenvironment, which has been associated with lack of response to immune checkpoint therapy. We observed that FGFR3 activating mutations were exclusively present in non-T cell-inflamed tumors. In order to further substantiate our findings, we analyzed an independent cohort of non-T cell inflamed bladder cancers.

### Methods

Ninety-three samples were analyzed from a validation data set (GSE 31684) with gene expression profiling. Affymetrix microarray files were downloaded from the GEO database and preprocessed to generate normalized gene expression values for 20,390 genes. Consensus clustering of samples was conducted using 725 genes from our prior TCGA analysis, and repeated using a refined 160 gene set developed across



## Tumor Microenvironment

Presenting author underlined; *Primary author in italics*

multiple cancer types by methods previously described. Immune subtypes were called based on gene expression. Differentially expressed genes were filtered by FDR-adjusted P-value < 0.01 and fold change  $\geq 1.5$ .

### Results

We first evaluated the performance of our refined gene expression signature, which has recently been adapted for application across all solid tumor types. Comparing previous and current gene sets derived from our 13 gene T cell-inflamed signature, we found our classification to be robust with 89% (83/93) concordance in immune subtype calling. We noted a higher proportion of samples were non-T cell-inflamed compared with bladder cancers in TCGA (48% vs. 33%). We confirmed a strong inverse correlation between expression of CD8A and FGFR3 ( $P < 0.0001$ ). Furthermore, FGFR3 overexpressing tumors by median dichotomization had significantly lower expression of PD-L1, IDO1, LAG3, and TIM3 (all  $P \leq 0.01$ ). The association between FGFR3 and FOXP3 was not significant ( $P = 0.41$ ). CD8A was concordantly expressed with PD-L1, IDO1, LAG3, FOXP3, and TIM3 ( $P < 0.0001$ ), consistent with data from TCGA. Finally, differentially expressed genes were compiled and enriched pathways were identified by Ingenuity Pathway Analysis. In non-T cell-inflamed tumors from this data set, activation of  $\beta$ -catenin, PPARG and SMARCA4 pathways was observed ( $P < 0.0001$ ).

### Conclusions

In summary, we confirm the fidelity of our gene expression classification of non-T cell-inflamed bladder cancers across different gene expression platforms and data sets. In addition to activating mutations, FGFR3 overexpression occurs preferentially in the non-T cell-inflamed immune subtype lacking PD-L1 expression.

### 433 Abstract Travel Award Recipient

#### Reprogramming of the ovarian cancer microenvironment by poly-I:C and selective TLR3 ligand, rintatolimod

Marie-Nicole Theodoraki<sup>1</sup>, Frances-Mary Mogundo<sup>2</sup>, Robert P Edwards<sup>2</sup>, Pawel Kalinski<sup>3</sup>

<sup>1</sup>University of Pittsburgh, Pittsburgh, PA, USA

<sup>2</sup>Magee-Womens Research Institute, Ovarian Cancer Center of Excellence, and Peritoneal/Ovarian Cancer Specialty Care Center, Hillman Cancer Center, University of Pittsburgh, Pittsburgh, PA, USA

<sup>3</sup>Department of Surgery; University of Pittsburgh Cancer Institute; Department of Infectious Diseases and Microbiology, University of Pittsburgh, Pittsburgh, PA, USA

### Background

Despite aggressive surgery and chemotherapy, the 5-year survival rate for patients with ovarian cancer is very low, 37% for stage III and 25% for stage IV [1]. Previously, we

have demonstrated a high level of synergy among TLR-3 ligands, IFN $\alpha$  and COX-2 blockers in inducing chemokines, which attract the desirable cytotoxic T cells, Th1-cells and NK cells in colorectal cancer microenvironments and limited local production of CCL22, the chemokine implicated in the accumulation of T regulatory cells [2]. In this study, we investigated an optimized combinatorial adjuvant to reprogram the tumor microenvironment (TME) of ovarian cancer.

### Methods

Ovarian cancer specimens were divided into 4-mm biopsies and cultured for 24 hours in the presence of IFN $\alpha$ , indomethacin (COX-1/2 inhibitor) or/and one of two synthetic TLR3 ligands Poly-I:C (non-selective activator of TLR3) rintatolimod (Ampligen), or their combinations. Biopsies were harvested for mRNA as well as for confocal microscopy and culture supernatants were analyzed for CCL5, CXCL10 and CCL22 concentration. Alternatively, established ovarian cancer cell lines (PE01 and PE04) or monocyte-derived macrophages were used in analogous experiments. Chemotaxis assays were performed using pre-activated CD8+ T cells and supernatants from the differentially treated ovarian cancer specimens.

### Results

We observed that the combination of TLR-3 ligands, IFN $\alpha$  and COX1/2 blockers selectively induce the desirable chemokines CCL5 and CXCL10 and suppressed CCL22 in ovarian cancer with similar results in the macrophages and ovarian cancer cell lines. Unexpectedly, IFN $\alpha$  + poly-I:C but not IFN $\alpha$  + rintatolimod, also promoted the expression of the MDSC attractant CXCL12, which was reversed through addition of COX-2 inhibitors. Furthermore, the induction of CCL5 was enhanced by the addition of COX1/2 inhibitor. Compared to poly-I:C, the positive effects of the selective TLR-3 ligand, rintatolimod, were not dependent on the addition of indomethacin.

### Conclusions

We demonstrate the feasibility of selective modulation of the ovarian TME, using combinations of different clinical reagents, in order to improve the local balance between tumor-infiltrating T effector and T regulatory cells. We show for the first time, that poly-I:C induces undesirable COX2-dependent suppressive factors, which can be eliminated through addition of the COX-1/2 inhibitor, indomethacin, or through usage of the selective TLR-3 ligand, rintatolimod.

### References

1. Holschneider CH, Berek JS: **Ovarian cancer: epidemiology, biology, and prognostic factors.** *Semin Surg Oncol* 2000, **19**:3-10.

## Tumor Microenvironment

Presenting author underlined; *Primary author in italics*

2. Muthuswamy R, Berk E, Junecko BF *et al*: **NF-kappaB hyperactivation in tumor tissues allows tumor-selective reprogramming of the chemokine microenvironment to enhance the recruitment of cytolytic T effector cells.** *Cancer Res* 2012, **72**:3735-3743.

**434**

### **TLR9 expression in prostate cancer cells results in leukemia inhibitory factor (LIF)-mediated accumulation of pSTAT3+ myeloid-derived suppressor cells**

Haejung Won, Dayson Moreira, Chan Gao, Xingli Zhao, Priyanka Dutttagupta, Jeremy Jones, Massimo D'Apuzzo, Sumanta Pal, Marcin Kortylewski

City of Hope, Duarte, CA, USA

#### **Background**

Inflammation plays pivotal roles in carcinogenesis and formation of the immunosuppressive microenvironment of prostate tumors. However, molecular mechanisms of crosstalk between cancer cells and immune cells at the tumor site are only partly understood. Our recent study demonstrated that advanced, castration-resistant prostate cancer (CRPC) cells express innate immune receptor, Toll-Like Receptor 9 (TLR9). TLR9 signaling through NF-kB/RELA and STAT3 promoted tumor propagating potential and self-renewal of prostate cancer cells. Here, we evaluated the effect of cancer cell-intrinsic TLR9 signaling on the composition of tumor microenvironment.

#### **Methods**

For temporal control of TLR9 expression, we introduced tetracycline-inducible TLR9 expression system (Tet-On) into mouse Ras/Myc-driven (RM9) prostate cancer cells.

#### **Results**

The induction of TLR9 expression in RM9 tumors *in vivo* correlated with the accumulation of polymorphonuclear myeloid-derived suppressor cells (PMN-MDSCs; CD11b<sup>+</sup>Ly6C<sup>INT</sup>Ly6G<sup>HI</sup>). The PMN-MDSC in TLR9<sup>HI</sup>-tumors showed elevated levels of activated STAT3, a master regulator of immunosuppressive MDSC activities. Accordingly, tumor-associated PMN-MDSCs isolated from TLR9<sup>HI</sup>, but not from TLR9<sup>LO</sup>- RM9 tumors, expressed high level of immunosuppressive mediators such as Arginase-1 and IL-10, and showed augmented suppressive effects on T cell proliferation. TLR9 expression in mouse and human (LNCaP and PC3) prostate cancer cells resulted in altered cytokine/chemokine secretion with significant upregulation of an IL-6 family cytokine, leukemia inhibitory factor (LIF). Our preliminary analysis confirmed elevated levels of LIF in plasma from prostate cancer patients compared to healthy subjects. On molecular level, TLR9 triggered direct binding of the NF-kB and STAT3 to the LIF promoter as

verified by chromatin immunoprecipitation (ChIP) assays. The antibody-mediated neutralization of LIF significantly inhibited tumor growth *in vivo* with concomitant reduction in the accumulation of pSTAT3<sup>+</sup> PMN-MDSCs. Finally, we used an oligonucleotide-based approach to inhibit STAT3 in TLR9 expressing RM9 tumor cells and in tumor-associated myeloid cells such as PMN-MDSCs. Local injection of CpG-STAT3 inhibitor reduced growth of RM9 prostate tumors at the treated and in the distant site suggesting generation of systemic antitumor immune responses.

#### **Conclusions**

Collectively, TLR9 signaling in prostate cancer cells induces tolerogenic tumor microenvironment through altering cytokine and chemokine and subsequent activation of STAT3 in tumor-infiltrated myeloid cells. In addition, the results suggest therapeutic potential of targeting TLR9+ prostate cancer cells and tumor-associated PMN-MDSC to eliminate both tumorigenic and tolerogenic effects of STAT3 signaling in the tumor microenvironment.

**435**

### **Immune modulation of the cancer microenvironment for enhancing cancer immunotherapy in ovarian clear cell carcinoma**

Tomonori Yaguchi, Juri Sugiyama, Hiroshi Nishio, Taeko Hayakawa, Yutaka Kawakami

Division of Cellular Signaling, Institute for Advanced Medical Research, Keio University School of Medicine, Shinjuku-ku, Tokyo, Japan

#### **Background**

To enhance the anti-tumor effects of current immunotherapies including immune checkpoint blockade therapies, it is important to reverse the cancer-induced immunosuppression. Ovarian clear cell carcinoma (OCCC), the second most major subtype of ovarian cancer in Japan, produces high amounts of immunosuppressive cytokines such as IL-6 and IL-8, which were correlated with poor prognoses. A transcriptional factor HNF-1 $\beta$  preferentially activated in human OCCC contributes to various malignant phenotypes including chemoresistance and glucose metabolism. In this study, we have investigated roles of HNF-1 $\beta$  in the immunosuppressive activity of human OCCC.

#### **Methods**

We have evaluated the number of tumor-infiltrating T cells in human OCCC tissues. We have evaluated the contribution of HNF-1 $\beta$  activation in OCCC to the suppression of DC function through the production of IL-6 *in vitro* and *in vivo*. Finally, we have screened an existing drug library for agents which have an activity to suppress IL-6 production from OCCC and evaluated their effects *in vivo*.



## Tumor Microenvironment

Presenting author underlined; Primary author in italics

### Results

Tumor-infiltrating T cells in OCCC were significantly fewer than those in other types of cancers including serous ovarian cancers. HNF-1 $\beta$  knockdown and overexpression experiments revealed that HNF-1 $\beta$  induced IL-6 and IL-8 production via NF- $\kappa$ B and STAT3 activation in OCCC. Suppressing activities of human OCCC cell line culture supernatants on human monocyte-derived dendritic cells (DC) were reduced *in vitro* by knockdown of HNF-1 $\beta$  partly through decrease of IL-6. Knockdown of HNF-1 $\beta$  in a human OCCC cell line resulted in the restoration of T cell stimulatory activity of murine DC in nude mice implanted with human OCCC partly through decrease of human IL-6 *in vivo*. From the drug screening, various existing drugs having activity to inhibit STAT-3 or NF- $\kappa$ B were found to suppress IL-6 production from OCCC and to restore immuno-competence of cancer-bearing mice.

### Conclusions

HNF-1 $\beta$  activation in human OCCC is a possible upstream event for induction of immunosuppression by IL-6 and IL-8 production via NF- $\kappa$ B and STAT3 activation and that combination of drugs targeting HNF-1 $\beta$ /STAT3/NF- $\kappa$ B pathway may enhance the efficacy of current immunotherapies for OCCC patients.

436

### Targeting fibroblast activation protein in combination with radiation

*Kayla McCarty*, David Friedman, Benjamin Cottam, Pippa Newell, Michael Gough, Marka Crittenden, *Kristina Young*

Earle A. Chile Research Institute, Portland, OR, USA

### Background

Pancreatic ductal adenocarcinoma (PDAC) is characterized by a fibrotic stroma and poor immune infiltrate, in part driven by cancer-associated fibroblasts (CAFs). CAFs, which selectively express fibroblast activation protein (FAP), contribute to immune escape via sequestration of anti-tumor CD8<sup>+</sup> T cells, upregulation of immune checkpoint ligand expression, and immunosuppressive cytokine production and polarization of tumor infiltrating immune cells.

### Methods

We established syngeneic pancreatic tumors in immune competent C57BL/6 mice using Panc02 cells. From days 7-20, mice were treated with FAP inhibitor UAMC-1110 or control. Radiation (RT) was delivered exclusively to the tumor using a 1cm collimator on the Small Animal Radiation Research Platform, 10Gy x 3 daily fractions on day 14, 15, and 16. FAP knockout mice were challenged with Panc02 or Panc02-SIY cells and radiated 10Gy x 3 on days 14-16. Tumors were measured, and mice followed for survival. Using the same

treatment groups above, tumors were harvested for flow cytometry and multiparameter immunofluorescence on day 14, 23, and 43. Splenocytes were harvested and pulsed with SIY peptide and tested for intracellular cytokine production on day 14 and 23. Tumor infiltrating macrophages were FACS sorted and western blot was performed to determine M1 vs M2 polarization. Tumor cytokines were assessed using cytokine bead assay.

### Results

UAMC-1110 alone had no effect on tumor growth or survival. RT caused a transient growth delay, resulting in a survival advantage. Combination treatment with radiation and UAMC-1110 resulted in two temporally distinct growth delays: an initial tumor growth delay significant over radiation alone at day 22, and a second late response at day 43; but did not translate to a survival advantage over RT. At day 14, UAMC-1110 treatment resulted in fewer macrophages. At day 23, RT increased CD11b<sup>+</sup> tumor infiltrates, MDSCs, and CD3<sup>+</sup> infiltrates. Tumor immune infiltrates were equivalent at day 43. Radiation and combination treatment with UAMC-1110 increased collagen deposition. FAP knockout mice had equivalent response to radiation compared to wildtype control. FAP KO tumors had fewer macrophages and MDSCs, and more antigen-specific T cells following radiation, but not prior to radiation.

### Conclusions

We tested a novel specific FAP inhibitor with radiation in a murine PDAC model. We found FAP inhibition favorably altered tumor immune infiltrate, and increase antigen-specific T cells following radiation, but was insufficient to result in a survival advantage. While FAP may be selectively expressed by CAFs, inhibition of its function is not seem sufficient to influence *in vivo* radiosensitivity. We propose a more comprehensive targeting of CAFs may be required to influence radiation response.

### Acknowledgements

KHY received an ASCO Young Investigator Award and an RSNA Research Seed Grant which funded this work.

437

### Arginase 2 blockage and reduction of PD-L1 expression in renal cell carcinoma

*Sufyan Jarushi*<sup>1</sup>, Brashonda Ross<sup>2</sup>, Sarah Normand<sup>3</sup>, Matthew Nguyen<sup>4</sup>, *Arnold Zea*<sup>1</sup>

<sup>1</sup>LSUHSC-NO, New Orleans, LA, USA

<sup>2</sup>Dillard University-NO, New Orleans, LA, USA

<sup>3</sup>Rhodes College, New Orleans, LA, USA

<sup>4</sup>Tulane University, New Orleans, LA, USA



## Tumor Microenvironment

Presenting author underlined; *Primary author in italics*

### Background

Tumors may evade the immune system, in part by exploiting interactions between T cells and the tumor. Renal cell carcinoma (RCC) is a poorly responsive tumor to conventional cytotoxic chemotherapies, although it is sensitive to IL-2, which still remains as the treatment of choice. The FDA has approved novel PD-1 immunotherapies, which have shown survival benefits for patients with metastatic RCC. However, preclinical studies and early phase clinical trials suggest that resistance mechanisms exploited by tumors may limit the effectiveness of these therapies. We believe that the heterogeneity of RCC tumors can contribute to the poor responses in RCC. In this work, we are studying the role the enzyme arginase 2 (ARG2) plays in the expression of PD-L1 in RCC tumors. Different levels of ARG2 expression in RCC contributes proportionally to the generation of T cell dysfunction. The understanding of this mechanism will be crucial for probing human immune responses and tumor biology in order to understand what distinguishes responder vs. non-responder patients. Therefore, our hypothesis is that the expression of PD-L1 in RCC tumors is regulated by ARG2 and blocking this enzyme will reduce its expression, resulting in improved antitumor activity.

### Methods

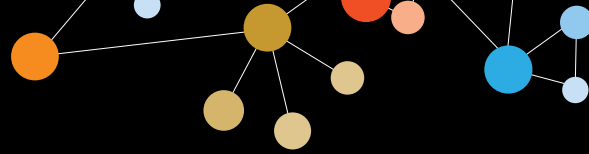
Three murine RCC cell lines, CL-2 (low-ARG2), CL-19 (high-ARG2), and Renca (median-ARG2) were cultured at different time points: 1, 3, 6, and 24h in the presence or absence of IFN $\gamma$  and ARG2 inhibitor BEC. Expression of PD-L1 was assessed by flow cytometry, tumor cell survival by MTT assay, ARG activity by enzymatic assays and supernatants for L-arginine by HPLC.

### Results

PD-L1 expression was similar between CL-2 and CL-19 cell lines (17-20%) that significantly increased up to 95% after 6h of IFN $\gamma$  stimulation (2.5 U/ML). Interestingly, we observed a constitutive high expression of PD-L1 in Renca cells (85-90%) in non-stimulated cells. When cells were treated with ARG2 inhibitor, PD-L1 expression decreased 5 fold in CL-2 and CL19 cells but had not effect on Renca cells. High concentrations of IFN $\gamma$  (10U/ML) had cytotoxic effects in CL-2 and CL-19 but not in Renca cells.

### Conclusions

These results suggest that 1) RCC heterogeneity plays an important role in the expression of immune checkpoints and in pathways that can disable T cells. This finding can contribute to determine what patients may benefit or not from anti PD-1 therapy. 2) The role of IFN $\gamma$  in this process is unclear and is currently being investigated.



## Late-Breaking Abstracts - Adoptive Cellular Therapy

Presenting author underlined; *Primary author in italics*

**438**

### **Chemo-immunotherapy with cyclophosphamide and tumor reactive CD4<sup>+</sup> T cells lead to destruction of tumor vasculature and eventual tumor eradication**

Tsadik Habtetsion, Gang Zhou

Augusta University, Augusta, GA, USA

#### **Background**

CD4<sup>+</sup> T cells are critical components of anti-tumor immunity and play a pivotal role in orchestrating anti-tumor immune responses. Mounting evidence from preclinical and clinical studies indicates that CD4<sup>+</sup> T cells in combination with chemotherapy can control tumor growth and recurrence. CD4<sup>+</sup> T cells are suggested to mediate tumor rejection through mechanisms that include cytotoxic effects on tumor cells, inhibition of angiogenesis, and reprogramming of the tumor microenvironment.

#### **Methods**

In this project, we set out to study the cellular and molecular mechanisms underlying the therapeutic effect of chemo-immunotherapy in the form of cyclophosphamide (CTX) and tumor specific CD4<sup>+</sup> T cells in a murine model of colorectal cancer. Mice were injected subcutaneously with colorectal cancer cells. When the tumor reached 140-160mm<sup>2</sup> in area, mice were injected with a low dose of cyclophosphamide followed by adoptive transfer of tumor reactive CD4<sup>+</sup> T cells.

#### **Results**

In a murine model of colorectal cancer, we show that the combination therapy of CTX and tumor reactive CD4<sup>+</sup> T cells resulted in enhanced necrosis of tumor cells *in vivo*, leading to eventual eradication of advanced tumors. By using immunofluorescence staining and blood perfusion imaging, we demonstrated that the combination therapy leads to destruction of the established tumor vasculature and reduced blood supply to tumor tissue. Furthermore, we assessed blood vessel permeability in the tumor tissue and found that the combination therapy increased extravasation of Evans blue dye, suggesting an increase in vascular permeability.

#### **Conclusions**

In summary, our findings suggest that the combination therapy of CTX + CD4<sup>+</sup> T cells leads to destruction of the tumor vasculature, resulting in extensive necrosis of tumor tissue and eventual tumor regression. These findings may provide new insights into mechanisms of tumor rejection by CD4<sup>+</sup> T cells

**439**

### **Preclinical development of tumor-infiltrating lymphocyte therapy for pancreatic cancer**

Donastas Sakellariou-Thompson, Cara Haymaker, Caitlin Creasy, Mark Hurd, Naohiro Uraoka, Jaime Rodriguez Canales, Scott Koptez, Patrick Hwu, Anirban Maitra, Chantale Bernatchez

University of Texas MD Anderson Cancer Center, Houston, TX, USA

#### **Background**

Immunotherapy has become an effective cancer therapy, particularly in the case of checkpoint blockade and adoptive T cell therapy (ACT). ACT exploits the presence of tumor-infiltrating lymphocytes (TIL) by exponentially expanding their numbers *ex vivo* and re-infusing them into the patient in an autologous setting. With the effectiveness of TIL therapy already well established in multiple phase II studies in melanoma, there is a push to translate it to other cancers in dire need of improved therapies. Pancreatic ductal adenocarcinoma (PDAC) is one such cancer for which the current therapy, surgery and chemotherapy, provides an overall 5-year survival rate of only 5%. The presence of TIL is correlated with increased survival in PDAC, which suggests that TIL could effectively control the disease and provides a rationale to test TIL therapy in this setting.

#### **Methods**

To assess the feasibility, we characterized the immune component of PDAC, explored the ability to grow and expand TIL from tumor fragments, and analyzed the clonality of these expanded TIL.

#### **Results**

Flow cytometry analysis detected low, CD4-rich T cell infiltration. These TIL were able to be expanded *ex vivo* and the addition of an agonistic anti-41BB antibody to the cultures preferentially increased total TIL outgrowth, particularly that of CD8<sup>+</sup> TIL. The success rate of TIL growth was increased from 23% to 50% for cultures grown without and with anti-41BB respectively. Sequencing of the T cell receptor CDR3-beta chain found specific T cell clones enriched at the tumor site in comparison to the blood. IHC staining for MHC class I (MHCI) on PDAC tumor samples showed that it is widely expressed but at low levels generally.

#### **Conclusions**

In conclusion, it is possible to expand CD8<sup>+</sup> T cells from PDAC bearing TCR sequences highly enriched in the tumor. Additionally, expanded TIL would be able to target tumor cells as they are shown to express MHCI. Although there are barriers yet to overcome, the initial data suggest the feasibility of TIL therapy for PDAC.

## Late-Breaking Abstracts - Adoptive Cellular Therapy

*Presenting author underlined; Primary author in italics*

440

### Synthetic biology approaches to enhance adoptive cell therapy safety and precision

*Scott M Coyle*<sup>1</sup>, Kole T Roybel<sup>1</sup>, Levi J Rupp<sup>1</sup>, Stephen P Santoro<sup>1</sup>, Stephanie Secrest<sup>1</sup>, Michael Spelman<sup>1</sup>, Hanson Ho<sup>1</sup>, Tina Gomes<sup>1</sup>, Tiffany Tse<sup>1</sup>, Chia Yung-Wu<sup>2</sup>, Jack Taunton<sup>3</sup>, Wendell Lim<sup>3</sup>, Peter Emtage<sup>1</sup>

<sup>1</sup>Cell Design Labs, San Francisco, CA, USA

<sup>2</sup>Amgen, San Francisco, CA, USA

<sup>3</sup>University of California San Francisco, San Francisco, CA, USA

#### Background

Chimeric antigen receptor T cells (CAR-T) have shown impressive efficacy against numerous hematological malignancies, yet a high percentage of individuals receiving these therapies experience toxicity in the form of cytokine release syndrome (CRS) and/or normal tissue destruction. Furthermore, solid tumors represent a substantive challenge for CAR therapy due to a lack of tumor-specific antigens and general inability of T cells to overcome immunosuppressive tumor microenvironments. We have sought to circumvent these obstacles by utilizing synthetic biology approaches to augment CAR-T function and specificity.

#### Methods

We developed two platform technologies that aim to mitigate toxicity associated with CAR-T therapy and endow T cells with environmental sensing capabilities that enhance tumor discrimination from normal tissue and/or confer the ability to generate customizable response outputs. Firstly, we engineered an "ON-switch" CAR that consists of two protein modules that undergo heterodimerization and become competent for signaling only in the presence of a small-molecule dimerizing agent [1]. In addition, we created a "synthetic Notch" (synNotch) receptor, which we previously described in the context of combinatorial antigen sensing [2], that is capable of driving expression of any number of downstream polypeptides in response to antigen engagement.

#### Results

Here we describe advances in our ON-switch CAR design that allow for dose-dependent antigen-specific T cell activation in the presence of an FDA-approved non-immunosuppressive small molecule dimerizer. Furthermore, we demonstrate that our synNotch T cells are able to deliver therapeutic payloads capable of, but not limited to, modulating the tumor microenvironment and changing the cell-intrinsic transcriptional properties of the synNotch T cells.

#### Conclusions

We have successfully identified a heterodimerizing switch receptor that specifically activates T cells in the presence

of an FDA-approved non-immunosuppressive small molecule. The ability to control the potency of the CAR-mediated immune response in this way may reduce the toxicity associated with CAR-T therapy. Furthermore, we have demonstrated that synNotch T cells are able to sculpt the anti-tumor immune response in both a T cell intrinsic (transcriptional programming) and T cell extrinsic (therapeutic payload) manner, providing a customizable platform for altering T cell function and the tumor microenvironment.

#### References

1. Wu C-Y, Roybal KT, Puchner EM, Onuffer J, Lim, WA: **Remote control of therapeutic T cells through a small molecule-gated chimeric receptor.** *Science* 2015 **350**: aab4077.
2. Roybal KT, Rupp LJ, Morsut L, Walker WJ, McNally KA, Park JS, Lim W: **Precision Tumor Recognition by T Cells With Combinatorial Antigen-Sensing Circuits.** *Cell* **164**: 770–779.

## Late-Breaking Abstracts - Biomarkers and Immune Monitoring

Presenting author underlined; Primary author in italics

441

### Evaluation of anticancer immunity in patients with thyroid cancer with a focus towards developing effective combination immunotherapy

Tarsem Moudgil<sup>1</sup>, Carmen Ballesteros-Merino<sup>1</sup>, Traci Hilton<sup>2</sup>, Christopher Paustian<sup>2</sup>, Rom Leidner<sup>3</sup>, David Page<sup>5</sup>, Walter Urba<sup>5</sup>, Bernard Fox<sup>1</sup>, *Bryan Bell*<sup>3</sup>, Ashish Patel<sup>1</sup>

<sup>1</sup>Providence Portland Medical Center, Portland, OR, USA

<sup>2</sup>UbiVac, Portland, OR, USA

<sup>3</sup>Earle A. Chiles Research Institute, Robert W. Franz Cancer Center, Providence Portland Medical Center, Portland, OR, Portland, OR, USA

<sup>5</sup>Earle A. Chiles Research Institute, Providence Cancer Center, Portland, OR, USA

#### Background

Thyroid cancer is the most common endocrine-related cancer with 64,330 diagnoses expected this year. While the majority of these cancers are curable, almost 2% of these cancers are anaplastic thyroid cancers, which are highly aggressive and almost uniformly lethal. At the same time, the thyroid is known for being inherently immunogenic. For these reasons and due to an active surgical practice providing regular resections of thyroid cancers, we undertook a study of thyroid cancer with the idea of developing an immunotherapy for this disease.

#### Methods

We have developed a thyroid cancer tumor bank to complement our Oral, Head and Neck Cancer Program. This tumor bank cryopreserves enzymatically isolated viable cells from resected tumors (n=16). We are also attempting to develop primary cell lines and are isolating and assessing autologous tumor-specific functions of tumor-infiltrating lymphocytes (TIL) (n=7).

#### Results

To date we have established 3 tumor cell lines from thyroid cancer specimens and identified PD-L1 expression on 2 of 2 tested. While numbers are small, preliminary analyses suggest that TIL cultures can be generated from 85% of thyroid cancer specimens and that autologous tumor-reactive TIL can be detected in 43% (n=7) of thyroid cancers. Since not every tumor appears to contain TIL capable of recognizing autologous tumor, strategies to prime tumor-specific T cells represents an area of interest. DPV-003 is a microvesicle vaccine, DRibble, that contains more than 80 proteins that are overexpressed by thyroid cancer (TCGA provisional RNASeq n=509 pts). The vaccine also contains a number of DAMPs and agonist activity for multiple TLRs packed into stable double membrane microvesicles that are targeted to CLEC9A+ antigen presenting cells. We are also developing

a second thyroid-specific DRibble vaccine from a cell line derived from an anaplastic thyroid cancer.

#### Conclusions

Almost half of thyroid cancers evaluated, including one anaplastic thyroid cancer, contain T cells capable of recognizing autologous cancer cells and secreting IFN-g. However, the other 50% of thyroid cancers appear to lack tumor-reactive T cells and may benefit from combination immunotherapy strategies that include a vaccine.

#### Acknowledgements

Support: Steve and Cindy Harder, Robert W. and Elsie Franz, Wes and Nancy Lematta, Lynn and Jack Loacker, and The Chiles foundation (BAF).

442

### Development and clinical translation of 89Zr-Df-IAB22M2C for detecting CD8+ T Cells for immunotherapy applications

*Tove Olafsen*<sup>1</sup>, Daulet Satpayev<sup>2</sup>, Michael Torgov<sup>1</sup>, Filippo Marchioni<sup>1</sup>, Jason Romero<sup>1</sup>, Ziyue Karen Jiang<sup>1</sup>, Charles Zamilpa<sup>1</sup>, Jennifer S Keppler<sup>1</sup>, Alessandro Mascioni<sup>1</sup>, Fang Jia<sup>1</sup>, Chen-Yu Lee<sup>1</sup>, Jean Gudas<sup>1</sup>

<sup>1</sup>ImaginAb Inc., Inglewood, CA, USA

<sup>2</sup>AdicetBio, Inc., Menlo Park, CA, USA

#### Background

Immunotherapies are changing the landscape for cancer treatment; however, the field is hampered by the lack of biomarkers that can be used for patient selection and for monitoring treatment responses rapidly and non-invasively. To address this need, ImaginAb is developing <sup>89</sup>Zr-Df-IAB22M2C, an ~80 kDa minibody (Mb) with high affinity to the CD8 glycoprotein (binding EC<sub>50</sub> = 0.4 nM) conjugated with desferrioxamine (Df) and radiolabeled with the positron emitting radionuclide Zirconium-89 (<sup>89</sup>Zr; T<sub>1/2</sub> 78.4 hours) for imaging CD8+ T cells in humans.

#### Methods

A comprehensive preclinical program that included evaluation of the *in vitro* and *in vivo* pharmacodynamics of IAB22M2C (unconjugated Mb), Df-IAB22M2C (conjugated Mb intermediate), Zr-Df-IAB22M2C (Zr chelated, conjugated non-radiolabeled form of final drug) and <sup>89</sup>Zr-Df-IAB22M2C (radioactive final drug product) was conducted to demonstrate the safety and potential efficacy of the probe.

#### Results

*In vitro* studies using human PBMCs from 10 individual human donors showed no measurable or reproducible impact on proliferation, activation or depletion of CD8+ T cells and no consistent release of cytokines when donor CD8+ T cells were exposed to soluble or immobilized Mb

## Late-Breaking Abstracts - Biomarkers and Immune Monitoring

Presenting author underlined; Primary author in italics

protein. Studies that evaluated the effect of saturating concentrations of  $^{89}\text{Zr}$ -Df-IAB22M2C on proliferation and viability of CD8+ T cells *in vitro*, also showed no impact on these parameters. Preclinical imaging and biodistribution studies demonstrated favorable pharmacokinetics and the ability of  $^{89}\text{Zr}$ -Df-IAB22M2C to detect infiltrating CD8+ T cells in a mouse hu-PBMC NSG<sup>TM</sup> GvHD model and in Matrigel<sup>TM</sup> plugs implanted with different numbers of human CD8+ T cells. Radiation dosimetry studies conducted in hu-CD34 NSG<sup>TM</sup> mice and the results GLP dosimetry analysis showed that on average, the organs receiving the largest dose equivalent were the kidneys at 8.0 rem/mCi (2.2 mSv/MBq) followed by the liver at 7.9 rem/mCi (2.1 mSv/MBq) and LLI wall at 6.5 rem/mCi (1.8 mSv/MBq). A GLP toxicology study was conducted in cynomolgus monkeys that included multiple dose cohorts of Zr-Df-IAB22M2C and a vehicle control. The results showed that doses up to 25 mg/kg of Zr-Df-IAB22M2C administered weekly to cynomolgus monkeys did not result in any treatment-related findings in survival, clinical signs, body weights, food consumption, ophthalmic examinations, electro-cardiology, blood pressure, heart rate, clinical and anatomic pathology, peripheral blood lymphocyte population, and cytokine levels.

### Conclusions

$^{89}\text{Zr}$ -Df-IAB22M2C has the desired sensitivity and safety profile for imaging CD8+ T cells and the first-in-human studies will commence in the Q4 2016.

443

### Combinatorial CD8+ and PD-L1+ cell densities correlate with response and improved survival in non-small cell lung cancer (NSCLC) patients treated with durvalumab

Sonja Althammer<sup>1</sup>, Keith Steele<sup>2</sup>, Marlon Rebelatto<sup>2</sup>, Tze Heng Tan<sup>1</sup>, Tobias Wiestler<sup>1</sup>, Guenter Schmidt<sup>1</sup>, Brandon Higgs<sup>2</sup>, Xia Li<sup>2</sup>, Li Shi<sup>2</sup>, Xiaoping Jin<sup>2</sup>, Joyce Antal<sup>2</sup>, Ashok Gupta<sup>2</sup>, Koustubh Ranade<sup>2</sup>, Gerd Binning<sup>1</sup>

<sup>1</sup>Definiens AG, Munich, Bayern, Germany

<sup>2</sup>MedImmune, Gaithersburg, MD, USA

### Background

Immunotherapies have improved patient responses and survival, though not all patients benefit. Effective biomarkers may help to improve outcomes. Durvalumab is a human IgG1 monoclonal antibody that inhibits PD-L1 binding to PD-1 and CD80, restoring antitumor immunity [1, 2]. PD-L1 expression on tumor or tumor-infiltrating immune cells measured manually with different immunohistochemistry (IHC) assays can enrich for patients responding to anti-PD-1/PD-L1 agents. Tumor-infiltrating cytotoxic CD8+ T cells may also have potential predictive utility for therapeutic response. We explored automated image analysis and pattern recognition

of tumor biopsies to determine whether CD8+ and PD-L1+ cell densities could better identify patients most likely to respond to durvalumab than PD-L1 IHC alone.

### Methods

CP1108/NCT01693562 was a nonrandomized phase I/II trial evaluating durvalumab in advanced NSCLC and other solid tumors [3]. By 29APR2016, 304 previously treated NSCLC patients, median 3 prior lines, received 10 mg/kg of durvalumab q2w  $\leq$ 12 months. Baseline archived or fresh tumor biopsies were analyzed for PD-L1 (Ventana/SP263) and CD8 (Ventana/SP239) by IHC. For the marker combination, slides were scored using the product of PD-L1+ and CD8+ cell densities with Definiens' Developer XD 2.1.4 software. For PD-L1 alone,  $\geq$ 25% tumor cells stained for PD-L1 at any intensity were scored positive. Clinical outcomes (ORR, PFS and OS) were analysed based on CD8+ and PD-L1+ densities (n=163 available) and PD-L1 alone in pre-treatment biopsies using a discovery (n=84) and validation (n=79) set. Datasets were matched on baseline PD-L1 status, histology, ECOG, lines of therapy, and response.

### Results

Patients with high pretreatment CD8+ and PD-L1+ densities (prevalence=36%) had better ORR, OS, and PFS compared to those with low CD8+ and PD-L1+ densities (Table 1), as well as high PD-L1 expression alone.

### Conclusions

Automated image analysis of CD8+ and PD-L1+ cell densities in baseline tumor biopsies may identify patients with improved outcomes to durvalumab.

### Trial Registration

ClinicalTrials.gov identifier NCT01693562.

### References

1. MedImmune/AstraZeneca. Data on file.
2. Ibrahim R, Stewart R, Shalabi A: **PD-L1 blockade for cancer treatment: MEDI4736**. *Semin Oncol* 2015, **42**:474-483.
3. Rizvi NA, Brahmer JR, Ou SHI, Segal NH, Khleif S, Hwu WJ, *et al*: **Safety and clinical activity of MEDI4736, an anti-programmed cell death-ligand 1 (PD-L1 antibody, in patients with non-small lung cancer (NSCLC)**. *J Clin Oncol* 2015, **33**(Suppl.):Abstract 8032.



## Late-Breaking Abstracts - Biomarkers and Immune Monitoring

Presenting author underlined; Primary author in italics

**Table 1. Clinical outcomes in CD8+/PD-L1+ or PD-L1 NSCLC patient subsets**

Patient subset	n	ORR % (95% CI)	Median OS, months (95% CI)	pOS	Median PFS, months (95% CI)	pPFS
High <sup>1</sup> CD8+/PD-L1+ Discovery	26	42 (23, 63)	17.9 (8.2, NR)	0.01	5.3 (2.6, 13.6)	0.0002
Low CD8+/PD-L1+ Discovery	58	7 (2, 17)	8.8 (4.1, 12.9)		1.4 (1.2, 1.4)	
High <sup>1</sup> CD8+/PD-L1+ Validation	33	37 (20, 55)	24.3 (14.0, NR)	0.0005	7.3 (3.1, 11.1)	0.001
Low CD8+/PD-L1+ Validation	46	7 (0, 18)	6.5 (4.2, 9.4)		2.6 (1.4, 3.7)	
High <sup>1</sup> PD-L1 Discovery	46	27 (15, 41)	17.1 (8.9, NR)	0.02	2.8 (1.4, 5.3)	0.005
Low PD-L1 Discovery	35	6 (0, 19)	7.6 (3.4, 12.9)		1.4 (1.2, 1.4)	
High <sup>1</sup> PD-L1 Validation	47	28 (16, 43)	14.5 (6.5, 25.3)	0.3	4.8 (2.6, 7.3)	0.3
Low PD-L1 Validation	32	6 (0, 21)	7.6 (5.7, 15.5)		2.8 (1.4, 6.5)	

<sup>1</sup>≥20%; <sup>2</sup>≥25% tumor cells; NR=Not reached; pOS=OS log-rank p-value; pPFS=PFS log-rank p-value

444

### High dose interleukin- 2 (HD IL-2) select trial in melanoma: a tissue and blood collection protocol to identify predictive biomarkers of benefit to HD IL-2 in patients with advanced melanoma

Ryan J Sullivan<sup>1</sup>, Yujin Hoshida<sup>2</sup>, Theodore Logan<sup>3</sup>, Nikhil Khushalani<sup>4</sup>, Anita Giobbie-Hurder<sup>5</sup>, Kim Margolin<sup>6</sup>, Joanna Roder<sup>7</sup>, Rupal Bhatt<sup>8</sup>, Henry Koon<sup>9</sup>, Thomas Olencki<sup>10</sup>, Thomas Hutson<sup>11</sup>, Brendan Curti<sup>12</sup>, Shauna Blackmon<sup>13</sup>, James W Mier<sup>8</sup>, Igor Puzanov<sup>14</sup>, Heinrich Roder<sup>7</sup>, John Stewart<sup>15</sup>, Asim Amin<sup>16</sup>, Marc S Ernstoff<sup>14</sup>, Joseph I Clark<sup>17</sup>, Michael B Atkins<sup>18</sup>, Howard L Kaufman<sup>19</sup>, Jeffrey Sosman<sup>20</sup>, Sabina Signoretti<sup>8</sup>, David F McDermott<sup>8</sup>

<sup>1</sup>Medical Oncology Department, Massachusetts General Hospital, Boston, MA, USA

<sup>2</sup>Hess Center for Science and Medicine; Tisch Cancer Institute, New York, NY, USA

<sup>3</sup>Simon Cancer Center, Indiana University, Indianapolis, IN, USA

<sup>4</sup>H. Lee Moffitt Cancer Center, Tampa, FL, USA

<sup>5</sup>Department of Biostatistics & Computational Biology, Boston, MA, USA

<sup>6</sup>Department of Medical Oncology, City Of Hope, Duarte, CA, USA

<sup>7</sup>Biodesix, Inc., Boulder, CO, USA

<sup>8</sup>Beth Israel Deaconess Medical Center, Boston, MA, USA

<sup>9</sup>Case Western Reserve University, Cleveland, OH, USA

<sup>10</sup>The Ohio State University, Columbus, OH, USA

<sup>11</sup>Texas Oncology-Baylor Charles A. Sammons Cancer Center, Dallas, TX, USA

<sup>12</sup>Earle A. Chiles Research Institute, Providence Cancer Center, Portland, OR, USA

<sup>13</sup>Massachusetts General Hospital Cancer Center, Boston, MA, USA

<sup>14</sup>Roswell Park Cancer Institute, Buffalo, NY, USA

<sup>15</sup>Wake Forest Baptist Medical Center, Winston Salem, NC, USA

<sup>16</sup>Levine Cancer Institute, Carolinas HealthCare System, Charlotte, NC, USA

<sup>17</sup>Loyola University Medical Center, Maywood, IL, USA

<sup>18</sup>Georgetown-Lombardi Comprehensive Cancer Center, Washington, DC, USA

<sup>19</sup>Rutgers Cancer Institute of New Jersey, New Brunswick, NJ, USA

<sup>20</sup>Robert Lurie Comprehensive Cancer Center of Northwestern University, Chicago, IL, USA

### Background

HD IL-2 provides objective responses in 15-20% and durable complete remission in 5-8% of patients with metastatic melanoma (MM). We previously identified a gene expression-based tumor subclass characterized by immune related genes (Class 2; C2) associated with durable response to HD IL-2 compared to the remaining tumors that overexpressed lineage-associated genes (Class 1; C1). The primary objective of the HD IL-2 select trial in melanoma was to prospectively validate the favorable gene expression signature (C2). Secondary objectives were to seek serum and tissue biomarkers of durable response.

### Methods

170 patients with MM were enrolled at 15 Cytokine Working Group sites from 2010 to 2014. All patients had formalin-fixed paraffin-embedded (FFPE) tumor tissues identified and blood drawn prior to HD IL-2. Tumor assessments used WHO criteria and investigator-assessed outcomes. RNA extracted from FFPE tumor tissues was used for whole transcriptome profiling by RNA sequencing (114 samples yielded sufficient RNA, 101 passed default Quality Control (QC)). Pretreatment serum from 114 patients served as the test set and was analyzed using matrix-assisted laser desorption/ionization (MALDI) and machine-based learning algorithms to identify a predictive protein expression signature.

### Results

Thirty-one of 170 pts (18.2%) responded, and median overall survival was 21.3 months, with a 40 month median follow-up. Analysis of RNAseq from 101 patients whose specimens passed QC showed that a C2 signature was associated with response to HD IL-2 (normalized enrichment score 1.70, false discovery rate 0.004). Using MALDI, a protein expression signature enriched for acute phase proteins (including CRP, IL-6, and SAA) was defined in the pre-treatment serum and used to classify 39 patients into group A (non-acute phase protein expression) and 75 patients in group B (acute phase protein expression). Complete response rate in group A was 21% and zero in group B (p = 0.0001). Two-year PFS rate was 29% in group A compared to 4 % in group B (p = 0.0005).

**Late-Breaking Abstracts - Biomarkers and Immune Monitoring**

Presenting author underlined; Primary author in italics

**Conclusions**

In this prospective biomarker validation study, HD IL-2 produced durable remissions and prolonged survival in patients with MM. A tumor-derived gene expression signature enriched for immune-related genes was associated with response. Additionally, preliminary data with a serum protein signature appears to identify patients most likely to have a complete response.

**Trial Registration**

ClinicalTrials.gov identifier NCT01288963.

**445****Pharmacodynamic gene expression changes from talimogene laherparepvec (T-VEC) plus ipilimumab in a phase Ib study for metastatic melanoma**

Abraham A Anderson<sup>1</sup>, Igor Puzanov<sup>2</sup>, Mohammed M Milhem<sup>3</sup>, Robert HI Andtbacka<sup>4</sup>, David Minor<sup>5</sup>, Kevin Gorski<sup>1</sup>, Daniel M Baker<sup>1</sup>, Omid Hamid<sup>6</sup>, Howard L Kaufman<sup>7</sup>

<sup>1</sup>Amgen Inc., Thousand Oaks, CA, USA

<sup>2</sup>Roswell Park Cancer Institute, Buffalo, NY, USA

<sup>3</sup>University of Iowa Hospitals and Clinics, Iowa City, IA, USA

<sup>4</sup>University of Utah, Huntsman Cancer Institute, Salt Lake City, UT, USA

<sup>5</sup>California Pacific Melanoma Center, San Francisco, CA, USA

<sup>6</sup>The Angeles Clinic & Research Institute, Los Angeles, CA, USA

<sup>7</sup>Rutgers Cancer Institute of New Jersey, New Brunswick, NJ, USA

**Background**

T-VEC is a herpes simplex virus type-1 based oncolytic immunotherapy designed to selectively replicate in tumors, produce GM-CSF, and stimulate antitumor immune responses. Ipilimumab is a checkpoint inhibitor that promotes T cell activation by blocking negative signaling through CTLA-4. Both agents have demonstrated activity as monotherapy in advanced melanoma. Based on the potential complementary MOA of the agents, tumor cell lysis and antigen presentation (T-VEC) in combination with T cell checkpoint inhibition, we hypothesized that improved efficacy was possible when the agents are used in combination. Because the safety profiles are non-overlapping, the combination was not anticipated to have significant increased toxicity. To address these hypotheses, a phase Ib/II study evaluating the safety and efficacy of T-VEC plus ipilimumab for Stage III-IV metastatic melanoma was initiated. The phase Ib study was completed (N=19) with no DLTs (primary endpoint) or new safety signals with combination treatment, and an ORR of 50% [1]. Phase Ib also included biomarker analyses investigating potential pharmacodynamic markers for T-VEC monotherapy and in combination with ipilimumab.

**Methods**

Nineteen patients received T-VEC at 10<sup>6</sup> PFU/mL at week 1, then 10<sup>8</sup> PFU/mL Q2W from week 4. Ipilimumab was given at 3 mg/kg Q3W starting at week 6 for 4 infusions. Peripheral blood was obtained (Paxgene RNA) at baseline and at weeks 4, 6, 9, and 15. Gene expression (Agilent Microarray) was analyzed for changes in expression level with treatment. Pharmacodynamic markers were identified with a linear mixed effects model. False discovery was controlled with permutation testing.

**Results**

Gene expression was measured in 16 patients in phase Ib. Most treatment effects on expression were seen after ipilimumab treatment, but there were a few effects in the initial T-VEC phase that passed false discovery controls. These T-VEC effects included *SELV*, *SYNPO*, *ZBTB32*, *IQCF2*, *CDC27*, *KLK1*, *PRR20B*, *CHST6*, and *IGH*. *ZBTB32* has been reported to control the proliferative burst of virus-specific natural killer cells responding to infection. The combination effects were enriched for genes involved in lymphoid tissue structure and development and immune cell trafficking. 185 of these genes had signs of a T-VEC effect in the monotherapy phase. These included increases in *GZMM*, *PDCD1*, *CD8B*, *CD8A*, and *CTLA4* and decreases in *IL18*, *IRAK3*, and *TXNRD1*.

**Conclusions**

This hypothesis-generating microarray analysis identified genes upregulated in circulating peripheral blood cells after T-VEC monotherapy and combination treatment. We plan to further evaluate these genes and other potential pharmacodynamic markers in phase II.

**Trial Registration**

ClinicalTrials.gov identifier NCT01740297.

**References**

1. Puzanov I, Milhem MM, Minor D, Hamid O, Li A, Chen L, *et al*: **Talimogene laherparepvec in combination with ipilimumab in previously untreated, unresectable stage IIIB-IV melanoma.** *J Clin Oncol* 2016, **34**:2619-2626.



## Late-Breaking Abstracts - Clinical Trials in Progress

Presenting author underlined; Primary author in italics

446

### Phase I study of alpha-tocopherlyoxyacetic acid in patients with advanced cancer: immune response and pharmacokinetics results

Emmanuel Akporiaye<sup>1</sup>, Brendan Curti<sup>2</sup>, Yoshinobu Koguchi<sup>2</sup>, Rom Leidner<sup>3</sup>, Kim Sutcliffe<sup>3</sup>, Kristie Conder<sup>3</sup>, Walter Urba<sup>2</sup>

<sup>1</sup>Veana Therapeutics Inc, Portland, OR, USA

<sup>2</sup>Earle A. Chiles Research Institute, Providence Cancer Center, Portland, OR, USA

<sup>3</sup>Earle A. Chiles Research Institute, Robert W. Franz Cancer Center, Providence Portland Medical Center, Portland, OR, USA

#### Background

Alpha-tocopherlyoxyacetic acid ( $\alpha$ -TEA) targets tumor cell mitochondria to release reactive oxygen species (ROS) that induce immunogenic cell death (ICD), antigen release, and enhanced antigen cross-presentation in pre-clinical models.  $\alpha$ -TEA is being evaluated for safety and tolerability in a first-in-human phase I trial in patients with advanced cancers (NCT02192346). Tumor types in the ongoing trial include renal cancer, esophageal adenocarcinoma, thyroid cancer, duodenal cancer, and squamous cell carcinoma of the head and neck.

#### Methods

$\alpha$ -TEA lysine salt is administered orally to patients and given daily in escalating doses for 28 days. Immune monitoring of peripheral whole blood was conducted for all 12 patients at baseline, and at 1 week and 4 weeks post-treatment. Plasma levels of  $\alpha$ -TEA have been determined so far in patients receiving 2.4 mg/kg and 4.8 mg/kg  $\alpha$ -TEA at 1, 4, 8, and 24 hours after the first dose. Additional samples were evaluated on days 8, 15, 22, and 29 before the planned  $\alpha$ -TEA dose on those days.

#### Results

Twelve patients have been treated so far at 2.4 mg/kg and 4.8 mg/kg dose levels. Eight patients have stable disease, lasting from 1 to 22+ months. One patient showed more than a 2-fold increase in the number of activated (CD38+ HLA-DR+) effector CD8+ T cells 1 week post-treatment. A second patient showed more than a 2-fold increase in the number of activated effector memory CD8+ T cells 4 weeks post-treatment. Both patients experienced stable disease over 5 and 22 months, respectively. Evaluation of  $\alpha$ -TEA levels at the 2.4 mg/kg and 4.8 mg/kg doses revealed a proportional increase in  $\alpha$ -TEA plasma levels over a 28-day interval without any indication that steady state plasma levels were reached. Of the 12 patients, 6 developed atrial fibrillation (AF) after starting  $\alpha$ -TEA. The earliest event occurred 7 days post-treatment, but AF was more common 29-56 days post-

treatment. Four of the 6 patients had a medical history of AF. These were grade 2 events by CTCAE 4.0 criteria and managed with appropriate medication without further sequelae.

#### Conclusions

$\alpha$ -TEA treatment resulted in stable disease in 80% of patients lasting between 1 and 22+ months. AF was observed commonly in patients with a medical history of AF, and was managed with appropriate medication. No clinically meaningful grade 3 or 4 toxicities were observed. Plasma  $\alpha$ -TEA levels increased proportionally without any indication that steady state levels were achieved.  $\alpha$ -TEA may function through enhancing pre-existing CD8+ T cell-mediated anti-tumor activity.

447

### Intratumoral Flt3L and poly-ICLC combined with low dose radiotherapy: a novel in situ vaccine for incurable indolent lymphomas

Thomas Marron<sup>1</sup>, Nina Bhardwaj<sup>1</sup>, Linda Hammerich<sup>1</sup>, Fiby George<sup>2</sup>, Seunghye Kim-Schulze<sup>2</sup>, Tibor Keler<sup>3</sup>, Tom Davis<sup>3</sup>, Elizabeth Crowley<sup>3</sup>, Andres Salazar<sup>4</sup>, Joshua Brody<sup>5</sup>

<sup>1</sup>Icahn School of Medicine at Mount Sinai, New York, NY, USA

<sup>3</sup>CellDex Therapeutics, Hampton, NJ, USA

<sup>4</sup>Oncovir, Inc., Washington, DC, USA

<sup>5</sup>Mount Sinai School of Medicine, New York, NY, USA

#### Background

Lymphomas are the 5<sup>th</sup> most common cancer in the United States, and unlike more aggressive lymphomas, indolent non-Hodgkin lymphoma (iNHL) and is incurable with standard therapy. A previous trial of *in situ* vaccination in iNHL combined intratumoral injection of a TLR9 ligand with radiation to induce a systemic immune response against tumor. This approach induced tumor-specific CD8+ T cell responses and durable clinical remissions of patients' untreated sites of disease were seen in a minority of patients. One limitation in this previous trial may have been the scarcity of intratumoral dendritic cells (DCs); DCs are uniquely able to endocytose dying tumor cells for cross-presentation to tumor antigen-specific CD8+ T cells. In our novel iteration of *in situ* vaccine, intratumoral FMS-like tyrosine kinase 3 ligand (Flt3L) is introduced as a priming step to increase the presence of intratumoral DCs. Flt3L induced tumor leukocyte infiltration and regression in lymphoma tumors in pre-clinical trials, and CDX-301- a formulation of Flt3L - was previously shown to mobilize BDCA-1 and BDCA-3 myeloid DC subsets in an early phase clinical trials. These DC subsets respond to several TLR agonists and cross-present antigens more effectively than plasmacytoid DCs (pDCs). While pDCs are high expressers of TLR9, responsive to CpG, myeloid dendritic

## Late-Breaking Abstracts - Clinical Trials in Progress

Presenting author underlined; Primary author in italics

cells express a wider array of TLRs, including high levels of TLR3.

### Methods

This phase I/II trial tests the hypothesis that this novel *in situ* vaccination will induce clinical remissions at distant (untreated) tumor sites in two cohorts of patients with either previously untreated or relapsed/refractory iNHL (n=15 per group). Intratumoral CDX-301 25ug/kg is injected into a palpable lymph node for 9 days, followed by 2Gy local radiotherapy on day 9 and 10 to the target lymph node. To activate local DCs, poly-ICLC 2mg is injected on day 10, 14, 17, and weekly thereafter for a total of 8 treatments.

### Results

Exploratory endpoints include measuring induction of systemic tumor-specific immune response in pre- and post-vaccine blood and tissue samples. Using flow cytometry and CyTOF, we have confirmed that CD1c+ (BDCA1<sup>+</sup>) and CD141+ (BDCA3<sup>+</sup>) DCs home to treated tumors following treatment with Flt3L and T cells attain a mature effector phenotype. Tissue from initial bx is being sequenced, and candidate neoantigens being determined *in silico*; these neoantigens are then being synthesized and tested for potential to activate patient pre- and post-vaccination T cells.

### Conclusions

This trial is in process.

### Trial Registration

ClinicalTrials.gov identifier NCT01976585.

**448**

### Preliminary safety and efficacy data for radiotherapy and PD-L1 checkpoint blockade in metastatic non-small cell lung cancer: is timing everything?

Arta Monjazeb<sup>1</sup>, Megan E Daly<sup>2</sup>, Jonathan Riess<sup>2</sup>, Tianhong Li<sup>2</sup>, William J Murphy<sup>1</sup>, Karen Kelly<sup>2</sup>

<sup>1</sup>University of California, Davis, Sacramento, CA, USA

<sup>2</sup>University of California Davis Comprehensive Cancer Center, Sacramento, CA, USA

### Background

Inhibition of the PD-1/PD-L1 checkpoint pathway can induce rapid and durable responses in patients with non-small cell lung cancer (NSCLC). Unfortunately the majority of patients fail to respond and there is interest in exploring combinatorial strategies to improve response rates. One such strategy is combining checkpoint inhibition with radiotherapy (RT). We report here our pre-clinical data for combining radiotherapy with PD-L1 checkpoint blockade. These data demonstrate a clear influence of the sequencing of combinatorial therapy on its efficacy. Based on these data, we have initiated a clinical trial testing sequencing strategies

of radiotherapy with PD-L1 inhibition in patients with metastatic NSCLC.

### Methods

Using syngeneic mouse tumor models, we tested the synergy of combining RT with PD-L1 inhibition and the influence of the sequencing of these therapies on efficacy. Based on this preclinical work, we have initiated a phase II clinical trial testing this combinatorial strategy with three cohorts. The three cohorts are concurrent therapy, radiotherapy followed by PD-L1 checkpoint blockade, and PD-L1 blockade followed by radiotherapy. We report here the preliminary safety, efficacy, and correlative science data from interim analysis of the safety run-in for this trial.

### Results

In studies using syngeneic mouse tumor models, we find that PD-L1 inhibition provides no added benefit to radiotherapy alone when administered after radiotherapy. Conversely, priming of the immune system with anti-PD-L1 prior to RT provides significant synergy of the combinatorial therapy. Our clinical trial has completed enrollment to the safety-run in of 6 patients. In total, 2 patients experienced grade 3 dose limiting toxicities meeting the criteria for completion of the safety-run in without the need for dose de-escalation. One patient experienced asymptomatic grade 3 lymphopenia and one patient experienced both grade 3 lymphopenia and grade 3 failure to thrive. At twelve weeks post-treatment initiation, 83% of patients experienced response or disease stability. Three patients (50%) had abscopal responses by RECIST criteria, two patients (33%) had stable disease, and one patient (17%) had progressive disease.

### Conclusions

Pre-clinical data suggests that sequencing may be key to the success of combinatorial strategies of PD-L1 blockade and RT. The safety run-in for combining PD-L1 checkpoint inhibition with RT suggests that the combination is safe and tolerable in metastatic NSCLC. The trial will continue to accrual to evaluate different sequencing strategies for combining RT and PD-L1 checkpoint blockade. Further study is needed to evaluate the efficacy and optimal sequencing of RT + PD-L1 checkpoint blockade.



## Late-Breaking Abstracts - Clinical Trials: Cutting-Edge (Completed Trials)

Presenting author underlined; Primary author in italics

449

### **Efficacy and safety of nivolumab plus ipilimumab in metastatic urothelial carcinoma: first results from the phase I/II CheckMate 032 study**

Padmanee Sharma<sup>1</sup>, Margaret K Callahan<sup>2</sup>, Emiliano Calvo<sup>3</sup>, Joseph W Kim<sup>4</sup>, Filippo de Braud<sup>5</sup>, Patrick A Ott<sup>6</sup>, Petri Bono<sup>7</sup>, Rathi N Pillai<sup>8</sup>, Michael Morse<sup>9</sup>, Dung T Le<sup>10</sup>, Matthew Taylor<sup>11</sup>, Pavlina Spiliopoulou<sup>12</sup>, Johanna Bendell<sup>13</sup>, Dirk Jaeger<sup>14</sup>, Emily Chan<sup>15</sup>, Scott J Antonia<sup>16</sup>, Paolo A Ascierto<sup>17</sup>, Delphine Hennicken<sup>18</sup>, Marina Tschaika<sup>18</sup>, Alex Azrilevich<sup>18</sup>, Jonathan Rosenberg<sup>2</sup>

<sup>1</sup>University of Texas MD Anderson Cancer Center, Houston, TX, USA

<sup>2</sup>Memorial Sloan Kettering Cancer Center, New York, NY, USA

<sup>3</sup>START Madrid, Centro Integral Oncológico Clara Campal, Madrid, Spain

<sup>4</sup>Yale Cancer Center, New Haven, CT, USA

<sup>5</sup>Istituto Nazionale dei Tumori-Università degli Studi di Milano, Milano, Lombardia, Italy

<sup>6</sup>Dana-Farber Cancer Institute, Boston, MA, USA

<sup>7</sup>Comprehensive Cancer Center, Helsinki University Hospital and University of Helsinki, Helsinki, Finland

<sup>8</sup>Emory Winship Cancer Institute, Atlanta, GA, USA

<sup>9</sup>Duke University Medical Center, Durham, NC, USA

<sup>10</sup>Sidney Kimmel Comprehensive Cancer Center at Johns Hopkins University, Baltimore, MD, USA

<sup>11</sup>Oregon Health & Science University, Portland, OR, USA

<sup>12</sup>Beatson West of Scotland Cancer Centre, Glasgow, United Kingdom

<sup>13</sup>Sarah Cannon Research Institute and Department of Medical Oncology, Tennessee Oncology, Nashville, TN, USA

<sup>14</sup>Heidelberg University Hospital, Heidelberg, Baden-Württemberg, Germany

<sup>15</sup>Vanderbilt-Ingram University Medical Center, Nashville, TN, USA

<sup>16</sup>H. Lee Moffitt Cancer Center, Tampa, FL, USA

<sup>17</sup>Istituto Nazionale Tumori Fondazione Pascale, Naples, Italy, Napoli, Italy

<sup>18</sup>Bristol-Myers Squibb, Princeton, NJ, USA

#### **Background**

Nivolumab is a programmed death-1 (PD-1) immune checkpoint inhibitor associated with clinical benefit in previously treated patients with metastatic urothelial carcinoma [1]. Preclinical and clinical data indicate that the combination of nivolumab plus ipilimumab, an anti-cytotoxic T-lymphocyte antigen-4 (CTLA-4) antibody, can improve antitumor activity in other tumor types. Here, we report the first efficacy and safety results of combined nivolumab plus ipilimumab given at two different dosing schedules in CheckMate 032, an open-label, multicenter, phase I/II

study of patients with metastatic urothelial carcinoma who progressed after prior platinum-based therapy.

#### **Methods**

Patients with locally advanced or metastatic urothelial carcinoma previously treated with platinum-based therapy were included in the study. Patients were treated with either of two combination schedules, nivolumab 1 mg/kg + ipilimumab 3 mg/kg (N1I3) or nivolumab 3 mg/kg + ipilimumab 1 mg/kg (N3I1) every 3 weeks for four cycles, followed by nivolumab 3 mg/kg every 2 weeks; or they were treated with nivolumab monotherapy 3 mg/kg (N3) every 2 weeks. All patients were treated until disease progression or unacceptable toxicity. The primary endpoint was investigator-assessed objective response rate (ORR) by RECIST v1.1. Secondary endpoints included safety and duration of response (DoR).

#### **Results**

Minimum follow-up was 3.9 months in the N1I3 (n=26) group, 14.5 months in the N3I1 group (n=104), and 13.8 months in N3 group (n=78). ORR was 38.5% (95% confidence interval [CI], 20.2-59.4), 26.0% (95% CI, 17.9-35.5), and 25.6% (95% CI, 16.4-36.8) in the N1I3, N3I1, and N3 groups, respectively. Median DoR has not been reached in any treatment group. The frequency of drug-related grade 3-4 adverse events was 30.8% (N1I3), 31.7% (N3I1), and 23.1% (N3). Treatment-related adverse events led to discontinuation in 7.7% (N1I3), 13.5% (N3I1), and 3.8% (N3) of patients. One death was reported in the N3I1 group (pneumonitis) and two deaths were reported in the N3 group (pneumonitis and thrombocytopenia).

#### **Conclusions**

Second-line treatment with N1I3 may provide the most favorable benefit-risk ratio among the regimens studied. If these interim results are confirmed with longer follow-up, further development of the N1I3 combination in metastatic urothelial carcinoma is warranted.

#### **Trial Registration**

ClinicalTrials.gov identifier NCT01928394.

#### **References**

1. Sharma P, Bono P, Kim JW, *et al*: **Efficacy and safety of nivolumab monotherapy in metastatic urothelial cancer (mUC): Results from the phase I/II CheckMate 032 study.** *J Clin Oncol* 2016, **34**(15 suppl): Abstract 4501.



## Late-Breaking Abstracts - Coinhibition & Costimulation

Presenting author underlined; Primary author in italics

450

### Computational identification, functional characterization, and antibody blockade of a new immune checkpoint in the TIGIT family of interacting molecules

*Ofer Levy*<sup>1</sup>, *Christopher Chan*<sup>2</sup>, Gady Cojocaru<sup>1</sup>, Spencer Liang<sup>2</sup>, Eran Ophir<sup>1</sup>, Sudipto Ganguly<sup>3</sup>, Amir Toporik<sup>1</sup>, Maya Kotturi<sup>2</sup>, Tal Fridman Kfir<sup>1</sup>, Benjamin M. Murter<sup>3</sup>, Kathryn Logronio<sup>2</sup>, Liat Dassa<sup>1</sup>, Ling Leung<sup>2</sup>, Shirley Greenwald<sup>1</sup>, Meir Azulay<sup>1</sup>, Sandeep Kumar<sup>2</sup>, Zoya Alteber<sup>1</sup>, Xiaoyu Pan<sup>4</sup>, Arthur Machlenkin<sup>1</sup>, Yair Benita<sup>1</sup>, Andrew W. Drake<sup>2</sup>, Ayelet Chajut<sup>1</sup>, Ran Salomon<sup>1</sup>, Ilan Vankin<sup>1</sup>, Einav Safyon<sup>1</sup>, John Hunter<sup>2</sup>, Zurit Levine<sup>1</sup>, Mark White<sup>2</sup>

<sup>1</sup>Compugen Ltd., Holon, Israel

<sup>2</sup>Compugen Inc, USA, South San Francisco, CA, USA

<sup>3</sup>Johns Hopkins University, Baltimore, MD, USA

<sup>4</sup>Bloomberg~Kimmel Institute for Cancer Immunotherapy, Johns Hopkins University, Baltimore, MD, USA

#### Background

While antibody blockade of the CTLA-4 and PD-1 pathways has emerged as an effective treatment modality for cancer, the majority of patients do not derive long-term benefit, suggesting a need for targeting of additional immune checkpoints. Employing our unique computational algorithms to define new members of the B7/CD28 family, we identified PVRIG, which is expressed by multiple subsets of T and NK cells. We report here its expression pattern, functional characterization, and anti-tumor activity of blocking antibodies targeting this molecule

#### Methods

Utilizing Compugen's Predictive Discovery platform we identified PVRIG as a potential novel immune checkpoint, after which a retroviral cell screening library was used to identify its cognate binding counterpart. Target effects on T cell modulation were assessed with primary and tumor-derived T cell assays, taking advantage of target overexpression, knockdown, and antagonist antibody approaches. Antibodies against the human protein were screened for their ability to enhance T cell activation *in vitro*, while antibodies targeting the mouse orthologue were assessed *in vivo* for effects on tumor growth inhibition in syngeneic models

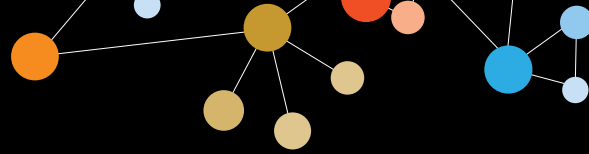
#### Results

A PVRIG-Fc-fusion protein was found to bind PVRL2, with binding specificity confirmed both by ELISA and flow cytometry analysis. PVRIG demonstrated unique expression kinetics upon T cell activation, with detection of the target on memory T cells, as well as on NK cells and  $\gamma\delta$  T cells. A panel of high affinity human antibodies with the ability to block interaction of PVRIG with PVRL2 were generated, which

when tested *in vitro* were shown to enhance activation of both primary CD4+ and tumor-derived CD8+ T cells through a PVRL2-dependent mechanism. The lead antibody, COM-701, is currently in preclinical development. Since COM-701 is not mouse cross-reactive, *in vivo* studies were conducted with a surrogate blocking anti-mouse PVRIG antibody. When combined with anti-PD-L1 blockade, anti-mouse PVRIG inhibits growth of established tumors in both the CT26 and MC38 colorectal cancer models. Combination testing with additional immune checkpoint inhibitors, as well as in PVRIG knockout mice, is ongoing.

#### Conclusions

We describe the identification of PVRIG as a novel immune checkpoint on T cells, as well the development of a high affinity antagonistic antibody, COM-701, that is currently in preclinical development. COM-701 is able to enhance human T cell activation, and a surrogate antibody with similar characteristics shows synergy with PD-L1 *in vivo* in multiple syngeneic models. Overall, our data demonstrate the utility of targeting PVRIG in addition to other B7 family checkpoints for the treatment of cancer.



## Late-Breaking Abstracts - Combinations: Immunotherapy/Immunotherapy

Presenting author underlined; Primary author in italics

451

### **Tissue factor is a novel oncotarget in triple negative breast cancer and BRAF- mutated melanoma for immunotherapy using a second generation ICON (L-ICON) in monotherapy and combination therapy**

Zhiwei Hu<sup>1</sup>, Rulong Shen<sup>2</sup>, Amanda Campbell<sup>2</sup>, Elizabeth McMichael<sup>2</sup>, Lianbo Yu<sup>2</sup>, Bhuvanewari Ramaswam<sup>2</sup>, Cheryl A London<sup>2</sup>, Tian Xu<sup>3</sup>, William Carson<sup>2</sup>

<sup>1</sup>The Ohio State University Wexner Medical Center and The OSU James Comprehensive Cancer Center, Columbus, OH, USA

<sup>2</sup>The Ohio State University, Columbus, OH, USA

<sup>3</sup>Yale University, New Haven, CT, USA

#### **Background**

The objective of this study is to identify tissue factor (TF) as a novel oncotarget for triple negative breast cancer (TNBC) and BRAF mutated melanoma, both of which are very difficult to treat in clinic, and to develop a novel TF-targeting agent for immunotherapy. To achieve this goal, Hu developed a second generation TF-targeting ICON, named L-ICON, which consists of only the light chain (1-152 aa) of FVII fused to an IgG1Fc. The effects of L-ICON were evaluated as monotherapy or combination therapy with interleukin 15 (IL-15) for the malignancies.

#### **Methods**

TF expression was determined by immunohistochemistry or by flow cytometry. L-ICON protein (GenBank accession no. KY760097) and replication-deficient adenoviral vectors have been developed. Binding activity of L-ICON was determined. Its ADCC effect was evaluated by an ADCC effector assay and coagulation activity by FVII chromogenic activity assay. L-ICON efficacy in monotherapy and combination therapy with IL-15 was tested in mouse models of murine and human breast cancer (4T1 and TNBC MDA-MB-231) and melanoma (B16F10 and BRAF mutated SK-Mel-28).

#### **Results**

TF is over-expressed on TNBC cells and the tumor neovasculature in over 85% of TNBC patients (n=14) when using standard paraffin-embedded tumor tissues or in nearly 60% of TNBC patients (n=157) when employing tissue microarray slides (Figure 1). Importantly, TF expression is not detected in normal breast tissues (Figure 1). L-ICON has several important improvements over its first generation ICON (Figures 2, 3), including (i) more than 50% reduction in molecular mass, (ii) complete elimination of coagulation activity, (iii) stronger binding activity to TNBC and (iv) more effective as monotherapy *in vivo* in orthotopic and subcutaneous mouse models of human TNBC (MDA-MB-231) and murine cancer 4T1 (an animal stage IV human breast

cancer) and B16F10. L-ICON monotherapy and combination with IL-15 were effective for the treatment of SK-Mel-28 in SCID mouse models.

#### **Conclusions**

TF is a novel marker and oncotarget in TNBC and BRAF-mutated melanoma. L-ICON, a novel TF-targeting ICON, was effective in monotherapy and combination therapy with IL-15 for the treatment of murine and human TNBC and melanoma *in vitro* and *in vivo* in preclinical mouse models.

#### **Acknowledgements**

This work was partly supported by a startup fund from OSUMC, a Seed Award from the OSUCCC TT Program, a Phase 1 L-Pilot Award from OSU CCTS via NCATS Award Number UL1TR001070. IL-15 was obtained from the NCI Preclinical Repository. Z.H. is the inventor of L-ICON and its uses (US Patent Application # 62/082,891).

452

### **Beta-adrenergic blockade improves the immunotherapeutic response to melanoma**

Kathleen M Kokolus<sup>1</sup>, Elizabeth A Repasky<sup>2</sup>, Todd D Schell<sup>1</sup>, Joseph D Drabick<sup>1</sup>

<sup>1</sup>The Pennsylvania State University College of Medicine, Hershey, PA, USA

<sup>2</sup>Roswell Park Cancer Institute, Buffalo, NY, USA

#### **Background**

Recent developments in immunotherapy have made enormous strides towards expanding the scope of cancer treatment by targeting a patient's own immune cells. Despite these advances, malignant melanoma remains a significant clinical issue with a high proportion of patients remaining unresponsive to therapy and improved, but still low, complete response rates. The body's response to stress is closely integrated with the immune response, yet few cancer treatment strategies account for the relationship between these biological systems. When the stress response is activated, neurotransmitters, including norepinephrine, which bind  $\beta$ -adrenergic receptors ( $\beta$ ARs) located on the surface of immune cells, are released, leading to regulation of various immune cell functions.  $\beta$ AR signaling can be prevented pharmaceutically with  $\beta$ AR antagonists ( $\beta$ -blockers) and considerable literature suggests that these drugs, which are commonly prescribed for other indications including hypertension, are associated with positive outcomes in cancer patients. We examined the effects of  $\beta$ AR blockade on the efficacy of two immunotherapies approved to treat metastatic melanoma: IL-2, which promotes T cell proliferation and  $\alpha$ PD-1, which impacts T cell activation.

**Late-Breaking Abstracts - Combinations: Immunotherapy/Immunotherapy**

Presenting author underlined; *Primary author in italics*

**Methods**

C57BL/6J mice with established B16.F10 melanomas were treated with  $\beta$ -blockers and immunotherapy ( $\alpha$ PD-1, IL-2 or  $\alpha$ PD-1/IL-2) and tumor growth was monitored throughout each treatment regimen. The accumulation of immune cells within the tumors and lymphoid tissues were evaluated by flow cytometry at multiple time points following treatment.

**Results**

Blockade of  $\beta$ AR signaling beginning after tumors were established had no significant impact on tumor growth. In contrast, attenuation of tumor growth by each immune-based therapy was improved in the presence of  $\beta$ -blockers. We observed significantly extended survival in mice treated with  $\alpha$ PD-1 or  $\alpha$ PD-1/IL-2 combined with  $\beta$ -blockers compared to immunotherapy only mice. Most importantly, the combination of  $\beta$ -blockers,  $\alpha$ PD-1 and IL-2 produced a highly significant delay in tumor growth and prolonged survival compared to  $\alpha$ PD-1/IL-2 without  $\beta$ -blockers.

**Conclusions**

Blocking  $\beta$ AR signaling improved the efficacy of at least two types of immunotherapy, but was most effective when administered with dual-immunotherapy. We suggest that each therapeutic component may improve a unique aspect of the immune response to maximally delay melanoma progression. Due to the availability of all three components for use in humans, this therapeutic regimen can potentially be clinically translated to expand the population of metastatic melanoma patients who experience long term benefits from immune-based therapies.

**Acknowledgements**

This work was supported by CURE Grant SAP #4100072562 (Pennsylvania Department of Health) and NIH/NCI 5T32 CA060395 (KMK). IL-2 was generously provided by Prometheus Laboratories Inc.

**453****Sequentially targeting upregulated TIM-3 and CTLA-4 does not rescue the attenuated therapeutic efficacy of combination immunotherapy with OX40 costimulation and PD-1 blockade**

David J Messenheimer<sup>1</sup>, Shawn Jensen<sup>2</sup>, Bernard Fox<sup>2</sup>

<sup>1</sup>Earle A. Chiles Research Institute, Portland, OR, USA

<sup>2</sup>Providence Cancer Center, Portland, OR, USA

**Background**

Combination immunotherapy targeting checkpoint molecules has shown substantial results against solid tumors. However as novel therapies targeting costimulatory molecules are introduced into the clinic, successful combination with checkpoint blockade remains uncertain. Some strongly

immunogenic preclinical models have shown benefit when combining anti-OX40 and anti-PD-1 treatment. In contrast, using a PD-1 refractory mammary tumor model we have demonstrated that a significant anti-tumor effect generated with OX40 costimulation is significantly attenuated with the addition of PD-1 blockade. We noted high levels of inflammatory cytokines in the serum of combination treated mice, and also saw a significant increase in inhibitory receptors TIM-3, LAG-3, and CTLA-4 on CD4<sup>+</sup> and CD8<sup>+</sup> T cells in the periphery of treated mice. We hypothesized that the upregulation of these other inhibitory receptors were limiting the efficacy of anti-OX40 plus anti-PD-1 combination treatment, and tested whether sequentially blocking these receptors could augment therapeutic efficacy.

**Methods**

Established orthotopically transplanted MMTV-PyMT mammary tumors in FVB/NJ mice were treated with three doses of anti-OX40 and anti-PD-1 every other day. Serum was taken at time points and tested for cytokine concentration and spleens were taken two days after treatment to measure surface expression of inhibitory and costimulatory receptors. Combination treated mice were then followed by three doses of anti-TIM-3 with or without anti-CTLA-4.

**Results**

The addition of anti-TIM-3 and CTLA-4 provided no additional impact to tumor growth compared to that provided by anti-OX40 and anti-PD-1 (n = 7/group, two independent experiments).

**Conclusions**

These data demonstrate that TIM-3 and CTLA-4 blockade was not sufficient to augment the inhibitory effects of the concurrent combination of anti-OX40 and anti-PD-1, and suggest that targeting inhibitory receptors upregulated after initial immunotherapy treatment will require more sophisticated biomarkers and immune monitoring. Alternatively, we noted significant increases in some costimulatory receptors (ICOS, 4-1BB) and targeting these receptors may provide an alternative to blocking inhibitory pathways. Additionally there may be a tipping point where providing additional antibodies targeting costimulatory or checkpoint molecules may be ineffective. T cells may become so heavily deregulated or over-stimulated that they become permanently exhausted. In support of this we have previously shown that anti-OX40 combined sequentially with anti-PD-1 provides superior therapeutic effect compared to concurrent combination, with complete tumor regression in ~30% of animals treated. Sequentially treated animals generated T cells capable of significantly more long-term proliferation, suggesting that timing is critical when combining immunotherapies.

## Late-Breaking Abstracts - Combinations: Immunotherapy/Immunotherapy

Presenting author underlined; Primary author in italics

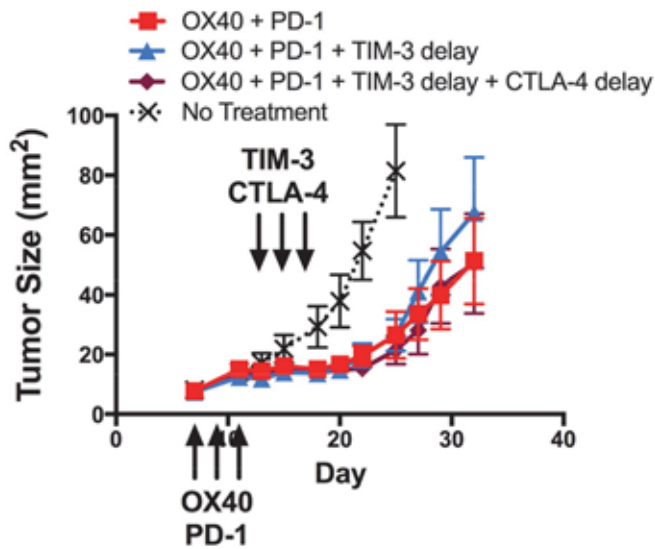


**Figure 1.** The addition of anti-TIM + anti-CTLA-4 provides no benefit to anti-OX40 + anti-PD-1 combination treatment.

454

### Novel IL-2/mAb complexes mediate potent anti-tumor immunity which is augmented with anti-PD-1 mAb therapy

Mark Rubinstein<sup>1</sup>, Kristina Andrijauskaitė<sup>1</sup>, Marzena Swiderska-syn<sup>1</sup>, Kristin Lind<sup>2</sup>, Agnes Choppin<sup>2</sup>, Marina K Roell<sup>2</sup>

<sup>1</sup>Medical University of South Carolina, Charleston, SC, USA

<sup>2</sup>XOMA Corporation, Berkeley, CA, USA

#### Background

Recent success and FDA approval of immune checkpoint inhibitors (CI) in a growing number of cancers are transforming cancer treatment and revitalizing interest in immunotherapies. However, while efficacy is observed in patients with advanced metastatic diseases treated with CI, not all patients respond and most responses are incomplete. Preclinical studies suggest that combinations of additional modalities will provide opportunities to improve patient responses. As both IL-2 and CI therapy can independently augment anti-tumor immunity in patients, likely in mechanistically distinct ways, we hypothesized we could improve anti-tumor immunity by combining IL-2 and anti-PD-1 mAb therapy.

#### Methods

To improve IL-2 efficacy and therapeutic index, we generated novel anti-IL-2 mAbs which, when complexed with IL-2 (IL-2/mAb) offer advantages over standard IL-2 therapy [1-3]. First, binding to an anti-IL-2 mAb increases IL-2 half-life and biological activity. Second, depending on the epitope at which the mAb binds to IL-2, antibody binding can modulate

which IL-2 receptor subunits (alpha, beta, or gamma) are engaged. Antibodies that interfere with binding of IL-2R $\alpha$  can reduce activation of high-IL-2R $\alpha$ -expressing cell types, such as suppressive Tregs, and steer activity toward cell types expressing only IL-2R $\beta$  and  $\gamma$ . In this way, these complexes may have more effective anti-tumor activity [1-3]. We screened antibody phage libraries to identify antibodies that shift IL-2 receptor binding and activity differentially on different cell types *in vitro* and *in vivo*. Complexes of these antibodies were tested *in vivo* for their effects on T cell frequency and activation, and in a subcutaneous Lewis lung carcinoma model for their ability to mediate anti-tumor immunity, both alone and in combination with anti-PD-1 mAb.

#### Results

In normal mice, IL-2/mAb complexes potently expanded CD8<sup>+</sup> T cells and NK cells with minimal expansion of Tregs. As single agent therapy, IL-2/mAb complexes or anti-PD-1 mAb reduced tumor growth, although most mice succumb to tumor growth eventually. Combination of IL-2/mAb complexes with anti-PD-1 mAb therapy resulted in durable, complete responses in nearly half of the mice.

#### Conclusions

While immune based therapies such as anti-PD-1 mAb can be highly effective in select patients, even in those patients that obtain clinical benefit, disease may recur. Our results suggest that the addition of IL-2/mAb complexes to therapy with anti-PD-1 mAb could broadly increase the percentage of patients deriving benefit from immune-based therapy.

#### References

1. Sato, *et al: Biotherapy* 1993, **6(3)**:225-231.
2. Boyman, *et al: Science* 2006, **311**:1924-1927.
3. Létourneau, *et al: PNAS* 2010, **107**:2171-2176.

455

### The combination of an IL-15/IL-15R $\alpha$ complex (ALT-803) and anti-PD-1 mAb leads to superior anti-tumor immunity in a murine lung tumor model

John Wrangle<sup>1</sup>, Kristina Andrijauskaitė<sup>1</sup>, Marzena Swiderska-syn<sup>1</sup>, Peter Rhode<sup>2</sup>, Hing Wong<sup>2</sup>, Mark Rubinstein<sup>1</sup>

<sup>1</sup>Medical University of South Carolina, Charleston, SC, USA

<sup>2</sup>Altos BioScience Corporation, Miramar, FL, USA

#### Background

Administration of antibodies that block the PD-1/PD-L1 pathway has demonstrated unprecedented success in mediating clinical responses in patients with advanced cancer. These antibodies are thought to act by blocking the ability of PD-L1 to mediate an inhibitory signal to PD-1 expressing T cells during antigen-recognition. These



**Late-Breaking Abstracts - Combinations: Immunotherapy/Immunotherapy**

Presenting author underlined; Primary author in italics

antibodies are now FDA-approved for multiple cancers including non-small cell lung cancer (NSCLC) in patients with disease that has progressed during or after platinum-based chemotherapy. In these patients, one in five patients can attain a clinical response while on checkpoint inhibitor therapy. While promising, this therapy fails to induce a durable clinical response in most patients. To overcome this limitation, we hypothesized that combinatorial therapy with anti-PD-1 mAb and a lymphocyte growth factor would more effectively augment the expansion of tumor-reactive lymphocytes. This would also provide a means to not only remove inhibitory pathways but directly augment the function of tumor-reactive lymphocytes. We chose to use an IL-15/IL-15Ra complex (ALT-803) composed of an IL-15 mutant (N72D) that was pre-associated with the soluble IL-15Ra/Fc fusion protein. This superagonist complex has been shown to potently expand and activate CD8<sup>+</sup> T cells and NK cells in various animal models.

**Methods**

To assess the efficacy of combination therapy, we injected C57BL/6 mice subcutaneously with Lewis lung carcinoma. Mice with established tumors were treated with anti-PD-1 mAb and/or IL-15/IL-15Ra complex, and we monitored tumor progression and changes in immune cell populations in the periphery and tumor.

**Results**

The combination of anti-PD-1 mAb and the IL-15/IL-15Ra complex was substantially more effective at inducing complete responses compared with administration of either agent alone. Effective therapy was associated with the expansion of CD8<sup>+</sup> T cells and NK cells, and the acquisition of the ability of CD8<sup>+</sup> T cells to produce IFN $\gamma$  after activation. Interestingly, *in vitro*, IFN $\gamma$  led to upregulation of both MHC and PD-L1 on tumor cells, suggesting a mechanistic basis for the improved efficacy of the combination therapy.

**Conclusions**

Our results suggest that the efficacy of anti-PD-1 mAb therapy may be improved by co-administration of the IL-15/IL-15Ra complex. Our results also suggest a mechanistic basis for why the combination may be superior to single agent therapy. To determine if this combination would be of value in human patients, we have initiated a phase Ib/II clinical trial (NCT02523469) to assess the combination of anti-PD-1 mAb (nivolumab) in combination with ALT-803 in patients with refractory advanced NSCLC.

**456****Preliminary efficacy from a phase I/II study of the natural killer cell-targeted antibody lirilumab in combination with nivolumab in squamous cell carcinoma of the head and neck**

Rom Leidner<sup>1</sup>, Hyunseok Kang<sup>2</sup>, Robert Haddad<sup>3</sup>, Neil H Segal<sup>4</sup>, Lori J Wirth<sup>5</sup>, Robert L Ferris<sup>6</sup>, F Stephen Hodi<sup>3</sup>, Rachel E Sanborn<sup>7</sup>, Thomas F Gajewski<sup>8</sup>, William Sharfman<sup>9</sup>, Dan McDonald<sup>10</sup>, Shivani Srivastava<sup>10</sup>, Xuemin Gu<sup>10</sup>, Penny Phillips<sup>10</sup>, Chaitali Passey<sup>10</sup>, Tanguy Seiwert<sup>8</sup>

<sup>1</sup>Earle A. Chiles Research Institute, Robert W. Franz Cancer Center, Providence Portland Medical Center, Portland, OR, USA

<sup>2</sup>Johns Hopkins Sidney Kimmel Comprehensive Cancer Center, Baltimore, MD, USA

<sup>3</sup>Dana-Farber Cancer Institute, Boston, MA, USA

<sup>4</sup>Memorial Sloan Kettering Cancer Center, New York, NY, USA

<sup>5</sup>Massachusetts General Hospital, Boston, MA, USA

<sup>6</sup>University of Pittsburg, Pittsburg, PA, USA

<sup>7</sup>Earle A. Chiles Research Institute, Providence Cancer Center, Portland, OR, USA

<sup>8</sup>University of Chicago Medical Center, Chicago, IL, USA

<sup>9</sup>The Sidney Kimmel Comprehensive Cancer Center, Johns Hopkins University School of Medicine, Lutherville, MD, USA

<sup>10</sup>Bristol-Myers Squibb, Princeton, NJ, USA

**Background**

Natural killer (NK) cells and the innate immune system play a critical role in immunosurveillance, control of tumor growth, and metastasis. NK-cell activation is negatively regulated by inhibitory killer-cell immunoglobulin-like receptors (KIRs); therefore, blocking KIR function may potentiate an anti-tumor immune response and complement other immunology therapies that enhance T cell activity. We present preliminary efficacy results in patients with squamous cell carcinoma of the head and neck (SCCHN) from a phase I/II study of lirilumab, a fully human monoclonal antibody that blocks inhibitory KIRs on NK cells, in combination with nivolumab, a fully human IgG4 monoclonal antibody that targets the PD-1 receptor, in patients with solid tumors (NCT01714739).

**Methods**

During dose escalation, patients with advanced solid tumors who progressed after  $\geq 1$  prior therapy received lirilumab 0.1–3.0 mg/kg once every 4 weeks (Q4W) plus nivolumab 3.0 mg/kg Q2W. Cohort expansion was initiated at the maximum dose of lirilumab 3.0 mg/kg Q4W plus nivolumab 3.0 mg/kg Q2W in patients with advanced solid tumors. Key study endpoints include safety (primary), objective response rate



## Late-Breaking Abstracts - Combinations: Immunotherapy/Immunotherapy

Presenting author underlined; Primary author in italics

(ORR), disease control rate (DCR), duration of response (DOR), and biomarker assessments.

### Results

As of the August 30, 2016 data cutoff, 159 patients were treated with the lirilumab plus nivolumab combination. Treatment-related adverse events (TRAEs) and grade 3–4 TRAEs were reported in 72% (114/159) and 15% (24/159) of patients, respectively. Discontinuations due to TRAEs occurred in 8% (12/159). Of the 41 patients with SCCHN treated, 29 were evaluable for response. In this heavily pretreated, checkpoint inhibitor-naïve group, ORR was 24% (7/29; confirmed and unconfirmed) and DCR was 52% (15/29). Maximum reduction in target lesions are presented in Figure 1 for 26 patients with available tumor assessments. Two patients classified as stable disease per RECIST v1.1 showed unconventional responses, with 100% and 37% reductions in target lesions. Among evaluable patients, five (17%) had reductions in tumor burden > 80%. Responses appear durable, with the median DOR not reached (Figure 2). Updated efficacy and preliminary biomarker analyses (including PD-L1 and HPV status) will be presented.

### Conclusions

Preliminary efficacy of lirilumab plus nivolumab in patients with advanced platinum-refractory SCCHN demonstrates clinical benefit, with encouraging response rates that were deep and durable responses in some patients. This combination demonstrated a manageable safety profile similar to that observed with nivolumab monotherapy. Further evaluation of this novel combination of an NK-cell inhibitor and an immune checkpoint inhibitor is ongoing.

### Trial Registration

ClinicalTrials.gov identifier: NCT01714739

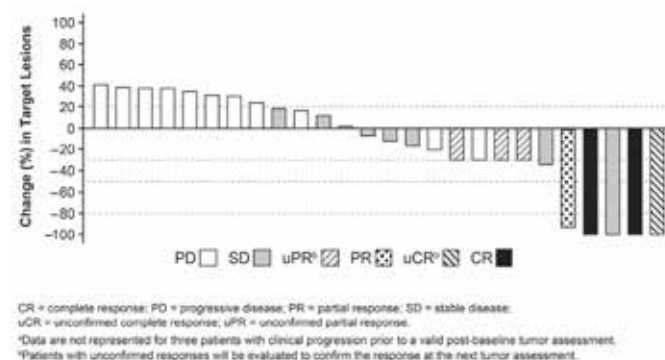


Figure 1. Maximum percent reduction in target lesions from baseline.<sup>a</sup>

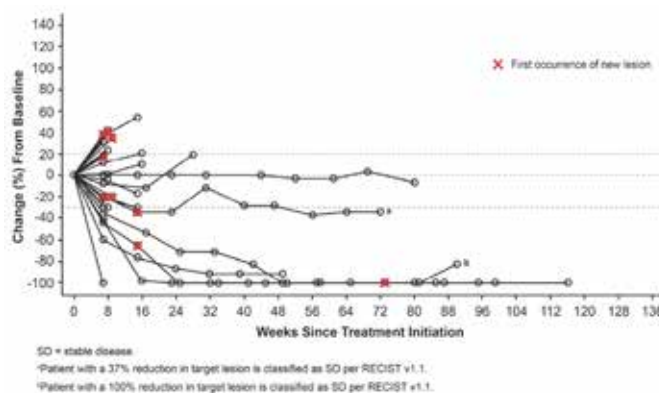


Figure 2. Percent change from baseline in target lesions over time.

### 457

#### Functional dichotomy of PI3K isoforms in CD4 T cells provides a strategy for selectively targeting regulatory T cells to enhance anti-tumor immunotherapy

*Shamim Ahmad*<sup>1</sup>, *Mason Webb*<sup>1</sup>, Rasha Abu-Eid<sup>1</sup>, Rajeev Shrimali<sup>1</sup>, Vivek Verma<sup>1</sup>, Atbin Doroodchi<sup>1</sup>, Zuzana Berrong<sup>1</sup>, David Yashar<sup>1</sup>, Raed Samara<sup>2</sup>, Mikayel Mkrtychyan<sup>1</sup>, Samir Khleif<sup>1</sup>

<sup>1</sup>Georgia Cancer Center, Augusta, GA, USA

<sup>2</sup>Qiagen, Frederick, MD, USA

### Background

The PI3K-Akt signaling pathway modulates diverse biological responses including signaling, proliferation and survival of T cells. The identification of a signaling pathway, which differentially regulates regulatory T cells (Tregs) and conventional T cells (Tconvs), is crucial for selectively modulating these two subsets. The differential role of class IA PI3K isoform in regulating the survival and apoptosis of Tregs and Tconvs has not been elucidated yet.

### Methods

For *in vitro* experiments sorted Tregs and Tconvs were labeled with CellTrace™ Violet Cell Proliferation stain (VCT) according to the manufacturer's protocol (Life Technologies, NY). Cells were stimulated with and without inhibitors. For *in vivo* experiments C57BL/6 Mice were injected subcutaneously (s.c.) with TC-1 tumor cells and monitored for development of tumors. Vaccine was given weekly s.c. For therapeutic experiments vaccine was given weekly throughout the experiment. CAL-101 treatment was provided on the day when tumor size reached 3-4 mm 5-6 day before vaccination.

### Results

Here, we report that PI3Kd isoform is sufficient for TCR downstream signaling, proliferation, and survival for either Tconvs or Tregs. In Tregs, however, PI3Kd is a dominant

**Late-Breaking Abstracts - Combinations: Immunotherapy/Immunotherapy**

Presenting author underlined; *Primary author in italics*

isoform, where Tregs are fully dependent on PI3K $\delta$  to regulate these properties as PI3K $\alpha$  and PI3K $\beta$  do not play any role in these biologic processes. On the other hand, in Tconvs, the two other isoforms, PI3K $\alpha$  and PI3K $\beta$  combined, provide redundant pathway to PI3K $\delta$  in the regulation of TCR signaling, proliferation and survival. This redundant role provided by PI3K $\alpha$  and PI3K $\beta$  isoforms to PI3K $\delta$  in Tconvs offers a selective therapeutic approach to inhibit Tregs, where by inhibiting PI3K $\delta$ , signaling, proliferation, and survival are inhibited in Tregs, while PI3K $\alpha$  and PI3K $\beta$ , will provide a path for Tconvs to proliferate and function. Importantly, we demonstrate that our findings translate to therapeutic efficacy *in vivo*, where the inhibition of PI3K $\delta$ , enhanced anti-tumor efficacy of antigen-specific vaccine by decreasing the suppressive Tregs and increasing the number of vaccine-induced CD8 T cells, thus showing synergistic therapeutic effect against tumors. Our findings provide a strategy for the selective targeting of Tregs in the frame of cancer combination immunotherapy.

**Conclusions**

These findings provide a new insight into CD4 T cell biology and offer a new strategy for selective targeting of Tregs in the frame of development of anti-cancer immunotherapies.

## Late-Breaking Abstracts - Immunotherapy/Standard of Care

Presenting author underlined; Primary author in italics

458

### **Pembrolizumab in combination with chemoradiotherapy (CRT) for locally-advanced squamous cell carcinoma of the head and neck (SCCHN): Interim safety analysis (ISA)**

Steven Powell<sup>1</sup>, Mark Gitau<sup>2</sup>, Christopher Sumei<sup>1</sup>, Andrew Terrell<sup>2</sup>, Michele Lohr<sup>1</sup>, Ryan K Nowak<sup>1</sup>, Steven McGraw<sup>3</sup>, Ash Jensen<sup>2</sup>, Miran Blanchard<sup>2</sup>, Kathryn A Gold<sup>4</sup>, Ezra EW Cohen<sup>4</sup>, Christie Ellison<sup>1</sup>, Lora Black<sup>1</sup>, John Lee<sup>5</sup>, William Chad Spanos<sup>1</sup>

<sup>1</sup>Sanford Cancer Center, Sioux Falls, SD, USA

<sup>2</sup>Sanford Roger Maris Cancer Center, Fargo, ND, USA

<sup>3</sup>Sanford Health, Sioux Falls, SD, USA

<sup>4</sup>Moore's Cancer Center, University of California, San Diego, La Jolla, CA, USA

<sup>5</sup>NantKwest, Inc., Culver City, CA, USA

#### Background

Blockade of the programmed death receptor 1 (PD-1) interaction with its ligands (PD-L1, PD-L2) represents an active therapeutic approach in recurrent and metastatic SCCHN [1]. This immune checkpoint may allow immune escape during standard treatment, including CRT [2]. Standard CRT in SCCHN has substantial toxicity and the safety of adding PD-1 inhibition is unknown. We report the first ISA of weekly cisplatin-based CRT in combination with pembrolizumab, a humanized IgG4 monoclonal antibody inhibitor of the PD-1:PD-L1/2 interaction.

#### Methods

This is an open-label phase IB trial of pembrolizumab used in combination with cisplatin-based, definitive CRT in patients with stage III-IVB SCCHN. The treatment schema is outlined in Figure 1. Key inclusion and exclusion criteria are in Figure 2. The primary endpoint of safety is assessed by dose-limiting grade  $\geq 3$  adverse events (AEs) and immune-related AEs (irAEs) per NCI-CTCAE v4.0 criteria. Efficacy is measured by RECIST v1.1 complete response (CR) rate on 100-day post-CRT imaging and/or pathologic CR for those who undergo salvage surgery. Planned enrollment is 39 patients based on a hypothesized CR rate of  $>60\%$  and a two-stage Simon minimax design (type I error rate of 0.05 and power of 0.80). Secondary endpoints will include overall response, survival, and quality-of-life assessments.

#### Results

At the time of ISA, 27 patients have been enrolled. Patient and disease characteristics are in Table 1. At data cut-off on 9/14/2016, 22 patients have completed CRT. Of those patients, 3 required cisplatin dose reductions and 6 required a dose discontinuation. Acute grade (G)  $\geq 3$  AEs for those completing CRT are in Table 2. Median cumulative cisplatin dose is 225 mg/m<sup>2</sup>. There were no radiation dose-limiting toxicities. Two patients (9%) discontinued pembrolizumab

due to irAEs (G2 peripheral motor neuropathy and G3 transaminase elevation). No deaths have occurred.

#### Conclusions

This represents one of the first studies to evaluate the safety of concurrent CRT and PD-1 inhibition in SCCHN. Acute CRT-related toxicities are comparable to other SCCHN CRT studies. No new immunologic safety signals were seen. Further investigation of this approach is warranted.

#### Acknowledgements

Funding supported by the Merck Investigator Studies Program.

#### Trial Registration

ClinicalTrials.gov identifier: NCT02586207

#### References

- Seiwert TY, *et al*: **Safety and clinical activity of pembrolizumab for treatment of recurrent or metastatic squamous cell carcinoma of the head and neck (KEYNOTE-012): an open-label, multicentre, phase 1b trial.** *Lancet Oncol* 2016, **17(7)**:956-965.
- Parikh F, *et al*: **Chemoradiotherapy-induced upregulation of PD-1 antagonizes immunity to HPV-related oropharyngeal cancer.** *Cancer Res* 2014, **74(24)**:7205-7216.

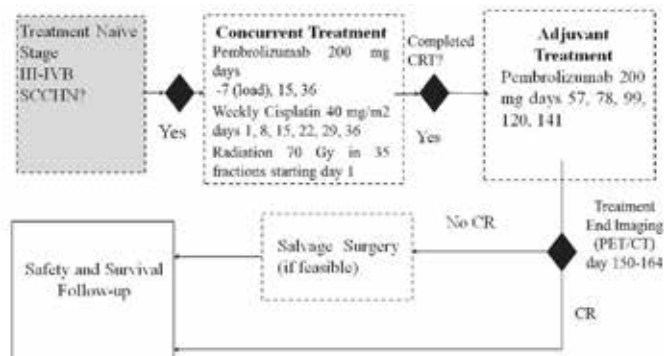


Figure 1. Clinical Trial Schema

INCLUSION	EXCLUSION
Squamous cell carcinoma of the oral cavity (excluding lip), oropharynx, hypopharynx, or larynx	Prior chemotherapy, radiotherapy, or immunotherapy for SCCHN
Stage III, IVA, or IVB	Stage IVC (distant metastases) disease
Age $\geq 18$	Concurrent active malignancy (excluding skin basal cell and squamous cell carcinomas)
ECOG PS 0-1	Active infections
RECIST 1.1 measurable disease	Active pneumonitis
Adequate organ function	History of HIV or active Hepatitis B or C

## Late-Breaking Abstracts - Immunotherapy/Standard of Care

Presenting author underlined; Primary author in italics

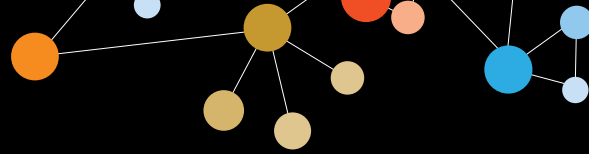
**Figure 2.** Key Inclusion and Exclusion Criteria

**Table 1:** Patient and Disease Characteristics

Demographics	
Median Age (range)	61.7 yrs (36-80 yrs)
Sex (n, %)	Male (23, 85%) Female (4, 15%)
Race (n, %)	White/Non-Hispanic (25, 92.6%) White/Hispanic (1, 3.7%) Native American (1, 3.7%)
Disease Characteristics	
Stage (n, %)	III (1, 3.7%) IVA (25, 92.6%) IVB (1, 3.7%)
Primary Site (n, %)	Oropharynx (22, 81.5%) <i>HPV (p16) positive (20, 74.1%)</i> <i>HPV (p16) negative (2, 7.4%)</i> Larynx (4, 14.8%) Hypopharynx (1, 3.7%)

**Table 2:** Acute Grade  $\geq 3$  Adverse Events with  $>1$  Occurrence

Adverse Event	Grade (n, %)
Lymphocyte count decreased	G3 (10, 45%), G4 (5, 23%)
White blood cell decreased	G3 (11, 50%)
Dysphagia	G3 (10, 45%)
Neutrophil count decreased	G3 (8, 36%)
Mucositis oral	G3 (4, 18%)
Hyponatremia	G3 (3, 14%)
Weight loss	G3 (3, 14%)
Hypophosphatemia	G3 (3, 14%)
Dehydration	G3 (2, 9%)
Anemia	G3 (2, 9%)
Radiation Dermatitis	G3 (2, 9%)
Platelet count decreased	G3 (2, 9%)



## Late-Breaking Abstracts - Diet, Exercise and/or Stress and Impact on the Immune System

Presenting author underlined; Primary author in italics

459

### **Exercise training reduces splenic accumulation of MDSCs and delays tumor progression in a therapeutic breast cancer model**

Erik Wennerberg<sup>1</sup>, Emily Schwitzer<sup>2</sup>, Claire Lhuillier<sup>1</sup>, Graeme Koelwyn<sup>3</sup>, Rebecca Hiner<sup>2</sup>, Lee Jones<sup>2</sup>, Sandra Demaria<sup>4</sup>

<sup>1</sup>Weill Cornell Medicine, New York, NY, USA

<sup>2</sup>Memorial Sloan Kettering Cancer Center, New York, NY, USA

<sup>3</sup>New York University School of Medicine, New York, NY, USA

<sup>4</sup>Department of Radiation Oncology, Weill Cornell Medicine, New York, NY, USA

#### **Background**

Epidemiological studies show a correlation between physical activity and cancer-related mortality [1]. However, the contribution of immune mediated anti-tumor immunity to the beneficial effects of exercise has yet to be defined [2]. We sought to investigate if forced running would have a therapeutic benefit in mice bearing a poorly immunogenic breast cancer and investigate the immunological changes occurring in response to exercise.

#### **Methods**

On day 0 Balb/c mice were inoculated with 4T1 breast cancer cells subcutaneously in the right flank (n=6/group). Starting on day 7, once tumors were palpable, mice were subjected to 30 minutes of forced treadmill running (18 cm/sec) five days per week. Control mice remained sedentary throughout the study. Analysis of immune cells in spleen and tumor was performed at day 17 and 32 and spontaneous lung metastases were evaluated at day 32.

#### **Results**

We observed a significantly delayed primary tumor growth (tumor volume on day 31: 1167±174 mm<sup>3</sup> in sedentary versus 847±124 mm<sup>3</sup> in exercised mice, p < 0.01) and a tendency for reduced metastatic burden in the lungs of exercised compared to sedentary mice. The progressive marked increase in myeloid-derived suppressor cells (MDSCs) and splenomegaly seen in sedentary 4T1 tumor-bearing mice was less pronounced in exercised mice. This difference was significant on day 17; with spleen weight (520±110 mg in sedentary versus 330±30 mg in exercised mice, p < 0.01) and MDSC frequency in spleen leukocytes (22.7±2.6 % in sedentary versus 14.3±2.7 % in exercised mice, p < 0.001) were significantly lower in exercised mice compared to sedentary mice. Furthermore, on day 32, the CD8+ T cell/Treg and CD8+ T cell/MDSC ratio showed a tendency to increase in tumors from exercised mice.

#### **Conclusions**

Our data demonstrate that exercise can slow tumor progression in a therapeutic setting. While the mechanisms of this effect require further investigation, the observed decrease in the proportion of immunosuppressive immune cells in spleen and tumor of exercised mice is likely to play a role. Importantly, the ability of exercise to reduce immunosuppression locally and systemically supports testing exercise in combination with immunotherapy as a therapeutic modality that can increase responses without increasing toxicity.

#### **References**

1. Ballard-Barbash R, Friedenreich CM, Courneya KS, Siddiqi SM, McTiernan A, Alfano CM: **Physical activity, biomarkers, and disease outcomes in cancer survivors: a systematic review.** *Natl Cancer Inst* 2012, **104**:815-840.
2. Koelwyn GJ, Wennerberg E, Demaria S, Jones LW: **Exercise in Regulation of Inflammation-Immune Axis Function in Cancer Initiation and Progression.** *Oncology* 2015, **29**(12).



## Late-Breaking Abstracts - Not Listed/Other

Presenting author underlined; *Primary author in italics*

460

### **Systemic immunotherapeutic efficacy of an immunocytokine, NHS-muLL12, in a superficial murine orthotopic bladder cancer model**

Vandever Amanda, John W Greiner, Jeffrey Schlom

Laboratory of Tumor Immunology and Biology, Center for Cancer Research, National Cancer Institute, Bethesda, MD, USA

#### **Background**

Interleukin-12 is one of the most powerful proinflammatory cytokines capable of supporting T and NK cell function, inducing IFN $\gamma$  while driving a T $\subscript{H}$ 1 adaptive immune response. Its success as an antitumor agent in preclinical models has yet to be realized in a clinical setting due to systemic toxicity. An IL-12 delivery system has been developed to maximize deposition of the cytokine directly in the tumor microenvironment (TME), while mitigating the dose-limiting systemic effects.

#### **Methods**

NHS-IL12 is a novel immunocytokine, consisting of two molecules of human or murine IL-12 fused to a tumor necrosis-targeting human IgG1 (NHS76). NHS76 recognizes exposed chromatin-DNA found in necrotic human/murine tumors. Previous studies have shown selective tumor uptake of NHS-IL12 in necrotic subcutaneous murine tumors. Urothelial bladder cancer is known to respond favorably to immunotherapeutic agents due to many somatic mutations and TILs, and response to Bacillus Calmette-Guerin (BCG).

#### **Results**

We evaluated the use of NHS-muLL12 in a murine orthotopic bladder cancer model. MB49<sup>Luc</sup> cells, instilled into the bladder form superficial, multifocal tumors which can be monitored with a luciferase-based intravital imaging system. NHS-muLL12 is a very potent anti-tumor agent in both MB49 tumor models, reducing tumor volume in a dose-dependent manner. In the intravesical bladder model, antitumor effects were seen at 2.5mg/kg administered as three separate systemic injections. Mice were cured of tumor when treated at 20mg/kgx3 NHS-muLL12 with durable tumor-free long-term survival. Immune analyses revealed TAA-specific CTLs and IFN- $\gamma$  responses, indicating the development of a specific anti-tumor immune response. An immune memory response protected mice following re-challenge with MB49 tumor cells. Anti-tumor efficacy required CD4+ or CD8+ T cells as depletion of either abrogated the anti-tumor effects. Evaluation of TILs by FACS, revealed that NHS-muLL12 significantly reduced the number of immune suppressive cells such as MDSCs, 24 hours post-treatment, which continued to the end of the study. Immunofluorescence

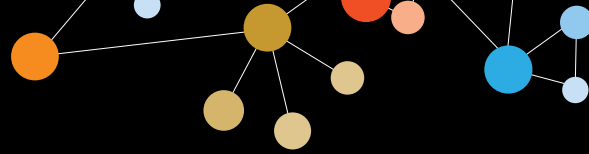
showed correlative treatment-related modulation of CD4+ and CD8+ T cells as well as MDSCs and Tregs within the TME. Gene expression of RNA from bladder tumors, identified various immune components with immunosuppressive or immune potentiating roles, modulated by NHS-muLL12 treatment.

#### **Conclusions**

These data support the possibility that NHS-muLL12 abrogates an immune-suppressive response within the TME, which might permit T cells to execute their antitumor effects. NHS-huLL12 (MSB0010360N; M9241), is currently being evaluated against solid tumors in a phase I clinical trial (NCT01417546).

#### **Acknowledgements**

We acknowledge the kind contribution of NHS-muLL12 from EMD Serono, Billerica, MA.



## Late-Breaking Abstracts - Therapeutic Cancer Vaccines

*Presenting author underlined; Primary author in italics*

**461**

### **Intracellular trafficking of self-assembled immune signals**

Michelle Bookstaver, Christopher M Jewell

Fischell Department of Bioengineering, University of Maryland - College Park, College Park, MD, USA

#### **Background**

We recently exploited electrostatic interaction to design self-assembling nanostructures comprised entirely from peptide antigens and toll-like receptor (TLR) agonists as adjuvants. These materials simplify vaccine composition and exhibit unique properties such as direct control over the absolute and relative concentrations of each component and co-delivery of the signals to antigen presenting cells. In pre-clinical models of melanoma, this approach leads to significantly enhanced anti-tumor immunity. Here, we study how the physicochemical features (e.g., peptide charge) and relative concentration of each component impact the internalization, trafficking, and processing of the immune signals in antigen presenting cells.

#### **Methods**

FITC-labeled SIINFEKL peptide was modified with three or nine arginines, for use as a cationic anchor to support self-assembly with a polyanionic nucleic acid-based TLR3 agonist, polyIC. Hollow capsules built from these signals were synthesized by coating a sacrificial CaCO<sub>3</sub> core with alternating layers of modified SIINFEKL and PolyIC. After deposition, the core was removed using EDTA and capsules were washed with buffer, resulting in stable capsules formed from immune signals. Capsule size was determined by image analysis and component loading levels were determined by fluorimetry using FITC-labeled peptide and Cy5-labeled TLRa. Stability studies were carried out by incubating capsules in media as a function of different pH and ionic strengths. For uptake and trafficking studies, murine splenocytes were isolated and treated with different concentrations of capsules. Cells were analyzed by flow cytometry and imaging in the presence or absence of inhibitors of endocytic processes and during staining with markers for surface proteins and intracellular organelles.

#### **Results**

Capsules loaded with FITC-SIINFEKL-R<sub>9</sub> and PolyIC were 1-2µm in diameter and exhibited similar size and shape for 2 weeks when in buffer. These materials exhibited tunable loading with a composition of 15.5% peptide and 84.5% TLRa used for trafficking studies. FITC-SIINFEKL-R<sub>9</sub> and PolyIC capsules were efficiently internalized through energy dependent processes (i.e., endocytosis) when incubated with primary dendritic cells within 1 hour of treatment. These

effects were also found to be dose-dependent and did not impact viability of treated cells.

#### **Conclusions**

Initial studies reveal capsules comprised of FITC-SIIN-R<sub>9</sub> and PolyIC are uptaken by primary immune cells quickly and effectively. Ongoing studies will assess the uptake of capsules by endocytosis in the presence of inhibitors to decipher the endocytic pathway and trafficking of capsules through lysosomes and endosomes.

#### **Acknowledgements**

This work was supported in part by NSF CAREER # 1351688 and Alliance for Cancer Gene Therapy # 15051543.

**462**

### **Analysis of B and T cell responses in non-small cell lung cancer (NSCLC) patients enrolled in a phase II trial of cyclophosphamide with allogenic DRibble vaccine (DPV-001)**

Christopher Paustian<sup>1</sup>, Andrew Gunderson<sup>1</sup>, Brian Boulmay<sup>2</sup>, Rui Li<sup>3</sup>, Bradley Spieler<sup>4</sup>, Kyle Happel<sup>4</sup>, Tarsem Moudgil<sup>5</sup>, Zipei Feng<sup>6</sup>, Carmen Ballesteros-Merino<sup>3</sup>, Christopher Dubay<sup>6</sup>, Brenda Fisher<sup>7</sup>, Yoshinobu Koguchi<sup>8</sup>, Sandra Aung<sup>1</sup>, Eileen Mederos<sup>4</sup>, Carlo B. Bifulco<sup>3</sup>, Michael McNamara<sup>9</sup>, Keith Bahjat<sup>9</sup>, William Redmond<sup>9</sup>, Augusto Ochoa<sup>4</sup>, Hong-Ming Hu<sup>10</sup>, Adi Mehta<sup>11</sup>, Fridtjof Lund-Johansen<sup>11</sup>, Bernard Fox<sup>6</sup>, Walter Urba<sup>8</sup>, Rachel E. Sanborn<sup>8</sup>, *Traci Hilton*<sup>1</sup>

<sup>1</sup>UbiVac, Portland, OR, USA

<sup>2</sup>Section of Hematology/Oncology, Louisiana State University, New Orleans, LA, USA

<sup>3</sup>Robert W. Franz Cancer Research Center, Earle A. Chiles Research Institute, Providence Cancer Center, Portland, OR, USA

<sup>4</sup>Louisiana State University Stanley S. Scott Cancer Center, New Orleans, LA, USA

<sup>5</sup>PPMC, Portland, OR, USA

<sup>6</sup>Providence Cancer Center, Portland, OR, USA

<sup>7</sup>Providence Medical Center, Portland, OR, USA

<sup>8</sup>Earle A. Chiles Research Institute, Providence Cancer Center, Portland, OR, USA

<sup>9</sup>Providence Medical Center, Portland, OR, USA

<sup>10</sup>UbiVac, Providence Medical Center, Portland, OR, USA

<sup>11</sup>Oslo University Hospital, Oslo, Norway

#### **Background**

DRibble vaccines are microvesicles derived from proteasome-blocked autophagosomes. The DPV-001 DRibble vaccine is derived from an adenocarcinoma and a mixed histology cancer cell line. By mass spectroscopy they contain more than 130 potential NSCLC antigens, many as prospective altered-peptide ligands, which could intensify their immunogenicity. In preclinical models, DRibble immunotherapy provided

## Late-Breaking Abstracts - Therapeutic Cancer Vaccines

Presenting author underlined; Primary author in italics

significant cross-protection against 8 of 9 tumors tested. Additionally, Dribble vaccines are effective in treating established tumors in preclinical combination immunotherapy models. We hypothesize that the efficacy of DRibbles' vaccination can be attributed to their capacity to present tumor-derived short-lived proteins (SLiPs) and defective ribosomal products (DRiPs) that are typically not processed and presented by professional antigen presenting cells. These SLiPs and DRiPs embody a prospective pool of tumor antigens against which the host may be less tolerant.

### Methods

Thirteen definitively-treated stage III NSCLC patients were vaccinated at 3-week intervals. Patients were randomized such that some patients' intradermal vaccines were combined with administration of imiquimod or GM-CSF as an adjuvant. PBMCs and serum were collected at baseline and at each vaccination. For one patient, PBMCs from the baseline visit and week 12 were tested against that patient's autologous tumor cell line to measure increased tumor specific T cell activation. Studies are currently underway to evaluate changes in TCR repertoires. CD4+ and CD8+ T cells from multiple time points were sorted and TCR sequencing is being performed to look at alterations in the T cell repertoire. The primary outcome measure of this clinical trial was to discover if vaccine alone, vaccine plus imiquimod, or vaccine plus GM-CSF generated the greatest number of strong antibody response.

Serum from the baseline visit and week 12 was analyzed for increased antibody response to >9000 human proteins using ProtoArrays and Microsphere Affinity Proteomics. Where sufficient tumor was available, whole exome sequencing was done to evaluate whether antibody and T cell responses were directed to mutations, altered peptide ligands or overexpressed normal proteins.

### Results

Compared to vaccination alone or vaccination with GM-CSF, vaccination with DPV-001 plus imiquimod significantly ( $p < 0.05$ ) increased the number of antibody responses that were four-fold higher at week twelve. In the one patient where autologous tumor was available, vaccination increased the tumor-specific release of TNF-alpha by peripheral blood CD4 T cells.

### Conclusions

Based on these studies, future trials will combine the adjuvant imiquimod with DRibble vaccine.

### Trial Registration

ClinicalTrials.gov identifier: NCT01909752

463

### An open-label phase I/IIa escalating dose study to evaluate safety and T cell immunogenicity of PDS0101 in subjects with cervical intraepithelial neoplasia (CIN) and high-risk HPV infection

*Frank Bedu-Addo*<sup>1</sup>, Greg Conn<sup>1</sup>, Michael King<sup>1</sup>, Panna Dutta<sup>1</sup>, Robert Shepard<sup>2</sup>, Mark Einstein<sup>3</sup>

<sup>1</sup>PDS Biotech, New Brunswick, NJ, USA

<sup>2</sup>PDS Biotech, Miami Beach, FL, USA

<sup>3</sup>Rutgers, NJ Medical School, Newark, NJ, USA

### Background

Current HPV vaccines are effective at preventing infection. However, there are no therapeutic vaccines to treat the infection or commonly associated diseases e.g. CIN, cervical, anal and oral cancers. A therapy that is simple, effective and safe enough to be administered to CIN and early-stage cancer patients could be important in achieving the goal of effective cancer prevention and treatment of pre-metastatic cancer. We assessed whether PDS0101, a combination of modified multi-epitope HPV16 peptides (HPVmix) and escalating doses of the synthetic Versamune® T cell activating platform could facilitate antigen cross-presentation and safe immune activation leading to strong HPV-specific CD8+ T cell induction in CIN.

### Methods

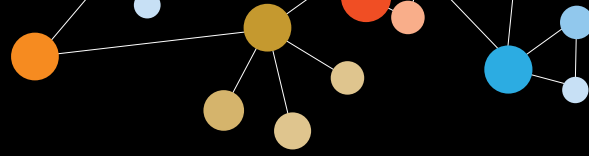
Safety and immunogenicity were assessed in an open label dose escalation study. Groups of 3-6 subjects received either low dose (1mg), medium dose (3mg) or high dose (10mg) of Versamune® cationic lipid with 2.4mg of HPVmix. Each subject received one SC dose every 3 weeks for a total of 3 doses. T cell response was evaluated by IFN-γ and granzyme-b ELISpot using blood drawn from the subjects pre-vaccination, 2 weeks after each vaccination and 90 days after vaccination 3. The trial is registered at ClinicalTrials.gov (number NCT02065973).

### Results

No serious adverse events were reported. No IND safety reports were submitted. No subjects withdrew. Strong HPV-specific T cell responses occurred at all 3 doses, even in those subjects with low pre-vaccination T cell responses. PDS0101 vaccination led to strong T cell responses evaluated by both IFN-γ and granzyme-b ELISpot. **Conclusions:** PDS0101 is safe and effectively performs antigen cross-presentation as demonstrated by HPV-specific T cell responses, including inducing active cytolytic T cells. Clinical benefit in CIN2/3 and cancer will be evaluated in larger phase II trials.

### Conclusions

PDS0101 is safe and effectively performs antigen cross-presentation as demonstrated by HPV-specific T cell



## **Late-Breaking Abstracts - Therapeutic Cancer Vaccines**

Presenting author underlined; *Primary author in italics*

responses, including inducing active cytolytic T cells. Clinical benefit in CIN2/3 and cancer will be evaluated in larger phase II trials.

### **Trial Registration**

ClinicalTrials.gov identifier: NCT02065973

**Late-Breaking Abstracts - Tumor Microenvironment**

Presenting author underlined; *Primary author in italics*

**464****Effects of TLR7 agonist imiquimod combined with local radiotherapy on the tumor microenvironment in women with metastatic breast cancer in a prospective trial**

Sylvia Adams<sup>1</sup>, Ena Wang<sup>2</sup>, Ping Jin<sup>3</sup>, Yelena Novik<sup>1</sup>, Debra Morrison<sup>1</sup>, Ruth Oratz<sup>1</sup>, Franco M Marincola<sup>2</sup>, David Stroncek<sup>4</sup>, Judith Goldberg<sup>1</sup>, Sandra Demaria<sup>5</sup>, Silvia C Formenti<sup>5</sup>

<sup>1</sup>Perlmutter Cancer Center, New York University School of Medicine, NYC, NY, USA

<sup>2</sup>Sidra Medical and Research Center, Doha, Qatar

<sup>3</sup>National Institutes of Health Clinical Center Department of Transfusion Medicine, Bethesda, MD, USA

<sup>4</sup> National Institutes of Health Clinical Center, Bethesda, MD, USA

<sup>5</sup>Weill Cornell Medicine, Department of Radiation Oncology, New York, NY, USA

**Background**

Application of TLR7 activator imiquimod (IMQ) onto BCC of the skin leads to an early tumoral transcriptional profile of immunological rejection (ICR) preceding complete remission as shown in a randomized trial [1]. Here we employed the same methodology evaluating serial FNA tumor biopsies from breast cancer patients treated on a clinical trial of the combination of IMQ and radiotherapy (RT), to delineate dynamic changes associated with ICR in breast cancer and to understand the contribution of each treatment modality to antitumor immunity *in vivo*. We previously demonstrated synergy of IMQ/RT in the poorly immunogenic TSA model with enhanced T cell-mediated inhibition of treated and untreated tumors [2].

**Methods**

Clinical trial (NCT01421017): for patients with metastatic breast cancer to the skin. Treatment: topical IMQ to one metastasis, IMQ and RT to another metastasis. IMQ self-applied 5xX/per week x 8weeks, RT started with first IMQ (6Gyx5 over 10 days). Cyclophosphamide (200mg/m<sup>2</sup> IV) was administered a week before in a subset of patients. An untreated, measurable lesion (skin or distant metastases) outside the IMQ and radiation fields was observed as systemic response read-out per RECIST1.1. Local response defined as PR or CR in treated lesions. FNA of IMQ and IMQ/RT treated metastases: at baseline, 2 and 3 weeks, RNA isolation/amplification performed per SOPs. Gene expression: Affymetrix Human GeneArray 1.0 ST/Partek Genomics suite software with special emphasis on expected immune signature.

**Results**

Serial FNA samples are available from 18 patients. Gene expression profiles of baseline biopsy treated with IMQ/RT identified 2309 differentially expressed genes ( $p < 0.005$ ) between CR and PR. Among them, ICR genes such as GZMB, GZMH, PRF1, GNLY, CD8A and TBX21 are over expressed in CR. Significant altered gene expression was observed in progressing lesions (week 3 vs baseline, 1854 genes) in contrast to responding metastases (PR: 53 genes, CR: 23 genes) post IMQ/RT suggesting active wound healing and tumor progression signature. For the IMQ alone treated metastases, differential gene expression was observed at baseline distinguishing subsequent PR and PD ( $n=189$ ,  $p < 0.005$ ). Systemic response was observed as a marked baseline gene expression difference ( $n=1177$ ,  $p < 0.005$ ) predicting abscopal phenomena (CR, PR, SD and PD).

**Conclusions**

The ICR signature in tumors before IMQ-RT treatment is positively correlated with complete local response, which validates the ICR hypothesis in metastatic breast cancer. Systemic response consistent with induction and/or boosting of adaptive immunity is predicted by significant enrichment of immune signature.

**Acknowledgements**

1R01CA161891

**Trial Registration**

ClinicalTrials.gov identifier: NCT01421017

**References**

1. Panelli: *Genome Biol* 2008.
2. Dewan: *CCR* 2012.

**465****Immunescore as a prognostic marker in stage I-III colon cancer: results of a SITC-led global validation study**

Jérôme Galon<sup>1</sup>, Bernhard Mlecnik<sup>1</sup>, Florence Marliot<sup>1</sup>, Fang-Shu Ou<sup>2</sup>, Carlo B Bifulco<sup>3</sup>, Alessandro Lugli<sup>4</sup>, Inti Zlobec<sup>4</sup>, Tilman T Rau<sup>4</sup>, Iris D Nagtegaal<sup>5</sup>, Elisa Vink-Borger<sup>5</sup>, Arndt Hartmann<sup>6</sup>, Carol Geppert<sup>6</sup>, Michael H. Roehrl<sup>7</sup>, Prashant Bavi<sup>7</sup>, Pamela S Ohashi<sup>7</sup>, Julia Y Wang<sup>7</sup>, Linh T Nguyen<sup>7</sup>, SeongJun Han<sup>7</sup>, Heather L MacGregor<sup>7</sup>, Sara Hafezi-Bakhtiari<sup>7</sup>, Bradley G Wouters<sup>7</sup>, Yutaka Kawakami<sup>8</sup>, Boryana Papivanova<sup>8</sup>, Mingli Xu<sup>8</sup>, Tomonobu Fujita<sup>8</sup>, Shoichi Hazama<sup>9</sup>, Nobuaki Suzuki<sup>9</sup>, Hiroaki Nagano<sup>9</sup>, Kiyotaka Okuno<sup>10</sup>, Kyogo Itoh<sup>11</sup>, Eva Zavadova<sup>12</sup>, Michal Vocka<sup>12</sup>, Jan Spacek<sup>12</sup>, Lubos Petruzella<sup>12</sup>, Bohuslav Konopasek<sup>12</sup>, Pavel Dundr<sup>12</sup>, Helena Skalova<sup>12</sup>, Toshihiko Torigoe<sup>13</sup>, Noriyuki Sato<sup>13</sup>, Tomohisa Furuhashi<sup>13</sup>, Ichiro Takemasa<sup>13</sup>, Marc Van den Eynde<sup>14</sup>, Anne Jouret-Mourin<sup>14</sup>, Jean-Pascal Machiels<sup>14</sup>, Tessa Fredriksen<sup>1</sup>, Lucie Lafontaine<sup>1</sup>, Bénédicte Buttard<sup>1</sup>, Sarah Church<sup>1</sup>, Pauline Maby<sup>1</sup>, Helen Angell<sup>1</sup>, Mihaela Angelova<sup>1</sup>, Angela Vasaturo<sup>1</sup>,





## Late-Breaking Abstracts - Tumor Microenvironment

Presenting author underlined; Primary author in italics

Gabriela Bindea<sup>1</sup>, Anne Berger<sup>1</sup>, Christine Lagorce<sup>1</sup>, Prabhu S Patel<sup>15</sup>, Hemangini H Vora<sup>15</sup>, Birva Shah<sup>15</sup>, Jayendrakumar B Patel<sup>15</sup>, Kruti N Rajvik<sup>15</sup>, Shashank J Pandya<sup>15</sup>, Shilin N Shukla<sup>15</sup>, Yili Wang<sup>16</sup>, Guanjun Zhang<sup>16</sup>, Giuseppe V Masucci<sup>17</sup>, Emilia K Andersson<sup>17</sup>, Fabio Grizzi<sup>18</sup>, Luigi Laghi<sup>18</sup>, Gerardo Botti<sup>19</sup>, Fabiana Tatangelo<sup>19</sup>, Paolo Delrio<sup>19</sup>, Gennaro Cilberto<sup>19</sup>, Paolo A Ascierto<sup>19</sup>, Franco Marincola<sup>20</sup>, Daniel J Sargent<sup>2</sup>, Bernard A Fox<sup>3</sup>, Franck Pages<sup>1</sup>

<sup>1</sup>INSERM, Université Pierre et Marie Curie, Université Paris Descartes, Paris, France

<sup>2</sup>Mayo Clinic, Rochester, MN, USA

<sup>3</sup>Earle A. Chiles Research Institute, Providence Cancer Center, Portland, Oregon, USA

<sup>4</sup>Institute of Pathology, University of Bern, Bern, Switzerland

<sup>5</sup>Radboud University Nijmegen Medical Center, Nijmegen, Netherlands

<sup>6</sup>University Erlangen-Nürnberg, Erlangen, Germany

<sup>7</sup>Princess Margaret Cancer Centre, University Health Network, Toronto, ON, Canada

<sup>8</sup>Division of Cellular Signaling, Institute for Advanced Medical Research, Keio University School of Medicine, Tokyo, Japan

<sup>9</sup>Department of Gastroenterological, Breast and Endocrine Surgery, Yamaguchi University Graduate School of Medicine, Ube, Japan

<sup>10</sup>Department of Surgery, Kinki University Faculty of Medicine, Osaka-Sayama, Japan

<sup>11</sup>Division of Clinical Research, Research Center for Innovative Cancer Therapy, Kurume University School of Medicine, Kurume, Japan

<sup>12</sup>First Faculty of Medicine, Charles University and General University Hospital, Prague, Czech Republic

<sup>13</sup>Sapporo Medical University, Sapporo, Japan

<sup>14</sup>Institut Roi Albert II, Cliniques universitaires St-Luc, Université Catholique de Louvain, Brussels, Belgium

<sup>15</sup>The Gujarat Cancer & Research Institute, Ahmedabad, India

<sup>16</sup>Institute for Cancer Research, Xi'an Jiaotong University, Xi'an, China

<sup>17</sup>Karolinska Institutet, Karolinska University, Stockholm, Sweden

<sup>18</sup>Humanitas Clinical and Research Center, Rozzano, Italy

<sup>19</sup>Istituto Nazionale Tumori Fondazione Pascale, Naples, Italy

<sup>20</sup>Sidra Medical and Research Center, Doha, Qatar

### Background

Increasing evidence has illustrated that enhanced lymphocytic infiltration is a powerful prognostic marker in colon cancer (CC). The Immunoscore (IM) methodology was developed as a standardized assay to quantify the *in situ* immune cell infiltrate.

### Methods

The Society for Immunotherapy of Cancer (SITC) led an international consortium, initiated with 23 expert centers

from 17 countries, to evaluate the Immunoscore in routine clinical settings. CC patients (pts) stages I/II/III with no prior neo-adjuvant treatment were included in this study. Overall, 3855 pts split into a training set (TS), internal validation set (IVS), and external validation set (EVS) were quantified for IM using immunohistochemistry with CD3/CD8 antibodies and digital pathology quantification of whole slide sections. All statistical analyses were pre-defined and performed by external statisticians. The primary endpoint was time-to-recurrence (TTR); multivariate analyses were performed using Cox models adjusted for IM, age, gender, T-stage, N-stage, and stratified by participating center.

### Results

Across centers, the median recurrent follow-up was 126.6 months. Pt characteristics: 51.5% male, median age 69 years, and 17%/54%/29% stage I/II/III, respectively. Among pts with stages I-III CC in the TS, TTR was shorter among 152 pts (22%) with Low-IM CC vs. 548 pts with High-IM CC (HR [95% CI], 0.41 [0.28-0.61];  $P < 0.0001$ ). In the IVS, TTR was also shorter among 155 pts with Low-IM CC vs. 481 pts with High-IM CC (0.41 [0.27-0.65];  $P < 0.0001$ ). In the EVS, TTR was also shorter among 225 pts with Low-IM CC vs. 744 pts with High-IM CC (0.51 [0.38-0.68];  $P < 0.0001$ ). These results were independent of age, sex, tumor stage, and sidedness. Among secondary objectives, Immunoscore groups (High, Int, Low) predicted time to recurrence in the TS (0.19 [0.10-0.37];  $P < 0.0001$ ), IVS (0.27 [0.14-0.53];  $P < 0.0001$ ), and EVS (0.33 [0.22-0.49];  $P < 0.0001$ ). In stage II CC pts (1433), the difference in TTR was significant between the Low and High-Immunoscore groups (0.36 [0.23-0.56];  $P < 0.0001$ ). In multivariate models, Immunoscore grouping (2, 3, or 5) was significant (C-index : 0.73 [0.66-0.80], all  $P < 0.0001$ ). Multivariate models including MSI and sidedness were performed and will also be presented. Reproducibility of the IM assay was validated across centers.

### Conclusions

The primary and secondary endpoints of the global Immunoscore study were reached. Overall, TTR was significantly longer in pts with stages I-III CC defined as High-IM. Moreover, a subgroup of patients with high-risk stage II CC was also identified by Low-IM.

### Acknowledgements

This initiative was supported by a variety of sources, including funding from Definiens, Prometheus, and a grant from the Czech Ministry of Health, 15-28188A and League against cancer.

**Late-Breaking Abstracts - Tumor Microenvironment**

Presenting author underlined; Primary author in italics

466

**Phase II study of intratumoral plasmid interleukin 12 (pIL-12) with electroporation in combination with pembrolizumab in stage III/IV melanoma patients with low tumor infiltrating lymphocytes**

Alain Algazi<sup>1</sup>, Katy Tsai<sup>1</sup>, Michael Rosenblum<sup>1</sup>, Prachi Nandoskar<sup>1</sup>, Robert HI Andtbacka<sup>2</sup>, Amy Li<sup>1</sup>, John Nonomura<sup>3</sup>, Kathryn Takamura<sup>3</sup>, Mary Dwyer<sup>3</sup>, Erica Browning<sup>3</sup>, Reneta Talia<sup>3</sup>, Chris Twitty<sup>3</sup>, Sharron Gargosky<sup>3</sup>, Jean Campbell<sup>3</sup>, Carmen Ballesteros-Merino<sup>4</sup>, Carlo B. Bifulco<sup>4</sup>, Bernard Fox<sup>4</sup>, Mai Le<sup>5</sup>, Robert H Pierce<sup>3</sup>, Adil Daud<sup>1</sup>

<sup>1</sup>University of California, San Francisco, San Francisco, CA, USA<sup>2</sup>Huntsman Cancer Institute, University of Utah, Salt Lake City, UT, USA<sup>3</sup>OncoSec Medical Inc., San Diego, CA, USA<sup>4</sup>Robert W. Franz Cancer Research Center, Earle A. Chiles Research Institute, Providence Cancer Center, Portland, Oregon, USA<sup>5</sup>Doctor Hope, LLC, San Diego, CA, USA**Background**

Low tumor infiltrating lymphocytes (TIL) are predictive for poor response to immunotherapy with anti-PD-1/PD-L1 agents. We have shown that melanoma patients with a low frequency of PD-1hiCTLA-4+TIL are unlikely to respond to pembrolizumab (Daud2016). Intratumoral electroporation of pIL-12 (IT-pIL12-EP) leads to an IFN-g signature suggestive of increased TIL as well as regression in both treated and untreated lesions. We hypothesize that combination IT-pIL12-EP and pembrolizumab will improve clinical outcomes in this low-response population. Preliminary results from a multi-center, phase II, open-label trial testing this hypothesis are presented.

**Methods**

Melanoma stage III/IV patients with accessible lesions were consented and enrolled if they had a TIL status of hiCTLA-4+ in the CD45+CD8+CD3+ gate by flow cytometry (FC). Patients were treated with pembrolizumab (200mg every 3 weeks) concurrently with IT-pIL12-EP on days 1, 5 and 8 every 6weeks. Patients were evaluated for overall response rate (ORR) every 12weeks by RECISTv1.1. Pre and post-treatment blood and tumor specimens were collected, and analyzed for immune phenotyping, gene expression, TCR diversity, and changes in the tumor microenvironment with multispectral immunohistochemistry.

**Results**

Interim ORR data is available on 15 patients. 13/15 patients had a frequency of PD-1hi CTLA-4+ TIL of < 22% (low TIL status), phenotypes associated with a low probability of response to anti-PD-1 (Daud 2016). These 15 patients age

39-89 years, were 53% male, 66% stage III and 34% stage IV. Treatment was well tolerated; 38% of adverse events (AE) were classified as treatment site reactions (grade 1-2) that resolved. One SAE of cellulitis resolved with 5d antibiotics. One grade 3 AE of diarrhea resolved with corticosteroids. The ORR was 40% (4CR, 2PR) by RECISTv1.1. Analysis of tumor biopsies and blood demonstrated meaningful immunological changes including an increased number and ratio of CD8+:PD-L1+ and CD8+:FoxP3+TIL, tumoral RNA signatures indicating an increase in CD8 and IFN-γ-related gene expression and concordant immune phenotypes in the periphery.

**Conclusions**

The combination IT-pIL12-EP with pembrolizumab in patients with an anti-PD-1 non-responsive phenotype engendered a 40% clinical response with associated positive immune-based biomarker data and an excellent safety profile. These data suggests that IT-pIL12-EP modulates the tumor microenvironment to enable an effective anti-PD-1 mAb response in patients otherwise unlikely to respond.

**Acknowledgements**

We thank Merck and Oncosec for supporting this trial with pembrolizumab and IT-pIL-12, respectfully.

**Trial Registration**

ClinicalTrials.gov identifier: NCT02493361

**References**

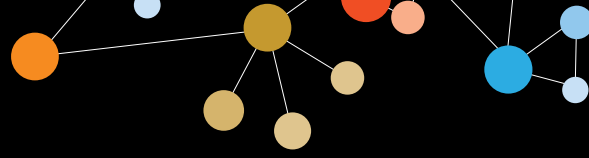
1. Daud AI, Loo K, Pauli ML, Sanchez-Rodriguez R, Sandoval PM, Taravati K, et al: **Tumor immune profiling predicts response to anti-PD-1 therapy in human melanoma**. *J Clin Invest* 2016, **126(9)**:3447-3452.

467

**Defining critical features of the immune microenvironment in melanoma**

Robyn Gartrell<sup>1</sup>, Douglas Marks<sup>1</sup>, Edward Stack<sup>2</sup>, Yan Lu<sup>1</sup>, Daisuke Izaki<sup>3</sup>, Kristen Beck<sup>4</sup>, Dan Tong Jia<sup>4</sup>, Paul Armenta<sup>4</sup>, Ashley White-Stern<sup>4</sup>, Yichun Fu<sup>4</sup>, Zoe Blake<sup>1</sup>, Howard L Kaufman<sup>5</sup>, Bret Taback<sup>1</sup>, Basil Horst<sup>1</sup>, *Yvonne M Saenger*<sup>6</sup>

<sup>1</sup>Columbia University Medical Center, New York, NY, USA<sup>2</sup>Perkin Elmer, Hopkinton, MA, USA<sup>3</sup>Columbia University, New York, NY, USA<sup>4</sup>Columbia University College of Physicians and Surgeons, New York, NY, USA<sup>5</sup>Rutgers Cancer Institute of New Jersey, New Brunswick, NJ, USA<sup>6</sup>New York Presbyterian/Columbia University Medical Center, New York, NY, USA



## Late-Breaking Abstracts - Tumor Microenvironment

Presenting author underlined; Primary author in italics

### Background

Precise biomarkers are urgently needed to characterize the tumor immune micro-environment, both for prognostication and to predict the benefit of immuno-therapeutic intervention. HLA-DR on tumor cells and Ki67 on cytotoxic (CD8+) T cells have been proposed as biomarkers of anti-PD1 activity. Multiplex immunohistochemistry (mIHC) allows for automated quantitation of phenotypes and spatial distributions of immune cell populations within formalin fixed paraffin embedded (FFPE) tissues.

### Methods

In order to test whether mIHC can better characterize the tumor immune microenvironment, we screened databases at the Herbert Irving Cancer Center (HICC) at Columbia University for early stage melanoma patients with available FFPE primary melanoma tissue and documented clinical follow up. We identified a preliminary population of 31 stage II-III melanoma patients diagnosed between 2000 and 2012, with characteristics shown in Table 1 for whom pathology from the primary biopsy was shown. Clinical follow up was available on 18 patients of whom 9 patients were alive with no evidence of recurrence, 1 had died of another malignancy, and 7 had died of melanoma. 15 patients had more than 24 months of survival information available but no detailed clinical information. 5µm slides from either the primary biopsy or subsequent wide local excision procedure were stained using Opal multiplex IHC for DAPI, CD3 (LN10, Leica), CD8 (4B11, Leica), CD68 (KP1, Biogenex), SOX10 (BC34, Biocare), HLA-DR (LN-3, Abcam) and Ki67 (MIB1, Abcam). Cell phenotypes within representative fields pre-selected by a trained dermato-pathologist and were visualized using the Mantra quantitative pathology workstation (Perkin Elmer), and analysis of spatial distribution of CD3+CD8+ cells analyzed as shown in Figures 1 and 2 using inForm® image analysis software (Perkin Elmer), and Spotfire software (TIBCO).

### Results

CD3+CD8+ cells are closer to both tumor (SOX10+) and CD68+ cells when they express HLA-DR ( $p < 0.001$ ). Conversely, CD3+CD8+ cells are significantly farther from Sox10+ cells when they express Ki-67. Among patients with clinical follow up, CD8+CD3+ cells in non-recurrent patients were closer to HLA-DR+Sox10+ cells than they were in recurrent patients( $p < 0.001$ ).

### Conclusions

If proximity is a surrogate for interaction, these data may indicate that HLA-DR expression enhances interaction with T cells for both CD68+ infiltrating cells and Sox10+ tumor cells. In addition, CD8+CD3+ cells were closer to HLA-DR+Sox10+ cells in patients who did not recur, which is interesting in light of recent data showing that expression of HLA-DR by tumor

cells increases likelihood of response to anti-PD1. Further staining and analysis of annotated tumor samples from the complete HICCC cohort 2000-2012 is ongoing and results will be updated at time of presentation.

**Table 1. Melanoma Patient Cohort Demographics**

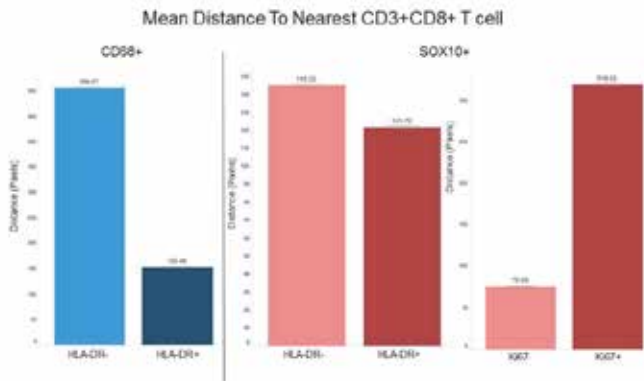
Melanoma Patient Characteristics		
Characteristics	Patients (N=32)	
<b>Clinical Characteristics:</b>		
<b>Gender</b>		
Male, no. (%)	22	(19.5)
Female, no. (%)	10	(8.8)
Age median (years), (range)	74	(35-90)
<b>Location of Tumor</b>		
Trunk, no (%)	9	(29.0)
Extremity, no (%)	22	(71.0)
<b>Stage</b>		
II, no (%)	24	(75.0)
III, no (%)	8	25.0
<b>Pathological characteristics</b>		
Depth (mm), median (range)	2.8	(0.7-11)
<b>Ulceration</b>		
Absent	15	(46.9)
Present	10	(31.3)
Not reported	7	(21.9)
<b>Patient Follow-Up,</b>		
Median (Months), (range)	42.5	(4-151)
Alive, no. (%)	20	(69.0)
Dead, no. (%)	9	(31.0)

Table 1: Demographic Characteristics of Melanoma

Late-Breaking Abstracts - Tumor Microenvironment

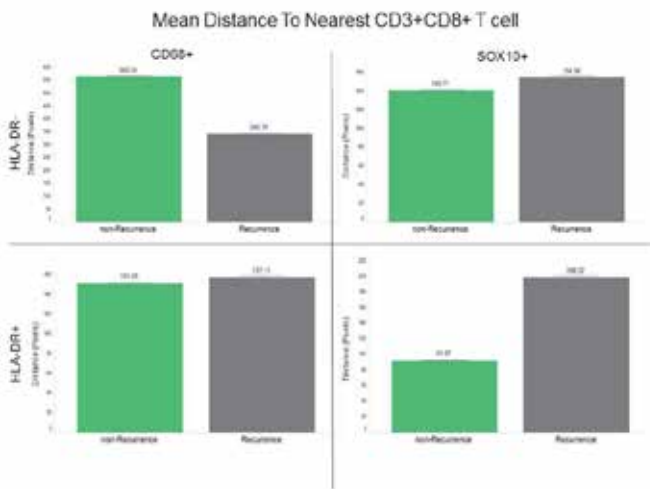
Presenting author underlined; Primary author in italics

Figure 1: Mean Distance From HLA-DR+ cells to Nearest CD3+CD8+



Distance between CD3+CD8+ T cells and nearest neighbor, Left: Mean distance from CD3+CD8+ to CD68+HLA-DR- (light blue) or CD68+HLA-DR+ (dark blue), Center: Mean distance from CD3+CD8+ to SOX10+HLA-DR- (pink) or SOX10+HLA-DR+ (red), Right: Mean distance from CD3+CD8+ to SOX10+Ki67- (pink) or SOX10+Ki67+ (red).

Figure 2: Mean Distance To Nearest CD3+CD8+ T cell by Recurrence Status



Distance between CD3+CD8+ T cells and nearest neighbor by recurrence status, Top Left: Mean distance from CD3+CD8+ to CD68+HLA-DR- by recurrence status, Lower Left: Mean distance from CD3+CD8+ to CD68+HLA-DR+ by recurrence status. Top Right: Mean distance from CD3+CD8+ to SOX10+HLA-DR- by recurrence status, Bottom Right: Mean distance from CD3+CD8+ to SOX10+HLA-DR+ by recurrence status.

468

Immune profiling via multiplexed immunofluorescence shows that Imprime based anti-cancer efficacy involves profound changes in macrophage polarization, type 1 IFN signaling and the formation of immune cell clusters

Steven Leonardo, Keith Gorden, Ross B Fulton, Kathryn Fraser, Takashi O Kangas, Richard Walsh, Kathleen Ertelt, Jeremy Graff, Mark Uhlik

Biothera Pharmaceuticals Inc., Eagan, MN, USA

Background

Imprime PGG (Imprime) is a soluble, intravenously (iv) administered yeast 1,3/1,6 β-glucan PAMP (pathogen-associated molecular pattern). As a PAMP, Imprime triggers innate immune function, including direct tumor killing, repolarization of the immunosuppressive tumor microenvironment (flipping immunosuppressive M2 macrophages to an anti-tumor M1 state), and T cell expansion and activation via dendritic cell maturation and antigen presentation. Clinically, Imprime has demonstrated promising efficacy in clinical trials when combined with tumor-targeting or anti-angiogenic antibodies. Phase II studies with pembrolizumab are starting in both metastatic triple negative breast cancer and metastatic melanoma. Herein, we have employed multiplexed immunofluorescence to profile the immune microenvironment in preclinical tumor tissues.

Methods

The B16F10 experimental metastasis model was used to interrogate Imprime’s anti-tumor activity *in vivo*. B16F10 melanoma cells were injected into the tail vein of syngeneic C57BL/6 mice, seeding the lungs with B16 foci. Outgrowth of these metastatic foci was assessed after treatment with the tumor-targeting anti-trypt1 antibody TA99, Imprime, or the combination. At various times post tumor injection, lungs were examined via multiplexed immunofluorescence (IFC) for markers of immune infiltration and activation. IFC was performed using 7-color staining (Opal technology, PerkinElmer) combined with *in situ* hybridization (RNAScope, ACD). Images were acquired with the Vectra3 multispectral imaging system and cells segmented using Inform (PerkinElmer). Imaging data were transformed into “.fcs” files and analyzed using Flowjo flow cytometry software (Treestar). Relational parameters such as immune cell clustering and tumor infiltration were performed via custom algorithms in R.





## Late-Breaking Abstracts - Tumor Microenvironment

Presenting author underlined; Primary author in italics

### Results

TA99 alone suppressed the outgrowth of B16 lung metastases by 54% when compared to vehicle treatment. The combination of Imprime with TA99 reduced the number of metastases even more profoundly (96% vs vehicle). IFC analyses showed that Imprime specifically accumulates in the tumor stroma, binds to macrophages and elicits increased iNOS production, indicating the re-polarization of these macrophages to a more M1-like, inflammatory state. Imprime-treatment also triggered the formation of large immune cell clusters, possibly representing resolved tumor nests or the establishment of tertiary lymphoid tissues, both of which have been identified as predictors of successful anti-tumor immune responses. Finally, Imprime treatment and localization at the tumor site corresponds with substantial upregulation of the gene *Mx1*- a type 1 interferon-responsive gene.

### Conclusions

Imprime is a potent immunomodulator that induces a coordinated immune attack *in vivo* demonstrated by immune cell binding, M1 re-polarization and a type-1 interferon signature that coincides with reduced outgrowth of established lung metastases.

469

### Local convection-enhanced delivery of PD-1 blockade antibody in *de novo* murine model of glioblastoma

Jennifer S Sims, Liang Lei, Takashi Tsujiuchi, Jeffrey N Bruce, Peter Canoll

Columbia University Medical Center, New York, NY, USA

### Background

Systemic delivery of anti-PD1 antibody therapy has proven relatively safe in glioma patients, but therapeutic response remains unpredictable and persistently low. Checkpoint blockade antibodies face numerous potential confounders in these tumors, such as the blood-brain barrier, poor local or lymph node presentation of tumor antigens, and unknown dependency on PD-1/PD-L1 activity during tumor progression. Here, we conducted a pilot study using intracranial convection-enhanced delivery (CED) of anti-PD1 (mDX400) into a *de novo* murine glioma model to dissect tumor and immune perturbations following local treatment, and to compare the efficacy of treating during early or late tumor progression.

### Methods

Transgenic C57BL/6-PTEN(f1/f1) mice were injected with a retrovirus expressing PDGFb and cre recombinase, inducing tumorigenesis as previously described. In this model, with a median survival of 80 days post-tumor induction (D80), convergence to a stereotyped subset of genomic

rearrangements occurs by approximately D35. Intracranial osmotic pumps filled with mDX400 or isotype control antibody solution were implanted at the tumor site for 14-day windows spanning (D28-D42) or following (D42-D56) this developmental transition, then removed. Tumor burden was monitored by bioluminescence (luciferase reporter), and mice were sacrificed upon presentation of tumor-related morbidity. Tissue was formalin-fixed for histopathology and cryopreserved for gene expression analysis.

### Results

During both treatment windows, tumor burden decreased differentially in mDX400-treated mice. While survival time between mDX400- and isotype-treated mice was nearly identical for D28-D42 (both median D70), for mice treated between D42-D56, median survival differed (D88 vs. D68), but without statistical significance between the groups ( $p=0.25$ ). Interestingly, the D42-D56 mDX400 group produced several "long-term survivors", who lived up to 158 days with stable tumor burden. While substantial T cell infiltration was detected in the end-stage tumors of both mDX400- and isotype-treated mice by immunohistochemistry (CD3e), expression of immune signaling pathways (e.g., Fc receptor and Toll-like receptor families, phagosome/lysosome components), was significantly higher among three long-surviving mDX400-treated mice than in three isotype-treated mice.

### Conclusions

Our pilot study of mDX400 administration by CED identified an impact on tumor burden during and following therapy, but a lack of survival benefit for D28-D42 treatment. While additional experiments are needed to statistically evaluate survival benefit for the later treatment window, differentially high intratumoral expression of genes reflecting immune activation among mDX400-treated, long-surviving mice demonstrates that molecular study in this model may elucidate intratumoral conditions associated with response to anti-PD1 blockade in glioma.

### Acknowledgements

This pre-clinical study is supported by Merck & Co. Investigator-Initiated Sponsored Projects grant LKR146174.





# Journal for ImmunoTherapy of Cancer

The Official Journal of the *Society for Immunotherapy of Cancer*



## CALL FOR SUBMISSIONS



To support our members' continued efforts to improve the lives of people with cancer, **all members' article processing charges are waived through 2016!**

Pedro J. Romero, MD, JITC Editor-in-Chief, welcomes submissions to the journal sections listed below.

## ABOUT THE JOURNAL

**International • Open Access • Peer Reviewed**

The *Journal for ImmunoTherapy of Cancer* (JITC) is the official online journal of the Society for Immunotherapy of Cancer (SITC).

An outlet devoted to and created by today's leaders in the field, JITC provides rapid dissemination of cutting-edge tumor immunology and cancer immunotherapy discoveries—from basic research through clinical application—by contributors from around the world.

## INDEXING

JITC is currently indexed in five major indexing databases including: PubMed, PubMed Central, the Directory of Open Access Journals (DOAJ), Thomson Reuters' Emerging Sources Citation Index (ESCI) and Elsevier's Scopus database.

## JOURNAL SECTIONS



### Basic Tumor Immunology

*Cornelis J.M. Melief, MD, PhD*



### Case Reports

*Alfred Zippelius, MD*



### Clinical/Translational Cancer Immunotherapy

*F. Stephen Hodi, Jr., MD*



### Clinical Trials Monitor

*Leisha A. Emens, MD, PhD*



### Commentary/Editorials

*Christian Capitini, MD*

**New Section Coming Soon:  
Guidelines and Consensus Statements  
featuring SITC's Cancer Immunotherapy Guidelines**



### Immunotherapy Biomarkers

*Lisa H. Butterfield, PhD*



### Reviews

*Bernard A. Fox, PhD*



### Reviews

*Thomas F. Gajewski, MD, PhD*

Visit [sitcancer.org/journal](http://sitcancer.org/journal) to submit your research and for instant online access to SITC's 31<sup>st</sup> Annual Meeting Abstracts, the 2016 JITC Best Paper Award publications and more.



Society for Immunotherapy of Cancer

SAVE THE DATES

# SITC 2017

November 8-12

NATIONAL HARBOR  
MARYLAND

Gaylord National Hotel  
& Convention Center

## *Thank You to Our Organizers!*

### **SITC 32<sup>nd</sup> Annual Meeting**

Charles G. Drake, MD, PhD – *Columbia University Herbert Irving Comprehensive Cancer Center*

Susan M. Kaech, PhD – *Yale University*

Marcela V. Maus, MD, PhD – *Massachusetts General Hospital Cancer Center*

Laura S. Wood, RN, MSN, OCN – *Cleveland Clinic Taussig Cancer Center*

### **Workshop on Single Cell Techniques in Immunology and Cancer Immunotherapy**

Nir Hacohen, PhD – *Massachusetts General Hospital*

### **Primer on Tumor Immunology and Cancer Immunotherapy™**

Nina Bhardwaj, MD, PhD – *The Tisch Cancer Institute at The Mount Sinai Medical Center*

### **Grant Writing Workshop on Cancer Immunotherapy Protocol Development**

*Organized by the Early Career Scientist Committee*



Society for Immunotherapy of Cancer